

Blue carbon: Beyond the inventory

Edited by

Joanne S. Porter, William Richard Turrell, Hilary Anne Kennedy,
William Edward Newns Austin and Catherine Lovelock

Published in

Frontiers in Marine Science



FRONTIERS EBOOK COPYRIGHT STATEMENT

The copyright in the text of individual articles in this ebook is the property of their respective authors or their respective institutions or funders. The copyright in graphics and images within each article may be subject to copyright of other parties. In both cases this is subject to a license granted to Frontiers.

The compilation of articles constituting this ebook is the property of Frontiers.

Each article within this ebook, and the ebook itself, are published under the most recent version of the Creative Commons CC-BY licence. The version current at the date of publication of this ebook is CC-BY 4.0. If the CC-BY licence is updated, the licence granted by Frontiers is automatically updated to the new version.

When exercising any right under the CC-BY licence, Frontiers must be attributed as the original publisher of the article or ebook, as applicable.

Authors have the responsibility of ensuring that any graphics or other materials which are the property of others may be included in the CC-BY licence, but this should be checked before relying on the CC-BY licence to reproduce those materials. Any copyright notices relating to those materials must be complied with.

Copyright and source acknowledgement notices may not be removed and must be displayed in any copy, derivative work or partial copy which includes the elements in question.

All copyright, and all rights therein, are protected by national and international copyright laws. The above represents a summary only. For further information please read Frontiers' Conditions for Website Use and Copyright Statement, and the applicable CC-BY licence.

ISSN 1664-8714
ISBN 978-2-8325-4057-2
DOI 10.3389/978-2-8325-4057-2

About Frontiers

Frontiers is more than just an open access publisher of scholarly articles: it is a pioneering approach to the world of academia, radically improving the way scholarly research is managed. The grand vision of Frontiers is a world where all people have an equal opportunity to seek, share and generate knowledge. Frontiers provides immediate and permanent online open access to all its publications, but this alone is not enough to realize our grand goals.

Frontiers journal series

The Frontiers journal series is a multi-tier and interdisciplinary set of open-access, online journals, promising a paradigm shift from the current review, selection and dissemination processes in academic publishing. All Frontiers journals are driven by researchers for researchers; therefore, they constitute a service to the scholarly community. At the same time, the *Frontiers journal series* operates on a revolutionary invention, the tiered publishing system, initially addressing specific communities of scholars, and gradually climbing up to broader public understanding, thus serving the interests of the lay society, too.

Dedication to quality

Each Frontiers article is a landmark of the highest quality, thanks to genuinely collaborative interactions between authors and review editors, who include some of the world's best academicians. Research must be certified by peers before entering a stream of knowledge that may eventually reach the public - and shape society; therefore, Frontiers only applies the most rigorous and unbiased reviews. Frontiers revolutionizes research publishing by freely delivering the most outstanding research, evaluated with no bias from both the academic and social point of view. By applying the most advanced information technologies, Frontiers is catapulting scholarly publishing into a new generation.

What are Frontiers Research Topics?

Frontiers Research Topics are very popular trademarks of the *Frontiers journals series*: they are collections of at least ten articles, all centered on a particular subject. With their unique mix of varied contributions from Original Research to Review Articles, Frontiers Research Topics unify the most influential researchers, the latest key findings and historical advances in a hot research area.

Find out more on how to host your own Frontiers Research Topic or contribute to one as an author by contacting the Frontiers editorial office: frontiersin.org/about/contact

Blue carbon: Beyond the inventory

Topic editors

Joanne S. Porter — Heriot-Watt University, United Kingdom
William Richard Turrell — Marine Scotland, United Kingdom
Hilary Anne Kennedy — Bangor University, United Kingdom
William Edward Newns Austin — University of St Andrews, United Kingdom
Catherine Lovelock — The University of Queensland, Australia

Citation

Porter, J. S., Turrell, W. R., Kennedy, H. A., Austin, W. E. N., Lovelock, C., eds. (2024).
Blue carbon: Beyond the inventory. Lausanne: Frontiers Media SA.
doi: 10.3389/978-2-8325-4057-2

Table of contents

- 05 **Sounding Out the Carbon: The Potential of Acoustic Backscatter Data to Yield Improved Spatial Predictions of Organic Carbon in Marine Sediments**
Corallie A. Hunt, Urška Demšar, Ben Marchant, Dayton Dove and William E. N. Austin
- 25 **Future Mangrove Carbon Storage Under Climate Change and Deforestation**
Mark Chatting, Ibrahim Al-Maslamani, Mark Walton, Martin W. Skov, Hilary Kennedy, Y. Sinan Husrevoglu and Lewis Le Vay
- 39 **Blue Carbon Storage in a Northern Temperate Estuary Subject to Habitat Loss and Chronic Habitat Disturbance: Cowichan Estuary, British Columbia, Canada**
Tristan J. Douglas, Goetz Schuerholz and S. Kim Juniper
- 63 **Blue Carbon Ecosystems in Brazil: Overview and an Urgent Call for Conservation and Restoration**
Marcelo O. Soares, Luis Ernesto Arruda Bezerra, Margareth Copertino, Beatriz Diniz Lopes, Kcrishna Vilanova de Souza Barros, Cristina Almeida Rocha-Barreira, Rafaela Camargo Maia, Natalia Beloto and Luiz C. Cotovicz Jr.
- 79 **Implication of Macroalgal Bloom to Soil Organic Carbon Stock in Seagrass Meadows - A Case Study in South Hainan, China**
Shunyang Chen, Shiquan Chen, Bin Chen, Zhongjie Wu, Wenshuo An, Lizhen Luo, Jing Wang, Limei Xie, Jing Zhang and Guangcheng Chen
- 87 **Variability in the Net Ecosystem Productivity (NEP) of Seaweed Farms**
Yoichi Sato, Gregory N. Nishihara, Atsuko Tanaka, Dominic F. C. Belleza, Azusa Kawate, Yukio Inoue, Kenjiro Hinode, Yuhei Matsuda, Shinichiro Tanimae, Kandai Tozaki, Ryuta Terada and Hikaru Endo
- 99 **Nordic Blue Carbon Ecosystems: Status and Outlook**
Dorte Krause-Jensen, Hege Gundersen, Mats Björk, Martin Gullström, Martin Dahl, Maria E. Asplund, Christoffer Boström, Marianne Holmer, Gary T. Banta, Anna Elizabeth Løvgren Graversen, Morten Foldager Pedersen, Trine Bekkby, Helene Frigstad, Solrun Figenschau Skjellum, Jonas Thormar, Steen Gyldenkærne, Jennifer Howard, Emily Pidgeon, Sunna Björk Ragnarsdóttir, Agnes Mols-Mortensen and Kasper Hancke
- 123 **Towards Incorporation of Blue Carbon in Falkland Islands Marine Spatial Planning: A Multi-Tiered Approach**
Narissa Bax, David K. A. Barnes, Santiago E. A. Pineda-Metz, Tabitha Pearman, Markus Diesing, Stefanie Carter, Rachel V. Downey, Chris D. Evans, Paul Brickle, Alastair M. M. Baylis, Alyssa M. Adler, Amy Guest, Kara K. S. Layton, Paul E. Brewin and Daniel T. I. Bayley

- 136 **Review of Evaluation and Valuation Methods for Cetacean Regulation and Maintenance Ecosystem Services With the Joint Cetacean Protocol Data**
Jack Michael Sheehy, Nicola L Taylor, Nadescha Zwerschke, Mark Collar, Vicky Morgan and Eugenia Merayo
- 158 **A Guide to International Climate Mitigation Policy and Finance Frameworks Relevant to the Protection and Restoration of Blue Carbon Ecosystems**
Mathew A. Vanderklift, Dorothée Herr, Catherine E. Lovelock, Daniel Murdiyarso, Jacqueline L. Raw and Andrew D. L. Steven
- 172 **Mangroves Cover Change Trajectories 1984-2020: The Gradual Decrease of Mangroves in Colombia**
Paulo J. Murillo-Sandoval, Lola Fatoyinbo and Marc Simard
- 186 **Spatially Explicit Seagrass Extent Mapping Across the Entire Mediterranean**
Dimosthenis Traganos, Chengfa Benjamin Lee, Alina Blume, Dimitris Poursanidis, Hrvoje Čižmek, Julie Deter, Vesna Mačić, Monica Montefalcone, Gérard Pergent, Christine Pergent-Martini, Aurora M. Ricart and Peter Reinartz
- 199 **Is All Seagrass Habitat Equal? Seasonal, Spatial, and Interspecific Variation in Productivity Dynamics Within Mediterranean Seagrass Habitat**
Emma A. Ward, Charlotte Aldis, Tom Wade, Anastasia Miliou, Thodoris Tsimpidis and Tom C. Cameron
- 216 **Assessing the potential vulnerability of sedimentary carbon stores to bottom trawling disturbance within the UK EEZ**
Kirsty E. Black, Craig Smeaton, William R. Turrell and William E. N. Austin
- 233 **Using citizen science to estimate surficial soil Blue Carbon stocks in Great British saltmarshes**
Craig Smeaton, Annette Burden, Paulina Ruranska, Cai J. T. Ladd, Angus Garbutt, Laurence Jones, Lucy McMahon, Lucy C. Miller, Martin W. Skov and William E. N. Austin
- 249 **Sedimentary carbon on the continental shelf: Emerging capabilities and research priorities for Blue Carbon**
Carolyn A. Graves, Lisa Benson, John Aldridge, William E. N. Austin, Franck Dal Molin, Vera G. Fonseca, Natalie Hicks, Clare Hynes, Silke Kröger, Philip D. Lamb, Claire Mason, Claire Powell, Craig Smeaton, Sarah K. Wexler, Clare Woulds and Ruth Parker
- 271 **Salt marsh-atmosphere CO₂ exchanges in Patos Lagoon Estuary, Southern Brazil**
Ronald B. Souza, Margareth S. Copertino, Gilberto Fisch, Marcelo F. Santini, Walter H. D. Pinaya, Fabiane M. Furlan, Rita de Cássia M. Alves, Osmar O. Möller Jr. and Luciano P. Pezzi



Sounding Out the Carbon: The Potential of Acoustic Backscatter Data to Yield Improved Spatial Predictions of Organic Carbon in Marine Sediments

Corallie A. Hunt^{1*}, Urška Demšar¹, Ben Marchant², Dayton Dove³ and William E. N. Austin^{1,4}

¹ School of Geography and Sustainable Development, University of St Andrews, St Andrews, United Kingdom, ² British Geological Survey, Keyworth, United Kingdom, ³ British Geological Survey, The Lyell Centre, Edinburgh, United Kingdom, ⁴ Scottish Marine Institute, Scottish Association for Marine Science, Oban, United Kingdom

OPEN ACCESS

Edited by:

Martin Zimmer,
Leibniz Centre for Tropical Marine
Research (LG), Germany

Reviewed by:

Natascha Maria Oppelt,
University of Kiel, Germany
Zvi Steiner,
GEOMAR Helmholtz Center for Ocean
Research Kiel, Germany

*Correspondence:

Corallie A. Hunt
cah24@st-andrews.ac.uk

Specialty section:

This article was submitted to
Global Change and the Future Ocean,
a section of the journal
Frontiers in Marine Science

Received: 10 August 2021

Accepted: 22 October 2021

Published: 11 November 2021

Citation:

Hunt CA, Demšar U, Marchant B,
Dove D and Austin WEN (2021)
Sounding Out the Carbon:
The Potential of Acoustic Backscatter
Data to Yield Improved Spatial
Predictions of Organic Carbon
in Marine Sediments.
Front. Mar. Sci. 8:756400.
doi: 10.3389/fmars.2021.756400

Marine sediments hold vast stores of organic carbon (OC). Techniques to spatially map sedimentary OC must develop to form the basis of seabed management tools that consider carbon-rich sediments. While the natural burial of carbon (C) provides a climate regulation service, the disturbance of buried C could present a significant positive feedback mechanism to atmospheric greenhouse gas concentrations. We present a regional Scottish case study that explores the suitability of integrating archived seafloor acoustic data (i.e., multibeam echosounder bathymetry and backscatter) with physical samples toward improved spatial mapping of surface OC in a dynamic coastal environment. Acoustic backscatter is a proxy for seabed sediments and can be collected over extensive areas at high resolutions. Sediment type is also an important predictor of OC. We test the potential of backscatter as a proxy for OC which may prove useful in the absence of exhaustive sediment data. Overall, although statistically significant, correlations between the variables OC, sediment type, and backscatter are relatively weak, likely reflecting a combination of limited and asynchronous data, sediment mobility over time, and complex environmental processing of OC in shelf sediments. We estimate linear mixed models to predict OC using backscatter and Folk sediment type as covariates. Our results show that incorporating backscatter in the model improves the precision of OC predictions by 14%. Backscatter discriminates between coarse and fine sediments, and therefore low and high OC regimes; however, was not able to discriminate amongst finer sediments. Although sediment type is a stronger predictor of OC, these data are available at a much lower spatial resolution and do not account for fine-scale variability. The resulting maps display varying spatial distributions of OC reflecting the different scales of the predictor variables, demonstrating a need for further methodological development. Backscatter shows considerable promise as a high-resolution predictor variable to improve the precision

of surface OC maps, or to reduce the number of OC measurements required to achieve a specified precision. Applications of such maps have potential in improved C-stock estimates and the design of conservation and management strategies that consider marine sediments as valuable C stores.

Keywords: organic carbon, sedimentary carbon, multibeam, folk classification, acoustic backscatter, carbon stocks, spatial models, climate mitigation

INTRODUCTION

The marine environment has a significant role within the global carbon (C) cycle with 93% of the earth's C stored and cycled here, providing an essential energy source for marine biodiversity (Nellemann et al., 2009). Carbon captured by coastal and marine ecosystems is known as blue carbon (BC). The marine environment can store disproportionate amounts of organic carbon (OC) within marine organisms and associated sediments compared to terrestrial C stores, such as forest and peat (Duarte et al., 2005; Donato et al., 2011; McLeod et al., 2011; Goldstein et al., 2020). Marine sediments are currently overlooked within current BC definitions and accounting frameworks because they do not directly sequester C via photosynthesis (Lovelock and Duarte, 2019). However, they are a regional and global repository for OC and act to bury, and thus remove, OC from the active C cycle over geological timescales (Smith et al., 2015; Sayedi et al., 2020). This natural process provides an indirect and valuable climate regulation service (Luisetti et al., 2019). Activities that physically disturb seabed sediments cause the resuspension and exposure of buried OC to oxygen, which can be remineralised back to aqueous CO₂ (Aller, 1994; Macreadie et al., 2019). The management of these activities, such as benthic trawling (Paradis et al., 2017), could be key to maintaining sediments as part of the suite of nature-based solutions for mitigating against climate change (Sala et al., 2021). Assessments of the spatial distribution of sedimentary OC are key to understanding the processes that influence how C is processed and where it is more likely to be accumulating, i.e., carbon hotspots (Diesing et al., 2021).

Spatial maps of sedimentary OC have been developed that improve global and national-scale C-stock estimates within the marine environment (Diesing et al., 2017; Atwood et al., 2020; Smeaton et al., 2020). Maps can be produced by estimating an average OC content per sediment type, often Folk-classified, and scaling up to the areal extent of the sediment coverage (e.g., Smeaton et al., 2020), or through a modelled approach using existing data and a suite of predictor variables to estimate C content in places not directly measured (e.g., Diesing et al., 2017). These studies have progressed our understanding of the large-scale spatial distribution of sedimentary OC, however, uncertainties in stock estimates over large areas can also be high (Burrows et al., 2014; Diesing et al., 2017). Data for sedimentary OC are generally limited at the spatial scales required for effective seabed management strategies (Burrows et al., 2017; Pınarbaşı et al., 2017) and consequently maps at higher spatial resolutions (e.g., regional-scale) are needed (Pace et al., 2021). Following a successful demonstration study using multibeam echosounder (MBES)

data that produced a high-resolution map of OC (Hunt et al., 2020), we suggest that acoustic backscatter could be an effective predictor variable to improve OC maps, as has been demonstrated within habitat modelling studies (De Falco et al., 2010; Lucieer et al., 2013).

Physically sampling (i.e., “ground-truthing”) the seabed is a logistically-challenging, time-consuming, and expensive exercise. In contrast, acoustic mapping via MBES offers the opportunity to acquire spatially continuous, high-resolution imagery of seabed depth and morphology (i.e., MBES bathymetry) and a measure of seabed texture, composition, and hardness (i.e., MBES backscatter) (Lurton and Lamarche, 2015) at a lower expense. MBES data are regularly used to characterise the seabed because acoustic backscatter intensity acts as a proxy for substrate composition (Collier and Brown, 2005; McGonigle and Collier, 2014) by responding to complexities in substrate texture and hardness. Point sample measurements can be maximised by interpolating information, such as habitat type, over extensive areas, giving continuous maps which are useful for seabed conservation and management (Lecours, 2017). Application of this technology has been demonstrated in a range of studies to map different structures and habitats, including: geological features, such as evidence of glacial bedforms (Dove et al., 2015), horse-mussel (*Modiolus modiolus*) reef extents (Lindenbaum et al., 2008), and in one study, backscatter strength was found to be sufficiently distinct to identify at least six different seafloor habitats across the study sites, including a mixture of geological and biological substrates (Parnum and Gavrilov, 2012). However, despite the advantages of this technology, the complex nature of acoustic scattering within the marine environment means fundamental challenges still remain, for instance with delineating between gradual changes in substrate textures, and thus ground-truthing is still a necessary activity to interpret the signal (Misiuk et al., 2018; Diesing et al., 2020).

The basis for using backscatter as a predictor of OC comes from extrapolating empirical relationships between sediment grain size and OC (Hedges and Keil, 1995; Burdige, 2007) and between sedimentary properties and backscatter reflectance (Collier and Brown, 2005; Che Hasan et al., 2014). In this study, we explore the potential of ground-truthing an archive MBES dataset to predict the spatial distribution of OC within surface sediments. Interpolating OC measurements over an exhaustive surface could support improved C stock estimates and identify localised hotspots that may be lost within larger scale (e.g., national) mapping (Lecours et al., 2015). Under its statutory obligations to maritime safety, the United Kingdom Hydrographic Office (UKHO) collects hydrographic, oceanographic, and geophysical data in

waters of national responsibility to maintain high-resolution bathymetric charts. Systematic surveys are undertaken by the Civil Hydrography Programme (CHP) that uses acoustic systems to map the seabed. This data archive of MBES with ground truth samples presents a potentially cost-effective opportunity to extend the methodology of Hunt et al. (2020), to predict the surface distribution of OC more widely. Other studies have already shown the viability of using these archived MBES data to improve the mapping of seabed substrate (e.g., Diesing et al., 2014).

With a growing body of work supporting the role that coastal and shelf seabed sediments play in the long-term storage of C (Smith et al., 2015; Legge et al., 2020), considerations of how to incorporate marine C stocks in national C accounts are being developed (Luisetti et al., 2020). For a maritime nation such as Scotland, which has a considerably larger seabed area than landmass, marine carbon stocks form a significant proportion of the national carbon inventory (Avelar et al., 2017) and as such, spatial information is integral to informed management to protect sediments as nature-based solutions for climate change mitigation and biodiversity benefits (Shafiee, 2021). Diverse mitigation strategies against GHG emissions are needed to achieve targets set under the Paris Agreement to contain global temperature rise below two degrees relative to pre-industrial temperatures (United Nations/Framework Convention on Climate Change, 2015).

This study presents a potential methodological approach to mapping marine carbon stores that go beyond the current inventory. We explore the potential of archived MBES and sedimentary datasets as a cost-effective opportunity to improve regional-scale OC maps as tools to support decision-makers. We take an archive MBES survey dataset collected within the Moray Firth on the east coast of Scotland with the following aims: (1) to ground-truth the MBES dataset and explore the patterns of OC distribution; (2) to compare the effectiveness of using acoustic backscatter data to spatially predict OC against sediment type (Folk classification), a common and readily available predictor for OC; (3) to apply fitted linear mixed models (LMMs) to generate a regional-scale map of OC in a geostatistical framework; (4) to estimate a regional surface (10 cm) OC stock over the MBES area; and (5) to discuss the opportunities and limitations of using MBES to spatially map OC.

REGIONAL SETTING

Our study site is located within the Moray Firth Region, an embayment in the North Sea off the east coast of Scotland, United Kingdom (**Figure 1**). The inner part of this coastal zone is characterised as estuarine and is fed by three large estuaries, the Beaully, Cromarty and Dornoch Firths to the southwest of the site. Moving eastwards, the Moray Firth extends into the North Sea and is characterised by a shallow shelf. The seabed bathymetry generally slopes away from the coast to an average depth of 50 m within 15 km in the inner Moray Firth. Beyond this, the shelf

maintains a gradual slope to the central northern North Sea to depths between 150 and 250 m. A notable bathymetric feature within our study area is a narrow, deep trough orientated in a NNE-SSW direction that separates the Smith Bank from the immediate coastal zone reaching 80 m depths (Chesher and Lawson, 1983).

The seabed of the Moray Firth comprises a thin cover of Holocene sediments which are relict glacial and post-glacial accretions from offshore sources (**Figure 1**) (BGS (British Geological Survey), 1987; Reid and McManus, 1987). Following glacial melt at the start of the Holocene a rapid rise in sea level resulted in a source of lithic material to the area of predominantly sandy facies (Andrews et al., 1990). Sediments here are also sourced from fluvial contributions of the Dornoch and Cromarty Firths, limited to the south-west of the site and composed of muddy sands (Chesher and Lawson, 1983). Coarser, gravelly sands are found along the southern and northern coastlines in shallow water areas. Biogenic carbonate material is a final source of material which accumulates from calcareous seabed biota within the shallow coastal waters and which influences sediment composition (Holmes et al., 2004).

Sediment distribution is driven by local hydrodynamic regimes interacting with broader scale bathymetric variation. Due to the relatively shallow nature of the seabed, near-bed currents are mainly driven by wind and tidal interactions; the dominant current direction is from the north and north-east as NE Atlantic waters are channelled into the northern North Sea through the narrow channels between the Scottish mainland and offshore islands (Holmes et al., 2004).

MATERIALS AND METHODS

To investigate the suitability of acoustic backscatter data to act as a proxy for sediment type, and thereby a predictor of OC on the shelf, we first ground truth an MBES survey and generate a sedimentary C dataset to examine relationships between backscatter, sediment type and OC. We fit LMMs for the two covariates, including the backscatter over a range of scales, and use geostatistical interpolation to predict OC across the footprint. We compare how well each of the covariates predicts spatial OC and calculate surficial stock estimates for the best models. We use an existing MBES dataset as a cost-effective way to re-purpose marine datasets. In this section, we describe each of these steps in detail; the flow diagram in **Figure 2** provides a summary for reference.

Multibeam Echosounder Survey

The Civil Hydrography Programme (CHP) acoustic datasets are made available through the respective bathymetry¹ (UKHO hosted) and backscatter² (BGS hosted) Data Archive Centres. The “HI1150 survey: Tarbat Ness to Sarclet Head” MBES dataset was

¹<https://datahub.admiralty.co.uk/portal/apps/sites/#/marine-data-portal/pages/seabed-mapping-services>

²<https://www.bgs.ac.uk/map-viewers/geoindex-offshore/>

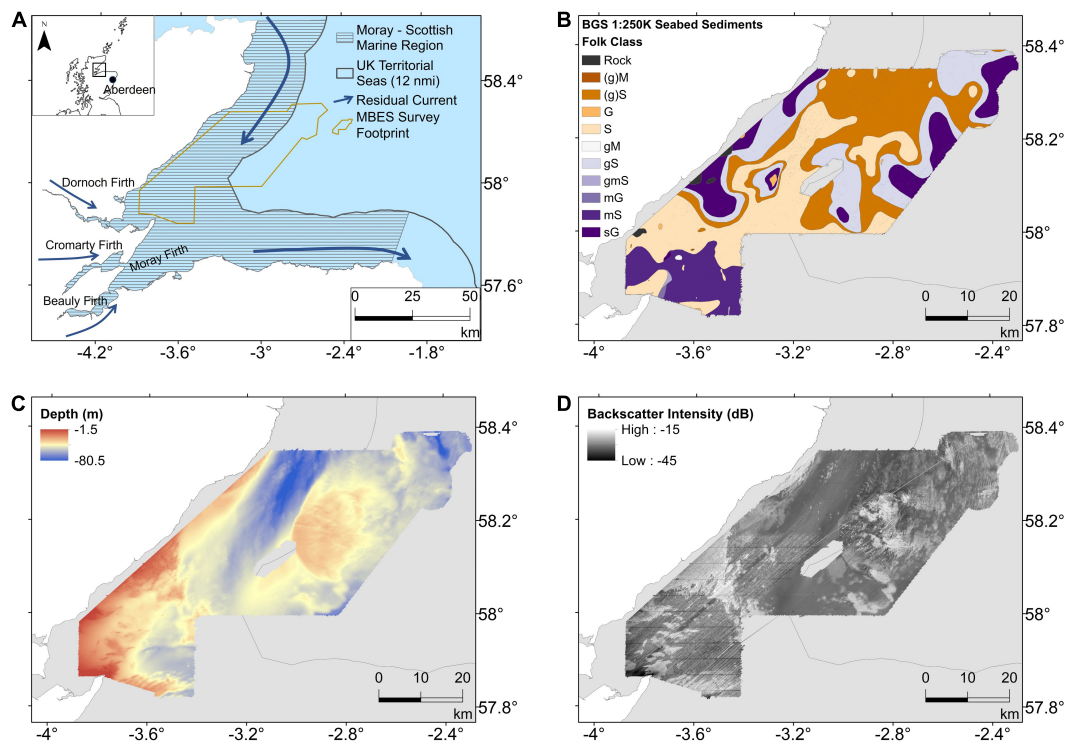


FIGURE 1 | (A) Location map for the survey area within the Moray Firth on the east coast of Scotland. The inset map shows the location in the context of Scotland. **(B)** Folk sediment map from the BGS 1:250K Seabed Sediment product DigSBS250 (accessed from: https://mapapps2.bgs.ac.uk/geoindex_offshore/home.html). Folk codes as follows: (g)M, slightly gravelly mud; (g)S, slightly gravelly sand; G, gravel; S, sand; gM, gravelly mud; gS, gravelly sand; gmS, gravelly muddy sand; mG, muddy gravel; mS, muddy sand; sG, sandy gravel. **(C,D)** H1150 MBES survey results. The rasters are presented at a 6 m × 6 m pixel resolution and the ArcGIS tool, “Focal Statistics” (circular neighbourhood, 3 m) has been applied to smooth noise. **(C)** Bathymetry (m). **(D)** Acoustic Backscatter Intensity (dB). The white area represents land, and the light-grey area represents the sea.

selected given that, firstly, physical sediment samples collected during the survey are archived at the National Geological Repository (NGR) in Keyworth, United Kingdom, and available to subsample for grain size and C analysis; and secondly, the typical sediment type (muddy-sands to sands) across the area was compatible to further sampling using a Day grab. These CHP MBES bathymetry and backscatter data are of high quality and have been processed to a very high standard, IHO Order 1a (IHO, 2020). This requires the data to meet strict accuracy and quality requirements, e.g., line spacing, sounding density, vertical accuracy, and cross-line calibration. The survey report is available from the UKHO Data Archive Centre. The 2006 MBES survey employed a Kongsberg Simrad EM710 (70–100 kHz) for the offshore leg, and a hull-mounted EM3002D (300 kHz) sensor for the inshore survey to account for two depth zones. A Trimble (RTK) GPS was used for positioning. Depth checks between the nadir beams of the MBES systems against a single beam echosounder agreed within a few centimetres, except in areas of rapidly varying terrain (e.g., rock or sand waves). Further to this, the backscatter data are processed to drastically reduce angle-range effects, ensuring accurate intensities are recorded across track. Bathymetry and backscatter data were processed using Caris HIPS/SIPS software. The total survey area covers approximately 2,640 km² (Figures 1C,D).

Multibeam Echosounder Data Iso Cluster Classification

The bathymetry and backscatter data were classified using the unsupervised Iso Cluster tool in ArcGIS to inform our sampling strategy across the MBES survey footprint. These variables have shown strong discriminatory power for classifying seabed substrates (Calvert et al., 2015). Prior to classification, the bathymetry raster data were resampled to 6 m resolution for consistency with the backscatter dataset and both rasters were normalised from 0 to 1 (Calvert et al., 2015). We used the BGS 1:250K Folk sediment map (Figure 1B) to support our selection of five classes representing the four sediment types plus rock of the modified Folk classification (Long, 2006) (Figure 3). Equal numbers of sediment samples were proposed from each class with the sampling locations dispersed across the class footprint (Figure 3). Backscatter and bathymetry data were further processed to remove noise and account for potential sample location error, using the “Focal Statistics” tool in ESRI ArcGIS v10.7 (3-pixel × 3-pixel circular neighbourhood), prior to extracting the raster values at each sample location.

Multiscale Backscatter Data

Studies have shown that the spatial scales of terrain and ecological attributes are an important consideration in sedimentary

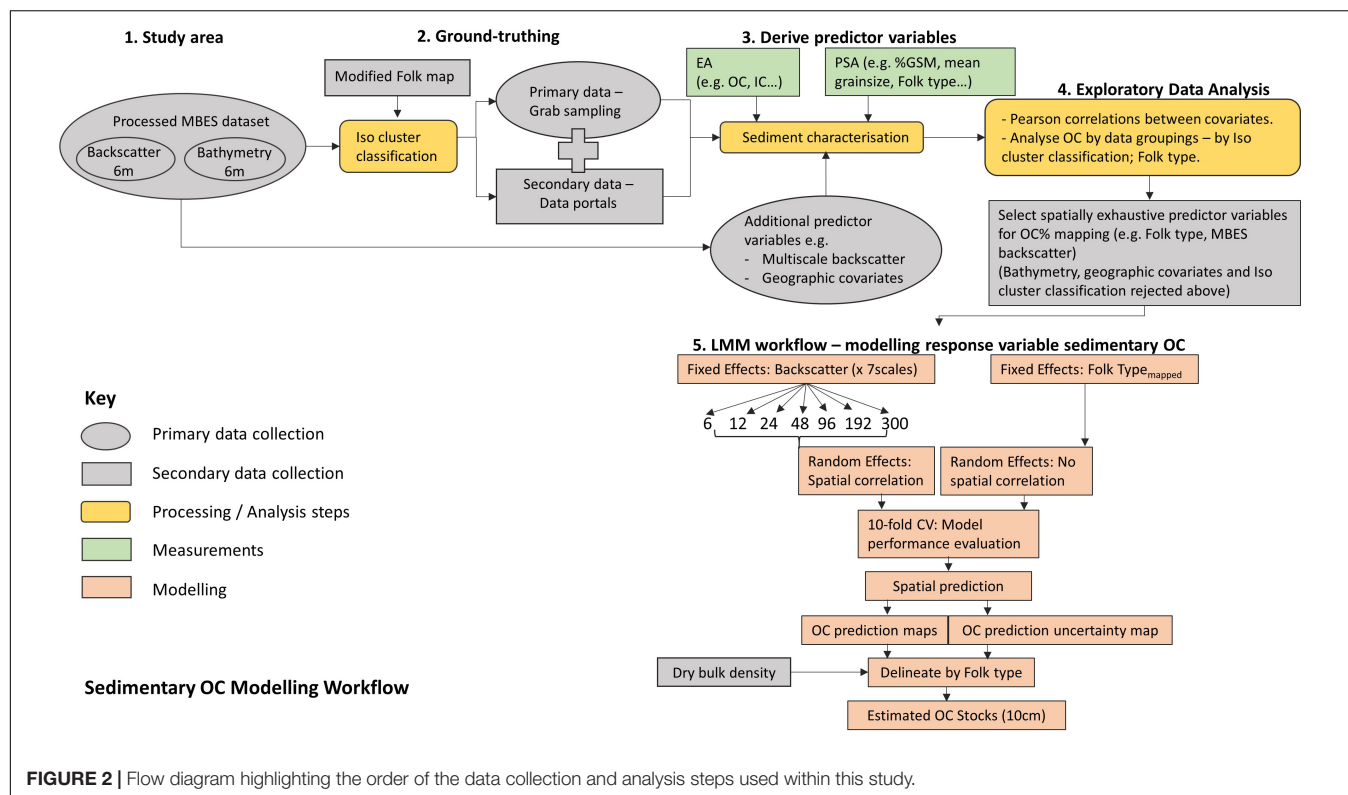
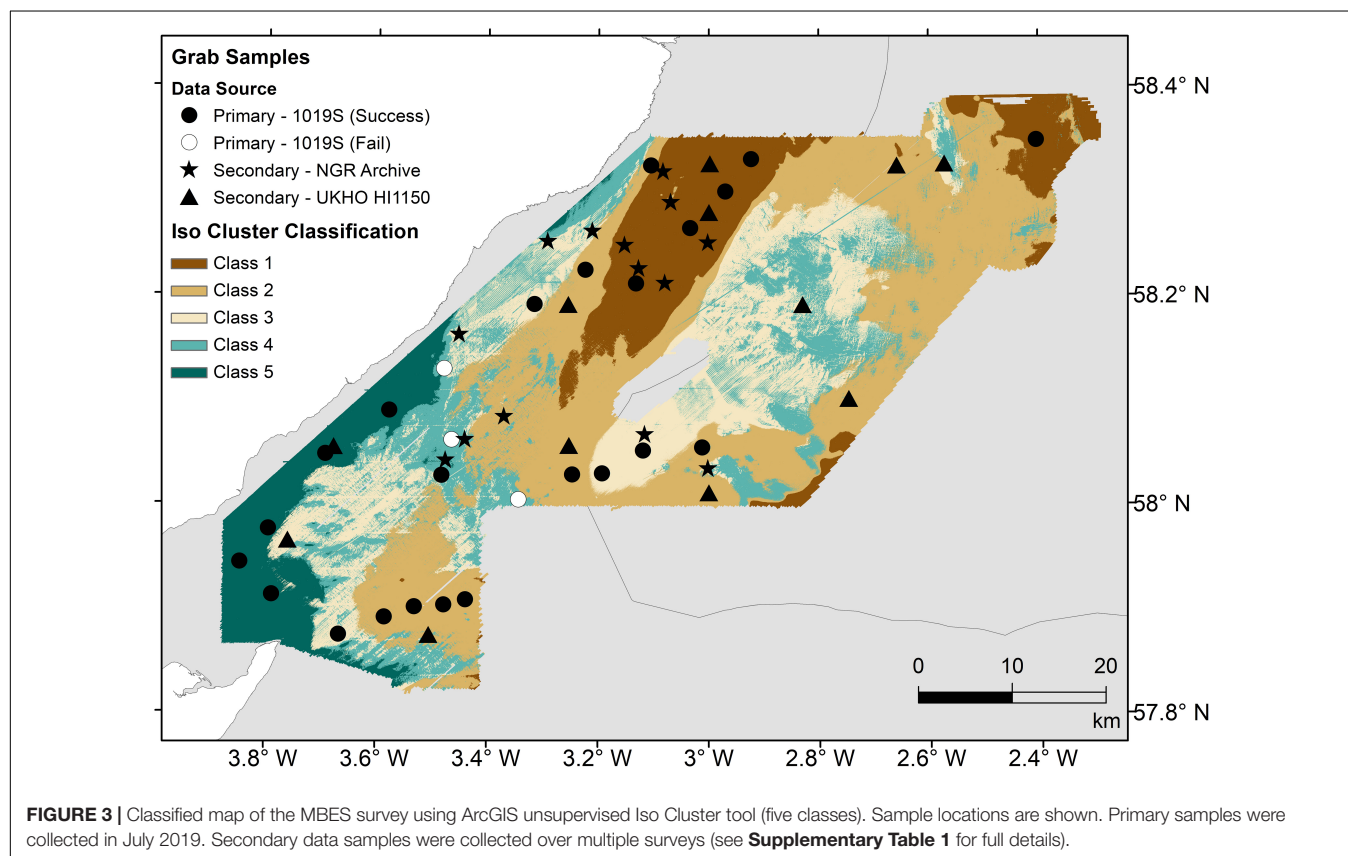


FIGURE 2 | Flow diagram highlighting the order of the data collection and analysis steps used within this study.



modelling and mapping studies since different environmental processes operate at different scales (Wilson et al., 2007; Misiuk et al., 2018). To investigate if there was an optimum scale at which backscatter and OC were correlated, we re-gridded the original data (6 m resolution) to the following spatial scales: 12, 24, 48, 96, 192, and 300 m resolution using the bilinear algorithm in the ArcGIS Resample tool. The backscatter values at the sample point locations, and as averaged over a 300 m grid, were extracted and used as predictor variables in the modelling component (see section “Spatial Analysis – Linear Mixed Models”).

Sediment Characterisation

Primary Data Collection

Twenty-three grab samples were successfully collected by FRV *Scotia* (1019S) in July 2019 using a Day grab (0.1 m²) (Figure 3). Three grabs failed where the sediment was too coarse to sample (all within “Class 4”). A full list of samples and accompanying metadata is found in **Supplementary Table 1**. Samples were collected according to the United Kingdom’s Joint Nature Conservation Committee (JNCC) marine monitoring protocols (Davies et al., 2001). A full-depth scoop of sediment (~10 cm depth) was collected from the Day grab, homogenised, and frozen until analysis.

Secondary Data

We supplemented our dataset using complementary secondary data spatially located within the MBES footprint. Physical material was subsampled from the NGR. This included the 11 retained samples collected during the H1150 MBES survey and additional archive material collected during national seabed surveys from the 1970s (Fannin, 1989). We also searched national databases (e.g., ICES) for sedimentary datasets with associated OC and grain size information, however, due to differences in analytical methods and reporting formats of the OC sediment fraction and grain size statistics, we decided to only use the physical secondary samples available for laboratory analysis, to maintain consistency with our primary data. There will be some uncertainty in OC amounts from archive samples attributable to the possible loss of labile material during long-term storage, which could manifest in an underestimation in OC predictions. We also note that the location uncertainty of archive samples is approximately 100 m because these were collected prior to the availability of Global Positioning Systems (Lark et al., 2012). Despite the uncertainties, the increased dataset nevertheless allows us to better characterise the regional sedimentary properties. An inventory of secondary data is found in **Supplementary Table 2** and includes a further 29 samples.

Carbon Analysis

Sediment samples were oven-dried at 50°C until constant weight, cooled, and ground to a homogenous powder. 40 mg ± 5 mg of sediment was weighed out into pre-baked steel crucibles. Carbon analysis was carried out using an *Elementar SoliTOC Cube Elemental Analyser*. This instrument measures *in situ* organic and inorganic C within a sample, thus the typical pre-acidification step to remove carbonates is not required to measure the organic component. This is advantageous for coastal sediments

comprising inorganic material because the acidification step can result in loss of sample through effervescent reaction (Verardo et al., 1990). The machine was calibrated against the standard reference material, B2290 (TOC/ROC/TIC silty soil standard) from Elemental Analysis, United Kingdom. The standard measurements deviated from the reference value by: TOC = 0.14%; ROC = 0.003%; and TIC = 0.29%. The measured C was normalised to the proportion of the sediment composition <2 mm. This represents the fraction of the bulk sediment viable for analysis; we assume that there is no OC associated with the sedimentary fraction >2 mm (i.e., “gravel” or rock).

Sediment Grain Size

Particle size analysis was undertaken for the 23 primary sediment samples using the protocol outlined in Mason (2011) to split the bulk material into coarse (>2 mm) and fine (<2 mm) components prior to analysis. The coarse material was sieved at 1/2 phi intervals (5.6, 4.0, 2.8, and 2.0 mm). The <2 mm fraction was analysed in a Coulter LS230 laser granulometer. The machine was calibrated using two sizes of glass bead reference standards (Vasquashene C100 and Vasquashene 590/840). Samples were treated with 3 ml of 5% Calgon solution to aid dispersion of aggregates prior to analysis (Blott et al., 2004). The results from the fine and coarse fractions were combined into a full particle size distribution as per Mason (2011). Grain size statistics were derived using GRADISTAT (Blott and Pye, 2001), although we only consider mean grain size in this study.

Dry Bulk Density

The dry bulk density (DBD) values of the sediment types have been derived from Smeaton et al. (2021) who collated sedimentary DBD data from across the United Kingdom Exclusive Economic Zone (EEZ). Where available, we first extracted region-specific data for the Moray Firth and aggregated the higher sediment classifications into the modified Folk sediment types (Kaskela et al., 2019). The average DBD value for each type is used in C-stock calculations and can be found in **Supplementary Table 3**.

Observed Sediment Type – Harmonising the Data

We only had access to the bulk sediment of the 23 primary grab samples and therefore could only generate full particle size distributions for these samples. The secondary sediment samples were available for subsampling in conservative amounts from the NGR archive, and we could not assume the sub-samples were representative of the bulk sediment to establish a quantitative grain size breakdown. We instead relied on composition metadata available from the BGS Offshore Geindex³, to harmonise the primary and secondary data by deriving a modified Folk classification based on the % gravel, % sand, and % mud composition of each sample (Kaskela et al., 2019; Smeaton and Austin, 2019). Every data point has thus been described according to the modified 5 Folk

³http://mapapps2.bgs.ac.uk/geoindex_offshore/home.html

classification (Mud-muddy sand; Sand; Mixed sediment; Coarse sediment; and Rock) (Kaskela et al., 2019). This allowed us to investigate how the composition of sediment affects the acoustic backscatter response.

Modified BGS Folk Sediment Map

As above, we converted the United Kingdom seabed Folk sediment polygon shapefile (1:250,000) (BGS (British Geological Survey), 1987) into a modified Folk sediment raster within ArcGIS by aggregating and reclassifying the default 16 Folk classes into 5 Folk classes based on Kaskela et al. (2019). The raster was projected into UTM Zone 30N and resampled to a 300 m resolution to align with the maximum backscatter raster scale (see section “Multiscale Backscatter Data”). We cross-checked the observed sediment type at each grab sample location (see section “Observed Sediment Type – Harmonising the Data”) against this reclassified sediment map to see how well it represented the sediment types described by the point sample data. Values of modified Folk type were extracted at each sample location (“mapped” Folk opposed to “observed” Folk) and used as a covariate within the spatial models. The modified Folk raster was also used as a continuous predictor variable for OC in our spatial predictions (see section “Spatial Analysis – Linear Mixed Models”).

Exploratory Analysis – Drivers of Organic Carbon Variation

Spatial information was extracted for each sample location using ArcGIS V10.7 including, geographical northing and easting and distance from the coast (calculated as the planar distance in metres from the target sample to the closest point on the coastline). These variables are included as potential predictors of sediment type and OC (Diesing et al., 2017). The appropriateness of using MBES and sedimentary data as explanatory variables to spatially predict OC was explored in the following ways; (i) by comparing the summary statistics of the sample data grouped by Iso Cluster class and by modified Folk type (**Supplementary Tables 4, 5**) and (ii) by exploring statistical associations between sedimentary properties and backscatter variables using Pearson correlation coefficients (**Supplementary Figure 1 and Supplementary Table 6**) (Serpetti et al., 2012). The relationship between modified Folk type, a categorical variable, and OC was compared using a one-way analysis of variance (ANOVA) (**Supplementary Table 7**). These analyses provided the supporting evidence for whether backscatter was a viable proxy for characterising sediments in this area (i.e., do sediment types have characteristic signatures?), and for insights into the significant predictors of OC here.

Spatial Analysis – Linear Mixed Models

We applied geostatistical methodology (Webster and Oliver, 2007) to explore how the observed relationships between OC and its drivers of variation could be used to map OC across our study region and how predictions of OC and their uncertainty could be upscaled to the entire study region. Non-spatial statistical methodologies such as linear regression require the assumption that the model errors or residuals are independent. In

contrast, spatial analyses acknowledge that these residuals could be spatially correlated (i.e., residuals from proximal locations are more likely to be similar than those from disparate locations). This means that there is a spatial pattern to the observed data beyond that which can be explained by the covariates. This unexplained spatial pattern can be predicted using geostatistical methods (Webster and Oliver, 2007) thus improving the accuracy of the maps that result. The spatial correlation can also lead to the underlying model consistently under- or over-estimating the true values across broad portions of the study region. This in turn implies that the uncertainty of upscaled predictions of OC (e.g., the average across the study area) can be larger than if the residuals were independent.

We explored the spatial relationships between OC and the strongest drivers of variation as per the Pearson correlation coefficients, by estimating a series of LMMs by residual maximum likelihood. This is a commonly used method in terrestrial spatial C stock studies (Lark et al., 2006; Rawlins et al., 2009). LMMs divide variation in the modelled variable between the fixed effects (i.e., an assumed linear relationship between the response variable, in this case OC, and the explanatory covariates) and a random-effects component (i.e., the variation in the model residuals which can be spatially correlated). A comprehensive explanation of this type of geostatistical model can be found in Lark et al. (2006).

The model covariates must be known at all locations where the OC is to be predicted. We thus used the “mapped” modified Folk sediment type as a proxy for mean grain size and composition data in the fixed effects and compared its performance with the backscatter data processed to different scales. At the model estimation and validation stage, we also consider the “observed” Folk class to explore the effectiveness of this predictor if it were known precisely at each location. This covariate cannot be used to predict OC at locations where it was not measured, however. For each covariate, we consider both independent and spatially correlated random effects. In the geostatistical literature, independent residuals are said to have arisen from a pure nugget model. We use an exponential function (Webster and Oliver, 2007) to represent the degree of spatial correlation when it is present in the model. The appropriateness of the different combinations of fixed and random effects was assessed via the Akaike Information Criterion (AIC, Akaike, 1973) which weighs model complexity against model fit. The model which leads to the lowest AIC is thought to have the appropriate degree of complexity to best model the observed data (Villanneau et al., 2011).

The best-fitting models were used to predict OC and its uncertainty across the study region using the best linear unbiased predictor (BLUP) (Lark et al., 2006). This is a spatial interpolation method, sometimes referred to as kriging, which combines the fixed and random effects. We also simulated 1,000 realisations of OC according to each fitted model using the Cholesky decomposition approach (Webster and Oliver, 2007). Each of the realisations reflects the degree of spatial correlation in the estimated model. If the average OC across the study region is calculated for each realisation, then the variation between these averages reflects the uncertainty in predicting OC at this scale.

The relatively small number of samples in this study meant it was difficult to split the data into a training and validation set. Instead, the models were validated by a 10-fold cross-validation procedure (Webster and Oliver, 2007). In this process, a tenth of the observations are removed from the dataset and the other observations are used to predict OC at the locations of those that have been removed. The process is repeated 10 times with different observations removed each time so that each observation is removed once. The predicted values are compared with the observed values and the bias can be assessed by calculating the mean error (ME):

$$ME = \frac{1}{n} \sum_{i=1}^n \{z(x_i) - \hat{z}(x_i)\},$$

and the accuracy by calculating the root mean squared error (RMSE),

$$RMSE = \left[\frac{1}{n} \sum_{i=1}^n \{z(x_i) - \hat{z}(x_i)\}^2 \right]^{\frac{1}{2}},$$

or the correlation between predicted and observed values, where $z(x_i)$ is the observed OC and $\hat{z}(x_i)$ is the prediction of OC at location x_i and n the number of observations.

In addition to a prediction of OC at each location, the BLUP also produces a measure of uncertainty of the prediction referred to as the prediction or kriging variance, an important consideration for decision-makers (Lark et al., 2012). The degree to which the kriging variances $\hat{\sigma}^2$ relate to the prediction uncertainty can be explored by calculating the standardised squared prediction errors (θ) at each site:

$$\theta_i = \frac{\{z(x_i) - \hat{z}(x_i)\}^2}{\hat{\sigma}^2(x_i)}.$$

If the random effects are normally distributed and the LMM correctly describes the variation of OC, then the expected mean and variance of the θ_i are equal to 1.

Organic Carbon Stock Estimates

Surface (10 cm) OC stock estimates were calculated for the best-fitting model surface maps using the methodological steps outlined in Burrows et al. (2014). The modified Folk class raster was first converted into a corresponding map of average DBD using the values identified from section “Dry Bulk Density.” Combined with the maps of predicted OC, OC stocks and densities were derived per pixel area. For each spatial model, we calculated the OC stock over each Folk class area by aggregating the predicted OC mass for all relevant pixels. The uncertainty of these stocks was determined by repeating the stock calculation process for each of the 1,000 realisations of OC simulated from each LMM. The standard deviation of the stock predictions that resulted approximates the standard error. This approximate standard error does not account for uncertainty in estimating the DBD for each Folk class.

RESULTS

Data Characteristics

Backscatter Signal

The backscatter data (Figure 1D) highlight discrete areas of high intensities within an otherwise generally homogenous signal, broadly reflecting the sediment structure described in section “Regional Setting.” High backscatter intensities follow the coastline, coincident with rock and coarse sediments (Figure 1B). The area overlying the Smith Bank is characterised by higher backscatter (~ -16 to -21 dB), likely a signature of the coarser sand and gravel material described by previous surveys (Holmes et al., 2004). There are additional areas of high backscatter (~ -16 to -23 dB) associated with bathymetric-high features known as drumlins (streamlined subglacial landforms comprised of coarse and over-consolidated sediments), leaving the Dornoch Firth. The upstanding ridges will be more exposed to currents and therefore likely to consist of coarse-grained material, flanked by winnowed finer sediments within the troughs. Much of the remaining area is represented by lower backscatter intensities ranging between -28 and -34 dB correlating with observations of sand-dominant sediment facies (Andrews et al., 1990).

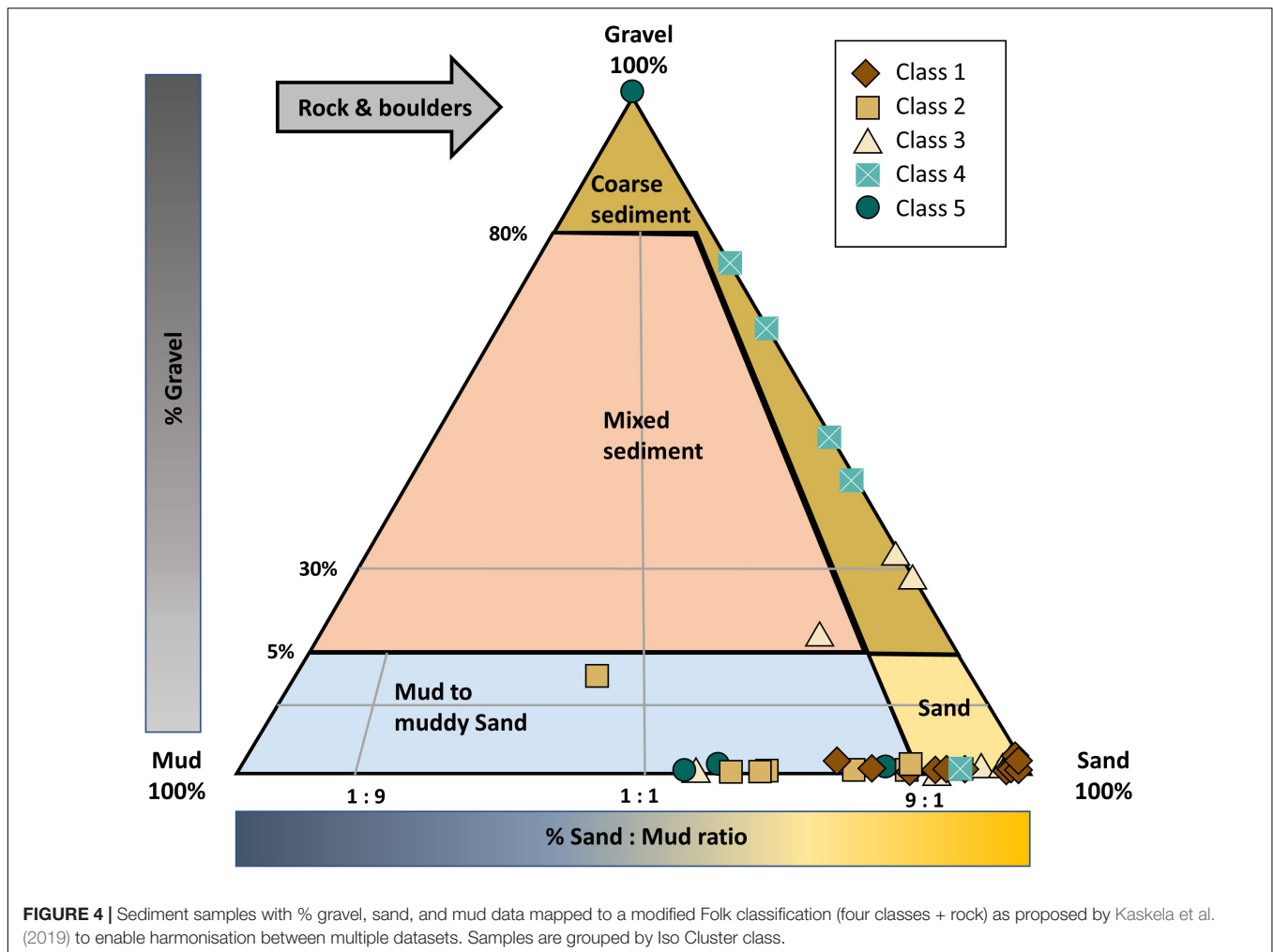
Sediment Type

Our grab samples were predominantly classified as sands and muddy sands, with a smaller proportion classified as coarse and mixed sediments (Figure 4 and Supplementary Table 1). Generally, it is difficult to sample a coarser sediment matrix successfully and these sediment types are often under-represented in sedimentary C studies. The three failed grabs during 1019S (all within “Class 4”) were likely due to coarse sediments. This assumption is supported by Figure 4, which clearly delineates the coarse sediment found within “Class 4” compared to the other classes. “Class 5” has a varied mixture of sediment types which could indicate poor sorting of sediments closer to the coastline. Despite having different compositions, the mean grain size of sediments collected within Classes 1, 2, 3, and 5 (following removal of outlier GB12) are broadly similar ($\sim 150 \mu\text{m}$) and classify as fine to medium sands with a mean backscatter intensity ($\sim -31 \text{ dB} \pm 1$) (Supplementary Table 4). The mean grain size for “Class 4” is significantly higher ($\sim 2 \text{ mm}$) characterised as a coarse sediment and matched by high mean backscatter intensity (-20.4 dB).

We chose to reclassify our primary grab samples to a modified Folk class (see section “Observed Sediment Type – Harmonising the Data”) to incorporate secondary data in our study. The observed Folk type broadly agrees with the modified Folk map over the study area (Figure 5), with 60% overall accuracy (Supplementary Table 8). The main source of disagreement comes from grab samples of muddy sands being incorrectly classed as sands and coarse sediments by the BGS Folk map indicating there is heterogeneity over finer scales than is captured by broad Folk sediment classifications.

Sedimentary Organic Carbon

Organic carbon values are consistent with other studies from the coastal shelf environment on the east coast of Scotland



(Serpetti et al., 2012); values range from 0 to 1.55% content, with an overall mean value of 0.87% and a standard deviation of 0.37% (Supplementary Table 1). Enriched OC values are found closer to the estuary, characterised by muddier sediments, and within the deeper water (defined by “Class 1”) suggesting that depth could be a factor in OC accumulation (Supplementary Table 4). “Class 4” has the lowest range of values recorded – the average OC content within this class is $0.65\% \pm 0.41$ (Supplementary Table 4) and mean grain size ~ 2 mm. When grouped by Folk type (Supplementary Table 5) the muddy sands are enriched in OC% (mean = $1.04\% \pm 0.27$) and coarse sediments have the lowest average value at $0.38\% \pm 0.27$. Sands have the largest variability in OC% (between 0.18 and 1.31%) with higher values overlapping those found in the muddy sands.

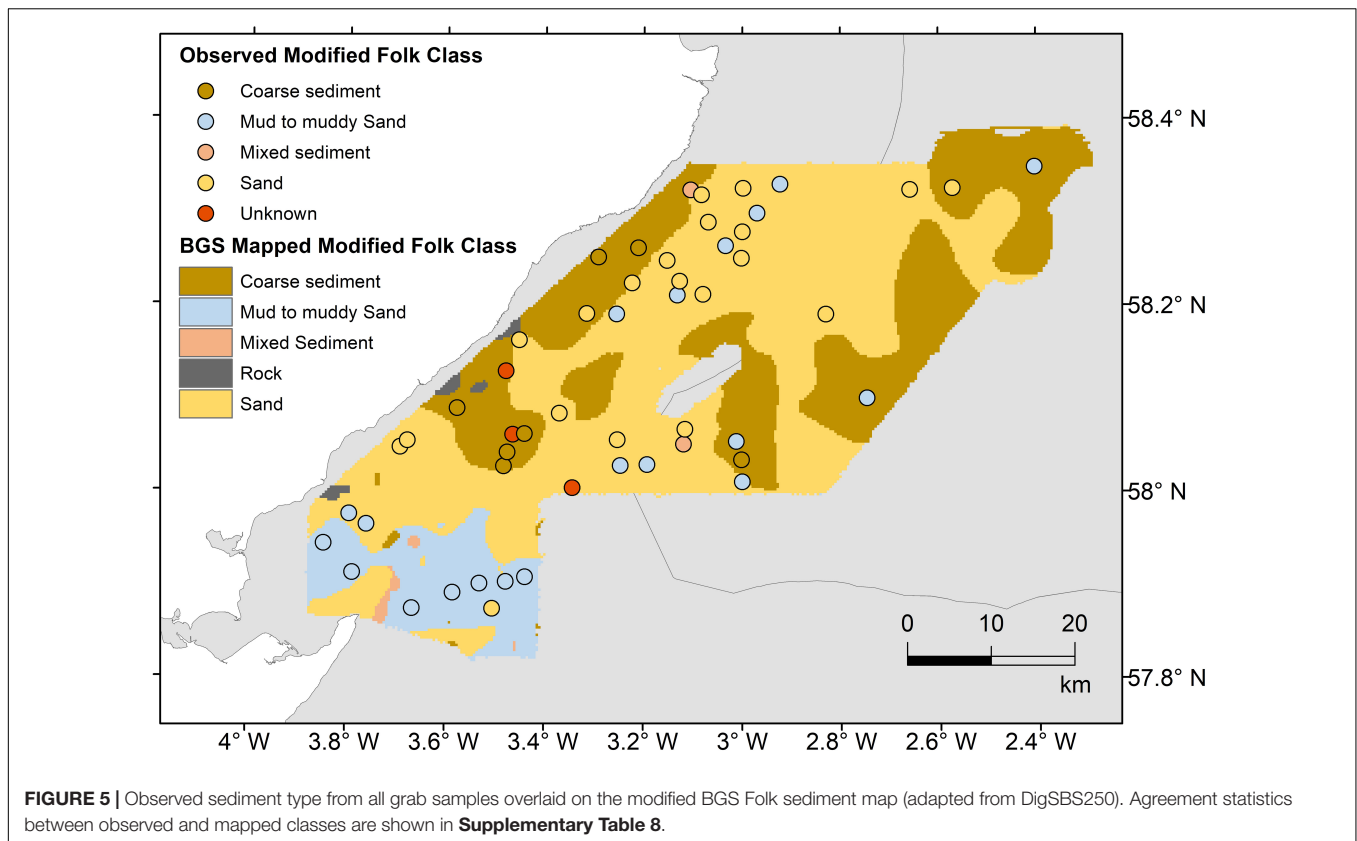
Exploratory Analysis

Effectiveness of Iso Cluster Classification

The objective of the unsupervised Iso Cluster classification of MBES bathymetry and backscatter was to identify distinct seabed substrates to guide a representative sampling strategy. Grouping the sample variables by Class highlights some issues with our approach. The bathymetry data appeared to drive the

final classification demonstrated by each class having a distinct depth range, except for Classes 3 and 4 (Figure 6A). The distinction between Class 3 and 4 was subsequently made using backscatter intensity. However, in this study, bathymetry shows limited discriminatory power to separate between sediment types (Figure 6B) indicating that our classification approach did not meet the objectives. This could be due to limited data, and it is possible that finer-scale sampling would have shown a response to small-scale bathymetric and geomorphological variation. “Class 4” (Figure 6A) is an exception and is distinctive from the others exhibiting similar characteristics to those of coarse sediment (Figure 6B) demonstrating the strong effect of increased grain size on acoustic backscatter (Goff et al., 2000).

Grouping the data instead by sediment type ($n = 49$) shows more distinct trends (Figure 6B). Coarse sediments have distinct signatures for all variables specifically, the lowest OC% values, a mean grain size > 2 mm, the highest backscatter intensities, and are within shallower depths. Mixed sediments are characterised by slightly larger mean grain sizes than sands due to the presence of gravel. This is also reflected in higher backscatter intensities for mixed sediments relative to muddy sands and sands. Despite having distinctly different mean grain sizes (note that mean grain



size is only available for ($n = 23$ samples), muddy sands and sands are characterised by similar mean backscatter values (~ 32 dB) and depth ranges. Backscatter has thus provided a distinction between coarse sediments from muddy sands (M-mS) and sands (S); however, these sediment types are indistinguishable from each other based on backscatter intensity alone. Mean grain size ($n = 23$) is a more useful indicator in this respect than sediment type.

Other than “Class 4” (coarse sediment), the Iso Cluster classification has not been able to differentiate sediment types, and OC contents satisfactorily. Thus, we have chosen not to use the Iso Cluster classification as a predictor (categorical) variable in further analysis and instead, we use Folk sediment type which demonstrates better coupling to OC content and backscatter.

Predictor Variable Correlations

Backscatter is significantly correlated with mean grain size ($r = 0.72$) and most influenced by the gravel content ($r = 0.76$) (Figure 7A and Supplementary Table 6), correlations that are in keeping with other studies (Goff et al., 2000; Sutherland et al., 2007; McGonigle and Collier, 2014). OC has a significant, negative correlation with both mean grain size ($r = -0.68$) and with backscatter but this is much weaker ($r = -0.47$). The relationship appears to be driven in part by sediment composition highlighted by relationships with both % gravel ($r = -0.65$) and % mud ($r = 0.48$) (Figure 7B and Supplementary Figure 1). Backscatter does not separate OC values around -30 to -34 dB (Figure 7B), which is problematic because

this backscatter range corresponds to varying compositions of muddy-sands and sands represented by similar mean grain size but with different associated OC values, ranging from ~ 0.3 to 1.4%. However, despite our low sample numbers, we do see the general trends that we would broadly expect given the empirical relationships between these predictor variables (Hunt et al., 2020); increased backscatter intensities correlate to reduced OC contents as a function of sediment type becoming coarser. There are clearly environmental complexities, beyond which our dataset parameters can elucidate.

Water depth is weakly correlated to OC ($r = -0.3$) with no overall trends and therefore depth is not a reliable predictor of OC in this study (Supplementary Figure 1). Geographic covariates, distance from the coast, easting, and northing, are not correlated with OC and not used further.

Spatial Analysis: Linear Mixed Models

In total, nine LMMs of OC variation with single fixed effects were estimated as summarised in Table 1. All model validation statistics can be found in Supplementary Table 9. The lowest AIC is achieved by using the observed Folk classification derived from our samples as the fixed effects, followed by the classified Folk map values. Inclusion of sediment type and backscatter information as a covariate (fixed effect) improved the model performance by 17–19% (mapped and observed) and 14%, respectively, compared to the constant fixed effect model according to the relative decrease in the RMSE values

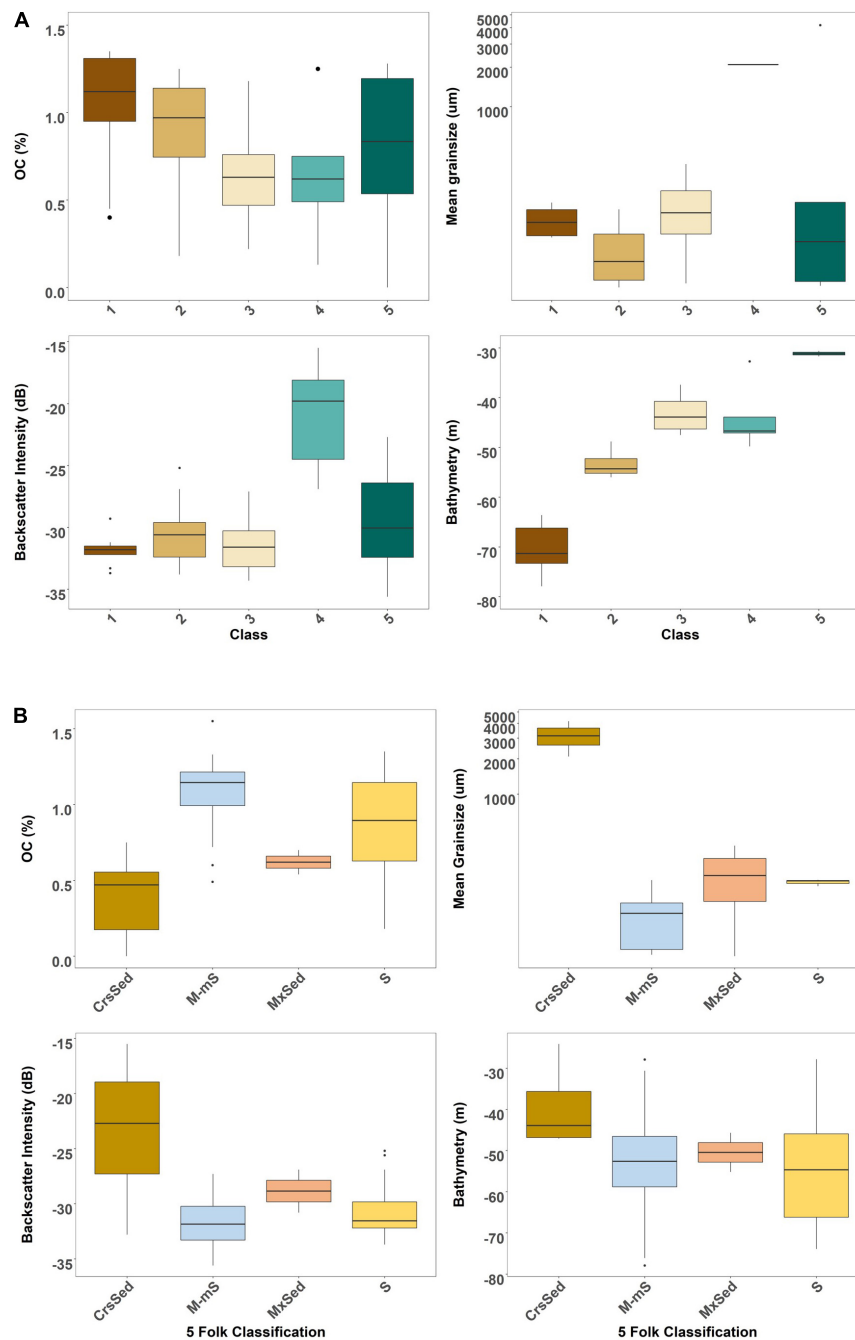


FIGURE 6 | Box plots characterising the core variables from the ground truth samples by **(A)** Iso Cluster classification and **(B)** modified Folk sediment type (Key for modified Folk type: CrsSed, coarse sediment; M-mS, muds to muddy sands; MxSed, mixed sediment; S, sand).

(**Supplementary Figure 2**). Of all the scales for backscatter, the data at the 48 m resolution lead to a more accurate model, indicating that backscatter resolution may be an important consideration for OC mapping, however, the differences in accuracy are modest and more data would be required to support this hypothesis. The fixed effects selected to spatially predict the OC were M5b (backscatter – 48 m) and M8b (Folk-mapped) because these variables are known across the study site.

While including exponential spatial correlation in the random effects did not improve any model fits according to the AIC alone, it does lead to small improvements in the model accuracy (**Supplementary Table 9**). Further, the upscaled prediction uncertainty values for the pure nugget are unrealistically small, approximately 1% of the total stock estimate (**Supplementary Table 10**). This results from a cancelling-out effect of positive and negative errors at different prediction

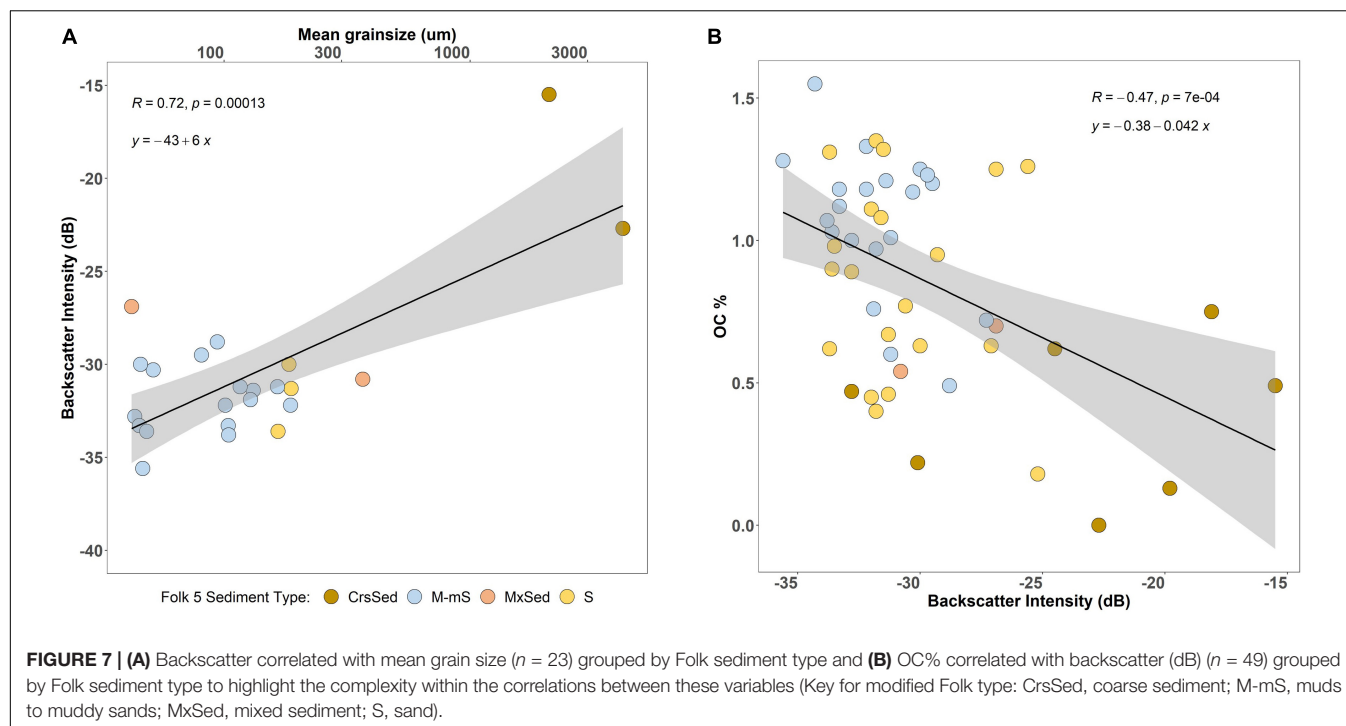


TABLE 1 | Matrix summarising linear mixed model permutations fitted to the observed data to predict OC%.

		Fixed effects								
		Constant (mean OC)	Bck-6	Bck-12	Bck-24	Bck-48	Bck-96	Bck-192	Folk5-Map	Folk5-Obs
Random effects	Without spatial autocorrelation (pure nugget)	M1a	M2a	M3a	M4a	M5a	M6a	M7a	M8a	M9a
	With spatial autocorrelation (exponential)	M1b	M2b	M3b	M4b	M5b	M6b	M7b	M8b	M9b

The random effects considered both a non-spatial (pure nugget) and spatial autocorrelation (exponential) covariance function. Bck-X, backscatter intensity (dB)-resolution of data (m); Folk5-Map, modified BGS 250K Folk sediment map classification; Folk5-Obs, observed modified Folk type at sample locations.

locations. The failure of the spatially correlated random effects to improve the AIC is likely to reflect the relatively small sample size meaning that there is limited evidence to assess the spatial correlation. It cannot be interpreted as evidence of an absence of spatial correlation. We therefore included spatial correlation in our spatial predictions of OC (**Figure 8**).

Only one of the observed OC values was made at a location with a “Mixed sediment” mapped Folk classification. Therefore, the expected OC % for the “Mixed sediment” class could not be estimated. For the purposes of spatial prediction, the expected OC % for this Folk class was assumed to equal the average of the expected values for the other three classes. Mixed sediment covers around 1% of the study area so this assumption is unlikely to substantially influence the predicted maps or site-wide stocks.

All models quantify the uncertainty satisfactorily according to the variances of the θ_i values which are close to 1; the spatial variation of this uncertainty can be seen in the standard error maps in **Figure 8**. Highest uncertainties arise from the constant fixed-effects model. The predicted OC using M5b ranges from

0.2 to 1.4% and is highly variable across the site. Lowest values of OC and associated prediction uncertainty are concurrent with high intensities in backscatter characterised by coarse sediments and rock (assumed to be 0%). For M8b, predicted OC shows very little variation within Folk sediment type boundaries and ranges from approximately 0.5–1.2%, the highest values characterised by the area of muddy-sands. The maps have relatively large standard errors which reflect the large degree of small-scale variation in OC. These uncertainties could be reduced if more data were collected.

Organic Carbon Stock Calculations

Table 2 outlines the estimated OC stocks calculated from the spatial predictions of OC for model M5b (estimated 3.00 ± 0.159 Mt OC) and model M8b (estimated 3.08 ± 0.164 Mt OC). The total OC stocks derived from the two models are within the prediction error of each other, differing by approximately 0.08 Mt. The Folk model predicts the higher stock value presumably a result of not capturing finer-scale sediment heterogeneity

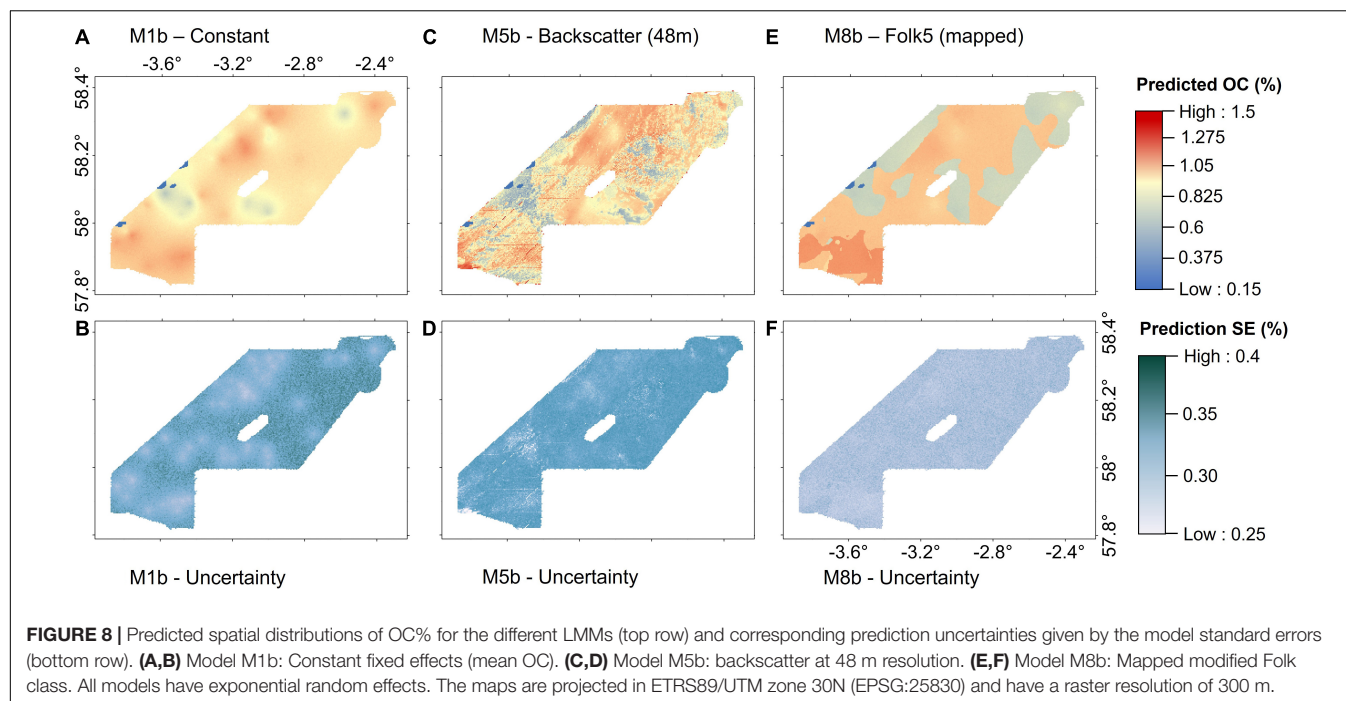


FIGURE 8 | Predicted spatial distributions of OC% for the different LMMs (top row) and corresponding prediction uncertainties given by the model standard errors (bottom row). **(A,B)** Model M1b: Constant fixed effects (mean OC). **(C,D)** Model M5b: backscatter at 48 m resolution. **(E,F)** Model M8b: Mapped modified Folk class. All models have exponential random effects. The maps are projected in ETRS89/UTM zone 30N (EPSG:25830) and have a raster resolution of 300 m.

TABLE 2 | Calculation of organic carbon stock using **(A)** predictions from the linear mixed model with backscatter at 48 m resolution as a fixed effect covariate including exponential random effects and **(B)** predictions from the linear mixed model with mapped Folk class as a fixed effect including exponential random effects.

(A) Model: M5b (backscatter)

Folk class	DBD (kg/m ³)	Area (m ² × 10 ⁹)	Mean OC (%)	Mean SE (%)	OC stock (Mt)	Stock SE (±) (Mt)	OC density (kg m ⁻²)
Mixed sediment	1154	0.01	0.72	0.12	0.0076	0.0012	0.83
Coarse sediment	1454	0.86	0.73	0.05	0.915	0.066	1.06
Mud – muddy sand	1141	0.27	0.87	0.06	0.266	0.018	0.99
Sand	1438	1.49	0.85	0.04	1.814	0.093	1.22
Rock	NA	0.01	NA	NA	NA	NA	NA
Total	–	2.64	–	–	3.0022	±0.159	–

(B) Model: M8b (Folk class)

Folk class	DBD (kg/m ³)	Area (m ² × 10 ⁹)	Mean OC (%)	Mean SE (%)	OC stock (Mt)	Stock SE (±) (Mt)	OC density (kg m ⁻²)
Mixed sediment	1154	0.01	0.88	0.08	0.009	0.0009	1.01
Coarse sediment	1454	0.86	0.56	0.08	0.700	0.099	0.81
Mud – muddy sand	1141	0.27	1.12	0.10	0.341	0.031	1.28
Sand	1438	1.49	0.95	0.06	2.034	0.124	1.36
Rock	NA	0.01	NA	NA	NA	NA	NA
Total	–	2.64	–	–	3.085	±0.164	–

Standard error (SE) relates only to uncertainty in predicting OC %; bulk densities (DBD) are assumed to be known exactly. (1 Mt = 1 million tonnes which is the equivalent of 1 Tg).

with sediment boundaries (Figure 5). The limitation of this backscatter dataset to differentiate between sands and muddy sands (similar intensity values) could be leading to an under- and over-estimation for OC in muddy-sands and sands, respectively (Figure 7). Both models agree that sands contribute most to the total stocks (~60–66%) due to their coverage. Estimated values for OC density are within the values estimated by other studies for United Kingdom coastal sediments, although in contrast to Smeaton et al. (2021), the two models predict that

sands have the highest OC density rather than the muddy sediments (Table 2).

DISCUSSION

We have explored the potential of using archived MBES backscatter data in combination with primary and secondary ground-truth data to map OC at high resolutions over a regional

area. We see promising trends between the predictor variables, yet the correlation between backscatter and OC is relatively weak, which suggests that backscatter cannot be solely used to predict OC. However, we show that the inclusion of this variable improves the carbon prediction accuracy or equivalently reduces the number of OC measurements required to achieve a specified precision. Comparing two exhaustive parameters, sediment type and backscatter, we have modelled two regional distribution maps of OC over an MBES footprint (2,640 km²) within the Moray Firth with spatially explicit uncertainties (**Figure 8**). We have used these maps to estimate surficial OC stocks across the area (**Table 2**). The stock estimates are in good agreement with each other; however, the spatial distribution pattern of OC varies. This is a result of the differences in how the covariate data were acquired. The BGS Folk sediment map is currently the United Kingdom's best national seabed map based on interpolated point data and expert judgement, whereas backscatter is a form of high-resolution remote sensing. Further samples and additional complementary predictor variables are needed to resolve the finer-scale variability of OC and to understand which of the maps is most representative; this would also serve to reduce the relatively large standard errors of OC (**Figure 8**). In this section, we discuss the limitations and opportunities of acoustic backscatter as a predictor variable for OC. We briefly analyse the spatial distribution of OC of this Scottish east coast embayment and its role in C-processing, and we consider the implications for such OC maps in seabed management and C-accounting frameworks.

Acoustic Backscatter as a Predictor of Sedimentary Organic Carbon

While backscatter has a significant, negative correlation with the OC content in surface sediments (**Supplementary Table 6**), the strength of the relationship is relatively weak, and thus offers limited power to predict OC directly. This is a similar finding within habitat or substrate mapping studies using MBES data, which show that backscatter can improve models as part of a suite of predictor variables (De Falco et al., 2010; Lucieer et al., 2013). The inclusion of backscatter in the geostatistical model M5b leads to a prediction accuracy improvement for OC of approximately 14%. This is a promising finding and is similar to improvements seen in substrate mapping accuracy when backscatter variables were incorporated (Lucieer et al., 2013; Biondo and Bartholomä, 2017). The resolution of the backscatter variable did not impact the overall performance of the LMMs, however, this does not mean that there is no difference and is likely a function of the limited sample size for the survey area. High-resolution backscatter data as a spatial covariate has the potential to increase the resolution of OC maps (Hunt et al., 2020). Fine-scale variability can be incorporated into these maps beyond which can be accounted for by current sediment maps (Smeaton et al., 2021).

The backscatter data differentiates between areas of coarse and fine sediments; however, it is not able to distinguish between muddy-sand and sandy sediments. Distinguishing between coarse and fine sediments is still a useful finding with respect to OC mapping because OC varies as a function of sediment type

(Hedges and Keil, 1995), with significantly lower quantities of OC within coarse sediments (**Figure 6**). High-intensity backscatter is characteristic of coarse or poorly-sorted material (Collier and Brown, 2005; Biondo and Bartholomä, 2017), which are likely to result from dynamic or erosive processes, and therefore unimportant areas for C storage. This visual aid can help prioritise ground-truthing toward the finer-grained sediments associated with deposition and enrichment in organic matter (Diesing et al., 2021). The difficulties of the backscatter to delineate between finer materials could be due to a limitation of the MBES survey technology and post-processing methods employed over a decade ago, however, similar challenges have been identified in very recent studies, indicating that further development is still required within this field (Diesing et al., 2020). As a result, there are likely to be some systematic over- and under-estimations of OC for sands and muddy-sands, which have similar intensities. Sediment composition can also cause conflicting interpretation of the backscatter signal and OC content. For example, a muddy gravel can have a very high backscatter signal, particularly as gravel or shell hash disproportionately affects the scattering effect (Goff et al., 2000, 2004), but counter-intuitively, also a relatively high OC content governed by the presence of mud (Serpetti et al., 2012). Increased ground-truthing or camera-tow coverage would help to better characterise the sedimentary environment in these areas (Hunt et al., 2020).

The dominant oceanographic characteristics of the inner Moray Firth are of a dynamic coastal system and the seabed is comprised of glacially relict, re-worked sediments (Reid and McManus, 1987). These factors will influence OC quantity and quality and could help to explain why the correlation between backscatter intensity as a proxy for OC is less convincing than backscatter as a proxy for sediment grain size. There are numerous variables that can influence the availability of OC within sediments including, oxygen penetration levels (Janssen et al., 2005; Hicks et al., 2017), water temperature (Burdige, 2011), sedimentation rate (de Haas et al., 1997), reactivity of OM (Burdige, 2007; Bianchi, 2011), disturbance levels (e.g., through benthic fishing activities: De Borger et al., 2020), and age/transportation times (Bao et al., 2019), which cannot be explained by backscatter alone. Equally, the relationship between backscatter and sediment type is complex (Diesing et al., 2020) and return signals can be influenced by the survey itself, including factors such as instrument type and acoustic frequency settings, weather conditions, and data processing techniques, and by physical environmental characteristics including sediment density and bioturbation from benthic fauna (Feldens et al., 2018).

Nevertheless, our results show that when backscatter measurements are combined with OC values within a geostatistical framework, the precision of the carbon predictions improves, and this method allows the prediction uncertainty to be quantified. In the absence of appropriate or exhaustive sedimentary datasets, our models show that acoustic backscatter data could be used to generate an improved picture of the spatial distribution of OC with appropriate ground-truthing. The backscatter data highlight some interesting finer-scale variations

that could provide insights into geomorphological features and sedimentary processes, which may also have implications for carbon storage, such as sand ripples, moraines, or trenches.

Folk Type as a Predictor of Sedimentary Organic Carbon

Sediment Folk type was a stronger covariate than backscatter for predicting OC in this study, and is commonly used within sedimentary OC studies (Smeaton et al., 2020), however, there are limitations with using such categorical data. Much of the United Kingdom archive sediment data is classified using the Folk scale based on broad composition information (Lark et al., 2012) which can be associated with a wide range of OC values. The current BGS 250K Folk sediment map for the United Kingdom doesn't pick up the heterogeneity in sediment type at smaller scales as highlighted by the 60% agreement between our observed samples and the Folk map (Figure 5). Sediment heterogeneity can have a large influence on C storage and should be accounted for Smeaton and Austin (2019). Areas of disagreement may be attributed to analytical improvements in sediment grain size detection for fine sediments (e.g., with laser sizing technology available) and/or legacy sample location inaccuracies which did not have the benefit of Global Positioning Systems (GPS) (Lark et al., 2012). In addition, large temporal differences exist between the samples collected in the 1970s, from which the BGS Folk sediment map was derived, compared to the samples for this study, during which time there is likely to have been considerable sediment movement. The improvement in LMM prediction accuracy of OC using sediment type is a clear indication of the importance of understanding sediment type and distribution. The confidence in substrate maps is also improved where remote sensing has been undertaken (Kaskela et al., 2019). Statistical relationships between our data variables (Supplementary Figure 1) show that grain size, and component fractions (e.g., % mud, gravel) were a stronger predictor of OC than sediment type, however, limited data coverage prevented us from using it as a covariate within the spatial modelling. We would therefore recommend that *in situ* sediment ground-truthing of MBES surveys is retained and submitted for comprehensive grain size analysis using laser-sizer technology (Blott et al., 2004), which would also allow complementary continuous predictions of % mud, sand and gravel at higher resolutions (Misiuk et al., 2018). See further recommendations in section "Recommendations."

Opportunities Presented by Multibeam Echosounder Surveys

Our study explores the development of a new methodology to map OC. There are several reasons why MBES backscatter as a predictor for OC may be a preferable option to traditional point sampling and interpolation methods. Sampling at sea is logistically challenging, expensive, and recognised as a carbon-intensive activity (Turrell, 2020). Within a decadal timescale, the Irish national seabed mapping project (INSS) has used acoustic systems to map at least 80% of the seabed of the Irish EEZ, generating new opportunities for environmental and commercial research toward sustainable development of

the marine environment (Guinan et al., 2020). "Piggy-backing" ground-truthing sampling onto such national-scale surveys has the potential to collect valuable datasets of seabed properties, including surficial OC. Often, as with this study, data for mapping projects are collated from different sources and temporal scales (Wilson et al., 2018; Atwood et al., 2020) which can increase the uncertainty in calculating and interpreting results.

Acoustic backscatter, collected as part of MBES surveys, is a spatially continuous measurement, which can uncover relative differences in seabed properties over multiple scales (Brown and Blondel, 2009), and can improve upon traditional sediment class maps. To highlight this point, the final OC map based on Folk type for instance shows rigid boundaries which are almost certainly overly simplistic (Figure 8).

Additionally, beyond the primary backscatter and bathymetry measurements, acoustic remote sensing data can provide a wealth of additional terrain and seabed geomorphology information (Lecours et al., 2016b; Masetti et al., 2018). The geomorphology of the seabed can provide important clues as to the dominant (local) physical processes, such as whether current and hydrodynamic regimes will enhance erosion or deposition. This information is commonly used within an ecological context, for instance, habitat modelling studies (Wilson et al., 2007; Lecours et al., 2017) and recently, has been used to predict the distribution of seabed sediments (Misiuk et al., 2018). As already noted, OC is associated with fine-grained material (Hedges and Keil, 1995), which is more likely to settle in low-energy environments; thus, it may be possible to identify relationships between seabed terrain attributes or geomorphological features that may indicate a depositional environment. For instance, the slope of the seabed is linked to dynamic ocean processes such as the steering or acceleration of currents, which can impact sediment transport and stability (Dolan, 2012) and as such, there is a higher probability that harder substrates will dominate steeper slopes (Dove et al., 2020). In the past decade, a suite of toolboxes have been developed to enable researchers to derive geomorphological parameters from high-resolution bathymetry data (Lecours et al., 2016a). Further research including terrain attribute predictors for sediment deposition could prove invaluable for improving the picture of sedimentary OC on the shelf (Diesing et al., 2021).

Finally, the United Kingdom is in a favourable position of having wide-scale sediment mapping across the EEZ with high confidence (Kaskela et al., 2019). Other maritime nations may not be in such a position and the use of MBES allows both substrates and OC to be investigated and mapped in parallel (Smeaton et al., 2021) and OC stocks to be subsequently calculated (Avelar et al., 2017).

Recommendations

We recognise that this study was constrained by a combination of temporally asynchronous primary and secondary data and a limited number of spatial OC observations (approximately one grab per 51 km²), which will have likely contributed to the weaker relationships seen (e.g., O'Carroll et al., 2017). However, despite this, we believe the results for this approach to mapping OC are promising. Looking forward, we would recommend that future national MBES surveys collect and preserve ground-truth

samples for sediment and OC analysis. Standard protocols and analytical procedures should be developed by the community to allow efficient re-use of data and comparative studies to maximise the opportunities. Secondary datasets can be used to enhance studies and data repository initiatives focussed on compiling contemporary sedimentary data, such as the MOSAIC initiative, will undoubtedly serve to improve understanding of sedimentary C processes (van der Voort et al., 2021). Sampling designs for ground-truthing could potentially be improved by incorporating primary MBES and secondary terrain attribute information at different scales before classification (Misiuk et al., 2018). The classification approach prior to sampling in this study versus that of Hunt et al. (2020) was less successful in differentiating substrates due to the influence of bathymetry, thus sampling approaches could consider the environment being surveyed; for instance, a higher proportion of samples could be collected within homogenous backscatter areas in dynamic coastal settings and/or camera tows are additional cost-effective tools to improve substrate classification (Kenny et al., 2003) prior to sampling. Small gradient changes in substrates present mapping challenges (Diesing et al., 2020), and could have a large impact on the overall C processing dynamics (Hicks et al., 2017).

Spatial Patterns of Sedimentary Organic Carbon Stocks in the Moray Firth

Organic carbon content ranges from ~0.2 to 1.5% (Figure 8) and we estimate that the total stock of sedimentary OC within the surface 10 cm for the MBES survey area is between 3.0 and 3.1 Mt of OC (Table 2). The MBES footprint covers an area of 2,640 km² and represents ~7% of Scotland's coastal and inshore waters area; 39,325 km² (Smeaton et al., 2021). The average OC density for our study area is thus estimated at approximately 1,144 tonnes OC km⁻² which is in good agreement with the upper estimates calculated by [Smeaton et al. (2021); 1,060 ± 128 tonnes km⁻²]. This is not distributed uniformly across the survey area, and we see variation in response to sediment type and potentially with localised hydrographic processes. For instance, the two predictive maps generally show the spatial agreement of enriched OC values to the southwest of the site in proximity to the estuarine systems (Figure 8). This region accumulates muddy sand, presumably from fluvial sources, in combination with a diminishing supply of carbonate muds that are transported onshore from the northeast (Reid and McManus, 1987). An interesting observation in our data relates to the slightly elevated levels of OC seen in the sediments of the deeper water to the north of the study area (outlined as “Class 1” in Figure 3). This local region is dominated by sands, which are permeable sediments and are known to be centres of efficient OC recycling (Huettel and Rusch, 2000) so the relatively elevated values of OC are unexpected for this sediment type. Given that the region falls within a deep channel it is possible that the local topography might be creating a localised area of deposition from currents arriving from the northeast (Goward Brown et al., 2017). To investigate these ideas further, techniques to elucidate the provenance and therefore fate of sedimentary OC can help in developing appropriate management strategies (Gerald et al., 2019).

Implications for Marine Spatial Planners, National Carbon Accounts, and Going Beyond the Inventory

Maps of the spatial distribution of sedimentary OC hotspots can be valuable to marine spatial planners who have a strategic goal to manage the seabed in a sustainable manner (Frazão Santos et al., 2019). Relative to large-scale mapping products of recent studies (Lee and Phrampus, 2019; Atwood et al., 2020; Legge et al., 2020; Smeaton et al., 2021), we would argue that regional-scale OC mapping data may be more practical for planners when considering the spatial conflicts between anthropogenic activities, environmental change, and vulnerable C stores. Protection of the seabed through spatial instruments such as marine protected areas (MPAs) can provide multiple benefits beyond C protection and supporting data are critical to identifying priority areas (Sala et al., 2021).

Marine shelf sea sediments are beyond the current C accounting frameworks for inclusion in NDCs, national GHG inventories and other actionable climate policies. However, there is a growing interest in the incorporation of these very significant C sinks and stores into accounting frameworks (Luisetti et al., 2020), as well as recognition of their vulnerability. Sediments are long-term stores of C on scales that have provided climate regulation services (Berner and Raiswell, 1983) but are vulnerable to human activities that cause disturbance and result in GHG emissions from the remineralisation of buried C (Macreadie et al., 2019). As explained by Howard et al. (2017), reporting an ecosystem as part of national GHG inventories would require in part an assessment of current C stocks and the geographic area covered. High-resolution OC maps will therefore have a valuable role in improved marine C accounting. Further research in sedimentary C hotspots, the source, and vulnerability of this C is necessary to determine appropriate accounting and sustainable seabed management measures (Luisetti et al., 2020).

CONCLUSION

Mapping the spatial distribution of sedimentary OC at regional scales is important for targeted seabed management measures which can protect C-rich sediment stores, in addition to promoting biodiversity, and food provisioning services. We have utilised an existing MBES dataset to investigate the potential of acoustic backscatter as a proxy for sediment type and therefore, to map associated OC. We use LMMs, a common technique in soil mapping studies, to estimate OC, comparing Folk sediment type and backscatter as fixed effect covariates. This study shows that the use of acoustic backscatter as a predictor covariate for OC improves the accuracy of the spatial model for OC by 14% and has good potential to delineate low – high C areas as a function of sediment type, at finer-scale resolutions than current UK seabed substrate maps. Inclusion of spatial autocorrelation in the models improves the quantification of uncertainty, which is an important consideration for decision-makers. We predict

that the MBES footprint within the Moray Firth holds between 3.0 and 3.1 Mt of OC in the top 10 cm, an estimate in good agreement with other modelling studies. This study would have benefited from more ground-truthing to better characterise the acoustic backscatter at lower intensities and to increase our understanding of the effect of spatial autocorrelation on OC. Despite the relatively limited dataset, the results for OC mapping using backscatter are promising and support the case for further research in this area. MBES data could play a pivotal role in improved spatial predictions for OC across regional scales, allowing inclusion of OC stocks into national C accounts and thus supporting broader thinking of marine carbon within nature-based solutions for climate mitigation, biodiversity preservation, and sustainable fisheries.

DATA AVAILABILITY STATEMENT

The original contributions presented in the study are included in the article/**Supplementary Material**; further inquiries can be directed to the corresponding author.

AUTHOR CONTRIBUTIONS

CH conceived the study with UD and WA. CH led the research design with support from DD, UD, and WA. CH undertook the fieldwork, laboratory work, and data analysis. Statistical modelling was undertaken by BM with support from CH and DD. CH wrote the first draft of the manuscript as part of her Ph.D. at the University of St Andrews under the supervision of WA, UD, and DD. All authors contributed to manuscript revisions and approved the final submitted version.

FUNDING

This research was partly supported by BGS National Capability funding from the Natural Environment Research Council (NERC), under UK Research and Innovation (UKRI) (Grant

Code: Seafloor and Coast – NEE6334S; Digital Labs – NEE75765). CH received joint funding from the University of St Andrews and the MASTS pooling initiative (The Marine Alliance for Science and Technology for Scotland) for her Ph.D. research, and their support is gratefully acknowledged. MASTS is funded by the Scottish Funding Council (grant reference HR09011) and contributing institutions. Additionally, funding for analyses for this study was supported by a Scottish Government grant for Blue Carbon research.

ACKNOWLEDGMENTS

We would like to thank the Scottish Blue Carbon Forum (SBCF) for their support of this research to further the understanding of Scotland's marine sedimentary OC inventory with respect to its significant marine carbon stores. We wish to thank Scottish Government for providing a berth and access to sampling equipment aboard RV Scotia (1019S) to allow Ph.D. student CH to collect the primary data for this study. We are grateful to the captain, crew, and fellow research scientists aboard the RV Scotia for assisting in primary sample collection, which was financially supported by the Scottish Government. We wish to thank the NGR for allowing us to subsample their repository through their in-kind sample loan scheme: Loan No. 263406. BM and DD publish with the permission of the Executive Director of the BGS (UKRI). We would like to thank William Hiles for the laboratory support. We thank the SBCF steering group – Bill Turrell and Cathy Tilbrook – for constructive comments on an early draft of the manuscript. Finally, we thank the two reviewers, NO and ZS, and the editor, MZ, for providing constructive comments that have improved this manuscript.

SUPPLEMENTARY MATERIAL

The Supplementary Material for this article can be found online at: <https://www.frontiersin.org/articles/10.3389/fmars.2021.756400/full#supplementary-material>

REFERENCES

- Akaike, H. (1973). "Information theory and an extension of the maximum likelihood principle," in *Proceedings of the Second International Symposium on Information Theory*, eds B. N. Petrov and F. Csaki (Budapest: Akademiai Kiado), 267–281.
- Aller, R. C. (1994). Bioturbation and remineralization of sedimentary organic matter: effects of redox oscillation. *Chem. Geol.* 114, 331–345. doi: 10.1016/0009-2541(94)90062-0
- Andrews, I. J., Long, D., Richards, P. C., Thomason, A. R., Brown, S., Chesher, J. A., et al. (1990). *United Kingdom Offshore Regional Report: The Geology of the Moray Firth*. London: HMSO.
- Atwood, T. B., Witt, A., Mayorga, J., Hammill, E., and Sala, E. (2020). Global patterns in marine sediment carbon stocks. *Front. Mar. Sci.* 7:165. doi: 10.3389/fmars.2020.00165
- Avelar, S., van der Voort, T. S., and Eglinton, T. I. (2017). Relevance of carbon stocks of marine sediments for national greenhouse gas inventories of maritime nations. *Carbon Balance Manag.* 12:10. doi: 10.1186/s13021-017-0077-x
- Bao, R., Zhao, M., McNichol, A., Galy, V., McIntyre, C., Haghipour, N., et al. (2019). Temporal constraints on lateral organic matter transport along a coastal mud belt. *Org. Geochem.* 128, 86–93. doi: 10.1016/j.orggeochem.2019.01.007
- Berner, R. A., and Raiswell, R. (1983). Burial of organic carbon and pyrite sulfur in sediments over phanerozoic time: a new theory. *Geochim. Cosmochim. Acta* 47, 855–862. doi: 10.1016/0016-7037(83)90151-5
- BGS (British Geological Survey) (1987). *Caithness Sheet 58 N – 04 W Sea Bed Sediments and Quaternary. 1250 000 UTM Series United Kingdom Continental Shelf – Seabed Sediments Quaternary*. Available online at: <https://webapps.bgs.ac.uk/data/maps/maps.cfc?method=viewRecord&mapId=11263> (accessed May 20, 2021).
- Bianchi, T. S. (2011). The role of terrestrially derived organic carbon in the coastal ocean: a changing paradigm and the priming effect. *Proc. Natl. Acad. Sci. U.S.A.* 108, 19473–19481. doi: 10.1073/pnas.1017982108
- Biondo, M., and Bartholomä, A. (2017). A multivariate analytical method to characterize sediment attributes from high-frequency acoustic backscatter and

- ground-truthing data (Jade Bay, German North Sea coast). *Cont. Shelf Res.* 138, 65–80. doi: 10.1016/j.csr.2016.12.011
- Blott, S. J., and Pye, K. (2001). GRADISTAT: a grain size distribution and statistics package for the analysis of unconsolidated sediments. *Earth Surf. Process. Landforms* 26, 1237–1248. doi: 10.1016/S0167-5648(08)70015-7
- Blott, S. J., Croft, D. J., Pye, K., Saye, S. E., and Wilson, H. E. (2004). “Particle size analysis by laser diffraction,” in *Forensic Geoscience: Principles, Techniques and Applications*, eds K. Pye and D. J. Croft (London: Geological Society), 63–73.
- Brown, C. J., and Blondel, P. (2009). Developments in the application of multibeam sonar backscatter for seafloor habitat mapping. *Appl. Acoust.* 70, 1242–1247. doi: 10.1016/j.apacoust.2008.08.004
- Burdige, D. J. (2007). Preservation of organic matter in marine sediments: controls, mechanisms, and an imbalance in sediment organic carbon budgets? *Chem. Rev.* 107, 467–485. doi: 10.1021/cr050347q
- Burdige, D. J. (2011). Temperature dependence of organic matter remineralization in deeply-buried marine sediments. *Earth Planet. Sci. Lett.* 311, 396–410. doi: 10.1016/j.epsl.2011.09.043
- Burrows, M. T., Hughes, D. J., Austin, W. E. N., Smeaton, C., Hicks, N., Howe, J. A., et al. (2017). *Assessment of Blue Carbon Resources in Scotland's Inshore Marine Protected Area Network*, NatureScot Commissioned Report 761. Edinburgh: NatureScot.
- Burrows, M. T., Kamenos, N., Hughes, D. J., Stahl, H., Howe, J. A., and Tett, P. (2014). *Assessment of Carbon Budgets and Potential Blue Carbon Stores in Scotland's Coastal and Marine Environment*. Scottish Natural Heritage Commissioned Report No. 761. Edinburgh: NatureScot.
- Calvert, J., Strong, J. A., Service, M., McGonigle, C., and Quinn, R. (2015). An evaluation of supervised and unsupervised classification techniques for marine benthic habitat mapping used multibeam echosounder data. *ICES J. Mar. Sci.* 72, 1498–1513. doi: 10.1093/icesjms/fsr174
- Che Hasan, R., Ierodiconou, D., Laurenson, L., and Schimel, A. (2014). Integrating multibeam backscatter angular response, mosaic and bathymetry data for benthic habitat mapping. *PLoS One* 9:e97339. doi: 10.1371/journal.pone.0097339
- Chesher, J. A., and Lawson, D. (1983). *The Geology of the Moray Firth*. London: HMSO.
- Collier, J. S., and Brown, C. J. (2005). Correlation of sidescan backscatter with grain size distribution of surficial seabed sediments. *Mar. Geol.* 214, 431–449. doi: 10.1016/j.margeo.2004.11.011
- Davies, J., Baxter, J., Bradley, M., Connor, D., Khan, J., Murray, E., et al. (eds) (2001). *Marine Monitoring Handbook, March 2001*. Peterborough: JNCC.
- De Borger, E., Tiano, J., Braeckman, U., Rijnsdorp, A. D., and Soetaert, K. (2020). Impact of bottom trawling on sediment biogeochemistry: a modelling approach. *Biogeosci. Discuss.* 2020, 1–32.
- De Falco, G., Tonielli, R., Di Martino, G., Innangi, S., Simeone, S., and Michael Parnum, I. (2010). Relationships between multibeam backscatter, sediment grain size and *Posidonia oceanica* seagrass distribution. *Cont. Shelf Res.* 30, 1941–1950. doi: 10.1016/j.csr.2010.09.006
- de Haas, H., Boer, W., and van Weering, T. C. E. (1997). Recent sedimentation and organic carbon burial in a shelf sea: the North Sea. *Mar. Geol.* 144, 131–146. doi: 10.1016/S0025-3227(97)00082-0
- Diesing, M., Green, S. L., Stephens, D., Lark, R. M., Stewart, H. A., and Dove, D. (2014). Mapping seabed sediments: comparison of manual, geostatistical, object-based image analysis and machine learning approaches. *Cont. Shelf Res.* 84, 107–119. doi: 10.1016/j.csr.2014.05.004
- Diesing, M., Kröger, S., Parker, R., Jenkins, C., Mason, C., and Weston, K. (2017). Predicting the standing stock of organic carbon in surface sediments of the North–West European continental shelf. *Biogeochemistry* 135, 183–200. doi: 10.1007/s10533-017-0310-4
- Diesing, M., Mitchell, P. J., O'keeffe, E., Gavazzi, G. O. A. M., and Bas, T. L. (2020). Limitations of predicting substrate classes on a sedimentary complex but morphologically simple seabed. *Remote Sens.* 12:3398. doi: 10.3390/rs12203398
- Diesing, M., Thorsnes, T., and Bjarnadóttir, L. R. (2021). Organic carbon densities and accumulation rates in surface sediments of the North Sea and Skagerrak. *Biogeosciences* 18, 21392160. doi: 10.5194/bg-18-2139-2021
- Dolan, M. F. J. (2012). *Calculation of Slope Angle from Bathymetry Data using GIS – Effects of Computation Algorithm, Data Resolution and Analysis Scale*. NGU Report 2012.041. Trondheim: NGU.
- Donato, D. C., Kauffman, J. B., Murdiyarso, D., Kurnianto, S., Stidham, M., and Kanninen, M. (2011). Mangroves among the most carbon-rich forests in the tropics. *Nat. Geosci.* 4, 293–297. doi: 10.1038/ngeo1123
- Dove, D., Arosio, R., Finlayson, A., Bradwell, T., and Howe, J. A. (2015). Submarine glacial landforms record Late Pleistocene ice-sheet dynamics, Inner Hebrides, Scotland. *Quat. Sci. Rev.* 123, 76–90. doi: 10.1016/j.quascirev.2015.06.012
- Dove, D., Weijerman, M., Grüss, A., Acoba, T., and Smith, J. R. (2020). “Substrate mapping to inform ecosystem science and marine spatial planning around the main Hawaiian Islands,” in *Seafloor Geomorphology as Benthic Habitat*, 2nd Edn, eds P. T. Harris and E. Baker (Amsterdam: Elsevier), 619–640. doi: 10.1016/b978-0-12-814960-7.00037-3
- Duarte, C. M., Middelburg, J. J., and Caraco, N. (2005). Major role of marine vegetation on the oceanic carbon cycle. *Biogeosciences* 2, 1–8. doi: 10.5194/bgd-1-659-2004
- Fannin, N. (1989). *Offshore Investigations 1966-87*, British Geological Survey Technical Report WB/89/2. Nottingham: British Geological Survey.
- Feldens, P., Schulze, I., Papenmeier, S., Schöнке, M., and Schneider von Deimling, J. (2018). Improved interpretation of marine sedimentary environments using multi-frequency multibeam backscatter data. *Geosciences* 8, 1–14. doi: 10.3390/geosciences8060214
- Frazão Santos, C., Ehler, C. N., Agardy, T., Andrade, F., Orbach, M. K., and Crowder, L. B. (2019). *Marine Spatial Planning*, 2nd Edn. Amsterdam: Elsevier Ltd. doi: 10.1016/B978-0-12-805052-1.00033-4
- Geraldi, N. R., Ortega, A., Serrano, O., Macreadie, P. I., Lovelock, C. E., Krause-Jensen, D., et al. (2019). Fingerprinting blue carbon: rationale and tools to determine the source of organic carbon in marine depositional environments. *Front. Mar. Sci.* 6:263. doi: 10.3389/fmars.2019.263
- Goff, J. A., Kraft, B. J., Mayer, L. A., Schock, S. G., Sommerfield, C. K., Olson, H. C., et al. (2004). Seabed characterization on the New Jersey middle and outer shelf: correlatability and spatial variability of seafloor sediment properties. *Mar. Geol.* 209, 147–172. doi: 10.1016/j.margeo.2004.05.030
- Goff, J. A., Olson, H. C., and Duncan, C. S. (2000). Correlation of side-scan backscatter intensity with grain-size distribution of shelf sediments, New Jersey margin. *Geo Mar. Lett.* 20, 43–49. doi: 10.1007/s003670000032
- Goldstein, A., Turner, W. R., Spawn, S. A., Anderson-Teixeira, K. J., Cook-Patton, S., Fargione, J., et al. (2020). Protecting irrecoverable carbon in Earth's ecosystems. *Nat. Clim. Chang.* 10, 287–295. doi: 10.1038/s41558-020-0738-8
- Goward Brown, A. J., Neill, S. P., and Lewis, M. J. (2017). Tidal energy extraction in three-dimensional ocean models. *Renew. Energy* 114, 244–257. doi: 10.1016/j.renene.2017.04.032
- Guinan, J., McKeon, C., O'keeffe, E., Monteys, X., Sacchetti, F., Coughlan, M., et al. (2020). Infomar data supports offshore energy development and marine spatial planning in the Irish offshore via the emodnet geology portal. *Q. J. Eng. Geol. Hydrogeol.* 54:qjehg2020-033. doi: 10.1144/qjehg2020-033
- Hedges, J. I., and Keil, R. G. (1995). Sedimentary organic matter preservation: an assessment and speculative synthesis. *Mar. Chem.* 49, 81–115.
- Hicks, N., Ubbara, G. R., Silburn, B., Smith, H. E. K., Kröger, S., Parker, E. R., et al. (2017). Oxygen dynamics in shelf seas sediments incorporating seasonal variability. *Biogeochemistry* 135, 35–47. doi: 10.1007/s10533-017-0326-9
- Holmes, R., Bulat, J., Henni, P., Holt, J., James, C., Kenyon, N., et al. (2004). *DTI Strategic Environmental Assessment Area 5 (SEA5): Seabed and Superficial Geology and Processes. CR/04/064N*. Nottingham: British Geological Survey.
- Howard, J., Sutton-Grier, A., Herr, D., Kleypas, J., Landis, E., Mcleod, E., et al. (2017). Clarifying the role of coastal and marine systems in climate mitigation. *Front. Ecol. Environ.* 15:42–50. doi: 10.1002/fee.1451
- Huettel, M., and Rusch, A. (2000). Transport and degradation of phytoplankton in permeable sediment. *Limnol. Oceanogr.* 45, 534–549. doi: 10.4319/lo.2000.45.3.0534
- Hunt, C., Demšar, U., Dove, D., Smeaton, C., Cooper, R., and Austin, W. E. N. (2020). Quantifying marine sedimentary carbon : a new spatial analysis approach using seafloor acoustics, imagery, and ground-truthing data in Scotland. *Front. Mar. Sci.* 7:588. doi: 10.3389/fmars.2020.00588
- IHO (2020). *International Hydrographic Organization Standards for Hydrographic Surveys S-44*. Monte Carlo: IHO.
- Janssen, F., Huettel, M., and Witte, U. (2005). Pore-water advection and solute fluxes in permeable marine sediments (II): benthic respiration at three

- sandy sites with different permeabilities (German Bight, North Sea). *Limnol. Oceanogr.* 50, 779–792. doi: 10.4319/lo.2005.50.3.0779
- Kaskela, A., Kotilainen, A., Alanen, U., Cooper, R., Green, S., Guinan, J., et al. (2019). Picking up the pieces—harmonising and collating seabed substrate data for European maritime areas. *Geosciences* 9:84. doi: 10.3390/geosciences9020084
- Kenny, A. J., Cato, I., Desprez, M., Fader, G., Schuttenhelm, R. T. E., and Side, J. (2003). An overview of seabed-mapping technologies in the context of marine habitat classification. *ICES J. Mar. Sci.* 60, 411–418. doi: 10.1016/S1054-3139(03)00006-7
- Lark, R. M., Cullis, B. R., and Welham, S. J. (2006). On spatial prediction of soil properties in the presence of a spatial trend: the empirical best linear unbiased predictor (E-BLUP) with REML. *Eur. J. Soil Sci.* 57, 787–799. doi: 10.1111/j.1365-2389.2005.00768.x
- Lark, R. M., Dove, D., Green, S. L., Richardson, A. E., Stewart, H., and Stevenson, A. (2012). Spatial prediction of seabed sediment texture classes by cokriging from a legacy database of point observations. *Sediment. Geol.* 281, 35–49. doi: 10.1016/j.sedgeo.2012.07.009
- Lecours, V. (2017). On the use of maps and models in conservation and resource management (warning : results may vary). *Front. Mar. Sci.* 4:288. doi: 10.3389/fmars.2017.00288
- Lecours, V., Dolan, M. F. J., Micallef, A., and Lucieer, V. L. (2016b). A review of marine geomorphometry, the quantitative study of the seafloor. *Hydrol. Earth Syst. Sci.* 20, 3207–3244. doi: 10.5194/hess-20-3207-2016
- Lecours, V., Brown, C. J., Devillers, R., Lucieer, V. L., and Edinger, E. N. (2016a). Comparing selections of environmental variables for ecological studies: a focus on terrain attributes. *PLoS One* 11:e0167128. doi: 10.1371/journal.pone.0167128
- Lecours, V., Devillers, R., Schneider, D. C., Lucieer, V. L., Brown, C. J., and Edinger, E. N. (2015). Spatial scale and geographic context in benthic habitat mapping : review and future directions. *Mar. Ecol. Prog. Ser.* 535, 259–284. doi: 10.3354/meps11378
- Lecours, V., Devillers, R., Simms, A. E., Lucieer, V. L., and Brown, C. J. (2017). Towards a framework for terrain attribute selection in environmental studies. *Environ. Model. Softw.* 89, 19–30. doi: 10.1016/j.envsoft.2016.11.027
- Lee, T. R., and Phrampus, B. J. (2019). A machine learning (kNN) approach to predicting global sea floor total organic carbon. *Glob. Biogeochem. Cycles* 33, 37–46. doi: 10.1029/2018GB005992
- Legge, O., Johnson, M., Hicks, N., Jickells, T., Diesing, M., Aldridge, J., et al. (2020). Carbon on the Northwest European shelf: contemporary budget and future influences. *Front. Mar. Sci.* 7:143. doi: 10.3389/fmars.2020.00143
- Lindenbaum, C., Bennell, J. D., Rees, E. I. S., Mclean, D., Cook, W., Wheeler, A. J., et al. (2008). Small-scale variation within a *Modiolus modiolus* (Mollusca: Bivalvia) reef in the Irish Sea: I. Seabed mapping and reef morphology. *J. Mar. Biol. Assoc. U. K.* 88, 133–141. doi: 10.1017/S0025315408000374
- Long, D. (2006). *BGS Detailed Explanation of Seabed Sediment Modified Folk Classification*. Peterborough: Joint Nature Conservation Committee.
- Lovelock, C. E., and Duarte, C. M. (2019). Dimensions of blue carbon and emerging perspectives. *Biol. Lett.* 15, 1–5. doi: 10.1098/rsbl.2018.0781
- Lucieer, V., Hill, N. A., Barrett, N. S., and Nichol, S. (2013). Do marine substrates “look” and “sound” the same? Supervised classification of multibeam acoustic data using autonomous underwater vehicle images. *Estuar. Coast. Shelf Sci.* 117, 94–106. doi: 10.1016/j.ecss.2012.11.001
- Luisetti, T., Ferrini, S., Grilli, G., Jickells, T. D., Kennedy, H., Kröger, S., et al. (2020). Climate action requires new accounting guidance and governance frameworks to manage carbon in shelf seas. *Nat. Commun.* 11:4599. doi: 10.1038/s41467-020-18242-w
- Luisetti, T., Turner, R. K., Andrews, J. E., Jickells, T. D., Kröger, S., Diesing, M., et al. (2019). Quantifying and valuing carbon flows and stores in coastal and shelf ecosystems in the UK. *Ecosyst. Serv.* 35, 67–76. doi: 10.1016/j.ecoser.2018.10.013
- Lurton, X., and Lamarche, G. (eds.). (2015). *Backscatter Measurements by Seafloor-Mapping Sonars. Guidelines and Recommendations, 200p, GeoHab Backscatter Working Group*. Available online at: <https://geohab.org/wp-content/uploads/2018/09/BWSG-REPORT-MAY2015.pdf>
- Macreadie, P. I., Atwood, T. B., Seymour, J. R., Fontes, M. L. S., Sanderman, J., Nielsen, D. A., et al. (2019). Vulnerability of seagrass blue carbon to microbial attack following exposure to warming and oxygen. *Sci. Total Environ.* 686, 264–275. doi: 10.1016/j.scitotenv.2019.05.462
- Masetti, G., Mayer, L. A., and Ward, L. G. (2018). A bathymetry- and reflectivity-based approach for seafloor segmentation. *Geosciences* 8:14. doi: 10.3390/geosciences8010014
- Mason, C. (2011). *NMBAQC's Best Practice Guidance. Particle Size Analysis (PSA) for Supporting Biological Analysis*. National Marine Biological AQC Coordinating Committee.
- McGonigle, C., and Collier, J. S. (2014). Interlinking backscatter, grain size and benthic community structure. *Estuar. Coast. Shelf Sci.* 147, 123–136. doi: 10.1016/j.ecss.2014.05.025
- McLeod, E., Chmura, G. L., Bouillon, S., Salm, R., Björk, M., Duarte, C. M., et al. (2011). A blueprint for blue carbon: toward an improved understanding of the role of vegetated coastal habitats in sequestering CO₂. *Front. Ecol. Environ.* 9:552–560. doi: 10.1890/110004
- Misiuk, B., Lecours, V., and Bell, T. (2018). A multiscale approach to mapping seabed sediments. *PLoS One* 13:e0193647. doi: 10.1371/journal.pone.0193647
- Nellemann, C., Corcoran, E., Duarte, C., Valdes, L., De Young, C., Fonseca, L., et al. (2009). *Blue Carbon. A Rapid Response Assessment*. Birkeland: Birkeland Trykkeri AS.
- O'Carroll, J. P. J., Kennedy, R., Ren, L., Nash, S., Hartnett, M., and Brown, C. (2017). A comparison of acoustic and observed sediment classifications as predictor variables for modelling biotope distributions in Galway Bay, Ireland. *Estuar. Coast. Shelf Sci.* 197, 258–270. doi: 10.1016/j.ecss.2017.08.005
- Pace, M. C., Bailey, D. M., Donnan, D. W., Narayanaswamy, B. E., Smith, H. J., Speirs, D. C., et al. (2021). Modelling seabed sediment physical properties and organic matter content in the Firth of Clyde. *Earth Syst. Sci. Data* [Preprint]. doi: 10.5194/essd-2021-23
- Paradis, S., Puig, P., Masqué, P., Juan-Díaz, X., Martín, J., and Palanques, A. (2017). Bottom-trawling along submarine canyons impacts deep sedimentary regimes. *Sci. Rep.* 7:43332. doi: 10.1038/srep43332
- Parnum, I., and Gavrilov, A. (2012). “High-frequency seafloor acoustic backscatter from coastal marine habitats of Australia,” in *Proceedings of the Acoustical Society of Australia*, (Fremantle, WA).
- Pınarbaşı, K., Galparsoro, I., Borja, Á., Stelzenmüller, V., Ehler, C. N., and Gimpel, A. (2017). Decision support tools in marine spatial planning: present applications, gaps and future perspectives. *Mar. Policy* 83, 83–91. doi: 10.1016/j.marpol.2017.05.031
- Rawlins, B. G., Marchant, B. P., Smyth, D., Scheib, C., Lark, R. M., and Jordan, C. (2009). Airborne radiometric survey data and a DTM as covariates for regional scale mapping of soil organic carbon across Northern Ireland. *Eur. J. Soil Sci.* 60, 44–54. doi: 10.1111/j.1365-2389.2008.01092.x
- Reid, G., and McManus, J. (1987). Sediment exchanges along the coastal margin of the Moray Firth, Eastern Scotland. *J. Geol. Soc. London* 144, 179–185.
- Sala, E., Mayorga, J., Bradley, D., Cabral, R. B., Atwood, T. B., Auber, A., et al. (2021). Protecting the global ocean for biodiversity, food and climate. *Nature* 592, 397–402. doi: 10.1038/s41586-021-03371-z
- Sayed, S. S., Abbott, B. W., Thornton, B. F., Frederick, J. M., Vonk, J. E., Overduin, P., et al. (2020). Subsea permafrost carbon stocks and climate change sensitivity estimated by expert assessment. *Environ. Res. Lett.* 15:124075. doi: 10.1088/1748-9326/abcc29
- Serpenti, N., Heath, M., Rose, M., and Witte, U. (2012). High resolution mapping of sediment organic matter from acoustic reflectance data. *Hydrobiologia* 680, 265–284. doi: 10.1007/s10750-011-0937-4
- Shafiee, R. T. (2021). *Blue Carbon*. Available online at: <https://digitalpublications.parliament.scot/ResearchBriefings/Report/2021/3/23/e8e93b3e-08b5-4209-8160-0b146bafec9d#> (accessed May 15, 2021).
- Smeaton, C., and Austin, W. E. N. (2019). Where's the carbon : exploring the spatial heterogeneity of sedimentary carbon in mid-latitude fjords. *Front. Earth Sci.* 7:269. doi: 10.3389/feart.2019.00269
- Smeaton, C., Austin, W., and Turrell, W. R. (2020). Re – evaluating Scotland's sedimentary carbon stocks. *Scott. Mar. Freshw. Sci.* 11:16. doi: 10.7489/12267-1
- Smeaton, C., Hunt, C. A., Turrell, W. R., and Austin, W. E. N. (2021). Marine sedimentary carbon stocks of the United Kingdom's exclusive economic zone. *Front. Earth Sci.* 9:593324. doi: 10.3389/feart.2021.593324
- Smith, R. W., Bianchi, T. S., Allison, M., Savage, C., and Galy, V. (2015). High rates of organic carbon burial in fjord sediments globally. *Nat. Geosci.* 8, 450–453. doi: 10.1038/NGEO2421

- Sutherland, T. F., Galloway, J., Loschiavo, R., Levings, C. D., and Hare, R. (2007). Calibration techniques and sampling resolution requirements for groundtruthing multibeam acoustic backscatter (EM3000) and QTC VIEWTM classification technology. *Estuar. Coast. Shelf Sci.* 75, 447–458. doi: 10.1016/j.ecss.2007.05.045
- Turrell, W. R. (2020). A compendium of marine related carbon stores, sequestrations and emissions. *Scott. Mar. Freshw. Sci.* 11, 1–70. doi: 10.7489/12261-1
- United Nations/Framework Convention on Climate Change (2015). *Adoption of the Paris Agreement, 21st Conference of the Parties*. Paris: United Nations.
- van der Voort, T. S., Blattmann, T., Usman, M., Montluçon, D., Loeffler, T., Tavagna, M. L., et al. (2021). MOSAIC (Modern Ocean Sediment Archive and Inventory of Carbon): a (radio)carbon-centric database for seafloor surficial sediments. *Earth Syst. Sci. Data Discuss.* 13, 2135–2146. doi: 10.5194/essd-2020-199
- Verardo, D. J., Froelich, P. N., and McIntyre, A. (1990). Determination of organic carbon and nitrogen in marine sediment using the Carlo Erba NA-1500 Analyzer. *Deep Sea Res. A* 37, 157–165.
- Villanneau, E. J., Saby, N. P. A., Marchant, B. P., Jolivet, C. C., Boulonne, L., Caria, G., et al. (2011). Which persistent organic pollutants can we map in soil using a large spacing systematic soil monitoring design? A case study in Northern France. *Sci. Total Environ.* 409, 3719–3731. doi: 10.1016/j.scitotenv.2011.05.048
- Webster, R., and Oliver, M. A. (2007). *Geostatistics for Environmental Scientists*, 2nd Edn. Chichester: John Wiley & sons, Inc.
- Wilson, M. F. J., O'Connell, B., Brown, C., Guinan, J. C., and Grehan, A. J. (2007). Multiscale terrain analysis of multibeam bathymetry data for habitat mapping on the continental slope. *Mar. Geod.* 30, 3–35. doi: 10.1080/01490410701295962
- Wilson, R. J., Speirs, D. C., Sabatino, A., and Heath, M. R. (2018). A synthetic map of the north-west European Shelf sedimentary environment for applications in marine science. *Earth Syst. Sci. Data* 10, 109–130. doi: 10.5194/essd-10-109-2018

Conflict of Interest: The authors declare that the research was conducted in the absence of any commercial or financial relationships that could be construed as a potential conflict of interest.

Publisher's Note: All claims expressed in this article are solely those of the authors and do not necessarily represent those of their affiliated organizations, or those of the publisher, the editors and the reviewers. Any product that may be evaluated in this article, or claim that may be made by its manufacturer, is not guaranteed or endorsed by the publisher.

Copyright © 2021 Hunt, Demšar, Marchant, Dove and Austin. This is an open-access article distributed under the terms of the Creative Commons Attribution License (CC BY). The use, distribution or reproduction in other forums is permitted, provided the original author(s) and the copyright owner(s) are credited and that the original publication in this journal is cited, in accordance with accepted academic practice. No use, distribution or reproduction is permitted which does not comply with these terms.



Future Mangrove Carbon Storage Under Climate Change and Deforestation

Mark Chatting^{1,2}, Ibrahim Al-Maslamani^{3*}, Mark Walton⁴, Martin W. Skov², Hilary Kennedy², Y. Sinan Husrevoglu⁵ and Lewis Le Vay⁴

¹ Environmental Science Centre, Qatar University, Doha, Qatar, ² School of Ocean Sciences, Bangor University, Menai Bridge, United Kingdom, ³ Office for Research and Graduate Studies, Qatar University, Doha, Qatar, ⁴ Centre for Applied Marine Science, Bangor University, Menai Bridge, United Kingdom, ⁵ Institute of Marine Sciences, Middle East Technical University, Mersin, Turkey

OPEN ACCESS

Edited by:

Iris Eline Hendriks,
Spanish National Research Council
(CSIC), Spain

Reviewed by:

Frida Sidik,
Ministry for Marine Affairs
and Fisheries of the Republic
of Indonesia, Indonesia
Inés Mazarrasa,
Environmental Hydraulics Institute
(IH Cantabria), Spain

*Correspondence:

Ibrahim Al-Maslamani
almaslamani@qu.edu.qa

Specialty section:

This article was submitted to
Global Change and the Future Ocean,
a section of the journal
Frontiers in Marine Science

Received: 23 September 2021

Accepted: 12 January 2022

Published: 10 February 2022

Citation:

Chatting M, Al-Maslamani I,
Walton M, Skov MW, Kennedy H,
Husrevoglu YS and Le Vay L (2022)
Future Mangrove Carbon Storage
Under Climate Change
and Deforestation.
Front. Mar. Sci. 9:781876.
doi: 10.3389/fmars.2022.781876

Mangroves are important sinks of organic carbon (C) and there is significant interest in their use for greenhouse gas emissions mitigation. Adverse impacts on organic carbon storage potential from future climate change and deforestation would devalue such ambitions, thus global projections of future change remains a priority research area. We modeled the effects of climate change on future C stocks and soil sequestration rates (CSR) under two climate scenarios (“business as usual”: SSP245 and high-emissions: SSP585). Model results were contrasted with CO₂ equivalents (CO₂e) emissions from past, present and future rates of deforestation on a country specific scale. For C stocks, we found climate change will increase global stocks by ~7% under both climate scenarios and that this gain will exceed losses from deforestation by the end of the twenty-first century, largely due to shifts in rainfall. Major mangrove-holding countries Indonesia, Malaysia, Cuba, and Nigeria will increase national C stocks by > 10%. Under the high-end scenario, while a net global increase is still expected, elevated temperatures and wider temperature ranges are likely increase the risk of countries’ C stocks diminishing. For CSR, there will likely be a global reduction under both climate change scenarios: 12 of the top 20 mangrove-rich countries will see a drop in CSR. Modeling of published country level mangrove deforestation rates showed emissions have decreased from 141.4 to 6.4% of annual CSR since the 1980’s. Projecting current mangrove deforestation rates into the future resulted in a total of 678.50 ± 151.32 Tg CO₂e emitted from 2012 to 2095. Reducing mangrove deforestation rates further would elevate the carbon benefit from climate change by 55–61%, to make the proposition of offsetting emissions through mangrove protection and restoration more attractive. These results demonstrate the positive benefits of mangrove conservation on national carbon budgets, and we identify the nations where incorporating mangrove conservation into their Nationally Defined Contributions offers a particularly rewarding route toward meeting their Glasgow Agreement commitments.

Keywords: mangrove carbon stocks, mangrove sequestration rates, blue carbon, soil carbon, mangrove deforestation, mangrove emissions, climate change

INTRODUCTION

Mangroves, tidal marshes and seagrass meadows accumulate organic rich soils that can often extend to many meters depth and provide long-term storage of organic carbon (C). Termed “blue carbon” ecosystems (BCE), these habitats occupy a relatively small area of the global ocean (~0.2%), but are major contributors to marine sediment organic carbon burial (Duarte et al., 2013). Mangroves are of particular interest as they store and sequester comparatively high amounts of C in both biomass and soils (Donato et al., 2011; Ezcurra et al., 2016; Almahasheer et al., 2017; Kauffman et al., 2017). Mangroves store up to five times as much organic carbon as tropical upland forests (Donato et al., 2011). A combination of high productivity and slow soil decomposition rates significantly increases mangroves’ ability to capture and store organic carbon, particularly in their soils (Alongi, 2012). Aboveground net primary productivity (NPP) rates in mangroves ($8.1 \text{ t DW ha}^{-1} \text{ yr}^{-1}$) rival those of highly productive tropical terrestrial forests ($11.1 \text{ t DW ha}^{-1} \text{ yr}^{-1}$) (Alongi, 2012). In addition, complex mangrove root structures and waterlogged soils trap allochthonous organic material on top of deep carbon rich peat composed mainly of dead root material, sometimes extending up to 10 m depth (McKee et al., 2007); soil carbon can comprise up to 90% of mangrove organic carbon stocks (Cooray et al., 2021). As a result, mangroves have received a great deal of scientific interest as natural systems for offsetting greenhouse gas (GHG) emissions (Donato et al., 2011; Fourqurean et al., 2012).

Historic rates of mangrove deforestation posed a serious risk of significant GHG emissions; since the 1950’s it has been estimated that up to 50% of the world’s mangroves have been deforested, largely due to land-use change (Alongi, 2002). Despite estimates of recent global mangrove loss slowing to 4.0% of global coverage between 1996 and 2016 (Richards et al., 2020), it has been estimated that > 300 million Mg of CO₂e were emitted as a result of mangrove deforestation between 2000 and 2012 (Hamilton and Friess, 2018). Between 2000 and 2016, 87% of mangrove loss in the West Coral triangle, where the vast majority of the world’s mangroves organic carbon is stored, was due to mangrove to agri/aquaculture land-use conversion (Adame et al., 2021). Mangrove conservation and restoration programs on a national scale have been identified as an efficient means of offsetting GHG emissions (Murdiyarso et al., 2015; Taillardat et al., 2018; Cameron et al., 2019), although the prevention of further forest loss, by far, outweighs gains from restoration (Kauffman et al., 2017).

While the potential for GHG emissions from mangrove deforestation are well documented (Lovelock et al., 2011; Kauffman et al., 2014; Lang’at et al., 2014; Atwood et al., 2017; Hamilton and Friess, 2018), the effects of climate change on global mangrove C stocks are less frequently addressed (Adame et al., 2021) and are therefore a priority research area for blue carbon science (Macreadie et al., 2019). Sea level rise has been identified as potentially the most significant climate change factor affecting mangrove distribution and C stocks (Macreadie et al., 2019; Lovelock and Reef, 2020). Sea level rise would cause changes to inundation periods and durations, potentially

increasing tree mortality (Ward et al., 2016). It has been estimated that 96% of coastal wetlands, which includes mangroves, could be lost in the Middle East this century due to sea level rise (Blankespoor et al., 2014). Where mangroves occur adjacent to human settlements, coastal “squeeze” may occur, between rising sea level and expanding human settlements/agriculture behind the mangrove (Lovelock and Reef, 2020). Worst case estimates have projected lost C sequestration of 3.4 Pg by 2100 due to coastal “squeeze” (Lovelock and Reef, 2020). Change in climatic regimes could also prove a significant factor in changing overall stocks in mangroves through altering forest biomass and productivity and its subsequent contribution to soil C stocks and soil sequestration rates (CSR). Recent evidence from extreme climatic regions of global mangrove distribution (Almahasheer et al., 2017; Kauffman and Bhomia, 2017; Schile et al., 2017; Chatting et al., 2020) shows that under extreme salinity, heat and reduced rainfall, total C stocks and CSR may be reduced when compared to tropical humid mangroves (Sheppard et al., 2010). In addition, it is well established that climate change will not have spatially uniform impacts around the world (Giorgi et al., 2019; Soares et al., 2019). The Asian and American tropics are forecast to experience an increase in the frequency of extreme precipitation events (Giorgi et al., 2019), while reductions in precipitation in northern areas of African tropics suggest that expansion of semi-arid conditions is possible (Soares et al., 2019). Little is known about what the sum effect of these regional changes in temperature and precipitation regimes could be on regional mangrove C stocks or CSR (Wang et al., 2020) and whether any regions are at risk of significant losses in stocks and reductions in CSR.

Here we use predictive models to forecast how climate change and forest degradation singularly and in combination affect future C stocks and CSR in mangroves. Data collated from previously published literature were used to develop predictive models to estimate the difference between current and future global total C stocks (biomass + soil) and CSR. We contrasted the impacts of climate change against GHG emissions from past, present and forecasted future rates of mangrove deforestation to examine the carbon benefits from current conservation efforts on a country-specific scale.

MATERIALS AND METHODS

Literature Data

In order to predict mangrove CSR globally and on a country-specific scale, two separate databases of previously published data were compiled. Measured soil C stocks and CSR estimates were compiled from previous work. Keywords “mangrove” AND “soil” OR “sediment” AND “carbon stocks” OR “sequestration rate” OR “burial rate” were searched in Google Scholar¹ only, as Google scholar search results are a superset of Web of Science and Scopus, two commonly used search databases in meta-analysis studies (Martín-Martín et al., 2018). In addition, publicly available unpublished datasets were searched in the

¹<http://scholar.google.com/>

Centre for International Forestry Research (CIFOR) online repository² (Sasmito et al., 2019). When studies reported interval measurements of C stocks (e.g., 0–15 cm, 15–30 cm, 30–50 cm and 50–100 cm) from sampled cores, these were used to calculate soil C stocks to 100 cm depth (C_{100}). Individual sampling site measurements were used to maximize the amount of data to later be used in predictive modeling and to reflect the high variability in soil C stocks. When unavailable, however, study means were collated, which is likely to have overestimated C stocks in sites where this was carried out as it does not take into account C decay with soil depth. Moreover, as 31 of the 88 collated studies reported sampled core data, our calculations of C_{100} are likely to be overestimates. Soil C sequestration rates were obtained from studies using Pb^{210} , Cs^{137} dating methods or if organic carbon sequestration was calculated from total sediment accretion. When studies reported data graphically, images of graphics were captured and points were digitized in plot digitizer software by manually overlaying points onto graphical points. When soil stocks or characteristics (dry bulk density (DBD) and soil C%) were reported, they were included and soil C stocks were calculated from the following equation then multiplied by 100 to estimate C_{100} stocks (Donato et al., 2011):

$$\text{Soil C (g cm}^{-3}\text{)} = 3.0443 \times \text{DBD}^{-1.313}$$

Where studies' reported measurement uncertainties (standard deviation with associated n and standard error) as well as DBD to soil C (g cm^{-3}) conversion equation uncertainties, these were included in the database to later be propagated in model development. Site longitude and latitude were extracted from studies when reported. For studies that did not report site coordinates, any maps included were used in combination with Google Earth images to obtain site coordinates. Only intact mature mangroves were included; data from mangroves reported as degraded, newly colonized or planted were excluded from the dataset.

Estimating Current Soil Stocks and Sequestration Rates

Statistical models were developed to predict mangrove soil organic carbon where it had not been measured. A suite of climatic variables commonly used in species distribution modeling and in previous global mangrove modeling efforts (O'Donnell and Ignizio, 2012; Hutchison et al., 2014; **Supplementary Table 1**) were calculated from historical climate datasets for all global mangrove points using a global mangrove presence/absence mask reported by Hamilton and Casey (2016). Previous global soil C mangrove modeling studies have incorporated non-climatic predictors, such as tidal range, river discharge and geomorphological setting (Rovai et al., 2018; Sanderman et al., 2018). However, only climatic predictors were used here, given the identified need to better understand how the magnitude of projected climate change will affect future mangrove C stocks and CSR. Global historical climate datasets used were monthly precipitation (P_{mean}) (from 1901 to

2010), mean monthly air temperatures (T_{mean}) (from 1901 to 2010), daily maximum temperatures (T_{max}) and daily minimum temperatures (T_{min}) (from 1979 to 2010). These datasets were obtained from the Global Precipitation Climatology Centre (Schneider et al., 2011) (GPCC) and National Center for Environmental Prediction (NCEP) (Kalnay et al., 1996) and aligned to the period from 1982–2018, the longest concurrent period of all datasets (the last 36 years). Means of the aligned period were then calculated to be used in model development. The ability of climate datasets to explain variation in soil C stocks data was also compared to models that contained non-climate predictors previously used in modeling studies, for example tidal range (Carrere et al., 2013) and river discharge (Fekete et al., 2002).

Parametric (multiple linear regression) and machine learning (random forest) approaches were contrasted to test which better predicted current soil C_{100} stocks and CSR datasets. Measurement and conversion equation uncertainties that were compiled from literature were included as inverse weights in linear and random forest modeling to account for reported sampling uncertainty. Log10 transformation was performed on response data for linear regression analyses to comply with regression assumptions and predictors were chosen based on stepwise regression. Linear regression multicollinearity was addressed by removing explanatory variables with a variance inflation factor > 3.3 (Kock and Lynn, 2012). Random forest models were built using the randomForest package in R. Random forests are not subject to assumptions of normality and multicollinearity, therefore, all predictors were used and response data were not transformed. Both linear and random forest model out of sample performance was tested by k-fold cross validation using an 80–20% training-test split (Rovai et al., 2018; Masih, 2019). All statistical analyses was performed using R 3.6.2 software.

Present Day Stocks and Soil Sequestration Rates

The global mangrove mask reported by Hamilton and Casey (2016) was assumed to be present day global mangrove coverage. For the purposes of this study, 2012 was selected as it was the latest previously published global mangrove extent map. As the study aimed to estimate national scale stocks and CSR, the original $\sim 30 \times 30$ m pixel spatial resolution was converted to $\sim 3,000 \times 3,000$ m by resampling points. This level of resolution was selected as it reduced computational time significantly, still represented a high enough detail to discern country level changes in climate and was comparable to previous global and country level mangrove modeling work. For example, Rovai et al. (2018) used a ~ 25 km pixel resolution when predicting mangrove soil organic carbon stocks globally, Zeng et al. (2021) used a 1 km spatial resolution when investigating country level emissions in mangroves; and Hutchison et al. (2014) aboveground mangrove biomass to a 30 arc-second (1 km) resolution. Aboveground biomass (Mg ha^{-1}) for all global mangrove pixels was estimated using a previously developed climate predictive model (AGB t

²<http://data.cifor.org>

$\text{ha}^{-1} = 0.295\text{Bio10} + 0.658\text{Bio11} + 0.023\text{Bio16} + 0.195\text{Bio17} - 120.3$ (Hutchison et al., 2014). Where Bio 10 and 11 are the mean temperatures of the warmest and coldest quarters of the year, respectively, and Bio16 and 17 are precipitation in the wettest and driest quarters, respectively. Below ground biomass was estimated using a total above to below ground biomass allocation ratio of 0.5 (Hamilton and Friess, 2018). Model residuals reported by Hutchison et al. (2014) were used to propagate aboveground biomass standard errors. Uncertainties were multiplied by 1.96 and either added or subtracted from mean predicted values to calculate upper and lower 95% confidence intervals (CI's) for above and below ground model outputs (Zuur et al., 2013). Above and below ground tree biomass estimates and CI's were then converted into above and below ground tree C stock using 0.48 and 0.39 conversion factors, respectively (Schile et al., 2017). Using our newly derived predictive model, soil C_{100} stocks and CSR and their associated uncertainties were applied to all global mangrove pixels. 95% CI's were calculated in the same way as aboveground biomass. Hectare level total stocks estimates, CSR and upper and lower confidence bounds were grouped by country. Country level total C stocks and 95% CI's were then calculated by summing all hectare value estimates within each country.

Forecasted Stocks and Soil Sequestration Rates

Constant global mangrove coverage was assumed from 2012 to 2095, to estimate potential change in mangrove C. Future (year 2095) global total mangrove organic carbon stocks, CSR, climate data and associated 95% CI's were predicted in the same way as present day estimates, however, forecasted climate data for all global mangrove coverage pixels were used instead of historical datasets. To calculate future climate data, the latest Coupled Model Inter-comparison Project phase 6 (CMIP6) climate scenarios were used. Shared Socioeconomic Pathway 2 radiative forcing 4.5 (SSP245) and Shared Socioeconomic Pathway 5 radiative forcing 8.5 (SSP585) were selected as they represent mid and high-level GHG emissions futures, respectively. Scenario SSP245 was selected as it represents a "business as usual" scenario where historical patterns of development are continued and could be compared to a more extreme scenario (SSP585), which forecasts high economic development and increased reliance on fossil fuels, subsequently high GHG emissions (Riahi et al., 2017). Prior to applying C stocks and CSR models to climate data, an ensemble of climate datasets were bias corrected and mean weighted. For each ensemble member, bias correction of future datasets, based on their alignment with historical climate datasets, was performed using the following equations (Luo et al., 2018):

$$\text{Cor } P_{\text{mean } m, \text{ loc}} = \text{Hist } P_{\text{mean } m, \text{ loc}} \times \frac{\mu(\text{Obs } P_{\text{mean } m, \text{ loc}})}{\mu(\text{Hist } P_{\text{mean } m, \text{ loc}})}$$

$$\text{Cor } T_{\text{mean } m, \text{ loc}} = \text{Hist } T_{\text{mean } m, \text{ loc}} + [\mu(\text{Obs } T_{\text{mean } m, \text{ loc}}) - \mu(\text{Hist } T_{\text{mean } m, \text{ loc}})]$$

$$\text{Cor } T_{\text{max } m, \text{ loc}} = \text{Hist } T_{\text{max } m, \text{ loc}} + [\mu(\text{Obs } T_{\text{max } m, \text{ loc}}) - \mu(\text{Hist } T_{\text{max } m, \text{ loc}})]$$

Where $\text{Cor } P_{\text{mean } m, \text{ loc}}$, $\text{Cor } T_{\text{mean } m, \text{ loc}}$ and $\text{Cor } T_{\text{max } m, \text{ loc}}$ stand for corrected future precipitation and temperature on the m^{th} month in the loc^{th} location. Prefaces Obs and Hist refer to observed historical and hindcasted historical data. Weighting coefficients (Supplementary Table 3) for bias corrected climate data was calculated depending on their ability to hindcast historical observed datasets using the following equation (Muhling et al., 2011):

$$\text{Model weight} = \frac{n}{\sum_{i=1}^n \{e^{-\text{RMS}(i)^2}\}}$$

Where RMS is the model root mean square (RMS) and n is the number of climate forecast models. From weighting coefficients, a bias corrected, mean weighted ensemble climate forecast dataset was then calculated for each predictor (P_{mean} , T_{mean} , T_{max} , T_s and T_{min}). The ensemble was selected where climate forecasts (and hindcast data) for each scenario (SSP245 and SSP585) and each predictor were available. Datasets were downloaded from the World Climate Research Program.³ Global mangrove biomass C stocks, soil C stocks and soil sequestration rates were then predicted from the mean weighted climate forecast using the same predictive models as present day from 2059 to 2095 (36 years, as was done for present day). Future estimates of total C stocks (biomass C and soil C_{100}), CSR and 95% CI's were then, subtracted from current (2012) estimates on a pixel basis. The resulting differences per pixel and CI's were then summed per country to express change in total C stocks or soil sequestration rates on a country level with uncertainty levels. The resulting values were split into two groups depending on whether the country was forecasted to experience a net gain or loss in total mangrove C (factor: gain vs. loss). A binomial Generalized Linear Model (GLM, gain vs. loss in total mangrove C stock) was then used for each climate predictor to test for the probability of increase in a countries' total C stock with the associated change in climate predictor.

Mangrove Deforestation

Global and country level mangrove coverage for the years 1980, 1990, and 2000 were obtained from a previously published Food and Agricultural Organization of the UN report (FAO, 2007). Data in this report were gathered by a combination of questionnaires distributed worldwide to members of the International Society for Mangrove Ecosystems (ISME) and satellite imagery (FAO, 2007). From 2000 to 2010, high resolution (~30 m) satellite imagery has been used to estimate global mangrove coverage (Giri et al., 2011; Hamilton and Casey, 2016). Our pre 2000 estimates are based on the 2007 FAO report (FAO, 2007), however, there is much debate about the uncertainties surrounding these data (Friess and Webb, 2014). Even determining the trend of mangrove coverage in some countries during this period is difficult (FAO, 2007).

³<https://esgf-node.llnl.gov/search/cmip6/>

However, this period represents peak rates of global mangrove deforestation, some estimates of mangrove loss during this period are up to 30–50% (Alongi, 2002; Duke et al., 2007). In addition, the present report is the most comprehensive historical record of global mangrove coverage prior to 2000. As such, estimates of coverage change, and therefore emissions, from 2000 should be considered more accurate than prior to 2000 estimates as post-2000 estimates are based on high resolution satellite imagery. Estimates of country level mangrove coverage and deforestation from 2000 to 2012 were obtained from Hamilton and Casey (2016) using the Mangrove Forests of the World dataset (MFW) (Giri et al., 2011). A constant reference deforestation rate was assumed for the period 2012–2095 (Adame et al., 2018). Rates of loss were based on previous country specific rates for the period 2011–2012.

Country Level Emissions

Mean present day hectare level C stocks and 95% CI's for each country were calculated and multiplied by the number of hectares lost for each decadal period from 1980 to 2095 (Atwood et al., 2017). The current study assumed that deforestation of 1 hectare of mangrove results in 43% loss in soil C in addition to all tree C (Atwood et al., 2017; Adame et al., 2018), which was then divided by 10 to calculate an annual lost C over a 10 year period. Lost C from mangrove deforestation and change in C stocks from climate change were summed to calculate total potential change in C stocks in the twenty-first century from climate change and mangrove deforestation. To compare C stocks changes and emissions from mangrove deforestation, C was converted to CO₂ equivalents (CO₂e) by multiplying C stocks by 3.67 (Atwood et al., 2017; Adame et al., 2018; Hamilton and Friess, 2018). Emissions can be a number of gasses, CO₂e is the standard unit of measure of GHG emissions for mangrove deforestation (Atwood et al., 2017; Adame et al., 2018; Hamilton and Friess, 2018).

RESULTS

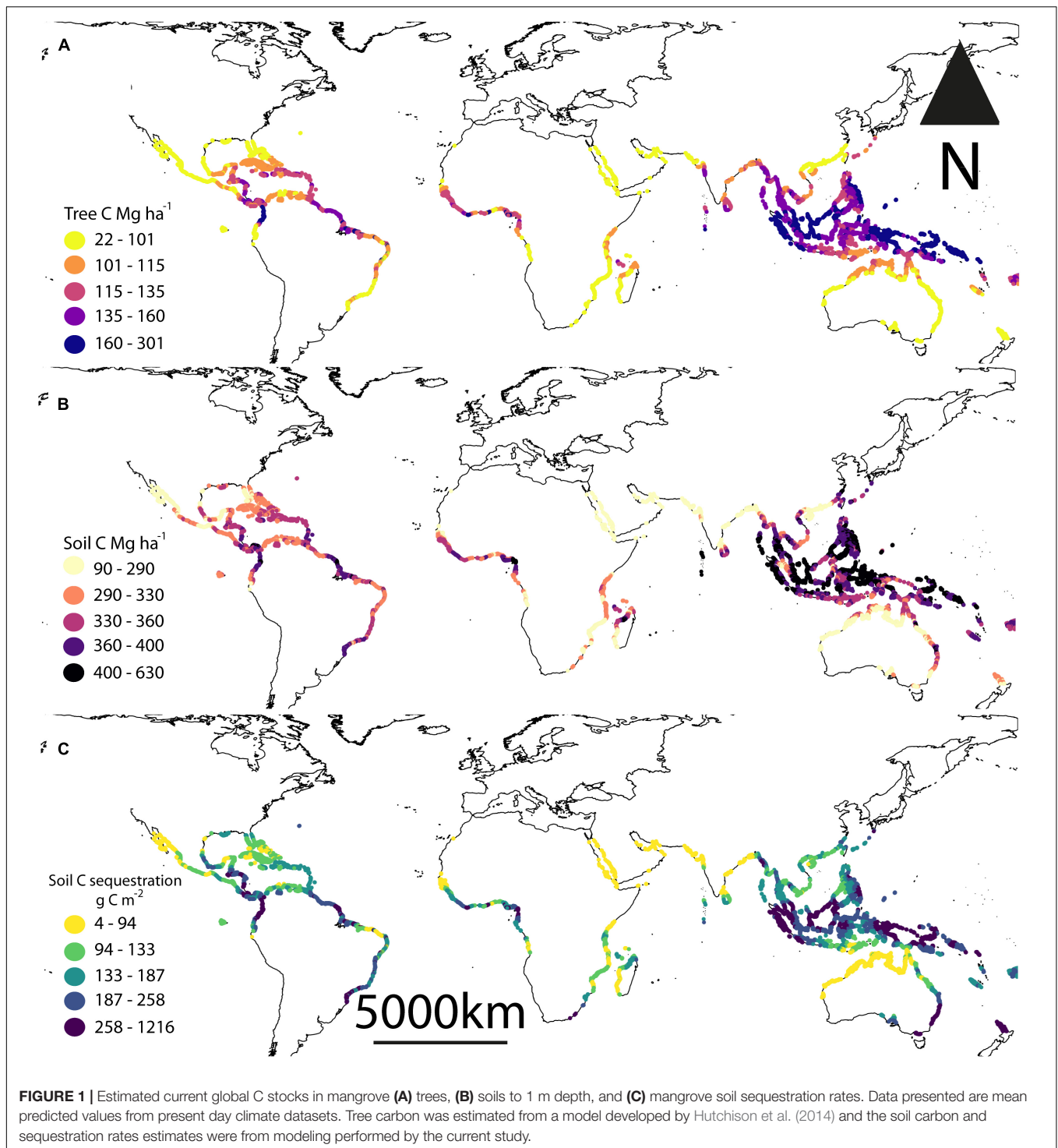
The literature search resulted in 785 data points of soil C₁₀₀ stocks from 87 individual studies conducted in 44 countries and 105 data points of soil C sequestration rates (CSR) from 31 individual studies in 17 countries (Supplementary Datasets 1, 2). Data points were available for seven out of the top ten countries reported by Sanderman et al. (2018) to hold the largest mangrove areas. Papua New Guinea, Myanmar and Cuba were the only countries in this list that lacked data.

Linear modeling only captured 27% of the variation in the soil C stocks (C₁₀₀) data [Regression: $F_{(3, 635)} = 79.21$, $p < 0.01$, $R^2 = 0.27$, standardized to 1 m depth], whereas random forest modeling captured over double that variation ($R^2 = 65\%$). The most important predictor was precipitation of the coldest quarter, which when dropped, accounted for 17.15% increase in the model's mean squared error (MSE, Supplementary Figure 1A). The final model selected to predict soil C₁₀₀ stocks was the random forest model as cross validation revealed it outperformed

the linear model in making out of sample predictions (CV Random forest: $R^2 = 0.65$, RMSE = 98.53 Mg C ha⁻¹; CV Linear model: $R^2 = 0.32$, RMSE = log10(0.24) Mg C ha⁻¹). Inclusion of tidal range and river discharge did not improve model performance (CV Random forest: $R^2 = 0.65$, RMSE = 98.85 Mg C ha⁻¹). The linear model captured 45% of the variation in the CSR data [Regression: $F_{(2, 91)} = 13.89$, $p < 0.01$, $R^2 = 0.45$], whereas random forest modeling captured less of the variation in CSR ($R^2 = 31\%$). However, the random forest model outperformed the linear model in making out of sample predictions (CV Random forest: $R^2 = 0.69$, RMSE = 113.44 g C m² yr⁻¹; Linear model: $R^2 = 0.46$, RMSE = log10(0.30) g C m² yr⁻¹). Therefore, the random forest model was selected to predict CSR. The most important predictor was precipitation of the wettest month, which accounted for a 7.64% increase in the model MSE (Supplementary Figure 1B).

We estimated mean per hectare total C stocks (biomass + soil) of 472.7 ± 56.4 Mg C (mean ± 1 standard error). The highest per hectare total C stocks were around Southeast Asia, particularly Indonesia and the Philippines (Figures 1A,B). Indonesia alone accounted for almost a quarter of current global C stocks ($24.27 \pm 0.61\%$), while the top 5 mangrove holding countries (Indonesia, Australia, the Philippines, Brazil and Mexico) held > 50% of the world's mangrove C stocks (Table 1). Similar to C stocks, the highest CSR were found in Southeast Asia (Figure 1C). The median predicted soil sequestration rate was 172.5 C m² yr⁻¹ (95% confidence interval: 101.4 – 321.7 C m² yr⁻¹). Indonesia again accounted for the majority of global annual mangrove CSR ($23.72 \pm 0.09\%$, Table 2).

When aggregated by country, the changes in total C stocks were spatially heterogeneous for both climate scenarios (SSP245 and SSP585). Under the business as usual scenario, reductions in total C stocks were predicted in countries that saw declines in precipitation. Decreases in precipitation of the wettest quarter (Binomial GLM: SE = 0.003, $p = 0.01$, Figure 2A) and the wettest month (Binomial GLM: SE = 0.001, $p = 0.01$, Figure 2B) were significant predictors of declines in countries' total C stocks. Egypt, Taiwan and Myanmar were predicted to have the three greatest reductions in precipitation in the wettest month of the year (-197.76 , -172.58 , and -166.66 mm, respectively) and wettest quarter of the year (-446.83 , -224.82 , and -576.60 mm, respectively). Under a high-end scenario (SSP585), it was an elevation in mean temperature or temperature ranges that caused the greatest reduction in C stocks. Countries forecast to experience significant increases in temperature seasonality (Binomial GLM: SE = 0.43, $p = 0.02$, Figure 2C) and higher mean annual temperatures (Binomial GLM: SE = 0.08, $p = 0.01$, Figure 2D) were also predicted to have diminished C stocks by 2095. Qatar, Bahrain and Sudan were predicted to have the three greatest changes in temperature seasonality (1.14 , 1.08 , and 0.94°C , respectively), with New Zealand, South Africa and Morocco experiencing the greatest increases in mean annual temperatures (7.77 , 5.07 , and 4.25°C , respectively). Changes in CSR were spatially heterogeneous and declines under scenario SSP245 were experienced in countries with predicted decreases in mean temperatures of the wettest



quarter of the year (Binomial GLM: SE = 0.18, $p = 0.05$, Figure 2E).

Global emissions from mangrove deforestation from 1980 to 2000 were more than three-times higher than those estimated from 2000 onward (Figure 3). Annual rates of mangrove deforestation dropped from 0.99% in the 1980's to 0.83% from in the 1990's, resulting in global emissions of 193.2 ± 44.4 Tg

CO₂e yr⁻¹ and 149.6 ± 33.3 Tg CO₂e yr⁻¹, respectively (Figures 3A,B). Emissions then dropped to 8.8 ± 2.0 Tg CO₂e yr⁻¹ (0.24% annual deforestation) between 2000 and 2010 (Figure 3C). To put that value into perspective, annual emissions from mangrove deforestation from 2000 to 2010 were 5.44–11.97% of total present day CSR. If countries continue current rates of mangrove deforestation (global average of 0.19%) from

TABLE 1 | Mean \pm 2 standard errors mangrove C stocks held by the 20 most mangrove-rich countries, and their forecasted gains under two climate scenarios (SSP245 and SSP585) based on bias-corrected and means-weighted forecasted climate data.

Country	Current total stocks (Tg C)	% of global total	Global cumulative%	SSP245		SSP585	
				Potential total stock change (Tg C)	% Of total country change	Potential total stock change (Tg C)	% of total country change
Indonesia	1,099.24 \pm 103.77	24.27 \pm 0.61	24.27 \pm 0.61	123.67 \pm 80.57	11.25 \pm 7.33	119.76 \pm 84.06	10.89 \pm 7.65
Australia	406.78 \pm 56.65	8.93 \pm 0.18	33.20 \pm 1.04	28.31 \pm 43.72*	6.96 \pm 10.75	41.61 \pm 47.65*	10.23 \pm 11.71
Philippines	325.13 \pm 30.13	7.18 \pm 0.19	40.38 \pm 1.66	18.72 \pm 22.41*	5.76 \pm 6.89	21.84 \pm 24.36*	6.72 \pm 7.49
Brazil	265.59 \pm 32.94	5.84 \pm 0.03	46.22 \pm 2.25	11.36 \pm 23.72*	4.28 \pm 8.93	8.64 \pm 24.24*	3.25 \pm 9.13
Mexico	174.14 \pm 26.21	3.82 \pm 0.12	50.04 \pm 2.72	8.83 \pm 18.63*	5.07 \pm 10.70	10.70 \pm 20.45*	6.15 \pm 11.75
Malaysia	170.47 \pm 16.66	3.76 \pm 0.08	53.80 \pm 3.27	20.48 \pm 12.54	12.01 \pm 7.35	18.61 \pm 13.01	10.92 \pm 7.63
Myanmar	154.59 \pm 33.68	3.36 \pm 0.34	57.16 \pm 3.48	-7.98 \pm 21.32*	-5.16 \pm 13.79	-3.55 \pm 21.73*	-2.30 \pm 14.06
Papua New Guinea	143.14 \pm 14.80	3.16 \pm 0.05	60.32 \pm 3.74	9.44 \pm 11.46*	6.60 \pm 8.01	13.46 \pm 11.92	9.40 \pm 8.33
Cuba	135.15 \pm 13.29	2.98 \pm 0.06	63.30 \pm 4.06	19.37 \pm 11.16	14.33 \pm 8.25	20.28 \pm 13.20	15.00 \pm 9.77
Nigeria	96.81 \pm 10.66	2.13 \pm 0.02	65.44 \pm 4.41	10.06 \pm 7.89	10.39 \pm 8.15	10.32 \pm 8.22	10.66 \pm 8.49
Thailand	94.27 \pm 9.37	2.08 \pm 0.04	67.52 \pm 4.79	-2.46 \pm 6.94*	-2.61 \pm 7.36	-3.67 \pm 7.59*	-3.89 \pm 8.05
Guinea-Bissau	92.21 \pm 12.75	2.02 \pm 0.03	69.54 \pm 5.14	2.18 \pm 9.89*	2.36 \pm 10.72	6.20 \pm 10.13*	6.73 \pm 10.98
India	87.16 \pm 11.72	1.92 \pm 0.03	71.45 \pm 5.47	-1.20 \pm 8.91*	-1.37 \pm 10.22	2.70 \pm 9.63*	3.10 \pm 11.04
Madagascar	82.27 \pm 11.22	1.81 \pm 0.03	73.27 \pm 5.76	-0.03 \pm 7.70*	-0.03 \pm 9.36	0.81 \pm 7.77*	0.98 \pm 9.44
United States	69.20 \pm 8.55	1.52 \pm 0.00	74.79 \pm 6.05	6.54 \pm 6.84*	9.45 \pm 9.88	9.94 \pm 7.75*	14.37 \pm 11.20
Mozambique	68.76 \pm 8.78	1.51 \pm 0.01	76.30 \pm 6.33	3.62 \pm 6.27*	5.26 \pm 9.12	4.59 \pm 6.82*	6.68 \pm 9.91
Colombia	68.08 \pm 12.23	1.49 \pm 0.09	77.79 \pm 6.52	1.17 \pm 8.78*	1.73 \pm 12.89	-1.07 \pm 8.53*	-1.57 \pm 12.53
Vietnam	61.15 \pm 6.74	1.35 \pm 0.01	79.14 \pm 6.72	-1.58 \pm 5.20*	-2.58 \pm 8.51	-0.23 \pm 5.61*	-0.37 \pm 9.17
Venezuela	61.10 \pm 7.26	1.35 \pm 0.01	80.48 \pm 6.93	2.50 \pm 5.44*	4.10 \pm 8.91	0.28 \pm 5.87*	0.45 \pm 9.61
Solomon Is.	55.98 \pm 5.74	1.23 \pm 0.02	81.72 \pm 7.16	2.87 \pm 4.78*	5.13 \pm 8.55	3.54 \pm 5.01*	6.32 \pm 8.95

Negative values imply losses in carbon, * denotes gains, losses or no change may be predicted.

2012 to 2095, a total of 678.50 ± 151.32 Tg CO₂e will be emitted due to mangrove deforestation, equivalent to mean global emissions of 8.18 ± 1.83 Tg CO₂e yr⁻¹. From 2012 to 2095, the top 23 emitting countries could account for over 90% of predicted global emissions from mangrove deforestation (Supplementary Table 1), with four countries (Indonesia, Brazil, Papua New Guinea and Malaysia) accounting for over 50% of all future emissions (Supplementary Table 2).

Our projections showed that, globally, increases in total C stocks (biomass + soil) induced by climate change would exceed emissions from mangrove deforestation between 2012 and 2095 (Table 3). Under a “business as usual” climate scenario these net gains represent an increase of $7.05 \pm 7.89\%$ (SSP245) or $7.71 \pm 9.47\%$ under a high-end scenario (SSP585) of present day global total C stocks. Total global losses from mangrove deforestation from 2012 to 2095 (Table 1) were estimated to be $61.4 \pm 10.1\%$ (SSP245) or $55.6 \pm 9.1\%$ (SSP585) of the potential gains in C stocks due to climate change. In contrast, CSR were forecast to decline by $2.60 \pm 3.57\%$ under scenario SSP245 and by $6.44 \pm 3.63\%$ under scenario SSP585 (Table 1).

DISCUSSION

Our study predicted a global net increase in mangrove C stocks under two climate projections (SSP245 and SSP585). Predicted climate change in Mainland Southeast Asia and southern Brazil

resulted in lower C stocks, whilst higher C stocks were predicted in the Caribbean, the Malay Archipelago, Australia, and West and East Africa (Supplementary Figure 2). Our results identify particularly mangrove C rich countries where significant gains will occur and can reinforce the value of mangroves as a practical tool for offsetting emissions to national governments. Under a “business as usual” scenario (SSP245), Indonesia, Malaysia, Cuba and Nigeria, all of which are currently in the top 10 mangrove holding countries (Hamilton and Casey, 2016), could hold > 10% higher C stocks than at present (Table 2). Under the high emissions scenario (SSP585), these countries plus the United States and Australia would have > 10% higher total C stocks (Table 2). These nations’ C stocks would also see significant benefit from reduced mangrove deforestation. The Malay Archipelago in particular, could emit 774.1 Tg CO₂e by 2100 from mangrove clearing and conversion to agri/aquaculture (Adame et al., 2021). Projections of C stocks in the current study are only to 1 m soil depth and are likely to be underestimates. Global mangrove soil C stocks to 2 m soil depth have been estimated to be almost double that of 1 m depth (Sanderman et al., 2018). Hence emissions from mangrove deforestation reported here (678.50 ± 151.32 Tg CO₂e from 2012 to 2095) are also likely to be underestimated. Other studies have projected up to 3,392 Tg CO₂e emissions by 2100, with 712 Tg CO₂e being lost in the West Coral Triangle alone (Adame et al., 2021).

Despite an overall gain in C stocks, a likely decrease in global soil sequestration rates (CSR) was predicted under both climate projections (SSP245 and SSP585), with a different spatial

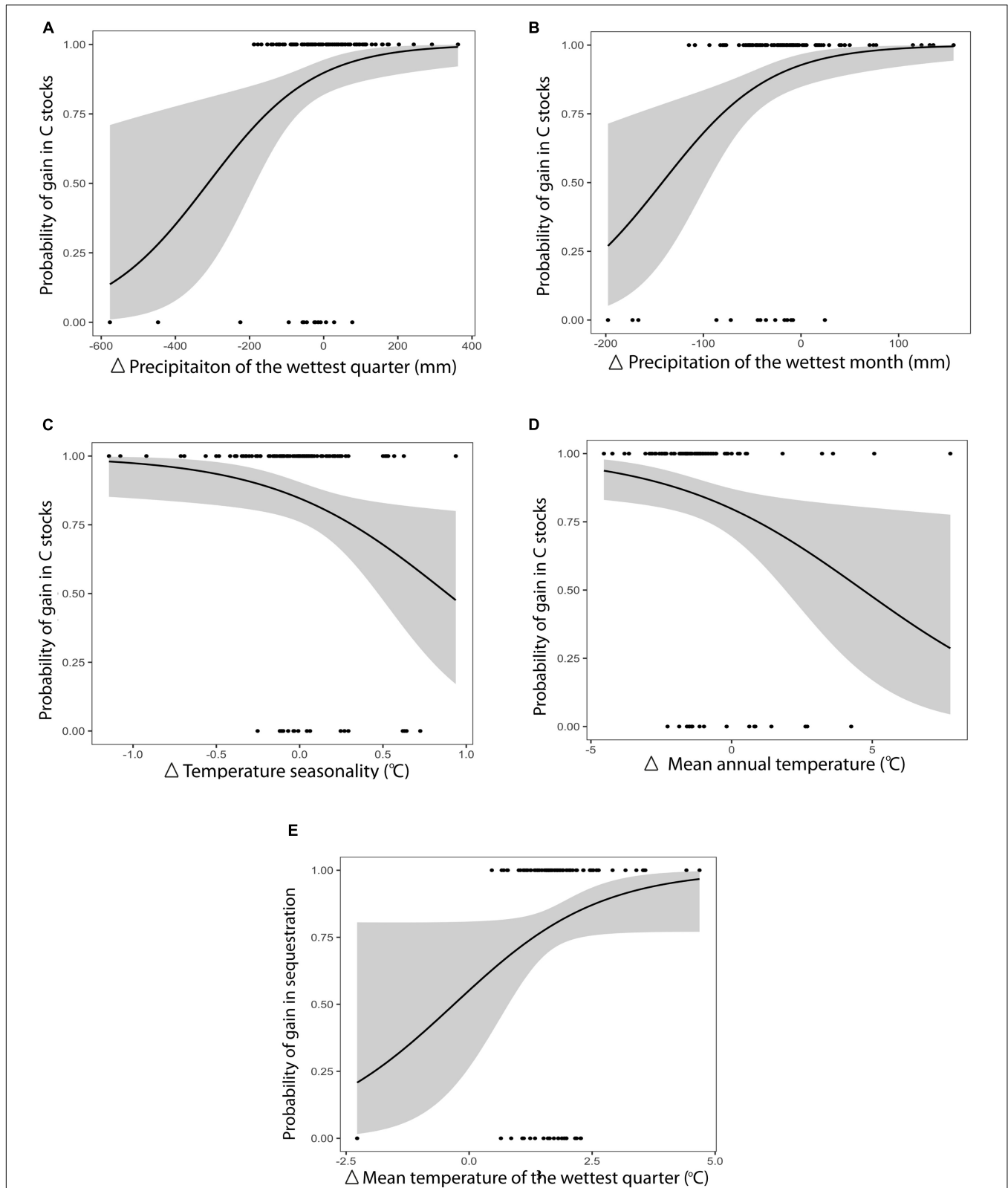
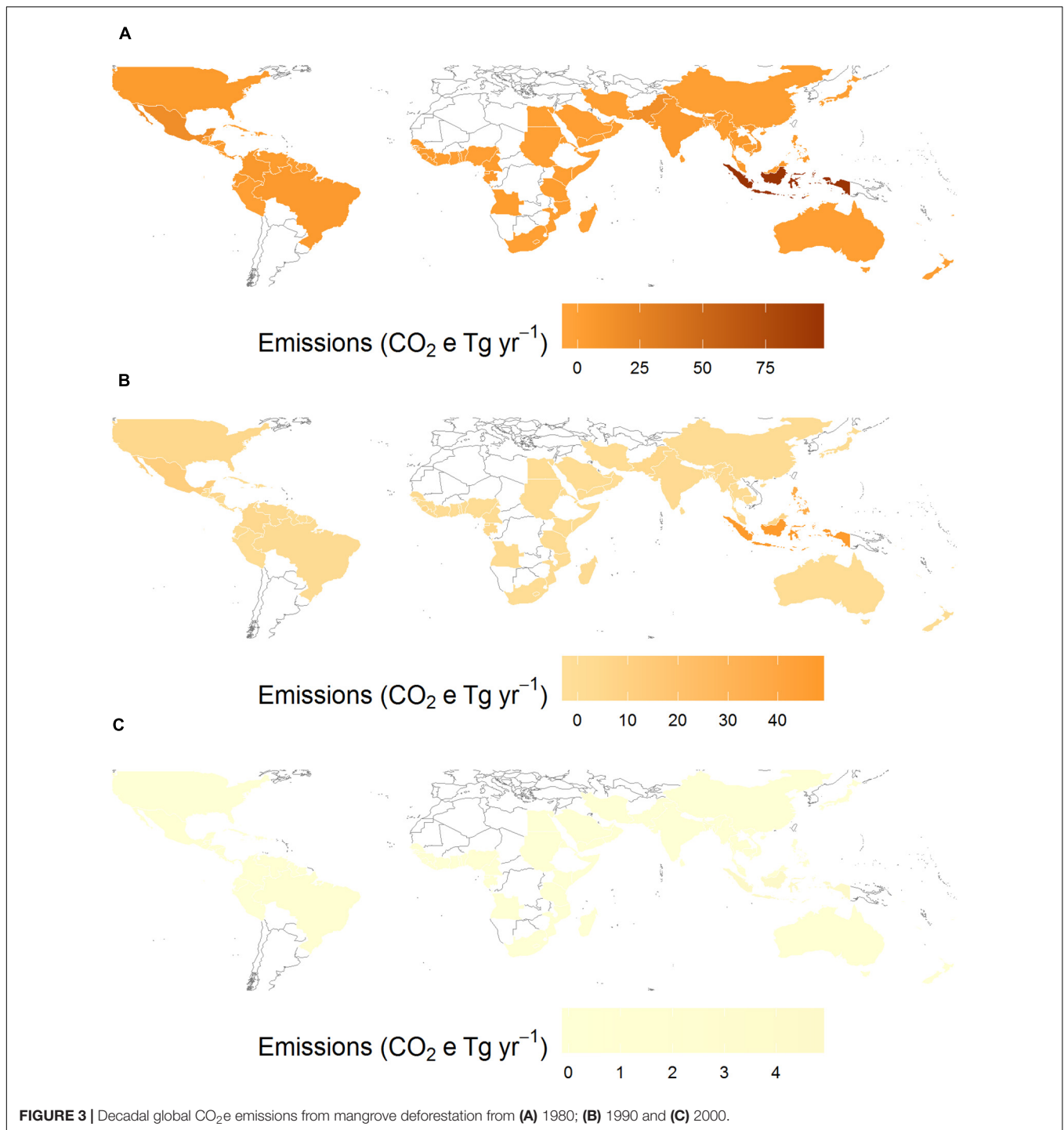


FIGURE 2 | Probability of countries experiencing gains in mangrove C stocks with change in twenty-first century climate. **(A,B)** Refer to significant differences under the “business as usual” scenario (SSP245), **(C,D)** refer to significant differences under the high emissions scenario (SSP585) and **(E)** refers to sequestration rates. Temperature seasonality refers to the annual variation of temperature. Black lines are the mean probability, while shaded areas represent 95% confidence intervals.



distribution to predicted gains in C stocks; depressed CSR were mainly forecast in the Malay Archipelago and the Southern Caribbean (**Supplementary Figure 2**). More than half of the top 20 mangrove holding countries would experience decreases in CSR. Some of these losses will be significant, Panama's annual CSR could reduce by $20.93 \pm 2.83\%$ under SSP245 or over a quarter ($25.77 \pm 2.92\%$) under SSP585 (**Table 2**). These reductions may be compounded by emissions from erosion,

which is expected to be the main driver for mangrove losses on the Caribbean coast of Panama by 2100 (Adame et al., 2021). Malaysia and Myanmar could experience total reductions in CSR by 17.43 and 21.96%, respectively (**Table 2**). These two countries' future emissions from mangrove losses are also expected to be largely driven by land-use change to agri/aquaculture (Adame et al., 2021) and would exacerbate the climate driven reductions in CSR. On a more positive note, even though overall reductions

TABLE 2 | Mean \pm 2 standard errors mangrove C sequestration rates of the 20 highest sequestering countries, and their forecasted gains under two climate scenarios (SSP245 and SSP585) based on bias-corrected and means-weighted forecasted climate data.

Country	Current total soil sequestration (Tg C yr ⁻¹)	% Of global total	Global cumulative%	SSP245		SSP585	
				Potential change in soil sequestration (Tg C yr ⁻¹)	% Of total country change	Potential change in soil sequestration (Tg C yr ⁻¹)	% Of total country change
Indonesia	4.34 \pm 0.19	23.72 \pm 0.09	23.72 \pm 0.09	-0.08 \pm 0.14*	-1.95 \pm 3.29	-0.37 \pm 0.14	-8.55 \pm 3.26
Australia	1.43 \pm 0.08	7.80 \pm 0.04	31.51 \pm 0.15	0.03 \pm 0.06*	2.29 \pm 4.06	0.05 \pm 0.06*	3.44 \pm 4.18
Philippines	1.20 \pm 0.06	6.56 \pm 0.01	38.06 \pm 0.23	-0.08 \pm 0.04*	-6.53 \pm 3.35	-0.09 \pm 0.04	-7.55 \pm 3.38
Brazil	1.03 \pm 0.05	5.62 \pm 0.00	43.69 \pm 0.30	0.02 \pm 0.04*	1.53 \pm 3.71	-0.08 \pm 0.04	-8.06 \pm 3.57
Myanmar	0.94 \pm 0.05	5.14 \pm 0.05	48.83 \pm 0.32	-0.13 \pm 0.04	-13.52 \pm 4.12	-0.17 \pm 0.04	-17.96 \pm 4.13
Malaysia	0.80 \pm 0.04	4.36 \pm 0.01	53.19 \pm 0.34	-0.14 \pm 0.03	-17.12 \pm 3.15	-0.17 \pm 0.02	-21.43 \pm 3.13
Mexico	0.68 \pm 0.04	3.71 \pm 0.02	56.89 \pm 0.35	-0.08 \pm 0.03	-11.74 \pm 3.81	-0.09 \pm 0.03	-12.78 \pm 4.15
Papua New Guinea	0.62 \pm 0.03	3.38 \pm 0.00	60.27 \pm 0.35	0.06 \pm 0.02	10.36 \pm 3.60	0.06 \pm 0.02	8.98 \pm 3.67
Colombia	0.43 \pm 0.02	2.33 \pm 0.03	62.59 \pm 0.37	0.01 \pm 0.01*	2.39 \pm 2.61	-0.01 \pm 0.01*	-1.26 \pm 2.63
Nigeria	0.42 \pm 0.02	2.30 \pm 0.01	64.90 \pm 0.38	-0.04 \pm 0.02	-9.28 \pm 3.57	-0.08 \pm 0.01	-19.14 \pm 3.46
Cuba	0.41 \pm 0.02	2.24 \pm 0.01	67.14 \pm 0.40	0.07 \pm 0.01	17.82 \pm 3.59	0.05 \pm 0.02	11.88 \pm 3.92
India	0.36 \pm 0.02	1.99 \pm 0.02	69.13 \pm 0.40	-0.02 \pm 0.02*	-5.29 \pm 4.47	0.00 \pm 0.02*	-0.02 \pm 4.65
Thailand	0.36 \pm 0.02	1.96 \pm 0.00	71.10 \pm 0.41	-0.01 \pm 0.01	-1.53 \pm 3.42	-0.02 \pm 0.01	-6.67 \pm 3.47
Guinea-Bissau	0.32 \pm 0.02	1.75 \pm 0.01	72.84 \pm 0.41	0.09 \pm 0.02	27.51 \pm 5.20	0.08 \pm 0.02	24.73 \pm 5.09
Madagascar	0.28 \pm 0.01	1.56 \pm 0.01	74.40 \pm 0.41	0.00 \pm 0.01*	-0.72 \pm 4.33	-0.03 \pm 0.01	-10.99 \pm 4.33
Guinea	0.28 \pm 0.02	1.52 \pm 0.02	75.92 \pm 0.43	0.00 \pm 0.01*	1.66 \pm 3.44	0.01 \pm 0.01*	2.65 \pm 3.80
Mozambique	0.25 \pm 0.01	1.35 \pm 0.01	77.27 \pm 0.44	-0.03 \pm 0.01	-10.24 \pm 3.33	-0.01 \pm 0.01*	-5.73 \pm 3.84
United States	0.24 \pm 0.01	1.34 \pm 0.01	78.61 \pm 0.44	0.01 \pm 0.01*	3.57 \pm 4.13	-0.01 \pm 0.01*	-2.98 \pm 4.14
Sierra Leone	0.24 \pm 0.01	1.29 \pm 0.02	79.89 \pm 0.46	-0.01 \pm 0.01*	-2.71 \pm 3.20	0.01 \pm 0.01*	2.93 \pm 3.66
Panama	0.23 \pm 0.01	1.27 \pm 0.00	81.17 \pm 0.47	-0.05 \pm 0.01	-20.93 \pm 2.83	-0.06 \pm 0.01	-25.77 \pm 2.92

Negative values imply declines in sequestration rates, * denotes gains, losses or no change may be predicted.

in global CSR were predicted, our study suggests global mangrove CSR has previously been underestimated. Our estimate of CSR (18.3 Tg C yr⁻¹) is more than double that of the most recent previous estimate (Alongi, 2020), which used the same global mangrove extent as us (8.6 Tg C yr⁻¹, mangrove extent: \sim 83,000 km²). Alongi (2020) used a median CSR value (103 gC m² a⁻¹) obtained from a literature study and multiplied this by the global coverage as opposed to our spatial modeling approach. The approach used by Alongi (2020) assumed all mangroves will have the same CSR, even though it has been shown to vary widely (1.0–1,722 gC m² a⁻¹) (Alongi, 2020). When global mangrove extent is standardized to 83,000 km², our CSR calculation is higher than most previous estimates (range: 8.3–18.8 Tg C yr⁻¹) (Chmura et al., 2003; Bouillon et al., 2008; McLeod et al., 2011; Breithaupt et al., 2012; Alongi, 2020). Mangroves have the ability to increase soil elevation, thus increasing soil C stores and, up to a point, keep pace with sea level rise (Ezcurra et al., 2016). Coastal wetlands that experienced rapid relative sea level rise (RSLR) during recent millennia have significantly greater soil organic carbon density than coastlines where relative sea level was stable (Rogers et al., 2019) and RSLR is considered to be an important driver in predicted increases in wetland soil organic carbon accumulation rates (Wang et al., 2020). Even though sediment accretion and increased surface elevation may reduce coastal flooding as a result of climate change driven sea level rise, accretion rates in mangroves are not likely to

compensate for increases in sea level of greater than 6.1 mm yr⁻¹ (Saintilan et al., 2020). As a result of the approach we used, we have been able to capture spatial variation in CSR and produce country-specific estimates, including those where CSR data are currently unavailable. Generally, model predictions have been shown to vary considerably from the IPCC's default estimates of greenhouse gas inventories, likely as a result of applying model predictions to locations where *in situ* measurements have not been taken, as opposed to applying a mean across all global mangroves.

Recent work has suggested higher temperatures would have “minimal impact” on organic carbon stocks (Macreadie et al., 2019). Our study showed that, under a high-emissions scenario, temperature increases would be high enough in some countries to impact national scale total C stocks and CSR. Under a business as usual scenario, temperature increases were not significant enough to detriment national scale mangrove C stocks. Peak photosynthesis productivity reduces above 38°C and increased temperatures would also increase evaporation rates which will in turn increase salinity stress (Clough and Rews, 1982). Our modeling showed, under SSP585, mean annual air temperatures could increase from 29.7 to 32.5°C, while maximum temperature of the warmest month could be as high as 44.2°C. Increases in mean temperatures and their annual variability, under the high-end scenario (SSP585), significantly increases the probability of a country experiencing losses in mangrove C stocks

TABLE 3 | Mean \pm 2 standard errors of the net effects of climate change and mangrove deforestation on total global mangrove carbon stocks and sequestration rates.

Global total stocks (Tg C)						
	Current day		Forecasted		Losses from deforestation	Net change
	Tree C stocks	Soil C stocks	Tree C stocks	Soil C stocks		
SSP245	1246.9 ± 427.1	3296.1 ± 114.8	1382.0 ± 450.6	3481.4 ± 121.3	196.7 ± 32.3	123.7 ± 1146.1
SSP585			1439.8 ± 502.5	3457.0 ± 125.6		157.1 ± 1202.3
Global Sequestration Rates (Tg C yr ⁻¹)						
	Current day	Forecasted	Net change			
SSP245	18.3 ± 0.9	17.8 ± 0.9	−0.5 ± 1.8			
SSP585		17.1 ± 0.9	−1.2 ± 1.8			

Forecasted stocks and sequestration rates represent global estimates for the year 2095. Soil C stocks are estimated to 1 m soil depth. Net change is forecasted stocks/sequestration rates minus current day stocks/sequestration rates minus losses from deforestation.

(Figures 2C,D). This is likely as a result of our study giving mangrove C stocks from arid regions at the climatic extremes of global mangrove distribution greater representation than previous modeling efforts. Apart from Sanderman et al. (2018), data from arid regions such as those of North Africa and the Arabian Peninsula, where mangroves have low organic carbon stocks and CSR (Eid and Shaltout, 2016; Almahasheer et al., 2017; Schile et al., 2017; Chatting et al., 2020), have not been incorporated into global models (Jardine and Siikamäki, 2014; Rovai et al., 2018).

Model predictions that global C stocks will increase while CSR will decrease may seem contradictory. However, total C stocks here are only quantified for the top 1 m of soil depth, in effect a measure of soil C density, with any change being the balance of gain by sequestration and losses by erosion and mineralization. Hence modeled C stocks may increase if climatic conditions result in increased soil C density, even if CSR declines. Over and above this effect, stocks throughout the whole soil depth profile could still increase substantially over time as more soil is accreted, even with lower sequestration rates (Alongi, 2012, 2015). Differences in estimates of global total mangrove C stocks and CSR largely arise from different methods calculating global mangrove extent (Breithaupt et al., 2012; Hamilton and Friess, 2018; Sanderman et al., 2018; Alongi, 2020). When projecting soil C stocks globally, our approach assumed pixels either had 100 or 0% mangrove coverage, similarly to Sanderman et al. (2018). However, this is unlike Hamilton and Friess (2018), where mangrove coverage was estimated to range from 0 to 100% per pixel. Global CSR estimates have ranged from 8.6 to 38.0 Tg C yr⁻¹ (Twilley et al., 1992; Jennerjahn and Ittekkot, 2002; Chmura et al., 2003; Duarte et al., 2005; Bouillon et al., 2008; Alongi, 2009, 2020; Breithaupt et al., 2012), where differences are mainly due to varying global mangrove extents used in calculation. Additional uncertainties arise when estimating change in C stocks and CSR at the end of the twenty first century. Our study assumed constant mangrove coverage from 2012 to 2095, however, on a global scale, mangroves in temperate regions have been forecast to expand to higher latitudes (Saintilan et al., 2014). Also, the interaction between sea level rise and coastal

human development will likely influence mangroves ability to migrate landward in response to sea level rise (Lovelock and Reef, 2020). Moreover, by subtracting future from present day C stocks and CSR and not incorporating estimated mangrove deforestation rates, this study assumed a constant rate of change from 2012 to 2095 and will lead to overestimates of C stocks and CSR. While this approach may be an oversimplification of the complex process by which mangroves sequester and store C, calculations of future estimates apply the same logic as has been performed for numerous estimates of present day C stocks (Hutchison et al., 2014; Hamilton and Friess, 2018; Rovai et al., 2018; Sanderman et al., 2018).

In addition to higher soil sequestration rates, our estimates of C emissions from mangrove deforestation between 2000 and 2010 are at the lower end of the 6.60–29.80 Tg CO₂e yr⁻¹ previously reported (Hamilton and Friess, 2018; Sanderman et al., 2018). A combination of higher global soil C sequestration rates than previously reported, coupled with comparatively low emissions estimates associated with mangrove deforestation (0.24% annually), largely due to significant reductions in deforestation rates, means that C emissions from mangrove deforestation are now < 12% of global annual soil sequestration rates. By contrast, in the 1980's global emissions from mangrove deforestation were almost three-times global mangrove annual soil C sequestration (Figure 3). Despite the great uncertainties surrounding historical estimates of mangrove deforestation rates (Friess and Webb, 2014), this decrease since the 1980's is a noteworthy success for mangrove conservation globally. Moreover, at a national level, our estimates show that, for many countries, rates of C sequestration in mangrove soils could be higher than previously thought, so that governments may choose to place greater value on their mangroves as a means of offsetting emissions. The outcomes of this modeling study demonstrate the positive effect of future mangrove protection and restoration on national C budgets, providing governments useful data on their mangrove soil sequestration rates in comparison to likely emissions and C stocks, which have not previously been available. Reducing emissions from mangrove deforestation is an achievable way to help countries

meet their Nationally Determined Contributions (NDC's) to the 2021 UN Climate Change Conference (COP26) and reach carbon neutrality. Indonesia has pledged almost 60% of their unconditional emissions reductions by 2030 to come from the forestry and other land use sector (Ministry of Environment and Forestry Directorate General of Climate Change, 2021). Globally, emissions from mangrove deforestation have been estimated to be as high as 19% of global total deforestation emissions (Pendelton et al., 2012) and blue carbon ecosystem restoration is estimated to be 3% of annual global fossil fuel emissions (Macreadie et al., 2021). Financing of mangrove conservation is a viable option for offsetting emissions where countries cannot directly reduce their own emissions (Zeng et al., 2021). Selling carbon credits gained from avoided mangrove deforestation in voluntary carbon markets has been shown to have similar returns on investment to investing in traditional asset classes (Cameron et al., 2019). Mangroves alone will not mitigate fully against climate change, however, their conservation can be used as a practical tool to facilitate countries moving toward carbon neutrality, as well as securing additional co-benefits through the enhancement of mangrove-derived ecosystem services.

DATA AVAILABILITY STATEMENT

The original contributions presented in the study are included in the article/**Supplementary Material**, further inquiries can be directed to the corresponding author/s.

AUTHOR CONTRIBUTIONS

MC, LL, MW, MWS, and IA-M conceived the study. MC and YSH performed all the modeling and statistical analyses. MC, LL, MW, MWS, HK, and IA-M wrote the manuscript draft. LL, MW, MWS, HK, and IA-M contributed to design of the work and critical evaluation of the manuscript during the extensive

drafting process. All authors helped write and edit the final version of the manuscript.

FUNDING

MC, LL, MW, MWS, IA-M, HK, and YSH were supported by the Qatar National Research Fund, National Priorities Research Program (NPRP) (Grant No. 7-1302-1-242), "Ecological processes underlying ecosystem function in arid mangroves."

ACKNOWLEDGMENTS

MC would like to thank the Environmental Science Centre at Qatar University for their continued support of his research endeavors.

SUPPLEMENTARY MATERIAL

The Supplementary Material for this article can be found online at: <https://www.frontiersin.org/articles/10.3389/fmars.2022.781876/full#supplementary-material>

Supplementary Figure 1 | Random forest variable importance and their % increase in MSE. These values refer to the % increase in the model mean squared error (MSE) when each predictor is excluded from the dataset for **(A)** soil C stocks and **(B)** soil C sequestration rates.

Supplementary Figure 2 | Estimated change in global C stocks in mangrove **(A)** trees and **(B)** soils, and sequestration rates **(C)** by the year 2095. As predicted from mean values from means weighted forecast climate datasets. Tree C was estimated from the predictive model developed by Hutchison et al. (2014), and the soil C and sequestration estimates were from modeling by the current study.

Supplementary Data Sheet 1 | Secondary literature data of soil carbon used in modeling analysis.

Supplementary Data Sheet 2 | Secondary literature data of soil sequestration rates used in modeling analysis.

REFERENCES

- Adame, M. F., Brown, C. J., Bejarano, M., Herrera-Silveira, J. A., Ezcurra, P., Kauffman, J. B., et al. (2018). The undervalued contribution of mangrove protection in Mexico to carbon emission targets. *Conserv. Lett.* 11:e12445. doi: 10.1111/conl.12445
- Adame, M. F., Connolly, R. M., Turschwell, M. P., Lovelock, C. E., Fatoyinbo, T., Lagomasino, D., et al. (2021). Future carbon emissions from global mangrove forest loss. *Glob. Chang. Biol.* 27, 2856–2866. doi: 10.1111/gcb.15571
- Almahsheer, H., Serrano, O., Duarte, C. M., Arias-Ortiz, A., Masque, P., and Irigoien, X. (2017). Low Carbon sink capacity of Red Sea mangroves. *Sci. Rep.* 7:9700. doi: 10.1038/s41598-017-10424-9
- Alongi, D. M. (2002). Present state and future of the world's mangrove forests. *Environ. Conserv.* 29, 331–349. doi: 10.1017/S0376892902000231
- Alongi, D. M. (2009). *The Energetics of Mangrove Forests*. New York: Springer Science & Business Media, doi: 10.1007/978-1-4020-4271-3
- Alongi, D. M. (2012). Carbon sequestration in mangrove forests. *Carbon Manag.* 3, 313–322. doi: 10.4155/cmt.12.20
- Alongi, D. M. (2015). The Impact of Climate Change on Mangrove Forests. *Curr. Clim. Chang. Rep.* 1, 30–39. doi: 10.1007/s40641-015-0002-x
- Alongi, D. M. (2020). Global Significance of Mangrove Blue Carbon in Climate Change Mitigation (Version 1). *Science* 2:57. doi: 10.3390/sci2030057
- Atwood, T. B., Connolly, R. M., Almahsheer, H., Carnell, P. E., Duarte, C. M., Lewis, C. J. E., et al. (2017). Global patterns in mangrove soil carbon stocks and losses. *Nat. Clim. Chang.* 7, 523–528. doi: 10.1038/ncclimate3326
- Blankespoor, B., Dasgupta, S., and Laplante, B. (2014). Sea level rise and coastal wetlands. *Ambio* 43, 996–1005. doi: 10.17226/10590
- Bouillon, S., Borges, A. V., Castañeda-Moya, E., Diele, K., Dittmar, T., Duke, N. C., et al. (2008). Mangrove production and carbon sinks: a revision of global budget estimates. *Global Biogeochem. Cycles* 22, 1–12. doi: 10.1029/2007GB003052
- Breithaupt, J. L., Smoak, J. M., Smith, T. J., Sanders, C. J., and Hoare, A. (2012). Organic carbon burial rates in mangrove sediments: strengthening the global budget. *Global Biogeochem. Cycles* 26:GB3011. doi: 10.1029/2012GB004375
- Cameron, C., Hutley, L. B., Friess, D. A., and Brown, B. (2019). High greenhouse gas emissions mitigation benefits from mangrove rehabilitation in Sulawesi, Indonesia. *Ecosyst. Serv.* 40:101035. doi: 10.1016/j.ecoser.2019.101035
- Carrere, L., Lyard, F., Cancet, M., Guillot, A., and Roblou, L. (2013). FES 2012: a new global tidal model taking advantage of nearly 20 years of altimetry. *20 Years Prog. Radar Altimetry* 710:13.
- Chatting, M., Le Vay, L., Walton, M., Skov, M. W., Kennedy, H., Wilson, S., et al. (2020). Mangrove carbon stocks and biomass partitioning in an extreme environment. *Estuar. Coast. Shelf Sci.* 244:106940. doi: 10.1016/j.ecss.2020.106940

- Chmura, G. L., Anisfeld, S. C., Cahoon, D. R., and Lynch, J. C. (2003). Global carbon sequestration in tidal, saline wetland soils. *Global Biogeochem. Cycles* 17:1111. doi: 10.1029/2002gb001917
- Clough, B. F., and Rews, T. J. (1982). "Physiological Processes in Mangroves," in *Mangrove Ecosystems in Australia: Structure, Function and Management*, ed. B. F. Clough (Canberra: Australian Institute of Marine Science in Association with Australian Natural University Press), 195–300.
- Cooray, P. L. I. G. M., Kodikara, K. A. S., Kumara, M. P., Jayasinghe, U. I., Madarasinghe, S. K., Dahdouh-Guebas, F., et al. (2021). Climate and intertidal zonation drive variability in the carbon stocks of Sri Lankan mangrove forests. *Geoderma* 389:114929.
- Donato, D. C., Kauffman, J. B., Murdiyarso, D., Kurnianto, S., Stidham, M., and Kanninen, M. (2011). Mangroves among the most carbon-rich forests in the tropics. *Nat. Geosci.* 4, 293–297. doi: 10.1038/ngeo1123
- Duarte, C. M., Losada, I. J., Hendriks, I. E., Mazarrasa, I., and Marbà, N. (2013). The role of coastal plant communities for climate change mitigation and adaptation. *Nat. Clim. Chang.* 3, 961–968. doi: 10.1038/nclimate1970
- Duarte, C. M., Middelburg, J. J., and Caraco, N. (2005). Major role of marine vegetation on the oceanic carbon cycle. *Biogeosciences* 2, 1–8. doi: 10.5194/bg-2-1-2005
- Duke, N. C., Meynecke, J. O., Dittmann, S., Ellison, A. M., Anger, K., Berger, U., et al. (2007). A World Without Mangroves? *Science* 317, 41b–42b. doi: 10.1126/science.317.5834.41b
- Eid, E. M., and Shaltout, K. H. (2016). Distribution of soil organic carbon in the mangrove *Avicennia marina* (Forssk.) Vierh. along the Egyptian Red Sea Coast. *Reg. Stud. Mar. Sci.* 3, 76–82. doi: 10.1016/j.rsma.2015.05.006
- Ezcurra, P., Ezcurra, E., Garcillán, P. P., Costa, M. T., and Aburto-Oropeza, O. (2016). Coastal landforms and accumulation of mangrove peat increase carbon sequestration and storage. *Proc. Natl. Acad. Sci.* 113, 4404–4409. doi: 10.1073/pnas.1519774113
- FAO (2007). *The World's Mangroves 1980-2005*. Rome: FAO.
- Fekete, B. M., Vörösmarty, C. J., and Grabs, W. (2002). High-resolution fields of global runoff combining observed river discharge and simulated water balances. *Global Biogeochem. Cycles* 16, 15–11. doi: 10.1029/1999gb001254
- Fourqurean, J. W., Duarte, C. M., Kennedy, H., Marbà, N., Holmer, M., Mateo, M. A., et al. (2012). Seagrass ecosystems as a globally significant carbon stock. *Nat. Geosci.* 5, 505–509. doi: 10.1038/ngeo1477
- Friess, D. A., and Webb, E. L. (2014). Variability in mangrove change estimates and implications for the assessment of ecosystem service provision. *Glob. Ecol. Biogeogr.* 23, 715–725. doi: 10.1111/geb.12140
- Giorgi, F., Raffaele, F., and Coppola, E. (2019). The response of precipitation characteristics to global warming from climate projections. *Earth Syst. Dyn.* 10, 73–89. doi: 10.5194/esd-10-73-2019
- Giri, C., Ochieng, E., Tieszen, L. L., Zhu, Z., Singh, A., Loveland, T., et al. (2011). Status and distribution of mangrove forests of the world using earth observation satellite data. *Glob. Ecol. Biogeogr.* 20, 154–159. doi: 10.1111/j.1466-8238.2010.00584.x
- Hamilton, S., and Casey, D. (2016). Creation of a high spatiotemporal resolution global database of continuous mangrove forest cover. *Glob. Ecol. Biogeogr.* 25, 729–738.
- Hamilton, S. E., and Friess, D. A. (2018). Global carbon stocks and potential emissions due to mangrove deforestation from 2000 to 2012. *Nat. Clim. Chang.* 8, 240–244. doi: 10.1038/s41558-018-0090-4
- Hutchison, J., Manica, A., Swetnam, R., Balmford, A., and Spalding, M. (2014). Predicting global patterns in mangrove forest biomass. *Conserv. Lett.* 7, 233–240. doi: 10.1111/conl.12060
- Jardine, S. L., and Siikamäki, J. V. (2014). A global predictive model of carbon in mangrove soils. *Environ. Res. Lett.* 9:104013. doi: 10.1088/1748-9326/9/10/104013
- Jennerjahn, T. C., and Ittekkot, V. (2002). Relevance of mangroves for the production and deposition of organic matter along tropical continental margins. *Naturwissenschaften* 89, 23–30. doi: 10.1007/s00114-001-0283-x
- Kalnay, E., Kanamitsu, M., Kistler, R., Collins, W., Deaven, D., Gandin, L., et al. (1996). The NCEP/NCAR 40-year reanalysis project. *Bull. Am. Meteorol. Soc.* 77, 437–495. doi: 10.1175/1520-04771996077<0437:TNYRP>2.0.CO;2
- Kauffman, B. J., Arifanti, V. B., Hernández Trejo, H., Jesús García, M. D. C., Norfolk, J., Cifuentes, M., et al. (2017). The jumbo carbon footprint of a shrimp: carbon losses from mangrove deforestation. *Front. Ecol. Environ.* 15, 183–188. doi: 10.1002/fee.1482
- Kauffman, J. B., and Bhomia, R. K. (2017). Ecosystem carbon stocks of mangroves across broad environmental gradients in West-Central Africa: global and regional comparisons. *PLoS One* 12:e0187749. doi: 10.1371/journal.pone.0187749
- Kauffman, J. B., Heider, C., Norfolk, J., and Payton, F. (2014). Carbon stocks of intact mangroves and carbon emissions arising from their conversion in the Dominican Republic. *Ecol. Appl.* 24, 518–527. doi: 10.1890/13-0640.1
- Kock, N., and Lynn, G. S. (2012). Lateral collinearity and misleading results in variance-based SEM: an illustration and recommendations. *J. Assoc. Inf. Syst.* 13, 546–580. doi: 10.17705/1jais.00302
- Lang'at, J. K. S., Kairo, J. G., Mencuccini, M., Bouillon, S., Skov, M. W., Waldron, S., et al. (2014). Rapid losses of surface elevation following tree girdling and cutting in tropical mangroves. *PLoS One* 9:e0118334. doi: 10.1371/journal.pone.0107868
- Lovelock, C. E., and Reef, R. (2020). Variable Impacts of Climate Change on Blue Carbon. *One Earth* 3, 195–211. doi: 10.1016/j.oneear.2020.07.010
- Lovelock, C. E., Ruess, R. W., and Feller, I. C. (2011). Co2 efflux from cleared mangrove peat. *PLoS One* 6:e21279. doi: 10.1371/journal.pone.0021279
- Luo, M., Liu, T., Meng, F., Duan, Y., Frankl, A., Bao, A., et al. (2018). Comparing bias correction methods used in downscaling precipitation and temperature from regional climate models: a case study from the Kaidu River Basin in Western China. *Water* 10:1046. doi: 10.3390/w10081046
- Macreadie, P., Costa, M., Atwood, T., Friess, D., Kelleway, J., Kennedy, H., et al. (2021). Blue carbon as a natural climate solution. *Nat. Rev. Earth Environ.* 2, 826–839. doi: 10.1038/s43017-021-00224-1
- Macreadie, P. I., Anton, A., Raven, J. A., Beaumont, N., Connolly, R. M., Friess, D. A., et al. (2019). The future of Blue Carbon science. *Nat. Commun.* 10:3998. doi: 10.1038/s41467-019-11693-w
- Martin-Martin, A., Orduna-Malea, E., Thelwall, M., and Delgado López-Cózar, E. (2018). Google Scholar, Web of Science, and Scopus: a systematic comparison of citations in 252 subject categories. *J. Informetr.* 12, 1160–1177. doi: 10.1016/j.joi.2018.09.002
- Masih, A. (2019). "Application of Random Forest Algorithm to Predict the Atmospheric Concentration of NO2," in *Conference: 2019 Ural Symposium on Biomedical Engineering, Radioelectronics and Information Technology (USBEREIT)*, (Piscataway: IEEE), 252–255. doi: 10.1109/USBEREIT.2019.8736679
- McKee, K. L., Cahoon, D. R., and Feller, I. C. (2007). Caribbean mangroves adjust to rising sea level through biotic controls on change in soil elevation. *Glob. Ecol. Biogeogr.* 16, 545–556. doi: 10.1111/j.1466-8238.2007.00317.x
- McLeod, E., Chmura, G. L., Bouillon, S., Salm, R., Björk, M., Duarte, C. M., et al. (2011). A blueprint for blue carbon: toward an improved understanding of the role of vegetated coastal habitats in sequestering CO2. *Front. Ecol. Environ.* 9, 552–560. doi: 10.1890/110004
- Ministry of Environment and Forestry Directorate General of Climate Change (2021). *Updated Nationally Determined Contribution Republic of Indonesia 2021*. Gedung Manggala: Ministry of Environment and Forestry Directorate General of Climate Change.
- Muhling, B., Lee, S., Lamkin, J., and Liu, Y. (2011). Predicting the effects of climate change on bluefin tuna (*Thunnus thynnus*) spawning habitat in the Gulf of Mexico. *ICES J. Mar. Sci.* 68, 1051–1062. doi: 10.1093/icesjms/fsr008
- Murdiyarso, D., Purbopuspito, J., Kauffman, J. B., Warren, M. W., Sasmito, S. D., Donato, D. C., et al. (2015). The potential of Indonesian mangrove forests for global climate change mitigation. *Nat. Clim. Chang.* 5, 1089–1092. doi: 10.1038/nclimate2734
- O'Donnell, M. S., and Ignizio, D. A. (2012). Bioclimatic Predictors for Supporting Ecological Applications in the Conterminous United States. *U.S. Geol. Surv.* 691:10. doi: 10.1016/j.mimet.2011.04.001
- Pendelton, L., Donato, D. C., Murray, B. C., Crooks, S., Jenkins, A. W., Sifleet, S., et al. (2012). Estimating Global "Blue Carbon" Emissions from Conversion and Degradation of Vegetated Coastal Ecosystems. *PLoS One* 7:e43542. doi: 10.1371/journal.pone.0043542
- Riahi, K., van Vuuren, D. P., Kriegler, E., Edmonds, J., O'Neill, B. C., Fujimori, S., et al. (2017). The Shared Socioeconomic Pathways and their energy, land use,

- and greenhouse gas emissions implications: an overview. *Glob. Environ. Chang.* 42, 153–168. doi: 10.1016/j.gloenvcha.2016.05.009
- Richards, D. R., Thompson, B. S., and Wijedasa, L. (2020). Quantifying net loss of global mangrove carbon stocks from 20 years of land cover change. *Nat. Commun.* 11:4260. doi: 10.1038/s41467-020-18118-z
- Rogers, K., Kelleway, J. J., Saintilan, N., Megonigal, J. P., Adams, J. B., Holmquist, J. R., et al. (2019). Wetland carbon storage controlled by millennial-scale variation in relative sea-level rise. *Nature* 567, 91–95. doi: 10.1038/s41586-019-0951-7
- Rovai, A. S., Twilley, R. R., Castañeda-Moya, E., Riul, P., Cifuentes-Jara, M., Manrow-Villalobos, M., et al. (2018). Global controls on carbon storage in mangrove soils. *Nat. Clim. Chang.* 8, 534–538. doi: 10.1038/s41558-018-0162-5
- Saintilan, N., Khan, N. S., Ashe, E., Kelleway, J. J., Rogers, K., Woodroffe, C. D., et al. (2020). Thresholds of mangrove survival under rapid sea level rise. *Science* 368, 1118–1121. doi: 10.1126/science.aba2656
- Saintilan, N., Wilson, N. C., Rogers, K., Rajkaran, A., and Krauss, K. W. (2014). Mangrove expansion and salt marsh decline at mangrove poleward limits. *Glob. Chang. Biol.* 20, 147–157. doi: 10.1111/gcb.12341
- Sanderman, J., Hengl, T., Fiske, G., Solvik, K., Adame, M. F., Benson, L., et al. (2018). A global map of mangrove forest soil carbon at 30 m spatial resolution. *Environ. Res. Lett.* 13:055002. doi: 10.1088/1748-9326/aabe1c
- Sasmito, S. D., Silanpää, M., Hayes, M. A., Bachri, S., Saragi-Sasmito, M. F., Sidik, F., et al. (2019). *SWAMP Dataset-Mangrove Soil Carbon-West Papua-2019, V2*. Bogor: Center for International Forestry Research (CIFOR). doi: 10.17528/CIFOR/DATA.00192
- Schile, L. M., Kauffman, J. B., Crooks, S., Fourqurean, J. W., Glavan, J., and Megonigal, J. P. (2017). Limits on carbon sequestration in arid blue carbon ecosystems. *Ecol. Appl.* 27, 859–874. doi: 10.1002/eap.1489
- Schneider, U., Becker, A., Finger, P., Meyer-Christoffer, A., Rudolf, B., and Ziese, M. (2011). *GPCC Full Data Reanalysis Version 6.0 at 0.5°: Monthly Land-Surface Precipitation from Rain-Gauges Built on GTS-Based and Historic Data*. doi: 10.5676/DWD_GPCC/FD_M_V7_050
- Sheppard, C., Al-Husiani, M., Al-Jamali, F., Al-Yamani, F., Baldwin, R., Bishop, J., et al. (2010). The Gulf: a young sea in decline. *Mar. Pollut. Bull.* 60, 13–38. doi: 10.1016/j.marpolbul.2009.10.017
- Soares, P. M. M., Careto, J. A. M., Cardoso, R. M., Goergen, K., and Trigo, R. M. (2019). Land-Atmosphere Coupling Regimes in a Future Climate in Africa: from Model Evaluation to Projections Based on CORDEX-Africa. *J. Geophys. Res. Atmos.* 124, 11118–11142. doi: 10.1029/2018JD029473
- Taillardat, P., Friess, D. A., and Lupascu, M. (2018). Mangrove blue carbon strategies for climate change mitigation are most effective at the national scale. *Biol. Lett.* 14:2018025. doi: 10.1098/rsbl.2018.0251
- Twilley, R. R., Chen, R. H., and Hargis, T. (1992). Carbon sinks in mangroves and their implications to carbon budget of tropical coastal ecosystems. *Water Air Soil Pollut.* 64, 265–288. doi: 10.1007/BF00477106
- Wang, F., Sanders, C. J., Santos, I. R., Tang, J., Schuerch, M., Kirwan, M. L., et al. (2020). Global blue carbon accumulation in tidal wetlands increases with climate change. *Natl. Sci. Rev.* 8:nwaa296. doi: 10.1093/nsr/nwaa296
- Ward, R. D., Friess, D. A., Day, R. H., and Mackenzie, R. A. (2016). Impacts of climate change on mangrove ecosystems: a region by region overview. *Ecosyst. Heal. Sustain.* 2:e01211. doi: 10.1002/ehs2.1211
- Zeng, Y., Friess, D. A., Sarira, T. V., Siman, K., and Koh, L. P. (2021). Global potential and limits of mangrove blue carbon for climate change mitigation. *Curr. Biol.* 31, 1737.e–1743.e. doi: 10.1016/j.cub.2021.01.070
- Zuur, A. F., Hilbe, J. M., and Ieno, E. N. (2013). *A Beginner's Guide to GLM and GLMM with R*. Newburgh: Highland statistics limited.
- Conflict of Interest:** The authors declare that the research was conducted in the absence of any commercial or financial relationships that could be construed as a potential conflict of interest.
- Publisher's Note:** All claims expressed in this article are solely those of the authors and do not necessarily represent those of their affiliated organizations, or those of the publisher, the editors and the reviewers. Any product that may be evaluated in this article, or claim that may be made by its manufacturer, is not guaranteed or endorsed by the publisher.

Copyright © 2022 Chatting, Al-Maslamani, Walton, Skov, Kennedy, Husrevoglu and Le Vay. This is an open-access article distributed under the terms of the Creative Commons Attribution License (CC BY). The use, distribution or reproduction in other forums is permitted, provided the original author(s) and the copyright owner(s) are credited and that the original publication in this journal is cited, in accordance with accepted academic practice. No use, distribution or reproduction is permitted which does not comply with these terms.



Blue Carbon Storage in a Northern Temperate Estuary Subject to Habitat Loss and Chronic Habitat Disturbance: Cowichan Estuary, British Columbia, Canada

Tristan J. Douglas^{1*}, Goetz Schuerholz² and S. Kim Juniper^{1,3,4}

OPEN ACCESS

Edited by:

Catherine Lovelock,
The University of Queensland,
Australia

Reviewed by:

Joanna Carey,
Babson College, United States
Savanna Barry,
University of Florida, United States

*Correspondence:

Tristan J. Douglas
tristanjohndouglas@gmail.com

Specialty section:

This article was submitted to
Ocean Solutions,
a section of the journal
Frontiers in Marine Science

Received: 18 January 2022

Accepted: 28 March 2022

Published: 27 April 2022

Citation:

Douglas TJ, Schuerholz G and
Juniper SK (2022) Blue Carbon
Storage in a Northern Temperate
Estuary Subject to Habitat Loss
and Chronic Habitat Disturbance:
Cowichan Estuary, British
Columbia, Canada.
Front. Mar. Sci. 9:857586.
doi: 10.3389/fmars.2022.857586

¹ School of Earth and Ocean Sciences, University of Victoria, Victoria, BC, Canada, ² Cowichan Estuary Restoration and Conservation Association, Duncan, BC, Canada, ³ Department of Biology, University of Victoria, Victoria, BC, Canada, ⁴ Ocean Networks Canada, University of Victoria Queenswood Campus, Victoria, BC, Canada

Vegetated coastal ecosystems can contribute greatly to long-term carbon sequestration and greenhouse gas emission mitigation, providing a strong argument for their protection and restoration. We investigated carbon sequestration in the Cowichan Estuary, a temperate estuary on Vancouver Island, Canada, in relation to habitat type (salt marsh, eelgrass, mudflats, and oyster shell beds) and habitat degradation. Stored organic carbon and inorganic carbon were quantified in the top 20 cm of sediment as well as in eelgrass and salt marsh vegetation. Sedimentation and carbon sequestration rates were quantified by ²¹⁰Pb radiometric dating, and organic matter sources and quality were assessed by $\delta^{13}\text{C}$, C:N ratios and photopigment content. We also examined the potential impact of habitat disturbance by industrial activity (log booms) on the estuary's carbon storage capacity. The salt marsh was the most important carbon reservoir, with a mean sediment organic carbon stock of $58.78 \pm 19.30 \text{ Mg C ha}^{-1}$. Sediment organic carbon stocks in the upper mudflats, lower mudflats, eelgrass meadow, and oyster shell beds were 19.30 ± 3.58 , 17.33 ± 3.17 , 18.26 ± 0.86 and $9.43 \pm 1.50 \text{ Mg C ha}^{-1}$, respectively. Carbon accumulation rates in the salt marsh and eelgrass meadows were 68.21 ± 21 and $38 \pm 26 \text{ g C m}^{-2} \text{ yr}^{-1}$, whereas ²¹⁰Pb profiles indicated that mudflat sediments were subject to erosion and/or mixing. While eelgrass was absent from the log boom area, likely due to disturbance, sediments there had similar carbon sequestration and bulk properties to adjacent mudflats. Carbon stocks in the eelgrass meadow were similar to those of the mudflats and consistent with the relatively low values reported for other temperate *Zostera marina* meadows, compared with tropical eelgrass meadows. Stable isotope evidence was suggestive of substantial outwelling and/or decomposition of eelgrass vegetation.

Finally, we compared the carbon sequestration potential of the estuary to selected sources and sinks of CO₂ in the surrounding region. We estimated that annual carbon sequestration in the estuary offsets approximately twice the greenhouse gas emission increases attributable to local population growth, and is equivalent to approximately twice that of a 20-year-old stand forest.

Keywords: Blue carbon, carbon sequestration, mudflat, sediment organic carbon, salt marsh, *Zostera mariana* (eelgrass), temperate estuarine ecosystem, seagrass

INTRODUCTION

The capacity of the world's coastal ecosystems to sequester carbon dioxide (CO₂) in biomass and biomass residues, termed “blue carbon,” has been a major focus of research in recent decades in the context of climate change mitigation. Estuarine and intertidal areas in particular have very high rates of carbon sequestration relative to the open ocean (Nelleman et al., 2009; Rogers et al., 2019). In these coastal habitats, photosynthesis by vascular plants, macroalgae, benthic diatoms, and phytoplankton produces and deposits organic matter at rates that often exceed microbial respiration, resulting in the net sequestration of organic carbon (OC) in sediments, where anoxic conditions may greatly restrict remineralization and release of (CO₂) into the atmosphere for millennia (Macreadie et al., 2017a). Sediment OC sequestration is additionally enhanced in coastal vegetated habitats by their ability to trap organic particles from river discharge and seawater flow (Van de Broek et al., 2018; Gerdali et al., 2019). Intertidal foundation plant species like salt marsh grasses and sedges, mangrove forests and seagrasses are particularly efficient natural carbon sinks. They are responsible for capturing and storing up to 70% of the OC permanently stored in marine systems despite only occupying 0.2% of the ocean surface (Nelleman et al., 2009; Duarte et al., 2013). Vegetated intertidal ecosystems rank among the most efficient sediment OC sinks on Earth, sequestering sediment OC at aggregated global rates that are disproportionately higher than terrestrial ecosystems, annually storing comparable quantities of sediment OC to terrestrial plants yet comprising only approximately 0.05% of the biomass and less than 3% the areal extent of forests. Recent global interest in blue carbon coastal ecosystems is based on the potential of vegetated habitats for climate change mitigation, coastal protection and wildlife enhancement (Duarte et al., 2005; Nelleman et al., 2009; Mcleod et al., 2011). Unvegetated mudflats, on the other hand, are generally under-represented in blue carbon budgets, despite often representing the largest areal component of intertidal systems with total sediment OC sequestration capacities that can be comparable to vegetated wetlands (Sanders et al., 2010; Phang et al., 2015). In addition, mudflats play important roles in nutrient recycling and supplying bioavailable OC to benthic populations (Van Duyl et al., 1999; Cook et al., 2004).

Salt marshes reportedly have the highest sediment OC burial rates per unit area of all intertidal blue carbon habitats, with a global average rate of $218 \pm 24 \text{ g C m}^{-2} \text{ yr}^{-1}$ (Chmura et al., 2003; Duarte et al., 2013; Ouyang and Lee, 2014), exceeding long-term

accumulation rates for temperate, tropical, and boreal forests, which range from 0.7 to $13.1 \text{ g C m}^{-2} \text{ yr}^{-1}$ (Zehetner, 2010; Mcleod et al., 2011). However, Chmura et al. (2003) and Ouyang and Lee (2014) reported salt marsh sediment OC sequestration rates that range widely around the globe, from 18 to $1713 \text{ g C m}^{-2} \text{ yr}^{-1}$. These estimates of salt marsh SOC accumulation rates were based on a limited number of locations ($n = 94$) and disproportionate representation from some temperate areas of the world such as Europe and eastern North America, with respect to western North America. Coastal wetlands of the cool, wet Pacific Northwest (British Columbia, Washington, Oregon) climate zone are particularly underrepresented in the global data set (Kauffman et al., 2020). Pacific Northwest salt marshes occur along saline to tidal freshwater gradients and, together with widespread seagrass beds, represent largely unquantified blue carbon sinks (Callaway et al., 2012).

Seagrasses, which have a wide latitudinal distribution, have a reported global average sediment OC burial rate of $138 \pm 38 \text{ g C m}^{-2} \text{ yr}^{-1}$, which is up to 35 times higher than in soils of temperate and tropical forests (Orth et al., 2006; Mcleod et al., 2011). Seagrasses have been estimated to capture up to 18% of the total carbon permanently stored in marine environments despite accounting for only 0.1 to 0.2% of the total ocean sea floor area globally (Gattuso et al., 1998; Duarte et al., 2005; Fourqurean et al., 2012a). However, most seagrass data used to develop worldwide blue carbon estimates are derived from tropical and subtropical regions. The seagrass *Zostera marina* (*Z. marina*), also known as “eelgrass”, is the predominant seagrass species in shallow areas of temperate estuaries along the Pacific coasts of Canada and the United States (Miyajima et al., 2015). The few published papers on carbon sequestration by *Z. marina* have reported sediment OC sequestration rates and sediment OC stocks orders of magnitude lower than global averages (Greiner et al., 2013; Miyajima et al., 2015; Spooner, 2015; Jankowska et al., 2016; Röhr et al., 2016; Poppe and Rybczyk, 2018; Prentice et al., 2019). Adequate regional and species-specific seagrass meadow data are therefore necessary to complete global blue carbon calculations and assess the relative importance of eelgrass habitats to regional blue carbon budgets.

Surficial mudflat sediments often host photosynthetic microbial biofilms, formed by eukaryotic algae and cyanobacteria, collectively known as ‘microphytobenthos’ (MPB) (Admiraal, 1984; Barranguet et al., 1997; Cahoon and Safi, 2002). The microphytobenthos can represent up to 50% of the total primary production in many estuaries (Underwood and Kromkamp, 1999; Pratt et al., 2015), and on a global scale, the

MPB represents one of the most important and largest components of marine/estuarine primary production (Pniewski and Sylwestrzak, 2018). The MPB forms biofilms by excreting extracellular polymeric substances (EPS), mainly polysaccharides, which enhance the stability of the sediment/water interface by reducing resuspension potential (Cahoon, 1999; Blanchard et al., 2000; de Brouwer et al., 2000). Further, biofilms are a major source of high-quality OC for populations of heterotrophic microbes, benthic invertebrates and shore birds (McKew et al., 2013; Schnurr et al., 2020).

Organic carbon generally represents a small fraction of buried material within intertidal habitats, often only 2–3% by weight, although this can be highly variable (Saderne et al., 2019). The remaining sediment is composed of siliciclastic and carbonate (CaCO_3) particles, with inorganic carbon (IC) concentrations often exceeding OC (Mazarrasa et al., 2015). Estuarine and other coastal ecosystems provide a variety of habitats for a diverse assortment of calcifying fauna and flora such as crustaceans, echinoderms, molluscs, calcified algae, and foraminifera, whose remains may be deposited onto the sediment and buried. Considerable uncertainty remains regarding the role of CaCO_3 as source or sink of atmospheric CO_2 , since carbonate shell production shifts the dissolved carbonate equilibrium in seawater and produces CO_2 with a ratio of ~ 0.6 mol of CO_2 emitted per mol of CaCO_3 precipitated (Ware et al., 1992). This has led to the argument that high CaCO_3 burial in shell beds may partially offset CO_2 sequestration associated with OC burial in some intertidal ecosystems (Howard et al., 2017). However, shellfish also facilitate atmospheric- CO_2 drawdown *via* filtration and rapid biodeposition of carbon-fixing primary producers (Fodrie et al., 2017). For the present, few generalizations can be made about the net result of CaCO_3

burial in sediments and CO_2 emission from carbonate formation for any given blue carbon system.

Our study site, the Cowichan Estuary, on the east coast of Vancouver Island, British Columbia, is a potentially informative field location for quantitatively addressing two important knowledge gaps related to blue carbon sequestration in the coastal zone. First, it hosts several types of intertidal habitat whose carbon storage capacities are poorly constrained, namely, temperate Pacific coastal salt marshes, temperate eelgrass meadows, mudflats, and shell beds. Second, the relatively simple and historically recent nature of agricultural and industrial activity in the estuary, together with substantial local and Indigenous knowledge, facilitate the quantitative evaluation of the impact of land use changes on habitat distribution and related carbon sequestration.

The Cowichan-Koksilah Estuary (hereafter referred to as the Cowichan Estuary) is the fourth largest estuary on Vancouver Island, with an intertidal/estuarine area about 4.9 km^2 , including vegetated intertidal lands (saltmarsh and eelgrass), mudflats, and oyster beds (Lambertsen, 1986) (Figure 1). The invasive Pacific oyster (*Crassostrea gigas*) is now the only oyster species in the Cowichan Estuary, outcompeting the Olympia oyster (*Ostrea lurida*), the only oyster species native to British Columbia (Schuerholz, 2018). As part of the traditional territory of the Coast Salish People, the Cowichan Estuary supported the largest Indigenous community on Vancouver Island prior to European settlement in Cowichan Bay in the mid-1800s, providing sustainable harvests of shellfish, salmon, herring roe and seaweed for centuries (Dyck, 2000; Schuerholz, 2006; Dale and Natcher, 2015). Like many estuaries in the province and globally, the ecological health of the Cowichan Estuary has been compromised by land use changes. Approximately 102.8 ha of

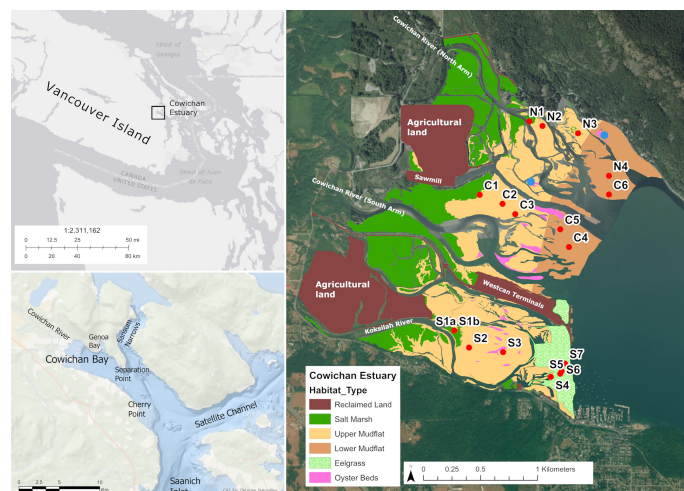


FIGURE 1 | Location map and sediment core sampling sites in the Cowichan Estuary on Vancouver Island, British Columbia, Canada. The rightmost map shows the four dominant habitats found at the Cowichan Estuary: the salt marsh at the landward edge (N1, C1, S1a, S1b), and the seagrass meadow at the seaward edge. The mudflat is in between the salt marsh and seagrass meadow, separated in the upper mudflat (N2, N3, C2, C3, C2, S3), the lower mudflat (N4, C4, C5, C6, S4). Pink shading outlines mapped oyster beds, with blue circles indicating oyster sediment sampling sites. Geo-referenced habitat polygons were delineated and classified by visual aerial photo interpretation of an unoccupied aerial vehicle (UAV)-acquired orthomosaic and verified using ground-based GIS waypoints.

intertidal area has been reclaimed for agricultural or industrial use (Schuerholz, 2017). Much of the salt marsh was dyked and drained for farming, and a shipping terminal, causeway and sawmill occupy infilled areas of salt marsh and mudflat (**Figure 1**). The distribution of eelgrass in the Cowichan Estuary has been strongly affected by sawmill activity. Log booming in the Cowichan Estuary has been documented since the late 1800s, when log storage was relocated from Cowichan Lake to Cowichan Bay with the construction of a sawmill (O'Donnell, 1988). By the 1980s, log handling, storage and boom assembly affected 129 hectares (45%) of the intertidal zone and was reported to be the major source of environmental impact in estuary (Cowichan Estuary Task Force, 1980). Today, logs for the mill continue to be transported by sea and stored in an approximately 20 ha area of the lower intertidal zone prior to processing. Log booms make physical contact with the seabed during low tides, destroying eelgrass meadows and preventing seedling recolonization (Leschen et al., 2010). The gradual loss of eelgrass has been described in several reports: interviews with First Nations elders and long-term residents of Cowichan Bay Village documented historic eelgrass distribution that extended throughout most of the lower intertidal zone (Cowichan Tribes, 2010); and research publications by Harris (1953) and Bell and Kallman (1976) respectively report on eelgrass distribution before and after the emergence of log booming. Currently, eelgrass covers approximately one third of the previously occupied area in the southern portion of the estuary, and no eelgrass remains on the northern mudflats where log storage is concentrated (**Figure 1**). Like eelgrass, the microphytobenthos in the lower intertidal zone may have been similarly impacted by the mechanical disturbance and shading of the seabed, with associated losses of MPB productivity potential resulting in decreased carbon sequestration.

We report here on stocks of organic and inorganic carbon in intertidal sediments of the Cowichan Estuary and their distribution among eelgrass, salt marsh, mudflat, and oyster bed habitats. We also investigated sedimentation and carbon accumulation rates and potential sources of organic matter in each habitat, and estimated the loss of blue carbon sequestration that has resulted from land reclamation for agriculture and current industrial activity in the estuary. Finally, we used our results to assess the contribution of blue carbon in the Cowichan Estuary to climate change mitigation by comparing annual sequestration of carbon dioxide equivalents (CO₂e) in the estuary to that of British Columbia forests, and local and regional greenhouse gas (GHG) emissions.

MATERIALS AND METHODS

Field Sampling and Sample Preparation Sediment Cores

A series of cores was the primary source of samples for quantitative and qualitative assessment of blue carbon stores in Cowichan Estuary sediments. Sampling sites were chosen to be representative of the major habitat types in the Estuary,

according to vegetation presence, vegetation type, tidal inundation, and anthropogenic disturbance. Habitat types were grouped as (1) salt marsh, (2) upper intertidal mudflat, (3) lower intertidal mudflat (the area affected by log booms and likely historical eelgrass habitat), and (4) eelgrass meadows in the lower intertidal zone (eelgrass also extended into the shallow subtidal zone). A total of eighteen sediment cores with 3–6 cores from each habitat type were collected from the Cowichan Estuary in May 2017 (**Figure 1** and **Table S1**). At low tide, sediment cores were collected by slowly inserting acrylic core tubes (50 cm length, 7.62 cm inner diameter) into the substrate at each site. The insertion procedure permitted the collection of sediment cores without visibly disturbing or compacting strata. Core tube penetration ranged from 24 cm to 38.5 cm, depending on sediment compactness; therefore, 20 cm was set as the maximum depth for all analyses except radiometric dating. Immediately after collection, the sediment cores were extruded from their tubes and systematically sectioned at depth intervals of 1 cm from the core surface to 10 cm, and at 2 cm intervals from 10 cm to the bottom of the core. The wet weights and volumes of individual sediment sections were recorded, following which they were subsampled, sealed in plastic containers, transported to the laboratory and frozen at -80°C until further analysis.

Plant Biomass

Separate aboveground and belowground vegetation samples from the salt marsh and eelgrass meadow were harvested to quantify sequestered carbon in living plant material. Sampling methods were designed to minimize destructive impact on each vegetated ecosystem. In the eelgrass meadow, aboveground plant material (*Zostera marina*) was harvested in five 1 m x 1 m (1 m²) quadrats by cutting eelgrass shoots at ground-level, leaving the roots undisturbed. In addition, a small number of eelgrass shoots with intact roots (n = 8) were carefully extracted by hand. Total belowground eelgrass biomass was then estimated from the quantitative relationship between shoot and root biomass, adapted from the methods of Touchette et al. (2003) and described below. Aboveground salt marsh material, predominantly Lyngbye's Sedge (*Carex lyngbyei* Hornem), was harvested by cutting shoots at ground level in five 0.25 m x 0.25 (0.0625 m²) quadrats. The denser belowground biomass in the salt marsh (roots and rhizomes) was estimated from material separated from sediment cores. Fine salt marsh root material could not be separated from sediments and was thus included in the analyses of salt marsh sediment organic material. Following sample collection, all plant material was rinsed with fresh water to remove sediments, carbonates, marine algae, detritus and other organisms, then oven dried and ground for OC estimation and elemental analysis as described for sediments below.

Oyster Beds

To quantify the bulk OC and IC stocks in the oyster shell beds, we collected oyster shell material and sediments from mapped oyster beds in the Cowichan Estuary. The high gravel content of the oyster bed sediments precluded coring, extruding, and fine-

resolution depth sampling. Instead, belowground oyster shells and shell debris were isolated from triplicate 25 cm x 25 cm x 20 cm (0.0125 m³ volume) excavated pits by sieving, removing gravel (2–4 mm granule and 4–64 mm pebble), and then drying and weighing the shell material. Three sediment samples of known volume were collected from each 0.0125 m³ pit at 1 cm, 10 cm, and 20 cm depth intervals for bulk OC and sediment IC measurements. Sample volumes ranged from 25 – 45 cm³ and were thus large enough to estimate gravel as a proportion of total sediment volume. Aboveground oyster shell density and mean shell weight data from the 2017 survey were used to calculate total aboveground oyster shell mass and IC content. Intact aboveground oyster shells with all barnacles and oyster flesh removed from a 2017 survey (Schuerholz, 2018) were rinsed, dried at 65°C, and pulverized in a mortar and pestle before being assessed for IC as described below.

Habitat Map

To determine the areal extent of each habitat type in the Cowichan Estuary, we and the Cowichan Estuary Restoration and Conservation Association (CERCA) produced a Cowichan Estuary habitat map in September 2017. Briefly, we collected red-green-blue (RGB) imagery and global information system (GIS) data by flying an unoccupied aerial vehicle (UAV) over the extent of the Cowichan Estuary, in addition to collecting ground-based GPS control point data. Data were processed into point clouds and an orthophoto in Agisoft Photoscan software (Agisoft, St. Petersburg, Russia) using photogrammetry and Structure from Motion (SfM) image processing workflows. A 2–4 cm resolution orthophoto was produced for the entire estuary with the exception of privately-held land by Western Forest Products and the Westcan Terminal leased Crown land. Geo-referenced habitat polygons were delineated and classified by visual aerial photo interpretation in accordance with Canada's Department of Fisheries and Oceans protocol for estuarine habitat mapping and verified using ground-based GIS waypoints. The total areal extent of each habitat type was calculated from the habitat polygons in ESRI ArcGIS[®] software. For more detail on the habitat mapping methodology implemented, see Schuerholz (2017).

Sediment Analysis

Bulk Density

The bulk density (BD) of each sediment section was determined from its calculated dry weight divided by its measured volume. The dry weight of each sediment section was calculated from the dry weight of a subsample from each section. First, frozen sediment sections were thawed and subsampled. Each subsample (≈ 4 g) was weighed wet, and then dried to a constant mass at $\leq 65^\circ\text{C}$ and re-weighed. Then, the dry weight/wet weight ratio of each subsample was then used to calculate the dry weight of its corresponding sediment section, using the previously determined section wet weight. Wet sediment volume (V) of the core sections were determined from the core radius (r) and the section thickness (h) using the formula for the volume of a cylinder.

Grain Size

Particle size analysis by Laser Diffraction (Laser PSA) was performed on a subset of samples ($n = 96$), at the Natural Resources Analytical Laboratory, University of Alberta, Canada, according to their protocol. Briefly, organic matter and IC in dried sediments <2 mm were removed by the addition of hydrogen peroxide and HCl, respectively. Samples were then dispersed by soaking overnight in 1% sodium hexametaphosphate (Calgon). Using a Laser PSA instrument, a total particle size range of 0.017 – 2000 μm was determined. Results were reported as full particle size distributions and sand/silt/clay size fractions were reported as % volume/volume.

²¹⁰Pb Sediment Dating

A subset of cores from each habitat type was selected for ²¹⁰Pb radioisotope dating using alpha spectrometry, assuming that similar sediment deposition rates had occurred within the same hydrogeomorphic location. Samples were analyzed by Chronos Scientific Inc (Ottawa, Ontario) for radionuclide analysis according to their protocol.

Carbon Stock Determinations

Sediment organic matter content was calculated as the weight loss on ignition at 550°C (LOI₅₅₀) for 5 hours (e.g., Hoogsteen et al., 2015). In a second step, ashed samples of sediment and whole oyster shells were combusted at 950°C for an additional 2 hours to determine the IC content. Organic carbon content and total nitrogen content in a subset of sediment samples ($n = 94$) was directly determined by elemental analysis using an Elementar Vario MicroCube elemental analyser in continuous flow mode, in the Géotop Research Centre, at the Université du Québec à Montréal (Montréal, Canada). This carbon content was used to convert organic matter content (LOI₅₅₀) to sediment OC (% by weight) in all samples (e.g., Prentice et al., 2020). Sediment OC density and sediment IC density were then calculated for each interval of the core sampled (e.g., Howard et al., 2014).

The mass of sediment OC and sediment IC in each core section sampled was calculated by multiplying each sediment carbon density value by the volume of the section (cm). To account for gravel in the oyster shell bed sediment, the volume of gravel in each sample was first measured by the water displacement method and then used to adjust sediment OC and sediment IC (Government of Western Australia, 2020). Core section totals to 20 cm depth were then added to determine the total mass of carbon in each core and converted into the Mg units (Tonnes) on a per hectare basis, as is commonly used in carbon stock assessment (Mg C/hectare_(20cm)) (e.g., Howard et al., 2014). The total carbon in the top 20 cm of each habitat type was estimated as the product of total sediment OC and sediment IC per core by each habitat area.

To determine the OC contained in macroscopic plant biomass, harvested aboveground eelgrass and saltmarsh vegetation was first dried and weighed. For the intact eelgrass plants, roots were separated from shoots, dried separately, and used to determine the relationship between shoot and root biomass by fitting a linear regression to root and shoot dry weight data from the individual plants. The OC content (% by

weight) of above- and below-ground plant material extracted from sediment cores was determined by elemental analysis, as described above. These values were then used to calculate the organic carbon content of dry harvested vegetation from the mean aboveground and belowground dry weights of the five quadrats, and then extrapolated to weights per hectare.

Total IC in aboveground oyster shells was determined from mean oyster shell IC content (% by weight) multiplied by the total shell weight of all oyster beds in the estuary, as estimated by Schuerholz (2017), based on mean oyster shell weight, mean oyster shell density, and total oyster shell bed habitat area.

Total ecosystem carbon stocks (TECS) were calculated for all habitats as described by Kauffman et al. (2020), where TECS are defined as the masses of all OC and IC in aboveground (vegetated habitats only) and belowground pools to a maximum depth of 20 cm, and expressed as:

$$TECS = \sum C_{AB} + C_{BB} + C_{SOC}$$

where C_{AB} is aboveground plant biomass C pool; C_{BB} is belowground biomass C pool and C_{SOC} is the sediment organic carbon pool.

Sediment Organic Carbon Burial Rates

Sediment organic carbon burial rates ($\text{Mg C ha}^{-1} \text{ yr}^{-1}$) were calculated using the same ^{210}Pb methods employed by Greiner et al. (2013) with the following equation:

$$\text{SedimentOC}_{\text{burial}} = \text{SedimentOC} * \text{MAR}$$

where SOC is sediment OC content (%), and MAR is sediment mass accumulation rate ($\text{g m}^{-2} \text{ yr}^{-1}$) derived from ^{210}Pb sediment dating. Sediment $\text{OC}_{\text{burial}}$ of each habitat-specific core was then multiplied by the habitat area in order to determine total annual sediment carbon burial per habitat. The same method was used to calculate the burial rates for sediment IC.

Organic Matter Quality and Sources

Photosynthetic Pigments

Sediment samples for pigment analysis were thawed overnight and mixed thoroughly, then approximately 2 g aliquots were added to 10 mL of refrigerated (4°C) 90% acetone in a 15-mL polypropylene centrifuge tube sonicated for 10 min, then incubated for 24 h in the dark at 2°C . The extracted samples were then centrifuged at 1500 rpm for 5 min. Supernatant containing extracted pigments was decanted into a clean 13 x 100 mm borosilicate culture tube. Concentrations of photosynthetic pigments (chl *a* and phaeopigments) were then measured spectrofluorometrically according to Heiri et al. (2001). Standards were prepared using 90% HPLC grade acetone and pure chlorophyll *a* (chl *a*) extracted from *Anacystis nidulans*. Sediment pellets were reweighted after ≥ 4 days of drying.

C:N and $\delta^{13}\text{C}$

The molar ratio of the total OC and nitrogen contents was used as an indicator of organic matter origins from terrestrial or

marine sources. C:N ratios were calculated from the above-cited elemental analyses. Selected sediment and vegetation tissue 'end-member' samples were analyzed to determine carbon stable isotope ratios $\delta^{13}\text{C}$, with the goal of identifying sources of OC stored in sediments. Dried, pre-weighed samples were analyzed at the Géotop Research Centre, at the Université du Québec à Montréal (Montréal, Canada), using a Micromass model Isoprime 100 isotope ratio mass spectrometer coupled to an Elementar Vario MicroCube elemental analyser in continuous flow mode.

Carbon Valuation and Greenhouse Gas Equivalents

Comparison to British Columbia Forests

Total Sediment OC stocks from the top 20 cm of the Cowichan Estuary habitats were compared to mature stands in the Pacific Northwest (PNW) as well as old- and second-growth forests of interior British Columbia (B.C.), Canada, as reported by Black et al. (2008). Soil OC represents 30-50% of forest TECS. Additionally, sediment OC burial rates in each habitat and the whole Cowichan Estuary were compared to a chronosequence of coastal Douglas-fir stands since 1998, ranging from clearcut-harvested stands which was a net source of carbon ($\sim 22 \text{ Mg CO}_2\text{e ha}^{-1} \text{ yr}^{-1}$) to $\sim 15 \text{ Mg CO}_2\text{e ha}^{-1} \text{ yr}^{-1}$ carbon sequestration in a 50-60-year-old forest. Because B.C. forest soil OC stocks have been reported to a depth of 1 m, they were divided by five to estimate SOC stocks to a depth of 20 cm, assuming homogeneous sediment OC distribution to a depth of 1 m, for comparison with sediment OC stocks from this study.

Greenhouse Gas Equivalents

To estimate the potential contribution of organic carbon sequestration in the Cowichan Estuary to mitigating regional GHG emissions, sediment organic carbon accumulation rates in this study were converted to equivalents in annual emissions by motor vehicles and per capita emission by B.C. residents, both for the entire estuary and for the different habitats. The United States Environmental Protection Agency (EPA) estimates annual emissions from individual motor cars at $4.6 \text{ Mg CO}_2 \text{ yr}^{-1}$ per vehicle, and B.C.'s annual emissions per capita are 12.6 Mg carbon dioxide equivalents (CO_2e), not including transportation or air travel emissions (Business Council of British Columbia, 2019). Calculated carbon sequestration rates from this study were then converted to CO_2e sequestration rates for regional-scale comparison with emissions from motor vehicles and residents.

Statistical Analysis

Sediment characteristics of the salt marsh, upper mudflat, lower mudflat, and eelgrass were compared statistically using R Studio version 1.3.1093 (cran.r-project.org). A Levene test of homogeneity of variance revealed that datasets had unequal variances. In addition, Shapiro-Wilk test showed that the datasets were not normally distributed, and the assumptions of the parametric t-test could not be met; thus, non-parametric tests were used. A Welch's unequal variance t-test was employed to

test for differences in the sediment characteristics between the habitats. Simple linear regressions and Pearson's correlation were used to determine statistical relationship between sediment properties. Natural log transformations of datasets were used when required to satisfy the assumptions of linear regression. Significance level of $\alpha = 0.05$ was set for all statistical analyses.

RESULTS

Sediment Physicochemical Properties

Bulk Density

Sediment BD generally increased with depth in all habitat types. Mean sediment BD values in the upper 20 cm were significantly different between all habitats (Welch's t-test, $p < 0.05$), most similar in the upper mudflat, lower mudflat, and eelgrass meadow, and notably lower in the salt marsh and at intermediate levels in the oyster shell beds (**Figure 2** and **Table S2**).

Sediment Organic Carbon

Concentrations of sediment organic matter and OC in the upper 20 cm were highest at the salt marsh stations ($8.96 \pm 1.06\%$ organic matter and $4.47 \pm 0.77\%$ OC), with a slight increasing trend from the eelgrass (2.49 ± 0.084 and $0.53 \pm 0.03\%$), to the lower mudflat (2.61 ± 0.10 and $0.57 \pm 0.06\%$), and the upper mudflat (3.13 ± 0.28 and $0.86 \pm 0.17\%$) stations. Sediment OC in the oyster shell bed sediments was $0.61 \pm 0.08\%$, comparable to mudflat and eelgrass sediments. Across all habitats, an inverse relationship was observed between bulk density and sediment OC ($p \leq 0.05$). None of the depth profiles for sediment OC concentration showed the typical exponential decay trend expected under

steady-state conditions of sediment OC accumulation and decomposition (Berner, 1980; Hargrave and Phillips, 1989). Generally, sediment OC content (% by weight) varied little with depth with the exception of the salt marsh cores where sediment OC increased from 2 to 12 cm and decreased from 12 to 20 cm (**Figure 2**). As a result of this homogeneity along depth profiles, mean sediment OC values over the full 20 cm are used here for comparison between all cores. Generally, sediment OC was low in all habitats compared to similar habitats globally (**Table 1**).

Granulometry

Upper mudflat, lower mudflat and eelgrass sediments were mostly sandy (82.56 ± 1.41 , 87.14 ± 1.28 , and $94.17 \pm 0.25\%$ sand, **Figure 3**), with a small fraction of silt ($<12\%$) and clay ($<6\%$). Salt marsh sediments had the highest fraction of silt and clay (32.39 ± 2.13 and $8.87 \pm 0.61\%$) and the lowest fraction of sand ($58.74 \pm 2.71\%$) compared to the other habitats. A general transition in mean grain size was observed from the high to the low intertidal zone, with decreasing clay and silt content and increasing sand content from salt marsh to lower mudflat stations. A positive relationship was observed between bulk density and percentage sand, as well as between sediment OC and clay and silt contents ($p \leq 0.05$). Average gravel content in the oyster shell bed sediments was $41.4 \pm 4.0\%$.

Carbon Stocks

Mean SOC stocks (i.e., the amount of OC stored per unit area, down to a fixed sediment depth) in the top 20 cm of sediment were comparable in the upper mudflat ($19.30 \pm 3.58 \text{ Mg C ha}^{-1}$), lower mudflat ($17.33 \pm 3.17 \text{ Mg C ha}^{-1}$) and eelgrass meadow ($18.26 \pm 0.86 \text{ Mg C ha}^{-1}$) cores (**Table 2S**). Saltmarsh sediments had the highest per-hectare carbon content ($58.78 \pm 31.45 \text{ Mg C ha}^{-1}$), approximately three-fold higher than all other habitats. When

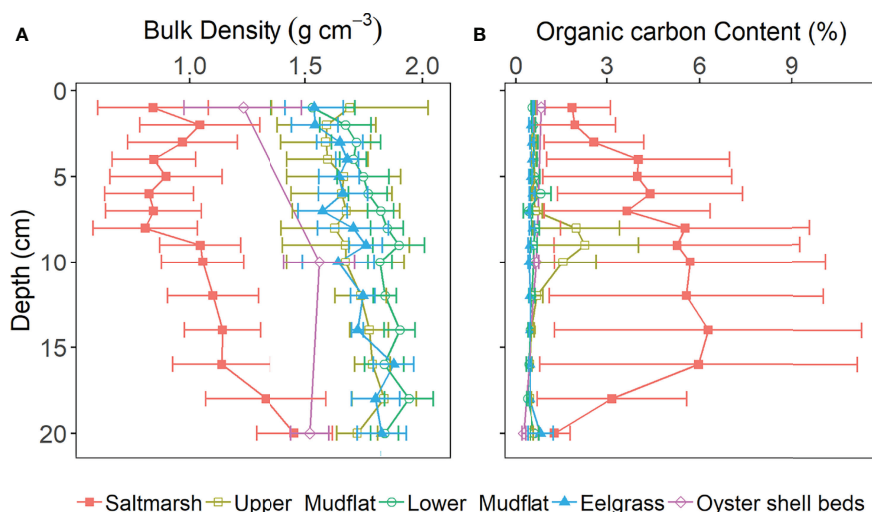


FIGURE 2 | Sediment core profiles of average (A) bulk density, and (B) carbon content (% by weight) in the top 20 cm of cores from salt marsh ($n = 4$), upper mudflat ($n = 6$), lower mudflat ($n = 5$), eelgrass ($n = 3$), and oyster shell bed ($n = 2$) stations at all sampling sites. All data are presented as the mean \pm standard error of the mean.

TABLE 1 | Comparison of sediment organic carbon (SOC) concentrations (% by weight) and stocks (Mg C ha⁻¹) at different salt marsh, mudflat and eelgrass environments.

Habitat	SOC (%)	SOC stock (Mg C ha ⁻¹)	Sedimentation rate	Reference
Salt marshes				
Australian coasts	–	2.8–192.6	–	Macreadie et al. (2017b)
Salada Lagoon, Gulf of Mexico	0.2–1.9	23.12 to 26.14	0.06 ± 0.01 to 1.03 ± 0.77 cm yr ⁻¹	Ruiz-Fernández et al. (2018)
Jiquilisco Bay, El Salvador	0.2–17.3	5.98 to 92.96	0.12 ± 0.09 to 0.40 ± 0.05	Ruiz-Fernández et al. (2018)
Estero de Urias Lagoon, Gulf of California, Mexico	6.7–16.8	61.06 to 72.4	0.07 ± 0.01 to 0.65 ± 0.09 cm yr ⁻¹	Ruiz-Fernández et al. (2018)
Sian Ka'an, Mexican Caribbean coast	0.7–3.1	23.38 ± 0.56	0.04 ± 0.01 to 0.3 ± 0.07	Ruiz-Fernández et al. (2018)
San Francisco Bay Tidal Wetlands	3.96–4.08	–	0.2–0.5 cm yr ⁻¹	Callaway et al. (2012)
Pacific Northwest Coast, United States: low marsh	4.79 ± 1.44	38.12 ± 1.46	–	Kauffman et al. (2020)
Pacific Northwest Coast, United States: high marsh	6.57 ± 1.52	52.36 ± 2.48	–	Kauffman et al. (2020)
Quintin Bay northeast Pacific, Mexico	–	51.8 to 64	0.01–0.03 g cm ⁻² yr ⁻¹	Cuellar-Martinez et al. (2019)
<i>Cowichan Estuary, Canada</i>	3.56 ± 0.50	49.1 ± 19.9	0.33 ± 0.10 cm yr ⁻¹	<i>This study</i>
Zostera marina meadows				
Baltic Sea	0.3 ± 0.0	4.62	–	Röhr et al. (2018)
Black Sea	3.5 ± 1.2	5.8	–	Röhr et al. (2018)
East and West Atlantic	0.7 and 0.3	11.08 and 10.8	–	Röhr et al. (2018)
East and West Pacific	0.4 and 1.1	13.88 and 18.74	–	Röhr et al. (2018)
Kattegatt-Skagerrak	2.5 ± 0.6	38.9	–	Röhr et al. (2018)
Mediterranean Sea	2.3 ± 0.0	70.34	–	Röhr et al. (2018)
Finland and Denmark	0.24 and 1.75	1.25 and 8.648	0.32–4.2 cm yr ⁻¹	Röhr et al. (2016)
Padilla Bay, Washington State	1.68 ± 0.09	–	0.08 ± 0.01 to 0.31 ± 0.03 cm yr ⁻¹	Poppe and Rybczyk (2018)
Pacific Northwest Coast, United States	0.635 ± 0.14	15.99 ± 0.88	–	Kauffman et al. (2020)
Clayoquot Sound, Canada	1.30	7.90 ± 2.83	–	Postlethwaite et al. (2018)
<i>Cowichan Estuary, Canada</i>	0.52 ± 0.040	17.9 ± 1.21	0.47 ± 0.32 cm yr ⁻¹	<i>This study</i>
Other seagrasses				
Oyster Harbour, Western Australia	1.6 to 16.9	–	0.066 ± 0.003 cm yr ⁻¹	Marbà et al. (2015)
Chek Jawa, Singapore	1.1 ± 0.1	27.6	–	Phang et al. (2015)
Abu Dhabi, UAE	0.6 ± 0.39	9.82 ± 1.4	–	Campbell et al. (2015)
Global	2 ± 0.1	32.7	–	Fourqurean et al. (2012a)
Florida Bay, USA	2.1 ± 0.3	32.7	–	Fourqurean et al. (2012b)
Shark Bay, Australia	1.9 ± 0.4	48.6	–	Fourqurean et al. (2012b)
Palau, Micronesia	16.7 ± 0.5	9.6 ± 0.86	–	Kauffman et al. (2011)
Quintin Bay northeast Pacific, Mexico	–	16.0 to 19.6	0.02–3.21 g cm ⁻² yr ⁻¹	Cuellar-Martinez et al. (2019)
Mudflats				
China	–	–	0.93 and 2.81 cm y ⁻¹	Ye et al. (2015)
Chek Jawa, Singapore	1.4 ± 0.2	24.8 to 28.6	–	Phang et al. (2015)
Indonesia	–	12.4 ± 2	–	Sasmito et al. (2020)
Australia	3–5	–	–	Cook et al. (2004)
	3.25–4.41	–	0.33 ± 0.4 cm y ⁻¹	Bernal and Mitsch (2013)
Tamandaré, Brazil	–	–	0.73 cm yr ⁻¹	Sanders et al. (2010)
<i>Cowichan Estuary, Canada</i>	0.82 ± 0.13 and 0.58 ± 0.048	19.1 ± 3.78 and 16.9 ± 4.36	0.40 ± 0.21 (mean salt marsh and eelgrass)	<i>This study</i>

Literature values have been divided by five to convert SOC stocks from 100 cm to 20 cm depth.

granule (2–4 mm) and pebble (4–64 mm) contents were accounted for, the oyster shell bed had a mean SOC stocks of 9.43 ± 1.50 Mg C ha⁻¹, approximately half those of the mudflats and eelgrass meadow.

Sediment Accretion, Mass Accumulation, and Carbon Sequestration Rates

Sediment accretion, mass accumulation, and carbon accumulation rates could only be determined for salt marsh

and eelgrass cores. The four mudflat cores analyzed showed no trends in ²¹⁰Pb_{ex} activity with depth, and thus could not be dated using the CRS model (Table 2 and Figure 4). Successfully dated salt marsh and eelgrass cores had low ²¹⁰Pb_{ex} activity ranges (0.12 to 10.30 and 0.86 to 5.13 Bq kg⁻¹, respectively) which resulted in high uncertainty values for sediment accretion, mass accumulation, carbon accumulation, and dates.

The salt marsh and eelgrass cores analyzed were both 32 cm in length. The maximum depth of excess ²¹⁰Pb (²¹⁰Pb_{ex}) was 28 cm

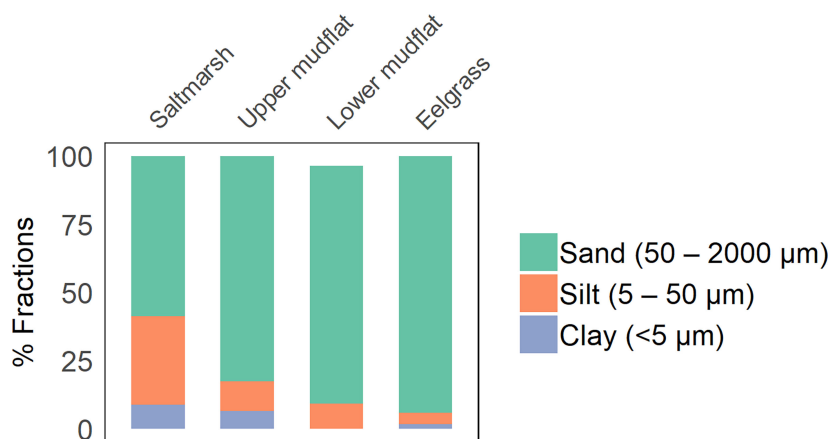


FIGURE 3 | Sediment grain size distribution in the top 20 cm of cores from salt marsh, upper mudflat, lower mudflat, and eelgrass stations at all sampling sites.

in the salt marsh core, corresponding to the year 1877 ± 52 years. The sediment accretion rate in the salt marsh core ranged from 0.095 to 0.733 cm yr^{-1} with an average 0.328 ± 0.103 cm yr^{-1} . Carbon accumulation rates ranged from 27 ± 19 to 122 ± 24 $\text{g C m}^{-2} \text{yr}^{-1}$, averaging 68 ± 21 $\text{g C m}^{-2} \text{yr}^{-1}$. The maximum depth of $^{210}\text{Pb}_{\text{ex}}$ in the eelgrass core was also 28 cm, with sediments at that depth dating from the year 1914 ± 31 years. Accretion rates in the eelgrass sediment ranged from 0.078 ± 0.038 to 0.900 ± 0.662 cm yr^{-1} at an average of 0.465 ± 0.317 cm yr^{-1} , while carbon accumulation rates ranged from 7 ± 3 to 68 ± 50 $\text{g C m}^{-2} \text{yr}^{-1}$, averaging 38 ± 26 $\text{g C m}^{-2} \text{yr}^{-1}$.

Aboveground and Belowground Biomass and Organic Carbon in Macroscopic Plant Material

The mean aboveground (herbaceous mass) and belowground (root mass) biomass stocks of the *Z. marina* that dominated the seagrass sites were respectively 0.44 ± 0.059 and 0.39 ± 0.077 Mg ha^{-1} , with area-integrated biomass stocks of 7.91 ± 1.07 Mg and 6.97 ± 1.39 Mg . Eelgrass biomass carbon stocks were 0.087 ± 0.012 and 0.074 ± 0.011 Mg C ha^{-1} in the below- and aboveground

biomass, with area-integrated stocks of 1.57 ± 0.21 and 1.50 ± 0.20 Mg C (Table 3). The aboveground and belowground biomass stocks of the salt marsh dominated by Lyngbye's sedge (*Carex lyngbyei* Hornem) were 4.67 ± 0.74 and 18.27 ± 7.02 Mg ha^{-1} . The salt marsh had area-integrated biomass stocks of 443.51 ± 70.56 aboveground and 1728.33 ± 655.17 Mg belowground, with average biomass OC stocks of 1.34 ± 0.21 and 7.144 ± 2.74 Mg C ha^{-1} , and area-integrated biomass carbon stocks of 126.53 ± 20.13 and 675.84 ± 259.61 Mg C . Total area-integrated biomass for both vegetated habitats was 805.44 Mg (see individual habitat stock values for associated standard errors).

Total Ecosystem Carbon Stocks

The term total ecosystem carbon stock (TECS) is defined here as the total sediment and vegetation OC stock per unit-area, excluding IC to remain consistent with established definition of ecosystem carbon stocks used by other contemporary blue carbon studies (Kauffman et al., 2020; Sharma et al., 2020). The TECS in the salt marsh was 67.26 Mg C ha^{-1} (1.34 ± 0.21 , 7.144 ± 2.74 , and 58.78 ± 14.19 Mg C ha^{-1} , respectively, for aboveground biomass, belowground biomass and sediment) (Table 2S,

TABLE 2 | Excess ^{210}Pb ($^{210}\text{Pb}_{\text{ex}}$) activity, depth of $^{210}\text{Pb}_{\text{ex}}$, sedimentation rates and carbon accumulation rates calculated with CRS dating model for each core with positive excess ^{210}Pb activity values, representing an approximately 100-year timeframe.

Site	Station	$^{210}\text{Pb}_{\text{ex}}$ range (Bq kg^{-1})	Depth of $^{210}\text{Pb}_{\text{ex}}$ (cm)	Mass accumulation rate ($\text{g m}^{-2} \text{yr}^{-1}$)	Sediment accretion rate (cm yr^{-1})	OC accumulation rate ($\text{g C m}^{-2} \text{yr}^{-1}$)	Habitat SOC accumulation rate (Mg C yr^{-1})
Salt marsh	N1	0.12 - 10.30	28	0.382 ± 0.120	0.328 ± 0.103	68.21 ± 21	64.53 ± 19.87
Upper Mudflat	C2	1.31 - 8.33	28	—	—	—	—
Upper Mudflat	C3	0.67 - 42.77	28	—	—	—	—
Lower Mudflat	C4	1.20 - 8.01	28	—	—	—	—
Lower Mudflat	C6	0.40 - 2.48	14	—	—	—	—
Eelgrass	S7	0.86 - 5.13	28	0.752 ± 0.517	0.465 ± 0.317	38 ± 26	6.84 ± 4.68

Table Legend: Means and Monte Carlo uncertainty are shown for each core.

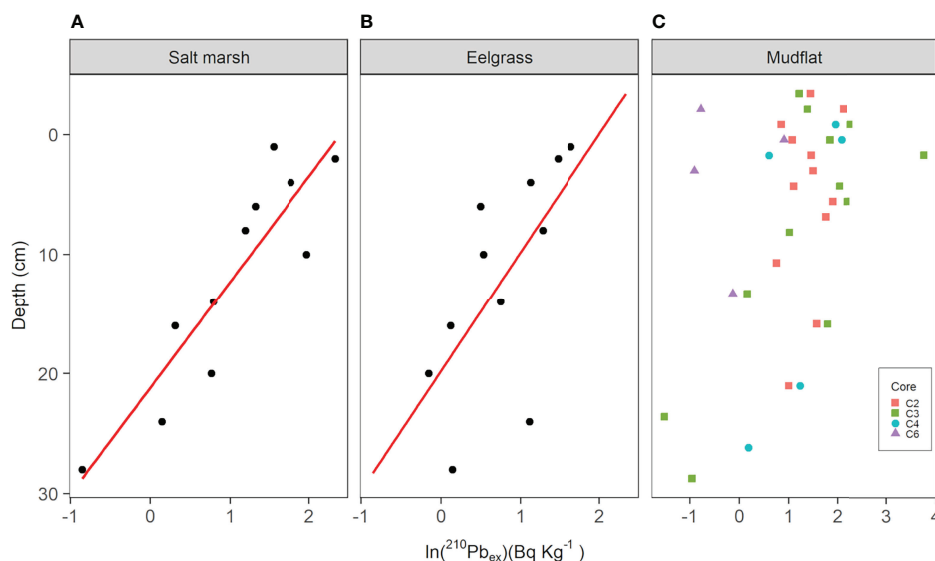


FIGURE 4 | Excess ^{210}Pb activity per unit mass of sediment (Bq kg^{-1}) depth profiles of sediment cores from the Cowichan Estuary. Panels **(A)** (salt marsh) and **(B)** (eelgrass) show natural log transformations of excess ^{210}Pb ($^{210}\text{Pb}_{\text{ex}}$) and linear regression lines used to estimate sediment accretion rate (SAR). Panel **(C)** shows natural log transformations $^{210}\text{Pb}_{\text{ex}}$ in mudflat cores C2, C3, C4, and C6, which were respectively collected from low to high tidal inundation, omitting values equal to or below the supported “background” ^{210}Pb threshold for each core.

Table 3 and **Figure 5**). The TECS were 19.30 and $17.33 \text{ Mg C ha}^{-1}$, respectively, in the upper mudflat and lower mudflat, and $21.33 \text{ Mg C ha}^{-1}$ in the eelgrass meadow (1.57 ± 0.21 , 1.50 ± 0.20 , and 18.26 ± 3.17 , respectively, for aboveground biomass, belowground biomass and sediment). The oyster shell bed TECS was $9.43 \pm 1.50 \text{ Mg C ha}^{-1}$, all of which was accounted for in the sediments. Carbon stocks in the salt marsh were generally three-fold higher than all other habitats, which were all approximately equal. Sediment OC stock dominated the total carbon storage in the eelgrass meadow, with combined aboveground and belowground biomass constituting 0.48% of TECS. In contrast, the salt marsh had the highest biomass contribution relative to total ecosystem carbon (12.61%).

When per-hectare TECS was multiplied by the area of each of the intertidal habitats, the upper mudflat total covered 52% of the land area (191 ha) and contained approximately 32% (3718.72 Mg C) of the Cowichan Estuary carbon stock (**Table 2S** and **Figure 5**). The salt marsh accounted for 25% (95 ha) of the land area, but 51% (6362.49 Mg C) of the TECS. The lower mudflat and eelgrass grass meadow respectively accounted for land areas

of 16% (60 ha) and 5% (18 ha), contributing 9% (1085.85 Mg C) and 3% (330.20 Mg C) of the TECS, respectively. The oyster beds accounted for approximately 2% of the estuary area and 0.65% (59.4 Mg C) of the TECS.

Organic Matter Characterization and Sources

Photosynthetic Pigments

At the saltmarsh sites, the depth-integrated total photosynthetic pigment concentration was $15.84 \pm 2.44 \mu\text{g/g}$, with a surface concentration of $35.77 \pm 16.38 \mu\text{g/g}$. The eelgrass sites had similar average depth-integrated and surface total pigment concentrations of 11.41 ± 1.23 and $34.78 \pm 0.77 \mu\text{g/g}$, respectively (**Table S3** and **Figure 6**). Pigment concentrations in upper and lower mudflat sediments were similar, and notably lower than those of the vegetated habitats, for both the depth-integrated (6.69 ± 0.58 and $6.58 \pm 0.58 \mu\text{g/g}$) and surface layer (14.65 ± 2.10 and $14.35 \pm 4.67 \mu\text{g/g}$) measures.

Depth-integrated chl *a* concentration increased from lower mudflat ($1.55 \pm 0.19 \mu\text{g/g}$) to upper mudflat ($2.49 \pm 0.32 \mu\text{g/g}$)

TABLE 3 | Total organic carbon (OC) stocks in salt marsh and eelgrass plant biomass.

Site	Vegetation	OC content (%)	Biomass carbon stock (Mg C ha^{-1})	Biomass carbon stock (Mg C)
Salt marsh	Aboveground	28.65 ± 6.11	1.34 ± 0.21	126.53 ± 20.13
	Belowground	39.10 ± 2.05	7.144 ± 2.74	675.84 ± 259.61
Eelgrass	Aboveground	19.87 ± 4.70	0.087 ± 0.012	1.57 ± 0.21
	Belowground	27.46 ± 11.63	0.074 ± 0.011	1.50 ± 0.20
Total				805.44

All data are presented as the mean \pm standard error of the mean.

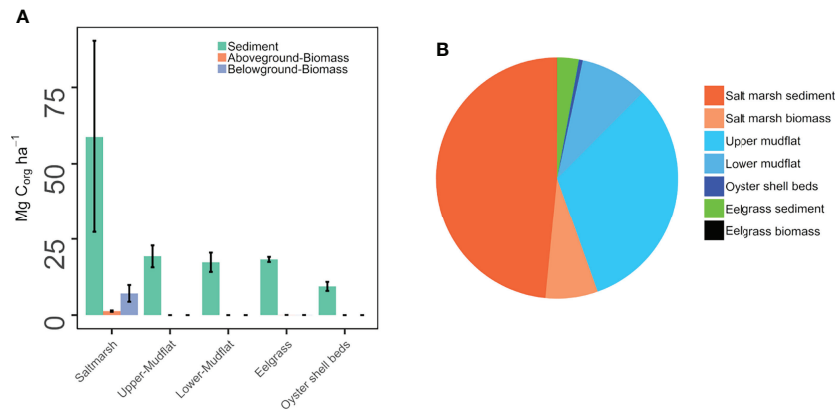


FIGURE 5 | Comparison of the total biomass and sediment organic carbon (OC) stocks in the salt marsh, upper mudflat, lower mudflat, eelgrass meadow, and oyster shell beds of the Cowichan Estuary. Panel **(A)** is per-hectare sediment and vegetation biomass organic carbon stocks; Panel **(B)** is total area-integrated sediment and vegetation biomass OC stocks. Bars represent standard errors.

stations, and eelgrass meadow ($2.63 \pm 0.37 \mu\text{g/g}$) to the salt marsh ($4.05 \pm 1.02 \mu\text{g/g}$). This trend of increasing chl *a* from low- to high-intertidal and unvegetated to vegetated habitats was more obvious in surface chl *a*, which increased from $4.43 \pm 0.04 \mu\text{g/g}$ in the lower

mudflat, to $8.80 \pm 2.08 \mu\text{g/g}$ in the upper mudflat, $10.02 \pm 0.81 \mu\text{g/g}$ in the eelgrass meadow, and $18.13 \pm 7.074 \mu\text{g/g}$ in the salt marsh.

Surface sediment chl *a*/Phaeopigment ratios were highest in the upper mudflat (1.67 ± 0.28), followed by the saltmarsh ($1.47 \pm$

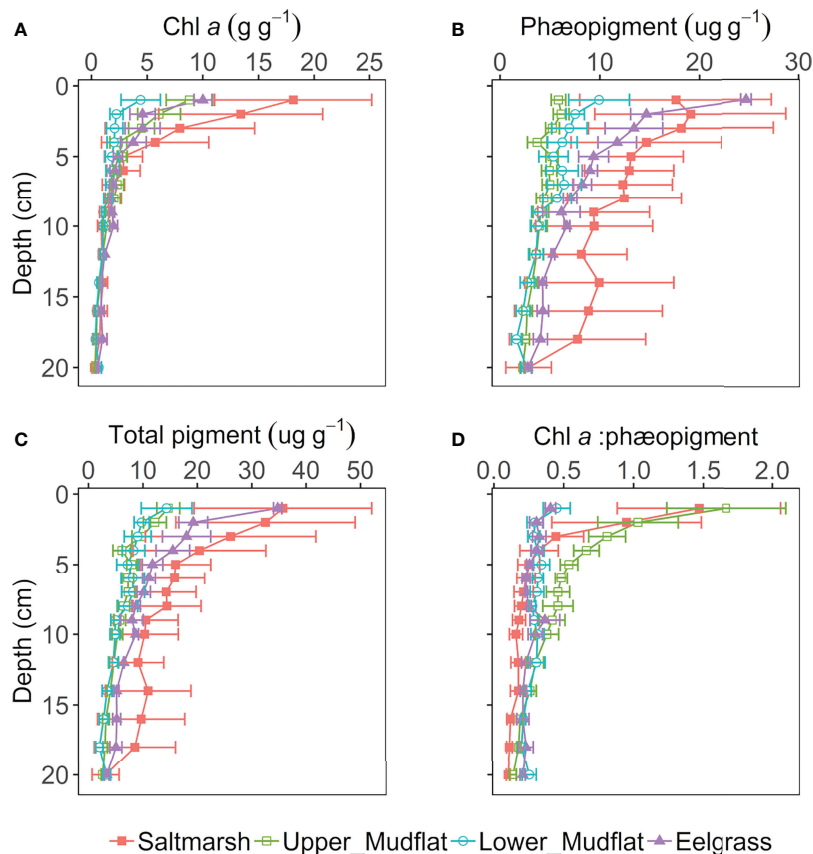


FIGURE 6 | Photosynthetic pigment depth profiles in the top 20 cm of sediment of the Cowichan Estuary: **(A)** chlorophyll *a* (chl *a*) ($\mu\text{g/g}$ dry sediment); **(B)** Phaeopigment ($\mu\text{g/g}$ dry sediment); **(C)** Total pigment ($\mu\text{g/g}$ dry sediment); **(D)** Chl *a*/phaeopigment ratio. Horizontal bars represent standard errors.

0.59). Lower mudflat and eelgrass sites had the lowest surface chl *a*/Phaeopigment ratios (0.45 ± 0.097 and 0.41 ± 0.037).

C:N and $\delta^{13}\text{C}$

Ranges of C:N ratios and $\delta^{13}\text{C}$ in cores from this study reflect the mixed nature of organic inputs in these sediments with both terrestrial- and marine-derived material (Table 4 and Figure 7). The highest average $\delta^{13}\text{C}$ enrichment (-22.6 ± 0.4 ‰) and lowest C:N (10.9 ± 1.2) were found in the eelgrass sediments suggesting a relatively high contribution of marine-derived OM and buried *Z. marina* biomass (McPherson et al., 2015). In contrast, salt marsh sediments were composed of more terrestrial material with the lowest $\delta^{13}\text{C}$ enrichment and highest C:N (-26.5 ± 0.1 ‰ and 20.2 ± 0.8) compared to the other habitats. The lower mudflat had slightly lower $\delta^{13}\text{C}$ (-25.8 ± 0.2 ‰) and higher C:N (12.2 ± 1.1) than the upper mudflat (-24.5 ± 0.1 ‰ and 11.7 ± 0.6), possibly reflecting the input of woody debris from log booms in the low intertidal zone.

Sediment and Oyster Shell Bed Inorganic Carbon Stocks

Inorganic carbon stocks, outside of the oyster shell beds, exhibited a generally positive relationship with tidal inundation, ranging from 6.26 ± 0.90 Mg C ha⁻¹ in the salt marsh and increasing to 11.15 ± 1.24 Mg C ha⁻¹ in the lower mudflats (Figure 1S and Table 2S). Statistically significant differences were found in the sediment IC densities between the salt marsh and all other all other habitats, as well as between the upper- and lower-mudflats, the eelgrass and lower mudflat, and the eelgrass and the oyster shell beds (Welch's t-test, $p < 0.05$). Together, the two mudflat IC stocks (1550.4 ± 117.2 and 669.0 ± 74.5 in the upper- and lower mudflat, respectively) contribute ~68% of the IC in the Cowichan Estuary, with the salt marsh and eelgrass meadow respectively accounting for 18% (591.9 ± 84.8 Mg C) and 5% (283.7 ± 19.2 Mg C).

The oyster shell beds represented approximately 9% (434.19 Mg C) of the IC in the intertidal sediments of the estuary despite covering under 2% of the intertidal area. Inorganic carbon accounted for $11.43 \pm 0.11\%$ of the shell material. Mean per-hectare aboveground oyster shell IC stock was 37.01 ± 0.34 Mg C ha⁻¹ and the total aboveground oyster shell IC stock for all of the oyster beds was 233.19 ± 2.16 Mg C. With buried shell material included in sediment IC (% by dry weight), the oyster shell bed sediments were statistically distinct from all other habitat types and mean per-hectare sediment IC stocks were highest in the oyster shell beds (31.91 ± 3.04 Mg C ha⁻¹).

Blue Carbon Valuation

Comparison With B.C. forests

The Cowichan Estuary salt marsh per-hectare sediment OC stock is up to to five and three times higher than values reported, respectively, for second- and old-growth forest in the interior of British Columbia, and comparable with the lower range of values for mature stands of Pacific Northwest coastal forest (Table 5). Cowichan Estuary eelgrass and mudflat per-hectare sediment OC stocks are approximately 1.5 times higher than to those of second growth forests and the lower limit of old growth forests of interior B.C., and around two times lower than estimates for mature stands of Pacific Northwest coastal forest.

Carbon Sequestration

Estimated areal rates of carbon sequestration for salt marsh and eelgrass meadow in the Cowichan Estuary were respectively 64.53 ± 19.87 and 6.84 ± 4.68 Mg C ha⁻¹ y⁻¹, similar to a 20-year-old stand of forest on coastal Vancouver Island, British Columbia. Together, these two blue carbon habitats (salt marsh and mudflat) in the Cowichan Estuary would have the capacity to sequester the annual equivalent emissions of 133 ± 72 vehicles and 49 ± 26 B.C. residents (Table 6).

TABLE 4 | Mean organic and nitrogen contents, CLN ratio, and $\delta^{13}\text{C}$ signatures in biomass, surface sediment (1 cm), and top 20 cm of sediment from salt marsh, upper mudflat, lower mudflat, and eelgrass meadow in the Cowichan Estuary.

Site	Total OC content (%)	Total nitrogen content (%)	C:N	$\delta^{13}\text{C}$ (‰)
Saltmarsh				
Sediment (1 cm)	1.08	0.085	14.9	-26.0
Sediment (20 cm)	1.936 ± 0.270	0.108 ± 0.013	20.2 ± 0.8	-26.5 ± 0.1
Aboveground biomass	28.7 ± 6.11	1.56 ± 0.42	22.2 ± 3.35	-25.6 ± 5.26
Belowground biomass	34.3 ± 3.12	0.74 ± 0.08	57.1 ± 8.11	-26.6 ± 5.53
Upper Mudflat				
Sediment (1 cm)	0.450	0.053	9.8	-23.6
Sediment (20 cm)	0.566 ± 0.047	0.056 ± 0.003	11.7 ± 0.6	-24.5 ± 0.1
woody debris	45.03 ± 2.05	0.26 ± 0.060	209.5 ± 39.2	-26.3 ± 0.03
Lower mudflat				
Sediment (1 cm)	0.410	0.048	10.0501	-25.3
Sediment (20 cm)	0.533 ± 0.075	0.049 ± 0.0030	12.2 ± 1.1	-25.8 ± 0.2
woody debris	40.8 ± 1.74	0.27 ± 0.026	194.3 ± 22.1	-27.2 ± 0.32
Eelgrass				
Sediment (1 cm)	0.894	0.090	11.6	-20.0
Sediment (20 cm)	0.612 ± 0.09	0.063 ± 0.005	10.9 ± 1.2	-22.6 ± 0.4
Aboveground biomass	17.6 ± 3.67	1.27 ± 0.29	16.1 ± 1.08	-12.2 ± 0.80
Belowground biomass	23.6 ± 6.22	0.71 ± 0.18	38.7 ± 0.66	-12.0 ± 0.24

All data except surface sediments are presented as the mean \pm standard error of the mean.

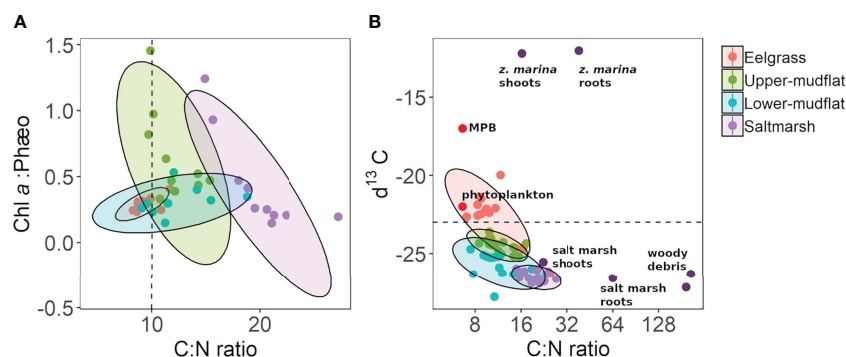


FIGURE 7 | Relationship between C:N ratio to sediment properties: **(A)** chlorophyll *a* (chl *a*)/phaeopigment ratio vs. C:N ratio, with hatched line on the x-axis to denote generally labile (C:N < 10) and recalcitrant (C:N > 10) material; **(B)** δ¹³C vs. C:N ratio plot of sediment cores collected from the Cowichan Estuary, with dark-purple labelled points denoting vegetation end-members from the Cowichan Estuary, with phytoplankton and microphytobenthos (MPB) δ¹³C and C:N estimates from literature (Redfield et al., 1963; France, 1995). The hatched line on the y-axis denotes marine (δ¹³C < 23‰) and terrestrial (δ¹³C > 23‰). Ellipses delineate the 95% confidence interval for each of the habitats, assuming a multivariate *t* distribution.

DISCUSSION

Evidence for Strong Hydrodynamics

We observed a number of habitat-related trends in sediment bulk properties in the Cowichan Estuary that we attribute to hydrodynamics. Most distinct were sediments from the salt marsh, where the high intertidal location and thick vegetation would act to minimize wave and current forces, compared to non-vegetated habitats and habitats lower in the intertidal zone. Salt marsh sediments were relatively carbon-rich, and high in moisture (low bulk density) and fine particles. In contrast, mudflat and eelgrass sediments had notably lower organic carbon and moisture contents, and a high percentage of sand. Alone, the relatively homogenous organic carbon profiles in the mudflat sediments could also be attributed to an irregular supply of organic matter or irregular rates of degradation (Alongi et al., 1996; Ruiz-Fernández et al., 2018). However, when combined with the non-trending ²¹⁰Pb depth profiles and the high percentage of coarser particles mixing and erosion forces are the most likely explanation (Winterwerp and Van Kesteren, 2004; Jacobs et al., 2011; Zhou et al., 2016). In addition, decreased chl *a* in the surface sediments of the lower mudflats

suggests that sediment instability may inhibit the formation of cohesive surface biofilms by epiphytobenthos (Cahoon, 1999; Blanchard et al., 2000; de Brouwer et al., 2000). The down-core trends in the eelgrass sediments also provide evidence for hydrodynamic mixing, possibly dampened by the vegetation. There was no depth-related organic matter decay trend in the eelgrass sediments. However, there was a discernible down-core trend in excess ²¹⁰Pb in the eel grass sediments that was weaker than the trend observed in the more thickly vegetated salt marsh.

Across intertidal ecosystems globally, reworking of sediment through burrowing and feeding activities of macrofauna, as well as an overabundance of bioturbators in some estuaries, can contribute to substantial remineralization of organic matter (Bentley et al., 2014; Coverdale et al., 2014). However, bioturbation rather than abiotic reworking is less likely to be the primary cause of sediment mixing in the Cowichan Estuary, as few potentially bioturbating macrofauna were observed in the mudflats during coring operations and other field activities. While interannual fluctuations in invertebrate species richness is common, the total macrofauna abundance and biomass is generally less pronounced (Beukema et al., 1993). Seasonally, a pattern of increasing invertebrate abundance has been observed

TABLE 5 | Comparison of sediment organic carbon (SOC) stocks, reported as carbon dioxide equivalents (CO₂e), in the top 1 m of Cowichan Estuary salt marsh and eelgrass meadow, mature stands in the Pacific Northwest (PNW), old- and second-growth forests of interior British Columbia, Canada.

Forest	TEC stock (Mg CO ₂ e ha ⁻¹)	SOC (30%) (Mg CO ₂ e ha ⁻¹)	SOC (50%) (Mg CO ₂ e ha ⁻¹)
Mature stands, PNW	549–828	164–248	275–414
Old growth forest, interior B.C.	237–309	71–92	119–155
Second growth forest, interior B.C.	147	44	73
Cowichan Estuary	SOC stock (Mg CO₂e ha⁻¹)	–	–
Salt marsh	215.6 ± 14.2	–	–
Upper mudflat	70.7 ± 4.4	–	–
Lower mudflat	63.5 ± 4.4	–	–
Eelgrass meadow	66.9 ± 0.6	–	–
Total	–	–	–

In the terrestrial habitats, 30–50% of carbon is stored in the soil and thus represent the upper and lower limits of SOC calculated from total ecosystem carbon stock (TECS). Forest data from Black et al., 2008.

TABLE 6 | Total annual carbon sequestration per habitat in the Cowichan Estuary compared to annual motor vehicle and B.C. resident CO₂e emission equivalents (CO₂e).

Habitat	Habitat Area (ha)	Carbon Accumulation (g CO ₂ e m ⁻² yr ⁻¹)	Cowichan habitat carbon accumulation (Mg CO ₂ e yr ⁻¹)	Annual motor vehicle emission equivalents	Annual per capita B.C. resident emission equivalents
Existing Habitat					
Salt marsh	94.6	250.3 ± 77.1	236.8 ± 72.0	15.8 ± 18.8	18.8 ± 5.8
Mudflat	251	139.5 ± 95.4	350.0 ± 217.5	52.1 ± 27.8	27.8 ± 19.0
Eelgrass	18	139.5 ± 95.4	25.1 ± 15.6	5.5 ± 3.7	2.0 ± 1.4
Total	363.40	—	612.0 ± 329.6	133.0 ± 71.6	48.6 ± 26.2
Reclaimed Habitat					
Salt marsh (agriculture)	91.7	250.3 ± 77.1	229.6 ± 70.7	49.9 ± 15.4	18.2 ± 5.6
Mudflat (Westcan Terminals)	11.09	139.5 ± 95.4	15.5 ± 10.6	3.4 ± 2.3	1.2 ± 0.8
Total including reclaimed area	466.39	—	857.0 ± 410.8	186.3 ± 89.3	68.0 ± 32.6

Separate data are shown for existing habitat and estimated areas of salt marsh and mudflat reclaimed for human use. All data except habitat area are presented as the mean ± standard error of the mean.

in late spring and early summer in temperate estuaries (Ysebaert, 2000). Sediment cores in this study were collected in May when macrofauna abundances would have likely been relatively high, yet sieved cores only occasionally produced polychaetes or crustaceans. Macrofaunal abundance may therefore be generally low in the Cowichan Estuary. Characterizing the exact role of bioturbation in sediment reworking in the Cowichan Estuary would require more detailed investigation of macrofauna species richness, biomass, and seasonal dynamics.

Cowichan Bay lacks a sill or any other geological features to shelter it from high-energy wave and current action from outside waters in the adjacent Satellite Channel. The Cowichan Estuary is exposed to strong tidal currents, and the associated mixing is known to play an important role in controlling water mass exchange (Davenne and Masson, 2001). A 1984 survey of the surface sediments of Cowichan Bay reported predominantly sandy sediments in most of the intertidal sample sites (>50–90% sand, $n = 22$ sites) and muddy sediments in the subtidal area extending into Satellite Channel (Luternauer, 1984), suggesting a hydrodynamic that favours the deposition of fine-grained sediment to the subtidal seafloor rather than within the estuary. Furthermore, Saanich Inlet, 6 km to the southeast of the Cowichan Estuary, receives the majority of its deposited terrigenous sediment from the Cowichan River *via* Satellite Channel (Gucluer and Gross, 1964). Erosion and/or export in the Cowichan Estuary may be enhanced by its many secondary tributary channels, as similar high sand content and deposition of coarse particles have been noted in sediment columns collected close to estuarine channels that are influenced by increased hydrodynamic energy conditions and tidal currents (Boldt et al., 2013; Nayak et al., 2018).

The observed patterns of decreasing total photosynthetic pigments, chl *a*, and chl *a*/phaeopigment ratios with depth at all stations offer insight into the relative time scales for the proposed hydrodynamic sediment mixing. Chlorophyll *a* is an indicator of fresh, recently produced and labile organic material (Gacia et al., 2002), as opposed to ²¹⁰Pb_{ex} and bulk sediment organic matter that degrade over longer periods of time (Fry et al., 1977; Arias-Ortiz et al., 2018). As such, deposited chl *a* is likely degrading in the

sediment faster than the sediment is being mixed vertically, resulting in a vertical decrease in chl *a* despite evidence of mixing in the profiles of sediment OC and other bulk properties (Figure 8). In both the datable sediment cores from the vegetated habitats and the non-datable cores from the mudflats, ²¹⁰Pb_{ex} activity was detectable to a depth of 28 cm, except for a lower mudflat core that lacked ²¹⁰Pb_{ex} activity below 14 cm. This depth threshold for ²¹⁰Pb_{ex} activity suggests the effects of sediment mixing in the mudflats do not occur deeper than 28 cm. While hydrodynamic-driven mixing does not necessarily penetrate up to 28 cm below the sediment surface, sediments at these depths have not been isolated from atmospheric input for sufficient time to produce statistically significant trends in ²¹⁰Pb_{ex} activity compared to the ~100-year-old sediment below this depth threshold. In the mudflats and eelgrass, this rate of mixing over the past ~100 year may be faster than the rate of measurable sediment OC loss, so that mixing obscures any evidence of decomposition (i.e., exponential decrease in sediment OC to the measured depth of 20 cm). In the eelgrass, the effects of hydrodynamic mixing may be dampened enough to allow for a detectable ²¹⁰Pb_{ex} decay profile to develop over the past ~100 years, but sediment instability and reworking over a longer time period prevent a sediment OC decay to develop in the anoxic sediments. As such, the establishment of photopigment decay profiles is likely to precede the rate at which mudflat sediments are mixed and measurable sediment OC decomposition can be detected. In the salt marsh, where the better defined ²¹⁰Pb_{ex} decay profile indicates more sediment stability than the eelgrass sites, the presence of refractory roots add another level of complexity to interpreting sediment OC trends since they are not expected to decay in the same manner as the more labile sediment OC in the other habitats, and furthermore involve substantial photosynthetic pumping of sediment OC to depth in the sediments (Vaughn et al., 2020).

Organic Carbon Stocks

Ecosystem organic carbon stocks in the Cowichan Estuary were dominated by sediment organic carbon which accounted for 87-

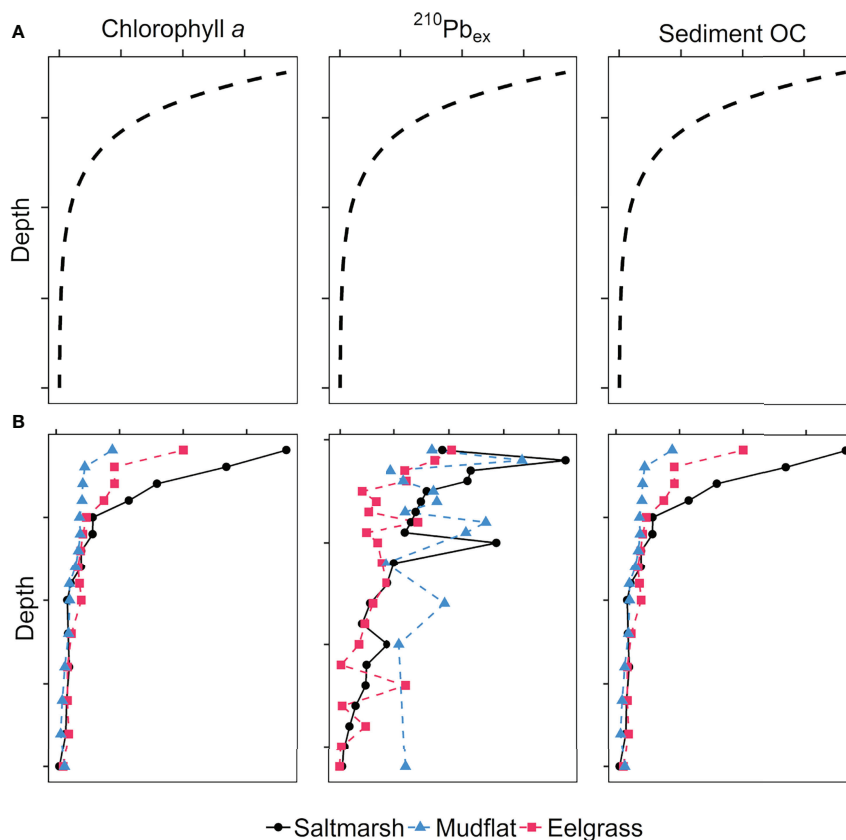


FIGURE 8 | Influence of hydrodynamic sediment mixing and relative rates of decay on profiles of chlorophyll *a*, excess ^{210}Pb , and bulk sediment organic carbon (OC) in deposited sediments in an intertidal system. Panel (A) shows idealized depth profiles with steady-state sediment accumulation where hydrodynamic mixing is minimal, resulting in exponential decay of (1) chlorophyll *a* followed by (2) excess ^{210}Pb and (3) organic matter decomposition; Panel (B) shows typical depth profiles in a system like the Cowichan Estuary where physical mixing is strong on unvegetated mudflats (dashed blue profiles), and dampened increasingly by eelgrass (dashed red profiles) and salt marsh vegetation (solid black profiles).

100% of total organic carbon stocks in the different habitats. Above- and belowground macroscopic plant material was not the primary contributor to ecosystem carbon stocks in either of the vegetated habitats. The high organic carbon concentrations in the salt marsh sediments resulted in a total area-integrated carbon stock that was approximately equal to that of the upper and lower mudflats combined, despite the spatial extent of the salt marsh being only about one third that of the mudflats. A substantially higher amount of plant biomass was observed in the saltmarsh compared to the eelgrass, especially in the root material. The eelgrass had a shoot: root ratio of approximately one, whereas the salt marsh had nearly five times as much macroscopic root biomass as aboveground herbaceous plant material, consistent with other studies reporting similar high belowground compared to aboveground salt marsh biomass (Valiela et al., 1976; Valiela et al., 1978; Tripathee and Schäfer, 2014). In salt marsh sediments, root material too fine to be separated from the sediment likely contributed to the high organic matter and low bulk density in cores, relative to the other habitats (Turner et al., 2004).

Salt marsh sediment organic carbon stocks were in the middle of the range reported for similar habitats globally (Table 1), with

the exception of some values reported for coastal Australian salt marshes, which were up to eight times higher than reported here (Macreadie et al., 2017b). Closer to the Cowichan Estuary, a multi-site blue carbon survey in the US Pacific Northwest yielded average salt marsh carbon stock estimates similar to ours (Kauffman et al., 2020). That study also separately sampled low marsh and high marsh areas, and reported 37% greater carbon stocks in high marsh compared with low marsh sediments. All of our saltmarsh cores from the Cowichan Estuary were collected from the lower marsh, which is predominantly populated by Lyngbye's sedge and submerged at high tide. Extrapolations to the entire salt marsh area may not accurately represent carbon storage nearer the riparian zone where bulrush (*Typha* sp., *Bolboschoenus maritimus*), and cordgrass (*Spartina patens*) are more abundant.

Compared to global averages for seagrasses, eelgrass carbon stocks measured here were low. However, such comparisons should be made with caution since global data are disproportionately dominated by tropical and subtropical seagrass species such as *Posidonia oceanica*, which can form thick, dense mats of roots and rhizomes and sequester orders of

magnitude more carbon (Mateo et al., 1997; Gacia et al., 2002; Serrano et al., 2012). Other studies of temperate *Z. marina* meadows have reported average sediment organic carbon concentrations, carbon stocks, and sequestration rates (Table 1 and Table 7) similar to what we observed in the Cowichan Estuary (Ruesink et al., 2010; Yang et al., 2013 and Ruesink et al., 2015). Several species-specific morphologies and habitat requirements have been proposed to explain low sediment organic carbon stocks in *Z. marina* meadows, including a low tolerance by the plant of sediment organic matter accumulations (Barko and Smart, 1983; Batiuk et al., 2000), sub-optimal light conditions in many temperate ecosystems, as well as seasonal *Z. marina* biomass patterns (Laugier et al., 1999). In a compilation of data from multiple studies worldwide, Fourqurean et al. (2012a) showed that the large majority of *Z. marina* are found in sediments with low organic carbon levels (average 2.5%). Whatever the underlying reason(s), our results agree with a growing literature consensus that low carbon stocks in *Z. marina* meadows are not anomalous but rather represent the carbon sequestration capacity of healthy *Z. marina*.

Despite low carbon burial levels, high annual rates of net primary productivity (NPP) have been reported for *Z. marina* in nearby Puget Sound, WA (Thom, 1990). Part of this discrepancy can be explained by high rates of decomposition (Kairis and

Rybczyk, 2010) and export of plant material. Since NPP in seagrass meadows is often greater than can be degraded or stored within the system, particulate and dissolved OC may be exported to adjacent coastal seawaters and sediments in a process known as “outwelling” (Odum and de la Cruz, 1967; Meziane et al., 1997; Meziane and Tsuchiya, 2000). Leaf shedding, which can be enhanced during strong hydrodynamic events (Cebrián, 2002), can cause aquatic macrophytes like *Z. marina* to export nutrient-rich detritus to neighbouring coastal systems (Pollard and Moriarty, 1991). In the K’ómoks Estuary on Vancouver Island, eDNA analysis revealed sloughed *Z. marina* material persisting along the approximately 500 m long wrack line, a fronting saltmarsh and a non-seagrass vegetated area (Hintz et al., 2016). Grazing and movement of macrobenthos such as crustaceans and snails also facilitate export of primary products, littoral particulate organic matter and biodeposits (Kharlamenko et al., 2001). Duarte and Cebrian (1996) reviewed carbon budgets for a variety of coastal habitats and estimated that seagrass ecosystems on average export 24.3% of their total NPP, with 50.3% lost to decomposition, 18.6% to herbivory, and only 15.9% stored in seagrass bed sediments.

To further investigate the effect of losses from outwelling, decomposition and herbivory on the carbon sequestration capacity of *Z. marina* in the Cowichan Estuary we applied a

TABLE 7 | Global sediment OC (SOC) sequestration rates reported for salt marshes and seagrasses globally, and carbon sequestration rates reported for *Z. marina* in the Northern Hemisphere.

Location	SOC sequestration (g C m ⁻² yr ⁻¹)	Reference
Global salt marshes	218 ± 24 (range = 18-1713) n = 96 sites	Chmura et al. (2003) Duarte et al. (2005) McLeod et al. (2011)
Cowichan Estuary salt marsh	74 ± 23	This study
Global Seagrasses	138 ± 38 (range = 45-190) n = 123 sites	Duarte et al. (2005) McLeod et al. (2011) Duarte et al. (2010) Kennedy et al. (2010)
Zostera marina meadows		
K’ómoks, British Columbia	3.0	Spooner (2015)
K’ómoks, British Columbia	5.0	Spooner (2015)
K’ómoks, British Columbia	13.0	Spooner (2015)
Finland	5.2	Röhr et al. (2016)
Limfjorden, Denmark	21.3	Röhr et al. (2016)
Funen, Denmark	49.1	Röhr et al. (2016)
Denmark	35.2	Röhr et al. (2016)
Padilla Bay, Washington	9.14 ± 0.59	Poppe and Rybczyk (2018)
Padilla Bay, Washington	11.34 ± 1.74	Poppe and Rybczyk (2018)
Seto Inland Sea, Japan	3.13	Miyajima et al. (2015)
Seto Inland Sea, Japan	7.10	Miyajima et al. (2015)
Seto Inland Sea, Japan	10.14	Miyajima et al. (2015)
Delmarva Peninsula, Virginia	36.68	Greiner et al. (2013)
Burnaby, British Columbia	33.98	Prentice et al. (2019)
Burnaby, British Columbia	36.74	Prentice et al. (2019)
Burnaby, British Columbia	3.47	Prentice et al. (2019)
Clayoquot Sound, B.C.	2.90-39.61	Postlethwaite et al. (2018)
Skagit County, Washington	43.88 ± 9.19	Lutz (2018)
Gulf of Gdańsk, Baltic Sea	0.84 ± 0.16	Jankowska et al. (2016)
Gulf of Gdańsk, Baltic Sea	2.78 ± 0.28	Jankowska et al. (2016)
Gulf of Gdańsk, Baltic Sea	3.85 ± 1.15	Jankowska et al. (2016)
Cowichan Estuary, Canada	38 ± 26	This study

two-source mixing model (Phillips and Gregg 2003; Limén et al., 2007) to our $\delta^{13}\text{C}$ data. The model enabled us to quantify the contribution of eelgrass tissue (shoots) to organic matter in the eelgrass sediments. The two $\delta^{13}\text{C}$ endmembers were eelgrass shoots (-12.2‰) and organic carbon in lower mudflat sediments (-25.8‰) that was sampled outside of the eelgrass meadow (Table 4). The percentage contribution of eelgrass shoots to sediment organic carbon in the eelgrass meadow was determined by solving for x in the following equation:

$$\delta^{13}\text{C}Sed_{eg} = 1 - x(\delta^{13}\text{C}Sed_{lm}) + x(\delta^{13}\text{C}EG_{sh})$$

Sed_{eg} , sediment in eelgrass meadow; Sed_{lm} , lower mudflat sediment; EG_{sh} , eelgrass shoots. The mixing model result indicated that 23.4% of the organic carbon in the eelgrass sediment could come from eelgrass shoots, with the remaining 77% from other sources, the same sources supplying the lower mudflat sediments outside of the eelgrass meadow. Eelgrass roots had a similar $\delta^{13}\text{C}$ signature (-12.0‰) to shoots and yielded a nearly identical result (23.2% contribution) when used in the mixing model in place of eelgrass shoots.

The non-depositional nature of the mudflat sediments may account for the observed lower carbon stocks compared with global averages. Several publications have reported sequestration capacities of intertidal mudflats to be comparable to adjacent vegetated habitats (Sanders et al., 2010; Phang et al., 2015). For example, Phang et al. (2015) reported nearly equal carbon stocks in seagrasses (138 Mg C ha^{-1}) and mudflats ($124\text{--}143 \text{ Mg C ha}^{-1}$) in a Singaporean estuary. In the Cowichan Estuary, a considerable portion of organic matter that would accumulate on the mudflats under less vigorous hydrodynamic conditions, may instead be exported and deposited elsewhere, such as on the subtidal seafloor in outer Cowichan Bay, where accumulations of fine-grained sediment have been noted (Luternauer, 1984).

Carbon Sequestration Rates in Vegetated Habitats

The sediment accretion rates determined from the ^{210}Pb profiles in cores from the vegetated habitats, together with corresponding sediment carbon density measurements, permitted the calculation of carbon accumulation rates for the seagrass meadow and the salt marsh in the Cowichan Estuary. The generally low levels of excess ^{210}Pb in sediments of these two habitats introduce a degree of uncertainty, and differences in sedimentation rates between the salt marsh and the eelgrass meadow should be interpreted with caution.

The higher organic carbon content of the salt marsh sediments in Cowichan Estuary resulted in this habitat having a higher carbon accumulation rate ($68.2 \pm 21 \text{ g C m}^{-2} \text{ yr}^{-1}$) than the eelgrass ($38 \pm 26 \text{ g C m}^{-2} \text{ yr}^{-1}$), despite having a slightly lower sediment accretion rate and mass accumulation rates (Table 2). The salt marsh carbon accumulation rate reported here is approximately one third of the global average (Table 1). However, there is a wide range of carbon sequestration rates in salt marshes in the global data set (18 to $1713 \text{ g C m}^{-2} \text{ yr}^{-1}$), and an underrepresentation of saltmarshes within the Pacific Northwest climate zone (Kauffman et al., 2020).

The average carbon accumulation rate estimated for the eelgrass meadow ($38 \pm 26 \text{ g C m}^{-2} \text{ yr}^{-1}$) was below the range reported globally for all seagrass species (45 to $190 \text{ g C m}^{-2} \text{ yr}^{-1}$) but comparable to or higher than average carbon sequestration rates reported in other *Z. marina* meadows (Table 7). Spooner (2015) reported *Z. marina* carbon accumulation rates three times lower (ranging from 0 to $13 \text{ g C m}^{-2} \text{ yr}^{-1}$) in the K'ómoks Estuary on Vancouver Island, located 170 km north of the Cowichan Estuary. Similarly, carbon accumulation rates of 3.13 to $11 \text{ g C m}^{-2} \text{ yr}^{-1}$ have been found in *Z. marina* meadows in Japan (Miyajima et al., 2015) and Padilla Bay, Washington State (Poppe and Rybczyk, 2018). Greiner et al. (2013) measured a carbon accumulation rate of $36.68 \text{ g C m}^{-2} \text{ yr}^{-1}$ *Z. marina* meadow in coastal bays of the US state of Virginia which had undergone restoration.

Blue Carbon Sources in the Cowichan Estuary

Between-habitat comparisons of sediments photosynthetic pigment concentrations, C:N ratios and $\delta^{13}\text{C}$ values provide some insights into the primary sources of organic carbon stocks for each habitat.

Beginning with the unvegetated upper and lower mudflats, we interpret the contrasting photopigment profiles between the two habitats to indicate that the upper mudflat had a more developed microphytobenthos than the lower mudflat. This is consistent with other studies that report a positive relationship between MPB biomass and emersion duration due to the increased exposure to favourable ambient conditions (i.e., light, warm temperatures, gas exchange into/out of biofilms) for MPB photosynthesis within the upper intertidal zone (van der Wal et al., 2010; Schnurr et al., 2020). In addition, in surface sediments (upper 1 cm), where microphytobenthos would be concentrated, chl *a*/phæopigment ratios were highest in the upper mudflat compared to all other habitats including the saltmarsh, indicating fresher OM in the upper mudflat relative to other habitats in the estuary. In contrast, the lower mudflat had the lowest total photopigment and chl *a* concentrations and the lowest chl *a*/phæopigment ratios. Microphytobenthos biomass in the Cowichan Estuary mudflats is low compared to similarly sandy estuarine sediments in the region. Ten cm depth-integrated chl *a* values in the Cowichan Estuary, converted from concentration per unit sediment dry weight calculations, were $377 \pm 53 \text{ mg m}^{-2}$ ($177\text{--}539$) in the upper mudflats and $207 \pm 34 \text{ mg m}^{-2}$ ($132\text{--}310$) in the lower mudflats. In contrast, Yin et al. (2016) reported 10 cm depth-integrated chl *a* values averaging $2,044 \text{ mg m}^{-2}$ ($160\text{--}4,200$) and 882 mg m^{-2} ($183\text{--}2,569$) at two sandy sites in the Fraser River Estuary (across the Strait of Georgia from the Cowichan Estuary), much higher than at two muddy sites in the Fraser River Estuary, which had average chl *a* concentrations of 84 mg m^{-2} ($41\text{--}174$) and 235 mg m^{-2} ($77\text{--}854$).

The extremely high C:N ratios ($\text{C:N} \geq 190$) of woody debris samples collected from mudflat sediments could have provided a means of identifying potential contributions of woody debris from log storage activity to sediment carbon storage in the

estuary. However, there were no significant differences (Welch's t-test, $p = 0.68$) in C:N ratios between the lower mudflat sediments (12.2 ± 1.1), where log boom activity was located, and sediments of the upper mudflat (11.7 ± 0.6). This observation excludes woody debris from log storage as a significant contributor to carbon storage in the estuary.

Consideration of only C:N ratios in salt marsh samples could lead to the conclusion that nitrogen-poor root material was likely responsible for the salt marsh sediments having the highest C:N ratio (20.0 ± 0.8) of all habitats. Sampled, larger pieces of macroscopic root material had a notably high C:N ratio (64.2 ± 8.84). However, a similar influence of the distinct $\delta^{13}\text{C}$ signature of root material (-22.1 ± 1.45) was not apparent in the salt marsh sediment $\delta^{13}\text{C}$ signature (-26.5 ± 0.1), which was indistinguishable from that of the aboveground saltmarsh vegetation (-25.6 ± 3.04). This leads us to suggest that our analysis of macroscopic root material may not have captured the stable isotope and C:N properties of the visibly abundant fine root material that was likely responsible for the high water and carbon contents of the salt marsh sediments. Compared to the other habitats, salt marsh sediment also had a $\delta^{13}\text{C}$ signature that was the most consistent with terrestrial vascular plant material, which is generally between -25‰ and -28‰ (Burdige, 2005). As such, the Lyngbye's sedge (*Carex lyngbyei*) growing on the lower salt marsh where we collected cores is a C_3 plant and likely a dominant source of the refractory, terrestrially derived material found in the salt marsh sediment.

Sediments in the eelgrass meadow were nitrogen rich (C:N = 10.9 ± 1.2), in comparison to samples of eelgrass shoots and roots whose C:N ratios were respectively 16.1 ± 1.08 and 38.7 ± 0.6 , consistent with reported values for *Z. marina* leaf biomass (C:N ratio = 19.7) and root-rhizome biomass (C:N ratio = 31.62) (Duarte, 1990; Pedersen and Borum, 1992; Fourqurean et al., 1997). The lower C:N ratio in the Cowichan Estuary eelgrass meadow sediments likely result from limited burial of *Z. marina* debris and a predominant input of the same nitrogen-rich, marine-derived material (microphytobenthos and phytoplankton) that accumulates in the mudflat sediments.

As discussed above, the stable isotope data indicate that eelgrass tissues make a minor but notable contribution to blue carbon storage in the eelgrass meadow. We were able to make this determination because of the enriched $\delta^{13}\text{C}$ signature of eelgrass shoots and roots, compared with other potential carbon sources in the estuary. As a polyphyletic group of aquatic angiosperms with C_3 or $\text{C}_3\text{-C}_4$ intermediate metabolisms (Touchette and Burkholder, 2000), seagrasses have much heavier isotopic signatures than terrestrial C_3 plants (Peterson and Fry, 1987), ranging from -23‰ to -3‰ (Hemminga and Mateo, 1996). *Z. marina* in particular generally has high ^{13}C enrichment, with $\delta^{13}\text{C}$ values in the range of -7 to -12‰ in leaves and rhizomes (Kim et al., 2014; McPherson et al., 2015), which are typically heavier than values reported for marine phytoplankton ($-22 \pm 3\text{‰}$) and marine macroalgae (-20‰ to -15‰), and MPB ($-17 \pm 4\text{‰}$) (France, 1995). The end member isotopic signatures for *Z. marina* shoot and roots here were

respectively $-12.2 \pm 0.80\text{‰}$ and $-12.0 \pm 0.24\text{‰}$. It is more likely that organic matter in the eelgrass sediment originates from a mixture of marine microalgae (phytoplankton and MPB), with a possible but less significant input of terrestrially-derived OM.

Sediment and Oyster Bed Inorganic Carbon Stocks

Particulate inorganic carbon (PIC) in the form of calcium carbonate (CaCO_3) often accumulates in the sediments of blue carbon ecosystems in addition to photosynthesized particulate organic carbon (POC) (Macreadie et al., 2017c). While PIC can represent a substantial carbon stock, the precipitation CaCO_3 can result in the depletion of carbonate (CO_3^{2-}) and reduction of total alkalinity (TA) in the water column, facilitating the return of CO_2 to the atmosphere (Ware et al., 1992; Saderne et al., 2019). Specifically, the production of one mole of CaCO_3 consumes two moles of TA and one mole of dissolved inorganic carbon (DIC), thereby increasing the partial pressure of carbon dioxide ($p\text{CO}_2$) and potentially resulting in CO_2 supersaturation and increased flux to the atmosphere. Because of this, there is concern that CaCO_3 precipitation partially offsets the sequestration of OC in blue carbon ecosystems and the current, rapid expansion of blue carbon scientific literature and CO_2 offset schemes report only organic carbon while omitting calcium carbonate cycling and sequestration (Macrae et al., 2017b).

The relationship between carbonate precipitation results and net release of CO_2 is defined as the molar ratio of CO_2 flux: CaCO_3 precipitation (Ψ) (Frankignoulle et al., 1994; Mazarrasa et al., 2015). Shallow-water coastal ecosystems may accumulate approximately two thirds of precipitated CaCO_3 in the benthic sediments, theoretically acting as net CO_2 sources with equal Ψ values for CaCO_3 precipitation and dissolution. However, the strong net primary production in these coastal areas may compensate for increases in $p\text{CO}_2$ due to calcification with the uptake of CO_2 during organic matter production. The sediments of the Cowichan Estuary habitat were generally dominated by sediment OC relative to sediment IC, and had sediment OC: sediment IC ratios of 9.80 ± 0.95 in the salt marsh, 2.99 ± 0.44 and 1.78 ± 0.18 in the upper and lower mudflats, and 1.87 ± 0.11 in the eelgrass meadow. Assuming that organic carbon and calcium carbonate accumulate in the sediment in proportion to their production, these high ratios indicate primary production is more than compensating for the calcification-associated CO_2 production in most of the estuary's habitats (Mazarrasa et al., 2015). In contrast, the oyster shell bed sediments had Ψ value of 0.62 ± 0.05 , suggesting that they act as a source of CO_2 . However, because the oyster beds account for less than 2% of the total area of the estuary, this venting of CO_2 can be considered negligible. Oyster shell beds growing on similar gravel banks from sandy intertidal flats with low sediment OC have been reported as net sources of CO_2 , resulting from predominantly carbonate deposition, whereas shallow subtidal saltmarsh fringing reefs with organic-carbon-rich sediments functioned as net carbon sinks, on par with vegetated coastal habitats (Fodrie et al., 2017).

Blue Carbon Valuation

The growing interest in blue carbon in recent decades has been founded on the widely reported high carbon sequestration capacities of coastal ecosystems, often estimated to be orders of magnitude greater than terrestrial ecosystems per unit area (Duarte et al., 2005; Mcleod et al., 2011; Atwood et al., 2020). Seagrass meadows have been reported to have global sequestration rates up to 35 times higher than temperate and tropical forests (Orth et al., 2006; Mcleod et al., 2011). Annual per-hectare sediment OC accumulation rates in the Cowichan Estuary were below global averages for each habitat examined, and the estuary as a whole sequesters carbon at approximately 30% that of an estuary of equal size and composition with global average sequestration rates for each habitat (**Table S4**). Compared to B.C. forests, the Cowichan Estuary, at 363 ha in size, stores about as much carbon in the top 20 cm of sediment as a second-growth forest in B.C. approximately 1.7 times larger in area (619 ha) and accumulates carbon at a rate between 1.39 ± 0.95 and $2.50 \pm 0.77 \text{ Mg C ha}^{-1} \text{ yr}^{-1}$, approximately equivalent of a 20-year-old stand forest.

Current annual sediment OC burial in the Cowichan Estuary is approximately equal to the annual GHG emission of 133 motor vehicles or 48 British Columbia residents (**Table 6**). The population of Cowichan Bay Village is 2,394 (City Population, 2020), meaning that the estuary can only offset the emissions produced by 2.05% of the local population per year. At the municipal level, current carbon sequestration in the Cowichan estuary offsets approximately twice the GHG emission increases from the 0.9% annual population growth of the Municipality of North Cowichan's 29,676-person population (Statistics Canada, 2017). If the historical extents of the salt marsh and mudflat were restored and the reclaimed sawmill, farms, and causeway were made available for carbon sequestration, the resulting carbon sequestration would increase to be equivalent to the annual emissions of 186 motor vehicles and 68 residents, or 2.8% of Cowichan Bay Village, and over GHG emission increases from the annual municipal population growth. The apparently small capacity of the Cowichan Estuary to mitigate anthropogenic GHG emissions even from local sources in a small rural village cannot be solely attributed to its below-average carbon sequestration rates. Even if each habitat in the Cowichan Estuary were to sequester carbon at reported average global rates, with the entire area of mudflat sequestering at the global average rate for seagrass meadows (**Table S3**), the equivalent emissions of only 461 motor vehicles and 168 people, or 14.25% of the local population, would be offset. Based on the estimations outlined in this valuation, over 20,000 ha of 20-year-old stand forest or a Cowichan Estuary more than 50 times its current size (363 ha) would be required to offset the emissions of Cowichan Bay Village. As such, preserving the areal extent of the Cowichan Estuary and restoring vegetated habitat should be prioritized in order to maintain and maximize its capability to offset GHG emissions. This highlights the current unsustainable level of per-capita GHG emissions, even at the scale of the local population in Cowichan Bay Village, which far exceed the natural capacity of

the estuary and other natural carbon reservoirs to trap and store greenhouse gasses.

CONCLUSIONS

The lack of a sill or any other geological feature preventing high-energy water exchange between the Cowichan Estuary and the open ocean likely results in strong hydrodynamic mixing, erosion, resuspension and/or export or deposited OM. This was reflected in the low sediment OC and scattered $^{210}\text{Pb}_{\text{ex}}$ vertical profiles of the unvegetated mudflats. Like the salt marsh, the eelgrass vegetation buffers hydrodynamic forces, stabilizing deposited material enough for an exponential decrease in $^{210}\text{Pb}_{\text{ex}}$ to be detected over a ~100 year period, but mixing and possible resuspension is still likely to occur on a broader timescale.

Our results point to epiphytobenthos and phytoplankton as the primary sources of organic carbon stored in the upper and lower mudflats and eelgrass sediments. This is evident in the similarly low C:N ratios, suggestive of labile cell material, and the marine stable isotope signatures in the upper and lower mudflat sediments, which are modified somewhat in the eelgrass sediments. The strong hydrodynamic and related outwelling of eelgrass material are also likely behind the modest contribution (23%) of eelgrass shoots and stems to the bulk ^{13}C signature of eelgrass sediments. A blue carbon evaluation of the subtidal area of outer Cowichan Bay would be of great interest for future research.

We found no evidence that log storage activity decreased carbon sequestration in the lower mudflat areas where logs make frequent contact with the seafloor. Carbon stocks in the mudflats were similar to those of the eelgrass meadow, despite being lower than global averages but consistent with recently reported low carbon stocks in *Z. marina* meadows in the Pacific Northwest. The salt marsh was the most important carbon reservoir in the Cowichan Estuary, which is consistent with a large body of studies that report salt marshes as having the highest carbon sequestration rates of all intertidal blue carbon habitats. However, the Cowichan Estuary salt marsh has a more modest carbon sequestration capacity compared to global averages; while the Cowichan estuary salt marsh's sequestration capacity is in the range of a 20-year-old forest stand, global average salt marsh carbon sequestration rates have been reported to exceed long-term accumulation rates in forests by many orders of magnitude (Zehetner, 2010; Mcleod et al., 2011). This point highlights the lack of temperate salt marsh representation in western North America in current global blue carbon estimates. Since approximately half of the historical salt marsh habitat in the Cowichan Estuary is currently reclaimed for agricultural and industrial use, consideration should be given to the role of the marsh system as a carbon reservoir in future land-use planning.

CO_2 emissions derived from carbonate deposition in the Cowichan Estuary are unlikely to significantly offset the CO_2 sink capacity associated with organic carbon burial. Sediment OC was generally three-fold higher than sediment IC. While the

oyster shell beds appear to be a net source of CO₂, they were very limited in overall area. Interestingly, the current area of oyster beds in the Cowichan Estuary represented a fraction of the former area, as a result of dredging of channels for moving logs from the lower intertidal zone to the sawmill.

Despite being the fourth largest estuary on Vancouver Island and the largest intertidal estuary in the Municipality of North Cowichan, the Cowichan Estuary can only offset the emissions produced by 2.05% of the local population of 2,394 in Cowichan Bay Village (City Population, 2020), highlighting the current unsustainable level of per-capita GHG emissions. Likewise, the Cowichan Estuary cannot significantly offset the emissions of the municipality's 29,676-person population, which is growing 0.9% per year. Current carbon sequestration in the Cowichan Estuary offsets approximately twice the GHG emission increases from the annual population growth Municipality of North Cowichan, and if all habitats were restored to their natural state and sequestered carbon at current rates, the estuary could have the capacity to offset over three times the GHG emission increases from the annual population growth. As such, preserving the areal extent of the Cowichan Estuary and restoring vegetated habitat should be prioritized in order to maintain and maximize its capability to offset GHG emissions.

DATA AVAILABILITY STATEMENT

The raw data supporting the conclusions of this article will be made available by the authors, without undue reservation.

AUTHOR CONTRIBUTIONS

TD contributed to conceptualization, fieldwork designing, laboratory methodology, investigation, writing the original

draft, data processing, statistical analyses, review and editing, and geospatial analysis. GS contributed to conceptualization, project administration, supervision, review and editing. SJ contributed to conceptualization, supervision, laboratory methodology, fieldwork designing, investigation, review and editing. All authors contributed to the article and approved the submitted version.

FUNDING

Funding for radiometric dating lab analyses was provided by the Cowichan Valley Regional District (CVRD) and the Cowichan Estuary Restoration and Conservation Association (CERCA). Funding for habitat mapping was funded by CERCA and the Fisheries and Oceans Canada (DFO). All other funding was provided by Ocean Networks Canada (ONC) and the BC Leadership Chair in Ocean Ecosystems and Global Change for their financial contributions.

ACKNOWLEDGMENTS

The authors thank S. Murdock, C.J. Stevens, B.D. Jameson, and V. Carnero-Bravo their technical assistance, and the Cowichan Estuary Restoration and Conservation Association for their support and collaboration. Special thanks to Grant Douglas for his assistance with the design and construction of field equipment.

SUPPLEMENTARY MATERIAL

The Supplementary Material for this article can be found online at: <https://www.frontiersin.org/articles/10.3389/fmars.2022.857586/full#supplementary-material>

REFERENCES

- Admiraal, W. (1984). The Ecology of Estuarine Sediment-Inhabiting Diatoms. *Prog. Phycol. Res.* 3, 269–322. doi: 10.1017/S0025315400019603
- Alongi, D. M., Tirendi, F., and Goldrick, A. (1996). OM Oxidation and Sediment Chemistry in Mixed Terrigenous-Carbonate Sands of Ningaloo Reef, Western Australia. *Marine Chem.* 54 (3–4), 203–219. doi: 10.1016/0304-4203(96)00037-0
- Arias-Ortiz, A., Masqué, P., Masqué, P., Masqué, P., Masqué, P., Garcia-Orellana, J., et al. (2018). Reviews and Syntheses: 210Pb-Derived Sediment and Carbon Accumulation Rates in Vegetated Coastal Ecosystems – Setting the Record Straight. *Biogeosciences* 15, 6791–6818. doi: 10.5194/bg-15-6791-2018
- Atwood, T. B., Witt, A., Mayorga, J., Hammill, E., and Sala, E. (2020). Global Patterns in Marine Sediment Carbon Stocks. *Front. Marine Sci.* 7 (10), 3389. doi: 10.3389/fmars.2020.00165
- Barko, J. W., and Smart, R. M. (1983). Effects of OM Additions to Sediment on the Growth of Aquatic Plants. *J. Ecol.* 71 (1), 161–175. doi: 10.2307/2259969
- Barranguet, C., Herman, P. M. J., and Sinke, J. J. (1997). Microphytobenthos Biomass and Community Composition Studied by Pigment Biomarkers: Importance and Fate in the Carbon Cycle of a Tidal Flat. *J. Sea Res.* 38, 59–70. doi: 10.1016/S1385-1101(97)00032-4
- Batiuk, R., Bergstrom, P., Kemp, M., Koch, E., Murray, L., Stevenson, C., et al. (2000). *Chesapeake Bay Submerged Aquatic Vegetation Water Quality and*
- Habitat-Based Requirements and Restoration Targets: A Second Technical Synthesis* (Annapolis, MD: US. EPA).
- Bell, M., and Kallman, R. (1976). *The Cowichan – Chemainus River Estuaries Status of Environmental Knowledge to 1975. Report of the Estuary Working Group Department of the Environment Regional Board Pacific Region* (West Vancouver, B. C: Fisheries and Marine Service Pacific Environment Institute).
- Bentley, S. J., Swales, A., Pyenson, B., and Dawe, J. (2014). Sedimentation, Bioturbation, and Sedimentary Fabric Evolution on a Modern Mesotidal Mudflat; a Multi-Tracer Study of Processes, Rates, and Scales. *Estuarine Coastal Shelf Sci.* 141, 58–68. doi: 10.1016/j.ecss.2014.02.004
- Bernal, B., and Mitsch, W. J. (2013). Carbon Sequestration in Freshwater Wetlands in Costa Rica and Botswana. *Biogeochemistry* 115 (1), 77–93. doi: 10.1007/s10533-012-9819-8
- Berner, R. A. (1980). *Early Diagenesis: A Theoretical Approach* (Princeton, USA: Princeton University Press), 245 pp.
- Beukema, J. J., Essink, K., Michaelis, H., and Zwarts, L. (1993). Year-To-Year Variability in the Biomass of Macrobenthic Animals on Tidal Flats of the Wadden Sea: How Predictable Is This Food Source for Birds? *Netherlands J. Sea Res.* 31 (4), 319–330. doi: 10.1016/0077-7579(93)90051-S
- Black, T. A., Jassal, R. S., Fredeen, A. L. Canadian Electronic Library (Firm), & University of Victoria (B.C.) Pacific Institute for Climate Solutions (2008). *Carbon Sequestration in British Columbia's Forests and Management Options* (Victoria, B.C: Pacific Institute for Climate Solutions, University of Victoria).

- Blanchard, G. F., Paterson, D. M., Stal, L. J., Richard, P., Galois, R., Huet, V., et al. (2000). The Effect of Geomorphological Structures on Potential Biostabilisation by Microphytobenthos on Intertidal Mudflats. *Continental Shelf Res.* 20, 1243–1125. doi: 10.1016/S0278-4343(00)00021-2
- Boldt, K. V., Nittrouer, C. A., and Ogston, A. S. (2013). Seasonal Transfer and Net Accumulation of Fine Sediment on a Muddy Tidal Flat: Willapa Bay, Washington. *Continental Shelf Res.* 60, S157–S172. doi: 10.1016/j.csr.2012.08.012
- Burdige, D. J. (2005). Burial of Terrestrial OM in Marine Sediments: A Reassessment. *Glob. Biogeochem.* 19 (4), 1–7. doi: 10.1029/2004GB002368
- Business Council of British Columbia. (2019). Available at: https://bcbc.com/insights-and-opinions/per-capita-emissions-what-does-it-really-mean#_ftn5.
- Cahoon, L. B. (1999). The Role of Benthic Microalgae in Neritic Ecosystems. *Oceanographic Marine Biol.* 37, 47–86. doi: 10.1201/9781482298550-4
- Cahoon, L. B., and Safi, K. A. (2002). Distribution and Biomass of Benthic Microalgae in Manukau Harbour, New Zealand, NZ. *J. Mar. Freshw. Res.* 36, 257–266. doi: 10.1080/00288330.2002.9517084
- Callaway, J. C., Borgnis, E. L., Turner, R. E., and Milan, C. S. (2012). Carbon Sequestration and Sediment Accretion in San Francisco Bay Tidal Wetlands. *Estuaries Coasts* 35 (5), 1163–1181. doi: 10.1007/s12237-012-9508-9
- Campbell, J. E., Lacey, E. A., Decker, R. A., Crooks, S., and Fourqurean, J. W. (2015). Carbon Storage in Seagrass Beds of Abu Dhabi, United Arab Emirates. *Estuaries Coasts* 38, 242–251. doi: 10.1007/s12237-014-9802-9
- Cebrián, J. (2002). Variability and Control of Carbon Consumption, Export, and Accumulation in Marine Communities. *Limnol. Oceanogr.* 47, 11–22. doi: 10.4319/lo.2002.47.1.0011
- Chmura, G. L., Anisfeld, S. C., Cahoon, D. R., and Lynch, J. C. (2003). Global Carbon Sequestration in Tidal, Saline Wetland Soils. *Glob. Biogeochem.* 17, 1111. doi: 10.1029/2002GB001917
- City Population (2020). Available at: https://www.citypopulation.de/en/canada/britishcolumbia/_/UA1410:cowichan_bay/.
- Cook, P. L. M., Revill, A. T., Clementson, L. A., and Volkman, J. K. (2004). Carbon and Nitrogen Cycling on Intertidal Mudflats of a Temperate Australian Estuary: III. Sources of OM. *Marine Ecology. Prog. Ser. (Halstenbek)* 280, 55–72. doi: 10.3354/meps280055
- Coverdale, T. C., Brisson, C. P., Young, E. W., Yin, S. F., Donnelly, J. P., and Bertness, M. D. (2014). Indirect Human Impacts Reverse Centuries of Carbon Sequestration and Salt Marsh Accretion. *PLoS One* 2014 (3), e93296. doi: 10.1371/journal.pone.0093296
- Cowichan Estuary Task Force. (1980). *Cowichan Estuary Task Force Report* (Victoria, BC, Province of British Columbia: Environment and Land Use Committee Secretariat).
- Cowichan Tribes. (2010). *Proceedings of the Cowichan Tribes Estuary Workshop*. Available at: <https://cowichanwatershedboard.ca/document/doc-cowichan-tribes-estuary-workshop-may-2010-proceedings/>.
- Cuellar-Martinez, T., Ruiz-Fernández, A. C., Sanchez-Cabeza, J., Pérez-Bernal, L., and Sandoval-Gil, J. (2019). Relevance of Carbon Burial and Storage in Two Contrasting Blue Carbon Ecosystems of a North-East Pacific Coastal Lagoon. *Sci. Total Environ.* 675, 581–593. doi: 10.1016/j.scitotenv.2019.03.388
- Dale, C., and Natcher, D. C. (2015). What Is Old Is New Again: The Reintroduction of Indigenous Fishing Technologies in British Columbia. *Dalen Environ.* 20 (11), 1309–1321. doi: 10.1080/13549839.2014.902371
- Davene, E., and Masson, D. (2001). *Water Properties in the Straits of Georgia and Juan De Fuca* (Vancouver Island, British Columbia: Institute of Ocean Sciences (IOS), Fisheries and Oceans Canada).
- de Brouwer, J. F. C., Bjelic, S., de Deckere, E. M. G. T., and Stal, L. J. (2000). Interplay Between Biology and Sedimentology in a Mudflat (Biezelingse Ham, Westerschelde, The Netherlands). *Continental Shelf Res.* 20, 1159–1177. doi: 10.1016/S0278-4343(00)00017-0
- Duarte, C. M. (1990). Seagrass Nutrient Content. *Marine Ecol. Prog. Ser.* 67, 201–207. doi: 10.3354/meps067201
- Duarte, C. M., and Cebrián, J. (1996). The Fate of Marine Autotrophic Production. *Limnol. Oceanogr.* 41, 1758–1766. doi: 10.4319/lo.1996.41.8.1758
- Duarte, C. M., Losada, I. J., Hendriks, I. E., Mazarrasa, I., and Marbà, N. (2013). The Role of Coastal Plant Communities for Climate Change Mitigation and Adaptation. *Nat. Climate Change* 3 (11), 961–968. doi: 10.1038/nclimate1970
- Duarte, C. M., Middelburg, J., and Caraco, N. (2005). Major Role of Marine Vegetation on the Oceanic Carbon Cycle. *Biogeosciences* 2, 1–8. doi: 10.5194/bg-2-1-2005
- Duarte, C. M., Marbà, N., Gacia, E., Fourqurean, J. W., Beggins, J., Barrón, C., et al. (2010). Seagrass Community Metabolism: Assessing the Carbon Sink Capacity of Seagrass Meadows. *Global Biogeochem. Cycles* 24 (4). doi: 10.1029/2010GB003793
- Dyck, J. (2000). To Take the Food From Our Mouths: The Cowichans' Fight to Maintain Their Fishery 1894–1914. *Native Stud. Rev.* 13 (1), 41–70.
- Fodrie, F. J., Rodriguez, A. B., Gittman, R. K., Grabowski, J. H., Lindquist, N. L., Peterson, C. H., et al. (2017). Oyster Reefs as Carbon Sources and Sinks. *Proc. R. Society. B Biol. Sci.* 284, 20170891. doi: 10.1098/rspb.2017.0891
- Fourqurean, J. W., Duarte, C. M., Kennedy, H., Marba, N., Holmer, M., and Mateo, A. M. (2012a). Seagrass Ecosystems as a Globally Significant Carbon Stock. *Nat. Geosci.* 5, 505–509. doi: 10.1038/ngeo1477
- Fourqurean, J. W., Kendrick, G. A., Collins, L. S., Chambers, R. M., and Vanderklift, M. A. (2012b). Carbon, Nitrogen and Phosphorus Storage in Subtropical Seagrass Meadows: Examples From Florida Bay and Shark Bay. *Marine Freshwater Res.* 63, 967. doi: 10.1071/MF12101
- Fourqurean, J. W., Moore, T. O., Fry, B., and Hollibaugh, J. T. (1997). Spatial and Temporal Variation in C:N:P Ratios, ¹⁵N and ¹³C of Eelgrass *Zostera Marina* as Indicators of Ecosystem Processes, Tomales Bay, California, USA. *Marine Ecol. Prog. Ser.* 157, 147–157. doi: 10.3354/meps157147
- France, R. L. (1995). Carbon-13 Enrichment in Benthic Compared to Planktonic Algae: Foodweb Implications. *Marine Ecol. Prog. Ser.* 124, 307–312. doi: 10.3354/meps124307
- Frankignoulle, M., Canon, C., and Gattuso, J. P. (1994). Marine Calcification as a Source of Carbon Dioxide: Positive Feedback of Increasing Atmospheric CO₂. *Limnol. Oceanogr.* 39, 458–466. doi: 10.4319/lo.1994.39.2.0458
- Fry, B., Scanlan, R. S., and Parkerv, P. L. (1977). Stable Carbon Isotope Evidence for Two Sources of OM in Coastal Sediments: Seagrass and Plankton. *Geochimica Cosmochimica Acta* 41, 1875–1877. doi: 10.1016/0016-7037(77)90218-6
- Gacia, E., Duarte, C. M., and Middleburg, J. J. (2002). Carbon and Nutrient Deposition in a Mediterranean Seagrass (*Posidonia Oceanica*) Meadow. *Limnol. Oceanogr.* 47, 23–32. doi: 10.4319/lo.2002.47.1.0023
- Gattuso, J. P., Frankignoulle, M., and Wollast, R. (1998). Carbon and Carbonate Metabolism in Coastal Aquatic Ecosystems, Annu. Rev. Ecol. Syst. 29, 405–434. doi: 10.1146/annurev.ecolsys.29.1.405
- Geraldi, N. R., Ortega, A., Serrano, O., Macreadie, P. I., Lovelock, C. E., Krause-Jensen, D., et al. (2019). Fingerprinting Blue Carbon: Rationale and Tools to Determine the Source of OC in Marine Depositional Environments. *Front. Marine Chem.* 10, 3389. doi: 10.3389/fmars.2019.00263
- Government of Western Australia's Department of Primary Industries and Regional Development. (2020). *Measuring and Reporting Soil Organic Carbon*. Available at: <https://www.agric.wa.gov.au/soil-carbon/measuring-and-reporting-soil-organic-carbon>.
- Greiner, J. T., McGlathery, K. J., Gunnell, J., and McKee, B. A. (2013). Seagrass Restoration Enhances “Blue Carbon” Sequestration in Coastal Waters. *PLoS One* 8, e72469. doi: 10.1371/journal.pone.0072469
- Guchler, S. M., and Gross, M. G. (1964). Recent Marine Sediments in Saanich Inlet, a Stagnant Marine Basin. *Limnol. Oceanogr.* 9 (3), 359–376. doi: 10.4319/lo.1964.9.3.0359
- Hargrave, B., and Phillips, G. (1989). Decay Times of OC in Sedimented Detritus in a Macrotidal Estuary. *Marine Ecology. Prog. Ser. (Halstenbek)* 56, 271–279. doi: 10.3354/meps056271
- Harris, R. D. (1953). *Eelgrass Status in 1953*. Canadian Wildlife Service (Delta, B.C.: Canadian Wildlife Service Unpublished Report), p. 3–4.
- Heiri, O., Lotter, A. F., and Lemcke, G. (2001). Loss on Ignition as a Method for Estimating Organic and Carbonate Content in Sediments: Reproducibility and Comparability of Results. *J. Paleolimnology* 25, 101e110. doi: 10.1023/A:1008119611481
- Hemminga, M. A., and Mateo, M. A. (1996). Stable Carbon Isotopes in Seagrasses: Variability in Ratios and Use in Ecological Studies. *Marine Ecol. Prog. Ser.* 140, 285–298. doi: 10.3354/meps140285
- Hintz, W., LeBlanc, J., Petrell, R., and Horgen, P. (2016). A DNA Diagnostic Approach for Following Sea Grass: Carbon Distribution in the K'o Moks Estuary and Key New Observations. *Comox Valley Project Watershed Soc.* 1–17.
- Hoogsteen, M. J. J., Lantinga, E. A., Bakker, E. J., Groot, J. C. J., and Tittoneil, P. A. (2015). Estimating Soil Organic Carbon Through Loss on Ignition: Effects of Ignition Conditions and Structural Water Loss. *Eur. J. Soil Sci.* 66 (2), 320–328. doi: 10.1111/ejss.12224

- Howard, J. L., Creed, J. C., Aguiar, M. V. P., and Fouquerean, J. W. (2017). CO₂ Released by Carbonate Sediment Production in Some Coastal Areas may Offset the Benefits of Seagrass 'Blue Carbon' Storage. *Limnol. Oceanogr.* 63, 160–172. doi: 10.1002/lno.10621
- Howard, J., Hoyt, S., Isensee, K., Pidgeon, E., and Telszewski, M. (2014). *Coastal Blue Carbon: Methods for Assessing Carbon Stocks and Emissions Factors in Mangroves, Tidal Salt Marshes and Seagrass Meadows Vol. 180 pp* (Arlington, USA: Conservation International, Intergovernmental Oceanographic Commission of UNESCO, International Union for Conservation of Nature).
- Jacobs, W., Le Hir, P., Van Kesteren, W., and Cann, P. (2011). Erosion Threshold of Sand-Mud Mixtures. *Continental Shelf Res.* 31, S14–S25. doi: 10.1016/j.csr.2010.05.012
- Jankowska, E., Michel, L. N., Zaborska, A., and Włodarska-Kowalczyk, M. (2016). Sediment Carbon Sink in Low-Density Temperate Eelgrass Meadows (Baltic Sea). *J. Geophys. Res. Biogeosci.* 121 (12), 2918–2934. doi: 10.1002/2016JG003424
- Kairis, P. A., and Rybczyk, J. M. (2010). Sea Level Rise and Eelgrass (*Zostera Marina*) Production: A Spatially Explicit Relative Elevation Model for Padilla Bay, WA. *Ecol. Modelling* 221 (7), 1005–1016. doi: 10.1016/j.ecolmodel.2009.01.025
- Kauffman, J. B., Giovanonni, L., Kelly, J., Dunstan, N., Borde, A., Diefenderfer, H., et al. (2020). Total Ecosystem Carbon Stocks at the Marine-Terrestrial Interface: Blue Carbon of the Pacific Northwest Coast, United States. *Global Change Biol.* 26 (10), 5679–5692. doi: 10.1111/gcb.15248
- Kauffman, J. B., Heider, C., Cole, T. G., Dwire, K. A., and Donato, D. C. (2011). Ecosystem Carbon Stocks of Micronesian Mangrove Forests. *Wetlands* 31, 343–352. doi: 10.1007/s13157-011-0148-9
- Kennedy, H., Beggins, J., Duarte, C. M., Fourqurean, J. W., Holmer, M., Marbà, N., et al. (2010). Seagrass Sediments as a Global Carbon Sink: Isotopic Constraints. *Glob. Biogeochem.* 24 (4). doi: 10.1029/2010GB003848
- Kharlamenko, V. I., Kiyashko, S. I., Imbs, A. B., and Vyshkvartzev, D. I. (2001). Identification of Food Sources of Invertebrates From the Seagrass *Zostera Marina* Community Using Carbon and Sulfur Stable Isotope Ratio and Fatty Acid Analyses. *Marine Ecology. Prog. Ser. (Halstenbek)* 220, 103–117. doi: 10.3354/meps220103
- Kim, M., Lee, S., Kim, H., Lee, S., Yoon, S., and Shin, K. (2014). Carbon Stable Isotope Ratios of New Leaves of *Zostera Marina* in the Mid-Latitude Region: Implications of Seasonal Variation in Productivity. *J. Exp. Marine Biol. Ecol.* 461, 286–296. doi: 10.1016/j.jembe.2014.08.015
- Lambertsen, G. K. British Columbia Ministry of Environment and Parks Planning and Assessment Branch (1986). *Cowichan Estuary Environmental Management Plan* (Victoria, B.C.: Ministry of Environment and Parks, Planning and Assessment Branch).
- Laugier, T., Rigollet, V., and de Casabianca, M. (1999). Seasonal Dynamics in Mixed Eelgrass Beds, *Zostera Marina* L. and *Z. Noltii* Hornem., in a Mediterranean Coastal Lagoon (Thau Lagoon, France). *Aquat. Bot.* 63 (1), 51–69. doi: 10.1016/S0304-3770(98)00105-3
- Leschen, A. S., Ford, K. H., and Evans, N. T. (2010). Successful Eelgrass (*Zostera Marina*) Restoration in a Formerly Eutrophic Estuary (Boston Harbor) Supports the Use of a Multifaceted Watershed Approach to Mitigating Eelgrass Loss. *Estuaries Coasts* 33 (6), 1340–1354. doi: 10.1007/s12237-010-9272-7
- Limén, H., Levesque, C., and Kim Juniper, S. (2007). POM in Macro-/Meiofaunal Food Webs Associated With Three Flow Regimes at Deep-Sea Hydrothermal Vents on Axial Volcano, Juan De Fuca Ridge. *Marine Biol.* 153 (2), 129–139. doi: 10.1007/s00227-007-0790-1
- Luternauer, J. L. (1984). *Skeena, Nanaimo and Cowichan River Deltas and Offshore Environs, British Columbia: Surficial Sediment Distribution and Locations of Other Available Data Types Collected by the Geological Survey of Canada* (Ottawa, ON: Geological Survey of Canada). Open File 1112.
- Lutz, M. D. (2018). *A Search for Blue Carbon in Central Salish Sea Eelgrass Meadows* (Bellingham, WA: M.S. Thesis, Western Washington University).
- Macreadie, P. I., Nielsen, D. A., Kelleway, J. J., Atwood, T. B., Seymour, J. R., Petrou, K., et al. (2017a). Can We Manage Coastal Ecosystems to Sequester More Blue Carbon? *Front. Ecol. Environ.* 15 (4), 206–213. doi: 10.1002/fee.1484
- Macreadie, P. I., Ollivier, Q. R., Kelleway, J. J., Serrano, O., Carnell, P. E., Lewis, C. J. E., et al. (2017b). Carbon Sequestration by Australian Tidal Marshes. *Sci. Rep.* 7, 44071. doi: 10.1038/srep44071
- Macreadie, P. I., Serrano, O., Maher, D. T., Duarte, C. M., and Beardall, J. (2017c). Addressing Calcium Carbonate Cycling in Blue Carbon Accounting: Addressing CaCO₃ Cycling in Blue CO₂ Accounting. *Limnol. Oceanogr. Lett.* 2 (6), 195–201. doi: 10.1002/lol2.10052
- Marbà, N., Arias-Ortiz, A., Masqué, P., Kendrick, G. A., Mazarrasa, I., Bastyan, G. R., et al. (2015). Impact of Seagrass Loss and Subsequent Revegetation on Carbon Sequestration and Stocks. *J. Ecol.* 103, 296–302. doi: 10.1111/1365-2745.12370
- Mateo, M. A., Romero, J., Pérez, M., Littler, M. M., and Littler, D. S. (1997). Dynamics of Millenary Organic Deposits Resulting From the Growth of the Mediter- Ranean Seagrass *Posidonia Oceanica*. *Estuarine. Coastal Shelf Sci.* 44, 103–110. doi: 10.1006/ecss.1996.0116
- Mazarrasa, I., Marbà, N., Lovelock, C. E., Serrano, O., Lavery, P. S., and Fourqurean, J. W. (2015). Seagrass Meadows as a Globally Significant Carbonate Reservoir. *Biogeosciences* 12, 4993–5003. doi: 10.5194/bg-12-4993-2015
- McKew, B. A., Dumbrell, A. J., Taylor, J. D., McGenity, T. J., and Graham, J. C. (2013). Underwood Differences Between Aerobic and Anaerobic Degradation of Microphytobenthic Biofilm-Derived OM Within Intertidal Sediments. *FEMS Microbiol. Ecol.* 84, 495–509. doi: 10.1111/1574-6941.12077
- McLeod, E., Chmura, G., Bouillon, S., Salm, R., Björk, M., Duarte, C. M., et al. (2011). A Blueprint for Blue Carbon: Toward an Improved Understanding of the Role of Vegetated Coastal Habitats in Sequestering CO₂. *Front. Ecol. Environ.* 9 (10), 552–560. doi: 10.1890/110004
- McPherson, M. L., Zimmerman, R. C., and Hill, V. J. (2015). Predicting Carbon Isotope Discrimination in Eelgrass (*Zostera Marina* L.) From the Environmental Parameters—Light, Flow, and [DIC]. *Limnol. Oceanogr.* 60 (6), 1875–1889. doi: 10.1002/lno.10142
- Meziane, T., Bodineau, L., Retiere, C., and Thoumelin, G. (1997). The Use of Lipid Markers to Define Sources of OM in Sediment and Food Web of the Intertidal Salt-Marsh-Flat Ecosystem of Mont-Saint-Michel Bay, France. *J. Sea Res.* 38, 47–58. doi: 10.1016/S1385-1101(97)00035-X
- Meziane, T., and Tsuchiya, M. (2000). Fatty Acids as Tracers of OM in the Sediment and Food Web of a Mangrove/Inter- Tidal Flat Ecosystem, Okinawa, Japan. *Mar. Ecol. Prog. Ser.* 200, 49–57. doi: 10.3354/meps200049
- Miyajima, T., Hori, M., Hamaguchi, M., Shimabukuro, H., Adachi, H., Yamano, H., et al. (2015). Geographic Variability in OC Stock and Accumulation Rate in Sediments of East and Southeast Asian Seagrass Meadows. *Glob. Biogeochem.* 29, 397–415. doi: 10.1002/2014GB004979
- Nayak, G. N., Volvoikar, S. P., and Hoskatta, T. (2018). Changing Depositional Environment and Factors Controlling the Growth of Mudflat in a Tropical Estuary, West Coast of India. *Environ. Earth Sci.* 77, 741. doi: 10.1007/s12665-018-7923-3
- Nellemann, C., Corcoran, E., Duarte, C. M., Valdés, L., De Young, C., Fonseca, L., et al. (2009). *Blue Carbon: A Rapid Response Assessment* (Birkeland Trykkeri AS, Birkeland: United Nations Environmental Programme, GRID-Arendal).
- O'Donnell, B. (1988). Indian and Non-Native Use of the Cowichan and Koksilah Rivers: An Historical Perspective. *Fisheries Oceans Canada Native Affairs Division Policy Program Plann.* 8, 40–84.
- Odum, E. P., and de la Cruz, A. A. (1967). *Particulate Organic Detritus in a Georgia Salt Marsh Estuarine Ecosystem*. Ed. M. Lauff (Washington, DC: Estuaries. Am. Assoc. Adv. Sci. Publ.), 383–388.
- Orth, R. J., Carruthers, T. J. B., Dennison, W. C., Duarte, C. M., Fourqurean, J. W., and Heck, K. L. (2006). A Global Crisis for Seagrass Ecosystems. *Bioscience* 56, 987–996. doi: 10.1641/0006-3568(2006)56[987:AGCFSE]2.0.CO;2
- Ouyang, X., and Lee, S. Y. (2014). Updated Estimates of Carbon Accumulation Rates in Coastal Marsh Sediments. *Biogeosciences* 11, 5057–5071. doi: 10.5194/bg-11-5057-2014
- Pedersen, M. F., and Borum, J. (1992). Nitrogen Dynamics of Eelgrass *Zostera Marina* During a Late Summer Period of High Growth and Low Nutrient Availability. *Marine Ecol. Prog. Ser.* 80, 65–73. doi: 10.3354/meps080065
- Peterson, B. J., and Fry, B. (1987). Stable Isotopes in Ecosystem Studies. *Annu. Rev. Ecol. Systematics* 18, 293–320. doi: 10.1146/annurev.es.18.110187.001453
- Phang, V. X. H., Chou, L. M., and Friess, D. A. (2015). Ecosystem Carbon Stocks Across a Tropical Intertidal Habitat Mosaic of Mangrove Forest, Seagrass Meadow, Mudflat and Sandbar. *Earth Surf Process Land* 40, 387–1400. doi: 10.1002/esp.3745

- Phillips, D. L., and Gregg, J. W. (2003). Source Partitioning Using Stable Isotopes: Coping With Too Many Sources. *Oecologia* 136 (2), 261–269. doi: 10.1007/s00442-003-1218-3
- Pniowski, F., and Sylwestrzak, Z. (2018). Influence of Short Periods of Increased Water Temperature on Species Composition and Photosynthetic Activity in the Baltic Periphyton Communities. *Biologia* 73 (11), 1067–1072. doi: 10.2478/s11756-018-0122-6
- Pollard, P. C., and Moriarty, D. J. W. (1991). OC Decomposition, Primary and Bacterial Productivity, and Sulphate Reduction, in Tropical Seagrass Beds of the Gulf of Carpentaria, Australia. *Mar Ecol. Prog. Ser.* 69, 149–159. doi: 10.3354/meps069149
- Poppe, K. L., and Rybczyk, J. M. (2018). Carbon Sequestration in a Pacific Northwest Eelgrass (*Zostera Marina*) Meadow. *Northwest Sci.* 92 (2), 80–91. doi: 10.3955/046.092.0202
- Postlethwaite, V. R., McGowan, A. E., Kohfeld, K. E., Robinson, C. L. K., and Pellatt, M. G. (2018). Low Blue Carbon Storage in Eelgrass (*Zostera Marina*) Meadows on the Pacific Coast of Canada. *PLoS One* 13 (6), e0198348–e0198348. doi: 10.1371/journal.pone.0198348
- Pratt, D. R., Lohrer, A. M., Thrush, S. F., Hewitt, J. E., Townsend, M., Cartner, K., et al. (2015). Detecting Subtle Shifts in Ecosystem Functioning in a Dynamic Estuarine Environment. *PLoS One* 10, e0133914. doi: 10.1371/journal.pone.0133914
- Prentice, C., Hessing-Lewis, M., Sanders-Smith, R., and Salomon, A. K. (2019). Reduced Water Motion Enhances OC Stocks in Temperate Eelgrass Meadows. *Limnol. Oceanogr.* 64 (6), 2389–2404. doi: 10.1002/lno.11191
- Prentice, C., Poppe, K. L., Lutz, M., Murray, E., Stephens, T. A., Spooner, A., et al. (2020). A Synthesis of Blue Carbon Stocks, Sources, and Accumulation Rates in Eelgrass (*Zostera Marina*) Meadows in the Northeast Pacific. *Glob. Biogeochem.* 34 (2), e2019GB006345. doi: 10.1029/2019GB006345
- Redfield, A. C., Ketchum, B. A., and Richards, F. A. (1963). "The Influence of Organisms on the Composition of Sea-Water," in *The Sea* (Vol 2). Ed. M. N. Hill (Wiley). pp. 26–77. Available at: <https://www.vliz.be/en/imis?module=ref&refid=28944&printversion=1&dropIMIStile=1>.
- Rogers, K., Macreadie, P. I., Kelleway, J. J., and Saintilan, N. (2019). Blue Carbon in Coastal Landscapes: A Spatial Framework for Assessment of Stocks and Additionality. *Sustainability Sci.* 14, 453–467. doi: 10.1007/s11625-018-0575-0
- Röhr, E., Boström, C., Canal-Vergés, P., and Holme, M. (2016). Blue Carbon Stocks in Baltic Sea Eelgrass (*Zostera Marina*) Meadows. *Biogeosciences* 13, 6139–6153. doi: 10.5194/bg-13-6139-2016
- Röhr, M. E., Holmer, M., Baum, J. K., Björk, M., Boyer, K., Chin, D., et al. (2018). Blue carbon storage capacity of temperate eelgrass (*zostera marina*) meadows. *Glob. Biogeochem.* 32 (10), 1457–1475. doi: 10.1029/2018GB005941
- Ruesink, J. L., Hong, J. S., Wisehart, L., Hacker, S. D., Dumbauld, B. R., Hessing-Lewis, M., et al. (2010). Congener Comparison of Native (*Zostera Marina*) and Introduced (*Z. Japonica*) Eelgrass at Multiple Scales Within a Pacific Northwest Estuary. *Biol. Invasions* 12, 1773–1789. doi: 10.1007/s10530-009-9588-z
- Ruesink, J. L., Yang, S., and Trimble, A. C. (2015). Variability in Carbon Availability and Eelgrass (*Zostera Marina*) Biometrics Along an Estuarine Gradient in Willapa Bay, WA, USA. *Estuaries Coasts* 38, 1908–1917. doi: 10.1007/s12237-014-9933-z
- Ruiz-Fernández, A. C., Carnero-Bravo, V., Sanchez-Cabeza, J. A., Pérez-Bernal, L. H., Amaya-Monterrosa, O. A., Bojórquez-Sánchez, S., et al. (2018). Carbon Burial and Storage in Tropical Salt Marshes Under the Influence of Sea Level Rise. *Sci. Total Environ.* 630, 1628–1640. doi: 10.1016/j.scitotenv.2018.02.246
- Saderne, V., Gerald, N. R., Macreadie, P. I., Maher, D. T., Middelburg, J. J., Serrano, O., et al. (2019). Role of Carbonate Burial in Blue Carbon Budgets. *Nat. Commun.* 10 (1), 1106–1106. doi: 10.1038/s41467-019-08842-6
- Sanders, C. J., Smoak, J. M., Naidu, A. S., Sanders, L. M., and Patchineelam, S. R. (2010). OC Burial in a Mangrove Forest, Margin and Intertidal Mud Flat. *Estuarine Coastal Shelf Sci.* 90, 168–172. doi: 10.1016/j.ecss.2010.08.013
- Sasmito, S. D., Kuzakov, Y., Lubis, A. A., Murdiyoso, D., Hutley, L. B., Bachri, S., et al. (2020). OC Burial and Sources in Soils of Coastal Mudflat and Mangrove Ecosystems. *Catena* (Giessen) 187, 104414. doi: 10.1016/j.catena.2019.104414
- Schnurr, P. J., Drever, M. C., Elner, R. W., Harper, J., and Arts, M. T. (2020). Peak Abundance of Fatty Acids From Intertidal Biofilm in Relation to the Breeding Migration of Shorebirds. *Front. Marine Sci.* 7, 63. doi: 10.3389/fmars.2020.00063
- Schuerholz, G. (2006). *Background to Cowichan Estuary* (Duncan BC, Canada: Cowichan Estuary Restoration and Conservation Association (CERCA). Available at: <http://www.cowichanestuary.com/background-to-cowichan-estuary/>.
- Schuerholz, G. (2017). *Cowichan Estuary Habitat Map* (Duncan BC, Canada: Cowichan Estuary Restoration and Conservation Association (CERCA). Available at: <https://www.cowichanestuary.com/projects-2>.
- Schuerholz, G. (2018). *Final Report on CERCA's Cowichan Estuary Oyster Research* (Duncan BC, Canada: Cowichan Estuary Restoration and Conservation Association (CERCA). Available at: <https://www.cowichanestuary.com/final-report-on-cerca-cowichan-estuary-oyster-research>.
- Serrano, O., Mateo, M. A., Renom, P., and Julià, R. (2012). Characterization of Soils Beneath a Posidonia Oceanica Meadow. *Geoderma* 185, 26–36. doi: 10.1016/j.geoderma.2012.03.020
- Sharma, S., MacKenzie, R. A., Tieng, T., Soben, K., Tulyasuwan, N., Resanond, A., et al. (2020). The Impacts of Degradation, Deforestation and Restoration on Mangrove Ecosystem Carbon Stocks Across Cambodia. *Sci. Total Environ.* 706, 135416. doi: 10.1016/j.scitotenv.2019.135416
- Spooner, A. M. (2015). *Blue Carbon Sequestration Potential in Zostera Marina Eelgrass Beds of the K'omoks Estuary, British Columbia* (Victoria, BC: M.S. Thesis, Royal Roads University).
- Statistics Canada. (2017). Cowichan Valley G, RDA [Census subdivision], British Columbia and British Columbia [Province] (table). *Census Profile. 2016 Census. Statistics Canada Catalogue no. 98-316-X2016001*. Ottawa. Released November 29, 2017. Available at: <https://www12.statcan.gc.ca/census-recensement/2016/dp-pd/prof/index.cfm?Lang=E> (accessed April 9, 2022).
- Thom, R. M. (1990). Spatial and Temporal Patterns in Plant Standing Stock and Primary Production in a Temperate Seagrass System. *Botanica Marina* 33, 497–510. doi: 10.1515/botm.1990.33.6.497
- Touchette, B. W., and Burkholder, J. M. (2000). Overview of the Physiological Ecology of Carbon Metabolism in Seagrasses. *J. Exp. Mar. Biol. Ecol.* 250 (1), 169–205. doi: 10.1016/S0022-0981(00)00196-9
- Touchette, B. W., Burkholder, J. M., and Glasgow, H. B. (2003). Variations in Eelgrass (*Zostera Marina* L.) Morphology and Internal Nutrient Composition as Influenced by Increased Temperature and Water Column Nitrate. *Estuaries* 26 (1), 142–155. doi: 10.1007/BF02691701
- Tripathee, R., and Schäfer, K. V. R. (2014). Above- and Belowground Biomass Allocation in Four Dominant Salt Marsh Species of the Eastern United States. *Wetlands (Wilmington N.C.)* 35 (1), 21–30. doi: 10.1007/s13157-014-0589-z
- Turner, R. E., Swenson, E. M., Milan, C. S., Lee, J. M., and Oswald, T. A. (2004). Below-Ground Biomass in Healthy and Impaired Salt Marshes: Salt Marsh Resilience Below-Ground. *Ecol. Res.* 19 (1), 29–35. doi: 10.1111/j.1440-1703.2003.00610.x
- Underwood, G. J. C., and Kromkamp, J. (1999). Primary Production by Phytoplankton and Microphytobenthos in Estuaries. *Adv. Ecol. Res.* 29, 93–153. doi: 10.1016/S0065-2504(08)60192-0
- Valiela, I., Teal, J. M., and Deuser, W. G. (1978). The Nature of Growth Forms in the Salt Marsh Grass *Spartina Alterniflora*. *Am. Nat.* 112 (985), 461–470. doi: 10.1086/283290
- Valiela, I., Teal, J. M., and Persson, N. Y. (1976). Production and Dynamics of Experimentally Enriched Salt Marsh Vegetation: Belowground Biomass. *Limnol. Oceanogr.* 21 (2), 245–252. doi: 10.4319/lo.1976.21.2.0245
- Van de Broek, M., Vandendriessche, C., Poppelmonde, D., Merckx, R., Temmerman, S., and Govers, G. (2018). Long-Term OC Sequestration in Tidal Marsh Sediments Is Dominated by Old-Aged Allochthonous Inputs in a Macrotidal Estuary. *Global Change Biol.* 24 (6), 2498–2512. doi: 10.1111/gcb.14089
- van der Wal, D., Wielemaker-van den Dool, A., and Herman, P. M. J. (2010). Spatial Synchrony in Intertidal Benthic Algal Biomass in Temperate Coastal and Estuarine Ecosystems. *Ecosystems (New York)* 13 (2), 338–351. doi: 10.1007/s10021-010-9322-9
- Van Duyl, F. C., de Winder, B., Kop, A. C., and Wollenzien, U. (1999). Tidal Coupling Between Carbohydrate Concentrations and Bacterial Activities in Diatom-Inhabited Intertidal Mudflats. *Mar Ecol. Prog. Ser.* 191, 19–32. doi: 10.3354/meps191019
- Vaughn, D. R., Bianchi, T. S., Shields, M. R., Kenney, W. F., and Osborne, T. Z. (2020). Increased OC Burial in Northern Florida Mangrove-Salt Marsh

- Transition Zones. *Glob. Biogeochem.* 34 (5), e2019GB006334. doi: 10.1029/2019GB006334
- Ware, J. R., Smith, S. V., and Reaka-kudla, M. L. (1992). Coral Reefs: Sources or Sinks of Atmospheric CO₂? *Coral Reefs* 11, 127–130. doi: 10.1007/BF00255465
- Winterwerp, J. C., and Van Kesteren, W. G. (2004). *Introduction to the Physics of Cohesive Sediment Dynamics in the Marine Environment* Vol. 56 (San Diego, CA: Elsevier).
- Yang, S., Wheat, E. E., Horwith, M. J., and Ruesink, J. L. (2013). Relative Impacts of Natural Stressors on Life History Traits Underlying Resilience of Intertidal Eelgrass (*Zostera Marina* L.). *Estuaries Coasts* 36, 1006–1013. doi: 10.1007/s12237-013-9609-0
- Ye, S., Laws, E. A., Yuknis, N., Ding, X., Yuan, H., Zhao, G., et al. (2015). Carbon Sequestration and Soil Accretion in Coastal Wetland Communities of the Yellow River Delta and Liaohe Delta, China. *Estuaries Coasts* 38 (6), 1885–1897. doi: 10.1007/s12237-014-9927-x
- Yin, K., Zetsche, E., and Harrison, P. J. (2016). Effects of Sandy vs Muddy Sediments on the Vertical Distribution of Microphytobenthos in Intertidal Flats of the Fraser River Estuary, Canada. *Environ. Sci. Pollution Res.* 23, 14196–14209. doi: 10.1007/s11356-016-6571-y
- Ysebaert, T. (2000). *Macrozoobenthos and Waterbirds in the Estuarine Environment: Spatio-Temporal Patterns at Different Scales*. PhD thesis (Antwerp: University of Antwerp), 180 p.
- Zehetner, F. (2010). Does OC Sequestration in Volcanic Soils Offset Volcanic CO₂ Emissions? *Quat. Sci. Rev.* 29, e1313–e1316. doi: 10.1016/j.quascirev.2010.03.003
- Zhou, Z., van der Wegen, M., Jagers, B., and Coco, G. (2016). Modelling the Role of Self-Weight Consolidation on the Morphodynamics of Accretional Mudflats. *Environ. Modelling Software* 76, 167–181. doi: 10.1016/j.envsoft.2015.11.002

Conflict of Interest: The authors declare that the research was conducted in the absence of any commercial or financial relationships that could be construed as a potential conflict of interest.

Publisher's Note: All claims expressed in this article are solely those of the authors and do not necessarily represent those of their affiliated organizations, or those of the publisher, the editors and the reviewers. Any product that may be evaluated in this article, or claim that may be made by its manufacturer, is not guaranteed or endorsed by the publisher.

Copyright © 2022 Douglas, Schuerholz and Juniper. This is an open-access article distributed under the terms of the Creative Commons Attribution License (CC BY). The use, distribution or reproduction in other forums is permitted, provided the original author(s) and the copyright owner(s) are credited and that the original publication in this journal is cited, in accordance with accepted academic practice. No use, distribution or reproduction is permitted which does not comply with these terms.



Blue Carbon Ecosystems in Brazil: Overview and an Urgent Call for Conservation and Restoration

Marcelo O. Soares^{1,2*}, Luis Ernesto Arruda Bezerra¹, Margareth Copertino^{3,4}, Beatriz Diniz Lopes¹, Kcrishna Vilanova de Souza Barros¹, Cristina Almeida Rocha-Barreira¹, Rafaela Camargo Maia⁵, Natalia Beloto¹ and Luiz C. Cotovicz Jr.^{1,6}

¹ Institute of Marine Sciences (LABOMAR), Federal University of Ceará (UFC), Fortaleza, Brazil, ² Reef Systems Group, Leibniz Center for Tropical Marine Research (ZMT), Bremen, Germany, ³ Federal University of Rio Grande (FURG), Rio Grande, Brazil, ⁴ Brazilian Network on Global Climate Change Research (Rede CLIMA), São José dos Campos, Brazil, ⁵ Instituto Federal de Educação, Ciência e Tecnologia do Ceará (IFCE), Acaraú, Brazil, ⁶ Department of Marine Chemistry, Leibniz Institute for Baltic Sea Research, Rostock, Germany

OPEN ACCESS

Edited by:

Joanne S. Porter,
Heriot-Watt University,
United Kingdom

Reviewed by:

Antoine De Ramon N'Yeurt,
University of the South Pacific, Fiji
Rebecca Borges,
University of Bremen, Germany

*Correspondence:

Marcelo O. Soares
marcelosoares@ufc.br

Specialty section:

This article was submitted to
Global Change and the Future Ocean,
a section of the journal
Frontiers in Marine Science

Received: 18 October 2021

Accepted: 11 March 2022

Published: 29 April 2022

Citation:

Soares MO, Bezerra LEA,
Copertino M, Lopes BD, Barros KvdS,
Rocha-Barreira CA, Maia RC,
Beloto N and Cotovicz LC (2022)
Blue Carbon Ecosystems in Brazil:
Overview and an Urgent Call for
Conservation and Restoration.
Front. Mar. Sci. 9:797411.
doi: 10.3389/fmars.2022.797411

In this article, we discuss knowledge and gaps regarding blue carbon ecosystems (BCEs) in Brazil, considering the urgency to apply protection actions and policies to safeguard their biodiversity and associated ecosystem services. We also indicate areas of further research to improve carbon stocks and sequestration rate estimates. We call attention to the shortage of studies on Brazilian BCEs relative to the growing knowledge on the Blue Carbon Framework accumulated worldwide over the last decade. Considering the extensive Brazilian Economic Exclusive Zone (known as “Blue Amazon”), knowledge concerning blue carbon stocks is vital at regional and global scales for mitigating global increases in atmospheric carbon dioxide (CO₂). The Blue Amazon has at least 1,100,000 ha of vegetated and non-vegetated coastal ecosystems (mangroves, salt marshes, seagrass meadows, and hypersaline tidal flats) that collectively contain vast amounts of stored carbon, making Brazil an ideal place to test mechanisms for evaluating, conserving, and restoring BCEs. Other poorly understood potential sinks and sources of carbon are macroalgal and rhodolith beds, mudflats, continental shelf sediments, and marine animal forests in shallow, mesophotic, and deep waters. The carbon fluxes between diverse environmental compartments, such as soil–air, soil–water, groundwater–water–surface water, air–water, and land–ocean, in BCEs across the Blue Amazon must be studied. We emphasize the importance of assessing the total carbon stock and the recent dismantling of environmental laws that pose great risks to these important BCEs. The conservation and recovery of these areas would enhance the carbon sequestration capacity of the entire country. Furthermore, we highlight priorities to improve knowledge concerning BCEs and their biogeochemical cycles in the Blue Amazon and to provide information to assist in the reduction of atmospheric levels of CO₂ for the United Nations Decade of Ocean Science (2021–2030).

Keywords: mangrove, seagrass meadow, salt marsh, carbon burial, carbon sink, South Atlantic

1 INTRODUCTION

Global climate change is perhaps the greatest challenge of modern civilization, and several efforts are being made towards impact adaptation and mitigation of excessive greenhouse gases (Steffen et al., 2018; Bertram et al., 2021). In addition to lowering emissions and decarbonizing the economy, nature-based solutions have been increasingly proposed owing to their low cost, efficiency, and associated co-benefits (McLeod et al., 2011; Gattuso et al., 2018; Taillardat et al., 2018). While terrestrial ecosystems have been the focus of nature-based solutions, the role of coastal and marine ecosystems remains unaccounted for in several national emission inventories and not included in the National Determined Contributions (NDC) (Duarte, 2017). Over the last decade, ocean and terrestrial ecosystems have sequestered approximately 52% of anthropogenic CO₂ emissions, with average rates of approximately 2.5 ± 0.6 and 3.4 ± 0.9 GtC year⁻¹, respectively (Friendlingstein et al., 2019). However, some processes and ecosystems, such as coastal areas, are not fully accounted for in the global carbon budget. The CO₂ that is captured from the atmosphere and sequestered in coastal and marine environments, mostly vegetated ecosystems such as mangroves, salt marshes, and seagrass meadows, is collectively known as blue carbon (BC) and consists of both organic and inorganic forms (Nellemann et al., 2009).

Coastal ecosystems sequester and stock larger amounts of carbon per unit area than terrestrial ecosystems. For this reason, the conservation and restoration of BC ecosystems (BCEs) are recognized among the key ocean-based activities towards climate change mitigation, adding to global efforts to limit global warming and achieve the goals of the Paris Agreement, with numerous co-benefits (Hoegh-Guldberg et al., 2019). The conservation and restoration of BCEs is crucial for marine CO₂ removal (Lezaun, 2021). Therefore, the loss and degradation (e.g., land use changes, trawling activities, changes in water quality, and increasing pollution) of BCEs lead to increases in atmospheric CO₂ emissions (Lovelock et al., 2017; O'Connor et al., 2019) and reductions in biosphere C sinks (net C accumulation in the long term) (Kauffmann et al., 2020), ultimately accelerating global climate change.

Mangroves, salt marshes, and seagrasses cover approximately ~36-185 million ha worldwide (Macreadie et al., 2021). However, some important marine ecosystems have not yet met the key criteria for inclusion within the BC framework (e.g., coral and oyster reefs) or show gaps in the scientific understanding of carbon stocks or greenhouse gas fluxes, with limited potential for management or accounting of carbon sequestration rates (e.g., macroalgal beds). Although the scale of greenhouse gas removal or emissions by plankton (Guidi et al., 2016), macroalgae forests (Krause-Jensen et al., 2018), mudflats, and marine animal forests (MAFs) (Rossi et al., 2017; Rossi et al., 2019) may be high, the long-term storage of fixed CO₂ is not completely understood for these systems (Lovelock & Duarte, 2019). However, as BC science is multifaceted and has a broad scope, it must explore all potential opportunities for climate change mitigation and adaptation in marine ecosystems, including large and poorly studied tropical regions such as Brazil.

The Blue Amazon is a concept created by the Brazilian Navy to draw attention to the vast Brazilian economic exclusive maritime zone (larger than the Brazilian Amazon) and existing natural resources (including BCEs), which are essential for economy and society (Wiesebron, 2013). However, while the roles of the Amazon Rainforest in biodiversity maintenance, carbon sequestration, and climate regulation are well understood and recognized globally (Gatti et al., 2021), the roles of the Blue Amazon are not. Brazil currently lacks plans to strengthen its climate change and conservation policies and management in this Blue Amazon. Brazil has a vital role in global climate change mitigation, mainly focusing on terrestrial carbon (Gatti et al., 2021). However, when devising climate actions and mitigation strategies, no considerable importance is given to the ocean and coast. Brazil has one of the world's longest coastlines (between 9th and 15th in rank) and maritime territories (11th in rank); it contains the second largest mangrove forest in a single country and has a high diversity of coastal and marine systems (Lacerda et al., 2019; Magris et al., 2020). However, the potential for carbon storage and sequestration in Brazil is not completely understood (Soares et al., 2017). As a result, Brazilian BCEs are not included in the country's climate-mitigation commitments (e.g., NDC documents) and adaptation plans.

Therefore, in this perspective article, we aim to discuss the knowledge gaps in BCEs and possible solutions for their protection and restoration in Brazil. First, we present a broad and general characterization of the Brazilian coast and its recognized BCEs, focusing on the distribution and stocks of vegetated coastal systems, such as mangroves, salt marshes, and seagrasses. We discuss the carbon stocks of other important coastal systems [e.g., macroalgal and rhodolith beds, hypersaline tidal flats (HTFs), mudflats, continental shelf, and MAFs] and their potential to be included as BCEs. Next, we discuss the main ongoing impacts and conservation policies that threaten carbon stocks. Finally, we conclude with suggestions for further research to improve carbon estimates, considering the urgency of applying environmental protection actions and policies to safeguard BCE biodiversity and associated ecosystem services, including for climate change mitigation.

2 BLUE CARBON ECOSYSTEMS IN BRAZIL

Brazil is recognized as a “mega-diverse country” by the United Nations Environmental Program (UNEP). Brazil's high biodiversity extends to multiple coastal and marine habitats observed across the long coastline (~9,000 km) and the vast maritime territory (up to 5,700,00 km²), ranging from equatorial (5°N) to warm-temperate latitudes (33°S) (Figure 1). One of the Brazilian sites of global conservation relevance is the Amazon Rainforest. However, the carbon sink of the Amazon Rainforest is declining due to deforestation and climate change, including the recent documentation of the occurrence of carbon sources to the atmosphere through burning in southeastern Amazonia, where deforestation,

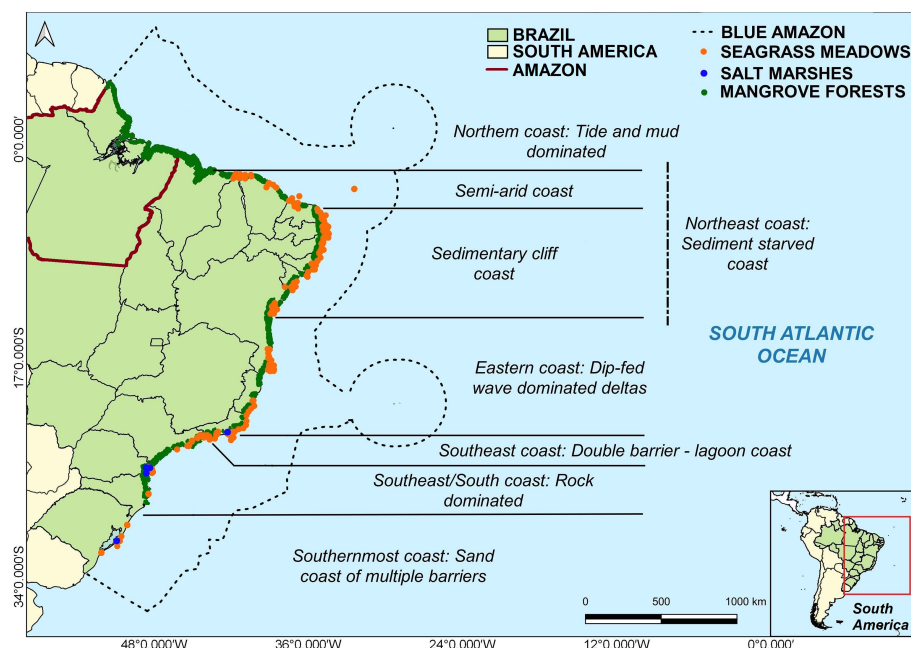


FIGURE 1 | Map showing the spatial distribution of major blue carbon ecosystems (BCEs) in the Brazilian coast. The dashed line presents the limits of the Blue Amazon (Brazilian Economic Exclusive Zone). The orange, blue, and green dots represent the seagrass meadows, salt marshes, and mangrove ecosystems, respectively. Sources: Wiesebron (2013); Copertino et al. (2016); Ferreira and Lacerda (2016); Schaeffer-Novelli et al. (2016), and Lacerda et al. (2019). Coastal geomorphological settings according to Muehe (2010).

warming, and moisture stress have been particularly enhanced (Gatti et al., 2021).

The jurisdictional maritime territory of Brazil, known as the “Blue Amazon” (Figure 1), contains vegetated and non-vegetated coastal and marine ecosystems (mangroves, salt marshes, seagrass meadows, MAFs, and other systems) (Table 1) that could collectively contain a vast amount of stored carbon, making Brazil an ideal place to test new mechanisms for evaluating, conserving, and restoring BCEs (Turra and Denadai, 2016; Bertram et al., 2021).

The extension of recognized Brazilian BCEs (at least 1,100,000 ha) (Table 1) needs to be better understood, quantified, acknowledged, and protected because of increasing human pressures operating on different spatial scales (local, regional, and global) (Copertino et al., 2016; Horta et al., 2016; Schaeffer-Novelli et al., 2016; Soares et al., 2017; Magris et al., 2020; Soares et al., 2021). In this context, we present a characterization of three actionable BCEs (mangroves, salt marshes, and seagrass meadows) in Brazil (Figure 2).

TABLE 1 | Dimensions and carbon burial rates of established and potential BCEs. Estimates for global area, global mean burial rate, and Brazilian ecosystem areas.

Vegetated BCEs	Global area (ha)	Global mean burial rates (Tg C y ⁻¹)	Brazilian area (ha)
Mangroves	8,148,400 ¹	31.0 - 34.4 ⁵	990,000 ⁸
Salt marshes	5,495,089 ²	4.8 - 87.2 ⁵	^A 28,886 ⁹ 10 11 12
Seagrass meadows	26,656,200 ³	48 - 112 ^{5 6}	^A 67,825 ^{13 14 15 16 17 18 19 20 21}
Macroalgal habitats	354,000,000 ⁴	0 - 42 ⁴	^B 1,144,232 ^{22 23 24 25}
Rhodolith beds	—	400 ⁷	^C 3,300,000 ²⁶
Non-vegetated BCEs			22,971,800 ²⁷
Hypersaline tidal flats	—	—	57,000 ²⁸
Continental Shelf	—	—	—
Marine animal forests	—	—	—

¹Hamilton and Casey, 2016; ²Mcowen et al., 2017; ³McKenzie et al., 2020; ⁴Krause-Jensen and Duarte, 2016; ⁵McLeod et al., 2011; ⁶Fourqurean et al., 2012; ⁷van de Heijden and Kamenos 2015; ⁸Diniz et al., 2019; ⁹Martinetto et al., 2016; ¹⁰Teixeira and Souza-Filho, 2009; ¹¹Rodrigues and Souza-Filho 2011; ¹²Flynn et al., 1998; ¹³Creed, 2003; ¹⁴Barros et al., 2014; ¹⁵Copertino et al., 2016; ¹⁶Howard et al., 2017a; ¹⁷Shaefer et al., 2018; ¹⁸Gorman et al., 2020a; ¹⁹Choi 2011, ²⁰Gama 2015; ²¹Silva 2017; ²²Horta, 2000; ²³Jorge et al., 2012; ²⁴Figueiredo et al., 2008; ²⁵Lanari et al., 2022; ²⁶Anderson et al., 2021; ²⁷Carvalho et al., 2020; ²⁸MapBiomass, 2021

^A Summing up available areal values from mapping and studies for distinct areas.

^B Potential habitats estimated by summing up the values of subtidal regions of marine protected areas (MPA's) where diverse macroalgal beds are registered. Data on MPA's shallow subtidal areas obtained from: (https://www.funbio.org.br/programas_e_projetos/gef-mar-funbio; <https://uc.socioambiental.org/pt-br/arp/932>; <https://www.parquedorecife.defora.com.br>).

^CHabitat range distribution of the deep kelp beds (*Laminaria abyssalis*) occurring at continental margin below tropical waters



FIGURE 2 | Blue carbon ecosystems in Brazil (South Atlantic). **(A)** Seagrass meadows - Cajueiro da Praia - Piauí state. Photo: K. Barros; **(B)** Mangrove forest - Rio Acaraú - Ceará state. Photo: R. C. Maia; **(C)** Salt marshes - Lagoa dos Patos - Rio Grande do Sul state. Photo: C.S.B. Costa.

2.1 Mangrove Forests

Mangroves have a mean total ecosystem carbon stock (TECS) of approximately $738.9 \text{ MgC ha}^{-1}$ (varying widely by site) and a total global mean C stock of 6.17 PgC . Tropical forests, on the other hand, have a mean TECS of approximately 314 MgC ha^{-1} and a total global mean carbon stock of 553 PgC (Alongi, 2020). Therefore, per plot, carbon stocks in mangrove forests are 2.35-fold those of in tropical rainforests. However, in terms of total carbon stocks, tropical forests have approximately 92-fold higher carbon levels than mangroves (Ahmed and Glaser, 2016; Kauffman et al., 2018a). For this review, we considered a global mangrove area of $8,148,400 \text{ ha}$, in which Brazil has the second largest mangrove area worldwide (Hamilton and Casey, 2016) (Table 1).

The aboveground (AGB) and belowground (BGB) biomass and TECS in Brazilian mangroves (Figure 2B) may present heterogeneity based on geomorphic and sedimentary settings, soil depth, tidal height, salinity, climate, environmental protection measures, and forest structure (Kauffman et al., 2018a; Kauffman et al., 2018b; Nóbrega et al., 2018; Rovai et al., 2018; Kauffmann et al., 2020; Hatje et al., 2020; Matos

et al., 2020; Rovai et al., 2020; Rovai et al., 2022) (Table 2). The belowground portion (including soils and roots) represents approximately 70%–86% of the total carbon stocks in mangroves (Hamilton and Friess, 2018; Kauffman et al., 2018a; Kauffmann et al., 2020).

In the last 5 years (2017–2021), mangroves from seven of Brazil's 15 coastal states have been studied and clarified the necessity of carbon research on the TECS, AGB, and BGB of Brazilian mangroves (Portillo et al., 2016; Kauffman et al., 2018a; Kauffman et al., 2018b; Pavani et al., 2018; Hamilton & Friess, 2018; Ferreira et al., 2019; Nóbrega et al., 2019; Portela et al., 2020; Rovai et al., 2020; Salum et al., 2020). There is also a shortage of information about TECS owing to the low spatial coverage of studies that include AGB and BGB portions simultaneously. Furthermore, the different biophysical typologies and the main drivers of the spatial heterogeneity of mangrove ecosystems along the Brazilian coast (Figure 1) remain poorly described.

Surveys of the TECS registered in Amazon mangroves (511 MgC ha^{-1}) do not significantly differ from the mangroves of semiarid tropical coasts in Brazil [413 MgC ha^{-1} (Kauffman et al.,

TABLE 2 | Carbon stock in different compartments (TECS, AGB, and BGB) of mangrove and tropical forest ecosystem.

Local	TECS (MgC ha^{-1})	Reference
World mangrove	738.9	Alongi (2020)
World tropical forest	314.2	Alongi (2020)
Brazilian mangrove	507	Hamilton and Friess (2018)
Brazilian mangrove	341	Rovai et al. (2022)
Amazon mangroves—Brazil	511	Kauffman et al. (2018a)
Semiarid tropical mangrove—Brazil	413	Kauffman et al. (2018a)
Northern coast São Paulo mangrove—Brazil	157.36	Pavani et al. (2018)
AGB (Mg C ha^{-1})		
Parnaíba river in Piauí state mangrove—Brazil	258	Portela et al. (2020)
Amazon mangrove—Brazil	159	Kauffman et al. (2018a)
Semiarid tropical mangrove—Brazil	72	Kauffman et al. (2018a)
Northern coast of São Paulo mangrove—Brazil	76.09	Pavani et al. (2018)
Southern coast of São Paulo mangrove—Brazil	52.7	Rovai et al. (2020)
BGB (Mg C ha^{-1})		
Northern coast of São Paulo mangrove—Brazil	22.7	Pavani et al. (2018)
Southern coast of São Paulo mangrove—Brazil	57.3	Rovai et al. (2020)
Rio de Janeiro preserved area mangrove—Brazil	104.41	Santos et al. (2017)

2018a) but differ from those of mangroves on the northern coast of São Paulo (157.36 MgC ha⁻¹) (Pavani et al., 2018)]. At the national level, mean TECS varies from 341 MgC ha⁻¹ and 507.83 MgC ha⁻¹ (Hamilton and Friess, 2018; Rovai et al., 2022). Regarding specific mangrove portions, the AGB of the Amazon mangroves (159 MgC ha⁻¹) is greater than that of semi-arid northeast mangroves (72 MgC ha⁻¹) and those of the northern (76.09 MgC ha⁻¹) and southern (52.7 MgC ha⁻¹) coasts of São Paulo, but inferior to that of the Parnaíba River (258 MgC ha⁻¹) (Kauffman et al., 2018a; Pavani et al., 2018; Portela et al., 2020; Rovai et al., 2020), illustrating matrix heterogeneity between sites (**Table 2**). Furthermore, the BGB portions of mangroves of the northern coast of São Paulo (22.07 MgC ha⁻¹) differ from those of the southern coast (57.3 MgC ha⁻¹) more than the Amazon mean for this compartment (104.41 MgC ha⁻¹) (Kauffman et al., 2018a; Pavani et al., 2018; Rovai et al., 2020). These trends could be due to various factors, such as vegetal composition, hydrologic fluxes (wave exposure and riverine inputs), edaphic factors, anthropogenic influences, and microphytobenthic productivity (Hamilton and Friess, 2018; Rovai et al., 2018; Pavani et al., 2018; Nóbrega et al., 2019; Gorman et al., 2020b). In this regard, a systematic review of BC stocks in Brazilian mangroves is a priority to highlight the importance of sites that have not yet been studied and provide information about AGB and BGB at each site.

The combined carbon stocks of Pará mangroves in the Amazon region are twice those of the upland evergreen forests and almost fivefold those of tropical dry forests (Kauffman et al., 2018a; Kauffman et al., 2018b). Amazon mangroves represent 27.9% of the total mangrove area of the country (Ferreira & Lacerda, 2016). These results demonstrate the global importance of Brazilian mangroves as carbon hotspots (Rovai et al., 2022) (**Table 1**). Mangroves in North Brazil (Amazon mangroves) are part of the world's largest continuous belt of mangroves (760,000 ha) (Souza Filho, 2005). In addition, mangroves between 5°N and 5°S represent almost 30% of the world's mangroves (Giri et al., 2011). However, despite recent scientific efforts, mangroves are not adequately represented in global C budgets because the C cycle in mangrove ecosystems is the result of complex and poorly documented processes (Bouillon et al., 2008), particularly in Brazil. In addition, other greenhouse gases (e.g., methane and nitrous oxide) emitted from mangrove-dominated waters and soils could partially offset CO₂ sequestration and organic C burial, especially in degraded/impacted mangroves (Rosentreter et al., 2018; Call et al., 2019).

Most of the research concerning C cycling in mangroves in Brazil and worldwide has focused on soil C stocks and burial rates, rather than on water fluxes. However, the fate of approximately 50% of the carbon fixed by mangrove vegetation is unknown (Bouillon et al., 2008). Studies have shown that mangrove carbon may be exported to the adjacent ocean (Maher et al., 2018; Santos et al., 2018). Thus, the C sequestration capacity of mangroves is likely underestimated.

The outwelling (lateral fluxes or horizontal exports) of dissolved and particulate carbon derived from BCEs has recently been described as a relevant process within the long-

term BC sequestration mechanism (Santos et al., 2021). From a global perspective, mangroves account for >10% of terrestrially derived refractory organic carbon exported to the ocean (Dittmar et al., 2006). Mangrove export (outwelling) is the main source of terrigenous organic carbon in the ocean off northern Brazil (Dittmar et al., 2006). Further studies are required on the rates of organic carbon mineralization along the mangrove–estuary–continental shelf continuum to emphasize its importance as a vital atmospheric CO₂ sink (Maher et al., 2018). In addition, the lateral export of dissolved inorganic carbon (DIC) and alkalinity can be greater than that of organic C burial as a long-term carbon sink (Maher et al., 2018; Santos et al., 2018). If the exported DIC remains in the water column after air–water equilibration, this carbon outwelling could represent an important and overlooked long-term carbon sink (Santos et al., 2018; Santos et al., 2021). Finally, this C outwelling along the land–ocean aquatic continuum has the potential to locally and/or regionally mitigate the process of ocean acidification by increasing coastal ocean pH (Sippo et al., 2016).

The northern and northeastern continental shelves of Brazil present widespread coral reef coverage (Leão et al., 2016; Soares et al., 2017; Soares et al., 2019) and the outwelling of carbon and alkalinity counteracting coastal acidification could be particularly relevant in shallow-water coral assemblages along the southwestern Atlantic coast (Cotovicz Jr. et al., 2020). However, estimates of carbon outwelling along the land–ocean continuum in Brazil (and elsewhere) are scarce (Cabral et al., 2021) and remain spatially and temporally limited. Therefore, it is important to calculate the outwelling from BCEs to correctly provide the actual sequestration capacities of BCEs, which may currently be underestimated. Future studies should examine the fate of carbon in coastal waters and oceans as long-term C reservoirs. The dissolved inorganic and organic C outwelling (lateral fluxes to the ocean) are potentially greater C sinks than organic C soil burial. Currently, these processes along the Brazilian coast are overlooked and require further investigation.

2.2 Salt Marshes

Salt marshes in Brazil occur along sheltered coastlines maybe associated or not with mangrove forests (Schaeffer-Novelli et al., 2016). Knowledge of salt marsh area extension (**Figures 1, 2C**), plant species composition, plant biomass standing crop, primary production, and associated surface soil parameters (carbon, organic matter, and grain size) is concentrated in subtropical and warm-temperate Brazilian estuaries and coastal bays (see Davy & Costa, 1992; Isacch et al., 2006; Martinetto et al., 2016; Schaeffer-Novelli et al., 2016 for reviews).

The most extensive salt marsh areas are found in southern Brazil, particularly in Rio Grande do Sul State (**Figure 1**), covering the margins of coastal lagoons and estuaries, and are dominated by mono- or multi-specific stands of *Spartina* (*S. alterniflora* and *S. densiflora*), *Sacocornia*, *Scirpus* (*S. maritimus* and *S. olney*), and *Juncus* (*J. kraussii* and *J. acutus*) (Costa et al., 2003). Large areas of salt and brackish marshes are also associated with tropical mangrove forests (Teixeira & Souza-Filho, 2009; Rodrigues & Souza-Filho, 2011) dominated by *Spartina* spp., *Distichlis* spp.,

Eleocharis spp., and *Schoenoplectus* spp. (Kauffman et al., 2018a). According to available data on cover extension based on mapping studies (Teixeira & Souza-Filho, 2009; Rodrigues and Souza-Filho 2011; Martinetto et al., 2016), the total Brazilian salt marsh area is approximately 26,300 ha (**Table 1**). However, this number is underestimated as the total area occupied by tropical salt marshes in the SW Atlantic is unknown.

The total biomass standing crop (from <1 to 30 MgC ha⁻¹) and surface soil organic matter (from <1% to 20%) content of these systems show high variability, depending on species composition, estuarine position, marsh level, terrestrial input, and climate. Most data on soil organic matter or carbon content are limited to surface or shallow core depths (up to 10–20 cm) and lack bulk density data and sedimentation rates. Moreover, data on carbon stocks of Brazilian salt marshes are restricted to two salt marsh areas more than 8,000 km apart that are influenced by distinct climates, tides, fluvial regimes, and community structures. The ecosystem carbon stocks (soil and biomass) observed in Amazonian tropical salt marshes (Pará, Brazil; for the top 1 m to 3 m soil depth) are between 196.7 ± 22.9 and 352.6 ± 29.0 (mean $257.3 \text{ Mg C ha}^{-1}$), which are slightly higher than those used by the IPCC as a referential mean (Kauffman et al., 2018a). The contribution of aboveground biomass to these carbon pools was less than 2%. Higher values have been found for the extensive salt marshes in southern Brazil (Patos Lagoon, Rio Grande do Sul State) (**Figure 1**), ranging from 263 up to 440 MgC ha⁻¹ (for the top 1 m), depending on the species and marsh level (Patterson et al., 2016). The aboveground biomass of these southern marshes (mean of 26.4 MgC ha⁻¹) may account for 10%–20% of the ecosystem carbon pool. Therefore, further studies on carbon stocks and sequestration in Brazilian salt marshes are needed to provide better support for science-based policies to protect these unique systems.

2.3 Seagrass Meadows

Seagrasses are distributed worldwide, on both temperate and tropical coasts, covering a total area of 26,656,200 ha (McKenzie et al. 2020), up to 164,678,900 ha according to one modeling estimation (Jayatilake and Costello, 2018). There is a notable lack of data on seagrass carbon stocks and sequestration rates from most of the South Atlantic Ocean (Nóbrega et al., 2018; Gorman et al., 2020a), including the Brazilian coastline (**Figure 1**). Seagrass meadows are suggested to be hotspots for BC storage in soils and may contain at least twice as much carbon per unit area as terrestrial soils (Fourqurean et al., 2012). However, the sedimentary inorganic carbon as carbonate could be close to sedimentary Corg levels, and as the production of carbonates may represent a CO₂ source, this can diminish the strength of seagrass sediments as CO₂ sinks in some ecosystems, including Brazilian seagrass meadows (Howard et al., 2017; Gullström et al., 2018). Most available data and global reviews concerning seagrass carbon pools are based on the Mediterranean, Australia, and North Atlantic coastlines (Fourqurean et al., 2012; Ricart et al., 2020) and are biased towards large persistent species and dense meadows. Less

knowledge is available regarding the stocks and sequestration capacity of small ephemeral species that dominate large extensions of the world's coasts and estuaries including in Brazil.

Although seagrass meadows have been highlighted as important carbon sinks since the 1980s, they are still neglected in global carbon cycle models and emission inventories, as well as in NDCs, owing to gaps and uncertainties about their stocks, carbonate chemistry, and water–air CO₂ fluxes (Duarte, 2017; Macreadie et al., 2014). The area of global seagrass meadows is highly controversial, with a large variability between estimates. Considering the range variability in worldwide seagrass area and the mean C stocks for the top meter of soil (108 Mg C ha^{-1}), the global carbon pool is generally considered to lie between 4.2 and 8.4 Pg (Fourqurean et al., 2012); however, a less conservative approach produces estimates of between 8 and 19.0 Pg. These uncertainties are due to the scarcity of data on most parts of the world's coasts, including South America. Approximately 50% of the seagrass soil carbon is derived from seagrass plants, with the remainder from other autochthonous and allochthonous sources (plankton, benthic algae, and terrestrial plants; Kennedy et al., 2010). Considering the loss rate of seagrass meadows (global loss rates accelerating from 0.9% year⁻¹ in the 1940s to 7% year⁻¹ towards the end of the 20th century) (Waycott et al., 2009; de los Santos et al., 2019), these systems may release an additional 11–90 Tg C year⁻¹ into the atmosphere (Fourqurean et al., 2012; Pendleton et al., 2012).

Seagrass meadows in Brazil occur discontinuously along the coast (**Figures 1, 2**), with species distribution and abundance being strongly influenced by regional oceanography, coastal currents, river runoff, and regional and local geomorphology (Copertino et al., 2016). Despite the increasing number of studies on seagrass ecology in Brazil, few have investigated seagrass soil carbon stocks/sequestration or other soil characteristics (Patterson et al., 2016; Howard et al., 2017; Nóbrega et al., 2018; Gorman et al., 2020a; Gorman et al., 2020b). One study comparing seagrass soil across the Brazilian coast (NE semi-arid coast and Southeast/South Brazilian coast) found significant differences according to their morphological, chemical, and physical properties, with distinct total organic carbon (TOC) contents (Nóbrega et al., 2018). Available data show that the percentage of TOC in seagrass soils varies according to latitude, with higher values in the northeast semi-arid coast (Ceará and Piauí states), according to measurements conducted within dense estuarine meadows ($2.5\% \pm 0.9\%$; Nóbrega et al., 2018).

Seagrass soil C stocks in *Halodule* spp. meadows measured from several sites across Eastern and Southeastern Brazil range from 0.2 to 1.7 Mg C ha⁻¹ (Howard et al., 2017), with an average ($0.67 \text{ Mg C ha}^{-1}$) lower than the global mean ($1.65 \text{ Mg C ha}^{-1}$; Fourqurean et al., 2012). Data from Northeast Brazil, taken from estuaries, show a higher mean ($\sim 2 \text{ Mg C ha}^{-1}$) and greater range of values ($0.7\text{--}4.0 \text{ Mg C ha}^{-1}$) (Nóbrega et al., 2018). The lack of seagrass mapping in most coastal regions hinders the accurate quantification of regional and global seagrass carbon pools. Summing up values from published and unpublished data and few mapped areas, the coastal seagrass area in Brazil covers at least 67,825 ha (**Table 1**). However, the total area coverage is

likely to be greater because many shallow turbid waters and clear deep waters (>10 m) have not been surveyed (Copertino et al., 2016).

Brazilian seagrasses are dominated by small seagrass genera (*Halodule*, *Halophila*, and *Ruppia*) that occur in dynamic patches and have high seasonal and annual variability in their abundance and distribution patterns. While local losses have been reported due to anthropogenic and natural impacts (Copertino et al., 2016), *H. wrightii* and *H. decipiens* have expanded the southern limit range distribution (Sordo et al., 2011; Gorman et al., 2020a). Although the distribution of seagrass species along the Brazilian coast is relatively well known, the general lack of mapping and better distribution of soil C stocks for most regions (particularly for the densest meadows thriving along the northeastern region) limit the estimation at the national scale. Roughly, multiplying average C stocks found by Patterson et al. (2016); Howard et al. (2017), and Nóbrega et al. (2018) by the estimated areal extent (Table 1) gives a total soil reservoir ranging between 200 and 3000 Mg C. This wide range is due to the high variability in C densities among the regions and can be considered a hypothesis to be tested.

3 OTHER POTENTIAL BLUE CARBON ECOSYSTEMS

The concept of BC and its rapidly growing scientific focus on mangroves, salt marshes, and seagrass ecosystems, justified by their large C reservoirs, high sequestration rates, long-term carbon storage, and potential to manage greenhouse gas emissions, support other adaptation policies (Lovelock & Duarte, 2019). In particular, mangroves and salt marshes are now recognized by the International Panel on Climate Change as potential nature-based solutions for atmospheric CO₂ reduction (IPCC 2021) and are eligible for inclusion in the greenhouse gas accounting guidance of this panel (IPCC 2014). While these vegetated coastal systems are established BCEs, other relevant systems do not meet key criteria (e.g., coral reefs) or have gaps in scientific knowledge and limited potential for management and accounting (e.g., macroalgal beds and HTFs) (Figure 3).

The Blue Amazon has large extensions of overlooked potential BC sinks, such as macroalgae (Aued et al., 2018), rhodolith beds (Horta et al., 2016), phytoplankton-dominated ecosystems (Guidi et al., 2016), hypersaline tidal flats, mudflats (Gorman et al., 2020b), and marine animal forests (Soares et al., 2017; Barbosa et al., 2019; Soares et al., 2019). In their review, Lovelock and Duarte (2019) framed some of these ecosystems as non-actionable since they do not fulfill key criteria and because of insufficient knowledge about their potential as long-term sinks (Figure 3). If such systems provide important C stocks and sequestration, whether for the ecosystem or beyond, they must be investigated before they can be included in the BC framework. This BC question is long-standing and controversial and requires resolution using empirical evidence (Macredie et al., 2021). In this context, we present other potential BC sinks that should be investigated and protected in the Blue Amazon.

3.1 Hypersaline Tidal Flats (Apicuns)

Hypersaline Tidal Flats (HTFs) are ecotones associated with mangrove ecosystems on arid and semiarid coasts (Figure 3). Despite carbon sequestration rates being lower in HTFs than in traditional BCEs (described in Section 2), worldwide HTF carbon stocks and long-term carbon sequestration rates can be substantial given their large area (Brown et al., 2021). Together with other vegetated systems, HTFs meet the requirements that define BC systems and can thus be included in global and regional management and mitigation policies (Lovelock & Duarte, 2019).

In Brazil, the HTFs, known as *apicuns*, occupy large areas in the supratidal zone (57,000 ha; MapBiomass 2021), in an intermediary position between mangroves (or salt marshes) and terrestrial environments (i.e., coastal plains), flooded monthly or with lower frequency (Schaeffer-Novelli et al., 2018; Albuquerque et al., 2014) (Figure 3). Low precipitation and tidal fluxes usually maintain hypersaline conditions (salinity > 100ppt). In Brazil apicuns and mangroves are contiguous ecological systems that present contrasting soils with very different physical, chemical, and mineralogical characteristics (Lacerda et al., 2019). The reduced tidal flooding associated with an evaporative environment and



FIGURE 3 | The Blue Amazon (Brazilian Economic Exclusive Zone, South Atlantic) contains potential and non-actionable BC ecosystems that could contain vast amounts of stored carbon. **(A)** Hypersaline tidal flat (E.g., Barra do Ceará-Ceará state. Photo: N. Beloto, 2020) **(B)** Macroalgal beds (E.g., Arquipélago de S. Pedro e S. Paulo-Pernambuco state. Photo: Dimas Gianuca, 2004); **(C)** Marine animal forest (E.g., Parque Estadual Marinho da Pedra da Risca do Meio - Ceará state. Photo: Marcus Davis, 2021).

hydric deficit seems to be the primary controlling factor for the formation of these wetlands, which are primarily vegetated by extreme halophytes or devoid of vegetation (Hadlich and Ucha, 2009). Active pedogenetic processes (e.g., salinization, sulfidation, and bioturbation) controlled by the above factors have important ecological roles, specifically regarding carbon and nutrient dynamics (Albuquerque et al., 2014). A sandy mineral apicun soil is deposited over former mangroves.

Mangrove leaves and microphytobenthos have been identified as important sources of organic material accumulated along the sediment columns of these systems. The reported soil carbon content of Brazilian HTFs is lower than 1% (Hadlich et al., 2010; Albuquerque et al., 2014; Brown et al., 2021). Rates of organic carbon burial for a Brazilian HTF (Guaratiba Bay, Rio de Janeiro) during the last century were estimated at $17.8 (\pm 0.8) \text{ g C m}^{-2} \text{ y}^{-1}$ (Brown et al., 2021). These rates are considerably lower than the global averages reported for salt marshes ($245 \pm 26 \text{ g m}^{-2} \text{ y}^{-1}$), mangrove forests ($163 \pm 40 \text{ g m}^{-2} \text{ y}^{-1}$), and seagrasses ($138 \pm 38 \text{ g m}^{-2} \text{ y}^{-1}$). Nevertheless, the importance of HTFs as carbon sinks may be substantial given their extensive coverage along Brazil, particularly on northern and northeast coast (MapBiomas 2021; Soares et al., 2021). HTFs are essential for Brazilian mangrove forests, as they act as reservoirs of nutrients and buffer zones, particularly where mangroves are likely to move inland with sea-level rise due to climate change (Schaeffer-Novelli et al., 2018).

3.2 Macroalgal Beds

Environments dominated by macroalgae occupy a global area of 354,000,000 ha and, considering the high sequestration rates ($173 \text{ T C year}^{-1}$), play an essential role in BC budgets (Krause-Jensen and Duarte, 2016). In addition, the burial process of macroalgae-derived organic carbon in shelf sediments and the deep ocean requires that these environments be included in BC estimates (Krause-Jensen et al., 2018), including for the Blue Amazon (Figures 1, 3). While the C stocks of some algal species have been evaluated for some Brazilian regions (e.g., *Sargassum*; Gouvêa et al., 2020), the contribution of most benthic macroalgae to the C budget and burial is unknown in the SW Atlantic. Nevertheless, it is likely that a large fraction of the organic matter produced by macroalgae is exported and buried in adjacent sediments and deep oceans (Krause-Jensen and Duarte, 2016; Macreadie et al., 2019; Gouvêa et al., 2020).

Macroalgal habitats (mainly algal turfs, frondose macroalgae, rhodolith beds, shallow subtidal sargassum beds, and deep-water kelp beds) occupy the sea bottoms along the Blue Amazon (Aued et al., 2018). Deep-water kelp beds (dominated by the endemic *Laminaria abyssalis*) are predicted to cover 3,300,000 ha of the Brazilian continental margin, between depths of 20 and 120 m, under cold water temperatures ($<15\text{--}19^\circ\text{C}$), and with a high nutrient supply of upwelling regimes (Anderson et al., 2021). Considering *L. abyssalis* demographic parameters ($0.22\text{--}2.20 \text{ ind/m}^2$) and individual dry weight (54 to 150 g) and the average C content for *Laminaria* species (30%–33%; King et al., 2020), we can expect average C stocks of up to $0.01 \text{ Mg C ha}^{-1}$. The minimum values of net primary productivity for *Laminaria* species in the Atlantic range between 100 and 300 g C

$\text{m}^{-2} \text{ year}^{-1}$ (King et al., 2020). Extrapolating to the area occupied by *L. abyssalis* in the southwestern Atlantic, it accounts for ecosystem sequestration rates of up to $312 \text{ Mg C year}^{-1}$.

The rhodolith beds of the Blue Amazon span over 22,971,800 ha, equivalent to the area of Australia's Great Barrier Reef (Horta et al., 2016; Carvalho et al., 2020). The most extensive area of rhodolith beds, covering 2,090,000 ha, is on the Abrolhos Bank (Amado-Filho et al., 2012). Distributed from 0 to $\sim 250 \text{ m}$ deep, these beds represent one of the largest carbonate depositional environments and play a fundamental role in the carbon cycle (Horta et al., 2016). The Abrolhos shelf boasts the world's largest expansion of rhodoliths and is able to produce $1 \text{ kg of CaCO}_3 \text{ m}^{-2} \text{ year}^{-1}$, which represents approximately 5% of the CaCO_3 burial/precipitation of the world's carbonate banks (Amado-Filho et al., 2012). Although there is a large distribution and abundance of rhodoliths and seaweeds on the Brazilian coastline (Carvalho et al., 2020), the specific processes of the carbon cycle in these environments have not been completely modeled.

Coralline algae, which form rhodolith beds, may act as a CO_2 sink in the processes of photosynthesis and CaCO_3 dissolution, and as a CO_2 source in the processes of respiration and CaCO_3 production (Gattuso et al., 1998), which may offset the C sequestration capacity in the short term. Using a modeling approach, the potential burial rate has been estimated to be $0.4 \times 10^9 \text{ Tg C year}^{-1}$ (Van de Heijden & Kamenos 2015). There is a need for more comprehensive studies involving the chemistry of coralline algae and refining the models with empirical data before evaluating the role of Brazilian rhodolith beds as true BCEs.

3.3 Plankton-Dominated Coastal Bays and Lagoons

Plankton (bacteria, viruses, phytoplankton, and zooplankton) represent communities in the biological carbon pump because they capture, transform, and export carbon from the upper layers of the ocean and coasts and transfer them for immobilization (Guidi et al., 2016) via benthic suspension feeders (e.g., sponges and octocorals) that compose MAFs (Rossi et al., 2017; Rossi and Rizzo, 2020), such as found across the Amazon Reef System (Soares et al., 2019). Other carbon may be deposited and sequestered through burial in sediments (Macreadie et al., 2019). However, only approximately 0.5% of the carbon fixed in the surface ocean is transferred and deposited on the sea floor.

In this way, higher rates of primary production associated with the eutrophication of Brazilian coastal bays in the tropics can generate large stocks of phytoplankton-derived dissolved and particulate organic carbon, which is permanently being produced, partially degraded, and buried in sediments (Cotovicz Jr. et al., 2018a). For example, the CO_2 sink efficiency of Guanabara Bay (Brazil) may be enhanced by eutrophication owing to its location (near the largest city of Rio de Janeiro) and geomorphological characteristics, such as tropical coastal embayment (Cotovicz Jr. et al., 2015). Recent studies conducted in eutrophic Brazilian coastal lagoons have demonstrated the same pattern of atmospheric CO_2 absorption and organic carbon storage in sediments (Cotovicz Jr. et al., 2021; Erbas et al., 2021). Large-scale exportation provided by plankton

along the tropical and subtropical pelagic marine environments has not been analyzed; however, recent results provided by the Tara Oceans Consortium in the South Atlantic indicate that Radiolaria, alveolate parasites, *Synechococcus*, copepods, and Rhizaria are drivers of carbon exportation (Guidi et al., 2016) to seafloor sediments and MAFs in the SW Atlantic.

3.4 Marine Animal Forests

Other neglected carbon sinks in the Blue Amazon are MAFs, which capture carbon *via* benthic-pelagic coupling (Rossi et al., 2017; Rossi and Rizzo, 2020). MAFs are important carbon immobilizers. Various MAFs, including gorgonian forests (Coppari et al., 2019), sponge gardens (Coppari et al., 2016) (**Figure 3C**), and inactive and passive benthic suspension feeders (Rossi et al., 2017), have been recognized as important systems for considering the BC budget. Ascension Island (South Atlantic, United Kingdom) and the surrounding seamounts in the South Atlantic have shallow MAFs with depths of less than 1,000 m. These MAFs are estimated to capture at least 0.41 MgC ha⁻¹, mainly in the form of deep coral reefs (Barnes et al., 2019). Thus, the Blue Amazon, which has seamounts, sponge gardens, octocoral forests, and an extensive seabed (Soares et al., 2017; Soares et al., 2019), should be considered during the estimation of carbon storage and immobilization in benthic ecosystems and associated sediments. These methodologies, applied to benthic suspension feeder communities (Barnes et al., 2019), mirror similar approaches used in terrestrial forestry studies (Coppari et al., 2016; Coppari et al., 2019) concerning C flux estimation (Rossi and Rizzo, 2020), and could be applied in the Blue Amazon to investigate the overlooked role of MAFs as carbon sinks in the SW Atlantic. However, the total area of the Brazilian MAFs has not been mapped (**Table 1**).

3.5 Continental Shelf

Perhaps the largest C sink, yet the most uncertain stock, lies within the Brazilian shelf sediments, which may receive a large part of the C exported from continental, coastal, and *in situ* pelagic biota inputs (e.g., Amazon River plume) (DeMaster et al., 1996; Sobrinho et al., 2021). Shelf sediments cover ~9% of global marine area and may account for more than 90% of stored carbon within some national inventories (Legge et al., 2020). Despite the large carbon pool, these marine areas are currently not protected by international agreements to promote their conservation.

Bottom trawling is likely to be the most widespread human pressure across the seabed globally, disturbing ecosystem functions and resuspending sediments (Rossi et al., 2019). Trawling affects up to 75% of continental shelf sediments globally, with almost 20 million km² of sediments subject to this pressure (Kaiser et al., 2002). Globally, bottom trawling may release approximately 1.5 billion metric tons of aqueous CO₂ annually, which is equal to that released on land through farming (Sala et al., 2021), plus the 22 Gt year⁻¹ of suspended sediments have high direct impacts on biodiversity. The Brazilian economic exclusive zone is a relevant area for carbon storage and must be considered as a BC research priority and conservation target (Soares et al., 2017). Recent studies have estimated that the

Amazon River Delta has an accumulated sedimentation rate above the global average. Moreover, the suspended material is transported horizontally by river plume fuel production to adjacent seafloor areas, which improves the relevance of the Amazon continental shelf to the global carbon budget (Sobrinho et al., 2021).

4 IMPACTS AND PROTECTION OF THE BCEs SEQUESTRATION

The extension and high biodiversity of the Blue Amazon provides great potential for carbon storage and sequestration, therefore contributing to climate mitigation and adaptation. However, their regional/global role as carbon sinks still needs to be better understood and recognized. Moreover, human impacts on these marine ecosystems must be avoided and managed because of the local and global relevance of ecosystem goods and services, including climate regulation. Climate change could modify the resistance or resilience of BCEs, potentially making them more sensitive to impacts from activities (e.g., bottom trawling and sewage pollution) and direct pressure may amplify climate change constraints in BCEs (Rossi et al., 2017).

In Brazil, BCEs are threatened by a plethora of human pressures such as coastal urbanization, heatwaves, global warming, oil and gas exploitation, eutrophication, ocean acidification, contamination by agricultural, industrial, and urban effluents, mining accidents, large oil spills, deforestation, and aquaculture activities (Pagliosa et al., 2012; Copertino et al., 2016; Soares et al., 2017; Lacerda et al., 2019; Magris et al., 2020; Soares et al., 2021). For example, deforestation for urbanization, salt exploration, and aquaculture has contributed to the loss of extensive mangrove areas and increased carbon emissions (Pagliosa et al., 2012; Kauffman et al., 2018b). In this way, aquaculture activities, such as shrimp farming, may remove 60% of the soil carbon stock and 85% of the living biomass carbon stock (Sasmitho et al., 2020). Shifts in hydrology, tidal exchange, disposal of effluents into mangrove soils, and water changes also have negative effects on BCEs (Macreadie et al., 2017), including in the Blue Amazon (Soares et al., 2017; Magris et al., 2020). Recently, the most extensive oil spill detected in tropical oceans has reached large areas of BCEs, such as mangroves, seagrasses, salt marshes, and rhodolith beds (Magris and Giarrizzo, 2020; Soares et al., 2020). For example, Brazilian estuaries (492,974 ha), mangroves (48,983 ha), seagrass meadows (32,477 ha), and tidal flats (6,364 ha) were severely affected by this oil spill along 3,000 km of coastline (Magris and Giarrizzo, 2020).

In addition to these local and regional pressures, the predicted impacts of climate change on Blue Amazon ecosystems, such as warming (Magris et al., 2015), ocean and coastal acidification (Cotovicz Jr. et al., 2018b; Perretti et al., 2018), rising sea levels (Godoy and Lacerda, 2015), and droughts (Marengo et al., 2017; Soares et al., 2021), also enhance the risks associated with the degradation of BCEs (Magris et al., 2020) and changes in the coverage of BC areas (e.g., retraction and expansion of mangroves) (Lacerda et al., 2019). Thus, the impacts of climate

change on BCEs and their C stocks are dependent on exposure to climate change factors and land use practices (Macreadie et al., 2019; O'Connor et al., 2019). These human activities in the Blue Amazon promote drastic changes in the rates and balance of carbon emissions due to the effects on the storage and sequestration of both the forest structure and burial in the soils (Pagliosa et al., 2012; Nóbrega et al., 2016; Kauffman et al., 2018b; Nóbrega et al., 2019).

Among BCEs, the only environments that have protection measures *via* legal instruments and coverage by coastal and marine protected areas (MPAs) are mangroves (Santos and Schiavetti, 2014). Other systems that are incorporated in MPAs (e.g., seagrass meadows within the Coral Coast MPA and Abrolhos Marine National Park) are also protected by instruments according to specific local, regional, or national laws. Coastal zones are formally protected by national and international legal provisions. For example, Brazilian mangroves are considered national heritage sites (Constitution of Brazil/1988) and permanent preservation areas (Forest Code/2012). Despite this apparent protection, the existing legal framework is insufficient as it does not require the development of public policies and management plans that ensure effective conservation (Ferreira and Lacerda, 2016). In recent years, the Brazilian federal government has made decisions that weakened and dismantled established environmental policies (Fearnside, 2019), modifying the protection of important areas (e.g., mangroves) and disregarding the inefficient use of natural resources (Bernardino et al., 2021).

Although protected by laws and MPAs, mangroves still suffer from illegal exploitation (Lacerda et al., 2019) and poor management effectiveness (Almeida et al., 2016). Shrimp aquaculture and urban development are likely to be the highest threats to mangrove forests in Brazil (Bernardino et al., 2021). The “Reducing Emissions from Deforestation and forest Degradation (REDD)” program could help to restore mangrove environments; however, technical and financial assistance and institutional support are required to implement REDD+ (Ahmed and Glaser, 2016). In addition to scientific gaps and uncertainties, the Blue Amazon suffers from a lack of political and a government agenda for downgrading already protected ecosystems. Therefore, the implementation of this type of instrument in coastal areas is still far from practical.

South America lost approximately 7.8% and 3.8% of its mangrove coverage between 1980–1990 and 1990–2000, respectively (Lacerda et al., 2019), including losses in Brazil (MAPBIOMAS 2021). In addition, it is important to highlight that Brazil has the third highest country-specific potential annual CO₂-equivalent emissions from mangrove soils (Atwood et al., 2017). BCE payments can be implemented in countries with moderate fossil fuel emissions and extensive coastlines, potentially contributing towards climate change mitigation at a national scale (Taillardat et al., 2018). Brazil's gross emission in 2020 was 2.16 billion tons of carbon dioxide equivalent (Gt CO₂; SEEG Brasil, 2021). Discounting carbon removal by secondary forests and protected areas, the national net emissions in the same year were 1.52 Gt CO₂. Considering only fossil fuel and cement production (land use change not included), Brazil

emitted 467.38 million tons CO₂, which represent 1.34% of global emissions (Ritchie and Roser, 2020).

In Brazil, 37.4% of emissions come from the energy sector, followed by the agriculture, land use change and forestry, industrial processes, and waste sectors, which contribute 32.6%, 22.6%, 4.2%, and 3.4% of greenhouse gas emissions, respectively (MCTIC – Ministério da Ciência e Tecnologia do Brasil 2017). In addition, the lack of knowledge regarding reliable and accurate estimates of BC cycling and national budgets is a lost opportunity for economic gains funding from voluntary carbon markets, non-carbon finance, and alternative livelihoods for local communities along the Brazilian coast (Zhao et al., 2020). Carbon credits can be generated for mangroves and coastal wetlands when degraded mangrove habitats are afforested or reforested. This could serve as a strategy to improve the quality of life of citizens and reduce social and economic inequalities using successful global case studies (Taillardat et al., 2018).

Despite the clear societal benefits of carbon sequestration, countries may wish to recognize the benefits in terms of economic value before making decisions about the protection of vulnerable ecosystems, aid policy decisions, widen the market for carbon management and trading (e.g., Nellemann et al., 2009; Luisetti et al., 2019), and include BC protection within national policies (Bertram et al., 2021). Under the increased human and climate pressures predicted for the next decades, damage costs caused by carbon release due to the disturbance of coastal and shelf sea sediments could be very high (e.g., up to US\$ 12.5 billion in UK; Luisetti et al., 2019). However, efforts to manage socio-economic pressures to maintain seabed carbon storage need to account for trade-offs with social welfare benefits, such as food security. Therefore, more robust evidence is needed to develop effective incentive mechanisms to preserve these valuable ecosystems within a sustainability governance framework in Brazil.

5 BCEs NATIONAL PRIORITIES

Surveys on carbon stocks and sequestration in mangroves and other BCEs are fundamental, and defining values and understanding how these ecosystems work in relation to the carbon cycle are essential for climate change compensation projects. This does not mean that surveillance actions should be in the background; however, having observed the political management of Brazil, it is noticeable that there is an inversion of national environmental agencies. Inspection actions are incipient and the budgets for these actions are not being utilized. As a consequence of such environmental liabilities, deforestation and degradation have continued, along with worsening conditions for indigenous people (Scantimburgo, 2018; Fearnside, 2019; Missiatto et al., 2021). The ridge-to-reef concept (Carlson et al., 2019) of ecosystem management can also be applied to Brazilian coastal and marine environments, considering the huge amount of deforestation and pollutants originating from land activities that impact mangroves, seagrass beds, salt marshes, and shallow-water animal forests. Therefore, the priority actions for

BCEs, and all terrestrial and marine areas of high importance, are political, especially for climate change mitigation and adaptation.

6 URGENT RECOMMENDATIONS AND FUTURE DIRECTIONS

The current mismanagement of carbon in the Blue Amazon highlights the need for urgent improvements in research, conservation actions, and science-based policies in the United Nations Decade of Ocean Science (2021–2030). We highlight that the knowledge concerning the ecosystem services of the Blue Amazon, such as C stock/sequestration and protection measures, is still incipient and needs to be improved. Importantly, attempts to measure and set targets for carbon sequestration in BCEs should be kept separate from emissions targets in other economic sectors (e.g., transport, industry, and agriculture), to avoid using BC as an offset of other required emission reductions (Climate Analytics 2017). Although it is essential to prevent the degradation of BCEs, carbon sequestration is not the only or most valuable ecosystem service for local populations along the Blue Amazon.

The wide range of potential benefits that emerge from coastal ecosystem conservation and restoration, beyond carbon sequestration, always have sufficient justification for schemes to incentivize their immediate protection (e.g., payment for ecosystem services), with substantial adaptation benefits for local communities, in addition to other ecosystem services. To maximize these benefits, schemes should be designed with the full set of ecosystem services in mind, in addition to carbon sequestration.

Another urgent problem regarding carbon mismanagement in the Blue Amazon is that other BCEs such as seagrass, tidal salt marshes, HTFs, MAFs, and rhodolith beds still have little protection from MPAs or legal provisions that prevent intense economic exploitation (Copertino et al., 2016; Horta et al., 2016; Soares et al., 2017; Magris et al., 2020). Therefore, it is necessary to increase legal protection and MPA coverage in all environments and improve the efficiency of public policies, such as the management effectiveness of mangrove protected areas (Almeida et al., 2016). Moreover, conservation actions that are advantageous for both BC and the structural complexity and diversity of marine species, such as initiatives in terrestrial forests (Silveira et al., 2019), are preferable to carbon-focused initiatives in coastal and marine environments. Thus, it is important to identify and provide effective protection to BC diversity hotspots along the southwestern Atlantic coast.

7 SUMMARY ACTIONS FOR RESEARCHERS AND POLICYMAKERS

- Promote research that provides information about C stocks, sequestration, and burial rates in Brazilian BCEs and that aims to understand carbon cycling in these environments.
- Reinforce surveillance actions in BCE areas, especially in those with high carbon sequestration and storage potential.

- Change the management of national and state environmental agencies to promote actions in BCEs and their dependent human communities favors.
- Establish goals for carbon sequestration in Brazilian BCEs together with economic sectors, considering carbon credit mechanisms.
- Consider all environmental goods and services provided by such unique environments, as well as carbon sequestration and storage, for the valorization of BCEs.
- Increase the legal protection of BCE areas, including environments that are still poorly measured or valued for their economic and environmental importance, such as seagrasses, HTFs, MAFs, and rhodolith beds.
- Establish the conservation and restoration of BCEs as a national priority for ocean-based carbon dioxide removal (CDR) and adaptation measures.

8 CONCLUSIONS

The Blue Amazon is potentially one of the largest carbon sinks on Earth but is largely overlooked. In addition, estimates of quantitative total carbon stocks, burial rates, and atmospheric exchanges of greenhouse gases in Brazilian BCEs are scarce. In this regard, systematic reviews and field/laboratory research on BC stocks in Brazilian coastal and marine ecosystems are a priority topic. It is important to publish future systematic reviews to demonstrate the gaps in current knowledge and original research to provide robust BC budgets of this extensive area.

It is necessary to improve the estimates of carbon stocks, fluxes, protection, and restoration of carbon both above- and belowground in already actionable BCEs (e.g., mangroves and seagrass meadows) and those still not-actionable (e.g., MAFs, HTFs, and macroalgal beds). However, the overall focus of current BC research on the estimations of total stocks and burial rates (habitat-bound carbon) has overlooked the mobile BC fraction, that is, carbon outwelling (lateral fluxes or horizontal exports of C to the ocean; Santos et al., 2021). Therefore, the sequestration capacity of BCEs can be largely underestimated (Santos et al., 2021; Rovai et al., 2022).

Understanding how climate change affects the carbon sequestration capacity in mature BC ecosystems (including Brazil) and during their restoration is a research priority (Macreadie et al., 2019). The role of rhodolith and fleshy macroalgal beds (sinks/donors) in BC cycling and the degree to which greenhouse gases are released following disturbance of BCEs are emerging scientific questions. Finally, we need to improve precision of the extent of BCEs, techniques to determine BC provenance, and understanding of the biotic and abiotic factors that influence sequestration in BCEs.

AUTHOR CONTRIBUTIONS

MOS: conceptualization, writing—original draft, writing—review and editing, methodology, and formal analysis. LB: writing—original draft, writing—review and editing, and formal analysis. BL: writing—original draft, writing—review

and editing, and formal analysis. KB: writing—original draft, writing—review and editing, and formal analysis. MC: writing—original draft, writing—review and editing, and formal analysis. RM: writing—original draft, writing—review and editing, and formal analysis. NB: writing—original draft, writing—review and editing, and formal analysis. LC: writing—original draft, writing—review and editing, and formal analysis. All authors contributed to the article and approved the submitted version.

FUNDING

This study was sponsored by Brazilian Long Term Ecological Research (Brazilian LTER) at Costa Semiárida do Brasil (PELD-CSB / CNPq Proc. 442337/2020-5), Alexander Von Humboldt Foundation (CAPES/AVH), and Brazilian Research Network on Global Climate Change (Rede CLIMA/ FINEP Grant 01.13.0353-00). MOS and LEAB are CNPq (Grants 313518/2020-3 and 310165/2020-2, respectively) and FUNCAP research fellows (Chief Scientist Program). MC was sponsored by CNPq (Edital

Universal Process 433602/2018-0; PELD-ELPA Proc. 403805/2012-0). NB received a PhD scholarship from CAPES. LC receives a visiting professor grant from UFC (FUNCAP, No. INT-00159-00009.01.00/19).

ACKNOWLEDGMENTS

The authors thank the editor JP and the three reviewers for their constructive comments and recommendations that improved the manuscript. MC is deeply indebted to The Blue Carbon Initiative and Blue Carbon Scientific Working Group for all intellectual and motivational support and to Conservation International and IOC-UNESCO for international travel awards. This study is a jointed contribution of the Brazilian Research Network on Global Climate Change (Rede CLIMA/ FINEP Grant 01.13.0353-00), Brazilian LTER (PELD-CSB and PELD-ELPA) and Institutional Program for Internationalization (CAPES – PrInt) from Federal University of Ceará and Federal University of Rio Grande.

REFERENCES

- Ahmed, N., and Glaser, M. (2016). Coastal Aquaculture, Mangrove Deforestation and Blue Carbon Emissions: Is REDD+ a Solution? *Mar. Pollut. Bull.* 66, 56–66. doi: 10.1016/j.marpol.2016.01.011
- Albuquerque, A. G. B. M., Ferreira, T. O., Cabral, R. L., Nóbrega, G. N., Romero, R. E., Meireles, A. J. A., et al. (2014). Hypersaline Tidal Flats (Apicum Ecosystems): The Weak Link in the Tropical Wetlands Chain. *Environ. Rev.* 22, 1–11. doi: 10.1139/er-2013-0026
- Almeida, L. T., Olimpio, J. L., Pantalena, A. F., Almeida, B. S., and Soares, M. O. (2016). Evaluating Ten Years of Management Effectiveness in a Mangrove Protected Area. *Ocean Coastal Manag.* 125, 29–37. doi: 10.1016/j.ocecoaman.2016.03.008
- Alongi, M. D. (2020). Global Significance of Mangrove Blue Carbon in Climate Change Mitigation. *Sci* 2 (3), 67. doi: 10.3390/sci2030067
- Amado-Filho, G. M., Moura, R. L., Bastos, A. C., Salgado, L. T., Sumida, P. Y., Guth, A. Z., et al. (2012). Rhodolith Beds Are Major CaCO₃ Bio-Factories in the Tropical South West Atlantic. *PloS One* 7 (4), e35171. doi: 10.1371/journal.pone.0035171
- Anderson, A. B., Assis, J., Batista, M. B., Serrão, E. A., Guabiroba, H. C., Delfino, S. D. T., et al. (2021). Global Warming Assessment Suggests the Endemic Brazilian Kelp Beds to be an Endangered Ecosystem. *Mar. Environ. Res.* 168, 105307. doi: 10.1016/j.marenvres.2021.105307
- Atwood, T. B., Connolly, R. M., Almahsheer, H., Carnell, P. E., Duarte, C. M., Lewis, C. J. E., et al. (2017). Global Patterns in Mangrove Soil Carbon Stocks and Losses. *Nat. Clim. Change* 7, 523–528. doi: 10.1038/nclimate3326
- Aued, A. W., Smith, F., Quimbayo, J. P., Cândido, D. V., Longo, G. O., Ferreira, C. E. L., et al. (2018). Large-Scale Patterns of Benthic Marine Communities in the Brazilian Province. *PloS One* 13(6), e0198452. doi: 10.1371/journal.pone.0198452
- Barbosa, R. V., Davies, A. J., and Sumida, P. Y. G. (2019). Habitat Suitability and Environmental Niche Comparison of Cold-Water Coral Species Along the Brazilian Continental Margin. *Deep-Sea Res. Part I- Oceanographic Res. Papers* 154, 103147. doi: 10.1016/j.dsr.2019.103147
- Barnes, D. K. A., Sands, C. J., Richardson, A., and Smith, N. (2019). Extremes in Benthic Ecosystem Services; Blue Carbon Natural Capital Shallower Than 1000m in Isolated, Small, and Young Ascension Island's EEZ. *Front. Mar. Sci.* 6. doi: 10.3389/fmars.2019.00663
- Barros, K., Costa, F., and Rocha-Barreira, C. (2014). A Halophila Baillonis Ascherson Bed on the Semi-arid Coast of Brazil. *Feddes Repert.* 125 (3-4), 93–97.
- Barros, K. V. S., Rocha-Barreira, C. A., and Magalhães, K. M. (2013). Ecology of Brazilian Seagrasses: Is Our Current Knowledge Sufficient to Make Sound Decisions About Mitigating the Effects of Climate Change? *Iheringia Sér. Bot.* 68 (1), 163–178. doi: 10.1016/j.marpol.2020.104389
- Bernardino, A. F., Nóbrega, G. N., and Ferreira, T. O. (2021). Consequences of Terminating Mangroves Protection in Brazil *Mar. Policy* 125:104389. doi: 10.1590/1678-4766e2017048
- Bertram, C., Quass, M., Reusch, T. B. H., Vafeidis, A. T., Wolff, C., and Rickels, W. (2021). The Blue Carbon Wealth of Nations. *Nat. Clim. Chang.* 11, 704–709. doi: 10.1038/s41558-021-01089-4
- Bouillon, S., Borges, A. V., Castañeda-Moya, E., Diele, K., Dittmar, T., Duke, N. C., et al. (2008). Mangrove Production and Carbon Sinks: A Revision of Global Budget Estimates. *Glob. Biogeochem. Cy.* 22, GB2013. doi: 10.1029/2007GB003052
- Brown, D. R., Marotta, H., Peixoto, R. B., Enrich-Prast, A., Barroso, G. C., Soares, M. L., et al. (2021). Hypersaline Tidal Flats as Important “Blue Carbon” Systems: A Case Study From Three Ecosystems. *Biogeosciences* 18 (8), 2527–2538. doi: 10.5194/bg-18-2527-2021
- Cabral, A., Dittmar, T., Call, M., Scholten, J., de Rezende, C. E., Asp, N., et al. (2021). Carbon and Alkalinity Outwelling Across the Groundwater-Creek-Shelf Continuum Off Amazonian Mangroves. *Limnol. Oceanogr. Lett.* 6, 369–378. doi: 10.1002/lol2.10210
- Call, M., Santos, I. R., Dittmar, T., Rezende, C. E., Asp, N. E., and Maher, D. T. (2019). High Pore-Water Derived CO₂ and CH₄ Emissions From a Macro-Tidal Mangrove Creek in the Amazon Region. *Geochim. Cosmochim. Acta* 247, 106–120. doi: 10.1016/j.gca.2018.12.029
- Carlson, R. R., Foo, S. A., and Asner, G. P. (2019). Land Use Impacts on Coral Reef Health: A Ridge-To-Reef Perspective. *Front. Mar. Sci.* 6. doi: 10.3389/fmars.2019.00562
- Carvalho, V. F., Assis, J., Serrão, E. A., Nunes, J. M., Anderson, A. B., Batista, M. B., et al. (2020). Environmental Drivers of Rhodolith Beds and Epiphytes Community Along the South Western Atlantic Coast. *Mar. Environ. Res.* 154, 104827. doi: 10.1016/j.marenvres.2019.104827
- Climate Analytics (2017) *Blue Carbon Briefing: The Dangers of Blue Carbon Offsets: From Hot Air to Hot Water*. Available at: https://climateanalytics.org/media/blue_carbon_briefing_16112017.pdf.
- Choi, K. F. (2011). Áreas Prioritárias Para a Conservação Do Peixe-Boi Marinho Trichechus Manatus No Ceará e Rio Grande do Norte (2011). *Dissertação (Mestrado em Ciências Marinhas e Tropicais)*, Instituto de Ciências do Mar, Universidade Federal do Ceará, Fortaleza 246f. Online access: <https://repositorio.ufc.br/handle/riufc/14762>.

- Copertino, M. S., Creed, J. C., Lanari, M. O., Magalhães, K., Barros, K., Lana, P. C., et al. (2016). Seagrass and Submerged Aquatic Vegetation (VAS) Habitats Off the Coast of Brazil: State of Knowledge, Conservation and Main Threats. *Braz. J. Oceanogr.* 64 (2), 53–80. doi: 10.1590/S1679-875920161036064sp2
- Copertino, M., and Seeliger, U. (2010). “Habitats De Ruppia Marítima E De Macroalgas,” in *O Estuário Da Lagoa Dos Patos: Um Século De Transformações, Ed. FURG*, 92–98. Rio Grande: FURG (Federal Universidade do Rio Grande).
- Coppari, M., Gori, A., Viladrich, N., Saponari, L., Canepa, A., Grinyó, J., et al. (2016). The Role of Mediterranean Sponges in Benthic-Pelagic Coupling Processes: *Aplysina Aerophoba* and *Axinella Polypoides* Case Studies. *J. Exp. Mar. Biol. Ecol.* 477, 57–68. doi: 10.1016/j.jembe.2016.01.004
- Coppari, M., Zanella, C., and Rossi, S. (2019). The Importance of Coastal Gorgonians in the Blue Carbon Budget. *Sci. Rep.* 9, 13550. doi: 10.1038/s41598-019-49797-410.1038/s41598-019-49797-4
- Costa, C. S., Marangoni, J. C., and Azevedo, A. M. G. Plant zonation in irregularly flooded salt marshes: relative importance of stress tolerance and biological interactions. *J. Ecol.*, v. 91, p. 951965, 2003
- Cotovicz, L. C. Jr., Chielle, R., and Marins, R. V. (2020). Air-Sea CO₂ Flux in an Equatorial Continental Shelf Dominated by Coral Reefs (Southwestern Atlantic Ocean). *Cont. Shelf Res.* 204, 104175. doi: 10.1016/j.csr.2020.104175
- Cotovicz, L. C. Jr., Knoppers, B. A., Brandini, N., Costa Santos, S. J., and Abril, G. (2015). A Strong CO₂ Sink Enhanced by Eutrophication in a Tropical Coastal Embayment (Guanabara Bay, Rio De Janeiro, Brazil). *Biogeosciences* 12, 6125–6146. doi: 10.5194/bg-12-6125-2015
- Cotovicz, L. C. Jr., Knoppers, B. A., Brandini, N., Poirier, D., Costa Santos, S. J., and Abril, G. (2018b). Aragonite Saturation State in a Tropical Coastal Embayment Dominated by Phytoplankton Blooms (Guanabara Bay - Brazil). *Mar. Pollut. Bull.* 129, 729–739. doi: 10.1016/j.marpolbul.2017.10.064
- Cotovicz, L. C. Jr., Knoppers, B. A., Brandini, N., Poirier, D., Costa Santos, S. J., Cordeiro, R. C., et al. (2018a). Predominance of Phytoplankton-Derived Dissolved and Particulate Organic Carbon in a Highly Eutrophic Tropical Coastal Embayment (Guanabara Bay, Rio De Janeiro, Brazil). *Biogeochemistry* 137, 1–14. doi: 10.1007/s10533-017-0405-y
- Cotovicz, L. C. Jr., Knoppers, B. A., Régis, C. R., Tremmel, D., Costa Santos, S. J., and Abril, G. (2021). Eutrophication Overcoming Carbonate Precipitation in a Tropical Hypersaline Coastal Lagoon Acting as a CO₂ Sink (Araruama Lagoon, SE Brazil). *Biogeochemistry* 156, 231–254. doi: 10.1007/s10533-021-00842-3
- Creed, J. C. (2003). “The Seagrasses of South America: Brazil, Argentina, and Chile,” in *World Atlas of Seagrasses*. Eds. E. P. Green and F. T. Short (Berkeley: The University California Press), 243–250.
- Davy, A., and Costa, C. S. B. (1992). “Development and Organisation of Salt Marsh Communities,” in *Coastal Plant Communities of Latin America*. Ed. U. Seeliger (San Diego, USA: Academic Press), 157–178.
- de los Santos, C. B., Krause-Jensen, D., Alcoverro, T., Marbà, N., Duarte, C. M., van Katwijk, M. M., et al. (2019). Recent Trend Reversal for Declining European Seagrass Meadows. *Nat. Commun.* 10, 3356. doi: 10.1038/s41467-019-11340-4
- DeMaster, D. J., Smith, W. O. Jr., Nelson, D. M., and Aller, J. Y. (1996). Biogeochemical Processes in Amazon Shelf Waters: Chemical Distributions and Uptake Rates of Silicon, Carbon and Nitrogen. *Cont. Shelf Res.* 16 (5-6), 617–643. doi: 10.1016/0278-4343(95)00048-8
- Diniz, C., Cortinhas, L., Nerino, G., Rodrigues, J., Sadeck, L., Adami, M., et al. (2019). Brazilian Mangrove Status: Three Decades of Satellite Data Analysis. *Remote Sens.* 11 (7), 808. doi: 10.3390/rs11070808
- Dittmar, T., Hertkorn, N., Kattner, G., and Lara, R. (2006). Mangroves, a Major Source of Dissolved Organic Carbon to the Oceans. *Global Biogeochem. Cy.* 20, GB1012. doi: 10.1029/2005GB002570
- Duarte, C. M. (2017). Reviews and Syntheses: Hidden Forests, the Role of Vegetated Coastal Habitats in the Ocean Carbon Budget. *Biogeosciences* 14, 301–310. doi: 10.5194/bg-14-301-2017
- Duarte, C. M., and Cebrian, J. (1996). The Fate of Marine Autotrophic Production. *Limnol. Oceanogr.* 41 (8), 1758–1766. doi: 10.4319/lo.1996.41.8.1758
- Duarte, C. M., Middelburg, J. J., and Caraco, N. (2005). Major Role of Marine Vegetation on the Oceanic Carbon Cycle. *Biogeosciences* 2 (1), 1–8. doi: 10.5194/bg-2-1-2005
- Erbas, T., Marques, A., and Abril, G. (2021). A CO₂ Sink in a Tropical Coastal Lagoon Impacted by Cultural Eutrophication and Upwelling. *Estuar. Coast Shelf Sci.* 263, 107633. doi: 10.1016/j.ecss.2021.107633
- Fearnside, P. M. (2019). “O Desmonte Da Legislação Ambiental,” In *Movimentos Socioambientais*. Ed. J. S. Weiss (Goiás: Editora Xapuri Socioambiental), 317–381.
- Ferreira, A. C., Bezerra, L. E. A., and Matthews-Cascon, H. (2019). Aboveground Carbon Stock in a Restored Neotropical Mangrove: Influence of Management and Brachyuran Crab Assemblage. *Wetlands Ecol. Manag.* 27, 1–20. doi: 10.1007/s11273-019-09654-7
- Ferreira, A. C., and Lacerda, L. D. (2016). Degradation and Conservation of Brazilian Mangroves, Status and Perspectives. *Ocean Coastal Manag.* 125, 38–46. doi: 10.1016/j.ocecoaman.2016.03.011
- Figueiredo, M. A. O., Horta, P. A., Pedrini, A. G., and Nunes, J. M. C. (2008). Benthic Marine Algae of the Coral Reefs of Brazil: A Literature Review. *Oecol. Bras.* 12 (2), 258–269. doi: 10.4257/oeco.2008.1202.07
- Flynn, M. N., Wakabara, Y., and Tararam, A. S. (1998). Macrobenthic associations of the lower and upper marshes of a tidal flat colonized by *Spartina alterniflora* in Cananea lagoon estuarine region. *Bull. Mar. Sci.* 63 (2), 427–442.
- Fourqurean, J. W., Duarte, C. M., Kennedy, H., Marbà, N., Holmer, M., Mateo, M. A., et al. (2012). Seagrass Ecosystems as a Globally Significant Carbon Stock. *Nat. Geosci.* 5 (7), 505–509. doi: 10.1038/ngeo1477
- Friedlingstein, P., Jones, M. W., O’Sullivan, M., Andrew, R. M., Hauck, J., Peters, G. P., et al. (2019). Global Carbon Budget 2019. *Earth Syst. Sci. Data* 11 (7), 17831838. doi: 10.5194/essd-11-1783-2019
- Gama, L. R. (2015). *Ecologia trófica e áreas de alimentação de Chelonia mydas (LINNAEUS, 1758), no litoral do Paraná, Brasil*. Dissertação de Mestrado, Universidade Estadual de Londrina, Londrina, 2015
- Gatti, L. V., Basso, L. S., Miller, J. B., Gloor, M., Domingues, L. G., Cassol, H. L. G., et al. (2021). Amazonia as a Carbon Source Linked to Deforestation and Climate Change. *Nature* 595, 388–393. doi: 10.1038/s41586-021-03629-6
- Gattuso, J.-P., Frankignoulle, M., and Wollast, R. (1998). Carbon and Carbonate Metabolism in Coastal Aquatic Ecosystems. *Annu. Rev. Ecol. Syst.* 29 (1), 405–434. doi: 10.1146/annurev.ecolsys.29.1.405
- Gattuso, J.-P., Magnan, A. K., Bopp, L., Cheung, W. W. L., Duarte, C. M., Hinkel, J., et al. (2018). Ocean Solutions to Address Climate Change and its Effects on Marine Ecosystems. *Front. Mar. Sci.* 5. doi: 10.3389/fmars.2018.00337
- Giri, C., Ochieng, E., Tieszen, L. L., Zhu, Z., Singh, A., Loveland, T., et al. (2011). Status and Distribution of Mangrove Forests of the World Using Earth Observation Satellite Data. *Global Ecol. Biogeogr.* 20, 154–159. doi: 10.1111/j.1466-8238.2010.00584.x
- Godoy, M. D. P., and Lacerda, L. D. (2015). Mangroves Response to Climate Change: A Review of Recent Findings on Mangrove Extension and Distribution. *Anais Acad. Bras. Cienc.* 87, 651–667. doi: 10.1590/0001-3765201520150055
- Gorman, D., Pavone, C. B., and Flores, A. A. V. (2020a). Changes to the Structure of Tropical Seagrass Meadows (*Halophila Decipiens*) in the Warm-Temperate Waters of the Southwest Atlantic. *Aquat. Bot.* 161, 103174. doi: 10.1016/j.aquabot.2019.103174
- Gorman, D., Sumida, P. Y. G., Figueira, R. C. L., and Turra, A. (2020b). Improving Soil Carbon Estimates of Mudflats in Aracá Bay Using Spatial Models That Consider Riverine Input, Wave Exposure and Biogeochemistry. *Estuar. Coastal Shelf Sci.* 238(5), 106734. doi: 10.1016/j.ecss.2020.106734
- Gouvêa, L. P., Assis, J., Gurgel, C. F. D., Serrão, E. A., Silveira, T. C. L., Santos, R., et al. (2020). Golden Carbon of *Sargassum* Forests Revealed as an Opportunity for Climate Change Mitigation. *Sci. Total Environ.* 729(10), 138745. doi: 10.1016/j.scitotenv.2020.138745
- Guidi, L., Chaffron, S., Bittner, L., Eveillard, D., Larhlimi, A., Roux, S., et al. (2016). Plankton Networks Driving Carbon Export in the Oligotrophic Ocean. *Nature* 532, 465–470. doi: 10.1038/nature16942
- Gullström, M., Lyimo, L. D., Dahl, M., Samuelsson, G. S., Eggertsen, M., Anderberg, E., et al. (2018). Blue Carbon Storage in Tropical Seagrass Meadows Relates to Carbonate Stock Dynamics, Plant–Sediment Processes, and Landscape Context: Insights From the Western Indian Ocean. *Ecosystems* 21, 551–566. doi: 10.1007/s10021-017-0170-8
- Hadlich, G. M., Celino, J. J., and Ucha, J. M. (2010). Physical-Chemical Differentiation Between Supratidal Salt Flats, Mangroves and Hillsides in the Todos Os Santos Bay, Northeast Brazil. *Geociências* 4 (29), 633–641.

- Hadlich, G. M., and Ucha, J. M. (2009). Apicuns: Aspectos Gerais, Evolução Recente E Mudanças Climáticas Globais. *Rev. Bras. Geomorf.* 2 (10), 13–20. doi: 10.20502/rbg.v10i2.126
- Hamilton, S. E., and Casey, D. (2016). Creation of a High Spatio-Temporal Resolution Global Database of Continuous Mangrove Forest Cover for the 21st Century (CGMFC-21). *Global Ecol. Biogeogr.* 25 (6), 729–738. doi: 10.1111/geb.12449
- Hamilton, S. E., and Friess, D. A. (2018). Global Carbon Stocks and Potential Emissions Due to Mangrove Deforestation From 2000 to 2012. *Nat. Climate Change* 8, 240–244. doi: 10.1038/s41558-018-0090-4
- Hatje, V., Masqué, P., Patire, V. F., Dorea, A., and Barros, F. (2020). Blue Carbon Stocks, Accumulation Rates, and Associated Spatial Variability in Brazilian Mangroves. *Limnol. Oceanogr.* 1 (1), 1–14. doi: 10.1002/lno.11607
- Hoegh-Guldberg, O., Caldeira, K., Chopin, T., Gaines, S., Haugan, P., Hemer, M., et al. (2019). *The Ocean as a Solution to Climate Change: Five Opportunities for Action* (Washington, DC: World Resources Institute).
- Hoeinghaus, D. J., Vieira, J. P., Costa, C., Bemvenuti, C. E., Winemiller, K. O., and Garcia, A. M. (2016). Estuary Hydrogeomorphology Affects Carbon Sources Supporting Aquatic Consumers Within and Among Ecological Guilds. *Hydrobiologia* 673, 79–92. doi: 10.1007/s10750-011-0751-z
- Horta, P. A. (2000). Macroalgas Do Infralitoral Do Sul e Sudeste Do Brasil: Taxonomia e Biogeografia. (2000). *Tese de Doutorado*, Universidade de São Paulo, São Paulo, 2000.
- Horta, P. A., Riul, P., Amado Filho, G. M., Gurgel, C. F. D., Berchez, F., Nunes, J. M. C., et al. (2016). Rhodoliths in Brazil: Current Knowledge and Potential Impacts of Climate Change. *Braz. J. Oceanogr.* 64 (2), 117–136. doi: 10.1590/S1679-875920160870064sp2
- Howard, J. L., Creed, J. C., Aguiar, M. V. P., and Fouquereau, J. W. (2017a). CO₂ Released by Carbonate Sediment Production in Some Coastal Areas may Offset the Benefits of Seagrass “Blue Carbon”. *storage Limnol. Oceanogr.* 63 (1), 160–172. doi: 10.1002/lno.10621
- Howard, J., Sutton-Grier, A., Herr, D., Kleypas, J., Landis, E., McLeod, E., et al. (2017b). Clarifying the Role of Coastal and Marine Systems in Climate Mitigation. *Front. Ecol. Environ.* 15, 42–50. doi: 10.1002/fee.1451
- Howard, J. L. (2018). “Patterns of Carbon Metabolism, Storage, and Remineralization in Seagrass Ecosystems”. *FIU Electronic Theses and Dissertations*. 3719. doi: 10.25148/etd.FIDC004080
- Intergovernmental Panel on Climate Change (IPCC) (2014). *Supplement to the 2006 IPCC Guidelines for National Greenhouse Gas Inventories* (Wetlands. Switzerland: IPCC).
- Isacch, J. P., Costa, C. S. B., Rodríguez-Gallego, L., Conde, D., Escapa, M., Gagliardini, D. A., et al. (2006). Distribution of Saltmarsh Plant Communities Associated With Environmental Factors Along a Latitudinal Gradient on the South-West Atlantic Coast. *J. Biogeogr.* 33 (5), 888–900. doi: 10.1111/j.1365-2699.2006.01461.x
- IPCC. (2021). Summary for Policymakers. *Climate Change 2021: The Physical Science Basis. Contribution of Working Group I to the Sixth Assessment Report of the Intergovernmental Panel on Climate Change* V. P. Masson-Delmotte, A. Zhai, S. L. Pirani, C. Connors, S. Péan, N. Berger, et al. Cambridge University Press.
- Jayathilake, D. R. M., and Costello, M. J. (2018). A Modelled Global Distribution of the Seagrass Biome. *Biol. Conserv.* 226, 120–126. doi: 10.1016/j.biocon.2018.07.009
- Jorge, R. R., Harari, J., and Fujii, M. T. (2012). Macroalgal Composition and its Association With Local Hydrodynamics in the Laje De Santos Marine State Park, Southwestern Atlantic, São Paulo, Brazil. *Braz. J. Oceanogr. Set* 2012 60 (3), 405–419. doi: 10.1590/S1679-87592012000300012
- Kaiser, M. J., Collie, J. S., Hall, J. S., Jennings, S., and Poiner, I. R. (2002). Modification of Marine Habitats by Trawling Activities: Prognosis and Solutions. *Fish Fish* 3, 114–136. doi: 10.1046/j.1467-2979.2002.00079.x
- Kauffman, J. B., Bernardino, A. F., Ferreira, T. O., Giovannoni, L. R., Gomes, L. E., Romero, D. J., et al. (2018a). Carbon Stocks of Mangroves and Salt Marshes of the Amazon Region, Brazil. *Biol. Lett.* 14, 20180208. doi: 10.1098/rsbl.2018.0208
- Kauffman, J. B., Bernardino, A. F., Ferreira, T. O., Bolton, N. W., Gomes, L. E. O., and Nóbrega, G. N. (2018b). Shrimp Ponds Lead to Massive Loss of Soil Carbon and Greenhouse Gas Emissions in Northeastern Brazilian Mangroves. *Ecol. Evol.* 8, 1–11. doi: 10.1002/ecs3.4079
- Kauffman, J. B., Adame, M. F., Arifanti, V. B., Schile-Beers, L. M., Bernardino, A. F., Bhomia, R. K., et al. (2020). Total Ecosystem Carbon Stocks of Mangroves Across Broad Global Environmental and Physical Gradients. *Ecol. Monogr.* 90 (2), e01405. doi: 10.1002/ecm.1405
- Kennedy, H., Beggins, J., Duarte, C. M., Fourqurean, J. W., Holmer, M., Marbà, N., et al. (2010). Seagrass Sediments as a Global Carbon Sink: Isotopic Constraints. *Global Biogeochem. Cycles* 24 (4), GB4026. doi: 10.1029/2010GB003848
- King, N. G., Moore, P. J., Pessarrodona, A., Burrows, M., and Moore, P. J. (2020). Ecological Performance Differs Between Range Centre and Trailing Edge Populations of a Cold-Water Kelp: Implications for Estimating Net Primary Productivity. *Mar. Biol.* 167, 137. doi: 10.1007/s00227-020-03743-5
- Krause-Jensen, D., and Duarte, C. M. (2016). Substantial Role of Macroalgae in Marine Carbon Sequestration. *Nat. Geosci.* 9 (10), 737–742. doi: 10.1038/ngeo2790
- Krause-Jensen, D., Lavery, P., Serrano, O., Marbà, N., Masque, P., and Duarte, C. M. (2018). Sequestration of Macroalgal Carbon: The Elephant in the Blue Carbon Room. *Biol. Lett.* 14 (6), 20180236. doi: 10.1098/rsbl.2018.0236
- Lacerda, L. D., Borges, R., and Ferreira, A. C. (2019). Neotropical Mangroves: Conservation and Sustainable Use in a Scenario of Global Climate Change. *Aquat. Conserv. Mar. Freshwater Ecosyst.* 29, 1347–1364. doi: 10.1002/aqc.3119
- Lanari, M., Copertino, M., and Horta, P. (2022). Functional redundancy and stability in a subtidal macroalgal community in the Southwestern Atlantic coast. *Mar. Environ. Res.* 173, 105519. doi: 10.1016/j.marenvres.2021.105519
- Leão, Z. M. A. N., Kikuchi, R. K. P., Ferreira, B. P., Sovierzoski, H. H., Oliveira, M. D. M., Maida, M., et al. (2016). Brazilian Coral Reefs in a Period of Global Change: a Synthesis. *Braz. J. Oceanogr.* 64, 97116. doi: 10.1590/S1679-875920160916064sp2
- Legge, O., Johnson, M., Hicks, N., Jickells, T., Diesing, M., Aldridge, J., et al. (2020). Carbon on the Northwest European Shelf: Contemporary Budget and Future Influences. *Front. Mar. Sci.* 7. doi: 10.3389/fmars.2020.00143
- Lezaun, J. (2021). Hugging the Shore: Tackling Marine Carbon Dioxide Removal as a Local Governance Problem. *Front. Clim.* 3. doi: 10.3389/fclim.2021.684063
- Lovelock, C. E., Atwood, T., Baldock, J., Duarte, C. M., Hickey, S., Lavery, P. S., et al. (2017). Assessing the Risk of Carbon Dioxide Emissions From Blue Carbon Ecosystems. *Front. Ecol. Environ.* 15 (5), 257–265. doi: 10.1002/fee.1491
- Lovelock, C. E., and Duarte, C. M. (2019). Dimensions of Blue Carbon and Emerging Perspectives. *Biol. Lett.* 15 (3), 20180781. doi: 10.1098/rsbl.2018.0781
- Luisetti, T., Turner, R. K., Andrews, J. E., Jickells, T. D., Kröger, S., Diesing, M., et al. (2019). Quantifying and Valuing Carbon Flows and Stores in Coastal and Shelf Ecosystems in the UK. *Ecosyst. Serv.* 35, 67–76. doi: 10.1016/j.ecoser.2018.10.013
- Macreadie, P. I., Anton, A., Raven, J. A., Beaumont, N., Connolly, R. M., Friess, D. A., et al. (2019). The Future of Blue Carbon Science. *Nat. Commun.* 10, 3998. doi: 10.1038/s41467-019-11693-w
- Macreadie, P. I., Baird, M. E., Trevathan-Tackett, S. M., Larkum, A. W. D., and Ralph, P. J. (2014). Quantifying and Modelling the Carbon Sequestration Capacity of Seagrass Meadows: a Critical Appraisal? *Mar Pollut Bull.* 83, 430–439. doi: 10.1016/j.marpolbul.2013.07.038
- Macreadie, P. I., Nielsen, D. A., Kelleway, J. J., Atwood, T. B., Seymour, J. R., Petrou, K., et al. (2017). Can We Manage Coastal Ecosystems to Sequester More Blue Carbon? *Front. Ecol. Environ.* 15 (4), 206–213. doi: 10.1002/fee.1484
- Magalhães, K. M., Barros, K. V. S., Lima, M. C. S., Rocha-Barreira, C. A., Rosa Filho, J., and Soares, M. O. (2020). Oil Spill + COVID-19: A Disastrous Year for Brazilian Seagrass Conservation. *Sci. Total Environ.* 764, 142872. doi: 10.1016/j.scitotenv.2020.142872
- Magris, R. A., Costa, M. D. P., Ferreira, C. E. L., Vilar, C. C., Joyeux, J.-C., Creed, J. C., et al. (2020). A Blueprint for Securing Brazil’s Marine Biodiversity and Supporting the Achievement of Global Conservation Goals. *Diversity Distrib* 27(2), 198–215. doi: 10.1111/ddi.13183
- Magris, R. A., and Giarrizo, T. (2020). Mysterious Oil Spill in the Atlantic Ocean Threatens Marine Biodiversity and Local People in Brazil. *Mar. Pollut. Bull.* 153, 110961. doi: 10.1016/j.marpolbul.2020.110961
- Magris, R. A., Heron, S. F., and Pressey, R. L. (2015). Conservation Planning for Coral Reefs Accounting for Climate Warming Disturbances. *PLoS ONE* 10 (11), e0140828. doi: 10.1371/journal.pone.0140828

- Maher, D. T., Call, M., Santos, I. R., and Sanders, C. (2018). Beyond Burial: Lateral Exchange is a Significant Atmospheric Carbon Sink in Mangrove Forests. *Biol. Lett.* 14, 20180200. doi: 10.1098/rsbl.2018.0200
- MAPBIOMAS (2021). *Manguezais, Praias, Dunas & Areais, Aquicultura E Apicuns Nos Últimos 36 Anos. Destaques do Mapeamento Anual Dos Manguezais, Praias, Dunas, Areais, Aquicultura E Apicuns No Brasil Entre 1985 a 2020. MapBiomas Coleção 6*. Available at: https://mapbiomas-br-site.s3.amazonaws.com/MapBiomas_Zona_Costeira_Outubro_2021_30102021_OK.pdf (Accessed January 25, 2022).
- Marengo, J. A., Torres, R. R., and Alves, L. M. (2017). Drought in Northeast Brazil – Past, Present, and Future. *Theor. Appl. Climatol.* 129, 1189–1200. doi: 10.1007/s00704-016-1840-8
- Martinetto, P., Montemayor, D. I., Alberti, J., Costa, C. S. B., and Iribarne, O. (2016). Crab Bioturbation and Herbivory May Account for Variability in Carbon Sequestration and Stocks in South West Atlantic Salt Marshes. *Front. Mar. Sci.* 3(122), 1–12. doi: 10.3389/fmars.2016.00122
- Matos, C. R. L., Berrêdo, J. F., Machado, W., Sanders, C. J., Metzger, E., and Cohen, M. C. L. (2020). Carbon and Nutrient Accumulation in Tropical Mangrove Creeks, Amazon Region. *Mar. Geol.* 429, 106317. doi: 10.1016/j.margeo.2020.106317
- McKenzie, L. J., Nordlund, L. N., Jones, B. L., et al (2020). The Global Distribution of Seagrass Meadows. *Environ. Res. Lett.* 15(7), 1–13. 074041. doi: 10.1088/1748-9326/ab7d06
- McLeod, E., Chmura, G. L., Bouillon, S., Salm, R., Björk, M., Duarte, C. M., et al. (2011). A Blueprint for Blue Carbon: Toward an Improved Understanding of the Role of Vegetated Coastal Habitats in Sequestering CO₂. *Front. Ecol. Environ.* 9(10), 552–560. doi: 10.1890/110004
- Mcowen, C., Weatherdon, L., Bochove, J., Sullivan, E., Blyth, S., Zockler, C., et al. (2017). A Global Map of Saltmarshes. *Biodivers. Data J.* 5, e11764. doi: 10.3897/BDJ.5.e11764
- MCTIC – Ministério da Ciência e Tecnologia do Brasil (2017) *Estimativas Anuais Da Emissão Dos Gases De Efeito Estufa*. Available at: <http://educaclima.mma.gov.br/wp-content/uploads/2019/08/Estimativas-Anuais-4-2017.pdf>.
- Missiatto, L. A. F., Silva, L. G., Carvalho, F. R., Denes, D. M., and Missiatto, H. M. (2021). A Colonialidade Nas Políticas Ambientais do Governo Bolsonaro E a Inversão Dos Órgãos De Defesa Do Meio Ambiente. *Rev. Interdisciplinar. Margens - Dossiê Margens Poder Insurgência América Latina* 15 (24), 85–102. doi: 10.18542/rmi.v15i24.10049
- Muehe, D. (2010). Brazilian coastal vulnerability to climate change. *Panam. J. Aquat. Sci.* 5(2), 173–183.
- Nellemann, C., Corcoran, E., Duarte, C. M., Valdés, L., De Young, C., Fonseca, L., et al. (2009). *Blue Carbon. A Rapid Response Assessment. GRID-Arendal: United Nations Environment Programme, GRID-Arendal* (Norway: Birkeland Trykkeri AS).
- Nóbrega, G. N., Ferreira, T. O., Neto, M. S., Mendonça, E. S., Romero, R. E., and Otero, X. L. (2019). The Importance of Blue Carbon Soils in Tropical Semiarid Mangroves: A Case Study in Northeastern Brazil. *Environ. Earth Sci.* 78, 369. doi: 10.1007/s12665-019-8368-z
- Nóbrega, G. N., Ferreira, T. O., Neto, M. S., Queiroz, H. M., Artur, A. G., Mendonça, E. S., et al. (2016). Edaphic Factors Controlling Summer (Rainy Season) Greenhouse Emissions (CO₂ and CH₄) From Semiarid Mangrove Soils (NE-Brazil). *Sci. Total Environ.* 542, A, 685–A, 693. doi: 10.1016/j.scitotenv.2015.10.108
- Nóbrega, G. N., Romero, D. J., Otero, X. L., and Ferreira, T. O. (2018). Pedological Studies of Subaqueous Soils as a Contribution to the Protection of Seagrass Meadows in Brazil. *Rev. Bras. Cienc. Solo* 42, 1–12. doi: 10.1590/18069657rbcs20170117
- O'Connor, J. J., Fest, B. J., Sievers, M., and Swearer, S. E. (2019). Impacts of Land Management Practices on Blue Carbon Stocks and Greenhouse Gas Fluxes in Coastal Ecosystems – A Meta-Analysis. *Global Change Biol.* 26 (3), 1354–1366. doi: 10.1111/gcb.14946
- Pagliosa, P. R., Rovai, A. S., and Fonseca, A. L. (2012). Carbon Mismanagement in Brazil. *Nat. Climate Change* 2, 764. doi: 10.1038/nclimate1718
- Patterson, E., Johnson, B., Dostie, P., and Copertino, M. (2016). Stocks and Sources of Carbon Buried in the Salt Marshes and Seagrass Beds of Patos Lagoon Estuary, Southern Brazil. *Geophys. Res. Abstr.* 18, EGU2016–10792.
- Pavani, B. F., Sousa Júnior, W. C., Inouye, C. E. N., Vieira, S. A., and Mello, A. Y. I. (2018). Estimating and Valuing the Carbon Release in Scenarios of Land-Use and Climate Changes in a Brazilian Coastal Area. *J. Environ. Manag.* 226, 416–427. doi: 10.1016/j.jenvman.2018.08.059
- Pendleton, L., Donato, D. C., Murray, B. C., Crooks, S., Jenkins, W. A., Sifleet, S., et al. (2012). Estimating Global “Blue Carbon” Emissions From Conversion and Degradation of Vegetated Coastal Ecosystems. *PloS One* 7 (9), e43542. doi: 10.1371/journal.pone.0043542
- Perretti, A. R., Albergaria-Barbosa, A. C. R., Kerr, R., and Cunha, L. C. (2018). Ocean Acidification Studies and the Uncertainties Relevance on Measurements of Marine Carbonate System Properties. *Braz. J. Oceanogr.* 66 (2), 234–242. doi: 10.1590/s1679-87592018000706602
- Portela, M. G. T., de Espindola, G. M., Valladares, G. S., Amorim, J. V. A., and Frota, J. C. O. (2020). Vegetation Biomass and Carbon Stocks in the Parnaíba River Delta, NE Brazil. *Wetlands Ecol. Manag.* 28, 607–622. doi: 10.1007/s11273-020-09735-y
- Portillo, J. T. M., Londe, V., and Moreira, F. W. A. (2016). Aboveground Biomass and Carbon Stock are Related With Soil Humidity in a Mangrove at the Piraquê-Açu River, Southeastern Brazil. *J. Coastal Conserv.* 21 (1), 139–144. doi: 10.1007/s11852-016-0482-4
- Ricart, A. M., York, P. H., Bryant, C. V., Rasheed, M. A., Ierodiaconou, D., and Macreadie, P. I. (2020). High Variability of Blue Carbon Storage in Seagrass Meadows at the Estuary Scale. *Sci. Rep.* 10 (5865), 1–12. doi: 10.1038/s41598-020-62639-y
- Ritchie, H., and Roser, M. (2020) *CO₂ and Greenhouse Gas Emissions*. Available at: <https://ourworldindata.org/co2-and-other-greenhouse-gas-emissions>.
- Rodrigues, S., and Souza-Filho, P. W. M. (2011). Use of Multi-Sensor Data to Identify and Map Tropical Coastal Wetlands in the Amazon of Northern Brazil. *Wetlands* 31(1), 11–23. doi: 10.1007/s13157-010-0135-6
- Rosentreter, J. A., Maher, D. T., Erler, D. V., Murray, R. H., and Eyre, B. D. (2018). Methane Emissions Partially Offset “Blue Carbon” Burial in Mangroves. *Sci. Adv.* 4, 6. doi: 10.1126/sciadv.aao4985
- Rossi, S., Coppari, M., and Viladrich, N. (2017). “Benthic-Pelagic Coupling: New Perspectives in the Marine Animal Forests,” in *Perspectives on the Marine Animal Forests*. Eds. S. Rossi, L. Bramanti, A. Gori and C. Orejas (Cham: Springer), 855–885. doi: 10.1007/978-3-319-21012-4_23
- Rossi, S., Isla, E., Bosch-Belmar, M., Galli, G., Gori, A., Gristina, M., et al. (2019). Changes of Energy Fluxes in Marine Animal Forests of the Anthropocene: Factors Shaping the Future Seascape. *ICES J. Mar. Sci.* 76 (7), 2008–2019. doi: 10.1093/icesjms/fsz147
- Rossi, S., and Rizzo, L. (2020). “Marine Animal Forests as C Immobilizers,” in *Perspectives on the Marine Animal Forest*. Eds. S. Rossi, L. Bramanti, A. Gori and C. Orejas (Cham: Springer), 333–400. doi: 10.1007/978-3-030-57054-5_11
- Rovai, A. S., Coelho-Jr, C., de Almeida, R., Cunha-Lignon, M., Menghini, R. P., Twilley, R. R., et al. (2020). Ecosystem-Level Carbon Stocks and Sequestration Rates in Mangroves in the Cananéia-Iguape Lagoon Estuarine System, Southeastern Brazil. *For. Ecol. Manag.* 479, 118553. doi: 10.1016/j.foreco.2020.118553
- Rovai, A. S., Twilley, R. R., Castañeda-Moya, E., Riul, P., Cifuentes-Jara, M., Manrow-Villalobos, M., et al. (2018). Global Controls on Carbon Storage in Mangrove Soils. *Nat. Climate Change* 8, 534–538. doi: 10.1038/s41558-018-0162-5
- Rovai, A. S., Twilley, R. R., Worthington, T. A., and Riul, P. (2022). Brazilian Mangroves: Blue Carbon Hotspots of National and Global Relevance to Natural Climate Solutions. *Front. Collect.* 4 (787533). doi: 10.3389/fc.2021.787533
- Sala, E., Mayorga, J., Bradley, D., Cabral, R. B., Atwood, T. B., Auber, A., et al. (2021). Protecting the Global Ocean for Biodiversity, Food and Climate. *Nature* 592, 397–402. doi: 10.1038/s41586-021-03371-z
- Salum, R. B., Souza-Filho, P. W. M., Simard, M., Silva, C. A., Fernandes, M. E. B., Cougo, M. F., et al. (2020). Improving Mangrove Above-Ground Biomass Estimates Using LiDAR. *Estuar. Coastal Shelf Sci.* 236, 106585. doi: 10.1016/j.ecss.2020.106585
- Santos, D. M. C., Estrada, G. C. D., Fernandez, V., Estevam, M. R. M., Souza, B. T. D., and Soares, M. L. G. (2017). First Assessment of Carbon Stock in the Belowground Biomass of Brazilian Mangroves. *Anais Da Academia Brasileira de Ciências* 89 (3), 15791589. doi: 10.1590/0001-3765201720160496
- Santos, I. R., Burdige, D. J., Jennerjahn, T. C., Bouillon, S., Cabral, A., Serrano, O., et al. (2021). The Renaissance of Odum's Outwelling Hypothesis in ‘Blue Carbon’ Science. *Estuar. Coastal Shelf Sci.* 255, 107361. doi: 10.1016/j.ecss.2021.107361

- Santos, I. R., Maher, D. T., Larkin, R., Webb, J., and Sanders, C. J. (2018). Carbon Outwelling and Outgassing vs. Burial in an Estuarine Tidal Creek Surrounded by Mangrove and Saltmarsh Wetlands. *Limnol. Oceanogr. Lett.* 2, 1–18. doi: 10.1002/lno.11090
- Santos, C. Z., and Schiavetti, A. (2014). Spatial Analysis of Protected Areas of the Coastal/Marine Environment of Brazil. *J. Nat. Conserv.* 22 (5), 453–461. doi: 10.1016/j.jnc.2014.05.001
- Sasmito, S. D., Sillanpää, M., Hayes, M. A., Bachri, S., Saragi-Sasmito, M. F., Sidik, F., et al. (2020). Mangrove Blue Carbon Stocks and Dynamics are Controlled by Hydrogeomorphic Settings and Land-Use Change. *Global Change Biol* 26 (5), 3028–3039. doi: 10.1111/gcb.15056
- Scantimburgo, A. (2018). O Desmonte Da Agenda Ambiental No Governo Bolsonaro. *Perspectivas* 52, 103–117.
- Schaeffer-Novelli, Y., Cintrón-Molero, G., Reis-Neto, A. S., Abuchahla, G. M. O., Neta, L. C. P., and Lira-Medeiros, C. F. (2018). The Mangroves of Aracá Bay through time: An interdisciplinary Approach for Conservation of Spatial Diversity at Large Scale. *Ocean & Coastal Management* 164, 60–67. doi: 10.1016/j.ocecoaman.2017.12.024
- Schaeffer-Novelli, Y., Soriano-Sierra, E. J., Vale, C. C., Bernini, E., Rovai, A. S., Pinheiro, M. A. A., et al. (2016). Climate Changes in Mangrove Forests and Salt Marshes. *Braz. Journ. Ocean.* 64 (sp2), 83–98. doi: 10.1590/S1679-875920160919064sp2
- SEEG–Brasil. (2016). Going against the world, Brazil increased emissions in the middle of the pandemic. <https://seeg.eco.br/en/press-release>
- Shaefer, C. E. G. R., Simas, F. N. B., Albuquerque, M. A., Souza, E., and Delpupo, K. K. (2010). Fosfatização de solos e evolução da paisagem no arquipélago de Abrolhos, BA. *Rem-Rev. Esc. Minas.* 63(4), 727–34. doi: 10.1590/S0370-44672010000400019
- Silva, G. C. M. (2017). Mapeamento de Bancos de Algas e Fanerógamas na área de Proteção Ambiental Dos Recifes de Corais: RN utilizando geotecnologias. *Tese de Doutorado em Desenvolvimento e Meio Ambiente, Centro de Biociências Universidade Federal do Rio Grande do Norte, Natal*, 112 f. Online access: <https://repositorio.ufrn.br/jspui/handle/123456789/24520>
- Silveira, E. M. O., Terra, M. C. N. S., Steege, H. T., Maeda, E. E., Júnior, F. W. A., and Scolforo, J. R. S. (2019). Carbon-Diversity Hotspots and Their Owners in Brazilian Southeastern Savanna, Atlantic Forest and Semi-Arid Woodland Domains. *For. Ecol. Manag.* 452, 117575. doi: 10.1016/j.foreco.2019.117575
- Sippo, J. Z., Maher, D. T., Tait, D. R., Holloway, C., and Santos, I. R. (2016). Are Mangroves Drivers or Buffers of Coastal Acidification? Insights From Alkalinity and Dissolved Inorganic Carbon Export Estimates Across a Latitudinal Transect. *Glob. Biogeochem. Cycles* 30, 753–766. doi: 10.1002/2015GB005324
- Soares, M. O., Campos, C. C., Carneiro, P. B. M., Barroso, H. S., Marins, R. V., Teixeira, C. E. P., et al. (2021). Challenges and Perspectives for the Brazilian Semi-Arid Coast Under Global Environmental Changes. *Perspect. Ecol. Conserv.* 19 (3), 267–278. doi: 10.1016/j.pecon.2021.06.001
- Soares, M. O., Lotufo, T. M. C., Vieira, L. M., Salani, S., Hajdu, E., Matthews-Cascon, H., et al. (2017). “Brazilian Marine Animal Forests: A New World to Discover in the Southwestern Atlantic,” in *Marine Animal Forests*. Eds. S. Rossi, L. Bramanti, A. Gori and C. Orejas (Cham: Springer), 73–110. doi: 10.1007/978-3-319-21012-4_51
- Soares, M. O., Tavares, T. C. L., and Carneiro, P. B. M. (2019). Mesophotic Ecosystems: Distribution, Impacts and Conservation in the South Atlantic. *Diversity Distrib.* 255 (2), 255–268. doi: 10.1111/ddi.1284610.1111/ddi.12846
- Soares, M. O., Teixeira, C. E. P., Bezerra, L. E. A., Paiva, S. V., Tavares, T. C. L., Garcia, T. M., et al. (2020). Oil Spill in South Atlantic (Brazil): Environmental and Governmental Disaster. *Mar. Policy* 115, 103879. doi: 10.1016/j.marpol.2020.103879
- Sobrinho, R. L., Bernardes, M. C., Rezende, C. E., Kim, J. H., Schouten, S., and Damsté, J. S. S. (2021). A Multiproxy Approach to Characterize the Sedimentation of Organic Carbon in the Amazon Continental Shelf. *Mar. Chem.* 232, 103961. doi: 10.1016/j.marchem.2021.103961
- Sordo, L., Fournier, J., Oliveira, V. M., Gern, F., Panizza, A. C., and Lana, P. C. (2011). Temporal Variations in Morphology and Biomass of Vulnerable *Halodule Wrightii* Meadows at Their Southernmost Distribution Limit in the Southwestern Atlantic. *Bot. Mar.* 54 (1), 13–21. doi: 10.1515/BOT.2011.007
- Souza Filho, P. W. M. (2005). Costa De Manguezais De Macromaré Da Amazônia: Cenários Morfológicos, Mapeamento E Quantificação De Áreas Usando Dados De Sensores Remotos. *Rev. Bras. Geofis.* 23, 427–435. doi: 10.1590/S0102-261X2005000400006
- Steffen, W., Rockström, J., Richardson, K., Lenton, T. M., Folke, C., Liverman, D., et al. (2018). Trajectories of the Earth System in the Anthropocene. *PNAS* 115 (33), 8252–8259. doi: 10.1073/pnas.1810141115
- Taillardat, P., Friess, D. A., and Lupascu, M. (2018). Mangrove Blue Carbon Strategies for Climate Change Mitigation are Most Effective at the National Scale. *Biol. Lett.* 14 (10), 20180251. doi: 10.1098/rsbl.2018.0251
- Teixeira, S. G., and Souza-Filho, P. W. M. (2009). Mapping Tropical Coastal Environments (Gulf of Maranhão, Brazil) Using Satellite Remote Sensing Images. *Rev. Bras. Geofis.* 27, 69–82. doi: 10.1590/S0102-261X2009000500006
- The Blue Carbon Initiative (2020) *About Blue Carbon*. Available at: <https://www.thebluecarboninitiative.org/about-blue-carbon>.
- Turra, A., and Denadai, M. R. (2016). Linking Biodiversity and Global Environmental Changes in Brazilian Coastal Habitats. *Braz. J. Oceanogr.* 64, 3–4. doi: 10.1590/S1679-87592016064sp2ed
- Van der Heijden, L. H., and Kamenos, N. A. (2015). Reviews and Syntheses: Calculating the Global Contribution of Coralline Algae to Total Carbon Burial. *Biogeosciences* 12 (21), 6429–6441. doi: 10.5194/bg-12-6429-2015
- Waycott, M., Duarte, C. M., Carruthers, T. J. B., Orth, R. J., Dennison, W. C., Olyarnik, S., et al. (2009). Accelerating Loss of Seagrasses Across the Globe Threatens Coastal Ecosystems. *PNAS* 106 (30), 12377–12381. doi: 10.1073/pnas.0905620106
- Wiesebron, M. (2013). Blue Amazon: Thinking the Defense of Brazilian Maritime Territory. *Austral. Braz. J. Strategy Int. Relat.* 2 (3), 101–124. doi: 10.22456/2238-6912.35039
- Zhao, C., Fang, C., Gong, Y., and Lu, Z. (2020). The Economic Feasibility of Blue Carbon Cooperation in the South China Sea Region. *Mar. Policy* 113, 103788. doi: 10.1016/j.marpol.2019.103788

Conflict of Interest: The authors declare that the research was conducted in the absence of any commercial or financial relationships that could be construed as a potential conflict of interest.

Publisher's Note: All claims expressed in this article are solely those of the authors and do not necessarily represent those of their affiliated organizations, or those of the publisher, the editors and the reviewers. Any product that may be evaluated in this article, or claim that may be made by its manufacturer, is not guaranteed or endorsed by the publisher.

Copyright © 2022 Soares, Bezerra, Copertino, Lopes, Barros, Rocha-Barreira, Maia, Beloto and Cotovicz. This is an open-access article distributed under the terms of the Creative Commons Attribution License (CC BY). The use, distribution or reproduction in other forums is permitted, provided the original author(s) and the copyright owner(s) are credited and that the original publication in this journal is cited, in accordance with accepted academic practice. No use, distribution or reproduction is permitted which does not comply with these terms.



Implication of Macroalgal Bloom to Soil Organic Carbon Stock in Seagrass Meadows - A Case Study in South Hainan, China

Shunyang Chen^{1,2†}, Shiquan Chen^{3†}, Bin Chen^{1,2,4}, Zhongjie Wu³, Wenshuo An^{1,2}, Lizhen Luo³, Jing Wang⁵, Limei Xie⁶, Jing Zhang⁵ and Guangcheng Chen^{1,2,4*}

¹ Third Institute of Oceanography, Ministry of Natural Resources, Xiamen, China, ² Observation and Research Station of Coastal Wetland Ecosystem in Beibu Gulf, Ministry of Natural Resources, Beihai, China, ³ Hainan Academy of Ocean and Fisheries Sciences, Haikou, China, ⁴ Key Laboratory of Marine Ecological Conservation and Restoration, Ministry of Natural Resources, Xiamen, China, ⁵ Society of Entrepreneurs and Ecology Foundation, Beijing, China, ⁶ Key Laboratory of the Ministry of Education for Coastal and Wetland Ecosystems, Xiamen University, Xiamen, China

OPEN ACCESS

Edited by:

Hilary Anne Kennedy,
Bangor University, United Kingdom

Reviewed by:

Ursula Felicitas Marianne Witte,
University of Aberdeen,
United Kingdom
Songlin Liu,
South China Sea Institute of
Oceanology (CAS), China

*Correspondence:

Guangcheng Chen
gc.chen@tio.org.cn

[†]These authors have contributed
equally to this work and share
first authorship

Specialty section:

This article was submitted to
Global Change and the Future Ocean,
a section of the journal
Frontiers in Marine Science

Received: 06 February 2022

Accepted: 19 April 2022

Published: 19 May 2022

Citation:

Chen S, Chen S, Chen B, Wu Z, An W,
Luo L, Wang J, Xie L, Zhang J and
Chen G (2022) Implication of
Macroalgal Bloom to Soil Organic
Carbon Stock in Seagrass Meadows -
A Case Study in South Hainan, China.
Front. Mar. Sci. 9:870228.
doi: 10.3389/fmars.2022.870228

The adverse impact of macroalgal blooms associated with nutrient enrichment on seagrass habitats and carbon storage potential is an ecological concern. In the present study, the soil carbon stock and sources were compared between a seagrass meadow where a serious macroalgal bloom occurred (site M) and an adjacent site without apparent macroalgae (site R) in a nutrient-enriched lagoon in South Hainan Island, China, to test whether macroalgal blooms associated with nutrient enrichment would impact the soil carbon in seagrass meadows. The soil organic carbon (OC) and total nitrogen contents in the top 30 cm at site M were significantly lower than those at site R. The soil OC stocks (top 30 cm) were 3.4 and 5.4 Mg C ha⁻¹ at site M and site R, respectively, and no difference was observed between sampling stations with different distances offshore at either site. Soil $\delta^{13}\text{C}$ was more enriched and closer to the $\delta^{13}\text{C}$ of seagrass tissues at site R than at site M. Bayesian stable isotope mixing model analyses suggested that seagrass-derived material contributed ~50% to soil OC at site R, while at site M, the contribution was reduced to ~25%. The results suggested that macroalgal blooms associated with nutrient enrichment could drive the loss of seagrass-derived OC and the OC stock in the soil, which is worthy of full attention for blue carbon conservation.

Keywords: soil carbon stock, soil $\delta^{13}\text{C}$, total nitrogen, carbon sources, *Enhalus acoroides*, priming effect

INTRODUCTION

Seagrass meadows are important blue carbon ecosystems that occur in all coastal areas of the world, except along Antarctic shores (Hemminga and Duarte, 2000). The organic carbon (OC) stored in the top metre of soils was estimated to range from 9.8 to 19.8 Pg C in global seagrass meadows, comparable to the organic carbon stored in the world's mangrove forests and tidal salt marshes

(Fourqurean et al., 2012). However, due to various anthropogenic impacts, seagrass meadows are disappearing or degraded (Dunic et al., 2021). A global assessment by Waycott et al. (2009) suggested that seagrasses disappeared at a rate of $110 \text{ km}^2 \text{ yr}^{-1}$ between 1980 and 2006, and the rates of decline have accelerated since 1990 relative to those before 1940. The decrease in seagrass extent has resulted in a loss of OC stored in seagrass soils, in an annual loss of between 63 and 297 Tg C , since the beginning of the twentieth century (Fourqurean et al., 2012).

Declines of seagrass populations have been observed in many estuarine embayments, which are often associated with anthropogenic nutrient loading (Waycott et al., 2009). Nutrient enrichment by nitrogen fertilization has been found to increase seagrass biomass and litter production (Armitage and Fourqurean, 2016; Howard et al., 2016; Qin et al., 2021), which provide more seagrass-derived detritus to be incorporated into the soil. However, increased availability of nutrients in the embayments may lead to blooms of macroalgae, phytoplankton and epiphytes, which reduces the light available for photosynthesis and decreases seagrass productivity and populations, leading to habitat loss and fragmentation (Burkholder et al., 2007; Han and Liu, 2014; Santos et al., 2020). Moreover, nutrient enrichment and macroalgal blooms may impact the quantity and quality of OC storage in seagrass soils by a 'priming effect', which trigger an extra decomposition of OC after providing exogenous inorganic nitrogen and labile OC to the soils (Kuzakov et al., 2000). The priming effect of exogenous OC input on the soil mineralization of OC have been found through experimental addition of algal OC to seagrass soil (Trevathan-Tackett et al., 2018; Liu et al., 2019), or through comparing the OC contents and compositions among sites subjected to different nutrient loadings (Liu et al., 2016; Jiang et al., 2018). These results suggest that macroalgal blooms in nutrient-enriched embayments may lead to the loss of soil OC in seagrass meadows, while few studies have examined this effect.

Seagrass meadows are commonly found in China either in the tropical/subtropical regions in the South China Sea or in the temperate northern provinces. Hainan Island within the tropical Indo-Pacific bioregion has been suggested to have the greatest extent and number of species of seagrass in China (Zheng et al., 2013), where seagrass mostly occurs in lagoons and on coral platforms (Wang et al., 2012). Due to threats from sea reclamation, marine aquaculture and harvest activities, a massive loss in the seagrass extent has taken place since the 2000s (Chen et al., 2015). In some embayment areas, the nutrient input from adjacent mariculture has resulted in nutrient enrichment, macroalgal blooms, and the degradation of seagrass meadows (Wang et al., 2012). In this study, we investigated the soil OC stocks and sources in seagrass meadows in a nutrient-enriched lagoon, namely, Xincun Bay in southeastern Hainan Island, to test whether macroalgal blooms would result in a loss of soil organic carbon. We hypothesized a lower soil organic carbon stock associated with the macroalgal bloom in the nutrient-enriched area, and the macroalgal bloom also resulted in a change in the carbon composition of the seagrass soil.

MATERIALS AND METHODS

Study Area

The Xincun Bay Lagoon is located southeast of Hainan Island, between $18^{\circ}22' - 18^{\circ}47' \text{ N}$ and $109^{\circ}45' - 110^{\circ}08' \text{ E}$ (Figure 1A). The region has a tropical monsoon climate, and the monthly mean temperature ranged from 20°C to 29°C from 2009 to 2018, with the highest temperature recorded in June (Weather China, 2022). The monthly mean precipitation ranges from 6–445 mm, and the annual precipitation is 2011 mm. Tides in the Xincun Bay area are mixed semidiurnal, with an annual tidal range of 1.34 m.

In the Xincun Bay Lagoon, seagrass meadows occur mainly along its southern coast on the sandy substrate. The seagrass is dominated by *Enhalus acoroides* in terms of biomass, while *Thalassia hemprichii* is also commonly found. However, nutrient enrichment of the lagoon area has occurred in recent decades due to various anthropogenic activities, including offshore restaurants and residences, marine aquaculture and shipping. The inorganic nitrogen concentration in the seawater around the seagrass sites increased by ~ 1.5 times between year 2005 and 2013 (Jiang et al., 2018). A recent study reported an inorganic nitrogen concentration of the seawater with a range of $0.10\text{--}0.38 \text{ mg N L}^{-1}$ in 2017 in the lagoon area (Fang et al., 2021). The nutrient enrichment has resulted in adverse impacts on seagrass ecosystems, e.g., habitat fragmentation and macroalgal blooms. A macroalgal biomass up to 19 g m^{-2} was reported at a seagrass site close to fish cage culture area in the Xincun Bay, ~ 5 time as that at a seagrass site with greater distance ($\sim 800\text{m}$ versus 3 km) off the culture area (Liu et al., 2016).

In this study, sampling was carried out at two *E. acoroides*-dominated seagrass sites (site M and site R) on the southern coast of the lagoon (Figure 1B). Site M had a longer semi-exchange time of seawater and stronger cumulative impacts of anthropogenic nutrient input than site R (Fang et al., 2020), where intensive overgrowth of macroalgae was observed (Figures 1C, D). The macroalgae was observed at this location in 2008, indicating that the algal bloom had been lasted for a decade before our sampling. Site R represented a reference site without apparent macroalgal blooms. The two seagrass sites had similar canopy coverage, density and biomass of *E. acoroides* (Table S1), while site M, as observed, presented more fragmentation of the seagrass canopy. At each of the two sites, two sampling stations (LW and SW) with different distances offshore were established. LW was designated the landward station of the *E. acoroides* zone, while SW ($\sim 150 \text{ m}$ away from LW) signified the seaward zone. The substrate was sandy at these two sites, consisting of $>90\%$ sand (Table S1).

Sample Collection

Soil cores were collected in January 2018 using PVC tubes (inner diameter 70 mm) with metal cutters on their bottom edges. The tubes were manually inserted into the soil at the *E. acoroides*-covered areas by gently turning the tube until a depth of 30 cm was reached at each sampling plot. At each sampling station, whole seagrass samples of *E. acoroides* (including leaves, roots

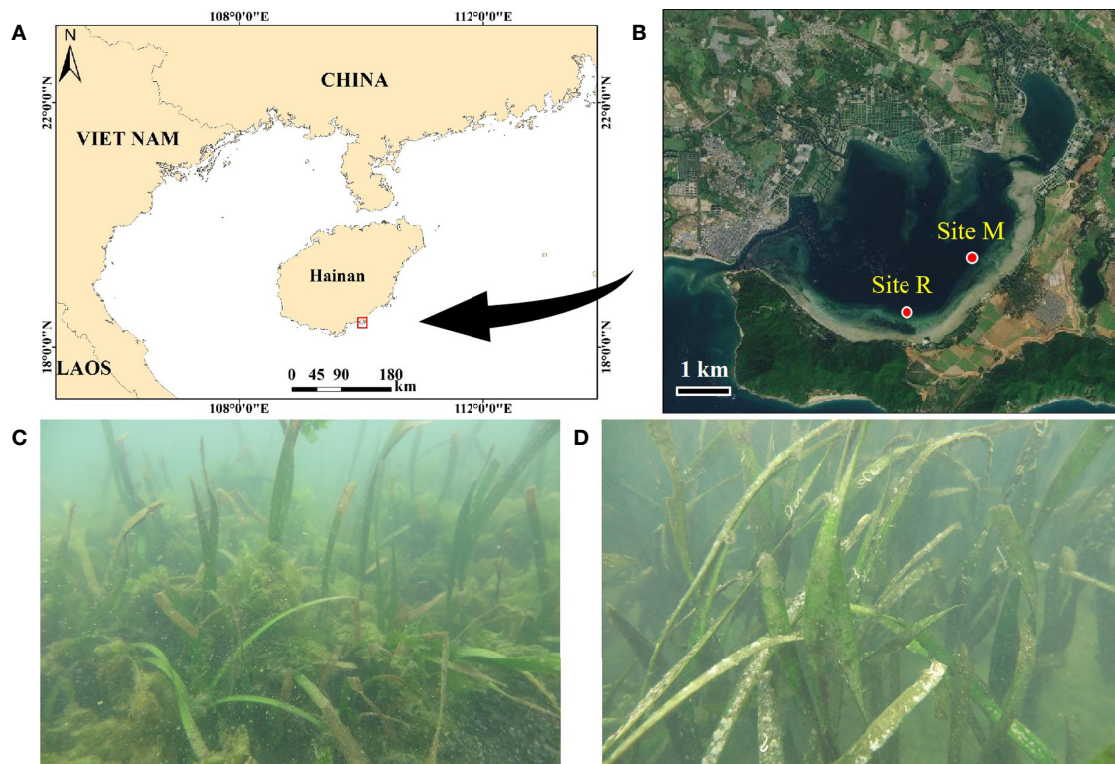


FIGURE 1 | Locations of Xincun Bay Lagoon (A) and the two seagrass sites (B), and respective typical scenes from the two seagrass sites, site M (C) and site R (D). Site M represents the nutrient enrichment site with macroalgal blooms, and site R represents the reference site without apparent macroalgal blooms. The panels A and B were created with image obtained from ArcGIS version 10.3 and National Platform for Common Geospatial Information Services (<https://map.tianditu.gov.cn>), respectively.

and rhizomes) were collected in three replicates and transported to the laboratory. Moreover, macroalgal samples of the dominant species, *Ulva lactuca* were collected at site M, and seawater was sampled in triplicates using plastic bottles in the central lagoon area during the high tide period to collect the suspended particulate organic matter (SPOM).

The soils were extruded in the laboratory by inserting a plunger at the bottom of the cores and carefully drawing the PVC liner down over the plunger. The soil cores were divided into subsections at 10 cm intervals. Each subsection was weighed and then sliced into two halves, with one half oven-dried at 60°C to determine the water content of fresh samples. The other half was then air-dried after removing visible animals, plant residues and stones (> 2 mm). The whole-plant tissues of seagrass were cleaned of epiphytes and sand and dried at 60°C for 24 h. The seawater samples, after passing through a 75 µm mesh, were filtered through a precombusted 0.7 µm GF/F filter to collect the SPOM. Epiphytes on seagrass leaves were scraped and rinsed using Milli-Q water and then filtered through a filter.

The OC, total nitrogen (TN) and $\delta^{13}\text{C}$ in the soil and plant samples were measured using a Thermo Flash EA 1112 HT-Delta V Advantages system. Air-dried subsamples of soils and seagrass tissues were placed into silver cups, acidified with diluted HCl (5%) and then oven-dried at 40°C to remove the carbonates.

Filtered samples of SPOM and epiphytes for isotope analysis were acidified by fumigation overnight over 1 mol L⁻¹ HCl to remove inorganic carbonates. The stable carbon isotopic composition is reported in the δ notation as the ratio of the heavy to the light stable isotope in the sample relative to that of a standard. The reproducibility of OC and stable isotopic analysis were 1.2% and 0.2‰, respectively.

Statistical Analysis and Estimation of Organic Carbon Sources

The normality and homogeneity of variables were checked using the Shapiro–Wilk test and Levene’s test, respectively, and if necessary, data were transformed with the Blom method to follow normality and homogeneity. A parametric three-way analysis of variance (ANOVA) was conducted to test for any effects of the sampling site, sampling station and soil depth and their interactive effects. Differences in the soil OC stocks and variables of the seagrass samples between the two sites and sampling stations were tested using two-way ANOVA. One-way ANOVA was used to compare the differences in variables among the carbon sources. The potential contributions of the primary sources (seagrass, SPOM, macroalgae and epiphyte at Site M; seagrass, SPOM and epiphyte at Site R) to the soil carbon composition were estimated using a Bayesian stable isotope mixing model, SIMMR.

RESULTS

Soil Characteristics and Organic Carbon Stock

The soil bulk density of the top 30 cm was comparable between the two seagrass sites and between the two sampling stations according to the three-way ANOVA test (**Figure 2A** and **Table S2**), while a difference was found between the surface (0–10 cm) and the 20–30 m layer (**Table S3**). The OC content in the top 30 cm of the soil showed significant differences with the seagrass site and soil depth. The degraded site had OC values ranging between 0.47 mg g^{-1} and 1.06 mg g^{-1} , which were lower than those measured at the site R ($0.80\text{--}1.86 \text{ mg g}^{-1}$). No significant difference in soil OC content was found with distance offshore (**Figure 2B**), and its value was significantly lower in the bottom layer than in the two upper layers. Similar spatial variation patterns of the soil OC density ($0.78\text{--}2.61 \text{ g cm}^{-3}$) to those of the soil OC content were observed in this study (**Figure 2C**), and higher values were measured at the site R and in the top 20 cm soil layers.

The mean soil TN content was $< 0.11 \text{ mg g}^{-1}$ at site M (**Figure 2D**), while at site R, the value was higher and reached 0.36 mg g^{-1} . In contrast, site R presented a significantly lower C:N ratio (in weight) than the values at site M (**Figure 2E**). There was no significant change in soil TN and the C:N ratio with either soil depth or sampling station.

The soil OC stock was higher at site R than at degraded site M ($F=22.661$, $p<0.01$) and was similar between the two sampling stations ($F=0.974$, $p>0.05$). The OC stocks were $3.5 \pm 0.4 \text{ Mg C ha}^{-1}$ (M-LW), $3.4 \pm 0.4 \text{ Mg C ha}^{-1}$ (M-SW), $5.8 \pm 0.8 \text{ Mg C ha}^{-1}$ (R-LW) and $5.1 \pm 1.1 \text{ Mg C ha}^{-1}$ (R-SW) in the top 30 cm soil at the four seagrass stations.

Characteristics of Primary Sources and Soil Organic Carbon Sources

The $\delta^{13}\text{C}$ and C:N ratios of the SPOM were $-21.89 \pm 0.32\text{‰}$ and 2.44 ± 0.14 , respectively, in the Xincun Bay lagoon. The seagrass

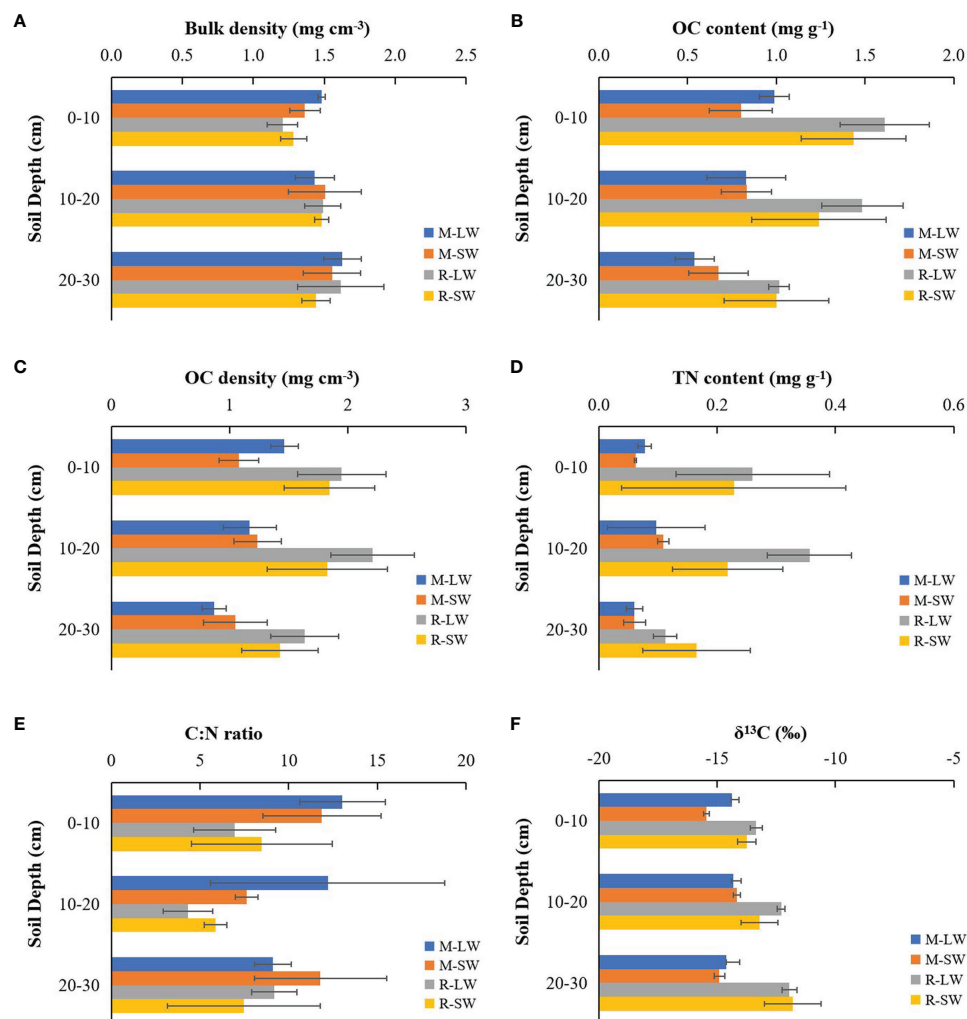


FIGURE 2 | Soil parameters of the two sampling stations at the two seagrass sites (M and R) in the Xincun Bay lagoon: **(A)** bulk density, **(B)** OC content, **(C)** OC density, **(D)** TN content, **(E)** C:N ratio and **(F)** $\delta^{13}\text{C}$. LW, landward station; SW, seaward station.

tissues had comparable $\delta^{13}\text{C}$, OC, TN contents and C:N ratios between the two seagrass sites and between the two sampling stations (Table 1 and Table S4). Seagrass tissues had the most enriched ^{13}C , and their $\delta^{13}\text{C}$ values were -8‰. The epiphytes had lower mean $\delta^{13}\text{C}$ and C:N ratios than the macroalgal and seagrass tissues; the macroalgal and seagrass tissues had comparable C:N ratios.

There were significant main effects of the seagrass site, sampling stations and soil depth on the soil $\delta^{13}\text{C}$, and a significant interaction of the seagrass site with sampling depth was found (Figure 2F and Table S3). The soil $\delta^{13}\text{C}$ were more enriched at site R and were closer to the $\delta^{13}\text{C}$ of the seagrass tissues at each soil layer. No significant difference in soil $\delta^{13}\text{C}$ with soil depth was found at site M, while the value became less negative when soil depth increased at site R. The soil $\delta^{13}\text{C}$ followed an increasing trend with soil OC ($r=0.553$, $p<0.01$). The SIMMR mixing model estimations showed a dissimilarity in the composition of carbon sources as assigned to the top 30 cm of the soil (Table 2). At site R, seagrass-derived material likely contributed more than the epiphytes and SPOM, and its respective proportional contribution was similar between the two stations. At site M, the seagrass reduced its contribution to the soil OC relative to its performance at site R, and macroalgae had a greater contribution than seagrass at both sampling stations.

DISCUSSION

The present study compared the ecosystem OC stocks and soil carbon sources between the two seagrass sites in the nutrient-enriched lagoon, and the results showed that the OC content in the top 30 cm soil at the degraded seagrass site where macroalgae overgrew (site M) was 37% lower than that at the site R less impacted by macroalgae, with a low soil OC stock and more negative $\delta^{13}\text{C}$ value. The results suggest that macroalgal blooms due to nutrient enrichment would impact the soil OC stock and the carbon composition of seagrass soil. We also found differences in the soil TN content and C:N ratio between the two seagrass sites.

The OC stocks in the Xincun Bay were 3.4 and 5.4 Mg C ha^{-1} in the top 30 cm of the soil at site M and site R, respectively, which were lower than the soil OC stocks at the same depth

reported in other seagrass meadows in the tropical and subtropical areas (Lavery et al., 2013; Miyajima et al., 2015; Serrano et al., 2021; Table S5), especially those in North Sulawesi in Indonesia (32–68 Mg C ha^{-1} , Chen et al., 2017) and the Colombian Caribbean (50–85 Mg C ha^{-1} , Serrano et al., 2021). The low soil OC stock in the Xincun Bay was attributed to the low OC content in the sandy seagrass soil. The soil OC contents (0.47–1.86 mg g^{-1}) at our sampling sites are comparable to those reported by Jiang et al. (2018) at other seagrass sites (0.5–2.3 mg g^{-1}) in Xincun Bay and are much lower than the values reported at other seagrass sites (Table S5) and the global average OC content, 25 mg g^{-1} , in seagrass soils (Fourqurean et al., 2012). Previous studies have suggested a low OC content strongly related to a high proportion of coarse grain size of seagrass soils (Dahl et al., 2016), and that the OC in coarse-grained soils is more refractory than in fine-grained soils (Howard et al., 2021).

The present study measured a lower soil OC content and stock at the site M where macroalgal bloom had occurred for no less than a decade than at the site R, and we consider that the macroalgal bloom due to nutrient enrichment may result in the loss of OC in seagrass soils. The macroalgal bloom reduces advective water exchange in seagrass meadows, and the rapid decomposition of macroalgal materials produces more labile carbon as a potential source of soil OC. Experimental additions of algal tissues to seagrass soils have shown promoted invertase and polyphenol oxidase activities in the soils (Liu et al., 2019) and stimulated metabolism and loss of recalcitrant components (lignin and lipids) in the seagrass litter (Liu et al., 2020) or in the soils (Trevathan-Tackett et al., 2018). During our sampling, we observed a deposited liquid layer with a dark brown colour over the soil surface from macroalgal decomposition at site M. The priming effect of the labile OC released from the rapid decomposition of macroalgae would stimulate the mineralization and loss of intrinsic OC in the seagrass soil at site M in this study. The soils in fertilized nutrient-enriched seagrass meadows were also found to present stimulated exocellular enzyme activities associated with carbon cycling (López et al., 1998; Liu et al., 2017), which are suggested to enhance the decomposition and consequent loss of soil OC in coastal wetlands (Luo et al., 2017). The soil OC contents at our sites before the macroalgal bloom were not available; however, we suspect that the soil OC content before macroalgal bloom at

TABLE 1 | $\delta^{13}\text{C}$, organic carbon (OC) content, total nitrogen (TN) content and C:N ratio (in weight) of macroalgae (*Ulva lactuca*), epiphytes and seagrass (*Enhalus acoroides*) samples in the Xincun Bay Lagoon.

Station	$\delta^{13}\text{C}$ (‰)	OC content (%)	TN content (%)	C:N ratio
<i>Ulva lactuca</i>	-12.29 ± 0.60	25.7 ± 0.7	2.60 ± 0.20	9.9 ± 0.5
Epiphytes				
Site M	-16.48 ± 0.47	na	na	3.8 ± 0.8
Site R	-14.78 ± 0.64	na	na	4.6 ± 0.2
<i>Enhalus acoroides</i>				
Site M-LW	-8.26 ± 0.48	35.5 ± 1.4	3.10 ± 0.09	11.4 ± 0.6
Site M-SW	-8.17 ± 0.72	34.5 ± 1.1	3.23 ± 0.51	10.9 ± 2.1
Site R-LW	-8.16 ± 0.28	35.1 ± 2.6	2.66 ± 0.31	13.4 ± 2.3
Site R-SW	-8.01 ± 0.18	35.3 ± 1.2	3.04 ± 0.41	11.8 ± 2.1

na, data not available.

TABLE 2 | Means and ranges of proportional contributions of the potential sources to the soil organic carbon at the two seagrass sites in the Xincun Bay Lagoon.

Station	SPOM	Seagrass	Macroalgae	Epiphytes
Site M-LW	19.1 (0-52)	22.3 (0-62)	29.6 (0-88)	29.0 (0-87)
Site M-SW	21.5 (0-55)	20.0 (0-58)	27.5 (0-83)	31.0 (0-92)
Site R-LW	16.1 (0-39)	50.0 (19-75)	–	33.9 (0-81)
Site R-SW	17.8 (0-42)	45.1 (13-71)	–	37.2 (0-87)

SPOM, suspended particulate organic matter.

site M was no less than that at site R, because site M had had a longer semi-exchange time of seawater and reduced wave energy, which favours the burial of more organic carbon in the soil (Mazarrasa et al., 2021). The lower soil OC content and stock at the site M therefore indicate a loss of OC relative to the site R.

Decrease in OC content with depth is a common feature of soil profile of OC in seagrass meadows (Fourqurean et al., 2012), as was found at the site R in this study. The upper layer at the site M as the interface of macroalgae and soil, receives high macroalgal OC loading. A more pronounced loss of soil OC therefore may be expected at the upper layer relative to the deeper layers, leading to different soil profile of OC at the site M from that at site R. This is contrarily to our result at the site M showing a lower OC content in the 20-30cm layer than the upper layers. We consider that the loss of soil OC in the deeper layer could also be apparent because the macroalgal OC could reach the deeper layer of the sandy soil through penetration and bioturbation, and trigger the mineralization of OC at a higher rate than that in the upper layers (Trevathan-Tackett et al., 2018). Soil profile of $\delta^{13}\text{C}$ at the two sites suggested a more pronounced impact of macroalgal bloom on the OC composition in the deeper layer. Moreover, the low OC content in the deeper layer may also be attributed to continuous burial of depleted OC by macroalgal bloom along with the sedimentation. However, the lack of dating of soil in this study would affect the interpretation of the observed differences in soil OC with seagrass site and soil depth; further studies are therefore deserved to investigate the priming effects of macroalgal bloom on the soil profile of OC content and composition, with the duration of macroalgal bloom and dating of soil considered.

Seagrasses contribute to the OC sequestration in their soils in the form of their above-/belowground litter, and ~16% of their net primary production was estimated to be buried in the soil pool of the global seagrass meadows (Duarte and Krause-Jensen, 2017). The seagrass canopy also enhances the deposition of imported organic matter by tides by trapping seston particles by seagrass leaves and reducing the particle-carrying capacity of the water (Chen et al., 2017). Studies have demonstrated that the soil OC sequestration and stock in seagrass meadows are highly related to the vegetation population (Serrano et al., 2019; Bedulli et al., 2020), while the loss of the seagrass canopy would result in the erosion of soil carbon stocks (Marbà et al., 2015). In this study, there was no significant difference in the seagrass population of the sampled patches between the two sites (Table S1); however, the fragmentation of the seagrass habitat, a finding also reported by Santos et al. (2020), would also contribute to the loss of OC in the seagrass soils at site M

because continuous meadows have a stronger carbon-holding capacity than patchy ones (Ricart et al., 2015; Ricart et al., 2017).

The soil $\delta^{13}\text{C}$ values measured at the two seagrass sites reflect a different carbon composition between these two sites. Organic carbon in seagrass soil is potentially derived from seagrass and allochthonous sources, including phytoplankton and epiphytes (Kennedy et al., 2004). Previous studies recognized seagrass tissue as the major contributor to the soil carbon pool under the seagrass canopy, with a global mean of ~50% of the carbon in the surface soil derived from seagrass sources (Kennedy et al., 2010). The soil $\delta^{13}\text{C}$ in this study fell within a narrow range between -11.8‰ and -13.8‰ at the site R, closer to the seagrass signature than the SPOM, indicating a potentially major contribution of seagrass material to the soil OC composition. The soil $\delta^{13}\text{C}$ was more negative at the degraded site M due to the incorporation of more ^{13}C -depleted sources (e.g., macroalgae) and mineralization of seagrass detritus in the soil, as reflected by the increase in soil OC with less negative $\delta^{13}\text{C}$. In our study, soil cores were collected in the *E. acoroides*-covered area, and *E. acoroides* and *U. lactuca* were sampled as the single sources of seagrass and macroalgal, representatively. During our sampling, *T. hemprichii* and another macroalgal *Enteromorpha* sp. were also found, and they had a similar $\delta^{13}\text{C}$ to those of *E. acoroides* and *U. lactuca*, respectively (Tables 1, S6). Other studies also reported a similar $\delta^{13}\text{C}$ of whole plant samples between *T. hemprichii* and *E. acoroides*, and a similar $\delta^{13}\text{C}$ of *Hypnea boergesenii*, another species ever observed in the seagrass sites, to that of *Ulva* species in the Xincun Bay (Liu et al., 2016; Jiang et al., 2018). Regarding the dominance of the *E. acoroides* and *U. lactuca* and the similarity in $\delta^{13}\text{C}$ between seagrass/macroalgae species, we consider that the carbon sources extrapolated using *E. acoroides* and *U. lactuca* signatures could be representative.

In the present study, we found a more rapid decline in the soil TN content than the OC content, leading to a higher soil C:N ratio at the degraded site, suggesting that nutrient enrichment and macroalgae would impact N metabolism in seagrass soil. We suspect that the soil microbes supplied with labile macroalgal or epiphytic sources with lower C:N ratios than the soil values would consume nitrogen in the seagrass soils. Further studies are needed to investigate the soil nitrogen metabolism in seagrass meadows under nutrient enrichment and macroalgal impacts.

CONCLUSION

In this study, we measured a lower soil OC content and stock at the nutrient-enriched seagrass site where macroalgae bloom than

at the site without apparent macroalgae located in the same lagoon and suggest that the degradation in the seagrass habitat and the macroalgal bloom due to nutrient enrichment drove the loss of seagrass-derived OC in the soil pool. The seagrass soils at Xincun Bay are relatively OC-poor and have low OC stocks, and we consider that the loss of the limited OC sequestered in the soil due to the priming effect of macroalgal bloom is worthy of full attention. Our results also suggest that nutrient enrichment and macroalgae would impact nitrogen metabolism, which deserves future detailed studies.

DATA AVAILABILITY STATEMENT

The original contributions presented in the study are included in the article/**Supplementary Material**. Further inquiries can be directed to the corresponding author.

AUTHOR CONTRIBUTIONS

GC contributed to the study conception. SYC, SQC, JW, JZ, LL, and WA performed the sample collection and data acquisition. LX, ZW, and BC performed the data analysis. All authors contributed to the article and approved the submitted version.

REFERENCES

- Armitage, A. R., and Fourqurean, J. W. (2016). Carbon Storage in Seagrass Soils: Long-Term Nutrient History Exceeds the Effects of Near-Term Nutrient Enrichment. *Biogeosciences* 13 (1), 313–321. doi: 10.5194/bg-13-313-2016
- Bedulli, C., Lavery, P. S., Harvey, M., Duarte, C. M., and Serrano, O. (2020). Contribution of Seagrass Blue Carbon Toward Carbon Neutral Policies in a Touristic and Environmentally-Friendly Island. *Front. Mar. Sci.* 7. doi: 10.3389/fmars.2020.00001
- Burkholder, J. M., Tomasko, D. A., and Touchette, B. W. (2007). Seagrasses and Eutrophication. *J. Exp. Mar. Biol. Ecol.* 350, 46–72. doi: 10.1016/j.jembe.2007.06.024
- Chen, G., Azkab, M. H., Chmura, G. L., Chen, S., Sastrosuwondo, P., Ma, Z., et al. (2017). Mangroves as a Major Source of Soil Carbon Storage in Adjacent Seagrass Meadows. *Sci. Rep.* 7, 42406. doi: 10.1038/srep42406
- Chen, S., Wang, D., Wu, Z., Zhang, G., Li, Y., Tu, Z., et al. (2015). Discussion of the Change Trend of the Seagrass Beds in the East Coast of Hainan Island in Nearly a Decade. *Mar. Environ. Sci.* 34 (1), 48–53. doi: 10.3969/j.issn.0253-4193.2015.06.01
- Dahl, M., Deyanova, D., Gütschow, S., Asplund, M. E., Lyimo, L. D., Karamfilov, V., et al. (2016). Sediment Properties as Important Predictors of Carbon Storage in *Zostera Marina* Meadows: A Comparison of Four European Areas. *PLoS One* 11 (12), e0167493. doi: 10.1371/journal
- Duarte, C. M., and Krause-Jensen, D. (2017). Export From Seagrass Meadows Contributes to Marine Carbon Sequestration. *Front. Mar. Sci.* 4. doi: 10.3389/fmars.2017.00013
- Dunic, J. C., Brown, C. J., Connolly, R. M., Turschwell, M. P., and Côté, I. M. (2021). Long-Term Declines and Recovery of Meadow Area Across the World's Seagrass Bioregions. *Global Change Biol.* 27, 4096–4109. doi: 10.1111/gcb.15684
- Fang, X., Li, X., Xiang, Y., Hao, C., Zhao, Y., and Zhang, Y. (2020). Cumulative Impact of Anthropogenic Nutrient Inputs on Lagoon Ecosystems - a Case Study of Xincun Lagoon, Hainan, China. *Reg. Stud. Mar. Sci.* 35, 101213. doi: 10.1016/j.rsma.2020.101213
- Fang, X., Li, X., Zhang, Y., Zhao, Y., Qian, J., Hao, C., et al. (2021). Random Forest-Based Understanding and Predicting of the Impacts of Anthropogenic Nutrient Inputs on the Water Quality of a Tropical Lagoon. *Environ. Res. Lett.* 16, 055003. doi: 10.1088/1748-9326/abf395

FUNDING

The work described in this paper was funded by the Provincial Natural Science Foundation of Fujian (2020J06030) and Hainan Provincial Basic and Applied Basic Research Fund for High-Level Talents in Natural Science (421RC662). The Scientific Research Foundation of the Third Institute of Oceanography, MNR (2020017) and the National Natural Science Foundation of China (42166006) also contribute to this work.

ACKNOWLEDGMENTS

The authors are grateful to Dr. Xijie Yin, Mr. Jiahui Chen, Mr. Pengfei Lin, and Mr. Yanmin Fu for their assistance with field sampling and laboratory analysis. We also appreciate the comments of two reviewers and those of Dr. Guanglong Qiu, which helped improve the manuscript.

SUPPLEMENTARY MATERIAL

The Supplementary Material for this article can be found online at: <https://www.frontiersin.org/articles/10.3389/fmars.2022.870228/full#supplementary-material>

- Fourqurean, J. W., Duarte, C. M., Kennedy, H., Marbà, N., Holmer, M., Mateo, M. A., et al. (2012). Seagrass Ecosystems as a Globally Significant Carbon Stock. *Nat. Geosci.* 5, 505–509. doi: 10.1038/ngeo1477
- Han, Q., and Liu, D. (2014). Macroalgal Blooms and Their Effects on Seagrass Ecosystems. *J. Ocean Univ. China (Oceanic Coast. Sea Res.)* 13 (5), 791–798. doi: 10.1007/s11802-014-2471-2
- Hemminga, M. A., and Duarte, C. M. (2000). *Seagrass Ecology* (Cambridge: Cambridge University Press).
- Howard, J. L., Lopes, C. C., Wilson, S. S., McGee-Absten, V., Carrión, C. I., and Fourqurean, J. W. (2021). Decomposition Rates of Surficial and Buried Organic Matter and the Lability of Soil Carbon Stocks Across a Large Tropical Seagrass Landscape. *Estuaries Coasts* 44, 846–866. doi: 10.1007/s12237-020-00817-x
- Howard, J. L., Perez, A., Lopes, C. C., and Fourqurean, J. W. (2016). Fertilization Changes Seagrass Community Structure But Not Blue Carbon Storage: Results From a 30-Year Field Experiment. *Estuaries Coasts* 39, 1422–1434. doi: 10.1007/s12237-016-0085-1
- Jiang, Z., Liu, S., Zhang, J., Wu, Y., Zhao, C., Lian, Z., et al. (2018). Eutrophication Indirectly Reduced Carbon Sequestration in a Tropical Seagrass Bed. *Plant Soil* 426, 135–152. doi: 10.1007/s11104-018-3604-y
- Kennedy, H., Beggins, J., Duarte, C. M., Fourqurean, J. W., Holmer, M., Marbà, N., et al. (2010). Seagrass Sediments as a Global Carbon Sink: Isotopic Constraints. *Global Biogeochem. Cycles* 24, GB4026. doi: 10.1029/2010GB003848
- Kennedy, H., Gaciab, E., Kennedy, D. P., Papadimitriou, S., and Duarte, C. M. (2004). Organic Carbon Sources to SE Asian Coastal Sediments. *Estuar. Coast. Shelf Sci.* 60, 59–68. doi: 10.1016/j.ecss.2003.11.019
- Kuzyakov, Y., Friedel, J. K., and Stahr, K. (2000). Review of Mechanisms and Quantification of Priming Effects. *Soil Biol. Biochem.* 32, 1485–1498. doi: 10.1016/S0038-0717(00)00084-5
- Lavery, P., Mateo, M.-Á., Serrano, O., and Rozaimi, M. (2013). Variability in the Carbon Storage of Seagrass Habitats and its Implications for Global Estimates of Blue Carbon Ecosystem Service. *PLoS One* 8 (9), e73748. doi: 10.1371/journal.pone.0073748
- Liu, S., Jiang, Z., Wu, Y., Deng, Y., Chen, Q., Zhao, C., et al. (2019). Macroalgal Bloom Decay Decreases the Sediment Organic Carbon Sequestration Potential

- in Tropical Seagrass Meadows of the South China Sea. *Mar. Pollut. Bull.* 138, 598–603. doi: 10.1016/j.marpolbul.2018.12.009
- Liu, S., Jiang, Z., Wu, Y., Zhang, J., Arbi, I., Ye, F., et al. (2017). Effects of Nutrient Load on Microbial Activities Within a Seagrass-Dominated Ecosystem: Implications of Changes in Seagrass Blue Carbon. *Mar. Pollut. Bull.* 117, 214–221. doi: 10.1016/j.marpolbul.2017.01.056
- Liu, S., Jiang, Z., Zhang, J., Wu, Y., Lian, Z., and Huang, P. (2016). Effect of Nutrient Enrichment on the Source and Composition of Sediment Organic Carbon in Tropical Seagrass Beds in the South China Sea. *Mar. Pollut. Bull.* 110, 274–280. doi: 10.1016/j.marpolbul.2016.06.054
- Liu, S., Trevathan-Tackett, S. M., Lewis, C., Huang, X., and Macreadie, P. I. (2020). Macroalgal Blooms Trigger the Breakdown of Seagrass Blue Carbon. *Environ. Sci. Technol.* 54 (22), 14750–14760. doi: 10.1021/acs.est.0c03720
- López, N. I., Duarte, C. M., Vallespinós, F., Romero, J., and Alcoverro, T. (1998). The Effect of Nutrient Additions on Bacterial Activity in Seagrass (*Posidonia Oceanica*) Sediments. *J. Exp. Mar. Biol. Ecol.* 224, 155–166. doi: 10.1016/S0022-0981(97)00189-5
- Luo, L., Han, M., Wu, R., and GU, J. (2017). Impact of Nitrogen Pollution/Deposition on Extracellular Enzyme Activity, Microbial Abundance and Carbon Storage in Coastal Mangrove Sediment. *Chemosphere* 177, 275–283. doi: 10.1016/j.chemosphere.2017.03.027
- Marbà, N., Arias-Ortiz, A., Masqué, P., Kendrick, G. A., Mazarrasa, I., Bastyan, G. R., et al. (2015). Impact of Seagrass Loss and Subsequent Revegetation on Carbon Sequestration and Stocks. *J. Ecol.* 103 (2), 296–302. doi: 10.1111/1365-2745.12370
- Mazarrasa, I., Lavery, P., Duarte, C. M., Lafratta, A., Lovelock, C. E., Macreadie, P. I., et al. (2021). Factors Determining Seagrass Blue Carbon Across Bioregions and Geomorphologies. *Global Biogeochem. Cycles* 35, e2021GB006935. doi: 10.1029/2021GB006935
- Miyajima, T., Hori, M., Hamaguchi, M., Shimabukuro, H., Adachi, H., Yamano, H., et al. (2015). Geographic Variability in Organic Carbon Stock and Accumulation Rate in Sediments of East and Southeast Asian Seagrass Meadows. *Global Biogeochem. Cycles* 29, 397–415. doi: 10.1002/2014GB004979
- Qin, L., Suonan, Z., Kim, S. H., and Lee, K. (2021). Coastal Sediment Nutrient Enrichment Alters Seagrass Blue Carbon Sink Capacity. *Environ. Sci. Technol.* 55, 15466–15475. doi: 10.1021/acs.est.1c03782
- Ricart, A. M., Pérez, M., and Romero, J. (2017). Landscape Configuration Modulates Carbon Storage in Seagrass Sediments. *Estuar. Coast. Shelf Sci.* 185, 69–76. doi: 10.1016/j.ecss.2016.12.011
- Ricart, A. M., York, P. H., Rasheed, M. A., Pérez, M., Romero, J., Bryant, C. V., et al. (2015). Variability of Sedimentary Organic Carbon in Patchy Seagrass Landscapes. *Mar. Pollut. Bull.* 100, 476–482. doi: 10.1016/j.marpolbul.2015.09.032
- Santos, R. O., Varona, G., Avila, C. L., Lirman, D., and Collado-Vides, L. (2020). Implications of Macroalgae Blooms to the Spatial Structure of Seagrass Seascapes: The Case of the *Anadyomene* Spp. (Chlorophyta) Bloom in Biscayne Bay, Florida. *Mar. Pollut. Bull.* 150, 110742. doi: 10.1016/j.marpolbul.2019.110742
- Serrano, O., Gómez-López, D. T., Sánchez-Valencia, L., Acosta-Chaparro, A., Navas-Camacho, R., González-Corredor, J., et al. (2021). Seagrass Blue Carbon Stocks and Sequestration Rates in the Colombian Caribbean. *Sci. Rep.* 11 (1), 11067. doi: 10.1038/s41598-021-90544-5
- Serrano, O., Lovelock, C. E., Atwood, T. B., Macreadie, P. I., Canto, R., Phinn, S., et al. (2019). Australian Vegetated Coastal Ecosystems as Global Hotspots for Climate Change Mitigation. *Nat. Commun.* 10, 4313. doi: 10.1038/s41467-019-12176-8
- Trevathan-Tackett, S. M., Thomson, A. C. G., Ralph, P. J., and Macreadie, P. I. (2018). Fresh Carbon Inputs to Seagrass Sediments Induce Variable Microbial Priming Responses. *Sci. Total Environ.* 621, 663–669. doi: 10.1016/j.scitotenv.2017.11.193
- Wang, D., Wu, Z., Chen, C., Lan, J., Chen, X., Wu, R., et al. (2012). Distribution of Sea-Grass Resources and Existing Threat in Hainan Island. *Mar. Environ. Sci.* 31 (1), 34–38. doi: 10.3969/j.issn.1007-6336.2012.01.008
- Waycott, M., Duarte, C. M., Carruthers, T. J. B., Orth, R. J., Dennison, W. C., Olyaynik, S., et al. (2009). Accelerating Loss of Seagrasses Across the Globe Threatens Coastal Ecosystems. *Proc. Natl. Acad. Sci. U.S.A.* 106, 12377–12381. doi: 10.1073/pnas.0905620106
- Weather China. (2022) *History.Shtml*. Available at: <http://www.weather.com.cn/forecast/history.sht-ml> (Accessed January 4, 2022).
- Zheng, F., Qiu, G., Fan, H., and Zhang, W. (2013). Diversity, Distribution and Conservation of Chinese Seagrass Species. *Biodivers. Sci.* 21 (5), 517–526. doi: 10.3724/SP.J.1003.2013

Conflict of Interest: The authors declare that the research was conducted in the absence of any commercial or financial relationships that could be construed as a potential conflict of interest.

Publisher's Note: All claims expressed in this article are solely those of the authors and do not necessarily represent those of their affiliated organizations, or those of the publisher, the editors and the reviewers. Any product that may be evaluated in this article, or claim that may be made by its manufacturer, is not guaranteed or endorsed by the publisher.

Copyright © 2022 Chen, Chen, Chen, Wu, An, Luo, Wang, Xie, Zhang and Chen. This is an open-access article distributed under the terms of the Creative Commons Attribution License (CC BY). The use, distribution or reproduction in other forums is permitted, provided the original author(s) and the copyright owner(s) are credited and that the original publication in this journal is cited, in accordance with accepted academic practice. No use, distribution or reproduction is permitted which does not comply with these terms.



Variability in the Net Ecosystem Productivity (NEP) of Seaweed Farms

Yoichi Sato^{1,2†}, Gregory N. Nishihara^{3,4†*}, Atsuko Tanaka^{5†}, Dominic F. C. Belleza^{4†}, Azusa Kawate⁴, Yukio Inoue⁴, Kenjiro Hinode⁶, Yuhei Matsuda⁴, Shinichiro Tanimae⁴, Kandai Tozaki⁷, Ryuta Terada⁸ and Hikaru Endo⁹

¹ Bio-Resources Business Development Division, Riken Food Co., Ltd., Tagajyo, Japan, ² RIKEN Nishina Center for Accelerator-Based Science, Wako, Japan, ³ Organization for Marine Science and Technology, Institute for East China Sea Research, Nagasaki University, Nagasaki, Japan, ⁴ Graduate School of Fisheries and Environmental Sciences, Nagasaki University, Nagasaki, Japan, ⁵ Department of Chemistry, Biology and Marine Science, Faculty of Science, University of the Ryukyus, Nishihara, Japan, ⁶ Kuroshio Biological Research Foundation, Otsuki, Japan, ⁷ Graduate School of Engineering and Science, University of the Ryukyus, Nishihara, Japan, ⁸ United Graduate School of Agricultural Sciences, Kagoshima University, Kagoshima, Japan, ⁹ Faculty of Fisheries, Kagoshima University, Kagoshima, Japan

OPEN ACCESS

Edited by:

Hilary Anne Kennedy,
Bangor University, United Kingdom

Reviewed by:

Victor Shelamoff,
University of Tasmania, Australia
John Gallagher,
University of Tasmania, Australia

*Correspondence:

Gregory N. Nishihara
greg@nagasaki-u.ac.jp

[†]These authors have contributed
equally to this work and share
first authorship

Specialty section:

This article was submitted to
Global Change and the Future Ocean,
a section of the journal
Frontiers in Marine Science

Received: 25 January 2022

Accepted: 22 April 2022

Published: 24 May 2022

Citation:

Sato Y, Nishihara GN, Tanaka A,
Belleza DFC, Kawate A, Inoue Y,
Hinode K, Matsuda Y, Tanimae S,
Tozaki K, Terada R and Endo H (2022)
Variability in the Net Ecosystem
Productivity (NEP) of Seaweed Farms.
Front. Mar. Sci. 9:861932.
doi: 10.3389/fmars.2022.861932

The important role of vegetated ecosystems in the sequestration of carbon has gained strong interest across a wide variety of disciplines. With evidence growing of the potential for macroalgae ecosystems to capture carbon, there is burgeoning interest in applying newfound knowledge of carbon capture rates to better understand the potential for carbon sequestration. Seaweed farms are expected to play a significant role in carbon capture; advocates for the expansion of seaweed farms are increasing in many countries. In general, seaweed farms are expected to be highly productive, although whether they are autotrophic or heterotrophic ecosystems and hence potential exporters of carbon, is under debate. Therefore, we present our investigation of three seaweed farms, two in northern Japan and one in southern Japan. We examine the frequency of autotrophic days and compare potential rates of carbon capture of the seaweed farms with two natural macroalgae ecosystems and one degraded site. We estimated potential carbon capture rates by calculating the net ecosystem productivity from continuous recordings of dissolved oxygen concentrations under natural environmental conditions. The net ecosystem production rates for the natural ecosystems in Arikawa Bay and Omura Bay were equivalent to 0.043 and 0.054 [g C m⁻² d⁻¹] m⁻¹, respectively. Whereas, for the degraded ecosystem in Tainoura Bay, it was -0.01 [g C m⁻² d⁻¹] m⁻¹. We reveal that the *Undaria pinnatifida* farm in Matsushima Bay experience autotrophy more often than natural ecosystems, although for seaweed farms producing *U. pinnatifida* in Hirota Bay and *Cladospirion okamuranus* at Bise Point, autotrophy was less frequently observed. Nevertheless, up to 14.1 g C m⁻² (0.110 g C m⁻² d⁻¹) was captured by the production of *U. pinnatifida* and 3.6 g C m⁻² (0.034 g C m⁻² d⁻¹) was captured by *C. okamuranus*, and the total yield of carbon captured during 2021 production season for these farms was 43,385 kg C.

Keywords: climate change, aquaculture, blue carbon, dissolved oxygen, seaweed, macroalgae

INTRODUCTION

Vegetated ecosystems are expected to play an important role in sequestering carbon. Interest and research in carbon sequestration by vegetated coastal ecosystems are driving the development of blue carbon strategies to mitigate the effects of climate change (McLeod et al., 2011; Siegel et al., 2021). Some evidence suggests that macroalgae ecosystems can capture carbon dioxide from the environment just as effectively as seagrass, mangrove, and salt marsh ecosystems (Hill et al., 2015; Trevathan-Tackett et al., 2015; Ortega et al., 2019; Gouvêa et al., 2020). Hence, it is expected that macroalgae ecosystems, which cover approximately 3.4 million km² of coastal ocean area, can capture approximately 1.5 Gt C yr⁻¹ (Krause-Jensen and Duarte, 2016). Estimates suggest that approximately 165 Mt C yr⁻¹ may be sequestered for time-scales relevant to the mitigation of climate change (Frontier et al., 2021). Hence, interest in developing seaweed aquaculture as a carbon mitigation tool can be attributed to their global coverage, high rates of productivity, and the perception that there is a high social and economic cost of carbon removal in terrestrial ecosystems (Chung et al., 2011; Boysen et al., 2017).

Approximately 48 million km² of ocean area is believed to be suitable for seaweed aquaculture and has the potential to create a carbon neutral industry by combining traditional fin-fish aquaculture with seaweed aquaculture (Froehlich et al., 2019). Based on annual landings of seaweed harvests from aquaculture farms, an estimated 0.7 Mt C yr⁻¹ was captured in the Asian-Pacific region (Sondak et al., 2017). The global seaweed aquaculture harvest is expected to capture 680 Mt C yr⁻¹ from the environment (Duarte, 2017).

In contrast to seagrass dominated ecosystems, which are expected to sequester some of the captured carbon locally within the sediment of their habitat, macroalgae dominated ecosystems are less able to sequester carbon locally because most macroalgae occur on rocky substrate. Macroalgae ecosystems are expected to export a large fraction of the carbon that is captured through photosynthesis and serve as a carbon source — captured carbon (i.e., about 11% of macroalgal net C production) is exported to adjacent environments and deposited in sediments for relevant time-scales (Krause-Jensen et al., 2018). Recent studies indicate that the biomass produced by macroalgae may continue to capture carbon through photosynthesis after becoming detached from the substrate or thallus as they are exported out of the local habitat and enhance the deposition of detritus away from rocky habitat and into sediments, which can facilitate carbon sequestration (Krumhansl and Scheibling, 2012; Pedersen et al., 2020; Frontier et al., 2021; Smale et al., 2021). The potential for mitigating greenhouse gases, especially carbon dioxide, with macroalgae ecosystems or macroalgae aquaculture is debatable (Muraoka, 2004; Hill et al., 2015; Fillbee-Dexter and Wernberg, 2020; Gallagher et al., 2021; Gallagher et al., 2022) and their status as climate mitigating carbon sinks requires careful inquiry (Howard et al., 2017). Nevertheless, macroalgae ecosystems and seaweed aquaculture are increasingly touted as a key blue carbon strategy (Krause-Jensen and Duarte, 2016; Duarte and Krause-

Jensen, 2017; Duarte et al., 2017; Krause-Jensen et al., 2018; Froehlich et al., 2019; Ortega et al., 2019; Fillbee-Dexter and Wernberg, 2020).

There is little field evidence regarding the amount of carbon removed by seaweed aquaculture farms. Nevertheless, *Saccharina japonica* farms in the Yellow Sea increased dissolved oxygen concentrations and exhibited a deficit in pCO₂ (Xiao et al., 2021). However, a recent study suggests that macroalgae ecosystems are generally heterotrophic and rather than exporting carbon to the deep ocean, these ecosystems are local producers of carbon dioxide due to the influence of allochthonous organic matter sources (Gallagher et al., 2022). Therefore, we explore the potential of seaweed farms in Japan to capture carbon and compare them to natural ecosystems dominated by macroalgae. We infer the potential of seaweed farms and natural ecosystems to capture carbon by estimating their net ecosystem production using continuous recordings of dissolved oxygen, evaluating the proportion of autotrophic days in these ecosystems, and by estimating carbon captured from the total yields of the farms. We expected that the seaweed farms were autotrophic more often than natural ecosystems, since natural ecosystems are expected to be primarily heterotrophic (Gallagher et al., 2022).

MATERIALS AND METHODS

Study Sites, Period, and Macroalgae Taxa

Our data was collected from two natural seaweed ecosystems, one degraded seaweed ecosystem, and three seaweed farms from six geographic location across Japan (**Figure 1**). The natural ecosystems that were examined were seaweed beds dominated by a variety of *Sargassum* taxa. The degraded ecosystem is one that was previously a seaweed abundant ecosystem that has degraded into a state of isoyake (i.e., a state where a seaweed ecosystem degraded into an ecosystem devoid of habitat forming seaweed; Fujita, 2010; Vergès et al., 2014; Eger et al., 2022). Two clusters of seaweed farms were monitored: *Undaria pinnatifida* farms in the north and a *Cladosiphon okamuranus* farm in the south (**Table 1** and **Figure 1**).

Matsushima Bay and Hirota Bay are located in northern Japan and are the sites of the *U. pinnatifida* farms (**Table 1** and **Figure 1**). Both bays have predominantly silty substrates. The seaweed farm at Matsushima Bay is in relatively shallow (ca. 5 m) and enclosed waters, whereas the seaweed farm at Hirota Bay is in deep water with depths ranging from 30 to 40 m. Both bays open to the east, where the mean fetch (number of vectors at the fixed limit) for Hirota Bay was 4832 m (37), whereas the mean fetch for Matsushima Bay was 3254 m (4). Both Matsushima Bay and Hirota Bay experience a similar range in salinity, ranging from 30 to 35 (Ichikawa et al., 2009; Jianxi et al., 2020). Besides *U. pinnatifida*, commercial cultivation of oysters, *Pyropia* spp., and *Saccharina* spp. are present in Matsushima Bay, while scallops are cultivated in Hirota Bay.

Bise Point is located in southern Japan and is the site of the *C. okamuranus* farm. Here, the farm is located within the lagoon of a coral reef in 3 to 6 m of water and faces the ocean to the east

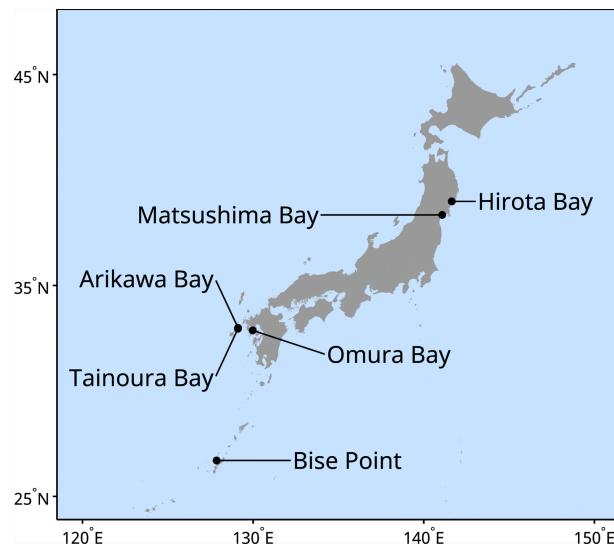


FIGURE 1 | Location of the sites monitored during the study.

with a mean fetch of 7336 m (62). Cultivation of *C. okamuranus* occurs in the lagoon to minimize exposure to strong hydrodynamic forces. Corals and seagrasses such as *Thalassia hemprichii*, *Cymodocea rotundata*, and *Halodule uninervis* can often be observed within the lagoon where salinity ranges from 32 to 35 (Higuchi et al., 2014).

Omura Bay, Arikawa Bay, and Tainoura Bay are located in Nagasaki Prefecture, in western Japan. Omura Bay is a highly enclosed bay, with a narrow and restricted entrance to the northeast. The study site has a mean fetch of 1584 m (3) and is a *Sargassum* spp. dominated ecosystem. The sediment at the site of Omura Bay is a mix of rock and sand. Salinity ranges from 30 to 35 (Nogami and Matsuno, 2001; Tsuchiya et al., 2018). Arikawa Bay and Tainoura Bay are in Nakadori Island, of the Goto Archipelago. Arikawa Bay is a wide north facing bay and is open to the ocean with a mean fetch of 2473 m (14). Tainoura Bay is a long narrow bay facing east with a mean fetch of 1016 (8) and is the site of an ecosystem degraded into an isoyake state, whereas Arikawa Bay is the site of a *Sargassum* spp. dominated ecosystem. Both bays have similar substrates, which is a mix of rock and sand.

All the sites examined in our study are located near large municipalities with armored shores. Although no major rivers drain into study sites, small streams and stormwater drains are present along the shore. Based on the mean fetch, we can rank the relative exposure of the sites from highest to lowest: Bise Point, Hirota Bay, Matsushima Bay, Arikawa Bay, Omura Bay, and Tainoura Bay. Data collection for the natural ecosystems occurred throughout the year; however, there are some gaps in the collection period due equipment malfunction and interruptions caused by tropical storms. Also, data collection for the seaweed farms were restricted to the production season

(Table 1). The period of seaweed production is variable and occurs for less than 6 months of the year. Variations in the production period also occurs due to the cultivation of different species and the differences in the environmental conditions. Therefore the comparisons made in this study are made with knowledge of this limitation.

Temperature and Dissolved Oxygen

Water temperature and dissolved oxygen concentrations were recorded with dataloggers (U26-001, Onset Computer Corporation, Bourne, MA, USA) at a rate of one sample every ten minutes. The U26-001 is an optical sensor that uses fluorescence to measure dissolved oxygen concentrations. Loggers were calibrated before and after deployment and referenced against a hand-held optical dissolved oxygen sensor (ProODO, Xylem Inc., Yellow Springs, OH, USA). In the natural and degraded ecosystems, one datalogger was placed directly above the sediment, another 50 cm above the sediment, and third 50 cm below the water surface (i.e., a total of three instruments and mean depth of 3 m for Omura Bay, 5 m for Arikawa Bay, and 8 m for Tainoura Bay). The dataloggers at the seaweed aquaculture farms were placed on the cultivation ropes and 1 m (Bise Point) and 2 m (Hirota Bay and Matsushima Bay) below the cultivation ropes (i.e., a total of two instruments). The instruments were placed so that the majority of the biomass of the seaweed were between the data loggers. Recordings were carried out for four to twenty days before the instruments were retrieved for maintenance and data offloading (e.g., Hinode et al., 2020). Calculations of productivity (as described below) is based on the ensemble mean of the dissolved oxygen time-series recorded by the dataloggers, to account for vertical heterogeneity.

TABLE 1 | Location, state, survey period, the number of recorded days (Survey days), the mean and standard deviation of the temperature during the survey period, and the mean fetch of the study sites.

Location	Latitude (N)	Longitude (E)	State	Start date	End date	Survey days	Temperature mean (°C)	Temperature standard deviation (°C)	Mean wind fetch (m) and the number of vectors at the upper limit in the parenthesis
Hirota Bay, Iwate	39.0240	141.7873	<i>Undaria pinnatifida</i>	2020-12-08	2021-04-15	129	9.7	1.8	4832 (37)
Matsushima Bay, Miyagi	38.3455	141.0808	<i>Undaria pinnatifida</i>	2019-10-17	2020-02-27	133	9.5	4.4	3254 (4)
Matsushima Bay, Miyagi	38.3455	141.0808	<i>Undaria pinnatifida</i>	2020-10-18	2021-03-14	145	8.3	4.4	3254 (4)
Arikawa Bay, Nagasaki	32.9883	129.1184	<i>Sargassum</i> spp.	2017-04-09	2017-04-30	22	16.5	0.57	2473 (14)
Arikawa Bay, Nagasaki	32.9883	129.1184	<i>Sargassum</i> spp.	2017-10-01	2018-04-30	136	16.8	3.9	2473 (14)
Arikawa Bay, Nagasaki	32.9883	129.1184	<i>Sargassum</i> spp.	2018-10-08	2019-04-30	178	17.1	2.6	2473 (14)
Arikawa Bay, Nagasaki	32.9883	129.1184	<i>Sargassum</i> spp.	2019-10-01	2020-04-21	178	17.6	3.1	2473 (14)
Arikawa Bay, Nagasaki	32.9883	129.1184	<i>Sargassum</i> spp.	2020-10-01	2021-04-29	159	17.7	3.31	2473 (14)
Tainoura Bay, Nagasaki	32.9513	129.1096	isoyake	2017-04-09	2017-04-30	22	16.8	0.6	1016 (8)
Tainoura Bay, Nagasaki	32.9513	129.1096	isoyake	2017-11-01	2018-04-30	101	16.7	2.9	1016 (8)
Tainoura Bay, Nagasaki	32.9513	129.1096	isoyake	2018-10-01	2019-04-30	185	17.7	2.8	1016 (8)
Tainoura Bay, Nagasaki	32.9513	129.1096	isoyake	2019-10-01	2020-04-30	187	18.1	3.1	1016 (8)
Omura Bay, Nagasaki	32.8700	129.9735	<i>Sargassum</i> spp.	2015-04-17	2015-04-22	6	15.8	0.4	1584 (3)
Omura Bay, Nagasaki	32.8700	129.9735	<i>Sargassum</i> spp.	2015-10-14	2016-04-30	27	16.2	4.8	1584 (3)
Omura Bay, Nagasaki	32.8700	129.9735	<i>Sargassum</i> spp.	2016-11-02	2017-02-02	14	15.5	5.5	1584 (3)
Bise Point, Okinawa	26.7043	127.8597	<i>Cladosiphon okamuranus</i>	2021-01-15	2021-04-30	105	21.8	0.9	7336 (62)

To determine wind fetch, 108 vectors with an upper limit of 10,000 m were generated in a 2π radial pattern around each coordinate. Rows are ordered from north to south.

Light and Wind Speed

To determine daylength and to calculate the air-sea gas flux of oxygen, the photosynthetic photon flux density (S-LIA-M003, Onset Computer Corporation, Bourne, MA, USA) and wind speed (S-BPB-CM50, Onset Computer Corporation, Bourne, MA, USA) were recorded to a datalogger (USB Microstation, Onset Computer Corporation, Bourne, MA, USA) at a rate of one sample every ten minutes. One set of instruments were deployed at each site. At the natural ecosystems, the measurements were taken one meter above the seawater surface by placing the equipment on a floating raft; however, at the seaweed aquaculture farms, the instruments were placed 10 m above ground at nearby boat harbors. Data was recorded for four to twenty days (e.g., Hinode et al., 2020).

Estimating Productivity

The gross ecosystem production (GEP) rates and ecosystem respiration (ER) rates were estimated from the diurnal fluctuations of the dissolved oxygen concentration with the open-water method (Hanson et al., 2008; Staehr et al., 2010; Champenois and Borges, 2012; Berg et al., 2019; Hinode et al., 2020), therefore the data includes not only the physiological processes of photosynthetic organisms, but also includes the respiration of non-photosynthetic organisms (see Gallagher et al., 2022 for details on the processes occurring in open systems). Briefly, the net ecosystem production (NEP) rate can be defined as $NEP = GEP + ER$, where GEP are positive values and ER are negative values. NEP rates (NEP_t) with respect to sampling time (i.e., $\Delta t = 10$ minutes) are calculated

as the time rate-of-change of the dissolved oxygen concentrations ($NEP_t = \frac{\Delta O_2}{\Delta t} + F_{O_2,t}$) determined from a smoother fitted with a generalized additive model (GAM) and the calculated flux ($F_{O_2,t}$) at the air-sea interface (Wanninkhof, 1992). The smoother for the GAM was a thin-plate spline, and the distribution was assumed to be Gaussian (Wood, 2011). Physical flux of dissolved oxygen within the water column cannot be evaluated by this method, however given the relative size of our measurement sites, our experience shows that any concentration gradients that could affect the measurements tend to sum to zero. Hence, we define the daily rates of NEP as the sum of the flux-corrected NEP rates ($NEP = \sum NEP_t$), and are approximations to NEP. The daily rates of ER are the sum of flux-corrected NEP rates occurring during the night (H_n), which were then normalized to 24 hours ($ER = \frac{H_n}{24} \sum NEP_t$). We assume that ER occurring during the night is representative of ER occurring over 24 hours. It is important to note that at the spatial scale of this study, unmeasured processes such as the physical flux of oxygen and the calcium carbonate cycle should be expected to influence GEP estimates, regardless of methodology (Holtgrieve et al., 2010; Staehr et al., 2012; Smith, 2013; Macreadie et al., 2017). Nevertheless, after assuming a 1:1 relationship between O_2 production and CO_2 consumption (Gauthier et al., 2018), we refer to NEP interchangeably with carbon capture potential, where the conversion rate of O_2 to C was 0.375. Units normalized to unit depth, given the vertical position of the data loggers, and are presented in $[g\ m^{-2}\ d^{-1}]\ m^{-1}$. It is important to recall that the vertical position of the data loggers was designed to maximize the fidelity of the dissolved oxygen fluctuations caused by photosynthetic and respiratory activity in the study system.

The total yield and carbon content of *U. pinnatifida* and *C. okamuranus* was determined for the 2021 production season. The percent carbon content for the seaweeds were determined from 5 haphazardly selected thalli for each taxa collected on 30 April 2021 for *C. okamuranus*, 14 March 2021 for *U. pinnatifida* from Matsushima Bay, and 15 April 2021 for *U. pinnatifida* from Hirota Bay. The whole thalli was analyzed for the *C. okamuranus* specimens. However, due to the large size of the *U. pinnatifida* specimens, a 20 mm diameter section of the frond was excised from the widest portion of the frond and used in the carbon content analysis. The seawater on the samples were carefully removed from their surfaces by blotting with a paper towel. The samples were dried in an oven (EYELA WFO-500, Tokyo Rikakikai Co., Ltd., Tokyo, Japan) for 12 hours at 80 °C. The dried samples were pulverized with a mortar and pestle, and the carbon content was measured with a CHN analyzer (Flash 2000, Thermofisher Scientific, Waltham, MA, USA).

Data Analysis

Inclement weather conditions caused periods of missing light and wind data. In the case of missing wind values, wind speeds were interpolated by fitting a generalized additive model to the wind, gust, and barometric pressure measurements publicly available from the Japan Meteorological Agency (<https://www.jma.go.jp/>). The smoother for the generalized additive model was

a tensor smooth of the three variables (i.e., wind speed, gust speed, and barometric pressure) with a normal distribution and an identity link-function. The Matsushima Bay observations referenced the wind and gust speed data from the Shiogama station and the barometric pressure from the Ishinomaki station, the Hirota Bay observations referenced the wind and gust speed data from the Kesen'numa station and the barometric pressure from the Ishinomaki station, the Bise Point observations referenced Nago station, and Arikawa Bay and Tainoura Bay observations referenced the Fukue station. No interpolation was needed for the Omura Bay observations. Interpolating light values resulted in poor estimates; however, the light data was only required to estimate day length, therefore the crepuscule function from the R package *maptools* was used to calculate day length for each study site (Bivand and Lewkin-Koh, 2021).

The relative wind exposure of each site was estimated by calculating the wind fetch with the *fetchR* package (Blake, 2020). A total of 108 vectors radiating out from each GPS coordinate (Table 1) were initially generated in a 2π radial pattern (see Supplement for details). The upper limit of the vectors was initialized to 10,000 m. Vectors that reached an obstruction (i.e., shoreline) was truncated and the mean values of these vectors were determined. Vectors that were not truncated (i.e., 10,000 m), were included and the numbers of untruncated vectors recorded. The mean wind fetch and number of untruncated vectors is a proxy for the physical conditions (e.g., wind and wave exposure) of the sites.

A generalized linear model (GLM) was used to analyze the effect of site (i.e., Hirota Bay, Matsushima Bay, Arikawa Bay, Tainoura Bay, Omura Bay, and Bise Point) on the daily NEP rates. A Student's t-distribution with an identity-link function was applied to the GLM. The variance for each site was modeled separately using a log-link function. The Student's t-distribution with 3 degrees-of-freedom, a location of 0, and a scale of 2.5 was the prior distribution that was applied to all parameters of the GLM. However, and a Gamma distribution with a shape of 2 and an inverse scale of 0.1 was applied to the degrees-of-freedom parameter for the GLM.

A GLM was also used to analyze the effect of site (i.e., Hirota Bay, Matsushima Bay, Arikawa Bay, Tainoura Bay, Omura Bay, and Bise Point) on the frequency of autotrophic days (i.e., positive rates of net ecosystem production). A Bernoulli distribution with a logit-link function was applied to this model and the prior distributions for the model parameters were similar to those applied in the GEP analysis. We did not include temperature or wind fetch as predictors in either of the GLMs, since they would be confounded with site.

All analyses were done with R version 4.1.2 (R Core Team, 2021) and days with missing values or erroneous measurements were excluded from the analysis. We used the *brms* package (Bürkner, 2017; Bürkner, 2018) to fit the model and ran four Markov chains for at least 4000 iterations each. The posterior distribution and convergence of the Markov chains were assessed visually. We report the mean and standard deviation of the observed rates of GEP, NEP, and ER. These values are unconditional with respect to the model and hence are not

restricted to distributional assumptions. As the data was not normally distributed, our discussion focuses on the conditional means estimated by the GLM, which are conditional on the model and data, and minimize the influence of the outliers. The value of the unconditional and conditional mean may differ in sign and magnitude (especially for values near zero) and likely indicates the effect of the scaled t-distribution of the model on the conditional mean.

RESULTS

The mean temperature observed during the study period across the sites ranged from 8.3 to 21.8°C (**Table 1**) and was lowest at the northern sites; however, the mean temperatures do not reflect yearly means for the seaweed aquaculture farms, since they were only collected during production season of *Undaria pinnatifida* and *Cladosiphon okamuranus*. From the 1726 daily observations, 169 observations were excluded from the analyses if the calculated values of GEP was less than zero or ER was greater than zero. An examination of the daily NEP rates indicated a symmetrical distribution with long tails, hence the use of a scaled t-distribution to model the error term in the GLM. However, the observations for all sites, except for Hirota Bay, (**Figure 2**) had a light negative skew (i.e., long tails to the left) when compared to the results of the model.

In general, the mean daily NEP rates of the observations were negative in all seaweed farms, the natural ecosystem of Omura Bay, and the degraded site of Tainoura Bay (**Table 2**). The NEP rates were most positive at Arikawa Bay and most negative at the

C. okamuranus farm at Bise Point. The mean daily GEP rates of the observations were highest at Bise Point, whereas it was the lowest at the *U. pinnatifida* farm at Hirota Bay. Natural ecosystems and the *U. pinnatifida* farm at Matsushima Bay had intermediate values of GEP and ER and followed similar patterns. ER rates reflected the GEP observations.

The GLMs clearly indicated that NEP and the frequency of autotrophic days differed among sites.

Unlike the mean values of the observations, the conditional means of the NEP from the GLM analysis followed a slightly different pattern. Applying a scaled t-distribution generally made little to no differences between the unconditional mean of the observation and the conditional means of the GLM. However, the long tails in the observations for Matsushima Bay and Omura Bay lead to slightly negative unconditional means (**Table 2**), whereas controlling for extreme values led to positive conditional means (**Table 3**).

These effects are observed because a scaled t-distribution dampens the effect of relatively extreme observations. The GLM results of the NEP observations indicated that the *C. okamuranus* farm at Bise Point had the least positive conditional mean value while the natural *Sargassum* spp. ecosystem at Omura Bay had the most positive conditional mean value (**Figure 2**). Leave-one-out cross validation indicated that the difference in the expected log pointwise predictive density (elpd) between the NEP GLM and a null model (i.e., no explanatory variables) was 143.2 ± 19.9 (mean \pm one standard error), supporting the NEP GLM over the null model (Vehtari et al., 2017). The GLM of the frequency of autotrophy indicated that the *C. okamuranus* farm at Bise Point was most often heterotrophic (26%); the *U. pinnatifida* farm at

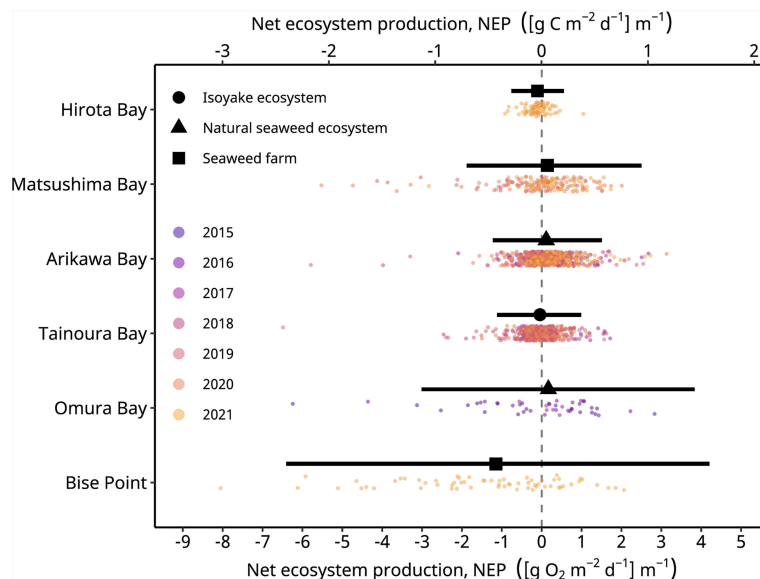


FIGURE 2 | The observed (colored points) and conditional mean of the net ecosystem production (black symbols) rates of the study sites. The black horizontal lines indicate the 95% highest density credible interval of the predicted values. Hirota Bay and Matsushima Bay are the *Undaria pinnatifida* aquaculture farms, Bise Point is the *Cladosiphon okamuranus* aquaculture farm, Arikawa Bay and Omura Bay are sites of the natural *Sargassum* spp. ecosystem, and Tainoura Bay is a site where a seaweed ecosystem has degraded into an isoyake state. The net ecosystem production in O₂ and C are calculated assuming a 1 to 1 molar ratio.

TABLE 2 | The mean and one standard deviation (SD) of the observed rates of gross ecosystem production (GEP), net ecosystem production (NEP), and the ecosystem respiration (ER) determined from three seaweed aquaculture farms (*Undaria pinnatifida* and *Cladosiphon okamuranus*) and three natural ecosystems in Japan.

Site	Species or State	GEP		NEP		ER	
		Mean	SD	Mean	SD	Mean	SD
Hirota Bay, Iwate	<i>Undaria pinnatifida</i>	0.39	0.39	-0.11	0.30	0.50	0.45
Matsushima Bay, Miyagi	<i>Undaria pinnatifida</i>	1.94	1.27	-0.05	1.12	1.98	1.70
Arikawa Bay, Nagasaki	<i>Sargassum</i> spp.	1.43	0.92	0.15	0.70	1.28	0.84
Tainoura Bay, Nagasaki	isoyake	0.77	0.54	-0.06	0.61	0.83	0.57
Omura Bay, Nagasaki	<i>Sargassum</i> spp.	3.73	1.91	-0.15	1.62	3.87	2.57
Bise Point, Okinawa	<i>Cladosiphon okamuranus</i>	3.87	3.01	-1.41	2.07	5.28	3.11

Rows are ordered from the north to south. Units of GEP, NEP, and ER are in $[g\ O_2\ m^{-2}\ day^{-1}]\ m^{-1}$.

TABLE 3 | The mean and 95% highest density credible interval for the expectations of the generalized linear model (GLM) of the net ecosystem production (NEP) and the autotrophic frequency.

Site	State	NEP GLM			Autotrophic frequency GLM		
		Mean	Lower	Upper	Mean	Lower	Upper
Hirota Bay, Iwate	<i>Undaria pinnatifida</i>	-0.11	-0.16	-0.06	0.34	0.24	0.44
Matsushima Bay, Miyagi	<i>Undaria pinnatifida</i>	0.11	-0.01	0.22	0.56	0.49	0.63
Arikawa Bay, Nagasaki	<i>Sargassum</i> spp.	0.11	0.07	0.15	0.59	0.55	0.63
Tainoura Bay, Nagasaki	isoyake	-0.05	-0.09	-0.02	0.42	0.37	0.46
Omura Bay, Nagasaki	<i>Sargassum</i> spp.	0.16	-0.20	0.54	0.59	0.46	0.73
Bise Point, Okinawa	<i>Cladosiphon okamuranus</i>	-1.10	-1.59	-0.65	0.26	0.16	0.37

Rows are ordered from north to south. Units of NEP are in $[g\ O_2\ m^{-2}\ day^{-1}]\ m^{-1}$.

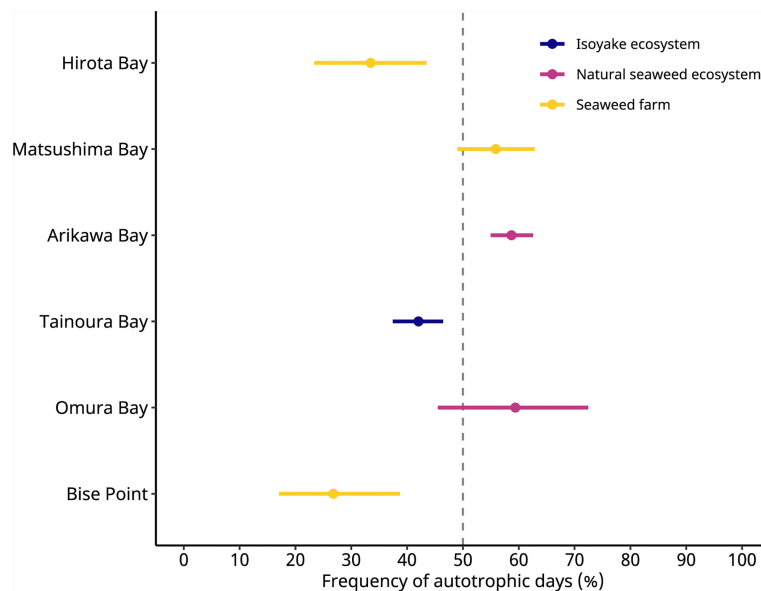


FIGURE 3 | The frequency of autotrophic days predicted by a generalized linear model. The colored points indicate the predicted values, and the colored lines indicate the 95% highest density credible interval. Hirota Bay and Matsushima Bay are the *Undaria pinnatifida* aquaculture farms, Bise Point is the *Cladosiphon okamuranus* aquaculture farm, Arikawa Bay and Omura Bay are sites of the natural *Sargassum* spp. ecosystem, and Tainoura Bay is a site where a seaweed ecosystem has degraded into an isoyake state.

Hirota Bay was the second most heterotrophic site (34%; **Figure 3** and **Table 3**). In contrast, the two *Sargassum* sp. ecosystems at Arikawa Bay and Omura Bay, and the *U. pinnatifida* farm at Matsushima Bay were most often autotrophic (> 50%). The GLM

of the autotrophic frequency had an elpd of 24.1 ± 7.6 , indicating support over the null model.

The total yield for each of the farms are known, and was 120, 40, and 6.8 tons for the *U. pinnatifida* farms in Hirota Bay,

Matsushima Bay, and the *C. okamuranus* farm at Bise Point, respectively (Table 4). The intensity of the carbon yield was calculated after determining the % carbon content of the cultivated seaweeds and ranged from 3.7 to 14.1 g C m⁻² (Table 4).

DISCUSSION

An ultimate goal would be to estimate the carbon sequestration rate of seaweed farms; however, without information regarding the export and import of carbon from allochthonous sources (see Gallagher et al., 2022), as well as the knowing the fate of cultivated seaweed, we can only estimate the carbon sequestration potential of our study sites. Nevertheless, we provide field estimates of the carbon sequestration potential of seaweed farm sites in Japan and also provide estimates of natural ecosystems and a degraded ecosystem for context. We expected NEP to be more positive in seaweed farms compared to the natural and degraded ecosystems, since natural ecosystems are expected to be primarily heterotrophic (Gallagher et al., 2022) and degraded ecosystem are deficient in primary producers, but our results were mixed and given the limitations of the data the model results provided should not be interpreted strictly as one system functioning more efficiently than the other. Nevertheless, the key finding of this study was that the field data clearly shows how seaweed aquaculture may not necessarily lead to carbon capture, and the potential to capture carbon may depend on taxa. For example, the conditional means of NEP for the *U. pinnatifida* farm at Matsushima Bay was 0.041 [g C m⁻² d⁻¹] m⁻¹ (Figure 2, Table 3). Among the seaweed farms, this site had the second highest rate of GEP (Table 2) and was autotrophic 56% of the time (Figure 3 and Table 3). In contrast, the *C. okamuranus* aquaculture farm at Bise Point had the highest rate of GEP among the aquaculture farms, however the NEP was most negative (Figure 1 and Tables 2, 3), and the aquaculture farm was only autotrophic 26% of the time (Figure 2 and Table 3).

Within taxa, the two *U. pinnatifida* seaweed farms clearly differed in NEP, where the conditional mean difference NEP between the Hirota Bay (-0.041 [g C m⁻² d⁻¹] m⁻¹) and Matsushima Bay (+0.041 [g C m⁻² d⁻¹] m⁻¹) differed by aquaculture farms was -0.083 (-0.13 to -0.038) [g C m⁻² d⁻¹] m⁻¹ (95% highest density credible interval). However, the intensity of carbon yield at Hirota Bay was 3.8 times greater than at Matsushima Bay (Table 4). We speculate that greater carbon yield intensities

occurring at the Hirota Bay farm stimulated the release of dissolved organic carbon and/or particulate organic carbon by *U. pinnatifida* (Wada et al., 2008; Chen et al., 2020). Although some of this material is exported out of the ecosystem (Krause-Jensen and Duarte, 2016), the release of this material can result in locally increased rates of ecosystem metabolism, through incorporation into the food-web (Sosik and Simenstad, 2013; Renaud et al., 2015; Paine et al., 2021). Additionally, it is unlikely that the *U. pinnatifida* produced at the aquaculture farms influenced the results, since both farms used the same cultivar provided by the authors (Sato et al., 2021a). Although the carbon yield intensity was also higher at Hirota Bay, compared to Matsushima Bay, evidence suggests that these differences were due to natural variation (Gao et al., 2014).

The GLM also indicated the *C. okamuranus* farm at Bise Point was heterotrophic (Table 3). In contrast to *U. pinnatifida*, which are cultivated on ropes, *C. okamuranus* are cultivated on nets (Sato et al., 2021b). However, the final yield intensity (i.e., 28 g m⁻²), was within the range of observed for *U. pinnatifida* at Hirota and Matsushima Bay (i.e., 52 g m⁻² and 15 g m⁻², respectively). Therefore, it is possible that stocking density may also influence the NEP of *C. okamuranus* farms, however since we could only examine one *C. okamuranus* farm site, the details remain to be revealed. Given that the *C. okamuranus* farm is deployed in the lagoon of a coral reef, characteristics of the ecosystem, such as the presence of corals and seagrasses nearby, may have led to a low NEP. Coral reef ecosystems were shown to be primarily heterotrophic in a number of studies (Falter et al., 2008; Miller et al., 2009; McGillis et al., 2011).

The potential for seaweed aquaculture farms to capture carbon from the environment and contribute to the mitigation of climate change was noted in a number of studies (Chung et al., 2017). It was suggested that seaweed aquaculture could potentially remove 1 g C m⁻² d⁻¹ from the environment based on aquaculture yields (Duarte et al., 2017; Froehlich et al., 2019), which is 1 to 2 orders of magnitude higher than our yield estimates (Table 4). A pioneering study on carbon flux in seaweed farms off the coast of the town Lido, China, also suggested that seaweed farms could absorb 1.2 g C m⁻² d⁻¹ (Jiang et al., 2013). Based on the conditional mean of NEP from the GLM analysis, the potential carbon capture rate was -0.041, +0.041, -0.41 [g C m⁻² d⁻¹] m⁻¹, for Hirota Bay, Matsushima Bay, and Bise Point, respectively.

There is an important caveat to these estimates of the seaweed farms examined in our study. Recall that measurements are limited to the production season of the seaweed farms (i.e., October to April), and do not provide a range of rates that would

TABLE 4 | The total yield and estimated amount of carbon captured by the seaweed farms at Hirota Bay, Matsushima Bay, and Bise Point during their respective cultivation season.

Site	Species	Yield (ton dry)	Farm area (m ²)	% Carbon content	Carbon yield intensity (g C m ⁻²)	Production duration (days)	Carbon capture rate (g C m ⁻² d ⁻¹)
Hirota Bay	<i>Undaria pinnatifida</i>	120	2,292,480	27.0	14.1	129	0.110
Matsushima Bay	<i>Undaria pinnatifida</i>	40	2,721,800	25.2	3.7	145	0.026
Bise Point	<i>Cladosiphon okamuranus</i>	6.8	246,581	13.3	3.7	105	0.035

occur over a year. Inclusion of the off-season (i.e., summer to autumn), would likely lead to a decrease in the frequency of autotrophic days, since respiration rates are higher during this period (Bordeyne et al., 2020). Macroalgae ecosystems are generally heterotrophic (Gallagher et al., 2022), and the GLM examining the frequency of autotrophic days also provides some support to these observations (**Figure 3**). Hence, we suggest that the NEP of seaweed farms are not exceptionally superior to natural ecosystems. Moreover, the limited production period of seaweed aquaculture must be considered when estimating their potential as a carbon mitigating system.

Since we measured oxygen production did not assess lateral flux of carbon, calcification rates, or the production of dissolved organic carbon our estimates of the potential to capture carbon should be considered carefully. Consider that at Bise Point, metabolic activity of nearby seagrasses may have influenced our oxygen observations. In seaweed ecosystems a significant portion of captured carbon is expected to be exported to adjacent ecosystems or as far as the deep ocean (Duarte and Cebrián, 1996; Krause-Jensen and Duarte, 2016; Ortega et al., 2019). Indeed, up to 50% of carbon captured by a *Sargassum horneri* ecosystem is believed to be exported out of the ecosystem (Watanabe et al., 2020). Additionally, many calcifying species produce calcium carbonate, with a net release of CO₂ into the environment during the calcification process, which can affect the net flux of CO₂, but not O₂ into the atmosphere (Frankignoulle et al., 1994).

In terms of blue carbon strategies, seaweed farms provides a large opportunity to mitigate climate change, given that it is easier and cheaper to scale-up, in contrast to the restoration of ecosystems, such as seagrass ecosystems (Gattuso et al., 2018; Lovelock and Duarte, 2019; Wu et al., 2020) and seaweed ecosystems (Eger et al., 2022). The net flux of carbon into seaweed farms was demonstrated in a number of studies (Tang et al., 2011; Jiang et al., 2013). However, to serve as a mitigation strategy, the carbon captured by seaweed aquaculture must be stored over long time scales. If all the seaweed produced by the farms could have been protected from conversion to CO₂, 43,384 kg of carbon would have been stored during the 2021 season (**Table 4**). Although we support past studies that suggests seaweed ecosystems can play a significant role in the mitigation of climate change and provide enough carbon capture capability to be included in carbon offset mechanisms, there remains a number of key questions that must be addressed before governments rush to develop seaweed farms to mitigate and offset carbon emissions. Uninformed expansion of seaweed farms can potentially cause a negative effect on surrounding and underlying ecosystems (Campbell et al., 2019). For example, in shallow water seaweed farms, the cultivation of carrageenophytes (e.g., *Kappaphycus* and *Eucheuma*) led to reductions in productivity and shoot density of the underlying seagrass ecosystems (Eklöf et al., 2005; Kelly et al., 2020; Moreira-Saporiti et al., 2021). Light reduction and the removal of nutrients by seaweed farms change the composition of phytoplankton (Jiang et al., 2020; Aldridge et al., 2021). Water flow and tidal exchange rates can decrease leading to increased

sedimentation rates and poor water exchange (Zeng et al., 2015). The expansion of seaweed farms can be associated with increased flux of plastic materials from discarded and lost equipment (e.g., synthetic polymer ropes) and plastic particles, exacerbating existing problems with marine plastic pollution (Derraik, 2002; Andrady, 2011; Krüger et al., 2020). An increase in the albedo of the sea surface may also occur, since seaweeds are better able to reflect short-wave radiation than the sea surface, enhancing local cooling of the environment (Bach et al., 2021). Steps towards a compromise between environmental disturbance and carbon capture *via* seaweed farms can be found in the proper site selection and monitoring of environmental conditions to optimize the timing of the grow-out period. For example, kelps cultured in exposed conditions exhibit the best growth performance with increased carbon content in their tissues (Peteiro and Freire, 2013; Visch et al., 2020). On the other hand, culturing seaweeds in nutrient limited waters leads to nutrient stress and a subsequent loss in seaweed biomass and a net increase in dissolved organic matter in the culture area (Yoshikawa et al., 2001; Paine et al., 2021). For temperate species, timing the grow-out and harvest phase is critical as warmer surface temperatures promote the growth of fouling organisms (Visch et al., 2020).

Reliable long-term field observations of carbon capture rates by macroalgae ecosystems remains scarce. Presently, most assessments of carbon capture rates rely on extrapolating from chambered photosynthesis experiments of using phytoelements or the whole thallus of macroalgae, measuring the CO₂ flux at the air-sea interface and the O₂ flux at the water-sediment interface using eddy covariance techniques (e.g., Berg et al., 2022), extrapolate from simulations and limited in temporal scope (e.g., Watanabe et al., 2020), extrapolate from O₂ mass-balances (e.g., Champenois and Borges, 2012; Hinode et al., 2020), measuring the O₂ flux at the water-sediment, and isotopic measurements (e.g., Holtgrieve et al., 2010; Staehr et al., 2012; Hoellein et al., 2013). All methods have both advantages and disadvantages, that must be considered prior to data interpretation. The method we used was comparatively inexpensive and can provide a long and continuous time-series of measurements, but introduces bias due to the assumptions used to estimate air-water flux of oxygen, the horizontal and vertical heterogeneity of dissolved oxygen concentrations and flux (Berg et al., 2022), and the assumption that night-time respiration adequately describes respiration rates during the day. However, all methods suffer from the inability to assess the carbon flux into and out of the system of interest and are unable to precisely assess whether or not the system is a carbon donor or carbon receiver (Hill et al., 2015). Methods to correct for advection and include more ecosystem level processes could enhance the accuracy of carbon flux estimates (Chung et al., 2013; Gruber et al., 2017; Gallagher et al., 2022). More critically, macroalgae can secrete organic carbon and about 18 to 62% of their productivity may be secreted as dissolved carbon, which can be respired by microbes (Wada et al., 2007; Wada et al., 2008; Paine et al., 2021).

The potential of seaweed farms to mitigate climate change remains to be determined. The effectiveness of aquaculture farms

to capture and remove carbon for relevant time-scales remains a challenge. Despite this, seaweed farms are still highly valuable for their contribution to the livelihood of coastal communities and have lesser detrimental impacts to the environment compared to other forms of aquaculture (Walls et al., 2017; Visch et al., 2020). We believe that the potential to capture carbon will not be homogenous across species and location, and that more studies to address carbon flux at organismal and ecosystem scales remain to be conducted. Despite these uncertainties, land-based aquaculture of seaweeds and the development of technology to lengthen the production season and yield should provide seaweed aquaculture with a unique opportunity to contribute to the mitigation of climate change (e.g., Sato et al., 2021a). However, the fate of the produced seaweeds will define the effectiveness of these strategies. Finally, detailed measurements of carbon capture from the aquaculture farms of carrageenophytes, chlorophytes such as *Ulva* spp. and *Monostroma* spp., some species of *Pyropia* spp., *Saccharina* spp., and *Sargassum* spp., are worthy of future investigation.

DATA AVAILABILITY STATEMENT

The raw data supporting the conclusions of this article will be made available by the authors, without undue reservation.

AUTHOR CONTRIBUTIONS

YS, GN, AT, RT, and HE conceptualized and supervised the research, YS, GN, AT, and RT acquired funding support, YS, GN,

and DB prepared the original draft of the manuscript, YS, GN, AT, RT, HE, and DB reviewed and edited the manuscript. YS, GN, AT, DB, AK, YI, KH, ST, YM, and KT conducted the research and collected data, YS, GN, DB, AK, YI, KH, ST, YM, and KT analyzed the model and prepared figures for the manuscript. GN administered the project. All authors contributed to the article and approved the submitted version.

FUNDING

This work was supported by JSPS KAKENHI Grant Number 20H03076, 16H02939, and 25450260.

ACKNOWLEDGMENTS

The authors would like to thank the Omura Bay Fisheries Cooperative and Arikawa Bay Fisheries Cooperative of Nagasaki, Shiogama City Fisheries Cooperative of Miyagi, Hirota Bay Fisheries Cooperative of Iwate, and the Motobu Fisheries Cooperative of Okinawa for their insights and cooperation which allowed us to conduct the field surveys in their seaweed aquaculture farms.

SUPPLEMENTARY MATERIAL

The Supplementary Material for this article can be found online at: <https://www.frontiersin.org/articles/10.3389/fmars.2022.861932/full#supplementary-material>

REFERENCES

- Aldridge, J. N., Mooney, K., Dabrowski, T., and Capuzzo, E. (2021). Modelling Effects of Seaweed Aquaculture on Phytoplankton and Mussel Production. Application to Strangford Lough (Northern Ireland). *Aquaculture* 536, 736400. doi: 10.1016/j.aquaculture.2021.736400
- Andrady, A. L. (2011). Microplastics in the Marine Environment. *Mar. Poll. Bull.* 62, 1596–1605. doi: 10.1016/j.marpolbul.2011.05.030
- Bach, L. T., Tamsitt, V., Gower, J., Hurd, C. L., Raven, J. A., and Boyd, P. W. (2021). Testing the Climate Intervention Potential of Ocean Afforestation Using the Great Atlantic *Sargassum* Belt. *Nat. Commun.* 12, 2556. doi: 10.1038/s41467-021-22837-2
- Berg, P., Delgard, M. L., Polsenaere, P., McGlathery, K. J., Doney, S. C., and Berger, A. C. (2019). Dynamics of Benthic Metabolism, O₂, and Pco₂ in a Temperate Seagrass Meadow. *Limnol. Oceanogr.* 64, 2586–2604. doi: 10.1002/lno.11236
- Berg, P., Huettel, M., Glud, R. N., Reimers, C. E., and Attard, K. M. (2022). Aquatic Eddy Covariance: The Method and Its Contributions to Defining Oxygen and Carbon Fluxes in Marine Environments. *Annu. Rev. Mar. Sci.* 14, 431–455. doi: 10.1146/annurev-marine-042121-012329
- Bivand, R., and Lewkin-Koh, N. (2021) *Maptools: Tools for Handling Spatial Objects. R Package Version 1.1-2*. Available at: <https://cran.r-project.org/package=maptools>.
- Blake, S. (2020) *Fetchr: Calculate Wind Fetch. R Package Version 2.1-2*. Available at: <https://cran.r-project.org/package=fetchr>.
- Bordeyne, F., Migné, A., Plus, M., and Davoult, D. (2020). Modelling the Annual Primary Production of an Intertidal Brown Algal Community Based on *in Situ* Measurements. *Mar. Ecol. Prog. Ser.* 656, 95–107. doi: 10.3354/meps13450
- Boysen, L. R., Lucht, W., and Gerten, D. (2017). Trade-Offs for Food Production, Nature Conservation and Climate Limit the Terrestrial Carbon Dioxide Removal Potential. *Global Change Biol.* 23, 4303–4317. doi: 10.1111/gcb.13745
- Bürkner, P.-C. (2017). Brms : An R Package for Bayesian Multilevel Models Using Stan. *J. Stat. Softw.* 80, 1–28. doi: 10.18637/jss.v080.i01
- Bürkner, P. C. (2018). Advanced Bayesian Multilevel Modeling With the R Package Brms. *R. J.* 10, 395–411. doi: 10.32614/rj-2018-017
- Campbell, I., Macleod, A., Sahlmann, C., Neves, L., Funderud, J., Øverland, M., et al. (2019). The Environmental Risks Associated With the Development of Seaweed Farming in Europe - Prioritizing Key Knowledge Gaps. *Front. Mar. Sci.* 6. doi: 10.3389/fmars.2019.00107
- Champanois, W., and Borges, A. (2012). Seasonal and Interannual Variations of Community Metabolism Rates of a *Posidonia Oceanica* Seagrass Meadow. *Limnol. Oceanogr.* 57, 347–361. doi: 10.4319/lo.2012.57.1.0347
- Chen, S., Xu, K., Ji, D., Wang, W., Xu, Y., Chen, C., et al. (2020). Release of Dissolved and Particulate Organic Matter by Marine Macroalgae and its Biogeochemical Implications. *Algal. Res.* 52, 102096. doi: 10.1016/j.algal.2020.102096
- Chung, I. K., Beardall, J., Mehta, S., Sahoo, D., and Stojkovic, S. (2011). Using Marine Macroalgae for Carbon Sequestration: A Critical Appraisal. *J. Appl. Phycol.* 23, 877–886. doi: 10.1007/s10811-010-9604-9
- Chung, I. K., Oak, J. H., Lee, J. A., Shin, J. A., Kim, J. G., and Park, K.-S. (2013). Installing Kelp Forests/Seaweed Beds for Mitigation and Adaptation Against Global Warming: Korean Project Overview. *ICES. J. Mar. Sci.* 70, 1038–1044. doi: 10.1093/icesjms/fss206
- Chung, I. K., Sondak, C. F. A., and Beardall, J. (2017). The Future of Seaweed Aquaculture in a Rapidly Changing World. *Eur. J. Phycol.* 52, 495–505. doi: 10.1080/09670262.2017.1359678

- Derraik, J. G. B. (2002). The Pollution of the Marine Environment by Plastic Debris: A Review. *Mar. Poll. Bull.* 44, 842–852. doi: 10.1016/S0025-326X(02)00220-5
- Duarte, C. M. (2017). Reviews and Syntheses: Hidden Forests, the Role of Vegetated Coastal Habitats in the Ocean Carbon Budget. *Biogeosciences* 14, 301–310. doi: 10.5194/bg-14-301-2017
- Duarte, C. M., and Cebrián, J. (1996). The Fate of Marine Autotrophic Production. *Limnol. Oceanogr.* 41, 1758–1766. doi: 10.4319/lo.1996.41.8.1758
- Duarte, C. M., and Krause-Jensen, D. (2017). Export From Seagrass Meadows Contributes to Marine Carbon Sequestration. *Front. Mar. Sci.* 4. doi: 10.3389/fmars.2017.00013
- Duarte, C. M., Wu, J., Xiao, X., Bruhn, A., and Krause-Jensen, D. (2017). Can Seaweed Farming Play a Role in Climate Change Mitigation and Adaptation? *Front. Mar. Sci.* 4. doi: 10.3389/fmars.2017.00100
- Eger, A. M., Marzinelli, E. M., Christie, H., Fagerli, C. W., Fujita, D., Gonzales, A. P., et al. (2022). Global Kelp Forest Restoration: Past Lessons, Present Status, and Future Directions. *Biol. Rev.* doi: 10.1111/brv.12850
- Eklöf, J. S., de la Torre Castro, M., Adelsköld, L., Jiddawi, N. S., and Kautsky, N. (2005). Differences in Macrofaunal and Seagrass Assemblages in Seagrass Beds With and Without Seaweed Farms. *Estuar. Coast. Shelf. Sci.* 63, 385–396. doi: 10.1016/j.ecss.2004.11.014
- Falter, J. L., Lowe, R. J., Atkinson, M. J., and Monismith, S. G. (2008). Continuous Measurements of Net Production Over a Shallow Reef Community Using a Modified Eulerian Approach. *J. Geophys. Res.* 113, C07035. doi: 10.1029/2007JC004663
- Fillbee-Dexter, K., and Wernberg, T. (2020). Substantial Blue Carbon in Overlooked Australian Kelp Forests. *Sci. Rep.* 10, 1–6. doi: 10.1038/s41598-020-69258-7
- Frankignoulle, M., Canon, C., and Gattuso, J.-P. (1994). Marine Calcification as a Source of Carbon Dioxide: Positive Feedback of Increasing Atmospheric CO₂. *Limnol. Oceanogr.* 39, 458–462. doi: 10.4319/lo.1994.39.2.0458
- Froehlich, H. E., Afflerbach, J. C., Frazier, M., and Halpern, B. S. (2019). Blue Growth Potential to Mitigate Climate Change Through Seaweed Offsetting. *Curr. Biol.* 29, 3087–3093.e3. doi: 10.1016/j.cub.2019.07.041
- Frontier, N., de Bettignies, F., Foggo, A., and Davoult, D. (2021). Sustained Productivity and Respiration of Degrading Kelp Detritus in the Shallow Benthos: Detached or Broken, But Not Dead. *Mar. Environ. Res.* 166, 105277. doi: 10.1016/j.marenvres.2021.105277
- Fujita, D. (2010). Current Status and Problems of Isoyake in Japan. *Bull. Fish. Res. Agen.* 32, 33–42.
- Gallagher, J. B., Shelamoff, V., and Layton, C. (2021). Missing the Forest for the Trees: A Reappraisal of Global Seaweed Carbon Sequestration. *bioRxiv*. doi: 10.1101/2021.09.05.459038
- Gallagher, J. B., Shelamoff, V., and Layton, C. (2022). Seaweed Ecosystems may Not Mitigate CO₂ Emissions. *ICES. J. Mar. Sci.* 79, 585–592. doi: 10.1093/icesjms/fsac011
- Gao, X., Endo, H., Taniguchi, K., and Agatsuma, Y. (2014). Effects of Experimental Thinning on the Growth and Maturation of the Brown Alga *Undaria Pinnatifida* (Laminariales; Phaeophyta) Cultivated in Matsushima Bay, Northern Japan. *J. Appl. Phycol.* 26, 529–535. doi: 10.1007/s10811-013-0071-y
- Gattuso, J. P., Magnan, A. K., Bopp, L., Cheung, W. W. L., Duarte, C. M., Hinkel, J., et al. (2018). Ocean Solutions to Address Climate Change and its Effects on Marine Ecosystems. *Front. Mar. Sci.* 5. doi: 10.3389/fmars.2018.00337
- Gauthier, P. P. G., Battle, M. O., Griffin, K. L., and Bender, M. L. (2018). Measurement of Gross Photosynthesis, Respiration in the Light, and Mesophyll Conductance Using 2H₂ 18O Labeling. *Plant Physiol.* 177, 62–74. doi: 10.1104/pp.16.00741
- Gouvêa, L. P., Assis, J., Gurgel, C. F. D., Serrão, E. A., Silveira, T. C. L., Santos, R., et al. (2020). Golden Carbon of Sargassum Forests Revealed as an Opportunity for Climate Change Mitigation. *Sci. Tot. Environ.* 729, 138745. doi: 10.1016/j.scitotenv.2020.138745
- Gruber, R. K., Lowe, R. J., and Falter, J. L. (2017). Metabolism of a Tide-Dominated Reef Platform Subject to Extreme Diel Temperature and Oxygen Variations. *Limnol. Oceanogr.* 62, 1701–1717. doi: 10.1002/lno.10527
- Hanson, P. C., Carpenter, S. R., Kimura, N., Wu, C., Cornelius, S. P., and Kratz, T. K. (2008). Evaluation of Metabolism Models for Free-Water Dissolved Oxygen Methods in Lakes. *Limnol. Oceanogr.: Methods* 6, 454–465. doi: 10.4319/lom.2008.6.454
- Higuchi, T., Takagi, K. K., Matoba, K., Kobayashi, S., Tsurumi, R., Arakaki, S., et al. (2014). The Nutrient and Carbon Dynamics That Mutually Benefit Coral and Seagrass in Mixed Habitats Under the Influence of Groundwater at Bise Coral Reef, Okinawa, Japan. *Int. J. Mar. Sci.* 4, 1–15. doi: 10.5376/ijms.2014.04.0001
- Hill, R., Bellgrove, A., Macreadie, P. I., Petrou, K., Beardall, J., Steven, A., et al. (2015). Can Macroalgae Contribute to Blue Carbon? An Australian Perspective. *Limnol. Oceanogr.* 60, 1689–1706. doi: 10.1002/lno.10128
- Hinode, K., Punchai, P., Saito, M., Nishihara, G. N., Inoue, Y., and Terada, R. (2020). The Phenology of Gross Ecosystem Production in a Macroalga and Seagrass Canopy is Driven by Seasonal Temperature. *Phycol. Res.* 68, 298–312. doi: 10.1111/pre.12433
- Hoellein, T. J., Bruesewitz, D. A., and Richardson, D. C. (2013). Revisiting Odu: A Synthesis of Aquatic Ecosystem Metabolism. *Limnol. Oceanogr.* 58, 2089–2100. doi: 10.4319/lo.2013.58.6.2089
- Holtgrieve, G. W., Schindler, D. E., Branch, T. A., and Teresa A'Mar, Z. (2010). Simultaneous Quantification of Aquatic Ecosystem Metabolism and Reaeration Using a Bayesian Statistical Model of Oxygen Dynamics. *Limnol. Oceanogr.* 55, 1047–1063. doi: 10.4319/lo.2010.55.3.1047
- Howard, J., Sutton-Grier, A., Herr, D., Kleypas, J., Landis, E., Mcleod, E., et al. (2017). Clarifying the Role of Coastal and Marine Systems in Climate Mitigation. *Front. Ecol. Environ.* 15, 42–50. doi: 10.1002/fee.1451
- Ichikawa, T., Sakai, T., Morozumi, K., and Suzuki, T. (2009). A Numerical Simulation of T-S Structure and Velocity Fields in Hirota Bay. *J. Advanced Mar. Sci. Technol. Soc.* 15, 125–135. doi: 10.14928/amstec.15.2.125
- Jiang, Z., Fang, J., Mao, Y., Han, T., and Wang, G. (2013). Influence of Seaweed Aquaculture on Marine Inorganic Carbon Dynamics and Sea-Air CO₂ Flux. *J. World Aquacult. Soc.* 44, 133–140. doi: 10.1111/jwas.12000
- Jiang, Z., Liu, J., Li, S., Chen, Y., Du, P., Zhu, Y., et al. (2020). Kelp Cultivation Effectively Improves Water Quality and Regulates Phytoplankton Community in a Turbid, Highly Eutrophic Bay. *Sci. Tot. Environ.* 707, 135561. doi: 10.1016/j.scitotenv.2019.135561
- Jianxi, H., Mizobata, K., and Kitade, Y. (2020). Effect of Wind on Seawater Exchange in Matsushima Bay. *La. Mer.* 58, 17–33. doi: 10.32211/lamer.58.1-2_17
- Kelly, E. L. A., Cannon, A. L., and Smith, J. E. (2020). Environmental Impacts and Implications of Tropical Carrageenophyte Seaweed Farming. *Conserv. Biol.* 34, 326–337. doi: 10.1111/cobi.13462
- Krause-Jensen, D., and Duarte, C. M. (2016). Substantial Role of Macroalgae in Marine Carbon Sequestration. *Nat. Geosci.* 9, 737–742. doi: 10.1038/ngeo2790
- Krause-Jensen, D., Lavery, P., Serrano, O., Marba, N., Masque, P., and Duarte, C. M. (2018). Sequestration of Macroalgal Carbon: The Elephant in the Blue Carbon Room. *Biol. Lett.* 14, 20180236. doi: 10.1098/rsbl.2018.0236
- Krüger, L., Casado-Coy, N., Valle, C., Ramos, M., Sánchez-Jerez, P., Gago, J., et al. (2020). Plastic Debris Accumulation in the Seabed Derived From Coastal Fish Farming. *Environ. Poll.* 257, 113336. doi: 10.1016/j.envpol.2019.113336
- Krumhansl, K. A., and Scheibling, R. E. (2012). Production and Fate of Kelp Detritus. *Mar. Ecol. Prog. Ser.* 467, 281–302. doi: 10.3354/meps09940
- Lovelock, C. E., and Duarte, C. M. (2019). Dimensions of Blue Carbon and Emerging Perspectives. *Biol. Lett.* 15, 1–5. doi: 10.1098/rsbl.2018.0781
- Macreadie, P. I., Serrano, O., Maher, D. T., Duarte, C. M., and Beardall, J. (2017). Addressing Calcium Carbonate Cycling in Blue Carbon Accounting. *Limnol. Oceanogr.* Lett. 2, 195–201. doi: 10.1002/lol2.10052
- McGillis, W. R., Langdon, C., Loose, B., Yates, K. K., and Corredor, J. (2011). Productivity of a Coral Reef Using Boundary Layer and Enclosure Methods. *Geophys. Res. Lett.* 38, L03611. doi: 10.1029/2010GL046179
- McLeod, E., Chmura, G. L., Bouillon, S., Salm, R., Björk, M., Duarte, C. M., et al. (2011). A Blueprint for Blue Carbon: Toward an Improved Understanding of the Role of Vegetated Coastal Habitats in Sequestering CO₂. *Front. Ecol. Environ.* 9, 552–560. doi: 10.1890/110004
- Miller, R. J., Reed, D. C., and Brzezinski, M. A. (2009). Community Structure and Productivity of Subtidal Turf and Foliose Algal Assemblages. *Mar. Ecol. Prog. Ser.* 388, 1–11. doi: 10.3354/meps08131
- Moreira-Saporiti, A., Hoeijmakers, D., Msuya, F. E., Reuter, H., and Teichberg, M. (2021). Seaweed Farming Pressure Affects Seagrass and Benthic Macroalgae Dynamics in Chwaka Bay (Zanzibar, Tanzania). *Reg. Environ. Change* 21, 1–12. doi: 10.1007/s10113-020-01742-2
- Muraoka, D. (2004). Seaweed Resources as a Source of Carbon Fixation. *Bull. Fish. Res. Agen. Suppl.* 1, 59–63.

- Nogami, M., and Matsuno, T. (2001). The Relationship Between Ocean Structure and Formation of the Second Thermocline in Ohmura Bay. *Oceanogr. Jap.* 10, 191–202. doi: 10.5928/kaiyou.10.191
- Ortega, A., Gerdali, N. R., Alam, I., Kamau, A. A., Acinas, S. G., Logares, R., et al. (2019). Important Contribution of Macroalgae to Oceanic Carbon Sequestration. *Nat. Geosci.* 12, 748–754. doi: 10.1038/s41561-019-0421-8
- Paine, E. R., Schmid, M., Boyd, P. W., Diaz-Pulido, G., and Hurd, C. L. (2021). Rate and Fate of Dissolved Organic Carbon Release by Seaweeds: A Missing Link in the Coastal Ocean Carbon Cycle. *J. Phycol.* 57, 1375–1391. doi: 10.1111/jpy.13198
- Pedersen, M. F., Filbee-Dexter, K., Norderhaug, K. M., Fredriksen, S., Frisk, N. L., Fagerli, C. W., et al. (2020). Detrital Carbon Production and Export in High Latitude Kelp Forests. *Oecologia* 192, 227–239. doi: 10.1007/s00442-019-04573-z
- Peteiro, C., and Freire, Ó. (2013). Biomass Yield and Morphological Features of the Seaweed *Saccharina Latissima* Cultivated at Two Different Sites in a Coastal Bay in the Atlantic Coast of Spain. *J. Appl. Phycol.* 25, 205–213. doi: 10.1007/s10811-012-9854-9
- R Core Team (2021) *R: A Language and Environment for Statistical Computing*. Available at: <https://www.r-project.org/>.
- Renaud, P. E., Løkken, T. S., Jørgensen, L. L., Berge, J., and Johnson, B. J. (2015). Macroalgal Detritus and Food-Web Subsidies Along an Arctic Fjord Depth-Gradient. *Front. Mar. Sci.* 2, doi: 10.3389/fmars.2015.00031
- Sato, Y., Hirano, T., Ichida, H., Fukunishi, N., Abe, T., and Kawano, S. (2021a). Extending the Cultivation Period of *Undaria Pinnatifida* by Using Regional Strains With Phenotypic Differentiation Along the Sanriku Coast in Northern Japan. *Phycology* 1, 129–142. doi: 10.3390/phycol.1020010
- Sato, Y., Nagoe, H., Ito, M., Konishi, T., Fujimura, H., Nishihara, G. N., et al. (2021b). Final Yield of the Brown Alga *Cladosiphon Okamurae* (Chordariaceae, Phaeophyta) may Depend on Nursery Quality. *Phycol. Res.* 69, 159–165. doi: 10.1111/pre.12453
- Siegel, D. A., Devries, T., Doney, S. C., and Bell, T. (2021). Assessing the Sequestration Time Scales of Some Ocean-Based Carbon Dioxide Reduction Strategies. *Environ. Res. Lett.* 16, 104003. doi: 10.1088/1748-9326/ac0be0
- Smale, D. A., Pessarrodona, A., King, N., and Moore, P. J. (2021). Examining the Production, Export, and Immediate Fate of Kelp Detritus on Open-Coast Subtidal Reefs in the Northeast Atlantic. *Limnol. Oceanogr.* doi: 10.1002/lno.11970
- Smith, S. V. (2013). Parsing the Oceanic Calcium Carbonate Cycle: A Net Atmospheric Carbon Dioxide Source or a Sink? *Le&O e-Books*. Association for the Sciences of Limnology and Oceanography (ASLO), Waco, TX. doi: 10.4319/svsmith.2013.978-0-9845591-2-1
- Sondak, C. F. A., Ang, P. O., Beardall, J., Bellgrove, A., Boo, S. M., Gerung, G. S., et al. (2017). Carbon Dioxide Mitigation Potential of Seaweed Aquaculture Beds (SABs). *J. Appl. Phycol.* 29, 2363–2373. doi: 10.1007/s10811-016-1022-1
- Sosik, E. A., and Simenstad, C. A. (2013). Isotopic Evidence and Consequences of the Role of Microbes in Macroalgae Detritus-Based Food Webs. *Mar. Ecol. Prog. Ser.* 494, 107–119. doi: 10.3354/meps10544
- Staehr, P. A., Bade, D., Van de Bogert, M. C., Koch, G. R., Williamson, C., Hanson, P., et al. (2010). Lake Metabolism and the Diel Oxygen Technique: State of the Science. *Limnol. Oceanogr.: Methods* 8, 628–644. doi: 10.4319/lom.2010.8.628
- Staehr, P. A., Testa, J. M., Kemp, W. M., Cole, J. J., Sand-Jensen, K., and Smith, S. V. (2012). The Metabolism of Aquatic Ecosystems: History, Applications, and Future Challenges. *Aquat. Sci.* 74, 15–29. doi: 10.1007/s00027-011-0199-2
- Tang, Q., Zhang, J., and Fang, J. (2011). Shellfish and Seaweed Mariculture Increase Atmospheric CO₂ Absorption by Coastal Ecosystems. *Mar. Ecol. Prog. Ser.* 424, 97–104. doi: 10.3354/meps08979
- Trevathan-Tackett, S. M., Kelleway, J., Macreadie, P. I., Beardall, J., Ralph, P., and Bellgrove, A. (2015). Comparison of Marine Macrophytes for Their Contributions to Blue Carbon Sequestration. *Ecology* 96, 3043–3057. doi: 10.1890/15-0149.1
- Tsuchiya, K., Ehama, M., Yasunaga, Y., Nakagawa, Y., Hirahara, M., Kishi, M., et al. (2018). Seasonal and Spatial Variation of Nutrients in the Coastal Waters of the Northern Goto Islands, Japan. *Bull. Coast. Oceanogr.* 55, 125–138. doi: 10.32142/engankaiyo.55.2_125
- Vehtari, A., Gelman, A., and Gabry, J. (2017). Practical Bayesian Model Evaluation Using Leave-One-Out Cross-Validation and WAIC. *Stat. Comput.* 27, 1413–1432. doi: 10.1007/s11222-016-9696-4
- Vergés, A., Steinberg, P. D., Hay, M. E., Poore, A. G. B., Campbell, A. H., Ballesteros, E., et al. (2014). The Tropicalization of Temperature Marine Ecosystems: Climate-Mediated Changes in Herbivory and Community Phase Shifts. *Proc. R. Soc. B.: Biol. Sci.* 281, 20140846. doi: 10.1098/rspb.2014.0846
- Visch, W., Nylund, G. M., and Pavia, H. (2020). Growth and Biofouling in Kelp Aquaculture (*Saccharina Latissima*): The Effect of Location and Wave Exposure. *J. Appl. Phycol.* 32, 3199–3209. doi: 10.1007/s10811-020-02201-5
- Wada, S., Aoki, M. N., Mikami, A., Komatsu, T., Tsuchiya, Y., Sato, T., et al. (2008). Bioavailability of Macroalgal Dissolved Organic Matter in Seawater. *Mar. Ecol. Prog. Ser.* 370, 33–44. doi: 10.3354/meps07645
- Wada, S., Aoki, M. N., Tsuchiya, Y., Sato, T., Shinagawa, H., and Hama, T. (2007). Quantitative and Qualitative Analyses of Dissolved Organic Matter Released From *Ecklonia Cava* Kjellman, in Oura Bay, Shimoda, Izu Peninsula, Japan. *J. Exp. Mar. Biol. Ecol.* 349, 344–358. doi: 10.1016/j.jembe.2007.05.024
- Walls, A. M., Kennedy, R., Edwards, M. D., and Johnson, M. P. (2017). Impact of Kelp Cultivation on the Ecological Status of Benthic Habitats and *Zostera Marina* Seagrass Biomass. *Mar. Poll. Bull.* 123, 19–27. doi: 10.1016/j.marpolbul.2017.07.048
- Wanninkhof, R. (1992). Relationship Between Wind Speed and Gas Exchange Over the Ocean. *J. Geophys. Res.* 97, 7373. doi: 10.1029/92JC00188
- Watanabe, K., Yoshida, G., Hori, M., Umezawa, Y., Moki, H., and Kuwae, T. (2020). Macroalgal Metabolism and Lateral Carbon Flows can Create Significant Carbon Sinks. *Biogeosciences* 17, 2425–2440. doi: 10.5194/bg-17-2425-2020
- Wood, S. N. (2011). Fast Stable Restricted Maximum Likelihood and Marginal Likelihood Estimation of Semiparametric Generalized Linear Models. *J. R. Stat. Soc. (B.)* 73, 3–36. doi: 10.1111/j.1467-9868.2010.00749.x
- Wu, J., Zhang, H., Pan, Y., Krause-Jensen, D., He, Z., Fan, W., et al. (2020). Opportunities for Blue Carbon Strategies in China. *Ocean. Coast. Manage.* 194, 105241. doi: 10.1016/j.ocecoaman.2020.105241
- Xiao, X., Agustí, S., Yu, Y., Huang, Y., Chen, W., Hu, J., et al. (2021). Seaweed Farms Provide Refugia From Ocean Acidification. *Sci. Tot. Environ.* 776, 145192. doi: 10.1016/j.scitotenv.2021.145192
- Yoshikawa, T., Takeuchi, I., and Furuya, K. (2001). Active Erosion of *Undaria Pinnatifida* Suringar (Laminariales, Phaeophyceae) Mass-Cultured in Otsuchi Bay in Northeastern Japan. *J. Exp. Mar. Biol. Ecol.* 266, 51–65. doi: 10.1016/S0022-0981(01)00346-X
- Zeng, D., Huang, D., Qiao, X., He, Y., and Zhang, T. (2015). Effect of Suspended Kelp Culture on Water Exchange as Estimated by *in Situ* Current Measurement in Sanggou Bay, China. *J. Mar. Syst.* 149, 14–24. doi: 10.1016/j.jmarsys.2015.04.002

Conflict of Interest: Author YS is employed by Riken Food Co., Ltd.

The remaining authors declare that the research was conducted in absence of any commercial or financial relationships that could be construed as a potential conflict of interest.

Publisher's Note: All claims expressed in this article are solely those of the authors and do not necessarily represent those of their affiliated organizations, or those of the publisher, the editors and the reviewers. Any product that may be evaluated in this article, or claim that may be made by its manufacturer, is not guaranteed or endorsed by the publisher.

Copyright © 2022 Sato, Nishihara, Tanaka, Belleza, Kawate, Inoue, Hinode, Matsuda, Tanimae, Tozaki, Terada and Endo. This is an open-access article distributed under the terms of the Creative Commons Attribution License (CC BY). The use, distribution or reproduction in other forums is permitted, provided the original author(s) and the copyright owner(s) are credited and that the original publication in this journal is cited, in accordance with accepted academic practice. No use, distribution or reproduction is permitted which does not comply with these terms.



Nordic Blue Carbon Ecosystems: Status and Outlook

Dorte Krause-Jensen^{1,2*}, Hege Gundersen³, Mats Björk⁴, Martin Gullström⁵, Martin Dahl⁵, Maria E. Asplund⁶, Christoffer Boström⁷, Marianne Holmer⁸, Gary T. Banta⁸, Anna Elizabeth Løvgren Graversen¹, Morten Foldager Pedersen⁹, Trine Bekkby³, Helene Frigstad³, Solrun Figenschau Skjellum³, Jonas Thormar¹⁰, Steen Gyldenkaerne^{1,11}, Jennifer Howard¹², Emily Pidgeon¹², Sunna Björk Ragnarsdóttir¹³, Agnes Mols-Mortensen^{14,15} and Kasper Hancke³

OPEN ACCESS

Edited by:

William Richard Turrell,
Marine Scotland, United Kingdom

Reviewed by:

Mat Vanderklift,
Commonwealth Scientific and
Industrial Research Organisation
(CSIRO), Australia
Alejandro H. Buschmann,
University of Los Lagos, Chile
W. Judson Kenworthy,
Independent researcher, Beaufort,
NC, United States

*Correspondence:

Dorte Krause-Jensen
dkj@ecos.au.dk

Specialty section:

This article was submitted to
Marine Ecosystem Ecology,
a section of the journal
Frontiers in Marine Science

Received: 02 January 2022

Accepted: 20 April 2022

Published: 31 May 2022

Citation:

Krause-Jensen D, Gundersen H, Björk M, Gullström M, Dahl M, Asplund ME, Boström C, Holmer M, Banta GT, Graversen AEL, Pedersen MF, Bekkby T, Frigstad H, Skjellum SF, Thormar J, Gyldenkaerne S, Howard J, Pidgeon E, Ragnarsdóttir SB, Mols-Mortensen A and Hancke K (2022) Nordic Blue Carbon Ecosystems: Status and Outlook. *Front. Mar. Sci.* 9:847544. doi: 10.3389/fmars.2022.847544

¹ Department of Ecoscience, Aarhus University, Silkeborg, Denmark, ² Arctic Research Centre, Aarhus University, Århus, Denmark, ³ Norwegian Institute for Water Research (NIVA), Oslo, Norway, ⁴ Department of Ecology, Environment and Plant Sciences, Stockholm University, Stockholm, Sweden, ⁵ School of Natural Sciences, Technology and Environmental Studies, Södertörn University, Huddinge, Sweden, ⁶ Department of Biological and Environmental Sciences, University of Gothenburg, Fiskebäckskil, Sweden, ⁷ Environmental and Marine Biology, Åbo Akademi University, Åbo, Finland, ⁸ Department of Biology, University of Southern Denmark, Odense M, Denmark, ⁹ Department of Science and Environment, Roskilde University, Roskilde, Denmark, ¹⁰ Flødevigen Research Station, Institute of Marine Research, His, Norway, ¹¹ Department of Environmental Science - Atmospheric Emissions, Aarhus University, Roskilde, Denmark, ¹² Conservation International, Arlington, VA, United States, ¹³ Icelandic Institute of Natural History, Borgum við Norðurslóð, Akureyri, Iceland, ¹⁴ TARI - Faroe Seaweed, Tórshavn, Faroe Islands, ¹⁵ Fiskaaling, Hvalvík, Faroe Islands

Vegetated coastal and marine habitats in the Nordic region include salt marshes, eelgrass meadows and, in particular, brown macroalgae (kelp forests and rockweed beds). Such habitats contribute to storage of organic carbon (Blue Carbon – BC) and support coastal protection, biodiversity and water quality. Protection and restoration of these habitats therefore have the potential to deliver climate change mitigation and co-benefits. Here we present the existing knowledge on Nordic BC habitats in terms of habitat area, C-stocks and sequestration rates, co-benefits, policies and management status to inspire a coherent Nordic BC roadmap. The area extent of BC habitats in the region is incompletely assessed, but available information sums up to 1,440 km² salt marshes, 1,861 (potentially 2,735) km² seagrass meadows, and 16,532 km² (potentially 130,735 km², including coarse Greenland estimates) brown macroalgae, yielding a total of 19,833 (potentially 134,910) km². Saltmarshes and seagrass meadows have experienced major declines over the past century, while macroalgal trends are more diverse. Based on limited salt marsh data, sediment C-stocks average 3,311 g C_{org} m⁻² (top 40–100 cm) and sequestration rates average 142 g C_{org} m⁻² yr⁻¹. Eelgrass C-stocks average 2,414 g C_{org} m⁻² (top 25 cm) and initial data for sequestration rates range 5–33 g C_{org} m⁻², quantified for one Greenland site and one short term restoration. For Nordic brown macroalgae, peer-reviewed estimates of sediment C-stock and sequestration are lacking. Overall, the review reveals substantial Nordic BC-stocks, but highlights that evidence is still insufficient to provide a robust estimate of all Nordic BC-stocks and sequestration rates. Needed are better quantification of habitat area, C-stocks and fluxes, particularly for macroalgae, as well as identification of target areas for BC management. The review also points to directives and regulations protecting Nordic marine vegetation, and local restoration

initiatives with potential to increase C-sequestration but underlines that increased coordination at national and Nordic scales and across sectors is needed. We propose a Nordic BC roadmap for science and management to maximize the potential of BC habitats to mitigate climate change and support coastal protection, biodiversity and additional ecosystem functions.

Keywords: eelgrass, salt marsh, macroalgae, area distribution, carbon stock, carbon sequestration, ecosystem services, management

INTRODUCTION

Vegetated coastal ecosystems including seagrass meadows, salt marshes, mangroves, and macroalgae are increasingly acknowledged for their contribution to sequestration and long-term storage of organic carbon (blue carbon, BC) and are, therefore, termed blue carbon habitats and ecosystems (Nellemann et al., 2009; Mcleod et al., 2011; Duarte et al., 2013; Krause-Jensen et al., 2018). Their capacity for long-term C-storage has made the management of these ecosystems relevant in relation to climate change mitigation; in addition, they constitute natural coastal protection by dampening wave energy and stabilizing and accreting sediments, thereby also contributing to climate change adaptation (Duarte et al., 2013; Macreadie et al., 2021). They also support biodiversity, including commercially important species, such as cod (Orth et al., 2020), and constitute coastal nutrient filters and sediment traps, which promote water quality and clarity (Aoki et al., 2020). These multiple functional roles and ecosystem services highlight the ecological and societal value of BC habitats (Barbier et al., 2011; Duarte et al., 2013; Smale et al., 2013; Gundersen et al., 2016). However, their location in the coastal zone where human pressures, such as eutrophication, fisheries and construction interact with climate change impacts such as heat waves and ocean acidification, render BC habitats among the most threatened on the globe (Orth et al., 2006; Waycott et al., 2009; Valiela et al., 2018; Dunic et al., 2021). Decline of the habitats due to diverse stressors put the C-reservoir at risk of erosion and to emit carbon dioxide (CO₂), and thereby turn the C-sinks into sources (Lovelock et al., 2017; Salinas et al., 2020; Moksnes et al., 2021).

Because of the multiple functions of vital BC ecosystems, actions to protect and restore these environments present win-win-win scenarios for buffering climate change, protecting biodiversity, and mitigating eutrophication, and for supporting human wellbeing (food security etc.) (Duarte et al., 2013; Gattuso et al., 2018; Hoegh-Guldberg et al., 2019; Macreadie et al., 2021). Such BC strategies are therefore natural climate solutions in parallel to forest protection and reforestation on land (Macreadie et al., 2021), which can supplement direct emission reductions. Protection of existing BC habitats preserves both the C-sequestration capacity and the sediment BC stocks, while restoration of lost BC habitats can regenerate the C-sequestration capacity and, over the long-term, rebuild C-stocks (e.g. Orth et al., 2020). As restoration can be challenging and costly, especially for seagrasses (van Katwijk et al., 2016),

prevention of loss has key management priority. At the global scale, the climate change mitigation potential of protection and restoration of mangroves, salt marshes and seagrass meadows could potentially represent 3% of current global emissions (Macreadie et al., 2021).

The C-sequestration capacity of salt marshes, seagrass meadows and mangroves exceeds that of green (terrestrial) forest ecosystems because of the combination of high ecosystem productivity, high potential for sedimentation of organic matter originating from the ecosystem itself (autochthonous) and from the surroundings (allochthonous), and the refractory nature of part of the organic matter and water-logged, anaerobic conditions limiting decomposition (Mcleod et al., 2011). The contribution of macroalgae to C-sequestration is more intricate to quantify than for seagrasses, salt marshes and mangroves. Unlike those systems that store C in sediments directly below them, macroalgal communities dominate rocky seafloor and their contribution to C-sequestration largely occurs through export to C-sinks beyond the habitat in fjord- and shelf sediments, and in the deep ocean, which is challenging to quantify (Krause-Jensen and Duarte, 2016; Pedersen et al., 2020). Management of macroalgal BC should consequently address both the macroalgal habitats and the BC sinks beyond the habitats (Krause-Jensen et al., 2018; Legge et al., 2020; Diesing et al., 2021).

The merit of protection and restoration of vegetated coastal ecosystems for climate action with co-benefits for biodiversity and human wellbeing underlines the importance of coordinated BC-strategies across sectors and regions. The Nordic region has a tradition of collaboration, e.g. under the auspices of the Nordic Council of Ministers, which is the official body for intergovernmental cooperation in the Nordic Region that seeks Nordic solutions wherever and whenever the countries can achieve more together than by working on their own. Such collaboration is also relevant regarding Nordic blue carbon ecosystems where joint efforts in science and management could benefit the region, and initiatives are already initiated. The study of vegetated coastal ecosystems has a long history in the Nordic region starting in the late 19th century (e.g., Rosenvinge, 1893; Ostenfeld, 1908; Waern, 1952) and shows a marked increase in research output over the past four decades to current levels of about 50 publications per year, as assessed by a bibliometric survey (**Figure S1; Table S2**). However, the peer-reviewed literature includes only a limited and recent focus on BC and has largely been conducted from a national angle. A first joint effort to quantify the distribution, biomass and C-storage

potential of seagrass meadows (dominated by eelgrass, *Zostera marina*), kelp forests (large canopy-forming brown macroalgae of the order Laminariales), and rockweed beds (brown macroalgae of the order Fucales) was recently supported by the Nordic Council of Ministers (Frigstad et al., 2021). But distribution maps, knowledge of status and trends, C-stocks and sequestration rates as well as knowledge of other ecosystem functions of seagrass meadows, salt marshes and macroalgal forests/beds are still incomplete. Blue carbon habitat restoration efforts are local and the information scattered.

The Nordic management of vegetated coastal habitats is related to European directives such as the Habitats Directive, Birds Directive, NATURA 2000 network of marine protected areas, Water Framework Directive, Marine Strategy Framework Directive and Nitrate Directive; regional conventions (HELCOM, OSPAR, ICES), collaboration platforms (Nordic Council of Ministers), as well as national and sub-national laws/regulations and management initiatives. However, BC aspects have received limited policy attention at the Nordic level. Recent declarations by the Nordic Council of Ministers highlight the ocean-climate nexus, the C-sink capacity of marine ecosystems, the coupling to biodiversity, and the need for Nordic collaboration (Gudbrandsson et al., 2019) to ensure that oceans and marine ecosystems are climate-resilient and sustainably managed. BC is also gaining focus at European and global levels. Hence, BC received unprecedented attention at the recent United Nations climate change conference COP26.

Here we present the state of knowledge related to Nordic BC habitats including environmental setting and policy framework, ecosystem extent and change, C-stocks and C-sequestration rates, and management status regarding protection and restoration of BC habitats. On this basis, we identify knowledge gaps and propose directions for research priorities, as well as cross-sectoral management and collaboration towards a Nordic BC-roadmap as a nature-based solution to combat multiple societal challenges. Our goal is to support Nordic management of vegetated coastal BC ecosystems to secure the multiple functions and services they provide. This contribution was initiated at the Nordic Blue Carbon Workshop with 77 participants from 18 countries, held in Copenhagen, Denmark, September 9–13, 2019, under The Blue Carbon Initiative (BCI) Scientific Working Group's 12th annual meeting.

THE NORDIC REGION AND ITS BLUE CARBON HABITATS

The Nordic region includes Norway, Sweden, Denmark, Finland, Iceland, the Faroe Islands, and Greenland. It covers 28 latitude degrees from Southern Denmark at 55°N to Northern Greenland at 83°N and extends across 58 longitude degrees from the west coast of Greenland in the Baffin Bay (73°E) to Finnmark, NE Norway, by the Barents Sea (31°E). The Nordic coastline is vast and is fringed by large shallow-water areas where light reaches the seafloor supporting potential growth of vegetation (**Figure S2**). According to Sayre et al. (2019, **Table S1**), the Nordic coastline is 224,087 km long, equaling about 9% of the global

coastline. This estimate is based on 30 m resolution mapping (i.e., 1:60 000 scale, Tobler 1987) and therefore excludes many small islands, which leads to a strong underestimation of island-rich archipelagos common across much of the region. Indeed, complex archipelagos with thousands of islands are important features of the region which hosts significant areas of BC habitats. For instance, the most updated estimate for Norway includes every island and calculates more than 100,000 km of coastline, which is almost twice the estimate of Sayre et al. (2019; 53,751 km). The average depth of the Baltic Sea, which is the world's largest estuary, is only 55 m. According to the EMODnet digital terrain model (emodnet-bathymetry.eu) at a 1/16 arc-minute resolution (which is approximately 125 m for the Nordic region), the extent of shallow areas with a water depth less than 10 m sums up to 50,330 km² for the Nordic countries (Svalbard and Jan Mayen included in the Norwegian estimate, but Greenland excluded due to lack of coverage by EMODnet). These shallow areas constitute on average 5.7% (3.25% if Svalbard is not included) of the countries' maritime Exclusive Economic Zone (from the VLIZ Maritime Boundaries Geodatabase), varying from <1% for Faroe Islands, Iceland, and Norway, to 5.5% for Sweden, 13% for Denmark, and 15% for Finland.

The region is characterized by physicochemical gradients with relevance to the BC habitats. In the northernmost areas, sea-ice cover affects both light availability and physical exposure and constitutes an important structuring factor, while the southernmost areas are only affected by ice during extreme winters (**Figure S2**). The region has a strong salinity gradient with high saline water and large tidal range along the Atlantic coastlines and near freshwater conditions with small or no tidal range in the Baltic Sea (**Figure S2**). Most Nordic countries, except Denmark, have large components of rocky shores (Young and Carilli, 2019). The levels of anthropogenic stressors such as land use and fishery also vary across the region, causing multi-stressor and cascading perturbations (Boström et al., 2014; Andersen et al., 2015; Reusch et al., 2018; Krause-Jensen et al., 2021). In addition, the area is strongly affected by climate change, which has led to a warming of the annual sea surface temperature of the Baltic Sea by up to 1.0°C per decade from 1990 to 2008 (BACC II author team, 2015 p. 9); this is much greater than the global average warming rate of the upper ocean of 0.11°C per decade from 1971 to 2010 (Rhein et al., 2014).

Nordic BC habitats reflect these regional environmental gradients (**Figure 1**). Salt marshes are common habitats along sheltered soft bottom shores and exhibit marked diversity from full marine tidal areas dominated by typical tidal marsh to brackish microtidal regions colonized by salt meadows and reed belts (**Figure 1**, see further details in the subsection on salt marshes). Deeper along the coastal slope, soft and sandy seafloors are colonized by meadows of seagrasses, dominated by eelgrass (*Zostera marina*), and increasingly mixed with other rooted vegetation and charophyte species in the more brackish regions towards the inner basins (Gulf of Bothnia) of the Baltic Sea and in the inner part of many estuaries (e.g. Boström et al., 2014; Wikström et al., 2016; **Figure 1**). Rocky shores are colonized by a variety of macroalgae with rockweed,



FIGURE 1 | Examples of characteristic Nordic BC habitats: Salt marsh (1st panel), rooted vegetation such as seagrass (2nd panel), intertidal macroalgae (3rd panel), and submerged macroalgae, such as kelp forests (4th panel).

particularly *Fucus* species dominating the shallow/tidal zone and *Laminaria*- and *Saccharina*-dominated kelp forests (**Figure 1**) with understory vegetation being abundant in the marine subtidal (e.g. Fredriksen et al., 2005).

GLOBAL, REGIONAL AND NATIONAL POLICIES RELATED TO NORDIC BLUE CARBON HABITATS

There is currently no specific BC policy or management strategy for BC habitats in the Nordic countries, but several policies and

directives address vegetated coastal habitats and provide an important basis for more targeted and coordinated BC management. Key examples are summarized below.

Global Scale

The Glasgow Climate Pact from the 26th Conference of the parties of the UNFCCC acknowledges the C-sink capacity of marine ecosystems. Several countries have included Blue Forests in their inventories and National Determined Contributions (NDCs) under the Paris Agreement based on the voluntary “2013 supplement to the 2006 IPCC Guidelines for National Greenhouse Gas Inventories: Wetlands”, which addresses saltmarshes, seagrasses and mangroves but not macroalgae.

However, none of the Nordic countries have yet included blue forests in their NDCs.

Protection of Nordic BC habitats and their services is, to some extent, also supported by global policy agreements under the Convention on Biological Diversity (CBD), the Ramsar convention for wetlands, the UNESCO Biosphere Reserves and Natural World Heritage sites, and the United Nations' Sustainable Development Goals (e.g. UN SDG 14.5 of 10% conservation of marine and coastal areas, and UN SDG 6.6 of protection and restoration of water-related ecosystems).

Regional Scale

The European Union's (EU) Habitat's Directive, Birds Directive, Water Framework Directive (WFD), and Marine Strategy Framework Directive (MSFD) as well as the Nitrate directive are all relevant for Nordic BC habitats. While Sweden, Denmark and Finland are EU members, Iceland and Norway are EEA EFTA members and have adopted the WFD *via* the EEA agreement. To some extent, national legislation in Iceland and Norway converges with, or are indirectly impacted by, the other EU directives as well. The Faroe Islands and Greenland are neither part of EU, nor the EEA EFTA and do not have obligations relative to e.g. the WFD, but EU and Greenland reinforce their partnership after the recent adoption of the new European strategy for the Arctic region. The WFD directly supports blue carbon habitats by defining the goal of good ecological status for coastal vegetation as a situation when "most disturbance sensitive macroalgal and angiosperm taxa associated with undisturbed conditions are present and the level of macroalgal cover and angiosperm abundance show slight signs of disturbance" (WFD, 2000/60/EC). The MSFD's requirement of "good environmental status (GES)" addresses the marine vegetation more indirectly *via* Descriptor 1 (biological diversity), Descriptor 4 (food webs) and Descriptor 6 (seafloor integrity). The WFD and the MSFD are closely connected; for example, marine vegetation and other so called "quality elements" targeted by the WFD are protected by management measures such as reduced eutrophication, and therefore also contributes to achieving GES within the MSFD with respect to several Descriptors.

At the regional level, the Baltic Sea Action Plan (2021) by the Helsinki Commission (HELCOM) also considers how mitigation by natural blue carbon processes can be maximized, but has no legal implications. HELCOM also defines eelgrass habitats and several macroalgal habitats in the Baltic Sea as being under threat and highlights the need for protection against e.g., eutrophication and anchoring (<https://helcom.fi/media/documents/HELCOM-Red-List-Biotope-Information-Sheets-BIS.pdf>). Moreover, in the North-East Atlantic, the inclusion of eelgrass beds in the OSPAR Convention's list of threatened species has been followed up by OSPAR Recommendation 2012/4 on furthering the protection and conservation of eelgrass beds (OSPAR 12/22/1, Annex 13). Greenland also accedes to the OSPAR. Moreover, the Arctic Council, with participants from several Nordic states (i.e. the Kingdom of Denmark including Greenland and Faroe Islands, as well as Iceland, Norway, Sweden and Finland), coordinates marine activities *via* working groups on the "Arctic monitoring and assessment program", "Protection of the Arctic marine

Environment", and the biodiversity working group of the Arctic Council: Conservation of Arctic Flora and Fauna (CAFF) and their Circumpolar Biodiversity Monitoring Programs (CMBP) on coastal and marine ecosystems. All these initiatives also to some extent address Nordic BC habitats.

National Scale

National management of BC habitats in EU member states must as a minimum fulfill the EU requirements and may also involve supplementary measures, which are treated in more detail in the management section (see below).

DISTRIBUTION AREA AND DYNAMICS OF NORDIC BLUE CARBON HABITATS

The total C-stocks and sequestration of coastal vegetation is connected to their area distribution. For some habitat types, like eelgrass meadows, the Nordic region has experienced major declines over the past century (Boström et al., 2014). For other BC habitats, like the kelp forests, the picture is more complex (Araújo et al., 2016). This section summarizes, by habitat type and country, the current knowledge on the distribution area of Nordic BC habitats (Table 1 and Figure 2A) and major changes over the past century.

Most Nordic countries conduct regular monitoring of BC habitats to document status and trends in relation to e.g. the Water framework directive and national programs (summarized in Table S3). However, except for the area of salt marshes, which is directly targeted by Habitats Directive monitoring, the monitored parameters are not necessarily related to the area distribution of the habitats, which is reflected in large knowledge gaps on BC habitat maps. For example, the Danish and Swedish national marine monitoring programs focuses on the depth limit and cover of eelgrass meadows and the cover of macroalgal communities (Riemann et al., 2016; Hammar et al. 2018) and the Greenland Ecosystem Monitoring (www.g-e-m.dk) focuses on the growth rate of kelps and rockweed as well as local depth distribution patterns. Norwegian coastal monitoring programs include regular measurements of the lower growth limit, coverage and status (e.g. the coverage of filamentous algae) for eelgrass and macroalgae on a fixed network of stations along the coast (Waldy et al., 2020) and additional kelp properties as part of the kelp harvesting strategy (Steen et al., 2016).

Salt Marshes

The Nordic region supports a range of habitat types that we here jointly refer to as "salt marshes" although they may also fit under terms such as "salt meadows", "coastal meadows", "tidal marshes" or "reed belts". They are dominated by herbs, grasses or low shrubs that are periodically inundated or saturated by tidal water (Adam, 1990; IPCC, 2014; Evans and Roekaerts, 2019). The use of different names for salt marshes and their heterogenous appearance make it challenging to get an overview of their total distribution. Comparison of these habitat across countries is also complicated by the existence of various national

TABLE 1 | Area estimates (km²) of coastal vegetated habitats (salt marshes, eelgrass and other rooted vegetation, macroalgae) across the Nordic region.

Vegetation type Country	Area km ²	Method	Notes	Reference
Salt marshes				
Greenland	nd	–	–	–
Iceland	65	Remote	Mainly via satellite	(Ottósson et al., 2016)
Faroe Islands	nd	–	–	–
Norway	57	Field	Likely underestimated	(Borgersen et al., 2020)
Denmark	410	Field and remote	1310, 1320, 1330	(Fredshavn et al., 2019)
Sweden	158	Field	1310, 1330, 1630	SLU*
Finland	330	Modelled pot, Remote	Common reed (<i>Phragmites australis</i>)	(Lehtomaa et al., 2018)
Finland	420	Remote	1630, salt meadows	(Lehtomaa et al., 2018)
Total	1,440			
Eelgrass				
Greenland	nd	–	Small areas in inner fjord branches.	(Olesen et al., 2015)
Iceland	>11	Field	Likely underestimated	(Ottósson et al., 2016)
Faroe Islands	nd	–	–	–
Norway	90	Field: 60 km ² mapped, multiplied by 1.5 to take unmapped areas into account		(Frigstad et al., 2021)
Denmark	1,345	Expert: 20% of historic area; based on data from Limfjorden & Øresund		(Boström et al., 2014)
Denmark	2,204	Modelled pot (GIS model of habitat suitability based on monitoring data; 100 m pixels)		(Staehr et al., 2019)
Denmark	nd	Remote	Based on satellite; 10 m pixels aggregated to 40 m.	Hansen LB (DHI) http://satlas.dk/marine-vegetation/
Sweden	400	Remote	Eelgrass and macroalgae combined. No area estimate Modelled by “the Symphony tool”, based on satellite (2008, 2016) w. field data, 10 m pixels aggregated to 250 m)	(Hammar et al. 2018)
Finland	15 (30)	Modelled pot (Habitat suitability modelling)	Maximum potential area of <i>Z. marina</i> . 15 added as a conservative estimate	(Downie et al., 2013; Boström et al., 2014)
Total	1,861 (2,735)			
Macroalgae (tidal and subtidal)				
Greenland	32,977	Modelled pot	Potential area of intertidal macroalgae (coarse estimate)	(Krause-Jensen et al., 2020)
Greenland	77,461	Modelled pot	Potential area of subtidal macroalgae (coarse estimate)	(Krause-Jensen et al., 2020)
Greenland	26,704 (24,401–27,877)	Modelled pot, rule based	Sugar kelp, dense (coarse estimate)	(Frigstad et al., 2021)
Iceland	>280	Field/Remote (pot. based on sediment, exposure)	Intertidal only	(Ottósson et al., 2016)
Iceland	495	Modelled, rule based	Intertidal and subtidal rockweed, dense	(Frigstad et al., 2021)
Iceland	2,328 (2,173–2,774)	Modelled, rule based	Subtidal kelp, dense (Tangle kelp 2,328; Sugar kelp 15)	(Frigstad et al., 2021)
Faroe Islands	245 (228–283)	Modelled, rule based	Subtidal kelp, dense (Tangle kelp 235; Sugar kelp 10)	(Frigstad et al., 2021)
Norway	3090	Modelled, rule based	Intertidal and subtidal rockweed, dense	(Frigstad et al., 2021)
Norway	7,417 (5,933–9,317)	Modelled, based on field observations	Subtidal kelp (Tangle kelp 3,810; sugar kelp 3,607)	(Frigstad et al., 2021)
Norway	5,355 (5,082–6,947)	Modelled, based on field observations	Subtidal kelp	(Gundersen et al., 2021)
Denmark	397	Remote/expert/modelled, rule based	Estimated area of tidal macroalgae (<i>Fucus</i> sp.) for Kattegat upscaled to national level	(Riemann et al., 2020; Frigstad et al., 2021)
Denmark	1,438	Field/Modelled pot	Suitable area for macroalgae in Kattegat (6.6% of Kattegat).	(Öberg, 2006)
Sweden	869	Survey/Modelled pot	Modelling of hard bottom as proxy for area of subtidal macroalgae	(Hammar et al. 2018) (based on the Geological Survey of Sweden)
Sweden	1,335	Modelled, rule based	Intertidal and subtidal rockweed, dense	(Frigstad et al., 2021)
Sweden	985 (904–2328)	Modelled, rule based	Subtidal kelp, dense (Tangle kelp 127; Sugar kelp 858)	(Frigstad et al., 2021)

(Continued)

TABLE 1 | Continued

Vegetation type Country	Area km ²	Method	Notes	Reference
Finland	240-580	Modelled pot	Pot. area of <i>Fucus vesiculosus</i> and <i>F. radicans</i>	(Sahla et al., 2020)
Total	16,532 (130,735)			
Grand sum	19,833 (134,910)			

*SLU, Swedish Species Information Centre; www.artdatabanken.se/en

Methods include "Field": upscaled from field observations; "Remote": based on remotely sensed data; "Modelled" or "Modelled potential (pot)", where the latter in some cases include habitat suitability modeling at a coarse scale without detailed documentation; "Expert": expert judgement based on field observations. Notes include information on species, habitat- or vegetation type (e.g. EU Habitats Directive Annex I habitat types #1310, 1320, 1330, 1630). References are provided. Details on area information: Values in bold mark the best available estimates of the realised distribution area. The area of Greenland macroalgae is not marked in bold as it represents coarser estimates than for other regions. For each vegetation type, the total Nordic area is calculated as the sum of national values marked in bold; in parenthesis follows the total potential area including the largest potential estimates and high-end-range of estimates for each country. In the case of Finland, area estimates for both eelgrass and other rooted vegetation are included in the total. nd, Not determined.

and international classification systems such as the European Nature Information System (EUNIS) in the EU (Evans and Roekaerts, 2019), the Nature in Norway (NiN) system in Norway (Borgersen et al., 2020; Halvorsen et al., 2020) and HELCOM for the Baltic Sea (Helcom, 2013) (details in Table S4).

There are strong gradients in "salt marsh" plant communities in the Nordic region related to gradients in tidal regime, salinity, and climate factors. A key management practice, grazing, which is often implemented to stimulate biodiversity, also markedly affect the marshes. Nordic EU member states map salt marshes as part of the Natura 2000 network, and Atlantic coastal meadows are categorized as vulnerable in the European Red List of Habitats (Janssen and Rodwell, 2016). Mapping is also taking place as part of national programs. Below is an overview of area information available for these habitats in the Nordic region. The European-funded project "NordSalt" (2021–2024, www.sdu.dk/en/forskning/nordsalt) will expand the information on salt marshes and their C-stocks and sequestration in the Nordic region.

Greenland

There is no overview of area distribution or changes in distribution of salt marshes at the Greenland scale. However, some local distribution studies exist (e.g., Glooschenko et al., 1993; Lepping and Daniëls, 2007; Bültmann and Daniëls, 2013), and salt marsh sediments have also been studied as archives of recent relative sea level change (Jensen et al., 2006; Woodroffe and Long, 2009; Long et al., 2012).

Iceland

Salt marshes in Iceland are classified into two habitat types. One is characterized by *Puccinellia maritima* (Atlantic lower shore communities under the EU habitat type 1330). The other is classified by *Carex* species (Icelandic *Carex lyngbyei* salt meadows). The latter is not accepted under EUNIS but proposed as a sub-type of Atlantic black sedge salt meadows that falls under Annex I at a higher level (see A2.5 – <https://eunis.eea.europa.eu/habitats/2931>). Together, the habitat types cover approximately 65 km², with the majority characterized by

P. maritima (Ottósson et al., 2016). The habitat mapping was done mainly by satellite image interpretations so estimation errors can be relatively high, especially for *Carex* habitats due to indistinct differences between similar habitats. No national monitoring of salt marshes exists in Iceland and long-term changes and dynamics are therefore unknown.

Faroe Islands

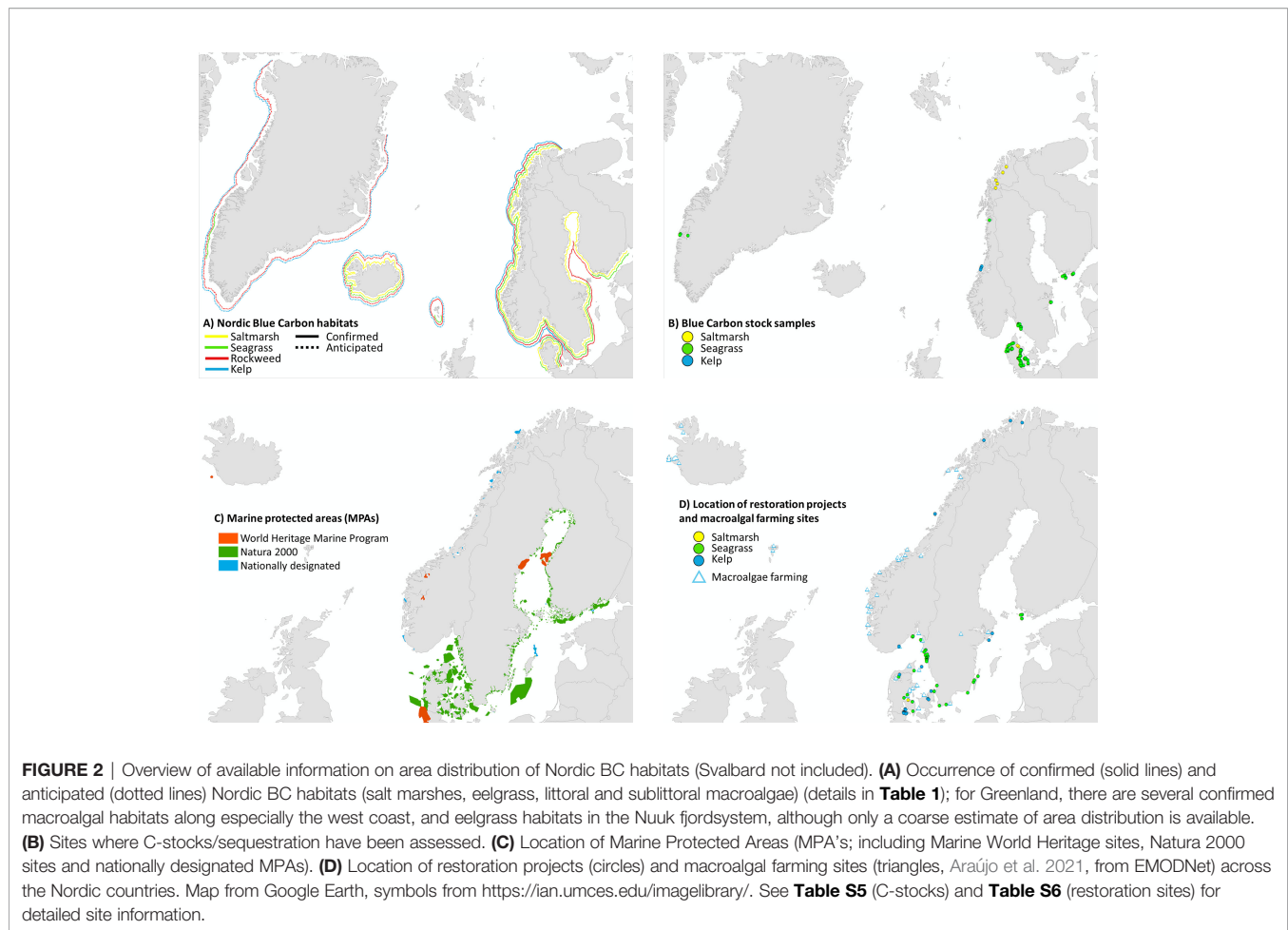
No overviews of distribution area or dynamics are available for the Faroe Islands (<https://kort.foroyakort.fo/kort/>). Salt marsh species such as *Carex lyngbyei*, *Glyceria fluitans*, *G. maxima* and *Puccinellia maritima* occur in the Faroe Islands but are all reported as very rare (reported 1–10 times) or rare (reported 11–25 times) (Jóhansen et al., 2000) indicating that salt marsh areas are negligible in extent.

Norway

Norway has no systematic mapping program for salt marshes, but some mapping efforts have been completed, e.g. in connection to mapping RAMSAR areas. Typical species in Norway are *Carex paleacea*, *C. vacillans*, *Glyceria fluitans*, *G. maxima*, *Phragmites australis*, *Schoenoplectus lacustris*, *S. tabernaemontani* and *Bolboschoenus maritimus*. Currently, 606 occurrences of salt marshes have been recorded in Norway with a total area of 57 km² (Borgersen et al., 2020). This is most likely an underestimate due to the lack of systematic mapping. The habitat is considered as of "least concern" in Norway's red list for habitats (Gundersen et al., 2018).

Denmark

Danish salt marshes are represented by the EU habitat types 1310, 1320 and 1330 (Table S4), with 1330 being the most widely distributed and categorized into two subtypes, salt marsh and salt swamp, depending on whether it is being grazed or not. The grazed plant communities are dominated by halophytic grasses and herbs, whereas the non-grazed ones are dominated by reeds such as *Phragmites australis*, *Schoenoplectus maritimus* and *Schoenoplectus tabernaemontani*. This division is the result of management practices with a long history of grazing preventing overgrowth by reed. The Wadden Sea has the largest tidal range



among Danish salt marshes and includes typical tidal *Spartina* spp. salt marshes (EU habitat type 1320). Many of these marshes were formed as part of land reclamation efforts (Jakobsen, 1954). All habitat types are monitored and mapped every six years under the Danish monitoring program NOVANA since 2007, with the most recent estimate representing a total of 410 km² (sum of the area of the EU habitat types 1310, 1320 and 1330; Fredshavn et al., 2019; **Table 1**, <https://naturdata.miljoeportal.dk/>). The saltmarsh area is estimated to have been twice as large as 150–200 years ago, with the loss caused primarily by expansion of agriculture (Vestergaard, 2000). EU habitat types 1310 and 1330 are categorized as having an unfavorable preservation status, the latter showing decline over the past 12 years, while 1320 has a favorable status (Fredshavn et al., 2019, **Table S4**).

Sweden

The extent of Swedish salt marshes is estimated at 158 km² based on data and information from the report of conservation status of habitats and species that is provided by the implementation of the EU Habitats Directive (under Article 17), which is synthesized and published every six years by the Swedish Species Information Centre, ArtDatabanken. The estimates include the EU habitat types 1310, 1330 and 1630

(**Table S4**), which are all categorized as having bad conservation status.

Finland

The majority of Finnish salt marshes belongs to the EU habitat type 1630 (Boreal Baltic coastal meadows). There are no overviews for habitat types 1310, 1320 or 1330 (**Table S4**), but 1330 is part of a recent classification (Pätsch et al., 2019). Traditionally managed (grazing, mowing) salt marshes have been classified (by IUCN) and their status assessed (improving, declining, stable) in the national red list of threatened habitat types (Lehtomaa et al., 2018). These marshes belong to the habitat type 1630 and are currently classified into six types: seashore meadows *Eleocharis parvula*-*E. acicularis*, *Eleocharis palustris*-*Schoenoplectus tabernaemontani*-*Bolboschoenus maritimus*, tall-sedge seashore meadows, low-graminoid seashore meadows, tall seashore meadows and salt patches. Of a total of about 6900 km² of traditionally managed salt meadows in the 18th century, only about 420 km² exist today (Lehtomaa et al., 2018). Reed belts have been favored by a dramatic decline in grazing by livestock as well as by eutrophication so the area of completely or partly preserved meadows of the habitat type 1630 is only 62 km², of which about 20 km² is overgrown by reed.

Hence, the habitat type 1630 is now classified as critically endangered (Schulman et al., 2008). It is estimated that about 121 km² of this habitat type can potentially be restored, and there are ongoing management initiatives (including grazing). Coastal reed belts with *Phragmites australis*, *Schoenoplectus* and *Bolboschoenus maritimus* or *Typha* are additional potential BC sinks not belonging to the habitat type 1630.

Seagrasses and Other Rooted Submerged Vegetation

In the Nordic region, there are two true seagrass species, eelgrass (*Zostera marina*) and dwarf eelgrass (*Z. noltei*). Eelgrass is by far the most dominant and subject to a long record of research, particularly in Denmark (Boström et al., 2014; Krause-Jensen et al., 2021). Other rooted vegetation, such as species of the genera *Ruppia*, *Zannichelia* and *Potamogeton*, may also occur in brackish areas. For the purposes of this paper, when the term seagrass or eelgrass is used for the Nordic region, we are referring to primarily eelgrass, occasionally including other species of rooted vegetation. Eelgrass meadows were historically very extended but experienced major declines in the 1930s due to the wasting disease, which decimated the North-Atlantic eelgrass meadows, and more recent declines due to multiple stressors (Krause-Jensen et al., 2021).

Greenland

Recent studies of eelgrass in the Nuuk fjord system at 64 °N show that the meadows are confined to inner, protected fjord branches with sandy seafloor where summer temperatures are relatively high (up to 13°C), although a sparse meadow grows in an area with maximum summer temperatures of 8°C (Olesen et al., 2015). These meadows support biomasses as high as those at lower latitudes but have lower productivity (Olesen et al., 2015). There is no assessment of the overall distribution area, but it is relatively small, limited by both availability of suitable sandy/soft seafloor in shallow protected settings and by low water temperatures (Olesen et al., 2015). Dating of sediments in eelgrass meadows in the Nuuk fjord system along with analyses of the origin of organic matter in these sediments, nevertheless, suggest that eelgrass has been expanding in these locations over the past century (Marbà et al., 2018).

Iceland

Macrovegetation on littoral sediments include eelgrass beds, which are most common along the west coast and in lagoons in the south-east while rare elsewhere (Boström et al., 2014). They cover roughly 1% (11 km²) of the coast (Ottósson et al., 2016), but this is likely an underestimate as the distribution area has only been partially explored. Lack of monitoring and mapping efforts prevent a detailed account of the status and trends.

Faroe Islands

Eelgrass is very rare in Faroe Islands. It has been reported less than 10 times (Jóhansen et al., 2000) but with no recent observations. The extent is therefore considered negligible with no overview of the distribution area or trend. Eelgrass

occurs in one of the fjords on the southernmost island, Suðuroy, where Ostenfeld (1905-08) already a century ago commented that this fjord was likely the only place where the species occurred.

Norway

Eelgrass meadows are the most common and widespread habitat-building species on soft seafloor in Norwegian fjords and bays. The largest occurrences of eelgrass meadows have been systematically mapped by the Norwegian National program for mapping of coastal biodiversity (Bekkby et al., 2013), and are found in sheltered and moderately wave exposed areas all the way from the Swedish border in southern Norway to the Barents Sea region in Finnmark. More than 3000 eelgrass meadows have been identified in Norway, covering 60 km² in total (Bekkby et al., 2013). Following the “red list” protocol (Gundersen et al., 2018), this area was multiplied by a factor of 1.5 to include meadows assumed to be present but not recorded, giving an estimate of 90 km² (Frigstad et al., 2021). The habitat is not considered threatened in Norway’s red list for habitats (from 2018), but the status and trends in the North Sea in particular are largely unknown and highly debated, as the methods used for monitoring do not capture changes in meadow size and lower growth limit (Gundersen et al., 2018). Degradation of the seagrass meadows in the Oslofjord has been documented (Dahl et al., 2008; Espeland and Knutsen, 2014).

Denmark

Denmark is the Nordic ‘hotspot’ for eelgrass due to the extensive coastline with gently sloping sandy shores in protected settings of intermediate salinity. The national Danish monitoring program assesses annually the cover and depth distribution of eelgrass across the country along transect lines from the shore to the deepest occurrence. Area surveys are not part of the monitoring program, except for the Wadden Sea eelgrass meadows. A first nationwide mapping of the submerged coastal vegetation (eelgrass, other rooted vegetation and macroalgae) has been produced based on optical satellite data from 2018, using advanced radiative transfer modelling and machine learning techniques. The map has 10 m resolution and represents depths down to 4–10 m, depending on local water clarity (<http://satlas.dk/marine-vegetation/>), but does not distinguish between eelgrass and macroalgae and provides yet no information on the distribution area. However, the potential distribution area of eelgrass in Danish coastal waters has been quantified at 2,204 km² based on a GIS modelling of where habitat requirements are fulfilled (Stæhr et al., 2019). This is about a third of the historic distribution area quantified at 6,726 km² around year 1900 (Petersen, 1914). Overviews for two key distribution areas (the Limfjord and Øresund) suggest that the current actual distribution area of eelgrass is probably only about 20% of the historic area, i.e. about 1,345 km² (Boström et al., 2014). Century-long records reveal shifting challenges to eelgrass over time with the wasting disease decimating the populations in the 1930s, eutrophication peaking in the 1980s causing additional decline, and bottom-trawling and warming further limiting the recovery during the past decades (Krause-Jensen et al., 2021).

Sweden

The area distribution of eelgrass in Swedish coastal waters is assessed at 400 km² using a model based on satellite remote sensing images (2008 and 2016) and associated ground truthing (>6000 sites) for field validation (the Symphony tool, Hammar et al. 2018) (Table 1). The spatial model described the probability of occurrence of seagrass (in 10 x 10 m pixels, aggregated into 250 x 250 m pixels); the probability level was set at 0.8, which means that there is at least 80% probability of finding the focal habitat in a pixel. The modelled coastal area encompasses primarily eelgrass (*Z. marina*), but also to some extent widgeon grass (*Ruppia* spp.) and occasionally some freshwater green algal species (principally along inner margins of *Z. marina*) (Boström et al., 2003). The model has been used efficiently in recent spatial risk assessment of global change impacts on eelgrass in Sweden (Perry et al., 2020). Satellite remote sensing has been shown useful to assess eelgrass coverage down to about 5–6 meters depth on the Swedish Skagerrak coast (Envall and Isaksson, 2012; Lundén and Gullström, 2013). In general, the cover of soft-bottom vegetation decreases with increasing total nitrogen concentrations and salinity (Wickström et al., 2016). Eelgrass meadows along the Swedish west coast experienced major declines over the period 1980s–2000s (Baden et al., 2003; Nyqvist et al., 2009) due to the combination of eutrophication and overfishing (Moksnes et al., 2008; Baden et al., 2010), and climate change is emerging as an additional stressor with increases in sea surface temperature, ocean acidification and wind-driven turbid conditions likely to cause interactive negative effects in risk areas in southern Sweden by the mid-end century (Perry et al., 2019; Perry et al., 2020).

Finland

There is no comprehensive area estimate of eelgrass coverage in Finland, but habitat suitability models suggest a maximum of 30 km² (Downie et al., 2013; Boström et al., 2014). As no national monitoring of eelgrass meadows exists, there are only few examples of long-term dynamics of Finnish eelgrass meadows. The available data suggest that these systems have been stable over time i.e. 1970–1990 (Boström et al., 2002). Finnish eelgrass meadows are often multi-specific, and eelgrass occurs here at the physiological boundary and is thus particularly vulnerable. Individual meadows are small, isolated clones with limited geneflow typically reaching over thousand years of age (Reusch et al., 1999; Reusch and Boström, 2011). The overall low reservoir of genetic diversity in the northern Baltic Sea combined with extremely limited sexual reproduction and inbreeding typically lead to reduced fitness (Reusch et al., 1999; Olsen et al., 2004). Thus, these populations are in urgent need of special conservation efforts as they lack potential for rapid adaptation and are likely to go extinct under extreme climate events.

Other submerged aquatic vegetation habitats that include plants of freshwater and/or marine origin are potentially more important BC habitats in Finland. These have been classified and their status assessed (Lehtomaa et al., 2018). They include habitats dominated by *Potamogeton* and/or *Stuckenia pectinata*, *Ranunculus* spp., *Zannichellia* spp. and/or *Ruppia*

spp., *Myriophyllum spicatum* and/or *M. sibiricum*, and exposed and sheltered habitats characterized by Charales and *Najas marina*.

Macroalgae – Intertidal and Subtidal

Macroalgae represent the largest BC habitat of the Nordic region with an estimated coverage of >10 000 km² (excluding area estimates from Greenland, which are very uncertain, Frigstad et al., 2021). Intertidal macroalgal habitats, largely defined by tidal range and the occurrence of hard substratum, are most conspicuous along the coasts of Greenland, Iceland, Faroe Islands, Norway and SW Sweden. The microtidal rocky south- and east coast of Sweden and the Finnish coast are also rich in habitats of *Fucus* sp. (Rinne & Salovius-Laurén, 2020; Sahla et al., 2020), which colonize the low-saline subtidal in addition to the intertidal zone (Törn et al., 2006). Here they penetrate deeper than in full marine settings because of reduced competition from other macroalgae (Nielsen et al., 1995; Middelboe et al., 1997). In contrast, most of the Danish coastline has only scattered stones and narrow tidal range and therefore limited distribution of intertidal macroalgal communities. The occurrence of subtidal macroalgae largely follows the pattern described for the intertidal habitats, i.e. dominating the rocky coastlines, although also growing on stone reefs, e.g. in the Kattegat. Sandy seafloors may also hold macroalgae such as Charales, floating macroalgae as well as macroalgal communities on scattered stones and shells. Overall, the macroalgal community of the region is characterized by steep declines in species diversity along the Baltic salinity gradient (Nielsen et al., 1995).

Greenland

Macroalgae occur along most of Greenland's coastline, but distribution records are relatively sparse, especially in the northernmost regions (Krause-Jensen et al., 2020). The depth limit and width of the belt of submerged macroalgae, dominated by kelps, increase from north towards south as the length of the open water period increases and more of the surface light potentially reaches the seafloor (Krause-Jensen et al., 2012). The deepest occurrence of kelps (> 60 m depth) is reported in clear waters along open coasts and offshore islands (Krause-Jensen et al., 2019). Intertidal macroalgae are also abundant along the Greenland coast, with potential for high biomasses even in northern regions (Høgslund et al., 2014; Ørberg et al., 2018; Sejr et al., 2021; Thyrring et al., 2021). Whereas no detailed mapping of macroalgae in Greenland exists, a first, coarse, spatial distribution model suggests a potential intertidal macroalgal distribution area of about 33,000 km² and a subtidal distribution area of 77,500 km² (Krause-Jensen et al., 2020). Also, Frigstad et al. (2021) estimated the total coverage of dense *Saccharina latissima* (sugar kelp) forests in Greenland to be 26,700 km² in a Nordic spatial model but emphasized that this is an undocumented estimate with high uncertainties due to unknown effects of sea ice cover, exposure, and substrate type. Macroalgal distribution and production is hypothesized to increase in parallel with increasing water temperatures and declining sea ice cover (Krause-Jensen et al., 2020).

Iceland

Rocky shores dominated by macroalgae cover 28% (280 km²) of the intertidal in Iceland (Ottósson et al., 2016). Sheltered intertidal areas that are dominated by *A. nodosum* cover >7% of the total intertidal area and >25% of all low to moderate energy littoral rocky shores. Breiðafjörður in West Iceland accounts for about 70% of intertidal areas (50 out of 70 km²), dominated by *A. nodosum* according to habitat mapping done in 2012–2014 (vistgerdakort.ni.is, 2018). More recent, in-depth studies expand this estimate to 91–107 km² (Gunnarsson et al., 2019). Frigstad et al. (2021) estimated a total coverage of 495 km² for rockweed and 2,328 km² for kelps, dominated by *Laminaria hyperborea* (tangle kelp), based on a spatial model covering the Nordic countries. No national monitoring of macroalgae exists so long-term trends and dynamics are unknown.

Faroe Islands

Kelps are widespread on the rocky shores of the Faroe Islands, and data from the FARCOS project in the 1990s (Bruntse et al., 1999) were recently used to model the potential kelp distribution around the Faroe Islands, predicting a coverage of 10 km² for sugar kelp and 235 km² for tangle kelp (Table 1, Frigstad et al., 2021). No estimates exist for the coverage of macroalgae in the littoral zone of the Faroe Islands.

Norway

Rockweeds cover the intertidal shores and the shallow subtidal areas along almost the entire Norwegian coast, with a total coverage estimated (modelled) to be 3,090 km² (Frigstad et al., 2021). Tangle kelp and sugar kelp are the two dominant species that form large subtidal kelp forests along the Norwegian coast. Tangle kelp is found in the wave-exposed areas and has been mapped systematically by the National program since 2007 (Bekkby et al., 2013), estimated to cover 3,810 km² (Frigstad et al., 2021). Sugar kelp forests colonize more sheltered areas, often in fjords, bays and in inner parts of archipelagos, and are mapped less systematically. These forests have been estimated to cover 3,607 km² by Frigstad et al. (2021) and 5,355 km² by Gundersen et al. (2021). Both estimates are adjusted for destructive sea urchin grazing in northern Norway (additionally 1592 km² of kelp forest is considered to be grazed by urchins, Gundersen et al., 2021). Tangle kelp forests are in the Norwegian “Red list” for habitats considered to be “near threatened” in northern Norway due to the intensive grazing by the green sea urchin *Strongylocentrotus droebachiensis* (Rinde et al., 2014). Sugar kelp is listed as endangered due to sea urchin grazing in the north and due to a combination of eutrophication and increasing frequency and intensity of marine heat waves in the south of Norway (Gundersen et al., 2018; Filbee-Dexter et al., 2020). For sugar kelp in southern Norway, a combination of increased water temperature and increased riverine inputs of terrestrial organic matter (increased light attenuation and sedimentation) has negatively affected the lower growth depth limit over the last decades (Frigstad et al., 2018). This trend is leading to a decrease in macroalgal area coverage, decreased primary production, and a subsequent decrease in macroalgal ecosystem services, including macroalgae-driven C-

sequestration (Filbee-Dexter and Wernberg, 2018; Wernberg et al., 2019).

Denmark

Although most of the Danish seafloor is soft, macroalgae occur on scattered stones along the shores as well as on offshore stone reefs. As a component of the national Danish monitoring program, the cover and species composition of macroalgal communities are assessed nationwide along shoreline depth gradients representing hard substratum, as well as on offshore stone reefs, but a map of overall macroalgal distribution in Denmark is lacking. However, recently, the area extent of *Fucus* sp., which is dominant in the tidal zone, was quantified for the Kattegat coast at about 54 km² based on analysis of aerial photos supported by monitoring data and drone/field surveys in test areas (Riemann et al., 2020). This area was upscaled to an estimated distribution area of intertidal algae in Denmark at 397 km², assuming similar area extent of *Fucus* per km of coastline as for the Kattegat (Frigstad et al., 2021). The distribution area of subtidal macroalgae in the Kattegat has been assessed at 1438 km² based on monitoring data, seafloor properties and modelling (Öberg, 2006). Large uncertainties in the area of hard substratum have so far prevented a reliable updated modeling of the subtidal macroalgal area (Frigstad et al., 2021).

Several stress factors, varying in space and time, affect Danish macroalgae. Vast macroalgal habitats have been lost due to extraction of stones for construction, a conservative estimate suggests that a total of 40 km² of exposed stone surface was removed from stone reefs in coastal Danish waters in the second half on the 20th Century (Dahl et al., 2003) before the practice was banned in 2010 (Dahl et al., 2016a). Bottom trawling for mussels and fish has added to the loss of stones. Eutrophication further limits the cover and diversity of both coastal and offshore stone reef macroalgal communities through light limitation and overgrowth by opportunistic species (Riemann et al., 2016).

Sweden

The area of hard bottom within the photic zone was modelled at 869 km² and used as a proxy for the extent of subtidal macroalgae (Hammar et al. 2018). The hard bottom model is based on geological mapping surveys conducted by the Geological Survey of Sweden (SGU). The model was set to 0.8, which means that there is at least 80% probability of finding the focal habitat in a pixel. In the Nordic model of Frigstad et al. (2021), the total coverage of tangle kelp and sugar kelp in Sweden were estimated at 127 and 858 km², respectively, all at the Swedish west coast. The differences in area estimates for subtidal macroalgae by the two models can e.g. be due to different resolution of the models. For *Fucus* sp., the total coverage in Sweden was estimated at 1335 km² using the same approach as for Denmark, assuming similar area extent per km of coastline as for the Kattegat (Riemann et al., 2020), excluding the northern east coast of Sweden with known low distributions of *Fucus* sp. (Frigstad et al., 2021).

Until today, there are no comprehensive overall estimates of macroalgal distribution or change in cover in Swedish marine waters. But long-term studies on depth distribution (based on

annual surveys) of macroalgal zonation, cover and community composition are available (e.g., Kautsky et al., 1986; Karlsson, 2007; Hammar et al. 2018) as well as scattered spatial surveys in localized areas (e.g., Blomqvist and Olsson, 2007; Gullström et al., 2009). A harmonized nation-wide macroalgae monitoring program is, however, ongoing since 2019, which aims to assess ecological status and spatiotemporal distribution of macroalgae on the west- and east coasts of Sweden (led by SWaM and following methodology in Lindegarth et al., 2016).

Finland

The Finnish Inventory Programme for the Underwater Marine Environment (VELMU) has systematically made inventories of macroalgae since 2011. Macroalgal monitoring started in 1993 and the monitoring of the lower depth limit of *Fucus* started in 2000. Based on habitat suitability modelling (GAM, EADM), the Finnish coastline (including Åland Islands) today supports about 240–580 km² of *Fucus* (including *F. radicans*) compared to >1000 km² in 1900 (Sahla et al., 2020).

Overall

The review identified the known area extent of BC habitats in the Nordic region, which was 1441 km² for salt marshes, 1,861 km² (potentially >2,735 km²) for seagrasses (mainly eelgrass) and 16,532 km² (potentially 130,735 km², including coarse Greenland estimates) for macroalgae. This sums up to 19,833 (potentially as much as 134,910 km²) of blue forests in the Nordic region (**Table 1** and **Figure 2A**). Although the numbers are associated with considerable uncertainty and contain major knowledge gaps, the area of Nordic marine forests is substantial. The overview reflects the increasing difficulty of mapping the habitats as the water depth increases and conceals the vegetation. Hence, actual distribution maps are very limited and the difference between documented and potential areas is huge for macroalgal habitats, which extend deepest among the BC habitats. Especially for Greenland, Faroe Island and Iceland, there is very limited documentation of area extent of BC habitats. The various estimates also represent major differences in terms of quantification of presence/absence versus dense vegetation, key macroalgal species (e.g. sugar kelp) versus overall macroalgal cover and regarding the pixel size and scale of the survey. Only unified mapping approaches across the Nordic region, such as the one carried out by Frigstad et al. (2021) offer direct comparison across part of the region but depend on further data input for data poor regions, such as Greenland. Whereas there has been very limited Nordic focus on particularly salt marshes in the BC context, Nordic EU member states quantify salt marsh areas as part of the requirements of the EU habitats directive.

In addition to the above-listed areas, EU member states report the areas and status/trends of the EU habitats directive's marine habitat types, several of which contain meadows of eelgrass and other rooted vegetation or macroalgae beds. However, in opposition to the directive's continental habitat types, the marine habitat types are defined based on geomorphology (e.g. "Estuaries, habitat type 1130", "Coastal lagoons, habitat type 1150" and "Large shallow inlets and bays, habitat type 1160")

and, hence, unfortunately, do not specifically target the vegetated habitats.

It is important to underline that the above estimates of the area of Nordic BC-habitats do not provide information on the extent of manageable areas with regard to restoration or protection against further loss and, hence, the extent of area that is relevant for climate change mitigation policies.

C-STOCKS AND SEQUESTRATION IN NORDIC BLUE CARBON HABITATS

Salt Marshes

Pioneering data on C-stocks and sequestration rates in Nordic salt marsh sediments are available from Denmark and Norway (**Figure 2B** and **Table S5**). C-stocks are 4228–8178 g C_{org} m⁻² for the upper 43 cm sediment in three microtidal salt marshes along the east coast of Jutland (**Table 2**, Graversen et al., 2022). C-sequestration rates at the same sites are 17–45 g C_{org} m⁻² yr⁻¹ (**Table 3**, Graversen et al., 2022). Sequestration rates of salt marshes in the German Wadden Sea, likely also representative for the Danish Wadden Sea, are quantified at 149 g C m⁻² yr⁻¹ over a 50 yr period and 112 g C m⁻² yr⁻¹ over longer term (Mueller et al., 2019), i.e. higher than those for Danish microtidal salt marshes. The estimates include the sequestration of both autochthonous and allochthonous carbon. In Arctic Norway, C-sequestration rates of five salt marshes are 19–603 g C m⁻² yr⁻¹, increasing e.g. with longer growing seasons; C-stocks in the corresponding sediments are limited to 367–1379 g m⁻², resulting from thin sediments, e.g. due to isostatic uplift (Ward, 2020). In addition to the C-sequestration within the habitats, there is also a scope for exported saltmarsh detritus ending up in other sink habitats such as seagrass meadows.

The evidence is still insufficient to provide a reasonable Nordic estimate of saltmarsh C-stocks and sequestration as the few data points represent only about 10 sites spanning sediment depths of 40–100 cm and showing 5–10 fold variation between estimates; the estimates of area extent add further uncertainty. Hence, the average sediment C-stock (3311 g C_{org} m⁻², **Table 2**) and C-sequestration rate (142 g C_{org} m⁻² yr⁻¹, **Table 3**) multiplied by the combined Nordic extent of salt marsh as quantified for Norway, Denmark, Sweden and Finland (1440 km², **Table 1**) gives only a vague indication of the potential C-stock (4.77 Tg C_{org}) and C-sequestration (0.20 Tg C_{org} per year, i.e. 0.75 million tonnes CO_{2e} yr⁻¹), which need further validation.

Seagrass Meadows

Data on C-stocks in eelgrass meadows are available for sites in Greenland, Denmark, Sweden and Finland (**Figure 2B** and **Table S5**). C-stocks for the upper 10 and 25 cm sediments are 197–4413 and 364–5046 g C_{org} m⁻², respectively, with higher stocks in the western Baltic Sea than in the eastern Baltic Sea and Greenland (**Table 2**, Röhr et al., 2018). The considerable variation in C-stocks both between and within regions relate to factors such as the degree of exposure and sediment characteristics with the highest stocks in sheltered settings with fine sediments (Röhr

TABLE 2 | Sediment organic C-stocks of Nordic BC habitats with indication of mean levels, standard deviation (sd), range, and number of observations (n).

Habitat type	C-stock (g C _{org} m ⁻²)				Sediment depth	Reference
Country	Mean	Sd	Range	N (sites)	(cm)	
Salt marshes						
Norway	629	335	367-1379	5 x 2*	>100	(Ward, 2020)
Denmark	5992	1401	4228-8178	6	43	(Graversen et al., 2022)
Eelgrass						
Greenland	413	201	197-595	3	10	(Marbà et al., 2018)
Norway	1453**	217		1	25	(Röhr et al., 2018)
Denmark	1013**	820	155-4413	50	10	(Kindeberg et al., 2018^)
Denmark	4324**	1188		10	25	(Röhr et al., 2016)
Sweden (W coast)	3806**	1117	1221-5046	15	25	(Dahl et al., 2016b; Dahl et al., 2020a; Dahl et al., 2020b; Moksnes et al., 2021);
Sweden (E Coast)	490**	213	364-735	3	25	(Dahl et al., 2016b)
Sweden - all data	3253**	1628	364-5046	18	25	(Dahl et al., 2016b; Dahl et al., 2020a; Dahl et al., 2020b; Moksnes et al., 2021)
Finland	627**	286	138-1425	10	25	(Röhr et al., 2016)

*Ward examined both high and low marsh at 5 sites. **Compaction not considered. [^]Includes Röhr et al., 2016 data.

The depth of the sediment representing the C-stock is listed with associated reference. Lacking information for a given country/habitat type indicates that we are not aware of any data.

et al., 2016; Dahl et al., 2016b; Kindeberg et al., 2018; Dahl et al., 2020b).

C-sequestration in eelgrass sediments has solely been quantified for meadows in Greenland (*via* Pb²¹⁰ dating) and over the first two years of a Danish eelgrass restoration (by repeated measure of sediment C-stocks in restored versus reference areas) (Table 3). These estimates range from an average of 5.1 g C_{org} m⁻² yr⁻¹ in Greenland to an average of 33 g C_{org} m⁻² yr⁻¹ associated with the eelgrass restoration in Denmark (Table 3). Sequestration has also been estimated for Danish and Finnish eelgrass meadows based on literature values on sediment accretion multiplied by measured C-densities (Röhr et al., 2016). In comparison with the initial sparse data from the Nordic region, a thorough recent study from the east coast of the USA reported net C-sequestration rate for eelgrass meadows (11.5 g C_{org} m⁻² yr⁻¹) that is compensated for the flux of greenhouse gasses (Oreska et al., 2020). Multiplying the estimated Nordic extent of eelgrass (1861 km², Table 1) by, respectively, the average C-stock (2414 g C_{org} m⁻², 25 cm depth,

Table 2) and the net C-sequestration rate (11.5 g C_{org} m⁻² yr⁻¹, Oreska et al., 2020), the total sediment C-stock is approximately 4.49 Tg C_{org} and the sequestration rate 0.021 Tg C_{org} per year (corresponding to 0.08 million tonnes CO_{2e} yr⁻¹). As for salt marshes, these estimates are very coarse and preliminary and need further validation.

Eelgrass also supports sediment C-stocks and C-sequestration beyond the habitats (Duarte and Krause-Jensen, 2017) as first documented by eelgrass tracer studies already a century ago, which concluded that the organic matter of sediments in Danish fjords then derived almost entirely from eelgrass (Boysen-Jensen, 1914). Moreover, findings of eelgrass in ancient sediments (5600-6200 ca. BP) from Blekinge, in the SE Sweden, suggest the capacity for sequestration over Millenia (Yu et al., 2004).

Macroalgal Habitats

Most macroalgae, including kelp and rockweed, attach to hard substrates, such as rocks and stones, where organic matter does not accumulate. Macroalgae export part of their photosynthetic

TABLE 3 | Sediment C-sequestration rates for Nordic BC habitats with indication of mean levels, standard deviation (sd), range and number of observations (n).

Habitat type	C-sequestration (g C _{org} m ⁻² yr ⁻¹)				Sediment depth	Dating method	Reference
Country	Mean	Sd	Range	N (site)	(cm)		
Salt marshes							
Norway	253	190	19-603	5 x 2*	4.75-10.75	²¹⁰ Pb	(Ward, 2020)
Denmark	30.3	14	17-45	3	14-30	²¹⁰ Pb	(Graversen et al., 2022)
Eelgrass							
Greenland	5.1	4.8	1.3-10.5	3	Ca. 10	²¹⁰ Pb	(Marbà et al., 2018)
Denmark	35.2		21-49	10	25	Not measured; sedimentation rate from literature: 2.02 mm yr ⁻¹	(Röhr et al., 2016)
Denmark	33	7.5 [^]	[^]	[^]	15	Repeated measure (0-2 yr) in restoration site versus reference site	(Lange et al., 2022)
Finland	5.2			10	25	Not measured; sedimentation rate from literature: 2.02 mm yr ⁻¹	(Röhr et al., 2016)
Macroalgae (tidal and subtidal)							
Norway	19.9**	5		4 (1)	40	²¹⁰ Pb	(Frigstad et al., 2021)

*Ward examined both high and low marsh at 5 sites.

**C-sequestration as particulate organic matter buried in coastal shelf sediments and the deep-sea based on a mass balance approach (aka Krause-Jensen and Duarte, 2016).: The estimate quantifies the macroalgal C-sequestration (which occurs beyond the habitat in adjacent soft sediments) relative to the macroalgal habitat area.

[^]Standard error, N not given, but representing detailed subsampling in large scale restoration plots.

We searched for data for each of the Nordic countries; hence if information is lacking for a given country/habitat type this indicates that we are not aware of any data. Sediment depth represent the depths used in the quantification of sequestration rates. Given rates are for particulate organic carbon (POC) sequestration only. Norway: no sequestration rates for eelgrass and other rooted vegetation. Sweden: Information exists only for eelgrass.

production as particulate and dissolved organic carbon (POC and DOC, respectively) to adjacent systems. This export supports secondary producers in the sea or on beaches (when washed ashore), while a small fraction is sequestered in C-sinks in marine sediments or the deep sea (Krause-Jensen and Duarte, 2016; Quirós et al., 2019; Ortega et al., 2020). This variety of export pathways and fates of macroalgal organic carbon makes it complex to constrain carbon budgets and sequestration rates for kelp and rockweed habitats. And because macroalgal C-sequestration in sediments occurs beyond the habitat, estimates are not directly comparable to those of sediment C-sinks in salt marshes and seagrass meadows.

In the Nordic region, the first studies documenting macroalgal export to sediment C-sinks are appearing. For northern Norway, the export rate of kelp to adjacent and off-shore sediments is quantified at levels close to the annual net kelp primary production, implying that most of the primary production is exported beyond the habitat. Part of this export supports sediment C-stocks and sequestration (Filbee-Dexter et al., 2018; Wernberg and Filbee-Dexter, 2018; Filbee-Dexter et al., 2020; Pedersen et al., 2020). For example, isotopic tracers show that macroalgae contribute to C-stocks in Danish eelgrass sediments (Thormar et al., 2016), environmental DNA (eDNA) document macroalgal C in coastal Greenland sediments (Ørberg et al., 2022), and eDNA supplemented with quantitative polymerase chain reaction (qPCR) document that macroalgae contribute to C-stocks and sequestration in coastal Norwegian sediments (Frigstad et al., 2021). An ongoing global study with Danish and Norwegian participation is quantifying the potential contribution of macroalgal farming to C-sequestration in sediments below the farms (www.oceans2050.com/seaweed). But no peer-reviewed sequestration rates of neither farmed or wild macroalgae are yet available from the Nordic region.

A first coarse, non-peer reviewed, estimate of the contribution of Nordic (excluding Greenland) kelp and rockweed habitats to C-sequestration was recently derived from the combined area of Nordic kelp forests (10,990 km²) and rockweed beds (5,556 km²), multiplied by an estimate of sequestration of Nordic macroalgal POC per macroalgal habitat area ($19.9 \pm 5 \text{ g C m}^{-2} \text{ yr}^{-1}$, Table 3, Frigstad et al., 2021). This POC-sequestration estimate is based on a mass balance approach similar to that developed for the global estimate of macroalgal C-sequestration (Krause-Jensen and Duarte, 2016) but with Nordic data on macroalgal NPP and POC export. On this basis, the sequestration of macroalgal POC in coastal shelf sediments and the deep sea was coarsely estimated at $0.328 \pm 0.082 \text{ Gg Tg C per year}$ (corresponding to $1.18 \pm 0.3 \text{ million tonnes CO}_2\text{e yr}^{-1}$, Frigstad et al., 2021). This first rough assessment needs further verification by peer-reviewed regional empirical data.

All in all, our review documents considerable Nordic information on sediment C-stocks of seagrass habitats, but limited information on C-sequestration rates for seagrass sediments and limited information on both sediment C-stocks and C-sequestration rates for other Nordic blue carbon habitats. While the compiled information represents sequestration of POC, DOC from BC habitats may also contribute to C-sequestration if being refractory or if exported to the deep sea

(e.g. Krause-Jensen and Duarte, 2016). Quantification of this component is associated with large uncertainties and major knowledge gaps about DOC export pathways, mineralization and sequestration rates at both Nordic and global scales (Paine et al., 2021). Coarse estimates suggest that DOC may contribute more than 14% of the total C-sequestration supported by seagrasses and up to 67% of the total C-sequestration supported by macroalgae (Krause-Jensen and Duarte, 2016; Duarte and Krause-Jensen, 2017; Frigstad et al., 2021 and references herein).

Another knowledge gap is the potential emission of greenhouse gases (GHG) from Nordic BC habitats. Natural GHG's that might escape from Nordic BC habitats are methane (CH₄) and nitrous oxide (N₂O), in addition of carbon dioxide (CO₂), which may reduce the net climate change mitigation capacity (Al-Haj and Fulweiler, 2020). For eelgrass, a recent study on Nordic eelgrass sediments showed only minor emissions of methane (Asplund et al., 2022), and a study from the east coast of the USA documented that restored eelgrass meadows still represent a net sink of CO₂ ($0.42 \text{ t CO}_2\text{e ha}^{-1} \text{ yr}^{-1}$) after including methane emission from the meadows (ca. 10% of the sequestration, Oreska et al., 2020). For salt marshes, the tidal regime as well as the salinity are important variables affecting the potential fluxes of methane or nitrous oxide emission and, thereby, the net C-sequestration capacity of marshes (Al-Haj and Fulweiler, 2020; Arias-Ortiz et al., 2021). Non-tidal and brackish salt marshes, such as those in the inner Baltic Sea, are likely especially prone to methane or nitrous oxide emission.

In addition to their C-sequestration capacity, marine vegetated habitats support a wide range of ecosystem functions and services such as (1) provisioning of biodiversity, including habitat and nursery grounds for economically important fish (birds in salt marshes), (2) a coastal nutrient filter that mitigates eutrophication, and (3) climate change buffering by natural coastal protection, alleviation of ocean acidification, and sediment accretion, (4) oxygen production, (5) protection of cultural heritage, and (6) aesthetical values. These aspects have received significant attention internationally (e.g. Costanza et al., 2014; Nordlund et al., 2016; Ruiz-Frau et al., 2017; Narayan et al., 2017) and will not be dealt with in any detail here. We solely underline that such functions are also documented in Nordic BC habitats (Table S6) and support the win-win aspect of the protection and restoration of BC habitats also in the Nordic region.

MANAGEMENT OF NORDIC BLUE CARBON HABITATS

This section gives an overview of the management of Nordic BC habitats in relation to protection against stressors, linking to the outlined policies, and with examples of concrete restoration initiatives. Most management addresses the BC habitats as such or BC sinks beyond the habitats both of which affect the capacity for climate change mitigation and adaptation as well as co-benefits of BC habitats.

Protection

Stressors differ somewhat between BC habitat types but include eutrophication and shading from coastal darkening, land-use changes/coastal development, physical disturbance from fisheries, overfishing, trawling, dredging, dumping, anchoring and harvest of macroalgae, as well as climate change (e.g., Baden et al., 2010; Baden et al., 2012; Boström et al., 2014; Reusch et al., 2018; Frigstad et al., 2020; Krause-Jensen et al., 2021). Protective measures involve nutrient management plans, establishment of marine protected areas (MPAs) involving various controls on fisheries, dumping and anchoring in BC habitats and in C-sink areas beyond the BC habitats (e.g., Legge et al., 2020; Luisetti et al., 2020). Protection also involves controls on harvest of macroalgae as well as harvest/grazing as part of the protection of saltmarshes.

Nutrient Management

Plans to reduce eutrophication are widely implemented across the Nordic region, e.g. in response to the European directives (WFD, 2000; MFS, 2008) and the HELCOM Baltic Sea Action Plan (<https://helcom.fi/baltic-sea-action-plan/nutrient-reduction-scheme/targets/>). In Denmark, for example, a first national Action Plan for the Aquatic Environment was enacted in 1987, followed by additional ones to achieve an overall objective of reducing total nitrogen and total phosphorus discharges by 50 and 80%, respectively. However, because 60% of the country is intensely cultivated, nutrient loadings remain a problem (Riemann et al., 2016).

Marine Protected Areas

MPAs in the Nordic region include sites designated under national laws as well as under the Natura 2000 network of nature protection areas. The latter encompasses Special Areas of Conservation under the Habitats Directive and Special Protection Areas under the Birds Directive (**Figure 2C**). Four of the Nordic MPAs are appointed UNESCO Marine World Heritage Sites: Surtsey (Iceland), West Norwegian Fjords – Geirangerfjord and Nærøfjord (Norway), Wadden Sea (Germany/Netherlands/Denmark) and High Coast/Kvarken Archipelago (Finland) of which the first three support documented BC habitats (UNESCO, 2020).

The current proportion (in %) of “protected” marine area varies across the Nordic region with 4.5% in Norway [Meld. St. 29 (2020–2021) - regjeringen.no], 9.8% in Finland, 12.8% in Sweden and 15.2% in Denmark (<https://biodiversity.europa.eu/countries/>). However, the 2021 Nordic ministerial declaration on biodiversity, oceans and climate, the EU biodiversity strategy, the first draft of the CBD post-2020 global biodiversity and the High-level panel for a Sustainable Ocean Economy all support regional and global goals of 30% MPAs.

The actual protection of habitats within MPAs also varies considerably as the term “protection” is subject to interpretation. For the Baltic Sea in general, trawling remains a major stressor despite various controls (de Liedekerke et al., 2020). In Denmark, fisheries have been allowed in most protected areas except in the Sound (Øresund) and except for a zone of 200 m surrounding

stone reefs and bubble reefs, which implies that only about 2% of the marine areas are protected from trawling; however, a new marine plan aims to increase the targets. In NW Sweden, ~7% of the eelgrass area is negatively affected by small-scale construction of docks and marinas, even though habitats located less than 100 m from the shoreline are protected against exploitation by national law, and ~50% of the eelgrass area is located within protected areas (Eriander et al., 2017).

Under the Habitats Directive, salt marshes are designated a habitat type and are therefore more directly protected than eelgrass meadows and kelp forests, which just form part of the habitat types “Large shallow inlets and bays”, “estuaries” or “mudflats”. The Finnish Nature Conservation Act hence protects coastal meadows but not (yet) eelgrass meadows. In Iceland, national laws specify protection of mudflats and, thereby, eelgrass and salt marshes.

Controls on Harvest of Marine Vegetation

The harvest of wild kelp (*Laminaria hyperborea*) in Norway amounts to ~150,000 metric tons per year (Steen, 2018), representing ~0.3% of the estimated standing stock of living biomass (55 million metric tons, Frigstad et al., 2021; Gundersen et al., 2021). Usually, the Norwegian harvest area is ~6% of a regional kelp resource (Norderhaug et al., 2020), but can exceed 75% at monitoring points (Steen et al., 2018). The harvested yield has been stable for the past 30 years but is foreseen to increase as the number of commercial actors have recently doubled (from 1 to 2). Kelp harvest is regulated by law and regulations, and the Norwegian coast is divided into harvesting zones by latitude minutes (1 nautical mile), where each zone is open for harvest every 5–6 years, to allow for kelp regrowth. There is no upper limit on biomass harvest by regulations, and each zone can theoretically be depleted every 5 years. In practice, commercial actors prioritize areas with a high biomass per area and bottom conditions that fit the harvesting equipment. This often results in a patchy harvest. Harvest may be restricted based on the outcome of monitoring conducted half a year prior to planned harvesting. If the commercial demand is increasing in the future, and more efficient harvesting equipment is developed, macroalgae biomass, habitats and ecosystems may be severely impacted without further legislation.

The rockweed *Ascophyllum nodosum* is also harvested commercially in Norway, with yearly landings around 20,000 metric tons (Directorate of Fisheries, Norway, www.fiskeridir.no/tall-og-analyse/aapne-data). The Marine Resource Act does not regulate this harvesting, as it largely takes place in the intertidal, which is private property, and can be conducted with permission from the landowners.

In Iceland, the harvest of macroalgae is mainly confined to Breiðafjörður. The harvest of *A. nodosum* amounts to 15,000–20,000 metric tons per year and 4,000–7,000 metric tons for *L. digitata* and *L. hyperborea* (Ingólfsson, 2010; Gunnarsson et al., 2019). The Marine & Freshwater Research Institute has advised that the annual harvest 2018–2022 of *A. nodosum* in Breiðafjörður should not exceed 40,000 metric tons, or around 3% annually of estimated rockweed biomass in the area (Hafro.is, 2018).

There is limited tradition for commercial exploitation of wild macroalgae in Denmark, as well as in the Baltic Sea in general, but a significant harvest of pristine communities of the drifting red algae *Furcellaria lumbricalis* took place in the central Kattegat in the 1940–1960s and decimated the population (Schramm, 1998; Weinberger et al., 2020).

For salt marshes, overgrowth and shadowing by tall grass (e.g. reeds) is being managed by grazing and hay harvest to increase biodiversity. In Denmark, around two thirds of the total area of mapped salt marshes (2016–2019) is managed by such practices. In Finland, abandonment of traditional agricultural activities (Lehikoinen et al., 2017) has rendered boreal coastal meadows endangered (Schulman et al., 2008), and the conservation status under the EU Habitats Directive was assessed as unfavorable or bad in 2007 and 2013. However, due to new management efforts, the total area of Finnish salt marshes has now increased from 60 to 62 km², and further supporting initiatives are in place *via* national funding (strategic nature conservation, restoration and management programme HELMI, 2020–2030) and EU funding (LIFE-project CoastNet LIFE, 2018–2025).

Restoration

The Nordic region holds several examples of active restoration of salt marshes, eelgrass meadows and kelp forests. Restoration can supplement protective measures and facilitate or speed up the natural recovery process. Below, we briefly summarize restoration techniques and provide (non-exhaustive) examples of restoration initiatives in the region (**Figure 2D** and **Table S7**). The Nordic restoration examples are typically individual projects that are not part of a coordinated large-scale effort and there is, as yet, no coordinated follow-up on restoration success, planning and guidance at national or Nordic scale.

Salt Marsh Restoration

As many former salt marsh areas were transformed to agriculture land by dikes, drainage and pumping, removal of these structures to reestablish the natural hydrology forms direct restoration measures. Such restoration links to “managed coastal realignment”, which is a new coastal protection strategy integrating coastal and nature protection by removing or abandoning coastal protection measures to reestablish natural processes and dynamics (Schernewski et al., 2018). There are examples from e.g. the southern Baltic Sea (Germany) and Denmark (Tryggevlev Nor) (Karnauskaitė et al., 2018) citing the database “Our Coast” and the European Maritime Spatial Planning (MSP) platform database (www.msp-platform.eu). However, as saltmarshes are not necessarily positively conceived by the public, and engineering solutions to coastal protection are probably more generally acknowledged, there is a need for thorough public communication and involvement to build confidence and develop best practices (Stewart-Sinclair et al., 2020).

Eelgrass Restoration

Over the past decade, several eelgrass restoration efforts have been undertaken in the Nordic region (**Figure 2D** and **Table S7**). The activities have benefitted from international experience,

which highlights (1) the need for careful site selection so that restoration takes place where eelgrass used to grow and where habitat requirements are presently fulfilled, (2) the importance of sufficient spatial scale of the restoration to increase the chance of building resilience in the new patches, and (3) ensuring sufficient time perspective (years) for monitoring the effects of the restoration (Bayraktarov et al., 2016; van Katwijk et al., 2016; Orth et al., 2020). Persistent Nordic restoration efforts confirm these recommendations and provide best practices for site selection and full-scale restoration (e.g. Moksnes et al., 2016; Lange et al., 2022). The most successful Nordic eelgrass restorations have involved eelgrass transplants rather than seeds, and have sometimes involved anchoring of shoots, stabilization of sediments by protective structures, sandcapping, enclosures to avoid bioturbation, traps to reduce crabs, or co-restoration with blue mussels in order to facilitate eelgrass survival and growth (Moksnes et al., 2016; Gagnon et al., 2021; van der Heide et al., 2021; Flindt et al., 2022; Lange et al., 2022) (**Table S7**). Target areas for restoration have been identified by modelling where eelgrass habitat requirements are fulfilled (e.g. Canal-Vergés et al., 2016; Flindt et al., 2016) supplemented with further site inspection and transplantation trials (Lange et al., 2022). However, because eelgrass restoration is labor intensive, costly and with no guarantee of success, protection of existing meadows is a management priority (Moksnes et al., 2016).

Macroalgal Restoration

The main threats to macroalgae include but are not limited to removal of anchoring stones, aggressive fishery practices, and destructive grazing by sea urchins. In the cases of macroalgal habitat loss due to removal of stones, restoration of the habitat requires the establishment of new reefs. The Blue Reef project in the Kattegat (www.blureef.dk) represents a successful example of macroalgal restoration. The experience gained from this and other projects led to a manual on best practices (Dahl et al., 2016a) and has inspired additional projects in Danish coastal waters (e.g. in Als Fjord and Limfjorden, and planned projects).

Restoration of macroalgae on barren grounds after destructive grazing by sea urchins has been carried out along the Norwegian coast by removing sea urchins, transplanting *Laminaria hyperborea* and *Saccharina latissima* kelp, planning sites of action taking interactions with other species, such as crabs, into account (Christie et al., 2019 and references therein). Based on this work, a strategy on how to recover kelp ecosystems from urchin barrens has been developed (Verbeek et al., 2021). “Green gravel” (i.e. small rocks seeded with kelp) has also recently been applied to restore sugar kelp (Fredriksen et al., 2020). The project MERCES has restored macroalgal habitats across Europe and concluded that active intervention (such as sea urchin removal) is required if the cause behind the habitat degradation and loss is not dealt with at a broader overall scale (Bekkby et al., 2020), e.g. by ensuring that intact fish populations control the sea urchin populations (Norderhaug et al., 2021). Internationally, Japan has the longest experience on macroalgal restoration including transplantation of kelp and removal of sea urchins, and their practice with country-wide restoration teams

TABLE 4 | Proposed Nordic science and management roadmap for Blue Carbon.**Science roadmap**

- * Establish maps of past and current **area distribution of Nordic BC habitats** and define strategies for future mapping, e.g. remote sensing techniques (satellites, airplanes, drones) and distribution modelling supported by field observations
- * Further quantification of **BC stocks, sequestration rates**, export pathways and overall carbon transport rates between sources and sinks. This also involves increased understanding of BC sinks beyond BC habitats
- * Estimate the **potential of BC strategies to increase BC areas and associated BC gain** via protection, restoration, and macroalgal farming, and identify key target areas for BC strategies based on knowledge on historic distribution, habitat suitability and connectivity
- * Quantify **co-benefits** of Nordic BC strategies for ecosystem biodiversity, ecological status and other Ecosystem Services
- * Database on **Nordic BC restoration** projects and associated synthesis and evaluation of restoration success and influencing factors
- * Identify ecological effects of **seaweed/kelp farming** and produce sustainability guidelines in order to support benefits and avoid negative effects
- * Quantify **effects of climate change** and its interaction with other stressors on BC habitat distribution and ecological status; and identify vulnerable habitats

Management roadmap

The management road map must be closely connected with the science agenda. Its principal duty includes but is not limited to:

- * Ensure **integrated/holistic management of BC habitats across sectors/ministries** (i.e. climate, coastal protection, biodiversity, eutrophication, fisheries) to address both the diversity of stressors and the full suite of benefits of BC habitats
- * **Coordinate mapping** of BC habitats for **monitoring** status and trends, and **target management** actions
- * **Promote protection of BC ecosystems** as a means to prevent further loss of BC habitats and associated BC stocks accumulated over long timespans (both BC-habitats and BC-sinks)
- * **Promote protection of C-sinks beyond BC habitats** by creating “carbon protecting zones” in areas of high organic C-burial in the shelf or open ocean sediments (cf. Diesing et al., 2021).
- * **Define science-based target areas for restoration** and **facilitate implementation** of restoration initiatives
- * Establish a **database for Nordic BC data** that is linked to existing data collection efforts.
- * **Facilitate sustainable macroalgal farming** via protocols and sound application/approval procedures
- * Promote **climate-smart management strategies** for the protection and restoration of BC habitats (including compounding impacts of climate with other stressors)
- * Data collected and strategies recommended through the BC Roadmap should align with and feed into requirements for **BC habitat integration into Nordic countries' Nationally Determined Contributions (NDCs) under the Paris Agreement (both for climate mitigation and adaptation commitments) and national GHG inventories.***
- * Establish a **Nordic BC task force** to lead coordination, provide technical guidance, promote knowledge exchange, and provide best practices.

* In addition to national scale climate commitments, voluntary carbon markets offer long-term private sector financing for climate mitigation at sub-national scales. The compliance markets are also gaining traction with the recent approval of Article 6 at COP26, which allows for nature-based carbon credits to be traded between countries. Existing methods such as the Verified Carbon Standard (VCS) - overseen and managed by Verra - provide access to carbon markets for the conservation and restoration of salt marshes, seagrasses and mangroves. Unfortunately, there is currently no methodology for macroalgae. Also, despite a methodology being available for seagrasses, no seagrass restoration project has been validated to date under Verra, probably due to the complexity of carbon flows and fluxes in the system and eelgrass restoration is relatively “new” compared to mangrove restoration.

Keywords are highlighted in bold.

including fishermen (Watanuki et al., 2010; see also annex of Duarte et al., 2020) may inspire similar action in the Nordic region.

Macroalgal farming could potentially benefit wild macroalgal forests by leading to reduced harvest of wild macroalgae. Moreover, sustainable macroalgal farming may contribute associated ecosystem services, including uptake of excess nutrients, and supporting C-sequestration and reduced emissions, provided that the farming follows best practice sustainability standards (Duarte et al., 2022). Sustainability standards are needed to avoid potential negative effects of the farming such as competition of resources or physically damaging native habitats, and/or spreading of non-native strains (Campbell et al., 2019). Verified standards for C-accounting and C-offsetting connected with seaweed farming are also lacking and would require challenging and careful documentation (Hurd et al., 2022). The interest in the exploitation of macroalgae through harvest of living biomass and beach cast as well as *via* seaweed farming is on the rise both in the Nordic Atlantic region and the Baltic region, although the low salinity of the Baltic Sea presents suboptimal growth conditions for most species (Weinberger et al., 2020; Araújo et al., 2021). Among the Nordic countries, Norway has the largest number of seaweed farms (>27) and a large potential for macroalgal cultivation both inshore and offshore (Broch et al.,

2019). The Norwegian seaweed cultivation industry is predicted to reach 4 million metric tons annually by 2030 and 20 million metric tons annually by 2050 (Olafsen et al., 2012). Macroalgal cultivation is also taking place in Denmark (6 farms), Faroe Island (2 farms), Greenland, Iceland and Sweden (one farm in each area) (Araújo et al., 2021).

KNOWLEDGE GAPS IN NORDIC BLUE CARBON SCIENCE AND MANAGEMENT

Scientific BC knowledge gaps include incomplete information on habitat area, changes in area, C-stocks, and C-sequestration rates and C-fluxes/budgets in general, including emission of methane and nitrous oxide. Another important information gap is to what extent it is possible to increase the C-sequestration of Nordic BC habitats *via* restoration and *via* protection against further loss, and thereby contribute to climate change mitigation. This is particularly the case for macroalgae for which information is lacking in each of the listed components, which prevents inclusion of macroalgal restoration and protection in BC policies. Salt marshes are also largely overlooked in BC context with very limited information on C-stocks and sequestration in the Nordic context, although areas are being assessed according to requirements of the Habitats Directive where this is relevant.

The degree of success of restoration projects and their resulting ecosystem effects on C-sequestration are also poorly quantified as are large-scale ecosystem effects of macroalgal farming. Moreover, the effects of climate change on BC habitats need further exploration, both regarding plant communities, their performance and vulnerability, and regarding BC stocks and decomposition rates. These gaps limit both the possibility to quantify the climate change mitigation potential of Nordic BC habitats and their role in marine C-budgets at the Nordic scale. However, the recently completed Nordic Blue Carbon project provided, as mentioned, a major step forward in this direction for eelgrass and macroalgal communities (Frigstad et al., 2021). A recently initiated Nordic collaboration on salt marshes (“NordSalt” funded by EU) will increase the knowledge on Nordic salt marsh distribution, dynamics, C-storage, and management.

Managerial gaps include lacking a Nordic BC managerial roadmap, poor/unclear protection status of BC habitats, and limited focus on integration of management across sectors (e.g. environment/fisheries/climate/food), including optimizing management measures in the face of climate change. Regarding effects of climate change on the habitats, there is a need for considering projected changes in habitat extent and species ranges in relation to global change scenarios for the Nordic region. Perry et al. (2020) identified some areas in Sweden particularly vulnerable to combined global change effects, which should be considered in management schemes. Also, shallow Danish eelgrass meadows are more vulnerable to warming than deeper, cooler areas and management should facilitate the colonization of deeper areas by continued nutrient load reductions and prevention of mussel trawling (Krause-Jensen et al., 2021). Regarding potential effects of the habitats on the climate, there is only scattered knowledge on the mitigation potentials of Nordic BC habitats in terms of climate change mitigation and co-benefits (Gundersen et al., 2016; Frigstad et al., 2021).

Last but not least, further integration across sectors is needed, both science-management integration, integrated management of stressors to increase protection against eutrophication, physical damage as well as climate change, and integrated management of the functions of BC habitats in relation to biodiversity, climate change mitigation and adaptation, and nutrient filter effect.

A NORDIC BLUE CARBON ROADMAP

The Nordic Blue Carbon project (nordicbluecarbon.no, Frigstad et al., 2021) recently highlighted policy recommendations, which we support and expand by also including salt marshes: “This group of scientists [...] urges for immediate and concerted policy actions to safeguard the Nordic Blue Carbon habitats, such as salt marshes, seagrass meadows, kelp forests and rockweed beds, especially through increased protection of coastal ecosystems by establishing marine protected areas and by increased efforts in reducing human pressures, such as nutrient pollution,

overfishing and habitat fragmentation. There is enough scientific evidence to underpin the importance of these coastal ecosystems to support this call for action.” A similar message “Blue Carbon can’t wait” was also recently communicated as an editorial of the Science magazine (Douve, 2021).

We propose a Nordic Blue Carbon roadmap for science and management along with a regional task force of Nordic experts to increase coordination and knowledge sharing, close the identified knowledge gaps, secure scientific data, and support the management of Nordic vegetated coastal and marine habitats as nature-based solutions to climate change with co-benefits for biodiversity and ecosystem health (Table 4). The science- and management roadmaps must be tightly connected, and linked to efficient communication to raise awareness to stimulate public and policy interest and involvement.

Among the key actions needed is to generate more evidence to understand and constrain the huge variability in C-storage and climate change mitigation potential of the Nordic BC habitats and understand how it varies along the steep environmental gradients. This involves better quantification of both areas and C-storage, as well as predictive models for the long-term C-storage capacity. Recent advances in remote sensing techniques (satellites and flying drones) facilitate large-scale spatial monitoring and enables mapping and monitoring of (at least the shallow) vegetation belts at Nordic scales, but further improvement is needed. Future BC strategies should also identify the best methods and key target areas for restoration and protection based on historical distribution and habitat suitability in present and future climate scenarios, and have focus on habitat connectivity to guide. In addition, we recommend to explore the potential for including BC habitat in the Nordic countries’ NDCs or national greenhouse gas inventories. Importantly, such initiatives should supplement and not reduce efforts to cut fossil GHG emissions. While IPCC guidelines exist for seagrass and saltmarsh habitats, they are still missing for macroalgae (the brown algae being most relevant to the Nordic region), and a further action point is to support the development of macroalgal BC guidelines (Table 4).

The large attendance of both scientists, managers and policy makers to the Nordic BC meeting in Copenhagen in 2019 already then demonstrated the scope for a Nordic BC collaboration and the relevance of a Nordic BC roadmap (Table S8). The work discussed here shows that while progress is being made and there is recognition that more data collection and dissemination is needed, there remains key knowledge gaps and challenges to realizing the full climate benefit and co-benefits of Nordic BC systems. Blue Carbon is clearly a concept at the intersection of science and policy, stressing the need of good science to advise and guide policy that will lead to climate mitigation, adaptation through conservation and restoration of these ecosystems. A strategic roadmap, supported by a formalized Nordic BC platform that provides coordination, prioritization, and knowledge exchange etc., will be essential in generating future joint Nordic BC collaborations and solutions towards climate change mitigation.

AUTHOR CONTRIBUTIONS

All authors contributed to the planning of the manuscript and provided information for their region and area of expertise. DK-J, HG and KH completed the first full draft, all authors approved the final version and JT also edited the references.

FUNDING

Velux Fonden provided support to DK-J, MH, AG, and GB through the project “Blå Skove (Blue Forests), no. 28421” and through support for the BCI workshop in Copenhagen. The Copenhagen workshop was also supported by NASA (grant number: 80NSSC19K1627) to BCI. The Norwegian Environment Agency and the Nordic Council of Ministers provided support via the Nordic Blue Carbon project (“Blue Carbon – climate adaptation, CO₂ uptake and sequestration of carbon in Nordic blue forests”; <https://nordicbluecarbon.no/>). DK-J also received funding from the Independent Research Fund Denmark (CARMA; grant number: 8021-00222B) regarding Greenland and from the European Commission H2020 (FutureMARES; grant number: 869300) regarding the

Baltic Sea. CB received financial support from the Åbo Akademi University Foundation Sr. We further acknowledge economic support from the Foundation for Baltic and East European studies (Östersjöstiftelsen) via the project ClimScape led by MG (grant number: 21-GP-0005). KH, HG, TB, SS, and HF received funding from the Norwegian Institute for Water Research (NIVA).

ACKNOWLEDGMENTS

All participants at the Blue Carbon Initiative’s (BCI) Nordic Blue Carbon workshop, Copenhagen, September 2019 are thanked for their contributions. Ole Geertz-Hansen is, in particular, thanked for information on marine management in Greenland.

SUPPLEMENTARY MATERIAL

The Supplementary Material for this article can be found online at: <https://www.frontiersin.org/articles/10.3389/fmars.2022.847544/full#supplementary-material>

REFERENCES

- Adam, P. (1990). *Saltmarsh Ecology* (Cambridge: Cambridge University Press). doi: 10.1017/CBO9780511565328
- Al-Haj, A. N., and Fulweiler, R. W. (2020). A Synthesis of Methane Emissions From Shallow Vegetated Coastal Ecosystems. *Glob. Change Biol.* 26, 2988–3005. doi: 10.1111/gcb.15046
- Andersen, J. H., Halpern, B. S., Korpinen, S., Murray, C., and Reker, J. (2015). Baltic Sea Biodiversity Status vs. Cumulative Human Pressures. *Estuar. Coast. Shelf Sci.* 161, 88–92. doi: 10.1016/j.ecss.2015.05.002
- Aoki, L. R., McGlathery, K. J., and Oreska, M. P. J. (2020). Seagrass Restoration Reestablishes the Coastal Nitrogen Filter Through Enhanced Burial. *Limnol. Oceanogr.* 65, 1–12. doi: 10.1002/lno.11241
- Araújo, R. M., Assis, J., Aguillar, R., Airoldi, L., Bárbara, I., Bartsch, I., et al. (2016). Status, Trends and Drivers of Kelp Forests in Europe: An Expert Assessment. *Biodivers. Conserv.* 25, 1319–1348. doi: 10.1007/s10531-016-1141-7
- Araújo, R., Vázquez Calderón, F., Sánchez López, J., Azevedo, I. C., Bruhn, A., Fluch, S., et al. (2021). Current Status of the Algae Production Industry in Europe: An Emerging Sector of the Blue Bioeconomy. *Front. Mar. Sci.* 7. doi: 10.3389/fmars.2020.626389
- Arias-Ortiz, A., Oikawa, P. Y., Carlin, J., Masqué, P., Shahan, J., Kanneg, S., et al. (2021). Tidal and Nontidal Marsh Restoration: A Trade-Off Between Carbon Sequestration, Methane Emissions, and Soil Accretion. *J. Geophys. Res. Biogeosci.* 126 (12), e2021JG006573.
- Asplund, M. E., Bonaglia, S., Boström, C., Dahl, M., Deyanova, D., Gagnon, K., et al. (2022). Methane Emissions From Nordic Seagrass Meadow Sediments. *Front. Mar. Sci.* 8. doi: 10.3389/fmars.2021.811533
- Baden, S., Boström, C., Tobiasson, S., Arponen, H., and Moksnes, P. O. (2010). Relative Importance of Trophic Interactions and Nutrient Enrichment in Seagrass Ecosystems: A Broad-Scale Field Experiment in the Baltic-Skagerrak Area. *Limnol. Oceanogr.* 55, 1435–1448. doi: 10.4319/lo.2010.55.3.1435
- Baden, S., Emanuelsson, A., Pihl, L., Svensson, C. J., and Åberg, P. (2012). Shift in Seagrass Food Web Structure Over Decades is Linked to Overfishing. *Mar. Ecol. Prog. Ser.* 451, 61–73. doi: 10.3354/meps09585
- Baden, S., Gullström, M., Lunden, B., Pihl, L., and Rosenberg, R. (2003). Vanishing Seagrass (*Zostera Marina*, L.) in Swedish Coastal Waters. *Ambio* 32, 374–377. doi: 10.1579/0044-7447-32.5.374
- Barbier, E. B., Hacker, S. D., Kennedy, C., Koch, E. W., Stier, A. C., and Silliman, B. R. (2011). The Value of Estuarine and Coastal Ecosystem Services. *Ecol. Monogr.* 81, 169–193. doi: 10.1890/10-1510.1
- Bayraktarov, E., Saunders, M. I., Abdullah, S., Mills, M., Beher, J., Possingham, H. P., et al. (2016). The Cost and Feasibility of Marine Coastal Restoration. *Ecol. Appl.* 26, 1055–1074. doi: 10.1890/15-1077
- Bekkby, T., Moy, F. E., Olsen, H., Rinde, E., Bodvin, T., Bøe, R., et al. (2013). “The Norwegian Programme for Mapping of Marine Habitats – Providing Knowledge and Maps for ICZMP,” in *Global Challenges in Integrated Coastal Zone Management*. Eds. E. Moksness, E. Dahl and J. Støttrup. Oxford, UK: John Wiley & Sons, Ltd, 19–30. doi: 10.1002/9781118496480.ch2
- Bekkby, T., Papadopoulou, N., Fiorentino, D., McOwen, C. J., Rinde, E., Boström, C., et al. (2020). Habitat Features and Their Influence on the Restoration Potential of Marine Habitats in Europe. *Front. Mar. Sci.* 7. doi: 10.3389/fmars.2020.00184
- Blomqvist, M., and Olsson, P. (2007). *Översyn Av Det Nationella Marina Övervakningsprogrammet För Vegetationsklädda Bottenar* (Stockholm, Sweden: Swedish Environmental Protection Agency). Available at: <http://www.diva-portal.se/smash/get/diva2:717044/FULLTEXT01.pdf>.
- Borgersen, G., Rinde, E., Moy, S., and Gundersen, H. (2020) *Are There Saltmarshes in Norway? An Assessment of the Term Against Norwegian Habitat Types (NiN)*. NIVA Report 7558-2020. Available at: <https://hdl.handle.net/11250/2718857>.
- Boström, C., Baden, S., Bockelmann, A. C., Dromph, K., Fredriksen, S., Gustafsson, C., et al. (2014). Distribution, Structure and Function of Nordic Eelgrass (*Zostera Marina*) Ecosystems: Implications for Coastal Management and Conservation. *Aquat. Conserv.* 24, 410–434. doi: 10.1002/aqc.2424
- Boström, C., Baden, S. P., and Krause-Jensen, D. (2003). “The Seagrasses of Scandinavia and the Baltic Sea,” in *World Atlas of Seagrasses*. Eds. E. P. Green and F. T. Short (Berkeley, USA: University of California Press), 27–37.
- Boström, C., Bonsdorff, E., Kangas, P., and Norkko, A. (2002). Long-Term Changes of a Brackish-Water Eelgrass (*Zostera Marina* L.) Community Indicate Effects of Coastal Eutrophication. *Estuar. Coast. Shelf Sci.* 55, 795–804. doi: 10.1006/ecss.2001.0943
- Boysen-Jensen, P. (1914). Studies Concerning the Organic Matter of the Sea Bottom. *Rep. Dan. Biol. Stat.* 22, 1–39.
- Broch, O. J., Alver, M. O., Bekkby, T., Gundersen, H., Forbord, S., Handa, A., et al. (2019). The Kelp Cultivation Potential in Coastal and Offshore Regions of Norway. *Front. Mar. Sci.* 5. doi: 10.3389/fmars.2018.00529

- Bruntse, G., Lein, T. E., and Nielsen, R. (1999). *Marine Benthic Algae and Invertebrate Communities From the Shallow Waters of the Faroe Islands - A Baseline Study* (Tórshavn, The Faroe Islands: Kalbak Marine Biological Laboratory, the Faroe Islands).
- Bültmann, H., and Daniëls, F. J. (2013) Greenland Data Stored in the Arctic Vegetation Archive (AVA) in Münster. (Eds). D. A. Walker, A. L. Breen, M. K. Reynolds and M. D. Walker In: *Arctic Vegetation Archive (AVA) Workshop, Krakow, Poland, April 14-16, 2013. CAFF Proceedings Report 10* (Iceland: CAFF). Available at: www.researchgate.net/publication/257021400_Arctic_Vegetation_Archive_AVA_Workshop_Proceedings (Accessed 2021-12-15).
- Campbell, I., Macleod, A., Sahlmann, C., Neves, L., Funderud, J., Øverland, M., et al. (2019). The Environmental Risks Associated With the Development of Seaweed Farming in Europe-Prioritizing Key Knowledge Gaps. *Front. Mar. Sci.* 6. doi: 10.3389/fmars.2019.00107
- Canal-Vergés, P., Petersen, J. K., Rasmussen, E. K., Erichsen, A., and Flindt, M. R. (2016). Validating GIS Tool to Assess Eelgrass Potential Recovery in the Limfjorden (Denmark). *Ecol. Model.* 338, 135–148. doi: 10.1016/j.ecolmodel.2016.04.023
- Christie, H., Andersen, G. S., Bekkby, T., Fagerli, C. W., Gitmark, J. K., Gundersen, H., et al. (2019). Shifts Between Sugar Kelp and Turf Algae in Norway: Regime Shifts or Fluctuations Between Different Opportunistic Seaweed Species? *Front. Mar. Sci.* 6. doi: 10.3389/fmars.2019.00072
- Costanza, R., de Groot, R., Sutton, P., van der Ploeg, S., Anderson, S. J., Kubiszewski, I., et al. (2014). Changes in the Global Value of Ecosystem Services. *Global Environ. Change* 26, 152–158. doi: 10.1016/j.gloenvcha.2014.04.002
- Dahl, M., Asplund, M. E., Björk, M., Deyanova, D., Infantes, E., Isaeus, M., et al. (2020a). The Influence of Hydrodynamic Exposure on Carbon Storage and Nutrient Retention in Eelgrass (*Zostera Marina* L.) Meadows on the Swedish Skagerrak Coast. *Sci. Rep.* 10, 13666. doi: 10.1038/s41598-020-70403-5
- Dahl, M., Asplund, M. E., Deyanova, D., Franco, J. N., Koliji, A., Infantes, E., et al. (2020b). High Seasonal Variability in Sediment Carbon Stocks of Cold-Temperate Seagrass Meadows. *J. Geophys. Res. Biogeosci.* 125, e2019JG005430. doi: 10.1029/2019JG005430
- Dahl, M., Deyanova, D., Gutschow, S., Asplund, M. E., Lyimo, L. D., Karamfilov, V., et al. (2016b). Sediment Properties as Important Predictors of Carbon Storage in *Zostera Marina* Meadows: A Comparison of Four European Areas. *PLoS One* 11, e0167493. doi: 10.1371/journal.pone.0167493
- Dahl, K., Lundsteen, S., and Helmig, S. (2003). *Stenrev, Havbundens Oaser* (Copenhagen, Denmark: Gads Forlag). Available at: http://www2.dmu.dk/1_viden/2_Publikationer/3_miljobib/rapporter/MB02.pdf.
- Dahl, E., Naustvoll, L. J., Steen, H., and Bodvin, T. (2008) *Utreddning Om Bruk Av Ålegras Som Biologisk Kvalitetselement I Forbindelse Med Vannforskriften*. Norwegian Pollution Control Authority Ta2464/2008. Available at: <https://evalueringsportalen.no/evaluering/eu-s-rammedirektiv-for-vann-utredning-om-bruk-av-aalegress-til-klassifisering-av-okologisk-tilstand/ta2464.pdf/@online>.
- Dahl, K., Støttrup, J. G., Stenberg, C., Berggreen, U. C., and Jensen, J. H. (2016a). *Best Practice for Restoration of Stone Reefs in Denmark (Codes of Conduct)* (Aarhus, Denmark: Aarhus University, DCE – Danish Centre for Environment and Energy. Technical Report no. 91). Available at: <http://dce2.au.dk/pub/TR91.pdf>.
- de Liedekerke, V., Thoreson, O., Owen, S., and Berggren, H. G. (2020). *A Sea Under Pressure: Bottom Trawling Impacts in the Baltic* (Solna, Sweden: WWF-Baltic Ecoregion Programme). Available at: www.wwfbaltic.org/report/a-sea-under-pressure-bottom-trawling-impacts-in-the-baltic/.
- Diesing, M., Thorsnes, T., and Bjarnadottir, L. R. (2021). Organic Carbon Densities and Accumulation Rates in Surface Sediments of the North Sea and Skagerrak. *Biogeosciences* 18, 2139–2160. doi: 10.5194/bg-18-2139-2021
- Douville, F. (2021). Blue Carbon Can't Wait. *Science* 373, 601. doi: 10.1126/science.abl7128
- Downie, A. L., von Numers, M., and Boström, C. (2013). Influence of Model Selection on the Predicted Distribution of the Seagrass *Zostera Marina*. *Estuar Coast Shelf S* 121, 8–19. doi: 10.1016/j.ecss.2012.12.020
- Duarte, C. M., Agusti, S., Barbier, E., Britten, G. L., Castilla, J. C., Gattuso, J.-P., et al. (2020). Rebuilding Marine Life. *Nature* 580, 39–51. doi: 10.1038/s41586-020-2146-7
- Duarte, C. M., Bruhn, A., and Krause-Jensen, D. (2022). A Seaweed Aquaculture Imperative to Meet Global Sustainability Targets. *Nat. Sustainability* 5, 185–193. doi: 10.1038/s41893-021-00773-9
- Duarte, C. M., and Krause-Jensen, D. (2017). Export From Seagrass Meadows Contributes to Marine Carbon Sequestration. *Front. Mar. Sci.* 4. doi: 10.3389/fmars.2017.00013
- Duarte, C. M., Losada, I. J., Hendriks, I. E., Mazarrasa, I., and Marbà, N. (2013). The Role of Coastal Plant Communities for Climate Change Mitigation and Adaptation. *Nat. Climate Change* 3, 961–968. doi: 10.1038/nclimate1970
- Dunic, J. C., Brown, C. J., Connolly, R. M., Turschwell, M. P., and Côté, I. M. (2021). Long-Term Declines and Recovery of Meadow Area Across the World's Seagrass Bioregions. *Glob. Change Biol.* 27, 4096–4109. doi: 10.1111/gcb.15684
- Envall, M., and Isaksson, I. (2012). *Ålgräsutbredning (Zostera Sp.) I Västra Götalands Län Sommaren 2008. Länsstyrelsen I Västra Götalands Län, Vattenvårdsenheten. Report No. 2012:58. Länsstyrelsen report series, Västra Götalands län, Sweden*
- Eriander, L., Laas, K., Bergström, P., Gipperth, L., and Moksnes, P. O. (2017). The Effects of Small-Scale Coastal Development on the Eelgrass (*Zostera Marina* L.) Distribution Along the Swedish West Coast - Ecological Impact and Legal Challenges. *Ocean Coast. Manage.* 148, 182–194. doi: 10.1016/j.ocecoaman.2017.08.005
- Espeland, S. H., and Knutsen, H. (2014). Rapport fra høstundersøkelsene med strandnot i Indre Oslofjord 2014. *Havforskningsinstituttet* 31-2014, 1–15.
- Evans, D., and Roekarts, M. (2019). *Interpretation Manual of the Habitats Listed in Resolution No. 4 (1996) Listing Endangered Natural Habitats Requiring Specific Conservation Measures. Fourth Draft Version 2019* (Council of Europe, Strasbourg). Available at: <https://rm.coe.int/interpretation-manual-of-the-habitats-listed-in-resolution-no-4-1996-/168098c68c>
- Filbee-Dexter, K., and Wernberg, T. (2018). Rise of Turfs: A New Battlefield for Globally Declining Kelp Forests. *Bioscience* 68, 64–76. doi: 10.1093/biosci/bix147
- Filbee-Dexter, K., Wernberg, T., Grace, S. P., Thormar, J., Fredriksen, S., Narvaez, C. N., et al. (2020). Marine Heatwaves and the Collapse of Marginal North Atlantic Kelp Forests. *Sci. Rep.* 10, 13388. doi: 10.1038/s41598-020-70273-x
- Filbee-Dexter, K., Wernberg, T., Norderhaug, K. M., Ramirez-Llodra, E., and Pedersen, M. F. (2018). Movement of Pulsed Resource Subsidies From Kelp Forests to Deep Fjords. *Oecologia* 187, 291–304. doi: 10.1007/s00442-018-4121-7
- Flindt, M. R., Oncken, N. S., Kuusemäe, K., Lange, T., Aaskoven, N., Winter, S., et al. (2022). Sand-Capping Stabilizes Muddy Sediment and Improves Benthic Light Conditions in Eutrophic Estuaries: Laboratory Verification and the Potential for Recovery of Eelgrass (*Zostera Marina*). *J. Sea Res.* 181, 102177. doi: 10.1016/j.seares.2022.102177
- Flindt, M. R., Rasmussen, E. K., Valdemarsen, T., Erichsen, A., Kaas, H., and Canal-Vergés, P. (2016). Using a GIS-Tool to Evaluate Potential Eelgrass Reestablishment in Estuaries. *Ecol. Model.* 338, 122–134. doi: 10.1016/j.ecolmodel.2016.07.005
- Fredriksen, S., Christie, H., and Saethre, B. A. (2005). Species Richness in Macroalgae and Macrofauna Assemblages on *Fucus Serratus* L. (Phaeophyceae) and *Zostera Marina* L. (Angiospermae) in Skagerrak, Norway. *Mar. Biol.* 1, 2–19. doi: 10.1080/17451000510018953
- Fredriksen, S., Filbee-Dexter, K., Norderhaug, K. M., Steen, H., Bodvin, T., Coleman, M. A., et al. (2020). Green Gravel: A Novel Restoration Tool to Combat Kelp Forest Decline. *Sci. Rep.* 10, 3983. doi: 10.1038/s41598-020-60553-x
- Fredshavn, J., Nygaard, B., Ejrnæs, R., Damgaard, C., Therkildsen, O. R., Elmeros, M., et al. (2019) *Bevaringsstatus for Naturtyper Og Arter - 2019. Habitatdirektivets Artikel 17-Rapportering. Aarhus Universitet, DCE - Nationalt Center for Miljø Og Energi. Scientific Report No. 340*. Available at: <http://dce2.au.dk/pub/SR340.pdf>.
- Frigstad, H., Andersen, G. S., Trannum, H. C., Naustvoll, L. J., Kaste, Ø., and Hjermann, D. Ø. (2018) *Synthesis of Climate Relevant Results From Selected Monitoring Programs in the Coastal Zone. Part 2: Quantitative Analyses. Norwegian Institute for Water Research. NIVA Report 7311-2018*. Available at: <http://hdl.handle.net/11250/2595792>.
- Frigstad, H., Gundersen, H., Andersen, G. S., Borgersen, G., Kvile, K. Ø., Krause-Jensen, D., et al. (2021). “Blue Carbon – Climate Adaptation, CO₂ Uptake and

- Sequestration of Carbon in Nordic Blue Forests – Results From the Nordic Blue Carbon Project.” (Copenhagen: Nordic Council of Ministers), TemaNord2020: 541. doi: 10.6027/temanord2020-541
- Frigstad, H., Harvey, T., Deininger, A., and Poste, A. (2020). *Increased Light Attenuation in Norwegian Coastal Waters – a Literature Review*. NIVA-Report 7551-2020 (Grimstad: Norwegian Institute for Water Research). Available at: <https://hdl.handle.net/11250/2711599>.
- Gagnon, K., Christie, H., Dideren, K., Fagerli, C. W., Govers, L. L., Gräfnings, M. L. E., et al. (2021). Incorporating Facilitative Interactions Into Small-Scale Eelgrass Restoration-Challenges and Opportunities. *Restor. Ecol.* 29, e13398. doi: 10.1111/rec.13398
- Gattuso, J.-P., Magnan, A. K., Bopp, L., Cheung, W. W. L., Duarte, C. M., Hinkel, J., et al. (2018). Ocean Solutions to Address Climate Change and Its Effects on Marine Ecosystems. *Front. Mar. Sci.* 5. doi: 10.3389/fmars.2018.00337
- Glooschenko, W. A., Tarnocai, C., Zoltai, S., and Glooschenko, V. (1993). “Wetlands of Canada and Greenland,” in *Wetlands of the World: Inventory, Ecology and Management*, vol. I. Eds. D. F. Whigham, D. Dykxjová and S. Hejný (Dordrecht: Springer Netherlands), 415–514. doi: 10.1007/978-94-015-8212-4
- Graversen, A. E. G., Banta, G. T., Masque, P., and Krause-Jensen, D. (2022). Carbon Sequestration is Not Inhibited by Livestock Grazing in Danish Salt Marshes. *Limnol. Oceanogr.* doi: 10.1002/(ISSN)1939-5590
- Gudbrandsson, G. I., Wermelin, L., Mikkonen, K., Elvestuen, O., Lövin, I., Gunell, C., et al. (2019). “Nordic Ministerial Declaration on Oceans and Climate – for adoption at the Nordic Ministerial Meeting in Stockholm, 30 October 2019” (Stockholm: Nordic Council of Ministers for the Environment and Climate). Available at: www.norden.org/en/declaration/nordic-ministerial-declaration-oceans-and-climate.
- Gullström, M., Isæus, M., Berglund, J., Blomqvist, M., Karlsson, A., Nygård, L., et al. (2009). *Övervakning Av Makrovegetation I Bottniska Viken – En Vägledning (in English: Monitoring of Macrovegetation in Bothnian Bay – a Guide)* (Meddelande: Länsstyrelsens Västerbotten), 6. Available at: <http://naturvardsverket.diva-portal.org/smash/record.jsf?pid=diva2:770191>.
- Gundersen, H., Bekkby, T., Oug, E., Norderhaug, K. M., Fredriksen, S., and Rinde, E. (2018). *Marine Shallow Waters. Norwegian Redlist for Habitats 2018* (Trondheim: Norwegian Biodiversity Information Centre). Available at: www.artsdatabanken.no/Pages/259183.
- Gundersen, H., Bryan, T., Chen, W., and Moy, F. E. (2016). Ecosystem Services. In *The Coastal Zone of the Nordic Countries* 552 (Copenhagen: Nordic Council of Ministers), 127. doi: 10.6027/TN2016-552
- Gundersen, H., Rinde, E., Bekkby, T., Hancke, K., Gitmark, J. K., and Christie, H. (2021). Variation in Population Structure and Standing Stocks of Kelp Along Multiple Environmental Gradients and Implications for Ecosystem Services. *Front. Mar. Sci.* 8. doi: 10.3389/fmars.2021.578629
- Gunnarsson, K., Burgos, J., Gunnarsdóttir, L., Egilsdóttir, S., Georgsdóttir, G. I., and Madrigal, V. F. P. (2019). *Klõþang Í Breiðafirði: Útbreiddsla Og Magn. Haframsóknastofnun HV 2019-16*. Available at: www.hafogvatn.is/static/research/files/hv2019-16.pdf.
- Hammar, L., Schmidtbauer Crona, J., Kågesten, G., Hume, D., Pålsson, J., Aarsrud, M., et al. (2018). Symphony: Integrat planeringsstöd för statlig havsplanering utifrån en ekosystemansats. (Swedish: Swedish Agency for Marine and Water Management report) 2018:1. Available at: <http://urn.kb.se/resolve?urn=urn:nbn:se:havochvatten:diva-170>
- Høgslund, S., Sejr, M. K., Wiktor, J., Blicher, M. E., and Wegeberg, S. (2014). Intertidal Community Composition Along Rocky Shores in South-West Greenland: A Quantitative Approach. *Polar Biol.* 37, 1549–1561. doi: 10.1007/s00300-014-1541-7
- Hafo.is (2018) *State of Marine Stocks and Advise 2018 - Klõþang – Rockweed*. Available at: www.hafogvatn.is/static/extras/images/thang2018318234.pdf.
- Halvorsen, R., Skarpaas, O., Bryn, A., Bratli, H., Erikstad, L., Simensen, T., et al. (2020). Towards a Systematics of Ecodiversity: The EcoSyst Framework. *Global Ecol. Biogeogr.* 29, 1887–1906. doi: 10.1111/geb.13164
- HELCOM (2013). ‘HELCOM HUB – Technical Report on the HELCOM Underwater Biotope and Habitat Classification,’ in *Baltic Sea Environment Proceedings 139*. Helsinki: HELCOM. Available at: www.helcom.fi/Lists/Publications/BSEP139.pdf.
- Hoegh-Guldberg, O., Caldeira, K., Chopin, T., Gaines, S., Haugan, P., Hemer, M., et al. (2019). *The Ocean as a Solution to Climate Change: Five Opportunities for Action. Report* (Washington, DC: World Resources Institute). Available at: <http://www.oceanpanel.org/climate>.
- Hurd, C. L., Law, C. S., Bach, L. T., Britton, D., Hovenden, M., Paine, E., et al. (2022). Forensic Carbon Accounting: Assessing the Role of Seaweeds for Carbon Sequestration. *J. Phycol.* doi: 10.1111/jpy.13249
- Ingólfsson, A. (2010). Náttúruverndargildi Íslensku Fjörunnar Og Aðsteðjandi Hættur. *Náttúrufræðingurinn* 79, 19–28.
- IPCC (2014). *2013 Supplement to the 2006 IPCC Guidelines for National Greenhouse Gas Inventories: Wetlands*. Eds. T. Hiraiishi, T. Krug, K. Tanabe, N. Srivastava, J. Baasansuren, M. Fukuda and T. G. Troxler (Switzerland: IPCC).
- Jakobsen, B. (1954). The Tidal Area in South-Western Jutland and the Process of the Salt Marsh Formation. *Geografisk Tidsskrift* 53, 49–61.
- Janssen, J. A. M., and Rodwell, J. S. (2016). *European Red List of Habitats : Part 2. Terrestrial and Freshwater Habitats* (Luxembourg: Publications Office of the European Union). doi: 10.2779/091372
- Jensen, L. A., Schmidt, L. B., Hollesen, J., and Elberling, B. (2006). Accumulation of Soil Organic Carbon Linked to Holocene Sea Level Changes in West Greenland. *Arct. Antarct. Alp. Res.* 38, 378–383. doi: 10.1657/1523-0430(2006)38[378:AOSOC]2.0.CO;2
- J. Jóhansen, A. M. Fosaa and S. Rasmussen (Eds.) (2000). *Føroya Flora* (Føroya skúlabókagrunnur: Tórshavn).
- Karlsson, J. (2007). *Övervakning Av Vegetationsklådda Hårdbottnar Vid Svenska Västskusten 1993-2006* (Gothenburg, Sweden: Tjárnö marinbiologiska laboratorium, Göteborgs Universitet). Available at: <http://naturvardsverket.diva-portal.org/smash/record.jsf?pid=diva2:657799>.
- Karnauskaitė, D., Schernewski, G., Schumacher, J., Grunert, R., and Povilanskas, R. (2018). Assessing Coastal Management Case Studies Around Europe Using an Indicator Based Tool. *J. Coast. Conserv.* 22, 549–570. doi: 10.1007/s11852-018-0597-x
- Kautsky, N., Kautsky, H., Kautsky, U., and Waern, M. (1986). Decreased Depth Penetration of *Fucus Vesiculosus* (L.) Since the 1940's Indicates Eutrophication of the Baltic Sea. *Mar. Ecol. Prog. Ser.* 28, 1–8. doi: 10.3354/meps028001
- Kindeberg, T., Ørberg, S. B., Röhr, M. E., Holmer, M., and Krause-Jensen, D. (2018). Sediment Stocks of Carbon, Nitrogen, and Phosphorus in Danish Eelgrass Meadows. *Front. Mar. Sci.* 5. doi: 10.3389/fmars.2018.00474
- Krause-Jensen, D., Archambault, P., Assis, J., Bartsch, I., Bischof, K., Filbee-Dexter, K., et al. (2020). Imprint of Climate Change on Pan-Arctic Marine Vegetation. *Front. Mar. Sci.* 7. doi: 10.3389/fmars.2020.617324
- Krause-Jensen, D., and Duarte, C. M. (2016). Substantial Role of Macroalgae in Marine Carbon Sequestration. *Nat. Geosci.* 9, 737–742. doi: 10.1038/Ngeo2790
- Krause-Jensen, D., Duarte, C. M., Sand-Jensen, K., and Carstensen, J. (2021). Century-Long Records Reveal Shifting Challenges to Seagrass Recovery. *Glob. Change Biol.* 27, 563–575. doi: 10.1111/gcb.15440
- Krause-Jensen, D., Marbà, N., Olesen, B., Sejr, M. K., Christensen, P. B., Rodrigues, J., et al. (2012). Seasonal Sea Ice Cover as Principal Driver of Spatial and Temporal Variation in Depth Extension and Annual Production of Kelp in Greenland. *Glob. Change Biol.* 18, 2981–2994. doi: 10.1111/j.1365-2486.2012.02765.x
- Krause-Jensen, D., Lavery, P., Serrano, O., Marbà, N., Masque, P., and Duarte, C. M. (2018). Sequestration of Macroalgal Carbon: The Elephant in the Blue Carbon Room. *Biol. Letters* 14 (6), 20180236. doi: 10.1098/rsbl.2018.0236
- Krause-Jensen, D., Sejr, M. K., Bruhn, A., Rasmussen, M. B., Christensen, P. B., Hansen, J. L. S., et al. (2019). Deep Penetration of Kelps Offshore Along the West Coast of Greenland. *Front. Mar. Sci.* 6. doi: 10.3389/fmars.2019.00375
- Lange, T., Oncken, N. S., Svane, N., Steinfurth, R. C., Kristensen, E., and Flindt, M. R. (2022). Large-Scale Eelgrass Transplantation: A Measure for Carbon and Nutrient Sequestration in Estuaries. *Marine Ecol. Prog. Ser.* 685, 97–109. doi: 10.3354/meps13975
- Legge, O., Johnson, M., Hicks, N., Jickells, T., Diesing, M., Aldridge, J., et al. (2020). Carbon on the Northwest European Shelf: Contemporary Budget and Future Influences. *Front. Mar. Sci.* 7. doi: 10.3389/fmars.2020.00143
- Lehikoinen, P., Lehikoinen, A., Mikkola-Roos, M., and Jaatinen, K. (2017). Counteracting Wetland Overgrowth Increases Breeding and Staging Bird Abundances. *Sci. Rep.* 7, 41391. doi: 10.1038/srep41391
- Lehtomaa, L., Ahonen, I., Hakamäki, H., Häggblom, M., Jantunen, J., Jutila, H., et al. (2018). “Perinnebiotoopit. [Traditional Rural Biotoopes],” in *Suomen Luontotyypien Uhanalaisuus 2018. Luontotyypien Punainen Kirja – Osa 2: Luontotyypien Kuvaukset. (Threatened Habitat Types in Finland 2018. Red*

- List of Habitats – Part II: Descriptions of Habitat Types*). Eds. T. Kontula and A. Raunio (Finnish Environment Institute and Ministry of the Environment. Finnish Environment), 659–757.
- Lepping, O., and Daniels, F. J. A. (2007). Phytosociology of Beach and Salt Marsh Vegetation in Northern West Greenland. *Polarforschung* 76, 95–108. doi: 10.1001/epic.29958.d001
- Lindgarth, M., Carstensen, J., Drakare, S., Johnson, R. K., Sandman, A. N., Söderpalm, A., et al. (2016). *Ecological Assessment of Swedish Water Bodies; Development, Harmonisation and Integration of Biological Indicators. Final Report of the Research Programme WATERS. Deliverable 1.1-4. WATERS Report No. 2016* (Sweden: Havsmiljöinstitutet), 10.
- Long, A. J., Woodroffe, S. A., Milne, G. A., Bryant, C. L., Simpson, M. J. R., and Wake, L. M. (2012). Relative Sea-Level Change in Greenland During the Last 700 Yrs and Ice Sheet Response to the Little Ice Age. *Earth Planet Sci. Lett.* 315, 76–85. doi: 10.1016/j.epsl.2011.06.027
- Lovelock, C. E., Atwood, T., Baldock, J., Duarte, C. M., Hickey, S., Lavery, P. S., et al. (2017). Assessing the Risk of Carbon Dioxide Emissions From Blue Carbon Ecosystems. *Front. Ecol. Environ.* 15, 257–265. doi: 10.1002/fee.1491
- Luisetti, T., Ferrini, S., Grilli, G., Jickells, T. D., Kennedy, H., Kröger, S., et al. (2020). Climate Action Requires New Accounting Guidance and Governance Frameworks to Manage Carbon in Shelf Seas. *Nat. Commun.* 11, 4599. doi: 10.1038/s41467-020-18242-w
- Lundén, B., and Gullström, M. (2013). Satellite Remote Sensing for Monitoring of Vanishing Seagrass in Swedish Coastal Waters. *Nor. Geogr. Tidskr.* 57, 121–124. doi: 10.1080/00291950310001379
- Macreadie, P. I., Costa, M. D. P., Atwood, T. B., Friess, D. A., Kelleway, J. J., Kennedy, H., et al. (2021). Blue Carbon as a Natural Climate Solution. *Nat. Rev. Earth Env.* 2, 826–839. doi: 10.1038/s43017-021-00224-1
- Marbà, N., Krause-Jensen, D., Masque, P., and Duarte, C. M. (2018). Expanding Greenland Seagrass Meadows Contribute New Sediment Carbon Sinks. *Sci. Rep.* 8, 14024. doi: 10.1038/s41598-018-32249-w
- McLeod, E., Chmura, G. L., Bouillon, S., Salm, R., Björk, M., Duarte, C. M., et al. (2011). A Blueprint for Blue Carbon: Toward an Improved Understanding of the Role of Vegetated Coastal Habitats in Sequestering CO₂. *Front. Ecol. Environ.* 9, 552–560. doi: 10.1890/110004
- Middelboe, A. L., Sand-Jensen, K., and Brodersen, K. (1997). Patterns of Macroalgal Distribution in the Kattegat-Baltic Region. *Phycologia* 36, 208–219. doi: 10.2216/i0031-8884-36-3-208.1
- Moksnes, P.-O., Gipperth, L., Eriander, L., Laas, K., Cole, S., and Infantes, E. (2016). *Handbok För Restaurering Av Älgräs I Sverige – Vägledning. Havs Och Vattenmyndigheten. Report No. 2016. 9*, Vattenmyndigheten (the Swedish Agency for Marine and Water Management), Göteborg, Sweden. Available at: <http://urn.kb.se/resolve?urn=urn:nbn:se:havochvatten:diva-108> Vattenmyndigheten (the Swedish Agency for Marine and Water Management), Göteborg, Sweden, Available from www.researchgate.net/publication/311512377_Handbook_for_eelgrass_restoration_in_Sweden_-_A_guideline.
- Moksnes, P. O., Gullström, M., Tryman, K., and Baden, S. (2008). Trophic Cascades in a Temperate Seagrass Community. *Oikos* 117, 763–777. doi: 10.1111/j.0030-1299.2008.16521.x
- Moksnes, P. O., Röhr, M. E., Holmer, M., Eklöf, J. S., Eriander, L., Infantes, E., et al. (2021). Major Impacts and Societal Costs of Seagrass Loss on Sediment Carbon and Nitrogen Stocks. *Ecosphere* 12, e03658. doi: 10.1002/ecs2.3658
- MSFD (2008). *Directive 2008/56/EC of the European Parliament and of the Council of 17 June 2008 Establishing a Framework for Community Action in the Field of Marine Environmental Policy* (Marine Strategy Framework Directive. Official Journal of the European Union).
- Mueller, P., Ladiges, N., Jack, A., Schmiedl, G., Kutzbach, L., Jensen, K., et al. (2019). Assessing the Long-Term Carbon-Sequestration Potential of the Semi-Natural Salt Marshes in the European Wadden Sea. *Ecosphere* 10, e02556. doi: 10.1002/ecs2.2556
- Narayan, S., Beck, M. W., Wilson, P., Thomas, C. J., Guerrero, A., Shepard, C. C., et al. (2017). The Value of Coastal Wetlands for Flood Damage Reduction in the Northeastern USA. *Sci. Rep.* 7, 9463. doi: 10.1038/s41598-017-09269-z
- Nellemann, C., Corcoran, E., Duarte, C. M., Valdres, L., Young, C. D., Fonseca, L., et al. (2009). *Blue Carbon: The Role of Healthy Oceans in Binding Carbon* Bergen: UN Environment, GRID-Arendal. Available at: <https://portals.iucn.org/library/sites/library/files/documents/2009-052.pdf>.
- Nielsen, R., Kristiansen, A., Mathiesen, L., and Mathiesen, H. (1995). Distributional Index of the Benthic Macroalgae of the Baltic Sea Area. *Acta Bot. Fenn.* 155, 1–51.
- Norderhaug, K. M., Nedreaas, K., Huserbråten, M., and Moland, E. (2021). Depletion of Coastal Predatory Fish Sub-Stocks Coincided With the Largest Sea Urchin Grazing Event Observed in the NE Atlantic. *Ambio* 50, 163–173. doi: 10.1007/s13280-020-01362-4
- Norderhaug, K. M., van Son, T. C., Nikolioudakis, N., Thormar, J., Moy, F., Knutsen, J. A., et al. (2020). *Biomassemodell for Stortare - Ressursmodell for Fremtidens Forvaltning. Rapport Fra Havforskningen 2020-7* (Norway: Institute of Marine Research). Available at: <https://hdl.handle.net/11250/2685899>.
- Nordlund, L. M., Koch, E. W., Barbier, E. B., and Creed, J. C. (2016). Seagrass Ecosystem Services and Their Variability Across Genera and Geographical Regions. *PLoS One* 11, e0163091. doi: 10.1371/journal.pone.0163091
- Nyqvist, A., André, C., Gullström, M., Baden, S. P., and Åberg, P. (2009). Dynamics of Seagrass Meadows on the Swedish Skagerrak Coast. *Ambio* 38, 85–88. doi: 10.1579/0044-7447-38.2.85
- Öberg, J. (2006). Primary Production by Macroalgae in Kattegat, Estimated From Monitoring Data, Seafloor Properties, and Model Simulations. *Cont. Shelf Res.* 26, 2415–2432. doi: 10.1016/j.csr.2006.07.005
- Ørberg, S. B., Krause-Jensen, D., Geraldi, N. R., Ortega, A., Díaz-Rúa, R., and Duarte, C. M. (2022). Fingerprinting Arctic and North Atlantic Macroalgae with eDNA—Application and perspectives. *Environmental DNA* 4 (2), 385–401. doi: 10.1002/edn3.262
- Olafsen, T., Winther, U., Olsen, Y., and Skjermo, J. (2012). *Verdiskaping Basert På Produktive Hav I 2050. Rapport Fra Arbeidsgruppe Oppnevnt Av Det Kongelige Norske Videnskabers Selskap (DKNVS) Og Norges Tekniske Vitenskapsakademi (NTVA)*. Available at: www.sintef.no/globalassets/upload/fiskeri_og_havbruk/publikasjoner/verdiskaping-basert-pa-produktive-hav-i-2050.pdf.
- Olesen, B., Krause-Jensen, D., Marbà, N., and Christensen, P. B. (2015). Eelgrass *Zostera Marina* in Subarctic Greenland: Dense Meadows With Slow Biomass Turnover in Cold Waters. *Mar. Ecol. Prog. Ser.* 518, 107–121. doi: 10.3354/meps11087
- Olsen, J. L., Stam, W. T., Coyer, J. A., Reusch, T. B. H., Billingham, M., Boström, C., et al. (2004). North Atlantic Phylogeography and Large-Scale Population Differentiation of the Seagrass *Zostera Marina* L. *Mol. Ecol.* 13, 1923–1941. doi: 10.1111/j.1365-294X.2004.02205.x
- Oreska, M. P. J., McGlathery, K. J., Aoki, L. R., Berger, A. C., Berg, P., and Mullins, L. (2020). The Greenhouse Gas Offset Potential From Seagrass Restoration. *Sci. Rep.* 10, 7325. doi: 10.1038/s41598-020-64094-1
- Ortega, A., Geraldi, N. R., and Duarte, C. M. (2020). Environmental DNA Identifies Marine Macrophyte Contributions to Blue Carbon Sediments. *Limnol. Oceanogr.* 65 (12), 3139–3149. doi: 10.1002/lno.11579
- Orth, R. J., Carruthers, T. J. B., Dennison, W. C., Duarte, C. M., Fourqurean, J. W., Heck, K. L., et al. (2006). A Global Crisis for Seagrass Ecosystems. *Bioscience* 56, 987–996. doi: 10.1641/0006-3568(2006)56[987:Agcfse]2.0.Co;2
- Orth, R. J., Lefcheck, J. S., McGlathery, K. S., Aoki, L., Luckenbach, M. W., Moore, K. A., et al. (2020). Restoration of Seagrass Habitat Leads to Rapid Recovery of Coastal Ecosystem Services. *Sci. Adv.* 6, eabc6434. doi: 10.1126/sciadv.abc6434
- Ostenfeld, C. H. (1908). The Land-Vegetation of the Færøes: With Special Reference to the Higher Plants. *Bot. Færøes* 3, 867–1026.
- J. G. Ottósson, A. Sveinsdóttir and M. Harðardóttir (Eds.) (2016). *Vistgerðir Á Íslandi. Fjölrit Náttúrufræðistofnunar Nr. 54* (Náttúrufræðistofnun Íslands: Garðabær). Available at: http://utgafa.ni.is/fjolrit/fjolrit_54.pdf.
- Paine, E. R., Schmid, M., Boyd, P. W., Diaz-Pulido, G., and Hurd, C. L. (2021). Rate and Fate of Dissolved Organic Carbon Release by Seaweeds: A Missing Link in the Coastal Ocean Carbon Cycle. *J. Phycol.* 57, 1375–1391. doi: 10.1111/jpy.13198
- Pätsch, R., Schaminée, J. H. J., Janssen, J. A. M., Hennekens, S. M., Bruchmann, I., Jutila, H., et al. (2019). Between Land and Sea? A Classification of Saline and Brackish Grasslands of the Baltic Sea Coast. *Phytocoenologia* 49, 319–348. doi: 10.1127/phyto/2019/0339
- Pedersen, M. F., Filbee-Dexter, K., Norderhaug, K. M., Fredriksen, S., Frisk, N. L., Fagerli, C. W., et al. (2020). Detrital Carbon Production and Export in High Latitude Kelp Forests. *Oecologia* 192, 227–239. doi: 10.1007/s00442-019-04573-z
- Perry, D., Hammar, L., Linderholm, H. W., and Gullström, M. (2020). Spatial Risk Assessment of Global Change Impacts on Swedish Seagrass Ecosystems. *PLoS One* 15, e0225318. doi: 10.1371/journal.pone.0225318

- Perry, D., Staveley, T., Deyanova, D., Baden, S., Dupont, S., Hernroth, B., et al. (2019). Global Environmental Changes Negatively Impact Temperate Seagrass Ecosystems. *Ecosphere* 10, e02986. doi: 10.1002/ecs2.2986
- Petersen, C. G. J. (1914). "Om Bændeltangens (Zostera Marina) Aarsproduktion I De Danske Farvande. Kap. IX," in *Mindeskraft I Anledning Af Hundredeaaret for Japetus Stenstrup's Fødsel*. Eds. H. Jungersen and E. Warming (København: Bianco Lunos Bogtrykkeri), 1–20.
- Queirós, A. M., Stephens, N., Widdicombe, S., Tait, K., McCoy, S. J., Ingels, J., et al. (2019). Connected Macroalgal-Sediment Systems: Blue Carbon and Food Webs in the Deep Coastal Ocean. *Ecol. Monogr.* 89 (3), p.e01366. doi: 10.1002/ecm.1366
- Reusch, T. B. H., and Boström, C. (2011). Widespread Genetic Mosaicism in the Marine Angiosperm *Zostera Marina* is Correlated With Clonal Reproduction. *Evol. Ecol.* 25, 899–913. doi: 10.1007/s10682-010-9436-8
- Reusch, T. B. H., Boström, C., Stam, W. T., and Olsen, J. L. (1999). An Ancient Eelgrass Clone in the Baltic. *Mar. Ecol. Prog. Ser.* 183, 301–304. doi: 10.3354/meps183301
- Reusch, T. B. H., Dierking, J., Andersson, H. C., Bonsdorff, E., Carstensen, J., Casini, M., et al. (2018). The Baltic Sea as a Time Machine for the Future Coastal Ocean. *Sci. Adv.* 4, eaar8195. doi: 10.1126/sciadv.aar8195
- Rhein, M., Rintoul, S. R., Aoki, S., Campos, E., Chambers, D., Feely, R. A., et al. (2014). "Observations: Ocean," in *Climate Change 2013: The Physical Science Basis. Contribution of Working Group I to the Fifth Assessment Report of the Intergovernmental Panel on Climate Change*. Eds. T. F. Stocker, D. Qin, G.-K. Plattner, M. Tignor, S. K. Allen and J. Boschung (Cambridge, United Kingdom and New York, NY, USA: Cambridge University Press), 255–316. doi: 10.1017/CBO9781107415324.010
- Riemann, B., Abay, A. T., Ankjær, T., Bruhn, A., Dahl, K., Galatius, A., et al. (2020). *Regional Havplanlægning I Det Vestlige Kattegat – Natur-, Erhvervs- Og Samfundsmæssige Forhold Og Scenarier* (Aarhus Universitet, DCE – Nationalt Center for Miljø og Energi. Scientific Report no. 403). Available at: <https://dce2.au.dk/pub/SR403.pdf>.
- Riemann, B., Carstensen, J., Dahl, K., Fossing, H., Hansen, J. W., Jakobsen, H. H., et al. (2016). Recovery of Danish Coastal Ecosystems After Reductions in Nutrient Loading: A Holistic Ecosystem Approach. *Estuar Coast* 39, 82–97. doi: 10.1007/s12237-015-9980-0
- Rinde, E., Christie, H., Fagerli, C. W., Bekkby, T., Gundersen, H., Norderhaug, K. M., et al. (2014). The Influence of Physical Factors on Kelp and Sea Urchin Distribution in Previously and Still Grazed Areas in the NE Atlantic. *PLoS One* 9, e100222. doi: 10.1371/journal.pone.0100222
- Rinne, H., and Salovius-Lauren, S. (2020). The Status of Brown Macroalgae *Fucus* Spp. And its Relation to Environmental Variation in the Finnish Marine Area, Northern Baltic Sea. *Ambio* 49, 118–129. doi: 10.1007/s13280-019-01175-0
- Röhr, M. E., Boström, C., Canal-Vergés, P., and Holmer, M. (2016). Blue Carbon Stocks in Baltic Sea Eelgrass (*Zostera Marina*) Meadows. *Biogeosciences* 13, 6139–6153. doi: 10.5194/bg-13-6139-2016
- Röhr, M. E., Holmer, M., Baum, J. K., Björk, M., Boyer, K., Chin, D., et al. (2018). Blue Carbon Storage Capacity of Temperate Eelgrass (*Zostera Marina*) Meadows. *Global Biogeochem. Cycles* 32, 1457–1475. doi: 10.1029/2018gb005941
- Rosenvinge, L. K. R. (1893). Grønlands Havalger. *Medd. Grønland* 3, 765–981.
- Ruiz-Frau, A., Gelcich, S., Hendriks, I. E., Duarte, C. M., and Marbà, N. (2017). Current State of Seagrass Ecosystem Services: Research and Policy Integration. *Ocean Coast. Manage.* 149, 107–115. doi: 10.1016/j.ocecoaman.2017.10.004
- Sahla, M., Tolvanen, H., Ruuskanen, A., and Kurvinen, L. (2020). Assessing Long Term Change of *Fucus* Spp. Communities in the Northern Baltic Sea Using Monitoring Data and Spatial Modeling. *Estuar Coast Shelf S.* 245, 107023. doi: 10.1016/j.ecss.2020.107023
- Salinas, C., Duarte, C. M., Lavery, P. S., Masque, P., Arias-Ortiz, A., Leon, J. X., et al. (2020). Seagrass Losses Since Mid-20th Century Fuelled CO₂ Emissions From Soil Carbon Stocks. *Glob. Change Biol.* 26, 4772–4784. doi: 10.1111/gcb.15204
- Sayre, R., Noble, S., Hamann, S., Smith, R., Wright, D., Breyer, S., et al. (2019). A New 30 Meter Resolution Global Shoreline Vector and Associated Global Islands Database for the Development of Standardized Ecological Coastal Units. *J. Oper. Oceanogr.* 12, S47–S56. doi: 10.1080/1755876x.2018.1529714
- Schernewski, G., Bartel, C., Kobarg, N., and Karnaushkaite, D. (2018). Retrospective Assessment of a Managed Coastal Realignment and Lagoon Restoration Measure: The Geltinger Birk, Germany. *J. Coast. Conserv.* 22, 157–167. doi: 10.1007/s11852-017-0496-6
- Schramm, W. (1998). "Seaweed Ressources of the Baltic Sea and the German Coasts of the North Sea," in *Seaweed Ressources of the World*. Eds. A. T. Critchley and H. Ohno (Japan International Collaboration Agency), 226–232.
- Schulman, A., Alanen, A., Hægström, C.-A., Huhta, A.-P., Jantunen, J., Kekäläinen, H., et al. (2008). "Perinnebiotoopit," in *Suomen Luontotyyppien Uhanalaisuus – Osa 2: Luontotyyppien Kuvaukset (Assessment of Threatened Habitat Types in Finland – Part 2: Habitat Type Descriptions)*, SYKE Report 2/2011. Eds. A. Raunio, A. Schulman and T. Kontula (Helsinki: Suomen ympäristökeskus), 397–465.
- Sejr, M. K., Mouritsen, K. N., Krause-Jensen, D., Olesen, B., Blicher, M. E., and Thyrring, J. (2021). Small Scale Factors Modify Impacts of Temperature, Ice Scour and Waves and Drive Rocky Intertidal Community Structure in a Greenland Fjord. *Front. Mar. Sci.* 7. doi: 10.3389/fmars.2020.607135
- Smale, D. A., Burrows, M. T., Moore, P., O'Connor, N., and Hawkins, S. J. (2013). Threats and Knowledge Gaps for Ecosystem Services Provided by Kelp Forests: A Northeast Atlantic Perspective. *Ecol. Evol.* 3, 4016–4038. doi: 10.1002/ecs3.774
- Staehr, P. A., Göke, C., Holbach, A. M., Krause-Jensen, D., Timmermann, K., Upadhyay, S., et al. (2019). Habitat Model of Eelgrass in Danish Coastal Waters: Development, Validation and Management Perspectives. *Front. Mar. Sci.* 6. doi: 10.3389/fmars.2019.00175
- Steen, H. (2018). Assessment of C-Fields for Kelp Harvesting in Sør-Trøndelag and Nord-Trøndelag in 2018. *IMR Report Series* (Bergen: Institute of Marine Research. Rapport fra Havforskningen no. 32-2018). Available at: www.hi.no/hi/nettrapporter/rapport-fra-havforskningen/2018/32-2018_rapport-tarehostefelt-trondelag.
- Steen, H., Moy, F. E., Bodvin, T., and Husa, V. (2016). Regrowth After Kelp Harvesting in Nord-Trøndelag, Norway. *ICES J. Mar. Sci.* 73, 2708–2720. doi: 10.1093/icesjms/fsw130
- Steen, H., Norderhaug, K. M., and Moy, F. E. (2018). *Tareundersøkelser I Nordland I 2018. Institute of Marine Research. Rapport Fra Havforskningen No. 44-2018*.
- Stewart-Sinclair, P. J., Purandare, J., Bayraktarov, E., Waltham, N., Reeves, S., Statton, J., et al. (2020). Blue Restoration - Building Confidence and Overcoming Barriers. *Front. Mar. Sci.* 7. doi: 10.3389/fmars.2020.541700
- The BACC II Author Team (2015). *Second Assessment of Climate Change for the Baltic Sea Basin* (Cham: Springer International Publishing). doi: 10.1007/978-3-319-16006-1
- Thormar, J., Hasler-Sheetal, H., Baden, S., Boström, C., Clausen, K. K., Krause-Jensen, D., et al. (2016). Eelgrass (*Zostera Marina*) Food Web Structure in Different Environmental Settings. *PLoS One* 11, e0146479. doi: 10.1371/journal.pone.0146479
- Thyrring, J., Wegeberg, S., Blicher, M. E., Krause-Jensen, D., Hogslund, S., Olesen, B., et al. (2021). Latitudinal Patterns in Intertidal Ecosystem Structure in West Greenland Suggest Resilience to Climate Change. *Ecography* 44, 1156–1168. doi: 10.1111/ecog.05381
- Tobler, W. (1987). Measuring spatial resolution. *Proceedings, Land Resources Information Systems Conference*, Beijing, pp. 12–16.
- Torn, K., Krause-Jensen, D., and Martin, G. (2006). Present and Past Depth Distribution of Bladderwrack (*Fucus Vesiculosus*) in the Baltic Sea. *Aquat. Bot.* 84, 53–62. doi: 10.1016/j.aquabot.2005.07.011
- UNESCO (2021). *UNESCO Marine World Heritage: Custodians of the Globe's Blue Carbon Assets* (Paris, France: United Nations Educational, Scientific and Cultural Organization).
- Valiela, I., Lloret, J., Bowyer, T., Miner, S., Remsen, D. P., Elmstrom, E., et al. (2018). Transient Coastal Landscapes: Rising Sea Level Threatens Salt Marshes. *Sci. Total Environ.*, 640–641, 1148–1156. doi: 10.1016/j.scitotenv.2018.05.235
- van der Heide, T., Temmink, R. J. M., Fivash, G. S., Bouma, T. J., Boström, C., Dideren, K., et al. (2021). Coastal Restoration Success via Emergent Trait-Mimicry is Context Dependent. *Biol. Conserv.* 264, 109373. doi: 10.1016/j.biocon.2021.109373
- van Katwijk, M. M., Thorhaug, A., Marbà, N., Orth, R. J., Duarte, C. M., Kendrick, G. A., et al. (2016). Global Analysis of Seagrass Restoration: The

- Importance of Large-Scale Planting. *J. Appl. Ecol.* 53, 567–578. doi: 10.1111/1365-2664.12562
- Verbeek, J., Louro, I., Christie, H., Carlsson, P. M., Matsson, S., and Renaud, P. E. (2021). *Restoring Norway's Underwater Forests a Strategy to Recover Kelp Ecosystems From Urchin Barrens* (Oslo: SeaForester, NIVA, Akvaplan-niva). Available at: www.niva.no/en/reports/restoring-norways-underwater-forests/_/attachment/download/bd43a73d-631d-46da-abdefe2e9774243:9ab75e57c149a6523927382b1fb17c272aaed95d/Restoring%20Norway's%20Underwater%20Forests_light.pdf.
- Vestergaard, P. (2000). *Strandenge – En Beskyttet Naturtype*. Miljø-Og Energiministeriet, Skov- Og Naturstyrelsen (Copenhagen, Denmark: G.E.C. Gads Forlag).
- Vistgerdakort.ni.is (2018) *Vistgerdakort*. Available at: <https://vistgerdakort.ni.is/>.
- Waern, M. (1952). *Rocky-Shore Algae in the Öregrund Archipelago*. [Dissertation] (Uppsala, Sweden: Sv. växtgeografiska sällsk).
- Walday, M. G., Fagerli, C. W., Frigstad, H., Staalstrøm, A., Kaurin, M., Christensen, G., et al. (2020). *Evaluering Av ØKOKYST - Stasjonsnett Og Klassegrenser*. NIVA Report No. 7547-2020 (Oslo: Norwegian Institute of Water Research). Available at: <https://hdl.handle.net/11250/2683488>.
- Ward, R. D. (2020). Carbon Sequestration and Storage in Norwegian Arctic Coastal Wetlands: Impacts of Climate Change. *Sci. Total Environ.* 748, 141343. doi: 10.1016/j.scitotenv.2020.141343
- Watanuki, A., Aota, T., Otsuka, E., Kawai, T., Iwahashi, Y., Kuwahara, H., et al. (2010). Restoration of Kelp Beds on an Urchin Barren: Removal of Sea Urchins by Citizen Divers in Southwestern Hokkaido. *Bull. Fish. Res. Agen. (Japan)* 32, 83–87.
- Water Framework Directive (2000). Directive 2000/60/EC of the European Parliament and the Council of 23 October 2000 Establishing a Framework for Community Action in the Field of Water Policy. *Off. J. Eur. Communities L* 327, 1–73. <https://www.legislation.gov.uk/euadr/2000/60/contents>
- Waycott, M., Duarte, C. M., Carruthers, T. J. B., Orth, R. J., Dennison, W. C., Olyarnik, S., et al. (2009). Accelerating Loss of Seagrasses Across the Globe Threatens Coastal Ecosystems. *Proc. Natl. Acad. Sci.* 106, 12377–12381. doi: 10.1073/pnas.0905620106
- Weinberger, F., Paalme, T., and Wikström, S. A. (2020). Seaweed Resources of the Baltic Sea, Kattegat and German and Danish North Sea Coasts. *Bot. Mar.* 63, 61–72. doi: 10.1515/bot-2019-0019
- Wernberg, T., Krumhansl, K., Filbee-Dexter, K., and Pedersen, M. F. (2019). “Status and Trends for the World's Kelp Forests,” in *World Seas: An Environmental Evaluation. Volume III: Ecological Issues and Environmental Impacts*, 2. ed. Ed. C. Sheppard (Amsterdam: Elsevier), 57–78. doi: 10.1016/B978-0-12-805052-1.00003-6
- Wickström, S. A., Carstensen, J., Blomqvist, M., and Krause-Jensen, D. (2016). Cover of Coastal Vegetation as an Indicator of Eutrophication Along Environmental Gradients. *Mar. Biol.* 163, 257. doi: 10.1007/s00227-016-3032-6
- Woodroffe, S. A., and Long, A. J. (2009). Salt Marshes as Archives of Recent Relative Sea Level Change in West Greenland. *Quat. Sci. Rev.* 28, 1750–1761. doi: 10.1016/j.quascirev.2009.02.009
- Young, A. P., and Carilli, J. E. (2019). Global Distribution of Coastal Cliffs. *Earth Surface Processes Landforms* 44, 1309–1316. doi: 10.1002/esp.4574
- Yu, S. Y., Berglund, B. E., Andren, E., and Sandgren, P. (2004). Mid-Holocene Baltic Sea Transgression Along the Coast of Blekinge, SE Sweden Ancient Lagoons Correlated With Beach Ridges. *GFF* 126, 257–272. doi: 10.1080/11035890401263257
- Ørberg, S. B., Krause-Jensen, D., Mouritsen, K. N., Olesen, B., Marbà, N., Larsen, M. H., et al. (2018). Canopy-Forming Macroalgae Facilitate Recolonization of Sub-Arctic Intertidal Fauna and Reduce Temperature Extremes. *Front. Mar. Sci.* 5. doi: 10.3389/fmars.2018.00332

Conflict of Interest: The authors declare that the research was conducted in the absence of any commercial or financial relationships that could be construed as a potential conflict of interest.

Publisher's Note: All claims expressed in this article are solely those of the authors and do not necessarily represent those of their affiliated organizations, or those of the publisher, the editors and the reviewers. Any product that may be evaluated in this article, or claim that may be made by its manufacturer, is not guaranteed or endorsed by the publisher.

Copyright © 2022 Krause-Jensen, Gundersen, Björk, Gullström, Dahl, Asplund, Boström, Holmer, Banta, Graversen, Pedersen, Bekkby, Frigstad, Skjellum, Thormar, Gyldenkerne, Howard, Pidgeon, Ragnarsdóttir, Mols-Mortensen and Hancke. This is an open-access article distributed under the terms of the Creative Commons Attribution License (CC BY). The use, distribution or reproduction in other forums is permitted, provided the original author(s) and the copyright owner(s) are credited and that the original publication in this journal is cited, in accordance with accepted academic practice. No use, distribution or reproduction is permitted which does not comply with these terms.



Towards Incorporation of Blue Carbon in Falkland Islands Marine Spatial Planning: A Multi-Tiered Approach

Narissa Bax^{1,2,3*†}, David K. A. Barnes^{4†}, Santiago E. A. Pineda-Metz⁵, Tabitha Pearman², Markus Diesing⁶, Stefanie Carter², Rachel V. Downey⁷, Chris D. Evans^{8,9}, Paul Brickley^{2,10}, Alastair M. M. Baylis², Alyssa M. Adler¹¹, Amy Guest^{2,10}, Kara K. S. Layton¹⁰, Paul E. Brewin^{2,12} and Daniel T. I. Bayley^{2,13}

OPEN ACCESS

Edited by:

Joanne S Porter,
Heriot-Watt University,
United Kingdom

Reviewed by:

Lida Teneva,
Independent Researcher,
Sacramento, CA, United States
Craig Smeaton,
University of St Andrews,
United Kingdom

*Correspondence:

Narissa Bax
nbax@saeri.ac.fk

[†]These authors share first authorship

Specialty section:

This article was submitted to
Marine Ecosystem Ecology,
a section of the journal
Frontiers in Marine Science

Received: 09 February 2022

Accepted: 29 April 2022

Published: 10 June 2022

Citation:

Bax N, Barnes DKA, Pineda-Metz SEA, Pearman T, Diesing M, Carter S, Downey RV, Evans CD, Brickley P, Baylis AMM, Adler A, Guest A, Layton KKS, Brewin PE and Bayley DTI (2022) Towards Incorporation of Blue Carbon in Falkland Islands Marine Spatial Planning: A Multi-Tiered Approach. *Front. Mar. Sci.* 9:872727. doi: 10.3389/fmars.2022.872727

¹ Centre for Marine Socioecology, Institute for Marine and Antarctic Studies, University of Tasmania, Hobart, TAS, Australia,

² South Atlantic Environmental Research Institute, Stanley, Falkland Islands, ³ Tasmanian Museum and Art Gallery (TMAG),

Hobart, TAS, Australia, ⁴ British Antarctic Survey (BAS), Cambridge, United Kingdom, ⁵ Alfred Wegener Institute Helmholtz

Centre for Polar and Marine Research (AWI), Bremerhaven, Germany, ⁶ Geological Survey of Norway, Trondheim, Norway,

⁷ Australian National University, Canberra, ACT, Australia, ⁸ Environment Centre Wales, UK Centre for Ecology and Hydrology

(UKCEH), Wallingford, United Kingdom, ⁹ UK Centre for Ecology and Hydrology, Bangor, United Kingdom, ¹⁰ School of

Biological Sciences, University of Aberdeen, Aberdeen, United Kingdom, ¹¹ Duke University, Nicholas School of the

Environment, Durham, NC, United States, ¹² Shallow Marine Surveys Group, Stanley, Falkland Islands, ¹³ Centre for

Biodiversity & Environment Research, University College London, Bloomsbury, London, United Kingdom

Ecosystem-based conservation that includes carbon sinks, alongside a linked carbon credit system, as part of a nature-based solution to combating climate change, could help reduce greenhouse gas levels and therefore the impact of their emissions. Blue carbon habitats and pathways can also facilitate biodiversity retention, aiding sustainable fisheries and island economies. However, robust blue carbon research is often limited at the scale of regional governance and management, lacking both incentives and facilitation of policy-integration. The remote and highly biodiverse coastal ecosystems and surrounding continental shelf can be used to better inform long-term ecosystem-based management in the vast South Atlantic Ocean and sub-Antarctic, to synergistically protect both unique biodiversity and inform on the magnitude of nature-based benefits they provide. Understanding key ecosystem information such as their location, extent, and condition of habitat types, will be critical in understanding carbon pathways to sequestration, threats to this, and vulnerability. This paper considers the current status of blue carbon data and information available, and what is still required before blue carbon can be used as a conservation management tool integrated in national Marine Spatial Planning (MSP) initiatives. Our research indicates that the data and information gathered has enabled baselines for a number of different blue carbon ecosystems, and indicated potential threats and vulnerability that need to be managed. However, significant knowledge gaps remain across habitats, such as salt marsh, mudflats and the mesophotic zones, which hinders meaningful progress on the ground where it is needed most.

Keywords: Falkland Islands, kelp, land-ocean carbon, mesophotic biodiversity, Marine Managed Areas, blue carbon, marine spatial planning, sub-Antarctic

INTRODUCTION

To synergistically tackle nature loss and climate change, the few remaining intact carbon-rich habitats need to be prioritised in conservation efforts (Smith et al., 2022). By protecting these carbon- and species-rich habitats, there is a reduction in carbon release and subsequent contribution to the climate change crisis (Pörtner et al., 2021). The cumulative consequences of anthropogenic climate change, habitat destruction and marine resource extraction are evident globally, even in the most isolated oceans and coastlines (Halpern et al., 2019; Bergstrom et al., 2021; Ward et al., 2022). The comparative isolation and reduced exposure from human pressures on islands and offshore shelf habitats imparts some level of biodiversity protection, but even these are impacted by climate change, marine debris, and non-native species threats (e.g. Barnes et al., 2018a; Hughes et al., 2020). Isolation does not absolve the need for management, nor does it guarantee the long-term sustainability of ecosystem services such as marine carbon capture to sequestration ('blue carbon'; Bax et al., 2021; Bayley et al., 2021). Indeed, remote islands present unique physical and economic barriers to conservation planning. These constraints are evident in a lack of governmental capacity and ecosystem-based knowledge (Queirós et al., 2021), due in part to constraints on financial resourcing for science and marine management (Bax et al., 2022). A comparatively high carbon footprint and associated 'risk footprint' (e.g., fuel transport, site contamination/remediation and oil spill mitigation), pose additional logistical complexities for carbon off-setting in remote environments (Brooks et al., 2018; Brooks et al., 2019). Overcoming these limitations is particularly pressing as CO₂ emissions continue to rise, and biodiversity continues to decline globally (Pörtner et al., 2021). Identifying locations with multiple intact blue carbon ecosystems such as seagrass, saltmarsh, mangrove, macroalgae and deeper seabed habitats is only one part of the challenge. Once these locations are identified, the additional tasks exist of securing adequate resourcing to support their conservation and ensuring this best mitigates threats.

Incorporating blue carbon as a conservation management tool is timely, as the global United Nations Framework Convention on Climate Change (UNFCCC) recommendations for the Conference of the Parties (COP26) in November 2021 noted that 'marine ecosystems' are also recognised as 'carbon sinks' in Article 21 of the final decision. This UNFCCC recommendation emphasises the importance of the protection, conservation, and restoration of terrestrial and marine ecosystems alongside the urgent and considerable reduction of greenhouse gas (GHG) emissions (UNFCCC, 2021a). Article 6 of the Paris Agreement outlines how governments can assist in achieving their Nationally Determined Contributions (NDCs) to carbon reduction and removal targets. This legislation includes international transactions in carbon reduction credits, and could encourage the private sector to contribute to GHG emissions reductions through "non-market approaches" under the Paris Climate Agreement (UNFCCC, 2021b). If such approaches are embraced, economists predict that the revenue from carbon markets could exceed USD 1 trillion by 2050 (IETA and the

University of Maryland, 2021). These economic incentives pave the way for carbon credits linked to blue carbon and marine biodiversity conservation management in the near future. Momentum is therefore growing for robust blue carbon research to facilitate policy-climate-integration and inform accurate carbon accounting across multiple habitats through for example, an understanding of the distribution of carbon sequestering habitat for Marine Spatial Planning (MSP) that addresses ocean climate-driven change ('climate-smart MSP') (see Queirós et al., 2021).

A BROADER BLUE CARBON DEFINITION

Many marine ecosystems are officially recognised as highly efficient carbon sinks. However, when Nellemann et al. (2009) originally defined blue carbon as carbon captured by marine living organisms, they put the spotlight on shallower, relatively accessible mangroves, salt marshes, and seagrasses. Blue carbon research continues to narrowly focus on these coastal ecosystem types because they are actionable; many nearshore systems which remove significant amounts of CO₂ and store fixed carbon long-term, are subjected to undesirable anthropogenic impacts, and can be managed to maintain or enhance carbon stocks. Such management aligns with climate change mitigation and adaptation policies (Lovelock and Duarte, 2019). Other potential blue carbon ecosystem types have only been considered recently, such as macroalgae (Krause-Jensen and Duarte, 2016), and seafloor blue carbon (Barnes, 2015; Bax et al., 2021). However, significant knowledge gaps currently preclude them from being considered as actionable blue carbon ecosystems. These important overlooked blue carbon ecosystems should be reassessed as actionable or non-actionable, once knowledge gaps have been filled.

Here we consider the situation in the Falkland Islands (FI), as an exemplar of global challenges faced. In order to identify and fill key knowledge gaps, this paper discusses the major ecosystems, from terrestrial (green carbon) sequestration and fluvial loss in the shallow sea across the water column, until its potential burial in seabed sediment to provide a framework across the carbon cycle (**Figure 1**). Proposed Marine Management Areas (MMAs) are being consulted upon in 2022 and would encompass 15% of FI marine waters if implemented. This paper provides a foundation for future work on these important ecosystems.

INCORPORATING 'BLUE CARBON' HABITATS INTO MARINE SPATIAL PLANNING IN THE FALKLANDS ISLANDS

The FI in the South West Atlantic, are positioned as a unique ecotone between the southern tip of South America and the Sub-Antarctic. The two main islands (East and West Falkland) are surrounded by over 700 smaller outer islands, and the FI coastline represents some of the world's remaining pristine

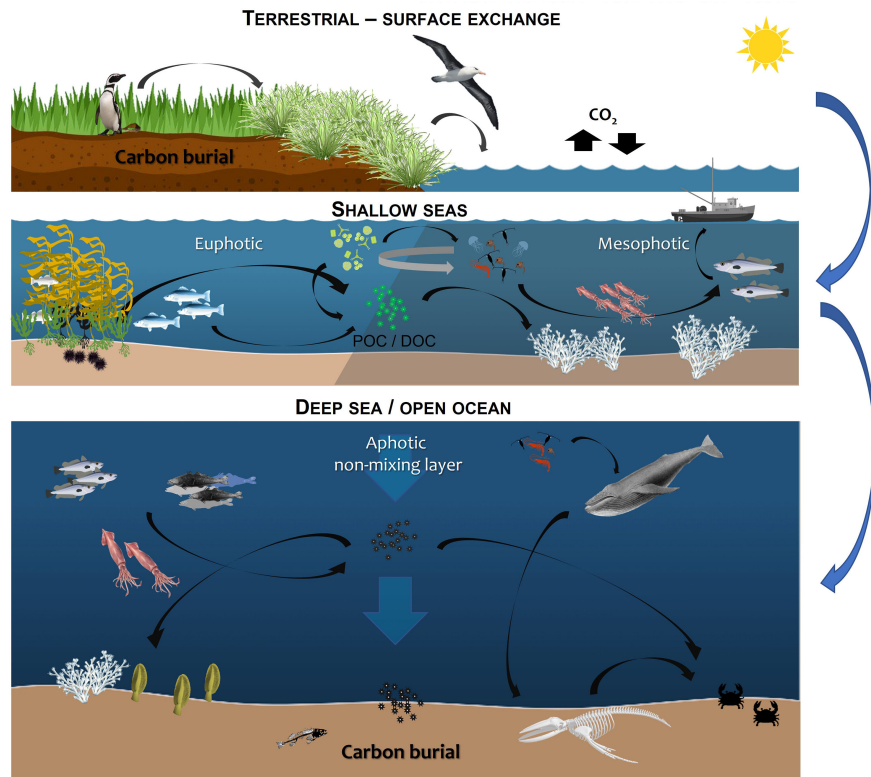


FIGURE 1 | Overview of blue carbon habitats considered here including tidal marsh, mud flats and terrestrial input, the mesophotic zone (30 - 150 metres) and seafloor (carbon storage and sequestration potential) (see SI for an overview of the habitat data available and limitations of the methodology).

kelp ecosystems (van Tussenbroek, 1993; Friedlander et al., 2020; Mora-Soto et al., 2021), with higher biodiversity and species richness than neighbouring South America or the Sub-Antarctic island South Georgia (Figuerola et al., 2017; Beaton et al., 2020). The Falklands Interim Conservation and Management Zone (FICZ; established in 1986) and the Falklands Outer Conservation Zone (FOCZ; established in 1990) extending to 200 nautical miles (~370 km), gave the FI sovereignty over its fisheries and marine waters (Harte and Barton, 2007). The total resident human population is 3203 (Census preliminary results, Falkland Islands Government press statement, 2021), and the Falkland Islands Government launched an Environment Strategy 2021 – 2040, recognising “the central and universal role that the natural environment plays in the sustainable development of our health and wellbeing, our economy and our nation as a whole” (Falkland Islands Government, 2021).

To balance the need for regional economic security and biodiversity conservation, a holistic approach to MSP was initiated in 2014 (Brickle et al., 2019). The MSP process in the FI included an Assessment of Fishing Closure Areas as Sites for wider management (Golding et al., 2017). This process prioritised marine wilderness areas as potential MMAs (Brickle et al., 2019). The proposed MMAs represent an ecosystem-based approach to management planning objectives. The proposed MMAs, if designated, will include protection of kelp forests in

nearshore waters, where they are recognised as structurally complex habitats, providing important ecosystem services (Bayley et al., 2021). In deeper waters, the proposed MMAs encompass the eastern slope of the Burdwood Bank, which is rich in unique and fragile Vulnerable Marine Ecosystems (VME) indicators (Auster et al., 2011; Brewin et al., 2020). Consequently, the MMAs could help to ensure the long-term resilience of multiple habitats and dependent species, as well as the sustainability of economically important fisheries by protecting connectivity between neighbouring biodiversity refugia (Briggs and Bowen, 2013). However, the data gaps common to highly biodiverse, but funding-limited remote island locations hinder the inclusion of management tools, such as the incorporation of blue carbon into MSP presently.

THE FIRST ANNUAL FLUX MEASUREMENTS OF DISSOLVED ORGANIC CARBON IN FALKLANDS RIVERS

The FI terrestrial ecosystems have amongst the highest proportional peat cover recorded anywhere in the world (Carter et al., 2020), making them extraordinarily carbon rich.

It is estimated that its peatlands hold an organic carbon stock of 934 Mt C (Upson et al., 2016), although this is possibly a slight overestimate (SAERI unpublished data). These terrestrial carbon stocks are unlikely to be uniformly distributed, and global soil maps suggest that the South West Atlantic region has variable stocks that are up to 100% peat cover (Poggio et al., 2021 and FAO mapping respectively). Peat run-off impacts neighbouring coastal ecosystems *via* natural processes of organic carbon (OC), from soils to rivers, and subsequent transport into estuaries and then ocean basins (Dinsmore et al., 2010; Evans et al., 2016). These natural processes are sensitive to climate, seasonality and hydrology, and can also be altered or intensified by land-management impacts, including peatland degradation. Recent data from four East Falkland rivers show very high inputs of dissolved organic carbon (DOC) to estuaries (Evans et al., unpublished data), with DOC concentrations approaching those observed in tropical 'blackwater' rivers (Moore et al., 2011). Assuming that measured DOC concentrations in these rivers (which drain a substantial part of the landmass of East FI) are representative of the overall land area, we calculated that the annual flux of DOC carbon in Falkland rivers may be around 0.05 Mt C yr⁻¹ (equivalent to 0.17 Mt CO₂ yr⁻¹ if subsequently oxidised). It appears that the majority of DOC exported from the terrestrial ecosystems is exported to the coastal ocean, but its subsequent fate and impact currently remains unclear. Visual observations have also documented the covering of seabed floors with particulate organic matter (POM) from eroded peat areas and peaty runoff discolouring the intertidal zone after rainfall events, but neither have been quantified (SMSG/SAERI unpublished data). The introduction of grazing animals following European settlement in the 1760s has changed the natural peatlands significantly, causing widespread soil erosion and drainage (Wilson et al., 1993; Otley et al., 2008), which climate change could be exacerbating (Upson et al., 2016). This can be devastating as peat fires alter carbon accumulation potential, can burn for months, producing peat-fire derived emissions (Turetsky et al., 2015). These combined impacts could increase dissolved and particulate export of terrestrial OC to the ocean, with implications such as altered biogeochemical cycles and aquatic light regimes. Research into the land-ocean carbon cycle is therefore required to understand the current impact of fluvial OC transport on the near-shore blue carbon cycle.

UNDESCRIBED COASTAL BLUE CARBON HABITATS

Globally, salt marshes and mudflats are recognised as important blue carbon habitats (e.g. Newton et al., 2021), and conservation measures for carbon accounting and accreditation can be quantifiably applied in some locations (Burden et al., 2019). In the FI, these habitats are limited in extent for two reasons: 1) the tidal range is generally small – a maximum of 1.90 m during spring tides at Stanley, East Falkland, (National Oceanography Centre, 2022) with lower amplitudes south of East Falkland and

higher ones west of West Falkland (Glorioso and Flather, 1995); and 2) coastal areas tend to be steep, so the effect of tides are therefore not visible across large areas. Consequently, salt marsh and mudflat extent is neither mapped nor quantified, limiting any inclusion in conservation management. The application of high-resolution satellite imagery is essential to map these small habitats scattered around the coastline – considering the global loss of these important ecosystems due to ongoing climate change, their disproportionate contribution to blue carbon stocks, and the potential for cross-habitat subsidies in estuaries (Bulmer et al., 2020), baseline information is urgently needed.

THE FIRST SEDIMENT ORGANIC CARBON CONTENT ESTIMATES ACROSS THE FALKLANDS CONSERVATION ZONES

Estimates of organic carbon stocks are required to gauge the importance of a system in the marine organic carbon cycle. Additionally, organic carbon stocks are a measure of the potential vulnerability to human-induced disturbance (Jennerjahn, 2020). Existing seabed sediment maps provide hints to where sizable organic carbon stocks might be expected, as organic carbon content scales with grain size. There are no maps available for this specific geographic region. However, predictive mapping of carbonates and grain size are available (Brewin et al., 2020) and comparative datasets from neighbouring geographies for the Argentinian and FI Island continental shelves do provide insight. For example, Parker et al. (1997) describe most of the continental shelf as either sand or gravel, and open-access seafloor type datasets support this assessment (Petschick et al., 1996; Servicio de Hidrografía Naval 2022). This is clearly an area of much needed future research to inform assessments on organic carbon stocks in surface sediments (upper 10 cm of the sediment column).

A more direct way to estimate organic is to spatially predict them with geostatistical or machine learning methods. This requires observations and suitable predictor variables and has been successfully demonstrated at regional scales (e.g., Diesing et al., 2017; Wilson et al., 2018; Diesing et al., 2021; Pace et al., 2021). The amount of suitable observations within the Falklands Conservation Zones (FCZs) that could be retrieved from relevant databases (PANGAEA, <https://www.pangaea.de/>, MOSAIC, <http://mosaic.ethz.ch/> and dbSEABED <http://instaar.colorado.edu/~jenkins/dbseabed/>) is, however, very limited. To derive a first-order approximation of the size of the organic carbon pool in FCZs surface sediments, we utilise recently published global maps of organic carbon content (Lee et al., 2019) and stock (Atwood et al., 2020).

Atwood et al. (2020) provide a global map of organic carbon stocks, measured in Mg C km⁻², that can be clipped to the FCZs which covers close to half a million km² (SI.1 Table 1). Mean values are then derived for the inner and outer zones with zonal statistics in ESRI ArcGIS, and these are multiplied by the surface area, yielding a pool size of 167 Tg and 138 Tg for the inner and outer zones, respectively. Conversely, using global predictions of

organic carbon content and porosity (Lee et al., 2019) gives pool sizes of 98 Tg and 89 Tg for the inner and outer zones, respectively. These differing estimates indicate that dedicated predictive models based on newly collected data will be necessary to narrow down the uncertainty in the organic carbon pool size (see SI for limitations of this methodology).

Seafloor ecosystems store and sequester from external sources across pelagic food chains with important linkages to macroalgal beds onshore (Bayley et al., 2021). In this manner, seafloor biota do not only bury their own carbon, but trap carbon from multiple sources (Laffoley and Grimsditch, 2009). Knowledge on source-to-sink pathways, organic carbon reactivity (Smeaton and Austin, 2022) and burial rates is essential to understand long-term storage and sequestration capacity. Therefore, without the collection and analysis of new sample data and investment, it is difficult to know how vulnerable the FI carbon stores are to depletion, or where additional carbon sequestration might be possible.

CARBON STORAGE IN FALKLAND ISLANDS KELP ECOSYSTEMS

Kelp forests dominate the FI coastal zone (Beaton et al., 2020), creating habitat for commercially important species and rapidly cycling carbon from the surrounding waters. Existing worldwide, kelps boast high growth rates and productivity (Wernberg et al., 2018). Despite disagreement in the literature on macroalgae's status as 'blue carbon', there is growing evidence for their ability to sequester biomass to surrounding deeper waters by drifting to stable sediment beyond the turbulent mixing layer, and potentially having a substantial role in global carbon cycles (Krause-Jensen and Duarte, 2016; Smale et al., 2018; Froehlich et al., 2019; Filbee-Dexter and Wernberg, 2020).

As knowledge around macroalgal distribution and potential sequestration rates becomes more robust (Queirós et al., 2019; Blain et al., 2021; Pedersen et al., 2021; Smale et al., 2021), kelp's likely role in global carbon storage becomes evident. Bayley et al. (2021), conservatively estimated that kelp in the FI may sequester in the order of 0.299 Mt of CO₂ annually (equating to ~£31.07 million per year at 2020 carbon price). However, a range of assumptions are included in such estimates, particularly relating to total carbon sequestered and the appropriate valuation of carbon credits. The financial value of carbon credits are only eligible for trading if they result from a management activity that illustrates net sequestration gain. For example, through the identification of a degraded location and its restoration. Limiting a nascent area of the blue carbon market, which is not currently accredited.

Due to the large size of blades that extend to the sea surface or sub-surface, it is possible to map the extent of *Macrocystis pyrifera* presence with good confidence. This is a method which has been applied to FI coasts (Golding et al., 2019; Mora-Soto et al., 2020; Houskeeper et al., 2022). However, this method is still limited by factors such as water clarity, wave action, and water depth. Alongside *M. pyrifera*, smaller kelp

species found around the archipelago include the two 'tree kelps', *Lessonia vadosa* and *Lessonia flavicans*, and the 'bull kelp' *Durvillaea antarctica* (Beaton et al., 2020; Mora-Soto et al., 2021). Smaller *Lessonia* species do not raft at the surface and often occur in deeper water or are obscured within the understory, making them difficult to map accurately (Golding et al., 2019). The larger *D. antarctica* can raft, however, its distribution is restricted to a thin band along exposed coasts, which can be difficult to access. Additionally, kelps undergo changes in extent and biomass according to annual/seasonal cycles and wave exposure, making survey timing important (Graham et al., 2007; Beaton et al., 2020). However, estimates of typical biomass, carbon storage per thali, and average net primary production are currently highly uncertain, and include regional taxonomic uncertainty for the *Lessonia* species (Bayley et al., 2021).

With these limiting factors in mind, confidence in kelp distribution may be improved through the collection of acoustic data (multibeam bathymetry/backscatter, side-scan sonar) (Golding et al., 2019). These data will help identify presence and type of vegetated benthic habitat, and the environmental factors which drive their distribution (Kenny et al., 2003; Ratray et al., 2013; Ratray et al., 2015). Combining above-water instrumentation with systematic in-water benthic surveys and use of remote-sensing tools will improve species distribution modelling estimates (Jayatilake and Costello, 2020; Mora-Soto et al., 2020). This will be particularly useful for quantifying vertical distribution of kelps, which can extend to ~60 m depth (Graham et al., 2007).

Once kelp source extent and condition are parameterised, mapping of source-to-sink pathways and quantification of carbon already sequestered within deep sea sediments will be necessary. Sediment depth, type, rate of sedimentation, bioturbation and average anthropogenic or natural disturbance will all influence the amount of carbon stored locally, now and in the future (Macreadie et al., 2017; Green et al., 2018; van de Velde et al., 2018; Atwood et al., 2020).

BLUE CARBON AND PLANKTONIC AND PELAGIC ORGANISMS

Pelagic ecosystem function is integral to global biogeochemical cycling and plays a major role in modulating atmospheric CO₂ concentrations (Howard et al., 2017). The southern Patagonian Shelf, a component of the Patagonian Large Marine Ecosystem, is one of the most productive marine ecosystems globally (Marrari et al., 2017). However, our understanding of regional phytoplankton, zooplankton and bacteria is hampered by a lack of knowledge of the taxa dynamics across the Patagonian Shelf, and particularly within the FCZs (e.g. Sabatini et al., 2004), where there are no oceanographic circulation models available to date. Consequently taxa dynamics are only inferred by proxies such as chlorophyll, which is a measure of phytoplankton biomass in surface waters (NASA satellite data). In contrast, pelagic fish communities in this region are relatively well known

(Arkhipkin et al., 2012; Arkhipkin et al., 2013a; Arkhipkin et al., 2013b), due to a long history of fishing pressure across the region. For example, the squid (*Illex argentinus*) represents the world's second largest cephalopod fishery, and during peak intensity it is a visible feature from space (NASA Earth Observatory 2022). *Illex argentinus* is primarily harvested by squid jigging in the FCZs, the high seas of the Southwest Atlantic, and Argentine Exclusive Economic Zone (to a value of \$597 million USD; range \$301–2,396 million USD based on 2005–2016 data, see Harte et al., 2018). Species at mid to low trophic positions play a key role in the trophodynamics of this ecosystem (e.g. *Sprattus fuegensis*, *Patagonotothen ramsayi*, *Micromesistius australis*, and *Munida gregaria*) and are considered to be a “wasp waist” structured ecosystem (Laptikhovsky et al., 2013; Riccialdelli et al., 2020). Therefore, there is an increasing awareness of the contribution of these fisheries' to important large-scale processes, such as carbon storage, and how ecosystem-based management can help sustain them. However, more knowledge and increased fisheries-science collaboration is required to quantify the specific trophic pathways and fate of carbon transferred through passive settlement to deep marine sediments, or transported *via* active migration of fish to neighbouring regions (Saba et al., 2021; Wing et al., 2021).

Carbon transported to the deep sea through these trophic pathways can remain sequestered for millennia (Howard et al., 2017). However, overfishing and the use of sediment-disturbing bottom trawl nets in particular prevent and reverse blue carbon sequestration over large time scales (van de Velde et al., 2018; Mariani et al., 2020). For example, Mariani et al. (2020) show that through historical extraction and fuel consumption, ocean fisheries have released ≥ 0.73 billion metric tons of CO₂ (GtCO₂) into the atmosphere since 1950. Globally, 43.5% of that blue carbon extracted by these fisheries in the high seas comes from areas that would be economically unprofitable without subsidies (not a component in FI Fisheries). Maintaining well managed fisheries will reduce blue carbon loss to the atmosphere by sustaining the natural carbon pump through healthy fish stocks and increase natural carcass deadfall to the deep sea (Higgs et al., 2014; Honjo et al., 2014). Roughly 60% of the FICZ has fishing restrictions in place presently (SI.1 Table 3) and future monitoring could inform on the effectiveness of these restrictions and closures for protecting carbon stores. Whilst, the proposed FI MMAs could preserve existing carbon storage and stock densities through conserving local marine ‘wilderness’ areas.

BLUE CARBON POTENTIAL OF HABITATS EXTENDING INTO THE MESOPHOTIC ZONE

Mesophotic ecosystems are largely unexplored in the FI and the lower depth limit of most light-dependent species is unknown (Goodwin et al., 2011; Goodwin et al., 2012; Brewin et al., 2020). These habitats constitute complex biodiversity at depths between 30 m to 150 m (Hinderstein et al., 2010) and we calculate that the

projected areal extent of this habitat is over c. 50,000 km² (SI.1 Table 3). However, despite this substantial area, only incidental nearshore surveys have been conducted to explore these depths to date. For example, surveys in 2020 and 2021 recorded the presence of stylasterid coral (hydrocoral) gardens, rhodolith beds (coralline algae nodules), and reef-like aggregations of parchment worms below 40 m during Remote Operated Vehicle (ROV) and drop cameras surveys (SAERI unpublished data). These observations constitute the discovery of carbon rich taxa in the mesophotic zone. Without investments in time and resources, observational data cannot be meaningfully quantified or included in distribution models and conservation planning at present. For example, a search of the Ocean Biodiversity Information System (OBIS) database for VME indicator taxa (FAO, 2008; CCAMLR, 2009) to identify potential benthic sequesters across the FCZs, showed that 26% of all the OBIS VME records are found in the mesophotic zone (Figure 2). However, the upper mesophotic zone (30 – 60 m) has only 0.5% of these, and 29% (c. 700 records) of OBIS VME records do not include depth information at all. These gaps highlight that there is much to be discovered in the FI marine environment, and much that needs to be done to progress the available information into broader application. Investments in nearshore marine science voyages and technology to survey the seafloor through multibeam echo sounder and backscatter data and sampling by means such as with Remote Operated Vehicles (ROVs) are needed to gain a baseline understanding. This will be an important first step to gain an understanding of undiscovered blue carbon habitats and biodiversity in areas where fisheries do and do not operate. Sampling in areas where fisheries operate could be undertaken in collaboration with existing ship-based data collections, and would aid in validating onshore to offshore carbon pathways and natural fluctuations through time. However, demonstrating permanence (removal of carbon from the biological to the geological carbon cycle), and identifying an intervention to increase carbon drawdown at scale is a substantial research effort, across much of the FCZs and central plateau region of the southern proposed Burdwood Bank MMA to understand mesophotic blue carbon (c. 11% SI.1. Table 3).

BENTHIC HABITATS OFFSHORE WITH LONG-TERM CARBON STORAGE AND SEQUESTRATION POTENTIAL

The FI benthic slope habitats share close affinities with the Sub-Antarctic, one of the world's most important geographic regions for the sequestration of anthropogenic CO₂ by marine ecosystems (Thomalla et al., 2011; Swart et al., 2015; Pörtner et al., 2021). Marine organic carbon accumulation is predicted to be primarily on shelf and slope habitats globally (e.g., Muller-Karger et al., 2005), where biodiversity is greatest, and where it is often vulnerable to the impacts of fishing gear and biomass extraction (Mariani et al., 2020). The biota on continental shelves at high southern latitudes are effective at sequestering carbon and

unlike other carbon sinks, they are increasing with climate change (for example around Antarctica: Barnes et al., 2018a; Bax et al., 2021; Cavanagh et al., 2021). A better understanding of these potentially rare and sizable (in terms of area) negative feedbacks on climate change, is valuable in social carbon costs. Seabed biomass shallower than 1000 m in some South Atlantic habitats can accumulate carbon of considerable mitigation potential (Barnes et al., 2021). The eastern Burdwood Bank (adjacent to the Namuncurá MPA), is a proposed MMA, and preliminary research suggests it hosts high carbon storage and sequestration potential (Bax and Cairns, 2014). Furthermore, carbon and biodiversity rich habitats including abundant stylasterid and scleractinian coral assemblages add to the conservation significance of this region (Bax et al., 2014; Cairns and Polonio, 2013). Cold water corals are debated as 'blue carbon' habitats as they re-emit some CO₂ when building their CaCO₃ skeletons (Laffoley and Grimsditch, 2009). Much seafloor life has importance as ecosystem engineers and sediment creators, but their vulnerability to climate change (Figuerola et al., 2021, Rogers et al., 2021) and bottom fishing mean a focus on maintaining ecosystem function at the site of sequestration - where it is most crucial to long-term climate mitigation - includes conservation of VME indicator taxa (such as corals) and the ecosystem services a biodiverse seafloor habitat can provide.

If research on ecosystem function at the site of sequestration is prioritised, a quantification and forecasting approach to blue carbon in locations like the Burdwood Bank could potentially lead to future investments in biodiversity conservation offshore, which includes economic gains by sustaining ecosystem services to inform national emission targets. However, there are a number of limitations to ground truthing long term carbon sequestration estimates on the seafloor (100s - 1000s of years), and the climate mitigation potential of benthic ecosystems in a policy-specific context (Bax et al., 2021). Primarily, this ground-truthing relies on seabed mapping technology with the capacity to discriminate between benthic habitats and model species distributions at multiple spatial scales. Investment at this scale is lacking, and large swaths of seafloor have never been sampled, or examined by multibeam echosounder, and in some cases these data are under commercial licence and not openly available for use (Figure 2). The limited spatial extent of ground-truthed data, coupled with the low resolution of environmental data used in these models, is the main limitation of habitat maps (Guisan and Thuiller, 2005; Ross et al., 2015), and we present a synthesis of high resolution bathymetry available to date (Figure 2 limitations outlined in SI).

The wealth of VME indicator taxa recorded from across the FI (Figure 2), including high sponge diversity (Goodwin et al., 2011), scleractinian coral reefs (Cairns and Polonio, 2013; Brewin et al., 2020), sea pen fields, coral gardens (Brewin et al., 2020), chemosynthetic communities (Noble, 2014 unpublished data) and field-like aggregations of deep-sea stylasterid (lace) corals across the plateau (Bax and Cairns, 2014; Bax, 2014); highlight that there is much to discover by investing in seafloor science in the FI. In an attempt to inform protection of these blue carbon habitats, spatial overlap between functional group

records and VME indicator taxa were compared (SI.1 Table 2). Considering the proportion of soft sediment on the FCZs (Petschick et al., 1996; Parker et al., 1997; Servicio de Hidrografía Naval 2022; Gerdes and Montiel, 1999), and the areal extent of VME indicator taxa of the FCZs c. 175, 000 km² (SI.1 Table 2), future work could align these groupings with geographic data sets in the Southern Ocean where core estimates have been contrasted against seabed images to clarify blue carbon gains (Zwerschke et al., 2022). However, whilst an imaging research approach is non-invasive and helps to clarify seafloor community ecology, it can fail to include infaunal species data. These data are often only available based on generalised biomass estimates (e.g., Brey and Gerdes, 1999) and species lists from adjacent regions (e.g., Gerdes and Montiel, 1999; Rios et al., 2003) limiting our capacity to understand basic seafloor biodiversity composition.

FUTURE SEAFLOOR BLUE CARBON PRIORITY RESEARCH AREAS

Future work would be most informative if bathymetric data were ground-truthed with seabed core sampling to clarify carbon content and production estimates, combined with carbon dating technology, through time (Atwood et al., 2020). Data from the Magellan and Beagle Channel region (including shelf estimates) provide comparable carbon content and production estimates to the eastern Weddell Sea (Brey and Gerdes, 1999). Ideally this information can be overlaid with VME and infaunal assemblage mapping, biogeochemistry, and population genetics to estimate blue carbon connectivity from key model sequesters (e.g., corals, sponges and echinoderms). This type of information would validate carbon storage and sequestration estimates based on functional groups at finer temporal and spatial scales (e.g., per population, per area, per year over time) both offshore (e.g., Barnes and Sands, 2017; Barnes et al., 2021) and nearshore (e.g., Morley et al., 2022). However, such estimates also rely on knowledge of a taxon's traits such as feeding strategy, mobility and lifestyle, which is lacking for most benthic taxa (www.SCAR-MarBIN.be). Therefore, an accurate estimation of carbon storage rates (such as annual increments) across areas for the purpose of carbon accreditation is currently difficult at the scales needed by policy (unless undertaken on a taxon by taxon basis (e.g. bryozoans, see Barnes, 2015).

FORWARD LOOK

The preservation of nature as a functional carbon sink, is based upon the long-term burial capacity of seafloor biota and the continued efficiency of external sources of carbon such as macroalgal beds and pelagic ecosystems. This recognition imparts the need for a multi-tiered approach to blue carbon research that includes fisheries management and terrestrial blue carbon pathways. This approach also focuses on ecosystem based preservation, as it is far more efficient and less costly to protect

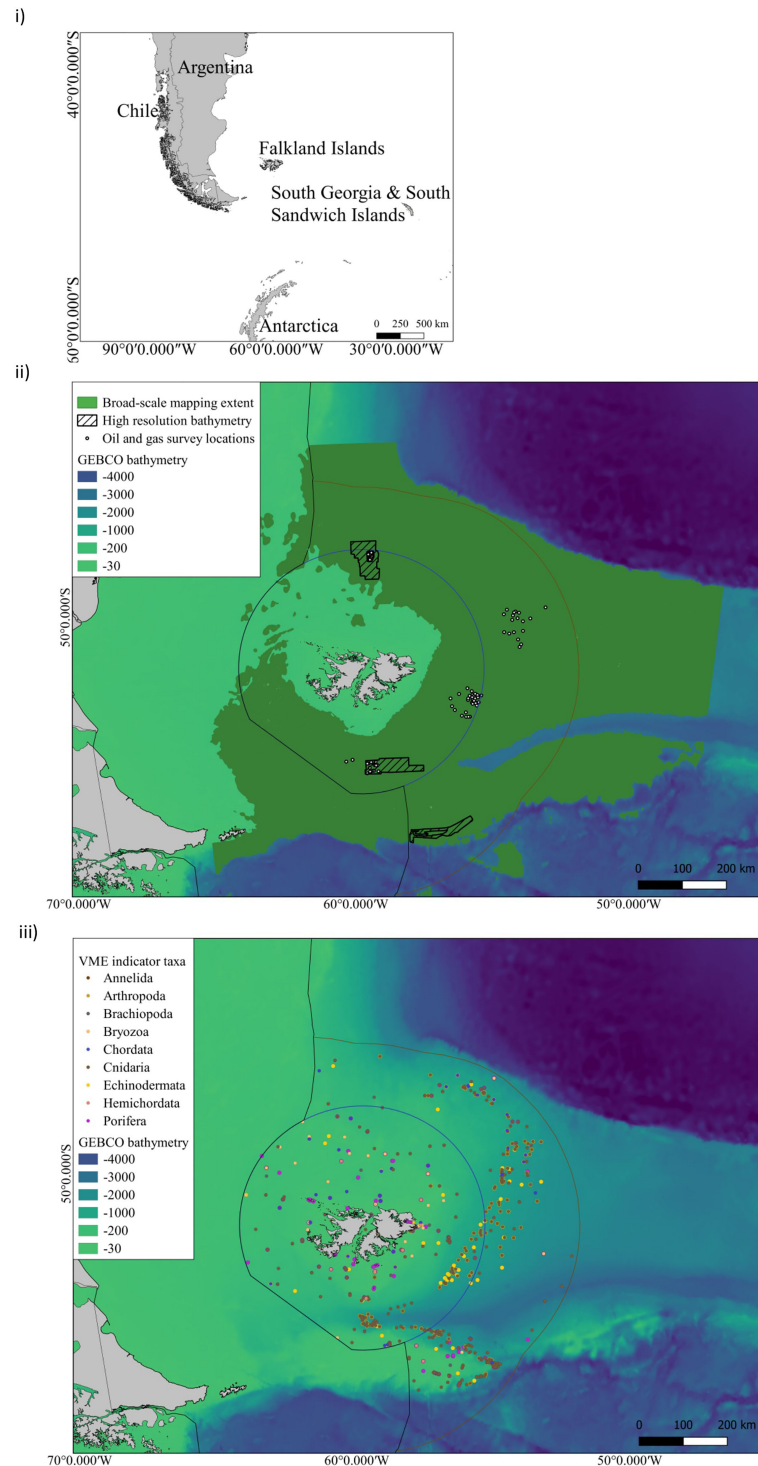


FIGURE 2 | i) The Falkland Islands geographic location in the South West Atlantic ii) Distribution of offshore surveys in FCZs: Broad-scale classification habitat maps and predictive maps of VME taxa as proxies of VMEs have been produced over the spatial extent indicated in dark green. These broad-scale maps have been based upon GEBCO bathymetry. Higher resolution mapping has been undertaken at oil and gas survey point locations shown by white circles ($2 \times 2 \text{ km}^2$). High-resolution bathymetry has been collected at these sites and within the hashed boxes. iii) VME indicator taxa compiled from OBIS, SAERI unpublished data and Brewin et al., 2020 (SI.1 Table 2) for the following taxa grouped by Phylum - Annelida - Serpulidae; Arthropoda - Bathylasmatidae; Brachiopoda; Bryozoa; Chordata - Ascidiacea; Cnidaria - Actiniaria, Alcyonacea, Pennatulacea, Scleractinia, Antipatharia, Hydroidolina, Stylasteridae; Echinodermata - Crinoidea, Ophiurida, Cidaroida; Hemichordata; Porifera.

habitats while healthy than to restore once degraded, with compromised carbon storage and sequestration capabilities (Barnes et al., 2021; Bax et al., 2021; Bayley et al., 2021). In the context of blue carbon, understanding key ecosystem information like the location, extent, and condition of broad scale habitat types, will be critical in understanding sequestration pathways and capacity. In turn, blue carbon habitats and pathways can facilitate strategic and adaptive planning aimed at retaining biodiversity, maintaining sustainable fisheries, and preserving ecosystem services and economies for generations to come (Bertram et al., 2021). However, before this utility of blue carbon as a MSP tool can be realised, a substantial knowledge and understanding base is required.

MPAs and spatial management are an important part of sustainable futures, especially if MSP can keep pace with climate change and remain both locally and globally relevant (Queirós et al., 2021). As the UN Ocean Decade for Sustainable Development (2021 - 2030) progresses, there is an increasing emphasis on negotiations for a new UN treaty on Biodiversity Beyond National Jurisdictions (BBNJ), where greater than 50% of earth's biodiversity resides (FAO, 2020). The total area of fishing footprint determined by Brewin et al. (2020) for both the FCZs and ABNJ is 36 924 km², and the total footprint of actual fished ground in the ABNJ is almost twice as large as the FICZ (23 928 km²) and FOCZ (12 997 km²). Therefore, whilst this paper focuses on knowledge gaps within the FCZs, as extractive industries expand globally, the FI also provides a test-case for the necessity of protection and sustainable practice in jurisdictional waters - to mitigate the threat of unregulated fleets in Areas Beyond National Jurisdiction (ABNJ). Furthermore, by filling the common knowledge gaps outlined here, all conservation and monitoring strategies south of 40° would benefit and could potentially replicate multi-tier approaches. In this manner, the inclusion of blue carbon research into MSP must also grapple with a contiguous managed area that includes ABNJ fisheries across a vast area extending into the Scotia arc in the sub-Antarctic. Given the diversity of habitats and high endemism to consider (Morley et al., 2022), a precautionary and informed management approach to conservation will be imperative.

DATA AVAILABILITY STATEMENT

The datasets presented in this study can be found in online repositories. The names of the repository/repositories and accession number(s) can be found in the article/**Supplementary Material**.

AUTHOR CONTRIBUTIONS

NB, DTIB, and KL formed the original concept for a blue carbon synthesis paper. NB wrote the draft manuscript. NB, DKAB, MD, SP-M and DTIB contributed to the introduction and manuscript framing. AB and NB contributed to the main text on FI policy and MSP. SC and CE contributed text on terrestrial carbon and

fluvial input. TP and RD provided maps and compiled available bathymetry, VME and OBIS data for this publication. RD calculated areal extent estimates. MD provided the first marine carbon stock estimates for the FICZs. DTIB, AG and AA contributed text on FI kelp ecosystems. NB and RD contributed text on FI mesophotic ecosystems. DTIB, PB, NB and SP-M contributed text on pelagic blue carbon and fisheries. NB, TP, RD, MD, DKAB and SP-M contributed text on seafloor blue carbon. DTIB created the visual abstract and paper figure. All co-authors were invited to review and edit content prior to manuscript submission. NB formed this multi-disciplinary collaboration as part of the Sub-Antarctic Blue Carbon and Natural Archives Network and as part of her research agenda as MCPC at SAERI to support research on the proposed MMAs in the FI. All authors contributed to the article and approved the submitted version.

FUNDING

We are grateful to the John Ellerman foundation for funding the Marine and Coastal Program Coordinator (NB) at the South Atlantic Environmental Research Institute (SAERI), SAERI is a registered charity in England and Wales. All authors contributed their time in kind to progress research and conservation. RD is funded by an Australian Government Research Training Program for her PhD research. DOC flux measurements reported were supported by the UK Natural Environment Research Council LOCATE project (NE/N018087/1). The author contributions (SC, CDE) on terrestrial carbon were supported by the Darwin Initiative through UK Government funding for projects DPLUS083 and DPLUS116. AG is funded by the Falkland Islands Government CDS Fund, John Cheek Trust, RBC Ltd for her PhD program. Funding for open access publication was provided by the British Antarctic Survey.

ACKNOWLEDGMENTS

We gratefully acknowledge our collaborators and colleagues, the organisations and individuals who contributed their time and expertise to marine spatial planning in the Falkland Islands, Alex Blake and Jorge Ramos at Falkland Island Fisheries for spatial estimates of fisheries in FCZs, Jack Ingledew for providing GIS and metadata assistance, and Chester Sands for providing input on an earlier draft of the manuscript. This paper is dedicated to the Falklands' future generations and the important marine biodiversity they will inherit.

SUPPLEMENTARY MATERIAL

The Supplementary Material for this article can be found online at: <https://www.frontiersin.org/articles/10.3389/fmars.2022.872727/full#supplementary-material>

REFERENCES

- Arkhipkin, A., Barton, J., Wallace, S., and Winter, A. (2013a). Close Cooperation Between Science, Management and Industry Benefits Sustainable Exploitation of the Falkland Islands Squid Fisheries. *J. Fish Biol.* 83 (4), 905–920. doi: 10.1111/jfb.12098
- Arkhipkin, A., Brickle, P., and Laptikhovsky, V. (2013b). Links Between Marine Fauna and Oceanic Fronts on the Patagonian Shelf and Slope. *Arquipelago Life Mar. Sci.* 30, 19–37. doi: 10.1111/jfb.12098
- Arkhipkin, A., Brickle, P., Laptikhovsky, V., and Winter, A. (2012). Dining Hall at Sea: The Eastern Patagonian Shelf is a Destination for Feeding Migrations of Nektonic Predators. *J. Fish Biol.* 81, 882–902. doi: 10.1111/j.1095-8649.2012.03359.x
- Atwood, T. B., Witt, A., Mayorga, J., Hammill, E., and Sala, E. (2020). Global Patterns in Marine Sediment Carbon Stocks. *Front. Mar. Sci.* 7. doi: 10.3389/fmars.2020.00165
- Auster, P. J., Gjerde, K., Heupel, E., Watling, L., Grehan, A., and Rogers, A. D. (2011). Definition and Detection of Vulnerable Marine Ecosystems on the High Seas: Problems With the “Move-on” Rule. *ICES J. Mar. Sci.* 68 (2), 254–264. doi: 10.1093/icesjms/fsq074
- Barnes, D. K. A. (2015). Antarctic Sea Ice Losses Drive Gains in Benthic Carbon Drawdown. *Curr. Biol.* 25 (18), R789–R790. doi: 10.1016/j.cub.2015.07.042
- Barnes, D. K. A., Bell, J. B., Bridges, A. E., Ireland, L., Howell, K. L., Martin, S. M., et al. (2021). Climate Mitigation Through Biological Conservation: Extensive and Valuable Blue Carbon Natural Capital in Tristan Da Cunha's Giant Marine Protected Zone. *Biology* 10, 1339. doi: 10.3390/biology10121339
- Barnes, D. K. A., Fleming, A., Sands, C. J., Quartino, M. L., Deregis, D., Chester, J., et al. (2018a). Icebergs, Sea Ice, Blue Carbon and Antarctic Climate Feedbacks. *Philos. Trans. R. Soc. A* 376 (2122), 20170176. doi: 10.1098/rsta.2017.0176
- Barnes, D. K. A., Morlet, S. A., Bell, J., Brewin, P., Brigden, K., Collins, M., et al. (2018b). Marine Plastics Threaten Giant Atlantic Marine Protected Areas. *Curr. Biol.* 28, R1137–R1138. doi: 10.1016/j.cub.2018.08.064
- Barnes, D. K. A., and Sands, C. J. (2017). Functional Group Diversity is Key to Southern Ocean Benthic Carbon Pathways. *PLoS One* 12 (6), 1–14. doi: 10.1371/journal.pone.0179735
- Bax, N., and Cairns, S. D. (2014). Stylasteridae (Cnidaria; Hydrozoa). Biogeographic Atlas of the Southern Ocean.
- Bax, N. (2014). Deep-Sea Stylasterid Corals in the Antarctic, Sub-Antarctic and Patagonian Benthos: Biogeography, Phylogenetics, Connectivity and Conservation (Doctoral dissertation, University of Tasmania).
- Bax, N., Novaglio, C., Maxwell, K. H., Meyers, K., McCann, J., Jennings, S., et al. (2022). Ocean Resource Use: Building the Coastal Blue Economy. *Rev. Fish Biol. Fish.* 32 (1), 189–207. doi: 10.1007/s11160-021-09636-0
- Bax, N., Sands, C. J., Gogarty, B., Downey, R. V., Moreau, C. V. E., Moreno, B., et al. (2021). Perspective: Increasing Blue Carbon Around Antarctica is an Ecosystem Service of Considerable Societal and Economic Value Worth Protecting. *Glob. Change Biol.* 27 (1), 5–12. doi: 10.1111/gcb.15392
- Bayley, D. T. I., Brickle, P., Brewin, P. E., Golding, N., and Pelembe, T. (2021). Valuation of Kelp Forest Ecosystem Services in the Falkland Islands: A Case Study Integrating Blue Carbon Sequestration Potential. *One Ecosyst.* 6, e62811. doi: 10.3897/oneeco.6.e62811
- Beaton, E. C., Küpper, F. C., van West, P., Brewin, P. E., and Brickle, P. (2020). The Influence of Depth and Season on the Benthic Communities of a *Macrocystis Pyrifera* Forest in the Falkland Islands. *Polar Biol.* 43, 573–586. doi: 10.1007/s00300-020-02662-x
- Bergstrom, D. M., Wienecke, B. C., van den Hoff, J., Hughes, L., Lindenmayer, D. B., Ainsworth, T. D., et al. (2021). Combating Ecosystem Collapse From the Tropics to the Antarctic. *Glob. Change Biol.* 27 (9), 1692–1703. doi: 10.1111/gcb.15539
- Bertram, C., Quaas, M., Reusch, T. B., Vafeidis, A. T., Wolff, C., and Rickels, W. (2021). The Blue Carbon Wealth of Nations. *Nat. Climate Change* 11 (8), 704–709. doi: 10.1038/s41558-021-01089-4
- Blain, C. O., Hansen, S. C., and Shears, N. T. (2021). Coastal Darkening Substantially Limits the Contribution of Kelp to Coastal Carbon Cycles. *Glob. Change Biol.* 27, 5547–5563. doi: 10.1111/gcb.15837
- Brewin, P. E., Farrugia, T. J., Jenkins, C., and Brickle, P. (2020). Straddling the Line: High Potential Impact on Vulnerable Marine Ecosystems by Bottom-Set Longline Fishing in Unregulated Areas Beyond National Jurisdiction. *ICES J. Mar. Sci.* 78 (6), 2132–2145. doi: 10.1093/icesjms/fsaa106
- Brey, T., and Gerdes, D. (1999). Benthic Community Productivity in the Magellan Region and in the Weddell Sea. *Sci. Mar.* 63 (1), 145–148. doi: 10.3989/scimar.1999.63s1145
- Brickle, P., Barton, J., Simovic, D., Golding, N., de Lecea, A., and Brewin, P. (2019). Marine Ecosystem Protection in the Falkland Islands. *Mar. Biol. Mag.* 13, 20–21.
- Briggs, J. C., and Bowen, B. W. (2013). Marine Shelf Habitat: Biogeography and Evolution. *J. Biogeogr.* 40 (6), 1023–1035. doi: 10.1111/jbi.12082
- Brooks, S. T., Jabour, J., and Bergstrom, D. M. (2018). What is ‘Footprint’ in Antarctica: Proposing a Set of Definitions. *Antarct. Sci.* 30 (4), 227–235. doi: 10.1017/S0954102018000172
- Brooks, S. T., Jabour, J., Van Den Hoff, J., and Bergstrom, D. M. (2019). Our Footprint on Antarctica Competes With Nature for Rare Ice-Free Land. *Nat. Sustain.* 2 (3), 185–190. doi: 10.1038/s41893-019-0237-y
- Bulmer, R. H., Stephenson, F., Jones, H. F., Townsend, M., Hillman, J. R., Schwendenmann, L., et al. (2020). Blue Carbon Stocks and Cross-Habitat Subsidies. *Front. Mar. Sci.* 7, 380. doi: 10.3389/fmars.2020.00380
- Burden, A., Garbutt, A., and Evans, C. D. (2019). Effect of Restoration on Saltmarsh Carbon Accumulation in Eastern England. *Biol. Lett.* 15 (1), 20180773. doi: 10.1098/rsbl.2018.0773
- Cairns, S. D., and Polonio, V. (2013). New Records of Deep-Water Scleractinia Off Argentina and the Falkland Islands. *Zootaxa* 3691 (1), 58–86. doi: 10.11646/zootaxa.3691.1.2
- Carter, S., Aitkenhead, M., Evans, C., Jungblut, A., McAdam, J., McNee, M., et al. (2020). Soil Map and Online Database as Climate Change Mitigation Tools. *Darwin Plus*, 083.
- Cavanagh, R. D., Melbourne-Thomas, J., Grant, S. M., Barnes, D. K., Hughes, K. A., Halfter, S., et al. (2021). Future Risk for Southern Ocean Ecosystem Services Under Climate Change. *Front. Mar. Sci.* 7, 1224. doi: 10.3389/fmars.2020.615214
- CCAMLR (2009). *VME Taxa Classification Guide* (Australia: Commission for the Conservation of Antarctic Marine Living Resources).
- Census preliminary results, Falkland Islands Government press statement (2021). Available at: www.falklands.gov.fk/census (Accessed February 1, 2022).
- Diesing, M., Kröger, S., Parker, R., Jenkins, C., Mason, C., and Weston, K. (2017). Predicting the Standing Stock of Organic Carbon in Surface Sediments of the North-West European Continental Shelf. *Biogeochemistry* 135, 183–200. doi: 10.1007/s10533-017-0310-4
- Diesing, M., Thorsnes, T., and Bjarnadóttir, L. R. (2021). Organic Carbon Densities and Accumulation Rates in Surface Sediments of the North Sea and Skagerrak. *Biogeosciences* 18, 2139–2160. doi: 10.5194/bg-18-2139-2021
- Dinsmore, K. J., Billett, M. F., Skiba, U. M., Rees, R. M., Drewer, J., and Helfter, C. (2010). Role of the Aquatic Pathway in the Carbon and Greenhouse Gas Budgets of a Peatland Catchment. *Glob. Change Biol.* 16 (10), 2750–2762. doi: 10.1111/j.1365-2486.2009.02119.x
- Evans, C. D., Renou-Wilson, F., and Strack, M. (2016). The Role of Waterborne Carbon in the Greenhouse Gas Balance of Drained and Re-Wetted Peatlands. *Aquat. Sci.* 78 (3), 573–590. doi: 10.1007/s00027-015-0447-y
- Falkland Islands Government (2021) *Falkland Islands Environment Strategy 2021–2040* (Stanley, Falkland Islands). Available at: <https://www.fig.gov.fk/policy/environment/environment-strategy> (Accessed February 10, 2022).
- FAO. (2008). International Guidelines for the Management of Deep-Sea Fisheries in the High-Seas. *Food and Agriculture Organization of the United Nations*. Adopted in Rome, Italy on 29 August 2008.
- FAO (2020) *Common Oceans, A Partnership for Sustainability in the ABNJ* (Food and Agriculture Organization of the United Nations). Available at: <http://www.fao.org/in-action/commonoceans/en/> (Accessed April 01, 2022).
- Figuerola, B., Barnes, D. K. A., Brickle, P., and Brewin, P. E. (2017). Bryozoan Diversity Around the Falkland and South Georgia Islands: Overcoming Antarctic Barriers. *Mar. Environ. Res.* 126, 81–94. doi: 10.1016/j.marenvres.2017.02.005
- Figuerola, B., Hancock, A. M., Bax, N., Cummings, V. J., Downey, R., Griffiths, H. J., et al. (2021). A Review and Meta-Analysis of Potential Impacts of Ocean Acidification on Marine Calcifiers From the Southern Ocean. *Front. Mar. Sci.* 8. doi: 10.3389/fmars.2021.584445
- Filbee-Dexter, K., and Wernberg, T. (2020). Substantial Blue Carbon in Overlooked Australian Kelp Forests. *Sci. Rep.* 10, 12341. doi: 10.1038/s41598-020-69258-7

- Friedlander, A. M., Ballesteros, E., Bell, T. W., Caselle, J. E., Campagna, C., Goodell, W., et al. (2020). Kelp Forests at the End of the Earth: 45 Years Later. *PLoS One* 15 (3), e0229259. doi: 10.1371/journal.pone.0229259
- Frøehlich, H. E., Afflerbach, J. C., Frazier, M., and Halpern, B. S. (2019). Blue Growth Potential to Mitigate Climate Change Through Seaweed Offsetting. *Curr. Biol.* 29, 3087–3093.e3. doi: 10.1016/j.cub.2019.07.041
- Gerdes, D., and Montiel, A. (1999). Distribution Patterns of Macrozoobenthos: A Comparison Between the Magellan Region and the Weddell Sea (Antarctica). *Sci. Mar.* 63 (1), 149–153. doi: 10.3989/scimar.1999.63s1149
- Glorioso, P. D., and Flather, R. A. (1995). A Barotropic Model of the Currents Off SE South America. *J. Geophys. Res. Oceans* 100 (C7), 13427–13440. doi: 10.1029/95JC00942
- Golding, N., and Augé, A. (2017). Marine Spatial Planning Phase II: Project Delivery Report. 1–123.
- Golding, N., Black, B., Blake, D., Brewin, P., Harte, M., Havercroft, H., et al. (2019). *Long-Term Coastal Habitat Mapping & Monitoring Handbook. Examples Based on Work Undertaken in the Falkland Islands & South Georgia* (DPLUS065 Coastal Habitat Mapping project). Available at: https://www.south-atlantic-research.org/wp-content/uploads/2020/05/DPLUS065_MonitoringHandbook_Final.pdf.
- Goodwin, C., Brewin, P. E., and Brickle, P. (2012). Sponge Biodiversity of South Georgia Island With Descriptions of Fifteen New Species. *Zootaxa* 3542, 1–48. doi: 10.11646/zootaxa.3542.1.1
- Goodwin, C., Jones, J., Neely, K., and Brickle, P. (2011). Sponge Biodiversity of the Jason Islands and Stanley, Falkland Islands With Descriptions of Twelve New Species. *J. Mar. Biol. Assoc. UK* 91 (2), 275–301. doi: 10.1017/S0025315410001542
- Graham, M. H., Vásquez, J. A., and Buschmann, A. H. (2007). Global Ecology of the Giant Kelp *Macrocystis*: From Ecotypes to Ecosystems. *Oceanogr. Mar. Biol.* 45, 39–88. doi: 10.1201/9781420050943.ch2
- Green, A., Chadwick, M. A., and Jones, P. J. S. (2018). Variability of UK Seagrass Sediment Carbon: Implications for Blue Carbon Estimates and Marine Conservation Management. *PLoS One* 13, 1–18. doi: 10.1371/journal.pone.0204431
- Guisan, A., and Thuiller, W. (2005). Predicting Species Distribution: Offering More Than Simple Habitat Models. *Ecol. Lett.* 8 (9), 993–1009. doi: 10.1111/j.1461-0248.2005.00792
- Halpern, B. S., Frazier, M., Afflerbach, J., Lowndes, J. S., Micheli, F., O'Hara, C., et al. (2019). Recent Pace of Change in Human Impact on the World's Ocean. *Sci. Rep.* 9, 11609. doi: 10.1038/s41598-019-47201-9
- Harte, M., and Barton, J. (2007). Balancing Local Ownership With Foreign Investment in a Small Island Fishery. *Ocean Coast Manage.* 7, 523–537. doi: 10.1016/j.ocecoaman.2007.03.001
- Harte, M., Borberg, J., and Sylvia, G. (2018). *Argentine Shortfin Squid (Illex Argentinus) Value Chain Analysis With an Emphasis on the Falkland Islands. Final Report for the South Atlantic Overseas Territories Natural Capital Assessment* (Joint Nature Conservation Committee (JNCC)). Available at: <https://data.jncc.gov.uk/data/3d406e7f-3bb0-4bed-9bfc-584398a2aaef/ot-ncasup-sat-28-fi-mar2019.pdf>.
- Higgs, N. D., Gates, A. R., and Jones, D. O. B. (2014). Fish Food in the Deep Sea: Revisiting the Role of Large Food-Falls. *PLoS One* 9, e96016. doi: 10.1371/journal.pone.0096016
- Hinderstein, L. M., Marr, J. C. A., Martinez, F. A., Dowgiallo, M. J., Puglise, K. A., Pyle, R. K., et al. (2010). Theme Section on “Mesophotic Coral Ecosystems: Characterization, Ecology, and Management”. *Coral Reefs* 29, 247–251. doi: 10.1007/s00338-010-0614-5
- Honjo, S., Eglinton, T., Taylor, C., Ulmer, K., Sievert, S., Bracher, A., et al. (2014). Understanding the Role of the Biological Pump in the Global Carbon Cycle: An Imperative for Ocean Science. *Oceanography* 27, 10–16. doi: 10.5670/oceanog.2014.78
- Houskeeper, H. F., Rosenthal, I. S., Cavanaugh, K. C., Pawlak, C., Trouille, L., Byrnes, J. E. K., et al. (2022). Automated Satellite Remote Sensing of Giant Kelp at the Falkland Islands (Islas Malvinas). *PLoS One* 17, e0257933. doi: 10.1371/journal.pone.0257933
- Howard, J., Sutton-Grier, A., Herr, D., Kleypas, J., Landis, E., Mcleod, E., et al. (2017). Clarifying the Role of Coastal and Marine Systems in Climate Mitigation. *Front. Ecol. Environ.* 15, 42–50. doi: 10.1002/fee.1451
- Hughes, K. A., Pescott, O. L., Peyton, J., Adriaens, T., Cottier-Cook, E. J., Key, G., et al. (2020). Invasive non-Native Species Likely to Threaten Biodiversity and Ecosystems in the Antarctic Peninsula Region. *Glob. Change Biol.* 26, 2702–2716. doi: 10.1111/gcb.14938
- IETA and the University of Maryland (2021) *The Potential Role of Article 6 Compatible Carbon Markets in Reaching Net-Zero*. Available at: https://www.ieta.org/resources/Resources/Net-Zero/Final_Net-zero_A6_working_paper.pdf (Accessed February 7, 2022).
- Jayathilake, D. R. M., and Costello, M. J. (2020). A Modeled Global Distribution of the Kelp Biome. *Biol. Conserv.* 252, 108815. doi: 10.1016/j.biocon.2020.108815
- Jennerjahn, T. C. (2020). Relevance and Magnitude of “Blue Carbon” Storage in Mangrove Sediments: Carbon Accumulation Rates vs. Stocks, Sources vs. Sinks. *Estuar. Coast Shelf Sci.* 247, 107027. doi: 10.1016/j.ecss.2020.107027
- Kenny, A., Cato, I., Desprez, M., Fader, G., Schuttenhelm, R., and Side, J. (2003). An Overview of Seabed-Mapping Technologies in the Context of Marine Habitat Classification. *ICES J. Mar. Sci.* 60, 411–418. doi: 10.1016/S1054-3139(03)00006-7
- Krause-Jensen, D., and Duarte, C. M. (2016). Substantial Role of Macroalgae in Marine Carbon Sequestration. *Nat. Geosci.* 9, 737–742. doi: 10.1038/ngeo2790
- Laffoley, D., and Grimsditch, G. D. (2009). *The Management of Natural Coastal Carbon Sinks*. Gland (SwissPrinters IRL). Available at: <https://books.google.com/books?hl=en&lr=&id=NZzLOHYvvO4C&oi=fnd&pg=PR5&dq=Laffoley,+D.,+and+Grimsditch,+G.+D.+&ots=8fBTkOtmPw&sig=VxLB3iHVFxC1ivnwNNftwUjgBEM>.
- Lapikhovskiy, V., Arkhipkin, A., and Brickle, P. (2013). From Small Bycatch to Main Commercial Species: Explosion of Stocks of Rock Cod Patagonotothen Ramsayi (Regan) in the Southwest Atlantic. *Fish. Res.* 147, 399–403. doi: 10.1016/j.fishres.2013.05.006
- Lee, T. R., Wood, W. T., and Phrampus, B. J. (2019). A Machine Learning (kNN) Approach to Predicting Global Seafloor Total Organic Carbon. *Glob. Biogeochem. Cycles* 33, 37–46. doi: 10.1029/2018GB005992
- Lovelock, C. E., and Duarte, C. M. (2019). Dimensions of Blue Carbon and Emerging Perspectives. *Biol. Lett.* 15, 20180781. doi: 10.1098/rsbl.2018.0781
- Macreadie, P. I., Nielsen, D. A., Kelleway, J. J., Atwood, T. B., Seymour, J. R., Petrou, K., et al. (2017). Can We Manage Coastal Ecosystems to Sequester More Blue Carbon? *Front. Ecol. Environ.* 15, 206–213. doi: 10.1002/fee.1484
- Mariani, G., Cheung, W. W. L., Lyet, A., Sala, E., Mayorga, J., Velez, L., et al. (2020). Let More Big Fish Sink: Fisheries Prevent Blue Carbon Sequestration-Half in Unprofitable Areas. *Sci. Adv.* 6, 1–9. doi: 10.1126/sciadv.abb4848
- Marrari, M., Piola, A. R., and Valla, D. (2017). Variability and 20-Year Trends in Satellite-Derived Surface Chlorophyll Concentrations in Large Marine Ecosystems Around South and Western Central America. *Front. Mar. Sci.* 4, 372. doi: 10.3389/fmars.2017.00372
- Moore, S., Gauci, V., Evans, C. D., and Page, S. E. (2011). Fluvial Organic Carbon Losses From a Bornean Blackwater River. *Biogeosciences* 8, 901–909. doi: 10.5194/bg-8-901-2011
- Mora-Soto, A., Capsey, A., Friedlander, A. M., Palacios, M., Brewin, P. E., Golding, N., et al. (2021). One of the Least Disturbed Marine Coastal Ecosystems on Earth: Spatial and Temporal Persistence of Darwin's Sub-Antarctic Giant Kelp Forests. *J. Biogeogr.* 48, 2562–2577. doi: 10.1111/jbi.14221
- Mora-Soto, A., Palacios, M., Macaya, E. C., Gómez, I., Huovinen, P., Pérez-Matus, A., et al. (2020). A High-Resolution Global Map of Giant Kelp (*Macrocystis Pyrifera*) Forests and Intertidal Green Algae (Ulvophyceae) With Sentinel-2 Imagery. *Remote Sens.* 12, 694. doi: 10.3390/rs12040694
- Morley, S. A., Souster, T. A., Vause, B. J., Gerrish, L., Peck, L. S., and Barnes, D. K. (2022). Benthic Biodiversity, Carbon Storage and the Potential for Increasing Negative Feedbacks on Climate Change in Shallow Waters of the Antarctic Peninsula. *Biology* 11 (2), 320. doi: 10.3390/biology11020320
- Muller-Karger, F. E., Varela, R., Thunell, R., Luerssen, R., Hu, C., and Walsh, J. J. (2005). The Importance of Continental Margins in the Global Carbon Cycle. *Geophys. Res. Lett.* 32, 1–4. doi: 10.1029/2004GL021346
- NASA Earth Observatory (2022) *Something Fishy in the Atlantic Night*. Available at: <https://earthobservatory.nasa.gov/features/Malvinas> (Accessed February 7, 2022).
- National Oceanography Centre (2022) *Tidal Predictions for Port Stanley* (Accessed February 3, 2022).
- Nellemann, C., Corcoran, E., Duarte, C. M., Valdeís, L., De Young, C., Fonseca, L., et al. (2009). *Blue Carbon: The Role of Healthy Oceans in Binding Carbon: A Rapid Response Assessment* (UN Environment, GRID-Arendal). Available at: https://com.unh.edu/sites/default/files/publications/Nellemann_2010_BlueCarbon_book.pdf.

- Newton, T. L., Gehrels, W. R., Fyfe, R. M., and Daley, T. J. (2021). Reconstructing Sea-Level Change in the Falkland Islands (Islas Malvinas) Using Salt-Marsh Foraminifera, Diatoms and Testate Amoebae. *Mar. Micropaleont.* 162, 101923. doi: 10.1016/j.marmicro.2020.101923
- Otley, H., Munro, H., Clausen, A., and Ingham, B. (2008). *Falkland Islands State of the Environment Report 2008* (Stanley: Falkland Islands Government and Falklands Conservation).
- Pace, M. C., Bailey, D. M., Donnan, D. W., Narayanaswamy, B. E., Smith, H. J., Speirs, D. C., et al. (2021). Modelling Seabed Sediment Physical Properties and Organic Matter Content in the Firth of Clyde. *Earth Syst. Sci. Data* 13, 5847–5866. doi: 10.5194/essd-13-5847-2021
- Parker, G., Paterlini, C. M., and Violante, R. A. (1997). “El Fondo Marino,” in *El Mar Argentino Y Sus Recursos Marinos*. Ed. E. E. Boschi (Mar del Plata: INIDEP), 65–87.
- Pedersen, M., Filbee-Dexter, K., Frisk, N., Sárosy, Z., and Wernberg, T. (2021). Carbon Sequestration Potential Increased by Incomplete Anaerobic Decomposition of Kelp Detritus. *Mar. Ecol. Prog. Ser.* 660, 53–67. doi: 10.3354/meps13613
- Petschick, R., Kuhn, G., and Ginge, F. (1996). *Data From: Grain Size Distribution of Surface Sediments of the South Atlantic* (PANGAEA). doi: 10.1594/PANGAEA.51464
- Poggio, L., de Sousa, L. M., Batjes, N. H., Heuvelink, G. B. M., Kempen, B., Ribeiro, E., et al. (2021). SoilGrids 2.0: Producing Soil Information for the Globe With Quantified Spatial Uncertainty. *SOIL* 7, 217–240. doi: 10.5194/soil-7-217-2021
- Pörtner, H.-O., Scholes, R. J., Agard, J., Archer, E., Bai, X., Barnes, D. K. A., et al. (2021). *IPBES-IPCC Co-Sponsored Workshop Report on Biodiversity and Climate Change (Version 2)* (IPBES-IPCC). doi: 10.5281/ZENODO.4782538
- Queirós, A. M., Stephens, N., Widdicombe, S., Tait, K., McCoy, S. J., Ingels, J., et al. (2019). Connected Macroalgal-Sediment Systems: Blue Carbon and Food Webs in the Deep Coastal Ocean. *Ecol. Monogr.* 89, 1–21. doi: 10.1002/ecm.1366
- Queirós, A. M., Talbot, E., Beaumont, N. J., Somerfield, P. J., Kay, S., Pascoe, C., et al. (2021). Bright Spots as Climate-Smart Marine Spatial Planning Tools for Conservation and Blue Growth. *Global Change Biol.* 27 (21), 5514–5531. doi: 10.1111/gcb.15827
- Rattray, A., Ierodiaconou, D., Monk, J., Versace, V. L., and Laurenson, L. J. B. (2013). Detecting Patterns of Change in Benthic Habitats by Acoustic Remote Sensing. *Mar. Ecol. Prog. Ser.* 477, 1–13. doi: 10.3354/meps10264
- Rattray, A., Ierodiaconou, D., and Womersley, T. (2015). Wave Exposure as a Predictor of Benthic Habitat Distribution on High Energy Temperate Reefs. *Front. Mar. Sci.* 2. doi: 10.3389/fmars.2015.00008
- Ricciardelli, L., Becker, Y. A., Fioramonti, N. E., Torres, M., Bruno, D. O., Rey, A. R., et al. (2020). Trophic Structure of Southern Marine Ecosystems: A Comparative Isotopic Analysis From the Beagle Channel to the Oceanic Burdwood Bank Area Under a Wasp-Waist Assumption. *Mar. Ecol. Prog. Ser.* 655, 1–27. doi: 10.3354/meps13524
- Rios, C., Mutschke, E., and Morrison, E. (2003). Benthic Sublittoral Diversity in the Strait of Magellan. *Chile. Rev. Biol. Mar. Oceanogr.* 38 (1), 1–12. doi: 10.4067/S0718-19572003000100001
- Rogers, A. D., Baco, A., Escobar-Briones, E., Gjerde, K., Gobin, J., Jaspars, M., et al. (2021). Marine Genetic Resources in Areas Beyond National Jurisdiction: Promoting Marine Scientific Research and Enabling Equitable Benefit Sharing. *Front. Mar. Sci.* 8, 600.
- Ross, L. K., Ross, R. E., Stewart, H. A., and Howell, K. L. (2015). The Influence of Data Resolution on Predicted Distribution and Estimates of Extent of Current Protection of Three ‘Listed’ Deep-Sea Habitats. *PloS One* 10 (10), e0140061. doi: 10.1371/journal.pone.0140061
- Saba, G. K., Burd, A. B., Dunne, J. P., Hernández-León, S., Martin, A. H., Rose, K. A., et al. (2021). Toward a Better Understanding of Fish-Based Contribution to Ocean Carbon Flux. *Limnol. Oceanogr.* 66, 1639–1664. doi: 10.1002/lno.11709
- Sabatini, M., Reta, R., and Matano, R. (2004). Circulation and Zooplankton Biomass Distribution Over the Southern Patagonian Shelf During Late Summer. *Cont. Shelf Res.* 24, 1359–1373. doi: 10.1016/j.csr.2004.03.014
- Servicio de Hidrografía Naval (2022) *Calidad De Fondo*. Available at: <http://www.hidro.gob.ar/DA/SHNCfondo.asp> (Accessed 24.01.2022).
- Smale, D. A., Moore, P. J., Queirós, A. M., Higgs, N. D., and Burrows, M. T. (2018). Appreciating Interconnectivity Between Habitats is Key to Blue Carbon Management. *Front. Ecol. Environ.* 16, 71–73. doi: 10.1002/fee.1765
- Smale, D. A., Pessarrodona, A., King, N., and Moore, P. J. (2021). Examining the Production, Export, and Immediate Fate of Kelp Detritus on Open-Coast Subtidal Reefs in the Northeast Atlantic. *Limnol. Oceanogr.* 1–14. doi: 10.1002/lno.11970
- Smeaton, C., and Austin, W. E. N. (2022). Quality Not Quantity: Prioritizing the Management of Sedimentary Organic Matter Across Continental Shelf Seas. *Geophys. Res. Lett.* 49, e2021GL097481. doi: 10.1029/2021GL097481
- Smith, P., Arneth, A., Barnes, D. K. A., Ichii, K., Marquet, P. A., Popp, A., et al. (2022). How do We Best Synergize Climate Mitigation Actions to Co-Benefit Biodiversity? *Glob. Change Biol.* 28, 1–8. doi: 10.1111/gcb.16056
- Swart, S., Thomalla, S. J., and Monteiro, P. M. S. (2015). The Seasonal Cycle of Mixed Layer Dynamics and Phytoplankton Biomass in the Sub-Antarctic Zone: A High-Resolution Glider Experiment. *J. Mar. Syst.* 147, 103–115. doi: 10.1016/j.jmarsys.2014.06.002
- Thomalla, S. J., Fauchereau, N., Swart, S., and Monteiro, P. M. S. (2011). Regional Scale Characteristics of the Seasonal Cycle of Chlorophyll in the Southern Ocean. *Biogeosciences* 8, 2849–2866. doi: 10.5194/bg-8-2849-2011
- Turetsky, M. R., Benscoter, B., Page, S., Rein, G., van der Werf, G. R., and Watts, A. (2015). Global Vulnerability of Peatlands to Fire and Carbon Loss. *Nat. Geosci.* 8 (1), 11–14. doi: 10.1038/ngeo2325
- UNFCCC. (2021a). *Nationally Determined Contributions Under the Paris Agreement. Synthesis Report by the Secretariat*. Available at: <https://unfccc.int/documents/306848> (Accessed February 7, 2022).
- UNFCCC. (2021b). *Negotiations on Action for Climate Empowerment*. Available at: <https://unfccc.int/topics/education-and-outreach/the-big-picture/education-and-outreach-in-the-negotiations> (Accessed February 7, 2022).
- Upson, R., McAdam, J., and Clubbe, C. (2016). *Climate Change Risk Assessment for Plants and Soils of the Falkland Islands and the Services They Provide* (Royal Botanic Gardens Kew and UK Falkland Islands Trust). doi: 10.13140/RG.2.2.15660.67203
- van de Velde, S., Van Lancker, V., Hidalgo-Martinez, S., Berelson, W. M., and Meysman, F. J. R. (2018). Anthropogenic Disturbance Keeps the Coastal Seafloor Biogeochemistry in a Transient State. *Sci. Rep.* 8, 1–10. doi: 10.1038/s41598-018-23925-y
- van Tussenbroek, B. I. (1993). Plant and Frond Dynamics of the Giant Kelp, *Macrocystis Pyrifera*, Forming a Fringing Zone in the Falkland Islands. *Eur. J. Phycol.* 28 (3), 161–165. doi: 10.1080/09670269300650251
- Ward, D., Melbourne-Thomas, J., Pecl, G. T., Evans, K., Green, M., McCormack, P. C., et al. (2022). *Safeguarding Marine Life: Conservation of Biodiversity and Ecosystems* (Reviews in Fish Biology and Fisheries), 1–36. Available at: <https://link.springer.com/article/10.1007/s11160-022-09700-3>.
- Wernberg, T., Krumhansl, K., Filbee-Dexter, K., and Pedersen, M. F. (2018). *Status and Trends for the World's Kelp Forests. 2nd ed.* (Elsevier Ltd). doi: 10.1016/B978-0-12-805052-1.00003-6
- Wilson, P., Clark, R., McAdam, J. H., and Cooper, E. A. (1993). Soil Erosion in the Falkland Islands: An Assessment. *Appl. Geogr.* 13 (4), 329–352. doi: 10.1016/0143-6228(93)90036-Z
- Wilson, R. J., Speirs, D. C., Sabatino, A., and Heath, M. R. (2018). A Synthetic Map of the North-West European Shelf Sedimentary Environment for Applications in Marine Science. *Earth Syst. Sci. Data* 10, 109–130. doi: 10.5194/essd-10-109-2018
- Wing, S. R., Durante, L. M., Connolly, A. J., Sabadel, A. J., and Wing, L. C. (2021). *Overexploitation and Decline in Kelp Forests Inflate the Bioenergetic Costs of Fisheries* (Global Ecology and Biogeography). Available at: <https://onlinelibrary.wiley.com/doi/abs/10.1111/geb.13448>.
- Zwerschke, N., Sands, C. J., Roman-Gonzalez, A., Barnes, D. K. A., Guzzi, A., Jenkins, S., et al. (2022). Quantification of Blue Carbon Pathways Contributing to Negative Feedback on Climate Change Following Glacier Retreat in West Antarctic Fjords. *Global Change Biol.* 28, 8–20. doi: 10.1111/gcb.15898

Conflict of Interest: The authors declare that the research was conducted in the absence of any commercial or financial relationships that could be construed as a potential conflict of interest.

Publisher's Note: All claims expressed in this article are solely those of the authors and do not necessarily represent those of their affiliated organizations, or those of

the publisher, the editors and the reviewers. Any product that may be evaluated in this article, or claim that may be made by its manufacturer, is not guaranteed or endorsed by the publisher.

Copyright © 2022 Bax, Barnes, Pineda-Metz, Pearman, Diesing, Carter, Downey, Evans, Brickle, Baylis, Adler, Guest, Layton, Brewin and Bayley. This is an open-

access article distributed under the terms of the Creative Commons Attribution License (CC BY). The use, distribution or reproduction in other forums is permitted, provided the original author(s) and the copyright owner(s) are credited and that the original publication in this journal is cited, in accordance with accepted academic practice. No use, distribution or reproduction is permitted which does not comply with these terms.



Review of Evaluation and Valuation Methods for Cetacean Regulation and Maintenance Ecosystem Services With the Joint Cetacean Protocol Data

OPEN ACCESS

Edited by:

William Richard Turrell,
Marine Scotland, United Kingdom

Reviewed by:

Jan Marcin Weslawski,
Polish Academy of Sciences, Poland
Sonia Mendes,
Joint Nature Conservation Committee,
United Kingdom
Laura Malinauskaitė,
University of Iceland, Iceland

*Correspondence:

Jack Michael Sheehy
jms9@hw.ac.uk

[†]These authors have contributed
equally to this work and share
last authorship

Specialty section:

This article was submitted to
Marine Ecosystem Ecology,
a section of the journal
Frontiers in Marine Science

Received: 09 February 2022

Accepted: 20 April 2022

Published: 21 June 2022

Citation:

Sheehy JM, Taylor NL, Zwierschke N,
Collar M, Morgan V and Merayo E
(2022) Review of Evaluation and
Valuation Methods for Cetacean
Regulation and Maintenance
Ecosystem Services With the Joint
Cetacean Protocol Data.
Front. Mar. Sci. 9:872679.
doi: 10.3389/fmars.2022.872679

Jack Michael Sheehy^{1*}, Nicola L Taylor^{2†}, Nadescha Zwierschke^{3†}, Mark Collar^{4†},
Vicky Morgan^{5†} and Eugenia Merayo^{4†}

¹ International Centre for Island Technology, Heriot-Watt University, Stromness, United Kingdom, ² Marine Species, Joint Nature Conservation Committee, Peterborough, United Kingdom, ³ Marine Ecosystems, Joint Nature Conservation Committee, Peterborough, United Kingdom, ⁴ Marine Natural Capital, Joint Nature Conservation Committee, Peterborough, United Kingdom, ⁵ Marine Ecosystems and Natural Capital, Joint Nature Conservation Committee, Peterborough, United Kingdom

Cetaceans provide a range of ecosystem services of value to anthropogenic interests. Following the Common International Classification of Ecosystem Services (CICES) these are categorised as regulation and maintenance, provisioning, and cultural values. This study focuses on those of importance to climate change mitigation through regulation and maintenance. Under regulation and maintenance, cetaceans can store, transport, and influence stocks of carbon through: climate regulation through carbon sequestration, enhanced biodiversity and ecosystem potential, and enhanced primary productivity. 'Climate regulation through carbon sequestration' can be quantified as carbon fixation through living biomass and 'whale-falls'. Cetacean populations store significant stocks of carbon in living biomass. After death, sinking whale carcasses, 'whale-falls', provide a significant transfer of biomass and nutrients to benthic sediments and support deep sea ecosystems. During their lifespan, cetaceans also disperse nutrients through feeding and excretion both horizontally through the 'whale-conveyor' and vertically through the 'whale pump'. As nutrient limitations hinder phytoplankton growth, these processes can be quantified as the increased potential of phytoplankton carbon fixation from cetacean driven nutrient cycling. Enhanced biodiversity, ecosystem potential, and primary productivity can be quantified as carbon fixation through nutrient cycling. This study reviews the evaluative and valutive techniques used in cetacean ecosystem service research and adapts and applies them to the Joint Cetacean Protocol (JCP) data which details cetacean abundance and distribution in Europe. They are then reviewed with

regards to their robustness, application in markets, and in decision making processes. Cetacean populations are estimated to contain 2 Mt C, cycle 60,000 t N yr⁻¹, and impact carbon fluxes by as much as 22 Mt C yr⁻¹ in the survey area. The values highlight key areas for cetacean conservation: the Outer Hebrides, west of south Wales, around the Isle of Man, to the east of England, and to the north-east of the Shetland Islands. There is, however, large uncertainty in the evaluative processes used; nutrient cycling models presented in this study don't capture removal of excess nutrients, or the values of enhanced biodiversity and ecosystem potential. As such, they are not sufficiently robust to quantify market values but highlight key areas for future research on climate change mitigation through conservation. Key areas of future research include phytoplankton uptake rates of nitrogen and phosphorus in nutrient limited waters, quantification of 'enhanced biodiversity and ecosystem potential', and nutrient removal from coastal waters.

Keywords: ecosystem services, cetacean, valuation, evaluation, blue carbon, climate change

1 INTRODUCTION

Whilst climate change is the result of anthropogenic activity and carbon emissions, the underlying factors of climate change are driven by economic, ecologic, and societal issues. Global policy therefore attempts to address climate change through an integrated approach of eco-social economics where common metrics (finance) are used to value natural capital and ecosystem services (Cisneros-Montemayor et al., 2019). There is debate on the suitability of ecologic valuations with regard to social equity (Peskett et al., 2008; FPP, 2011; Barbesgaard, 2016) and ecologic concerns (Fearnside, 1995; Fearnside, 2005; Fearnside, 2016). However, when carefully implemented, such valuations can aid conservation agendas and help communicate the value of natural capital to policy makers (Cavanagh et al., 2016; Dasgupta, 2021). Where values of natural capital are outside markets, they are often used to guide management of natural resources; in the ocean they are used in Marine Spatial Planning (MSP) processes (Price and Warren, 2016; Geraldi et al., 2019; Macreadie et al., 2019; Porter et al., 2020).

To value stocks of marine carbon, it's first necessary to understand the complex biogeochemical and physical processes that influence global carbon fluxes and concentrations of atmospheric carbon. The ocean is of key importance as a major carbon sink and holds 98.5% of the carbon in the ocean-atmosphere system (Houghton, 2003). Marine carbon will flux between atmospheric carbon, in different forms in marine waters, and/or into benthic sediments and habitats. If carbon is stored for more than 100 years or transported below depths of 1000m or into sediments, this may be considered sequestered (Caldeira et al., 2002; Lovelock and Duarte, 2019). As atmospheric carbon contributes to climate change, and creates costs through climate change impacts, sequestered marine carbon may then be valued as the avoidance of that carbon in the atmosphere contributing to climate change impacts. Carbon therefore has an estimated value (Pearce, 2003; Watkiss et al., 2005) and this underpins carbon

offsetting, 'blue carbon', and economic valuations of carbon stocks and fluxes (Ullman et al., 2013).

Marine carbon is defined as either being organic or inorganic, and as dissolved or particulate¹ (Thompson et al., 2017):

- **Organic:** the carbon found in living plants and animals, in organic rich detritus, as dissolved organic carbon (DOC), and as particulate organic carbon (POC).
- **Inorganic:** the carbon dissolved in seawater that forms carbonates, dissolved inorganic carbon (DIC) and the calcareous skeletons, and hard shell material, formed by living organisms otherwise referred to as particulate inorganic carbon (PIC).

The relative global stocks of marine carbon are:

- **DIC:** There is roughly 38,000 Gt C of global DIC as carbonic acid, bicarbonates, and carbonates (Olson et al., 1985; Hansell and Carlson, 2015). DIC is mostly stored in the deep sea, which is often defined as waters greater than 100m in depth (Bishop, 2009). DIC fluxes with atmospheric carbon, in addition to POC, and between deep and shallow waters.
- **DOC:** Global estimates of DOC range from 662 Gt C to 740 Gt C in marine waters (Bishop, 2009; Hansell et al., 2009) and 150 Gt C in mixed surface marine sediments (Hedges, 1992). Photosynthesis is predominantly responsible for fixing DOC into POC and by extension DIC (Hedges, 1992) but microbial action may account for 30-50% of primary production (Jiao et al., 2010; Hansell and Carlson, 2015).
- **POC:** There is 22 Gt C mostly as inert matter and detritus with roughly 2 Gt C of that as organic carbon in living marine organisms (Olson et al., 1985; Hedges, 1992; SOEST, 2011). Global POC fluxes from primary productivity in surface waters to deeper waters and sediments are estimated to be between 8.5 Gt C yr⁻¹ and 14.3 Gt C yr⁻¹ (Xie et al., 2019).
- **PIC:** There is roughly 0.02 Gt C of PIC, mostly CaCO₃, as a global average; it is important to note that CaCO₃ production will generally occur in blooms and create high spatial and temporal variability (Balch et al., 2005). PIC is believed to

represent one quarter of all marine sediments (Broecker and Peng, 1983; Balch et al., 2005; Seibold and Berger, 2017).

There are three main processes or ‘pumps’ which drive ocean-atmosphere carbon fluxes and nutrient cycling, and they are determined by both biotic and abiotic factors (Heinze et al., 1991; Bishop, 2009; Henson, 2020). They can be summarised as:

- **A physical/solubility pump:** driven by abiotic factors such as solubility, ventilation, and transport.
- **A biological soft tissue pump:** driven by a mix of abiotic factors and biotic processes such as photosynthesis, respiration, and heterotrophy.
- **A calcium carbonate pump:** driven by a mix of abiotic and biotic factors.

There is also a fourth pump, though it is generally considered to be part of the biological pump:

- **A microbial carbon pump:** this describes the production of DOC by microbial processes and can account for 30-50% of marine primary production (Ducklow et al., 1995; Biddanda and Benner, 1997; Jiao et al., 2010; Hansell and Carlson, 2015).

1.1 The Biological Pump

The biological pump describes the processes by which inorganic carbon (carbon dioxide) is fixed in the ocean through photosynthesis and then transported, and potentially sequestered, in the deep ocean (De La Rocha and Passow, 2013). This pump is principally driven by phytoplankton activity, photosynthesis, and respiration. It may be calculated without respiration to estimate Primary Productivity (PP), or also include respiratory requirements to estimate Net Primary Productivity (NPP). NPP is the foundation of the marine trophic chain and is determined by physical processes, such as tidal mixing (Marshall, 1997; Marshall et al., 1997), in addition to localised and regional nutrient concentrations which may limit phytoplankton growth (Parekh et al., 2006; Archer and Jokulsdottir, 2013). Nitrogen, phosphorus, and iron are the most common nutrients limiting phytoplankton growth (Roman and McCarthy, 2010; Zhao et al., 2019).

In the Southern Ocean, phytoplankton growth is limited by the availability of iron, therefore, processes which increase iron availability in the photic zone can increase NPP, the efficiency of the biological pump, and the export of carbon from the atmosphere to the deep ocean (Lavery et al., 2010; Ratnarajah et al., 2014). In the North Sea, in near coastal shallow waters, there is a terrigenous influx of nitrogen (Painting et al., 2018) and higher turbidity due to tidal mixing (Zhao et al., 2019); here light is the limiting factor for NPP (Zhao et al., 2019). Further away from shore in the North Sea, however, tidal mixing infuses nutrients into the surface (photic) waters and nitrogen availability is the limiting factor in NPP (Zhao et al., 2019).

1.2 Cetacean Ecosystem Services

Cetaceans have long been understood to provide a wide range of important ecosystem services (Katona and Whitehead, 1988;

Apollonio, 2002; Springer et al., 2003) but techniques to evaluate and value specific services relevant to climate change are relatively novel (Lavery et al., 2010; Roman and McCarthy, 2010; Ratnarajah et al., 2016; Chami et al., 2020). Whilst there are a number of different methods with which to value ecosystem services, the Common International Classification of Ecosystem Services (CICES) is the most currently accepted for cetaceans (Haines-Young and Potschin, 2018). Using this framework, Cook et al. (2020) state that cetacean ecosystem services fall into the following categories:

- Provisioning:
 - o Food products (meat, blubber, skin, and intestines).
 - o Whale bones, teeth, and baleen.
 - o Oil-based products derived from blubber.
- Regulation and maintenance:
 - o Enhanced biodiversity and evolutionary potential.
 - o Climate regulation through carbon sequestration.
- Cultural:
 - o Tourism (whale watching).
 - o Music and arts (entertainment).
 - o Religious and/or sacred.
 - o Educational.
 - o Aesthetics.
 - o Community cohesiveness and cultural identity.
 - o Existence.
 - o Bequest.

Whilst provisioning and cultural values are key components of cetacean ecosystem valuation, this paper focuses on cetacean regulation and maintenance ecosystem services for their relevance to climate change mitigation.

1.3 Cetacean Regulation and Maintenance Ecosystem Services

In CICES, Cook et al. (2020b) state the valuation methods appropriate for subsets of the regulation and maintenance category:

- Climate regulation (carbon sequestration) – marginal abatement/damage costs.
- Enhanced biodiversity and ecosystem potential – production function or contingent valuation.
- Enhanced primary production – production function or contingent valuation.

These methods evaluate fluxes of marine carbon either as stocks or through facilitating primary production and carbon fixation through photosynthesis. Cetaceans can influence stocks of carbon in living biomass, in ‘whale-falls’, and by facilitating the cycling and mixing of nutrients essential for phytoplankton growth. Valuation of cetacean ecosystem services is then based on carbon market values. Most values provided in research are purely theoretical with no market value, such as the \$2 million whale (Chami et al., 2020), as there are limited pathways for cetacean ecosystem services to be included in markets. Given sufficiently robust data, however, cetacean derived carbon could meet the criteria of Standard Setting Organisations (SSOs) for

blue carbon accreditation. There are five criteria for SSOs to blue carbon accreditation; baseline, additionality, leakage, permanence, and co-benefits (Ullman et al., 2013).

Climate regulation has been valued as carbon storage in living biomass (Chami et al., 2020). Large whales can weigh between 30 tonnes to 160 tonnes (Lockyer, 1976), and a 40 tonne grey whale contains roughly 2 t C (tonnes of carbon) (Smith and Baco, 2003). If anthropogenic protection restores cetacean populations, and their stocks of carbon in living biomass, this can reduce the concentration of atmospheric carbon and mitigate climate change. The increase in carbon stocks in cetacean living biomass could be accredited as carbon sequestered and removed from the atmosphere.

Climate regulation has also been evaluated as carbon sequestration through 'whale-falls' (Pershing et al., 2010). A grey whale carcass containing roughly 2 t C can provide an equivalent input to benthic habitats of ~2000 years of organic carbon compared to baseline activity (Smith and Baco, 2003). Soft tissues, however, are recycled over approximately 2 years back into trophic chains, shallow waters, and microbial loops (Higgs et al., 2011). Therefore, unless the carcass is transported to waters deeper than 1000m, this carbon will not be considered sequestered; only the skeleton is likely to remain on the benthos for over 100 years (Schuller et al., 2004). If benthic habitats are protected from disturbance, cetacean whale-fall carbon could be sequestered. Restoration of cetacean populations can therefore increase carbon sequestration through whale-falls, reduce atmospheric carbon, and mitigate climate change. The increase of this carbon export to benthic habitats could be accredited, given robust abundance and distribution data, as a probability of mortality and sinking of whale carcasses over protected benthic habitats. This could be as a portion of the entire carcass in waters greater than 1000m, or just the skeletal carbon in depths less than 1000m.

Enhanced biodiversity, evolutionary potential, and primary productivity has been evaluated together as nutrient cycling driving phytoplankton growth and carbon capture (Lavery et al., 2013; Ratnarajah et al., 2014; Ratnarajah et al., 2016; Ratnarajah et al., 2018). Cetacean feeding and excretion facilitates nitrogen retention in the photic zone which supports phytoplankton growth. This vertical cycling of nutrients is known as the 'whale-pump' and been noted to enhance NPP in the Gulf of Maine (Roman and McCarthy, 2010). The Gulf of Maine has an average NPP of 290 g C m⁻² yr⁻¹ (Townsend, 1998) and primary productivity enhancement from cetacean driven nutrient cycling may recycle 196,000 t N (tonnes of nitrogen) annually (Roman and McCarthy, 2010). Lateral movement of nutrients, notably nitrogen, from high latitude feeding grounds to low latitude calving areas also facilitates phytoplankton growth; this is known as the 'whale conveyor' (Roman et al., 2014). Cetaceans may therefore also provide ecosystem services for enhanced biodiversity, evolutionary potential, and primary productivity through the removal and transport of excess nutrients from coastal to offshore waters using valuations for nitrogen and phosphorus removal (Watson et al., 2020).

The whale-pump, cycling iron, has been shown to be self-sustaining in the iron depleted waters of the Southern Ocean. In this environment, cetacean driven nutrient cycling creates a positive feedback loop that increases both phytoplankton and cetacean biomass due to differences in cetacean and planktonic faecal dispersion; planktonic faeces sink into deeper waters and/or the benthos whilst cetacean faeces persist in the photic zone (Lavery et al., 2010). Cetacean nutrient cycling of iron allows a greater amount of carbon to be fixed through phytoplankton growth than is released through cetacean consumption and respiration (Lavery et al., 2014; Ratnarajah et al., 2014; Ratnarajah et al., 2016; Ratnarajah et al., 2018). In the North Sea, nitrogen availability may limit NPP (Zhao et al., 2019) and cetacean driven nutrient cycling might increase nitrogen availability and NPP. The marginal increase in NPP, and carbon fixation, with greater cetacean populations could be accredited as carbon removed from the atmosphere.

1.4 Scope of Research

The scope of this research is matched to data from the Joint Cetacean Protocol (JCP) (Paxton et al., 2016) used by the Joint Nature Conservation Committee (JNCC) in 'Management Units for cetaceans in UK waters' (IAMMWG, 2015). This is the most comprehensive dataset of cetacean abundance and distribution in Europe and the result of larger SCANS (Small Cetaceans in European Atlantic waters and the North Sea) surveys (Hammond, 2006; Hammond et al., 2009; Hammond et al., 2018). Within the survey area, JCP data include abundance and distribution estimates for harbour porpoise (*Phocoena phocoena*), Atlantic white-sided dolphin (*Lagenorhynchus acutus*), short-beaked common dolphin (*Delphinus delphis*), white-beaked dolphin (*Lagenorhynchus albirostris*), bottlenose dolphin (*Tursiops truncatus*), and minke whale (*Balaenoptera acutorostrata*). Average mass values and total population estimates for the survey area are detailed in **Table 1**. The survey area is shown in **Figure 1**.

The survey area includes both the North Sea, Skagerrak, and the Celtic sea; it encompasses a total area of 1.09 million km² (Paxton et al., 2016). Whilst the survey area overlaps with the territorial waters of France, Belgium, the Netherlands, Germany, Denmark, Sweden, and Norway, it's predominantly relevant to UK and Ireland waters. Provisioning as a cetacean ecosystem service is closely tied to localised cultural values and practices (Donovan, 1982; Simmonds et al., 2002; Kenny et al., 2018) and there is no consumption of whales for food in the UK and Ireland. With regards to other provisioning uses, they are of limited use in a modern context and/or replaced with other, and cheaper, alternatives (Cook et al., 2020b). Cetacean cultural values have been much studied (Cook et al., 2020b; Malinauskaite et al., 2021a) but there are limited data relevant to the UK or Ireland (Parsons et al., 2003; O'Connor et al., 2009a). As such, this study focuses on cetacean regulation and maintenance ecosystem services for their relevance to climate change, and reviews evaluative and valutive methods through application to JCP abundance and distribution estimates.

TABLE 1 | JCP population sizes and average mass values

Species	Mass (kg)	Population
Harbour porpoise (HP)	31	353,455
Atlantic white-sided dolphin (WSD)	170	69,293
Short-beaked common dolphin (CD)	80	56,556
White-beaked dolphin (WBD)	250	15,895
Bottlenose dolphin (BND)	188	17,516
Minke whale (MW)	6566	23,528

The CICES regulation and maintenance category is evaluated and tentatively valued based on cetacean derived carbon through:

- Stocks in cetacean living biomass.
- Cetacean driven nutrient cycling enhancing PP.
- Cetacean driven nutrient cycling enhancing NPP.

This paper does not attempt to evaluate or value whale-falls as there are no depths exceeding 1000m in the study area, see **Figure 2**. Therefore, only skeletal carbon could be considered sequestered in the study area. Unfortunately, whilst there is literature on cetacean skeletal compositions (Tont et al., 1977; Lees and Escoubes, 1987; Higgs et al., 2011), there is no clear detailing of cetacean skeletal carbon content. There are therefore insufficient data on carbon content

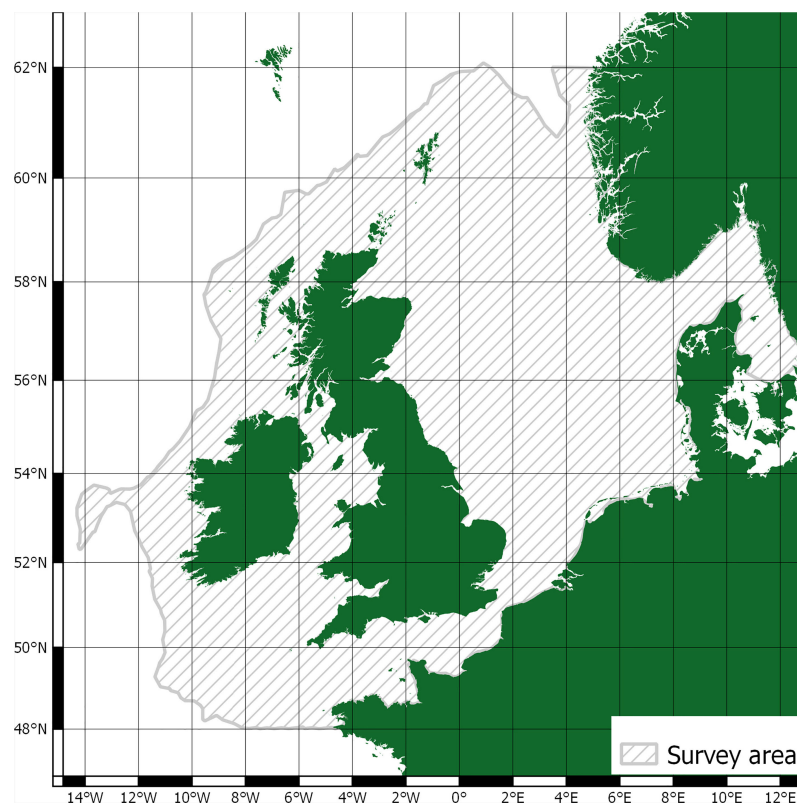
of cetacean skeletons to infer any meaningful analysis. Additionally, whilst there are protected areas within the survey area, it is unclear on the level of benthic protection they offer (Dunckley and Solandt, 2021).

This paper does not attempt to value cetacean ecosystem services through removal of nitrogen from near coastal waters. Whilst this may form an important part of cetacean regulation and maintenance ecosystem services, the JCP data don't detail cetacean abundance and distribution at a sufficient resolution to accurately detail their impact on near coastal nutrient cycling and nutrient removal.

Benefits to fisheries due to cetacean driven nutrient cycling increasing NPP are also not valued in this study as by Chami et al. (2020). There are insufficient data to support analysis of correlations between fisheries value due to cetacean driven nutrient cycling and cetacean abundance and distribution. In this study potential benefits to fisheries from cetacean driven nutrient cycling on NPP are determined to already be incorporated into fisheries value, even if they are not, as yet, quantified.

This paper is framed with the following research questions:

- What are the current stocks, and potential value, of carbon in cetacean living biomass in the survey area?
- What are the estimates, and potential value, of cetacean driven nutrient cycling enhancing PP?

**FIGURE 1** | Survey area.

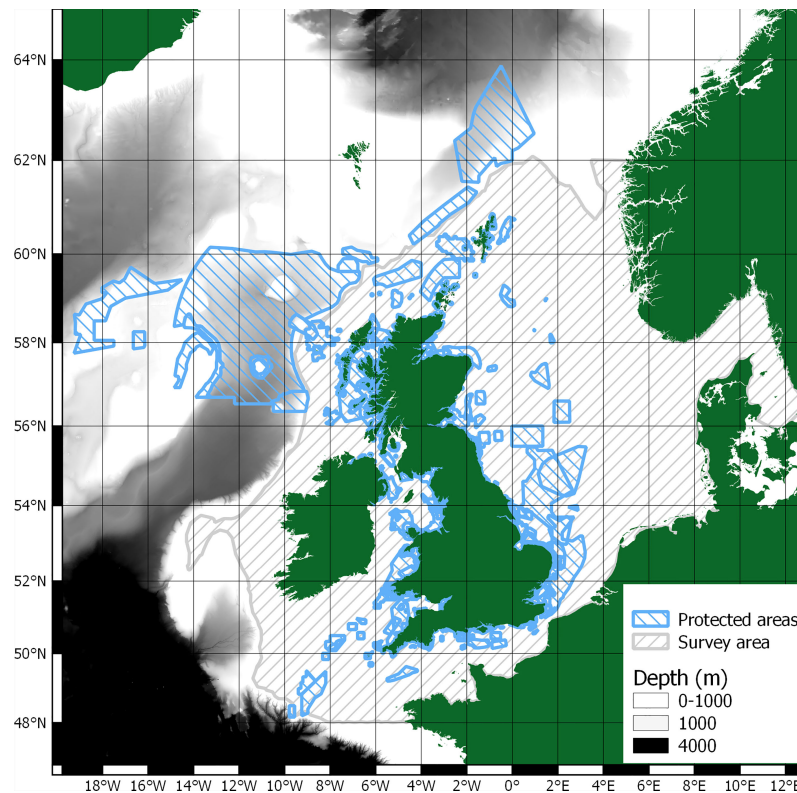


FIGURE 2 | Survey area, protected areas, and >1000m depth bathymetry.

- What are the estimates, and potential value, of cetacean driven nutrient cycling, including cetacean consumption and respiratory requirements, enhancing NPP ?
- What is needed to translate these potential values into market values?
- Can these estimates, and potential values, be used to inform MSP processes?

1.4.1 Survey Area Carbon and Nitrogen Stocks and Fluxes

To give context to the cetacean regulation and maintenance ecosystem services in determining marine carbon stocks and fluxes, estimates for ecosystem services in the survey area are provided here for reference. Whilst the survey area used in this study encompasses a total area of 1.09 million km² (Paxton et al., 2016), there are limited data that use these same parameters. As such, average measurements for other areas, within the survey area, are extrapolated to the whole survey area used in this study:

- 1.82 Mt C (million tonnes of carbon) of fish biomass in the survey area, extrapolated from an average 1.67 g C m⁻² in fish biomass. This was calculated from 10 Mt of fish biomass in a 750,000 km² area of the North Sea and Skagerrak (Waldy and Kroglund, 2008), and an average 12.5% carbon in fish biomass (Mariani et al., 2020).

- 2.18 Mt C of benthic biomass in the survey area. This was calculated from average North Sea benthos of 2 g C m⁻² (Barrio Froján et al., 2012; Zhang et al., 2019).
- An average 315,000 t N yr⁻¹ of total terrigenous inputs to the survey area. This was calculated from terrigenous North Sea nitrogen inputs of 150,000 t N yr⁻¹ to 230,000 t N yr⁻¹ and Celtic Sea terrigenous inputs of 100,000 t N yr⁻¹ to 150,000 t N yr⁻¹ (Painting et al., 2018).
- 255.06 Mt C yr⁻¹ of NPP, extrapolated from average North Sea NPP of 234 g C m⁻² yr⁻¹ (Capuzzo et al., 2018).
- An average 10.45 Mt C yr⁻¹ of NPP due to physical tidal mixing in the survey area, extrapolated from North Sea values which range from -40 g C m⁻² yr⁻¹ to +60 g C m⁻² yr⁻¹ (Zhao et al., 2019).

2 METHODS

This section describes the evaluative and valiative methods used for cetacean ecosystem services through:

- Carbon stocks in cetacean living biomass.
- Cetacean driven nutrient cycling removing nitrogen.
- Cetacean driven nutrient cycling enhancing PP.
- Cetacean driven nutrient cycling enhancing NPP.

2.1 Cetacean Average Mass Values

Cetacean average mass values are used to calculate carbon storage through living biomass and for nutrient cycling potential based on daily energy requirements and daily rations. Values are used in line with other literature (Barlow et al., 2008; Pershing et al., 2010), and extrapolated from the population age distribution model used by Lavery et al. (2014) where these data are not available.

Data extrapolated from Lavery et al. (2014) are based on average mass of population subsets and the proportional structure of those subsets within the population. Demographic parameters of cetacean populations can be found in other literature (Pershing et al., 2010), but only Lavery et al. (2014) and Mackintosh and Wheeler (1929) provide mass data for proportional subsets of cetacean populations; Lavery et al. (2014) model their population structure on the model used by Mackintosh and Wheeler (1929). These values are also used due to the absence of more relevant data for cetaceans included in this study and survey area. To derive average mass values, the mass and proportions of each population subset in a stable population were averaged. A conversion factor to adjust adult female mass² to average population mass value, to match data in Lavery et al. (2014), was then calculated. The conversion factor was calculated as 0.7241 to adjust the blue whale adult female mass of 120,000kg to the average blue whale population mass of 86,900kg. Adult mass values are taken from those most relevant to the UK where available (WDG, 2021a; WDG, 2021b) then rounded down to the nearest ten for simplicity. This gives values similar to average mass for species detailed in current literature (Barlow et al., 2008; Pershing et al., 2010). Bottlenose dolphin populations are known to differ in size between coastal and offshore populations but are treated here as one uniform population to standardise it to JCP cetacean distribution and abundance data (Paxton et al., 2016).

Average mass values of cetacean species, and their population size distributed across the study area are detailed in **Table 1**.

2.2 Carbon Stocks in Cetacean Living Biomass

Wet weight biomass is first converted to dry weight biomass. Dry weight biomass is taken to be 40% of wet weight (Jelmert and Oppen-Berntsen, 1996; Pershing et al., 2010) and further comprised of:

- 20% protein, with a carbon content of 54%.
- 20% fat, with a carbon content of 77%.

Stocks of carbon in living biomass are evaluated as:

$$\text{Living biomass (t C ind}^{-1}\text{)}$$

$$= \text{mass (tons)} \times \text{wet weight biomass to dry weight carbon}$$

²Adult female mass values were found to be the most readily available data for cetaceans (Barlow et al., 2008; Pershing et al., 2010; WDG, 2021a; WDG, 2021b).

$$\text{Living biomass (t C ind}^{-1}\text{)}$$

$$= \text{mass} \times (0.4 \times ((0.2 \times 0.54) + (0.2 \times 0.77)))$$

$$\text{Living biomass (t C ind}^{-1}\text{)} = \text{mass} \times 0.1048$$

Stocks of carbon were summed to give population totals per species, in addition to a cumulative value for all cetacean species included in this study. Stocks of carbon in living biomass were mapped to JCP distribution and abundance data to highlight spatial variability.

2.3 Cetacean Driven Nutrient Cycling Enhancing Primary Productivity

This is evaluated as the amount of nitrogen recycled through cetacean feeding and excretion. This is calculated based on cetacean average mass values, dietary requirements, nitrogen content within prey, and the ratio of retained nitrogen. From this, the increased potential carbon fixation due to phytoplankton growth that may occur from the replenishment of recycled nitrogen is evaluated.

2.3.1 Dietary Requirements

There are a number of ways to calculate dietary requirements, often referred to as annual consumption of wet weight (Lockyer, 1981; Trites and Pauly, 1998; Reilly et al., 2004; Barlow et al., 2008; Lavery et al., 2014). Models either estimate the average daily ration directly (kg of wet weight) or calculate them from estimates of Average Daily Metabolic Requirements (ADMR in kJ d⁻¹) (Barlow et al., 2008). ADMR is often modelled from Basal Metabolic Rate (BMR in kJ d⁻¹) and cetaceans, as homeotherms, have a BMR related to their average mass using the Kleiber function (Kleiber, 1975):

$$BMR = A \times M^B$$

- M – average mass.
- A – A value.
- B – B value.

The Kleiber function uses A and B values of 293.1 and 0.75 respectively. Other studies, however, may adjust these values to be more specific to marine mammals and/or to adjust from metabolic requirement values taken from animals in captivity; this may be referred to as the Field Metabolic Rate (FMR in kJ d⁻¹) (Barlow et al., 2008). Various values for A and B used in literature include:

- A = 0.1, B = 0.8 (Trites and Pauly, 1998).
- A = 0.42, B = 0.67 (Lavery et al., 2014).
- A = 1.66, B = 0.556 (Reilly et al., 2004).
- A = 70.5, B = 0.7325 (Lockyer, 1981).
- A = 80, B = 1 (Blix and Folkow, 1995).
- A = 863.6, B = 0.783 (Sigurjónsson and Víkingsson, 1997).
- A = 2529.2, B = 0.524 (Boyd, 2002).

Other models use the standard A and B values as used in the Kleiber function, 293.1 and 0.75, then adjust the total BMR by 2.5 or 3 times; these models are known as 2.5BMR and 3BMR

respectively. The 3BMR using the Kleiber function (Kleiber, 1975) was used in this study. This is believed to be the most accurate (Barlow et al., 2008; Roman and McCarthy, 2010) and provides values in a mid-range of the other models using alternate adjustment factors (Kenney et al., 1997; Costa and Williams, 1999; Hooker et al., 2002; Laidre et al., 2004; Croll et al., 2007) and A and B values (Trites and Pauly, 1998; Reilly et al., 2004; Lavery et al., 2014). This method also aligns with existing research on nitrogen cycling from cetacean ecosystem services (Roman and McCarthy, 2010).

3BMR is then the daily ration adjusted to provide an ADMR/FMR:

$$ADMR / FMR / 3BMR = 3 \times (293.1 \times mass^{0.75})$$

The ADMR/FMR was then divided by the energy provided in kJ per kg of prey (Leaper and Lavigne, 2007; Barlow et al., 2008). This converts the ADMR/FMR into a daily required wet weight of food; energy content of prey is generally accepted as 5450 kJ kg⁻¹ for fish and squid and 3900 kJ kg⁻¹ for crustacea. Given data constraints, with no further data on nitrogen composition of cetacean prey, it is assumed that cetacean diets are composed solely of zooplankton, squid, and/or fish. An additional assimilation efficiency of 80% was used to account for energetic losses in consumption (Leaper and Lavigne, 2007; Barlow et al., 2008). Annual consumption of wet weight (Q) was calculated as:

$$\begin{aligned} \text{Annual consumption wet weight (Q)} \\ = \frac{3 \times (293.1 \times mass^{0.75})}{(0.8 \times ((3900 \times d_z) + (5450 \times (1 - d_z)))) \times 365} \end{aligned}$$

- d_z – the proportion of dietary zooplankton.

2.3.2 Faecal Nitrogen Concentrations

To derive the faecal nitrogen concentrations, based on other literature (Roman and McCarthy, 2010), it is assumed that

- 80% of ingested nitrogen is metabolised and excreted.
- Fish and crustaceans are approximately 15% protein, which is 17% nitrogen by weight.

All consumption is deemed to be compositionally similar between prey; fish and crustaceans. Faecal nitrogen was calculated as:

$$N_d = Q \times 0.8 \times 0.15 \times 0.17$$

$$N_d = Q \times 0.0204$$

- N_d – the total annual amount of defecated nitrogen (dry weight) (kg yr⁻¹).
- Q – the total annual prey consumption in wet weight (kg yr⁻¹).
- 0.8 – adjustment for metabolic efficiency.
- 0.15 – the proportion of weight as protein.
- 0.17 – the proportion of protein as nitrogen.

This calculates the replenishment of nitrogen from cetacean recycling that may be used to enhance primary productivity.

2.3.3 Carbon Fixation Evaluation

The dry weight of faecal nitrogen was then used to calculate the amount of carbon fixation:

$$C_{fixed} = \left(\frac{N_d}{M_N} \right) \times M_C \times r$$

- C_{fixed} – the carbon fixed by phytoplankton primary productivity generated by nutrient cycling (kg C ind⁻¹ yr⁻¹).
- N_d – the total annual amount of defecated nitrogen (dry weight) (kg N ind⁻¹ yr⁻¹).
- M_N – the molecular mass of nitrogen equal to 14.0067 (g mol⁻¹).
- M_C – the molecular mass of carbon equal to 12.011 (g mol⁻¹).
- r is the uptake ratios of C:N from available literature. The Redfield ratio states C:N:P ratios as 106:16:1 (Biddanda and Benner, 1997). This is equal to 6.625 (mol mol⁻¹).

Fluxes of carbon from cetacean driven nutrient cycling driving Primary Productivity (PP) are evaluated as:

$$\begin{aligned} PP \text{ (t C ind}^{-1} \text{ yr}^{-1}) \\ = C_{fixed} \text{ (kg C ind}^{-1} \text{ yr}^{-1}) \times \text{kg to t conversion} \end{aligned}$$

$$PP \text{ (t C ind}^{-1} \text{ yr}^{-1}) = C_{fixed} \text{ (kg C ind}^{-1} \text{ yr}^{-1}) \times 0.001$$

Carbon fluxes were summed and mapped to JCP distribution and abundance data as with carbon stocks in living biomass.

2.4 Cetacean Driven Nutrient Cycling Enhancing Net Primary Productivity

The Modified Surplus-Yield (MS-Y) model (Lavery et al., 2014) has been used to evaluate the differences in cetacean activity enhancing Primary Productivity (PP) against the Primary Productivity Requirements (PPR) of the cetaceans for consumption and respiration. This model was based on iron in the iron depleted waters of the Southern Ocean. In this study, we adapt that model from iron, to nitrogen, to create a Nitrogen Modified Surplus-Yield (N MS-Y) model. It is summarised as:

$$N \text{ MS} - Y = PP - PPR = NPP$$

If N MS-Y is positive, it suggests cetacean driven nutrient cycling fixes more carbon through PP than they remove through nutritional requirements. If negative, it suggests cetaceans provide an ecosystem disservice and contribute to atmospheric carbon emissions. Negative values may, however, also highlight the transport and removal of nutrients, and/or highlight data gaps for cetacean driven nutrient cycling. The differences between carbon fixation and release are valued based on carbon value.

PP is calculated using the same process detailed previously.

2.4.1 Annual Primary Productivity Requirements (PPR)

PPR was calculated from dietary requirements the same as for the PP. In conjunction with this, PPR is the sum of the total prey consumed by cetaceans at trophic levels, the carbon content of prey, and the trophic transfer efficiency between trophic levels (Pauly and Christensen, 1995; Trites and Pauly, 1998; Barlow et al., 2008).

2.4.1.1 Prey Proportions

The prey proportions of the species detailed in this study are taken from Pauly et al. (1998), as in Barlow et al. (2008), and adjusted where necessary for UK species³. They are detailed in **Table 2**.

The eight prey categories are abbreviated as:

- BI – benthic invertebrates.
- LZ – large zooplankton.
- SS – small squid.
- LS – large squid.
- SP – small pelagic fish.
- MP – mesopelagic fish.
- MF – miscellaneous fish.
- HV – higher vertebrates.

2.4.1.2 Carbon Consumption

PPR was then calculated as the sum of all individual species' PPR:

$$PPR_i = Q_i \sum_{g=1}^8 d_{i,g} c_g \left(\frac{1}{T_e} \right)^{(L_g-1)}$$

- PPR_i – calculated for each species (i) (kg C yr^{-1}).
- Q_i – the total prey consumption in wet weight per species (kg yr^{-1}).
- $d_{i,g}$ – the proportion of prey (g) in the diet (d) of species (i).
- c_g – the dry weight proportion of carbon (c) per wet weight of each prey group (g), equal to 0.11 (Pauly and Christensen, 1995; Barlow et al., 2008).
- T_e – the trophic transfer efficiency, equal to 0.1 (Barlow et al., 2008).
- L_g – the trophic level of the prey category.

2.4.2 Nitrogen Modified Surplus Yield

The final calculation for the N MS-Y model is:

$$N \text{ MS} - Y = PP - PPR$$

- N MS-Y – the difference in carbon fixation and consumption ($\text{kg C ind}^{-1} \text{ yr}^{-1}$).

Stocks of carbon from cetacean driven nutrient cycling driving PP against PPR are evaluated as:

TABLE 2 | Cetacean dietary prey proportions and trophic levels.

			Prey proportions						
	BI	LZ	SS	LS	SP	MP	MF	HV	
Trophic levels									
Species	2.2	2.2	3.2	3.7	2.7	3.2	3.3	4	Trophic level
HP	0.05		0.1	0.1	0.3		0.45	0	4.2
WSD			0.3	0.05	0.3	0.2	0.15	0	4.2
CD	0	0	0.15	0.15	0.1	0.4	0.2	0	4.2
WBD	0	0	0.15	0.15	0.1	0.4	0.2	0	4.2
BND			0.2	0.05	0.15		0.6	0	4.2
MW		0.65			0.3		0.05	0	4.2

$$N \text{ MS} - Y \left(t \text{ C ind}^{-1} \text{ yr}^{-1} \right)$$

$$= N \text{ MS} - Y \left(\text{kg C ind}^{-1} \text{ yr}^{-1} \right) \times \text{kg to t conversion}$$

$$N \text{ MS} - Y \left(t \text{ C ind}^{-1} \text{ yr}^{-1} \right)$$

$$= N \text{ MS} - Y \left(\text{kg C ind}^{-1} \text{ yr}^{-1} \right) \times 0.001$$

Carbon fluxes were summed and mapped to JCP distribution and abundance data as with carbon stocks in living biomass and cetacean driven nutrient cycling enhancing PP.

2.5 Valuations of Cetacean Regulation and Maintenance Ecosystem Services

Cetacean regulation and maintenance ecosystem services are all tentatively valued through their estimated impacts on carbon stocks. Carbon is converted to CO_2 with a conversion factor of 11/3 (Chami et al., 2020). CO_2 values are taken as for 2010 to match available data (Paxton et al., 2016); 2010 value was £13 tCO_2e (DECC, 2011). They are then standardised to 2020 US\$ in line with National Ecosystem Assessment (NEA) guidelines (UK NEA, 2014). 2010 conversion value from £ to \$ was 1.55 (ofx.com, 2019). Inflation was accounted for over this period⁴ with a factor of 1.19 (Inflation Calculator, 2016). Values are applied to individuals per species, then summed for total population values, in addition to a combined total population value.

Living biomass carbon stocks per individual per species are valued as:

$$\text{Living biomass } (\$ \text{ t CO}_2 \text{ ind}^{-1}) = \text{living biomass}$$

$$(t \text{ C ind}^{-1}) \times \text{CO}_2 \text{ conversion} \times 2020 \text{ US\$ conversion}$$

$$\text{Living biomass } (\$ \text{ t CO}_2 \text{ ind}^{-1}) = \text{living biomass}$$

$$(t \text{ C ind}^{-1}) \times \left(\frac{11}{3} \right) \times (13 \times 1.55 \times 1.19)$$

$$\text{Living biomass } (\text{tCO}_2 \text{ ind}^{-1}) = \text{living biomass}$$

$$(t \text{ C ind}^{-1}) \times 3.6667 \times 23.9785$$

³ Atlantic white-sided dolphins are assumed to have the same dietary proportions as Pacific white-sided dolphins. White-beaked dolphin are assumed to have the same dietary proportions as common dolphin species.

⁴ All future references to \$ are as 2020 US\$ standardised using the same method unless otherwise indicated.

$$\text{Living biomass (tCO}_2 \text{ ind}^{-1}) = \text{living biomass (t C ind}^{-1}) \times 87.9212$$

Stocks of carbon from cetacean driven nutrient cycling driving PP per individual per species are valued as:

$$PP (\$ \text{ t CO}_2 \text{ ind}^{-1} \text{ yr}^{-1}) = PP (\text{t C ind}^{-1} \text{ yr}^{-1}) \times \text{CO}_2 \text{ conversion} \times 2020 \text{ US\$ conversion}$$

$$PP (\$ \text{ t CO}_2 \text{ ind}^{-1} \text{ yr}^{-1}) = PP (\text{t C ind}^{-1} \text{ yr}^{-1}) \times 87.9212$$

Stocks of carbon from cetacean driven nutrient cycling in the N MS-Y model per individual per species are valued as:

$$N \text{ MS-Y } (\$ \text{ t CO}_2 \text{ ind}^{-1} \text{ yr}^{-1}) = N \text{ MS-Y } (\text{t C ind}^{-1} \text{ yr}^{-1}) \times \text{CO}_2 \text{ conversion} \times 2020 \text{ US\$ conversion}$$

$$N \text{ MS-Y } (\$ \text{ t CO}_2 \text{ ind}^{-1} \text{ yr}^{-1}) = N \text{ MS-Y } (\text{t C ind}^{-1} \text{ yr}^{-1}) \times 87.9212$$

3 RESULTS

3.1 Carbon Stocks in Cetacean Living Biomass

Carbon stocks in cetacean living biomass, and potential value, is detailed in **Table 3** and shown in **Figure 3**.

Stocks of carbon in cetacean living biomass total 19,809 t C. This is dominated by minke whales, which account for 82% of all cetacean carbon stocks in living biomass in JCP data. Carbon stocks in cetacean living biomass are greatest to the west of Scotland and around the Outer Hebrides. Whilst being generally spread around the total distribution range, there are additional concentrations of cetacean carbon stocks to the east of England, around the Isle of Man, and to the west of Wales.

3.2 Cetacean Driven Nutrient Cycling Enhancing Primary Productivity

Carbon fluxes driven by cetacean nutrient cycling are detailed in **Table 4** and shown in **Figure 4**. The potential value of carbon in these fluxes is detailed in **Table 5**.

The total nitrogen taken up by cetaceans is equal to 60,745 t N yr⁻¹. The total nitrogen recycled back into the environment is 48,596 t N yr⁻¹. Converting this into potential benefits to PP, equates to a total of 276,075 t C yr⁻¹ across the survey area. The minke whale population accounts for 65% of this estimate. Carbon fluxes are mostly concentrated around the Outer Hebrides, but other key areas can be found west of Wales, along the east coast of England, and to the north-east of the Shetland Islands.

3.3 Cetacean Driven Nutrient Cycling Enhancing Net Primary Productivity

Carbon fluxes driven by cetacean nutrient cycling are detailed separately for PP and PPR in **Table 6**. Carbon fluxes using the N MS-Y model are detailed, with their potential values, in **Table 7**. Carbon fluxes using the N MS-Y model are shown in **Figure 5**.

The N MS-Y models suggest that the cetaceans in this study cumulatively contribute to atmospheric emissions of 21 Mt C annually. The contributions of cetaceans in this model are relatively evenly spread between species, rather than dominated by one species. Whilst harbour porpoise populations bear the greatest influence on these values, owing to their large population, they have the lowest impact per individual. Key areas of activity are to the east of England, around the Outer Hebrides, and north-east of the Shetland Islands. They match the cumulative and more even distribution of value between all cetacean species distribution and abundance data.

3.4 Summary and Context of Results

Summary results for cetacean populations contributions to regulation and ecosystem services are detailed with wider ecological processes in **Tables 8–10**.

Stocks of carbon in living biomass are minimal compared to other stocks of carbon in living biomass; there is estimated to be roughly 100 times as much carbon in stocks of fish (Walday and Kroglund, 2008) and another 100 times as much carbon in benthic biomass (Barrio Froján et al., 2012; Zhang et al., 2019).

Modelling of cetacean driven nutrient cycling suggests a modest impact on recycling nitrogen. In the survey area, cetaceans ingest just under 20% of the amount that is input into the marine environment from terrigenous sources annually (Painting et al., 2018). Cetaceans are estimated to recycle a total of just under 50,000 t N yr⁻¹ and remove a total of just over 12,000 t N yr⁻¹ from the marine environment in the survey area. These equate to 15% and 4% of annual terrigenous nitrogen inputs.

Modelling of cetacean driven nutrient cycling against consumption and respiration requirements suggest a more complex interaction of ecosystem services. Just considering PP, cetacean contributions are 0.11% of total NPP. The estimates of PPR dominate the N MS-Y equation, however, which cause both to have a negative and similar relative contribution with regards to NPP, roughly 8.5% of total NPP (Capuzzo et al., 2018). This suggests cetaceans have a negative effect on NPP, and using an average value for tidal mixing across the survey area (Zhao et al., 2019), suggests cetaceans impact NPP twice as much as tidal mixing.

TABLE 3 | Stocks and valuations of carbon in living biomass.

Species	Mass (t)	Living biomass (t C ind ⁻¹)	Living biomass (t C)	Living biomass (\$ t CO ₂ ind ⁻¹)	Living biomass (\$ t CO ₂)
HP	0.031	0.00	1,148	0.29	100,960
WSD	0.17	0.02	1,235	1.57	108,541
CD	0.08	0.01	474	0.74	41,689
WBD	0.25	0.03	416	2.30	36,615
BND	0.188	0.02	345	1.73	30,342
MW	6.566	0.69	16,190	60.50	1,423,445
Total			19,809		1,741,592

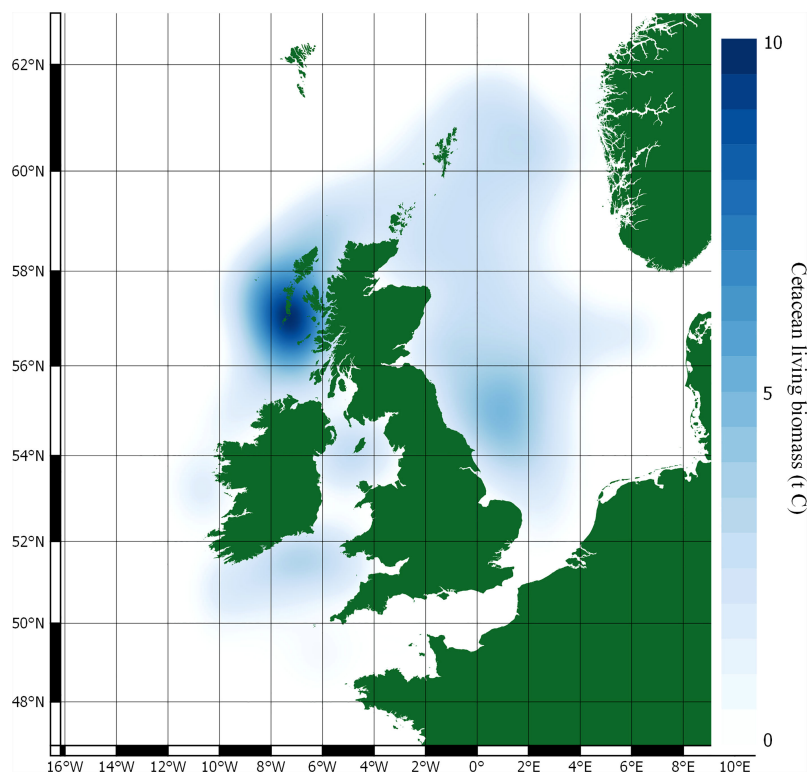


FIGURE 3 | Carbon stocks in cetacean living biomass.

TABLE 4 | Cetacean driven nitrogen fluxes.

Species	Nitrogen consumed/ removed (t N ind ⁻¹ yr ⁻¹)	Nitrogen consumed/ removed (t N yr ⁻¹)	Nitrogen excreted/ recycled (t N ind ⁻¹ yr ⁻¹)	Nitrogen excreted/ recycled (t N yr ⁻¹)
HP	0.02	8,716	0.0197	6,973
WSD	0.09	6,124	0.0707	4,899
CD	0.05	2,840	0.0402	2,272
WBD	0.12	1,876	0.0944	1,501
BND	0.10	1,669	0.0762	1,335
MW	1.68	39,520	1.3437	31,616
Total		60,745		48,596

3.5 Valuation of Cetacean Regulation and Maintenance Ecosystem Services

When valuated, carbon stocks in cetacean living biomass cumulatively sum up to just under \$2 million. As they are standing stocks, assuming no change in population growth or mortality, they represent a potential value only. At most they represent a baseline for SSO accreditation. Cetaceans may account for a potential total value of \$24 million per year of phytoplankton growth in the survey area. Minke whales contribute the greatest amount in this model, contributing \$671 per whale per year to phytoplankton growth. If the N MS-Y model is valuated, however, they suggest cetaceans account for carbon emissions at a cost of just under \$2 billion per year.

3.6 Data Uncertainty

There are significant areas of uncertainty in modelling and evaluative techniques used in this study. This uncertainty is compounded with each subsequent analysis and valuation.

3.6.1 Carbon Stocks in Cetacean Living Biomass

Average mass values for populations of cetacean species are used. Whilst these are guided by the most relevant research (Lavery et al., 2010) there is still uncertainty on how proportions of population subsets may impact these average mass calculations. All cetacean populations were assumed to be in a stable state, rather than a depleted state, as defined in (Lavery et al., 2010). It is unclear, however, on the status, and population structure, of the cetacean populations included in this study. Carbon content per mass unit is assumed to be a specific value and proportional between all species detailed. Cetacean species, however, are known to differ in body content; blubber may vary significantly between cetacean species (Pershing et al., 2010).

3.6.2 Cetacean Driven Nutrient Cycling Enhancing Primary Productivity

Cetacean driven impacts on nitrogen, and by extension PP, are underpinned by cetacean population average mass values (see section 3.6.1 Carbon stocks in cetacean living biomass). From this, dietary proportions of zooplankton are used to calculate metabolic rates and daily ration. Zooplankton only feature in the

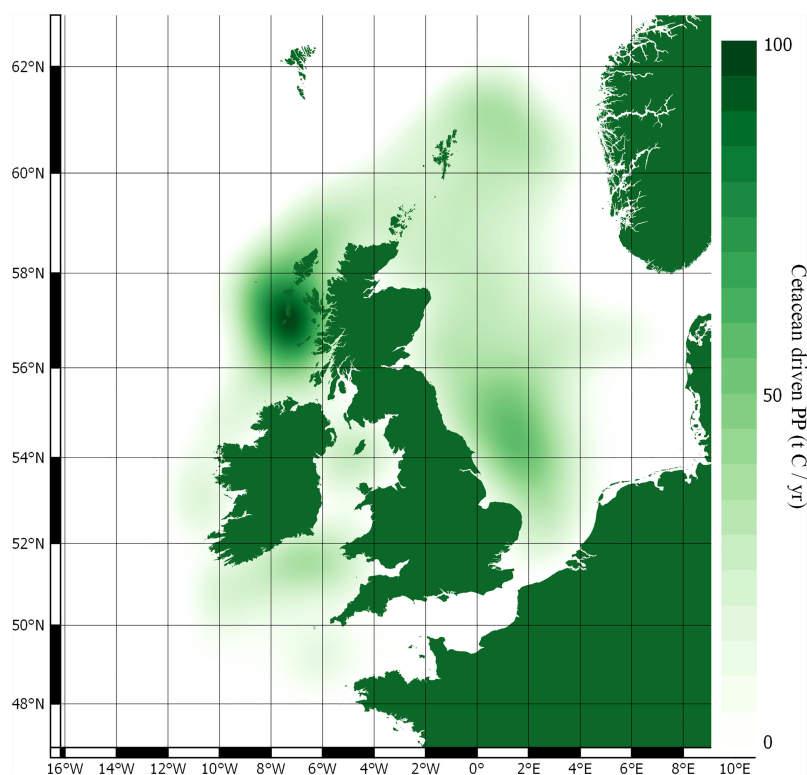


FIGURE 4 | Cetacean driven PP carbon fluxes.

TABLE 5 | Cetacean driven primary productivity and valuations.

Species	PP (t C ind ⁻¹ yr ⁻¹)	PP (t C yr ⁻¹)	PP (\$ t CO ₂ ind ⁻¹ yr ⁻¹)	PP (t C ind ⁻¹ yr ⁻¹)
HP	0.11	39,615	10	3,482,986
WSD	0.40	27,831	35	2,446,934
CD	0.23	12,906	20	1,134,730
WBD	0.54	8,525	47	749,569
BND	0.43	7,587	38	667,037
MW	7.63	179,611	671	15,791,596
Total		276,075		24,272,851

TABLE 6 | Cetacean driven primary productivity and primary productivity requirements.

Species	PP (t C ind ⁻¹ yr ⁻¹)	PP (t C yr ⁻¹)	PPR (t C ind ⁻¹ yr ⁻¹)	PPR (t C yr ⁻¹)
HP	0.11	39,615	18	6,516,725
WSD	0.40	27,831	57	3,982,863
CD	0.23	12,906	45	2,564,612
WBD	0.54	8,525	107	1,694,108
BND	0.43	7,587	76	1,338,290
MW	7.63	179,611	258	6,080,990
Total		276,075		22,177,589

diet of minke whales in this study, and taken as an average 65% of their diet in line with other research (Barlow et al., 2008). Whilst this is an average value, there is uncertainty of spatial and

seasonal variability with diet for all cetacean species. All cetacean species' diets in the study are assumed to be composed solely of zooplankton, squid, and/or fish. Energy content for zooplankton is assumed to be a standard value, as is the energy content of squid and fish. There is also then uncertainty on spatial and temporal variability for dietary energy content. The PP calculation used in this study uses the 3BMR method, but as detailed in section 2.3.1 Dietary requirements, there are a large number of other potential values that could be used. It is unclear which might be the most applicable to the cetaceans in this study and/or the survey area.

Dietary requirements form the basis to calculate the amount of nitrogen ingested, stored, and cycled by cetacean feeding and excretion. This is assumed to be standard for all prey items and all cetacean species. Nitrogen removal is a key, and valued,

TABLE 7 | Cetacean driven N MS-Y carbon fluxes and valuations.

Species	N MS-Y (t C ind ⁻¹ yr ⁻¹)	N MS-Y (t C yr ⁻¹)	N MS-Y (\$ t CO ₂ ind ⁻¹ yr ⁻¹)	N MS-Y (\$ t CO ₂ yr ⁻¹)
HP	-18	-6,477,110	-1,611	-569,475,071
WSD	-57	-3,955,032	-5,018	-347,731,033
CD	-45	-2,551,706	-3,967	-224,348,955
WBD	-106	-1,685,582	-9,324	-148,198,365
BND	-76	-1,330,703	-6,679	-116,997,002
MW	-251	-5,901,380	-22,053	-518,856,178
Total		-21,901,513		-1,925,606,604

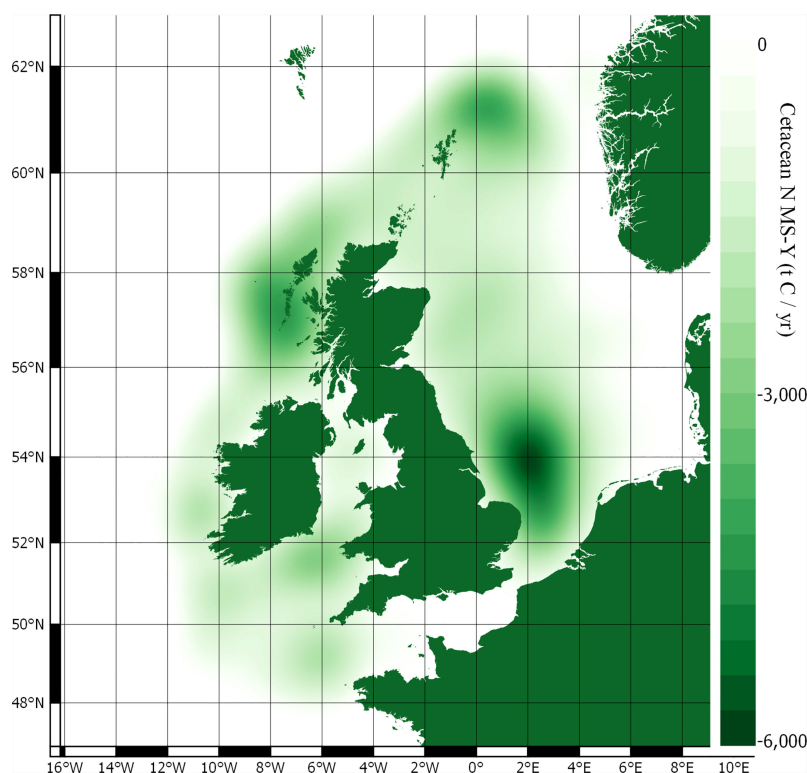


FIGURE 5 | Cetacean driven N MS-Y carbon fluxes.

TABLE 8 | Summary of survey area carbon stocks.

Living biomass stocks (Mt C)	Cetaceans	Fish	Benthos
Total	0.02	1.82	2.18
References		(Walday and Kroglund, 2008)	(Barrio Froján et al., 2012; Zhang et al., 2019)

TABLE 9 | Summary of survey area nitrogen fluxes.

Nitrogen fluxes (1,000 t N yr ⁻¹)	Cetacean nitrogen ingested	Cetacean nitrogen recycled	Terrigenous inputs
Total	60.75	48.60	315.00
References			(Painting et al., 2018)

ecosystem service (Watson et al., 2020). Nitrogen removal is valued at £295 kg⁻¹, and whilst this could have been included in this study, it is likely only to be applicable to near coastal waters where nitrogen is not limited, but rather in excess, due to terrigenous nitrogen inputs (Painting et al., 2018; Watson et al., 2020).

The estimates for cycled nitrogen are used to calculate how much carbon will be fixed through PP. Crucially at this stage, the model assumes nitrogen uptake by phytoplankton to be a standard value in line with Redfield ratios (Biddanda and

Benner, 1997). Where this approach is used for cetacean regulation and maintenance ecosystem service modelling in the Southern Ocean (Lavery et al., 2010; Ratnarajah et al., 2016), uptake ratios specific for iron in an iron depleted environment are used; this dramatically influences the cetacean driven PP. The survey area is known to have nutrient limitations for NPP (Zhao et al., 2019). There are, however, no known values of uptake for nitrogen or phosphorus by phytoplankton when these nutrients are limited. Additionally, nutrient limitations have spatial and temporal variability in the survey area (Zhao et al., 2019); this variability is not captured in evaluations used in this study.

Finally, the evaluation of cetacean driven PP is adapted from the modified surplus yield (MS-Y) model used for baleen whales in the Southern Ocean. It is unclear how applicable it is to the survey area, the cetaceans in this study, and to non-baleen species. In the Southern Ocean models, iron concentrations from cetacean defecation are used. There are, however, no data

TABLE 10 | Summary of survey area carbon fluxes.

NPP fluxes (Mt C yr ⁻¹)	Cetacean PP	Cetacean PPR	Cetacean N MS-Y	Tidal mixing	NPP
Total	0.28	22.18	-21.90	10.45	255.06
References				(Zhao et al., 2019)	(Capuzzo et al., 2018)

for nitrogen, or phosphorus, concentrations from cetacean defecation. As such, a standard estimate of 80% ingested nitrogen is assumed to be metabolised and excreted (Roman and McCarthy, 2010); there is uncertainty on how accurate this is with regards to specific cetacean species, population subsets and their proportion within the population, and for spatial and seasonal variability. This is also the basis of the N MS-Y model.

3.6.3 Cetacean Driven Nutrient Cycling Enhancing Net Primary Productivity

The PPR, like the PP, is also estimated using average mass values, dietary zooplankton proportions, and 3BMR. From this, prey categories and proportions are used to estimate productivity requirements with an assumed standard dry weight of carbon per wet weight of prey group. Prey categories and proportions are taken from the most relevant research (Pauly and Christensen, 1995; Barlow et al., 2008) but it is again uncertain if these are applicable to the cetaceans in this study and for this survey area. The model uses trophic levels for each prey group, and also assumes a standard trophic transfer efficiency between each level. The dry weight of carbon per wet weight of prey group is also assumed to be a standard value. There is uncertainty on the robustness of this and whether there is spatial and temporal variability in these values, whether this model is applicable to the cetaceans in this study, and whether this model is applicable for the survey area used in this study.

The model then evaluates 'enhanced primary production' but does not seem to include a value for 'enhanced biodiversity and ecosystem potential' as in CICES (Cook et al., 2020b). There is currently no quantification methodology to quantify the latter. Any model of cetacean driven nutrient cycling impacting NPP is therefore lacking a key additional value to robustly estimate cetacean regulation and maintenance ecosystem services.

3.6.4 Joint Cetacean Protocol (JCP) Data

The evaluative techniques in this study are applied to the JCP cetacean abundance and distribution data (Paxton et al., 2016). JCP data use elements of predictive modelling; data used include day of year, year, depth, slope, and sea surface temperature (Paxton et al., 2016). The evaluations in this study are then mapped to the point density values provided by the JCP data. JCP data, however, also provide lower (2.5%) and upper (97.5%) confidence limits for cell densities. All evaluative techniques used in this study, then mapped to JCP data, are subject to the uncertainty inherent in the JCP data (Paxton et al., 2016).

Whilst the JCP data detail estimates of cetacean distribution and abundance, data detailing distribution of linked ecosystem processes are not available. There is spatial and temporal variability in cetacean activity, nutrient cycling from physical processes, nutrient limitations, and phytoplankton growth and uptake ratios of nutrients. Finally, the JCP data provide estimates of cetacean abundance and distribution for 2010. They are, therefore, slightly outdated and it is unclear how relevant this data is now. All these various factors compound key uncertainties in data, evaluative techniques, mapping, and potential valuation of cetacean regulation and maintenance ecosystem services.

4 DISCUSSION

The results show large variability in both the evaluations, and potential valuations, of cetacean ecosystem services. The variability highlights the uncertainty inherent in the models as described in section 3.6 Data uncertainty. This section appraises the significance of the results, the potential accreditation process of valuations presented in this study with SSO criteria, and details future research that would best support future evaluation and valuation of cetacean regulation and maintenance ecosystem services.

4.1 Carbon Stocks in Cetacean Living Biomass

Carbon stocks in living biomass are of minor significance in comparison to other marine stocks of carbon in the survey area (Walday and Kroglund, 2008; Barrio Froján et al., 2012; Zhang et al., 2019). Whilst there are some species unaccounted for in JCP data with regards to abundance and distribution, such as Risso's dolphin *Grampus griseus*, these are likely to have little impact on the stocks; the majority of cetacean species in the survey area are included in JCP data. The minke whale population dominates the carbon stocks in living biomass and account for 82% of carbon. However, since the calculations involve all cetacean species detailed in the JCP data, the distribution of this carbon highlights key areas of cetacean activity. These key areas are therefore likely to be on the west coast of Scotland, around the Outer Hebrides and Isle of Man, to the west of Wales, and off the east coast of England.

Whilst the stocks of cetacean carbon, in comparison to other marine stocks, are relatively minor, the valuation details a potential value of just under \$2 million in the UK. This is largely driven by minke whales and, given their large size, it is expected that other large cetacean species would likely have significant value if mapped. This value assumes that removal of cetaceans wouldn't result in greater biomass, and carbon stocks, in other species in the trophic chain. This is supported by research that indicates removal of large species can decrease total community biomass by 30% due to differences in relative metabolic efficiency between large and small organisms (Pershing et al., 2010). It is unclear, however, if this would be applicable in the survey area and to what degree cetaceans influence total community biomass.

It is important to note that this potential combined value of just under \$2 million is not an annual ecosystem service value. It only represents the value of carbon stocks in UK cetacean populations for 2010, and at most represent baseline data if considered for SSO accreditation (Ullman et al., 2013). They are also only taken for 2010, therefore, inferences regarding population changes can't be made. As such, these stocks of carbon would likely not meet the criterion of permanence with no other data to robustly support population stability or recovery. If additionality and permanence can be proved through policy and management this may lead to carbon accreditation. To prove these criteria, international coordination of cetacean protection and restoration would need to coincide with more large scale survey efforts such as

SCANS (Hammond et al., 2018). This would provide a future series of robust data to complement the baseline values presented in this study. Any carbon valued through this process would also need to meet other criteria of leakage and co-benefits (Ullman et al., 2013). Leakage is inherently difficult with mobile trans-national species. It is unclear how such a valuation might work across international boundaries, with different policy agendas, and to whom that value might be assigned if ownership of cetacean populations, and their protection, is uncertain. This study does not attempt to quantify the co-benefits of cetacean living biomass and their importance to ecologic and societal considerations but these are likely to be significant (Roman et al., 2014; Malinauskaite et al., 2021b). Cetacean based tourism alone was valued at \$21.4 million in 2008 (O'Connor et al., 2009b); without considering growth and adjusting for inflation, this is 2020 US \$73.5 million. Cetacean populations are likely to have more market applicable values through cultural values (Cook et al., 2020a; Malinauskaite et al., 2021a) than the potential values highlighted here for carbon stocks.

4.2 Carbon Stocks in Whale-Falls

Whale-falls are not evaluated in this study due to lack of data. This reflects uncertainty regarding the transport and sequestration of soft tissue carbon into deep waters in other potential blue carbon such as kelp (Krumhansl and Scheibling, 2012; Bayley et al., 2017). It is unclear whether this transport of carbon to the deep sea or benthos would meet the permanence criterion; isotopic, or eDNA, analysis to identify the carbon source might be required (Hopkinson, 2018).

There is a significant protected area just beyond the survey area to the west of the Outer Hebrides in waters deeper than 1000m, see **Figure 2**. As such, whale-falls in this area might provide significant sequestration of carbon if cetacean abundance and distribution can also be determined, see section 1.4 Scope of research.

Whale-falls incorporated into carbon accreditation are likely to be the most tangible of all potential values for cetacean derived carbon. There would, however, be uncertainty on where to set the baseline; the baseline might include existing protected areas. Additionally, permanence, and leakage could be met through the additional protection of skeletal carbon in protected areas. Alternatively, new protected areas might be based on cetacean distributions and likelihood of mortality. Co-benefits would likely be realised by protecting the wider ecosystem by protecting the benthos, and/or used to engage communities. A statistics approach to data, reliant on probabilities of cetacean-falls rather than verifiable data, would need to be accepted by SSOs. This, however, has already some pathways through tier assessment accreditation which recognises the data constraints that might otherwise impede blue carbon projects (Troxler et al., 2018). Additionally, there is advancement of probability-based data in carbon accreditation process with recommendations for a general 50% reduction in carbon seagrass quantification rather than identification of the carbon source. This simplifies and reduces costs inherent in autochthonous and allochthonous carbon analysis (Kennedy et al., 2010).

4.3 Cetacean Driven Removal of Excess Nutrients From Coastal Waters

Cycling of nutrients is a key component of ecosystem function (Townsend, 1998; Zhao et al., 2019) and cetacean contributions to nutrient cycling have been evaluated (Roman and McCarthy, 2010) and valued (Chami et al., 2020). This study shows that UK cetaceans recycle more than twice the amount of nitrogen than in the Gulf of Maine (Townsend, 1998; Roman and McCarthy, 2010). This is arguably a more pronounced enhancement than in the Gulf of Maine as the average PP is lower in the North Sea. In the survey area, cetaceans recycle 48,000 t N yr⁻¹ in waters with an average PP of 234g C m⁻² yr⁻¹ (Capuzzo et al., 2018) whilst in the Gulf of Maine cetaceans recycle 19,600 t N yr⁻¹ (Roman and McCarthy, 2010) in waters with an average PP of 290g C m⁻² yr⁻¹ (Townsend, 1998).

In coastal areas this could assist in removal of excess nutrients and has been valued as an ecosystem service in other contexts (Watson et al., 2020). It is unclear, however, on the appropriate value that could be assigned to this process. A price of £295 kg⁻¹ has been used for nitrogen removal (Watson et al., 2020) but this has been for sessile habitats where there is less uncertainty due to spatial and temporal variability from cetacean mobility. It is also uncertain how this value could be integrated into markets. If applied to data used in this study, estimating ingestion of 60,745 t N yr⁻¹, this would equate to just under \$23 billion⁵ yr⁻¹ using 2020 £ to \$ conversion values (ofx.com, 2019). Currently, however, this represents a value outside market mechanisms and requires more supporting data.

The evaluation and valuation of this ecosystem service was not investigated further or detailed in this study as there is currently too much uncertainty for which subset of the JCP data it could be mapped. If cetacean nutrient cycling of nitrogen is used to generate PP, it is unclear if cetacean nutrient cycling could also be used to value removal of nitrogen. In addition to nitrogen, there is also cycling of phosphorus which can also be valued (Watson et al., 2020) and which is also a limiting factor for PP in the survey area (Zhao et al., 2019). There is uncertainty on where to separate the subsets of data if one subset (close to shore) is valued for nitrogen removal and the other subset (farther offshore) is valued for nitrogen cycling. An arbitrary distance from a shoreline could be used or it could be combined with spatial data on inputs of terrigenous nitrogen (Painting et al., 2018), and spatial data of nitrogen limited waters (Zhao et al., 2019), to detail which portions of cetacean populations are valued for which ecosystem service. Alternatively, due to cetacean mobility, the whole population could be valued for both services with transport of nitrogen from the coast to offshore waters to then enhance offshore PP. It is also unclear on which aspects of the nitrogen cycling should be valued; valuation could be applied to nitrogen ingestion, nitrogen retention, and/or nitrogen cycling and transport. Nitrogen retention would apply to 20% of nitrogen ingested, whilst nitrogen cycling and transport could be applied to either 80% or 100% of the estimated nitrogen ingested.

When compared against terrigenous nitrogen inputs into the survey area (Painting et al., 2018), cetaceans will recycle or

⁵Billion in this paper refers to a thousand million, standardising it to US\$.

transport, at most, 20% of this input using the models in this study. There must therefore be key elements of nitrogen cycling in the survey area which are currently unaccounted. These elements could include uptake and cycling by other biota, such as fish and benthos which have a much larger biomass than cetaceans in the survey area (Walday and Kroglund, 2008; Barrio Froján et al., 2012; Zhang et al., 2019). They might also include physical processes (Zhao et al., 2019) and/or other aspects of biological pumps, calcium carbonate pumps, or microbial pumps driving nutrient fluxes (see section 1 Introduction).

4.4 Cetacean Driven Nutrient Cycling Enhancing Primary Productivity

Extrapolating cetacean driven nutrient cycling to then calculate potential carbon fixation through PP allows for this process to also be valued through carbon. This study used the Redfield ratios of nutrients in phytoplankton due to lack of data on uptake rates specific to nutrient limitations in the environment. Compared to other nutrient cycling processes, cetacean driving nutrient cycling enhancing PP is of minor value. This study calculates that cetaceans enhance PP by $0.28 \text{ Mt C yr}^{-1}$ which is just 2.64% of carbon fixed due to the average value of tidal mixing at $10.45 \text{ Mt C yr}^{-1}$ (Zhao et al., 2019). Compared to total NPP in the survey area, extrapolated to be $255.06 \text{ Mt C yr}^{-1}$ (Capuzzo et al., 2018), cetacean driven nutrient cycling contributes just 0.11%.

Cetacean driven contributions to PP are mostly concentrated around the Outer Hebrides but other key areas can be found west of Wales, along the east coast of England, and to the north-east of the Shetland Islands. These areas are somewhat aligned with existing protection, but this analysis suggests additional protection should be focused here with an increase of areal extent and in protective measures. These values also partially align with spatial distributions of nitrogen limited waters in the North Sea (Capuzzo et al., 2018; Zhao et al., 2019). It is unclear if this also holds true to the west of Scotland, where cetacean driven PP is most concentrated; there is limited data on spatial limitations of nutrients for the survey area outside the North Sea.

Valuating carbon fixation and applying them to JCP cetacean abundance and distribution data suggests the carbon cycled through this ecosystem service is worth \$24 million per year in the survey area. It is, however, unlikely these values could be accredited through SSOs. Data would need to robustly show the importance of this nutrient recycling to primary productivity. Whilst there are data that highlight the importance of cetaceans for ecosystem function through regulation and maintenance (Apollonio, 2002; Springer et al., 2003; Reisewitz et al., 2006; Springer et al., 2008; Pershing et al., 2010; Wilmers et al., 2012; Roman et al., 2014), the contributions of this process are difficult to quantify. Furthermore, ecosystem complexity, environmental factors, and regional differences may preclude extrapolation of data to other areas. If robust data can be produced, they may only have value if additionality, permanence, non-leakage, and co-benefits criteria are met. These are the same barriers to accreditation as with cetacean living biomass carbon. If cetacean driven PP is viewed in conjunction with valuation of carbon stocks in living biomass, it is unclear whether this would be viewed as 'double-counting' or the result of positive feedback; increased cetacean populations, with

larger carbon stocks, would have a greater impact on PP, which would cycle back to allow greater cetacean population growth.

4.5 Cetacean Driven Nutrient Cycling Enhancing Net Primary Productivity

Scientific robustness requires that cetacean driven nutrient cycling enhancing PP also needs to be balanced against the PPR of cetaceans. This has been calculated for cetaceans in the Southern Ocean, with recycled iron, and modelling of nutrient recycling is positive and self-sustaining. In the original research, this has only been evaluated with regards to carbon fluxes (Lavery et al., 2010; Roman and McCarthy, 2010; Lavery et al., 2014; Ratnarajah et al., 2018). Extrapolations of this research have, however, been valued to attach monetary values to these processes (Chami et al., 2020).

The N MS-Y model indicates a negative contribution from cetaceans on NPP of $-21.90 \text{ Mt C yr}^{-1}$ in the survey area. Relative to other processes impacting NPP, this is roughly twice the average value of tidal mixing at $10.45 \text{ Mt C yr}^{-1}$ (Zhao et al., 2019). Relative to total NPP of $255.06 \text{ Mt C yr}^{-1}$ (Capuzzo et al., 2018), this would account for 8.5% in the survey area. Compared to the much larger stocks of carbon in other forms of biomass (Walday and Kroglund, 2008; Barrio Froján et al., 2012; Zhang et al., 2019) in the survey area, cetaceans may have a limited impact on NPP.

Whilst the individual contributions are dominated by minke whales again, the total value is more evenly spread between the cetacean species included. The individual contributions from minke whales are offset by the much larger abundances of other species. The largest values come from the harbour porpoise population, though their individual contributions are the smallest. The N MS-Y model shows hotspots of activity similar to that of PP, around the Outer Hebrides, the east of England, and the north-east of the Shetland Islands.

When valued, the model suggests that UK cetacean populations provide an ecosystem disservice of just under \$2 billion per year. Valuations of cetacean ecosystem disservices, however, are unlikely to gain accreditation due to excessive uncertainty. Even if policy pathways become available (Herr and Landis, 2016), accreditation processes would have the same obstacles as for living biomass and nutrient cycling driving primary productivity. If values for carbon stocks in living biomass, cetacean driven PP, and N MS-Y are contradictory, they highlight greater uncertainty in the evaluative methods which will need to be addressed before any carbon could be accredited. There is a significant body of research which highlights the importance of cetaceans in ecosystem function through regulation and maintenance ecosystem services (Apollonio, 2002; Springer et al., 2003; Reisewitz et al., 2006; Springer et al., 2008; Pershing et al., 2010; Wilmers et al., 2012; Roman et al., 2014). As such, the N MS-Y model here is deemed to be inaccurate and missing key data, see section 3.6.3 Cetacean driven nutrient cycling driving phytoplankton growth and carbon capture against cetacean consumption and respiration.

There are a number of points to consider when reviewing the N MS-Y model results. Since the North Sea, and other waters included in the survey area, are not iron deficient, recycled

nitrogen was used as the basis of the analysis. Nitrogen, and phosphorus, limit phytoplankton growth in the North Sea (Zhao et al., 2019). Integrating the specific spatial distributions of these limitations, however, was beyond the scope of this research. The Southern Ocean also used environment specific uptake rates for iron but such data are not available for nitrogen, or phosphorus, in the survey area detailed in this study. Without these data, the N MS-Y model uses the Redfield ratios, and likely significantly underestimates cetacean driven nutrient cycling on PP. Other data constraints increase uncertainty in the evaluation.

Under CICES, the regulation and maintenance category has been evaluated as enhanced biodiversity, evolutionary potential, and primary productivity together. We find, however, that only primary productivity has been evaluated with enhanced biodiversity and evolutionary potential lacking any established methods of quantification. Where cetaceans have been removed from ecosystems, there is evidence of reduced productivity, biodiversity, and ecosystem function (Apollonio, 2002; Springer et al., 2003; Reisewitz et al., 2006; Springer et al., 2008; Pershing et al., 2010; Wilmers et al., 2012; Roman et al., 2014) but it is difficult to extrapolate these data to other environments due to site specific differences. This research suggests that negative values presented in the MS-Y modelling do not accurately detail cetacean ecosystem disservices. It is unclear, however, if negative values derived in MS-Y modelling are due to wider ecosystem effects and transfer of nutrients beyond the survey area, i.e. the whale conveyor, or if values fail to account for enhanced biodiversity and ecosystem potential. They may also be the result of failing to account for inputs and recycling of other key nutrients, such as phosphorus, which may act cumulatively to impact primary productivity (Ho et al., 2003; Stubbins, 2016).

There is too much uncertainty in the modelling to accurately quantify carbon fixation for the purposes of valuation or SSO accreditation. Research should focus on reducing quantification uncertainty in these ecosystem services to facilitate their valuation, conservation, and benefits from an eco-social economics perspective (Cisneros-Montemayor et al., 2019). This paper does not support any conclusions based off the N MS-Y values presented here or state that removal of cetaceans would increase ecosystem function in the survey area.

4.6 Future Research

This study presents a complex model composed of different evaluative processes. As such, there are areas where future research could focus to more accurately detail cetacean regulation and maintenance ecosystem services specific to each evaluation.

4.6.1 Carbon Stocks in Cetacean Living Biomass

Population structures of cetaceans included in the JCP data would better inform average mass values. The growth, or decline, of populations would be needed to prove 'additionality' as an SSO criterion and could also be used to characterise 'stable' or 'depleted' population structures (Lavery et al., 2010). Carbon content per mass unit could also be detailed for specific species, in addition to the population subsets of species. This would also

help inform carbon sequestration through 'whale-falls' by better informing sinking rates (Pershing et al., 2010) and skeletal carbon content. Future research could further investigate species specific sinking rates (Pershing et al., 2010), spatial mortality of migratory species, benthic protective status from trawl data (Dunkley and Solandt, 2021), and cetacean skeletal carbon composition (Nishiwaki, 1950). Bycatch might also be incorporated into future valuations to better understand carbon fluxes through whale-falls. If carbon stocks in living biomass are able to be accredited, values applied to cetaceans could then also be used to support sustainable fishing practices; cetacean by-catch would have an associated cost or fine.

4.6.2 Cetacean Driven Nutrient Cycling Enhancing Primary Productivity

Whilst there are data on dietary prey compositions of cetaceans (Barlow et al., 2008), they are taken from the west coast of north America; it is unclear how relevant they are to cetacean populations in the survey area. Dietary composition of cetaceans relevant to Europe would better inform ecosystem service modelling. If spatial and temporal variability in cetacean diet could also be detailed this could provide more insight into PP and PPR calculations. A better understanding of the specifics of energy content in diet would also ensure the estimates of cetacean metabolic rates are more robust. This could also be used to better inform research as to which values for metabolic rates in the Kleiber function (Kleiber, 1975) are the most relevant for the survey area.

More robust dietary requirements would provide insight into cetacean driven nutrient cycling. Future research could then focus on spatial and temporal variability of nitrogen removal from near shore coastal areas (Painting et al., 2018). Given the high value associated with this ecosystem service, £295/kg (Watson et al., 2020), this is suggested as a priority even if it is unclear on how this value might be brought into markets. Research could focus on near shore cetacean activity, the transport of nutrients offshore through the 'whale-conveyor' (Roman et al., 2014), cetacean faecal nutrient concentrations, spatial and temporal variability in nutrients (Painting et al., 2018), spatial and temporal variability in nutrient limitations (Zhao et al., 2019), and the importance of these nutrients in regard to limiting factors for PP (Capuzzo et al., 2018; Zhao et al., 2019). In addition to nitrogen, research into the cycling of phosphorus would provide additional values to cetacean regulation and maintenance ecosystem services (Painting et al., 2018; Zhao et al., 2019; Watson et al., 2020).

Focusing on the value of nutrient cycling to PP, uptake rates of environmentally limited nutrients, nitrogen and phosphorus, would be key to future evaluations and valuations. This study did not apply an uptake ratio for uptake of nitrogen by phytoplankton; it is argued in this study that this lack of data precludes any meaningful valuation of this ecosystem service in the survey area. Future research that details this factor with spatial and temporal nutrient limitations could underpin robust evaluations along with potential valuation and accreditation. Finally, previous research has focused on baleen whales (Lavery et al., 2010; Ratnarajah et al., 2016; Chami et al., 2019)

and it is unclear how appropriate it is to apply this process to non-baleen species. Evaluations of these species were included to provide an overall picture of cetacean nutrient cycling and PP, but species-specific models, using species-specific data as detailed earlier in this section, would be more accurate.

4.6.3 Cetacean Driven Nutrient Cycling Enhancing Net Primary Productivity

Species specific prey categories, proportions, and dry weight of carbon per wet weight of prey group could be used to better estimate PPR. The trophic levels and transfer efficiency between each level might also be species specific, location specific, and exhibit spatial and temporal variability. Finally, there is as yet no way to evaluate 'enhanced biodiversity and ecosystem potential' as in CICES (Cook et al., 2020b). Research into this area, based off data that details their importance in ecosystem function (Apollonio, 2002; Springer et al., 2003; Reisewitz et al., 2006; Springer et al., 2008; Pershing et al., 2010; Wilmers et al., 2012; Roman et al., 2014), could provide a key value that could be integrated into other values of cetacean ecosystem services (Villa et al., 2002).

4.6.4 Net Primary Productivity and Fisheries Value

Data constraints precluded the analysis of correlations of fisheries value between PP, PPR, and N MS-Y values. Future research could test the relative strength of correlations between PP and PPR from MS-Y models. If PP more closely correlates to fisheries value than PPR, it could support evaluations of cetacean nutrient cycling as a positive benefit to ecosystem function.

5 CONCLUSIONS

This study provides evaluations of a number of cetacean regulation and maintenance ecosystem services. There are, however, large uncertainties in the evaluative processes due to data constraints and lack of evaluative methods for 'enhanced biodiversity and ecosystem potential'. This uncertainty is compounded with subsequent valuations of these processes. We do not suggest that any valuations presented for nutrient cycling here are robust for accreditation, either as benefits or as costs. The N MS-Y model is a preliminary application of valuating cetacean nutrient cycling from which future research might build.

Outputs of this study can, however, be used to assist decision making processes and marine management by highlighting key areas of cetacean activity. These areas, for all aspects of cetacean regulation and maintenance ecosystem services, are concentrated by the Outer Hebrides in Scotland, along the east coast of England, and to the west of south Wales. These hotspots are mostly synched with protected areas but suggest that additional protection might be a consideration for the Outer Hebrides, west of south Wales, around the Isle of Man, to the east of England, and to the north-east of the Shetland Islands.

Whilst the values presented in this study are not considered sufficiently robust for accreditation, they may provide a basis of valuation from which future research can build. For SSO accreditation, values here might provide a baseline from which future research could detail additionality. These values also

highlight key areas for future ecosystem service research, and may be used to support cetacean regulation and maintenance ecosystem service evaluation and valuation from a policy perspective. They might also be used to drive public interest in cetacean research, and supplement other valuations such as the \$2 million whale (Chami et al., 2020). With more robust evaluative processes, they may be used in an integrated approach to ecosystem service valuation, which combine different values and areas of ecosystem services (Villa et al., 2002). Added values for carbon might be able to support community engagement and conservation agendas by highlighting their importance to climate change mitigation alongside societal and cultural values (Cisneros-Montemayor et al., 2019).

DATA AVAILABILITY STATEMENT

The datasets analysed for this study can be found in the 'Revised Phase III Data Analysis of Joint Cetacean Protocol Data Resources' (<https://hub.jncc.gov.uk/assets/01adfabd-e75f-48ba-9643-2d594983201e>).

ETHICS STATEMENT

This study used existing data on abundance and distribution from the JCP and only applied desk-based modelling to these data. This study did not involve interaction with live animals, as such, an ethics review was not required.

AUTHOR CONTRIBUTIONS

JS developed the paper concept from analysis of existing literature and policy to modelling and mapping of cetacean ecosystem services. JS led writing of the manuscript and NT, NZ, MC, VM, and EM provided expert input. All authors contributed to manuscript revision and approved the submitted version.

FUNDING

This work was supported by the Natural Environment Research Council grant number NE/S007342/1.

ACKNOWLEDGMENTS

The authors would like to acknowledge the support of Marine Alliance for Science and Technology Scotland (MASTS), the Scottish Universities Partnership for Environmental Research Doctoral Training Partnership (SUPER DTP), and the Joint Nature Conservation Committee (JNCC) in supporting policy internships and novel research. The authors would also like to acknowledge data used through the EMODnet Bathymetry Consortium (2020): EMODnet Digital Bathymetry (DTM) (<https://doi.org/10.12770/bb6a87dd-e579-4036-abe1-e649cea9881a>).

REFERENCES

- Apollonio, S. (2002). *Hierarchical Perspectives on Marine Complexities*, New York: Chichester, West Sussex: Columbia University Press. Available at: <https://doi.org/10.7312/apoll12488>
- Archer, D., and Jokulsdottir, T. (2013). "Biological Fluxes in the Ocean and Atmospheric pCO₂", in *The Oceans and Marine Geochemistry: Elsevier, Treatise on Geochemistry* H. D. Holland and K. K. Turekian (eds) Oxford, UK: Elsevier Inc., pp. 281–292. doi: 10.1016/B978-0-08-095975-7.00610-0.
- Balch, W. M., Gordon, H. R., Bowler, B. C., Drapeau, D. T., and Booth, E. S. (2005). Calcium Carbonate Measurements in the Surface Global Ocean Based on Moderate-Resolution Imaging Spectroradiometer Data. *J. Geophys. Res. C Ocean*. 110, 1–21. doi: 10.1029/2004JC002560
- Barbesgaard, M. (2016). Blue Carbon: Ocean Grabbing in Disguise?, *Transnational Institute, Afrika Kontakt, Indonesia Traditional Fisheries Union*. 1–11. doi: 10.1111/cobi.12310.
- Barlow, J., Kahru, M., and Mitchell, B. G. (2008). Cetacean Biomass, Prey Consumption, and Primary Production Requirements in the California Current Ecosystem. *Mar. Ecol. Prog. Ser.* 371, 285–295. doi: 10.3354/meps07695
- Barrio Foján, C. R. S., Bolam, S. G., Eggleton, J. D., and Mason, C. (2012). Large-Scale Faunal Characterisation of Marine Benthic Sedimentary Habitats Around the UK. *J. Sea. Res.* 69, 53–65. doi: 10.1016/j.seares.2012.02.005
- Bayley, D., Marengo, I., and Pelembe, T. (2017). Giant kelp 'Blue carbon' storage and sequestration value in the Falkland Islands. Natural Capital in the UK's Overseas Territories Report Series – Supplementary Report (South Atlantic Region). Contracted report to JNCC. Available at: <https://hub.jncc.gov.uk/assets/72c89fdc-a14b-4176-b543-81fe1ecd94bc> [Accessed November 7, 2019].
- Biddanda, B., and Benner, R. (1997). Carbon, Nitrogen, and Carbohydrate Fluxes During the Production of Particulate and Dissolved Organic Matter by Marine Phytoplankton. *Limnol. Oceanogr.* 42, 506–518. doi: 10.4319/lo.1997.42.3.0506
- Bishop, J. K. B. (2009). Autonomous Observations of the Ocean Biological Carbon Pump. *Oceanography* 22, 182–193. doi: 10.5670/oceanog.2009.48
- Blix, A. S., and Folkow, L. P. (1995). Daily Energy Expenditure in Free Living Minke Whales. *Acta Physiol. Scand.* 153, 61–66. doi: 10.1111/j.1748-1716.1995.tb09834.x
- Boyd, I. L. (2002). Energetics: Consequences for Fitness. In: *Marine Mammal Biology: An Evolutionary Approach*. Available at: <https://www.wiley.com/en-us/Marine+Mammal+Biology%3A+An+Evolutionary+Approach-p-9780632052325> (Accessed May 21, 2021).
- Broecker, W. S., and Peng, T. H. (1983). *Tracers in the Sea*. New York: Eldigio Press doi: 10.1016/0016-7037(83)90075-3.
- Caldeira, K., Wickett, M. E., and Duffy, P. B. (2002). Depth, Radiocarbon, and the Effectiveness of Direct CO₂ Injection as an Ocean Carbon Sequestration Strategy. *Geophys. Res. Lett.* 29, 13–11. doi: 10.1029/2001gl014234
- Capuzzo, E., Lynam, C. P., Barry, J., Stephens, D., Forster, R. M., Greenwood, N., et al. (2018). A Decline in Primary Production in the North Sea Over 25 Years, Associated With Reductions in Zooplankton Abundance and Fish Stock Recruitment. *Glob. Change Biol.* 24, e352–e364. doi: 10.1111/gcb.13916
- Cavanagh, R. D., Broszeit, S., Pilling, G. M., Grant, S. M., Murphy, E. J., and Austen, M. C. (2016). Valuing Biodiversity and Ecosystem Services: A Useful Way to Manage and Conserve Marine Resources? *Proc. R. Soc. B. Biol. Sci.* 283 (1844):20161635. doi: 10.1098/rspb.2016.1635
- Chami, R., Cosimano, T., Fullenkamp, C., and Oztosun, S. (2019). Nature's Solution to Climate Change: A Strategy to Protect Whales can Limit Greenhouse Gases and Global Warming. *Financ. Dev.* 56 (4), 34–38. <https://www.imf.org/external/pubs/ft/fandd/2019/12/natures-solution-to-climate-change-chami.htm>
- Chami, R., Fullenkamp, C., Berzaghi, F., Español-Jiménez, S., Marcondes, M., and Palazzo, J. (2020). On Valuing Nature-Based Solutions to Climate Change: A Framework with Application to Elephants and Whales. *Economic Research Initiatives at Duke (ERID) Working Paper No.* 297. Elsevier BV doi: 10.2139/ssrn.3686168.
- Cisneros-Montemayor, A. M., Moreno-Báez, M., Voyer, M., Allison, E. H., Cheung, W. W. L., Hessing-Lewis, M., et al. (2019). Social Equity and Benefits as the Nexus of a Transformative Blue Economy: A Sectoral Review of Implications. *Mar. Policy* 109, 103702. doi: 10.1016/j.marpol.2019.103702
- Cook, D., Malinauskaite, L., Davíðsdóttir, B., and Ögmundardóttir, H. (2020a). A Contingent Valuation Approach to Estimating the Recreational Value of Commercial Whale Watching – the Case Study of Faxaflói Bay, Iceland. *Tour. Manage. Perspect.* 36, 100754. doi: 10.1016/j.tmp.2020.100754
- Cook, D., Malinauskaite, L., Davíðsdóttir, B., Ögmundardóttir, H., and Roman, J. (2020b). Reflections on the Ecosystem Services of Whales and Valuing Their Contribution to Human Well-Being. *Ocean. Coast. Manage.* 186, 105100. doi: 10.1016/j.ocecoaman.2020.105100
- Costa, D. P., and Williams, T. M. (1999). "Marine Mammal Energetics", in *Encyclopedia of Marine Mammals*. Washington, DC: Smithsonian Institution Press, p. 1355. Available at: <https://vpn.gw.ulg.ac.be/science/book/DanaInfo=www.sciencedirect.com+9780123735539#ancs18>
- Croll, D. A., Kudela, R., and Tershy, B. R. (2007). "Ecosystem Impact of the Decline of Large Whales in the North Pacific," in *Whales, Whaling, and Ocean Ecosystems*, 202–214. doi: 10.1525/california/9780520248847.003.0016
- Danielsson, L. G. (1982). On the Use of Filters for Distinguishing Between Dissolved and Particulate Fractions in Natural Waters. *Water Res.* 16, 179–182. doi: 10.1016/0043-1354(82)90108-7
- Dasgupta, P. (2021) *The Economics of Biodiversity: The Dasgupta Review*. Available at: www.gov.uk/official-documents (Accessed February 17, 2021).
- DECC (2011) *A Brief Guide to the Carbon Valuation Methodology for UK Policy Appraisal*. Available at: <http://www.decc.gov.uk/> (Accessed June 12, 2021).
- De La Rocha, C. L., and Passow, U. (2013). "The Biological Pump", in H. Holland and K. Turekian (eds) *The Oceans and Marine Geochemistry: Elsevier, Treatise on Geochemistry/Treatise on Geochemistry: Second Edition*. Oxford, UK: Elsevier Inc., pp. 93–122. doi: 10.1016/B978-0-08-095975-7.00604-5
- Donovan, G. P. (1982). *International Whaling Commission Aboriginal/Subsistence Whaling (with special reference to the Alaska and Greenland fisheries) Reports of the International Whaling Commission Special Issue 4 Cambridge 1982*. Great Britain University Press, Cambridge.
- Ducklow, H. W., Carlson, C. A., Bates, N. R., Knap, A. H., and Michaels, A. F. (1995). Dissolved Organic Carbon as a Component of the Biological Pump in the North Atlantic Ocean. *Philos. Trans. - R. Soc. Lond. B.* 348, 161–167. doi: 10.1098/rstb.1995.0058
- Dunkley, F., and Solandt, J.-L. (2021). Marine Un-Protected Areas: Marine Conservation Society. Ross-on-Wye, UK.
- Fearnside, P. M. (1995). Hydroelectric Dams in the Brazilian Amazon as Sources of 'Greenhouse' Gases. *Environ. Conserv.* 22, 7–19. doi: 10.1017/S0376892900034020
- Fearnside, P. M. (2005). Brazil's Samuel Dam: Lessons for Hydroelectric Development Policy and the Environment in Amazonia. *Environ. Manage.* 35, 1–19. doi: 10.1007/s00267-004-0100-3
- Fearnside, P. M. (2016). Environmental and Social Impacts of Hydroelectric Dams in Brazilian Amazonia: Implications for the Aluminum Industry. *World Dev.* 77, 48–65. doi: 10.1016/j.worlddev.2015.08.015
- FPP (2011) *Lessons From the Field: REDD + and the Rights of Indigenous Peoples and Forest Dependent Communities: Forest Peoples Programme*. Available at: <http://www.forestpeoples.org/sites/fpp/files/news/2011/09/Minam> (Accessed April 4, 2020).
- Geraldi, N. R., Ortega, A., Serrano, O., Macreadie, P. I., Lovelock, C. E., Krause-Jensen, D., et al. (2019). Fingerprinting Blue Carbon: Rationale and Tools to Determine the Source of Organic Carbon in Marine Depositional Environments. *Front. Mar. Sci.* 6. doi: 10.3389/fmars.2019.00263
- Haines-Young, R., and Potschin, M. (2018). Common International Classification of Ecosystem Services (CICES) V5.1 and Guidance on the Application of the Revised Structure. Available at: <https://cices.eu/resources/> [Accessed February 15, 2021].
- Hammond, P. S. (2006). Small Cetaceans in the European Atlantic and North Sea (SCANS-II): Final Report. LIFE Project Number, LIFE04NAT/GB/000245, Final Report. *Mamm. Species*. Available at: <http://marine.gov.scot/sma/content/small-cetaceans-european-atlantic-and-north-sea-scans-ii>
- Hammond, P. S., Lacey, C., Gilles, A., Viquerat, S., Börjesson, P., Herr, H., et al. (2018). *Estimates of cetacean abundance in European Atlantic waters in summer 2016 from the SCANS-III aerial and shipboard surveys, Diseases of Aquatic Organisms*. Available at: <https://marine.gov.scot/sma/content/estimates-cetacean-abundance-european-atlantic-waters-summer-2016-scans-iii-aerial-and> (Accessed: 15 February 2021).
- Hammond, P. S., Macleod, K., Gillespie, D., Swift, R., Winship, A., Burt, M. L., et al. (2009). Cetacean Offshore Distribution and Abundance in the European Atlantic (CODA). Available at: <http://marine.gov.scot/sma/content/cetacean->

- offshore-distribution-and-abundance-european-atlantic-coda [Accessed February 15, 2021].
- Hansell, D., Carlson, C., Repeta, D., and Schlitzer, R. (2009). Dissolved Organic Matter in the Ocean. *Oceanography* 22 (4), 202–211.
- Hedges, J. I. (1992). Global Biogeochemical Cycles: Progress and Problems. *Mar. Chem.* 39, 67–93. doi: 10.1016/0304-4203(92)90096-S
- Heinze, C., Maier-Reimer, E., and Winn, K. (1991). Glacial Pco₂ Reduction by the World Ocean: Experiments With the Hamburg Carbon Cycle Model. *Paleoceanography* 6, 395–430. doi: 10.1029/91PA00489
- Henson, S. (2020) *Biological Components of the Ocean Carbon Cycle - National Oceanography Centre*. Available at: http://projects.noc.ac.uk/greenhouse_gas_science/greenhouse-gases-oceans (Accessed June 8, 2020).
- Herr, D., and Landis, E. (2016). Coastal Blue Carbon Ecosystems Opportunities for Nationally Determined Contributions. *Policy Brief. Natl. Wetl. Newsl.* 36, 1–28. doi: 10.2305/IUCN.CH.2015.10.en
- Higgs, N. D., Little, C. T. S., and Glover, A. G. (2011). Bones as Biofuel: A Review of Whale Bone Composition With Implications for Deep-Sea Biology and Palaeoanthropology. *Proc. R. Soc. B: Biol. Sci.* 278, 9–17. doi: 10.1098/rspb.2010.1267
- Hooker, S. K., Whitehead, H., and Gowans, S. (2002). Ecosystem Consideration in Conservation Planning: Energy Demand of Foraging Bottlenose Whales (Hyperoodon Ampullatus) in a Marine Protected Area. *Biol. Conserv.* 104, 51–58. doi: 10.1016/S0006-3207(01)00153-7
- Hopkinson, C. S. (2018). “Net Ecosystem Carbon Balance of Coastal Wetland-Dominated Estuaries”, in *A Blue Carbon Primer* (CRC Press), 51–65. doi: 10.1201/9780429435362-5
- Ho, T. Y., Quigg, A., Finkel, Z. V., Milligan, A. J., Wyman, K., Falkowski, P. G., et al. (2003). The Elemental Composition of Some Marine Phytoplankton. *J. Phycol.* 39, 1145–1159. doi: 10.1111/j.0022-3646.2003.03-090.x
- Houghton, R. A. (2003). “The Contemporary Carbon Cycle,” in *Treatise on Geochemistry* (Pergamon:Oxford, UK), 473–513. doi: 10.1016/B0-08-043751-6/08168-8
- IAMMWG (2015) *Management Units for Cetaceans in UK Waters (January 2015)* (JNCC Peterborough: JNCC Report No. 547) (Accessed June 15, 2021).
- Inflation Calculator (2016) *Inflation Calculator | Find US Dollar's Value from 1913–2015*. Available at: <https://www.usinflationcalculator.com/> (Accessed June 11, 2021).
- Jelmer, A., and Oppen-Berntsen, D. O. (1996). Whaling and Deep-Sea Biodiversity. *Conserv. Biol.* 10, 653–654. doi: 10.1046/j.1523-1739.1996.10020653.x
- Jiao, N., Herndl, G. J., Hansell, D. A., Benner, R., Kattner, G., Wilhelm, S. W., et al. (2010). Microbial Production of Recalcitrant Dissolved Organic Matter: Long-Term Carbon Storage in the Global Ocean. *Nat. Rev. Microbiol.* 8, 593–599. doi: 10.1038/nrmicro2386
- Katona, S., and Whitehead, H. (1988). Are Cetacea Ecologically Important? *Oceanogr. Mar. Biol. Annu. Rev.* 26, 553–568.
- Kennedy, H., Beggins, J., Duarte, C. M., Fourqurean, J. W., Holmer, M., Marbá, N., et al. (2010). Seagrass Sediments as a Global Carbon Sink: Isotopic Constraints. *Global Biogeochem. Cycle* 24(4). doi: 10.1029/2010GB003848
- Kenney, R. D., Scott, G. P., Thompson, T. J., and Winn, H. E. (1997). Estimates of Prey Consumption and Trophic Impacts of Cetaceans in the USA Northeast Continental Shelf Ecosystem. *J. Northw. Atl. Fish. Sci.* 22, 155–171. doi: 10.2960/J.v22.a13
- Kenny, T. A., Hu, X. F., Kuhnlein, H. V., Wesche, S. D., and Chan, H. M. (2018). Dietary Sources of Energy and Nutrients in the Contemporary Diet of Inuit Adults: Results From the 2007–08 Inuit Health Survey. *Public Health Nutr.* 21, 1319–1331. doi: 10.1017/S1368980017003810
- Kleiber, M. (1975). *The Fire of Life. An Introduction to Animal Energetics*. New York: Krieger.
- Krumhansl, K. A., and Scheibling, R. E. (2012). Production and Fate of Kelp Detritus. *Mar. Ecol. Prog. Ser.* 467, 281–302. doi: 10.3354/meps09940
- Laidre, K. L., Heide-Jørgensen, M. P., Jørgensen, O. A., and Treble, M. A. (2004). Deep-Ocean Predation by a High Arctic Cetacean. *ICES J. Mar. Sci.* 61, 430–440. doi: 10.1016/j.jcesjms.2004.02.002
- Lavery, P. S., Mateo, M. A., Serrano, O., and Rozaimi, M. (2013). Variability in the Carbon Storage of Seagrass Habitats and Its Implications for Global Estimates of Blue Carbon Ecosystem Service. *PLoS One* 8, e73748. doi: 10.1371/journal.pone.0073748
- Lavery, T. J., Roudnew, B., Gill, P., Seymour, J., Seuront, L., Johnson, G., et al. (2010). Iron Defecation by Sperm Whales Stimulates Carbon Export in the Southern Ocean. *Proc. R. Soc. B. Biol. Sci.* 277, 3527–3531. doi: 10.1098/rspb.2010.0863
- Lavery, T. J., Roudnew, B., Seymour, J., Mitchell, J. G., Smetacek, V., and Nicol, S. (2014). Whales Sustain Fisheries: Blue Whales Stimulate Primary Production in the Southern Ocean. *Mar. Mammal. Sci.* 30, 888–904. doi: 10.1111/mms.12108
- Leaper, R., and Lavigne, D. (2007). How Much do Large Whales Eat? *J. Cetacean. Res. Manage.* 9(3), 179.
- Lees, S., and Escoubes, M. (1987). Vapor Pressure Isotherms, Composition and Density of Hyperdense Bones of Horse, Whale and Porpoise. *Connect. Tissue Res.* 16, 305–322. doi: 10.3109/03008208709005617
- Lockyer, C. (1976). Body Weights of Some Species of Large Whales. *ICES J. Mar. Sci.* 36, 259–273. doi: 10.1093/icesjms/36.3.259
- Lockyer, C. (1981). Growth and Energy Budgets of Large Baleen Whales From the Southern Hemisphere. *Mamm. Seas.* 3 (FAO Fish. Ser. no. 5), 379–487.
- Loomis, J. B., and Larson, D. M. (1994). Total Economic Values of Increasing Gray Whale Populations: Results From a Contingent Valuation Survey of Visitors and Households. *Mar. Resour. Econ.* 9, 275–286. doi: 10.1086/mre.9.3.42629085
- Lovelock, C. E., and Duarte, C. M. (2019). Dimensions of Blue Carbon and Emerging Perspectives. *Biol. Lett.* 15, 23955–26900. doi: 10.1098/rsbl.2018.0781
- Mackintosh, N. A., and Wheeler, J. F. G. (1929). Southern Blue and Fin Whales. *Discovery Rep.* 1, 257–540. <https://www.biodiversitylibrary.org/part/236587>
- Macreadie, P. I., Anton, A., Raven, J. A., Beaumont, N., Connolly, R. M., Friess, D. A., et al. (2019). The Future of Blue Carbon Science. *Nat. Commun.* 10, 1–13. doi: 10.1038/s41467-019-11693-w
- Mariani, G., Cheung, W. W. L., Lyet, A., Sala, E., Mayorga, J., Velez, L., et al. (2020). Let More Big Fish Sink: Fisheries Prevent Blue Carbon Sequestration-Half in Unprofitable Areas. *Sci. Adv.* 6(44). doi: 10.1126/sciadv.abb4848
- Marshall, D. (1997). Subduction of Water Masses in an Eddying Ocean. *J. Mar. Res.* 55, 201–222. doi: 10.1357/0022240973224373
- Marshall, J., Adcroft, A., Hill, C., Perelman, L., and Heisey, C. (1997). A Finite-Volume, Incompressible Navier Stokes Model for, Studies of the Ocean on Parallel Computers. *J. Geophys. Res. C Ocean.* 102, 5753–5766. doi: 10.1029/96JC02775
- Nishiwaki, M. (1950). *On the Body Weight of Whales, The Scientific reports of the Whales Research Institute*. Tokyo: Scientific Reports Whales Research Institute.
- O'Connor, S., Campbell, R., Cortez, H., and Knowles, T. (2009a). *Whale Watching Worldwide Tourism Numbers, Expenditures and Expanding Economic Benefits*. Available at: www.ecolarge.com (Accessed February 16, 2021).
- O'Connor, S., Campbell, R., Cortez, H., and Knowles, T. (2009b). *Whale Watching Worldwide Tourism Numbers, Expenditures and Expanding Economic Benefits*. Available at: https://www.mmc.gov/wp-content/uploads/whale_watching_worldwide.pdf (Accessed May 11, 2021).
- ofx.com. (2019). *Monthly Average Rates | OFX. ofx.com*. Available at: <https://www.ofx.com/en-au/forex-news/historical-exchange-rates/monthly-average-rates/> (Accessed June 11, 2021).
- Olson, J. S., Garrels, R. M., Berner, R. A., Armentano, T. V., Dyer, M. I., and Yaalon, D. H. (1985). “The Natural Carbon Cycle”, in J. R. Trabalka (ed.) *Atmospheric Carbon Dioxide and the Global Carbon Cycle*. Washington, DC: US Department of Energy Report DOE/ER-0239., pp. 175–214.
- Painting, S., Collingridge, K., Garcia, L., Barry, J., Leaf, S., Best, M., et al. (2018). *Nutrient Inputs in Water and Air* (UK Marine Online Assessment Tool). Available at: <https://moat.cefas.co.uk/pressures-from-human-activities/eutrophication/nutrient-inputs/> (Accessed April 11, 2022).
- Parekh, P., Follows, M. J., Dutkiewicz, S., and Ito, T. (2006). Physical and Biological Regulation of the Soft Tissue Carbon Pump. *Paleoceanography* 21 (3). doi: 10.1029/2005PA001258
- Parsons, E. C. M., Warburton, C. A., Woods-Ballard, A., Hughes, A., and Johnston, P. (2003). The Value of Conserving Whales: The Impacts of Cetacean-Related Tourism on the Economy of Rural West Scotland. *Aquat. Conserv. Mar. Freshw. Ecosyst.* 13, 397–415. doi: 10.1002/aqc.582
- Pauly, D., and Christensen, V. (1995). Primary Production Required to Sustain Global Fisheries. *Nature* 374, 255–257. doi: 10.1038/374255a0
- Pauly, D., Trites, A. W., Capuli, E., and Christensen, V. (1998). Diet Composition and Trophic Levels of Marine Mammals. *ICES J. Mar. Sci.* 55, 467–481. doi: 10.1006/jmsc.1997.0280
- Paxton, C. G. M., Scott-Hayward, L., Mackenzie, M., Rexstad, E., and Thomas, L. (2016) *Revised Phase III Data Analysis of Joint Cetacean Protocol Data Resources*. Available at: <http://jncc.defra.gov.uk/page-6991> (Accessed April 20, 2021).

- Pearce, D. (2003). The Social Cost of Carbon and its Policy Implications. *Oxf. Rev. Econ. Policy* 19, 362–384. doi: 10.1093/oxrep/19.3.362
- Pershing, A. J., Christensen, L. B., Record, N. R., Sherwood, G. D., and Stetson, P. B. (2010). The Impact of Whaling on the Ocean Carbon Cycle: Why Bigger was Better. *PLoS One* 5, e12444. doi: 10.1371/journal.pone.0012444
- Peskett, L., Huberman, D., Bowen-Jones, E., Edwards, G., Brown, J., Brown, D., et al. (2008). *Making REDD Work for the Poor A Poverty Environment Partnership (PEP) Report Making REDD Work for the Poor Prepared on Behalf of the Poverty Environment Partnership (PEP)*. IUCN: International Union for Conservation of Nature.
- Porter, J. S., Austin, W. E. N., Burrows, M. T., Clarke, D., Davies, G., Kamenos, N., et al. (2020). Blue Carbon Audit of Scottish Waters. *Scott. Mar. Freshw. Ser.* 11 (3), 96pp. doi: 10.7489/12262-1
- Price, J. T., and Warren, R. (2016). *Literature Review of the Potential of “Blue Carbon” Activities to Reduce Emissions*. 1104872/AVOID2 WPE.2 Report 1. <https://docslib.org/doc/10123770/blue-carbon-activities-to-reduce-emissions>
- Ratnarajah, L., Bowie, A. R., Lannuzel, D., Meiners, K. M., and Nicol, S. (2014). The Biogeochemical Role of Baleen Whales and Krill in Southern Ocean Nutrient Cycling. *PLoS One* 9, e114067. doi: 10.1371/journal.pone.0114067
- Ratnarajah, L., Melbourne-Thomas, J., Marzloff, M. P., Lannuzel, D., Meiners, K. M., Chever, F., et al. (2016). A Preliminary Model of Iron Fertilisation by Baleen Whales and Antarctic Krill in the Southern Ocean: Sensitivity of Primary Productivity Estimates to Parameter Uncertainty. *Ecol. Modell.* 320, 203–212. doi: 10.1016/j.ecolmodel.2015.10.007
- Ratnarajah, L., Nicol, S., and Bowie, A. R. (2018). Pelagic Iron Recycling in the Southern Ocean: Exploring the Contribution of Marine Animals. *Front. Mar. Sci.* 5, doi: 10.3389/fmars.2018.00109
- Reilly, S., Hedley, S., Borberg, J., Hewitt, R., Thiele, D., Watkins, J., et al. (2004). Biomass and Energy Transfer to Baleen Whales in the South Atlantic Sector of the Southern Ocean. *Deep. Res. Part II. Top. Stud. Oceanogr.* 51, 1397–1409. doi: 10.1016/j.dsr2.2004.06.008
- Reisewitz, S. E., Estes, J. A., and Simenstad, C. A. (2006). Indirect Food Web Interactions: Sea Otters and Kelp Forest Fishes in the Aleutian Archipelago. *Oecologia* 146, 623–631. doi: 10.1007/s00442-005-0230-1
- Ridgwell, A., and Arndt, S. (2015). ‘Why Dissolved Organics Matter: DOC in Ancient Oceans and Past Climate Change’, in D. A. Hansell and C. A. Carlson (eds) *Biogeochemistry of Marine Dissolved Organic Matter: Second Edition*. Copyright © 2014 Elsevier Inc. All rights reserved.: Academic Press, pp. 1–20. doi: 10.1016/B978-0-12-405940-5.00001-7
- Roman, J., Estes, J. A., Morissette, L., Smith, C., Costa, D., McCarthy, J., et al. (2014). Whales as Marine Ecosystem Engineers. *Front. Ecol. Environ.* 12, 377–385. doi: 10.1890/130220
- Roman, J., and McCarthy, J. J. (2010). The Whale Pump: Marine Mammals Enhance Primary Productivity in a Coastal Basin. *PLoS One* 5, 13255. doi: 10.1371/journal.pone.0013255
- Schuller, D., Kadko, D., and Smith, C. R. (2004). Use of ²¹⁰Pb/²²⁶Ra Disequilibria in the Dating of Deep-Sea Whale Falls. *Earth Planet. Sci. Lett.* 218, 277–289. doi: 10.1016/S0012-821X(03)00690-3
- Seibold, E., and Berger, W. (2017). ‘Sources and Composition of Marine Sediments’ in *The Sea Floor. Springer Textbooks in Earth Sciences, Geography and Environment*. Springer, Cham, pp. 45–61. doi: 10.1007/978-3-319-51412-3_4
- Sigurjónsson, J., and Víkingsson, G. A. (1997). Seasonal Abundance of the Estimated Food Consumption by Cetaceans in Icelandic and Adjacent Waters. *J. Northw. Atl. Fish. Sci.* 22, 271–287. doi: 10.2960/J.v22.a20
- Sillanpää, M., Matilainen, A., and Lahtinen, T. (2015). ‘Characterization of NOM’, in *Natural Organic Matter in Water: Characterization and Treatment Methods* (Oxford, UK:Elsevier Inc), 17–53. doi: 10.1016/B978-0-12-801503-2.00002-1
- Simmonds, M. P., Haraguchi, K., Endo, T., Cipriano, F., Palumbi, S. R., and Troisi, G. M. (2002). Human Health Significance of Organochlorine and Mercury Contaminants in Japanese Whale Meat. *J. Toxicol. Environ. Heal. - Part A*. 65, 1211–1235. doi: 10.1080/152873902706125714
- Smith, C. R., and Baco, A. R. (2003). ‘Ecology of Whale Falls at the Deep-Sea Floor’, in *Oceanography and Marine Biology*, Vol 41 (CRC Press), 311–354.
- SOEST (2011) *The Carbon Cycle: School of Ocean and Earth Science and Technology*. Available at: www.royalsoc.ac.uk (Accessed June 10, 2020).
- Springer, A. M., Estes, J. A., Van Vliet, G. B., Williams, T. M., Doak, D. F., Danner, E. M., et al. (2003). Sequential Megafaunal Collapse in the North Pacific Ocean: An Ongoing Legacy of Industrial Whaling? *Proc. Natl. Acad. Sci. U. S. A.* 100, 12223–12228. doi: 10.1073/pnas.1635156100
- Springer, A. M., Estes, J. A., Van Vliet, G. B., Williams, T. M., Doak, D. F., Danner, E. M., et al. (2008). Mammal-Eating Killer Whales, Industrial Whaling, and the Sequential Megafaunal Collapse in the North Pacific Ocean: A Reply to Critics of Springer Et Al 2003. *Mar. Mammal. Sci.* 24, 414–442. doi: 10.1111/j.1748-7692.2008.00185.x
- Stubbins, A. (2016). A Carbon for Every Nitrogen. *Proc. Natl. Acad. Sci. U. S. A.* 113, 10736–10738. doi: 10.1073/pnas.1612995113
- Thompson, K., Miller, K., Johnston, P., and Santillo, D. (2017). Storage of carbon by marine ecosystems and their contribution to climate change mitigation Greenpeace Research Laboratories Technical Report (Review) 03-2017. Exeter, UK Available at: <https://www.greenpeace.to/greenpeace/wp-content/uploads/2017/05/Carbon-in-Marine-Ecosystems-Technical-Report-March-2017-GRL-TRR-03-2017.pdf> [Accessed April 1, 2020].
- Tont, S. A., Percy, W. G., and Arnold, J. S. (1977). Bone Structure of Some Marine Vertebrates. *Mar. Biol.* 39, 191–196. doi: 10.1007/BF00387004
- Townsend, D. W. (1998). Sources and Cycling of Nitrogen in the Gulf of Maine. *J. Mar. Syst.* 16, 283–295. doi: 10.1016/S0924-7963(97)00024-9
- Trites, A. W., and Pauly, D. (1998). Estimating Mean Body Masses of Marine Mammals From Maximum Body Lengths. *Can. J. Zool.* 76, 886–896. doi: 10.1139/z97-252
- Troxler, T. G., Kennedy, H. A., Crooks, S., and Sutton-Grier, A. E. (2018). ‘Introduction of Coastal Wetlands into the IPCC Greenhouse Gas Inventory Methodological Guidance’, in *A Blue Carbon Primer* (CRC Press), 217–234. doi: 10.1201/9780429435362-16
- UK NEA (2014) *UK National Ecosystem Assessment Follow-On: Synthesis of Key Findings*. Available at: <http://uknea.unep-wcmc.org/Resources/tabid/82/Default.aspx> (Accessed February 16, 2021).
- Ullman, R., Bilbao-Bastida, V., and Grimsditch, G. (2013). Including Blue Carbon in Climate Market Mechanisms. *Ocean Coast. Manag.* 83, 15–18. doi: 10.1016/j.ocecoaman.2012.02.009
- Villa, F., Wilson, M. A., de Groot, R., Farber, S., Costanza, R., and Boumans, R. M. J. (2002). Designing an Integrated Knowledge Base to Support Ecosystem Services Valuation. *Ecol. Econ.* 41, 445–456. doi: 10.1016/S0921-8009(02)00093-9
- Walday, M., and Kroglund, T. (2008). The North Sea -bottom Trawling and Oil/gas Exploitation. Copenhagen: European Environment Agency. https://www.eea.europa.eu/publications/report_2002_0524_154909
- Watkiss, P., Anthoff, D., Downing, T. E., Hepburn, C. J., Hope, C., Hunt, A., et al. (2005) *The Social Costs of Carbon Review – Methodological Approaches for Using SCC Estimates in Policy Assessment*. Available at: www.defra.gov.uk (Accessed April 2, 2020).
- Watson, S. C. L., Preston, J., Beaumont, N. J., and Watson, G. J. (2020). Assessing the Natural Capital Value of Water Quality and Climate Regulation in Temperate Marine Systems Using a EUNIS Biotope Classification Approach. *Sci. Total. Environ.* 744, 140688. doi: 10.1016/j.scitotenv.2020.140688
- WDG (2021a) *Atlantic White-Sided Dolphin - Whale and Dolphin Conservation*. Available at: <https://uk.whales.org/whales-dolphins/species-guide/atlantic-white-sided-dolphin/> (Accessed May 19, 2021).
- WDG (2021b) *White-Beaked Dolphin - Whale and Dolphin Conservation*. Available at: <https://uk.whales.org/whales-dolphins/species-guide/white-beaked-dolphin/> (Accessed May 19, 2021).
- Wilmers, C. C., Estes, J. A., Edwards, M., Laidre, K. L., and Konar, B. (2012). Do Trophic Cascades Affect the Storage and Flux of Atmospheric Carbon? An Analysis of Sea Otters and Kelp Forests. *Front. Ecol. Environ.* 10, 409–415. doi: 10.1890/110176
- Xie, F., Tao, Z., Zhou, X., Lv, T., and Wang, J. (2019). Spatial and Temporal Variations of Particulate Organic Carbon Sinking Flux in Global Ocean From 2003 to 2018. *Remote Sens.* 11, 2941. doi: 10.3390/rs11242941
- Zhang, W., Wirtz, K., Daewel, U., Wrede, A., Kröncke, I., Kuhn, G., et al. (2019). The Budget of Macrobenthic Reworked Organic Carbon: A Modeling Case Study of the North Sea. *J. Geophys. Res. Biogeosci.* 124, 1446–1471. doi: 10.1029/2019JG005109
- Zhao, C., Daewel, U., and Schrum, C. (2019). Tidal Impacts on Primary Production in the North Sea. *Earth Syst. Dyn.* 10, 287–317. doi: 10.5194/esd-10-287-2019

Conflict of Interest: The authors declare that the research was conducted in the absence of any commercial or financial relationships that could be construed as a potential conflict of interest.

The reviewer SM declared a shared affiliation with the authors NT, NZ, MC, VM, and EM

Publisher's Note: All claims expressed in this article are solely those of the authors and do not necessarily represent those of their affiliated organizations, or those of the publisher, the editors and the reviewers. Any product that may be evaluated in

this article, or claim that may be made by its manufacturer, is not guaranteed or endorsed by the publisher.

Copyright © 2022 Sheehy, Taylor, Zwerschke, Collar, Morgan and Merayo. This is an open-access article distributed under the terms of the Creative Commons Attribution License (CC BY). The use, distribution or reproduction in other forums is permitted, provided the original author(s) and the copyright owner(s) are credited and that the original publication in this journal is cited, in accordance with accepted academic practice. No use, distribution or reproduction is permitted which does not comply with these terms.



A Guide to International Climate Mitigation Policy and Finance Frameworks Relevant to the Protection and Restoration of Blue Carbon Ecosystems

Mathew A. Vanderklift^{1*}, Dorothee Herr², Catherine E. Lovelock³, Daniel Murdiyarso^{4,5}, Jacqueline L. Raw⁶ and Andrew D. L. Steven⁷

OPEN ACCESS

Edited by:

Catherine Sarah Longo,
Marine Stewardship Council (MSC),
United Kingdom

Reviewed by:

Anna R. Armitage,
Texas A&M University at Galveston,
United States
Mats Björk,
Stockholm University, Sweden
Iris Eline Hendriks,
Spanish National Research Council
(CSIC), Spain
Junhong Bai,
Beijing Normal University, China

*Correspondence:

Mathew A. Vanderklift
mat.vanderklift@csiro.au

Specialty section:

This article was submitted to
Ocean Solutions,
a section of the journal
Frontiers in Marine Science

Received: 09 February 2022

Accepted: 31 May 2022

Published: 07 July 2022

Citation:

Vanderklift MA, Herr D,
Lovelock CE, Murdiyarso D, Raw JL
and Steven ADL (2022) A Guide to
International Climate Mitigation Policy
and Finance Frameworks Relevant
to the Protection and Restoration
of Blue Carbon Ecosystems.
Front. Mar. Sci. 9:872064.
doi: 10.3389/fmars.2022.872064

¹ CSIRO Oceans and Atmosphere, Indian Ocean Marine Research Centre, Crawley, WA, Australia, ² Global Marine and Polar Programme, IUCN, Gland, Switzerland, ³ School of Biological Sciences, The University of Queensland, St Lucia, QLD, Australia, ⁴ Center for International Forestry Research, Jl. CIFOR, Bogor, Indonesia, ⁵ Department of Geophysics and Meteorology, IPB University, Bogor, Indonesia, ⁶ DSI-NRF Research Chair in Shallow Water Ecosystems, Department of Botany and Institute for Coastal and Marine Research, Nelson Mandela University, Gqeberha, South Africa, ⁷ CSIRO Oceans and Atmosphere, Queensland Biosciences Precinct, University of Queensland, Brisbane, QLD, Australia

The protection, management and restoration of vegetated ecosystems on land and in the ocean ('natural climate solutions') can be a useful strategy for reducing net greenhouse gas emissions to help limit global warming. Their potential contribution to reducing net emissions has led to the development of policies and financial incentives for their protection and restoration. These have in turn created a set of expectations among some stakeholders, and interest in expanding these to encompass other ecosystems. However, there are specific rules about how abatement is calculated in international policy and climate finance, and the frameworks and terminology associated with them are often complex. This can be a barrier to stakeholders who want to leverage the potential of natural climate solutions, sometimes leading to incongruence between realised and anticipated benefits. In this article, we attempt to outline some of the key international policy and carbon market frameworks for coastal 'blue carbon' ecosystems, and the extent to which different ecosystems are accommodated. Currently, among the coastal ecosystems, only mangrove forests, seagrass meadows, and tidal marshes are typically considered in international policy and carbon market frameworks. The defining feature of these ecosystems is that the foundation species are plants that grow in sediment (soil). They are the only coastal ecosystems currently included in IPCC guidelines for national greenhouse gas inventories, and in compliance and voluntary carbon markets. There is interest in potentially including other marine ecosystems, such as kelp forests and unvegetated tidal flats, into carbon accounting frameworks, but there are unresolved questions about whether sequestration and storage of carbon by these ecosystems meets the rigorous standards required. Voluntary carbon markets have greater flexibility than mechanisms linked to national greenhouse gas inventories, and so might be early

implementers of expanding methods to include other ecosystems. Incorporating coastal ecosystems into national greenhouse gas inventory is a useful action countries can take that will likely help generate incentives for protection and restoration of these important ecosystems.

Keywords: coastal wetlands, greenhouse gas inventory, restoration, carbon market, international climate policy

NATURAL CLIMATE SOLUTIONS

Effective protection, management, and restoration of vegetated ecosystems on land and in the ocean can help reduce net emissions of greenhouse gases (GHGs) to limit global warming (Howard et al., 2017; Fuss et al., 2018). These ‘natural climate solutions’ (NCS; Griscom et al., 2017) are part of an increasing emphasis on nature-based solutions (NbS) to multiple global problems (Seddon et al., 2020). Estimates of the potential global contribution of NCS are large, amounting to gigatons (Gt) per year and contributing substantially to the net emissions reduction required by 2030 to have a high probability of staying below 1.5°C of warming (Griscom et al., 2017). (See **Box 1** for a glossary with definitions of abbreviations and key terms used in this article.)

Harnessing natural ecosystems to achieve net emissions reductions can be achieved in two main ways. Firstly, emissions of naturally occurring GHG (carbon dioxide, methane, and nitrous oxide) occur when vegetated ecosystems are cleared or degraded, so protecting these ecosystems from such damage prevents those emissions. In the language of climate

policy, this is referred to as avoided emissions (or avoided loss). In addition, restoring ecosystems — for example through revegetation — can lead to increased carbon sequestration (also called removal) because it can increase the mass of carbon stored in ‘sinks’ or ‘reservoirs’. In vegetated ecosystems these sinks are aboveground (branches, stems) and belowground biomass (roots and rhizomes), and soil (Hiraishi et al. 2014). Restoring ecosystems can also help avoid GHG emissions that occur in some land use activities (IPCC, 2013; Kroege et al., 2017; IPCC, 2019a). Improving the management of ecosystems that are used more intensively by humans, for example by improving forestry and farming practices, is another way of reducing net emissions (Cook-Patton et al., 2021). In some cases, this might include modifying landscapes through afforestation. The reduction of net emissions, either through reducing GHG emissions or increasing sequestration, is referred to as abatement (**Box 1**).

The potential contribution of vegetated ecosystems to reducing net GHG emissions has led to the development of policies and financial incentives for their protection and restoration. These in turn have led to a set of expectations

BOX 1 | Glossary: list of key terms and abbreviations used in this article, in alphabetical order with definitions.

Avoidance: actions that prevent the release of greenhouse gases into the atmosphere

Abatement: in climate policy, the act of reducing net emissions (it is also used to refer to the quantity of net emissions reduction)

Additionality: a principle that requires that a net reduction in emissions happens only because of specific finance (like sale of carbon credits), and would not happen without it

AFOLU: Agriculture, Forestry and Other Land Use, used in the context of IPCC guidelines which refer to GHG emissions from these sectors

Emissions factor: in carbon accounting a value representing the average mass of emissions or removals of a GHG (in CO₂-e: see **Box 2**) resulting from an activity

GHG: Greenhouse gas

IPCC: Intergovernmental Panel on Climate Change, an entity of the United Nations; it is not part of the UNFCCC, but was established by the United Nations Environment Programme (UNEP) and the World Meteorological Organization (WMO) four years before the UNFCCC

Leakage: An increase in net GHG emissions outside a project or jurisdiction that occurs because of activities within it

LULUCF: Land use, land-use change, and forestry, referring to emissions and removals of greenhouse gases resulting from direct human interventions in these systems

Mitigation: in climate policy, an intervention to reduce the magnitude and effects of climate change

NDC: Nationally Determined Contributions, reports submitted to the UNFCCC that outline a country's commitments to reduce emissions and adapt to climate change

Net emissions: the sum of emissions minus sequestration

NbS: Nature-based solutions, actions that involve protecting, sustainably managing, or restoring ecosystems (natural or modified) to address societal challenges; NCS (see below) are NbS that are focussed primarily on climate change mitigation

NCS: Natural Climate Solutions, conservation, restoration, and/or improved land management actions that increase carbon storage or avoid GHG emissions in forests, wetlands, grasslands, or agricultural lands (Griscom et al., 2017)

Permanence: the risk that carbon stored or emissions avoided from a project activity will be released (back) into the atmosphere after a defined period

REDD+: Reducing emissions from deforestation and forest degradation, a framework created through the UNFCCC to guide activities that reduce emissions from deforestation and forest degradation, as well as the sustainable management of forests and the conservation and enhancement of forest carbon stocks in developing countries

Reservoir: a component of Earth's climate system where a GHG or carbon is stored.

Sequestration: removal of carbon dioxide from the atmosphere into long-term reservoirs (in blue carbon ecosystems, long-lived plant biomass or soil); usage typically implies a temporal aspect which distinguishes it from stock (see below)

Stock: the amount of carbon in a reservoir (see above)

UNFCCC: United Nations Framework Convention on Climate Change, an international environmental treaty to combat “dangerous human interference with the climate system”, in part by stabilizing greenhouse gas concentrations in the atmosphere.

among some stakeholders. The expectations vary among the diverse suite of stakeholders, and can include inflated expectations of financial benefits (e.g. Pascual et al., 2014; Rakotomahazo et al., 2019), and aspirations to expand policy and finance frameworks to encompass ecosystems that are not currently included. However, there is specific guidance on how abatement should be calculated — including by countries when they report their GHG emissions to the United Nations Framework Convention on Climate Change (UNFCCC) and in the way net emissions reductions are accounted for in carbon markets. This guidance is based on information about GHG emissions and removals in different land uses and ecosystems. The rules and terminology used in accounting for carbon in international policy frameworks and carbon markets are often complex and many of the stakeholders who want to leverage the potential of natural climate solutions to achieve specific aims are unfamiliar with them, which can lead to incongruence between anticipated and realised benefits.

Here, we outline some of the key international policy and finance frameworks for coastal ‘blue carbon’ ecosystems, and the extent to which different ecosystems are accommodated (**Figure 1**). Blue carbon ecosystems are receiving increasing attention for their disproportionately high abatement potential relative to the area they cover, as well as the other benefits that they provide (such as protection from floods and damaging waves, and habitat for a wide variety of species, including fish that are caught for food or recreation: Menéndez et al., 2020; Friess et al., 2021). As a result, they are increasingly being incorporated into international policy frameworks and financial instruments (McLeod et al., 2011; Windham-Myers et al., 2018). There are growing expectations of potential financial benefits, and discussion about what ecosystems are included in existing frameworks, as well as how frameworks could be modified to encompass those ecosystems not currently included (e.g. Steven et al., 2019; Luisetti et al., 2020).

COASTAL ‘BLUE CARBON’ ECOSYSTEMS

All marine vegetation, as well as some other organisms (such as corals), convert inorganic carbon to organic carbon through photosynthesis. However, only mangrove forests, seagrass meadows and tidal marshes are typically considered ‘blue carbon’ ecosystems in current policy frameworks (Howard et al., 2017; Lovelock and Duarte, 2019).¹ The defining feature of these coastal ecosystems is that the foundation species are plants that grow in sediment² that is submerged at least part of the time by tidal water. Through photosynthesis these plants take

up CO₂ [and, in the case of seagrass, bicarbonate (HCO₃⁻)] and use it to create organic carbon substrates that are needed to maintain and grow new leaves, stems, roots and so on. Woody plant biomass can persist for many years, in some circumstances for centuries. Further, when a plant dies — or when part of a plant, say a leaf, is detached and falls to the sediment surface — a fraction of the organic carbon is incorporated into the sediment where it can persist for long periods, in some cases for millennia. Because the sediment of blue carbon ecosystems is typically inundated by water (through which oxygen moves more slowly than air), the rates of decomposition are very low, which facilitates accumulation of the organic matter. Indeed, in many of these ecosystems the carbon stock in the sediment is greater than that in the plant biomass (Alongi, 2014). In addition, unlike freshwater wetlands, the higher concentration of sulphate in seawater acts to reduce the anaerobic formation and release of methane (Bridgman et al., 2013), such that methane emissions from saline coastal wetlands tend to be lower than for other wetlands (Kroeger et al., 2017; although emissions can sometimes be high even in coastal wetlands — see Rosentreter et al., 2021).

The potential contribution of the three main blue carbon ecosystems (mangrove forests, seagrass meadows and tidal marshes) to global climate mitigation is a relatively modest proportion of the total abatement needed, perhaps a little more than ~1 Gt or so per year (Herr and Landis, 2016; Griscom et al., 2017) — to give this some context, global emissions were ~35 Gt in 2021 (Liu et al., 2022). However, actions to protect and restore blue carbon ecosystems could be an important contributor to abatement in some countries, such as those in which degradation of these ecosystems is a large contributor to emissions (Murdijarso, 2019). In addition, these ecosystems offer a suite of other benefits, including reductions in the height of damaging storm waves, reducing inundation by storm surges, provision of habitat for species that are important for food and livelihoods, and more.

There is great interest in potentially including macroalgae and other marine ecosystems into blue carbon accounting frameworks (e.g. Krause-Jensen and Duarte, 2016; Sala et al., 2021), but there are unresolved questions about whether removal and sequestration of carbon by these ecosystems meets the rigorous standards required to incorporate potential abatement into policy and finance frameworks. Not all ecosystems create or store carbon in the same way, and not all do it equally effectively (Jobbagy and Jackson, 2000; McLeod et al., 2011). Here, we briefly outline the main international policy and climate finance (with focus on carbon markets) frameworks and how different ecosystems can be considered in the context of those frameworks.

INTERNATIONAL POLICY FRAMEWORKS

The main global entity through which countries cooperate to develop international policies that explicitly address the problem of increasing greenhouse gas concentrations is the United Nations Framework Convention on Climate Change (UNFCCC). Here, we briefly review a subset of the main

¹ Here we use the term tidal marsh to be consistent with Intergovernmental Panel on Climate Change terminology, but they are also often called salt marshes, or even tidal salt marshes: French (2019) Tidal salt marshes: sedimentology and geomorphology, in *Coastal Wetlands*, eds. G.M.E. Perillo, E. Wolanski, D.R. Cahoon & C.S. Hopkins. Elsevier, 479–517.

² Here we use the term sediment because that is most familiar to many marine scientists but note that other authors also use the term soil, which corresponds to Intergovernmental Panel on Climate Change terminology.

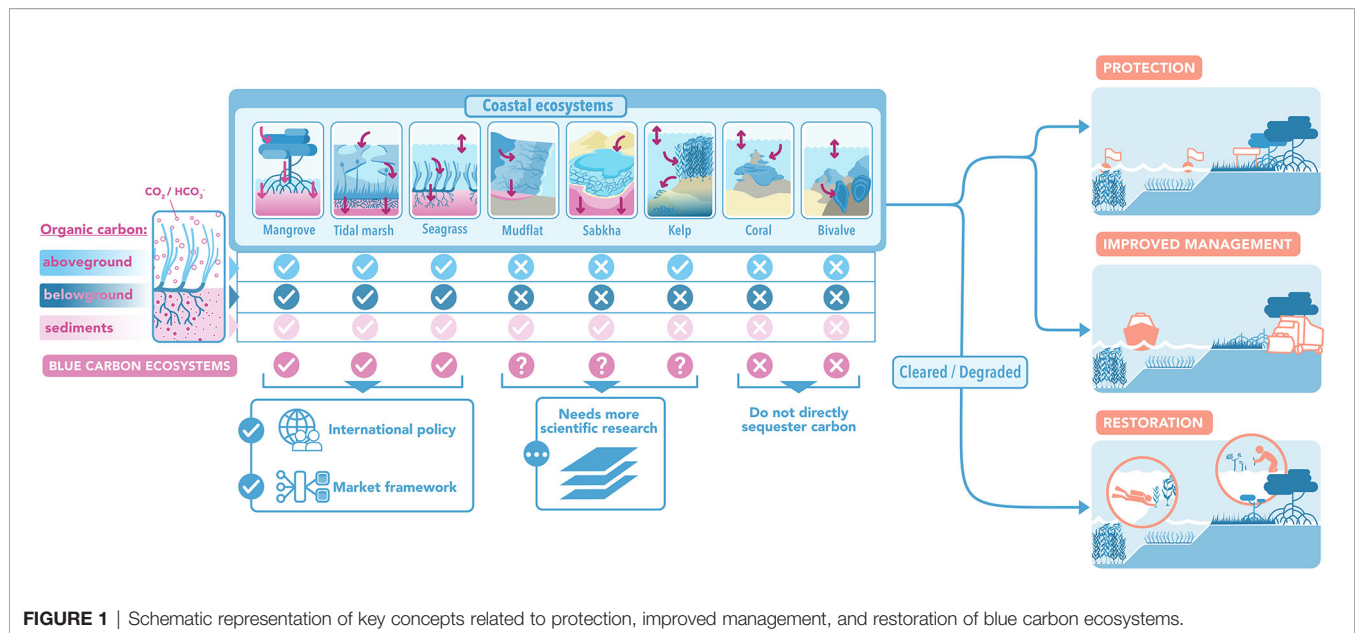


FIGURE 1 | Schematic representation of key concepts related to protection, improved management, and restoration of blue carbon ecosystems.

UNFCCC mechanisms relevant to protection and restoration of coastal blue carbon ecosystems (for a more detailed review see Herr et al., 2019b).

As a framework convention, the UNFCCC establishes the mechanisms to achieve its objectives through a suite of legal instruments agreed to at the annual Conference of Parties — the (now expired) Kyoto Protocol and the Paris Agreement are well-known examples.³ These decisions are diverse, and include aspects such as the magnitude of ambition (originally focussing on mitigation but increasingly also encompassing adaptation), different strategies to achieve that ambition, and ways of generating the finance to enable them (Kuyper et al., 2018).

Multiple processes and mechanisms have been implemented in the years since the establishment of the UNFCCC (Bodansky and Rajamani, 2018). Blue carbon ecosystems are relevant to a number of the current ones, including several that are still being negotiated (Dobush et al., 2021; Herr and Hamilton, 2021). We don't attempt to review all of them, but Nationally Determined Contributions (NDC) and REDD+ (Reducing emissions from deforestation and forest degradation), are worth noting because they have received attention in the context of blue carbon. NDC are plans that are submitted to the UNFCCC Secretariat by each of the Parties to the Paris Agreement. In the context of the UNFCCC, a Party is essentially a country, which is assigned into one of three groups according to the level of commitments that they are able to make.⁴ NDC are an obligation on Parties to the Paris Agreement, which describe voluntary commitments that are consistent with the principle enshrined in the original convention text that countries have 'common but differentiated responsibilities'. As such, each country sets its own emissions

reduction targets, and outlines plans to achieve them (as well as adapt to climate change) in their NDC. Blue carbon ecosystems can contribute towards mitigation and adaptation efforts, and there are a wide variety of actions that could be built into these national plans (Herr and Landis, 2016; Lecerf et al., 2021). Among these is the opportunity to incorporate coastal wetlands in national greenhouse gas inventories (outlined below), which in turn creates a set of incentives for increased protection and restoration of blue carbon ecosystems.

REDD+ is a mechanism created and modified through the UNFCCC process that focuses on using forest management to reduce emissions (from forest clearing or degradation) and increase removal of atmospheric CO₂ into sinks (primarily trees). It is characterised by payments that are contingent on achieving specific results — thus embedding financial incentives into the approach (Angelsen and McNeill, 2012). Seagrass meadows and tidal marshes are not forests, but some mangroves are considered forests, depending on a country's definition of what a forest is. Notwithstanding that some definitions do not resonate well in particular cultural circumstances (Putz, 2010), the UNFCCC has a general operational definition of a forest: "...a minimum area of land of 0.05-1.0 hectares with tree crown cover (or equivalent stocking level) of more than 10-30 per cent with trees having the potential to reach a minimum height of 2-5 metres at maturity *in situ*" (Schoene et al., 2007). However, within this broad definition, countries can elect to further refine their definition of a forest. If mangroves happen to fit the national definition of a forest, then they can be included in REDD+, although so far there have been relatively few mangrove projects. Countries that participate in REDD+ should establish a Forest Reference Emission Level (FREL), which sets the baseline mass of net emissions (in tCO₂-e: see **Box 2**) against which to evaluate changes; these are typically calculated from national estimates over multiple years (Romijn et al., 2013).

³ If you are confused about the difference between a protocol, an agreement and other instruments, you aren't alone, see: https://treaties.un.org/Pages/overview.aspx?path=overview/definition/page1_en.xml.

⁴ <https://unfccc.int/parties-observers>

BOX 2 | tCO₂-e

Different greenhouse gases — carbon dioxide, methane, nitrous oxide, and so on — absorb different proportions of infrared radiation, and so their contribution to atmospheric warming isn't proportional to their concentration in the atmosphere (Lashof and Ahuja, 1990). In addition, the different gases persist in the atmosphere for different lengths of time. Because of this, in an effort to allow for a common standard to account for emissions, each is assigned a 'global warming potential' (Smith and Wigley, 2000), based on the amount of warming expected over a specified duration (usually 100 years), relative to carbon dioxide (IPCC, 1990). This is used to calculate 'carbon dioxide equivalent', CO₂-e: in carbon accounting this is expressed as a unit of mass, so tCO₂-e is a measure of the mass of CO₂ that would generate an equivalent amount of warming. Relative to carbon dioxide the warming potential of methane and nitrous oxide are 25 and 298 times greater.

UNFCCC mechanisms also guide international cooperation, facilitating countries to assist each other in meeting their commitments. One way in which they can do so is through formally recognised internationally transferred mitigation outcomes (ITMOs), in which one country assists another (say, through providing financial assistance), and in return receives the right to claim some of the net emissions reductions. ITMOs are also quantified in units of tCO₂-e. Their use can be complicated and has been somewhat contentious (Allen et al., 2021). One contentious aspect is the possibility that some emission reductions could be counted by more than one country, which would inflate estimates of net emissions reduction globally (called 'double counting', for example if a project in one country is funded through ODA from another and both want to count the emission reductions achieved from the project to offset their emissions). To avoid this, rules agreed to through the UNFCCC stipulate that, if the country in which the project occurs wishes to sell their emissions reductions they cannot count them towards their own target but the buyer (the donor country) can.

The UNFCCC also provides a framework for a variety of mechanisms to generate finance to implement actions that are intended to reduce net emissions, especially in developing countries. These include establishing formal entities to receive donations and disburse the funds (such as the Green Climate Fund), and establishing agreed rules for transfer of funds between countries (Romano et al., 2018). These have been implemented in various ways since the UNFCCC was formed, and international climate finance is now substantially influenced by the mechanisms introduced in the Paris Agreement (and subsequently outlined in detail in the rules drafted afterwards, the so-called 'Paris Rulebook'). In particular, the way that international carbon markets are used to generate finance to support international cooperation is outlined in several parts of Article 6 of the Paris Agreement (Schneider, 2019). These rules are especially relevant to protection and restoration of blue carbon ecosystems, which tend to occur disproportionately in developing countries (Herr et al., 2018). We review how carbon markets work later in this article.

Other international agreements also deal with natural climate solutions in a way that is relevant for protection and restoration of blue carbon ecosystems, each with a different and complementary focus. For example, the Convention on Biological Diversity focuses on conservation of biological diversity (including ecosystems), the Sendai Framework for Disaster Risk Reduction focuses on preventing and reducing disaster risk (including through harnessing the benefits provided by natural ecosystems), the Convention on Wetlands of

International Importance especially as Waterfowl Habitat⁵ focuses on conservation of wetlands, and the UNESCO World Heritage Convention is focussed on protection and preservation of particular sites considered to be of outstanding value to humanity. Actions implemented under these agreements can also contribute to reducing net emissions. The extent to which these agreements complement each other, and UNFCCC agreements, is an important area but none have a specific focus on climate mitigation. The Sustainable Development Goals, a set of broad goals and associated targets established by the United Nations General Assembly, does have specific targets related to climate change, but one of which is to implement the UNFCCC. Since none are specifically focussed on climate mitigation, we don't discuss them further.

NATIONAL GREENHOUSE GAS INVENTORY

One of the main tools the UNFCCC uses to assess how successful (or not) countries are at reducing net greenhouse gas emissions is the national GHG inventory (Troxler et al., 2019). These are designed to account for GHG emissions by sources and removals by sinks from all sectors of a country's economy. These inventories are submitted more frequently and in greater detail by certain countries (essentially, developed countries: Perugini et al., 2021). From 2024 all Parties to the Paris Agreement will need to submit a Biennial Transparency Report (which should include a report on that country's GHG inventory report, among other things) every two years. Developed countries will still need to submit national GHG inventories each year.

The UNFCCC has adopted detailed methods and standardised reporting procedures for GHG inventories that have been produced by the Intergovernmental Panel on Climate Change (IPCC). GHG inventories include emissions and removals of three naturally occurring GHG that are particularly relevant to blue carbon ecosystems — carbon dioxide (CO₂), methane (CH₄), nitrous oxide (N₂O) — as well as four types of synthetically-produced fluorinated gases.

In preparing GHG inventories for submission to the UNFCCC, countries are required to calculate emissions sources and sinks from multiple sectors (UNFCCC, 2009; UNFCCC, 2016). Coastal wetlands are included in a sector called land-use change and forestry (LULUCF), which since 2006 has been combined with agriculture to create a single consolidated

⁵ more typically known as the Ramsar Convention after the city in Iran where it was originally signed.

sector: Agriculture, Forestry, and Other Land Use (AFOLU: **Box 3**)⁶. AFOLU activities contribute towards a significant net source of global GHG emissions – approximately 23% of CO₂-e (5.2 ± 2.6 Gt CO₂ yr⁻¹) from 2007–2016 (IPCC, 2019b). Countries don't need to report on everything that IPCC gives guidance on though. Land can be both a source and a sink of GHG, making estimates of emissions and removals in the AFOLU sector complex.

The IPCC guidelines contain detailed instructions for calculating GHG emissions and removals from a suite of managed and natural ecosystems, including (since 2013) coastal wetlands (mangroves, tidal marshes, and seagrasses: the three blue carbon ecosystems). Current guidelines provide methods to calculate GHG emissions and removals for these ecosystems under four activities (**Figure 2**):

- Forest management practices in mangroves.
- Extraction activities (which includes excavation, dredging, construction of ponds for aquaculture or salt production).
- Drainage activities (in which the soil is intact but water levels on the landscape are reduced, usually to facilitate agricultural production).
- Rewetting, revegetation, or creation (rehabilitation and restoration of ecosystems).

For each of these activities, GHG emissions and removals can be estimated with different 'tiers' of certainty (Troxler et al., 2019). At the coarsest resolution are 'Tier 1' assessments, which accommodate estimates generated from global datasets (called 'default values') to calculate GHG emissions and removals for a country. These default values are estimated from available scientific literature at the time and are assumed to be generally representative. At the next level of resolution, 'Tier 2' assessments use national data should it be available, while 'Tier 3' assessments are the highest resolution and involve site-specific data at finer spatial resolutions or nationally implemented models (e.g. Richards and Evans, 2004). Countries can apply different tiers to different activities depending on data availability.

The IPCC provides guidance for obtaining data, as well as default values for Tier 1 assessments. However, they recommend that Tier 2 or Tier 3 assessments are done where possible, because the default values may not accurately reflect emissions and removals for the country being assessed. Estimating net GHG emissions can involve estimating the difference in carbon

stocks based on emissions factors for specific activities (which are supplied by the IPCC), estimating the difference in carbon stocks measured at two points in time, or measuring or modelling the GHG flux between the soil and vegetation and the atmosphere or water (Troxler et al., 2019).

Since the IPCC issued guidance for including wetlands into national GHG inventory (Hiraishi et al 2014 ; IPCC, 2019a), scientists have continued to refine the estimates of removals and emissions and to publish new data. This has enabled higher resolution estimates (e.g. Murdiyarso et al., 2015; Kauffman et al., 2017; Vinh et al., 2019) and improved models (e.g. Atwood et al., 2017; Rovai et al., 2018; Adame et al., 2021). The data and models underpinning national GHG inventories are continually improving, there are still some data gaps that need to be addressed, especially regarding flux of GHGs in blue carbon ecosystems, spatial patterns in emissions and removals within and among ecosystems, and the contribution of seagrasses.

So far, few countries have included coastal wetlands in their national GHG inventory, although capacity building and other activities to enable widespread reporting has been increasing (Green et al., 2021). If a country includes mangroves in the FREL through REDD+, they should report them using the same methods under forests, not wetlands, in their national GHG inventory (Green et al., 2021).

CLIMATE FINANCE AND CARBON MARKETS

Climate finance can occur in multiple forms. It can include grants, or loans, or even investment into private companies, such as through purchasing shares (Romano et al., 2018). It can also occur in forms intended to generate profit for the investors (such as bonds), or by risk transfer mechanisms like insurance. Some, such as results-based payments under REDD+ (which mostly occurs in the form of Official Development Assistance grants from developed countries: European Commission Directorate-General for Climate Action, 2018) require rigorous processes for measuring net abatement following a similar process as GHG inventories (Michel et al., 2016). One of the most widely used mechanisms for generating climate finance is carbon markets, developed in part due to a recognition that grants and donations alone were unlikely to generate sufficient finance, but also in response to a worldview which favoured an economic ideology based on letting the private sector attempt to resolve problems (Newell and Paterson, 2010).

⁶The other sectors are Energy, Industrial Processes and Product Use, Waste and Other.

BOX 3 | Classification and delineation of coastal wetlands as land cover categories

Coastal wetlands are defined within the AFOLU sector as areas that "consist of organic and mineral soils that are covered or saturated, for all or part of the year, by tidal freshwater, brackish or saline water and are vegetated by vascular plants" (Hiraishi et al 2014). This includes blue carbon ecosystems – mangroves, tidal marshes, and seagrasses. Each country must have a clear definition of the ecosystems that are represented by coastal wetlands so that the land cover category can be appropriately assigned within the AFOLU inventory consistently over time. These definitions might be different between countries depending on the type of coastal wetlands and their national extent.

Estimating CO₂ emissions and removals using the IPCC guidance requires information on the extent of area encompassed by each ecosystem. The boundaries of blue carbon ecosystems can extend landward beyond the extent of frequent tidal inundation, such as with supratidal salt marshes, and seaward to any depth at which seagrass could occur. The boundaries and extent can be challenging to quantify in these ecosystems — for example, seagrasses are difficult to map because they are underwater, and it can be difficult to delineate boundaries between high intertidal marshes and terrestrial vegetation.

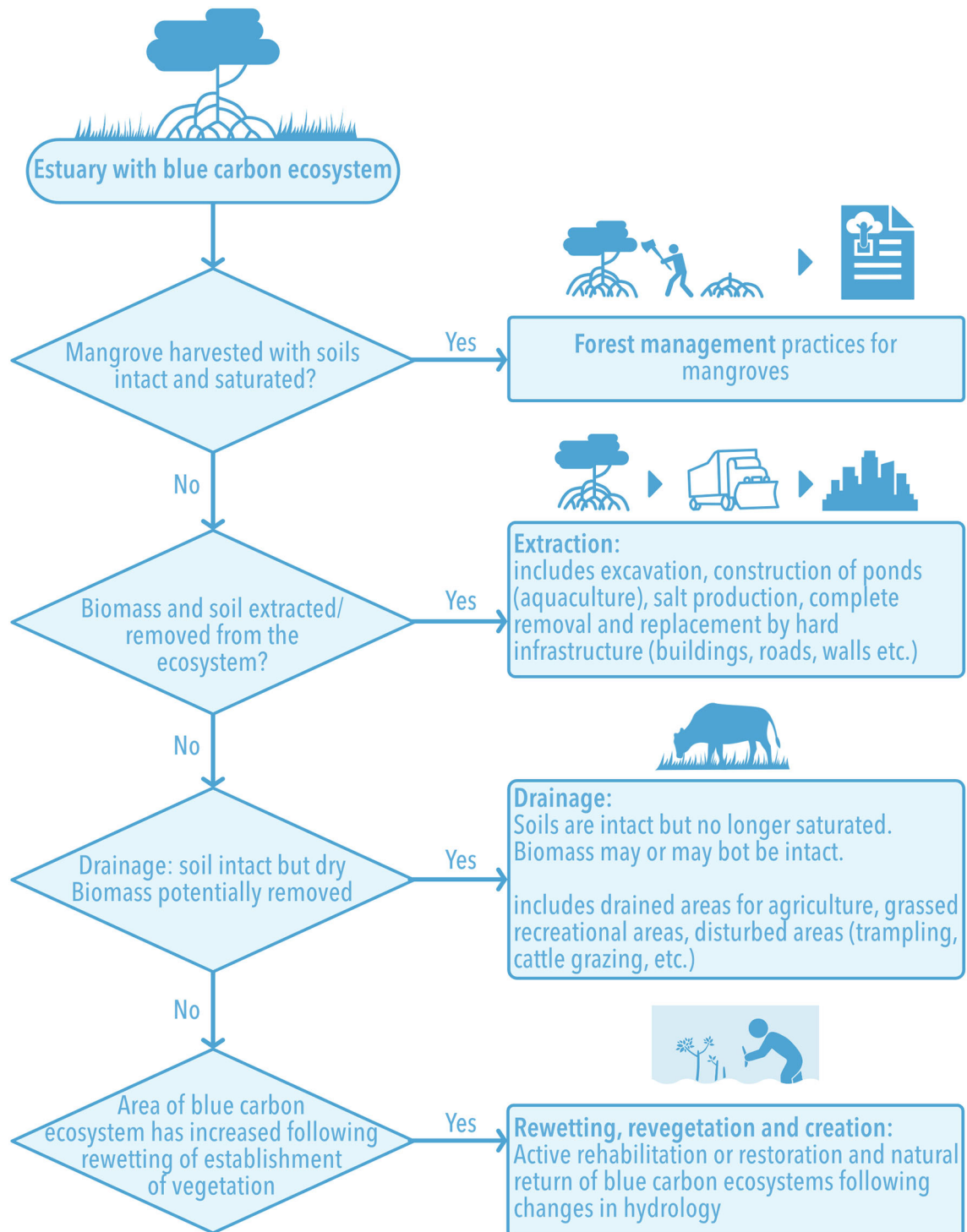


FIGURE 2 | Decision tree to assign reported changes in blue carbon ecosystems to the emissions and removals categories provided by the Hiraishi et al 2014 Wetlands Supplement. Adapted from (Hiraishi et al 2014).

Carbon markets are mechanisms which are designed to allow emitters (say, a company) to account for emissions that they cannot reduce by paying for emissions reductions (or ‘offsets’) elsewhere. Specifically, they are frameworks to trade (i.e. buy and sell) those emissions reductions, and can be broadly categorised into compliance and voluntary markets (Vanderkluft et al., 2019; Streck, 2020). The units traded have different names in different schemes, but they are typically referred to under the general term ‘carbon credit’; each credit represents one tonne of carbon dioxide equivalent (tCO₂-e: see **Box 2**).

Each credit therefore reflects a unit of mass that represents a net emissions reduction that has been achieved by either reducing emissions (say, by replacing fossil fuel with renewable energy or by not clearing a patch of mangrove forest) or by removing CO₂ from the atmosphere and sequestering the carbon in biomass or soil (say, by restoring a degraded mangrove forest). Each credit has a unique serial number, which is listed on one or more public registries. Once the owner of the credit wishes to claim it for emissions reductions, the credit is ‘retired’ (also sometimes called ‘surrendered’) and a note to that effect is made against the serial number. It is then taken off the market so that it can no longer be sold or given away, preventing the possibility that a single credit might be claimed more than once.

Compliance markets are used in some jurisdictions to enforce the requirements of legislation or regulations. For example, in the European Union’s (EU) Emissions Trading Scheme (ETS) — an example of a ‘cap-and-trade’ scheme — emitters must stay below a quantity of emissions that is established by EU regulations, and they can use offsets generated by projects that reduce emissions to help achieve this (Bayer and Aklin, 2020). In some jurisdictions (such as in California and New Zealand), credits can also be generated by projects that sequester carbon through improved forest management (Shrestha et al., 2021). Compliance markets can be a central part of a country’s emissions reduction policy, in which case the net emissions reductions that they yield are incorporated into the country’s GHG inventory. The types of emission reduction activities that are eligible must therefore align with categories defined in the IPCC guidelines.

The nature of compliance markets is such that purchasers tend to favour low-cost credits. The lowest cost credits are usually generated by projects that replace fossil-fuel based energy production with methods based on renewable energy (Hamrick and Gallant, 2017; Donofrio et al., 2020). The costs of projects that involve NCS, such as protection and restoration of blue carbon ecosystems, are typically much higher (de Groot et al., 2013), and so demand for them is unlikely to be substantial in compliance markets. In contrast, buyers in a voluntary market typically do so because they are motivated by reasons other than the need to meet regulatory requirements (Peters-Stanley et al., 2013). In these cases, buyers are often prepared to pay higher prices for the credits, which makes credits generated by coastal blue carbon projects feasible. Indeed, there are now multiple projects in mangrove and tidal marsh ecosystems using methods accredited according to the rules of several different international standards (e.g. Needelman et al., 2018). In addition, these buyers are not necessarily constrained by the need to adhere to the

categories used in national GHG inventory (although they can if they choose to), which can lend greater flexibility.

NCS often generate additional benefits beyond their contribution to climate mitigation (usually called ‘co-benefits’), such as enhanced fisheries production or reduction in the height of damaging storm waves. These co-benefits are often attractive to buyers in a voluntary market; credits from projects that also generate co-benefits tend to be preferred by buyers, who might also be willing to pay higher prices for the offsets. In general, quantification of these co-benefits is not as well understood as carbon abatement (Palomo et al., 2019; Orth et al., 2020), and warrants further research and development, including methods to value these benefits and the trade-offs among them.

The broad dichotomy between compliance and voluntary markets can be more complicated, because voluntary markets can be part of a broader regulated market (such as in South Africa and Colombia: Hanna and Nicolas, 2019), or they might be completely separate. Also, not all credits are traded on an open market; one of the largest blue carbon projects is a mangrove reforestation project in Sumatra (which generated >270,000 of tCO₂-e by 2019: Anon, 2020) — credits generated by this project are not traded on an open market but are used to offset emissions of the companies which provided the finance for project implementation (Anon, 2015; Herr et al., 2019a).

In both compliance and voluntary markets, there are rules that need to be followed. In regulated markets those rules will typically be established by the regulators (for example in Australia, they must abide by ‘offsets integrity standards’ that are established in legislation: Bell-James, 2016; Kelleway et al., 2020). In voluntary markets they are established by the organisations that produce voluntary market standards. They tend to share a set of common rules, although there is some variation in the way that these are applied (e.g. Richards and Huebner, 2014). The Taskforce on Scaling Voluntary Carbon Markets (Taskforce on Scaling Voluntary Carbon Markets, 2021) has suggested these be developed into a set of principles that all projects should abide by.

The principles common across standards are that abatement should be real, measurable and credible, that it should be additional (that is, it would not occur without the incentive provided by carbon finance), that the net CO₂ reduction that the credit represents must not be reversed (at least not for a very long period of time; this is called ‘permanence’), and that it should not cause an increase in net emissions either in another source or somewhere else (this is called ‘leakage’). These principles are designed to ensure that (net) emissions are genuinely reduced. The International Carbon Reduction and Offset Alliance (ICROA) includes all of these in a set of best practice integrity principles⁷ for using carbon credits to offset unavoidable emissions. These principles are used by standards that together represent the bulk of offsets traded in the voluntary market, as well as offsets traded under schemes such as the Clean Development Mechanism and Australia’s Emissions Reduction Fund.

⁷https://www.icroa.org/resources/Documents/ICROA_cobp_carbon_management_service_executive_summary_2021.pdf

The principle that abatement should be real, measurable and credible means that the methods for calculating the abatement that can be attributed to a particular activity are typically conservative. Often, like the methods for calculating emissions for national GHG inventory described earlier, they can involve a mixture of surrogate data like emissions factors, direct measurements, and models. The models are typically based on extensive data collected at different places, and account for the fact that the rates and net result of processes vary from place to place. They can also be cheaper than methods that require regular (and potentially expensive) measurements.

As described earlier, compliance markets will often be used to reduce emissions in sectors that are covered by a country's GHG inventory, so the eligible sectors and activities will tend to reflect those defined by the IPCC. Voluntary markets might allow greater flexibility, raising the possibility that other sectors or activities might be included. However, they will still need to adhere to the rules applying to carbon accounting; examination of those rules in the context of different ecosystems can reveal why we focus on some ecosystems and not others, and why our ability to include them remains uncertain (Table 1).

HOW DO BLUE CARBON PROJECTS FIT INTO CARBON MARKETS?

Many stakeholders (including scientists) are interested in whether projects in different ecosystems might be eligible for carbon market finance. Some ecosystems are covered by methods developed under voluntary carbon market standards. For example, there are several methods produced by the carbon accounting organisation Verra that are applicable to mangrove, tidal marsh and seagrass ecosystems. Of the ecosystems that are not included, it is possible that some could be, but development of methods is hampered by insufficient information. In some offsetting schemes the net emissions reductions need to be linked to a GHG inventory, and so are constrained by the ecosystems and activities that are included in IPCC guidance. Many voluntary market standards don't have this constraint, and so have more flexibility to include other ecosystems or other activities — but they still need to adhere to the same principles. Some ecosystems can be immediately discounted and considering them in the context of the main carbon market principles reveals why (see also Howard et al., 2017; Lovelock and Duarte, 2019).

Additionality

The additionality principle is intended to ensure that net emissions reduction occurs because of the implementation of project activities — in a carbon market this in turn means that it could not have been done without the finance generated by the sale of the credits. Additionality is typically assessed from this perspective for an individual project to ensure that activities would not occur without the finance, but in some restoration contexts additionality is assumed because the rate of restoration is lower than the rate of loss for an ecosystem (Needelman et al., 2018; Zeng et al., 2021). This can be complex, and problems include ensuring that protection and restoration would not occur in the absence of finance (which can be particularly difficult to assess for protection), as well as the moral hazard associated with providing more opportunities to those who have been the poorest stewards of nature.

Coral and bivalve reefs, where the process of calcification in seawater produces a net release of CO₂ (Table 1: Frankignoulle et al., 1995; Lovelock and Duarte, 2019), would fail to meet the first principle of additionality. Coastal vegetated ecosystems — mangroves, tidal marshes and seagrasses — are composed of photosynthesising vascular plants, producing a net uptake of CO₂, so they could meet this principle, providing that the activities would not otherwise happen without the financial incentive.

Permanence

The principle of permanence requires that the net GHG reduction must not be reversed. This risk tends to be lower for blue carbon ecosystems because they are less susceptible to some of the risks that terrestrial ecosystems are prone to, such as fire — although they are not immune to risks associated with severe weather events, or even climate change itself. The carbon fixed by plants through photosynthesis is stored in their biomass, and some of these meet the principle of permanence — although the duration of time considered 'permanent' varies among standards, it is typically at least 25–30 years, and often 100 years (Richards and Huebner, 2012). The carbon in the sediment these plants grow in can be thousands of years old (Rogers et al., 2019), and so easily passes the test of permanence. In carbon markets, the requirement to demonstrate permanence is typically applied regardless of whether a project sets out to avoid emissions from degradation of the ecosystem, or to enhance sequestration by restoring the ecosystem.

These frameworks assume that carbon removal and sequestration occurs within the boundaries of a defined project

TABLE 1 | Assessment of confidence in coastal ecosystems in the context of principles central to verifying offsets through carbon markets.

Criterion	Existing IPCC guidance	Additionality	Permanence
Mangroves	Y	Y	Y
Tidal marsh	Y	Y	Y
Seagrass	Y	Y	Y
Kelp	N	Y _a	Y _a
		I _b	I _b
Mudflats	N	Y	I
Coral/bivalve reef	N	N	–

Y, yes; N, no; I, insufficient evidence. a = carbon removals within the project area; b = carbon exported from the project area (see Box 4).

area. Removals can in some cases also include allochthonous organic carbon that is brought into the area (for example by currents or wind), if it can be shown that this organic carbon would have been remineralised and returned to the atmosphere if the project had not occurred (Needelman et al., 2018). Carbon exported from the area is not accounted for, because there is no easy way of knowing its fate — including whether it is additional or permanent. IPCC guidelines recognise that this is a gap in knowledge requiring more information (at least for coastal wetlands, for inland wetlands it is considered to be an emissions source: Hiraishi et al., 2014).

Carbon exported from coastal wetlands might be sequestered elsewhere. This can include small particles originating from mangrove, marsh or seagrass plants as well as dissolved organic or inorganic carbon, and even alkalinity (Huxham et al., 2018; Maher et al., 2018). Extending from methods that focus on measuring the organic carbon sequestered within a project area to methods that can account for carbon fixed in one place and sequestered in another will be challenging. Demonstrating that abatement achieved using such methods is real, measurable and credible will involve overcoming current impediments to quantifying carbon export to and sequestration in distant places. Simple models might be developed that can aid this, but these will require substantial, locally relevant data. This would help resolve the role that unvegetated sediments (such as intertidal and subtidal mudflats and sabkha) might play as NCS: they can contain substantial organic carbon, but most originates elsewhere (Phang et al., 2015; Sasmito et al., 2020). Little is known about permanence of organic carbon in these systems.

Kelp and other seaweed ecosystems pose a challenge from the perspective of permanence (Table 1). They photosynthesise and represent substantial carbon fixation. However, they tend to be short-lived — even a long-lived seaweed typically lives for only a few years. In addition, natural kelp stands tend to grow on rock, which doesn't accumulate organic matter (this also creates a challenge to including them in national GHG inventory, because the IPCC guidelines currently only include wetlands as ecosystems with organic or mineral soils. Instead, most kelp carbon is exported from the place where it is fixed, through

erosion of fronds or dislodgement of entire individuals (de Bettignies et al., 2013). Nevertheless, it is possible to envisage how methods to account for the emissions reduction potential of kelps (and other seaweeds) might be developed (Box 4).

Leakage

Leakage from project areas can be challenging to assess. It requires understanding whether a protection or restoration activity is likely to cause an unintended increase in emissions, either directly from an increase in GHG emissions within the project area, or indirectly through displacement of an activity to somewhere else — say, through construction of aquaculture ponds elsewhere that cause a mangrove forest to be destroyed (Thamo and Pannell, 2016). In the latter case, the risk is assessed through examining the likelihood that the activity will cause such displacement, regardless of whether it is a mangrove, tidal marsh or seagrass.

Unintended increased emissions of GHG can occur from an activity designed to restore a blue carbon ecosystem. If the increased emissions are in the form of methane or nitrous oxide, both of which have global warming potentials much greater than CO₂ (see Box 2; Smith and Wigley, 2000), this could conceivably create leakage. Emissions of these GHG occur naturally in ecosystems (Lovelock et al., 2017). Methane and nitrous oxide are released by microbial decomposition of organic matter, and are influenced by conditions such as temperature, salinity, and the amount of organic matter. Methane emissions tend to be more pronounced where salinity is low, but can sometimes be high in mangrove and tidal marsh ecosystems (Rosentreter et al., 2021), while nitrous oxide emissions can be high in places where nitrogen inputs have been substantial (Roughan et al., 2018). Methane emissions in seagrasses tend to be low, and although nitrous oxide emissions can sometimes be high, one study showed that net abatement of seagrass restoration was still substantial (Oreska et al., 2020). Accounting for GHG emissions in seagrass meadows is further complicated by poor understanding of whether gases dissolved in seawater (where they don't contribute to warming) are transferred to the atmosphere (where they do) in these

BOX 4 | Kelp carbon and carbon markets

Protection and restoration of natural ecosystems carbon market finance is built around a concept in which only GHG emissions avoided or carbon sequestered within a defined project boundary are included. This presents a challenge for building accounting methods for kelp and other seaweed (Luisetti et al., 2020), which tend to be short-lived (years or less), and export carbon to adjacent ecosystems. During transport, some is consumed by organisms from decomposers to herbivores (Ince et al., 2007; Vanderkluft and Wernberg, 2008), but a proportion can travel to places where it might be sequestered, on continental shelves or even the deep sea (Krause-Jensen and Duarte, 2016).

It is possible that kelp detritus is sequestered into sediments in these places, but evidence regarding the proportion that might be expected to be sequestered is limited. Evidence of transport to distant areas alone is not sufficient, because kelp detritus is readily consumed by many consumers. It is possible that kelp transported to depths below the pycnocline might be considered permanently sequestered because material at those depths is not readily returned to shallower depths (Krause-Jensen and Duarte, 2016), but the fate of carbon during transport, and even after arriving at those depths, remains poorly understood (Boyd et al., 2019).

These challenges should not present impediments to developing methods for avoided loss of naturally-occurring kelp. In a method for avoided loss, the total carbon stock of all biomass can be included — including components that are typically short-lived (like leaves). In a similar way, the carbon stock in a kelp forest under threat could be accounted for — although this will in many instances be less than that of vascular plant ecosystems because there is no sediment component. Methods for mangrove and seagrass restoration can also account for the total stock restored (e.g. Needelman et al., 2018), which could similarly apply for kelp forests, although again the absence of sediment means that this might be significantly less than that of the blue carbon ecosystems (Figure 3).

Farming kelp might also offer opportunities for other ways of reducing net emissions, such as use in biofuels. These possibilities are still in early stages of exploration, and much remains to be understood before they can be deployed as effective solutions.

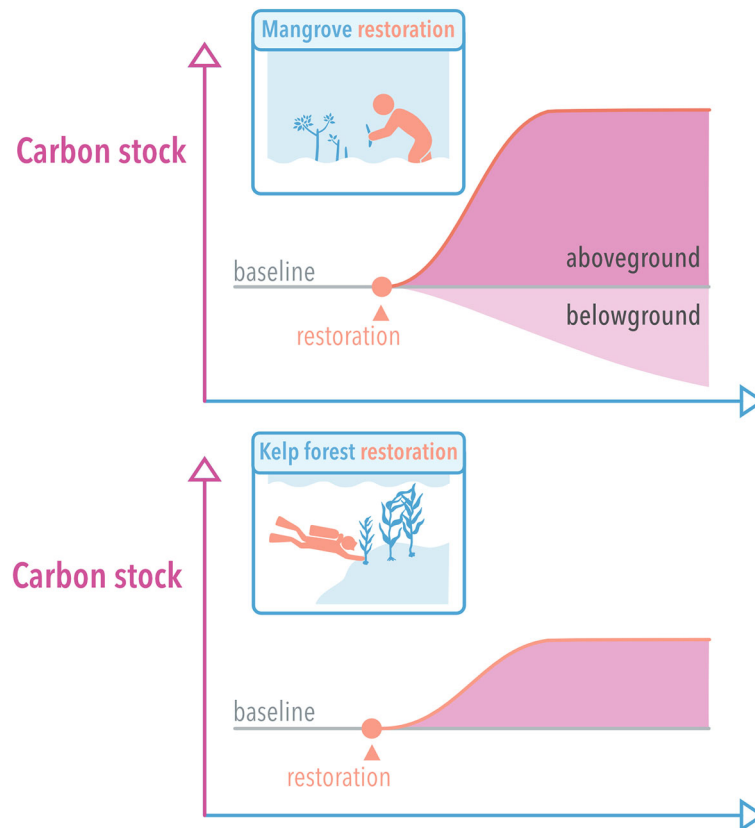


FIGURE 3 | Schematic representation of carbon stock changes for two distinct types of ecosystem (mangrove and kelp) in the context of restoration. The pink shaded area is the carbon that could be attributed to the project activity. Adapted from Olander and Ebeling, 2011.

ecosystems (Van Dam et al., 2021). Transport of detached kelp onto shorelines can result in substantial emissions.

A restoration activity which causes a transition from one ecosystem or land use to another is also likely to generate emissions associated with that transition when the original plants die (Lovelock et al., 2022). Typically, this should be small relative to the amount of sequestration for projects to be feasible.

CONCLUSION

The protection and restoration of coastal blue carbon ecosystems can make a modest but important contribution as natural climate solutions (NCS) for achieving net reductions of greenhouse gas emissions. This potential has generated a lot of interest among scientists, restoration practitioners, policymakers, investors and others — each of whom has different expectations about what the individual and collective benefits are. However, to effectively achieve their potential as NCS, protection and restoration efforts often need to work within policy and finance frameworks — which can mean that the expected benefits are not realised. For example, some activities are not eligible to receive financial support through

carbon markets. Or, they might be eligible, but the amount of abatement that they can claim is less than expected because calculations are conservative. This article was intended to explain some of the main international policy and finance frameworks that such projects should consider.

Of course, there are many reasons to undertake activities that protect and restore coastal blue carbon ecosystems. Doing so will usually contribute to climate mitigation, and if accounting for carbon is not a primary aim, then these frameworks are less relevant. Such activities will typically also generate other desirable outcomes, from enhancing habitat for a variety of species to supporting livelihoods or creating more enjoyable places to spend time. Sometimes stakeholders might want to formally quantify or seek credit for these benefits (and nascent methods for doing so exist, although they are not as mature as methods for accounting for carbon abatement), but again this need not always be the desired outcome.

Some protection and restoration activities for the three coastal wetlands included in the IPCC guidance (i.e. mangroves, tidal marshes and seagrasses) are well understood and are being increasingly implemented. Other activities, other ecosystems, and even some potential carbon pools are less well understood. More information on these is needed. However,

there is sufficient information to support implementation of many activities. One of the most useful at a national level is to incorporate coastal wetlands into national GHG inventory — this is likely to create a variety of incentives for enhancing protection, better management, and restoration of blue carbon ecosystems. NDC can be used to communicate this (as well as other commitments) through the framework of the Paris Agreement. Countries who do so should receive greater benefits both in meeting GHG reduction and in the suite of other benefits that tend to occur alongside. Pilot-scale restoration activities — which can be part of markets if desired — are also a low-risk way of promoting action.

REFERENCES

- Adame, M. F., Connolly, R. M., Turschwell, M. P., Lovelock, C. E., Fatoyinbo, T., Lagomasino, D., et al. (2021). Future Carbon Emissions From Global Mangrove Forest Loss. *Global Change Biol.* 27, 2856–2866. doi: 10.1111/gcb.15571
- Allen, M., Tanaka, K., Macey, A., Cain, M., Jenkins, S., Lynch, J., et al. (2021). Ensuring That Offsets and Other Internationally Transferred Mitigation Outcomes Contribute Effectively to Limiting Global Warming. *Environ. Res. Lett.* 16, 074009. doi: 10.1088/1748-9326/abfcf9
- Alongi, D. M. (2014). Carbon Cycling and Storage in Mangrove Forests. *Annu. Rev. Mar. Sci.* 6, 195–219. doi: 10.1146/annurev-marine-010213-135020
- Angelsen, A., and McNeill, D. (2012). “The Evolution of REDD+,” in *Analysing REDD+: Challenges and Choices*. Eds. A. Angelsen, M. Brockhaus, W. D. Sunderlin and L. V. Verchot (Bogor, Indonesia: CIFOR).
- Anon (2015). *Mangrove Restoration and Coastal Greenbelt Protection in the East Coast of Aceh and North Sumatra Province, Indonesia* (Medan: Project description).
- Anon (2020). *Coastal Carbon Corridor: Mangrove Restoration and Coastal Greenbelt Protection in the East Coast of Aceh and North Sumatra Province, Indonesia* (Essen – Germany: Verification Report VCS Version 3).
- Atwood, T. B., Connolly, R. M., Almahasheer, H., Carnell, P. E., Duarte, C. M., Ewers Lewis, C. J., et al. (2017). Global Patterns in Mangrove Soil Carbon Stocks and Losses. *Nat. Climate Change* 7, 523–528. doi: 10.1038/nclimate3326
- Bayer, P., and Aklın, M. (2020). The European Union Emissions Trading System Reduced CO₂ Emissions Despite Low Prices. *Proc. Natl. Acad. Sci.* 117, 8804–8812. doi: 10.1073/pnas.1918128117
- Bell-James, J. (2016). Developing a Framework for ‘Blue Carbon’ in Australia: Legal and Policy Considerations. *UNSW Law J.* 39, 1583–1611.
- Bodansky, D., and Rajamani, L. (2018). “The Evolution and Governance Architecture of the United Nations Climate Change Regime,” in *Global Climate Policy: Actors, Concepts, and Enduring Challenges*. Eds. U. Luterbacher and D. F. Sprinz (Cambridge, MA: The MIT Press), 13–66.
- Boyd, P. W., Claustre, H., Levy, M., Siegel, D. A., and Weber, T. (2019). Multi-Faceted Particle Pumps Drive Carbon Sequestration in the Ocean. *Nature* 568, 327–335. doi: 10.1038/s41586-019-1098-2
- Bridgman, S. D., Cadillo-Quiroz, H., Keller, J. K., and Zhuang, Q. (2013). Methane Emissions From Wetlands: Biogeochemical, Microbial, and Modeling Perspectives From Local to Global Scales. *Global Change Biol.* 19, 1325–1346. doi: 10.1111/gcb.12131
- Cook-Patton, S. C., Drever, C. R., Griscom, B. W., Hamrick, K., Hardman, H., Kroeger, T., et al. (2021). Protect, Manage and Then Restore Lands for Climate Mitigation. *Nat. Climate Change* 11, 1027–1034. doi: 10.1038/s41558-021-01198-0
- de Bettignies, T., Wernberg, T., Lavery, P. S., Vanderkluft, M. A., and Mohring, M. B. (2013). Contrasting Mechanisms of Dislodgement and Erosion Contribute to Production of Kelp Detritus. *Limnol. Oceanogr.* 58, 1680–1688. doi: 10.4319/lo.2013.58.5.1680
- de Groot, R. S., Blignaut, J., van der Ploeg, S., Aronson, J., Elmqvist, T., and Farley, J. (2013). Benefits of Investing in Ecosystem Restoration. *Conserv. Biol.* 27, 1286–1293. doi: 10.1111/cobi.12158
- Dobush, B.-J., Gallo, N. D., Guerra, M., Guilloux, B., Holland, E., Seabrook, S., et al. (2021). A New Way Forward for Ocean-Climate Policy as Reflected in the UNFCCC Ocean and Climate Change Dialogue Submissions. *Climate Policy*, 22, 1–18. doi: 10.1080/14693062.2021.1990004
- Donofrio, S., Maguire, P., Zwick, S., and Merry, W. (2020). *Voluntary Carbon and the Post-Pandemic Recovery* (Washington, DC: Forest Trends Association).
- European Commission Directorate-General for Climate Action (2018). *Study on EU Financing of REDD+ Related Activities, and Results-Based Payments Pre and Post 2020: Sources, Cost-Effectiveness and Fair Allocation of Incentives* (Publications Office).
- Frankignoulle, M., Pichon, M., and Gattuso, J.-P. (1995). “Aquatic Calcification as a Source of Carbon Dioxide,” in *Carbon Sequestration in the Biosphere*. Ed. M. A. Beran (Berlin, Heidelberg: Springer Berlin Heidelberg), 265–271.
- French, J. (2019). “Tidal Salt Marshes: Sedimentology and Geomorphology,” in *Coastal Wetlands*. Eds. G. M. E. Perillo, E. Wolanski, D. R. Cahoon and C. S. Hopkins (Amsterdam: Elsevier), 479–517.
- Friess, D. A., Yando, E. S., Alemu, I. J. B., Wong, L. W., Soto, S. D., and Bhatia, N. (2021). Ecosystem Services and Disservices of Mangrove Forests and Salt Marshes. *Oceanogr. Mar. Biol. Annu. Rev.* 58, 107–141.
- Fuss, S., Lamb, W. F., Callaghan, M. W., Hilaire, J., Creutzig, F., Amann, T., et al. (2018). Negative Emissions-Part 2: Costs, Potentials and Side Effects. *Environ. Res. Lett.* 13, 102083. doi: 10.1088/1748-9326/aabf9f
- Green, C., Lovelock, C., Sasmito, S., Hagger, V., and Crooks, S. (2021). *Coastal Wetlands in National Greenhouse Gas Inventories: Advice on Reporting Emissions and Removal From Management of Blue Carbon Ecosystems*.
- Griscom, B. W., Adams, J., Ellis, P. W., Houghton, R. A., Lomax, G., Miteva, D. A., et al. (2017). Natural Climate Solutions. *Proc. Natl. Acad. Sci.* 114, 11645–11650. doi: 10.1073/pnas.1710465114
- Hamrick, K., and Gallant, M. (2017). *Unlocking Potential: State of the Voluntary Carbon Markets* (Washington DC: E. Marketplace).
- Hanna, W.-H., and Nicolas, K. (2019). The Potential Impacts of a Domestic Offset Component in a Carbon Tax on Mitigation of National Emissions. *Renewable Sustain. Energy Rev.* 101, 453–460. doi: 10.1016/j.rser.2018.11.026
- Herr, D., Blum, J., Himes-Cornell, A., and Sutton-Grier, A. (2019a). An Analysis of the Potential Positive and Negative Livelihood Impacts of Coastal Carbon Offset Projects. *J. Environ. Manage.* 235, 463–479. doi: 10.1016/j.jenvman.2019.01.067
- Herr, D., Chagas, T., Krämer, N., Conway, D., and Streck, C. (2018). *Coastal Blue Carbon and Article 6: Implications and Opportunities* (Amsterdam, The Netherlands: IUCN).
- Herr, D., and Hamilton, J. (2021). *Building on the Ocean-Climate Dialogue: Options for Strengthening Action on the Ocean Under the UNFCCC*.
- Herr, D., and Landis, E. (2016). *Coastal Blue Carbon Ecosystems: Opportunities for Nationally Determined Contributions* (Switzerland: IUCN).
- Herr, D., Vegh, T., and Von Unger, M. (2019b). “State of International Policy for Blue Carbon Actions,” in *A Blue Carbon Primer: The State of Coastal Wetland Carbon Science, Practice, and Policy*. Eds. L. Windham-Myers, S. Crooks and T. G. Troxler (Boca Raton: CRC Press), 199–215.
- Hiraishi, T., Krug, T., Tanabe, K., Srivastava, N., Baasansuren, J., Fukuda, M., et al. (2014). *2013 Supplement to the 2006 IPCC Guidelines for National Greenhouse Gas Inventories* (Wetlands. Switzerland: IPCC).
- Howard, J., Sutton-Grier, A., Herr, D., Kleypas, J., Landis, E., McLeod, E., et al.

AUTHOR CONTRIBUTIONS

MV and AS contributed to conception and design of the study. All authors wrote sections of the manuscript, contributed to manuscript revision, read, and approved the submitted version.

ACKNOWLEDGMENTS

We thank Raymundo Marcos-Martinez for helpful comments that improved the manuscript, and Antoine Minne for producing the graphics.

- (2017). Clarifying the Role of Coastal and Marine Systems in Climate Mitigation. *Front. Ecol. Environ.* 15, 42–50. doi: 10.1002/fee.1451
- Huxham, M., Whitlock, D., Githaiga, M., and Dencer-Brown, A. (2018). Carbon in the Coastal Seascape: How Interactions Between Mangrove Forests, Seagrass Meadows and Tidal Marshes Influence Carbon Storage. *Curr. Forest. Rep.* 4, 101–110. doi: 10.1007/s40725-018-0077-4
- Ince, R., Hyndes, G. A., Lavery, P. S., and Vanderklift, M. A. (2007). Marine Macrophytes Directly Enhance Abundances of Sandy Beach Fauna Through Provision of Food and Habitat. *Estuar. Coast. Shelf. Sci.* 74, 77–86. doi: 10.1016/j.ecss.2007.03.029
- IPCC (1990). *Climate Change: The IPCC Scientific Assessment* (Cambridge: Intergovernmental Panel on Climate Change).
- IPCC (1996). *Revised 1996 IPCC Guidelines for National Greenhouse Gas Inventories* (Geneva: IPCC/OECD/IEA).
- IPCC (2013). *Supplement to the 2006 IPCC Guidelines for National Greenhouse Gas Inventories: Wetlands*. Eds. T. Hiraiishi, T. Krug, K. Tanabe, N. Srivastava, J. Baasansuren, M. Fukuda and T. G. Troxler (Geneva).
- IPCC (2019a). *2019 Refinement to the 2006 IPCC Guidelines for National Greenhouse Gas Inventories*. Eds. E. Calvo Buendia, K. Tanabe, A. Kranjc, J. Baasansuren, M. Fukuda, S. Ngarize, A. Osako, Y. Pyrozhenko, P. Shermanau and S. Federici (Geneva).
- IPCC (2019b). “Summary for Policymakers,” in *Climate Change and Land: An IPCC Special Report on Climate Change, Desertification, Land Degradation, Sustainable Land Management, Food Security, and Greenhouse Gas Fluxes in Terrestrial Ecosystems*. Eds. P. R. Shukla, J. Skea, E.C. Buendia, V. Masson-Delmotte, H.-O. Pörtner, D. C. Roberts, P. Zhai, R. Slade, S. Connors, R.v. Diemen, M. Ferrat, E. Haughey, S. Luz, S. Neogi, M. Pathak, J. Petzold, J.P. Pereira, P. Vyas, E. Huntley, K. Kissick, M. Belkacemi and J. Malley
- Jobbagy, E. G., and Jackson, R. B. (2000). The Vertical Distribution of Soil Organic Carbon and its Relation to Climate and Vegetation. *Ecol. Appl.* 10, 423–436. doi: 10.1890/1051-0761(2000)010[0423:TVDOSO]2.0.CO;2
- Kauffman, J. B., Arifanti, V. B., Hernández Trejo, H., Carmen Jesús García, M., Norfolk, J., Cifuentes, M., et al. (2017). The Jumbo Carbon Footprint of a Shrimp: Carbon Losses From Mangrove Deforestation. *Front. Ecol. Environ.* 15, 183–188. doi: 10.1002/fee.1482
- Kelley, J. J., Serrano, O., Baldock, J. A., Burgess, R., Cannard, T., Lavery, P. S., et al. (2020). A National Approach to Greenhouse Gas Abatement Through Blue Carbon Management. *Global Environ. Change* 63, 102083. doi: 10.1016/j.gloenvcha.2020.102083
- Krause-Jensen, D., and Duarte, C. M. (2016). Substantial Role of Macroalgae in Marine Carbon Sequestration. *Nat. Geosci.* 9, 737–742. doi: 10.1038/ngeo2790
- Kroeger, K. D., Crooks, S., Moseman-Valtierra, S., and Tang, J. (2017). Restoring Tides to Reduce Methane Emissions in Impounded Wetlands: A New and Potent Blue Carbon Climate Change Intervention. *Sci. Rep.* 7, 11914. doi: 10.1038/s41598-017-12138-4
- Kuyper, J., Schroeder, H., and Linnér, B.-O. (2018). The Evolution of the UNFCCC. *Annu. Rev. Environ. Resour.* 43, 343–368. doi: 10.1146/annurev-environ-102017-030119
- Lashof, D. A., and Ahuja, D. R. (1990). Relative Contributions of Greenhouse Gas Emissions to Global Warming. *Nature* 344, 529–531. doi: 10.1038/344529a0
- Lecerf, M., Herr, D., Thomas, C., Elverum, C., Delrieu, E., and Picourt, L. (2021). *Coastal and Marine Ecosystems as Nature-Based Solutions in New or Updated Nationally Determined Contributions*. Ocean & Climate Platform, Conservation International, IUCN, GIZ, Rare, The Nature Conservancy and WWF.
- Liu, Z., Deng, Z., Davis, S. J., Giron, C., and Ciais, P. (2022). Monitoring Global Carbon Emissions in 2021. *Nat. Rev. Earth Environ.* 3, 217–219. doi: 10.1038/s43017-022-00285-w
- Lovelock, C. E., Adame, M. F., Bradley, J., Dittman, S., Hagger, V., Hickey, S. M., et al. (2022). An Australian blue carbon method to estimate climate change mitigation benefits of coastal wetland restoration. *Restoration Ecology*. doi: 10.1111/rec.13739
- Lovelock, C. E., Atwood, T., Baldock, J., Duarte, C. M., Hickey, S., Lavery, P. S., et al. (2017). Assessing the Risk of Carbon Dioxide Emissions From Blue Carbon Ecosystems. *Front. Ecol. Environ.* 15, 257–265. doi: 10.1002/fee.1491
- Lovelock, C. E., and Duarte, C. M. (2019). Dimensions of Blue Carbon and Emerging Perspectives. *Biol. Lett.* 15, 20180781. doi: 10.1098/rsbl.2018.0781
- Luisetti, T., Ferrini, S., Grilli, G., Jickells, T. D., Kennedy, H., Kroger, S., et al. (2020). Climate Action Requires New Accounting Guidance and Governance Frameworks to Manage Carbon in Shelf Seas. *Nat. Commun.* 11, 4599. doi: 10.1038/s41467-020-18242-w
- Maher, D. T., Call, M., Santos, I. R., and Sanders, C. J. (2018). Beyond Burial: Lateral Exchange is a Significant Atmospheric Carbon Sink in Mangrove Forests. *Biol. Lett.* 14, 20180200. doi: 10.1098/rsbl.2018.0200
- McLeod, E., Chmura, G. L., Bouillon, S., Salm, R., Bjork, M., Duarte, C. M., et al. (2011). A Blueprint for Blue Carbon: Toward an Improved Understanding of the Role of Vegetated Coastal Habitats in Sequestering CO₂. *Front. Ecol. Environ.* 9, 552–560. doi: 10.1890/110004
- Menéndez, P., Losada, I. J., Torres-Ortega, S., Narayan, S., and Beck, M. W. (2020). The Global Flood Protection Benefits of Mangroves. *Sci. Rep.* 10, 4404. doi: 10.1038/s41598-020-61136-6
- Michel, J., Kallweit, K., and von Pfeil, E. (2016). “Reduced Emissions From Deforestation and Forest Degradation (REDD),” in *Tropical Forestry Handbook*. Eds. L. Pancel and M. Köhl (Berlin, Heidelberg: Springer Berlin Heidelberg), 3065–3091.
- Murdiyarso, D. (2019). “The Nexus Between Conservation and Development in Indonesian Mangroves,” in *A Blue Carbon Primer: The State of Coastal Wetland Carbon Science, Practice, and Policy*. Eds. L. Windham-Myers, S. Crooks and T. G. Troxler (Boca Raton: CRC Press), 295–305.
- Murdiyarso, D., Purbopuspito, J., Kauffman, J. B., Warren, M. W., Sasmito, S. D., Donato, D. C., et al. (2015). The Potential of Indonesian Mangrove Forests for Global Climate Change Mitigation. *Nat. Climate Change* 5, 1089–1092. doi: 10.1038/nclimate2734
- Needelman, B. A., Emmer, I. M., Emmett-Mattox, S., Crooks, S., Megonigal, J. P., Myers, D., et al. (2018). The Science and Policy of the Verified Carbon Standard Methodology for Tidal Wetland and Seagrass Restoration. *Estuar. Coast.* 41, 2159–2171. doi: 10.1007/s12237-018-0429-0
- Newell, P., and Paterson, M. (2010). *Climate Capitalism: Global Warming and the Transformation of the Global Economy* (Cambridge: Cambridge University Press).
- Olander, J., and Ebeling, J. (2011). “Building Forest Carbon Projects: Step-by-Step Overview and Guide,” in *Building Forest Carbon Projects*. Eds. J. Ebeling and J. Olander (Washington, D.C.: Forest Trends).
- Oreska, M. P. J., McGlathery, K. J., Aoki, L. R., Berger, A. C., Berg, P., and Mullins, L. (2020). The Greenhouse Gas Offset Potential From Seagrass Restoration. *Sci. Rep.* 10, 7325. doi: 10.1038/s41598-020-64094-1
- Orth, R. J., Lefcheck, J. S., McGlathery, K. S., Aoki, L., Luckenbach, M. W., Moore, K. A., et al. (2020). Restoration of Seagrass Habitat Leads to Rapid Recovery of Coastal Ecosystem Services. *Sci. Adv.* 6, eabc6434. doi: 10.1126/sciadv.abc6434
- Palomo, I., Dujardin, Y., Midler, E., Robin, M., Sanz, M. J., and Pascual, U. (2019). Modeling Trade-Offs Across Carbon Sequestration, Biodiversity Conservation, and Equity in the Distribution of Global REDD+ Funds. *Proc. Natl. Acad. Sci.* 116, 22645–22650. doi: 10.1073/pnas.1908683116
- Pascual, U., Phelps, J., Garmendia, E., Brown, K., Corbera, E., Martin, A., et al. (2014). Social Equity Matters in Payments for Ecosystem Services. *BioScience* 64, 1027–1036. doi: 10.1093/biosci/biu146
- Perugini, L., Pellis, G., Grassi, G., Ciais, P., Dolman, H., House, J. I., et al. (2021). Emerging Reporting and Verification Needs Under the Paris Agreement: How can the Research Community Effectively Contribute? *Environ. Sci. Policy* 122, 116–126. doi: 10.1016/j.envsci.2021.04.012
- Peters-Stanley, M., Gonzalez, G., and Yin, D. (2013). *Covering New Ground State of the Forest Carbon Markets 2013* (Washington, DC: Forest Trends’ Ecosystem Marketplace).
- Phang, V. X. H., Chou, L. M., and Friess, D. A. (2015). Ecosystem Carbon Stocks Across a Tropical Intertidal Habitat Mosaic of Mangrove Forest, Seagrass Meadow, Mudflat and Sandbar. *Earth Surf. Proc. Landf.* 40, 1387–1400. doi: 10.1002/esp.3745
- Putz, F. E. (2010). The Importance of Defining ‘Forest’: Tropical Forest Degradation, Deforestation, Long-Term Phase Shifts, and Further Transitions. *Biotropica* 42, 10–20. doi: 10.1111/j.1744-7429.2009.00567.x
- Rakotomahazo, C., Ravaoarinarotsihoarana, L. A., Randrianandrasaziky, D., Glass, L., Gough, C., Georges, G., et al. (2019). Participatory Planning of a Community-Based Payments for Ecosystem Services Initiative in Madagascar’s Mangroves. *Ocean. Coast. Manage.* 175, 43–52. doi: 10.1016/j.ocecoaman.2019.03.014
- Richards, G. P., and Evans, D. M. W. (2004). Development of a Carbon Accounting Model (FullCAM Vers. 1.0) *Aust. Contin. Aust. Forest.* 67, 277–283. doi: 10.1080/00049158.2004.10674947

- Richards, K. R., and Huebner, G. E. (2012). Evaluating Protocols and Standards for Forest Carbon-Offset Programs, Part A: Additionality, Baselines and Permanence. *Carb. Manage.* 3, 393–410. doi: 10.4155/cmt.12.38
- Richards, K. R., and Huebner, G. E. (2014). Evaluating Protocols and Standards for Forest Carbon-Offset Programs, Part A: Additionality, Baselines and Permanence. *Carb. Manage.* 3, 393–410. doi: 10.4155/cmt.12.38
- Rogers, K., Kelleway, J. J., Saintilan, N., Megonigal, J. P., Adams, J. B., Holmquist, J. R., et al. (2019). Wetland Carbon Storage Controlled by Millennial-Scale Variation in Relative Sea-Level Rise. *Nature* 567, 91–95. doi: 10.1038/s41586-019-0951-7
- Romano, A. A., Scandurra, G., Carfora, A., and Ronghi, M. (2018). *Climate Finance as an Instrument to Promote the Green Growth in Developing Countries* (Cham, Switzerland: Springer).
- Romijn, E., Ainembabazi, J. H., Wijaya, A., Herold, M., Angelsen, A., Verchot, L., et al. (2013). Exploring Different Forest Definitions and Their Impact on Developing REDD+ Reference Emission Levels: A Case Study for Indonesia. *Environ. Sci. Policy* 33, 246–259. doi: 10.1016/j.envsci.2013.06.002
- Rosentreter, J. A., Al-Haj, A. N., Fulweiler, R. W., and Williamson, P. (2021). Methane and Nitrous Oxide Emissions Complicate Coastal Blue Carbon Assessments. *Global Biogeochem. Cycle.* 35, e2020GB006858. doi: 10.1029/2020GB006858
- Roughan, B. L., Kellman, L., Smith, E., and Chmura, G. L. (2018). Nitrous Oxide Emissions Could Reduce the Blue Carbon Value of Marshes on Eutrophic Estuaries. *Environ. Res. Lett.* 13, 044034. doi: 10.1088/1748-9326/aab63c
- Rovai, A. S., Twilley, R. R., Castañeda-Moya, E., Riul, P., Cifuentes-Jara, M., Manrow-Villalobos, M., et al. (2018). Global Controls on Carbon Storage in Mangrove Soils. *Nat. Climate Change* 8, 534–538. doi: 10.1038/s41558-018-0162-5
- Sala, E., Mayorga, J., Bradley, D., Cabral, R. B., Atwood, T. B., Auber, A., et al. (2021). Protecting the Global Ocean for Biodiversity, Food and Climate. *Nature* 592, 397–402. doi: 10.1038/s41586-021-03371-z
- Sasmito, S. D., Kuzakov, Y., Lubis, A. A., Murdiyarto, D., Hutley, L. B., Bachri, S., et al. (2020). Organic Carbon Burial and Sources in Soils of Coastal Mudflat and Mangrove Ecosystems. *Catena* 187, 104414. doi: 10.1016/j.catena.2019.104414
- Schneider, H. (2019). “The Role of Carbon Markets in the Paris Agreement: Mitigation and Development,” in *Climate Change and Global Development: Market, Global Players and Empirical Evidence*. Eds. T. Sequeira and L. Reis, 109–132. Switzerland: Springer Nature
- Schoene, D., Killmann, W., Lüpke, H. v., and LoycheWilkie, M. (2007). Definitional Issues Related to Reducing Emissions From Deforestation in Developing Countries. *Forest. Climate Change Work. Pap.* 5, pp 29.
- Seddon, N., Chaussou, A., Berry, P., Girardin, C. A. J., Smith, A., and Turner, B. (2020). Understanding the Value and Limits of Nature-Based Solutions to Climate Change and Other Global Challenges. *Philos. Trans. R. Soc. B: Biol. Sci.* 375, 20190120. doi: 10.1098/rstb.2019.0120
- Shrestha, A., Eshpeter, S., Li, N., Li, J., Nile, J. O., and Wang, G. (2021). Inclusion of Forestry Offsets in Emission Trading Schemes: Insights From Global Experts. *J. Forest. Res.* 33, 279–287. doi: 10.1007/s11676-021-01329-5
- Smith, S. J., and Wigley, M. L. (2000). Global Warming Potentials: 1. Climatic Implications of Emissions Reductions. *Clim. Change* 44, 445–457. doi: 10.1023/A:1005584914078
- Steven, A. D. L., Vanderklift, M. A., and Bohler-Muller, N. (2019). A New Narrative for the Blue Economy and Blue Carbon. *J. Indian Ocean. Reg.* 15, 123–128. doi: 10.1080/19480881.2019.1625215
- Streck, C. (2020). Who Owns REDD Plus ? Carbon Markets, Carbon Rights and Entitlements to REDD Plus Finance. *Forests* 11, 15. doi: 10.3390/f11090959
- Taskforce on Scaling Voluntary Carbon Markets (2021). *Taskforce on Scaling Voluntary Carbon Markets: Final Report*.
- Thamo, T., and Pannell, D. J. (2016). Challenges in Developing Effective Policy for Soil Carbon Sequestration: Perspectives on Additionality, Leakage, and Permanence. *Climate Policy* 16, 973–992. doi: 10.1080/14693062.2015.1075372
- Troxler, T. G., Kennedy, H. A., Crooks, S., and Sutton-Grier, A. E. (2019). “Introduction of Coastal Wetlands Into the IPCC Greenhouse Gas Inventory Methodological Guidance,” in *A Blue Carbon Primer: The State of Coastal Wetland Carbon Science, Practice, and Policy*. Eds. L. Windham-Myers, S. Crooks and T. G. Troxler (Boca Raton: CRC Press), 217–234.
- UNFCCC (2009). *UNFCCC Resource Guide for Preparing the National Communications of Non-Annex I Parties: Module 3 - National Greenhouse Gas Inventories*.
- UNFCCC (2016). *Compendium on Greenhouse Gas Baselines and Monitoring: National-Level Mitigation Actions*.
- Van Dam, B., Polsenaere, P., Barreras-Apodaca, A., Lopes, C., Sanchez-Mejia, Z., Tokoro, T., et al. (2021). Global Trends in Air-Water CO₂ Exchange Over Seagrass Meadows Revealed by Atmospheric Eddy Covariance. *Global Biogeochem. Cycle.* 35, e2020GB00684. doi: 10.1029/2020GB006848
- Vanderklift, M. A., Marcos-Martinez, R., Butler, J. R. A., Coleman, M., Lawrence, A., Prislán, H., et al. (2019). Constraints and Opportunities for Market-Based and Protection of Blue Carbon Ecosystems. *Mar. Policy* 107, 103429. doi: 10.1016/j.marpol.2019.02.001
- Vanderklift, M. A., and Wernberg, T. (2008). Detached Kelps From Distant Sources are a Food Subsidy for Sea Urchins. *Oecologia* 157, 327–335. doi: 10.1007/s00442-008-1061-7
- Vinh, T. V., Allenbach, M., Joanne, A., and Marchand, C. (2019). Seasonal Variability of CO₂ Fluxes at Different Interfaces and Vertical CO₂ Concentration Profiles Within a *Rhizophora* Mangrove Forest (Can Gio, Viet Nam). *Atmos. Environ.* 201, 301–309. doi: 10.1016/j.atmosenv.2018.12.049
- Windham-Myers, L., Crooks, S., and Troxler, T. G. (2018). *A Blue Carbon Primer: The State of Coastal Wetland Carbon Science, Practice, and Policy* (Boca Raton: CRC Press).
- Zeng, Y., Friess, D. A., Sarira, T. V., Siman, K., and Koh, L. P. (2021). Global Potential and Limits of Mangrove Blue Carbon for Climate Change Mitigation. *Curr. Biol.* 31, 1737–1743.e1733. doi: 10.1016/j.cub.2021.01.070

Conflict of Interest: The authors declare that the research was conducted in the absence of any commercial or financial relationships that could be construed as a potential conflict of interest.

Publisher’s Note: All claims expressed in this article are solely those of the authors and do not necessarily represent those of their affiliated organizations, or those of the publisher, the editors and the reviewers. Any product that may be evaluated in this article, or claim that may be made by its manufacturer, is not guaranteed or endorsed by the publisher.

Copyright © 2022 Vanderklift, Herr, Lovelock, Murdiyarto, Raw and Steven. This is an open-access article distributed under the terms of the Creative Commons Attribution License (CC BY). The use, distribution or reproduction in other forums is permitted, provided the original author(s) and the copyright owner(s) are credited and that the original publication in this journal is cited, in accordance with accepted academic practice. No use, distribution or reproduction is permitted which does not comply with these terms.



Mangroves Cover Change Trajectories 1984-2020: The Gradual Decrease of Mangroves in Colombia

Paulo J. Murillo-Sandoval^{1,2*}, Lola Fatoyinbo^{1*} and Marc Simard³

¹ Biospheric Sciences Laboratory, The National Aeronautics and Space Administration (NASA) Goddard Space Flight Center, Greenbelt, MD, United States, ² Departamento de Topografía, Facultad de Tecnología, Universidad del Tolima, Ibagué, Colombia, ³ Jet Propulsion Laboratory, California Institute of Technology, Pasadena, CA, United States

OPEN ACCESS

Edited by:

Catherine Lovelock,
The University of Queensland,
Australia

Reviewed by:

Rodolfo Rioja-Nieto,
Rodolfo Rioja Nieto, Mexico
Anusha Rajkaran,
University of the Western Cape,
South Africa

*Correspondence:

Paulo J. Murillo-Sandoval
pjmurillos@ut.edu.co
Lola Fatoyinbo
lola.fatoyinbo@nasa.gov

Specialty section:

This article was submitted to
Marine Ecosystem Ecology,
a section of the journal
Frontiers in Marine Science

Received: 09 March 2022

Accepted: 22 June 2022

Published: 20 July 2022

Citation:

Murillo-Sandoval PJ,
Fatoyinbo L and Simard M
(2022) Mangroves Cover Change
Trajectories 1984-2020: The Gradual
Decrease of Mangroves in Colombia.
Front. Mar. Sci. 9:892946.
doi: 10.3389/fmars.2022.892946

Awareness of the significant benefits of mangroves to human lives and their role in regulating environmental processes has increased during the recent decades. Yet there remains significant uncertainty about the mangrove change trajectories and the drivers of change at national scales. In Colombia, the absence of historical satellite imagery and persistent cloud cover have impeded the accurate mapping of mangrove extent and change over time. We create a temporally consistent Landsat-derived dataset using the LandTrendr algorithm to track the historical land cover and mangrove conversion from 1984-2020 across Colombia. Over this period, mangrove extent decreased by ~48,000ha (14% of total mangrove area). We find a gradual reduction of mangrove extent along the Pacific coast since 2004, whereas, in the Caribbean, mangrove cover declined around during 1984-1988 and also after 2012. Our time-series analysis matches with drivers of mangrove change at three local sites. For instance, hydroclimatic events, dredging activities, and high sediment loads transported by the rivers have collectively improved mangrove recovery in some sites. In contrast, human activities pressure linked to agricultural expansion and road construction have degraded mangroves. The transition from dense mangrove to other vegetation types is the most significant conversion affecting mangrove cover in Colombia, impacting an area of $38,469 \pm 2,829$ ha. We anticipate increased mangrove loss, especially along the Pacific coast, resulting from intensified human activity. Prioritization of conservation areas is needed to support local institutions, maintain currently protected areas, and develop strategies (e.g. payment for ecosystem services) to preserve one of the most pristine mangrove regions in the Western Hemisphere.

Keywords: Landsat, Colombia, mangrove, Landtrendr, land cover change (LCC)

1 INTRODUCTION

Mangroves are complex ecosystems with various benefits to humans and the environment (de Jong et al., 2021). They are well-recognized for their ecosystem services, especially for communities living in tropical and subtropical regions (Guo et al., 2021). While mangroves are known to provide services such as coastal protection (Yang et al., 2008; Shahbudin et al., 2012), carbon storage (Fatoyinbo et al., 2018; Tang et al., 2018), and biodiversity conservation (Polidoro et al., 2010), they continue to be impacted by human activities. Common land cover change trajectories result from mangrove

conversion to aquaculture, agriculture, and urbanization (Goldberg et al., 2020). Other change trajectories include subtle changes ranging from selective logging and forest degradation as well as mangrove gain or recovery (Bhargava et al., 2021; Vélez-Castaño et al., 2021).

Tracking land change trajectories in mangrove is needed to identify their human and natural drivers and evaluate their impacts. Initial efforts to produce consistent global mangrove extent maps focused on finite epochs (Giri et al., 2011; Hamilton and Casey, 2016). Applications of the Landsat archive is commonly used to track local mangrove gain (Gilani et al., 2021), loss (Thampanya et al., 2006; Bhargava et al., 2021), and degradation (Lee et al., 2021). While research utilizing the extensive record of Landsat imagery for monitoring mangroves remains less exploited (Pasquarella et al., 2016), these approaches and publicly available datasets already provide a much better understanding of the location of coarse drivers (Thomas et al., 2017) of mangroves change (Goldberg et al., 2020) and specific periods of loss and gain (Luijendijk et al., 2018; Mentaschi et al., 2018). The increased availability of complementary remote sensing datasets from radar has also been successfully used to produce global change maps, albeit with a coarser and more limited time-span (Bunting et al., 2018; Thomas et al., 2018).

Earth Observation technologies provide an objective means of monitoring the status of mangrove forests. However, tracking mangrove dynamics is difficult for many reasons. For instance, cloud cover and the restricted access to historical optical satellite imagery in tropical regions limit our ability to accurately evaluate mangrove extent and change. Additionally, most current mangroves datasets fail to recognize their historical dynamism because they primarily focus on bi-temporal or decadal analysis aggregating the outcomes at coarse spatial scales. Finally, there is often a discrepancy in mangrove extent area, loss, and gain at national levels (Ruiz-Luna et al., 2008; Mejía-Rentería et al., 2018; Suyadi et al., 2018; Alban et al., 2020) which can potentially affect the design of policies to improve conservation outcomes (Hamilton et al., 2018).

To our knowledge, there is no country-specific continuous assessment of the change in the extent of mangroves in Colombia (Bernal et al., 2017; Mejía-Rentería et al., 2018), and large uncertainties about historical mangrove change trajectories remain unknown (Mejía-Rentería et al., 2018). Previous studies have estimated mangrove extent in Colombia ranging from ~500,000 ha in 1966 (IGAC, 1966) to 214,000 ha in 2000 (Giri et al., 2011), suggesting a mangrove loss of 57% in 45 years (López-Angarita et al., 2016). However, these estimates are highly uncertain because of the diverse methodologies employed and the lack of reference validation (Zambrano Escamilla and Rubiano-Rubiano, 1996). Most previous mangrove research in Colombia has focused on localized studies. National assessments are scarce due to the limited availability of cloud-free optical imagery and the lack of a consistent method to exploit remote sensing archives. The Caribbean coast has more research given its accessibility since colonial times whereas accessibility has limited the number of studies along the Pacific coast (Castellanos-Galindo et al., 2021b).

Recent efforts by different Colombian agencies have contributed to a better assessments of mangrove extent (IDEAM, 2010; INVEMAR, 2014). Projects such as *Sistema de Información para la gestión de los manglares en Colombia* – (SIGMA) by the Colombian government seek to establish a platform for research and conservation strategies for these ecosystems (<http://sigma.invemar.org.co/geovisor>). Given the increasing global demand from commodities such as rice, shrimp, and oil palm cultivation and the current post-conflict opportunities in Colombia (Murillo-Sandoval et al., 2020), it is imperative to identify the past and current mangrove change trajectories. While large areas in Colombia are profitable for establishing Blue Carbon projects based on carbon prices (Zeng et al., 2021), the ability to facilitate management and conservation priorities depends on the capacity to monitor the condition of mangroves quantitatively. Thus, understanding historical changes in extent is the initial step for developing carbon accounting and resource management systems.

This paper combines Landsat imagery with the LandTrendr algorithm (Kennedy et al., 2010) to develop consistent temporal land cover maps at annual steps between 1984 and 2020. We quantify land change trajectories associated with mangrove gain, changes from mangrove to other vegetation types, mangrove to open water, as well as urban and agricultural expansion. We highlight sites where these changes are evident and describe potential drivers using previous research studies. Different sites highlight diverse mangrove change trajectories, and social and environmental conditions that contribute to test our remote sensing method at the National level. The contributions of this study are threefold: we initially reduce the uncertainty about the current extent and distribution of mangroves in Colombia using 36 years of satellite data. Additionally, our methodology produces consistent land change maps and is compatible with national agencies' requirements to monitor mangroves regularly (i.e., SIGMA). Finally, we identify the location of mangrove change and qualitatively identify specific natural and human drivers. We specifically ask:

1. What is the current and historical extent of mangroves in Colombia?
2. What were the mangrove change trajectories and specific transitions of gain and loss?
3. How can the most dynamic locations of mangroves change be attributed to specific human-induced activities and natural drivers?

2 STUDY AREA

Approximately 70% of Colombia's mangroves are found along the Pacific coast, with 30% on the Caribbean coast (Bernal et al., 2017). Colombia hosts 1.5% of global mangrove carbon stock (Simard et al., 2019a). Low alluvial plains characterize the Pacific coast fed by many large rivers from the Western Andes. The coastline is about 1600 km long and considered one of the rainiest places on the Earth (Mejía et al., 2021). With an average

precipitation of ~8000 mm, frequent cloud cover seriously hampers optical remote sensing studies (Fagua and Ramsey, 2019). The environmental conditions and poor accessibility have contributed to keeping the remaining mangroves mostly undisturbed across large swaths of the Pacific coast. This condition has allowed the development of some of the tallest mangroves forests in South America, with canopies reaching 54 meters (Simard et al., 2019a) and trees measured *in situ* reaching 57 meters (Castellanos-Galindo et al., 2021a).

In contrast, the Caribbean coast is drier than the Pacific, with annual precipitation reaching ~2500 mm along the ~1300 km coastline. Under microtidal conditions in the Caribbean, mangroves are mainly located on small deltas and coastal lagoons. The Caribbean is more developed than the Pacific coast, with many small cities and five large commercial ports (Riohacha, Santa Marta, Barranquilla, Cartagena, and Turbo) (Correa and Morton, 2010). Human pressure on mangrove forests has been more extensive on the Caribbean than on the Pacific coast. With more consistent cloud-free satellite observations, the availability of studies in the Caribbean is more extensive (Simard et al., 2008; Villate Daza et al., 2020; Vélez-Castaño et al., 2021).

The geomorphological setting of mangroves in Colombia varies greatly with small and large deltas, estuaries, lagoons, open coasts, and carbonate islands. The environmental conditions between the Caribbean and the Pacific coasts also contribute to diverse mangrove structure (Blanco-Libreros et al., 2022). The meso- and macro-tidal Pacific coast is dominated by alluvial plains and large river deltas where mangrove have developed under high rainfall conditions (Castellanos-Galindo et al., 2021b). In contrast, the microtidal Caribbean coast is mainly a dry environment in which mangroves occur in medium to small deltas, coastal lagoons, and some marginal areas along the coast (Correa and Morton, 2010).

In Colombia, the protected mangrove areas cover 67,000 ha, corresponding to 23% of the total mangrove area. There are seven mangrove species (Palacios and Cantera, 2017): *Avicennia germinans* (black mangrove), *Rhizophora mangle* (red mangrove), *Laguncularia racemosa* (white mangrove), *Conocarpus erectus*, (button mangrove) and *Pelliciera rhizophorae* (piñuelo) are the five found in the Caribbean. Along the Pacific, we find these five species as well as *Rhizophora racemosa* and *Mora oleifera*.

2.1 Case Study Sites

We selected three sites with diverse human activities and natural processes that have affected mangrove cover. The selected sites are important to test our method and link them to specific drivers of mangrove change. First, in the Caribbean, *Ciénaga Grande de Santa Marta* (CGSM) is the largest lagoon–delta complex in Colombia (1280 km²) (Botero and Salzwedel, 1999). Mangrove extent here has dramatically decreased due to the construction of roads (Botero and Salzwedel, 1999). These roads resulted in the diversion, diking, and drainage of freshwater courses and subsequent die-off of 60 to 90% of the mangrove areas (Bernal et al., 2017). Dredging activities increased freshwater input into the CGSM that temporally improved mangrove recovery. Second, the Gulf of Urabá, also known as the Darien region, is

the most extensive sea inlet on the Colombian coasts (Blanco et al., 2012). The Western part is mainly affected by natural conditions, while its Eastern part has suffered the impact of anthropogenic activities such as large agricultural expansion linked to land grabbing processes (Ballvé, 2013). Finally, Sanquianga is the largest protected area along the Pacific coast of South America and is located on the new Patía-Sanquianga delta plain. In 1972 water diversion and channelization changed this northern estuarine system into an active delta plain mainly for easier extraction of logged trees (Restrepo, 2012; Bernal et al., 2017). This diversion shifted more than 90% of the Patía River discharged through the Sanquianga River with diverging impacts on mangrove cover (Restrepo, 2012).

3 DATA AND METHODS

We divide the methods into four parts (see **Figure 1**). First, we combine Sentinel 1 (S1) and Sentinel 2 (S2) to create a 10m-resolution land cover base map for 2020 (Section 3.1) trained with official map sources. This base map allows the collection of enough training data for time-series analysis. Second, we apply the LandTrendr algorithm to remove year-to-year variability, interpolate missing data and enhance spectral separability between land cover classes using temporally consistent and multivariate descriptions of the landscape (Section 3.2). Third, we identify sites where mangrove loss and gain are evident and explain these changes using available reports and previous research (Section 3.3). Finally, an accuracy assessment and area estimation are provided (Section 3.4).

3.1 Base Map 2020

We employ Synthetic Aperture Radar (SAR) data from Sentinel 1 A and B Sensors and optical data from Sentinel 2 to create a new land cover map with a spatial resolution of 10m across Colombia. First, we build a cloud-free Sentinel-2 image composite including data collected in 2019–2020. Our predictors based on the image composites include the mean, percentile 20th, 80th, and the standard deviation for each spectral optical band in Sentinel-2 and VV and VH polarizations for Sentinel-1A/B. Additionally, we include several vegetation indices and Gray-Level Co-occurrence Matrix (GLCM) indicators (see **Supplementary**). Second, we collect training data (first training, see **Figure 1**). The training data comes from the official Colombian Corine Land Cover map 2012 (CLC) (IDEAM, 2010). The CLC map identifies the five most common land cover classes along the Colombian coasts as agriculture, dense forest, mangroves, water, and scrub-shrub wetland associations.

We created a mask of 2012 to 2020 class persistence using the Global Forest Cover disturbance, tree canopy cover datasets (Hansen et al., 2013), and JRC Global Surface Water (Pekel et al., 2016). This allowed the selection of training samples on S1 and S2 image composite for year 2020 based on classes identified in 2012 Corine Land cover map. We applied a Simple Non-Iterative Clustering (SNIC) algorithm available in Google Earth Engine to S1 and S2 image composite and spectral

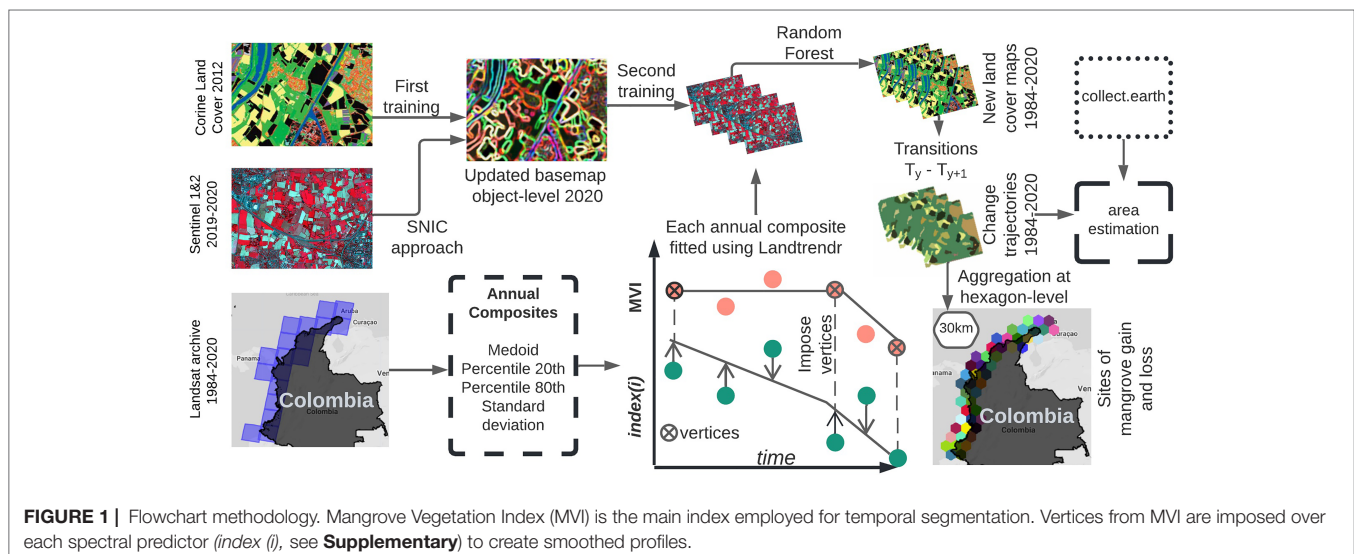
indices (see **Supplementary**). SNIC is an object-based image segmentation approach useful to group neighboring pixels with similar characteristics into clusters (Tassi and Vizzari, 2020). We randomly sampled 1000 SNIC clusters per class and confirmed class labels through visual inspection of Planet data in the Collect Earth application. This process removed 549 samples that could not be assigned (e.g., cloud cover or not available imagery). A total of 4451 samples were divided into training (70%) and validation (30%). We found the Mangrove Vegetation Index (MVI) as the dominant metric for spatial segmentation to delineate mangroves from non-mangroves (Baloloy et al., 2020). After image segmentation, mean values of each predictor were assigned to each cluster and classified with the RandomForest algorithm to produce a new base land cover for 2020 (Breiman, 2001). Our method is highly automated using the Google Earth Engine platform (Gorelick et al., 2017).

3.2 Landsat Preprocessing and LandTrendr Setup

In this section, we created a new spectral dataset after a linear fit using LandTrendr algorithm (Kennedy et al., 2010). This process creates a temporally consistent dataset that provides a better temporal stabilization of spectral metrics to build consistent land cover maps. We analyzed 7853 Landsat Tier 1 images in the GEE Catalog between 1984 and 2020. For each image, we applied a series of steps. First, after using the standard cloud and shadow masking procedure, we visually removed 238 images with artifacts that would affect the creation of annual composites. Second, we produced homogenous spectral values for Landsat 4 through 8 using Roy's parameters (Roy et al., 2016). Third, topographic effects were reduced using the Dymond-Shepherd physical correction (Shepherd and Dymond, 2003). Fourth, a negative 2 km buffer around each image was applied to remove scene edge artifacts. Finally, we clumped the spectral data to eliminate undesirable outliers.

After preprocessing, we created annual image composites using four methods: medoid, percentile 20th, 80th, and standard deviation. Medoid is a well-recognized method for building radiometrically consistent Landsat composites with the smallest average heterogeneity in tropical regions (Van doninck and Tuomisto, 2018). Instead of minimum and maximum values, we use the 20th and 80th percentiles to reduce sensitivity to shadows and atmospheric contamination effects (Zhang and Roy, 2017). Additionally, the 20th percentile is helpful in differential vegetated areas that are persistent green throughout the year (Lyburner et al., 2020). Standard deviation highlights dynamic and stable surfaces. While the scarcity of enough observations in the early years (e.g., 80 and 90) can affect the performance of percentiles (Xie et al., 2020), missing Landsat observations mostly occur in mountainous regions and few locations on the coast. These are spatially filled using an average window (8 x 8 pixels) procedure.

We applied the LandTrendr (LT) algorithm on each of these composite datasets. While extensively used for tracking forest disturbances and agents of change (Kennedy et al., 2010; Zhu, 2017; Kennedy et al., 2018), its usability for building consistent landcover maps is less common (Murillo-Sandoval et al., 2021). LT identifies breakpoints (vertices) where the temporal progression of spectral values is approximated to be linear to reduce noise. We simplify chronosequences into representative temporal trajectories that improve land cover maps creation through linear fit smoothing. LT needs different parameters to identify breaks; here, we use previous parametrization available for Colombian forest (see **Supplementary**) (Murillo-Sandoval et al., 2021). We increased the spectral separability among land cover classes by imposing the timing of the vertices detected using MVI onto a set of spectral predictors (see **Supplementary Figure 1**). This process provides temporal stabilization of spectral metrics removing ephemeral changes across years for each composite method. The algorithm also interpolates temporal data gaps due to clouds, cloud shadows, and Landsat-7 SLC errors.



We randomly sampled our new base land cover map in 2020 (section 3.1) for the five landcover classes incorporating the predictors from different Landsat composite methods (second training, see **Figure 2**). Additionally, we added more training data using purposive sampling in 1990, 2000, and 2010 to have a complete temporal description of land changes. The additional training data was verified using Landsat images and high-resolution images in Google Earth. A set of ten individual landcover maps per year were created employing a RandomForest. This iterative process decreases salt-pepper effects; the mode from these maps produced the final map per year.

3.3 Quantifying Land Change Trajectories

Land cover change maps are a proxy for detecting mangrove loss and gain processes and infer types of land use conversion. We derived five land change trajectories based on our land cover maps. The first conversion is from dense mangrove to scrub-shrub vegetation. The Instituto Geografico Agustín Codazzi (IGAC) defines dense mangroves in Colombia as tree height > 15m that follows a continuous woody pattern with tree cover > 70%. The scrub-shrub vegetation is also defined as tree height < 4m that has been human or naturally intervened (IGAC, 1999). This conversion of mangrove to other vegetation type indicates mangrove loss. Loss and mangrove gain can be natural or anthropogenic processes that evolve in shorelines (Bhargava et al., 2021). The transition from mangroves to open water (Mentaschi et al., 2018) is considered mangrove loss. Mangrove gain is related to new mangroves expanding into the coastal ocean or inland. To determine mangrove gain, we consider the conversions from water, agriculture, and scrub-shrub vegetation to mangrove. Mangrove loss includes conversion of mangrove to open water, other vegetation types, and urban and agriculture areas. The latter two are human-driven conversions that affects the development of other land cover types (IDEAM, 2010). To reduce misclassification with tiny settlements, we employ the new ESA 2020 (Zanaga et al., 2021) urban layer to separate settlements from agriculture. Finally, classes such as permanent water and other non-mangrove-related transitions were calculated for the mapping process but not included in the area estimation assessment.

We create a difference map between 1984 and 2020 to identify the locations of mangroves gain and mangrove loss. We use spatial aggregation based on hexagons of 30 km diameter to visualize mangrove gain and loss, and identify three locations that experience mangrove gain and loss: *Ciénaga Grande de Santa Marta*, the Gulf of Urabá, and the Sanquianga Protected Area. We identify potential drivers of mangrove change in these regions using expert knowledge and available research.

3.4 Accuracy and Area Estimation Assessment

Good practices in remote sensing tasks recommend using unbiased estimators on stratified data using reference observations (Olofsson et al., 2020). Using an established procedure (Olofsson et al., 2014), the accuracy assessment was derived from the change map between 1984 and 2020. A random stratification sampling of 1,230 points was distributed among the five types of change trajectory and stable mangroves classes. The allocation follows 800 samples for mangroves (65% proportion area), 150 to mangrove to other vegetation types and mangrove gain, 50 to mangrove to open water and agriculture, and 30 to urban areas. While using a multi-sample approach can highlight more detail into the area estimation, developing an annual assessment would increase the number of needed samples to $\sim 1230 \times 35 = 43,050$. Therefore, the choice of 1,230 points is merely practical and conservative, involving available human resources and making a careful effort to keep precision in the reference process.

We use a sampling unit of 30 m pixel size of the Landsat image for the reference process. We utilized CollectEarth (<https://collect.earth/>) which links the samples with the reference observation through a visual process. CollectEarth offers a set of tools for connecting each sampled point with its reference using Landsat images subsets, Landsat time-series plots, and high-resolution images from OpenStreetMap and Planet. Additionally, CollectEarth offers a degradation tool widget that tracks forest disturbances and helps in assigning the reference class to each sampled point. After reference data collection, we constructed error matrices and reported the estimated areas for each class. The bias in the mapped area (pixel counts) is assumed

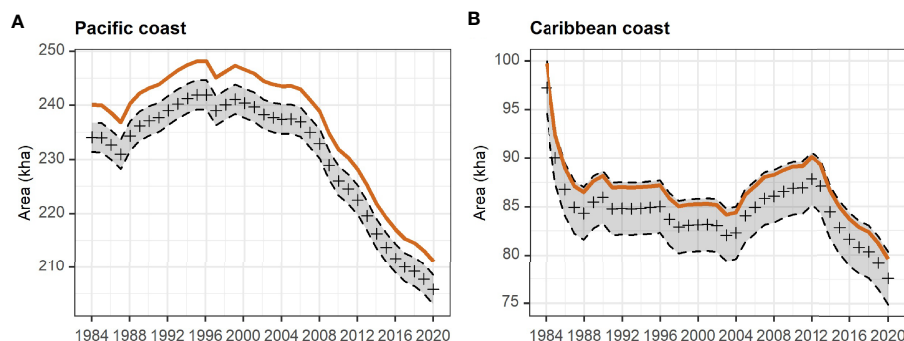


FIGURE 2 | Mangroves area for the Pacific and Caribbean coasts. Area estimates with 95% confidence intervals (dashed lines). Brown line represents the area mapped (pixel counts), and cross symbols represent the area estimated.

to be uniformly distributed in time and space. Consequently, the coefficient between the mapped area and the estimated area (unbiased) for the full stratification is multiplied by the mapped area in a given year for each class to obtain the estimated area (Olofsson et al., 2016).

4 RESULTS

4.1 Colombian Mangroves Extent and Change Trajectories

In this paper, we provide a consistent method and historical examination of mangrove extent in Colombia. Our Landsat-based analysis reveals that mangroves had declined throughout the entire study area from $331,356 \pm 2,708$ ha in 1984 to $283,419 \pm 2,708$ ha in 2020. In other words, Colombia lost 14% ($\sim 47,937$ ha) of its mangrove in 36 years (0.38% per annual change). The base map produced with Sentinel-1 and Sentinel-2 supports the current extent in 2020, with a mangrove cover of $287,678 \pm 34,107$ ha. The Pacific coast held $234,345 \pm 2,644$ ha, with mangroves decreasing by about $\sim 32,000$ ha since 2004 (Figure 2A). The map bias, the difference between the mapped area and estimated area, is 5898ha, an overestimation that falls outside confidence intervals (Figure 2A). In contrast, the Caribbean coast has $75,689 \pm 853$ ha, with two notable periods

of decline of $\sim 15,000$ ha between 1984–1988 and $\sim 10,000$ ha between 2012–2020 (Figure 2B). Our mapped area is within the limits of confidence intervals (Figure 2B). Producer's accuracy was greater than 90% for all classes except for urban that reaches 40%. User's accuracy was also greater than 90% for all classes, excluding agriculture, with a value of 79%.

The decrease in mangrove extent (Figure 3E) is mainly associated with mangrove to other vegetation types followed by mangrove to open water, adding a loss of $56,439 \pm 47,477$ ha (Figures 3A, B). These two conversions gradually rise on the Pacific coast, whereas, in the Caribbean, they remain relatively constant from 1988 to 2004 (see Supplementary Figures). Other change trajectories such as agricultural and urban expansion into mangroves have a minor contribution in mangroves loss from 1984 to 2020; however, they have a higher area uncertainty: $11,285 \pm 10,688$ ha for agriculture (Figure 3C) and $2,824 \pm 1,478$ ha for urban areas (Figure 3D). In contrast to mangroves loss, mangrove gain reaches $46,541 \pm 1,068$ ha (Figure 3F).

4.2 Locations of Mangroves Loss and Gain

The Landsat-based difference map between 1984 and 2020 shows the long-term mangrove gain and loss changes (Figure 4). Mangrove gain indicates new mangroves expanding into the coastal ocean or inland. Mangroves loss results from mangrove conversion to other vegetation types, open water, agricultural

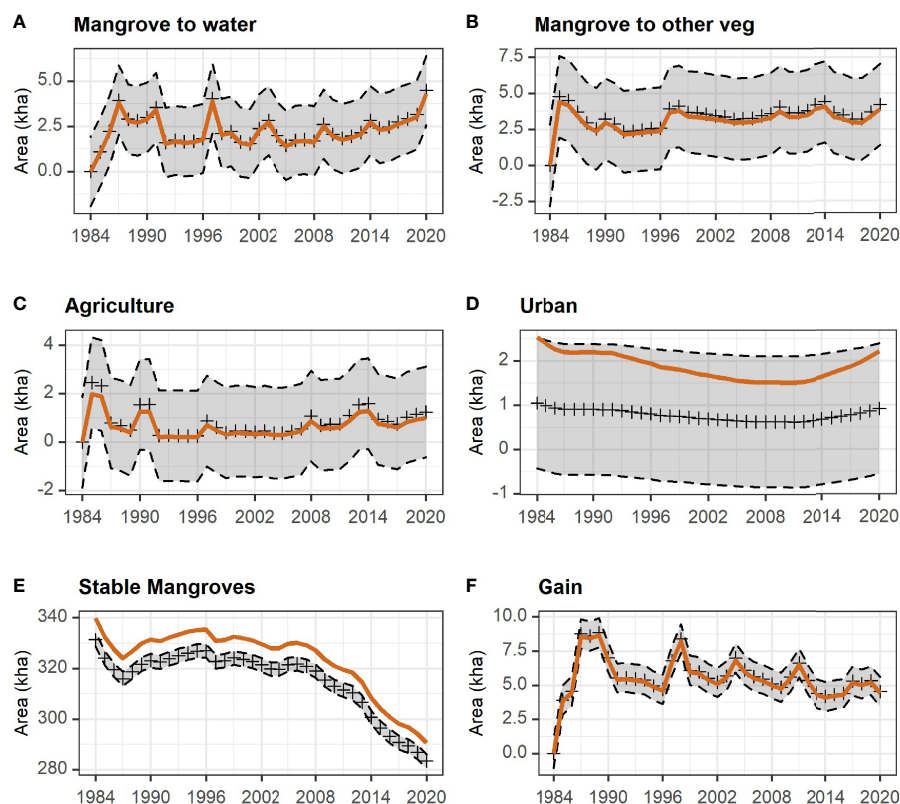


FIGURE 3 | National level estimated and mapped areas for five trajectories of change and stable mangroves. Area estimates with 95% confidence intervals (dashed lines). Brown line represents the area mapped (pixel counts) and cross symbols represent the area estimated.

and urban. We found changes in mangrove extent in all coastal departments over the 36 years of analysis, except in the department of Guajira in the Caribbean and Chocó in the Pacific (Figure 4). While the Department of Guajira has little mangrove areas to start with, the Department of Chocó has a significant portion of Colombia's mangroves. Diverse changes are presenting in our three local sites: CGMS, the gulf of Urabá and Sanquianga.

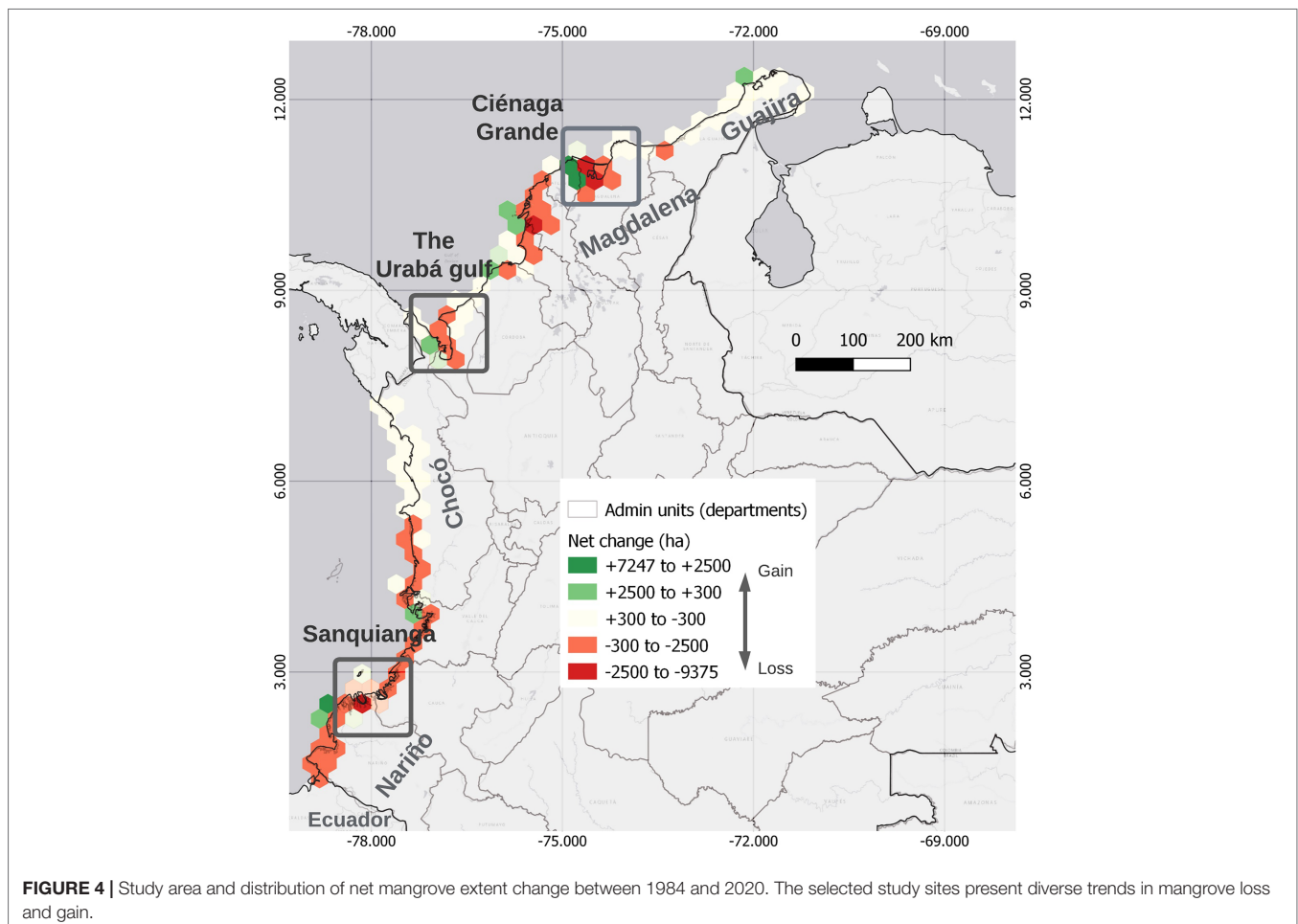
4.2.1 Ciénaga Grande de Santa Marta

The construction of roads around 1950 and consequent water diversion caused the destruction of more than 60% of mangrove cover in CGSM due to an increase in salinity (Botero and Salzwedel, 1999). However, during our analyzed period 1984–2020, the main trajectory is linked to mangrove gain (Figure 5). By 1984 mangrove cover was steady with episodes of loss and gains until 2004 and increased between 2004 and 2012 by $6,614 \pm 74$ ha (Figure 5C). From 2012 onward, mangrove extent decreased linked to the transition from mangrove to other vegetation and mangrove to water, by 2020 mangrove extent reaches $39,996 \pm 451$ ha. The CGSM shows prominent locations with mangrove to open water mainly located near the coast, while mangrove gain is widely distributed across the lagoon, and mangrove to other vegetation is situated in the periphery. A complete table

with areas of annual change for each transition is available in **Supplementary Material (Table SP7)**.

4.2.2 The Gulf of Urabá

In total, our Landsat analysis indicates a mangrove area of $6,342 \pm 71$ ha in the Gulf of Uraba in 2020. Mangrove to other vegetation in 1999 is the main trajectory of change with a large value of 261 ± 19 ha in 1999, followed by mangrove to open water of $78 \text{ ha} \pm 8 \text{ ha}$ (Figure 6C). On the Western coast, extensive mangrove gain is mapped in the mouth of the Atrato delta. While many mouths in the Atrato delta show mangroves gain, the mouth called El Roto experienced the most significant expansion of mangroves in the last 36 years with 735 ± 16 ha of mangrove gain with an annual increase rate of 32 ha per year (Figure 6). On the other hand, mangrove to open water is visible in the Northwest coast, with a yearly retreat of -14 meters per year (Figure 6A). Contrarily to the natural processes presented on the Western coast of Urabá, mangrove loss due to urbanization is presented along the eastern coast is significant around Turbo city and across the whole East Coast, putting pressure over smaller mangrove areas. In addition, some location shows mangroves gain with areas where mangroves have migrated in small river deltas. The development of large channels to drain the excess water from



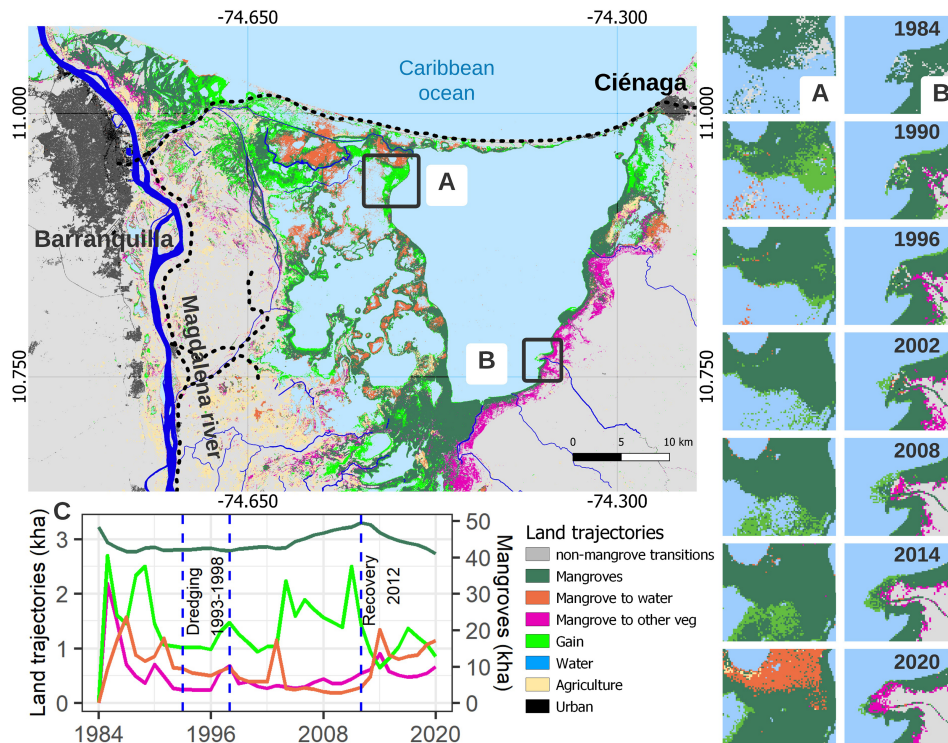


FIGURE 5 | Map difference between 1984 and 2020 in Ciénaga Grande de Santa Marta. Black dotted lines represent the roads constructed to join Barranquilla and Ciénaga cities between 1956 to 1960 and the road parallel to Magdalena River constructed in 1970. **(A)** Image subsets represented mangrove gain with mangrove to open water detected in 2020. **(B)** Image subsets show mangrove to other vegetation inland and gain since 2008. **(C)** The time series plot shows the land trajectories of change and dredging period between 1993–1998 and mangrove recovery from 2004 to maximum in 2012.

large banana plantations led to a large load of sediment deposits contributing to mangrove expansion (**Figure 6B**). More detail about areas of change is available in **Supplementary Material (Table SP8)**.

4.2.3 Sanquianga Protected Area

Mangrove change trajectories indicate more mangrove gain than mangrove to open water and mangrove to other vegetation. Mangrove cover in Sanquianga slightly increased from 2000 to 2014 (see change values in SP **Table SP9**), currently holding $41,138 \pm 464$ ha of pristine mangroves in 2020. Additionally, two peaks of mangrove gain occurred in 1987–1988 and 1997–1998, coinciding with intense El Niño events. The warmer circumstances during El Niño favored mangrove growth, reproduction, and respiration (Riascos et al., 2018). The combined impact of these two climatic events increased mangrove gain by about 3,000ha. However, abrupt La Niña events followed these El Niño events in 1988–1989 and 1998–1999, reducing these overall gains (**Figure 7B**). Mangrove to open water and mangrove to other vegetation within the official limits of Sanquianga park are located on the shorelines and dispersed in small areas across the protected area. Both processes account for an annual loss of 500ha during the analysis period. Interestingly, mangrove to other vegetation is prone to happen inland outside the protected area, meaning pressure over the remaining mangrove.

5 DISCUSSION

5.1 Mangrove Dynamics at National Scale

We produce historical maps of mangrove extent in Colombia using the temporal smoothing profiles derived from LandTrendr (LT) onto Landsat imagery. Using LT fitted spectral information significantly reduced noise from phenological changes, atmospheric conditions, and illumination conditions, leading to a better representation of changes on mangrove cover. Our methodology provides historical trajectories of mangrove to open water and other vegetation types, and mangrove gain, improving previous national and global datasets efforts. Our estimate of mangrove cover for 2020 is 283419 ± 2708 ha is 26%, 42%, and 20% higher than global datasets by Giri et al. (2011); Hamilton & Casey (2016), and Global Mangroves Watch in 2016 (Bunting et al., 2018) respectively. We identify mangrove patches often missed by global datasets, especially on the Pacific coast. Global datasets are very conservative and with few available imagery they often miss large portions of the mangroves distribution, this aspect has been well-documented in previous studies (Mejía-Rentería et al., 2018). However, our current Landsat mangrove cover map in 2020 is 1% smaller than the available dataset produced by national agencies (IDEAM, 2010; INVEMAR, 2014). Our method offers a quick and effective way to monitor local and regional

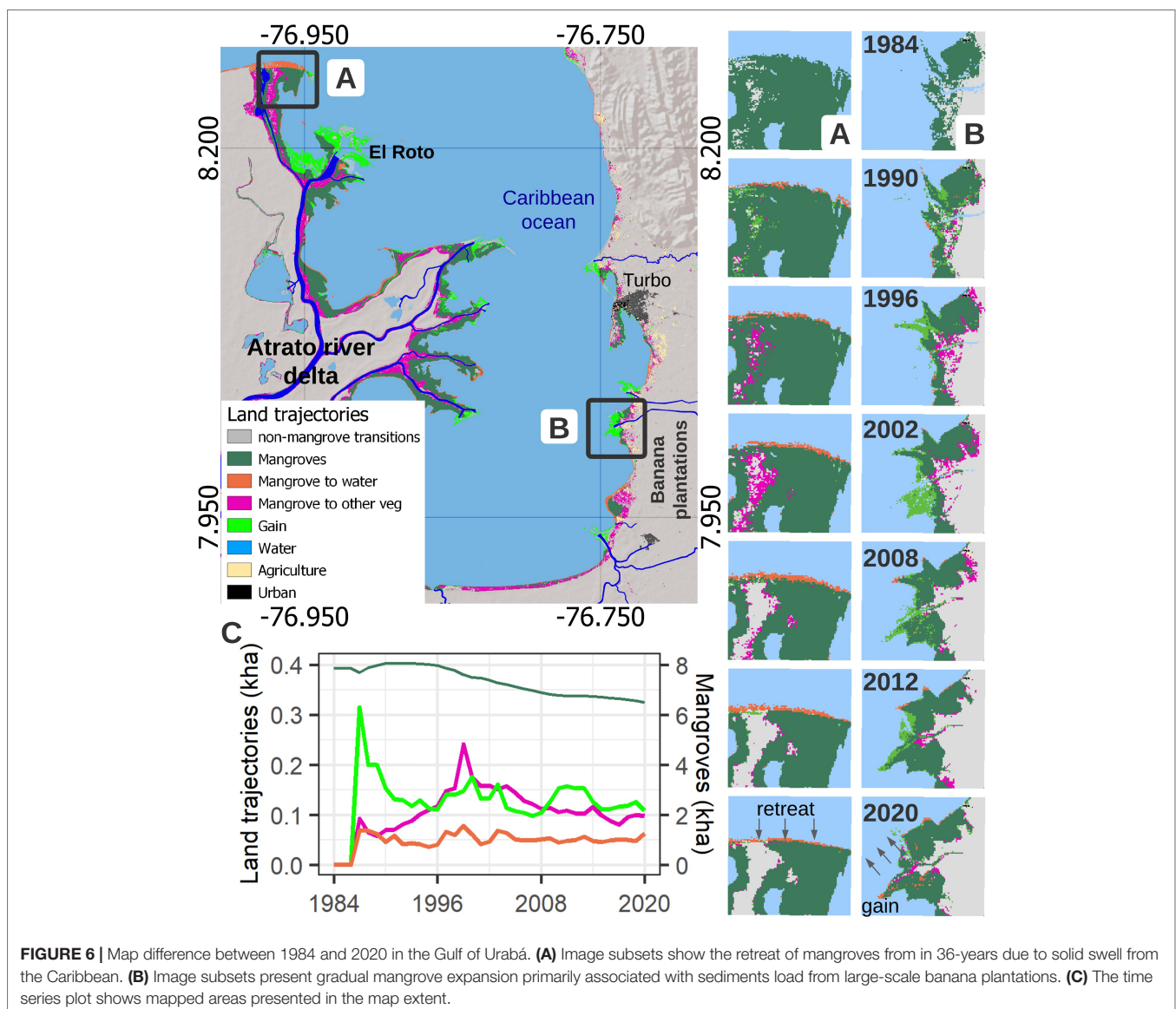
mangrove change and provide time-effective information about mangrove status. The method can be incorporated within the official *Sistema de Información para la gestión de los manglares en Colombia* (SIGMA).

While Colombia has large persistent areas of mangroves, the net 14% decline in both coasts and the more recent increase in mangrove losses on the Pacific is a big concern. The conversion from mangrove to other vegetation is by far the most common trajectory of mangrove loss, and it is generally located inland in the landward mangrove zones. The Pacific coast shows a gradual decline mostly from the middle of Choco to the Southern of the country since 2014 to the present. In contrast, in the Caribbean coast, two periods of mangrove loss indicate that changes are widely distributed along the entire coastline. While we observed both mangrove gain and losses in Colombia, there has been a net decrease in mangrove area since 1984 due to human activities associated with the gradual expansion of agricultural activities,

selective logging and mining (Mejía-Rentería et al., 2018; INVEMAR, 2020).

5.2 Potential Drivers of Mangrove Change at Local Scale

Our empirical contribution investigates mangrove change trajectories based on previous studies in three mangrove sites. The construction of roads surrounding the Cienaga Grande de Santa Marta region started in 1950. The consequent reduction in hydrologic connectivity, combined with warmer periods, resulted in hypersaline conditions that caused conversion of mangrove to other vegetation types and prevented mangrove recovery (Jaramillo et al., 2018). To re-establish the necessary hydrological conditions for mangroves recovery, five of the pre-existing natural tributaries were dredged between 1993 and 1998 to improve freshwater and reduce salinity (Botero and Salzwedel,

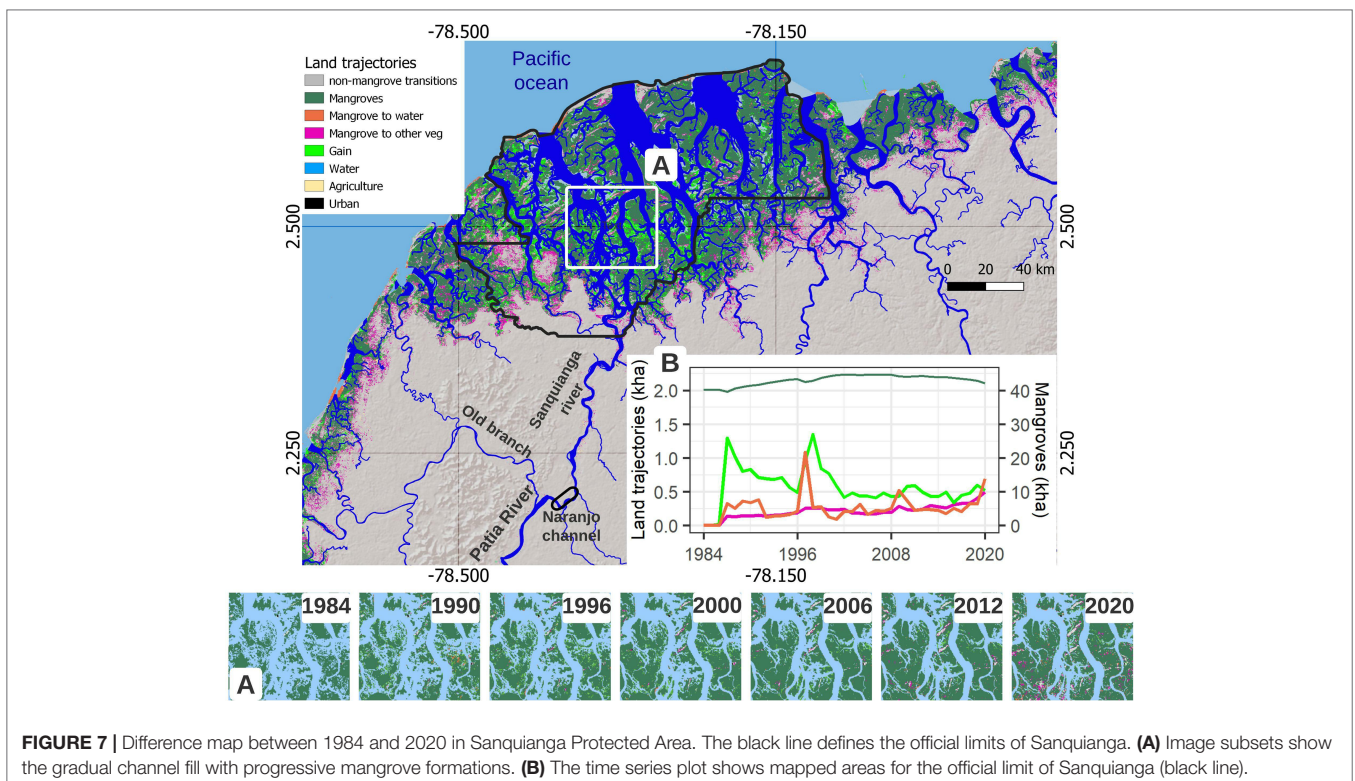


1999). Our analysis shows that mangrove extent increased in 2004, suggesting that dredging activities were successful. In addition, the persistent La Niña event between 1999 and 2001 also enhanced freshwater into the CGSM and boosted mangrove gain. The positive increase in mangroves after 2012 was altered by the intense El Niño events in 2015–2016 and 2018–2019 that reduced the mangrove recovery trend (Blanco et al., 2006). In CGSM, the increased streamflow in the Magdalena River combined with dredging operations reduce salinity that contribute to mangrove growth during a short timeframe (Blanco et al., 2006; Jaramillo et al., 2018).

In the Gulf of Urabá, diverging mangrove processes have occurred along its Eastern and Western coasts. First, on the Western side, mangrove gain dominates trajectory in Atrato river delta mouth. Here mangrove gain is driven by high sediment load discharge of the Atrato River fed by high precipitation rates Chocó Region (Blanco et al., 2012). Some authors also linked the expansion of mangroves in the Atrato delta with legal gold mining peaks and periods of heavy rain associated with La Niña events (Vélez-Castaño et al., 2021). Erosion only occurs in limited areas mainly due to the low sinuosity of the Atrato River, which is a highly vegetated floodplain with resilient riverbanks. A larger area of erosion led to a retreat of the mangroves due to north-to-south coastal drift and extreme swell events that constantly hit the coast in a perpendicular orientation (Vélez-Castaño et al., 2021). On the Eastern coast, the role of armed conflict has shaped land distribution and consequently the expansion of agriculture affecting mangroves extent (Muñoz-mora et al., 2015). Through different strategies such as paper falsification, direct threats,

and killing, illegal actors have taken land from small farmers and established large-scale agricultural projects (Grajales, 2011; Ballvé, 2013). The increase in bananas, plantain crops, and the expansion of pasture lands are the leading cause of transition of mangrove to other vegetation and deforestation (Figure 6). The struggles between small and large landholders remain in Urabá (Truth Commission - Forensic Architecture, 2021). However, disentangling these drivers and their relative impact would require field monitoring, local testimonies, and participative research that was beyond the scope of this study.

In Sanquianga, water diversion in 1972 converted this estuarine system into a new active delta. The higher discharged contributed to a widening of the Sanquianga River, leading to active sedimentation and channel filling (Restrepo, 2012). Consequently, pioneer mangroves gradually colonized the fine sediments, and morphological changes associated with channel fill are detected in the Landsat time-series (Figure 7A). While an evident mangrove gain is observed through the 36-years analysis, the conversion of mangrove to open water and to other vegetation types are minimal along Sanquianga's shoreline. Episodes of sea-level rise associated with the El Niño events (Restrepo, 2012) may have increased shoreline loss. Sanquianga shows a persistent mangrove extent, indicating the system is currently balanced in terms of mangrove gain and loss. In addition, the growth of coca crops surrounding Sanquianga affects mangrove cover, given the contamination of water by wasted chemicals (Parra and Restrepo-Angel, 2014). The presence of illegal groups also limits the livelihoods of communities. As losing access to gathering cockles, coca's economy is the only farming alternative



putting more pressure over mangroves, increasing communities vulnerability, and shifting social and economic outcomes (UNODC, 2017; Treviño and Murillo-Sandoval, 2021).

5.3 Limitations and Future Work

Our remote sensing analysis capture commonly absent mangrove patches in previous global datasets, however some uncertainties remain. For instance, we do not use pixel-based tidal masking to remove effects from extreme climate events. The temporal variability in mangrove to open water and mangrove gain presented in (Figures 3A, F) may be potentially minimized after modeling tidal effects. The tidal masking helps delineate better shorelines (Bishop-Taylor et al., 2021) to update mangrove change trajectories. Our accuracy assessment shows that urban, and agriculture (primarily pasturelands) shows high uncertainty and low accuracy (see **Supplementary**). Although these classes have a small area proportion, adding urban more training data and other higher spatial resolution dataset might help track these minor transitions.

Future research in Colombia to track mangrove status from aerial and satellite imagery should incorporate the role of natural processes and the participation of communities and institutions (i.e., institutional framework) (Ostrom and Nagendra, 2006). Multidisciplinary approaches that consider social sciences are often missed, even if the role of local testimonies is known to be invaluable (e.g., Truth Commission - Forensic Architecture, 2021). Local community involvement highlight otherwise overlooked problems and provides insight into complex and unintended environmental and social aspects (Treviño and Murillo-Sandoval, 2021). Another relevant aspect is the role of *causality*. Future studies require regular ground validation and sensors to monitor river discharge, tracking sediments, weather stations, and sea-level rises. Although expensive, causality analysis disentangles specific processes that lead to better policy-making decisions. Additionally, forest structure is an important factor that can be detected from space to provide a more accurate estimate of carbon stocks (Simard et al., 2019b) and support assessment of mangrove vulnerability to certain drivers of mangrove degradation and loss. However, *in situ* ground data collection is needed to reduce uncertainty and provide better estimates to build blue carbon initiatives.

The Landsat archive and the temporal smoothing profiles derived from LandTrendr are practical to track historical trends and inform mangrove gain and loss. However, discrimination of mangrove forests from subsistence agriculture, coca farming and small settlements could potentially be improved with better spatial, spectral and temporal resolutions offers by new local and global datasets such as UAVSAR and NISAR respectively. Finally, identifying governance opportunities through public-private partnerships is essential, given the need to keep carbon safe and reduce deforestation (Furumo and Lambin, 2020). Consequently, reviews highlighting the

synergy between stakeholders provide crucial elements to extrapolate into other locations such as the efforts in Cispatá, the first long-term sustainable financing strategy in the Colombian Caribbean (Verra, 2021; Kuwae et al., 2022).

6 CONCLUSIONS

We produced a consistent high-resolution (30m) dataset to track annual mangrove extent change in Colombia from 1984 to 2020. Analysis of potential natural and human-induced drivers of change in three sites shows the response of the mangrove landscape. While many large mangroves remain unchanged, a 14% net decline in mangrove extent poses concern about their future status. Human activities such as gold mining, pasturelands expansion, and coca farming expansion can seriously affect mangrove cover. Colombia's mangrove ecosystems include some of the largest and relatively undisturbed mangrove extensions in the Western Hemisphere and require consistent monitoring to support management strategies that consider hydrological, climatic, and socioeconomic factors.

The three sites selected in this study *Ciénaga Grande de Santa Marta*, Gulf of Urabá, and Sanquianga, have been found to be profitable for blue carbon projects, and they could be financially sustainable based on current carbon prices over a 30-year time frame (Zeng et al., 2021). Despite the high carbon density in these locations, realistic conservation strategies are needed. For instance, the role of armed conflict processes, narcotrafficking, and local community participation is commonly ignored in these estimations. Moreover, the potential extent of mangrove blue carbon financing depends on a suite of conservation approaches and community participation that minimize current and future threats (Zeng et al., 2021).

DATA AVAILABILITY STATEMENT

The datasets presented in this article are not readily available. However, all methods details are included in the article and **Supplementary Material**. Additional inquiries can be asked to the corresponding author. A GitHub repository with all code and examples to be tested at local and regional levels is available in <https://paulomur.github.io/mangroves/>. Requests to access the datasets should be directed to pjmurillos@ut.edu.co.

AUTHOR CONTRIBUTIONS

PM-S conceptualization, methodology, writing-original draft; and LF and MS contributed to the writing, review, and supervision of the paper. All authors contributed to the article and approved the submitted version.

FUNDING

The United States Silva Carbon program provided funding. LF and MS were funded by SilvaCarbon and NASA's LCLUC programs.

ACKNOWLEDGMENTS

We thank members of IDEAM (Gustavo Galindo and Andres Zuluaga) for early discussions about mapping changes strategy. We also thank Cheryl Doughty for her review and useful

comments in the manuscript. Part of this work was performed at the Jet Propulsion Laboratory, California Institute of Technology, under contract with the National Aeronautics and Space Administration (NASA).

SUPPLEMENTARY MATERIAL

The Supplementary Material for this article can be found online at: <https://www.frontiersin.org/articles/10.3389/fmars.2022.892946/full#supplementary-material>

REFERENCES

- Alban, J.D.T.De, Jamaludin, J., de Wen, D. W., Than, M. M., and Webb, E. L. (2020). Improved Estimates of Mangrove Cover and Change Reveal Catastrophic Deforestation in Myanmar. *Environ. Res. Lett.* 15 (3), 34034. doi: 10.1088/1748-9326/ab666d
- Ballvé, T. (2013). Grassroots Masquerades: Development, Paramilitaries, and Land Laundering in Colombia. *Geoforum* 50, 62–75. doi: 10.1016/j.geoforum.2013.08.001
- Baloloy, A. B., Blanco, A. C., Sta. Ana, R. R. C., and Nadaoka, K. (2020). Development and Application of a New Mangrove Vegetation Index (MVI) for Rapid and Accurate Mangrove Mapping. *ISPRS J. Photogrammetry Remote Sens.* 166, 95–117. doi: 10.1016/j.isprsjprs.2020.06.001
- Bernal, B., Sidman, G. and Pearson, T. (2017). *Assessment of Mangrove Ecosystems in Colombia and Their Potential for Emissions Reductions and Restoration*. Arlington. Winrock International.
- Bhargava, R., Sarkar, D. and Friess, D. A. (2021). A Cloud Computing-Based Approach to Mapping Mangrove Erosion and Progradation: Case Studies From the Sundarbans and French Guiana. *Estuar. Coast. Shelf Sci.* 248, 106798. doi: 10.1016/j.ecss.2020.106798
- Bishop-Taylor, R., Nanson, R., Sagar, S., and Lymburner, L. (2021). Mapping Australia's Dynamic Coastline at Mean Sea Level Using Three Decades of Landsat Imagery. *Remote Sens. Environ.* 267, 112734. doi: 10.1016/j.rse.2021.112734
- Blanco, J. F., Estrada, E. A., Ortiz, L. F., and Urrego, L. E. (2012). Ecosystem-Wide Impacts of Deforestation in Mangroves: The Urabá Gulf (Colombian Caribbean) Case Study. *ISRN Ecol.*, 2012:1–14. doi: 10.5402/2012/958709
- Blanco-Libreros, J. F., López-Rodríguez, S. R., Valencia-Palacios, A. M., Perez-Vega, G. F., and Álvarez-León, R. (2022). Mangroves From Rainy to Desert Climates: Baseline Data to Assess Future Changes and Drivers in Colombia. *Front. Forests Global Change* 5. doi: 10.3389/ffgc.2022.772271
- Blanco, J. A., Vilorio, E. A. and Narváez B, J. C. (2006). 'ENSO and Salinity Changes in the Ciénaga Grande De Santa Marta Coastal Lagoon System, Colombian Caribbean'. *Estuarine Coast. Shelf Sci.* 66 (1–2), 157–167. doi: 10.1016/j.ecss.2005.08.001
- Botero, L. and Salzwedel, H. (1999). Rehabilitation of the Cienaga Grande De Santa Marta, a Mangrove-Estuarine System in the Caribbean Coast of Colombia. *Ocean Coast. Manage.* 42 (2–4), 243–256. doi: 10.1016/S0964-5691(98)00056-8
- Breiman, L. (2001). Random Forests. *Mach. Learn.* 45 (1), 5–32. doi: 10.1023/A:1010933404324
- Bunting, P., Rosenqvist, A., Lucas, R. M., Rebelo, L.-M., Hilarides, L., Thomas, N., et al. (2018). The Global Mangrove Watch—A New 2010 Global Baseline of Mangrove Extent. *Remote Sens.* 10, 1–19. doi: 10.3390/rs10101669
- Castellanos-Galindo, G. A., Casella, E., Tavera, H., Zapata Padilla, L. A., and Simard, M. (2021a). Structural Characteristics of the Tallest Mangrove Forests of the American Continent: A Comparison of Ground-Based, Drone and Radar Measurements. *Front. Forests Global Change* 4, 1–11. doi: 10.3389/ffgc.2021.732468
- Castellanos-Galindo, G. A., Kluger, L. C., Camargo, M. A., Cantera, J., Mancera Pineda, J. E., Blanco-Libreros, J. F., et al. (2021b). Mangrove Research in Colombia: Temporal Trends, Geographical Coverage and Research Gaps. *Estuarine Coast. Shelf Sci.* 248. doi: 10.1016/j.ecss.2020.106799
- Correa, I. and Morton, R. (2010). Caribbean Coast of Colombia. *Encyclopedia World's Coast. Landforms* 2010, 259–264. doi: 10.1007/978-1-4020-8639-7_41
- de Jong, S. M., Shen, Y., de Vries, J., Bijnaar, G., van Maanen, B., Augustinus, P., et al. (2021). Mapping Mangrove Dynamics and Colonization Patterns at the Suriname Coast Using Historic Satellite Data and the LandTrendr Algorithm. *Int. J. Appl. Earth Observat. Geoinform.* 97, 102293. doi: 10.1016/j.jag.2020.102293
- Fagua, J. C. and Ramsey, R. D. (2019). Geospatial Modeling of Land Cover Change in the Chocó-Darien Global Ecoregion of South America; One of Most Biodiverse and Rainy Areas in the World. *PLoS One* 14 (2), e0211324. doi: 10.1371/journal.pone.0211324
- Fatoyinbo, T., Feliciano, E. A., Lagomasino, D., Lee, S. K., and Trettin, C. (2018). Estimating Mangrove Aboveground Biomass From Airborne {LiDAR} Data: A Case Study From the Zambezi River Delta. *Environ. Res. Lett.* 13 (2), 25012. doi: 10.1088/1748-9326/aa9f03
- Furumo, P. R. and Lambin, E. F. (2020). Scaling Up Zero-Deforestation Initiatives Through Public-Private Partnerships: A Look Inside Post-Con Fict Colombia. *Global Environ. Change* 62, 13. doi: 10.1016/j.gloenvcha.2020.102055
- Gilani, H., Naz, H. I., Arshad, M., Nazim, K., Akram, U., Abrar, A., et al. (2021). Evaluating Mangrove Conservation and Sustainability Through Spatiotemporal, (1990–2020) Mangrove Cover Change Analysis in Pakistan. *Estuarine Coast. Shelf Sci.* 249, 107128. doi: 10.1016/j.ecss.2020.107128
- Giri, C., Ochieng, E., Tieszen, L. L., Zhu, Z., Singh, A., Loveland, T., et al. (2011). Status and Distribution of Mangrove Forests of the World Using Earth Observation Satellite Data. *Global Ecol. Biogeogr.* 20 (1), 154–159. doi: 10.1111/j.1466-8238.2010.00584.x
- Goldberg, L., Lagomasino, D., Thomas, N., and Fatoyinbo, T. (2020). Global Declines in Human-Driven Mangrove Loss. *Global Change Biol.* 26 (10), 5844–5855. doi: 10.1111/gcb.15275
- Gorelick, N., Hancher, M., Dixon, M., Ilyushchenko, S., Thau, D., and Moore, R. (2017). Google Earth Engine: Planetary-Scale Geospatial Analysis for Everyone. *Remote Sens. Environ.* 202, 18–27. doi: 10.1016/j.rse.2017.06.031
- Grajales, J. (2011). The Rifle and the Title: Paramilitary Violence, Land Grab and Land Control in Colombia. *J. Peasant Stud.* 38 (4), 771–792. doi: 10.1080/03066150.2011.607701
- Guo, Y., Liao, J. and Shen, G. (2021). Mapping Large-Scale Mangroves Along the Maritime Silk Road From 1990 to 2015 Using a Novel Deep Learning Model and Landsat Data. *Remote Sens.* 13 (2), 1–20. doi: 10.3390/rs13020245
- Hamilton, S. E. and Casey, D. (2016). Creation of a High Spatio-Temporal Resolution Global Database of Continuous Mangrove Forest Cover for the 21st Century (CGMFC-21). *Global Ecol. Biogeogr.* 25 (6), 729–738. doi: 10.1111/geb.12449
- Hamilton, S. E., Castellanos-Galindo, G. A., Millones-Mayer, M., and Chen, M. (2018). "Remote Sensing of Mangrove Forests: Current Techniques and Existing Databases," in *Threats to Mangrove Forests: Hazards, Vulnerability, and Management*. Eds. Makowski, C. and Finkl, C. W. (Cham: Springer International Publishing), 497–520. doi: 10.1007/978-3-319-73016-5_22
- Hansen, M. C., Potapov, P. V., Moore, R., Hancher, M., Turubanova, S. A., and Tyukavina, A. (2013). High-Resolution Global Maps of Forest Cover Change. *Science* 342 (6160), 850–853. doi: 10.1126/science.1244693
- IDEAM (2010). *Leyenda Nacional De Coberturas De La Tierra. Metodología CORINE Land Cover Adaptada Para Colombia Escala 1:100000* (Bogota, Colombia: IDEAM). I. de H. M. y E. A. de C.

- IGAC (1966). *Mapa General De Bosques, República De Colombia* (Bogotá, Colombia: IGAC).
- IGAC (1999). *Paisajes Fisiográficos De Orinoquía - Amazonía, Análisis Geográficos*, Vol. 27. 361.
- INVERMAR (2014). *Informe Del Estado De Los Ambientes Y Recursos Marinos Costeros En Colombia Año 2014 Instituto de Investigaciones Marinas y Costeras*. (Santa Marta, Colombia). Available at: www.invermar.org.co.
- INVERMAR (2020). *Informe Del Estado De Los Ambientes Y Recursos Marinos Y Costeros En Colombia 2020*, INVERMAR (Santa Marta: Serie de Publicaciones Periódicas No.3).
- Jaramillo, F., Licero, L., Åhlen, I., Manzoni, S., Rodríguez-Rodríguez, J. A., Guittard, A., et al. (2018). Effects of Hydroclimatic Change and Rehabilitation Activities on Salinity and Mangroves in the Ciénaga Grande De Santa Marta, Colombia. *Wetlands* 38 (4), 755–767. doi: 10.1007/s13157-018-1024-7
- Kennedy, R. E., Ohmann, J., Gregory, M., Roberts, H., Yang, Z., Bell, D. M., et al. (2018). An Empirical, Integrated Forest Biomass Monitoring System. *Environ. Res. Lett.* 13, 1–10. doi: 10.1088/1748-9326/aa9d9e
- Kennedy, R. E., Yang, Z., and Cohen, W. B. (2010). Detecting Trends in Forest Disturbance and Recovery Using Yearly Landsat Time Series: 1. LandTrendr - Temporal Segmentation Algorithms. *Remote Sens. Environ.* 114 (12), 2897–2910. doi: 10.1016/j.rse.2010.07.008
- Kuwae, T., Watanabe, A., Yoshihara, S., Suehiro, F., and Sugimura, Y. (2022). Implementation of Blue Carbon Offset Crediting for Seagrass Meadows, Macroalgal Beds, and Macroalgae Farming in Japan. *Mar. Policy* 138, 104996. doi: 10.1016/j.marpol.2022.104996
- Lee, C. K. F., Duncan, C., Nicholson, E., Fatoyinbo, T. E., Lagomasino, D., Thomas, N., et al. (2021). Mapping the Extent of Mangrove Ecosystem Degradation by Integrating an Ecological Conceptual Model With Satellite Data. *Remote Sens.* 13 (11), 1–19. doi: 10.3390/rs13112047
- López-Angarita, J., Roberts, C. M., Tilley, A., Hawkins, J. P., and Cooke, R. G. (2016). Mangroves and People: Lessons From a History of Use and Abuse in Four Latin American Countries. *For. Ecol. Manage.* 368, 151–162. doi: 10.1016/j.foreco.2016.03.020
- Luijendijk, A., Hagenaars, G., Ranasinghe, R., Baart, F., Donchyts, G., and Aarninkhof, S. (2018). The State of the World's Beaches. *Sci. Rep.* 8 (1), 1–11. doi: 10.1038/s41598-018-24630-6
- Lymburner, L., Bunting, P., Lucas, R., Scarth, P., Alam, I., Phillips, C., et al. (2020). Mapping the Multi-Decadal Mangrove Dynamics of the Australian Coastline. *Remote Sens. Environ.* 238, 111185. doi: 10.1016/j.rse.2019.05.004
- Mejía, J. F., Yepes, J., Henao, J. J., Poveda, G., Zuluaga, M. D., Raymond, D. J., et al. (2021). Towards a Mechanistic Understanding of Precipitation Over the Far Eastern Tropical Pacific and Western Colombia, One of the Rainiest Spots on Earth. *J. Geophysical Res.: Atmosph.* 126 (5), e2020JD033415. doi: 10.1029/2020JD033415
- Mejía-Rentería, J. C., Castellanos-Galindo, G. A., Cantera-Kintz, J. R., and Hamilton, S. E. (2018). A Comparison of Colombian Pacific Mangrove Extent Estimations: Implications for the Conservation of a Unique Neotropical Tidal Forest. *Estuarine Coast. Shelf Sci.* 212, 233–240. doi: 10.1016/j.ecss.2018.07.020
- Mentaschi, L., Voudoukas, M. I., Pekel, J. F., Voukouvalas, E., and Feyen, L. (2018). Global Long-Term Observations of Coastal Erosion and Accretion. *Sci. Rep.* 8 (1), 1–11. doi: 10.1038/s41598-018-30904-w
- Muñoz-mora, J. C., Johansson, S. L., Giraldo-ramírez, J., and Fortou, J. A. (2015). *This Land is My Land: Understanding the Relationship Between Armed Conflict This Land Is My Land: Understanding the Relationship Between Armed Conflict*. Work. Pap. ECARES ECARES 2015-17, ULB -- Univ. Libr. Bruxelles.
- Murillo-Sandoval, P. J., et al. Van Dexter, K., Van Den Hoek, J., Wrathall, D., and Kennedy, R. E. (2020). The End of Gunpoint Conservation: Forest Disturbance After the Colombian Peace Agreement. *Environ. Res. Lett.* 15, 1–12 (3). doi: 10.1088/1748-9326/ab6ae3
- Murillo-Sandoval, P. J., Gjerdseth, E., Correa-ayram, C., Wrathall, D., Hoek, J., Van Den, Davalos, L. M., et al. (2021). No Peace for the Forest: Rapid, Widespread Land Changes in the Andes-Amazon Region Following the Colombian Civil War. *Global Environ. Change* 69, 1–12. doi: 10.1016/j.gloenvcha.2021.102283
- Olofsson, P., Foody, G. M., Herold, M., Stehman, S. V., Woodcock, C. E., and Wulder, M. A. (2014). Good Practices for Estimating Area and Assessing Accuracy of Land Change. *Remote Sens. Environ.* 148, 42–57. doi: 10.1016/j.rse.2014.02.015
- Olofsson, P., Holden, C. E., Bullock, E. L., and Woodcock, C. E. (2016). 'Time Series Analysis of Satellite Data Reveals Continuous Deforestation of New England Since the 1980s'. *Environ. Res. Lett.* 6, 1–8. doi: 10.1088/1748-9326/11/6/064002
- Olofsson, P., Arévalo, P., Espejo, A. B., Green, C., Lindquist, E., McRoberts, R. E., et al. (2020). Mitigating the Effects of Omission Errors on Area and Area Change Estimates. *Remote Sens. Environ.* 236, 111492. doi: 10.1016/j.rse.2019.111492
- Ostrom, E. and Nagendra, H. (2006). Insights on Linking Forests, Trees, and People From the Air, on the Ground, and in the Laboratory. *Proc. Natl. Acad. Sci.* 103 (51), 19224–19231. doi: 10.1073/pnas.0607962103
- Palacios, M. L. and Cantera, J. R. (2017). Mangrove Timber Use as an Ecosystem Service in the Colombian Pacific. *Hydrobiologia* 803 (1), 345–358. doi: 10.1007/s10750-017-3309-x
- Parra, A. S. and Restrepo-Angel, J. D. (2014). El Colapso Ambiental En El Rio Patia, Colombia: Variaciones Morfológicas Y Alteraciones En Los Ecosistemas De Manglar. *Latin Am. J. Aquat. Res.* 42 (1), 40–60. doi: 10.3856/vol42-issue1-fulltext-4
- Pasquarella, V. J., Holden, C. E., Kaufman, L., and Woodcock, C. E. (2016). From Imagery to Ecology: Leveraging Time Series of All Available Landsat Observations to Map and Monitor Ecosystem State and Dynamics. *Remote Sens. Ecol. Conserv.*, 2, 1–19. doi: 10.1002/rse2.24
- Pekel, J.-F., Cottam, A., Gorelick, N., and Belward, A. S. (2016). High-Resolution Mapping of Global Surface Water and its Long-Term Changes. *Nature* 540 (7633), 418–422. doi: 10.1038/nature20584
- Polidoro, B. A., Carpenter, K. E., Collins, L., Duke, N. C., Ellison, A. M., Ellison, J. C., et al. (2010). The Loss of Species: Mangrove Extinction Risk and Geographic Areas of Global Concern. *PLoS One* 5 (4), 1–10. doi: 10.1371/journal.pone.0010095
- Restrepo, A. J. D. (2012). Assessing the Effect of Sea-Level Change and Human Activities on a Major Delta on the Pacific Coast of Northern South America: The Patia River. *Geomorphology* 151–152, 207–223. doi: 10.1016/j.geomorph.2012.02.004
- Riascos, J. M., Cantera, J. R. and Blanco-Libreros, J. F. (2018). Growth and Mortality of Mangrove Seedlings in the Wettest Neotropical Mangrove Forests During ENSO: Implications for Vulnerability to Climate Change. *Aquat. Bot.* 147, 34–42. doi: 10.1016/j.aquabot.2018.03.002
- Roy, D. P., Kovalsky, V., Zhang, H. K., Vermote, E. F., Yan, L., Kumar, S. S., et al. 2016. Characterization of Landsat-7 to Landsat-8 Reflective Wavelength and Normalized Difference Vegetation Index Continuity. *Remote Sens. Environ.*, 185, 57–70. doi: 10.1016/j.rse.2015.12.024
- Ruiz-Luna, A., Acosta-Velázquez, J. and Berlanga-Robles, C. A. (2008). On the Reliability of the Data of the Extent of Mangroves: A Case Study in Mexico. *Ocean Coast. Manage.* 51 (4), 342–351. doi: 10.1016/j.ocecoaman.2007.08.004
- Shahbudin, S., Zuhairi, A. and Kamaruzzaman, B. Y. (2012). Impact of Coastal Development on Mangrove Cover in Kilim River, Langkawi Island, Malaysia. *J. Forest. Res.* 23 (2), 185–190. doi: 10.1007/s11676-011-0218-0
- Shepherd, J. D. and Dymond, J. R. (2003). Correcting Satellite Imagery for the Variance of Reflectance and Illumination With Topography. *Int. J. Remote Sens.* 24 (17), 3503–3514. doi: 10.1080/01431160210154029
- Simard, M., Rivera-Monroy, V. H., Mancera-Pineda, J. E., Castañeda-Moya, E., and Twilley, R. R. (2008). A Systematic Method for 3D Mapping of Mangrove Forests Based on Shuttle Radar Topography Mission Elevation Data, ICESat/GLAS Waveforms and Field Data: Application to Ciénaga Grande De Santa Marta, Colombia. *Remote Sens. Environ.* 112 (5), 2131–2144. doi: 10.1016/j.rse.2007.10.012
- Simard, M., Fatoyinbo, T., Smetanka, C., Rivera-Monroy, V. H., Castañeda-Moya, E., Thomas, N., et al. (2019a). 'Global Mangrove Distribution, Aboveground Biomass, and Canopy Height' (ORNL Distributed Active Archive Center). doi: 10.3334/ORNLDAAC/1665
- Simard, M., Fatoyinbo, T., Smetanka, C., Rivera-Monroy, V. H., Castañeda-Moya, E., Thomas, N., et al. (2019b). Mangrove Canopy Height Globally Related to Precipitation, Temperature and Cyclone Frequency. *Nat. Geosci.* 12 (1), 40–45. doi: 10.1038/s41561-018-0279-1
- Suyadi, Gao, J., Lundquist, C. J., and Schwendenmann, L. (2018). Sources of Uncertainty in Mapping Temperate Mangroves and Their Minimization Using Innovative Methods. *Int. J. Remote Sens.* 39 (1), 17–36. doi: 10.1080/01431161.2017.1378455

- Tang, W., Zheng, M., Zhao, X., Shi, J., Yang, J., and Trettin, C. C. (2018). Big Geospatial Data Analytics for Global Mangrove Biomass and Carbon Estimation. *Sustainability*. 10, 1–17. doi: 10.3390/su10020472
- Tassi, A. and Vizzari, M. (2020). Object-Oriented LULC Classification in Google Earth Engine Combining SNIC, GLCM, and Machine Learning Algorithms. *Remote Sens.* 12, 1–17. doi: 10.3390/rs12223776
- Thampanya, U., Vermaat, J. E., Sinsakul, S., and Panapitukkul, N. (2006). Coastal Erosion and Mangrove Progradation of Southern Thailand. *Estuarine Coast. Shelf Sci.* 68 (1), 75–85. doi: 10.1016/j.ecss.2006.01.011
- Thomas, N., Lucas, R., Bunting, P., Hardy, A., Rosenqvist, A., and Simard, M. (2017). Distribution and Drivers of Global Mangrove Forest Change 1996–2010. *PLoS One* 12 (6), 1–14. doi: 10.1371/journal.pone.0179302
- Thomas, N., et al. (2018). Mapping Mangrove Extent and Change: A Globally Applicable Approach. *Remote Sens.* 10 (9), 1–20. doi: 10.3390/rs10091466
- Treviño, M. and Murillo-Sandoval, P. J. (2021). Uneven Consequences: Gendered Impacts of Shrimp Aquaculture Development on Mangrove Dependent Communities. *Ocean Coast. Manage.* 210, 1–13. doi: 10.1016/j.ocecoaman.2021.105688
- Truth Commission - Forensic Architecture (2021). in *Dispossession and the Memory of the Earth: Land Dispossession in Nueva Colonia*. Bogota, Colombia. Available at: <https://forensic-architecture.org/investigation/land-dispossession-in-nueva-colonia>.
- UNODC (2017) *Colombia Survey of Territories Affected by Illicit Crops – 2016*. Available at: https://www.unodc.org/documents/crop-monitoring/Colombia/Colombia_Coca_survey_2016_English_web.pdf.
- Van doninck, J. and Tuomisto, H. (2018). A Landsat Composite Covering All Amazonia for Applications in Ecology and Conservation. *Remote Sens. Ecol. Conserv.* 4 (3), 197–210. doi: 10.1002/rse2.77
- Vélez-Castaño, J. D., Betancurth-Montes, G. L. and Cañón-Barriga, J. E. (2021). Erosion and Progradation in the Atrato River Delta: A Spatiotemporal Analysis With Google Earth Engine. *Rev. Facultad Ingeniería* 99, 83–98. doi: 10.17533/udea.redin.20200688
- Verra (2021) *Verra Has Registered Its First Blue Carbon Conservation Project*. Available at: <https://verra.org/>.
- Villate Daza, D. A., Sánchez Moreno, H., Portz, L., Portantiolo Manzolli, R., Bolívar-Anillo, H. J., and Anfuso, G. (2020). Mangrove Forests Evolution and Threats in the Caribbean Sea of Colombia. *Water*, 12, 1–20. doi: 10.3390/w12041113
- Xie, S., Liu, L. and Yang, J. (2020). Time-Series Model-Adjusted Percentile Features: Improved Percentile Features for Land-Cover Classification Based on Landsat Data. *Remote Sens.* 12(18), 1–24. doi: 10.3390/rs12183091
- Yang, S. L., Li, H., Ysebaert, T., Bouma, T. J., Zhang, W. X., Wang, Y. Y., et al. (2008). Spatial and Temporal Variations in Sediment Grain Size in Tidal Wetlands, Yangtze Delta: On the Role of Physical and Biotic Controls. *Estuarine Coast. Shelf Sci.* 77 (4), 657–671. doi: 10.1016/j.ecss.2007.10.024
- Zambrano Escamilla, C. H. and Rubiano-Rubiano, D. J. (1996). *Memoria De Los Mapas De Los Bosques De Manglar Del Caribe Colombiano: 1996. Proy. PD 171/91 Rev. 2 (F) Fase I 'Conservación Y Manejo Para El Usos Múltiple Y El Desarrollo De Los Manglares En Colombia', MMA/OIMT. Tech. Rep. 8, 1–41 + 81 Cartas (1 :100000)* (SantaFé de Bogotá: MINAMBIENTE).
- Zanaga, D., Van De Kerchove, R., De Keersmaecker, W., Souverijns, N., Brockmann, C., Quast, R., et al. (2021). *ESA WorldCover 10 M 2020 V100*. doi: 10.5281/zenodo.5571936
- Zeng, Y., Friess, D. A., Sarira, T. V., Siman, K., and Koh, L. P. (2021). Global Potential and Limits of Mangrove Blue Carbon for Climate Change Mitigation. *Curr. Biol.* 31 (8), 1737–1743.e3. doi: 10.1016/j.cub.2021.01.070
- Zhang, H. K. and Roy, D. P. (2017). Using the 500 M MODIS Land Cover Product to Derive a Consistent Continental Scale 30 M Landsat Land Cover Classification. *Remote Sens. Environ.* 197, 15–34. doi: 10.1016/j.rse.2017.05.024
- Zhu, Z. (2017). Change Detection Using Landsat Time Series: A Review of Frequencies, Preprocessing, Algorithms, and Applications. *ISPRS J. Photogrammetry Remote Sens.* 130, 370–384. doi: 10.1016/j.isprsjprs.2017.06.013

Conflict of Interest: The authors declare that the research was conducted in the absence of any commercial or financial relationships that could be construed as a potential conflict of interest.

Publisher's Note: All claims expressed in this article are solely those of the authors and do not necessarily represent those of their affiliated organizations, or those of the publisher, the editors and the reviewers. Any product that may be evaluated in this article, or claim that may be made by its manufacturer, is not guaranteed or endorsed by the publisher.

Copyright © 2022 Murillo-Sandoval, Fatoyinbo and Simard. This is an open-access article distributed under the terms of the Creative Commons Attribution License (CC BY). The use, distribution or reproduction in other forums is permitted, provided the original author(s) and the copyright owner(s) are credited and that the original publication in this journal is cited, in accordance with accepted academic practice. No use, distribution or reproduction is permitted which does not comply with these terms.



Spatially Explicit Seagrass Extent Mapping Across the Entire Mediterranean

Dimosthenis Traganos^{1*}, Chengfa Benjamin Lee¹, Alina Blume¹, Dimitris Poursanidis², Hrvoje Čižmek³, Julie Deter^{4,5}, Vesna Mačić⁶, Monica Montefalcone⁷, Gérard Pergent⁸, Christine Pergent-Martini⁸, Aurora M. Ricart^{9,10} and Peter Reinartz¹¹

¹German Aerospace Center (DLR), Remote Sensing Technology Institute -, Berlin, Germany, ²Foundation for Research and Technology - Hellas (FORTH), Institute of Applied and Computational Mathematics, Heraklion, Greece, ³Marine Explorers Society - 20000 Leagues, Zadar, Croatia, ⁴Andromède Océanologie, Manguio, France, ⁵MARBEQ, Univ Montpellier, CNRS, IFREMER, IRD, labcom InToSea, Montpellier, France, ⁶Institute of Marine Biology, University of Montenegro, Kotor, Montenegro, ⁷Department of Earth, Environment and Life Sciences (DISTAV), University of Genoa, Genoa, Italy, ⁸EqEL – UMR CNRS 6134 SPE, University of Corsica Pascal Paoli, Corte, France, ⁹Bodega Marine Laboratory-University of California, Davis, Bodega Bay, CA, United States, ¹⁰Bigelow Laboratory for Ocean Sciences, East Boothbay, ME, United States, ¹¹German Aerospace Center (DLR), Earth Observation Center (EOC), Weßling, Germany

OPEN ACCESS

Edited by:

Catherine Lovelock,
The University of Queensland,
Australia

Reviewed by:

Maria Laura Zoffoli,
National Research Council (CNR),
Italy

Konstantinos Topouzelis,
University of the Aegean, Greece

*Correspondence:

Dimosthenis Traganos
dimosthenis.traganos@dlr.de

Specialty section:

This article was submitted to
Global Change and
the Future Ocean,
a section of the journal
Frontiers in Marine Science

Received: 08 February 2022

Accepted: 22 June 2022

Published: 22 July 2022

Citation:

Traganos D, Lee CB, Blume A, Poursanidis D, Čižmek H, Deter J, Mačić V, Montefalcone M, Pergent G, Pergent-Martini C, Ricart AM and Reinartz P (2022) Spatially Explicit Seagrass Extent Mapping Across the Entire Mediterranean. *Front. Mar. Sci.* 9:871799. doi: 10.3389/fmars.2022.871799

The seagrass *Posidonia oceanica* is the main habitat-forming species of the coastal Mediterranean, providing millennial-scale ecosystem services including habitat provisioning, biodiversity maintenance, food security, coastal protection, and carbon sequestration. Meadows of this endemic seagrass species represent the largest carbon storage among seagrasses around the world, largely contributing to global blue carbon stocks. Yet, the slow growth of this temperate species and the extreme projected temperature and sea-level rise due to climate change increase the risk of reduction and loss of these services. Currently, there are knowledge gaps in its basin-wide spatially explicit extent and relevant accounting, therefore accurate and efficient mapping of its distribution and trajectories of change is needed. Here, we leveraged contemporary advances in Earth Observation—cloud computing, open satellite data, and machine learning—with field observations through a cloud-native geoprocessing framework to account the spatially explicit ecosystem extent of *P. oceanica* seagrass across its full bioregional scale. Employing 279,186 Sentinel-2 satellite images between 2015 and 2019, and a human-labeled training dataset of 62,928 pixels, we mapped 19,020 km² of *P. oceanica* meadows up to 25 m of depth in 22 Mediterranean countries, across a total seabed area of 56,783 km². Using 2,480 independent, field-based points, we observe an overall accuracy of 72%. We include and discuss global and region-specific seagrass blue carbon stocks using our bioregional seagrass extent estimate. As reference data collections, remote sensing technology and biophysical modelling improve and coalesce, such spatial ecosystem extent accounts could further support physical and monetary accounting of seagrass condition and ecosystem services, like blue carbon and coastal biodiversity. We envisage that effective policy uptake of these holistic seagrass accounts in national climate strategies and financing could accelerate transparent natural climate solutions and coastal resilience, far beyond the physical location of seagrass beds.

Keywords: Mediterranean, Sentinel-2, *Posidonia oceanica*, Coastal ecosystem accounting, Google Earth Engine Seagrass, Earth Observation, Blue Carbon

INTRODUCTION

The Mediterranean coastal seascape hosts 18% of all known marine species, 31% of the global tourism, and 2% of the global population across 48,300 km of coastline (Coll et al., 2010; UNEP/MAP, 2012). Seagrasses—marine flowering plants forming submerged meadows up to 40 m deep—and especially the endemic and most common species in the basin *Posidonia oceanica*—have been the bioengineers of this structurally complex seascape framework for millennia (Arnaud-Haond et al., 2012). Covering less than 2% of the total Mediterranean seabed, the *P. oceanica* seagrass meadows provide a plethora of ecosystem services valued between 57,000 to 184,000 €/ha/year (Paoli et al., 2018; Rigo et al., 2021) and are globally significant carbon sinks, with greater organic carbon density than the observed one in estuarine mangroves, peatlands or tropical forests (IUCN, 2021). The large efficiency of such vegetated coastal ecosystems in absorbing and storing carbon, and thus reducing atmospheric carbon dioxide concentration, has led to initiatives to include them in climate change mitigation strategies like REDD+ (Reducing Emissions from Deforestation and Forest Degradation) (Duarte et al., 2013). Such initiatives are further supported by the observation that *P. oceanica* seagrass meadows could have sequestered up to 42% of the carbon emitted by all Mediterranean countries since the onset of the Industrial Revolution (Pergent et al., 2014).

Due to numerous anthropogenic impacts, including coastal development, eutrophication, anchoring, and illegal fishing, the Mediterranean seascape has experienced a net loss of 6,990 ha in the coverage of *P. oceanica* meadows between 1869 and 2016, with, however, a reversed decline trend since the 1990s (de los Santos et al., 2019). A regional climate warming of 1.5°C above pre-industrial levels coupled with *P. oceanica*'s slow growth (1 cm yr⁻¹) (Marbà and Duarte, 1998) would accelerate its loss (Jordà et al., 2012) with associated risks to biodiversity, food security, livelihoods, tourism, and, ultimately, coastal protection. The observed decline of the *P. oceanica* meadows and the lack of suitable spatially explicit monitoring necessitate accurate and continuous mapping and monitoring of their extent, trajectory of change, and condition. Such monitoring efforts can enable a better understanding and detection of hotspots of sensitivity and resilience not only for effective management and protection but also for climate change mitigation and adaptation strategies across the basin.

In the past five years, advances in Earth Observation technology—high spatial and temporal satellite data archives—as well as cloud computing power and artificial intelligence (AI) have enabled data-driven measurements, monitoring, and change detection in the distribution, trends, and health of the coastal environment, from a regional to global scale (Bunting et al., 2018; Murray et al., 2019; Purkis et al., 2019; Lyons et al., 2020). Such large-scale Earth Observation efforts require consistent, accurate, and well-distributed reference data of extensive magnitude in space and time to calibrate and validate their mapping products. These mapping products could enable seascape management and conservation at national and global scales, and climate

change mitigation schemes like the Nationally Determined Contributions (United Nations Framework Convention on Climate Change, 2021); and could support the efficacy of the Sustainable Development Goals relevant to the coastal marine environment—namely Goal 6, 13 and 14—by 2030 (United Nations, 2015).

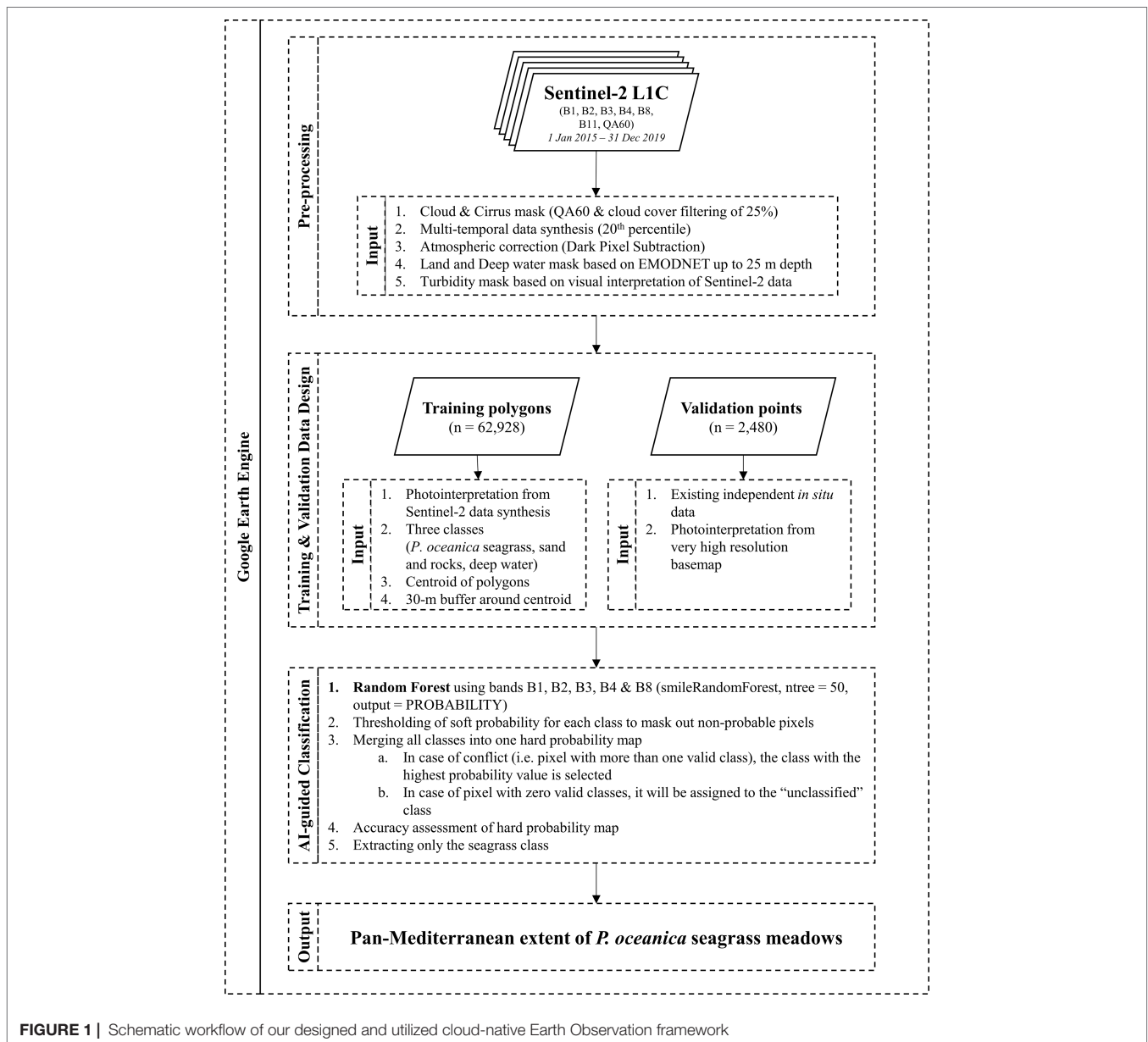
In this study, we have expanded an end-to-end cloud-native—built and run entirely within a cloud computing environment—Earth Observation algorithmic framework (Traganos et al., 2018) using the cloud geospatial platform of the Google Earth Engine (GEE) (Gorelick et al., 2017). We utilized this algorithmic framework to map, for the first time, the *P. oceanica* seagrass ecosystem extent at its whole bioregion scale of 56,783 km² that includes 22 countries. The GEE cloud geospatial platform enabled the storage, processing, and analysis of a mosaic of 279,186 open satellite Sentinel-2 images (Gascon et al., 2017) between 2015 and 2019, the mosaic classification *via* the cloud-based machine learning (ML) algorithm of the Random Forests (RF) (Gislason et al., 2006), and the development of an inventory of human-labeled training data to guide the ML-based classification. For the latter, we annotated 1,748 training blocks consisting of 62,928 100-m² pixels indicative of the different Mediterranean benthic classes i.e., seagrass meadows, rocky reefs and sandy bottom, and optically deep water. Optically deep waters are regions where the remote sensing signal does not provide any bottom information due to the light attenuation from the water column. To validate the mapping results, we collected and utilized an independent (both spatially and source-wise) inventory of existing field-based data (2,480 points).

METHODS

The Cloud-Native Earth Observation Framework

As part of this study, we improved a recent cloud-native algorithmic framework (Traganos et al., 2018). This framework was built upon the advances in Earth Observation technology in terms of open petabyte-scale satellite datasets, high-performance cloud computational power, supervised machine learning, web-based visualization capabilities, and human-guided design of large-scale training data suitable for the supervision of the ML component—all of which are powered by the cloud infrastructure of the GEE.

The cloud-native existence of the evolved Earth Observation framework (**Figure 1**) allowed a time- and cost-efficient scalability in three dimensions: space (e.g., region, country, basin), time (e.g., monthly, seasonal, annual, multiannual), and satellite data input. The time dimension here encompassed multi-temporal analytics based on the combination of metadata selection and statistical analysis of all available satellite images within a given period. The result of multi-temporal analytics is a pseudo-image whose pixels contain the least amount of clouds, aerosols, waves, and reflection from the sea surface—all of the above being common natural obstacles within satellite scenes over coastal waters.



The Multi-Temporal Sentinel-2 Satellite Image Mosaic

The aforementioned three components were adjusted according to our mapping task. To map the basin-scale seagrass distribution of *P. oceanica*, we scaled up the framework (Traganos et al., 2018) throughout the first 25 m of the depth of the Mediterranean, a total of 56,783 km². We identified this depth range utilizing the EMODnet Bathymetry Digital Terrain Model (DTM) for the European Seas of 2018 (<https://www.emodnet.eu/new-high-resolution-digital-terrain-model>), which is a composite of bathymetric datasets from different sources at ~115m x 115 m resolution. We empirically selected the 25 m cut off depth as the most representative deep limit of seabed detection of the Sentinel-2 satellite—guided by water quality and human expert knowledge—in both the western and eastern basin part of the

Mediterranean (Poursanidis et al., 2019) (Supplementary Table S2; Figures S3–S8). This depth limit is a balance between removing as many optically deep water pixels as possible without accidentally misidentifying and removing seagrass pixels, since both classes have similar spectral values. A deeper limit would include many more optically deep pixels, which could lead to potential false positives of seagrass presence; while a shallower limit would conversely mask many potential true positives of *P. oceanica* seagrass regions, especially within the optically shallower eastern basin.

Additionally, we manually masked extensive regions of turbid waters (mainly in north Italy, Egypt, Syria, and southeast Turkey), which would obscure the seabed detection. Finally, pixels from 279,186 satellite image tiles of Sentinel-2—100x100 km² images—acquired between 23 June 2015 and

31 December 2019 synthesized the multi-annual mosaic at 10 m resolution—a full-archive synthesis of Sentinel-2 images over the Mediterranean at the time of its creation. The multi-temporal synthesis was essentially a statistical reduction of all land, cloud and deep-water-filtered images to the 25th percentile per pixel, a reduction deemed necessary to automatically filter out natural interferences like remaining clouds, haze, waves, sunglint and similar. As these Sentinel-2 images are top-of-the-atmosphere satellite data, we also employed the modified dark pixel subtraction method (Traganos et al., 2018) to account for the atmospheric effect in these data.

Training Data

Before describing the artificial intelligence component in the heart of our cloud-native framework, it is important to describe our training data design—essentially, the type of data that guides the AI. The training data were labeled following human-guided photointerpretation of the Sentinel-2 image mosaic by an expert on both Earth Observation image analysis and the nature of the Mediterranean coastal seascape. The expert spent 100 working hours within the cloud geospatial environment to annotate polygons indicative of the presence of three habitat classes: a) seagrasses (*P. oceanica*), b) optically deep water, and c) rocky and sandy seabed (**Table 1**). We decided to design polygons on *P. oceanica* seagrass meadows and not on other Mediterranean seagrass species (e.g., *C. nodosa*, *Z. marina*) as the sparse natural distribution of the latter species would have caused confusion on the 10 m spatial resolution of Sentinel-2. Therefore, it is expected that the spectral similarities between *P. oceanica* and other seagrass beds may have caused over-estimations and misclassification of the former class in our mapping effort. The human photointerpreter designed the training data by choosing polygons from all depths (shallow to deep), distribution (eastern and western basin), and density gradient (sparse to dense) of the studied habitats.

Sequentially, the final training dataset consisted of 1,748 polygons which were first reduced to centroids (**Figure 2**) and then were grown to blocks of a 30-m circular radius buffer around the centroids i.e., ~36 Sentinel-2-pixel blocks of 3,600 m² each (**Table 1**). This means that we allocated 1.1 training point for each square kilometer of the mapped seabed, on average (62,928 training pixels for all 56,783 km² of seabed area). This ensured a robust plethora of training blocks of pure pixels for each class.

Artificial Intelligence

We employed the training data to guide the Random Forests artificial intelligence framework (Breiman, 2001) and classify the multi-annual Sentinel-2 mosaic at 10 m resolution. RF is an ensemble supervised machine learning classification algorithm that incorporates numerous self-learning decision trees that can handle both collinearity and non-linearity between predictor variables (e.g., the often non-linear border of *Poceanica* seagrass meadows with the unconsolidated fine sediments). The rationale behind choosing RF was two-fold: a) their robustness against overtraining and noisy data (Gislason et al., 2006) that could still arise from our training data design; and b) their high accuracies in multi-scale coastal habitat mapping in local and serverless environments (Traganos and Reinartz, 2018a; Traganos and Reinartz, 2018b; Poursanidis et al., 2019; Lyons et al., 2020).

We parameterized and ran the RF within the GEE platform using the probability mode. This essentially creates an intermediate soft probability of presence or *soft classification* of each class varying between 0 and 100. This means that each pixel in this intermediate continuous layer represent probability of presence between 0 and 100%. We ran a series of quantitative and qualitative analyses to determine the best threshold value for the presence of seagrasses in both the western and eastern part of the basin. Then, we merged all classes into one hard probability habitat map containing all pixels—the *hard classification*. In contrast to the continuous soft probability layer, the hard probability/classification layer is a thematic product with each pixel representing a different class. This allowed us to delve into our classification experiments, further decreasing a possible over-estimation resulting from potential noise in the training data. Based on our analyses, the ideal threshold values for the soft-to-hard transformation were 45 in the West Mediterranean and 77 in the East. **Figure 3** displays the spectral ranges of the training and validation data in both Western and Eastern Mediterranean across our utilized Sentinel-2 bands.

Validation Data and Accuracy Assessment

To assess the accuracy of our bioregional map, we synthesized existing independent field-based validation data of *P. oceanica* seagrass meadows and neighboring habitats. During this synthesis, we collected high-resolution seagrass habitat maps developed previously in the Mediterranean by trained experts and scientists in the seagrass domain resulting in *in situ* data of total coverage of 3,274 km². **Table 2** indicates information on the coverage, temporal range, and source of the reference data.

TABLE 1 | Name and definition of the human-labeled classes along with the number of designed training pixel blocks and points.

Class name	Class definition	Number of Blocks	Number of Points	Total area (km ²)
Seagrass	Seabed covered by <i>P. oceanica</i> seagrass meadows	401	14,436	1.4
Optically deep water	Areas where the seabed is not visible on the Sentinel-2 mosaic	300	10,800	1.1
Seabed covered with sand or rocks	Areas with fine unconsolidated sediments or exposed hard bare substrates	1,047	37,692	3.8
		1,748 (total)	62,928 (total)	6.3

The training points were used to guide the pan-Mediterranean mapping with the aid of the ML classifier of Random Forests.

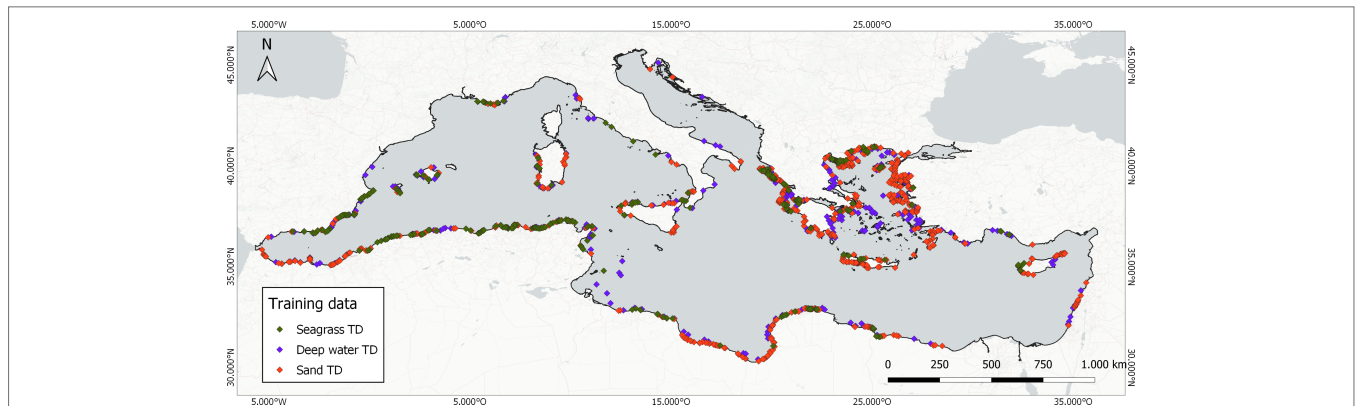


FIGURE 2 | Distribution of the centroids of the 1,748 image-annotated training data blocks indicative of the presence of the three mapped classes.

In addition to approaching our annotated data with as much independence as possible to reduce possible bias, the reference data featured higher quality and finer spatial resolution (Finegold et al., 2016) following field collection by trained experts *via* snorkeling, diving, and/or with the use of other technical equipment.

An independent analyst (not being the same person who annotated the training data) randomly selected data for the three habitat classes from the total amount of training data (3.8% on average), which resulted in 680 points for the seagrass class, 350 points for the optically deep water class, and 1,450 points

for the sandy and rocky class (**Figure 4**). We decided to have a merged sandy and rocky class as the latter class was poorly represented across the entire basin based on both its natural distribution and the validation data availability and thus would have caused a rather biased representation in the confusion matrix and classification. The design was performed on a local GIS environment using three sources of data for guidance: a) the outline of the EMODnet DTM 0–25 m extent to ensure that all validation points fall within these limits; b) the higher spatial resolution satellite base maps of Google Earth Pro and the BING imagery platform independently from the Sentinel-2 data; and

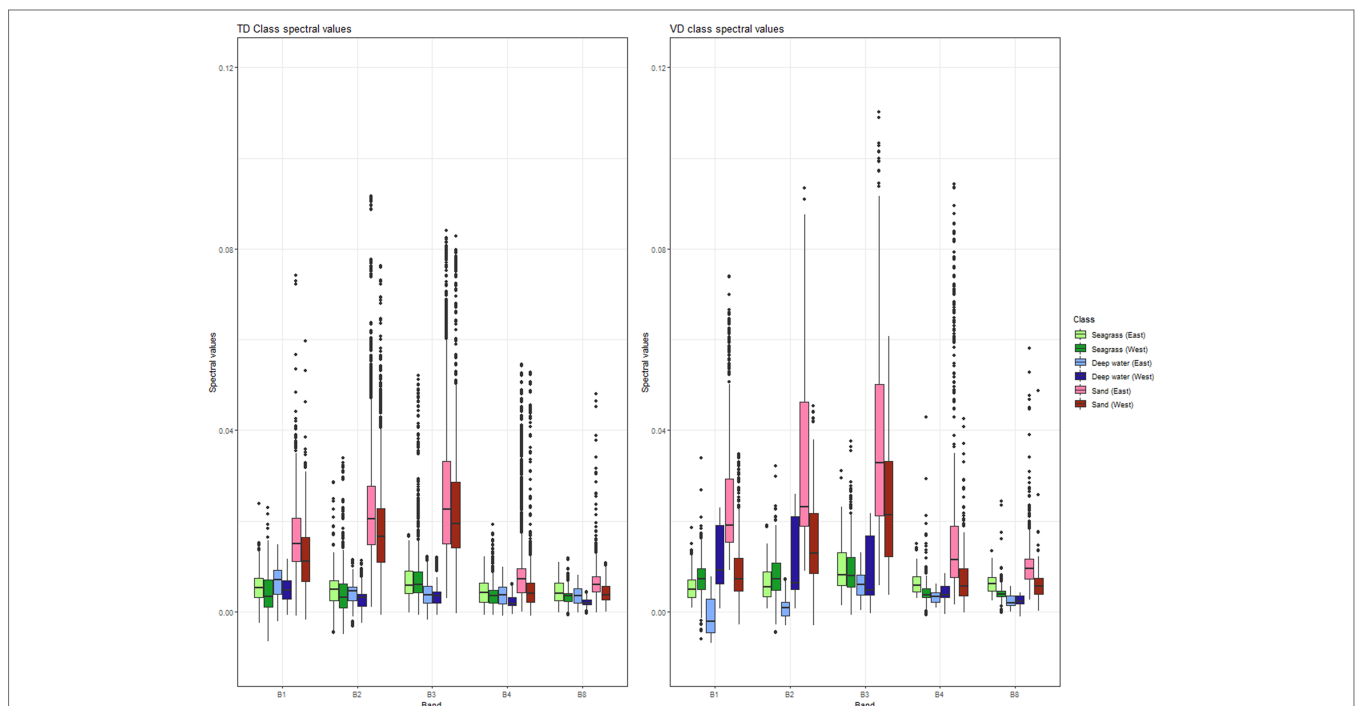


FIGURE 3 | Spectral ranges of the training and validation data in both eastern and western Mediterranean across the B1–B4, and B8 bands of our multi-temporal Sentinel-2 data mosaic. Bright and dark hues of each color code reflect eastern and western reference data and green, blue, and red hues reflect the seagrass, deep water, and sand classes respectively. The split into eastern and western regions was in consideration of their dissimilar spectral reflectances (**Supplementary Figure S8**). This is more pronounced in the validation data where many of the interquartile ranges (the boxes of the boxplots) within each class in all the bands have either a small or no overlap. The lines within the boxes indicate the median.

TABLE 2 | Analytical information about the herein employed independent validation (reference) data.

Country	Coverage (km ²)	Temporal Range	Citation
Croatia	63.6	2012-2017	Čižmek (2017)
France	2,166.1	2010-2016	Andromède Océanologie (2019)
France	569.8	2010-2016	Pergent-Martini et al. (2015)
Montenegro	98.6	2010-2018	DFS Montenegro Engineering (2012)
Spain	142.8	2008-2017	Ricart (2016); Atlas of Posidonia (2019) GENCAT (2021)
Turkey	233.2	2016-2018	Duman et al. (2019)
	3,274 (Total)		

c) a hot-spot map based on the training data to ensure spatial independency between the latter and the validation data to further reduce potential spatial bias.

To assess the accuracy of our habitat mapping approach, we employed standard quantitative metrics in Earth Observation analysis: the Overall Accuracy—the proportion of area that is classified correctly; the Producer's Accuracy—informing whether map classes were under-estimations; and the User's Accuracy—reflecting whether the classified map is overestimated. We reported these metrics through the cross-tabulation of the labeled classes populated by the classification results and the reference data; the so-called “error matrix” (**Supplementary Table S1**).

RESULTS

The Pan-Mediterranean Extent of *P. oceanica* Seagrass Meadows

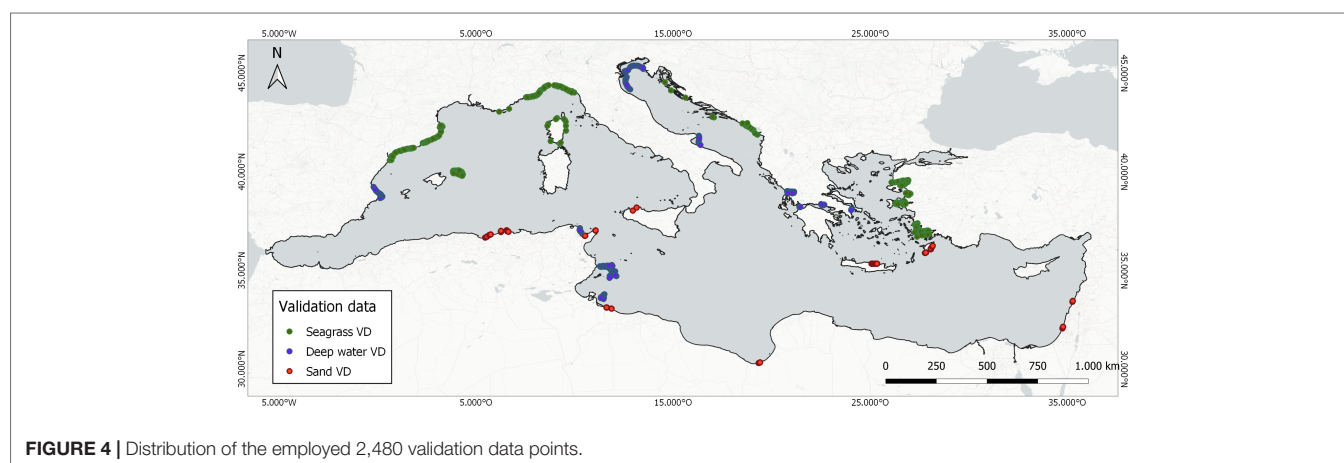
We estimated a basin-wide seagrass area of 19,020 km² between 0 and 25 m of depth in 22 countries with 72% overall accuracy—4,325 km² in the Eastern basin (overall accuracy of 79%) and 14,694 km² in the Western basin (overall accuracy of 64%). The producer's and user's accuracies of our seagrass product are 55% and 62% respectively (**Supplementary Table S1**). Our coverage estimate at the basin scale is 55.3% larger than the seagrass area synthesis in Telesca et al. (2015) (12,247 km²), 34.2% larger than the higher-confidence area synthesis of McKenzie et al. (2020) (14,167 km²), and around 1/6 of the MaxEnt-based modeled estimate of Jayatilake and Costello

(2018) (118,913 km²). **Figure 5** shows the bioregional extent of *P. oceanica* seagrass meadows across the entire Mediterranean.

Country-Scale *P. oceanica* Seagrass Area Inventories

Table 3 depicts the country-scale *P. oceanica* seagrass extent estimates across 22 Mediterranean countries between 0 and 25 m of depth, based on the spatial resolution of 10 m of Sentinel-2 data. The three countries with the largest *P. oceanica* seagrass meadows were Tunisia (6,369 km²), Italy (3,261 km²), and Greece (2,878 km²) (**Table 3**). The three countries with the largest seagrasses by km of Mediterranean coastline were Tunisia (3.4 km²/km), Montenegro (0.8 km²/km), and Croatia (0.5 km²/km). The 13 European countries with a Mediterranean coastline counted a total *P. oceanica* seagrass area of 10,932 km² (57.5% of the total seagrass bioregional area). The five African countries have an estimated total seagrass area of 7,310 km² (38.4% of the total bioregional seagrass area) and the five Asian countries a total seagrass extent of 778 km² (4.1% of the pan-Mediterranean seagrass extent).

In comparison to the data gaps in *P. oceanica* seagrass meadows in Telesca et al. (2015) (46.7% featured missing data on seagrasses), our baseline spatially explicit estimate features: a greater coverage of the coastline of several countries (e.g., +92% in Greece, +89% in Libya, +86% in Croatia, and +84% in Algeria), one additional country-scale estimate (Bosnia and Herzegovina), and one additional overseas territory (UK - Gibraltar). Finally, in relation to the country-scale seagrass area of Greece, we estimated a 13.7% larger area than the estimation of 2,510 km² (Traganos

**FIGURE 4** | Distribution of the employed 2,480 validation data points.

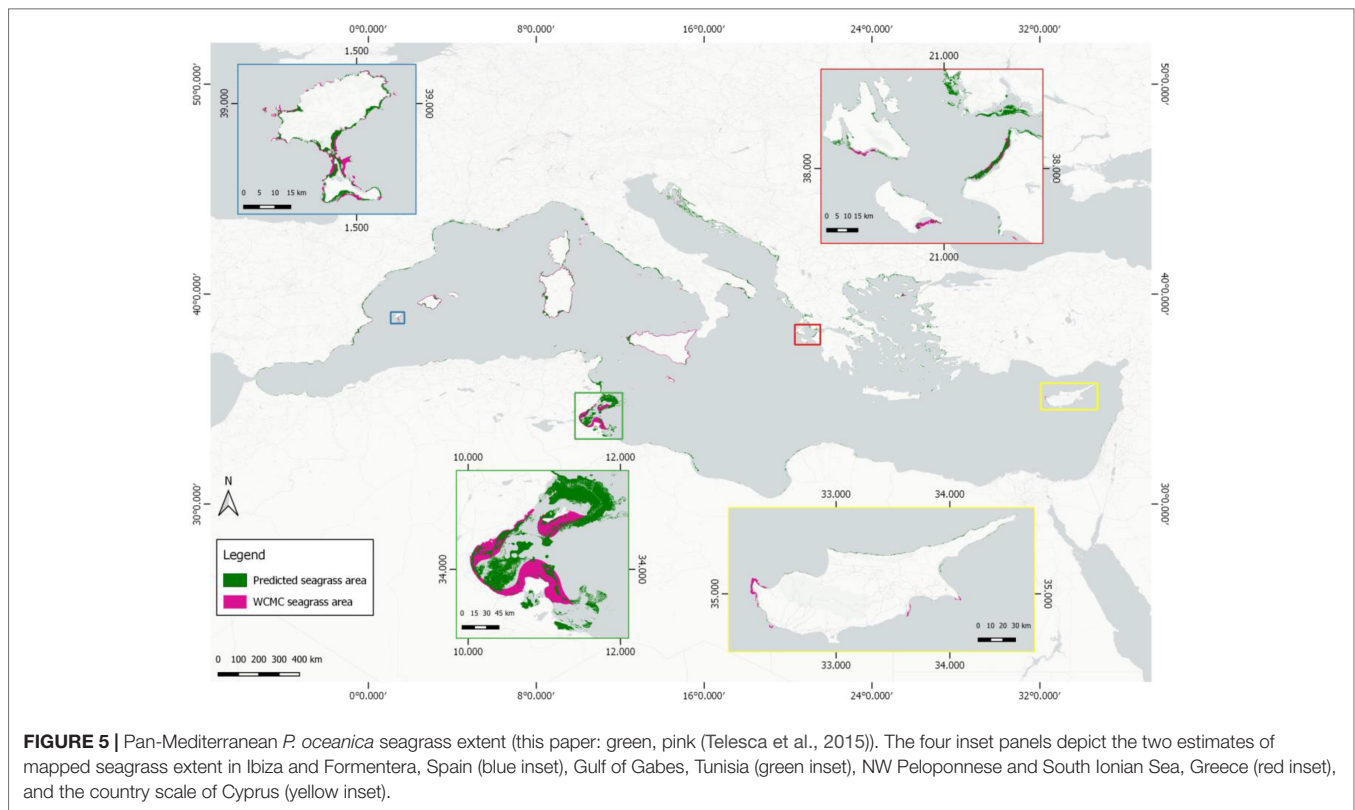


TABLE 3 | Country-scale *P. oceanica* seagrass mapping estimates (km²) in the entire Mediterranean basin.

Country	Coastline length ¹ (km)	0-25 m coastal area (km ²)	Seagrass area - this paper 0-25 m deep (km ²)	Seagrass area ⁴ (km ²)	Seagrass area (km ²) relative to coastline length (km)	Seagrass area (%) of total 0-25 m coastal area
Albania	397.95	1,035.62	149.56	48.03	0.38	14.44
Algeria	1,487.57	401.79	167.91	40.72	0.11	41.79
Bosnia & Herzegovina ²	15.11	8.36	6.90	NA	0.46	82.56
Croatia	4,165.41	2,870.70	2,029.99	314.37	0.49	70.71
Cyprus	442.27	682.11	44.45	90.40	0.1	6.52
Egypt	1,214.31	1,309.97	2.96	NA	0.002	0.23
France	2,299.10	1,723.78	900.28	940.30*	0.39	52.23
Greece	14,772.08	9,621.20	2,877.78	449.39	0.2	29.91
Israel	137.27	357.20	10.43	0	0.08	2.92
Italy	8,914.69	7,929.72	3,261.23	3376.11	0.37	41.13
Lebanon	190.80	178.06	26.94	0	0.14	15.13
Libya	1,441.92	8,249.06	622.03	12.35	0.43	7.54
Malta	153.61	38.45	29.44	58.60	0.19	76.55
Monaco	4.23	0.42	0.41	Included in France*	0.1	98.87
Montenegro	173.46	211.39	146.62	N/A	0.84	69.36
Morocco	551.68	490.63	148.03	N/A	0.27	30.17
Slovenia ³	37.60	0.00021	0.00021	0.09	0.000006	99.98
Spain	3,227.89	3,579.31	1,480.88	1726.69	0.46	41.37
Syria ³	147.57	0.00	0.00	0	0.000	0.00
Tunisia	1,871.04	15,178.60	6,369.05	5186.85	3.4	41.96
Turkey	3,411.52	2,910.61	740.59	2.87	0.22	25.44
UK (Gibraltar)	16.49	5.17	4.20	N/A	0.26	81.23
Total	45,073.55	56,782.1	19,019.6	12,247.07	-	-

¹Mediterranean coastline. ²Bosnia and Herzegovina has a very short coastline length of 20 km considered in this study due to the depth masking beyond 25 m.

³Slovenia and Syria have an almost non-existent seagrass area due to the manual exclusion of turbid waters from our satellite mosaic. ⁴Based on Telesca et al., 2015. Included for comparison are the basin and country-scale.

P. oceanica seagrass area estimates in Telesca et al. (2015), the Mediterranean-wide seagrass area synthesis in McKenzie et al. (2020) — 14,167 km² (Moderate-High Confidence), and the MaxEnt-based modeled potential seagrass area in Jayatilake and Costello (2018) — 118,913 km².

et al., 2018) that also used Sentinel-2 multi-temporal data within GEE.

DISCUSSION

Using a cloud-native Earth Observation framework for big-satellite-data processing and analysis, we showcase here the first data-driven, spatially explicit seagrass extent accounting across an entire bioregional scale. Featuring a plethora of cutting-edge frameworks and algorithms in Earth Observation such as multi-temporal data analytics, machine learning, cloud computing, and big-data processing, we map 19,020 km² of area of the seagrass *Posidonia* across the entire basin using 10 m 279,186 open Sentinel-2 satellite image tiles (2015–2019) and 65,408 reference data points. Undoubtedly, the most important novelty of our mapping effort is the fact that we designed, synthesized, and employed a single and consistent data source—the multi-temporal Sentinel-2 data mosaic—within the moderately small temporal window of 4 years to account the bioregion-wide seagrass ecosystem extent.

The present mapping effort covers important gaps in the previous charting of the Mediterranean seagrasses. The previous Mediterranean-wide effort (Telesca et al., 2015) mapped 55.3% fewer seagrasses than our effort, lacking data on their distribution in 46.7% of the entire Mediterranean and 93% of the entire Eastern basin. Additionally, this effort featured multiple data sources based primarily on experts' knowledge spanning 39 years (1972–2011) in contrast to the 4 years in this present study. An additional synthesis (McKenzie et al., 2020) used an existing inventory (UNEP-WCMC and Short, 2018) and only quantitative polygons with accompanied accuracy to calculate 14,167 km² of Mediterranean seagrasses—that is 34.2% less than our calculation. The reliance of the two latter studies on multiple data sources and interpolated expert knowledge may have led to a possible under-estimation of the seagrass extent throughout the Mediterranean basin (United Nations Environment Programme, 2020). This was also highlighted in a recent national-scale seagrass mapping venture in the Greek territorial waters (Traganos et al., 2018) which yielded four times more seagrass habitats than the inventory of UNEP-WCMC and Short (2018). Last but not least, we calculated only one-sixth of the modeled-based area of Jayatilake and Costello (2018) (118,913 km²), which nonetheless was *not* an actual seagrass area estimate, but rather the potential regional occurrence of seagrasses in the basin according to their habitat suitability. Such model-guided output could complement the ability of the two former data syntheses to guide the scalability of data-driven mapping approaches like the one presented here. It is also worth noting that our basin-wide mapping estimate features a producer's accuracy of 55% which increases the uncertainty in the aforementioned comparisons.

Our cloud-native framework was built on the latest technological advances in Earth Observation: cloud

computing power, AI, and open and free satellite data. More specifically, we describe below four important technological innovations alongside their associated benefits and space for improvement, if applicable:

- a) Scalability: We can scale up the cloud-native framework in terms of space (region, country, basin), time (monthly, seasonally, annually, multi-annually), as well as satellite data input depending on the final goal. The framework could be tuned to also ingest the multi-decadal satellite data archive of NASA/USGS Landsat series within GEE (Dwyer et al., 2018). The spatial scalability is demonstrated by the adaptation of the present Earth Observation system to ingest two orders of magnitude of Sentinel-2 tiles (1,000 to 100,000s) across tens of thousands of km² to map both the Greece-wide (Traganos et al., 2018) and the pan-Mediterranean seascape here.
- b) Time efficiency: Through the high-performance computation within the Google Earth Engine, our framework requires less than 5 minutes (the maximum allocated time for on-demand interactive computations in the platform) to run its end-to-end big data processing to classify seagrasses; we estimate that just downloading 279,186 Sentinel-2 tiles, with an approximate size of 600MB/tile, would have taken somewhat less than 6 months on a 100 Mbps Fast Ethernet connection and 167.5TB of disk space, rendering the present venture unfathomable within a local server.
- c) Multi-temporal Analytics: The cloud-native availability of the public satellite data archive of Sentinel-2 allowed the implementation of all available images within a selected period (> 4 years in this study) in a multi-temporal fashion. Following a statistical and metadata-based approach, this enabled the automated reduction of natural optical interferences (e.g., clouds, sunglint, waves, etc.) that impede the traditional off-the-shelf single-image approaches. In the future, the availability of larger temporal stacks within the cloud will enable more accurate multi-annual mapping analytics through the improved filtering of the aforementioned interferences.
- d) Artificial intelligence: The Google Earth Engine platform contains a large set of available, ready-to-use, and easily-tuned ML algorithms, which ease the implementation and tuning of the AI component in the heart of our cloud-native algorithmic pipeline. Paired with hundreds of thousands of human-labeled training data, our selected algorithm of the Random Forests enabled a better classification result in comparison to the majority of applications in our targeted domain, most of which employ local-scale unsupervised and/or supervised classifiers in local servers. Looking into near-future potential AI developments, we expect that ensemble—voting systems consisting of several different ML classifiers which output the most voted class per pixel—and deep learning architectures could bring further breakthroughs in data-driven approaches in seagrass mapping. All of the above will be achieved by increasing automation and accuracy in the image annotation and

streamlining of seagrass data and related reference data (Zhang, 2015; Islam et al., 2020). Nevertheless, deep learning techniques in Earth Observation have not yet reached the necessary maturity to provide a clear understanding of whether the extra scientific effort for a theoretically greater accuracy justifies the needed extra vast manual annotation and processing power compared to ML classifiers. Nor, in any way, have cloud-native earth observation frameworks within a coastal aquatic context matured.

We identify here four main challenges and associated uncertainties of the present framework along with potential solutions:

a) Over- and under-estimation of seagrass class: We carried out an intensive training data design to differentiate *P. oceanica* from other seagrass species present in the basin (e.g., *Cymodocea nodosa* and *Zostera marina*) and optically deep water. Nonetheless, based on a qualitative and quantitative assessment, clusters of over and under-estimation of the seagrass extent were inevitably identified. This could arise from several reasons. On one hand, over-estimation could have been produced from the pre-processing of our satellite mosaic to the level of the surface reflectance, accounting for the effect of the atmosphere and water surface media, but not of the water column medium. This causes spectral similarities across habitats with increasing depths (e.g., *P. oceanica* seagrass features a similar color to other seagrass habitats and also optically deep water on the satellite mosaic) leading to misclassifications of the *P. oceanica* class. We quantitatively confirmed the similar spectral ranges of the classes of *P. oceanica* meadows and deep water in **Figure 4**. The differences in spectral reflectances between the training and validation data for these two classes would further accentuate such misclassifications, namely the over-estimation of seagrass areas in our study. On the other hand, the possible under-estimation of our seagrass product is highlighted by two facts. First, its producer's accuracy is 7% less than its user's accuracy. This indicates that most of the *P. oceanica* in the map was also *P. oceanica* in the validation data, but that the map failed to capture a fair amount of this class. Second, masking out all depths deeper than 25 m (deemed necessary to reduce over-estimations due to the spectral confusion between seagrass and optically deep water) may have produced under-estimations. The mean lower depth limit of *P. oceanica* in the majority of the basin is around 35 m which means that our mapped area omitted 10 m of potential *P. oceanica* vertical habitat suitability. We evaluated the magnitude of this possible under-estimation, estimating 12,267 km² of coastal area between 25 and 35 m of depth. Using the seagrass coverage percentage per country of the total coastal area in the first 25 of depth, we estimated 3,964 km² of

potential additional *P. oceanica* meadows across 22,984 km² at basin scale. This corresponds to 20.8% of possible under-estimation at the basin scale (**Supplementary Table S2**). The latter estimate is only 3.6% larger than the recent Mediterranean-wide estimate of Pergent-Martini et al. (2021) (22,161 km²) which was based on national seagrass areas. This increases the confidence in our cloud-based method and estimate as well as the calculation of the potential under-estimation here. Using the potential under-estimation of 3,964 km², the true bioregional blue carbon storage of *P. oceanica* beds increases to 872.7 million MgC, considering a Tier 2 assessment (**Supplementary Table S4**). Last but not least, other sources of over- and under-estimation of seagrass meadows and resulting uncertainties in our analysis could be potential confusion with macroalgae, existent seagrasses in waters of low to medium turbidity, varying seagrass density at the sub-pixel level, and, finally, relatively larger temporal differences between our mapping and implemented validation data (**Table 2**).

One way to alleviate these over and under-estimation trends could be to map bathymetry along with the habitat mapping and use cut-off depths for the optical presence of a certain class; for such a vast and diverse optical environment as the Mediterranean, this could be problematic due to the differences in optical properties between the western and eastern part. A second approach to solve this problem could be through forward modeling within the cloud to estimate the “true” seabed reflectance of seagrasses combined with the use of specific spectral indices that could allow differentiation between the seagrass and neighboring classes. A third way to resolve this could be the development of statistical thresholding on the attenuation coefficient layer which in turn will output only the optically shallow regions, offering the two-fold benefit of reduced computational power and improved detection accuracy.

b) Multi-temporal Analytics: Modern solutions are sometimes the forebears of equally modern problems. Our multi-temporal analytics employs a deep satellite image stack spanning more than 4 years. This allows us to address and correct natural optical interferences more efficiently. Yet, in baseline mapping estimations, this also means that such an approach would not detect any potential change within and across seagrasses or neighboring habitats over the studied period. Assuming no habitat loss, the slow growth of *P. oceanica* seagrass species is an advantage here. However, short-lived seagrasses in tropical regions undergo changes in much smaller time scales which would render obligatory the reduction of the temporal selection to monthly or seasonal composites to reflect their natural cycles. Nonetheless, tropical regions experience substantially more cloudy days than the Mediterranean, and thus the reduction of the time dimension would allow more

clouds and cloud shadows to negatively impact our detection capabilities. Currently, this trade-off between change detection through multi-temporal analytics and the correction of environmental noise poses a very interesting scientific question in multi-temporal coastal aquatic mapping efforts within primarily tropical systems.

- c) Training data: Large-scale mapping requires large-scale training data. The case of sufficient training data is one of the emerging issues due to the transition of seagrass mapping from the local to the cloud environment, and from the local to the bioregional mapping scale. Due to the absence of suitable and standardized training data to guide our ML component, we spent a labor-intensive effort to annotate an inventory that would match the multi-temporal Sentinel-2 mosaic. One possible approach to increase the time efficiency could be to design a machine or deep learning framework that, using the same satellite input with the mapping, could generate training data in a more automated way. Yet, to some extent, humans would still have to be involved in assessing the produced training data before these could be fed into the AI-based mapping. Anterior designed and implemented systems for semi-automated and automated interpretation of coastal and marine habitats do exist (Beijbom et al., 2015; González-Rivero et al., 2016; Griffin et al., 2017; Evans et al., 2018; Williams et al., 2019) and could be paired with our cloud-native framework in future endeavors.
- d) Validation data: Large-scale mapping data also requires equally large-scale validation data. The four most important characteristics of suitable reference data for the validation of the Earth Observation mapping approaches include independence to the data source and location, higher quality and higher resolution than the training data in use, and temporal consistency of the source information with the mapping products. It was also very time-consuming to collect such reference data and transform them into a suitable format for the validation process (e.g., designing points within existing polygons in areas with sparse or no training data). Arguably, we could render the validation data design more time-efficient by developing a central user-friendly cloud-native tool (e.g., within Google Earth Engine), which could be used by experienced seagrass and seascape scientists for the design of large-scale, high-quality validation data on high-resolution satellite base maps such as the ones within Google Earth and/or Google Maps.

At present, we infer that based on the observed producer's and user's accuracy of our produced seagrass mapping data, which fluctuates between 40.2 and 69.1%, considerable efforts must be placed to improve our multi-temporal analytics and reference data design. Such efforts will enable the quantification of additional seagrass biophysical parameters with at least

moderate confidence (e.g., leaf area index, above-ground biomass, cover, density, fragmentation, carbon stocks). These efforts would have to rely on not only a greater wealth of available and/or new field data collections to train AI frameworks, but also optical data of higher spatial resolution to detect and map sparser features than the 100 m² pixel of Sentinel-2. It is without doubt that near-future collaborations with seagrass and coastal habitat scientists in and beyond the Mediterranean would expand our mapping capacity beyond just seagrass extent.

Our cloud-native framework can be adapted to account seagrasses and other coastal aquatic ecosystems beyond the geographic limits of the Mediterranean in both temperate and tropical waters. New mapping efforts using our framework can enrich the sparsity of existing large-scale coastal habitat mapping results. Notable examples focused only on tropical marine systems of >10,000 km² include the pan-Caribbean seagrass mapping of Purkis et al. (2019), the merged geomorphic-benthic habitat product of Wabnitz et al. (2008) across 65,000 km², and the coincident geomorphic and benthic habitat mapping of Lyons et al. (2020) across four orders of spatial magnitude. The latter multiscale Earth Observation framework is the only one, to the best of our knowledge, that can be compared to the herein framework as both use the same technological pillars (cloud computing, artificial intelligence, and satellite data) to produce scalable benthic habitat mapping products. Nevertheless, a qualitative and quantitative comparison of all the aforementioned mapping results would enable a better technical understanding of the challenges around these endeavors. Additionally, this would allow us to overcome the arising challenges towards continental and global-scale seagrass mapping following the examples of existing related global-scale EO frameworks and products: the Global Forest Watch (Hansen et al., 2013), the Global Mangrove Watch (Bunting et al., 2018), and the planetary-scale mapping of surface water (Pekel et al., 2016), and tidal flats (Murray et al., 2019).

Applying our pan-Mediterranean seagrass extent estimate of 19,020 km² between 0 and 25 m and the region-specific seagrass carbon storage of Fourqurean et al. (2012), we estimate a 722.2 million MgC of blue carbon storage for all *P. oceanica* seagrass meadows in all 22 countries (Supplementary Table S3). Furthermore, applying our extrapolated bioregional extent estimate of 22,984 km² between 0 and 35 m, we estimate 872.7 million MgC of *P. oceanica* seagrass blue carbon storage (Supplementary Table S4). While these bioregional and their underlying national blue carbon accounts are based on a single region-specific seagrass carbon estimate—and not on more accurate and dense country-specific data—we envisage that a broader availability of the latter data at the nationwide scale will unlock standardized, spatially explicit monitoring programs of seagrass blue carbon in and beyond the basin. These monitoring programs and their provided spatial accounts are expected to aid effective blue carbon policy actions and much-needed investments, especially in countries with large yet unaccounted seagrass carbon sinks (Macreadie et al., 2019; Macreadie et al., 2021). Within the era of *Space Renaissance* that we are currently

traversing, the stability and frequency of the cultural heritages that constitute the Copernicus Sentinel and Landsat satellite data collections could facilitate the transformation of comparable cloud-native frameworks into powerful, global decision support and knowledge systems that will:

- a) Enhance the effective protection and management of seagrasses and their vital ecosystem services and functions.
- b) Strengthen climate change resilience through the promotion and assessment of the role of seagrasses as a nature-based solution to climate change.
- c) Assist the accounting of the seagrass-related Sustainable Development Goals and enforce their alignment with Nationally Determined Contributions and Ecosystem-based Adaptation approaches.

Namely, a new project entitled “Global Seagrass Watch” is established to impel this Earth Observation framework into a long-term standardized ecosystem accounting system. Its near-future implementation will empower scientists, governments, and policymakers to develop tangible solutions beyond their standard operating procedures in terms of communication, partnerships, and actions for the entirety of the coastal seascape environment.

The latest advances in Earth Observation, namely the democratization and widespread availability of satellite data, AI, and cloud-based, large-scale satellite data processing paired with human-labeled reference data, allowed the adaptation of the cloud-native framework of this project in an innovative and scalable way. This scalability yielded in the present study bioregional seagrass ecosystem accounts with increased accuracy, cost and time-efficiency, as well as automation. Following the availability of suitable reference data and big satellite data analytics, we envisage that the present spatially-explicit seagrass ecosystem accounting effort will assist in paving the way towards future national to bioregional-scale accurate accounting of seagrass extent and related blue carbon stocks following recent mapping efforts (Murray et al., 2019; Serrano et al., 2019; Lyons et al., 2020) and needs (Macreadie et al., 2019).

DATA AVAILABILITY STATEMENT

The original contributions presented in the study are included in the article/**Supplementary Material**. Further inquiries can be directed to the corresponding author.

REFERENCES

- Andromède Océanologie (2019) *Seabed Map, Donia Project*. Available at: www.medtrix.fr.
- Arnaud-Haond, S., Duarte, C. M., Diaz-Almela, E., Marbà, N., Sintès, T. and Serrão, E. A. (2012). Implications of Extreme Life Span in Clonal Organisms: Millenary Clones in Meadows of the Threatened Seagrass *Posidonia Oceanica*. *PLoS One* 7 (2), e30454. doi: 10.1371/journal.pone.0030454
- Atlas of *Posidonia* (2019). Available at: <https://ideib.caib.es/posidonia/> [Accessed July 5, 2022].
- Beijbom, O., Edmunds, P. J., Roelfsema, C., Smith, J., Kline, D. I., Neal, B. P., et al. (2015). Towards Automated Annotation of Benthic Survey Images:

AUTHOR CONTRIBUTIONS

DT conceived the idea, designed the work, annotated the training data, and wrote the manuscript with the input of all co-authors. CL and DT designed, developed, and executed the cloud-based Earth Observation framework. DP coordinated the collection and design of the *in situ* validation data. HC, JD, VM, MM, GP, CP-M, and AR provided their validation data. AB ran the Tier 1 and Tier 2 blue carbon accounting. CL, AB, and DT designed all figures and tables. All authors contributed to the article and approved the submitted version.

FUNDING

DT acknowledges support from both a DLR-DAAD Research Fellowship (No. 57186656) and the DLR-funded Global Seagrass Watch Project. CL acknowledges support from a DLR-DAAD Research Fellowship (No. 57478193).

ACKNOWLEDGMENTS

In France, data used to build the 1:10000 marine habitat map were collected by Andromède Océanologie, Agence de l'Eau RMC, Conservatoire du Littoral, DREAL PACA; Egis Eau, ERAMM, GIS Posidonie, IFREMER, Institut océanographique Paul Ricard, Nice Côte d'Azur, TPM, Programme CARTHAM—Agence des Aires Marines Protégées, ASCONIT Consultants, COMEX-SA, EVEMAR, *IN VIVO*, Sentinelle, Stareso, Programme MEDBENTH, Université de Corse (EQEL), Ville de St Cyr-sur-mer, Ville de Cannes, Ville de Marseille, Ville de St Raphaël and Ville de St Tropez. We acknowledge and appreciate the assistance of an anonymous proof-reader towards improving the quality of this manuscript.

SUPPLEMENTARY MATERIAL

The Supplementary Material for this article can be found online at: <https://www.frontiersin.org/articles/10.3389/fmars.2022.871799/full#supplementary-material>

- Variability of Human Experts and Operational Modes of Automation. *PLoS One* 10 (7), e0130312. doi: 10.1371/journal.pone.0130312
- Breiman, L. (2001). Random Forests. *Mach. Learn.* 45 (1), 5–32. doi: 10.1023/A:1010933404324
- Bunting, P., Rosenqvist, A., Lucas, R. M., Rebelo, L.-M., Hilarides, L., Thomas, N., et al. (2018). The Global Mangrove Watch — A New 2010 Global Baseline of Mangrove Extent. *Remote Sens. Ecol. Conserv.* 10 (10), 1669. doi: 10.3390/rs10101669
- Çiżmek H. (2017). *Marine Habitat Mapping Along Eastern Adriatic Coast*.
- Coll, M., Piroddi, C., Steenbeek, J., Kaschner, K., Ben Rais Lasram, F., Aguzzi, J., et al. (2010). The Biodiversity of the Mediterranean Sea: Estimates, Patterns, and Threats. *PLoS One* 5 (8), e11842. doi: 10.1371/journal.pone.0011842

- de los Santos, C. B., Krause-Jensen, D., Alcoverro, T., Marbà, N., Duarte, C. M., van Katwijk, M. M., et al. (2019). Recent Trend Reversal for Declining European Seagrass Meadows. *Nat. Commun.* 10 (1), 3356. doi: 10.1038/s41467-019-11340-4
- DFS Montenegro Engineering (2012). *Start Up of "Katiëccaron;" MPA in Montenegro and Assessment of Marine and Coastal Ecosystems Along the Coast*. Duarte, C. M., Losada, I. J., Hendriks, I. E., Mazarrasa, I. and Marbà, N. (2013). The Role of Coastal Plant Communities for Climate Change Mitigation and Adaptation. *Nat. Climate Change* 3 (11), 961–968. doi: 10.1038/nclimate1970
- Duman, M., Eronat, A. H., İIhan, T., Talas, E. and Küçüksezgin, F. (2019). Mapping Posidonia Oceanica (Linnaeus) Meadows in the Eastern Aegean Sea Coastal Areas of Turkey: Evaluation of Habitat Maps Produced Using the Acoustic Ground Discrimination Systems. *Int. J. Environ. Geoinformatics* 6 (1), 67–75. doi: 10.30897/ijgeo.544695
- Dwyer, J. L., Roy, D. P., Sauer, B., Jenkerson, C. B., Zhang, H. K. and Lymburner, L. (2018). Analysis Ready Data: Enabling Analysis of the Landsat Archive. *Remote Sens.* 10 (9), 1363. doi: 10.3390/rs10091363
- Evans, S. M., Griffin, K. J., Blick, R. A., Poore, A. G. and Vergés, A. (2018). Seagrass on the Brink: Decline of Threatened Seagrass Posidonia Australis Continues Following Protection. *PLoS One* 13 (4), e0190370. doi: 10.1371/journal.pone.0190370
- Finegold, Y., Ortmann, A., Lindquist, E., d'Annunzio, R. and Sandker, M. (2016). *Map Accuracy Assessment and Area Estimation: A Practical Guide* (Rome: Food Agriculture Organization of the United Nations).
- Fourqurean, J. W., Duarte, C. M., Kennedy, H., Marbà, N., Holmer, M., Mateo, M. A., et al. (2012). Seagrass Ecosystems as a Globally Significant Carbon Stock. *Nat. Geosci.* 5 (7), 505–509. doi: 10.1038/ngeo1477
- Gascon, F., Bouzinac, C., Thépaut, O., Jung, M., Francesconi, B., Louis, J., et al. (2017). Copernicus Sentinel-2A Calibration and Products Validation Status. *Remote Sens.* 9 (6), 584. doi: 10.3390/rs9060584
- GENCAT (2021) *Herbassars. Zones D'envolvents*. Available at: <http://agricultura.gencat.cat/ca/details/Article/Herbassars.-Zones-denvolvents>.
- Gislason, P. O., Benediktsson, J. A. and Sveinsson, J. R. (2006). Random Forests for Land Cover Classification. *Pattern Recognition Lett.* 27 (4), 294–300. doi: 10.1016/j.patrec.2005.08.011
- González-Rivero, M., Beijbom, O., Rodríguez-Ramírez, A., Holtrop, T., González-Marrero, Y., Ganase, A., et al. (2016). Scaling Up Ecological Measurements of Coral Reefs Using Semi-Automated Field Image Collection and Analysis. *Remote Sens.* 8 (1), 30. doi: 10.3390/rs8010030
- Gorelick, N., Hancher, M., Dixon, M., Ilyushchenko, S., Thau, D. and Moore, R. (2017). Google Earth Engine: Planetary-Scale Geospatial Analysis for Everyone. *Remote Sens. Environ.* 202, 18–27. doi: 10.1016/j.rse.2017.06.031
- Griffin, K. J., Hedge, L. H., González-Rivero, M., Hoegh-Guldberg, O. I. and Johnston, E. L. (2017). An Evaluation of Semi-Automated Methods for Collecting Ecosystem-Level Data in Temperate Marine Systems. *Ecol. Evol.* 7 (13), 4640–4650. doi: 10.1002/ece3.3041
- Hansen, M. C., Potapov, P. V., Moore, R., Hancher, M., Turubanova, S. A., Tyukavina, A., et al. (2013). High-Resolution Global Maps of 21st-Century Forest Cover Change. *Science* 342 (6160), 850–853. doi: 10.1126/science.1244693
- Islam, K. A., Hill, V., Schaeffer, B., Zimmerman, R. and Li, J. (2020). Semi-Supervised Adversarial Domain Adaptation for Seagrass Detection Using Multispectral Images in Coastal Areas. *Data Sci. Eng.* 5, 111–125. doi: 10.1007/s41019-020-00126-0
- IUCN (2021). *Manual for the Creation of Blue Carbon Projects in Europe and the Mediterranean*. Ed. Otero, M., 144 pages. Center for Mediterranean Cooperation, Malaga, Spain
- Jayatilake, D. R. and Costello, M. J. (2018). A Modelled Global Distribution of the Seagrass Biome. *Biol. Conserv.* 226, 120–126. doi: 10.1016/j.biocon.2018.07.009
- Jordà, G., Marbà, N. and Duarte, C. M. (2012). Mediterranean Seagrass Vulnerable to Regional Climate Warming. *Nat. Climate Change* 2 (11), 821–824. doi: 10.1038/nclimate1533
- Lyons, M. B., Roelfsema, C. M., Kennedy, E. V., Kovacs, E. M., Borrego-Acevedo, R., Markey, K., et al. (2020). Mapping the World's Coral Reefs Using a Global Multiscale Earth Observation Framework. *Remote Sens. Ecol. Conserv.* 6 (4), 557–568. doi: 10.1002/rse2.157
- Macreadie, P. I., Anton, A., Raven, J. A., Beaumont, N., Connolly, R. M., Friess, D. A., et al. (2019). The Future of Blue Carbon Science. *Nat. Commun.* 10 (1), 1–13. doi: 10.1038/s41467-019-11693-w
- Macreadie, P. I., Costa, M. D. P., Atwood, T. B., Friess, D. A., Kelleway, J. J., Kennedy, H., et al. (2021). Blue Carbon as a Natural Climate Solution. *Nat. Rev. Earth Environ.* 2 (12), 826–839. doi: 10.1038/s43017-021-00224-1
- Marbà, N. and Duarte, C. M. (1998). Rhizome Elongation and Seagrass Clonal Growth. *Mar. Ecol. Prog. Ser.* 174, 269–280. doi: 10.3354/meps174269
- McKenzie, L. J., Nordlund, L. M., Jones, B. L., Cullen-Unsworth, L. C., Roelfsema, C. and Unsworth, R. K. (2020). The Global Distribution of Seagrass Meadows. *Environ. Res. Lett.* 15 (7), 074041. doi: 10.1088/1748-9326/ab7d06
- Murray, N. J., Phinn, S. R., DeWitt, M., Ferrari, R., Johnston, R., Lyons, M. B., et al. (2019). The Global Distribution and Trajectory of Tidal Flats. *Nature* 565 (7738), 222–225. doi: 10.1038/s41586-018-0805-8
- Paoli, C., Povero, P., Burgos, E., Daputo, G., Fanciulli, G., Massa, F., et al. (2018). Natural Capital and Environmental Flows Assessment in Marine Protected Areas: The Case Study of Liguria Region (NW Mediterranean Sea). *Ecol. Model.* 368, 121–135. doi: 10.1016/j.ecolmodel.2017.10.014
- Pekel, J.-F., Cottam, A., Gorelick, N. and Belward, A. S. (2016). High-Resolution Mapping of Global Surface Water and its Long-Term Changes. *Nature* 540 (7633), 418–422. doi: 10.1038/nature20584
- Pergent, G., Bazairi, H., Bianchi, C. N., Boudouresque, C. F., Buia, M., Calvo, S., et al. (2014). Climate Change and Mediterranean Seagrass Meadows: A Synopsis for Environmental Managers. *Mediterr. Mar. Sci.* 15 (2), 462–473. doi: 10.12681/mms.621
- Pergent-Martini, C., Pergent, G., Monnier, B., Boudouresque, C.-F., Mori, C. and Valette-Sansevin, A. (2021). Contribution of Posidonia Oceanica Meadows in the Context of Climate Change Mitigation in the Mediterranean Sea. *Mar. Environ. Res.* 165, 105236. doi: 10.1016/j.marenvres.2020.105236
- Pergent-Martini, C., Valette-Sansevin, A. and Pergent, G. (2015). *Cartographie Continue Des Habitats Marins En Corse / Résultats Cartographiques*.
- Poursanidis, D., Traganos, D., Reinartz, P. and Chrysoulakis, N. (2019). On the Use of Sentinel-2 for Coastal Habitat Mapping and Satellite-Derived Bathymetry Estimation Using Downscaled Coastal Aerosol Band. *Int. J. Appl. Earth Observation Geoinformation* 80, 58–70. doi: 10.1016/j.jag.2019.03.012
- Purkis, S. J., Gleason, A. C., Purkis, C. R., Dempsey, A. C., Renaud, P. G., Faisal, M., et al. (2019). High-Resolution Habitat and Bathymetry Maps for 65,000 Sq. Km of Earth's Remotest Coral Reefs. *Coral Reefs* 38 (3), 467–488. doi: 10.1007/s00338-019-01802-y
- Ricart, A. M. (2016). *Insights Into Seascape Ecology: Landscape Patterns as Drivers in Coastal Marine Ecosystems* (Barcelona, Spain: Universitat de Barcelona).
- Rigo, I., Paoli, C., Daputo, G., Pergent-Martini, C., Pergent, G., Oprandi, A., et al. (2021). The Natural Capital Value of the Seagrass Posidonia Oceanica in the North-Western Mediterranean. *Diversity* 13 (10), 499. doi: 10.3390/d13100499
- Serrano, O., Lovelock, C. E., Atwood, T. B., Macreadie, P. I., Canto, R., Phinn, S., et al. (2019). Australian Vegetated Coastal Ecosystems as Global Hotspots for Climate Change Mitigation. *Nat. Commun.* 10 (1), 1–10. doi: 10.1038/s41467-019-12176-8
- Telesca, L., Belluscio, A., Criscoli, A., Ardizzone, G., Apostolaki, E. T., Fraschetti, S., et al. (2015). Seagrass Meadows (Posidonia Oceanica) Distribution and Trajectories of Change. *Sci. Rep.* 5 (1), 1–14. doi: 10.1038/srep12505
- Traganos, D., Aggarwal, B., Poursanidis, D., Topouzelis, K., Chrysoulakis, N. and Reinartz, P. (2018). Towards Global-Scale Seagrass Mapping and Monitoring Using Sentinel-2 on Google Earth Engine: The Case Study of the Aegean and Ionian Seas. *Remote Sens.* 10 (8), 1227. doi: 10.3390/rs10081227
- Traganos, D. and Reinartz, P. (2018a). Interannual Change Detection of Mediterranean Seagrasses Using RapidEye Image Time Series. *Front. Plant Sci.* 9. doi: 10.3389/fpls.2018.00096
- Traganos, D. and Reinartz, P. (2018b). Mapping Mediterranean Seagrasses With Sentinel-2 Imagery. *Mar. Pollut. Bull.* 134, 197–209. doi: 10.1016/j.marpolbul.2017.06.075
- UNEP/MAP (2012). *State of the Mediterranean Marine and Coastal Environment* (Athens: UNEP/MAP – Barcelona Convention).
- UNEP-WCMCShort, F. T. (2018) *Global Distribution of Seagrasses (Version 6.0). Sixth Update to the Data Layer Used in Green and Short, (2003)*. Available at: <http://data.unep-wcmc.org/datasets/7>.

- United Nations (2015). *Transforming Our World: The 2030 Agenda for Sustainable Development* (New York, USA: United Nations).
- United Nations Environment Programme (2020). *Out of the Blue: The Value of Seagrasses to the Environment and to People* (Nairobi, Kenya: UNEP).
- United Nations Framework Convention on Climate Change (2021) *Nationally Determined Contributions (NDCs)*. Available at: <https://unfccc.int/process-and-meetings/the-paris-agreement/nationally-determined-contributions-ndcs/nationally-determined-contributions-ndcs> (Accessed 11 January 2022).
- Wabnitz, C. C., Andréfouët, S., Torres-Pulliza, D., Müller-Karger, F. E. and Kramer, P. A. (2008). Regional-Scale Seagrass Habitat Mapping in the Wider Caribbean Region Using Landsat Sensors: Applications to Conservation and Ecology. *Remote Sens. Environ.* 112 (8), 3455–3467. doi: 10.1016/j.rse.2008.01.020
- Williams, I. D., Couch, C. S., Beijbom, O., Oliver, T. A., Vargas-Angel, B., Schumacher, B. D., et al. (2019). Leveraging Automated Image Analysis Tools to Transform Our Capacity to Assess Status and Trends of Coral Reefs. *Front. Mar. Sci.* 6. doi: 10.3389/fmars.2019.00222
- Zhang, C. (2015). Applying Data Fusion Techniques for Benthic Habitat Mapping and Monitoring in a Coral Reef Ecosystem. *ISPRS J. Photogrammetry Remote Sens.* 104, 213–223. doi: 10.1016/j.isprsjprs.2014.06.005

Conflict of Interest: The authors declare that the research was conducted in the absence of any commercial or financial relationships that could be construed as a potential conflict of interest.

Publisher's Note: All claims expressed in this article are solely those of the authors and do not necessarily represent those of their affiliated organizations, or those of the publisher, the editors and the reviewers. Any product that may be evaluated in this article, or claim that may be made by its manufacturer, is not guaranteed or endorsed by the publisher.

Copyright © 2022 Traganos, Lee, Blume, Poursanidis, Čížmek, Deter, Mac'ic, Montefalcone, Pergent, Pergent-Martini, Ricart and Reinartz. This is an open-access article distributed under the terms of the Creative Commons Attribution License (CC BY). The use, distribution or reproduction in other forums is permitted, provided the original author(s) and the copyright owner(s) are credited and that the original publication in this journal is cited, in accordance with accepted academic practice. No use, distribution or reproduction is permitted which does not comply with these terms.



Is All Seagrass Habitat Equal? Seasonal, Spatial, and Interspecific Variation in Productivity Dynamics Within Mediterranean Seagrass Habitat

Emma A. Ward^{1,2,3*}, Charlotte Aldis¹, Tom Wade¹, Anastasia Miliou^{2*}, Thodoris Tsimpidis² and Tom C. Cameron^{1*}

¹School of Life Sciences, University of Essex, Colchester, United Kingdom, ²Archipelagos Institute of Marine Conservation, Pythagorio, Greece, ³Institute of Marine Sciences, School of Biological Sciences, University of Portsmouth, Portsmouth, United Kingdom

OPEN ACCESS

Edited by:

Hilary Anne Kennedy,
Bangor University, United Kingdom

Reviewed by:

Gregory N. Nishihara,
Nagasaki University, Japan
Dirk Jacob Koopmans,
University of Virginia, United States

*Correspondence:

Emma A. Ward
emma.ward3@myport.ac.uk
Anastasia Miliou
a.miliou@archipelago.gr
Tom C. Cameron
tcameron@essex.ac.uk

Specialty section:

This article was submitted to
Marine Ecosystem Ecology,
a section of the journal
Frontiers in Marine Science

Received: 07 March 2022

Accepted: 09 June 2022

Published: 25 July 2022

Citation:

Ward EA, Aldis C, Wade T, Miliou A,
Tsimpidis T and Cameron TC (2022)
Is All Seagrass Habitat Equal?
Seasonal, Spatial, and Interspecific
Variation in Productivity Dynamics
Within Mediterranean
Seagrass Habitat.
Front. Mar. Sci. 9:891467.
doi: 10.3389/fmars.2022.891467

Seagrass meadows' ability to capture carbon through sequestering autochthonous carbon via photosynthesis means they could represent a potential nature-based solution to rising carbon emissions. In multispecies seagrass communities, and due to species introduction or predicted range shifts, it is important to know which species deliver different carbon sequestration gains to inform conservation actions. Large benthic chamber experiments (volume = 262L) assessed the seasonal and spatial variation in metabolism dynamics of the endemic and dominant Mediterranean seagrass, *P. oceanica* whilst small benthic chamber experiments (volume = 7L) compared the dynamics between, *P. oceanica* the native *C. nodosa* and non-native *H. stipulacea*. Within shallow *P. oceanica* edge habitat lower Net Apparent Productivity (NAP) occurs in autumn ($\bar{x} = 1.3$, $SD \pm 2.95$ O₂ mmol m⁻² d⁻¹) compared to summer ($\bar{x} = 9.9$, $SD \pm 2.75$ O₂ mmol m⁻² d⁻¹) corresponding with periods of light limiting and light saturating conditions, but it remains overall autotrophic annually (2.3 C mol m⁻² yr⁻¹). However, spatial heterogeneity exists, the center areas of *P. oceanica* were more productive (NAP $\bar{x} = 19.7$, $SD \pm 3.83$ O₂ mmol m⁻² d⁻¹) compared to edge habitat with spatial changes in productivity relating to plant surface area (96%), shoot density (81%), blade length (72%) and seagrass percentage cover (64%). Under comparative conditions in a sparse multispecies area of the meadow the species demonstrated different capacities for carbon fixation. *H. stipulacea* was carbon positive and *P. oceanica* fluctuated between positive and negative carbon balance suggesting both can maintain a balance between carbon fixation and carbon utilised for metabolic activity. In contrast the *C. nodosa* here would be expected to deteriorate as it was utilising carbon more than it was fixing (NAP_N² ($\bar{x} = -0.0012$, $SD \pm 0.0007$ O₂ mmol cm⁻² d⁻¹). This study demonstrates that not all seagrass habitat is equal. If seagrass meadows are to play a part in mitigating CO₂ emissions, variability in primary productivity within seagrass meadows needs to be accounted for to produce accurate total fixed carbon estimates, and subsequently autochthonous carbon sequestration

estimates. This means seagrass meadow species composition and the condition of these meadows must be better understood.

Keywords: seagrass, productivity, carbon, nature based solutions, blue carbon, Mediterranean, restoration

1 INTRODUCTION

Seagrass meadows act as a major global carbon sink (Duarte et al., 2013), therefore restoration or expansion of seagrass beds represent a potential nature-based solution to rising carbon emissions. Seagrasses capture carbon through actively sequestering autochthonous carbon by photosynthesis and passively trapping allochthonous carbon within their architectural structure. Allochthonous carbon is typically considered more labile, therefore deposits of autochthonous carbon are those expected to lead to long-term stable carbon deposits (Mazarrasae et al., 2018). The metabolic rates of global seagrass communities favour net autotrophy, with temperate meadows typically favoured to have a higher net autotrophy than tropical meadows (Duarte et al., 2010), suggesting not all seagrass is equal in its ability to sequester carbon.

The temperate seagrass *Posidonia oceanica* forms vast monospecific meadows in the Mediterranean and is unique in its ability to form vertical mattes that can store sedimentary carbon for millennia (Mateo et al., 1997). It is perhaps why some herald these meadows to represent the global maximum in carbon sequestration among seagrasses (Lavery et al., 2013). Unlike terrestrial soils, *Posidonia* sediments have the potential to not become saturated with carbon over time because they can accrete vertically (Mateo et al., 1997; Samper-Villarreal et al., 2018). If the vertical accretion matches the rate of sea level rise, they potentially have a limitless capacity, which in part demonstrates their suitability for climate mitigation policy efforts (McKee et al., 2007; Howard et al., 2017). However, *P. oceanica* meadows have undergone severe regression in the last 50 years (34% loss), with only localised areas of persistence and growth (Telesca et al., 2015). The causes of decline for *P. oceanica* include water quality degradation, coastal modification, mechanical damage (i.e., bottom trawling, anchoring, mooring, culture farm occupation), extreme weather events and non-native macroalgae invasion (Santos et al., 2019).

At the Mediterranean scale, *P. oceanica* populations in the Western and Eastern basins maintain genetic differentiation due to present-day dispersal limits (Arnaud-Haond et al., 2007). There is a greater distribution of *P. oceanica* in the Eastern basin (713,992 ha) compared to the Western basin (510,715 ha) (Telesca et al., 2015). Despite the genetic variation between basins and larger coverage in the Eastern Mediterranean basin, the majority of *P. oceanica* metabolism estimates have come from the Western Mediterranean basin (Frankignoulle and Bouqueneau, 1987; Holmer et al., 2004; Gazeau et al., 2005; Barron and Duarte, 2009; Olive et al., 2015; Champenois and Borges, 2018). There is a single published study on *P. oceanica* metabolism in the Eastern Mediterranean basin, in the western region of the Aegean Sea (Apostolaki et al., 2010). Metabolism and carbon sequestration

estimations for *P. oceanica* are considered one of the most well researched amongst seagrass species (Nordlund et al., 2018), yet there are distinct local knowledge gaps and spatial biases, particularly within the Eastern Mediterranean basin that need to be addressed. In the Eastern Mediterranean basin, the sea surface has warmed by $0.05 \pm 0.009^{\circ}\text{C yr}^{-1}$ compared to just $0.03 \pm 0.008^{\circ}\text{C yr}^{-1}$ in the Western Mediterranean basin from 1985 to 2006 (Nykjaer, 2009). Given the Eastern Mediterranean basin is warming faster than the Western Mediterranean basin understanding if the metabolism and drivers of productivity are different in Eastern vs Western Mediterranean seagrass is important.

Seagrass metabolism is influenced by multiple variables including light (Champenois and Borges, 2018), nutrient availability (Holmer et al., 2008; Apostolaki et al., 2010), and temperature and ocean acidification (Berg et al., 2019); which leads to seasonal fluctuations in productivity. Seagrass depth distribution is determined by light availability, as under insufficient light conditions the plant does not meet the photosynthetic requirements needed to maintain positive metabolic and carbon balance (Ralph et al., 2007), moving away from a state of net autotrophy and net carbon storage. Although seagrass presence is a function of the accumulative light availability throughout the year as this will change seasonally from periods where light is limiting to periods where it is potentially light saturating. The optimal thermal conditions for *P. oceanica* are between 17 - 20°C (Champenois and Borges, 2018), therefore its metabolism both above and below these conditions, is not optimal for maximum oxygen production and is more likely to become heterotrophic. Annual patterns of *P. oceanica* metabolism therefore comprise periods that alternate from negative to positive carbon balance as temperature and light availability change with seasons (Alcoverro et al., 2001). Further to this *P. oceanica* meadows are known to undergo seasonal senescence, leading to the shedding of >85% of leaf material at the end of Summer (Ott, 1980; Cebrian and Duarte, 2001). If metabolism estimates were produced only during the summer months it would overestimate the meadow's net carbon sequestration capacity (Champenois and Borges, 2012). Notably as stable carbon stocks rely on autochthonous carbon deposits, we will also assess key environmental parameters that influence photosynthesis in these different seasons: for example change in light and temperature.

Seagrass meadows are not always a uniform habitat and whilst *P. oceanica* meadows can form continuous meadows, patchy coverage across meadows is common. Patchy *P. oceanica* creates complex seascapes, which are mosaics including habitats of sand, *P. oceanica* dead matte and live *P. oceanica* (Borg et al., 2006; Abadie et al., 2015). This complexity also acts within a *P. oceanica* meadow, because at the junction between the seagrass and adjacent habitats there are considerable edge effects,

resulting in distinct areas of central and edge *P. oceanica* habitat (Abadie et al., 2018). Meadows that experience a wave exposure gradient from low to high energy develop patchier meadow formation (Folkard, 2005; Pace et al., 2016). Anthropogenic factors have also increased patchiness including anchoring, impact from historic military activity, fishing practices and fish farming (Montefalcone et al., 2009; Abadie et al., 2015). When a *P. oceanica* meadow is described as patchy it has lower overall cover, more complex patch shapes and reduced within-patch architectural complexity (Pace et al., 2016). This patchiness influences the available surface of photosynthetically active plant material. It is therefore important that in this study we consider the spatial variation in canopy architecture of *P. oceanica* when considering its area based carbon sequestration potential, and not just take estimates from pristine intact meadows.

The Mediterranean temperate-tropical combination of seagrass species is considered a unique bioregion of seagrass diversity (Short et al., 2007). Alongside the dominant endemic *P. oceanica*, the next most prevalent species in the Aegean Sea is the native *Cymodocea nodosa*. The eastern region of the Aegean Sea also sits at a crossroad for alien species expansion (Pancucci-Papadopoulou et al., 2012), including the non-native seagrass *Halophila stipulacea*, introduced to the Mediterranean and first reported in 1894 off the Island of Rhodes in the south-eastern region of the Aegean Sea (Fritsch, 1895; also see *Halophila decipiens*, Gerakaris et al., 2019). *H. stipulacea* was listed amongst the '100 Worst Invasive Species' in the Mediterranean (Streftaris and Zenetos, 2006). However, there are discrepancies in whether it should be considered 'invasive' or not as no ecological consequences of its introduction and spread in the Mediterranean have been reported (Williams, 2007). Scarce research has focused on its potential impact or contribution to ecosystem services within Mediterranean coastal ecosystems, yet *H. stipulacea* habitat was recently suggested to support carbon sequestration (Apostolaki et al., 2019; Wesselmann et al., 2021). Given *H. stipulacea* is one of the longest monitored non-native species in the Mediterranean, there has been a clear lag from reporting its presence and rate of expansion, to understanding its impact within the communities where it has successfully established.

In the Mediterranean *H. stipulacea* can be found in single species meadows, multi-species meadows with the native *Cymodocea nodosa*, in the free spaces between patches of *P. oceanica* or in habitats previously devoid of seagrass (Boudouresque et al., 2009). Whilst there are reports of its 'invasive' behaviour on sandy substrata when it exists in high abundances, no displacement of native species has yet been reported (Tsiamis et al., 2010). Given that *H. stipulacea* has various contexts in which it can be found in the Mediterranean its contribution to community productivity may be context dependent. When *H. stipulacea* has colonised areas previously absent of seagrass its presence has increased the distribution of seagrass habitat in the Mediterranean, this is one reason why it can be considered a new potential blue carbon sink habitat (Apostolaki et al., 2019; Wesselmann et al., 2021). The potential of *H. stipulacea* to also influence the net productivity of mixed seagrass habitats, especially considering evidence it can

colonise patchy areas of bare ground where *P. oceanica* may have been present in the past (Telesca et al., 2015), will also be assessed in this study.

This study will firstly determine if seasonal differences in metabolism measurements occur for shallow *P. oceanica* meadows in the eastern region of the Aegean Sea and the relative influence of the concurrent seasonal changes in light, temperature, and seagrass canopy height, on net productivity. These seasonal measurements will provide a conservative estimate of annual total fixed carbon. Secondly in the summer we will assess if spatial variation in productivity exists between edge and central *P. oceanica* habitat and if various plant biometrics can be used to describe any variation in spatial plant productivity. Finally, we assess if variation in species-specific metabolism exists between both native seagrass species *P. oceanica* and *C. nodosa* in direct comparison to the non-native seagrass species *H. stipulacea*. Our results will contribute to suitable Mediterranean scale carbon budgets which take into account the variation in total fixed carbon produced by Mediterranean seagrass.

2 METHODS

2.1 Study Site

This study took place at Vroulia Bay (37.317460° N, 26.724704° E), Lipsi Island, which is part of the Dodecanese Islands, in the eastern region of the Greek Aegean Sea. The bay consists of a multispecies seagrass meadow, largely dominated by monospecific areas of *P. oceanica*. However, the bay also houses small monospecific patches of *C. nodosa* and *H. stipulacea*, as well as areas where two or all three of the species form mixed meadows (Supplementary Figure 1).

2.2 Experimental Design

This metabolism study exists in two parts. Firstly, and primarily, large benthic chamber experiments focus on the seasonal and spatial metabolism dynamics of *P. oceanica* from within monospecific shallow *P. oceanica* (2m depth). Seasonal *P. oceanica* sampling occurred in autumn (3rd – 9th November 2018), spring (12th – 19th April 2019) and summer (2nd – 12th July 2019); whilst spatial *P. oceanica* sampling occurred only in summer (2nd July – 12th August 2019).

Secondly small benthic chamber experiments from a deeper area (7m depth) of the same meadow where all three seagrass species are found mixed focus on comparative metabolism dynamics of *P. oceanica*, *C. nodosa* and *H. stipulacea*, in summer (20th June – 17th July 2019) (Full sampling regime available in; Supplementary Table 1).

2.2.1 Seasonal and Spatial *P. oceanica* Metabolism -Large Benthic Chamber Setup

Large dome-shaped clear PVC benthic chambers (diameter = 1 m, height = 50 cm, benthic surface area = 0.79 m², volume = 262 L) were deployed *via* free divers (Figure 1) in shallow monospecific *P. oceanica* (1.6 - 2 m depth). PME miniDOT[®] loggers were fitted to the apex of the chamber, to record dissolved

oxygen and temperature in 10 minutes intervals. HOBO Pedant[®] loggers were fixed and weighted flat to the seafloor within the benthic chambers to record relative irradiance in 5 minutes intervals. The HOBO loggers were calibrated under controlled light and temperature facilities in Essex before being sent out to the field site. In our experience pre-calibration differences between newly purchased HOBO loggers are always minimal. A submersible pump was secured to the inside of the chamber 30 cm from the seafloor to mix water at a flow rate of 480 L hr⁻¹ in 10 minute intervals (10 minutes on followed by 10 minutes off), as such the overall flow rate within the chamber was considered to be 240 L hr⁻¹. The benthic chambers were held in place by large chains and sank 5 cm into the sediment to create a seal. Given the morphology and typically large aboveground biomass of *P. oceanica*, the large benthic chambers combined with internal mixing support sufficient volume of water inside the chamber relative to vegetative biomass to prevent oxygen saturation (Olive et al., 2015), and prevent oxygen saturation (**Supplementary Figure 2**). The benthic chambers were deployed within the same 2 hour timeframe each morning (10:45 am -12:45 pm) then left *in situ* for 24 hour (autumn and summer) or 23 hour (spring) incubations.

The large *in situ* benthic chambers were deployed over edge habitat in autumn, spring and summer. For this study we consider patchy edge habitat to be within the fringing 1m of *P. oceanica* before the transition point from continuous *P. oceanica* (> 2m) to sand or the entirety of small *P. oceanica* patches (< 2m), because patches of *P. oceanica* < 2m in size are assumed to consist entirely of edge habitat due to the proximity of the centre of the small patch to the edge. Edge habitat creates a good seal at the base

of the large benthic chambers because of the high proportion of sand to low proportion of rhizome. Simultaneously a large benthic chamber was placed over the adjacent unvegetated habitat to collect bare sand incubations. We have used a sand-based control given we are studying patchy and shallow beds and therefore they are not sitting on as established matte, however a dead seagrass matte control achieved by cutting live material away from a chamber's area would be an alternative, in our case using bare sand incubations also limits any impacts to our study meadow. If it was not possible to simultaneously deploy the bare sand incubations, they were deployed the day after the first incubation was completed, although this only occurred once (**Supplementary Table 1**).

To achieve a comparison between fragmented edge seagrass habitat and the continuous central meadow, in summer benthic chambers were placed over *P. oceanica* within the meadow centre in addition to those deployed over edge habitat. Within dense areas of *P. oceanica* the rigid PVC benthic chamber likely cut the rhizomes and roots, however the stress caused is generally considered marginal (Champenois and Borges, 2012). The summer bare sand incubations collected simultaneously to the summer *P. oceanica* edge habitat (n = 4) were used as the control to summer central measurements (Full sampling regime available in; **Supplementary Table 1**).

2.2.2 Species Specific Productivity -Small Benthic Chamber Setup

An area within Vroulia bay was chosen where all three species were in proximity, therefore maintaining as much as possible similar *in situ* environmental conditions for each species (appx.



FIGURE 1 | Large benthic chamber setup (A) Deployed in autumn over *P. oceanica* edge habitat (B) Deployed in summer over dense central *P. oceanica* meadow. (C) Setup of the internal water pump (foreground) within bare sand incubation. External submersible pump battery pack in background. (D) Illustration of large benthic chamber set-up. Photographs © Emma A Ward, Illustration © Tom Wade.

7m depth). An area of patchy mixed meadow transitioned in areas from *P. oceanica* dominant to *C. nodosa* dominant, with scarce intermittent presence of clumps of *H. stipulacea*, as such this was chosen for the metabolism measurements focusing on *P. oceanica* and *C. nodosa* (**Supplementary Figure 1**). The use of the small chambers allowed for complimentary experimental questions to occur in the summer 2019 field season, but also enabled sampling to take place in the deeper multispecies area of the meadow where we could not safely deploy the large chambers with the equipment we had.

Care was taken to avoid placing benthic chambers over mixed species compositions and generally the benthic chambers only encompassed the intended dominant species. Two of five *C. nodosa* chambers covered a small amount of either *P. oceanica* or *H. stipulacea*. Nevertheless, in those instances *C. nodosa* represented 93% and 96% of the total seagrass plant surface area within the chamber and therefore these two replicates were still considered representative of *C. nodosa* patches. One of six *P. oceanica* chambers covered a small amount of *H. stipulacea* but *P. oceanica* represented 98% of the total plant surface area within the chamber and therefore was also considered representative of *P. oceanica*. Directly adjacent to the *P. oceanica* and *C. nodosa* was a monospecific area of *H. stipulacea*, which was utilised for the metabolism measurements focused on this species.

Three smaller clear dome PVC benthic chambers (diameter = 30 cm, height = 15 cm, benthic surface area = 0.071 m², volume = 7 L) were deployed by free divers, secured with a small chain and sank into the sediment to create a seal (**Figure 2**). The benthic incubations took place for each seagrass species consecutively; *H. stipulacea* 20th June – 5th July, *C. nodosa* 10th – 14th July and *P. oceanica* 14th – 17th July. A bare sand incubation was simultaneously deployed every day. The same oxygen, light and temperature loggers and temporal sampling methods were used as per the large domes described above. The benthic chambers were deployed within the same half an hour timeframe each morning (11:00 - 11:30 am) and left *in situ* for ~ 23 hours. As *H. stipulacea* and *C. nodosa* are smaller seagrass species with lower above ground biomass, the small benthic chamber design should sufficiently provide a suitable volume of water to vegetative biomass to prevent oxygen saturation. The

P. oceanica within this area of the bay is naturally patchy and short, which should also accommodate the smaller chamber size and volume (**Figure 2B**). There was no mixing present inside these small benthic chambers, given water motion reduces the thickness of the diffusion boundary-layer which in turn allows for a higher carbon availability on the plant surface (Koch, 1993), these smaller benthic chambers likely underestimate the carbon flux taking place *in situ* with water motion present.

2.2.3 Quantifying Seagrass Canopy Within the Benthic Chamber

The quantity of seagrass canopy enclosed within all benthic chambers was quantified; large benthic chambers a representative sample was selected, measured *in situ* and scaled up to reflect the full chamber; small chambers had all the leaf material collected and measured back at the lab.

For seasonal large benthic chambers, blade length (B_{length}) (cm) from 5 – 6 randomly selected blades were measured from the *P. oceanica* enclosed within the chambers to reflect canopy height and broadly represent the biomass enclosed within the chambers across seasons. In the summer several additional measurements were taken from the seagrass within the benthic chambers. *P. oceanica* coverage (*Cover*) (%) was estimated once the benthic chamber was deployed reflecting the percentage of seagrass cover within the entirety of the chamber. When the benthic incubations were complete three 20 x 20 cm quadrats were placed on the *P. oceanica* enclosed within the chamber to determine shoot density ($Shoot_D$) (m⁻²). To establish a proxy of the plant surface area for individual *P. oceanica* shoots enclosed ($Shoot_{SA}$) the following was also acquired; the number of blades (B_{Number}) (shoot⁻¹) from 5 - 6 randomly selected shoots; blade length (B_{length}) and blade width (B_{width}) (cm) from 5 – 6 randomly selected blades:

$$Shoot_{SA} = 2(B_{length} \times B_{width}) \times B_{Number}$$

Seagrass cover (%), $Shoot_D$ and B_{length} representative of canopy height were all used as standalone plant biometrics. However, in combination these seagrass biometrics and $Shoot_{SA}$ determine



FIGURE 2 | Small benthic chamber setup (A) Deployed over short patchy *P. oceanica* habitat (B) Aerial view above patchy *P. oceanica* chambers deployed. Photographs; A and B © Jente van Langerak.

plant surface area ($Plant_{SA}$) ($\text{cm}^2 \text{ m}^{-2}$) within each chamber, calculated as:

$$Plant_{SA} = Shoot_{SA} \times \left(Shoot_D \times \frac{Cover}{100} \right)$$

For the small benthic chambers all leaf material from within the chambers was collected by cutting the leaves leaving the rhizome and roots, this along with the small sample size within these chambers' limits damage to the overall sampling area. The aboveground leaf material was transported back to the lab where they were separated from any dead leaf litter and all individual leaves were photographed using a digital camera, on a white background. The planar surface area of all seagrass leaves within corresponding benthic chambers were determined, by Image J software, (modified from, Schneider et al., 2012). This was converted into plant surface area ($Plant_{SA}$) ($\text{cm}^2 \text{ m}^{-2}$) by doubling the planar surface area and dividing by the chamber benthic surface area (A) (m^2).

$$Plant_{SA} = \frac{2 \times \text{Planar surface area}}{A}$$

2.3 Community Metabolism Calculations

The record from the PME oxygen logger was used to calculate net community productivity for every 10-minute interval over each 24-hour period (NCP_{24}) (modified from Cole and Pace, 2000):

$$NCP_{24} = \Sigma \Delta DO$$

where DO is dissolved oxygen. This was applicable to the autumn and summer large benthic chamber *P. oceanica* samples when 24-hour incubations were completed.

The spring *P. oceanica* and mixed species incubations were completed across 23-hour incubations missing one hour of daylight incubation. HOBO Pendant[®] light intensity data was used to distinguish hours of daytime (H_d) from hours of night (H_n). Daytime NCP ($NCP_{Daytime}$) (Champerois and Borges, 2012; Rodriguez et al., 2016) was calculated whereby H_i is the daylight incubation time:

$$NCP_{Daytime} = \left(\frac{\Sigma \Delta DO}{H_i} \right) \times H_d$$

The change that occurred during the night-time dark period (H_n) were summed over the whole night to calculate CR_{Night} , which has a negative sign, as follows:

$$CR_{Night} = \Sigma \Delta DO \left[\text{during } H_n \right]$$

For 23-hour incubations the combination of the net community change during the daytime ($NCP_{Daytime}$) and night-time dark period (CR_{Night}) determine NCP across 24 hours (NCP_{24}):

$$NCP_{24} = NCP_{Daytime} + CR_{Night}$$

Since the benthic chamber incubations do not acquire a direct measurement of $CR_{Daytime}$, we assume the hourly value of CR_{Night} and $CR_{Daytime}$ are equal (Cole and Pace, 2000):

$$CR_{Daytime} = \left(\frac{CR_{Night}}{H_n} \right) \times H_d$$

This allows daily community respiration (CR_{24}) to be found:

$$CR_{24} = CR_{Daytime} + CR_{Night}$$

GPP_{24} is then calculated as:

$$GPP_{24} = NCP_{24} - CR_{24}$$

Measurements of metabolism (with units of $\text{O}_2 \text{ mg L}^{-1} \text{ d}^{-1}$) were converted to measurements of flux (with units of $\text{O}_2 \text{ mol m}^{-2} \text{ d}^{-1}$) (Olive et al., 2015), by multiplying by volume (V) and dividing by area (A) of the benthic chamber.

The photosynthetic and respiratory quotient of 1 mol of O_2 : 1 mol CO_2 is applied to terrestrial plants that use starch and sugars as respiratory substrates, as observed in *P. oceanica* (Alcoverro et al., 2001). The photosynthetic and respiratory quotient of 1 mol of O_2 : 1 mol CO_2 is conservatively applied to a wide number of seagrass species (Duarte et al., 2010) and therefore also used for *H. stipulacea* and *C. nodosa*. Therefore, the metabolism values are interchangeable as units of oxygen or carbon ($\text{O}_2 \text{ mol m}^{-2} \text{ d}^{-1}$ and $\text{C mol m}^{-2} \text{ d}^{-1}$).

2.4 Net Apparent Productivity Calculations

The net apparent productivity (NAP) of the seagrass and epiphytes (modified from Murray and Wetzel, 1987), was calculated as the difference between estimates for the NCP_{24} of the seagrass benthic chambers (NCP_{SG}) and the average NCP_{24} of the bare sand incubations (NCP_{BS}) (Murray and Wetzel, 1987) from the same corresponding season. Whilst there may be differences between the habitats beyond the presence and absence of vegetation the calculation of NAP is made on the assumption the prime difference between the vegetated and unvegetated benthic chambers is the presence of the seagrass and epiphytes. In fact, the expected contribution of epiphyte productivity is deemed minimal due to the overall high biomass of *P. oceanica* to that of the epiphytes (Cox et al., 2015), therefore the large benthic chamber NAP is assumed to primarily reflect the productivity of the *P. oceanica*.

$$NAP = NCP_{SG} - (\bar{x} NCP_{BS})$$

To account for seasonal changes in seagrass canopy the seasonal NAP measurements were also standardised by the concurrent seasonal canopy height (B_{length}) within the large

benthic chambers and presented separately as NAP canopy-height-normalised flux (NAP_N) (O_2 mmol m^{-2} cm^{-1} d^{-1}).

$$NAP_N = \frac{NAP}{B_{length}}$$

Accounting for the metabolism of the community within a seagrass meadow is important to determine the net productivity at a community level, but as the autotrophy within the community is largely attributed to the primary productivity of the seagrasses (Hemminga and Duarte, 2000), distinguishing the NAP and NAP_N enables a clearer determination of the influences driving this metabolic component of the community. Justifying the approach to distinguish between NCP (proxy of community metabolism) and NAP (proxy of plant productivity) within the seagrass meadow ecosystem, as seasonal community metabolism may partially mask the drivers in seagrass productivity. However, NCP estimates are widely accepted for benthic chamber metabolism studies within seagrass meadows (Duarte et al., 2010; Olive et al., 2015), because they clearly quantify the extent to which the overall community is a carbon sink or source. Hence, we also chose to present our results in NCP as it allows for closer comparisons to existing NCP estimates.

To determine the NAP of the small benthic chambers the average NCP of the bare sand incubations deployed at the same time as the corresponding seagrass species were used. Given each seagrass species were deployed consecutively the corresponding bare sand incubations were grouped; thus, 20th June – 5th July ($n = 6$) corresponding to *H. stipulacea*, 10th – 14th July ($n = 3$) for *C. nodosa* and 14th – 17th July ($n = 3$) for *P. oceanica*. Given the differences between these species typical above ground biomass comparative NAP is most appropriately discussed when accounting for these differences in biomass. NAP is therein presented standardised by the respective plant surface area as NAP_{N^2} (O_2 mmol cm^{-2} d^{-1}), calculated with the plant surface area from within the small benthic chambers (cm^2 m^{-2}).

$$NAP_{N^2} = \frac{NAP}{Plant_{SA}}$$

2.5 Data Analysis

2.5.1 Seasonal *P. oceanica* NCP, NAP and NAP_N

The three samples from winter and spring and four samples in summer, meant finding an appropriate data distribution suitable for the seasonal *P. oceanica* benthic chamber data is challenging, but Shapiro-Wilk tests confirmed that when grouped by Season both the NCP and NAP conform to normal distribution (autumn $W = 0.9903741$, $P > 0.05$; spring $W = 0.8167365$, $P > 0.05$; summer $W = 0.9591216$, $P > 0.05$) (Supplementary Figure 3). Whilst Bartlett's test confirmed equal variances across both the NCP and NAP seasonal groups ($K = 0.00952$, $P > 0.05$). Therefore, ANOVAs were appropriate and were used to assess

if there was a significant seasonal difference in *P. oceanica* NCP, NAP and NAP_N . Tukey *post hoc* tests were used in each case to test for pairwise differences between the seasons.

2.5.2 Influence of Environmental Conditions on *P. oceanica* NAP

The mean PME miniDOT water temperature was calculated across each incubation period. HOBO logger irradiance (lux) were converted to PAR (photosynthetic active radiation), according to the conversion factor appropriate to the light source 'daylight' (Thimijan and Heins, 1983), this converts the light intensity into a more useful measure than the standard lux reported by the logger. The Instantaneous PAR with the unit $\mu mol\ s^{-1}\ m^{-2}$ is used to calculate Daily Light Integral (DLI) given the time interval in seconds (t) between each PAR reading over each 24-hour period:

$$DLI = \Sigma \Delta t \times PAR$$

The DLI is presented with the unit $mol\ m^{-2}\ d^{-1}$.

To examine the change in *P. oceanica* NAP relative to the changing light environment, the photosynthesis-irradiance relationship was fit with a hyperbolic tangent function (Jassby and Platt, 1976), modified to account for respiration (Rheuban et al., 2014), as used for the seagrass species in question (Koopmans et al., 2020). The model fitted was:

$$Flux = P_{max} \tanh \frac{I}{I_k} - R_l$$

where P_{max} , I_k and R_l are fitting constants; P_{max} represents the maximum photosynthetic rate, I_k is the saturation irradiance, R_l is respiration, and I is available light. The parameters were estimated by non-linear least squares approach (nls function, R version 3.5.1), estimating approximate start values. The irradiance compensation point is the irradiance at which net oxygen production equals zero. If no light saturation is occurring, this function converges to a linear function, (Rheuban et al., 2014). To determine the most appropriate model for both the saturation curve and linear model an Akaike Information Criterion approach was used (Burnham and Anderson, 2002).

As there was no significant interaction between temperature and seasonal NAP ($F_{1,4} = 0.189$, $P > 0.05$), or significant effect when temperature is assessed as a covariate for change in seasonal NAP by ANCOVA ($F_{1,6} = 2.1154$, $P > 0.05$) (Supplementary Figure 4). The maximal model to assess for significant effect of temperature on NAP was by ANOVA.

2.5.3 Annual *P. oceanica* Productivity

Annual NAP and NCP was estimated by scaling up the three average seasonal daily NAP and NCP measurements; the November measurement was chosen to represent the period between October to January (123 days), April represented the period from February to May (120 days) and July represented June to September (122 days):

$$\begin{aligned}
 \text{NAP}_{\text{Annual}} &= \left(\text{NAP}_{\text{Daily}(\text{Nov})} \times 123 \right) \\
 &+ \left(\text{NAP}_{\text{Daily}(\text{Apr})} \times 120 \right) + \left(\text{NAP}_{\text{Daily}(\text{Jul})} \times 122 \right) \\
 \text{NCP}_{\text{Annual}} &= \left(\text{NCP}_{\text{Daily}(\text{Nov})} \times 123 \right) + \left(\text{NCP}_{\text{Daily}(\text{Apr})} \times 120 \right) \\
 &+ \left(\text{NCP}_{\text{Daily}(\text{Jul})} \times 122 \right)
 \end{aligned}$$

2.5.4 Influence of Spatial Dynamics on *P. oceanica* NAP

A Welch's t-test, to account for unequal sample size, is applied to determine if the NAP differs between the central meadow area and the meadow edge. Then linear regressions are applied to the summer NAP measurements to determine if the difference in central meadow and meadow edge relate to changes in plant surface area, percentage cover, shoot density and blade length. Comparison of the R^2 values provides an understanding of which seagrass biometric account for the variation in NAP and are the best spatial predictor for *P. oceanica* NAP.

2.5.5 Species Specific Productivity Comparison

The comparative species-specific NAP_N^2 data conforms to a normal distribution ($W_{1,7} = 0.922$, $P > 0.05$) and an ANOVA was used to assess if there was a significant difference in NAP_N^2 between seagrass species during summer. The NAP standardised for plant surface area also confirmed to normal distribution ($W_{1,7} = 0.968$, $P > 0.05$) therefore an ANOVA was used here also, and Tukey *post hoc* tests confirmed any pairwise differences between species.

3 RESULTS

3.1 Seasonal *P. oceanica* NCP, NAP and NAP_N

The *P. oceanica* meadow NCP is greater than the bare sand incubations in every season (Figure 3A). In autumn, the *P. oceanica* community is overall heterotrophic, as CR is greater than GPP (3 B and C). However, the oxygen deficit is still greater in the community without seagrass (NCP ($\bar{x} = -3.1$, $\text{SD} \pm 7.62 \text{ O}_2 \text{ mmol m}^{-2} \text{ d}^{-1}$), than in the *P. oceanica* community (NCP $\bar{x} = -1.8$, $\text{SD} \pm 2.95 \text{ O}_2 \text{ mmol m}^{-2} \text{ d}^{-1}$) (Figure 3A). There is a significant seasonal influence on *P. oceanica* NCP ($F_{2,7} = 10.924$, $P < 0.05$). Pairwise *post hoc* comparisons show NCP is significantly higher in spring (NCP $\bar{x} = 7.6$, $\text{SD} \pm 2.84 \text{ O}_2 \text{ mmol m}^{-2} \text{ d}^{-1}$) and summer (NCP $\bar{x} = 7.1$, $\text{SD} \pm 2.75 \text{ O}_2 \text{ mmol m}^{-2} \text{ d}^{-1}$), compared to autumn when it is heterotrophic (Tukey: $P < 0.05$). There is no significant difference in NCP between the spring and summer.

During the transition from autumn to spring there is a large increase in GPP (GPP $\bar{x} = 18.3$, $\text{SD} \pm 7.11 \text{ O}_2 \text{ mmol m}^{-2} \text{ d}^{-1}$ to GPP $\bar{x} = 62.3$, $\text{SD} \pm 43.53 \text{ O}_2 \text{ mmol m}^{-2} \text{ d}^{-1}$, Figure 3B) and a simultaneous increase in CR (CR $\bar{x} = 20.2$, $\text{SD} \pm 9.21 \text{ O}_2 \text{ mmol m}^{-2} \text{ d}^{-1}$ to CR $\bar{x} = 54.7$, $\text{SD} \pm 40.75 \text{ O}_2 \text{ mmol m}^{-2} \text{ d}^{-1}$, Figure 3C). However, the increase in GPP is greater than the increase in CR transitioning the *P. oceanica* meadow from heterotrophic in autumn to autotrophic in spring (Figures 3B, C). The *P. oceanica* meadow stays in an autotrophic state in the Summer (Figures 3B, C) registering its highest GPP (GPP $\bar{x} = 85.6$, $\text{SD} \pm 67.52 \text{ O}_2 \text{ mmol m}^{-2} \text{ d}^{-1}$, Figure 3B), but also its highest CR (CR $\bar{x} = 78.6$, $\text{SD} \pm 67.51 \text{ O}_2 \text{ mmol m}^{-2} \text{ d}^{-1}$, Figure 3C). The increase in GPP is

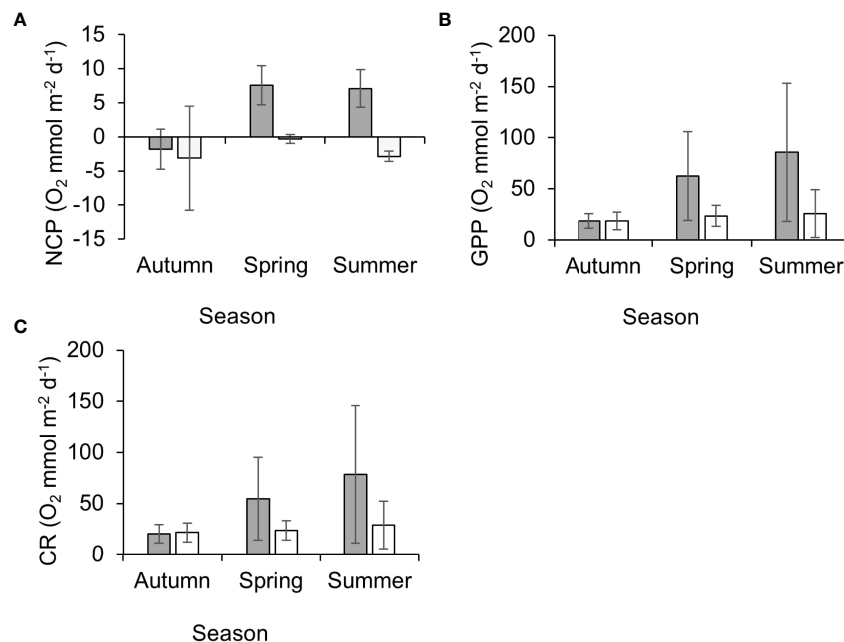


FIGURE 3 | (A) Net community productivity (NCP), **(B)** Gross primary productivity (GPP) and **(C)** Community respiration (CR) of *P. oceanica* meadow edge (grey) and bare sand incubations (White) determined across seasons with large benthic chambers; autumn (November), spring (April) and summer (July). Error bars represent standard deviation (autumn and spring $n = 3$, summer $n = 4$).

not as great as the increase in CR, therefore the NCP is lower in summer compared to spring (Figure 3A). Further to this, bare sand incubations have a higher metabolic rate in the summer (NCP $\bar{x} = -2.9$, SD ± 0.74 O₂ mmol m⁻² d⁻¹) compared to the spring (NCP $\bar{x} = -0.3$, SD ± 0.65 O₂ mmol m⁻² d⁻¹, Figure 3A).

Whilst the *P. oceanica* NCP is highest in spring, *P. oceanica* NAP is highest in summer (NAP $\bar{x} = 9.9$, SD ± 2.75 O₂ mmol m⁻² d⁻¹) (Figure 4A). There remains a significant seasonal difference in *P. oceanica* NAP ($F_{2,7} = 8.3885$, $P < 0.05$). However, Tukey *post hoc* comparisons found NAP is only significantly lower in autumn compared to summer (Tukey: $P < 0.05$). Although there is an observational difference in NAP between the autumn (NAP $\bar{x} = 1.3$, SD ± 2.95 O₂ mmol m⁻² d⁻¹) and spring (NAP $\bar{x} = 7.9$, SD ± 2.84 O₂ mmol m⁻² d⁻¹) the difference is not significant. There remains no significant difference in NAP between the periods of highest productivity in spring and summer.

The canopy height within the edge *P. oceanica* habitat is lowest during autumn ($\bar{x} = 15.4$, SD ± 2.84 cm), this increases into spring ($\bar{x} = 22.3$, SD ± 4.77 cm) and peaks during summer ($\bar{x} = 25.1$, SD ± 5.90 cm). *P. oceanica* NAP_N is lowest in autumn and most variable within autumn (NAP_N $\bar{x} = 0.01$, SD ± 0.201 O₂ mmol m⁻² cm⁻¹ d⁻¹) (Figure 4B). In comparison *P. oceanica* NAP_N in Summer (NAP_N $\bar{x} = 0.4$, SD ± 0.06 O₂ mmol m⁻² cm⁻¹ d⁻¹), is less varied and similar to spring (NAP_N $\bar{x} = 0.4$, SD ± 0.121 O₂ mmol m⁻² cm⁻¹ d⁻¹) (Figure 4B). Thus, the significant seasonal difference in NAP_N remains, between autumn and summer ($F_{2,7} = 6.3149$ $P < 0.05$). There is no significant difference in NAP_N between autumn and spring or spring and summer.

3.2 Influence of Environmental Conditions on *P. oceanica* NAP

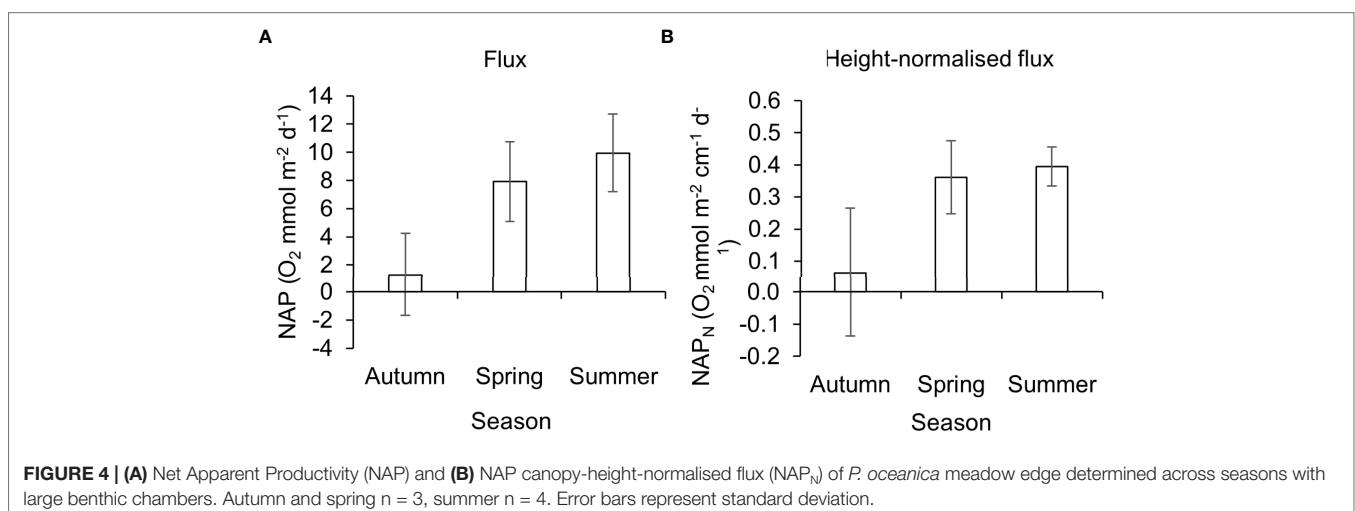
The daily light integral ranged from 4.7 mol photons m⁻² d⁻¹ during autumn to 25.2 mol photons m⁻² d⁻¹ in the summer. Variation in environmental conditions within each season allowed for some overlap in the irradiance encountered between seasons and the *P. oceanica* NAP resembled a saturation curve when plotted as a function of irradiance (Figure 5A), as did the

curve for NAP_N (Figure 5B). When fit to the NAP dataset the AIC value of the hyperbolic tangent function versus linear model (AIC = 58.77 vs 61.72) confirmed the use of a light saturation model for demonstrating the presence of light saturation opposed to that of a linear function. The model fitting constants for NAP are $P_{max} = 64.853$, $I_k = 3.609$ and $R_l = 55.646$. The DLI conditions in autumn (minimum = 4.7 mol photons m⁻² d⁻¹) sit near the predicted irradiance compensation point ($I_c = 4.6$ mol photons m⁻² d⁻¹) as such within the autumnal DLI range there are conditions where the plant may only just or may not maintain metabolic requirements due to low irradiance. In spring the seagrass transitions between light limiting and light saturating levels. The light saturating conditions occur throughout summer, when NAP (NAP $\bar{x} = 9.9$, SD ± 2.75 O₂ mmol m⁻² d⁻¹, Figure 4A) sits near the predicted maximum (9.21 O₂ mmol m⁻² d⁻¹, Figure 5A). The changes in the DLI account for 71% of the variation in *P. oceanica* NAP (Figure 4A). The period of summer light saturation also corresponds to when NAP_N is less varied (Figure 4B).

The water temperature was lowest in spring ($\bar{x} = 17.7$, SD ± 0.13 °C), increasing to a summer high ($\bar{x} = 23.6$, SD ± 0.40 °C). The autumn temperatures encountered sat at a relative mid-point ($\bar{x} = 20.7$, SD ± 0.45 °C) between spring and summer, yet the NAP was lowest in autumn. Therefore, the change in NAP and was not relative to the change in water temperature and not a statistically significant factor in our model (Supplementary Figure 4), with season (Temperature $F_{1,6} = 2.1154$, $P > 0.05$) or without season (Temperature $F_{1,8} = 0.7265$, $P > 0.05$).

3.3 Annual Productivity of *P. oceanica* Edge Habitat

The annual NAP of the *P. oceanica* edge habitat in this meadow was estimated at 2.3 C mol m⁻² yr⁻¹. However, the organisms present within the *P. oceanica* meadow have their own metabolic requirements (NCP without seagrass present -0.8 C mol m⁻² yr⁻¹), as such the net carbon gain at the community level for this *P.*



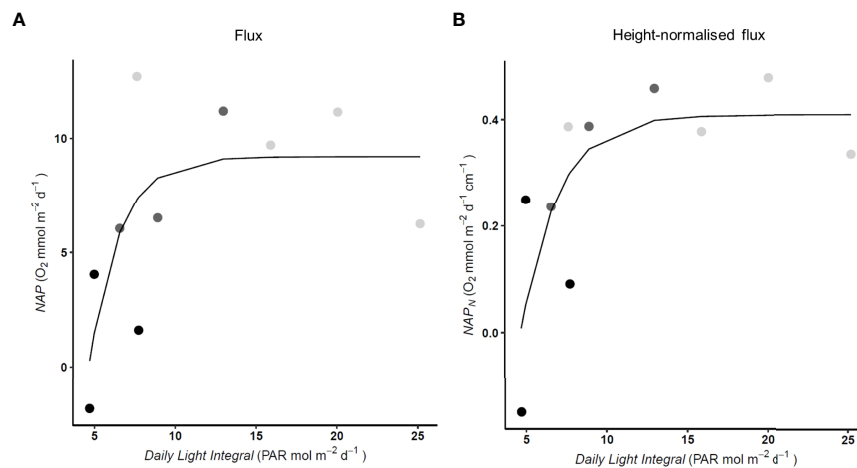


FIGURE 5 | (A) Net Apparent Productivity (NAP) ($R^2 = 0.713$) and **(B)** NAP canopy-height-normalised flux (NAP_N) ($R^2 = 0.711$) presented as a function of PAR given as the Daily Light Integral, for *P. oceanica* meadow edge determined across seasons with large benthic chambers. The irradiance compensation point (I_c) was $4.6 \text{ mol photons m}^{-2} \text{ d}^{-1}$. Replicate season denoted for visual reference autumn (●), spring (●) and summer (●).

oceanica meadow was less than the NAP produced annually by the *P. oceanica* ($NCP = 1.5 \text{ C mol m}^{-2} \text{ yr}^{-1}$).

3.4 Influence of Spatial Dynamics on *P. oceanica* NAP

The *P. oceanica* NAP in summer is significantly different between the central areas of the meadow and the meadow edge ($t_{(1,4)} = 3.7647, P < 0.05$). (Figure 6). The *P. oceanica* NAP is highest in the central areas of the meadow ($NAP \bar{x} = 19.7, SD \pm 3.83 \text{ O}_2 \text{ mmol m}^{-2} \text{ d}^{-1}$) and approximately two-fold that of the edge habitat ($NAP \bar{x} = 9.9, SD \pm 2.75 \text{ O}_2 \text{ mmol m}^{-2} \text{ d}^{-1}$). The *P. oceanica* NAP increases relative to the plant surface area of *P. oceanica* (LM: $F_{1,5} = 132.5, P < 0.01$) (Figure 6A). The plant surface area was the best predictor of NAP and accounted for more than 96% of the variation in NAP. As standalone biometrics of seagrass meadow metabolism, shoot density (m^2), blade length (cm) and seagrass cover (%), were all significant predictors of NAP (shoot density, LM: $F_{1,5} = 21.13, P < 0.01$; blade length, LM: $F_{1,5} = 12.98, P < 0.05$; percentage cover, LM: $F_{1,5} = 8.78, P < 0.05$) but they only accounted for 81%, 72% and 64% (Figures 6B–D) of the variation in NAP of the *P. oceanica*.

3.5 Species Specific Productivity

The seagrass benthic communities at 7m depth are all heterotrophic at the community level, ranging from the least heterotrophic with *H. stipulacea* present ($NCP \bar{x} = -4.8, SD \pm 4.7 \text{ O}_2 \text{ mmol m}^{-2} \text{ d}^{-1}$), followed by the community with *P. oceanica* present ($NCP \bar{x} = -7.5, SD \pm 8.9 \text{ O}_2 \text{ mmol m}^{-2} \text{ d}^{-1}$) and finally the most heterotrophic the *C. nodosa* dominant community ($NCP \bar{x} = -10.5, SD \pm 6.0 \text{ O}_2 \text{ mmol m}^{-2} \text{ d}^{-1}$) (Figure 7A). The difference spatially in above ground vegetative material between species is demonstrated through the increasing total plant surface between species from *H. stipulacea* ($\bar{x} = 5.1, SD \pm 1.4 \times 10^{-3} \text{ cm}^2 \text{ m}^{-2}$), to *C. nodosa* ($\bar{x} = 10.6, SD \pm 9.4 \times 10^{-3} \text{ cm}^2 \text{ m}^{-2}$) and culminating

in *P. oceanica* ($\bar{x} = 17.6, SD \pm 7.3 \times 10^{-3} \text{ cm}^2 \text{ m}^{-2}$) (Figure 7B). However, the plant surface area is also more uniform for *H. stipulacea* spatially across the habitat sampled, in comparison the plant surface area of both *C. nodosa* and *P. oceanica* show higher variation between samples (Figure 7B).

H. stipulacea NAP_N^2 appears to be the highest comparatively and the only seagrass species to on average maintain positive carbon balance ($\text{O}_2 > 0$) (Figure 7C). However, variation in NAP_N^2 for *H. stipulacea* ($NAP_N^2 \bar{x} = 0.0004, SD \pm 0.0011 \text{ O}_2 \text{ mmol cm}^{-2} \text{ d}^{-1}$) and *P. oceanica* ($NAP_N^2 \bar{x} = -0.0004, SD \pm 0.0009 \text{ O}_2 \text{ mmol cm}^{-2} \text{ d}^{-1}$) show both species fluctuate between positive and negative carbon balance within this area of the bay in Summer (Figure 7C). Whilst *C. nodosa* NAP_N^2 is the lowest and consistently negative ($NAP_N^2 \bar{x} = -0.0012, SD \pm 0.0007 \text{ O}_2 \text{ mmol cm}^{-2} \text{ d}^{-1}$). A significant difference in NAP_N^2 does occur between species ($F_{2,14} = 4.1922, P < 0.05$). Tukey *post hoc* comparisons confirm *C. nodosa* NAP_N^2 to be significantly lower than *H. stipulacea* NAP_N^2 (Tukey: $P < 0.05$). But there was no significant difference between the native species *C. nodosa* and *P. oceanica* NAP_N^2 and also no significant difference in NAP_N^2 between *H. stipulacea* and *P. oceanica*.

4 DISCUSSION

4.1 Seasonal *P. oceanica* NCP, NAP and NAP_N

We found strong seasonality in *P. oceanica* productivity, at both the community (NCP Spring $\bar{x} = 7.6, SD \pm 2.84$; Autumn $\bar{x} = -1.8, SD \pm 2.95 \text{ O}_2 \text{ mmol m}^{-2} \text{ d}^{-1}$) and plant level (NAP Summer $\bar{x} = 9.9, SD \pm 2.75$; Autumn ($\bar{x} = 1.3, SD \pm 2.95 \text{ O}_2 \text{ mmol m}^{-2} \text{ d}^{-1}$), which reinforces the need for seagrass carbon sequestration studies to consider year-round dynamics, thereby ensuring carbon storage estimates are not exaggerated by only reflecting summer peaks. Similar conclusions from studies of

net ecosystem productivity in freshwater lakes (Brentrup et al., 2020), temperate saltmarshes (Vazques-Lule & Vargas, 2021) and seagrass habitat (Champenois and Borges, 2012; Caffray et al., 2014), suggest that this should be the norm. Strong seasonality of *P. oceanica* NCP in the Western Mediterranean typically occurs after an October minimum coinciding with increases in aboveground biomass, followed by a decrease through summer and autumn when aboveground biomass is stable and then decreases (Champenois and Borges, 2012). Similarly in the Eastern Mediterranean but within the western region of the Aegean Sea strong seasonality in NCP is apparent with a marked decrease from June to August, before reaching its minimum in October. Therefore, our study adds to the evidence that single season measures of seagrass NCP are inappropriate, given autumnal lows are a typical artifact of *P. oceanica* studies across the Mediterranean.

Multi-season approaches enable the assessment of seasonal drivers such as irradiance (Gazeau et al., 2005; Champenois and Borges, 2012). During autumn, the overall irradiance reaching the plant is lower as the daylight period is shorter, the likelihood of cloud cover increases, and increased frequency of stormy conditions results in greater hydrodynamic activity reducing in-water visibility. Subsequently autumnal photosynthetic activity occurs when conditions are light limiting, promoting a greater variability in productivity. In contrast light saturating

levels present throughout summer, lead to a lower *P. oceanica* photosynthetic efficiency and saturation is evident in this study given the low variation in summer productivity. Long-term exposure to saturating irradiance decreases plant productivity and can lead to photoinhibition (Ralph and Burchett, 1995), though a decline from photoinhibition is not considered in this study. The saturation response alone has important considerations for modelling total fixed carbon, re-emphasising the importance of seasonality which is dependent on the concurrent irradiance levels. Physical disturbance to seagrass meadows such as autumnal and winter storms will seasonally reduce the available photosynthetically active plant material, i.e., as storms tear seagrass blades. Although we have considered seasonal changes in seagrass productivity (NAP) and presented this standardised by any seasonal changes in seagrass canopy height (NAP_N), we have not directly measured vegetative export from the meadow over winter, which can be vast enough to create seagrass exported onshore forms called banquettes (Gomez-Pujol et al., 2013); in short – large, heaped mounds of decaying seagrass on the shoreline. The seasonal storm export of biomass from these meadows needs to be determined, because the retention of plant material is intrinsically linked to its carbon sequestration potential. Senescence the shedding and loss of leaf material at the end of the summer season which can be at a scale of >85% of *P. oceanica* leaf production (Cebrian and Duarte, 2001), would also

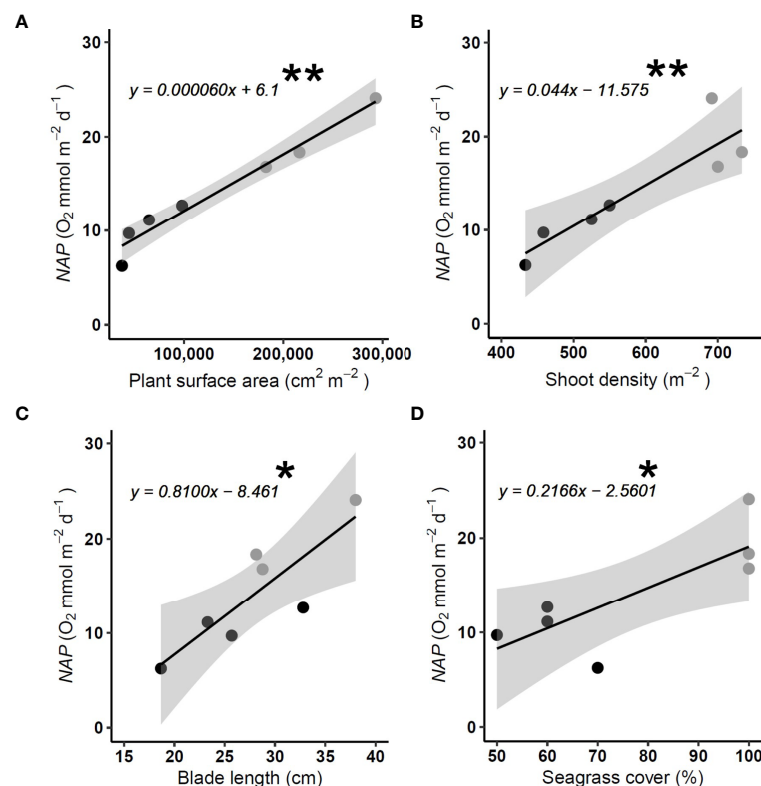


FIGURE 6 | Net apparent productivity (NAP) of *P. oceanica* meadow edge (Black) and meadow center (grey) determined in Summer with large benthic chambers, in relation to **(A)** *P. oceanica* blade surface area **(B)** *P. oceanica* shoot density (m⁻²) **(C)** *P. oceanica* blade length (cm) and **(D)** *P. oceanica* cover (%). Central meadow n = 3, meadow edge n = 4. Significant linear regression from edge and central meadow combined * = P < 0.05, ** = P < 0.01. Grey bands reflect the 95% confidence level interval for predictions from a linear model.

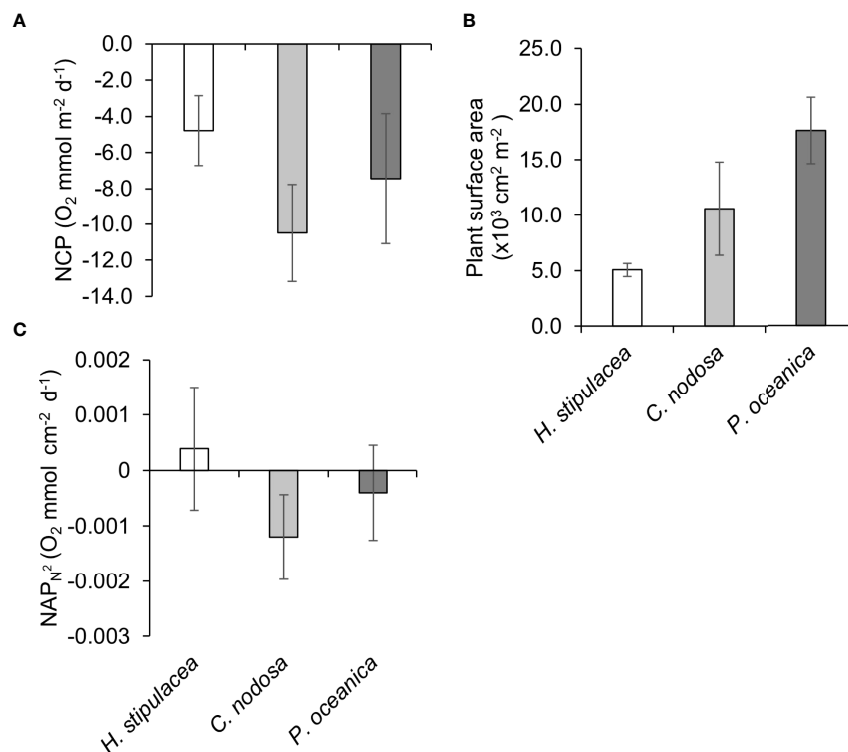


FIGURE 7 | (A) Net community productivity (NCP), **(B)** Plant surface Area **(C)** NAP plant-surface area-normalised flux (NAPN2), for sparse *H. stipulacea* (n = 6), *C. nodosa* (n = 5) and *P. oceanica* (n = 6) determined in summer by small benthic chambers. Error bars represent standard deviation.

lead to reduced productivity in autumn as less photosynthetically active material would remain within the meadow. In fact the canopy height of the shallow sparse *P. oceanica* within this meadow is notably reduced in the autumn with the loss of more mature longer blades and likely a contributory factor to the observed low productivity.

Given *P. oceanica* meadows within the eastern region of the Aegean Sea have been noted to be fragmented in response to elevated sea surface temperatures (Chefaoui et al., 2017), it is surprising we found no statistically significant influence of temperature on the productivity of shallow water *P. oceanica*. Other temperate seagrass species have been shown to transition to a negative carbon balance when exposed to high summer water temperatures (Marsh Jr. et al., 1986). Although our highest average daily water temperature was above optimal thermal conditions (23.9 vs 17 - 20 °C) for *P. oceanica* (Champenois and Borges, 2018), this was well below *P. oceanica* critical temperature limits (> 29 °C). The *in-situ* nature of this study does not allow for the independent control of water temperature or light intensity encountered at any time, and so they are often correlated making it challenging to differentiate between them. Shallow water *P. oceanica* has a greater tolerance to increased water temperatures than deeper *P. oceanica* (Marin-Guirao et al., 2016). This heat acclimation in shallow *P. oceanica* emerges by stabilising respiration, thereby establishing respiratory homeostasis (i.e., balanced photosynthetic carbon gains and

respiratory carbon losses; Marin-Guirao et al., 2016). This suggests that shallow *P. oceanica* may maintain net productivity gains at higher water temperatures for longer periods. It is also possible that the *P. oceanica* within the Eastern Mediterranean may have a greater acclimation to increased water temperature, as the Eastern Mediterranean basin has been exposed to higher sea surface temperatures for longer than the Western basin (since 1985) (Nykjaer, 2009). Ultimately any temperature effect on *P. oceanica* metabolism in this study was confounded by the strong irradiance effect and thus could not be disentangled.

4.2 Annual *P. oceanica* NCP and NAP

The annual net community productivity for *P. oceanica* meadows in our study was lower than recorded for two *P. oceanica* meadows previously studied in the western region of the Aegean Sea, even one negatively impacted by eutrophication (4.83 C mol m⁻² yr⁻¹) (Apostolaki et al., 2010), however that study used smaller chambers, which are more likely to cause oxygen saturation which can overestimate productivity. The annual NCP in our study was conservative as it was obtained from patchy *P. oceanica* edge habitat, this underestimates the meadows total fixed carbon which consisted of both dense and patchy habitat. However, in shallow water meadows, patchy edge habitat is a more prominent feature (Montefalcone et al., 2009), therefore it is an appropriate conservative annual NCP estimate. The annual

NCP of $1.5 \text{ C mol m}^{-2} \text{ yr}^{-2}$ calculated for shallow *P. oceanica* in the Eastern Mediterranean would benefit from sampling at a bimonthly or monthly regime to better ascertain the switch point when the meadow transitions from autotrophic to heterotrophic. However annual metabolism rates of *P. oceanica* in the Eastern Mediterranean are rare and therefore this estimation remains important.

Our measures of *P. oceanica* meadow centre productivity was two-fold that of the edge habitat, therefore shallow *P. oceanica* meadow can support annual total fixed carbon at between $2.3 - 4.6 \text{ C mol m}^{-2} \text{ yr}^{-2}$. The carbon sequestration potential of seagrass meadows ultimately relates to how much of the total fixed carbon produced by the seagrass, i.e., the productivity, accumulates as refractory material in the seagrass meadow. It has been estimated that *P. oceanica* has the capacity to sequester in the sedimentary compartment around 21% of the carbon fixed by primary production (Pergent-Martini et al., 2021). However, reduced current attenuation should promote significantly higher organic carbon concentration with distance from the edge (Oreska et al., 2017). The patchiness of shallow meadows may therefore render them less effective at attenuating currents and promoting settlement of organic particles leading to a lower capacity for the sequestration of photosynthetically fixed carbon. Despite a lower potential for patchy *P. oceanica* to fix and sequester the fixed carbon compared to other seagrass meadows they still actively contribute to carbon acquisition within the carbon cycle. If shallow patchy *P. oceanica* meadows transitioned to an unvegetated state this would result in the loss of this photosynthetic carbon fixation, transitioning from an autotrophic habitat to one that functions as a carbon source (i.e., bare sand habitat). Given a total of 7139.92 km^2 of *P. oceanica* is estimated to occur in the Eastern Mediterranean Basin (Telesca et al., 2015), and seagrass coverage within Greek waters has been estimated at 2619 km^2 (Topouzelis et al., 2018), *P. oceanica* within Greek waters represents around 36.7% of the total *P. oceanica* in the Eastern Mediterranean. The quantity of *P. oceanica* habitat within the Aegean Sea and Eastern Mediterranean means it represents a substantial blue carbon habitat irrespective of its fragmented nature (Chefaoui et al., 2018). The further loss of this habitat would risk current climate change targets therefore seagrass meadows need distinct conservation management strategies given their proximity to current threats including impacts from human infrastructure and coastal activities (Giakoumi et al., 2015).

4.3 Spatial Dynamics of *P. oceanica* NAP

Metabolism measurements are typically presented as an area-based unit (Apostolaki et al., 2010; Duarte et al., 2010; Olive et al., 2015). We have shown Net Apparent Productivity to be affected by spatial variation in plant aboveground biomass, this would suggest that reported estimates may benefit from additional information on canopy height and shoot density, particularly in the case of *P. oceanica*. Estimates should therefore potentially move away from denoting discrete areal measurements for meadows. Instead acquiring and mapping large scale data on canopy height (shoot size) and shoot density to enable comprehensive habitat wide total fixed carbon estimates. Acquiring seagrass biometric

data to support productivity estimates requires greater effort than collating presence-absence or coverage data, but simple plant biometrics of shoot density and leaf area index have been demonstrated as standalone predictors of carbon sequestration and community composition (Samper-Villarreal et al., 2016; Collier et al., 2021). High shoot density in shallow areas with a high degree of patchiness creates very specific nest-like patterns, these have their highest shoot density in the centre and decrease in density radially towards the edge of the patches (Zupo et al., 2005). Therefore, this distinction in spatial productivity between edge and central areas of *P. oceanica* may be a specific characteristic to consider for shallow meadows because overall shoot densities are highest in the shallow and decrease with depth (Olesen et al., 2002; Zupo et al., 2005). More work would be needed to determine if the same distinctions in shoot density and subsequent primary productivity exist between the edge and central areas of *P. oceanica* meadows in deeper waters. The use of chambers with a larger benthic surface area has a greater representation of community-scale metabolism, as trialled for heterogenic coral reef habitats (Yates and Halley, 2003). The use of a larger benthic chamber for *P. oceanica* metabolism measurements in this study (1m diameter) comprises community metabolism measurements influenced by fine scale variation in shoot density, compared to previous studies using smaller chambers (0.18m diameter), which house only a few shoots at similar densities within the benthic chamber (Gazeau et al., 2005; Barron et al., 2006).

4.4 Species Specific NCP and NAP_{N}^2

Whilst we found shallow central and edge *P. oceanica* meadow (2m) to be autotrophic in the Summer, *P. oceanica* at 7m depth, where it is found mixed with *C. nodosa* and *H. stipulacea*, fluctuated between positive and negative carbon balance. Such heterogeneity within the same bay highlights that adjacent *P. oceanica* patches may simultaneously undergo growth and loss. Given the health of the *P. oceanica* at 7m depth was decreased indicated by the reduced plant surface area ($\bar{x} = 17.6$, $\text{SD} \pm 7.3 \times 10^{-3} \text{ cm}^2 \text{ m}^{-2}$) relative to the shallow area where the plant surface area was higher (Ranging from $37.6 - 293.0 \times 10^{-3} \text{ cm}^2 \text{ m}^{-2}$) and given plant surface area acts as a predictor of productivity in the shallower areas, lower productivity and in this case the heterotrophic nature may be explained by these characteristics. It must also be considered that our results for this comparison are influenced by differences in chamber area, volume, and incubation time.

Based on our productivity assessments alone, the non-native *H. stipulacea* ability to fix carbon was comparable to *P. oceanica* (NAP_{N}^2 ($\bar{x} = 0.0004$, $\text{SD} \pm 0.0011$ vs ($\bar{x} = -0.0004$, $\text{SD} \pm 0.0009 \text{ O}_2 \text{ mmol m}^{-2} \text{ d}^{-1}$). *H. stipulacea*'s NAP is positive and the *P. oceanica* fluctuates between positive and negative carbon balance, suggesting that both can maintain a balance between carbon fixation and carbon utilised for carbon metabolic activity. Which explains why *H. stipulacea* has the capability to opportunistically colonise space previously occupied by *P. oceanica*. With regression of *P. oceanica* meadows well documented (Telesca et al., 2015), alongside *H. stipulacea* range

expansion (Georgiou et al., 2016), maintenance of Mediterranean seagrass meadow areal cover through replacement of current seagrass species cover is likely. Whilst *H. stipulacea* has persisted within the Mediterranean since 1894 and expanded its known range (Fritsch, 1895; van der Velde and den Hartog, 1992; Gambi et al., 2009; Tsiamis et al., 2010; Sghaier et al., 2011; Georgiou et al., 2016). *H. stipulacea* is known to disappear and recolonise as per a metapopulation (Gambi et al., 2009), making the persistence of its sedimentary carbon stocks questionable. While questions remain, *H. stipulacea* is considered to be making positive contributions to community blue carbon in the eastern Aegean (Apostolaki et al., 2019). In fact, carbon sequestration into the sedimentary compartment by *H. stipulacea* has been estimated to be greater than *P. oceanica* in the Eastern Mediterranean (Wesselmann et al., 2021). However, *H. stipulacea* carbon sequestration is not yet greater than *P. oceanica* carbon sequestration estimates in the Western Mediterranean (Mazarrasa et al., 2017). *H. stipulacea* productivity in the Mediterranean is lower than its native range, given irradiance was the driving factor in *H. stipulacea* productivity within its home range in the Gulf of Aquaba and its generally tropical origins (Cardini et al., 2018), under future climate change predictions of a warming Mediterranean *H. stipulacea* has potential to increase its productivity, whilst the same cannot be said for *P. oceanica*.

The replacement of *P. oceanica* by *C. nodosa* is well documented (Montefalcone et al., 2006; Montefalcone et al., 2007). This replacement is typically considered a result of *C. nodosa* being more tolerant to varying environmental conditions. Compared against six dominant native Mediterranean macrophytes *C. nodosa* presented the highest thermal optima (Savva et al., 2018). But the substitution of *P. oceanica* for *C. nodosa* is not exclusive, replacement of *P. oceanica* dead matte to algae dominated *Caulerpa* spp. habitats also occurs (Montefalcone et al., 2007). *C. nodosa* may not always be the 'winner' following loss or fragmentation of *P. oceanica* meadows. Whilst the *C. nodosa* and *H. stipulacea* in the deeper part of this meadow had different plant surface areas (*C. nodosa* \bar{x} = 10.6, SD \pm 9.4 cm²; *H. stipulacea* = \bar{x} = 5.1, SD \pm 1.4 cm²), when their biomass is comparable *C. nodosa* would be expected to deteriorate as it is utilising carbon more than it is fixing, whilst *H. stipulacea* would maintain a positive carbon balance. In the Southern Mediterranean replacement of *C. nodosa* by *H. stipulacea* under warmer environmental conditions has already been demonstrated to occur (Sghaier et al., 2014). Very shallow water will be readily heated by the sun, in the North Mediterranean this may provide warmer conditions closer to the tropical native range of *H. stipulacea*. Within our study site, but at a shallower location (0.5m depth), *H. stipulacea* was found mixed within dense *C. nodosa* beds and growing multiple paired leaves off a vertical stem (Pers. obv., **Supplementary Figure 5**). This is important given lateral growth is more typical of this species (Posluszny and Tomlinson, 1991; Winters et al., 2020). Vertical growth would give *H. stipulacea* the potential to increase its biomass relative to *C. nodosa*. However, *C. nodosa* colonisation has been shown to shift the benthic sediment community from autotrophic (e.g., microphytobenthic) to strongly heterotrophic when associated with mature stands of *C. nodosa* (Barron et al.,

2004). Therein the negative productivity documented here in association with *C. nodosa* could be representative of a strong benthic community shift towards respiration within the *C. nodosa* enclosed benthic chambers.

5 CONCLUSIONS

This study establishes that not all seagrass habitat is equal in its capacity to fix carbon, but the variability can in part be accounted for seasonally and spatially; using environmental predictors such as irradiance; plant biometrics such as plant surface area; and determining species specific assessments particularly in mixed species seagrass meadows. Here seagrass meadows in the eastern Mediterranean have been used as an archetype to demonstrate the high levels of spatio-temporal variability in these plants ability to fix carbon. Which highlights the importance of protecting Eastern Mediterranean seagrass meadows for their capacity to naturally fix carbon, even when shallow and patchy in nature. If the true value of natural ecosystems such as seagrass meadows are to be understood particularly for their capacity to sequester carbon, finetuning knowledge to account for the natural spatial and seasonal variation in these ecosystems needs to take place.

DATA AVAILABILITY STATEMENT

The raw data supporting the conclusions of this article is available to access at the following link: <http://researchdata.essex.ac.uk/153/>.

AUTHOR CONTRIBUTIONS

EW, TC, TW, CA, TT, and AM contributed to the study conception and design. EW and CA led the field-based studies, supported by TT and AM. TW led a preliminary pilot study integral to our final experimental design. EW and TC led on data analysis and the manuscript first draft. All authors were involved in the revision and final approval of this version of the manuscript.

FUNDING

The Erasmus+ Programme provided funding for TW and EW to complete student placements with Archipelagos Institute of Marine Conservation (AIMC). The University of Essex supported CA. AIMC, the University of Essex and the UKRI Natural Environment Research Council (NE/R016569) funded the collaboration, purchase of field equipment and time spent by TT, AM, and TCC on this project.

ACKNOWLEDGMENTS

Thank you to Jack Wade for technical support related to the design, assembly, and maintenance of the submersible pump system. The following interns from AIMC assisted with

fieldwork operations: Camilla Hansen, Jente van Langerak, Nikos Papagiannopoulos and Saulé Medelytė; The works presented here formed part of the study towards a Masters by Dissertation (EW) and Masters of Science (CA and TW) at the University of Essex.

REFERENCES

- Abadie, A., Gobert, S., Bonacorsi, M., Lejeune, P., Pergent, G. and Pergent-Martini, C. (2015). Marine Space Ecology and Seagrasses. Does Patch Types Matter in *Posidonia Oceanica* Seascapes? *Ecol. Indic.* 57, 435–446. doi: 10.1016/j.ecolind.2015.05.020
- Abadie, A., Pace, M., Gobert, S. and Borg, J. A. (2018). Seascape Ecology in *Posidonia Oceanica* Seagrass Meadows: Linking Structure and Ecological Processes for Management. *Ecol. Indic.* 87, 1–13. doi: 10.1016/j.ecolind.2017.12.029
- Alcoverro, T., Manzanera, M. and Romero, J. (2001). Annual Metabolic Carbon Balance of the Seagrass *Posidonia Oceanica*: The Importance of Carbohydrate Reserves. *Mar. Ecol. Prog. Ser.* 211, 105–116. doi: 10.3354/meps211105
- Apostolaki, E. T., Holmer, M., Marba, N. and Karakassis, I. (2010). Metabolic Imbalance in Coastal Vegetated (*Posidonia Oceanica*) and Unvegetated Benthic Ecosystems. *Ecosystems* 13, 459–471. doi: 10.1007/s10021-010-9330-9
- Apostolaki, E. T., Vizzini, S., Santinelli, V., Kaberi, H., Andolina, C. and Papatthanassiou, E. (2019). Exotic *Halophila Stipulacea* is an Introduced Carbon Sink for the Eastern Mediterranean Sea. *Nat. Sci. Rep.* 9, 9643. doi: 10.1038/s41598-019-45046
- Arnaud-Haond, S., Migliaccio, M., Diaz-Almela, E., Teixeira, S., van de Vliet, M. S., Alberto, F., et al. (2007). Vicariance Patterns in the Mediterranean Sea: East-West Cleavage and Low Dispersal in the Endemic Seagrass *Posidonia Oceanica*. *J. biogeography* 34, 963–976. doi: 10.1111/j.1365-2699.2006.01671.x
- Barron, C. and Duarte, C. M. (2009). Dissolved Organic Matter (DOM) Release in a *Posidonia Oceanica* Meadow. *Mar. Ecol. Prog. Ser.* 374, 75–84. doi: 10.3354/meps07715
- Barron, C., Duarte, C. M., Frankignoulle, M. and Borges, A. V. (2006). Organic carbon metabolism and carbonate dynamics in a Mediterranean seagrass (*Posidonia oceanica*) meadow. *Estuaries and Coasts*, 29, 417–426.
- Barron, C., Marbe, N., Terrados, J., Kennedy, H. and Duarte, C. M. (2004). Community Metabolism and Carbon Budget Along a Gradient of Seagrass (*Cymodocea Nodosa*) Colonization. *Limnol. Oceanogr.* 49, 1642–1651. doi: 10.4319/lo.2004.49.5.1642
- Berg, P., Delgard, M. L., Polsenaere, P., McGlathery, K. J., Doney, S. C. and Berger, A. C. (2019). Dynamics of Benthic Metabolism, O₂ and Pco₂ in a Temperate Seagrass Meadow. *Assoc. Sci. Limnol. Oceanogr.* 64, 2586–2604. doi: 10.1002/lno.11236
- Borg, J. A., Rowden, A. A., Attrill, M. J., Schembri, P. J. and Jones, M. B. (2006). Wanted Dead or Alive: High Diversity of Macroinvertebrates Associated With Living and 'Dead' *Posidonia Oceanica* Matte. *Mar. Biol.* 149, 667–677. doi: 10.1007/s00227-006-0250-3
- Boudouresque, C. F., Bernaud, G., Pergent, G., Shili, A. and Verlaque, M. (2009). Regression of Mediterranean Seagrasses Caused by Natural Processes and Anthropogenic Disturbances and Stress: A Critical Review. *Botanica Marina* 52, 395–418. doi: 10.1515/BOT.2009.057
- Brenttrup, J. A., Richardson, D. C., Carey, C. C., Ward, N. K., Bruesewitz, D. A. and Weathers, K. C. (2020). Under-Ice Respiration Rates Shift the Annual Carbon Cycle in the Mixed Layer of an Oligotrophic Lake From Autotrophy to Heterotrophy. *Inland waters* 11, 114–123. doi: 10.1080/20442041.2020.1805261
- Burnham, K. P. and Anderson, D. R. (2002). *Model Selection and Multimodel Inference: A Practical Information-Theoretic Approach*. 2nd ed (New York: Springer).
- Caffray, J. M., Murrell, M. C., Amacker, K. S., Harper, J. W., Phipps, S. and Woodrey, M. S. (2014). Seasonal and Inter-Annual Patterns in Primary Production, Respiration, and Net Ecosystem Metabolism in Three Estuaries in the Northeast Gulf of Mexico. *Estuaries Coasts* 37, 222–241. doi: 10.1007/s12237-013-9701-5
- Cebrian, J. and Duarte, C. M. (2001). Detrital Stocks and Dynamics of the Seagrass *Posidonia Oceanica* (L.) Delile in the Spanish Mediterranean. *Aquat. Bot.* 70, 295–309. doi: 10.1016/S0304-3770(01)00154-1
- Champanois, W. and Borges, A. V. (2012). Seasonal and Inter-Annual Variations of Community Metabolism Rates of a *Posidonia Oceanica* Seagrass Meadow. *Limnol. Oceanogr.* 57, 347–361. doi: 10.4319/lo.2012.57.1.0347
- Champanois, W. and Borges, A. V. (2018). Inter-Annual Variations Over a Decade of Primary Production of the Seagrass *Posidonia Oceanica*. *Limnol. Oceanogr.* 64, 32–45. doi: 10.1002/lno.11017
- Cardini, U., van Hoytema, N., Bednarz, V. N., Al-Rshaidat, M. M. D. and Wild, C. (2018). N₂ fixation and primary productivity in a red sea *Halophila stipulacea* meadow exposed to seasonality. *Limnology and Oceanography*, 63, 786–798.
- Chefaoui, R. M., Duarte, C. M. and Serrão, E. A. (2017). Paleoclimatic Conditions in the Mediterranean Explain Genetic Diversity of *Posidonia Oceanica* Seagrass Meadows. *Nat. Sci. Rep.* 7, 2732. doi: 10.1038/s41598-017-03006-2
- Chefaoui, R. M., Duarte, C. M. and Serrão, E. A. (2018). Dramatic loss of seagrass habitat under projected climate change in the Mediterranean Sea. *Global Change Biology*, 24, 4919–4928.
- Cole, J. J. and Pace, M. L. (2000). Persistence of Net Heterotrophy in Lakes During Nutrient Addition and Food Web Manipulations. *Limnol. Oceanogr.* 45, 1718–1730. doi: 10.4319/lo.2000.45.8.1718
- Collier, C. J., Langlois, L. M., McMahon, K. M., Udy, J., Rasheed, M., Lawrence, E., et al. (2021). What Lies Beneath: Predicting Seagrass Below-Ground Biomass From Above-Ground Biomass, Environmental Conditions and Seagrass Community Composition. *Ecol. Indic.* 121, 107156. doi: 10.1016/j.ecolind.2020.107156
- Cox, T. E., Schenone, S., Delille, J., Diaz-Castaneda, V., Alliouane, S., Gattuso, J.-P., et al. (2015). Effects of Ocean Acidification on *Posidonia Oceanica* Epiphytic Community and Shoot Production. *J. Ecol.* 103, 1594–1609. doi: 10.1111/1365-2745.12477
- Duarte, C. M., Losada, I. J., Hendriks, I. E., Mazarrasa, I. and Marba, N. (2013). The Role of Coastal Plant Communities for Climate Change Mitigation and Adaptation. *Nat. Climate Change* 3, 961–968. doi: 10.1038/nclimate1970
- Duarte, C. M., Marba, N., Gacia, E., Fourqurean, J. W., Beggins, J., Barron, C., et al. (2010). Seagrass Community Metabolism: Assessing the Carbon Sink Capacity of Seagrass Meadows. *Global Biogeochemical Cycles* 24, GB4032. doi: 10.1029/2010GB003793
- Folkard, A. M. (2005). Hydrodynamics of Model P. Oceanica Patches in Shallow Water. *Limnol. Oceanogr.* 50, 1592–1600. doi: 10.4319/lo.2005.50.5.1592
- Frankignoulle, M. and Bouqueneau, J. M. (1987). Seasonal Variation of the Diel Carbon Budget of a Marine Macrophyte Ecosystem. *Mar. Ecol. Prog. Ser.* 38, 297–299. doi: 10.3354/meps038197
- Fritsch, C. (1895). Über Die Auffindung Einer Marinen Hydrocharidae Im Mittelmeer. *Verhandlungen der Zoologisch Botanischen gesamtan Wien* 45, 104–106.
- Gambi, M. C., Barbieri, F. and Bianchi, C. N. (2009). New Record of the Alien Seagrass *Halophila Stipulacea* (Hydrocharitaceae) in the Western Mediterranean: A Further Clue to Changing Mediterranean Sea Biogeography. *Mar. Biodiversity Records* 2, e84. doi: 10.1017/S175526720900058X
- Gazeau, F., Duarte, C. M., Gattuso, J.-P., Barron, C., Navarro, N., Ruiz, S., et al. (2005). Whole System Metabolism and CO₂ Fluxes in a Mediterranean Bay Dominated by Seagrass Beds (Palma Bay, NW Mediterranean). *Biogeosciences* 2, 43–60. doi: 10.5194/bg-2-43-2005
- Georgiou, D., Alexandre, A., Luis, J. and Santos, R. (2016). Temperature is Not a Limiting Factor for the Expansion of *Halophila Stipulacea* Throughout the Mediterranean Sea. *Mar. Ecol. Prog. Ser.* 544, 159–167. doi: 10.3354/meps11582

SUPPLEMENTARY MATERIAL

The Supplementary Material for this article can be found online at: <https://www.frontiersin.org/articles/10.3389/fmars.2022.891467/full#supplementary-material>

- Gerakaris, V., Lardi, P. and Issaris, Y. (2019). First Record of the Tropical Seagrass Species *Halophila Decipiens* Ostenfeld in the Mediterranean Sea. *Aquat. Bot.* 160, 103151. doi: 10.1016/j.aquabot.2019.103151
- Giakoumi, S., Halpern, B. S., Michel, L. N., Gobert, S., Sini, M., Boudouresque, C.-F., et al. (2015). Towards a Framework for Assessment and Management of Cumulative Human Impacts on Marine Food Webs. *Conserv. Biol.* 29, 1228–1234. doi: 10.1111/cobi.12468
- Gomez-Pujol, L., Orfila, A., Alvarez-Ellacuria, A., Terrados, J. and Tintore, J. (2013). Posidonia Oceanica Beach-Cast Litter in Mediterranean Beaches: A Coastal Video Monitoring Study. *J. Coast. Res.* 65, 1768–1773. doi: 10.2112/SI65-299.1
- Hemminga, M. A. and Duarte, C. M. (2000). *Seagrass Ecology* (Cambridge: Cambridge University Press).
- Holmer, M., Argyrou, M., Dalsgaard, T., Danovaro, R., Diaz-Almela, E., Duarte, C. M., et al. (2008). Effects of Fish Farm Waste on *Posidonia Oceanica* Meadows: Synthesis and Provision of Monitoring and Management Tools. *Mar. Pollut. Bull.* 56, 1618–1629. doi: 10.1016/j.marpolbul.2008.05.020
- Holmer, M., Duarte, C. M., Boschker, H. T. S. and Barron, C. (2004). Carbon Cycling and Bacterial Carbon Sources in Pristine and Impacted Mediterranean Seagrass Sediments. *Aquat. Microbial Ecol.* 36, 227–237. doi: 10.3354/ame036227
- Howard, J., Sutton-Grier, A., Herr, D., Kleypas, J., Landis, E., McLeod, E., et al. (2017). Clarifying the Role of Coastal and Marine Systems in Climate Mitigation. *Front. Ecol. Environ.* 15, 42–50. doi: 10.1002/fee.1451
- Jassby, A. D. and Platt, T. (1976). Mathematical Formulation of the Relationship Between Photosynthesis and Light for Phytoplankton. *Limnol. Oceanogr.* 21, 540–547. doi: 10.4319/lo.1976.21.4.0540
- Koch, E. W. (1993). Hydrodynamics, Diffusion-Boundary Layers and Photosynthesis of the Seagrasses *Thalassia Testudinum* and *Cymodocea Nodosa*. *Mar. Biol.* 118, 767–776. doi: 10.1007/BF00347527
- Koopmans, D., Holtappels, M., Chennu, A., Weber, M. and de Beer, D. (2020). High Net Primary Production of Mediterranean Seagrass (*Posidonia Oceanica*) Meadows Determined With Aquatic Eddy Covariance. *Front. Mar. Sci.* 7. doi: 10.3389/fmars.2020.00118
- Lavery, P. S., Mateo, M.-A., Serrano, O. and Rozaimi, M. (2013). Variability in the Carbon Storage of Seagrass Habitats and Its Implications for Global Estimates of Blue Carbon Ecosystem Service. *PLoS One* 8, e73748. doi: 10.1371/journal.pone.0073748
- Marin-Guirao, L., Ruiz, J. M., Dattolo, E., Garcia-Munoz, R. and Proccini, G. (2016). Physiological and Molecular Evidence of Differential Short-Term Heat Tolerance in Mediterranean Seagrasses. *Nat. Sci. Rep.* 6, 28615. doi: 10.1038/srep28615
- Marsh, J. A., Jr., Dennison, W. C. and Alberte, R. S. (1986). Effects of Temperature on Photosynthesis and Respiration in Eelgrass (*Zostera Marina* L.). *J. Exp. Mar. Biol. Ecol.* 101, 257–267. doi: 10.1016/0022-0981(86)90267-4
- Mateo, M. A., Romero, J., Pérez, M., Littler, M. M. and Littler, D. S. (1997). Dynamics of Millenary Organic Deposits Resulting From the Growth of the Mediterranean Seagrass *Posidonia Oceanica*. *Estuar. Coast. Shelf Sci.* 44, 103–110. doi: 10.1006/ecss.1996.0116
- Mazarrasae, I., Samper-Villarreal, J., Serrano, O., Lavery, P. S., Lovelock, C. E., Marba, N., et al. (2018). Habitat Characteristics Provide Insights of Carbon Storage in Seagrass Meadows. *Mar. Pollut. Bull.* 134, 106–117. doi: 10.1016/j.marpolbul.2018.01.059
- Mazarrasa, I., Marba, N., Garcia-Orellana, J., Masque, P., Arias-Ortiz, A. and Duarte, C. M. (2017). Effect of Environmental Factors (Wave Exposure and Depth) and Anthropogenic Pressure in the C Sink Capacity of *Posidonia Oceanica* Meadows. *Limnol. Oceanogr.* 62, 1436–1450. doi: 10.1002/lno.10510
- McKee, K. L., Cahoon, D. R. and Feller, I. C. (2007). Caribbean Mangroves Adjust to Rising Sea Level Rise Through Biotic Controls on Change in Soil Elevation. *Global Ecol. Biogeography* 16, 545–556. doi: 10.1111/j.1466-8238.2007.00317.x
- Montefalcone, M., Albertelli, G., Bianchi, C. N., Mariani, M. and Morri, C. (2006). A New Synthetic Index and a Protocol for Monitoring the Status of *Posidonia Oceanica* Meadows: A Case Study at Sanremo (Ligurian Sea, NW Mediterranean). *Aquat. Conservation: Mar. Freshw. Syst.* 16, 29–42. doi: 10.1002/aqc.688
- Montefalcone, M., Morri, C., Peirano, A., Albertelli, G. and Bianchi, C. N. (2007). Substitution and Phase Shift Within the *Posidonia Oceanica* Seagrass Meadows of NW Mediterranean Sea. *Estuarine Coast. Shelf Sci.* 75, 63–71. doi: 10.1016/j.ecss.2007.03.034
- Montefalcone, M., Parravicini, V., Vacchi, M., Alvertelli, G., Ferrari, M., Morri, C., et al. (2009). Human Influence on Seagrass Habitat Fragmentation in NW Mediterranean Sea. *Estuarine Coast. shelf Sci.* 86, 292–298. doi: 10.1016/j.ecss.2009.11.018
- Murray, L. and Wetzel, R. L. (1987). Oxygen Production and Consumption Associated With the Major Autotrophic Components in Two Temperate Seagrass Communities. *Mar. Ecol. Prog. Ser.* 38, 231–239. doi: 10.3354/meps038231
- Nordlund, L. M., Jackson, E. L., Nakaoka, M., Samper-Villarreal, J., Beco-Carretero, P. and Creed, J. C. (2018). Seagrass Ecosystem Services – What's Next? *Mar. Pollut. Bull.* 134, 145–151. doi: 10.1016/j.marpolbul.2017.09.014
- Nykjaer, L. (2009). Mediterranean Sea Surface Warming 1985–2006. *Climate Res.* 39, 11–17. doi: 10.3354/cr00794
- Olesen, B., Enriquez, s., Duarte, C. M. and Sand-Jensen, K. (2002). Depth Acclimation of Photosynthesis, Morphology and Demography of *Posidonia Oceanica* and *Cymodocea Nodosa* in the Spanish Mediterranean Sea. *Mar. Ecol. Prog. Ser.* 236, 89–97. doi: 10.3354/meps236089
- Olive, I., Silva, J., Costa, M. M. and Santos, R. (2015). Estimating Seagrass Community Metabolism Using Benthic Chambers: The Effect of Incubation Time. *Estuaries Coasts* 39, 138–144. doi: 10.1007/s12237-015-9973-z
- Oreska, M. P. J., McGlathery, K. J. and Porter, J. H. (2017). Seagrass Blue Carbon Spatial Patterns at the Meadow-Scale. *PLoS One* 12, e0176630. doi: 10.1371/journal.pone.0176630
- Ott, J. A. (1980). Growth and Production in *Posidonia Oceanica* (L.) Delile. *Mar. Ecol. I*, 47–64. doi: 10.1111/j.1439-0485.1980.tb00221.x
- Pace, M., Borg, J. A., Galdies, C. and Malhotra, A. (2016). Influence of Wave Climate on Architecture and Landscape Characteristics of *Posidonia Oceanica* Meadows. *Mar. Ecol.* 38, e12387. doi: 10.1111/maec.12387
- Pancucci-Papadopoulou, M. A., Raitos, D. E. and Corsini-Foka, M. (2012). Biological Invasions and Climatic Warming: Implications for South-Eastern Aegean Ecosystem Functioning. *J. Mar. Biol. Assoc. United Kingdom* 92, 777–789. doi: 10.1017/S0025315411000981
- Pergent-Martini, C., Pergent, G., Monnier, B., Boudouresque, C.-F., Mori, C. and Valette-Sansevin, A. (2021). Contribution of *Posidonia Oceanica* Meadows in the Context of Climate Change Mitigation in the Mediterranean Sea. *Mar. Environ. Res.* 165, 105236. doi: 10.1016/j.marenvres.2020.105236
- Posluszny, U. and Tomlinson, P. B. (1991). Shoot Organization in the Seagrass *Halophila* (Hydrocharitaceae). *Can. J. Bot.* 69, 1600–1615. doi: 10.1139/b91-204
- Ralph, P. J. and Burchett, M. D. (1995). Photosynthetic Responses of the Seagrass *Halophila Ovalis* (R. Br.) Hook. F. @ to High Irradiance Stress, Using Chlorophyll a Fluorescence. *Aquat. Bot.* 51, 55–66. doi: 10.1016/0304-3770(95)00456-A
- Ralph, P. J., Durako, M. J., Enriquez, S., Collier, C. J. and Doblin, M. A. (2007). Impact of Light Limitation on Seagrasses. *J. Exp. Mar. Biol. Ecol.* 350, 176–193. doi: 10.1016/j.jembe.2007.06.017
- Rheuban, J. E., Berg, P. and McGlathery, K. J. (2014). Ecosystem Metabolism Along a Colonization Gradient of Eelgrass (*Zostera Marina*) Measured by Eddy Correlation. *Limnol. Oceanogr.* 59, 1376–1387. doi: 10.4319/lo.2014.59.4.1376
- Rodriguez, P., Bystrom, P., Geibrink, E., Hedstrom, P., Vasconcelos, F. R. and Karlsson, J. (2016). Do Warming and Humic River Runoff Alter the Metabolic Balance of Lake Ecosystems. *Aquat. Sci.* 78, 717–725. doi: 10.1007/s00027-015-0463-y
- Samper-Villarreal, J., Lovelock, C. E., Saunders, M. I., Roelfsema, C. and Mumby, P. J. (2016). Organic Carbon in Seagrass Sediments is Influenced by Seagrass Canopy Complexity, Turbidity, Wave Height, and Water Depth. *Limnol. Oceanogr.* 61, 938–952. doi: 10.1002/lno.10262
- Schneider, C. A., Rasband, W. S., and Eliceiri, K. W. (2012) NIH Image to ImageJ: 25 years of Image Analysis. *Nature Methods*. 9, 671–675.
- Samper-Villarreal, J., Mumby, P. J., Saunders, M. I., Barry, L. A., Zawadzki, A., Heijnis, H., et al. (2018). Vertical Accretion and Carbon Rates in Subtropical Seagrass Meadows Increased Following Anthropogenic Pressure From European Colonisation. *Estuarine Coast. Shelf Sci.* 202, 40–53. doi: 10.1016/j.ecss.2017.12.006

- Santos, C. B., Krause-Jensen, D., Alcoverro, T., Marba, N., Duarte, C. M., Katwijk, M. M., et al. (2019). Recent Trend Reversal for Declining European Seagrass Meadows. *Nat. Commun.* 10, 3356. doi: 10.1038/s41467-019-11340-4
- Savva, I., Bennett, S., Roca, G., Jorda, G. and Marba, N. (2018). Thermal Tolerance of Mediterranean Marine Macrophytes: Vulnerability to Global Warming. *Ecol. Evol.* 8, 12032–12043. doi: 10.1002/ece3.4663
- Sghaier, Y. R., Zakhama-Sraieb, R., Benamer, I. and Charfi-Cheikhrouha, F. (2011). Occurrence of the Seagrass *Halophila Stipulacea* (Hydrocharitaceae) in the Southern Mediterranean Sea. *Botanica Marina* 54, 575–582. doi: 10.1515/BOT.2011.061
- Sghaier, Y. R., Zakhama-Sraieb, R. and Charfi-Cheikhrouha, F. (2014). “Effects of the Invasive Seagrass *Halophila Stipulacea* on the Native Seagrass *Cymodocea Nodosa*,” in *Proceedings of the Fifth Mediterranean Symposium on Marine Vegetation* (Portorožˇ, SL: UNEP), 167–171.
- Short, F., Carruthers, T., Dennison, W. and Waycott, M. (2007). Global Seagrass Distribution and Diversity: A Bioregional Model. *J. Exp. Mar. Biol. Ecol.* 350, 3–20. doi: 10.1016/j.jembe.2007.06.012
- Streftaris, N. and Zenetos, A. (2006). Alien Marine Species in the Mediterranean –the 100 ‘Worst Invasives’ and Their Impact. *Mediterr. Mar. Sci.* 7, 87–118. doi: 10.12681/mms.180
- Telesca, L., Belluscio, A., Criscoli, A., Ardizzone, G., Apostolaki, E. T., Frascetti, S., et al. (2015). Seagrass Meadows (*Posidonia Oceanica*) Distribution and Trajectories of Change. *Nat. Sci. Rep.* 5, 12505. doi: 10.1038/srep12505
- Thimijan, R. W. and Heins, R. D. (1983). Photometric, Radiometric, and Quantum Light Unit of Measure: A Review of Procedures for Interconversion. *Am. Soc. Hortic. Sci.* 18, 818–822.
- Topouzelis, K., Makri, D., Stoupas, N., Papakonstantinou, A. and Katsanevakis, S. (2018). Seagrass mapping in Greek territorial waters using Landsat-8 satellite images. *International Journal of applied earth observation and geoinformation*, 67, 98–113.
- Tsiamis, K., Moñtesanto, B., Panayotidis, P., Katsaros, C. and Verlaque, M. (2010). Updated Records and Range Expansion of Alien Marine Macrophytes in Greece, (2009). *Mediterr. Mar. Sci.* 11, 61–79. doi: 10.12681/mms.91
- van der Velde, G. and den Hartog, C. (1992). Continuing Range Extension of *Halophila Stipulacea* (Forssk.) Aschers. (Hydrocharitaceae) in the Mediterranean -Now Found at Kefallinia and Ithaki (Ionian Sea). *Acta Botanica neerlandica* 41, 345–348. doi: 10.1111/j.1438-8677.1992.tb01341.x
- Vazquez-Lule, A. and Vargas, R. (2021). Biophysical Drivers of Net Ecosystem and Methane Exchange Across Phenological Phases in a Tidal Salt Marsh. *Agric. For. Meteorology* 300, 108309. doi: 10.1016/j.agrformet.2020.108309
- Wesselmann, M., Gerdali, N. R., Duarte, C. M., Garcia-Orellana, J., Diaz-Rua, R., Arias-Ortiz, A., et al. (2021). Seagrass (*Halophila Stipulacea*) Invasion Enhances Carbon Sequestration in the Mediterranean Sea. *Global Change Biol.* 27, 2592–2607. doi: 10.1111/gcb.15589
- Williams, S. L. (2007). Introduced Species in Seagrass Ecosystems: Status and Concerns. *J. Exp. Mar. Biol.* 350, 89–110. doi: 10.1016/j.jembe.2007.05.032
- Winters, G., Beer, S., Willette, D. A., Viana, I. G., Chiquillo, K. L., Beco-Carretero, P., et al. (2020). The Tropical Seagrass *Halophila Stipulacea* Reviewing What We Know From its Native and Invasive Habitats, Alongside Identifying Knowledge Gaps. *Front. Mar. Sci.* 7. doi: 10.3389/fmars.2020.00300
- Yates, K. K. and Halley, R. B. (2003) Measuring Coral Reef Community Metabolism Using New Benthic Chamber Technology. *Coral reefs* 22, 247–255. doi: 10.1007/s00338-003-0314-5
- Zupo, V., Mazzella, L., Buia, M. C., Gambi, M. C., Lorenti, M., Scipione, M. B., et al. (2005). A Small-Scale Analysis of the Spatial Structure of a *Posidonia Oceanica* Meadow Off the Island of Ischia (Gulf of Naples, Italy): Relationship With the Seafloor Morphology. *Aquat. Bot.* 84, 101–109. doi: 10.1016/j.aquabot.2005.08.006

Conflict of Interest: The authors declare that the research was conducted in the absence of any commercial or financial relationships that could be perceived as a potential conflict of interest.

Publisher’s Note: All claims expressed in this article are solely those of the authors and do not necessarily represent those of their affiliated organizations, or those of the publisher, the editors and the reviewers. Any product that may be evaluated in this article, or claim that may be made by its manufacturer, is not guaranteed or endorsed by the publisher.

Copyright © 2022 Ward, Aldis, Wade, Miliou, Tsimpidis and Cameron. This is an open-access article distributed under the terms of the Creative Commons Attribution License (CC BY). The use, distribution or reproduction in other forums is permitted, provided the original author(s) and the copyright owner(s) are credited and that the original publication in this journal is cited, in accordance with accepted academic practice. No use, distribution or reproduction is permitted which does not comply with these terms.



OPEN ACCESS

EDITED BY

Iris Eline Hendriks,
Spanish National Research Council
(CSIC), Madrid, Spain

REVIEWED BY

Hilmar Hinz,
University of the Balearic Islands, Spain
Christian Lønborg,
Aarhus University, Denmark

*CORRESPONDENCE

Kirsty E. Black
kb99@st-andrews.ac.uk

SPECIALTY SECTION

This article was submitted to
Global Change and the Future Ocean,
a section of the journal
Frontiers in Marine Science

RECEIVED 09 March 2022

ACCEPTED 07 July 2022

PUBLISHED 04 August 2022

CITATION

Black KE, Smeaton C, Turrell WR and
Austin WEN (2022) Assessing the
potential vulnerability of sedimentary
carbon stores to bottom trawling
disturbance within the UK EEZ.
Front. Mar. Sci. 9:892892.
doi: 10.3389/fmars.2022.892892

COPYRIGHT

© 2022 Black, Smeaton, Turrell and
Austin. This is an open-access article
distributed under the terms of the
[Creative Commons Attribution License
\(CC BY\)](https://creativecommons.org/licenses/by/4.0/). The use, distribution or
reproduction in other forums is
permitted, provided the original author
(s) and the copyright owner(s) are
credited and that the original
publication in this journal is cited, in
accordance with accepted academic
practice. No use, distribution or
reproduction is permitted which does
not comply with these terms.

Assessing the potential vulnerability of sedimentary carbon stores to bottom trawling disturbance within the UK EEZ

Kirsty E. Black^{1*}, Craig Smeaton¹, William R. Turrell²
and William E. N. Austin^{1,3}

¹School of Geography and Sustainable Development, University of St. Andrews, St. Andrews, United Kingdom, ²Marine Scotland Science, Aberdeen, United Kingdom, ³Scottish Association for Marine Science, Scottish Marine Institute, Oban, United Kingdom

It is estimated that within the UK exclusive economic zone (UK EEZ), 524 Mt of organic carbon (OC) is stored within seabed sediment. However, the stability and potential vulnerability of OC in these sediments under anthropogenic stressors, such as bottom trawling activity, remains poorly quantified. To improve our understanding of the areas where sedimentary OC is likely to be at greatest risk from trawling events, we have developed a carbon vulnerability ranking (CVR) to identify areas of the seabed where preventative protection may be most beneficial to help maintain current OC stocks while further research continues to shed light on the fate of OC after trawling (e.g., remineralization, transport, and consumption). Predictive maps of currently available fishing intensity, OC and sediment distribution, and sediment OC lability have been generated within ArcGIS using fuzzy set theory. Our results show that the west coast of Scotland represents one of the key areas where sedimentary OC is potentially at greatest risk from bottom trawling activity. This is due mainly to the high reactivity of these OC rich sediments combined with the pressures of repetitive trawling activity within inshore waters. Our research shows that these OC hotspots are potentially at risk of disturbance from bottom trawling activity and should be prioritized for the consideration of future safeguarding (management) measures to ensure emissions are minimized and to provide greater protection of this natural carbon capital resource.

KEYWORDS

organic carbon (OC), sediment, fishing gear, seabed, mapping, disturbance

1 Introduction

As marine sediments are deposited and accumulate on the seafloor, they act as a trap and long-term store ($> 10^3$ years) of large quantities of carbon (C). It is estimated that marine sediments contain $87,000 \pm 43,000$ Mt of organic carbon (OC) within global surficial sediments (Lee et al., 2019). It has also been predicted that globally, marine sediments may hold up to 3,117,000 Mt OC within the top 1 m (Atwood et al., 2020). These global stores of OC are estimated to increase by 160 Mt annually through accumulation and burial (Hedges and Keil, 1995). Due to the highly heterogeneous nature of sedimentary marine environments, OC is not uniformly stored but instead exhibits a high degree of spatial heterogeneity across the seabed (Hunt et al., 2020; Smeaton et al., 2021a). Under natural hydrodynamic processes, OC can accumulate and add to the long-term store within marine sediments (Bernier, 1982; Hedges and Keil, 1995). However, increasing anthropogenic activity which disturbs the seabed is potentially putting these OC stores at risk, notably through elevated rates of OC remineralisation to carbon dioxide (CO_2) (Duplisea et al., 2001), which may potentially contribute towards global emissions.

Fishing alongside other anthropogenic activities such as offshore drilling, aggregate dredging, aquaculture farming, and shipping exert significant pressure on benthic marine environments (Kavadas et al., 2015). Out of all these activities, bottom trawling is commonly recognised as the most frequent and widespread cause of anthropogenic disturbance and pressure on the seabed, putting coastal and shelf sea environments at risk (Kaiser et al., 2006; Rijnsdorp et al., 2016; Eigaard et al., 2017; Kenny et al., 2018). During bottom contact fishing disturbance, the resuspension of sediments occurs. This potentially results in the exposure of buried OC to oxygen-rich overlying waters, enhancing organic matter (OM) remineralisation processes (Arndt et al., 2013) and reducing the quantity of OC stored. In some regions where accumulation and deposition of OC is low or where OC is especially reactive (e.g. coastal inlets and fjords) (Smeaton and Austin, 2022), this could result in a more significant overall loss of OC from the sediment when disturbed. Resuspended OC rich sediment may also undergo lateral sediment transport, resulting in a loss of fine flocculant material from the trawl site (Epstein et al., 2022). Additional biological factors such as the reduction in biomass of flora and fauna may also negatively impact OC storage within sediments (Epstein et al., 2022).

However, it is worth noting that the loss of OC due to bottom trawling activity may be offset by a reduction of faunal bioturbation, reduced respiration rates, and an increase in primary production due to increased nutrient availability (Epstein et al., 2022). In addition to this, while sediment may be resuspended and laterally transported during trawling, this material may be deposited and stored elsewhere. Current studies

investigating the net impact of bottom trawling have shown mixed results, highlighting the need for further study within this field. It is estimated that 1.3% (4.9 million km^2) of the global seabed is trawled annually (Sala et al., 2021). Unlike the environmental threats to sedimentary OC stores, such as changes in ocean temperature and oxygen availability, direct anthropogenic pressures such as bottom trawling can be monitored and controlled to safeguard the most vulnerable OC stores. By managing marine protected areas (MPA's) and highly protected marine areas (HPMA's), it may be possible to alleviate some of this fishing pressure and protect marine life and sedimentary environments with a high OC storage capacity. However, globally, only 2.7% of the marine environment is currently under complete or high-level protection from fishing impacts, with the majority (577/1,013) of these protected areas being less than 10 km^2 (Marine Conservation Institute, 2021).

It is estimated that 52% (1,606,000 Mt) of the global 1 m OC stock is located within the 200-mile Exclusive Economic Zones (EEZ) (Atwood et al., 2020). In the case of the UK EEZ, it is estimated that these marine sediments store greater quantities of OC (524 Mt) than their terrestrial equivalents (Smeaton et al., 2021a).

The UK EEZ has one of the most comprehensively mapped seabeds in terms of available sedimentary datasets. In recent years, there have been multiple studies looking at the distribution and content of OC within marine sediments in the greater North Sea region (Diesing et al., 2017; Luisetti et al., 2019; Legge et al., 2020; Diesing et al., 2021). However, more recently, fjords, estuaries, and deep-water environments have been included in these efforts, allowing the first complete spatial dataset of OC in the UK EEZ to be developed (Smeaton et al., 2021a). This improved understanding of OC distribution within the UK EEZ allows the development of new tools to assess the vulnerability of these OC stores to anthropogenic disturbances.

In this study, we use a multi-criteria decision analysis approach using open-source data to calculate and spatially define the relative vulnerability of OC in marine sediments within the UK EEZ. We evaluate the impacts of different fishing gear pressures (e.g. otter trawls, beam trawls, and towed dredging) by creating a sedimentary OC vulnerability ranking (CVR) map. This CVR map details areas of the UK EEZ seabed where surficial OC stores are at the highest risk from bottom-contact fishing activity and may highlight areas that would benefit from some form of management intervention to deliver OC safeguarding alongside other criteria for marine protection. The calculations and outputs presented for the UK EEZ represent one of the first detailed mapping efforts to understand the potential vulnerability of sedimentary OC from bottom trawling.

Within this study, vulnerability is taken to be a relative measure of the probability that an aspect (i.e. OC content) of a pre-defined geographical area is likely to be damaged or disrupted by the impact of a particular hazard, in this case,

bottom trawling. In addition, we define the “loss” of OC from the seabed as the OC which is disturbed from its original depositional location after a trawling event, with the potential to be either transported and re-deposited, remineralised, or consumed. This model-based approach aims to determine which areas of the seabed contain OC that is most vulnerable to bottom trawling. However, our study does not determine the fate of these sediments after they are disturbed by trawling; neither do we consider ongoing natural processes at the seafloor. Instead, the results from this study are intended to support new decision making related to the monitoring, prioritisation of research, implementation of preventative management, and protection of the seabed within the UK EEZ.

2 Methods

2.1 Study area

The UK EEZ covers an area of 743,470 km² (including Rockall and the Isle of Man). Within this study, the term EEZ is used to define the entire area under the exclusive jurisdiction of the UK as a coastal state. Throughout the UK EEZ, there is considerable variation in sediments across both water depth and environment type (e.g. fjordic, coastal and inshore, continental shelf etc.) (See Figure 1A), all of which play a critical role in the

various biogeochemical processes which occur, most notably in the C cycle (Burrows et al., 2017; Smeaton and Austin, 2017; Smeaton et al., 2021a). The surficial sediments of the UK EEZ are estimated to hold 524.4 ± 68.4 Mt of OC (Smeaton et al., 2021a), much of this is concentrated in distinct accumulation hotspots such as fjords, estuaries, and coastal muds, where OC supply is enhanced by proximity to land and higher marine productivity rates (Figure 1B). The influence of fjordic and sheltered environments is most notable in the estimates for Scottish sedimentary OC stores, which are estimated to contain 356.5 ± 72.2 Mt OC compared to English sedimentary OC stores estimated to contain 142.1 ± 28.5 Mt OC (Smeaton et al., 2021a). There are also muddy sediment areas with higher OC content on the shelf. However, it is unknown whether or not OC is continuously deposited and stored within these sediments as elsewhere, such as in the southern North Sea, sediment accumulation rates are low (De Haas et al., 1997; De Haas et al., 2002; Diesing et al., 2021).

2.1.1 Benthic trawling activity

Benthic trawling activity is the most frequent and widespread cause of disturbance to the seabed (Jones, 1992; Amoroso et al., 2018), including within the UK EEZ (de Groot, 1984; Kaiser et al., 1996; Hiddink et al., 2006; Dunkley and Solandt, 2020). As of December 2019, the UK fishing fleet was the seventh-largest fleet within the EU by the number of vessels

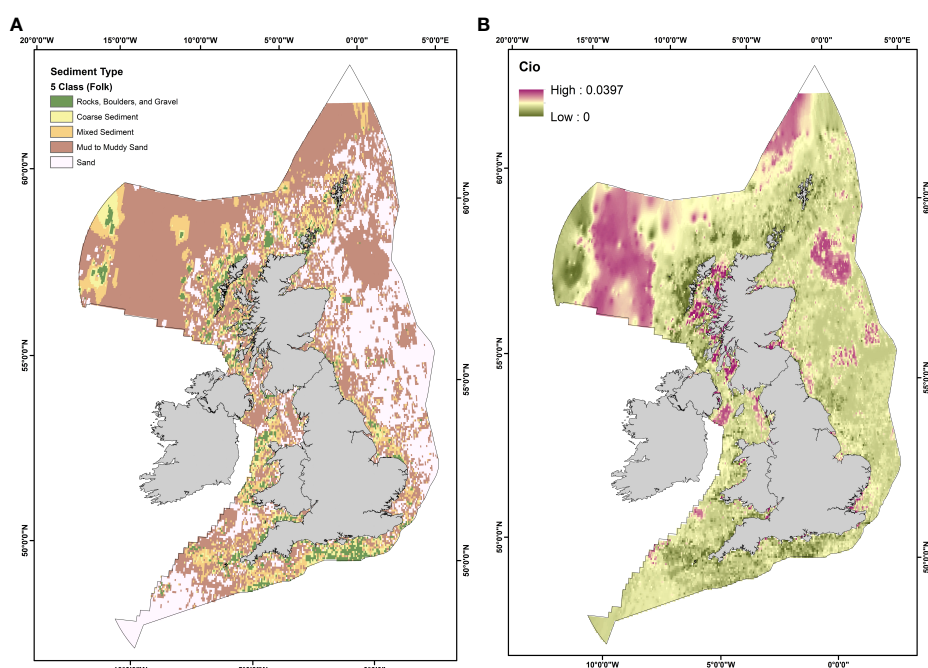


FIGURE 1

(A) Simplified five classification scheme sediment map of the UK EEZ, (B) Estimated Organic Carbon (OC) content (%) of marine sediments in the UK EEZ. Raster pixel resolution in both figures have been decreased for this study. For higher resolution rasters, see Smeaton et al. (2021a).

and the second-largest by gross tonnage (Uberoi et al., 2020). In 2020, the UK fishing fleet consisted of 4,301 active vessels; 61% were 10 metres or under in length and operated predominantly within inshore waters. The types of fishing gear used by British vessels vary with vessel size, power, and target species. Approximately 64% of vessels use static or passive gear types (e.g. pots, traps, hooks, drift and fixed nets etc.) (Quintana et al., 2021). Due to this, vessels under 10 meters in length only account for around 5% of the annual UK catch (Uberoi et al., 2021).

Under European legislation, all vessels greater than 12 meters in length must report their spatial fishing activity *via* vessel monitoring systems (VMS) to monitor fishing activity spatially and temporally within European waters (Gerritsen and Lordan, 2011; Rouse et al., 2017). By coupling logbook and VMS datasets, the International Council for the Exploration of the Sea (ICES) data centre can analyse this information to estimate the spatial and temporal distribution of bottom trawling activity and its pressure on the seabed within the OSPAR maritime region. Due to the lack of implementation of VMS on vessels under 12 meters in length, there is currently a large knowledge gap surrounding the spatial and temporal fishing patterns of the inshore fishing fleet.

As shown in Figure 2A, fishing activity (e.g., the total time spent fishing) typically occurs within coastal “hotspot” areas primarily on the west coast of Scotland, west of the Isle of Man, and off southwest and southern England. Figure 2B presents the

swept area ratio (SAR, see section 2.3.5) for all fishing gear types across the UK EEZ. However, this information can be broken down further to detail the specific gear usage patterns throughout UK waters.

Within the UK EEZ, bottom trawling activity can be grouped into one of the four main gear types: otter trawls (Figure 3A), beam trawls (Figure 3B), dredges (Figure 3C), and seine trawls (Figure 3D). All of these differ in the trawling technique used and the sediment penetration depth of the gears.

The activity of these four gear types for vessels >12 meters is reported by The Convention for the Protection of the Marine Environment of the North-East Atlantic (OSPAR Convention) and ICES as VMS data. As this data is only reported for vessels >12 meters, there is an underestimation of trawling occurring within British waters, particularly within coastal areas where vessels are typically under 12 meters. Otter trawls are the most widely used due to their compact nature, allowing for their use across various vessel sizes. As a result, they have a widely used spatial distribution throughout the entire UK EEZ (Figure 4B). Beam trawling activity occurs primarily within English and Welsh waters, with no records from vessels >12 meters reported within Scottish waters (Figure 4A). Dredging is concentrated mainly within coastal environments across the UK, predominantly around the entire Scottish coast, western Welsh coast, and western and southern English coast (Figure 4C). There is reduced dredging activity reported along the east coast of England. This study did not include seine fishing due

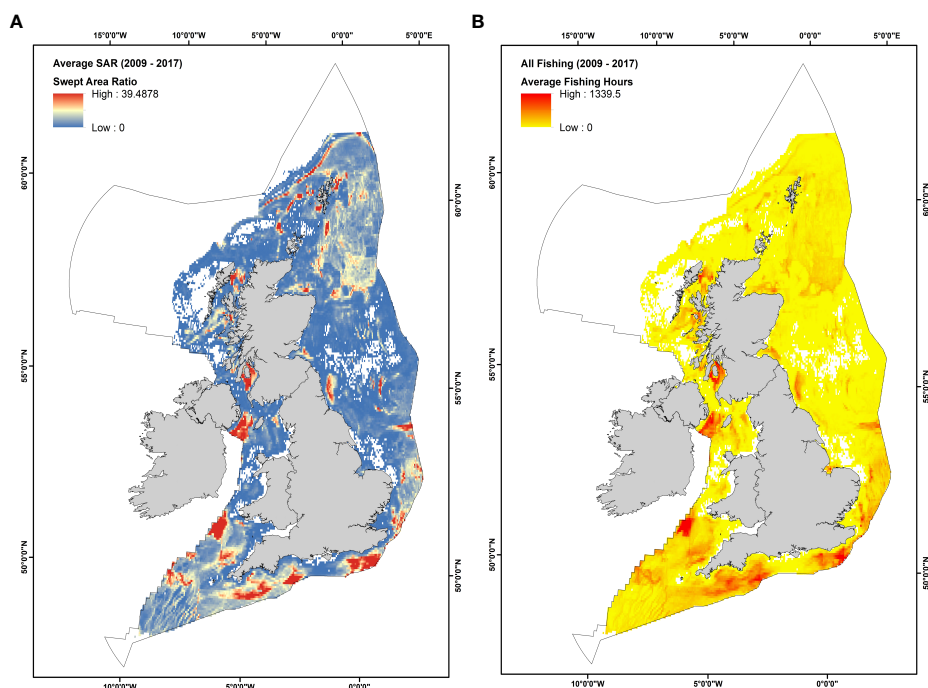


FIGURE 2

(A) Average fishing effort in hours within the UK EEZ between 2009 – 2017 for all bottom trawling types. (B) Average Swept Area ratio within the UK EEZ between 2009 – 2017 for all bottom trawling types (Data Source: OSPAR, 2016). White patches are areas of no data.

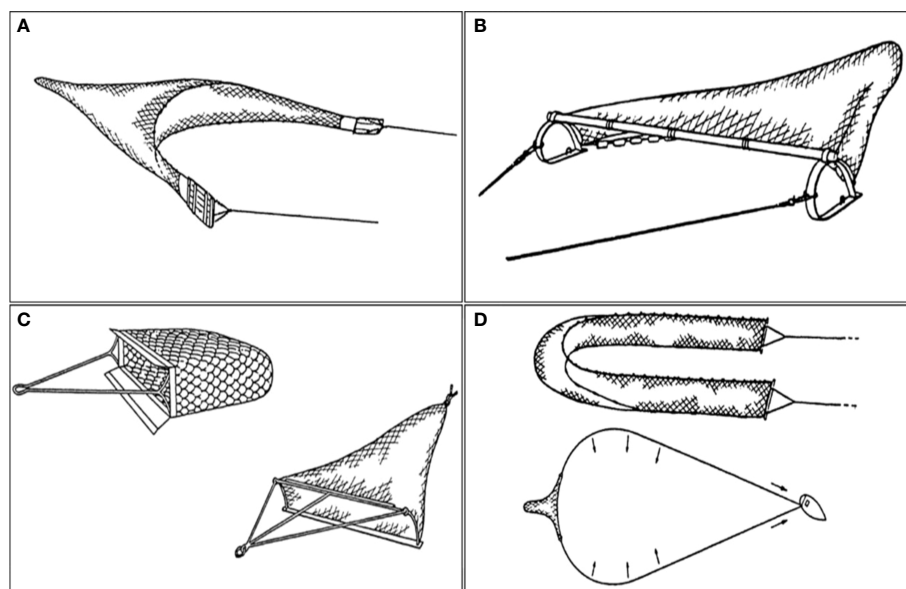


FIGURE 3

The four main bottom trawling gear types used within the UK EEZ. (A) Otter Trawl, (B) Beam Trawl, (C) Towed Dredge, and (D) Seine Trawl (Source: FAO, Technology Fact Sheets. <https://www.fao.org/fishery/en/geartype/104/en>).

to the limited data availability regarding gear penetration depth for Danish and Scottish seining gear (Eigaard et al., 2016).

2.2 Selection of criteria and data processing

Previously, attempts at estimating the impact of bottom trawling activity on sedimentary OC stores have been conducted at various scales, from local (Paradis et al., 2019; Tiano et al., 2019; Paradis et al., 2020) to global (Sala et al., 2021). However, due to the nature of the underlying calculations required to estimate these impacts, great care is required before any reliable estimates of risk can be made. Here, we present a revised methodology for generating sedimentary CVR maps to determine areas of seabed where OC is most at risk following disturbance by bottom trawling within the UK EEZ. Our methodology is modified after that of Sala et al. (2021). However, several significant modifications to the data, underlying assumptions, and methods of ranking used in this calculation have been made possible due to the availability of high-quality data sources for the UK EEZ (e.g. Smeaton et al., 2021a), which help overcome some of the limitations of applying the original methodology at the global scale (Epstein et al., 2021).

To estimate the potential vulnerability of OC in marine sediments, we used multiple data sources to generate a sufficient dataset to be implemented within a multi-criteria decision analysis (MCDA). MCDA is a process where conflicting

criteria may be evaluated against each other to aid in informed and effective decision-making processes. A complete list of the different types of data, their values, and references to data sources used within this study can be seen in Table 1.

In our mapping analysis, we first conducted a series of smaller calculations and intermediary steps to determine factors such as the spatial impact of fishing gear on the seabed with gear type and penetration depth and the proportion of material which may resettle after bottom trawling disturbance based on sediment type (Figure 5 orange and blue boxes). Combined with data on the estimated reactivity of marine sediments, these factors are then used to estimate the fraction of material that may be “lost” from the seabed during a trawling event (Figure 5. yellow boxes).

By combining the potential fraction of “lost” material with the amount of OC estimated to be contained within marine sediments, we can improve estimates for the amount of OC that may be “lost” during trawling events (Figure 5 red boxes). The estimated fraction that may be lost can then be combined with the fraction of OC currently estimated to be present in marine sediments across the entire UK EEZ to generate a multi-criteria map which identifies areas where OC is potentially most vulnerable to bottom trawling pressures (Figure 5. black box).

2.2.1 Grain size data

Information on the particle size characteristics of marine sediments is crucial when investigating their role and significance for long term OC storage. Sediment grain size is

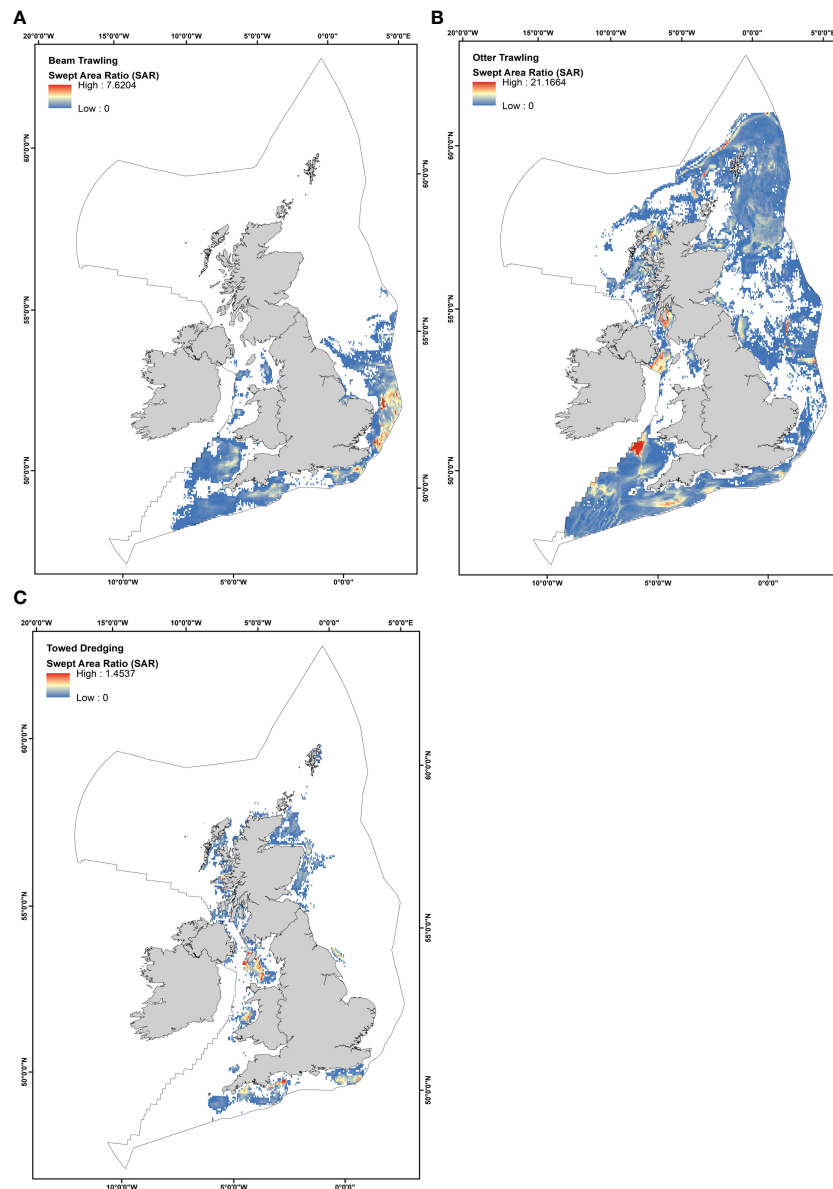


FIGURE 4

The average swept area ratio (SAR) within the UK EEZ between 2009–2017 for (A) Beam Trawling, (B) Otter Trawling, (C) Towed Dredging, and (D) All Fisheries (Beam, Otter, Dredge, and Seine).

routinely measured under OSPAR and the ICES commitments within the UK EEZ. As a result, the marine sedimentary environment of the UK EEZ is well mapped and studied, allowing a high-quality dataset of the spatial characteristics of the seabed to be used within our model (BGS, 2019; Smeaton et al., 2021a).

2.2.2 Sedimentary carbon data

Estimates and modelling of OC within the UK EEZ and North-East Atlantic have been steadily growing and improving

over the last few years (Diesing et al., 2017; Luisetti et al., 2019; Legge et al., 2020; Smeaton et al., 2020; Diesing et al., 2021; Smeaton et al., 2021a). As a result of these efforts, high-resolution bulk (top 10 cm) OC spatial estimates are now available for the entire UK EEZ (Smeaton et al., 2021a).

2.2.3 Sediment lability data

Just as OC content varies across sediment types, the lability of OM associated with the sediments also varies. Thermal analysis of sediments allows for data regarding the quantity,

TABLE 1 Parameters used for modelling the potential vulnerability of UK EEZ marine sediments under different fishing gear types and their sources.

Parameter	Description	Value/ Resolution	References	Source
(a) Spatially Variable Parameters				
SAR	Swept Area Ratio - an estimate of fishing intensity occurring on the seabed	Continuous Grid Resolution: 0.056° x 0.056°	(ICES, 2017)	https://odims.ospar.org/en/search/?search=fishing%20intensity
C	Estimated organic carbon stored in the top 10 cm of sediments	Continuous Grid Resolution: 0.01° x 0.01°	(Smeaton et al., 2021a)	https://data.marine.gov.scot/dataset/sediment-type-and-surficial-sedimentary-carbon-stocks-across-united-kingdom%E2%80%99s-exclusive
(b) Fixed Parameters				
P _{lab}	Estimated mean lability of organic matter as a function of grain size	Mud to Muddy Sand: 0.0223 Sand: 0.0065 Mixed Sediment: 0.011 Coarse Sediment: 0.0095 Gravel: 0.0104	(Smeaton and Austin, 2022)	Supplementary Material Table 1
k	First order degradation constant based on oceanic region	23.34	(Harvey et al., 1995; Soetaert et al., 1996, 1998; Luff and Moll, 2004; Soetaert and Middelburg, 2009; Provoost et al., 2013)	Supplementary Material Table 2
t	Time	1 year		
P _{depth}	Estimated average penetration depth of fishing gear, can be separated by type	Otter Trawling: 2.44 cm Beam Trawling: 2.72 cm Towed Dredging: 5.47 cm	(Hiddink et al., 2017)	
P _{layer}	Depth of sedimentary carbon data used in this study	10 cm	(Smeaton et al., 2021a)	
R	Submerged specific gravity of marine sediments at 12°C	0.658 g cm ⁻³	(Tenzer and Gladkikh, 2014)	
g	Acceleration due to gravity	9.81 ms ⁻²		
D	Mean grain size in a simplified 5 class folk scale	Mud to Muddy Sand: 0.063 mm Sand: 0.1875 mm Mixed Sediment: 0.375 mm Course Sediment: 1.25 mm Gravel: 2 mm	(Folk, 1954)	Supplementary Material Table 3
C ₁ and C ₂	C ₁ and C ₂ are both constants assigned under the assumption that the sediment grains are angular and natural in shape	C ₁ : 24 C ₂ : 1.2	(Ferguson and Church, 2004)	

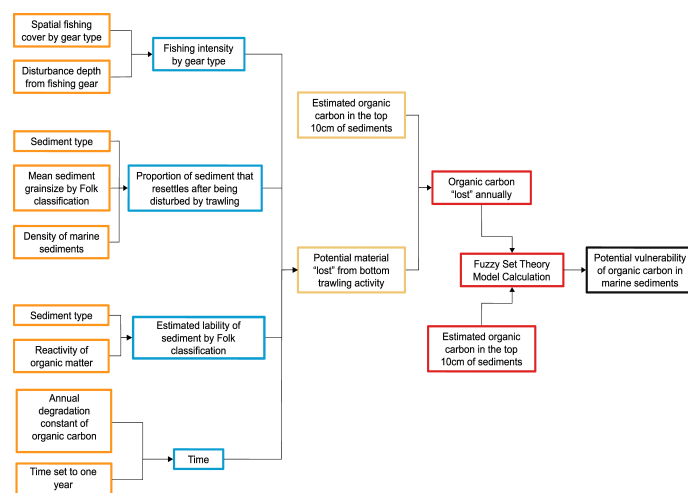


FIGURE 5

Simplified schematic of the workflow steps taken to generate the organic carbon vulnerability estimates. Coloured boxes represent different stages within the calculation. Preparation of the data used in this study was conducted within RStudio (Ver. 2021.09.1 + 372) and ArcGIS (Ver. 10.7). Rasters were rescaled where necessary to be on the same scale to ensure a single-pixel calculation overlay. Calculations and spatial analysis were conducted within ArcGIS using the raster calculator tool, fuzzy membership tool, and fuzzy overlay tool.

quality, and reactivity of OM to be obtained. The reactivity of OM can be split into three key components: the labile, the recalcitrant, and the refractory fractions. In simple terms, the labile fraction of OM represents the most biologically available material and is prone to degradation. In contrast, the refractory fraction is the least biologically available and least reactive. Recent analytical developments have allowed the quantification of the different OM pools (labile, recalcitrant, and refractory) within the marine sediment of the UK EEZ (Smeaton and Austin, 2022).

These new results highlight that the quantity of labile OM in the continental shelf sediments are strongly linked to sediment type. The high-resolution spatial data for sediment type within the UK EEZ makes it possible to de-evolve sediment classifications from a 16 Folk classification scheme to the simplified 5 Folk classification scheme (Supplementary Material Figure 1) (Kaskela et al., 2019; Smeaton et al., 2021a). Using this simplified classification scheme, we were able to assign mean sediment OM lability ($OM_{labile}\%$) for each class within the UK EEZ (sediment samples, $n = 375$, across a range of environmental types (Supplementary Material: Table 1) (Smeaton and Austin, 2022)).

2.2.4 Disturbed sediment exposure

Once sediment has been disturbed by bottom trawling, it will be resuspended from the seabed into the water column (e.g. Breimann et al., 2022). While in the water column, OC associated with the sediment will be exposed to chemical processes, such as remineralisation, which may lead to its

permanent loss from the seabed. Hence, the more time disturbed sediment remains in the water column, the greater the potential for OC to be lost. The length of time the sediment remains above the seabed is determined by the speed it falls out of the water and the height above the seabed to which it is raised by disturbance. However, it is not possible to model in detail the physical disturbance of sediment under all the different physical conditions associated with bottom trawling in UK water or elsewhere. Therefore, a theoretical fall speed can be estimated for any sediment type based on particle size, and this can be used to assess the relative difference in possible exposure during resuspension of disturbed sediment.

Using the universal settling speed calculation proposed by Ferguson and Church (2004), it is possible to calculate a theoretical rate of sediment resettling for each of the five sediment class types used in this study. Settlement speeds are then used to derive a non-dimensional relative estimate of potential exposure. However, it should be noted that this calculation does not consider external factors such as turbulence (Nielsen, 1993), currents and wave movement (Coughlan et al., 2021), which may be critical processes in natural and anthropogenically disturbed shelf systems.

2.2.5 Fishing data

Within the UK EEZ, specific gear types have significant regional patterns related to the fishing intensity (e.g., otter trawling, beam trawling, and towed dredging). VMS can be used to provide high quality temporal and spatial data about the type and intensity of fishing activity occurring across the UK

EEZ. Using OSPAR VMS fishing data, we can estimate the CVR of sediments for each of the three main fishing types on a $0.05^\circ \times 0.05^\circ$ cell resolution (C-square geocode system, see Rees, 2003). VMS datasets were chosen for this study instead of the alternative automatic identification systems (AIS) because VMS separates SAR data by gear type, unlike AIS data which reports trawling as a singular activity with no distinction of the gear type being used. Additionally, due to the ability of fishers to turn off AIS tracking systems and known issues with data reporting, AIS data is only accurately reported approximately 26% of the time spent fishing (Shepperson et al., 2018). By EU law, it is required that VMS always remains switched on for vessels >12 meters in length, making the spatial coverage of the fishing data more reliable. However, as previously noted, this data does not include the fishing activity for vessels under 12 meters in length. As a result, there may be some underestimation in fishing intensity, particularly within coastal areas from the inshore fleet, which are typically smaller vessels.

Using the reported VMS hours fished data combined with log-book records, it is possible to calculate the seabed swept area ratio (SAR) (Figure 2B) using Eq. 1.

$$SAR = \frac{\text{Gear Width} \times \text{Vessel Speed} \times \text{Time Spent Fishing}}{\text{Cell Area}} \quad \text{Eq. 1}$$

The SAR indicates the theoretical number of times a grid cell would be “swept” annually if the fishing effort was evenly distributed throughout a set grid cell area (ICES, 2020). Using the OSPAR VMS data, it is possible to establish the annual average SAR of each pixel. To avoid a single year bias, the SAR of each cell has been averaged from 2009 to 2017.

2.3 Calculation method

2.3.1 Model overview

MCDA is a GIS-based spatial analysis method that allows for both spatial and non-spatial data to be brought together to generate outputs that can inform about complex interactions within datasets. A CVR value for each pixel within a raster dataset was estimated using the MCDA method known as fuzzy set theory, which is a widely used modelling approach in complex systems where the information supplied to a model is vague, imprecise, or ambiguous (Kahraman and Kaya, 2010; Balezentienė et al., 2013). Fuzzy set theory is commonly used within spatial planning and evaluation as it allows spatial information to be treated as members of a set. This means that a degree of membership between different types of spatial information can be determined. Unlike other MCDA methodologies, the degree of membership from fuzzy set theory will take on values between 0 and 1, denoting the strength of the membership between the candidate objects being assessed. This allows for a ranking system to be used.

For example, the OC ranking of a pixel is a numerical ranking that highlights where sedimentary OC is most vulnerable, where 1 is the most vulnerable location, and 0 is the least vulnerable location. It should be noted that the use of fuzzy set theory estimates the possibility, i.e., the capacity of something being true/occurring, not the probability, which refers to the likelihood of something being true/occurring.

2.3.2 Data processing for model set up

In order to generate a MCDA map of the potential vulnerability of sedimentary C stores we must generate two key layers, the amount of OC currently in sediments before bottom trawling and the amount of OC estimated to remain in sediments after a bottom trawl pass. This was done using the following methodology. Firstly, the total fraction of OC present within each pixel, C_i^{in} , is estimated from the UK EEZ sediment OC mapping of Smeaton et al. (2021a), shown here as C_{i0}

$$C_i^{in} = C_{i0} \quad \text{Eq. 2}$$

While the fraction of total OC assumed to remain if the sediment in pixel i is exposed to fishing based disturbance using gear g is denoted as C_{ig}^{out} .

$$C_{ig}^{out} = C_{i0} (1 - La_{ig}) \quad \text{Eq. 3}$$

Where C_{i0} is from Eq. 2. La_{ig} is the estimated fraction of labile OM (%) which would be “lost” from the sediment annually in the presence of fishing activity by gear type g in pixel i (Eq. 4). Note that in Eq. 3, if $(1 - La_{ig})$ has a value of zero, there is no potential loss of OC from pixel i due to gear g . If it has a value of unity, then there is a theoretical potential for total loss of OC. La_{ig} may be calculated via Eq. 4:

$$La_i = SVR_{ig} \times PER_i \times Plab_i \times (1 - e^{-k_i t}) \quad \text{Eq. 4}$$

Where SVR_{ig} is the swept volume ratio calculated via Eq. 5 and PER_i is the potential exposure ratio calculated via Eq. 6 (See below). $Plab_i$ is the estimated mean lability of OM in each pixel as a function of sediment type using the UK EEZ sediment classification from Smeaton et al. (2021a) (Supplementary Table 1). The first-order degradation rate constant, k_i , was assigned based on the oceanic region and was estimated for this study to be 23.34 using an average of values for oxic sediment types in the North Sea (Table 1). It should be noted that k_i is assigned relative to the oceanic region being studied, meaning that its influence on the rate of loss for labile OM will vary geographically depending where this approach is being applied due to factors such as diffusive oxygen flux, the total OC content of surface sediments, and bottom water oxygen concentration (Seiter et al., 2005; Arndt et al., 2013; Paraska et al., 2014). Time, t , was set to one year.

The swept volume ratio, SVR_{ig} , from Eq. 4 may be calculated via Eq. 5:

$$SVR_{i,g} = SAR_{i,g} \times \frac{P_{depth,g}}{P_{layer}} \quad \text{Eq. 5}$$

Where $SAR_{i,g}$ (Eq. 1.) is the swept area ratio in pixel i by vessels using gear type g , from publicly available OSPAR VMS datasets (ICES, 2016). $P_{depth,g}$ is the estimated average penetration depth of gear type g from Hiddink et al., 2017. These depths are 2.44 cm for otter trawling, 2.72 cm for beam trawling, and 5.47 cm for towed dredging. P_{layer} is the depth of sediment used in this study for the carbon estimates, in this case, 10 cm.

The potential exposure ratio, PER_i , in Eq. 4 was estimated by creating a ratio of the settling of the largest sediment size-class speed (w_{max}) to the settling speeds (w_i) for each of the 5 sediment classes outlined in Table 1 so that:

$$PER_i = \frac{w_i}{w_{max}} \quad \text{Eq. 6}$$

The settling speed (w) for each sediment grain size class was calculated using the following equation from Ferguson and Church, 2004:

$$w = \frac{RgD^2}{C_1\nu + (0.75C_2R_gD^3)^{0.5}} \quad \text{Eq. 7}$$

Where R is the submerged specific gravity (0.658 g cm^{-3}) for marine sediments, using the density of marine sediment from Tenzer and Gladkikh (2014) and the density of seawater at 12°C , g is the acceleration due to gravity, and D is the mean diameter of the grain size within each of the sediment classes reported by Smeaton et al. (2021a). C_1 is constant with a value of 18, and C_2 is constant with a value of 1.0 (Ferguson and Church, 2004), ν is the kinematic viscosity of seawater at 12°C (Supplementary Material: Table 3). Several calculation steps were necessary to get the data ready to be applied to the fuzzy overlay model. First, the data fed into the model must undergo fuzzification to allow the source data to be rescaled to fit the 0 to 1 scale (Raines et al., 2010). This was applied using the fuzzy membership tool (membership type: linear) to the estimated OC stored in the top 10 cm of the sediment (C_i^{in}) and the predicted amount of total OC lost from the sediment due to bottom trawling (C_i^{out}) in each pixel for each gear type.

To model the CVR for the UK EEZ, fuzzy set theory models were run within ArcMap (ArcGIS 10.7). The final suitability map was generated using the fuzzy overlay tool (overlay function: AND), which allows for a continuous 0 to 1 scale map to be generated (Nyimbili and Erden, 2020). Finally, the model outputs were defuzzified via the reclassification tool, where classes were set for each gear type using the natural breaks (Jenks) classification method to develop a five-class vulnerability ranking of the seabed within the UK EEZ.

While it is possible to calculate the potential OC lost from benthic trawling, we have chosen not to calculate the benthic efflux of CO_2 because of the high levels of uncertainty and large-

scale assumptions that must be made. Recent studies within this field have attempted to calculate the efflux of CO_2 from bottom trawling (Luisetti et al., 2019; Sala et al., 2021). These studies assume that all the labile OC resuspended during a disturbance event is completely remineralised to aqueous CO_2 . From here, it is also assumed by Luisetti et al., 2019, that all remineralised OC is then released into the atmosphere in a singular process. These gross assumptions are unlikely to be correct and lead to vast overestimates in the amount of CO_2 lost from long term sedimentary OC stores upon disturbance. Processes such as elemental stoichiometry, biological turnover, solubility cycling, and carbonate cycling will all influence the fate of remineralised OC and should not be assumed to be negligible. More data on the efflux of OC across the sediment-water interface in natural and post-disturbance environments is needed before this type of calculation can be attempted with any confidence in the results.

3 Results

The spatial distribution of estimated CVR values across the UK EEZ was mapped using the methodology detailed above at a gridded resolution of $0.05^\circ \times 0.05^\circ$. An area of $743,470 \text{ km}^2$ of the UK seabed was mapped; the most northern tip of the UK EEZ (an area of approximately $24,000 \text{ km}^2$) remains unmapped due to limitations in data availability (Figure 2). However, there are no reported VMS fishing records for this area, and it can be assumed that the impact of bottom trawling in this area is low. Additionally, OC within this area is also reported to be low (Smeaton et al., 2021a), which would, in turn, reduce the overall CVR of the area.

The lack of VMS data available for inshore fisheries also means that their impact is underestimated and prevents us from reliably modelling the CVR within some inshore areas, particularly within fjords. The CVR of some of these inshore sediments must therefore be considered as conservative estimates at present. Our analysis of the areas of the UK EEZ seabed where OC is estimated to be most vulnerable from bottom trawling activity is calculated as a function of the predicted OC stored within surficial sediments and the relative lability of the OM in these sediments. Therefore, the methodology presented here represents the development of a new tool that can be used to assess the potential vulnerability of sedimentary OC stores from bottom trawling pressures.

Based on previous literature and knowledge, we hypothesised that OC is most at risk from anthropogenic pressure within coastal sediments where there is a constant supply of fresh labile matter and a naturally elevated OC store. Likewise, we can assume that as the distance from shore increases, the vulnerability of OC will decrease due to the decline in lability of overall OM accumulation (Smeaton and Austin, 2022). The CVR risk model estimates a typically lower CVR within sands, coarse sediments, mixed sediments, and

gravels/rocks compared to finer-grained sediment types. Our results show that distributions of CVR within the UK EEZ are associated with specific “hot spot” areas for the three major fishing gear types.

3.1 Model validation

Validation of the new model is a fundamental development step and is crucial for determining its predictive capabilities. Our CVR maps have been developed using multiyear spatial monitoring fisheries data (OSPAR, 2016), in addition to previously validated sedimentary OC quantity and sediment type datasets which have been tested *via* extensive ground-truthing efforts and Markov chain Monte Carlo (MCMC) simulations (Smeaton et al., 2021a). In addition to this, we utilise fuzzy set analysis MCDA techniques in place of traditional weighted overlay methods. Weighted overlay works as a Boolean operator where areas are defined as either being a member (1) or not being a member (0). These results fall within clear cut risk or no risk areas, offering no room for further

interpretation. However, fuzzy overlay addresses the possibility of inaccuracies within the attribute data used within the model by assigning a membership ranking between 0 and 1, thus accounting for uncertainties within the calculation where the datasets are more limited (e.g., the lability of sediments assigned as a function of sediment type).

3.2 Carbon vulnerability ranking

Within this model, the CVR is an estimate of those areas of the seabed where sedimentary OC is predicted to be the most susceptible to “loss” due to direct bottom trawling action by specific gears. Our model shows that the most vulnerable areas of the seabed are typically concentrated within inshore muddy sediments and impacted by otter and dredge trawling activity, while beam trawling impacts are spread across muddy, mixed, and coarse sediment types. Despite having the largest spatial coverage overall, otter trawling predominantly results in a low CVR for much of the UK EEZ, with a smaller estimate of areas where vulnerability is high or very high (Table 2 and Figure 6).

TABLE 2 Spatial area coverage of the carbon vulnerability ranking (CVR) by fishing type.

Fishing Type	Carbon Vulnerability Ranking	Area [km ²]					
		England	Scotland	Wales	Northern Ireland	Isle of Mann	Total
Otter Trawling	Very Low	10,547	6,456	466	221	–	17,689
	Low	52,014	60,503	3,896	735	233	117,380
	Medium	7,803	19,906	1,078	429	159	29,376
	High	1,789	10,621	368	894	184	13,855
	Very High	49	2,144	–	12	–	2,205
	Total Area fished by otter trawling	72,202	99,629	5,807	2,291	576	180,504
	Area unfished by otter trawling	155,542	362,341	27,056	14,636	3,392	562,966
Beam Trawling	EEZ Area	227,743	461,970	32,862	16,927	3,968	743,470
	Very Low	1,789	–	172	–	–	1,960
	Low	7,424	–	576	–	25	8,024
	Medium	20,298	–	2,732	12	37	23,079
	High	17,015	–	2,242	25	12	19,294
	Very High	1,127	–	208	123	–	1,458
	Total Area fished by beam trawling	47,653	–	5,929	159	74	53,814
Towed Dredging	Area unfished by beam trawling	180,091	461,970	26,933	16,768	3,895	689,656
	EEZ Area	227,743	461,970	32,862	16,927	3,968	743,470
	Very Low	1,005	1,531	490	110	184	3,320
	Low	5,133	5,476	1,397	319	588	12,912
	Medium	3,700	5,990	1,433	368	502	11,993
	High	257	1,531	37	86	12	1,923
	Very High	–	588	–	12	–	600
	Total Area fished by beam trawling	10,094	15,117	3,357	894	1,286	30,748
	Area unfished by beam trawling	217,649	446,854	29,506	16,033	2,682	712,723
	EEZ Area	227,743	461,970	32,862	16,927	3,968	743,470

The CVR for each finishing type is broken down by country/dependency. Note that there are no fishing records for beam trawlers over 12 meters in length for Scottish waters. Seine trawling has been excluded from this study due to a lack of data regarding trawl penetration depth, thus there will be additional areas.

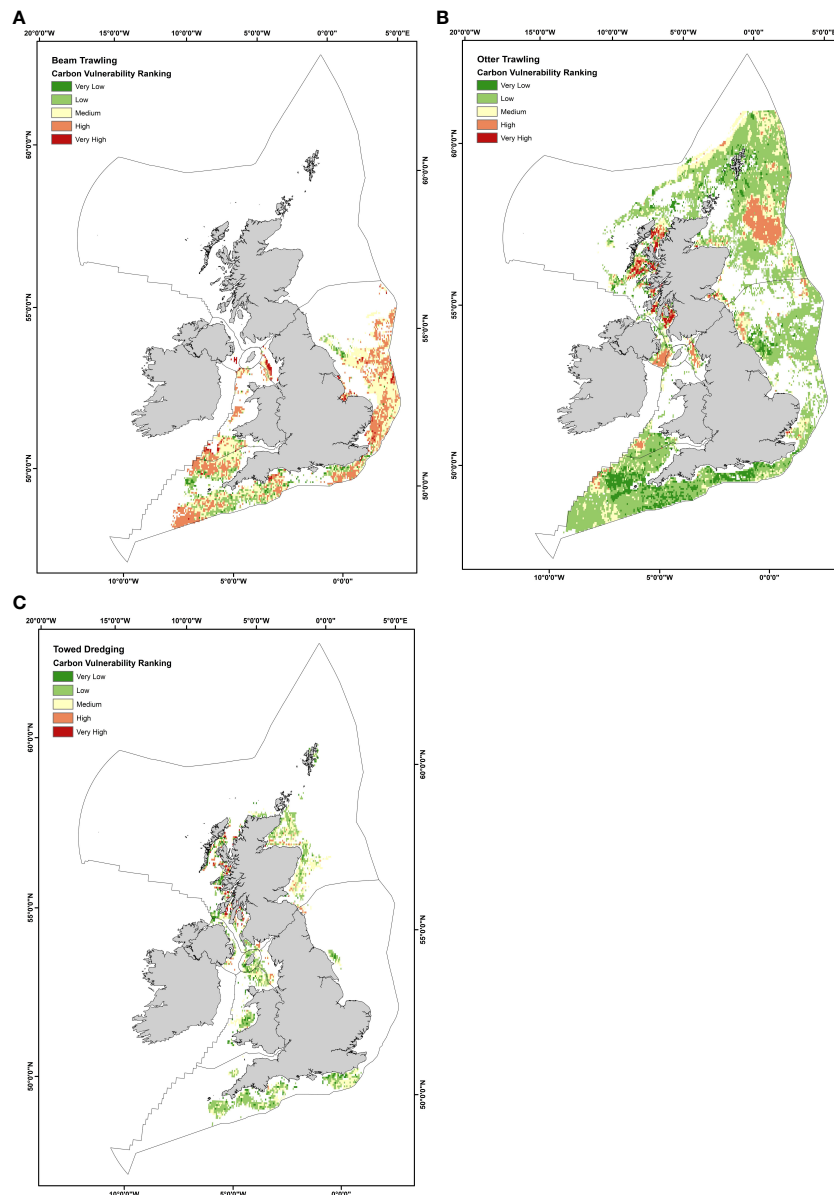


FIGURE 6

Carbon vulnerability ranking (CVR) by fishery type. All three fishing types are associated with regional hot spots where the CVR is very high. These hotspot areas typically coincide with muddy sediment types where labile organic matter content is high; a high swept area ratio also characterises these inshore fishing areas. (A) Beam Trawling, (B) Otter Trawling, (C) Towed Dredging.

Otter trawling has the highest proportion of very low, low, medium, and very high CVR areas compared to other fishery types (Table 2).

Beam trawling has an estimated total spatial coverage of 53,814 km², heavily concentrated within the English sector. Within the medium, high, and very high CVR categories, beam trawling has the highest estimated area coverage of 23,079 km², 19,294 km², and 1,458 km², respectively (Table 2 and Figure 6A). Medium CVR areas are scattered for beam

fisheries (Figure 6A). However, high CVR areas linked to beam trawling are more closely grouped across England's south-western, southern, and south-eastern coastline. Areas of very high CVR for beam trawling can be found on the west coast of the UK in the Irish Sea and on the east coast in the Wash.

Overall, otter trawling has the greatest estimated spatial coverage (180,504 km²) out of the three main fishery types considered within this study. However, despite this large footprint, a significant proportion of the actively fished area

from otter trawling is classified by our model to be within very low (17,689 km²), low (117,380 km²), and medium (29,376 km²) CVR categories (Table 2). It is estimated that approximately 13,855 km² of the seabed is categorised as having a high CVR, with a further 2,205 km² being estimated to have a very high CVR. For otter trawling, these high and very high CVR areas are predominantly located in hot spots across the fjordic west coast of Scotland (Figure 6B), where labile OC muddy sediments dominate, OC content is high, and repetitive trawl passes are common (Figure 2). Regions of high CVR can also be found in the Irish Sea and the Fladen Grounds (Northeast Scotland).

Dredging has the lowest estimated spatial coverage of 30,748 km² compared to the other two fishing types. Towed dredging across the UK EEZ is concentrated mainly in small areas of activity (Figure 6C), unlike the other two fisheries, which are spread across a much greater area. Our model estimates that approximately 3,320 km² of actively dredged seabed is categorised as having a very low ranking. A further 12,912 km² is estimated as being within the low CVR category (Table 2). An estimated 11,993 km² of the seabed is classified as having a medium CVR, with a further estimated 1,923 km² and 600 km² classified as having high to very high CVRs, respectively. Similarly, to otter trawling, hotspots of high to very high CVRs are located on the fjordic west coast of Scotland. Prevailing sediment type, high OC contents and the repetitive nature of fishing disturbances in this region drive high to very high CVRs (Figure 2).

4 Discussion

The main aim of this study was to determine the areas of the seabed where sedimentary OC might be most vulnerable to the impacts of benthic trawling activity within the UK EEZ. We present a new methodological approach to determine the potential vulnerability of the seabed across the UK EEZ using open-source data. The outputs of our model identify the fjords and coastal sediments on the west coast of Scotland as having the highest potential OC vulnerability to disturbances from bottom trawling. Three main determining factors occur in these environments. Firstly, sedimentary OC content is high (Smeaton and Austin, 2019). Secondly, there is a high level of repetitive trawling disturbance within these coastal areas (Figure 4). Thirdly, sediments in this region are largely fine-grained, meaning that they will remain in suspension longer once disturbed. This means that these OC rich sediments have a greater chance of being transported away from their original location and resettling elsewhere.

While we have developed a new OC vulnerability model using fuzzy set theory to identify where OC is potentially most vulnerable due to benthic trawling activity, these models all lack key information that may result in some over- and under-

estimations of CVRs. This is most likely the case with the sediment OM lability data (Smeaton and Austin, 2022). It is likely that sediment OM lability is higher within coastal and fjordic areas in comparison to muddy shelf sediments. This is due to differences in productivity between the two environments and the transportation of OM from coastal to shelf environments, and the ongoing degradation of this matter which occurs during this process. There is currently a data gap within UK EEZ sedimentary OM data, which restricts us from applying OM as a function of sediment type rather than as a spatially modelled estimate. Additionally, a lack of data to adequately monitor the impact of the inshore fishing fleet (i.e., vessels <12 meters) implies that the CVR of sediments in coastal waters may be underestimated. We have intentionally used a flexible modelling framework to account for these data limitations that can be adapted as new data sources are available. For example, previous evidence shows that fuzzy logic modelling frameworks have been successful within other data-poor conservation and safeguarding projects involving trawling datasets (Hattab et al., 2013).

It should also be remembered that the UK EEZ is a region with a long and ubiquitous history of fishing activity, implying that the sediments and surficial OC data used in this study may have already been subject to decades of modernised industrial fishing methods. Therefore, this study does not provide an undisturbed natural baseline for sedimentary OC. Instead, this study provides a present-day snapshot of the current state of the potential areas of OC vulnerability within the UK EEZ. Previous research has shown that the first pass of towed benthic gear on the seabed is the most destructive pass to benthic ecosystems, regardless of the hours spent fishing in the area (Lindgarth et al., 2000; Kaiser et al., 2006; Lambert et al., 2014; Rijnsdorp et al., 2018).

While previous attempts at understanding the impact of bottom trawling on sedimentary OC stores have provided an insight into the potential risk to C, they are conducted at too broad a scale and with too many uncertainties and assumptions to be utilised and implemented within policymaking. Instead, our adapted CVR methodology could provide a policy steppingstone, allowing for greater consideration about the sedimentary environment being investigated and the data availability at the regional scale.

Despite our use of improved data sets and the wealth of understanding of the UK EEZ, we have chosen not to estimate the efflux of CO₂ from the seabed arising from benthic disturbance because of the assumptions required to make this type of calculation and the misleading outputs that can arise. Cross-comparisons of this type of calculation with *in-situ* data are difficult due to the lack of studies investigating the post-disturbance effects of trawling on benthic CO₂ efflux and nutrient efflux within the UK EEZ, or elsewhere. In addition, we do not include the influence of nutrient release from the

sediments during trawling, which can result in increased primary productivity, indirectly resulting in increased OM and OC supply to the sediments. There is currently not enough supporting information about the efflux of nutrients in a post-trawl environment within the UK EEZ to confidently include this information within our calculations. Equally, these models do not account for the removal of benthic fauna during a trawling event.

Similarly, it is also challenging to estimate the accumulation of multiple years of fishing impact on sedimentary OC stores within the UK EEZ due to a lack of information about sediment accumulation rates and OC sequestration rates. Large assumptions would have to be made with this type of calculation. For example, based on current data, we would have to assume that there was a single accumulation rate throughout the UK EEZ and that OC is lost from the sediments at the same rate annually. However, we know this is not the case, especially within coastal fjordic environments where accumulation is reported to be high (Smeaton et al., 2016; Smeaton et al., 2021b) in comparison to the low accumulation rate reported within the North Sea (De Haas et al., 1997; De Haas et al., 2002; Evans et al., 2002; Scourse et al., 2002; Diesing et al., 2021). Recent research has allowed for the sediment accumulation rate to be modelled within the Greater North Sea region (Diesing et al., 2021), highlighting that these types of predictive models are possible. However, for multiyear sedimentary OC losses to be calculated with a high degree of confidence, the sediment accumulation rate across different sedimentary environments and marine environment types (e.g., fjords, inshore, offshore, deep sea) within the UK EEZ need to be spatially resolved.

4.1 Management of marine sedimentary organic carbon

We have shown that marine sediments within the UK EEZ combine with the distinction of fishing activity to produce a spatially variable pattern of OC vulnerability, organic-rich sediments from the fjordic complex of the west coast of Scotland being potentially most vulnerable. Our model can identify at-risk zones where OC is most likely to be vulnerable to bottom trawling activity. While marine sedimentary OC is not currently considered within the frameworks of national OC inventories for greenhouse gas reporting, there is growing interest in the potential and significance of including these stocks (Avelar et al., 2017). Further research into how sedimentary OC can be accounted for within nationally determined contributions is necessary, alongside new accounting guidance and frameworks (Luisetti et al., 2020).

Recent research has shown that marine sediments store significant amounts of OC both globally (Lee et al., 2019;

Atwood et al., 2020) and locally within the UK EEZ and greater North Sea region (Diesing et al., 2017; Luisetti et al., 2019; Diesing et al., 2021; Smeaton et al., 2021a). While OC in shelf sea sediments is prone to natural processes of recycling and remineralisation, it is possible that anthropogenic disturbances are driving enhanced OC loss. Our research maps the potential vulnerability of OC to bottom trawling activity. While this research considers estimated surficial OC stores of the UK EEZ and the anthropogenic impacts of fishing, further detail is needed about the role of and interaction with natural disturbances on these sediments (e.g., current, wave, tidal, and storm activity) to understand the full disturbance pattern. There has been some recent development in this natural disturbance field on sediment mobilisation (Coughlan et al., 2021), but further detail about the impact of natural forcing on OC storage is required. While there are other anthropogenic disturbances that impact the seabed across the UK EEZ, including commercial aggregate dredging, offshore structure construction, and sediment disposal activity, these happen on a localised basis. Thus the impact of these types of activity on sedimentary OC stores is thought to be minimal compared to widespread practices such as trawling (Kenny et al., 2018). Current literature surrounding the fate of OC under bottom trawling activity is conflicting, with some studies estimating that sediment OC may increase (Pusceddu et al., 2005; Martin et al., 2014; Sciberras et al., 2016), while others estimate a decrease (Jennings et al., 2001; Durrieu De Madron et al., 2005; Pusceddu et al., 2014; Oberle et al., 2016). Further research is needed to address some of these uncertainties.

A suggestion for the management of sedimentary OC stores has been to explore the use of MPA's and HPMA's as a tool to protect and enhance carbon stores (Roberts et al., 2017), with accumulating evidence in the literature to support the potential of MPA's to provide an area of enhanced mitigation, adaptation, and resilience towards climate change (Duffy et al., 2016; Roberts et al., 2017; Gaines et al., 2018). Our CVR results for the UK EEZ could be used to help inform potential MPA selection. This type of management approach, where measures limit the activity of bottom trawling may provide scope for the potential limitation of unintentional emissions and possible recovery of benthic communities (Hiddink et al., 2017). The net reaction and relative timescales for the response of benthic ecosystems and sediment OC stores following closure of the seabed to bottom trawling are yet to be determined.

5 Conclusion

We present a new workflow for predicting regions of the seabed where OC is potentially most vulnerable from disturbance. This study has allowed for the first detailed assessment of the relative vulnerability of sedimentary OC

towards fishing disturbance. Our model results highlight that coastal muddy sediments dominated by otter and beam trawling have the highest CVRs. We estimate the sedimentary OC stores on the west coast of Scotland to be amongst the most vulnerable areas of the seabed within the UK EEZ.

Data availability statement

Datasets generated/analysed for this study are included in the article/Supplementary Material. The GIS files generated in this study are available at Marine Scotland Data (<https://doi.org/10.7489/12426-1>).

Author contributions

The study was conceived jointly by KB and WA. KB led the development of the methodology used in this study with assistance from CS, WT, and WA. KB undertook the formal analysis and investigation of this study and wrote the first draft of the manuscript as part of her Ph.D. at the University of St Andrews under the supervision of WA. All authors contributed towards manuscript revisions and have approved the submitted version.

Funding

This work received joint funding from the University of St Andrews and Marine Scotland through the Scottish Blue Carbon Forum.

References

- Amoroso, R. O., Pitcher, C. R., Rijnsdorp, A. D., McConnaughey, R. A., Parma, A. M., Suuronen, P., et al. (2018). Bottom trawl fishing footprints on the world's continental shelves. *Proc. Natl. Acad. Sci. U. S. A.* 115, E10275–E10282. doi: 10.1073/pnas.1802379115
- Arndt, S., Jørgensen, B. B., LaRowe, D. E., Middelburg, J. J., Pancost, R. D., and Regnier, P. (2013). Quantifying the degradation of organic matter in marine sediments: A review and synthesis. *Earth Sci. Rev.* 123, 53–86. doi: 10.1016/j.earscirev.2013.02.008
- Atwood, T. B., Witt, A., Mayorga, J., Hammill, E., and Sala, E. (2020). Global patterns in marine sediment carbon stocks. *Front. Mar. Sci.* 7. doi: 10.3389/fmars.2020.00165
- Avelar, S., van der Voort, T. S., and Eglinton, T. I. (2017). Relevance of carbon stocks of marine sediments for national greenhouse gas inventories of maritime nations. *Carbon Balance Manage.* 12, 10. doi: 10.1186/s13021-017-0077-x
- Balezentiene, L., Streimikiene, D., and Balezentis, T. (2013). Fuzzy decision support methodology for sustainable energy crop selection. *Renew. Sustain. Energy Rev.* 17, 83–93. doi: 10.1016/j.rser.2012.09.016
- Berner, R. A. (1982). Burial of organic carbon and pyrite sulfur in the modern ocean: Its geochemical and environmental significance. *Am. J. Sci.* 282, 451–473. doi: 10.2475/ajs.282.4.451
- BGS (2019) *Offshore sediment index*. Available at: http://mapapps2.bgs.ac.uk/geoindex_offshore/home.html (Accessed 2.10.21).
- Breimann, S. A., O'Neill, F. G., Summerbell, K., and Mayor, D. J. (2022). Quantifying the resuspension of nutrients and sediment by demersal trawling. *Cont. Shelf Res.* 233, 104628. doi: 10.1016/j.csr.2021.104628
- Burrows, M. T., Hughes, D. J., Austin, W. E. N., Smeaton, C., Hicks, N., Howe, J. A., et al. (2017). Assessment of blue carbon resources in Scotland's inshore marine protected area network. *Scottish Nat. Herit. Commun. Rep.* 1–283.
- Coughlan, M., Guerrini, M., Creane, S., O'Shea, M., Ward, S. L., Van Landeghem, K. J. J., et al. (2021). A new seabed mobility index for the Irish Sea: Modelling seabed shear stress and classifying sediment mobilisation to help predict erosion, deposition, and sediment distribution. *Cont. Shelf Res.* 229, 1–17. doi: 10.1016/j.csr.2021.104574
- de Groot, S. J. (1984). The impact of bottom trawling on benthic fauna of the north Sea. *Ocean Manag.* 9, 177–190. doi: 10.1016/0302-184X(84)90002-7
- De Haas, H., Boer, W., and Van Weering, T. C. E. (1997). Recent sedimentation and organic carbon burial in a shelf sea: The north Sea. *Mar. Geol.* 144, 131–146. doi: 10.1016/S00253227(97)00082-0
- De Haas, H., Van Weering, T. C. E., and De Stigter, H. (2002). Organic carbon in shelf seas: sinks or sources, processes and products. *Cont. Shelf Res.* 22, 691–717. doi: 10.1016/S0278-4343(01)00093-0
- Diesing, M., Kröger, S., Parker, R., Jenkins, C., Mason, C., and Weston, K. (2017). Predicting the standing stock of organic carbon in surface sediments of the

Acknowledgments

We would like to acknowledge the support of The St Andrews Institutional Open Access Fund which supported the cost of Open Access.

Conflict of interest

The authors declare that the research was conducted in the absence of any commercial or financial relationships that could be construed as a potential conflict of interest.

Publisher's note

All claims expressed in this article are solely those of the authors and do not necessarily represent those of their affiliated organizations, or those of the publisher, the editors and the reviewers. Any product that may be evaluated in this article, or claim that may be made by its manufacturer, is not guaranteed or endorsed by the publisher.

Supplementary material

The Supplementary Material for this article can be found online at: <https://www.frontiersin.org/articles/10.3389/fmars.2022.892892/full#supplementary-material>

Key data used within this study can be found in the supplementary material. All GIS files will be made available on a data repository

north-west european continental shelf. *Biogeochemistry* 135, 183–200. doi: 10.1007/s10533-017-0310-4

Diesing, M., Thorsnes, T., and Bjarnadóttir, L. R. (2021). Organic carbon densities and accumulation rates in surface sediments of the north sea and skagerrak. *Biogeosciences* 18, 2139–2160. doi: 10.5194/bg-18-2139-2021

Duffy, J. E., Lefcheck, J. S., Stuart-Smith, R. D., Navarrete, S. A., and Edgar, G. J. (2016). Biodiversity enhances reef fish biomass and resistance to climate change. *Proc. Natl. Acad. Sci. U. S. A.* 113, 6230–6235. doi: 10.1073/pnas.1524465113

Dunkley, F., and Solandt, J.-L. (2020). *A case for a just transition to ban bottom trawl and dredge fishing in offshore marine protected areas*. Marine Conservation Society: Ross-on-Wye.

Duplisse, D. E., Jennings, S., Malcolm, S. J., Parker, R., and Sivy, D. B. (2001). Modelling potential impacts of bottom trawl fisheries on soft sediment biogeochemistry in the north Sea. *Geochem. Trans.* 2, 112–117. doi: 10.1186/1467-4866-2-112

Durrieu De Madron, X., Ferré, B., Le Corre, G., Grenz, C., Conan, P., Pujo-Pay, M., et al. (2005). Trawling-induced resuspension and dispersal of muddy sediments and dissolved elements in the gulf of lion (NW Mediterranean). *Cont. Shelf Res.* 25, 2387–2409. doi: 10.1016/j.csr.2005.08.002

Eigaard, O. R., Bastardie, F., Breen, M., Dinesen, G. E., Hintzen, N. T., Laffargue, P., et al. (2016). Estimating seabed pressure from demersal trawls, seines, and dredges based on gear design and dimensions. *ICES J. Mar. Sci.* 73, i27–i43

Eigaard, O. R., Bastardie, F., Hintzen, N. T., Buhl-Mortensen, L., Buhl-Mortensen, P., Catarino, R., et al. (2017). The footprint of bottom trawling in European waters: Distribution, intensity, and seabed integrity. *ICES J. Mar. Sci.* 74, 847–865. doi: 10.1093/icesjms/fsw194

Epstein, G., Hawkins, J. P., Norris, C. R., and Roberts, C. M. (2021). The potential for mobile demersal fishing to reduce carbon storage and sequestration in seabed sediments. *bioRxiv preprint*, 1–29. doi: 10.1101/2021.07.07.450307

Epstein, G., Middelburg, J. J., Hawkins, J. P., Norris, C. R., and Roberts, C. M. (2022). The impact of mobile demersal fishing on carbon storage in seabed sediments. *Glob. Change Biol.* 28, 2875–2894. doi: 10.1111/gcb.16105

Evans, J. R., Austin, W. E. N., Brew, D. S., Wilkinson, I. P., and Kennedy, H. A. (2002). Holocene Shelf sea evolution offshore northeast England. *Mar. Geol.* 191, 147–164. doi: 10.1016/S0025-3227(02)00529-7

Ferguson, R. I., and Church, M. (2004). A simple universal equation for grain settling velocity. *J. Sediment. Res.* 74, 933–937. doi: 10.1306/051204740933

Folk, R. L. (1954). The Distinction between Grain Size and Mineral Composition in Sedimentary-Rock. *Nomenclature. J. Geol.* 62, 344–359.

Gaines, S. D., Costello, C., Owashi, B., Mangin, T., Bone, J., Molinos, J. G., et al. (2018). Improved fisheries management could offset many negative effects of climate change. *Sci. Adv.* 4, 1–9. doi: 10.1126/sciadv.aao1378

Gerritsen, H., and Lordan, C. (2011). Integrating vessel monitoring systems (VMS) data with daily catch data from logbooks to explore the spatial distribution of catch and effort at high resolution. *ICES J. Mar. Sci.* 68, 245–252. doi: 10.1093/icesjms/fsq137

Harvey, H. R., Tuttle, J. H., and Bell, J. T. (1995). Kinetics of phytoplankton decay during simulated sedimentation: Changes in biochemical composition and microbial activity under oxic and anoxic conditions. *Geochim. Cosmochim. Acta* 59, 3367–3377. doi: 10.1017/journal.pone.0076430

Hattab, T., Lasram, F. B. R., Albouy, C., Sammar, C., Romdhane, M. S., Cury, P., et al. (2013). The use of a predictive habitat model and a fuzzy logic approach for marine management and planning. *PLoS One* 8, 1–13. doi: 10.1371/journal.pone.0076430

Hedges, J. I., and Keil, R. G. (1995). Sedimentary organic matter preservation: an assessment and speculative synthesis. *Mar. Chem.* 49, 81–115. doi: 10.1016/0304-4203(95)00008-F

Hiddink, J. G., Jennings, S., and Kaiser, M. J. (2006). Indicators of the ecological impact of bottom-trawl disturbance on seabed communities. *Ecosystems* 9, 1190–1199. doi: 10.1007/s10021-005-0164-9

Hiddink, J. G., Jennings, S., Sciberras, M., Szostek, C. L., Hughes, K. M., Ellis, N., et al. (2017). Global analysis of depletion and recovery of seabed biota after bottom trawling disturbance. *Proc. Natl. Acad. Sci. U. S. A.* 114, 8301–8306. doi: 10.1073/pnas.1618858114

Hunt, C., Demšar, U., Dove, D., Smeaton, C., Cooper, R., and Austin, W. E. N. (2020). Quantifying marine sedimentary carbon: A new spatial analysis approach using seafloor acoustics, imagery, and ground-truthing data in Scotland. *Front. Mar. Sci.* 7, doi: 10.3389/fmars.2020.00588

ICES (2016). *OSPAR request for further development of fishing intensity and pressure mapping*. ICES advice 2016.

ICES (2017). *EU request on indicators of the pressure and impact of bottom-contacting fishing gear on the seabed, and of tradeoffs in the catch and the value of landings*. ICES Spec. Req. advice ICES:Denmark, 1–29.

ICES (2020). *VMS/Log book data for fishing activities in the north East Atlantic and Baltic Sea for the provision of ICES advice on the spatial distribution and impact of fisheries 2009 to 2019* (No. H.4/NH/AB/av) (ICESCopenhagen).

Jennings, S., Kaiser, M. J., and Reynolds, J. D. (2001). “Fishing gears and techniques,” in *Marine fisheries ecology* (Oxford: Blackwell Publishing), 90–111.

Jones, J. B. (1992). Environmental impact of trawling on the sea bed: a review. *New Zeal. J. Mar. Freshw. Res.* 26, 59–67. doi: 10.1080/00288330.1992.9516500

Kahraman, C., and Kaya, I. (2010). Investment analyses using fuzzy probability concept. *Technol. Econ. Dev. Econ.* 16, 43–57. doi: 10.3846/tede.2010.03

Kaiser, M. J., Clarke, K. R., Hinz, H., Austen, M. C. V., Somerfield, P. J., and Karakassis, I. (2006). Global analysis of response and recovery of benthic biota to fishing. *Mar. Ecol. Prog. Ser.* 311, 1–14. doi: 10.3354/meps311001

Kaiser, M. J., Hill, A. S., Ramsay, K., Spencer, B. E., Brand, A. R., Veale, L., et al. (1996). Benthic disturbance by fishing gear in the Irish Sea: a comparison of beam trawling and scallop dredging. *Aquat. Conserv. Mar. Freshw. Ecosyst.* 6, 269–285. doi: 10.1002/(SICI)1099-0755(199612)6:4<269::AID-AQC202>3.0.CO;2-C

Kaskela, A. M., Kotilainen, A. T., Alanen, U., Cooper, R., Green, S., Guinan, J., et al. (2019). Picking up the pieces—harmonising and collating seabed substrate data for European maritime areas. *Geosciences* 9, 1–18. doi: 10.3390/geosciences9020084

Kavadas, S., Maina, I., Damalas, D., Dokos, I., Pantazi, M., and Vassilopoulou, V. (2015). Multi-criteria decision analysis as a tool to extract fishing footprints: Application to small scale fisheries and implications for management in the context of the maritime spatial planning directive. *Mediterr. Mar. Sci.* 16, 294–304. doi: 10.12681/mms.1087

Kenny, A. J., Jenkins, C., Wood, D., Bolam, S. G., Mitchell, P., Scougal, C., et al. (2018). Assessing cumulative human activities, pressures, and impacts on north Sea benthic habitats using a biological traits approach. *ICES J. Mar. Sci.* 75, 1080–1092. doi: 10.1093/icesjms/fsx205

Lambert, G. I., Jennings, S., Kaiser, M. J., Davies, T. W., and Hiddink, J. G. (2014). Quantifying recovery rates and resilience of seabed habitats impacted by bottom fishing. *J. Appl. Ecol.* 51, 1326–1336. doi: 10.1111/1365-2664.12277

Lee, T. R., Wood, W. T., and Phrampus, B. J. (2019). A machine learning (kNN) approach to predicting global seafloor total organic carbon. *Global Biogeochem. Cycles* 33, 37–46. doi: 10.1029/2018GB005992

Legge, O., Johnson, M., Hicks, N., Jickells, T., Diesing, M., Aldridge, J., et al. (2020). Carbon on the northwest european shelf: contemporary budget and future influences. *Front. Mar. Sci.* 7, 143. doi: 10.3389/fmars.2020.00143

Lindgarth, M., Valentinsson, D., Hansson, M., and Ulmestrand, M. (2000). Effects of trawling disturbances on temporal and spatial structure of benthic soft-sediment assemblages in gullmarsfjorden, Sweden. *ICES J. Mar. Sci.* 57, 1369–1376. doi: 10.1006/jmsc.2000.0903

Luff, R., and Moll, A. (2004). Seasonal dynamics of the North Sea sediments using a three-dimensional coupled sediment-water model system. *Cont. Shelf Res.* 24, 1099–1127

Luisetti, T., Ferrini, S., Grilli, G., Jickells, T. D., Kennedy, H., Kröger, S., et al. (2020). Climate action requires new accounting guidance and governance frameworks to manage carbon in shelf seas. *Nat. Commun.* 11, 1–10. doi: 10.1038/s41467-020-18242-w

Luisetti, T., Turner, R. K., Andrews, J. E., Jickells, T. D., Kröger, S., Diesing, M., et al. (2019). Quantifying and valuing carbon flows and stores in coastal and shelf ecosystems in the UK. *Ecosyst. Serv.* 35, 67–76. doi: 10.1016/j.ecoser.2018.10.013

Marine Conservation Institute (2021) *Marine protection atlas*. Available at: <https://mpatlas.org/countries/> (Accessed 8.19.21).

Martin, J., Puig, P., Masqué, P., Palanques, A., and Sá Nchez-Gó Mez, A. (2014). Impact of bottom trawling on deep-Sea sediment properties along the flanks of a submarine canyon. *PLoS One* 9, 1–11.

Nielsen, P. (1993). Turbulence effects on the settling of suspended particles. *J. Sediment. Petrol.* 63, 835–838. doi: 10.1306/d4267c1c2b26-11d78648000102c1865d

Nyimbili, H. P., and Erden, T. (2020). A combined model of gis and fuzzy logic evaluation for locating emergency facilities: a case study of istanbul. *8th Int. Conf. Cartogr. GIS* 1, 191–203.

Oberle, F. K. J., Storlazzi, C. D., and Hanebuth, T. J. J. (2016). What a drag: Quantifying the global impact of chronic bottom trawling on continental shelf sediment. *J. Mar. Syst.* 159, 109–119. doi: 10.1016/j.jmarsys.2015.12.007

OSPAR (2016) *Ospar data files including trawler data*. Available at: https://odims.ospar.org/odims_data_files/ (Accessed 6.18.19).

Paradis, S., Goni, M., Masqué, P., Duran, R., Arjona-Camas, M., Palanques, A., et al. (2020). Persistence of biogeochemical alterations of deep-sea sediments by bottom trawling geophysical research letters. *Geophys. Res. Lett.* 48, 1–12. doi: 10.1029/2020GL091279

Paradis, S., Pusceddu, A., Masqué, P., Puig, P., Moccia, D., Russo, T., et al. (2019). Organic matter contents and degradation in a highly trawled area during fresh particle inputs (Gulf of castellammare, southwestern Mediterranean). *Biogeochemistry* 16, 4307–4320. doi: 10.5194/bg-16-4307-2019

- Paraska, D. W., Hipsey, M. R., and Ursula Salmon, S. (2014). Sediment diagenesis models: Review of approaches, challenges and opportunities. *Environ. Model. Software* 61, 297–325. doi: 10.1016/j.envsoft.2014.05.011
- Pusceddu, A., Bianchelli, S., Martin, J., Puig, P., Palanques, A., Masque, P., et al. (2014). Chronic and intensive bottom trawling impairs deep-sea biodiversity and ecosystem functioning. *PNAS* 111, 8861–8866. doi: 10.1073/pnas.1405454111
- Pusceddu, A., Grémare, A., Escoubeyrou, K., Amouroux, J. M., Fiordelmondo, C., and Danovaro, R. (2005). Impact of natural (storm) and anthropogenic (trawling) sediment resuspension on particulate organic matter in coastal environments. *Cont. Shelf Res.* 25, 2506–2520. doi: 10.1016/j.csr.2005.08.012
- Provoost, P., Braeckman, U., Van Gansbeke, D., Moodley, L., Soetaert, K., Middelburg, J. J., et al. (2013). Modelling benthic oxygen consumption and benthic-pelagic coupling at a shallow station in the southern North Sea. *Estuar. Coast. Shelf Sci.* 120, 111.
- Quintana, M. M., Motova, A., Wilkie, O., and Patience, N. (2021). *Economics of the UK fishing fleet 2020* (Edinburgh: Seafood Industry Authority).
- Raines, G. L., Sawatzky, D. L., and Bonham-Carter, G. F. (2010). New fuzzy logic tools in ArcGIS. *ArcUser* 10, 8–13.
- Rees, T. (2003). C-squares, a new spatial indexing system and its applicability to the description of oceanographic datasets. *Oceanography* 16, 11–19. doi: 10.5670/oceanog.2003.52
- Rijnsdorp, A. D., Bastardie, F., Bolam, S. G., Buhl-Mortensen, L., Eigaard, O. R., Hamon, K. G., et al. (2016). Towards a framework for the quantitative assessment of trawling impact on the seabed and benthic ecosystem. *ICES J. Mar. Sci.* 73, i127–i138. doi: 10.1093/icesjms/fsv207
- Rijnsdorp, A. D., Bolam, S. G., Garcia, C., Hiddink, J. G., Hintzen, N. T., Van Denderen, P. D., et al. (2018). Estimating sensitivity of seabed habitats to disturbance by bottom trawling based on the longevity of benthic fauna. *Ecol. Appl.* 28, 1302–1312. doi: 10.1002/eap.1731
- Roberts, C. M., Leary, B. C. O., Mccauley, D. J., Maurice, P., Duarte, C. M., and Castilla, J. C. (2017). Marine reserves can mitigate and promote adaptation to climate change. *PNAS* 114, 6167–6175. doi: 10.1073/pnas.1701262114
- Rouse, S., Kafas, A., Hayes, P., and Wilding, T. A. (2017). Development of data layers to show the fishing intensity associated with individual pipeline sections as an aid for decommissioning decision-making. *Underw. Technol.* 34, 171–178. doi: 10.3723/ut.34.171
- Sala, E., Mayorga, J., Bradley, D., Cabral, R. B., Atwood, T. B., Auber, A., et al. (2021). Protecting the global ocean for biodiversity, food and climate. *Nature* 592, 397–402. doi: 10.1038/s41586-021-03371-z
- Sciberras, M., Parker, R., Powell, C., Robertson, C., Kroger, S., Bolam, S., et al. (2016). Impacts of bottom fishing on the sediment infaunal community and biogeochemistry of cohesive and non-cohesive sediments. *Limnol. Oceanogr.* 61, 2076–2089. doi: 10.1002/lno.10354
- Scourse, J. D., Austin, W. E. N., Long, B. T., Assinder, D. J., and Huws, D. (2002). Holocene Evolution of seasonal stratification in the Celtic Sea: Refined age model, mixing depths and foraminiferal stratigraphy. *Mar. Geol.* 191, 119–145. doi: 10.1016/S0025-3227(02)00528-5
- Seiter, K., Hensen, C., and Zabel, M. (2005). Benthic carbon mineralization on a global scale. *Global Biogeochem. Cycles* 19, 1–26. doi: 10.1029/2004GB002225
- Shepperson, J. L., Hintzen, N. T., Szostek, C. L., Bell, E., Murray, L. G., and Kaiser, M. J. (2018). A comparison of VMS and AIS data: The effect of data coverage and vessel position recording frequency on estimates of fishing footprints. *ICES J. Mar. Sci.* 75, 988–998. doi: 10.1093/icesjms/fsx230
- Smeaton, C., and Austin, W. E. N. (2017). Sources, sinks, and subsidies: Terrestrial carbon storage in mid-latitude fjords. *J. Geophys. Res. Biogeosci.* 122, 2754–2768. doi: 10.1002/2017JG003952
- Smeaton, C., and Austin, W. E. N. (2019). Where's the carbon: exploring the spatial heterogeneity of sedimentary carbon in mid-latitude fjords. *Front. Earth Sci.* 7, 1–16. doi: 10.3389/feart.2019.00269
- Smeaton, C., and Austin, W. E. N. (2022). Quality not quantity: Prioritizing the management of sedimentary organic matter across continental shelf seas. *Geophys. Res. Lett.* 49, 1–11. doi: 10.1029/2021GL097481
- Smeaton, C., Austin, W. E. N., Davies, A. L., Baltzer, A., Abell, R. E., and Howe, J. A. (2016). Substantial stores of sedimentary carbon held in mid-latitude fjords. *Biogeosciences* 13, 5771–5787. doi: 10.5194/bg-13-5771-2016
- Smeaton, C., Austin, W. E. N., and Turrell, W. R. (2020). *Re-evaluating Scotland's sedimentary carbon stocks* (Aberdeen: Marine Scotland Science).
- Smeaton, C., Hunt, C. A., Turrell, W. R., and Austin, W. E. N. (2021a). Marine sedimentary carbon stocks of the United Kingdom's exclusive economic zone. *Front. Earth Sci.* 9, 1–21. doi: 10.3389/feart.2021.593324
- Smeaton, C., Yang, H., and Austin, W. E. N. (2021b). Carbon burial in the mid-latitude fjords of Scotland. *Mar. Geol.* 441, 106618. doi: 10.1016/j.margeo.2021.106618
- Soetaert, K., Herman, P. M. J., and Middelburg, J. J. (1996). A model of early diagenetic processes from the shelf to abyssal depths. *Geochim. Cosmochim. Acta* 60, 1019–10140.
- Soetaert, K., Herman, P. M. J., Middelburg, J. J., and Heip, C. (1998). Assessing organic matter mineralization, degradability and mixing rate in an ocean margin sediment (Northeast Atlantic) by diagenetic modeling. *J. Mar. Res.* 56, 519–534.
- Soetaert, K., and Middelburg, J. J. (2009). Modeling eutrophication and oligotrophication of shallow-water marine systems: The importance of sediments under stratified and wellmixed conditions. *Hydrobiologia* 629, 239–254.
- Tenzer, R., and Gladkikh, V. (2014). Assessment of density variations of marine sediments with ocean and sediment depths. *Sci. World J.* 2014, 1–9. doi: 10.1155/2014/823296
- Tiano, J. C., Witbaard, R., Bergman, M. J. N., van Rijswijk, P., Tramper, A., van Oevelen, D., et al. (2019). Acute impacts of bottom trawl gears on benthic metabolism and nutrient cycling. *ICES J. Mar. Sci.* 76, 19171930. doi: 10.1093/icesjms/fsz060
- Uberoi, E., Hutton, G., Ward, M., and Ares, E. (2020). *UK Fisheries statistics 2020*. (London: UK parliament house of commons library).
- Uberoi, E., Hutton, G., Ward, M., and Ares, E. (2021). *UK Fisheries statistics: 2021* (London: UK Parliament House of Commons Library).



OPEN ACCESS

EDITED BY
Alberto Basset,
University of Salento, Italy

REVIEWED BY
Yining Chen,
Ministry of Natural Resources, China
Xiaoguang Ouyang,
Southern Marine Science and
Engineering Guangdong Laboratory
(Guangzhou), China

*CORRESPONDENCE
Craig Smeaton
cs244@st-andrews.ac.uk

[†]These authors share first authorship

SPECIALTY SECTION
This article was submitted to
Marine Ecosystem Ecology,
a section of the journal
Frontiers in Marine Science

RECEIVED 01 June 2022

ACCEPTED 18 July 2022

PUBLISHED 11 August 2022

CITATION
Smeaton C, Burden A, Ruranska P,
Ladd CJT, Garbutt A, Jones L,
McMahon L, Miller LC, Skov MW and
Austin WEN (2022) Using citizen
science to estimate surficial soil
Blue Carbon stocks in Great
British saltmarshes.
Front. Mar. Sci. 9:959459.
doi: 10.3389/fmars.2022.959459

COPYRIGHT
© 2022 Smeaton, Burden, Ruranska,
Ladd, Garbutt, Jones, McMahon, Miller,
Skov and Austin. This is an open-access
article distributed under the terms of
the [Creative Commons Attribution
License \(CC BY\)](https://creativecommons.org/licenses/by/4.0/). The use, distribution
or reproduction in other forums is
permitted, provided the original
author(s) and the copyright owner(s)
are credited and that the original
publication in this journal is cited, in
accordance with accepted academic
practice. No use, distribution or
reproduction is permitted which does
not comply with these terms.

Using citizen science to estimate surficial soil Blue Carbon stocks in Great British saltmarshes

Craig Smeaton^{1*†}, Annette Burden^{2†}, Paulina Ruranska¹,
Cai J. T. Ladd^{3,4}, Angus Garbutt², Laurence Jones²,
Lucy McMahon⁵, Lucy C. Miller¹, Martin W. Skov⁴
and William E. N. Austin^{1,6}

¹School of Geography and Sustainable Development, University of St Andrews, St Andrews, United Kingdom, ²UK Centre for Ecology and Hydrology, Bangor, United Kingdom, ³School of Geographical and Earth Sciences, University of Glasgow, Glasgow, United Kingdom, ⁴School of Ocean Sciences, Bangor University, Menai Bridge, United Kingdom, ⁵Department of Environment and Geography, Wentworth Way, University of York, York, United Kingdom, ⁶Scottish Association of Marine Science, Oban, United Kingdom

A new saltmarsh soil dataset comprising of geochemical and physical property data from 752 soil samples collected through a sampling program supported by citizen scientists has been brought together with existing data to make the first national estimates of the surficial (top 10 cm) soil OC stock for Great British (GB) saltmarshes. To allow the inclusion of secondary data in the soil stock estimate a new bespoke organic matter to organic carbon conversion for GB saltmarsh soil was developed allowing organic matter data measured using loss-on-ignition to be converted to organic carbon content. The total GB surficial soil OC stock is 2.320 ± 0.470 Mt; English saltmarshes hold 1.601 ± 0.426 Mt OC, Scottish saltmarshes hold 0.368 ± 0.091 Mt OC, and Welsh saltmarshes hold 0.351 ± 0.082 Mt OC. The stocks were calculated within a Markov Chain Monte Carlo framework allowing robust uncertainty estimates to be derived for the first time. Spatial mapping tools are available to accompany these stock estimates at individual saltmarsh habitats throughout GB. This data will aid in the protection and management of saltmarshes and represents the first steps towards the inclusion of saltmarsh OC in the national inventory accounting of blue carbon ecosystems.

KEYWORDS

saltmarsh, carbon, vegetation, soil, organic matter, citizen science, spatial mapping, Great Britain

Introduction

Saltmarsh ecosystems alongside other intertidal Blue Carbon habitats such as seagrass and mangroves (Nellemann and Corcoran, 2009) are recognized hotspots for the burial and long-term storage of organic carbon (OC). Globally, saltmarshes occupy an area of 54,951 km² (Mcowen et al., 2017) and their soils store between 0.4 – 6.5 Pg of OC (McLeod et al., 2011; Duarte et al., 2013). Annually, a further 0.9 – 31.4 Tg OC is buried in saltmarsh soils globally (Ouyang and Lee, 2014). The large quantities of OC stored, coupled with the high OC burial rates in these ecosystems, has resulted in saltmarshes now being considered core components of the coastal carbon (C) cycle (Bauer et al., 2013). The potential for saltmarshes and other intertidal environments to regulate global climate through the burial and storage of OC within their soils is now widely recognized (Macreadie et al., 2019; Macreadie et al., 2021). Yet, these systems are also at risk. With increasing climate instability, sea level rise, and anthropogenic pressure, saltmarsh's ability to trap and store OC will likely be severely reduced and a significant proportion of the OC stored within their soils may be lost by the end of this century (Crosby et al., 2016; Horton et al., 2018). Globally it is estimated that saltmarsh habitat is reducing by 1 – 2% yr⁻¹ (Duarte et al., 2008) with approximately 25% reduction of the global habitat since 1800 (Bridgham et al., 2006; McLeod et al., 2011). Yet, recent estimates suggest at a global scale much of the modern (1999–2019) habitat loss has been offset by the creation of new saltmarsh (Murray et al., 2022). Nevertheless, significant efforts are still required to preserve these saltmarshes and assure the significant quantities of OC held within their soil is not lost and remineralized, which would further exacerbate global climate change (Schuerch et al., 2018).

Quantifying the OC stored in saltmarsh soil is a crucial foundational step towards integrating saltmarsh OC into national C accounting, understanding the C and climate impact of habitat loss, and justifying habitat protection and restoration (Granek et al., 2010; Theuerkauf et al., 2015; Rogers et al., 2019). Yet the current global saltmarsh soil OC stocks are coarse, with estimates ranging between 0.4 – 6.5 Pg OC (McLeod et al., 2011; Duarte et al., 2013). This is largely driven by the unequal spatial distribution of current stock assessments with the majority focusing on tropical/sub-tropical areas such as Australia (Lovelock et al., 2014; Brown et al., 2016; Kelleway et al., 2016) and the Gulf of Mexico (Thorhaug et al., 2019; Vaughn et al., 2020). Only a few countries such as Australia (Young et al., 2021) and the USA (Hinson et al., 2017; Holmquist et al., 2018) have undertaken national saltmarsh OC stock assessments. A lack of stock assessments is particularly apparent across the temperate and boreal saltmarshes of the NE Atlantic region where data on saltmarsh OC stock is

extremely limited (Mueller et al., 2019a; Mueller et al., 2019b). The best current OC stock data for saltmarshes in Great Britain (GB) have generally been limited to single marshes (Andrews et al., 2008; Burden et al., 2013; Porter et al., 2020) or have been geographically constrained to single regions (Burden et al., 2019; Ford et al., 2019; Austin et al., 2021). Where full national saltmarsh soil OC stock estimates have been undertaken (Beaumont et al., 2014), these are still based on extrapolation from a relatively few well-studied sites. A recent systematic review found inconsistencies in the way data was gathered and reported, makes comparisons and consolidation of knowledge difficult (Mason et al., 2022). This limited and fragmented knowledge base could hinder the inclusion of OC held within GB saltmarshes into national Greenhouse Gas (GHG) reporting and C budgets.

Reliance on data from only a few sites makes assumptions about the homogeneity of soil C stocks across different biogeographic contexts fail to account for differences due to soil type or vegetation community, leading to uncertainty in soil carbon stock estimates (Kelleway et al., 2016; Kelleway et al., 2017). A challenge for structured surveys for habitats like saltmarshes - which are widely distributed around national coastlines, but often in multiple and fragmented locations - is the ability to reliably sample sufficient sites to gather a robust national picture of variation within and across sites. The rise of citizen involvement in data collection has made large-scale sampling feasible (Aavik et al., 2020), raised public engagement in science (Phillips et al., 2019), and influenced policy formulation and implementation (Couvet et al., 2008) within the conservation sciences. By following standardized sampling procedures, systematic observations, and simple methods (Conrad and Hilchey, 2011; Parsons et al., 2011), citizen-led data collection is now widely appreciated for its quality and includability in peer-review research (McKinley et al., 2017).

In this study, we undertake a national scale assessment to quantify the OC held within the surficial soils (top 10 cm) of the saltmarshes of GB. Utilizing the well-established relationship between regional vegetation composition and surficial soil OC (Ford et al., 2019; Austin et al., 2021; Penk and Perrin, 2022) we bring together the latest national saltmarsh mapping data (Haynes, 2016; Natural Resources Wales, 2016; Environment Agency, 2021) with a new GB wide soil dataset produced following a standardized sampling methodology by citizen scientists allowing, for the first time, the quantity of OC held within surficial soils to be estimated and mapped for all saltmarshes within GB and its constituent nations (Scotland, England, and Wales). As this study only focuses on the surficial (top 10 cm) soils the calculated OC stocks will be an underestimate of the full quantity of OC held at depth within

the soil of saltmarshes. Yet, the surficial soil OC stock estimates are key to understanding saltmarsh OC dynamics at national scales. The resulting broad spatial understanding of OC stocks can be used in prioritizing saltmarsh conservation, restoration, and management from a C storage viewpoint.

Saltmarshes of Great Britain

Saltmarsh habitat is widely distributed around the constituent nations (Scotland, England, and Wales) of GB (Figure 1A). The most extensive areas occur along estuaries in the counties of Hampshire, north Kent, Essex, Norfolk, Lincolnshire, and Lancashire (May and Hansom, 2003). The extent of saltmarsh habitat in the GB is estimated to be between 400 km² and 495 km² (Burd, 1989; Jones et al., 2011; Burden et al., 2020; Ladd, 2021). The marshes vary significantly in size from the small marshes found at the head of Scotland's fjords to the expansive coastal systems of the Solway Firth, Morecambe Bay, and the Wash (Supplementary Figure 1).

In GB, saltmarsh systems can be defined into six core types (Pye and French, 1993): estuarine, embayment, back-barrier,

and fringing marshes are found throughout GB, while loch-head and perched marshes are found in Scotland. Loch-head marshes are highly sheltered systems found at the landward end of Scotland's fjords. Perched saltmarshes form on sea cliffs and in the shelter of raised rocky outcrops, where shallow soils tend to develop in the wave splash-zone (Haynes, 2016).

Saltmarsh vegetation composition across GB is driven by climatic conditions, coastal processes and soil characteristics, and hydrological regimes. GB marshes are generally dominated by SM13 (*Puccinellia maritima*) and SM16 (*Festuca rubra*) vegetation communities as described by the British National Vegetation Classification (NVC) scheme (Rodwell, 1991). These communities occupy a significant proportion of GB saltmarshes but variations in several factors, notably sediment type, climate, biotic factors, and historical management (Adam, 1978) lead to a range of differing vegetation communities developing within and between marshes (Burd, 1989).

Although the variation in saltmarsh vegetation is continuous within and between sites, it is possible to recognize combinations of vegetation types which allow several distinct geo-regions to be identified. Following the approach of Adam (1978) where four geo-regions were identified across GB:

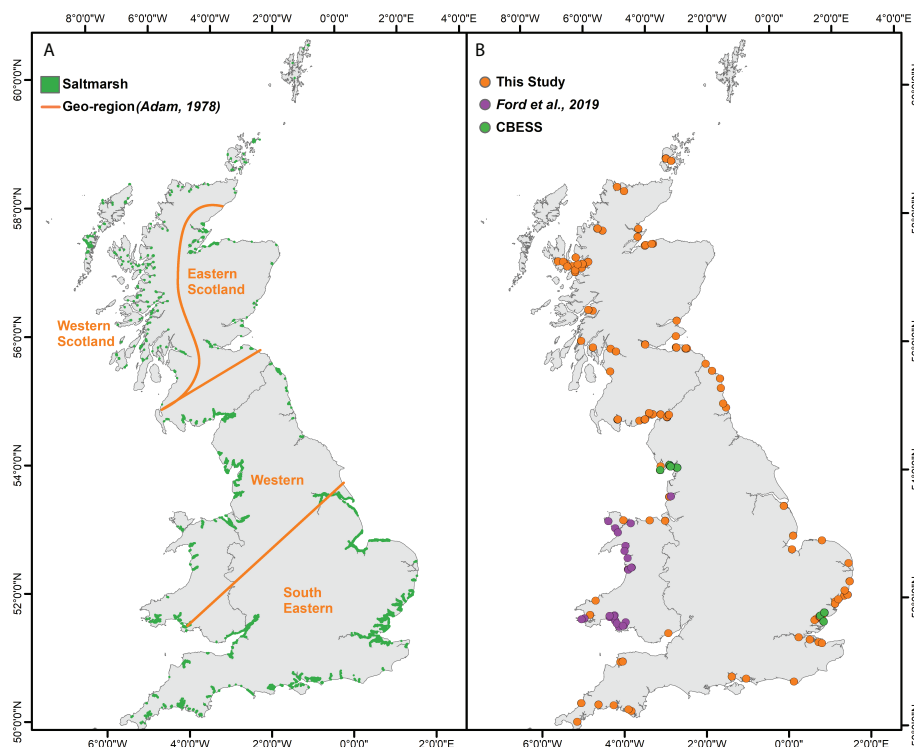


FIGURE 1
Saltmarshes of Great Britain. (A) Mapped extent of saltmarsh habitat across the nations of Great Britain (exaggerated by 1.5 times for visibility). Orange lines highlight the different saltmarsh vegetation geo-regions of Great Britain as described by Adam, 1978. (B) Sampling sites across Great British saltmarsh (orange dots) and the location of secondary data sources (green and purple dots).

Western Scotland: This geo-region contains all the loch-head and perched saltmarshes in GB. The marshes are generally small, on average occupying less than 0.1 km². The vegetation structure of the marshes in this geo-region is often simple in comparison to other areas. These marshes are dominated by *Puccinellia/Festuca* and *Juncus gerardii* communities. The pioneer and low marsh communities are generally dominated by *Salicornia* and *Suaeda* (Adam, 1978; Haynes, 2016).

Eastern Scotland: Saltmarshes within this geo-region are defined as embayment, fringing, and back-barrier, with large estuarine marshes mainly absent (Haynes, 2016). These marshes are dominated by four vegetation communities which occur in varying proportions: *Salicornia/Suaeda*, *Puccinellia*, *Puccinellia/Festuca*, and *Juncus gerardii* (Adam, 1978; Burd, 1989; Haynes, 2016).

Western: The marshes in the western geo-region are significantly larger than those in the Western and Eastern Scotland geo-regions (Supplementary Figure 1), with large estuarine marshes being common (Burd, 1989). These marshes are further differentiated by their sandy soils, resulting in greater importance of *P. maritima* in the pioneer zone due to reduced competition from *Spartina maritima* and *Aster tripolium*. Higher precipitation in this geo-region generally leads to more brackish high marshes with *Blysmetum rufi* and *Halimionetum portulacoidis* communities are commonly found.

South Eastern: The marshes within this geo-region are smaller than those in the Western region, with exception of the Wash marshes (Supplementary Figure 1). The prevailing substrate is fine silt, and marsh vegetation is predominantly *Spartina* (Burd, 1989). The mid-low marsh communities, *Puccinellia* and *Halimione*, *Puccinellia/Festuca* occupy significant proportions of the total area. Upper marsh communities are more common than in other geo-regions, with *Phragmites* common across much of the region.

Methods

Harmonization of saltmarsh classifications

In the last decade there has been a concerted effort in GB to measure areal extent and habitat composition. The classifications used in saltmarsh mapping differ in England to that of Wales and Scotland. In Scotland (Figure 2A) and Wales (Figure 2B), saltmarsh data is mapped to NVC communities (Rodwell, 1991). In England, saltmarsh is mapped to a set of saltmarsh zones (Spartina, Pioneer, Mid-Low, and High Marsh) following a modified version of the European nature information system (EUNIS) classification scheme currently used by the Environment Agency (Figure 2C). For the purposes of this study, we define the extent of the saltmarsh following the approach of the Environment Agency (2021), at the seaward end the demarcation between saltmarsh and intertidal flat is described as $\geq 5\%$ ground coverage of saltmarsh vegetation. The demarcation of the landward extent is defined when saltmarsh vegetation becomes $\geq 5\%$ of a predominantly terrestrial vegetation community.

Prior to undertaking OC stock calculations, the mapping data must be harmonized under a single classification scheme. The modified EUNIS scheme already utilized in the English marshes was determined to be best suited to this task. The EUNIS habitat classification system is a comprehensive pan-European systems for habitat classification. Using a hierarchical approach, the habitat types are identified by specific codes, with saltmarshes being classified as A2.5. These categories can be further broken down into high (A2.52), mid-high (A2.53), low-mid (A2.54), pioneer (A2.55) and *Spartina* dominated (A2.55443) saltmarsh zones. In this study a modified version of the EUNIS scheme is used where the mid-high and low-mid

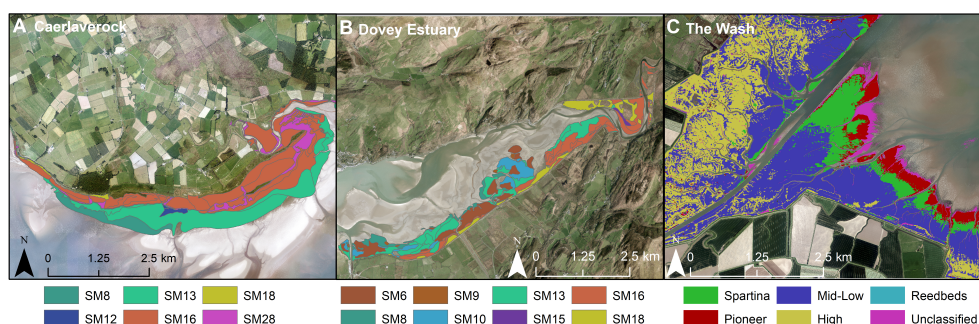


FIGURE 2
Examples of current saltmarsh mapping within (A) Scotland – Caerlaverock marsh (54.969555, -3.484984), (B) Wales – Dovey (Dyfi) Estuary (52.543454, -3.977258) and (C) England – The Wash (52.926668, 0.061452).

EUNIS marsh classifications are combined into the mid-low class. The Scottish and Welsh NVC (Rodwell, 2000) data can be easily converted to follow the modified EUNIS classification (Supplementary Table 1) allowing the data to be combined with the English saltmarsh data and to allow direct comparisons with neighboring European saltmarshes in the future.

Within the mapped data, some zones were recorded as mosaics of two or more NVC communities. In these cases, the first NVC community listed was chosen as the primary classification. The perched saltmarshes found in Scotland (Haynes, 2016) have been removed from the datasets, as these marshes are generally found on cliffs, largely devoid of any underlying soil (Haynes, 2016; Porter et al., 2020).

The field surveys and photographic data used to classify marshes was collected between 2010 – 2012 for Scotland (Haynes, 2016), 2006 – 2019 for England (Environment Agency, 2021) and 2006 – 2009 for Welsh sites (Natural Resources Wales, 2016). The marsh classes therefore represent a snapshot in time of GB saltmarsh extent and vegetation composition as they were when the surveys were completed. The classes may no longer be an accurate representation of the marshes as they are today, especially considering the highly dynamic nature of the intertidal habitats (Ladd et al., 2019; Ladd, 2021). However, these mapping products remain the best quality data currently available.

Soil sampling

A total of 752 soil samples were collected from saltmarshes across GB (Figure 1B) between 2018 – 2021 with the aim of quantifying surficial OC stocks. Of these, 393 surficial soil (top 10 cm) samples were collected from Scottish saltmarshes using a mix of either modified syringe samplers (60 ml syringe with end cut away, creating a 10 cm length barrel with a 3 cm diameter), or a 3 cm gouge corer by the project team. Both sampling methods are designed to reduce the effect of compaction of the fibrous layers of saltmarsh soil (Smeaton et al., 2020). Soil samples were collected in conjunction with detailed vegetation surveys designed to explore the relationship between vegetation and soil OC, alongside investigating the accuracy of current saltmarsh mapping and to assess potential changes in vegetation composition and aerial extent since mapping occurred. The vegetation surveys were undertaken following a standard protocol where, at each site, a 1 m² quadrat was placed on the marsh and percentage coverage of each plant species estimated. Vegetation composition was then assigned following the NVC scheme (Rodwell, 2000).

A further 369 samples were collected by volunteer citizen scientists as part of the “CarbonQuest” initiative. The citizen scientists were provided with a pack of five modified color-coded

syringe samplers and instructions to collect samples at equal distances along a land-to-sea transect and to freeze the samples upon collection. Sampling locations were recorded by extracting coordinates from image files associated with photographs taken of each soil core *in situ* with a GPS-enabled smart phone. Surveys were completed between August and October 2019, and all samples were received by the University of St Andrews by November 2019. Samples were stored at -20°C prior to analysis. The location data was quality-checked to assure the sampling protocol was followed and that samples were collected from appropriate locations (saltmarsh *vs* freshwater wetland). This was achieved by comparing the sampling locations to current saltmarsh maps and high resolution (25 cm) aerial photography. If the sample location did not overlap with known saltmarsh habitats, the sample was removed from the sample set and did not undergo laboratory analysis. As the identification and quantification of vegetation coverage and composition requires specialist expertise, it was not possible for all the citizen scientists to provide this level of detail. Therefore, each sample was assigned a classification (NVC, Simplified NVC, marsh zone) using the existing saltmarsh maps.

Soil physical property and geochemical analysis

The samples within the syringe tubes were visually inspected and the length of the sample measured to assure accurate quantification of sample volumes (cm³) was recorded. The samples were extruded from the syringe and the soil was described according to the British Columbia protocol for estimating soil texture (www.for.gov.bc.ca/isb/forms/lib/fs238.pdf). This approach uses simple qualitative measures (graininess, moistness, stickiness, and ability to hold a form without breaking apart when rolled) to classify the soil to one of twelve soil categories (Supplementary Table 2) which can be further simplified into sandy, non-sandy and organic (>40% organic matter (OM) classes (Ford et al., 2019).

The extruded soil samples alongside the samples collected using the gouge corer were oven dried at 60°C for 72 hrs and weighed. Using the dry mass and the sample volume (prior to drying) the dry bulk density was calculated following the approach of Dadey et al. (1992):

$$\begin{aligned} \text{Dry Bulk Density (g cm}^{-3}\text{)} \\ = \text{Dry Mass (g)} / \text{Volume before drying (cm}^3\text{)} \quad (\text{eq.1}) \end{aligned}$$

The dry samples were then milled to a fine powder and split into two subsamples to undergo loss on ignition (LOI) and elemental analysis. The quantity of OM within each sample was determined by LOI following the approach of Craft et al. (1991)

to allow for global comparison. Briefly, 1 g of milled sample was placed in a crucible and dried overnight at 105°C to remove any moisture the crucible was then transferred to furnace to be combusted at 450°C for 4 hrs. The sample was weighed before and after each stage allowing the OM content of the soil to be calculated.

The OC content of the soil was determined by placing 10 mg of sample into silver capsules. The samples were acidified with HCl (10%) to remove carbonate (CaCO_3). The acidified samples were dried overnight at 50°C and sealed. The OC contents of the sealed samples were measured using an Elemental Analyzer (Elementar Vario EL Cube; (Verardo et al., 1990; Nieuwenhuize et al., 1994). Triplicate measurements of samples ($n = 30$) produced standard deviations (1σ) of 0.04% for OC. Further quality control was assured by repeat analysis of high OC sediment standard (B2151) with reference values for C of $7.45 \pm 0.14\%$, the reference standards ($n = 76$) deviated from the known OC values by 0.08%.

Secondary soil data

Saltmarsh soil (top 10cm) dry bulk density and OM data for 265 sampling sites across the saltmarshes of Morecambe Bay and Essex were extracted from the Coastal Biodiversity and Ecosystem Service Sustainability (CBESS) project outputs (Ford et al., 2015; Ford et al., 2016a; Ford et al., 2016b; Ford et al., 2016c). This dataset was further supplemented by additional data from Morecambe Bay marshes (Baugh, 2019), the Ribble Estuary (Ford et al., 2012) and Welsh marshes (Ford et al., 2019).

Organic matter vs organic carbon

With the exception of Baugh (2019), the secondary datasets do not report the OC content of the soil but rather the OM content measured by LOI. To convert the OM data to OC different conversion factors can be applied, the most common of which is Van Bemmelen (1890) which assumes that 58% of OM is OC resulting in a 1.724 conversion factor to transform OM to OC (Van Bemmelen, 1890). Though widely used the Van Bemmelen (1890) approach is now considered problematic and is not supported by empirical measurements both in terrestrial and saltmarsh soils (Pribyl, 2010; Ouyang and Lee, 2020). In saltmarsh studies the OM to OC conversion developed by Craft et al. (1991) has been widely applied globally and in general performs well in organic rich systems such as those in North America. Yet, the performance of the Craft et al. (1991) conversion in organo-mineral systems such as the saltmarshes of GB is uncertain. Using the data collected from the saltmarshes of GB, a bespoke OM-OC conversion was

developed following the methodology of Craft et al. (1991). Using the new bespoke conversion factor the OM data compiled from the literature were converted to OC and integrated into the main dataset.

Quantifying soil OC stocks

The surficial (top 10cm) soil OC stocks were determined for the GB saltmarshes following the calculation steps outlined in Smeaton et al. (2020) (eq.2-4). For each of the four geo-regions, the mean (and standard deviation) soil dry bulk density and OC content were compiled for each NVC, simplified NVC and marsh zone. A hierarchical approach was used to populate each of the equations (eq 1-3). Where possible dry bulk density and OC data for each NVC (i.e., SM13a) for a given geo-region was utilized in the calculations. If no data was available, surrogate values were utilized in descending order: simplified NVC (i.e., SM13), marsh zone (i.e., mid-low), geo-region average values, and finally national average values. The areal extent of the NVC and marsh zones was taken from the marsh classifications (Section 3.1).

$$\text{Volume}(\text{m}^3) = \text{Area}(\text{m}^2) \times \text{Soil depth}(\text{m}) \quad (\text{eq.2})$$

$$\text{Mass}(\text{kg}) = \text{Volume}(\text{m}^3) \times \text{Dry bulk density}(\text{kg m}^{-3}) \quad (\text{eq.3})$$

$$\text{OC stock}(\text{kg}) = \text{Mass}(\text{kg}) \times \text{OC content}(\%) \quad (\text{eq.4})$$

The calculation steps (eq.2-4) were undertaken within a Markov Chain Monte Carlo (MCMC) framework allowing improved estimations of the uncertainties associated with the quantified OC stocks. MCMC analysis was applied using the OpenBUGS software package (Lunn et al., 2009) by taking 1,000,000 out of 100,000,000 random samples from a normal distribution of each variable (area, dry bulk density, OC content) to populate equations (eq.2-4). This process generates a significant quantity of solutions which follow a normal distribution. The application of standard descriptive statistical techniques to the pool of generated solutions allows the mean, standard deviation, minimum, maximum, and 5th, 50th (median), and 95th percentiles to be calculated.

$$\text{OC Storage}(\text{kg OC m}^{-2}) = \text{OC Stock}(\text{kg}) / \text{Area}(\text{m}^2) \quad (\text{eq.5})$$

For each of the four geo-regions and GB as a whole, the area normalized soil OC storage was calculated following equation 5 within the MCMC framework for each available NVC alongside the marsh zones. The outputs from these calculations were combined with the geospatial data (Section 3.1) to create a new bespoke geospatial dataset illustrating soil OC storage across the saltmarshes of GB, and allowing the quantification of individual marsh soil OC stocks.

TABLE 1 Areal extent (km²) of saltmarsh habitat across the nations of Great Britain, and the four geo-regions (Adam, 1978; Figure 1).

	Areal extent (km ²)			
	Scotland	England	Wales	Great Britain
Pioneer	3.32	13.75	1.16	17.36
Mid-Low	51.42	175.94	43.64	270.99
High	3.47	71.96	1.14	76.57
<i>Spartina</i>	0.12	25.15	6.70	32.83
Unclassified	—	49.01	4.88	53.89
Total	58.33	335.80	57.51	451.65
	Western Scotland	Eastern Scotland	Western	South Eastern
Pioneer	0.10	1.88	7.13	8.21
Mid-Low	15.87	14.91	131.28	108.85
High	0.43	1.08	38.16	36.89
<i>Spartina</i>	0.11	0.01	10.13	22.7
Unclassified	—	—	12.99	40.99
Total	16.51	17.96	199.69	217.64

The bold values represent the nations and the geo-regions.

Results and interpretation

Saltmarsh areal extent and vegetation

The GB wide mapping (Haynes, 2016; Natural Resources Wales, 2016; Environment Agency, 2021) estimates that saltmarsh habitat occupies an area of 451.65 km², in line with previous studies (Burd, 1989; Jones et al., 2011; Burden et al., 2020). English saltmarshes represent 74% of all saltmarsh habitat in GB, with Scottish and Welsh marshes each accounting for 13% of the areal coverage (Table 1). Across the four geo-regions (Adam, 1978), 92% of saltmarsh habitat can be found in the Western (44%) and South Eastern (48%) geo-regions, with the remaining 8% spread across the Western Scotland and Eastern Scotland regions (Table 1).

The differences in vegetation communities within each geo-region reflect the classification developed by Adam (1978). The clearest of these differences is the zonation of the marshes and the occurrence of *Spartina* (Table 1; Supplementary Figure 2). The marshes located in the Western Scotland and Eastern Scotland geo-regions are similar in that 96% and 86% of the total marsh area is classified as mid-low marsh vegetation respectively (Table 1). The differentiating factor between these two regions is the greater abundance of pioneer and high marsh vegetation found in the Eastern Scotland region when compared to Western Scotland (Table 1). The marshes of the Western and South Eastern regions are still dominated by mid-low marsh vegetation with 66% and 50% aerial coverage, but a greater proportion of the vegetation is classified as pioneer and high marsh (Table 1; Supplementary Figure 2). The presence of *Spartina* in these regions is also a defining factor, with 7% of the Western and 18% of geo-regions marshes being dominated

by *Spartina* in comparison only 0.7% and 0.1% of the marshes in the Western Scotland and Eastern Scotland regions (Table 1).

To determine the accuracy of the current saltmarsh maps (Haynes, 2016; Natural Resources Wales, 2016), NVC classifications (Rodwell, 1991) were derived from vegetation surveys carried out in Scotland (Miller et al., 2022) and Wales (Ford et al., 2019) and compared to the mapped NVC class in these areas. Of the simplified 584 NVCs derived from the vegetation surveys, 2% of the data points differ and these are confined to the highly dynamic (Ladd, 2021) pioneer zone. To account for lateral marsh dynamics (Ladd et al., 2019) since the vegetation classification surveys were done, an uncertainty value of 5% was applied to all areas used to determine soil OC stock to assure robust uncertainty estimates.

Saltmarsh soil physical and geochemical composition

Dry bulk density

The dry bulk density values are comparable to both global datasets from muddy and sandy intertidal soils and sediments (Bradley and Morris, 1990; Flemming and Delafontaine, 2000) and existing data from GB (Beaumont et al., 2014; Ford et al., 2019; Marley et al., 2019; Smeaton et al., 2020). Across the four geo-regions there are distinct differences, largely driven by the dominant substrate found in the estuary (e.g., mud vs sand). Both the Western Scotland and Eastern Scotland regions are dominated by soils defined as non-sandy and organic which is reflected in the dry bulk density data (Figures 3A, B). Average soil dry bulk density values of 0.39 ± 0.25 g cm⁻³ and 0.54 ± 0.30 g cm⁻³ are observed in the Western Scotland and Eastern Scotland regions

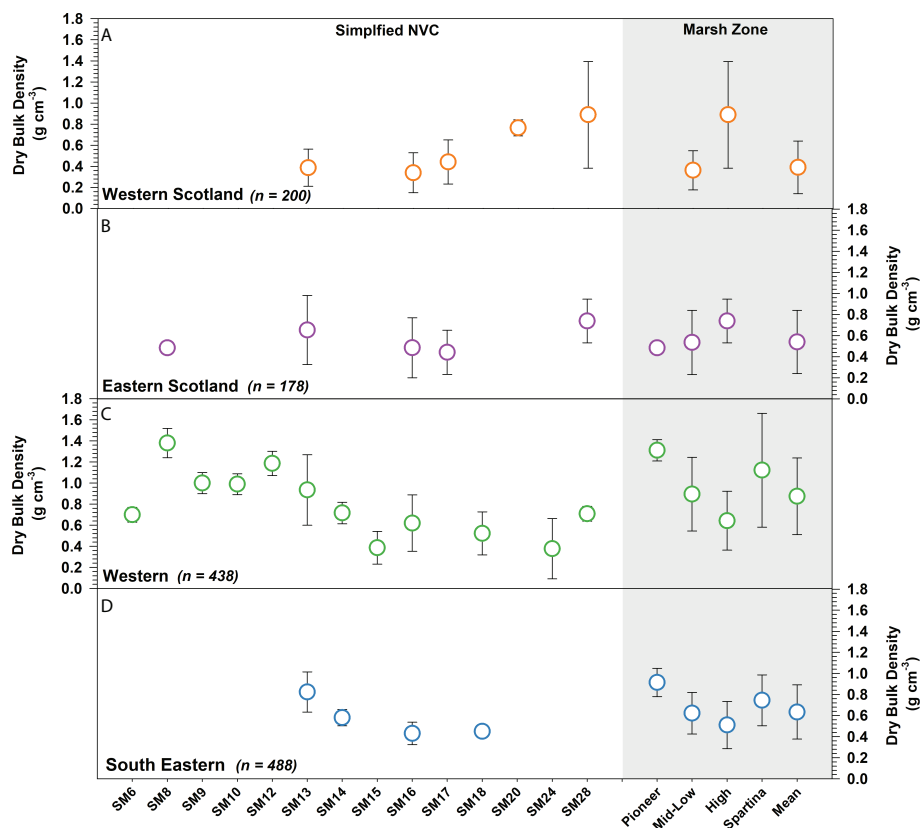


FIGURE 3
Soil dry bulk density (g cm^{-3}) values associated with different saltmarsh vegetation and zones across the four geo-regions (A–D) of Great Britain. Error bars represent 1s. Full breakdown of the OC data can be found in [Supplementary Figure 3](#) and [Supplementary Table 4](#).

respectively. The dry bulk density values found in the Western region are the highest observed ([Figure 3C](#)) reflecting the sandy nature of many of these systems ([Adam, 1978; Burd, 1989; Ford et al., 2019; Harvey et al., 2019](#)). The average soil dry bulk density from this region is $0.88 \pm 0.36 \text{ g cm}^{-3}$, almost double that measured in any other region. The highest values are found in the pioneer zone ($1.31 \pm 0.10 \text{ g cm}^{-3}$), decreasing as soils become more organic in the high marsh ([Figure 3C](#)). In the South Eastern region, soil dry bulk density varies little between marsh zones with an average value of $0.63 \pm 0.26 \text{ g cm}^{-3}$ observed. As with the Western geo-region, the highest values are found in the pioneer zone, decreasing across the transition landward to an average dry bulk density of $0.51 \pm 0.22 \text{ g cm}^{-3}$ in the high marsh.

Organic carbon

Organic matter vs organic carbon

A linear regression between LOI and OC ($p < 0.001$, $R^2 = 0.83$) produced a bespoke conversion for GB saltmarshes (eq.6).

$$\text{OC content}(\%) = 0.377 \times \text{OM}(\%) + 1.452 \quad (\text{eq.6})$$

Using this new conversion ([Figure 4](#)), the data compiled from the literature ([Section 3.4](#)) was converted from % OM data to % OC, which can be used alongside the data produced through elemental analysis ([Section 3.3](#))

Organic carbon content

The OC content of GB saltmarshes ranges between 0.02% in sandy soils to 59.7% in organic-rich soils ([Figure 5](#)). The values measured in this study are comparable to other data from GB ([Andrews et al., 2008; Burden et al., 2013; Beaumont et al., 2014; Marley et al., 2019; Smeaton et al., 2020](#)) and other temperate saltmarshes ([Mueller et al., 2019a; Mueller et al., 2019b; Penk and Perrin, 2022](#)).

All regions generally display a trend of increasing soil OC content upon moving from the pioneer to high marsh zones. Whilst these trends exist in all regions, the quantity of OC found in the soils varies. Western Scotland and Eastern Scotland contained the highest quantities of OC ([Figures 5A, B](#)), with average OC contents of $15.23 \pm 7.62\%$ and $14.39 \pm 8.73\%$ respectively. For both regions, soils associated with the

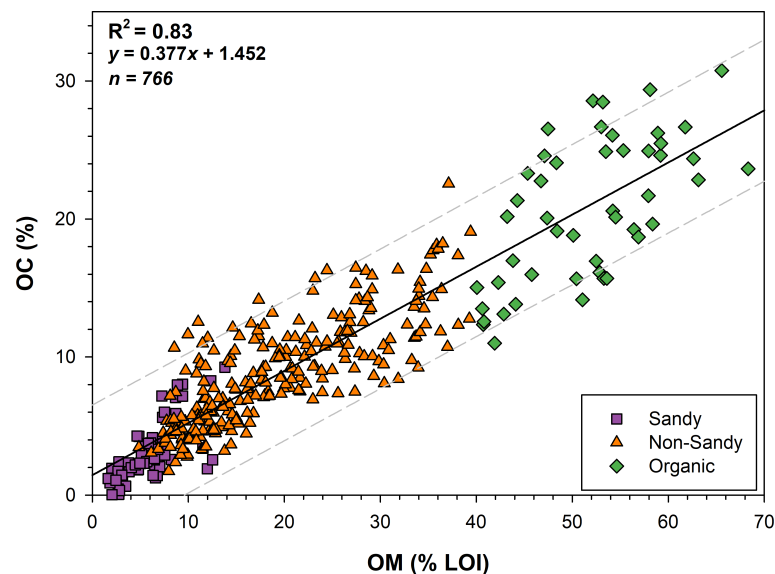


FIGURE 4

Correlation between the quantity of OM measured by loss on ignition (LOI) and OC content derived from elemental analysis for 766 saltmarsh soil samples of differing texture (sandy, non-sandy and organic) from across Great Britain ($p < 0.001$; $R^2 = 0.83$). Grey dotted lines represent the 95th percentile prediction bands.

vegetation classes SM13, SM16, and SM28 had the greatest OC content (Figure 5). The high OC content of the saltmarsh soils within these two geo-regions is potentially driven by high allochthonous OC input from the neighboring OC rich terrestrial environment (Lilly and Donnelly, 2012). The marshes within the Western Scotland region have the highest observed OC values (Figure 5A); within this region terrestrial derived OC has been shown to be the dominant component of near shore (fjords) sedimentary OC stores (Smeaton and Austin, 2017). Therefore it would not be unexpected that the high OC contents in the saltmarshes at head of these systems was due to the presence of large quantities of terrestrial OC. In comparison, the OC content of the Western region was considerably lower, with an average OC value of $5.85 \pm 4.72\%$. The low OC content of these soils is likely due to these marshes being dominated by sand. The physical properties (e.g., low porosity) of sandy soils generally do not provide the conditions (e.g., low oxygen) to preserve and retain OM (Yost and Hartemink, 2019) resulting in low OC contents (Figure 4). In the Western region, there is a distinct difference in OC content of the soils upon moving landward (Figure 5C), with the pioneer zone on average containing $3.91 \pm 2.40\%$ OC, with values reaching $7.31 \pm 3.92\%$ OC in the high marsh. For context, the highest values in the Western region are broadly comparable to OC values measured in the pioneer zone of the Eastern Scotland region (Supplementary Table 5). Saltmarsh soils within the South Eastern region contain similarly low quantities of OC, with an

average value of $6.53 \pm 3.21\%$. The highest soil OC content ($9.57 \pm 5.37\%$ OC) was again observed in the high marsh.

Data validation

Soil dry bulk density and OC content values were checked for outliers (Supplementary Figure 5). Two samples with very high OC contents ($>60\%$, all other samples $<35\%$) and two with very low bulk density were excluded.

Soil OC stocks of Great British saltmarshes

Surficial soils (top 10 cm) within GB saltmarshes hold an estimated 2.32 ± 0.47 Mt of OC. The Western geo-region saltmarsh soils hold the greatest quantity of OC (1.12 ± 0.36 Mt OC) followed by the South Eastern region (0.96 ± 0.29 Mt OC) with the soils within the Western Scotland and Eastern Scotland holding <0.15 Mt each (Figure 6A). Despite containing lower volumes of OC per soil unit area than any other geo-region, C stocks were highest in the western geo-region by virtue of having the largest marsh extent. The Western and South Eastern marsh extent is >10 times greater than that found in either the Western Scotland and Eastern Scotland regions (Table 1). The patterns observed in the geo-regions are closely

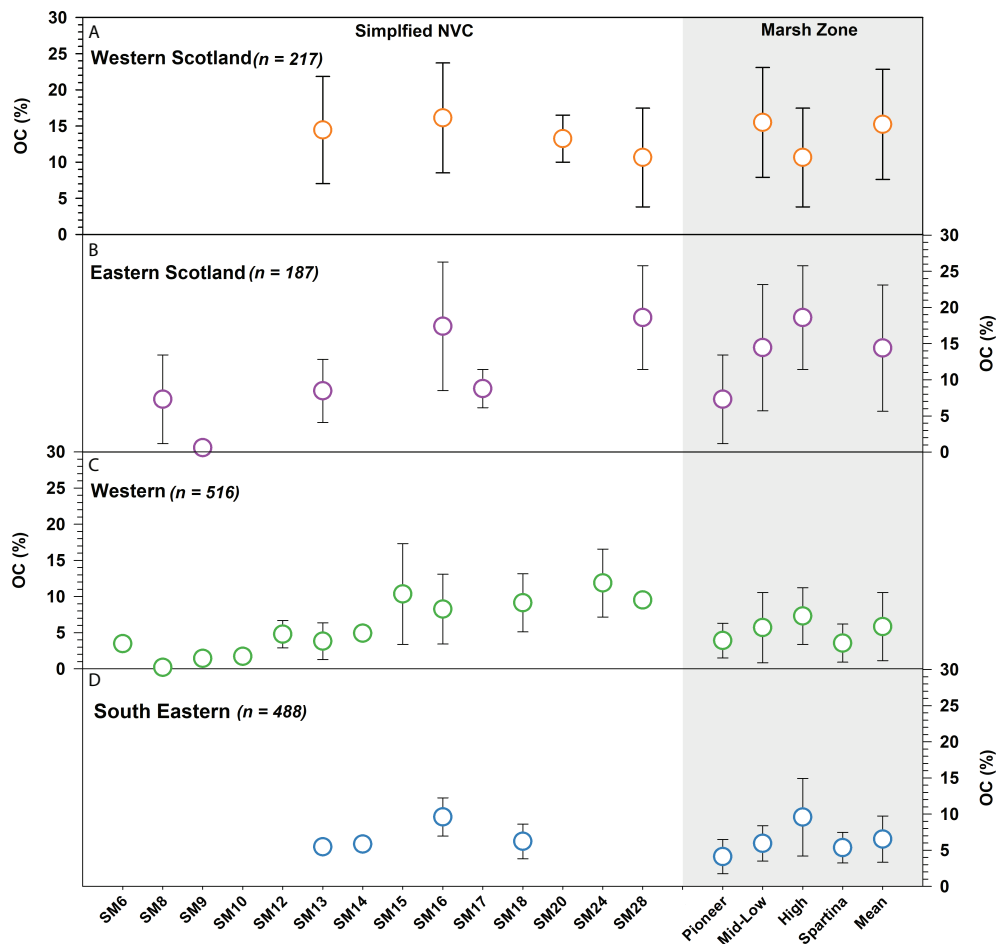


FIGURE 5

Soil OC content (%) values associated with different saltmarsh vegetation and zones across the four geo-regions (A–D) of Great Britain. Error bars represent 1s. Full breakdown of the OC data can be found in [Supplementary Figure 4](#) and [Supplementary Table 5](#).

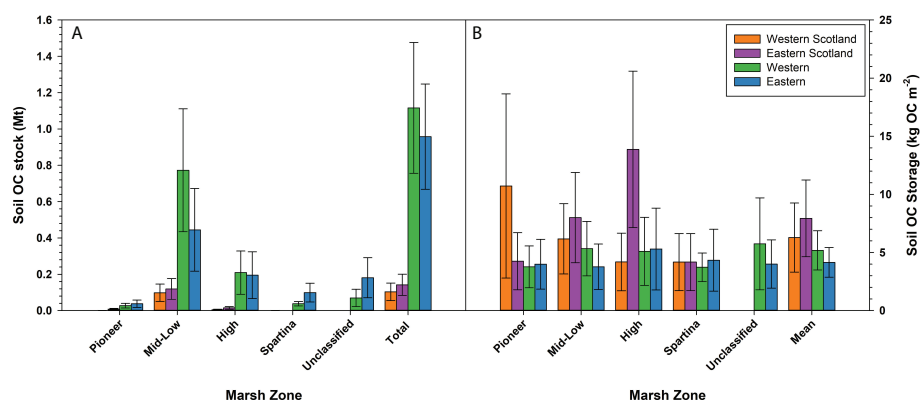


FIGURE 6

Saltmarsh surficial soil (A) OC stocks (Mt) and (B) soil OC storage (kg OC m⁻²) for the different saltmarsh zones within the four geo-regions of Great Britain. Error bars represent 1σ. Full statistical breakdown of the OC stocks can be found in [Supplementary Tables 6–10](#).

TABLE 2 Summary of surficial (top 10 cm) soil OC stocks (Mt) for the four saltmarsh geo-regions, and nations within Great Britain. Full statistical breakdown of the OC stocks can be found in [Supplementary Tables 6–10](#).

Geo-region	Surficial (top 10cm) soil OC stock (Mt)			
	Western Scotland	Eastern Scotland	Western	South Eastern
Pioneer	0.001 ± 0.0003	0.008 ± 0.005	0.027 ± 0.013	0.038 ± 0.020
Mid-Low	0.098 ± 0.048	0.119 ± 0.057	0.773 ± 0.339	0.445 ± 0.228
High	0.005 ± 0.003	0.015 ± 0.007	0.209 ± 0.119	0.195 ± 0.129
Spartina	0.0005 ± 0.0003	—	0.038 ± 0.012	0.099 ± 0.051
Unclassified	—	—	0.070 ± 0.048	0.181 ± 0.110
Total	0.105 ± 0.048	0.142 ± 0.058	1.116 ± 0.360	0.958 ± 0.290
Nation	Scotland	England	Wales	Great Britain
Pioneer	0.015 ± 0.005	0.062 ± 0.062	0.003 ± 0.0004	0.073 ± 0.025
Mid-Low	0.320 ± 0.090	0.836 ± 0.836	0.279 ± 0.008	1.435 ± 0.411
High	0.033 ± 0.008	0.371 ± 0.371	0.020 ± 0.008	0.424 ± 0.175
Spartina	0.0005 ± 0.0003	0.102 ± 0.102	0.018 ± 0.007	0.137 ± 0.053
Unclassified	—	0.230 ± 0.108	0.020 ± 0.013	0.251 ± 0.119
Total	0.368 ± 0.091	1.601 ± 0.426	0.351 ± 0.082	2.320 ± 0.470

The bold values represent the four nations of GB and four geo-regions.

mirrored in the national saltmarsh surficial (top 10 cm) soil OC stocks with the English marshes hold an estimated 1.601 ± 0.426 Mt of OC, whilst Scottish and Welsh marshes hold similar OC quantities (Table 2).

GB saltmarsh OC stocks have been estimated at 0.7 - 13 Mt OC (Beaumont et al., 2014; Luisetti et al., 2019; Legge et al., 2020), however differences in sampling depth make it difficult to directly compare these with each other and with this study at the GB scale (Table 3), therefore for fair comparisons it is important to compare like-for-like estimates (i.e. stocks derived from the top 10 cm of soil). Surficial soil (top 10 cm) OC stocks have been recently estimated for Scotland (Austin et al., 2021), Wales

(ABPmer, 2020), and GB (scaled from NW Europe to match the extent of GB marshes; Legge et al., 2020) at 0.368 ± 0.102 , 0.32, and 0.7 - 2.8 Mt OC respectively. The estimates for Scotland (Austin et al., 2021) were calculated using an early version of the data utilized in this study using a simplified calculation methodology, therefore the similarity in OC stocks is not surprising. The surficial (top 10 cm) saltmarsh soils of the Republic of Ireland are estimated to hold 0.265 Mt of OC (Penk, 2019). The saltmarshes of the Republic of Ireland occupy an area of 69.26 km², are within the same climatic zone, and have similar vegetation composition (Penk and Perrin, 2022) to GB saltmarshes. These Irish systems are similar in size to the

TABLE 3 Saltmarsh surficial soil OC stock estimates from this study in comparison to existing OC soil stocks from Great British and temperate saltmarsh systems. Note that Beaumont et al. (2014) estimates are for depths 0 - 50 or 0 - 100 cm.

Nation	Soil Depth(cm)	Soil OC Stock(Mt)	Soil OC Storage(kg OC m ⁻²)	Reference
Scotland	0-10	0.368 ± 0.091	6.31 ± 1.56	<i>This Study</i>
England		1.601 ± 0.426	4.50 ± 1.20	
Wales		0.351 ± 0.082	6.10 ± 1.43	
Great Britain		2.320 ± 0.470	5.14 ± 1.04	
Scotland	0-10	0.368 ± 0.102	6.0 ± 1.8	(Austin et al., 2021)
Wales	0-10	0.32	5.56	(ABPmer, 2020)
Republic of Ireland	0-10	0.265	3.8	(Penk and Perrin, 2022)
NW Europe	0-10	2.8 - 7.6	—	(Legge et al., 2020)
NW Europe (scaled to GB)		0.7 - 2.8		
Scotland	0-50 (100)	0.49	—	(Beaumont et al., 2014)
England		4.32		
Wales		0.57		
Northern Ireland		0.02		
Great Britain		5.41		

Scottish and Welsh saltmarshes and produce comparable OC stocks (Table 2).

Across the GB saltmarshes, the greatest quantity of OC is stored in the mid-low marsh zone, followed by the high marsh (Figure 6A). This is largely because the aerial extent of the mid-low marsh zone is 3 times greater than the high marsh extent. The disparity in the extent of the high to the mid-low marsh zones is a key indicator of coastal squeeze (Hughes and Paramor, 2004) which has primarily been driven by the need to expand agricultural land in Great Britain since the 17th century (Smout, 2003). Saltmarsh soils in the Western Scotland and Eastern Scotland geo-regions have the highest soil OC storage (i.e., OC stock normalized for area; Figure 6B) with values of 6.28 ± 2.97 kg OC m⁻² and 7.94 ± 3.30 kg OC m⁻² respectively. In the saltmarsh soils of Western and South Eastern regions where the largest stocks are located, we observe lower OC storage values of 5.18 ± 1.69 kg OC m⁻² and 4.15 ± 1.27 kg OC m⁻² respectively. These differences are potentially driven by local sediment loads, sedimentation rates, dilution of the OC by minerogenic input and by the underlying substrate. Marshes with sandy soil (Western and South Eastern) generally have higher dry bulk densities (Figure 3) than their muddy counterparts and fail to trap and store OM (Figure 5) (Kelleway et al., 2016). OC storage values reported here are comparable to previous studies in Scotland (4.4 to 6.5 kg OC m⁻²; Austin et al., 2021), Wales (5.56 kg OC m⁻²; ABPmer, 2020), and the Republic of Ireland (3.8 kg OC m⁻²; Penk, 2019).

Mapping soil OC storage and stocks

The new spatial mapping of OC storage allows the calculation of site-specific OC stocks, providing managers and policymakers a bespoke tool to assist in the management of these systems at both the local and national scale. By combining

current saltmarsh maps (Haynes, 2016; Natural Resources Wales, 2016; Environment Agency, 2021) with the calculated NVC and marsh zone specific OC densities (Supplementary Tables 11–14), it is possible to gain a geospatial understanding of OC across saltmarshes (Figure 7) and calculate saltmarsh specific surficial soil OC stocks (Figure 8). The OC density maps highlight changes in OC storage between saltmarshes and within the marshes themselves from the pioneer to high marsh zones (Figure 7).

Marshes in the Ribble Estuary (53.711340, -2.943835) hold the largest OC stock (139,916 tonnes OC) followed by the saltmarshes found in the the major estuaries of GB such as the Wash (52.926668, 0.061452), Morecambe Bay (54.175172, -2.849556) and the Solway Firth (54.969555, -3.484984). The saltmarshes in Essex, the Solent, Dornoch Firth and Cromarty Firth are smaller and hold less OC within their soils. A large number of small marshes within these areas does result in OC stocks equivalent to the largest marshes (Figure 8; Supplementary Data). Of the 438 marshes with surficial soil OC stocks, 229 marshes hold < 1000 tonnes OC in their surficial soils, with only 30 exceeding > 20,000 tonnes of OC (Supplementary Data). This results in large disparity in the distribution of OC across GB saltmarsh with 7% of saltmarshes accounting for 55% of soil OC storage.

The spatial mapping of OC density and marsh specific OC stocks are designed to assist environmental managers and policymakers in determining how best to protect and preserve these important coastal environments and how best to move forward with the inclusion of saltmarshes in national C accounting. To that end, data used to create these maps is freely available. It is envisaged that these decision support tools will evolve as new spatial mapping is introduced and/or when additional soil parameters (e.g., dry bulk density and OC content) become available.

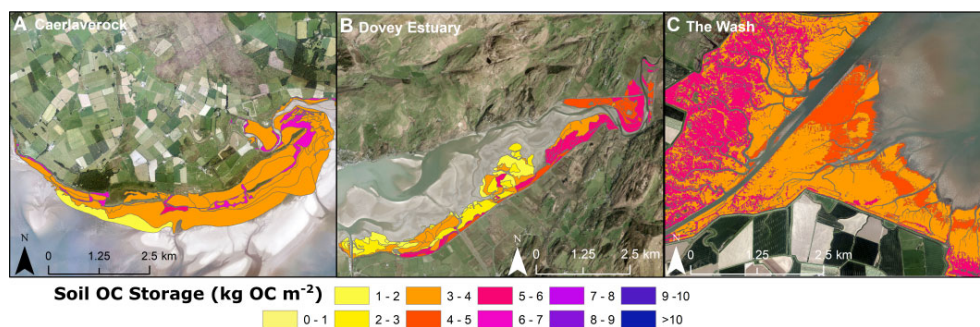


FIGURE 7

Examples of OC storage (kg OC m⁻²) mapped across (A) Scotland – Caerlaverock marsh (54.969555, -3.484984), (B) Wales – Dovey (Dyfi) Estuary (52.543454, -3.977258) and (C) England – The Wash (52.926668, 0.061452). Full geospatial dataset (Smeaton et al., 2022) can be found at: <https://catalogue.ceh.ac.uk/documents/cb8840f2-c630-4a86-9bba-d0e070d56f04>.

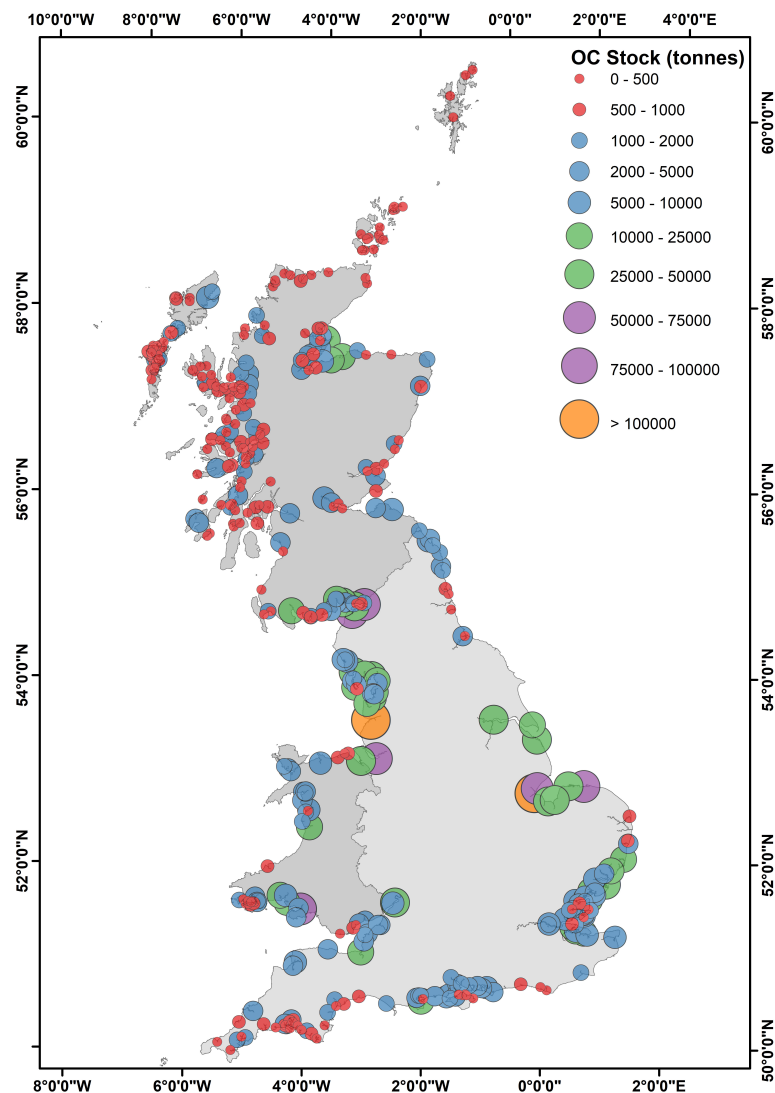


FIGURE 8

Mapped surficial soil OC stocks (tonnes) for individual saltmarshes across Great Britain. Size of circle represent the absolute magnitude of the stock (tonnes) while the colors highlight ranges: Red: < 1,000 tonnes OC, Blue 1,000 – 10,000 tonnes OC, Green: 10,000 – 50,000 tonnes OC, Purple: 50,000 – 100,000 and Orange > 100,000 tonnes OC. Full breakdown of OC stocks can be found in the [supplementary data](#).

Conclusion

There is a growing international awareness that the burial and storage of OC in saltmarshes may provide a nature-based solution to regulating atmospheric C. A fundamental opportunity therefore presents itself to society, namely, to manage and protect these important OC hotspots from increasing climatic and anthropogenic threats. Quantifying the magnitude of the surficial soil OC stocks and how it is spatially distributed across the GB saltmarshes is a critical foundational step towards this goal. The surficial soils (top 10 cm) of GB saltmarshes contain 2.32 ± 0.47 Mt OC. Across GB marshes

there is a disparity in OC stocks, the Scottish systems hold more carbon per unit area but the extreme differences in marsh extent result in the expansive marshes of England holding 69% of the total soil OC. The new spatial mapping products could not have readily been produced without the assistance of UK citizen scientists and are envisaged to provide decision support tools to assist in the management of these important C resources. The mapping has highlighted that a small number ($n = 30$) of large marshes located in the major estuaries (The Wash, Morecambe Bay and the Solway Firth) represent 55% of the total soil OC stock. This raises the fundamental question on how to best manage these ecosystems for C at a national scale, do we take a

holistic approach for all marshes, or do we focus our efforts on the C rich areas? Although this study provides an additional contribution to the quantification and understanding of GB saltmarsh soils and their OC stores as a significant component of UKs natural capital, this new understanding of surficial soil OC stocks only represents a first step towards answering this question. The mechanisms that govern the accumulation, preservation and long-term storage of OC in these systems remain poorly defined across GB saltmarshes.

Data availability statement

The datasets generated and analyzed for this study can be found in the Environmental Information Data Centre (www.eidc.ac.uk/) and the Marine Scotland Data (www.data.marine.gov.scot/) repository. The saltmarsh soil physical property and OC content data for England and Wales (Ruranska et al., 2022): www.catalogue.ceh.ac.uk/documents/e5554b83-910f-4030-8f4e-81967dc7047c and for Scotland, Ruranska et al. (2020): www.catalogue.ceh.ac.uk/documents/81a1301f-e5e2-44f9-afe0-0ea5bb08010f and Miller et al. (2022): <https://data.marine.gov.scot/dataset/physical-and-geochemical-properties-scottish-saltmarsh-soils>. The geospatial data layers (Smeaton et al., 2022) produced from this research can be found at: <https://catalogue.ceh.ac.uk/documents/cb8840f2-c630-4a86-9bba-d0e070d56f04>

Author contributions

The first draft of the manuscript was jointly developed by CS and AB with assistance from all authors. CL and MS organized and oversaw the citizen science sampling program. LCM, AG and WA undertook vegetation surveys and a soil sampling to ground-truth current mapping. PR and LCM conducted the physical and geochemical soil analysis under the supervision of CS and WA. CS carried out the calculations to estimate the soil OC stock with the support of AB, LJ, AG, LM and WA. All authors contributed to the manuscript revision and approved the submitted version.

References

- Aavik, T., Carmona, C. P., Träger, S., Kaldra, M., Reinula, I., Conti, E., et al. (2020). Landscape context and plant population size affect morph frequencies in heterostylous *primula veris*—results of a nationwide citizen-science campaign. *J. Ecol.* 108 (6), 2169–2183. doi: 10.1111/1365-2745.13488
- ABPmer (2020) *Estimating the carbon sink potential of the welsh marine environment, natural resource Wales commissioned report*. Available at: https://cdn.naturalresources.wales/media/692035/nrw-evidence-report-428_blue-carbon_v11-002.pdf.
- Adam, P. (1978). Geographical variation in British saltmarsh vegetation. *J. Ecol.*, 339–366. doi: 10.2307/2259141
- Andrews, J. E., Samways, G., and Shimmield, G. B. (2008). Historical storage budgets of organic carbon, nutrient and contaminant elements in saltmarsh sediments: Biogeochemical context for managed realignment, Humber estuary, UK. *Sci. Tot. Environ.* 405 (1–3), 1–13. doi: 10.1016/j.scitotenv.2008.07.044
- Austin, W., Smeaton, C., Riegel, S., Ruranska, P., and Miller, L. (2021). “Blue carbon stock in Scottish saltmarsh soils,” in *Scottish Marine and freshwater science*, vol. 12. (Marine Scotland). doi: 10.7489/12372-1
- (2016) *Natural resources Wales*. Available at: <https://lle.gov.wales/catalogue/item/SaltmarshExtents/?lang=en>.

Funding

This research was finically supported by the Natural Environment Research Council funded Carbon Storage in Intertidal Environments (C-SIDE) project (grant NE/R010846/1) with additional support from the Scottish Blue Carbon Forum.

Acknowledgments

We would like to extend a special thanks to the volunteer citizen scientists that undertook soil sampling across Great Britain creating a unique and invaluable resource that is the foundation of this research. Finally, we would like to thank the Editor and reviewers for providing helpful comments that have improved the manuscript.

Conflict of interest

The authors declare that the research was conducted in the absence of any commercial or financial relationships that could be construed as a potential conflict of interest.

Publisher's note

All claims expressed in this article are solely those of the authors and do not necessarily represent those of their affiliated organizations, or those of the publisher, the editors and the reviewers. Any product that may be evaluated in this article, or claim that may be made by its manufacturer, is not guaranteed or endorsed by the publisher.

Supplementary material

The Supplementary Material for this article can be found online at: <https://www.frontiersin.org/articles/10.3389/fmars.2022.959459/full#supplementary-material>

- Bauer, J. E., Cai, W. J., Raymond, P. A., Bianchi, T. S., Hopkinson, C. S., and Regnier, P. A. (2013). The changing carbon cycle of the coastal ocean. *Nature* 504 (7478), 61–70. doi: 10.1038/nature12857
- Baugh, L. (2019). *Spatial analysis of blue carbon in a UK saltmarsh: implications of carbon distribution, master's thesis* (United Kingdom: John Moores University, Liverpool). Available at: <https://researchonline.ljmu.ac.uk/id/eprint/10878>.
- Beaumont, N. J., Jones, L., Garbutt, A., Hansom, J. D., and Toberman, M. (2014). *The value of carbon sequestration and storage in coastal habitats* Vol. 137 (Estuarine, Coastal and Shelf Science), 32–40.
- Bradley, P. M., and Morris, J. T. (1990). "Physical characteristics of salt marsh sediments: Ecological implications," in *Marine ecology progress series*, vol. 61. (Oldendorf), 245–252.
- Bridgman, S. D., Megonigal, J. P., Keller, J. K., Bliss, N. B., and Trettin, C. (2006). *The carbon balance of north American wetlands* Vol. 26 (Wetlands), 889–916.
- Brown, D. R., Conrad, S., Akkerman, K., Fairfax, S., Fredericks, J., Hanrio, E., et al. (2016). Seagrass, mangrove and saltmarsh sedimentary carbon stocks in an urban estuary: cofts harbour, Australia. *Region. Stud. Mar. Sci.* 8, 1–6. doi: 10.1016/j.rsmas.2016.08.005
- Burd, F. (1989). "The saltmarsh survey of great Britain," in *An inventory of British saltmarshes, research and survey in nature conservation* (Peterborough: Nature Conservancy Council).
- Burden, A., Garbutt, A., and Evans, C. D. (2019). Effect of restoration on saltmarsh carbon accumulation in Eastern England. *Biol. Lett.* 15, 20180773. doi: 10.1098/rsbl.2018.0773
- Burden, A., Garbutt, R. A., Evans, C. D., Jones, D. L., and Cooper, D. M. (2013). "Carbon sequestration and biogeochemical cycling in a saltmarsh subject to coastal managed realignment," in *Estuarine, coastal and shelf science*, vol. 120, 12–20.
- Burden, A., Smeaton, C., Angus, S., Garbutt, A., Jones, L., Lewis, H., et al. (2020). "Impacts of climate change on coastal habitats, relevant to the coastal and marine environment around the UK," in *MCCIP science review 2020*.
- Conrad, C. C., and Hilchey, K. G. (2011). *A review of citizen science and community-based environmental monitoring: issues and opportunities* Vol. 176 (Environmental monitoring and assessment), 273–291.
- Couvet, D., Jiguet, F., Julliard, R., Levrel, H., and Teyssedre, A. (2008). *Enhancing citizen contributions to biodiversity science and public policy* Vol. 33 (Interdisciplinary science reviews), 95–103.
- Craft, C. B., Seneca, E. D., and Broome, S. W. (1991). *Loss on ignition and kjeldahl digestion for estimating organic carbon and total nitrogen in estuarine marsh soils: calibration with dry combustion* Vol. 14 (Estuaries), 175–179.
- Crosby, S. C., Sax, D. F., Palmer, M. E., Booth, H. S., Deegan, L. A., Bertness, M. D., et al. (2016). *Salt marsh persistence is threatened by predicted sea-level rise* Vol. 181 (Estuarine: Coastal and Shelf Science), 93–99. doi: 10.1016/j.ecss.2016.08.018
- Dadey, K. A., Janeczek, T., and Klaus, A. (1992). Dry-bulk density: its use and determination. *Proceedings of the ocean drilling program. Sci. Res. Vol.* 126
- Duarte, C. M., Dennison, W. C., Orth, R. J., and Carruthers, T. J. (2008). *The charisma of coastal ecosystems: addressing the imbalance* Vol. 31 (Estuaries and coasts), 233–238.
- Duarte, C. M., Losada, I. J., Hendriks, I. E., Mazarrasa, I., and Marbà, N. (2013). The role of coastal plant communities for climate change mitigation and adaptation. *Nat. Climate Change* 3 (11), 961–968. doi: 10.1038/nclimate1970
- Environment Agency (2021) *Saltmarsh extent and zonation*. Available at: <https://data.gov.uk/dataset/0e9982d3-1fef-47de-9af0-4b1398330d88/saltmarsh-extent-zonation#licence-info>.
- Flemming, B. W., and Delafontaine, M. T. (2000). *Mass physical properties of muddy intertidal sediments: some applications, misapplications and non-applications* Vol. 20 (Continental Shelf Research), 1179–1197.
- Ford, H., Garbutt, A., Duggan-Edwards, M., Harvey, R., Ladd, C., and Skov, M. W. (2019). Large-Scale predictions of salt-marsh carbon stock based on simple observations of plant community and soil type. *Biogeosciences* 16 (2), pp.425–pp.436. doi: 10.5194/bg-16-425-2019
- Ford, H., Garbutt, A., Jones, L., and Jones, D. L. (2012). "Methane, carbon dioxide and nitrous oxide fluxes from a temperate salt marsh: Grazing management does not alter global warming potential," vol. 113. (Estuarine, Coastal and Shelf Science), 182–191.
- Ford, H., Garbutt, A., and Skov, M. (2015). "Coastal biodiversity and ecosystem service sustainability (CBESS) dry weight root biomass from three soil depths on salt marsh sites at Morecambe bay and Essex," in *NERC environmental information data centre*. doi: 10.5285/a84622db-842d-40d2-aad8-e3f85bd306c9
- Ford, H., Garbutt, A., and Skov, M. (2016a). "Coastal biodiversity and ecosystem service sustainability (CBESS) soil organic matter content from three soil depths on saltmarsh sites at Morecambe bay and Essex," in *NERC environmental information data centre*. doi: 10.5285/90457ba1-f291-4158-82dc-425d7cbb1ac5
- Ford, H., Garbutt, A., and Skov, M. (2016b). "Coastal biodiversity and ecosystem service sustainability (CBESS) standing crop biomass on salt marsh sites at Morecambe bay and Essex," in *NERC environmental information data centre*. doi: 10.5285/87114da4-3189-471f-9832-00b3e759232f
- Ford, H., Garbutt, A., and Skov, M. (2016c). "Coastal biodiversity and ecosystem service sustainability (CBESS) soil bulk density from three soil depths on salt marsh sites at Morecambe bay and Essex," in *NERC environmental information data centre*. doi: 10.5285/814be4cf-0ff2-46dd-b296-c4d9b913b6e4
- Granek, E. F., Polasky, S., Kappel, C. V., Reed, D. J., Stoms, D. M., Koch, E. W., et al. (2010). Ecosystem services as a common language for coastal ecosystem-based management. *Conserv. Biol.* 24, 207–216. doi: 10.1111/j.1523-1739.2009.01355.x
- Harvey, R. J., Garbutt, A., Hawkins, S. J., and Skov, M. W. (2019). No detectable broad-scale effect of livestock grazing on soil blue-carbon stock in salt marshes. *Front. Ecol. Evol.* 7, 151. doi: 10.3389/fevo.2019.00151
- Haynes, T. A. (2016). "Scottish Saltmarsh survey national report," in *Scottish Natural heritage commissioned report*.
- Hinson, A. L., Feagin, R. A., Eriksson, M., Najjar, R. G., Herrmann, M., Bianchi, T. S., et al. (2017). The spatial distribution of soil organic carbon in tidal wetland soils of the continental united states. *Global Change Biol.* 23 (12), 5468–5480. doi: 10.1111/gcb.13811
- Holmquist, J. R., Windham-Myers, L., Bliss, N., Crooks, S., Morris, J. T., Megonigal, J. P., et al. (2018). Accuracy and precision of tidal wetland soil carbon mapping in the conterminous united states. *Sci. Rep.* 8 (1), 1–16. doi: 10.1038/s41598-018-26948-7
- Horton, B. P., Shennan, I., Bradley, S. L., Cahill, N., Kirwan, M., Kopp, R. E., et al. (2018). Predicting marsh vulnerability to sea-level rise using Holocene relative sea-level data. *Nat. Commun.* 9, 2687. doi: 10.1038/s41467-018-05080-0
- Hughes, R. G., and Paramor, O. A. L. (2004). On the loss of saltmarshes in south-east England and methods for their restoration. *J. Appl. Ecol.* 41 (3), 440–448. doi: 10.1111/j.0021-8901.2004.00915.x
- Jones, M. L. M., Angus, S., Cooper, A., Doody, P., Everard, M., Garbutt, A., et al. (2011). "Coastal margins," in *UK National ecosystem assessment. understanding nature's value to society* (Cambridge: Technical Report, UNEP-WCMC), 411–457.
- Kelleway, J. J., Saintilan, N., Macreadie, P. I., Baldock, J. A., and Ralph, P. J. (2017). Sediment and carbon deposition vary among vegetation assemblages in a coastal salt marsh. *Biogeosciences* 14 (16), 3763–3779. doi: 10.5194/bg-14-3763-2017
- Kelleway, J. J., Saintilan, N., Macreadie, P. I., and Ralph, P. J. (2016). Sedimentary factors are key predictors of carbon storage in SE Australian saltmarshes. *Ecosystems* 19 (5), 865–880. doi: 10.1007/s10021-016-9972-3
- Ladd, C. J. T. (2021). "Review on processes and management of saltmarshes across great britain." *Proc. Geol. Assoc.* 132, 269–283. doi: 10.1016/j.jpeola.2021.02.005
- Ladd, C. J., Duggan-Edwards, M. F., Bouma, T. J., Pages, J. F., and Skov, M. W. (2019). Sediment supply explains long-term and large-scale patterns in salt marsh lateral expansion and erosion. *Geophys. Res. Lett.* 46 (20), 11178–11187. doi: 10.1029/2019GL083315
- Legge, O., Johnson, M., Hicks, N., Jickells, T., Diesing, M., Aldridge, J., et al. (2020). Carbon on the northwest European shelf: Contemporary budget and future influences. *Front. Mar. Sci.* 7, 143. doi: 10.3389/fmars.2020.00143
- Lilly, A. B. N., and Donnelly, D. (2012). *Map of soil organic carbon in top soils of scotland. map prepared for EU project GS-SOIL-Assessment and strategic development of INSPIRE compliant geodata-services for European soil data*.
- Lovelock, C. E., Adame, M. F., Bennion, V., Hayes, M., O'Mara, J., Reef, R., et al. (2014). Contemporary rates of carbon sequestration through vertical accretion of sediments in mangrove forests and saltmarshes of south East Queensland, Australia. *Estuar. Coast.* 37 (3), 763–771. doi: 10.1007/s12237-013-9702-4
- Luisetti, T., Turner, R. K., Andrews, J. E., Jickells, T. D., Kröger, S., Diesing, M., et al. (2019). Quantifying and valuing carbon flows and stores in coastal and shelf ecosystems in the UK. *Ecosys. Serv.* 35, 67–76. doi: 10.1016/j.ecoser.2018.10.013
- Lunn, D., Spiegelhalter, D., Thomas, A., and Best, N. (2009). The BUGS project: Evolution, critique and future directions. *Stat. Med.* 28 (35), 3049–3067.
- Macreadie, P. I., Anton, A., Raven, J. A., Beaumont, N., Connolly, R. M., Friess, D. A., et al. (2019). The future of blue carbon science. *Nat. Commun.* 10, 3998. doi: 10.1038/s41467-019-11693-w
- Macreadie, P. I., Costa, M. D., Atwood, T. B., Friess, D. A., Kelleway, J. J., Kennedy, H., et al. (2021). Blue carbon as a natural climate solution. *Nat. Rev. Earth Environ.* 2 (12), 826–839. doi: 10.1038/s43017-021-00224-1
- Marley, A. R., Smeaton, C., and Austin, W. E. (2019). An assessment of the tea bag index method as a proxy for organic matter decomposition in intertidal environments. *J. Geophys. Res.: Biogeosci.* 124 (10), 2991–3004. doi: 10.1029/2018JG004957
- Mason, V. G., Wood, K. A., Jupe, L. L., Burden, A., and Skov, M. W. (2022). "UK Saltmarsh code: Systematic review and evidence synthesis," in *Initial report. report to the natural environment investment readiness fund*, vol. 36. (Bangor: UK Centre for Ecology & Hydrology).

- May, V. J., and Hansom, J. D. (2003). *Coastal geomorphology of great britain. geological conservation review series no. 28* (Joint Nature Conservation Committee, Peterborough).
- McKinley, D. C., Miller-Rushing, A. J., Ballard, H. L., Bonney, R., Brown, H., Cook-Patton, S. C., et al. (2017). Citizen science can improve conservation science, natural resource management, and environmental protection. *Biol. Conserv.* 208, 15–28. doi: 10.1016/j.biocon.2016.05.015
- McLeod, E., Chmura, G. L., Bouillon, S., Salm, R., Björk, M., Duarte, C. M., et al. (2011). A blueprint for blue carbon: Towards an improved understanding of the role of vegetated coastal habitats in sequestering CO₂. *Front. Ecol. Environ.* 9, 552–560. doi: 10.1890/110004
- Mcowen, C. J., Weatherdon, L. V., Van Bochove, J. W., Sullivan, E., Blyth, S., Zockler, C., et al. (2017). A global map of saltmarshes. *Biodivers. Data J.* 5. doi: 10.3897/BDJ.5.e11764
- Miller, L. C., Smeaton, C., Yang, H., and Austin, W. E. N. (2022). Physical and geochemical properties of Scottish saltmarsh soils. *Mar. Scotl. Data.* doi: 10.7489/12422-1
- Mueller, P., Do, H. T., Jensen, K., and Nolte, S. (2019a). "Origin of organic carbon in the topsoil of wadden Sea salt marshes," in *Marine ecology progress series*, vol. 62410(1). (Wadden Sea. Ecosphere), 39–50.
- Mueller, P., Ladiges, N., Jack, A., Schmiedl, G., Kutzbach, L., Jensen, K., et al. (2019b). Assessing the long-term carbon-sequestration potential of the semi-natural salt marshes in the European wadden Sea. *Ecosphere* 10 (1), e02556. doi: 10.1002/ecs2.2556
- Murray, N. J., Worthington, T. A., Bunting, P., Duce, S., Hagger, V., Lovelock, C. E., et al. (2022). High-resolution mapping of losses and gains of earth's tidal wetlands. *Science* 376 (6594), pp.744–pp.749. doi: 10.1038/s41586-018-0805-8
- C. Nellemann and E. Corcoran (Eds.) (2009). *Blue carbon: the role of healthy oceans in binding carbon: a rapid response assessment* (UNEP/Earthprint).
- Nieuwenhuize, J., Maas, Y. E., and Middelburg, J. J. (1994). Rapid analysis of organic carbon and nitrogen in particulate materials. *Mar. Chem.* 45 (3), 217–224. doi: 10.1016/0304-4203(94)90005-1
- Ouyang, X., and Lee, S. Y. (2014). Updated estimates of carbon accumulation rates in coastal marsh sediments. *Biogeosciences* 11 (18), 5057–5071. doi: 10.5194/bg-11-5057-2014
- Ouyang, X., and Lee, S. Y. (2020). Improved estimates on global carbon stock and carbon pools in tidal wetlands. *Nat. Commun.* 11 (1), pp.1–pp.7. doi: 10.1038/s41467-019-14120-2
- Parsons, J., Lukyanenko, R., and Wiersma, Y. (2011). Easier citizen science is better. *Nature* 471 (7336), 37–37. doi: 10.1038/471037a
- Penk, (2019). *Preliminary carbon stocks of Irish saltmarshes, environmental protection agency report 2018-CCRP-SS.25.*
- Penk, M. R., and Perrin, P. M. (2022). *Variability of plant and surface soil carbon concentration among saltmarsh habitats in Ireland* (Estuaries and Coasts), 1–15.
- Phillips, T. B., Ballard, H. L., Lewenstein, B. V., and Bonney, R. (2019). *Engagement in science through citizen science: Moving beyond data collection* Vol. 103 (Science Education), 665–690.
- Porter, J., Austin, W., Burrows, M., Clarke, D., Davies, G., Kamenos, N., et al. (2020). "Blue carbon audit of Orkney waters," in *Scottish Marine and freshwater science reports*, vol. 11. (Marine Scotland). doi: 10.7489/12262-1
- Pribyl, D. W. (2010). A critical review of the conventional SOC to SOM conversion factor. *Geoderma* 156 (3–4), 75–83. doi: 10.1016/j.geoderma.2010.02.003
- Pye, K., and French, P. W. (1993). "Cambridge Environmental research consultants Ltd.(United kingdom); ministry of agriculture, fisheries and food, London (United kingdom);," in *Erosion and accretion processes on British saltmarshes: Volume four-modelling of saltmarsh and mudflat processes* (Cambridge Environmental Research Consultants).
- Rodwell, J. S. (2000). *British Plant communities, maritime communities and vegetation of open habitats* Vol. 5 (Cambridge, UK: Cambridge University Press).
- Rodwell, J. S. (1991). *British plant communities: Volume 5, Maritime communities and vegetation of open habitats* 5, Cambridge University Press.
- Rogers, K., Macreadie, P. I., Kelleway, J. J., and Saintilan, N. (2019). Blue carbon in coastal landscapes: a spatial framework for assessment of stocks and additionality. *Sustain. Sci.* 14, 453–467. doi: 10.1007/s11625-018-0575-0
- Ruranska, P., Ladd, C. J. T., Smeaton, C., Skov, M. W., and Austin, W. E. N. (2022). *Dry bulk density, loss on ignition and organic carbon content of surficial soils from English and Welsh salt marshes 2019* (NERC EDS Environmental Information Data Centre). doi: 10.5285/e5554b83-910f-4030-8f4e-81967dc7047c
- Ruranska, P., Miller, L. C., Hindle, C., Ladd, C. J. T., Smeaton, C., Skov, M. W., et al. (2020). *Dry bulk density, loss on ignition and organic carbon content of surficial soils from Scottish salt marshes 2018-2019* (NERC Environmental Information Data Centre). doi: 10.5285/81a1301f-e5e2-44f9-afe0-0ea5bb08010f
- Schuerch, M., Spencer, T., Temmerman, S., Kirwan, M. L., Wolff, C., Lincke, D., et al. (2018). Future response of global coastal wetlands to sea-level rise. *Nature* 561, 231–234. doi: 10.1038/s41586-018-0476-5
- Smeaton, C., and Austin, W. E. (2017). Sources, sinks, and subsidies: Terrestrial carbon storage in mid-latitude fjords. *J. Geophys. Res.: Biogeosci.* 122 (11), 2754–2768.
- Smeaton, C., Burden, A., Ruranska, P., Ladd, C. J. T., Garbutt, A., Jones, L., et al. (2022). Spatial mapping of surficial soil organic carbon storage and stocks across Great British saltmarshes. *NERC EDS Environ. Inform. Data Centre.* doi: 10.5285/cb8840f2-c630-4a86-9bba-d0e070d56f04
- Smeaton, C., Barlow, N. L., and Austin, W. E. (2020). Coring and compaction: Best practice in blue carbon stock and burial estimations. *Geoderma* 364, 114180. doi: 10.1016/j.geoderma.2020.114180
- Smout, T. C. (2003). 'Landscape and history since 1500', *English historical review*, Vol. 118. 848–850.
- Theuerkauf, E. J., Stephens, J. D., Ridge, J. T., Fodrie, F. J., and Rodriguez, A. B. (2015). Carbon export from fringing saltmarsh shoreline erosion overwhelms carbon storage across a critical width threshold. *Estuar. Coast. Shelf. Sci.* 164, 367–378. doi: 10.1016/j.ecss.2015.08.001
- Thorhaug, A. L., Poulos, H. M., López-Portillo, J., Barr, J., Lara-Domínguez, A. L., Ku, T. C., et al. (2019). Gulf of Mexico estuarine blue carbon stock, extent and flux: Mangroves, marshes, and seagrasses: A north American hotspot. *Sci. Tot. Environ.* 653, 1253–1261. doi: 10.1016/j.scitotenv.2018.10.011
- Van Bemmelen, J. M. (1890). *Über die bestimmung des wassers, des humus, des schwefels, der in den colloidalen silikaten gebundenen kieselsäure, des mangans usw im ackerboden* Vol. 37 (Die Landwirtschaftlichen Versuchs-Stationen).
- Vaughn, D. R., Bianchi, T. S., Shields, M. R., Kenney, W. F., and Osborne, T. Z. (2020). Increased organic carbon burial in northern Florida mangrove-salt marsh transition zones. *Global Biogeochem. Cycle.* 34 (5), e2019GB006334. doi: 10.1029/2019GB006334
- Verardo, D. J., Froelich, P. N., and McIntyre, A. (1990). Determination of organic carbon and nitrogen in marine sediments using the Carlo erba NA-1500 analyzer. deep Sea research part a. *Oceanogr. Res. Paper.* 37 (1), 157–165. doi: 10.1016/0198-0149(90)90034-S
- Yost, J. L., and Hartemink, A. E. (2019). Soil organic carbon in sandy soils: A review. *Adv. Agron.* 158, 217–310. doi: 10.1016/bs.agron.2019.07.004
- Young, M. A., Serrano, O., Macreadie, P. I., Lovelock, C. E., Carnell, P., and Ierodiaconou, D. (2021). National scale predictions of contemporary and future blue carbon storage. *Sci. Tot. Environ.* 800, 149573. doi: 10.1016/j.scitotenv.2021.149573



OPEN ACCESS

EDITED BY

Tim Rixen,
Leibniz Centre for Tropical Marine
Research (LG), Germany

REVIEWED BY

Markus Diesing,
Geological Survey of Norway, Norway
Nicole Burdanowitz,
University of Hamburg, Germany

*CORRESPONDENCE

Carolyn A. Graves
carolyn.graves@cefias.co.uk

SPECIALTY SECTION

This article was submitted to
Ocean Solutions,
a section of the journal
Frontiers in Marine Science

RECEIVED 22 April 2022

ACCEPTED 08 August 2022

PUBLISHED 08 September 2022

CITATION

Graves CA, Benson L, Aldridge J,
Austin WEN, Dal Molin F, Fonseca VG,
Hicks N, Hynes C, Kröger S, Lamb PD,
Mason C, Powell C, Smeaton C,
Wexler SK, Woulds C and Parker R
(2022) Sedimentary carbon on the
continental shelf: Emerging
capabilities and research priorities for
Blue Carbon.
Front. Mar. Sci. 9:926215.
doi: 10.3389/fmars.2022.926215

COPYRIGHT

© 2022 Graves, Benson, Aldridge,
Austin, Dal Molin, Fonseca, Hicks,
Hynes, Kröger, Lamb, Mason, Powell,
Smeaton, Wexler, Woulds and Parker.
This is an open-access article
distributed under the terms of the
[Creative Commons Attribution License
\(CC BY\)](https://creativecommons.org/licenses/by/4.0/). The use, distribution or
reproduction in other forums is
permitted, provided the original
author(s) and the copyright owner(s)
are credited and that the original
publication in this journal is cited, in
accordance with accepted academic
practice. No use, distribution or
reproduction is permitted which does
not comply with these terms.

Sedimentary carbon on the continental shelf: Emerging capabilities and research priorities for Blue Carbon

Carolyn A. Graves^{1*}, Lisa Benson², John Aldridge²,
William E. N. Austin³, Franck Dal Molin², Vera G. Fonseca¹,
Natalie Hicks⁴, Clare Hynes², Silke Kröger², Philip D. Lamb²,
Claire Mason², Claire Powell², Craig Smeaton³,
Sarah K. Wexler⁵, Clare Woulds⁶ and Ruth Parker²

¹Centre for Environment Fisheries and Aquaculture Science, Weymouth, United Kingdom, ²Centre for Environment Fisheries and Aquaculture Science, Lowestoft, United Kingdom, ³School of Geography and Sustainable Development, University of St Andrews, St Andrews, United Kingdom, ⁴School of Life Sciences, University of Essex, Colchester, United Kingdom, ⁵Centre for Ocean and Atmospheric Sciences, School of Environmental Sciences, University of East Anglia, Norwich, United Kingdom, ⁶School of Geography, University of Leeds, Leeds, United Kingdom

Continental shelf sediments store large amounts of organic carbon. Protecting this carbon from release back into the marine system and managing the marine environment to maximize its rate of accumulation could both play a role in mitigating climate change. For these reasons, in the context of an expanding “Blue Carbon” concept, research interest in the quantity and vulnerability of carbon stored in continental shelf, slope, and deep ocean sediments is increasing. In these systems, carbon storage is physically distant from carbon sources, altered between source and sink, and disturbed by anthropogenic activities. The methodological approaches needed to obtain the evidence to assess shelf sea sediment carbon manageability and vulnerability within an evolving blue carbon framework cannot be transferred directly from those applied in coastal vegetated “traditional” blue carbon habitats. We present a toolbox of methods which can be applied in marine sediments to provide the evidence needed to establish where and when marine carbon in offshore sediments can contribute to climate mitigation, focusing on continental shelf sediments. These methods are discussed in the context of the marine carbon cycle and how they provide evidence on: (i) stock: how much carbon is there and how is it distributed? (ii) accumulation: how rapidly is carbon being added or removed? and (iii) anthropogenic pressures: is carbon stock and/or accumulation vulnerable to manageable human activities? Our toolbox provides a starting point to inform choice of techniques for future studies alongside consideration of their specific research questions and available resources. Where possible, a stepwise approach to analyses should be applied in which initial parameters are analysed to inform which samples, if any, will provide information of interest from more resource-intensive analyses. As studies increasingly address the knowledge gaps around continental shelf

carbon stocks and accumulation – through both sampling and modelling – the management of this carbon with respect to human pressures will become the key question for understanding where it fits within the blue carbon framework and within the climate mitigation discourse.

KEYWORDS

particulate organic carbon (POC), marine sediment analysis, carbon stock, carbon sequestration, carbon provenance, carbon vulnerability, carbon management

Introduction

Continental shelf sediments store large amounts of organic carbon (e.g., 21–73 Tmol C in the upper 10 cm of northwest European shelf sediments; Legge et al., 2020; Figure 1). This carbon is both allochthonous, sourced from terrestrial ecosystems (Santos et al., 2021), and autochthonous, derived from marine primary productivity. Organic carbon (C_{org}) is transported and transformed in the water column before reaching the seabed where it is further modified or buried (Najjar et al., 2018; LaRowe et al., 2020; Luisetti et al., 2020). Protecting this marine sedimentary carbon from release back into the marine system and managing the marine environment to maximize its accumulation and sequestration would contribute to climate change mitigation.

Blue carbon has become a high-profile topic in conservation and policy discussions, driving the need for a robust scientific evidence base on stocks and accumulation rates of marine carbon (e.g., Lovelock and Duarte, 2019; Macreadie et al., 2019; Christianson et al., 2022). As an emerging research area, blue carbon has been defined differently between studies, and there is ongoing discussion about which elements of marine carbon could and should be included in the blue carbon concept in different contexts (e.g., Krause-Jensen et al., 2018). Lovelock and Duarte (2019) set out criteria to determine if the carbon in a marine ecosystem should be considered as blue carbon from a climate mitigation perspective: removing greenhouse gases at a significant scale, providing long-term storage for fixed carbon dioxide (CO_2), the system being negatively impacted by

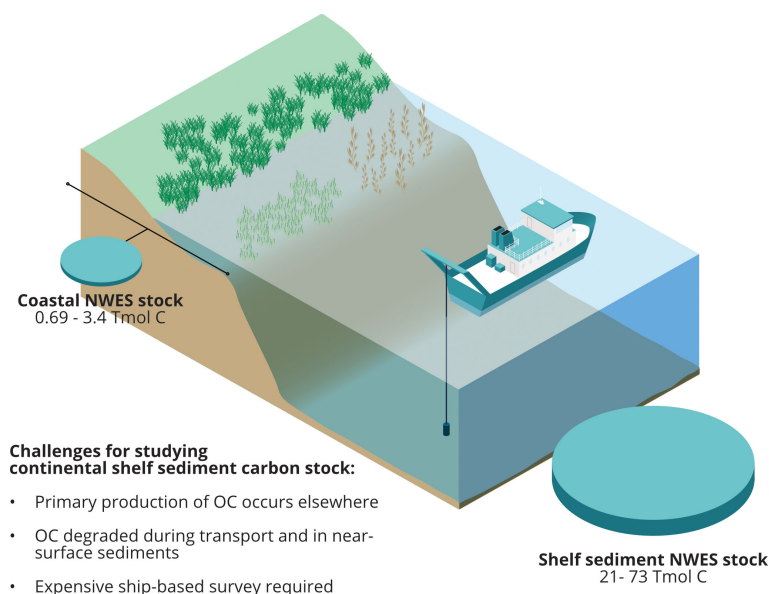


FIGURE 1

Estimates of marine organic carbon stocks for the northwest European shelf (NWES), from Legge et al., 2020, alongside schematic representation of carbon sampling in continental shelf highlighting some of the challenges compared to coastal blue carbon ecosystems. Cylinder volume is proportional to the mid-point of the coastal and shelf organic carbon stock estimates, with the full estimate range also given. Benthic stock is for the upper 10 cm of sediment. OC: organic carbon.

anthropogenic activities, and the ability to manage the system to maintain or enhance the carbon services without social or environmental harm. Systems which satisfy these conditions are said to be “actionable” if they can be incorporated into existing mitigation policies. Herein, we consider blue carbon to be the organic carbon stored in marine ecosystems which contributes to climate change mitigation in a manageable way.

The traditional blue carbon ecosystems which can currently be included in formal carbon accounting mechanisms (IPCC, 2008; IPCC, 2013) are mangroves, seagrass, and saltmarsh (e.g., Luisetti et al., 2019; Luisetti et al., 2020), but research is increasingly bringing additional systems into the blue carbon discourse, recognising that these habitats (and their carbon) are not isolated from marine carbon cycling in the rest of the ocean (Santos et al., 2021). Macroalgae, for example, are recognized as a significant biomass carbon store, but since carbon is not sequestered long term within the habitat itself it is difficult to include in blue carbon financing frameworks (Krause-Jensen and Duarte, 2016; Krause-Jensen et al., 2018; Dolliver and Connor, 2022; Duarte et al., 2022). Several recent studies and ongoing research aim to improve recognition of the carbon storage ecosystem service macroalgae provide by evidencing their role as a carbon-donor habitat to sediments, such as those considered here (e.g., Trevathan-Tackett et al., 2015; Pessarrodona et al., 2018; Wernberg and Filbee-Dexter, 2018; Kokubu et al., 2019; Ortega et al., 2019; Queirós et al., 2019; Filbee-Dexter et al., 2020).

Similarly, research interest in the quantity and vulnerability of carbon stored in continental shelf, slope and deep ocean sediments is increasing (e.g., Avelar et al., 2017; Atwood et al., 2020; Legge et al., 2020; Smeaton, et al., 2021a; Sala et al., 2021). In these systems, carbon is less directly coupled to primary productivity than in coastal blue carbon habitats. The methodological approaches needed to obtain the evidence to assess shelf sea sediment carbon manageability and vulnerability within an evolving blue carbon framework cannot be transferred directly from those applied in traditional blue carbon habitats: different issues need to be considered, a multi-tool approach taken, and new and emerging techniques used.

Here, we set out how to obtain the evidence needed to establish where and when marine carbon in offshore sediments can contribute to climate mitigation, focusing on continental shelf sediments. The key questions to be addressed in this context are: (i) stock: how much carbon is there and how is it distributed? (ii) accumulation: how rapidly is carbon being added or removed? and (iii) anthropogenic pressures: is carbon stock and/or accumulation vulnerable to manageable human activities? These blue carbon focused questions link directly to the marine carbon cycling questions of carbon provenance and carbon reactivity. This research will provide the foundation upon which to determine if carbon in shelf sediments can be incorporated, without social or environmental harm, into existing climate mitigation

frameworks and policy instruments and thus be considered actionable blue carbon.

Marine scientists have a range of measurement and analysis tools available to provide answers to these questions, from routine, rapid, low-cost analyses to highly specialized techniques which are still in development. We discuss these in turn as they relate to the underlying scientific questions. Together, they make up the marine sediment carbon toolbox from which appropriate sampling and analytical approaches can be chosen for the studies which will fill the evidence gaps identified and enable improved assessment of the role of the seabed in climate change regulation.

Carbon stocks

Quantifying stocks

The amount of organic carbon locked away from connection with the atmosphere, or – in the case of sediments, the ocean water column – is the fundamental parameter determining if and where shelf sea sediments satisfy the blue carbon criterion of “significant carbon storage”. The distribution of carbon stocks must be known in order to consider their importance, vulnerability and manageability.

The Blue Carbon Initiative¹'s manual designed to provide standardized guidance to managers for assessing carbon stocks and emissions factors (Howard et al., 2014), enumerates the three elements required to quantify stocks: (i) (total) organic soil thickness (depth to underlying hard substrate), (ii) dry bulk density, (iii) organic carbon content (%C_{org}). In the context of continental shelf sediments, dry bulk density and organic carbon content remain critical, while total soil (sediment) depth is unlikely to be determined and furthermore not immediately relevant in the context of climate mitigation. The depth of interest is that which is likely to be disturbed by human activities, and thus contains “vulnerable” carbon stocks. In traditional blue carbon ecosystems the organic soil thickness is expected to vary from between 10 cm to over 3 m (Howard et al., 2014), and IPCC guidelines recommend the use of 1 m as a standard depth for reporting stocks in the absence of information on total soil depth (IPCC, 2008; IPCC, 2013). In marine sediments, the relevant depth of vulnerability will be influenced by the natural setting (e.g., water depth, sediment type, fauna) and the influence of potential disturbances (bottom trawling, deep-sea mining, dredging and disposal, etc., see *Anthropogenic pressures*). Many, though certainly not all, existing datasets are limited to near-surface sediments (e.g., upper 10 cm; Diesing et al., 2017; Wilson et al., 2018; Smeaton et al., 2021a) due to standard sampling procedures in routine

1 <https://www.thebluecarboninitiative.org>

monitoring programmes. Significant (and unquantifiable) uncertainty in estimated stocks is introduced where data are extrapolated beyond their measurement depth (e.g., to 1 m, [Atwood et al., 2020](#)) as it is not expected that C_{org} content remains constant between near-surface and deeper sediments. Generally, C_{org} is expected to decrease with depth due to remineralization/diagenesis (e.g., [Burdige, 2007](#); [Arndt et al., 2013](#); [LaRowe et al., 2020](#)) such that extrapolating near-surface carbon stocks to e.g., 1 meter depth would yield an overestimation of stock, and that deeply buried organic matter may be less labile and less likely to be remineralized to release CO_2 if disturbed (see *Characterising stock reactivity*)

Determination of dry bulk density and organic carbon content in marine sediments are standard analyses which are routinely carried out by geologists, geochemists, and biogeochemists. Dry bulk density is the ratio of the mass of a dried sediment sample to its original volume. Porosity, the ratio of the volume of ‘voids’ (between sediment grains) to the total (wet) sediment mixture volume, is more frequently reported in marine sediments. Porosity is generally calculated by mass difference of wet and dried sediment, assuming a density for pore fluid (based on salinity) and sediment grains (typically 2650 kg cm^{-3} for quartz/feldspar) (e.g., [Jenkins, 2005](#); [Diesing et al., 2017](#)). Empirical relationships have been used to estimate bulk density from sediment grain size (% mud) and C_{org} content itself (e.g., [Diesing et al., 2017](#); [Silburn et al., 2017](#); [Atwood et al., 2020](#)). The organic carbon content of marine sediments is commonly determined by elemental analyzer, alongside total carbon, inorganic carbon, and organic matter carbon: nitrogen (C:N) ratio ([Verardo et al., 1990](#); [Nieuwenhuize et al., 1994](#); [Harris et al., 2001](#)). This well established method, and its advantages over the lower-cost loss on ignition (LOI) approach, which relies on determining a habitat and/or site-specific conversion between organic matter and organic carbon, is described in detail in [Howard et al. \(2014\)](#) in the context of its application in coastal blue carbon habitats. A methodologically simplified approach based on ramped thermal heating alongside CO_2 detection by infrared spectrometry has recently been applied to marine sedimentary carbon ([Smeaton et al., 2021a](#)).

Total carbon stocks are usually derived by extrapolating spatially limited observations over a relevant spatial area to generate an inventory. The validity of, or numerical uncertainty in, the estimated total stock then depends on how representative the sampled sites are of the larger area of interest ([Howard et al., 2014](#)). Where this is partially addressed by estimating a different stock for different spatial sub-units (e.g., [Burrows et al., 2014](#); [Watson et al., 2020](#); [Gregg et al., 2021](#)), additional uncertainty is introduced by the estimation of the extent of the area for each. It is important to recognize the large uncertainty in values obtained by multiplying estimated stock over a large estimated area (discussed for soil C_{org} in [Goidts et al., 2009](#)). Since measurements in marine sediments require sampling from a research vessel, at high cost, achieving adequate

spatial resolution for high confidence inventories is particularly challenging. Furthermore, there is a tendency for observations to be biased to near-coast and, because sediment coring is more challenging in coarse sediments, to higher mud-content sediments which are expected to contain high C_{org} (Figure 5 in [Smeaton et al., 2021a](#)). Linking carbon content to explanatory parameters (e.g., particle size, hydro-acoustic reflectance; [Hunt et al., 2020](#)) and applying statistical models or machine learning approaches to generate spatially resolved maps ([Serpetti et al., 2012](#); [Diesing et al., 2017](#); [Wilson et al., 2018](#); [Atwood et al., 2020](#); [Smeaton et al., 2021a](#)), can help to overcome issues of spatial bias in observations but assumes carbon processing, which controls stock, occurs in the same way across the region of interest. Co-measurement of the key physical and carbon content properties is a fundamental requirement for producing accurate stock assessments therefore determining additional sediment and environment parameters alongside carbon stocks adds significant value to carbon stock measurements.

Marine carbon stocks can also be determined by modelling. Process-based biogeochemical modelling studies focused on shelf sea carbon cycling (e.g., [Kühn et al., 2010](#); [Wakelin et al., 2012](#)) generally assume marine carbon ultimately derives from marine primary production and, crucially, that most organic detrital carbon in the benthic system is remineralized over an annual cycle. With this assumption, models typically predict stocks of benthic C_{org} one to two orders of magnitude lower than observed ([Aldridge et al., 2017](#)). This discrepancy is resolved if it is assumed the models follow only the relatively labile carbon most important for correctly modelling the annual recycling of carbon and nutrients, whilst most of the observed carbon stock is highly refractory: does not degrade significantly over annual timescales. However, this means that model results do not, at present, provide appropriate stock values for sediment carbon inventories. Long term storage (sequestration) of highly refractory (non-mineralizable) carbon has been implemented within models, for example by explicitly assuming a background flux ([Soetaert et al., 1996](#)) or assuming a fraction of more labile carbon becomes deeply buried and no longer undergoes degradation ([Butenschön et al., 2016](#)).

Characterising stock provenance

To apply the blue carbon accounting framework, organic carbon in marine sediments must be linked back to the source of photosynthesis to avoid “double-counting”. For example: macroalgal carbon being accounted for in a carbon valuation of the coastal macroalgae habitat, and then again in offshore marine sediments where it is eventually buried. To protect or enhance the carbon storage potential of shelf sediments, management measures need to be applied not only locally, but also to the key carbon source ecosystems. Furthermore, the vulnerability of organic carbon in marine sediment to

disturbance, in terms of release back towards the water column, is determined in part by its provenance as this influences how readily it is broken down and remineralized to CO₂.

The primary production of much of the organic carbon subsequently stored in marine sediments occurred elsewhere: on land or in coastal habitats. In shelf seas marine phytoplankton are an important organic carbon source, though much of this carbon is expected to be recycled back to CO₂ within ocean waters (e.g., [Humphreys et al., 2019](#); [Dang, 2020](#)). In shallow waters, even away from the coast, microphytobenthos also fix carbon at the sediment surface (e.g., [Reiss et al., 2007](#)). Fundamentally, linking stored carbon to its source(s) relies on constraining the properties of the source itself: potential sources should be identified and analysed wherever possible, which is more challenging when carbon storage occurs at a distance from the carbon source and molecular properties are modified between source and sink.

In being transported to marine sediments, and after having been deposited there, organic matter is typically transformed by physical ([Ausín et al., 2021](#)) and biogeochemical processes ([Middelburg, 2018](#); [Kharbush et al., 2020](#)). This chemical alteration makes it more difficult to identify the provenance of different components of sediment organic matter. Moreover, it often renders the organic material molecularly uncharacterizable. Within the sediments, interaction with the mineral surface ([Kleber et al., 2021](#)), and with iron minerals in particular ([Lalonde et al., 2012](#)) have been suggested as a key mechanisms for this. This fraction of the input organic carbon that is sequestered long-term in marine sediments, largely significantly altered from its original molecular form, is that which is largely resistant to remineralization to inorganic carbon. Organic carbon which is less altered, and thus more reactive/vulnerable to disturbance, can also be buried in marine sediments in environments of low biological activity (e.g., under low oxygen or low temperature conditions; [Canfield, 1994](#)).

Methods for determining the provenance of organic carbon in coastal blue carbon ecosystems (tidal marshes, mangrove and seagrass meadows) were recently reviewed by [Gerald et al., \(2019\)](#). These authors concluded that the more different properties of organic matter that can be determined - in other words: applying a multi-tool approach - the more likely it is a single source can be unambiguously identified. When characterizing organic matter, the methods that provide greater source specificity are those that are performed on the smallest fractions of the bulk material (e.g., compound-specific analyses; see Figure 2.1 in [Bianchi and Canuel, 2011](#)). Here we place relevant methodology in the context of continental shelf sediments and consider issues and sources of uncertainty.

Bulk organic matter characterization

The majority of organic carbon stored in marine sediments is molecularly uncharacterizable (termed MUC) and thus cannot be characterized in terms of the biochemical classes (such as

proteins or fats) that form living organisms. MUC can often not be extracted from the sediment (e.g., using solvent extraction or acid hydrolysis), and/or cannot be hydrolyzed into recognizable monomers that are amenable to quantification methods; it must be investigated using methods that consider the bulk organic carbon pool. These methods are particularly powerful if they can be related to or calibrated against other established source indicators, or a mechanistic understanding of organic matter transformation and preservation processes.

The most general and routinely used methods, both in marine sediments and in coastal blue carbon habitats, are bulk organic matter carbon to nitrogen ratio [or nitrogen to carbon, see [Perdue and Koprivnjak \(2007\)](#)], and $\delta^{13}\text{C}$ and $\delta^{15}\text{N}$. These analyses are typically used in combination as, for example marine sources of organic carbon can have $\delta^{13}\text{C}$ ratios between -20 ‰ and -30 ‰ which lie within the range of C3 terrestrial plants ([Meyers, 1994](#)), and C:N ratios of soils can fall in the range of those of marine carbon sources (e.g., [Zhao et al., 2015](#)). Information from bulk organic matter characterization can be combined using various mixing models: binary ([Thornton and McManus, 1994](#)), three end-member ([Gordon and Goni, 2003](#)), and Bayesian ([Smeaton and Austin, 2017](#)). Within these models, bulk elemental (C:N) and isotopic ratios of C_{org} sources (i.e., terrestrial soils, vegetation and marine algae) are used to constrain, though not unambiguously identify, the proportion of the C_{org} originating from each of the sources.

Different isotopic systems (e.g., $\delta^2\text{H}$, $\delta^{18}\text{O}$, $\delta^{34}\text{S}$) could potentially provide additional specific information on source and transformations of the organic matter in some settings but they have not yet been applied to marine sediment samples even within coastal ecosystems ([Gerald et al., 2019](#)) and significant methodological development is needed before they can provide additional information in the context of continental shelf carbon sources.

Pyrolysis gas chromatography mass spectrometry (py-GCMS) can be used to investigate the macromolecular composition of sedimentary organic matter, including compound classes such as lignins, cellulose, carbohydrates and proteins. The technique involves heating a sample (e.g., at 700 °C) in an anoxic environment to yield thermal degradation products which are analysed by GCMS. The method has the advantage of not needing solvent extraction, which makes sample preparation less laborious than many biomarker techniques (described in *Biomarkers*), while also looking at the whole organic carbon pool rather than only the extractable pool, which can constitute as little as ~5% of the total organic carbon ([Sparkes et al., 2016](#)).

For example, py-GCMS allowed [Kumar et al. \(2020\)](#) to identify that organic carbon in Ria Formosa Lagoon, Portugal, was dominantly from algal, bacterial and marine macrophyte sources, with very little from terrestrial sources, and that pollution was from spilled petroleum products and sewage. In the Siberian Arctic, py-GCMS allowed differentiation of types of terrestrial organic carbon, with nitriles and alkylbenzenes

derived from humified soils, and furfurals linked to much fresher/less degraded polysaccharides (Guo et al., 2004). In the Barents Sea, Stevenson and Abbott (2019) detected ecosystem shifts with distance from the ice edge, based on changing relative proportions of groups such as alkylphenols, alkylbenzenes, polysaccharides, and alkenes plus alkanes. However, uncertainties about the sources of these groups, and about whether groups are specific to particular sources (e.g., chitin is derived from shrimp and zooplankton, but also from peptidoglycan in bacteria), meant that analysis alongside ecological data was necessary to draw firmer conclusions.

One challenge posed by pyrolysis is that thermal degradation yields hundreds of different compounds, leading to complex chromatograms, and data that are difficult to interpret in terms of organic matter source and degradation state. This challenge has been tackled in some cases (Guo et al., 2004; Guo et al., 2009; Sparkes et al., 2016) by selecting and quantifying a sub-set of compounds (e.g., phenol and pyridine) that can be fairly confidently linked to specific sources (lignin and marine proteins, respectively). Although this means that only a sub-set of total organic carbon is being used to draw conclusions, the full pool is nonetheless being accessed by the analysis, and it does provide a systematic means of making comparisons between samples.

Cross referencing pyrolysis results with more established organic carbon source indicators can help to overcome the challenge of compound classes not being unique to certain organic carbon sources. Sparkes et al. (2016) determined marine versus terrestrial source from the ratio of phenols to pyridines in samples from the East Siberian Arctic Shelf. Through additional analysis of samples along offshore transects they were able to show that phenols were dominantly (although not exclusively) terrestrial, and pyridines were dominantly (but not exclusively) marine. They then showed that their pyrolysis-based index correlated well with other terrestrial versus marine indices, including $\delta^{13}\text{C}$, R'_{soil} , and the branched and isoprenoid tetraether (BIT) index, which allowed it's calibration even though the compounds on which it was based were not exclusive to either marine or terrestrial carbon sources.

Biomarkers

Biomarkers are organic molecules that may be traced unambiguously back to a specific biological origin. They constitute an important source-tracking tool for the characterization of aquatic organic matter (Derrien et al., 2019). Organic matter is a highly complex mixture of different types of compounds with varying physio-chemical properties originating from diverse sources. This includes allochthonous sources outside the aquatic system (e.g., higher plants from the terrestrial environment), autochthonous sources within the aquatic system (e.g., plankton and macrophytes such as seagrasses), and anthropogenic sources (e.g., sewage and oil

spills). The molecular biomarker approach to source-tracking involves targeting specific classes of organic compounds, such as lipids, pigments, lignin-phenols, carbohydrates, and proteins, which can inform on provenance of C_{org} present in marine depositional environments. As a targeted approach, biomarkers are selective by nature and thus represent a specific portion of the bulk organic matter pool.

Some lipids (e.g., sterols, fatty acids) and pigments (chlorophylls and degradation products, carotenoids) produced by specific organisms have been widely used to trace carbon sources within marine particulate organic matter; their recalcitrance makes them good indicators of material exported to marine sediments (Kharbush et al., 2020). Lipid biomarkers are widely considered to hold the most promise as indicators of organic carbon provenance (Derrien et al., 2017; Derrien et al., 2019; Gerdali et al., 2019). The lipids used in this context possess all the necessary qualities of a good biomarker, being ubiquitous, chemically and diagenetically stable, and structurally diverse. Lipids (commonly n-alkanes and fatty acids) have been used to track organic carbon provenance in numerous marine environments from diverse sources including anthropogenic, allochthonous, and autochthonous inputs (Derrien et al., 2019).

The n-alkanes are hugely abundant, simple, straight-chain lipid molecules produced by many lifeforms including terrestrial plants, aquatic plants, plankton, and bacteria. Their chain length provides the key diagnostic feature indicative of biological origin, whilst a predominance of an odd- or even- number of carbon atoms in the structure is also informative. Bacteria, algae, and plankton, for example, all produce short-chain n-alkanes (ca. $<\text{C}_{20}$), while plankton exhibit a predominance of an odd number of carbons (15, 17, or 19), and bacteria, an even number of carbon atoms (16, 18, 20). Mid chain n-alkanes (ca C_{20-25}) are associated with aquatic macrophytes such as seagrasses and saltmarsh plants. Long chain n-alkanes (C_{25-35}) are found in the leaf wax of vascular plants and have a predominance of an odd number of carbons (27, 29, 31) and are largely from terrestrial sources. These variations in the n-alkane structure with associated biological origins led to the development of the carbon preference index (CPI) broadly as an indicator of terrestrial versus petrogenic sources (Bray and Evans, 1961). The CPI has since been adapted and developed alongside many other n-alkane biomarker indices including the average chain length (ACL) and numerous other marine-aquatic-terrestrial discriminating ratios capable of identifying organic matter sources (Derrien et al., 2017). Similar indices also exist for other lipids such as fatty acids and are fully reviewed in Derrien et al. (2017).

Whilst biomarkers can identify a wide range of different inputs to bulk organic matter, including providing high resolution for mixed sources (Derrien et al., 2017), like any analytical tool they also have their limitations. For example, constraining the sources of organic matter using biomarkers can sometimes be a challenge within more complex marine

environments, such as those with significant coastal inputs in addition to marine and terrestrial sources. Advancing analytical methodologies include the very powerful combination of organic biomarkers, such as lipids, alongside the measurement of their specific isotopic signatures (typically stable C, H, N, O, S), termed compound-specific-isotope-analysis (CSIA). This technique imparts added value to the biomarker approach yielding increased specificity and the ability to discriminate between multiple and sometimes overlapping sources of organic matter. It utilizes the difference in isotopic composition of biomarkers from terrestrial, aquatic, and marine sources, which are all distinct and reflective of the CO₂ substrate (e.g., atmospheric, aquatic, marine) used for photosynthesis.

Sikes et al. (2009) combined the n-alkane lipid biomarkers with $\delta^{13}\text{C}$ to help resolve overlapping and masked sources of organic matter in surface sediments in the Hauraki Gulf, New Zealand. Bulk stable isotope analyses alone could not fully resolve the terrestrial signal, and n-alkane chain length indices were also insufficient due to overlapping and non-unique n-alkane signatures from confounding coastal sources (mangroves, seagrass) alongside the terrestrial and marine inputs. The differences in isotopic composition of biomarkers revealed by CSIA meant that the coastal input could be fully resolved from the terrestrial and marine signals. Sikes et al. (2009) thus demonstrated how an appreciable amount of purely terrestrial-derived organic matter was transported from input locations across the shelf and redistributed and buried in sediments including outer shelf locations towards the continental slope.

The ability to trace and quantify the allochthonous contribution to marine organic matter is essential for accurate carbon accounting (Kharbush et al., 2020). This involves understanding how terrestrial carbon moves through marine ecosystems: the traditional blue carbon ecosystems (mangroves, salt marshes, seagrass), as well as estuaries and continental shelf sediments, and how this carbon may subsequently be sequestered and stored. Lignin biomarkers are a powerful tool to probe the terrestrial contribution. Methodologies that continue to advance our understanding of the various distinct terrestrial inputs include the use of radiocarbon (as an addition to stable carbon and other elements) CSIA of lignin and other biomarkers. Tao et al. (2015) used the abundance and carbon isotope composition (^{13}C and ^{14}C) of n-alkane and fatty acid lipids and lignin-phenols to characterize source, composition, and age of suspended particulate organic carbon from the Yellow River, China. Natural allochthonous C_{org} inputs *via* rivers include recently biosynthesized biomass, pre-aged mineral-associated soil, and ‘ancient’ sedimentary rock sources. The latter two contain more refractory carbon as they have undergone prior processing and aging, and this has important implications for subsequent carbon cycling and storage in shelf sediments. Tao et al. (2015) found that, while bulk isotope measurements were relatively uniform for ^{13}C and showed old

^{14}C ages, it was only the differences in the ^{14}C ages of individual biomarkers that could fully reveal the various individual and very different terrestrial C_{org} sources. Linking the terrestrial C_{org} to its distinct source or sources informed on the nature of the exported C_{org}. In the case of the Yellow River, the refractory nature of much of the particulate organic carbon supports the high burial rates observed for terrestrial C_{org} in the delta area.

eDNA

Environmental DNA (eDNA) refers to traces of DNA left behind in the environment (soil, water, air, or sediment) by organisms through processes such as sloughing, shedding, or injury (Harrison et al., 2019). Since its first use to detect non-native species (Ficetola et al., 2008), eDNA has been used in a range of applications including rare and cryptic species identification, pathogen monitoring, fisheries stock assessments, diet studies, as well as characterizing the biodiversity of entire communities (Lallias et al., 2015; Deiner et al., 2017; Fonseca et al., 2017; Gilbey et al., 2021). DNA makes up approximately 3% of the cellular C_{org} in sediments (Landenmark et al., 2015) and therefore is adept at determining the provenance of marine carbon. Furthermore, eDNA techniques are fast, inexpensive, and capable of identifying carbon provenance to a finer taxonomic rank (species-level) than other techniques such as biomarkers, and stable isotopes (Reef et al., 2017).

At present, we are only aware of three published studies using eDNA to determine sources of C_{org} in marine sediments (Reef et al., 2017; Queirós et al., 2019; Ortega et al., 2020). Reef et al. (2017) used eDNA analysis, alongside stable isotope analysis, to identify the origin of C_{org} in seagrass meadows. Using a chloroplast gene, Reef et al. (2017) were able to identify traces of 150 plant taxa in the sediment. However, 88% of sequences belonged to seagrass, suggesting most C_{org} was autochthonous, originating within the system. Ortega et al. (2020) applied a similar approach using a ribosomal gene, in conjunction with stable isotope analysis, to identify sources of C_{org} in seagrass meadows and mangrove forests. A total of 40 plant taxa were identified, showing different communities of plants contributed to blue carbon in mangroves and seagrass meadows. In contrast to seagrass meadows in the Reef et al. (2017) study, Ortega et al. (2020) discovered substantial macroalgal input to stored carbon. The study also investigated if a quantitative relationship existed between i) detected eDNA and sediment eDNA, and ii) detected eDNA and sediment carbon content using mock community experiments. In both instances a high correlation was found, with an R² of 76% and 86% found in the sediment DNA and carbon experiments, respectively. This suggests that sedimentary eDNA studies may be able to provide interim information on C_{org} if a stable isotope analysis has yet to be conducted. The Queirós et al. (2019) study used a ribosomal gene to detect eDNA in the top centimeter of sediments, alongside stable isotope analysis and benthic-pelagic

process measurements, to understand the contribution of macroalgae to subtidal coastal ocean carbon stocks. One hundred and forty-eight plant taxa from surrounding coastal habitats were detected, suggesting a range of macroalgae species contribute to sedimentary C_{org} . A method for tracing macroalgal carbon in deeper marine sediments has been developed by the Norwegian Institute for Water Research (NIVA) to investigate long-term sequestration (burial) (d'Auriac et al., 2021). d'Auriac et al. (2021) quantified *L. hyperborea* and *S. latissimi*. eDNA levels in marine sediments down to 1.6 meters below the seafloor to estimate their contribution to the organic carbon stock and understand how it varied with time and since deposition.

Despite established protocols for sediment DNA-based biodiversity assessments (Fonseca and Lallias, 2016; Fonseca, 2018; Pawlowski et al., 2022) there remain technical considerations when conducting a marine carbon study. eDNA biodiversity assessments require the collection of a sediment sample, extracting the DNA from the sediment with no prior organism separation, followed by polymerase chain reaction (PCR) to create copies of the eDNA (called amplicons). These are then sequenced (obtaining the nucleotide composition of the eDNA), and the retrieved sequences are taxonomically assigned using either publicly available genetic databases such as BOLD (Ratnasingham and Hebert, 2007) or GenBank (Clark et al., 2016) or bespoke taxonomic libraries.

Every stage of the workflow has aspects that will affect the outcome of the assessment. Factors associated with sampling such as the body size of organisms in sediment, whereby larger organisms are more likely to be detected (Elbrecht et al., 2017), and seasonality and environmental conditions, which affect how quickly DNA decays (Jo and Minamoto, 2021). Similarly other sources of variation to be considered are habitat heterogeneity and sampling effort i.e., organism ability to disperse and its detectability and representativeness through enough biological replicates (Fonseca, 2018; Grey et al., 2018). Methodological considerations include the DNA extraction method, since different extraction techniques will reflect different components of existing biodiversity (Gerald et al., 2020). Further considerations of technical replicates are needed, such as the number of DNA extractions or PCR replicates used (more replicates give more robust biodiversity estimates) (Ficetola et al., 2015; Fonseca, 2018; Bruce et al., 2021).

During PCR, the primers (short single stranded sequences of DNA) are used to target the sections of eDNA to copy. DNA is copied more readily if there is greater similarity between the primer and the target eDNA. Therefore, DNA from different taxonomic groups will be copied at different rates (based on similarity to the primers) and the quantity of apparent DNA from each taxon will be distorted. This misrepresentation of biodiversity present is commonly referred to as "primer bias" and is inherent to most PCR-based approaches. In marine sediment carbon this means any given set of primers will not provide a complete picture of C_{org} origins; an assay to identify

terrestrial-plant DNA may not be capable of detecting phytoplankton DNA (or vice versa). In practice, this means a standardized primer set is unlikely to work for all marine sediment carbon applications, instead primers should be chosen with careful consideration given to the biodiversity present. Fortunately, it is possible to use multiple primers to test different aspects of biodiversity to ameliorate the effects of primer bias, though analysis cost increases with each additional primer.

The selection of genetic reference databases is also a key step in a marine sediment carbon study (Gerald et al., 2019). In essence, to identify taxa and assign taxonomic identities from DNA, the taxa must already be present, and correctly identified with the relevant DNA region, on a reference database. If absent or mislabeled, the DNA cannot be identified and can lead to an underestimation, or total exclusion, of C_{org} sources. This can be combatted in some instances by assigning higher taxonomic resolution (i.e., when species level identification is not possible, similarities to a closely related species on the database may facilitate genus or family level identification). Furthermore, a site-specific reference taxonomic database can be constructed but will require additional time and budget.

A final consideration whether or not the number of sequences produced corresponds to the amount of eDNA, biomass or C_{org} in the sample. Recent meta-analyses suggest that whilst some quantitative relationship between DNA and biomass exists, there is a high degree of variability, likely depending on a combination of the primers used and the community of organisms surveyed, e.g., unicellular or multicellular (Lamb et al., 2019; Yates et al., 2019). Thus, the sequences retrieved from eDNA would not correspond to the total amount of carbon from those taxa. Although molecular techniques are being refined to facilitate quantitative analysis, at present the extent to which sequences correspond to C_{org} using a mock community (Ortega et al., 2020) should be explicitly tested before molecular data are used in this manner.

Characterising stock reactivity

Not all organic carbon present in marine sediments at a given time will be stored over timescales greater than weeks to months to years (LaRowe et al., 2020). The total stock of organic carbon can be classified by its biogeochemical reactivity (Alderson et al., 2016), a key biogeochemical model parameter (Arndt et al., 2013). Organic matter reactivity or degradability (which can be defined as susceptibility to removal of a fraction by either biotic or abiotic processes, measured by lifetime e.g., Hansell, 2013) is understood to be a continuum (e.g., LaRowe et al., 2020) from labile (reactive; easily degraded; short lived) to recalcitrant (resistant to rapid microbial degradation; Hansell, 2013) and refractory. The term refractory is defined variability in different studies and used as "a one-fits-all word" for various

properties related to C_{org} reactivity, typically as the opposite of labile in a certain context, see discussion in [Hansell, 2013](#) and [Baltar et al., 2021](#). Understanding sedimentary organic matter's re-mineralization potential and ability to resist degradation ([Doetterl et al., 2016](#)) is vital in estimating its vulnerability to potential natural or anthropogenic disturbance and remineralization of the associated organic carbon.

The balance of organic carbon fractions with various reactivities determines the biodegradability of sedimentary organic matter and in turn the stability of the associated carbon. The rate of microbially-mediated degradation of organic matter can be impacted by the addition of more or of less labile material to a mixture (the priming effect; [Bianchi and Canuel, 2011](#)). If disturbed, the organic carbon in sediments dominated by labile organic matter is highly likely to be remineralized. Conversely if sediments dominated by recalcitrant organic matter are disturbed this material would likely be re-deposited as particulate organic carbon on or in the seabed. Only organic carbon of some intermediate degradability is thus relevant to the climate mitigation role of marine sediments.

Organic carbon reactivity is fundamentally linked to the organic matter's source, discussed in *Characterising stock provenance*. Black carbon, a refractory carbon fraction formed from incomplete combustion of organic carbon, accounts for 15–30% of the organic matter buried in marine sediments ([Middelburg et al., 1999](#)). The most refractory fraction of the black carbon is highly condensed soot, formed from combustion of fossil fuels at high temperatures ([Masiello, 2004](#)), which may remain in the atmosphere for months before eventually being buried in sediments. More degradable lightly charred black carbon formed during low temperature biomass burning may reach the marine environment *via* rivers through soil leaching or erosion ([Coppola et al., 2014](#)). Once deposited in sediments, factors including the depth of burial, microbial and redox conditions as well as subsequent disturbance influence the degree of black carbon's long-term storage. In general, small soot particles withstand degradation and result in long-term storage whereas lower formation temperature/larger size

fragments are more susceptible to biotic and chemical degradation ([Masiello, 2004](#)).

[Chew and Gallagher \(2018\)](#) show that black carbon can be a major component of organic carbon in seagrass, mangrove and saltmarsh sediment cores and because it is resistant to being re-released back into the atmosphere, as CO_2 for example, assert that it should be discounted from any blue carbon storage mitigations being proposed. Taking a different perspective, [Ren et al. \(2019\)](#) highlight that the relatively slow cycling of black carbon in Arctic Ocean sediments makes it an important fraction of inert carbon representing a significant sink of atmospheric CO_2 , which is likely to increase with global warming and increased melting of permafrost. There is thus a clear need to understand both the overall reactivity of the marine organic matter as well as to identify specific types and sources of organic carbon which are resistant to degradation.

Thermogravimetric analysis (TGA)

Organic matter recalcitrance can be defined in terms of the temperature at which mass is lost during combustion. TGA is an automated process which continuously measures the mass of a sample during ramped heating (e.g., from 0–1000°C at a rate of 10°C min⁻¹). Thermal decomposition through TGA allows the major organic matter fractions to be quantified. Within the literature, the thermal ranges which define these organic matter fractions are variable depending on environment and methodology ([Table 1](#)). Within marine sediments these organic matter fractions are thermally defined as labile (200–400°C), recalcitrant (400–550°C) and refractory (550–650°C) ([Capel et al., 2006](#); [Smeaton and Austin, 2022](#)). Focusing on the 200–650°C temperature range removes interference from absorbed water and non-organic material (i.e., calcite).

Most studies using this thermal approach characterize the organic matter into the three fractions, although some studies go further and use the thermal decomposition data to quantify specific components (e.g., hemicellulose, cellulose, lignin) ([Trevathan-Tackett et al., 2015](#); [Trevathan-Tackett et al., 2017](#)) or functional groups such as aliphatic and carboxyl groups ([Lopez-Capel et al., 2005](#); [Manning et al., 2005](#)) potentially

TABLE 1 Temperature ranges defining organic matter recalcitrance by thermogravimetric analysis in different environments.

Environment	Temperature Range (°C)			Reference
	Labile	Recalcitrant	Refractory	
Marine Sediments	200–400	400–550	550–650	(Capel et al., 2006 ; Smeaton and Austin, 2022)
Marine Sediment	130–280		280–520	(Kristensen, 1990)
Marine Sediment	160–300	300–400	400–600	(Loh et al., 2008)
Seagrass	200–400	400–500	550–650	(Trevathan-Tackett et al., 2015 and 2017)
Peatland	160–300	300–400	400–600	(Mauquoy et al., 2020)
Plant Material	300–350	400–500	430–530	(Kaloustian et al., 2001)
Soil	300–350	400–500	430–530	(Lopez-Capel et al., 2005 ; Manning et al., 2005)

allowing this approach to be applied to determine the provenance of the organic matter.

The quantification of the different thermal fractions allows the lability of organic matter to be estimated (Smeaton and Austin, 2022). A number of indices have been developed for this purpose ranging from the early Rp index (Kristensen, 1990), which used stepwise thermogravimetry (i.e., Loss on Ignition), to the Refractory index (R-index) and Carbon Reactivity Index (CRI), which utilize TGA data and provide an advanced understanding of the thermal characteristics of organic matter in different environments (Trevathan-Tackett, 2016; Smeaton and Austin, 2022). For example, a CRI value of 0 indicates that the material is fully biodegradable (high reactivity), while a value of 1 indicates that the substance is non-biodegradable (low reactivity) (Smeaton and Austin, 2022).

The gases evolved during TGA can be further analysed by coupling the system to an FTIR (Fourier transform infrared spectroscopy) or GCMS to provide greater understanding of (macro) molecular composition. Within marine sediments these approaches are largely focused on detecting and quantifying pollution (Oudghiri et al., 2015; Becker et al., 2020) but they have the potential to be powerful tools in characterizing organic matter. While understanding the recalcitrance of organic matter is one of the main applications of TGA, the continuous nature of the data produced results in their applicability to many areas including provenance studies (Oudghiri et al., 2015; Becker et al., 2020).

Amino acid index

The amino acid composition of organic matter in marine sediments can be used as an indicator (biomarker) of its degradation state. Total hydrolysable amino acids (THAA) are quantified by reverse-phase HPLC of their fluorescent derivatives (Dauwe and Middelburg, 1998), and their relative abundances used to generate an index for degradation state

which indicates the recalcitrance of the remaining material (Dauwe and Middelburg, 1998; Dauwe et al., 1999). This method was developed for North Sea continental shelf sediments, where phytoplankton primary productivity is the main source of organic matter. It has more recently been applied as part of a study of organic matter in the South Yellow Sea and East China Sea sediments (Chen et al., 2021), and in coastal blue carbon habitats (Vaughn et al., 2021). Recently, compound-specific radiocarbon analysis of amino acids has been proposed as a novel method for improving understanding of food webs and sedimentary organic carbon (Blattmann and Ishikawa, 2020; Blattmann et al., 2020).

Black carbon quantification

To measure black carbon, traditional methods require the removal of inorganic carbon using the same methodology as that used to prepare samples for organic carbon analysis, with either sulphurous acid (Verardo et al., 1990; Jablonski et al., 2002; Phillips et al., 2011) or hydrochloric acid (Komada, 2008; Brodie et al., 2011). Following removal of inorganic carbon, there are a number of methods used to quantify fractions of black carbon (Hammes et al., 2007; Table 2). Chew and Gallagher (2018) compare chemo-thermal oxidation (CTO) and chemical nitric acid oxidation (NAO) and conclude that the presence of thermally resistant phytoliths was responsible for differences in black carbon results from these two methods.

Newer instrumentation, based on the temperature gradient method is now being applied for carbon measurements (Smeaton, et al., 2021a) with the advantages that no acid carbonate removal is required to remove inorganic carbonates, and that measurements of particulate organic carbon, black carbon (residual oxidizable carbon (ROC)) as well as inorganic carbon can be derived from a single sample. Results have been shown to be comparable with the more traditional methods (Natali et al., 2020).

TABLE 2 Methods used to quantify black carbon, following removal of inorganic carbon (Hammes et al., 2007), including references where these methods have been applied.

Method	Black carbon fraction quantified/comments	Selected references
Chemo-thermal oxidation (CTO)	Refractory soot sediments and particulates. Possible interference from C _{org} charring.	Gustaffson et al. (2001), Fang et al. (2016), Chew and Gallagher (2018)
Dichromate/sulphuric acid oxidation	Soot and charring fractions. Variable results and methodology.	Maisello et al. (2002), Ren et al. (2019)
Nitric acid oxidation (NAO)	Degradable char black carbon.	Middelburg et al. (1999), Chew and Gallagher (2018)
BCPA derivatization	Dissolved black carbon especially. Method-inherent errors need correction.	Glaser et al. (1998) Ziolkowski et al. (2011)
$\Delta^{14}\text{C}$ with BCPA	Differentiates fractions from biomass burning and fossil fuel combustion.	Coppola et al. (2014), Coppola et al. (2019)
$\delta^{13}\text{C}$ with BCPA	Differentiates riverine and marine sources.	Wagner et al. (2019), Coppola et al. (2019)

The priming effect

Priming occurs when the rate of remineralization of stable organic matter is either increased or decreased by addition of labile organic matter (Sanches et al., 2021). As such, simply measuring the recalcitrance of organic matter in marine sediments may not fully capture the vulnerability of stored carbon when the system is disturbed, i.e., if the disturbance mixes stable organic matter with a labile fraction. Sanches et al. (2021) reviewed studies of priming in aquatic systems and found that the observed magnitude and direction of the effect depended on whether a lab or field-based approach was applied and on the proxies used to measure remineralization. Their meta-analysis concluded that, in general, priming has a positive effect (increased remineralization of stable organic matter with the addition of labile organic matter). They recommend using bacterial growth as a proxy (in preference to production or respiration) or CO₂ production as these approaches are most sensitive. For example, van Nugteren et al. (2009) added ¹³C-enriched diatoms to marine sediment slurries and measured evolved CO₂ to observe a 31% increase in remineralization.

Carbon accumulation rates

Quantification of the rate that carbon accumulates in shelf sediments is the key parameter for natural carbon accounting, for which carbon burial is the service of interest (Luisetti et al., 2020). In the context of blue carbon projects, “additionality” must be shown: that management activities lead to an increase in carbon sequestration relative to accumulation rates in the unmanaged system (e.g., Lafratta et al., 2020).

*The Blue Carbon Initiative*²'s manual designed to provide standardized guidance to managers for assessing carbon stocks and emissions factors (Howard et al., 2014), discusses carbon accumulation and loss in a chapter entitled ‘how to estimate CO₂ emissions’ – explicitly emphasizing the motivation of assessing impacts on the atmospheric CO₂ budget. The caveat of assuming all, or a given proportion of, sediment carbon accumulation or loss being in connection with the atmosphere is presented therein in this context (Howard et al., 2014). The simple surface elevation table (SET) method often applied in coastal blue carbon ecosystems is not appropriate in marine sediments. Instead, natural radiotracers, including carbon-14 (¹⁴C, radiocarbon), lead-210 (²¹⁰Pb), and thorium-230 (²³⁰Th, uranium-thorium dating), are routinely used to determine rates of marine sediment accumulation. ²¹⁰Pb and ²³⁰Th are both part of the ²³⁸U decay chain and are deposited from the atmosphere at a relatively constant rate with abundances in marine sediment decreasing with depth as they decay (Appleby and Oldfield, 1978). ¹⁴C is absorbed from the atmosphere into

the tissue of living organisms, and its abundance decays after death (Anderson et al., 1947; Libby et al., 1949). Other dating tools include tephra chronology (Cage et al., 2011; Davies, 2015), optical luminescence (OSL) dating (Madsen et al., 2005) and direct methods to measure the rate of particle accumulation on the seafloor, like sediment traps (which generally underestimate particle fluxes due to particle solubilization, zooplankton swimmers and hydrodynamics; Subha Anand et al., 2017).

Differentiation between radiotracer techniques is based predominantly on the time interval over which their decay rate (half-life) allows material to be dated. Radiocarbon based age-control is typically used to estimate long-term (100s–1000s of years) sediment accumulation rates, while radionuclide dating (i.e., ²¹⁰Pb) provides a chronological constraint of modern deposition over the last ~150 years. The limitations of different methods can be partially addressed by combining different radiotracers, but the dates obtained do not always agree (e.g., Jenkins, 2018: shorter-period dates tend to be higher than long-term dates; the Sadler effect; Sadler, 1981). For example, sedimentation rates from ¹⁴C are generally found to be lower (slower) than those derived from ²¹⁰Pb (Baskaran et al., 2017; Smeaton et al., 2021b) because of the effects of sediment compaction (Bird et al., 2004) and diagenetic processes (biogeochemical alteration) that can alter the organic matter (Arndt et al., 2013; LaRowe et al., 2020). Baskaran et al. (2017) suggest that short-lived radioisotopes are better suited to determining modern depositional rates than radiocarbon and recommend using ²¹⁰Pb where possible when determining sediment accumulation rates.

Radiotracers can also be applied to track carbon through the ocean and or sediment system. While not directly providing organic carbon burial rates, these more focused studies are an integral part of developing a broader understanding of marine carbon cycling. For example: the use of ¹⁴C and ³⁵S radiolabeling techniques to track microbial recycling of organic carbon in the sediments (Beulig et al., 2017).

Lead-210-derived sedimentation rates and dating

The process of assigning ages to organic carbon present in specific layers (depth intervals) of marine sediment can be achieved by measuring the activity concentration of co-occurring ²¹⁰Pb (Tolosa et al., 1996; Pappa et al., 2019). In relatively undisturbed depositional aquatic ecosystems ²¹⁰Pb abundance decreases exponentially with depth from the seawater-sediment interface due to the radioactive decay of the tracer, allowing the ²¹⁰Pb depth profile to estimate a sedimentation rate for any substances of interest associated with the sediment. Application of ²¹⁰Pb dating remains a challenge because of unresolved issues associated with the variety of radioanalytical methodologies available as well as

² <https://www.thebluecarboninitiative.org>

different modelling approaches that play an essential role in deriving sediment accumulation rates from radiotracer measurements (MacKenzie et al., 2011; Garcia-Tenorio et al., 2020).

Disturbances can complicate the straightforward determination of sediment accumulation rates from ^{210}Pb depth profiles. The surface 10–15 cm of the seabed are likely to be disturbed by, e.g., bioturbation, fishing activities and natural resuspension by bottom water currents (see *Anthropogenic pressures*). Furthermore, dating must account for the additional sources of ^{210}Pb within the sediment, from the *in-situ* decay of radium-226 (^{226}Ra) and, more problematically, from industrial activities including offshore oil and gas and other mineral processing industries (Sahu et al., 2014; Ahmad et al., 2021). The proportion of ^{210}Pb present in the sediment and from human activity (termed supported ^{210}Pb) does not decay at the same rate as the unsupported ^{210}Pb fraction from atmospheric deposition (Gulliver et al., 2001; Cook et al., 2004). Measuring ^{226}Ra in addition to ^{210}Pb enables the subtraction of supported ^{210}Pb from the total ^{210}Pb measured prior to estimating sedimentation rates and dating sediment layers.

With a half-life of 22.3 years, ^{210}Pb dating is limited to relatively recent sediment ages (up to 150 years). It can therefore be challenging to use this technique in low-sedimentation rate marine environments ($<0.15\text{ cm yr}^{-1}$) (De Haas et al., 1997). There are several ^{210}Pb dating models available, that can be applied and help interpret different ^{210}Pb core profiles (Arias-Ortiz et al., 2018; Blaauw et al., 2018). These models have been comprehensively described over the last forty years. The Constant Initial Concentration (CIC) (Robbins, 1978), Constant Rate of Supply (CRS) (Appleby and Oldfield, 1978) and Constant Flux: Constant Sedimentation (CF:CS) (Appleby and Oldfield, 1978) models are the most widely used to estimate sedimentation accumulation rates, but they are associated with numerous assumptions that can sometimes limit their appropriateness in more complex and disturbed aquatic ecosystems (Arias-Ortiz et al., 2018). Very often, the mass accumulation rate, expressed in $\text{mg cm}^{-2}\text{ yr}^{-1}$, is also estimated to account for compaction effect (Schmidt et al., 2014). More recently the advantages of a Bayesian approach, as applied in radiocarbon dating (Blaauw et al., 2018), is gaining attention (Aquino-López et al., 2020; Blaauw et al., 2021).

^{210}Pb in environmental matrices, including marine sediments, is commonly determined directly by gamma spectrometry. However, gamma spectrometers equipped with Well-type germanium (Ge) detectors that allow the direct determination of low levels of ^{210}Pb with little sample mass and preparation required are not commonly available. More common and cheaper flat end Ge detectors with much higher limits of detection can provide insufficient levels of accuracy and precision for measuring the very low levels of ^{210}Pb naturally present in the environment (Dal Molin et al., 2018). Alternatively, ^{210}Pb can also be determined indirectly by

measuring polonium-210 (^{210}Po), its granddaughter decay product, *via* alpha spectrometry. Although this alternative traditional radiometric technique requires samples to be digested in strong acid mixtures and treated prior to analysis, the limits of detection and level of accuracy and precision that can be achieved are more appropriate (Hassen et al., 2020). The underlying assumption, that ^{210}Pb is in secular equilibrium with ^{210}Po such that both radionuclides are present at the same concentration, can be verified by performing a second analysis of ^{210}Po at a later stage, i.e., generally, by determining ^{210}Po ingrowth from the decay of ^{210}Pb after three to four months.

To determine ^{226}Ra and correct for supported ^{210}Pb , gamma spectrometry is the most common technique. The sample must be placed in a radon proof container for a minimum of three weeks prior to analysis to ensure secular equilibrium is established before indirect measurement *via* its two decay products (bismuth-214 and lead-214). ^{226}Ra can be determined indirectly by either measuring emission of radon-222 gas, or directly by alpha-spectrometry, and more recently by ICP-MS, following appropriate sample preparation steps (IAEA, 2010).

Caesium-137 (^{137}Cs) is commonly used as a complementary tool to validate ^{210}Pb dating models. Characteristic abundance peaks of ^{137}Cs observed in marine sediments in the Northern hemisphere can be directly related to nuclear weapon testing events of the late 1950s and early 1960s, and more locally in the UK seas to peak discharges from Sellafield nuclear reprocessing plant in the late 1970s (Environment Agency et al., 2021). Caesium-137 can easily be measured by gamma spectrometry, however, because its concentration is constantly decreasing over time [half-life of 30 years and no major additional characteristic peak since Chernobyl; see Figure 7.9 in Environment Agency et al. (2021)], it is important to optimize the counting time to ensure reliable and accurate results by gamma spectrometry (Garcia-Tenorio et al., 2020).

Radiocarbon dating

The radioactive ^{14}C isotope has a half-life of $5,700 \pm 30$ years (Kutschera, 2013) which allows for the determination of the age of a carbon bearing material formed over the past 55,000 years (Hajdas et al., 2021). Since the detection of ^{14}C in 1977 using particle accelerators (Bennett et al., 1977), Accelerator Mass Spectrometry (AMS) has become the most used technique in ^{14}C analysis. In AMS, the $^{14}\text{C}/^{13}\text{C}$ or $^{14}\text{C}/^{12}\text{C}$ ratio in the sample is directly measured resulting in shorter measurement times (days to minutes) and reduced sample requirements (g to μg of C) than previous scintillation methods (Litherland et al., 2011). Recent developments in AMS technologies have resulted in ^{14}C detections at significantly lower energies (Synal et al., 2000), resulting in the reduction in size of AMS's and the establishment of new sample introduction techniques for direct analysis of CO_2

resulting from combustion (EA-AMS) (Haghipour et al., 2019), wet oxidation (Leonard et al., 2013), acid hydrolysis (Molnár et al., 2013) and laser ablation (LA-AMS; Welte et al., 2016).

The data produced by the AMS (Fraction ^{14}C or $F^{14}\text{C}$) allows for conventional ^{14}C ages to be calculated following the approach of Libby (1955) where conventional ^{14}C age = $-8,033 \ln(F^{14}\text{C})$. To determine the true age of the sample, the conventional ^{14}C age must be calibrated to a curve based on measurements of ^{14}C from samples of known age and location (e.g., northern hemisphere, southern hemisphere, or the marine environment). The IntCal radiocarbon calibration curves (Heaton et al., 2020; Hogg et al., 2020; Reimer, 2020) are a resource constructed from measurements of ^{14}C made in different laboratories on a range of dated samples. The last 13,900 years are constrained by dated tree rings (Reimer, 2020), while beyond this (13,900–55,000 years) lake and marine sediments, speleothems or corals are statistically integrated to create the most accurate representation of past atmospheric ^{14}C (Reimer, 2020).

Today, conventional ^{14}C ages are calibrated using advanced Bayesian statistical tools that include dedicated routines for the different calibration curves, the most commonly used modelling tools are OxCal (Ramsey, 1995; Ramsey et al., 2020) and MatCal (Lougheed and Obrochta, 2016). Calibrated ^{14}C ages are referred to as a calendar age counted backwards from 0 cal BP (before present) which corresponds to 1950 Common Era (CE, previously referred to as AD) or to calendar years Before Common Era (BCE, previously referred to as BC). Post 1950 CE correspond to the age of nuclear testing where atmospheric ^{14}C concentrations measured in CO_2 of air and dated tree rings, display significantly elevated ^{14}C concentration (bomb spike) hindering the use of conventional ^{14}C dating approaches (Hua et al., 2013; Santos et al., 2020). To calculate sedimentation and accumulation rates an age-depth model is constructed using the calibrated dates. Classical age-depth models can be constructed in software such as CLAM (Blaauw, 2010), but more commonly Bayesian statistical packages such as OxCal (Ramsey, 1995; Ramsey, 2009), and BACON (Blaauw and Christen, 2011), are applied to create models that fully account for uncertainties allowing for the calculation of sedimentation and accumulation rates.

There is a long history of using ^{14}C to chronologically constrain sedimentary records allowing the calculation of long-term (100s–1000s of years) sedimentation and accumulation rates on the seabed (Kershaw, 1986; Darby et al., 1997; Colman et al., 2002; Santschi and Rowe, 2008; Smeaton et al., 2021c). In marine sediments both organic matter and carbonate (inorganic) material (e.g., shells or foraminifera) can be dated, but organic matter cannot be used to constrain the age of the sediment as the carbon it contains originates from multiple (many unknown) sources with varying compositions and ages. Carbonate material is therefore the preferred sample medium for ^{14}C analysis and age constraint. Living benthic

foraminifera are found in the upper most layers of most sediments and therefore the shells of foraminifera buried after death provide material ideally suited for dating as they are representative of past surface sediments from their time of deposition. The number of foraminifera required to measure ^{14}C using a conventional AMS can vary but it is not uncommon to need between 500–1000 individuals, whereas the recent developments in AMS technology (Synal et al., 2000) means that far smaller numbers are now required (<100 individuals) with state-of-the-art systems allowing single foraminifera dating (Wacker et al., 2013; Lougheed et al., 2018). Shells can also be dated but greater care must be taken to ensure they are representative of past surficial sediments and not shells associated with mobile burrowing species (Cage and Austin, 2010; Baltzer et al., 2015).

When calibrating ^{14}C ages derived from material from the marine environment the marine reservoir effect must be considered. The marine reservoir effect occurs when the C in tissues of organisms or inorganic deposits reflects a mix of C sources and ages (Hajdas et al., 2021). The marine reservoir effect was previously accounted for by adding 400 years to an age calibrated using the northern hemisphere calibration curve (Reimer, 2020) which led to large uncertainties. With the production of the Marine20 calibration curve (Heaton et al., 2020) the marine reservoir age can now be robustly accounted for and is directly integrated into the calibration stage. The Marine20 calibration curve has significantly improved age calibration of marine samples, but it remains a global calibration; for greater accuracy local reservoir age corrections can be applied (i.e., Cage et al., 2006) if available.

Uranium/thorium paleo-dating of biologically derived fossil carbonates

For 500 to 100,000-year timescales, thorium-230 (^{230}Th) dating, also referred to as U/Th dating or ^{238}U -uranium-234 (^{234}U)- ^{230}Th dating, can be applied. This method relies on the disequilibrium due to solubility differences of uranium and thorium nuclides and involves calculating ages by studying the radioactive relationships between ^{238}U , ^{234}U , and ^{230}Th (Henderson and Anderson, 2003). It is appropriate in closed carbonate systems with no initial ^{230}Th , for example, fossil carbonates present within the terrestrial environment (e.g., rocks), but also marine carbonate formations such as corals (Cheng et al., 2000) and authigenic carbonates. It is very often used as a complementary method to ^{14}C dating of fossil carbonates and for validating results from ^{14}C dating.

Extending thorium-230 (^{230}Th) dating to marine sediments is challenging mainly due to the presence of additional ^{230}Th in materials scavenged from the seawater column. In addition, the typical levels of carbonates found in marine sediments as well as the potential post-depositional weathering, transport and

mixing processes can further limit its application (Chen et al., 2020). Nevertheless, modelling and state-of-the-art analytical tools can potentially overcome some of these challenges and thus provide valuable insights into sediment accumulation rates over longer timescales. Geibert et al. (2019) have recently presented an alternative approach using a CRS model, similarly to ^{210}Pb dating and assuming constant rate of supply of ^{230}Th from the seawater. Although alpha spectrometry can provide accurate measurement of all relevant U and Th isotopes, these techniques require labor intensive preparation steps and lengthy counting times in comparison to mass-spectrometry coupled with a laser ablation system. These state-of-the-art techniques have become the preferred analytical option (Robinson et al., 2004; Mas et al., 2020).

Anthropogenic pressures

Only carbon which is subject to manageable “undesirable human impacts”, satisfies the blue carbon criteria of Lovelock and Duarte (2019). The vulnerability of organic carbon in marine sediments to a given disturbance is a function of the organic matter’s source (*Characterising stock provenance*), and recalcitrance (*Characterising stock reactivity*). Pressures on, or conversely management and restoration of, terrestrial or coastal ecosystems which act as remote carbon sources (carbon donors) to marine sediments will affect carbon accumulation (Santos et al., 2021). Physical disturbance of the seabed which resuspends near-surface sediments into the oxic water column will recycle labile organic carbon into the ocean and potentially impact the atmospheric carbon system (Sala et al., 2021), although it can also simply re-distribute and redeposit sediments (Rijnsdorp et al., 2021). Seabed disturbance impacts the benthic faunal community, which plays a key role in the biogeochemical processes determining what fraction of deposited carbon is recycled (remineralized) or buried (stored) (de Borger et al., 2021a; de Borger et al., 2021b).

Bottom trawling is the most spatially significant anthropogenic process physically disturbing shelf sediments (Oberle et al., 2016b; Rijnsdorp et al., 2021), while wind farms have been shown to locally increase organic matter deposition (and recycling) because of faunal colonization of their structure (de Borger et al., 2021a). Other activities, including pipe and cable laying, aggregate extraction, and dredge disposal, are also expected to impact organic matter storage and deposition, although their impacts are more spatially restricted. Some continental shelf sediments are naturally subject to high disturbance, for example due to high-energy tidal bottom water currents (Thompson et al., 2019), which may locally dominate over bottom fishing disturbance (Diesing et al., 2013); these tend not to be sites with significant carbon stocks or accumulation (Diesing et al., 2021) and are therefore less vulnerable to anthropogenic disturbance from a carbon

perspective and not good sites for the implementation of management measures.

The impacts of trawling on carbon accumulation and storage are complex and differ between shelf and deeper water slope systems (Palanques et al., 2014; Pusceddu et al., 2014; Oberle et al., 2016b; Paradis et al., 2019). See Epstein et al. (2022) for a review. They depend on the properties of the carbon stock, the type of trawling equipment and frequency of trawling, as well as sediment type and faunal community (Legge et al., 2020). More research is required to improve understanding of these factors in the context of carbon storage across a range of settings. Recent work advancing towards this goal includes that of Bradshaw et al. (2021) and Morys et al. (2021) who made field measurements of the biogeochemical impacts of trawl disturbances in the Baltic Sea, and that of de Borger et al. (2021b) who modelled biogeochemical impacts of trawling scenarios at specific sampled sites in the North Sea. Global scale modelling of trawling impact (e.g., Hiddink et al., 2021; Sala et al., 2021) remains limited by the need to make broad-scale assumptions of the underlying processes and carbon characteristics which control carbon response to pressure.

In addition to their use in geochronology (see *Carbon accumulation rates*), radionuclides can also be used to evidence disturbance. In an upper section of mixed (typically bioturbated) sediments, ^{210}Pb activity is constant before being expected to decrease exponentially with depth (see *Lead-210-derived sedimentation rates and dating*) but this pattern is not observed where sediments have been physically disturbed. Physical seabed disturbance can also be confirmed qualitatively by measuring excess of thorium-234 (^{234}Th). ^{234}Th has a very short half-life (24.1 days) and is produced directly from the alpha decay of ^{238}U in the ocean. ^{238}U is a highly soluble and conservative radionuclide in seawater, whereas ^{234}Th is highly particle reactive. As ^{234}Th is preferentially adsorbed onto sinking particles, the natural secular equilibrium between the two radionuclides becomes disturbed. Consequently, an excess of ^{234}Th is expected in the upper layers of undisturbed sediment. An anthropogenic disturbance (e.g., man-made platforms or trawling) can be qualitatively confirmed if the excess of ^{234}Th is not as noticeable as in a separate sediment core collected nearby and known to be undisturbed (e.g., in a Marine Protected Areas; MPAs). ^{234}Th can be determined either by beta counting or gamma spectrometry (Buesseler et al., 2001), whereas ^{238}U is usually measured either by alpha spectrometry or ICP-MS (Forte et al., 2001).

Sampling studies investigating the impact of trawling on carbon accumulation make use of many of the analytical techniques detailed in the sections above. Oberle et al. (2016a) used 3D petroleum fingerprinting alongside ^{210}Pb dating to quantify the depth of disturbance across sites exposed to different trawling pressure. Paradis et al. (2019; 2021) measured both ^{210}Pb and ^{234}Th in a comparison of trawled and un-trawled continental margin sites. Sañé et al. (2013)

compared a number of biomarkers between trawled and un-trawled submarine canyon flank sites and found that labile amino acids in particular were less abundant in the disturbed sediments, providing evidence for increased carbon remineralization as a result of trawling disturbance and resulting differences in vulnerability to subsequent disturbance.

Even if the potential impact of trawling on sediment carbon at a particular site was well understood, data on trawling pressure (gear types, frequency) are often incomplete or not available at an appropriate spatial resolution. Trawling pressure maps are typically compiled from fishing GPS-based vessel track information (e.g., vessel monitoring systems, VMS) (e.g., Oberle et al., 2016b; Eigaard et al., 2017; Sala et al., 2021). These are limited by the temporal (and thus spatial) resolution of the fishing vessel location information, requiring application of interpolation techniques (see Russo et al., 2011) and resulting in estimated trawling intensity within spatial grid cells based on the number of times each was visited. Linking trawling pressure to sediment carbon is also complicated by the non-random distribution of trawling with respect to expected high carbon sites, e.g., trawling pressure tends to be higher in high-mud sediments, which are also highest in organic carbon (see Epstein et al., 2022 for further discussion).

Discussion

Gaining and improving understanding of the spatial distribution and variability of carbon stocks and accumulation rates and their vulnerability in shelf sea sediments is essential for their monitoring and management. As recent studies demonstrate (e.g., Sañé et al., 2013; Oberle et al., 2016a; Paradis et al., 2019; Paradis et al., 2021), layers of information derived from multiple analytical techniques are required in marine sediments to provide a mechanistic understanding in settings where carbon storage is physically distant from carbon sources, altered between source and sink, and disturbed by anthropogenic activities. We have outlined an extensive multidisciplinary toolbox of analysis techniques which are needed to achieve this understanding, summarized in Table 3.

The choice of techniques applied by any study will be determined by its specific research questions, and also by available resources. Table 3 provides a starting point with which to approach this decision. Where possible a stepwise approach to analyses should be applied by which initial parameters are analysed to inform which samples, if any, will provide information of interest from more resource-intensive analyses. It is important to distinguish between routine measurements and analyses (e.g., particle grain size, total organic carbon and C:N ratios) and emerging techniques and those which have not traditionally been applied in shelf sediments (e.g., eDNA, compound specific isotopic analyses) where ongoing method development must be considered.

Studies should aim to characterize the system by measuring more than the minimum parameters wherever possible to inform a process-level understanding. Associated explanatory parameters such as bottom water properties and pore water chemistry can allow modelling approaches to be applied, adding value to what can be obtained by measurements alone. Biogeochemical modelling can be used in two ways; to help interpret observations, and to allow scaling up and scenario exploration (for example of climate change). However, a clear understanding of which analytical outputs are needed to model a given scenario and which analytical tools can provide these outputs is needed to fully exploit modelling approaches. For example, scenario studies describing the vulnerability of carbon release to a given physical disturbance rely on knowledge of the lability of sediment carbon which must come from observation.

To assess the role of continental shelf sediments in the blue carbon framework, the analyses outlined herein – addressing the fundamental blue carbon questions of stock (its abundance, provenance, recalcitrance) and accumulation rate, and vulnerability – must be considered holistically. A key outstanding question is linking measurements to the physical and biogeochemical processes which control carbon stock and accumulation.

As studies increasingly address the knowledge gaps around continental shelf carbon stocks and accumulation – through both sampling and modelling – the management of this carbon with respect to human pressures will become the key question for understanding where it fits within the blue carbon framework and within the climate mitigation discourse (e.g., Christianson et al., 2022). Can the biogeochemical processes which mediate carbon cycling in near-surface sediments be controlled or protected such that carbon burial is maximized? Improved process understanding is required. Controlling trawling and other human activities which disturb the seabed where it acts as a carbon store appears to be a quick win, yet the impacts of disturbed sediment can extend beyond the trawled area on a regional scale (Palanques et al., 2014). If MPAs are to be used as a management tool to protect carbon stocks and accumulation in continental margin sediments (e.g., Roberts et al., 2017; Sala et al., 2021), their locations must be informed by well-mapped carbon stock and accumulation (e.g., Diesing et al., 2021) and process-level understanding (e.g., de Borger et al., 2021b).

Conclusions

The marine environment stores organic carbon in offshore as well as coastal ecosystems. In traditional coastal blue carbon habitats (saltmarsh, seagrass, mangrove) organic carbon is locally produced. Organic carbon in marine sediment is more allochthonous: it has largely been transported from terrestrial, coastal or near-surface sources and has been more significantly

TABLE 3 Summary of analyses presented and considerations for their application to improving understanding of blue carbon in continental shelf sediments.

Parameter or Analysis	Blue Carbon Relevance	Key considerations for application in shelf sediments
(organic) carbon content	fundamental measurement of carbon stock	Typically inter/extrapolated between sampled sites, which is improved by co-measurement of other sediment properties. Typically determined by EA (provides organic carbon) and not LOI (provides organic matter from which OC can be derived) in shelf sediments. Though more expensive than LOI, EA is a routinely applied analysis. In order to derive carbon stocks from percent organic carbon measurements, sediment dry bulk density must also be measured.
carbon to nitrogen ratio (C:N; N:C)	provenance	Informs on provenance only when considered alongside other OM properties. Readily determined by EA alongside OC quantification.
bulk organic matter stable isotopes	provenance	A commonly used analytical approach. When used in tandem with C:N ratios and isotopic mixing models, provides a quantitative method to estimate the proportion OM originating from different sources. Providing accurate estimates of the proportion of OC originating from different sources if (i) OM source values are well defined with minimal overlap, (ii) OM has gone through no decomposition during the transport and burial processes.
pyrolysis	provenance	Allows the whole OC pool to be analysed without requiring solvent extraction. Typically coupled with GC or GCMS to investigate compound classes.
biomarkers	provenance	n-Alkane lipid biomarkers (discussed in detail) and fatty acids, pigments, and lignin phenols (only briefly mentioned herein) provide a targeted approach capable of resolving mixed sources at high resolution. Able to discern source contributions with increased specificity (compared with bulk stable isotopes, for example) in complex environments with overlapping inputs. n-Alkane biomarkers are especially powerful when combined with Compound Specific Isotope Analysis.
eDNA	provenance	Primer choice will determine which taxa can be detected within sediment: it is unlikely that a single primer set will identify all sources of carbon. The availability and quality of reference sequences in genetic databases will affect the ease and accuracy of taxonomic assignment.
black carbon	recalcitrance	May be a significant fraction of the OC, with important implications for discussion of blue carbon. Traditional methods require acid digestion before analysis, which is avoided by temperature gradient methods.
TGA: thermogravimetric analysis	recalcitrance	A rapid low-cost approach to quantify the different OM pools (labile, recalcitrant and refractory) and characterize the reactivity of the OM in marine sediments. Can be used alongside other OM properties to assess the potential vulnerability of the OC within the marine sediments to remineralization.
amino acids	recalcitrance	Provides calculation of an index developed for OM primarily sourced from phytoplankton.
sedimentation rates by Pb-210	accumulation; disturbance (vulnerability)	A heterogeneous mineralogy and granulometry across a core will affect the application of this tool. Fine sieving will help obtain higher absolute Pb-210 concentrations. Depending on the sampling location, other fingerprinting tools from legacy human activities (including non-nuclear activities) might be available to validate any dating or sedimentation rate estimations.
radiocarbon dating (^{14}C)	Accumulation; provenance	Primary tool for gaining chronological control over long-term ($\times 10^3$ year) accumulation rates. In interpreting long-term OC accumulation rates calculated from ^{14}C factors such as compaction, changing C sources and material dated all need to be taken into consideration. Radiocarbon can also be used as a tracer to understand provenance of the OM and processes governing the transport, burial and degradation of the OM.
U/Th dating	accumulation	This approach is not applicable for dating sediment of less than 500 years and is only applicable to authigenic sediments rich in carbonates.
Th-234	disturbance (vulnerability)	Excess of Th-234 should be present only at the sediment-seawater interface. Its depth profile indicates efficient mixing of the upper sediments either by bioturbation or human activities. Comparison with another sediment sample collected from a nearby site and known to be undisturbed by human activities (e.g., MPAs) would be required to confirm a human disturbance qualitatively.

EA, Elemental Analyser; GC, Gas chromatography; GCMS, gas chromatography mass spectrometry; LOI, Loss on ignition; OC, organic carbon; OM, organic matter.

altered from its original form during transport and after deposition in near-surface sediments. Organic carbon stock and accumulation rates are smaller locally in subtidal marine sediment than in coastal blue carbon habitats, but larger when their expansive spatial extent is considered. Shelf sea sediments are subject to different anthropogenic pressures, most notably that of disturbance from bottom trawling, and require different carbon management approaches.

To establish if organic carbon stored in continental shelf sediments contributes to climate change mitigation in a manageable way, thus meeting the criteria for blue carbon,

organic carbon stock and accumulation rates must be determined alongside carbon properties which inform on its sources and stability and control its vulnerability. A multitude of analyses, brought together here as a toolbox, can be applied to answer these questions. Some analyses are already routinely applied in shelf sea sediments (e.g., percent of organic carbon content) while others continue to be developed for offshore sediment blue carbon application (e.g., eDNA). However, even for the relatively simple determination of stock, lack of co-measured dry bulk density or porosity is often a barrier to including legacy data in calculations and spatial modelling is

needed to integrate limited observations and provide a holistic picture. The field is advancing rapidly, with the application of eDNA to link coastal carbon sources to shelf sediment recipient sites and novel carbon reactivity indices being defined to inform on vulnerability. Consistency in methodology between studies through application of the toolbox we present will improve comparability and facilitate data aggregation to develop broad scale understanding.

The link between carbon stored in marine sediments, even at shelf sea water depths, and the atmospheric carbon system is moderated by the oceanic carbon cycle. More sediment carbon data collected alongside explanatory parameters (such as temperature and nutrient concentrations) are needed to better constrain the complex biogeochemical controls on the connectivity between these systems in the context of climate mitigation considerations.

Author contributions

RP and LB provided initial conceptualization of this work. CAG led a workshop attended by all authors (except SKW) where the manuscript was initiated. Workshop discussions provided the basis for the review. CAG facilitated subsequent manuscript drafting and editing. CAG, JA, FDM, VGF, NH, CH, PDL, CM, CS, SKW, and CW drafted sections of the text. All authors contributed to manuscript revision, read, and approved the submitted version.

References

- Ahmad, F., Morris, K., Law, G. T. W., Taylor, K. G., and Shaw, S. (2021). Fate of radium on the discharge of oil and gas produced water to the marine environment. *Chemosphere* 273, 129550. doi: 10.1016/j.chemosphere.2021.129550
- Alderson, D. M., Evans, M. G., Rothwell, J. J., and Boulton, S. (2016). Classifying sedimentary organics: It is a matter of quality rather than quantity. *Prog. Phys. Geogr.: Earth Environ.* 40 (3), 450–479. doi: 10.1177/0309133315625864
- Aldridge, J. N., Lessin, G., Amoudry, L. O., Hicks, N., Hull, T., Klar, J. K., et al. (2017). Comparing benthic biogeochemistry at a sandy and a muddy site in the Celtic sea using a model and observations. *Biogeochemistry* 135 (1–2), 155–182. doi: 10.1007/s10533-017-0367-0
- Anderson, E. C., Libby, W. F., Weinhouse, S., Reid, A. F., Kirshenbaum, A. D., and Grosse, A. V. (1947). Natural radiocarbon from cosmic radiation. *Phys. Rev.* 72, 931–936. doi: 10.1103/PhysRev.72.931
- Appleby, P. G., and Oldfield, F. (1978). The calculation of lead-210 dates assuming a constant rate of supply of unsupported 210Pb to the sediment. *Catena* 5 (1), 1–8. doi: 10.1016/S0341-8162(78)80002-2
- Aquino-López, M. A., Sanderson, N. K., Blaauw, M., Sanchez-Cabeza, J.-A., Ruiz-Fernandez, A. C., Aquino-López, J., et al. (2020). A simulation study to compare 210Pb dating data analyses. Available at: <http://arxiv.org/abs/2012.06819>.
- Arias-Ortiz, A., Masqué, P., Garcia-Orellana, J., Serrano, O., Mazarrasa, I., Marbá, N., et al. (2018). Reviews and syntheses: 210Pb-derived sediment and carbon accumulation rates in vegetated coastal ecosystems - setting the record straight. *Biogeosciences* 15 (22), 6791–6818. doi: 10.5194/bg-15-6791-2018
- Arndt, S., Jørgensen, B. B., LaRowe, D. E., Middelburg, J. J., Pancost, R., and Regnier, D. P. (2013). Quantifying the degradation of organic matter in marine sediments: A review and synthesis. *Earth-Sci. Rev.* 123, 53–86. doi: 10.1016/j.earscirev.2013.02.008
- Atwood, T. B., Witt, A., Mayorga, J., Hammill, E., and Sala, E. (2020). Global patterns in marine sediment carbon stocks. *Front. Mar. Sci.* 7. doi: 10.3389/fmars.2020.00165
- Ausin, B., Bruni, E., Haghipour, N., Welte, C., Bernasconi, S. M., and Eglinton, T. I. (2021). Controls on the abundance, provenance and age of organic carbon buried in continental margin sediments. *Earth Planet. Sci. Lett.* 558, 116759. doi: 10.1016/j.epsl.2021.116759
- Avellar, S., van der Voort, T. S., and Eglinton, T. I. (2017). Relevance of carbon stocks of marine sediments for national greenhouse gas inventories of maritime nations. *Carbon Balance Manage.* 12:10. doi: 10.1186/s13021-017-0077-x
- Baltar, F., Alvarez-Salgado, X. A., Aristegui, J., Benner, R., Hansell, D. A., Herndl, G. J., et al. (2021). What is refractory organic matter in the ocean? *Front. Mar. Sci.* 8: 642637. doi: 10.3389/fmars.2021.642637
- Baltzer, A., Mokeddem, Z., Goubert, E., Lartaud, F., Labourdette, N., Fournier, J., and Bourillet, J.-F. (2015). “The ‘Turritella Layer’: A Potential Proxy of a Drastic Holocene Environmental Change on the North–East Atlantic Coast,” in *Sediment fluxes in coastal areas* Eds: M. Maanan and M. Robin (Dordrecht:Springer), 3–21.
- Baskaran, M., Bianchi, T. S., and Filley, T. (2017). Inconsistencies between ¹⁴C and short-lived radionuclides-based sediment accumulation rates: effects of long-term remineralization. *J. Environ. Radioact.* 174, 10–16. doi: 10.1016/j.jenvrad.2016.07.028
- Becker, R., Altmann, K., Sommerfeld, T., and Braun, U. (2020). Quantification of microplastics in a freshwater suspended organic matter using different thermoanalytical methods – outcome of an interlaboratory comparison. *J. Anal. Appl. Pyrolysis* 148, 104829. doi: 10.1016/j.jaap.2020.104829
- Bennett, C. L., Beukens, R. P., Clover, M. R., Gove, H. E., Liebert, R. B., Litherlan, A. E., et al. (1977). Radiocarbon dating using electrostatic accelerators: Negative ions provide the key. *Science* 198, 508–510. doi: 10.1126/science.198.4316.508

Acknowledgments

This work was supported by Cefas internal Seedcorn self-investment funding under the project DP440: Blue carbon within climate mitigation and ecosystem service approaches to natural asset assessments, and by Cefas’ Ecosystem Theme science theme. We would like to thank two reviewers and editor Tim Rixen for their constructive comments which improved this review.

Conflict of interest

The authors declare that the research was conducted in the absence of any commercial or financial relationships that could be construed as a potential conflict of interest.

Publisher’s note

All claims expressed in this article are solely those of the authors and do not necessarily represent those of their affiliated organizations, or those of the publisher, the editors and the reviewers. Any product that may be evaluated in this article, or claim that may be made by its manufacturer, is not guaranteed or endorsed by the publisher.

- Beulig, F., Roy, H., Glombitza, C., and Jørgensen, B. B. (2017). Control on rate and pathway of anaerobic organic carbon degradation in the seabed. *Proc. Natl. Acad. Sci. U. S. A.* 115 (2), 367–372. doi: 10.1073/pnas.1715789115
- Bianchi, T. S., and Canuel, E. A. (2011). *Chemical biomarkers in aquatic ecosystems* (Princeton, NJ: Princeton University Press). doi: 10.23943/princeton/9780691134147.001.0001
- Bird, M. I., Fifield, L. K., Chua, S., and Goh, B. (2004). Calculating sediment compaction for radiocarbon dating of intertidal sediments. *Radiocarbon* 46, 421–435. doi: 10.1017/S0033822200039734
- Blaauw, M. (2010). Methods and code for “classical” age-modelling of radiocarbon sequences. *Quaternary Geochronol.* 5 (5), 512–518. doi: 10.1016/j.quageo.2010.01.002
- Blaauw, M., Aquino-Lopez, M., and Christen, J. A. (2021). “Bayesian improvements to 210Pb dating,” *EGU general assembly*, online, 19–30 Apr 2021, EGU21–E1596. doi: 10.5194/egusphere-egu21-1596
- Blaauw, M., and Christen, J. A. (2011). Flexible paleoclimate age-depth models using an autoregressive gamma process. *Bayesian Anal.* 6 (3), 457–474. doi: 10.1214/11-BA618
- Blaauw, M., Christen, J. A., Bennett, K. D., and Reimer, P. J. (2018). Double the dates and go for Bayes — Impacts of model choice, dating density and quality on chronologies. *Quaternary Sci. Rev.* 188, 58–66. doi: 10.1016/j.quascirev.2018.03.032
- Blattmann, T. M., Montluçon, D. B., Haghipour, N., Ishikawa, N. F., and Eglinton, T. I. (2020). Liquid chromatographic isolation of individual amino acids extracted from sediments for radiocarbon analysis. *Front. Mar. Sci.* 7, 174. doi: 10.3389/fmars.2020.00174
- Blattmann, T. M., and Ishikawa, N. F. (2020). Theoretical amino acid-specific radiocarbon content in the environment: Hypotheses to be tested and opportunities to be taken. *Front. Mar. Sci.* 7, 302. doi: 10.3389/fmars.2020.00302
- Bradshaw, C., Jakobsson, M., Brüchert, V., Bonaglia, S., Mörth, C. M., Muchowski, J., et al. (2021). Physical disturbance by bottom trawling suspends particulate matter and alters biogeochemical processes on and near the seafloor. *Front. Mar. Sci.* 8, 683331. doi: 10.3389/fmars.2021.683331
- Bray, E. E., and Evans, E. D. (1961). Distribution of n-paraffins as a clue to recognition of source beds. *Geochim. Cosmochim. Acta* 22 (1), 2–15. doi: 10.1016/0016-7037(61)90069-2
- Brodie, C. R., Leng, M. J., Casford, J. S. L., Kendrick, C. P., Lloyd, J. M., Yongqiang, Z., et al. (2011). Evidence for bias in C and N concentrations and $\delta^{13}\text{C}$ composition of terrestrial and aquatic organic materials due to pre-analysis acid preparation methods. *Chem. Geol.* 282 (3–4), 67–83. doi: 10.1016/j.chemgeo.2011.01.007
- Bruce, K., Blackman, R., Bourlat, S., Hellström, A., Bakker, J., Bista, I., et al. (2021). “A practical guide to DNA-based methods for biodiversity assessment”. Advanced books. doi: 10.3897/ab.e68634
- Buesseler, K. O., Benitez-Nelson, C., Rutgers van der Loeff, M., Andrews, J., Ball, L., Crossin, G., and Charette, M. A. (2001). An intercomparison of small- and large-volume techniques for thorium-234 in seawater. *Mar. Chem.* 74 (1), 15–28. doi: 10.1016/S0304-4203(00)00092-X
- Burdige, D. J. (2007). Preservation of organic matter in marine sediments: controls, mechanisms, and an imbalance in sediment organic carbon budgets? *Chem. Rev.* 107 (2), 467–485.
- Burrows, M. T., Kamenos, N. A., Hughes, D. J., Stahl, H., Howe, J. A., and Tett, P. (2014). *Assessment of carbon budgets and potential blue carbon stores in Scotland's coastal and marine environment. Project Report. Scottish Natural Heritage Commissioned Report No. 761.*
- Butenschön, M., Clark, J., Aldridge, J. N., Icarus Allen, J., Artioli, Y., Blackford, J., et al. (2016). ERSEM 15.06: A generic model for marine biogeochemistry and the ecosystem dynamics of the lower trophic levels. *Geosci. Model. Dev.* 9 (4), 1293–1339. doi: 10.5194/gmd-9-1293-2016
- Cage, A. G., and Austin, W. E. N. (2010). Marine climate variability during the last millennium: The Loch Sunart record, Scotland, UK. *Quaternary Sci. Rev.* 29 (13–14), 1633–1647. doi: 10.1016/j.quascirev.2010.01.014
- Cage, A. G., Davies, S. M., Wastegård, S., and Austin, W. E. N. (2011). Identification of the Icelandic Landnám tephra (AD 871±2) in Scottish fjordic sediment. *Quaternary Int.* 246, 168–176. doi: 10.1016/j.quaint.2011.08.016
- Cage, A. G., Heinemeier, J., and Austin, W. E. N. (2006). Marine radiocarbon reservoir ages in Scottish coastal and fjordic waters. *Radiocarbon* 48, 31–43. doi: 10.1017/S0033822200035372
- Canfield, D. E. (1994). Factors influencing organic carbon preservation in marine sediments. *Chem. Geol.* 114 (3–4), 315–329. doi: 10.1016/0009-2541(94)90061-2
- Capel, E. L., de la Rosa Arranz, J. M., González-Vila, F. J., González-Pérez, J. A., and Manning, D. A. C. (2006). Elucidation of different forms of organic carbon in marine sediments from the Atlantic coast of Spain using thermal analysis coupled to isotope ratio and quadrupole mass spectrometry. *Org. Geochem.* 37 (12), 1983–1994. doi: 10.1016/j.orggeochem.2006.07.025
- Chen, C. Y., McGee, D., Woods, A., Pérez, L., Hatfield, R. G., Edwards, R. L., et al. (2020). U-Th dating of lake sediments: Lessons from the 700 ka sediment record of lake Junin, Peru. *Quaternary Sci. Rev.* 244, 106422. doi: 10.1016/j.quascirev.2020.106422
- Chen, Y., Hu, C., Yang, G. P., and Gao, X. C. (2021). Source, distribution and degradation of sedimentary organic matter in the South Yellow Sea and East China Sea. *Estuar. Coast. Shelf Sci.* 255, 107372. doi: 10.1016/j.ecss.2021.107372
- Cheng, H., Adkins, J., Edwards, R. L., and Boyle, E. A. (2000). U-Th dating of deep-sea corals. *Geochim. Cosmochim. Acta* 64 (14), 2401–2416. doi: 10.1016/S0016-7037(99)00422-6
- Chew, S. T., and Gallagher, J. B. (2018). Accounting for black carbon lowers estimates of blue carbon storage services. *Sci. Rep.* 8(2553), 1–8. doi: 10.1038/s41598-018-20644-2
- Christianson, A. B., Cabré, A., Bernal, B., Baez, S. K., Leung, S., Pérez-Porro, A., et al. (2022). The promise of blue carbon climate solutions: Where the science supports ocean-climate policy. *Front. Mar. Sci.* 9, 851448. doi: 10.3389/fmars.2022.851448
- Clark, K., Karsch-Mizrachi, I., Lipman, D. J., Ostell, J., and Sayers, E. W. (2016). GenBank. *Nucleic Acids Res.* 44, D67–D72. doi: 10.1093/nar/gkv1276
- Colman, S. M., Baucom, P. C., Bratton, J. F., Cronin, T. M., McGeehin, J. P., Willard, D., et al. (2002). Radiocarbon dating, chronologic framework, and changes in accumulation rates of holocene estuarine sediments from Chesapeake Bay. *Quaternary Res.* 57 (1), 58–70. doi: 10.1006/qres.2001.2285
- Cook, G. T., MacKenzie, A. B., Muir, G. K. P., Mackie, G., and Gulliver, P. (2004). Sellafeld-derived anthropogenic ^{14}C in the marine intertidal environment of the NE Irish Sea. *Radiocarbon* 46 (2), 877–883. doi: 10.1017/S0033822200035918
- Coppola, A. I., Ziolkowski, L. A., Masiello, C. A., and Druffel, E. R. M. (2014). Aged black carbon in marine sediments and sinking particles. *Geophys. Res. Lett.* 41, 2427–2433. doi: 10.1002/2013GL059068
- Coppola, A. I., Seidel, M., Ward, N. D., Viviroli, D., Nascimento, G. S., and Haghipour, N. (2019). Carbon pools. *Nat. Commun.* 10, 4018. doi: 10.1038/s41467-019-11543-9
- Dal Molin, F., Warwick, P. E., and Read, D. (2018). Under-estimation of ^{210}Pb in industrial radioactive scales. *Anal. Chim. Acta* 1000, 67–74. doi: 10.1016/j.aca.2017.08.037
- Dang, H. (2020). Grand challenges in microbe-driven marine carbon cycling research. *Front. Microbiol.* 11. doi: 10.3389/fmicb.2020.01039
- Darby, D. A., Bischof, J. F., and Jones, G. A. (1997). Radiocarbon chronology of depositional regimes in the western Arctic Ocean. *Deep Sea Res. Part II: Top. Stud. Oceanogr.* 44 (8), 1745–1757. doi: 10.1016/S0967-0645(97)00039-8
- d'Auriac, M. A., Hancke, K., Gundersen, H., Frigstad, H., and Borgersen, G. (2021). *Blue carbon eDNA – a novel eDNA method to trace macroalgae carbon in marine sediments* (Oslo, Norway: Norwegian Institute for Water Research (NIWA)). doi: 10.13140/RG.2.2.10631.93607
- Dauwe, B., Middelburg, J. J., Herman, P. M. J., and Heip, C. H. R. (1999). Linking diagenetic alteration of amino acids and bulk organic matter reactivity. *Limnol. Oceanogr.* 44 (7), 1809–1814. doi: 10.4319/lo.1999.44.7.1809
- Dauwe, B., and Middelburg, J. J. (1998). Amino acids and hexosamines as indicators of organic matter degradation state in North Sea sediments. *Limnol. Oceanogr.* 43 (5), 782–798. doi: 10.4319/lo.1998.43.5.0782
- Davies, S. M. (2015). Cryptotephra: The revolution in correlation and precision dating. *J. Quaternary Sci.* 30(2)114–130. doi: 10.1002/jqs.2766
- de Borger, E., Ivanov, E., Capet, A., Braeckman, U., Vanaverbeke, J., Grégoire, M., and Soetaert, K. (2021a). Offshore windfarm footprint of sediment organic matter mineralization processes. *Front. Mar. Sci.* 8, 632243. doi: 10.3389/fmars.2021.632243
- de Borger, E., Tian, J., Braeckman, U., Rijnsdorp, A. D., and Soetaert, K. (2021b). Impact of bottom trawling on sediment biogeochemistry: A modelling approach. *Biogeosciences* 18, 2539–2557. doi: 10.5194/bg-18-2539-2021
- de Haas, H., Boer, W., and Van Weering, T. C. E. (1997). Recent sedimentation and organic carbon burial in a shelf sea: The North Sea. *Mar. Geol.* 144 (1–3), 131–146. doi: 10.1016/S0025-3227(97)00082-0
- Deiner, K., Bik, H. M., Mächler, E., Seymour, M., Lacoursière-Roussel, A., Altermatt, F., et al. (2017). Environmental DNA metabarcoding: Transforming how we survey animal and plant communities. *Mol. Ecol.* 26 (21), 5872–5895. doi: 10.1111/mec.14350
- Derrien, M., Brogi, S. R., and Gonçalves-Araújo, R. (2019). Characterization of aquatic organic matter: Assessment, perspectives and research priorities. *Water Res.* 163, 114908. doi: 10.1016/j.watres.2019.114908
- Derrien, M., Yang, L., and Hur, J. (2017). Lipid biomarkers and spectroscopic indices for identifying organic matter sources in aquatic environments: A review. *Water Res.* 112, 58–71. doi: 10.1016/j.watres.2017.01.023
- Diesing, M., Kröger, S., Parker, R., Jenkins, C., Mason, C., and Weston, K. (2017). Predicting the standing stock of organic carbon in surface sediments of the

North-West European continental shelf. *Biogeochemistry* 135 (1–2), 183–200. doi: 10.1007/s10533-017-0310-4

Diesing, M., Stephens, D., and Aldridge, J. (2013). A proposed method for assessing the extent of the seabed significantly affected by demersal fishing in the Greater North Sea. *ICES J. Mar. Sci.* 70 (6), 1085–1096. doi: 10.1093/icesjms/fst066

Diesing, M., Thorsnes, T., and Rún Bjarnadóttir, L. (2021). Organic carbon densities and accumulation rates in surface sediments of the North Sea and Skagerrak. *Biogeosciences* 18 (6), 2139–2160. doi: 10.5194/bg-18-2139-2021

Doetterl, S., Berhe, A. A., Nadeu, E., Wang, Z., Sommer, M., and Fiener, P. (2016). Erosion, deposition and soil carbon: A review of process-level controls, experimental tools and models to address C cycling in dynamic landscapes. *Earth-Sci. Rev.* 154, 102–122. doi: 10.1016/j.earscirev.2015.12.005

Dolliver, J., and Connor, N. O. (2022). Whole system analysis is required to determine the fate of macroalgal carbon: A systematic review. *J. Phycol.* 58(3), 364–376. doi: 10.1111/jpy.13251

Duarte, C. M., Gattuso, J.-P., Hancke, K., Gundersen, H., Filbee-Dexter, K., Pedersen, M. F., et al. (2022). Global estimates of the extent and production of macroalgal forests. *Global Ecol. Biogeogr.* 31(7), 1422–1439. doi: 10.1111/geb.13515

Eigaard, O. R., Bastardie, F., Hintzen, N. T., Buhl-Mortensen, L., Buhl-Mortensen, P., Catarino, R., et al. (2017). The footprint of bottom trawling in European waters: Distribution, intensity, and seabed integrity. *ICES J. Mar. Sci.* 74 (3), 847–865. doi: 10.1093/icesjms/fsw194

Elbrecht, V., Peinert, B., and Leese, F. (2017). Sorting things out assessing effects of unequal specimen biomass on DNA. *Ecol. Evol.* 7, 6918–6926. doi: 10.1002/ece3.3192

Environment Agency, Food Standards Agency, Food Standards Scotland, Northern Ireland Environment Agency, Natural Resources Wales and Scottish Environment Protection Agency (2021). Radioactivity in Food and the Environment 2020. *RIFE* 26. EA, FSA, FSS, NIEA, NRW and SEPA, Bristol, London, Aberdeen, Belfast, Cardiff and Stirling.

Epstein, G., Middelburg, J. J., Hawkins, J. P., Norris, C. R., and Roberts, C. M. (2022). The impact of mobile demersal fishing on carbon storage in seabed sediments. *Global Change Biol.*, 28(9), 2875–2894. doi: 10.1111/gcb.16105

Fang, Z., Yang, W., Chen, M., Zheng, M., and Hu, W. (2016). Abundance and sinking of particulate black carbon in the western Arctic and Subarctic Oceans. *Sci. Rep.* 6(29959), 1–11. doi: 10.1038/srep29959

Ficetola, G. F., Miaud, C., Pompanon, F., and Taberlet, P. (2008). Species detection using environmental DNA from water samples. *Biol. Lett.* 4 (4), 423–425. doi: 10.1098/rsbl.2008.0118

Ficetola, G. F., Pansu, J., Bonin, A., Coissac, E., Giguët-Covex, C., De Barba, M., et al. (2015). Replication levels, false presences and the estimation of the presence/absence from eDNA metabarcoding data. *Mol. Ecol. Resour.* 15 (13), 543–556. doi: 10.1111/1755-0998.12338

Filbee-Dexter, K., Pedersen, M. F., Fredriksen, S., Norderhaug, K. M., Rinde, E., Kristiansen, T., et al. (2020). Carbon export is facilitated by sea urchins transforming kelp detritus. *Oecologia* 192 (1), 213–225. doi: 10.1007/s00442-019-04571-1

Fonseca, V. G. (2018). Pitfalls in relative abundance estimation using edna metabarcoding. *Mol. Ecol. Resour.* 18 (5), 923–926. doi: 10.1111/1755-0998.12902

Fonseca, V. G., Sinniger, F., Gaspar, J. M., Quince, C., Creer, S., Power, D. M., et al. (2017). Revealing higher than expected meiofaunal diversity in Antarctic sediments: A metabarcoding approach. *Sci. Rep.* 7 (1), 1–11. doi: 10.1038/s41598-017-06687-x

Fonseca, V. G., and Lallias, D. (2016). Metabarcoding marine sediments: Preparation of amplicon libraries. *Methods Mol. Biol.* 1452, 183–196. doi: 10.1007/978-1-4939-3774-5_12

Forte, M., Rusconi, R., Margini, C., Abbate, G., Maltese, S., Badalamenti, P., and Bellinzona, S. (2001). Determination of uranium isotopes in food and environmental samples by different techniques: A comparison. *Radiat. Prot. Dosimetry* 97 (4), 325–328. doi: 10.1093/oxfordjournals.rpd.a006681

García-Tenorio, R., Rozmaric, M., Harms, A., Godoy, J. M.D.O., Barsanti, M., Schirone, A., et al. (2020). From radiometry to chronology of a marine sediment core: A 210Pb dating interlaboratory comparison exercise organised by the IAEA. *Mar. Pollut. Bull.* 159, 111490. doi: 10.1016/j.marpolbul.2020.111490

Geibert, W., Stimac, I., Rutgers van der Loeff, M. M., and Kuhn, G. (2019). Dating deep-sea sediments with 230Th excess using a constant rate of supply model. *Paleoceanography Paleoclimatology* 34 (12), 1895–1912. doi: 10.1029/2019PA003663

Geraldi, N. R., Ortega, A., Serrano, O., Macreadie, P. I., Lovelock, C. E., Krause-Jensen, D., et al. (2019). Fingerprinting blue carbon: Rationale and tools to determine the source of organic carbon in marine depositional environments. *Front. Mar. Sci.* 6. doi: 10.3389/fmars.2019.00263

Geraldi, N. R., Díaz-Rúa, R., Shea, L. A., and Duarte, C. M. (2020). Performance of extraction methods for extracellular DNA from sediments across marine habitats. *Environ. DNA* 2 (1), 91–98. doi: 10.1002/edn3.48

Gilbey, J., Carvalho, G., Castilho, R., Coscia, I., Coulson, M. W., Dahle, G., et al. (2021). Life in a drop: Sampling environmental DNA for marine fishery management and ecosystem monitoring. *Mar. Policy* 124, 104331. doi: 10.1016/j.marpol.2020.104331

Glaser, B., Haumaier, L., Guggenberger, G., and Zech, W. (1998). Black carbon in soils: The use of benzenecarboxylic acids as specific markers. *Org. Geochem.* 29 (4), 811–819. doi: 10.1016/S0146-6380(98)00194-6

Goidts, E., Van Wesemael, B., and Crucifix, M. (2009). Magnitude and sources of uncertainties in soil organic carbon (SOC) stock assessments at various scales. *Eur. J. Soil Sci.* 60 (5), 723–739. doi: 10.1111/j.1365-2389.2009.01157.x

Gordon, E. S., and Goni, M. A. (2003). Sources and distribution of terrigenous organic matter delivered by the Atchafalaya river to sediments in the northern Gulf of Mexico. *Geochim. Cosmochim. Acta* 67 (13), 2359–2375. doi: 10.1016/S0016-7037(02)01412-6

Gregg, R., Elias, J. L., Alonso, I., Crosher, I. E., Muto, P., and Morecroft, M. D. (2021). Carbon storage and sequestration by habitat: A review of the evidence (second edition) Natural England Research Report NERR094. in *Natural England research report*.

Grey, E. K., Bernatchez, L., Cassey, P., Deiner, K., Deveney, M., Howland, K. L., et al. (2018). Effects of sampling effort on biodiversity patterns estimated from environmental DNA metabarcoding surveys. *Sci. Rep.* 8 (1), 2–11. doi: 10.1038/s41598-018-27048-2

Gulliver, P., Cook, G. T., MacKenzie, A. B., Naysmith, P., and Anderson, R. (2001). Transport of Sellafield-derived 14C from the Irish Sea through the North Channel. *Radiocarbon* 43 (2B), 869–877. doi: 10.1017/S0033822200041539

Guo, L., Semiletov, I., Gustafsson, Ö., Ingri, J., Andersson, P., Dudarev, O., and White, D. (2004). Characterization of Siberian Arctic coastal sediments: Implications for terrestrial organic carbon export. *Global Biogeochem. Cycles* 18 (1), GB1036. doi: 10.1029/2003gb002087

Guo, L., White, D. M., Xu, C., and Santschi, P. H. (2009). Chemical and isotopic composition of high-molecular-weight dissolved organic matter from the Mississippi River plume. *Mar. Chem.* 114 (3–4), 63–71. doi: 10.1016/j.marchem.2009.04.002

Gustafsson, Ö., Bucheli, T. D., Kukulska, Z., Andersson, M., Largeau, C., Rouzaud, J. N., et al. (2001). Evaluation of a protocol for the quantification of black carbon in sediments. *Global Biogeochem. Cycles* 15 (4), 881–890. doi: 10.1029/2000GB001380

Haghipour, N., Ausin, B., Usman, M. O., Ishikawa, N., Wacker, L., Welte, C., et al. (2019). Compound-specific radiocarbon analysis by elemental analyzer-accelerator mass spectrometry: Precision and limitations. *Anal. Chem.* 91, 2042–2049. doi: 10.1021/acs.analchem.8b04491

Hajdas, I., Ascough, P., Garnett, M. H., Fallon, S. J., Pearson, C. L., Quarta, G., et al. (2021). Radiocarbon dating. *Nat. Rev. Methods Primers* 1, 1–26. doi: 10.1038/s43586-021-00058-7

Hammes, K., Schmidt, M. W.I., Smernik, R. J., Currie, L. A., Ball, W. P., Nguyen, T. H., et al. (2007). Comparison of quantification methods to measure fire-derived (black-elemental) carbon in soils and sediments using reference materials from soil, water, sediment and the atmosphere. *Global Biogeochem. Cycles* 21 (3), GB3016. doi: 10.1029/2006GB002914

Hansell, D. A. (2013). Recalcitrant dissolved organic carbon fractions. *Annu. Rev. Mar. Sci.* 5, 421–425. doi: 10.1146/annurev-marine-120710-100757

Harris, D., Horváth, W. R., and Van Kessel, C. (2001). Acid fumigation of soils to remove carbonates prior to total organic carbon or carbon-13 isotopic analysis. *Soil Sci. Soc. America J.* 65, 1853–1856. doi: 10.2136/sssaj2001.1853

Harrison, J. B., Sunday, J. M., and Rogers, S. M. (2019). Predicting the fate of eDNA in the environment and implications for studying biodiversity. *Proc. R. Soc. B: Biol. Sci.* 286 (1915), 20191409. doi: 10.1098/rspb.2019.1409

Hassen, N. E. H., Reguigui, N., Helali, M. A., Mejjad, N., Laissaoui, A., Benkdad, A., et al. (2020). Evaluating the historical sedimentation patterns in two different Mediterranean deep environments (Sardinia and Sicily Channels). *Mediterr. Mar. Sci.* 20 (3), 542–548. doi: 10.12681/mms.19558

Heaton, T., Blaauw, M., Blackwell, P., Ramsey, C. B., Reimer, P., and Scott, E. (2020). The IntCal20 approach to radiocarbon calibration curve construction: A new methodology using bayesian splines and errors-in-Variables. *Radiocarbon* 62 (4), 821–863. doi: 10.1017/RDC.2020.46

Henderson, G. M., and Anderson, R. F. (2003). The U-series toolbox for paleoceanography. *Uranium-series Geochem.* 52, 493–531. doi: 10.1515/9781501509308-017

Hiddink, J. G., van de Velde, S. J., McConnaughey, R. A., de Broger, E., and O'Neill, F. G. (2021). 'Quantifying the carbon benefits of ending bottom trawling'. Available at: https://figshare.com/articles/preprint/Quantifying_the_carbon_benefits_of_ending_bottom_trawling/16722808.

Hogg, A. G., Heaton, T. J., Hua, Q., Palmer, J. G., Turney, C. S., Southon, J., et al. (2020). SHCal20 southern hemisphere calibration, 0–55,000 years cal BP. *Radiocarbon* 62 (4), 759–778. doi: 10.1017/RDC.2020.59

- Howard, J., Hoyt, S., Isensee, K., Telszewski, M., and Pidgeon, E. (eds.) (2014). *Coastal Blue Carbon: Methods for assessing carbon stocks and emissions factors in mangroves, tidal salt marshes, and seagrasses*. Arlington, Virginia, USA: Conservation International, Intergovernmental Oceanographic Commission of UNESCO, International Union for Conservation of Nature.
- Hua, Q., Barbetti, M., and Rakowski, A. Z. (2013). Atmospheric radiocarbon for the period 1950–2010. *Radiocarbon* 55 (4), 2059–2072. doi: 10.2458/azu_js_rc.v55i2.16177
- Humphreys, M. P., Achterberg, E. P., Hopkins, J. E., Chowdhury, M. Z. H., Griffiths, A. M., Hartman, S. E., et al. (2019). Mechanisms for a nutrient-conserving carbon pump in a seasonally stratified, temperate continental shelf sea. *Prog. Oceanogr.* 177, 101961. doi: 10.1016/j.pocean.2018.05.001
- Hunt, C., Demšar, U., Dove, D., Smeaton, C., Cooper, R., and Austin, W. E. N. (2020). Quantifying marine sedimentary carbon: A new spatial analysis approach using seafloor acoustics, imagery, and ground-truthing data in Scotland. *Front. Mar. Sci.* 7, 588. doi: 10.3389/fmars.2020.00588
- IAEA (2010). *Analytical methodology for the determination of radium isotopes in environmental samples* (Vienna, Austria: IAEA).
- IPCC (2008). *IPCC guidelines for national greenhouse gas inventories—a primer*. Ed. H. S. Eggleston, et al. (Japan: National Greenhouse Gas Inventories Programme).
- IPCC (2013). *2013 Supplement to the 2006 IPCC guidelines for national greenhouse gas inventories: Wetlands*. Ed. T. Hiraishi, T. Krug, K. Tanabe, N. Srivastava, J. Baasansuren, M. Fukuda, et al. (Switzerland: IPCC).
- Jablonski, S. A., Mccray, E. L., Munson, J. M., and Blackwood, D. S. (2002). *Geochemical sediment analysis procedures*. Available at: <https://pubs.usgs.gov/of/2002/of02-371/>. (Accessed August 2022)
- Jenkins, C. (2005). 'Summary of the on CALCULATION methods used in dbSEABED'. Ed. B. J. Buczkowski, J. A. Reid, C. J. Jenkins, J. M. Reid, S. J. Williams and J. G. Flocks (Gulf of Mexico and Caribbean/Puerto Rico and U.S. Virgin Islands): Offshore Surficial Sediment Data Release: U.S. Geological Survey DataSeries 146.
- Jenkins, C. (2018). Sediment accumulation rates for the Mississippi Delta region: A time-interval synthesis. *J. Sediment. Res.* 88 (2), 301–309. doi: 10.2110/jsr.2018.15
- Jo, T., and Minamoto, T. (2021). Complex interactions between environmental DNA (eDNA) state and water chemistries on eDNA persistence suggested by meta-analyses. *Mol. Ecol. Resour.* 21 (5), 1490–1503. doi: 10.1111/1755-0998.13354
- Kaloustian, J., Pauli, A. M., and Pastor, J. (2001). Kinetic study of the thermal decompositions of biopolymers extracted from various plants. *J. Therm. Anal. Calorim.* 63, 7–20. doi: 10.1023/A:1010199831895
- Kershaw, P. (1986). Radiocarbon dating of Irish Sea sediments. *Estuar. Coast. Shelf Sci.* 23 (2), 295–303. doi: 10.1016/0272-7714(86)90029-6
- Kharbush, J. J., Close, H. G., Van Mooy, B. A. S., Arnosti, C., Smittenberg, R. H., Le Moigne, F. A. C., et al. (2020). Particulate organic carbon deconstructed: Molecular and chemical composition of particulate organic carbon in the ocean. *Front. Mar. Sci.* 7. doi: 10.3389/fmars.2020.00518
- Kleber, M., Bourq, I. C., Coward, E. K., Hansel, C. M., Myneni, S. C. B., and Numan, N. (2021). Dynamic interactions at the mineral–organic matter interface. *Nat. Rev. Earth Environ.* 2, 402–421. doi: 10.1038/s43017-021-00162-y
- Kokubu, Y., Rothäusler, E., Filippi, J. B., Durieux, E. D. H., and Komatsu, T. (2019). Revealing the deposition of macrophytes transported offshore: Evidence of their long-distance dispersal and seasonal aggregation to the deep sea. *Sci. Rep.* 9 (1), 4331. doi: 10.1038/s41598-019-39982-w
- Komada, T. (2008). Carbonate removal from coastal sediments for the determination of organic carbon and its isotopic signatures, $\delta^{13}\text{C}$ and $\Delta^{14}\text{C}$: Comparison of fumigation and direct acidification by hydrochloric acid. *Limnol. Oceanogr. Methods* 6(6), 254–262. doi: 10.4319/lom.2008.6.254
- Krause-Jensen, D., and Duarte, C. M. (2016). Substantial role of macroalgae in marine carbon sequestration. *Nat. Geosci.* 9 (10), 737–742. doi: 10.1038/ngeo2790
- Krause-Jensen, D., Lavery, P., Serrano, O., Marba, N., Masque, P., and Duarte, C. M. (2018). Sequestration of macroalgal carbon: The elephant in the blue carbon room. *Biol. Lett.* 14 (6), 20180236. doi: 10.1098/rsbl.2018.0236
- Kristensen, E. (1990). Characterization of biogenic organic matter by stepwise thermogravimetry (STG). *Biogeochemistry* 9, 135–159. doi: 10.1007/BF00692169
- Kühn, W., Pätsch, J., Thomas, H., Borges, A. V., Schiettecatte, L.-S., Bozec, Y., et al. (2010). Nitrogen and carbon cycling in the North Sea and exchange with the North Atlantic—a model study, part II: Carbon budget and fluxes. *Cont. Shelf Res.* 30 (16), 1701–1716. doi: 10.1016/j.csr.2010.07.001
- Kumar, M., Boski, T., González-Vila, F. J., de la Rosa, J. M., and González-Pérez, J. A. (2020). Discerning natural and anthropogenic organic matter inputs to salt marsh sediments of Ria Formosa lagoon (South Portugal). *Environ. Sci. Pollut. Res.* 27 (23), 28962–28985. doi: 10.1007/s11356-020-09235-9
- Kutschera, W. (2013). Applications of accelerator mass spectrometry. *Int. J. Mass Spectrom.* 349, 203–218. doi: 10.1016/j.jms.2013.05.023
- Lafratta, A., Serrano, O., Masqué, P., Mateo, M. A., Fernandes, M., Gaylard, S., et al. (2020). Challenges to select suitable habitats and demonstrate 'additionality' in Blue Carbon projects: A seagrass case study. *Ocean Coast. Manage.* 197, 105295. doi: 10.1016/j.ocecoaman.2020.105295
- Lallias, D., Hiddink, J. G., Fonseca, V. G., Gaspar, J. M., Sung, W., Neill, S. P., et al. (2015). Environmental metabarcoding reveals heterogeneous drivers of microbial eukaryote diversity in contrasting estuarine ecosystems. *ISME J.* 9 (5), 1208–1221. doi: 10.1038/ismej.2014.213
- Lalonde, K., Mucci, A., Ouellet, A., and Gélina, Y. (2012). Preservation of organic matter in sediments promoted by iron. *Nature* 483 (7388), 198–200. doi: 10.1038/nature10855
- Lamb, P. D., Hunter, E., Pinnegar, J. K., Creer, S., Davies, R. G., and Taylor, M. I. (2019). How quantitative is metabarcoding: A meta-analytical approach. *Mol. Ecol.* 28 (2), 420–430. doi: 10.1111/mec.14920
- Landenmark, H. K. E., Forgan, D. H., and Cockell, C. S. (2015). An estimate of the total DNA in the biosphere. *PLoS Biol.* 13 (6), 1–10. doi: 10.1371/journal.pbio.1002168
- LaRowe, D. E., Arndt, S., Bradley, J. A., Estes, E. R., Hoarfrost, A., Lang, S. Q., et al. (2020). The fate of organic carbon in marine sediments - new insights from recent data and analysis. *Earth-Sci. Rev.* 204, 103146. doi: 10.1016/j.earscirev.2020.103146
- Legge, O., Johnson, M., Hicks, N., Jickells, T., Diesing, M., Aldridge, J., et al. (2020). Carbon on the northwest European shelf: Contemporary budget and future influences. *Front. Mar. Sci.* 7, 143. doi: 10.3389/fmars.2020.00143
- Leonard, A., Castle, S., Burr, G. S., Lange, T., and Thomas, J. (2013). A wet oxidation method for AMS radiocarbon analysis of dissolved organic carbon in water. *Radiocarbon* 55, 545–552. doi: 10.1017/S0033822200057672
- Libby, W. F. (1955). *Radiocarbon Dating, 2nd edition* Chicago, University of Chicago Press: 175p.
- Libby, W. F., Anderson, E. C., and Arnold, J. R. (1949). Age determination by radiocarbon content — world-wide assay of natural radiocarbon. *Science* 109, 227–228. doi: 10.1126/science.109.2827.227
- Litherland, A., Zhao, X. L., and Kieser, W. (2011). Mass spectrometry with accelerators. *Mass Spectrom. Rev.* 30, 1037–1072. doi: 10.1002/mas.20311
- Loh, P. S., Reeves, A. D., Harvey, S. M., Overnell, J., and Miller, J. A. E. J. (2008). The fate of terrestrial organic matter in two Scottish sea lochs. *Estuar. Coast. Shelf Sci.* 76 (3), 566–579. doi: 10.1016/j.ecss.2007.07.023
- Lopez-Capel, E., Bol, R., and Manning, D. A. C. (2005). Application of simultaneous thermal analysis mass spectrometry and stable carbon isotope analysis in a carbon sequestration study. *Rapid Commun. Mass Spectrom.* 19 (22), 3192–3198. doi: 10.1002/rcm.2145
- Lougheed, B. C., Metcalfe, B., Ninnemann, U. S., and Wacker, L. (2018). Moving beyond the age–depth model paradigm in deep-sea palaeoclimate archives: Dual radiocarbon and stable isotope analysis on single foraminifera. *Climate Past* 14 (4), 515–526. doi: 10.5194/cp-14-515-2018
- Lougheed, B., and Obrochta, S. J. (2016). MatCal: open source bayesian 14C age calibration in MatLab. *J. Open Res. Software* 4, e42. doi: 10.5334/jors.130
- Lovelock, C. E., and Duarte, C. M. (2019). Dimensions of blue carbon and emerging perspectives. *Biol. Lett.* 15 (3), 20180781. doi: 10.1098/rsbl.2018.0781
- Luisetti, T., Turner, R. K., Andrews, J. E., Jickells, T. D., Kröger, S., Diesing, M., et al. (2019). Quantifying and valuing carbon flows and stores in coastal and shelf ecosystems in the UK. *Ecosyst. Serv.* 35, 67–76. doi: 10.1016/j.ecoser.2018.10.013
- Luisetti, T., Ferrini, S., Grilli, G., Jickells, T. D., Kennedy, H., Kröger, S., et al. (2020). Climate action requires new accounting guidance and governance frameworks to manage carbon in shelf seas. *Nat. Commun.* 11 (1), 4599. doi: 10.1038/s41467-020-18242-w
- MacKenzie, A. B., Hardie, S. M.L., Farmer, J. G., Eades, L. J., and Pulford, I. D. (2011). Analytical and sampling constraints in 210Pb dating. *Sci. Total Environ.* 409 (7), 1298–1304. doi: 10.1016/j.scitotenv.2010.11.040
- Macreadie, P. I., Anton, A., Raven, J. A., Beaumont, N., Connolly, R. M., Friess, D. A., et al. (2019). The future of blue carbon science. *Nat. Commun.* 10 (1), 3998. doi: 10.1038/s41467-019-11693-w
- Madsen, A. T., Murray, A. S., Andersen, T. J., Pejrup, M., and Breuning-Madsen, H. (2005). Optically stimulated luminescence dating of young estuarine sediments: A comparison with 210Pb and 137Cs dating. *Mar. Geol.* 214 (1–3), 251–268. doi: 10.1016/j.margeo.2004.10.034
- Manning, D. A. C., Lopez-Capel, E., and Barker, S. (2005). Seeing soil carbon: Use of thermal analysis in the characterization of soil C reservoirs of differing stability. *Mineral. Mag.* 69 (4), 425–435. doi: 10.1180/0026461056940260
- Mas, J. L., Aparicio, P., Galán, E., Romero-Baena, A., Miras, A., Yuste, A., and Martín, D. (2020). Determination of uranium and thorium isotopes in kaolinitic samples by ICP-MS/MS. *Appl. Clay Sci.* 196, 105736. doi: 10.1016/j.clay.2020.105736

- Masiello, C. A. (2004). New directions in black carbon organic geochemistry. *Mar. Chem.* 92, 201–213. doi: 10.1016/j.marchem.2004.06.043
- Masiello, C. A., Druffel, E. R. M., and Currie, L. A. (2002). Radiocarbon measurements of black carbon in aerosols and ocean sediments. *Geochim. Cosmochim. Acta* 66 (6), 1025–1036. doi: 10.1016/S0016-7037(01)00831-6
- Mauquoy, D., Payne, R. J., Babeshko, K. V., Bartlett, R., Boomer, I., Bowey, H., et al. (2020). Falkland Island peatland development processes and the pervasive presence of fire. *Quaternary Sci. Rev.* 240, 106391. doi: 10.1016/j.quascirev.2020.106391
- Meyers, P. A. (1994). Preservation of elemental and isotopic source identification of sedimentary organic matter. *Chem. Geol.* 114 (3–4), 289–302. doi: 10.1016/0009-2541(94)90059-0
- Middelburg, J. J. (2018). Reviews and syntheses: To the bottom of carbon processing at the seafloor. *Biogeosciences* 15 (2), 413–427. doi: 10.5194/bg-15-413-2018
- Middelburg, J. J., Nieuwenhuize, J., and Van Breugel, P. (1999). Black carbon in marine sediments. *Mar. Chem.* 65 (3–4), 245–252. doi: 10.1016/S0304-4203(99)00005-5
- Molnár, M., Hajdas, I., Janovics, R., Rinyu, L., Synal, H. A., Veres, M., and Wacker, L. (2013). C-14 analysis of groundwater down to the millilitre level. *Nucl. Instrum. Methods Phys. Res. Section B: Beam Interact. Mater. Atoms* 294, 573–576. doi: 10.1016/j.nimb.2012.03.038
- Morys, C., Brüchert, V., and Bradshaw, C. (2021). Impacts of bottom trawling on benthic biogeochemistry in muddy sediments: Removal of surface sediment using an experimental field study. *Mar. Environ. Res.* 169, 105384. doi: 10.1016/j.marenvres.2021.105384
- Najjar, R. G., Herrmann, M., Alexander, R., Boyer, E. W., Burdige, D. J., Butman, D., et al. (2018). Carbon budget of tidal wetlands, estuaries, and shelf waters of eastern North America. *Global Biogeochem. Cycles* 32 (3), 389–416. doi: 10.1002/2017GB005790
- Natali, C., Bianchini, G., and Carlino, P. (2020). Thermal stability of soil carbon pools: Inferences on soil nature and evolution. *Thermochim. Acta* 683, 178478. doi: 10.1016/j.tca.2019.178478
- Nieuwenhuize, J., Maas, Y. E., and Middelburg, J. J. (1994). Rapid analysis of organic carbon and nitrogen in particulate materials. *Mar. Chem.* 45 (3), 217–224. doi: 10.1016/0304-4203(94)90005-1
- Oberle, F. K. J., Storz, C. D., and Hanebuth, T. J. J. (2016b). What a drag: Quantifying the global impact of chronic bottom trawling on continental shelf sediment. *J. Mar. Syst.* 159, 109–119. doi: 10.1016/j.jmarsys.2015.12.007
- Oberle, F. K. J., Swarzenski, P. W., Reddy, C. M., Nelson, R. K., Baasch, B., and Hanebuth, T. J. J. (2016a). Deciphering the lithological consequences of bottom trawling to sedimentary habitats on the shelf. *J. Mar. Syst.* 159, 120–131. doi: 10.1016/j.jmarsys.2015.12.008
- Ortega, A., Gerdali, N. R., Alam, I., Kamau, A. A., Acinas, S. G., Logares, R., et al. (2019). Important contribution of macroalgae to oceanic carbon sequestration. *Nat. Geosci.* 12 (9), 748–754. doi: 10.1038/s41561-019-0421-8
- Ortega, A., Gerdali, N. R., and Duarte, C. M. (2020). Environmental DNA identifies marine macrophyte contributions to blue carbon sediments. *Limnol. Oceanogr.* 65 (12), 3139–3149. doi: 10.1002/lno.11579
- Oudghiri, F., García-Morales, J. L., and Rodríguez-Barroso, M. R. (2015). Novel use of TGA-FTIR technique to predict the pollution degree in marine sediments. *Infrared Phys. Technol.* 72, 52–57. doi: 10.1016/j.infrared.2015.07.006
- Palanques, A., Puig, P., Guillén, J., Demestre, M., and Martín, J. (2014). Effects of bottom trawling on the Ebro continental shelf sedimentary system (NW Mediterranean). *Cont. Shelf Res.* 72, 83–98. doi: 10.1016/J.CSR.2013.10.008
- Pappa, F. K., Tsabaris, C., Patiris, D. L., Eleftheriou, G., Ioannidou, A., Androulakis, E. G., et al. (2019). Temporal investigation of radionuclides and heavy metals in a coastal mining area at Ierissos Gulf, Greece. *Environ. Sci. Pollut. Res.* 26 (26), 27457–27469. doi: 10.1007/s11356-019-05921-5
- Paradis, S., Pusceddu, A., Masqué, P., Puig, P., Moccia, D., Russo, T., Iacono, L. O., et al. (2019). Organic matter contents and degradation in a highly trawled area during fresh particle inputs (Gulf of Castellammare, southwestern Mediterranean). *Biogeosciences* 16 (21), 4307–4320. doi: 10.5194/bg-16-4307-2019
- Paradis, S., Goñi, M., Masqué, P., Durán, R., Arjona-Camas, M., Palanques, A., et al. (2021). Persistence of biogeochemical alterations of deep-sea sediments by bottom trawling. *Geophys. Res. Lett.* 48, e2020GL091279. doi: 10.1029/2020GL091279
- Pawlowski, J., Bruce, K., Panksep, K., Aguirre, F. I., Amalfitano, S., Apothéloz-Perret-Gentil, L., et al. (2022). Environmental DNA metabarcoding for benthic monitoring: A review of sediment sampling and DNA extraction methods. *Sci. Total Environ.* 818, 151783. doi: 10.1016/j.scitotenv.2021.151783
- Perdue, E. M., and Koprivnjak, J. F. (2007). Using the C/N ratio to estimate terrigenous inputs of organic matter to aquatic environments. *Estuar. Coast. Shelf Sci.* 73 (1–2), 65–72. doi: 10.1016/j.ecss.2006.12.021
- Pessarrodona, A., Moore, P. J., Sayer, M. D. J., and Smale, D. A. (2018). Carbon assimilation and transfer through kelp forests in the NE Atlantic is diminished under a warmer ocean climate. *Global Change Biol.* 24 (9), 4386–4398. doi: 10.1111/gcb.14303
- Phillips, S. C., Johnson, J. E., Miranda, E., and Disenhorf, C. (2011). Improving CHN measurements in carbonate-rich marine sediments. *Limnol. Oceanogr.* 9, 194–203. doi: 10.4319/lom.2011.9.194
- Pusceddu, A., Bianchelli, S., Martín, J., Puig, P., Palanques, A., Masqué, P., and Danovaro, R. (2014). Chronic and intensive bottom trawling impairs deep-sea biodiversity and ecosystem functioning. *Proc. Natl. Acad. Sci. U. S. A.* 111 (24), 8861–8866. doi: 10.1073/pnas.1405454111
- Queirós, A. M., Stephens, N., Widdicombe, S., Tait, K., McCoy, S. J., Ingels, J., et al. (2019). Connected macroalgal-sediment systems: Blue carbon and food webs in the deep coastal ocean. *Ecol. Monogr.* 89 (3), 1–21. doi: 10.1002/ecm.1366
- Ramsey, C. B. (1995). Radiocarbon calibration and analysis of stratigraphy: The OxCal program. *Radiocarbon* 37, 425–430. doi: 10.1017/S0033822200030903
- Ramsey, C. B. (2009). Bayesian analysis of radiocarbon dates. *Radiocarbon* 51 (1), 337–360. doi: 10.1017/s0033822200033865
- Ramsey, C. B., Heaton, T. J., Schlögl, G., Staff, R. A., Bryant, C. L., Brauer, A., et al. (2020). Reanalysis of the atmospheric radiocarbon calibration record from Lake Suigetsu, Japan. *Radiocarbon* 62 (4), 989–999. doi: 10.1017/RDC.2020.18
- Ratnasingham, S., and Hebert, P. D. N. (2007). BOLD: The barcode of life data system: Barcoding. *Mol. Ecol. Notes* 7 (3), 355–364. doi: 10.1111/j.1471-8286.2007.01678.x
- Reef, R., Atwood, T. B., Samper-Villarreal, J., Adame, M. F., Sampayo, E. M., and Lovelock, C. E. (2017). Using eDNA to determine the source of organic carbon in seagrass meadows. *Limnol. Oceanogr.* 62 (3), 1254–1265. doi: 10.1002/lno.10499
- Reimer, P. (2020). Composition and consequences of the IntCal20 radiocarbon calibration curve. *Quaternary Res.* 96, 22–27. doi: 10.1017/qua.2020.42
- Reiss, H., Wiekling, G., and Kröncke, I. (2007). Microphytobenthos of the Dogger Bank: A comparison between shallow and deep areas using phytoplankton composition of the sediment. *Mar. Biol.* 150, 1061–1071. doi: 10.1007/s00227-006-0423-0
- Ren, P., Liu, Y., Shi, X., Sun, S., Fan, D., and Wang, X. (2019). Sources and sink of black carbon in Arctic Ocean sediments. *Sci. Total Environ.* 689, 912–920. doi: 10.1016/j.scitotenv.2019.06.437
- Rijnsdorp, A. D., Depestele, J., Molenaar, P., Eigaard, O. R., Ivanović, A., and O'Neill, F. G. (2021). Sediment mobilization by bottom trawls: A model approach applied to the Dutch North Sea beam trawl fishery. *ICES J. Mar. Sci.* 78 (5), 1574–1586. doi: 10.1093/icesjms/fsab029
- Robbins, J. A. (1978). “Geochemical and geophysical applications of radioactive lead,” in *The biogeochemistry of lead in the environment*. Ed. J. O. Nriagu (Amsterdam: North-Holland Biomedical Press), 285–393.
- Roberts, C. M., O'Leary, B. C., Mccauley, D. J., Cury, P. M., Duarte, C. M., Lubchenco, J., et al. (2017). Marine reserves can mitigate and promote adaptation to climate change. *Proc. Natl. Acad. Sci. United States America* 114 (24), 6167–6175. doi: 10.1073/pnas.1701262114
- Robinson, L. F., Belshaw, N. S., and Henderson, G. M. (2004). U and Th concentrations and isotope ratios in modern carbonates and waters from the Bahamas. *Geochim. Cosmochim. Acta* 68 (8), 1777–1789. doi: 10.1016/j.gca.2003.10.005
- Russo, T., Parisi, A., and Cataudella, S. (2011). New insights in interpolating fishing tracks from VMS data for different métiers. *Fish. Res.* 108 (1), 184–194. doi: 10.1016/j.fishres.2010.12.020
- Sadler, P. M. (1981). Sediment accumulation rates and the completeness of stratigraphic sections. *J. Geol.* 89.5, 569–584. doi: 10.1086/628623
- Sahu, S. K., Ajmal, P. Y., Bhangare, R. C., Tiwari, M., and Pandit, G. G. (2014). Natural radioactivity assessment of a phosphate fertilizer plant area. *J. Radiat. Res. Appl. Sci.* 7 (1), 123–128. doi: 10.1016/j.jrras.2014.01.001
- Sala, E., Mayorga, J., Bradley, D., Cabral, R. B., Atwood, T. B., Auber, A., et al. (2021). Protecting the global ocean for biodiversity, food and climate. *Nature* 592, 397–402. doi: 10.1038/s41586-021-03371-z
- Sanches, L. F., Guenet, B., dos Anjos Cristiano Marino, N., and de Assis Esteves, F. (2021). Exploring the drivers controlling the priming effect and its magnitude in aquatic systems. *J. Geophys. Res.: Biogeosci.* 126, e2020JG006201. doi: 10.1029/2020JG006201
- Sañé, E., Martín, J., Puig, P., and Palanques, A. (2013). Organic biomarkers in deep-sea regions affected by bottom trawling: Pigments, fatty acids, amino acids and carbohydrates in surface sediments from the La Fonera (Palamós) canyon, NW Mediterranean Sea. *Biogeosciences* 10 (12), 8093–8108. doi: 10.5194/bg-10-8093-2013
- Santos, G. M., Granato-Souza, D., Barbosa, A. C., Oelkers, R., and Andreu-Hayles, L. (2020). Radiocarbon analysis confirms annual periodicity in cedrela odorata tree rings from the equatorial Amazon. *Quaternary Geochronol.* 58, 101079. doi: 10.1016/j.quageo.2020.101079

- Santos, I. R., Burdige, D. J., Jennerjahn, T. C., Bouillon, S., Cabral, A., Serrano, O., et al. (2021). The renaissance of Odum's outwelling hypothesis in "Blue Carbon" science. *Estuar. Coast. Shelf Sci.* 255, 107361. doi: 10.1016/j.ecss.2021.107361
- Santschi, P. H., and Rowe, G. T. (2008). Radiocarbon-derived sedimentation rates in the Gulf of Mexico. *Deep Sea Res. Part II: Top. Stud. Oceanogr.* 55 (24–26), 2572–2576. doi: 10.1016/j.dsr2.2008.07.005
- Schmidt, S., Howa, H., Diallo, A., Martin, J., Cremer, M., Duros, P., et al. (2014). Recent sediment transport and deposition in the Cap-Ferret Canyon, South-East Margin of Bay of Biscay. *Deep-Sea Res. Part II: Top. Stud. Oceanogr.* 104, 134–144. doi: 10.1016/j.dsr2.2013.06.004
- Serpetti, N., Heath, M., Rose, M., and Witte, U. (2012). High resolution mapping of sediment organic matter from acoustic reflectance data. *Hydrobiologia* 680 (1), 265–284. doi: 10.1007/s10750-011-0937-4
- Sikes, E. L., Uhle, M. E., Nodder, S. D., and Howard, M. E. (2009). Sources of organic matter in a coastal marine environment: Evidence from n-alkanes and their $\delta^{13}C$ distributions in the Hauraki Gulf, New Zealand. *Mar. Chem.* 113 (3–4), 149–163. doi: 10.1016/j.marchem.2008.12.003
- Silburn, B. E., Sivyer, D. B., Kroeger, S., Parker, R., Mason, C., Nelson, P., et al. (2017). 'Shelf sea biogeochemistry sediment characterisation' (UK: British Oceanographic Data Centre - Natural Environment Research Council).
- Smeaton, C., and Austin, W. E. N. (2017). Sources, sinks, and subsidies: Terrestrial carbon storage in mid-latitude fjords. *J. Geophys. Res.: Biogeosci.* 122 (11), 2754–2768. doi: 10.1002/2017JG003952
- Smeaton, C., and Austin, W. E. (2022). Quality not quantity: Prioritizing the management of sedimentary organic matter across continental shelf seas. *Geophys. Res. Lett.* 49, e2021GL097481. doi: 10.1029/2021GL097481
- Smeaton, C., Cui, X., Bianchi, T. S., Cage, A. G., Howe, J. A., and Austin, W. E. N. (2021c). The evolution of a coastal carbon store over the last millennium. *Quaternary Sci. Rev.* 266, 107081. doi: 10.1016/j.quascirev.2021.107081
- Smeaton, C., Hunt, C. A., Turrell, W. R., and Austin, W. E. N. (2021a). Marine sedimentary carbon stocks of the United Kingdom's Exclusive Economic Zone. *Front. Earth Sci.* 9. doi: 10.3389/feart.2021.593324
- Smeaton, C., Yang, H., and Austin, W. E. N. (2021b). Carbon burial in the mid-latitude fjords of Scotland. *Mar. Geol.* 441, 106618. doi: 10.1016/j.margeo.2021.106618
- Soetaert, K., Herman, P. M. J., and Middelburg, J. J. (1996). A model of early diagenetic processes from the shelf to abyssal depths. *Geochim. Cosmochim. Acta* 60 (6), 1019–1040. doi: 10.1016/0016-7037(96)00013-0
- Sparkes, R. B., Selver, A. D., Gustafsson, Ö., Semiletov, I. P., Haghpor, N., Wacker, L., et al. (2016). Macromolecular composition of terrestrial and marine organic matter in sediments across the East Siberian Arctic Shelf. *Cryosphere* 10 (5), 2485–2500. doi: 10.5194/tc-10-2485-2016
- Stevenson, M. A., and Abbott, G. D. (2019). Exploring the composition of macromolecular organic matter in arctic ocean sediments under a changing sea ice gradient. *J. Anal. Appl. Pyrolysis* 140, 102–111. doi: 10.1016/j.jaap.2019.02.006
- Subha Anand, S., Rengarajan, R., Shenoy, D., Gauns, M., and Naqvi, S. W. A. (2017). POC export fluxes in the Arabian Sea and the Bay of Bengal: A simultaneous $^{234}Th/^{238}U$ and $^{210}Po/^{210}Pb$ study. *Mar. Chem.* 198, 70–87. doi: 10.1016/j.marchem.2017.11.005
- Synal, H.-A., Jacob, S., and Suter, M. (2000). The PSI/ETH small radiocarbon dating system. *Nucl. Instrum. Methods Phys. Res. Section B: Beam Interact. Mater. Atom* 2, 1–7.
- Tao, S., Eglinton, T. I., Montluçon, D. B., McIntyre, C., and Zhao, M. (2015). Pre-aged soil organic carbon as a major component of the Yellow River suspended load: Regional significance and global relevance. *Earth Planet. Sci. Lett.* 414, 77–86. doi: 10.1016/j.epsl.2015.01.004
- Thompson, C. E. L., Williams, M. E., Amoudry, L., Hull, T., Reynolds, S., Panto, A., and Fones, G. R. (2019). Benthic controls of resuspension in UK shelf seas: Implications for resuspension frequency. *Cont. Shelf Res.* 185, 3–15. doi: 10.1016/j.csr.2017.12.005
- Thornton, S. F., and McManus, J. (1994). Application of organic carbon and nitrogen stable isotope and C/N ratios as source indicators of organic matter provenance in estuarine systems: Evidence from the Tay Estuary, Scotland. *Estuar. Coast. Shelf Sci.* 38 (3), 219–233. doi: 10.1006/ecss.1994.1015
- Tolosa, I., Bayona, J. M., and Albaiges, J. (1996). Aliphatic and polycyclic aromatic hydrocarbons and sulfur/oxygen derivatives in northwestern Mediterranean sediments: Spatial and temporal variability, fluxes, and budgets. *Environ. Sci. Technol.* 30 (8), 2495–2503. doi: 10.1021/es950647x
- Trevathan-Tackett, S. M. (2016). *Dynamics of refractory carbon in seagrass meadows*. (PhD Thesis, University of Technology Sydney: Sydney Australia).
- Trevathan-Tackett, S. M., Kelleway, J., Macreadie, P. I., Beardall, J., Ralph, P., and Bellgrove, A. (2015). Comparison of marine macrophytes for their contributions to blue carbon sequestration. *Ecology* 96 (11), 3043–3057. doi: 10.1890/15-0149.1
- Trevathan-Tackett, S. M., Macreadie, P. I., Sanderman, J., Baldock, J., Howes, J. M., and Ralph, P. J. (2017). A global assessment of the chemical recalcitrance of seagrass tissues: Implications for long-term carbon sequestration. *Front. Plant Sci.* 8. doi: 10.3389/fpls.2017.00925
- van Nugteren, P., Moodley, L., Brummer, G.-J., Heip, C. H. R., Herman, P. M. J., and Middelburg, J. J. (2009). Seafloor ecosystem functioning: The importance of organic matter priming. *Mar. Biol.* 156, 2277–2287. doi: 10.1007/s00227-009-1255-5
- Vaughn, D. R., Bianchi, T. S., Shields, M. R., Kenney, W. F., and Osborne, T. Z. (2021). Blue carbon soil stock development and estimates within northern Florida wetlands. *Front. Earth Sci.* 9. doi: 10.3389/feart.2021.552721
- Verardo, D. J., Froelich, P. N., and McIntyre, A. (1990). Determination of organic carbon and nitrogen in marine sediments using the Carlo Erba NA-1500 analyzer. *Res. Part A. Oceanogr. Res. Papers* 37 (1), 157–165. doi: 10.1016/0198-0149(90)90034-S
- Wacker, L., Lippold, J., Molnár, M., and Schulz, H. (2013). Towards radiocarbon dating of single foraminifera with a gas ion source. *Nucl. Instrum. Methods Phys. Res. Section B* 294, 307–310. doi: 10.1016/j.nimb.2012.08.038
- Wagner, S., Brandes, J., Spencer, R. G. M., Ma, K., Rosengard, S. Z., Moura, J. M. S., and Stubbins, A. (2019). Isotopic composition of oceanic dissolved black carbon reveals non-riverine source. *Nat. Commun.* 10 (1), 1–8. doi: 10.1038/s41467-019-13111-7
- Wakelin, S. L., Holt, J. T., Blackford, J. C., Allen, J. I., Butenschön, M., and Artioli, Y. (2012). Modeling the carbon fluxes of the northwest European continental shelf: Validation and budgets. *J. Geophys. Res.: Oceans* 117 (5), 1–17. doi: 10.1029/2011JC007402
- Watson, S. C. L., Preston, J., Beaumont, N. J., and Watson, G. J. (2020). Assessing the natural capital value of water quality and climate regulation in temperate marine systems using a EUNIS biotope classification approach. *Sci. Total Environ.* 744, 140688. doi: 10.1016/j.scitotenv.2020.140688
- Welte, C., Wacker, L., Hattendorf, B., Christl, M., Fohlmeister, J., Breitenbach, S. F. M., et al. (2016). Laser ablation - accelerator mass spectrometry: An approach for rapid radiocarbon analyses of carbonate archives at high spatial resolution. *Anal. Chem.* 88 (17), 8570–8576. doi: 10.1021/acs.analchem.6b01659
- Wernberg, T., and Filbee-Dexter, K. (2018). Grazers extend blue carbon transfer by slowing sinking speeds of kelp detritus. *Sci. Rep.* 8 (1), 1–7. doi: 10.1038/s41598-018-34721-z
- Wilson, R. J., Speirs, D. C., Sabatino, A., and Heath, M. R. (2018). A synthetic map of the north-west European Shelf sedimentary environment for applications in marine science. *Earth System Sci. Data* 10 (1), 109–130. doi: 10.5194/essd-10-109-2018
- Yates, M. C., Fraser, D. J., and Derry, A. M. (2019). Meta-analysis supports further refinement of eDNA for monitoring aquatic species-specific abundance in nature. *Environ. DNA* 1 (1), 5–13. doi: 10.1002/edn3.7
- Zhao, Y., Wu, F., Fang, X., and Yang, Y. (2015). Topsoil C/N ratios in the Qilian Mountains area: Implications for the use of subaqueous sediment C/N ratios in paleo-environmental reconstructions to indicate organic sources. *Palaeogeogr. Palaeoclimatol. Palaeoecol.* 426, 1–9. doi: 10.1016/j.palaeo.2015.02.038
- Ziolkowski, L. A., Chamberlin, A. R., Greaves, J., and Druffel, E. R. M. (2011). Quantification of black carbon in marine systems using the benzene polycarboxylic acid method: A mechanistic and yield study. *Limnol. Oceanogr.: Methods* 9 (4), 140–140. doi: 10.4319/lom.2011.9.140



OPEN ACCESS

EDITED BY

Catherine Lovelock,
University of Queensland, Australia

REVIEWED BY

Robinson W. (Wally) Fulweiler,
Boston University, United States
Grace Cott,
University College Dublin, Ireland

*CORRESPONDENCE

Ronald B. Souza
ronald.buss@inpe.br

SPECIALTY SECTION

This article was submitted to
Global Change and the Future Ocean,
a section of the journal
Frontiers in Marine Science

RECEIVED 09 March 2022

ACCEPTED 23 August 2022

PUBLISHED 21 September 2022

CITATION

Souza RB, Copertino MS, Fisch G,
Santini MF, Pinaya WHD, Furlan FM,
Alves RdCM, Möller OO Jr. and
Pezzi LP (2022) Salt marsh-
atmosphere CO₂ exchanges in Patos
Lagoon Estuary, Southern Brazil.
Front. Mar. Sci. 9:892857.
doi: 10.3389/fmars.2022.892857

COPYRIGHT

© 2022 Souza, Copertino, Fisch, Santini,
Pinaya, Furlan, Alves, Möller and Pezzi.
This is an open-access article
distributed under the terms of the
[Creative Commons Attribution License
\(CC BY\)](https://creativecommons.org/licenses/by/4.0/). The use, distribution or
reproduction in other forums is
permitted, provided the original
author(s) and the copyright owner(s)
are credited and that the original
publication in this journal is cited, in
accordance with accepted academic
practice. No use, distribution or
reproduction is permitted which does
not comply with these terms.

Salt marsh-atmosphere CO₂ exchanges in Patos Lagoon Estuary, Southern Brazil

Ronald B. Souza^{1*}, Margareth S. Copertino^{2,3}, Gilberto Fisch⁴,
Marcelo F. Santini⁵, Walter H. D. Pinaya⁶, Fabiane M. Furlan⁷,
Rita de Cássia M. Alves⁷, Osmar O. Möller Jr.²
and Luciano P. Pezzi⁵

¹Earth System Numerical Modeling Division, National Institute for Space Research (INPE), Cachoeira Paulista, Brazil, ²Institute of Oceanography, Federal University of Rio Grande (FURG), Rio Grande, Brazil, ³Brazilian Network on Global Climate Change Research (Rede CLIMA), National Institute for Space Research (INPE), São José dos Campos, Brazil, ⁴Agricultural Science Department, University of Taubaté (UNITAU), Taubaté, Brazil, ⁵Earth Observation and Geoinformatics Division, National Institute for Space Research (INPE), São José dos Campos, Brazil, ⁶Secretariat of Aquaculture and Fisheries, Ministry of Agriculture, Livestock and Food Supply, Brasília, Brazil, ⁷State Center for Remote Sensing and Meteorology Research, Federal University of Rio Grande do Sul (CEPSRM/UFRGS), Porto Alegre, Brazil

Blue carbon ecosystems are recognized as carbon sinks and therefore for their potential for climate mitigation. While carbon stocks and burial rates have been quantified and estimated regionally and globally, there are still many knowledge gaps on carbon fluxes exchanged particularly at the interface vegetation-atmosphere. In this study we measured the atmospheric CO₂ concentrations in a salt marsh located in the Patos Lagoon Estuary, southern Brazil. Eddy correlation techniques were applied to account for the CO₂ exchange fluxes between the vegetation and the atmosphere. Our dataset refers to two sampling periods spanning from July up to November 2016 and from January to April 2017. By using time series analysis techniques including wavelet and cross-wavelet analysis, our results show the natural cycles of the CO₂ exchanges variability and the relationship of these cycles with other environmental variables. We also present the amplitudes of the salt marsh-atmosphere CO₂ fluxes' diurnal cycle for both study periods and demonstrate that the CO₂ fluxes are modulated by the passage of transient atmospheric systems and by the level variation of surrounding waters. During daytime, our site was as a CO₂ sink. Fluxes were measured as $-6.71 \pm 5.55 \mu\text{mol m}^{-2} \text{s}^{-1}$ and $-7.95 \pm 6.44 \mu\text{mol m}^{-2} \text{s}^{-1}$ for the winter-spring and summer-fall periods, respectively. During nighttime, the CO₂ fluxes were reversed and our site behaved as a CO₂ source. Beside the seasonal changes in sunlight and air temperature, differences between the two periods were marked by the level of marsh inundation, winds and plant biomass (higher in summer). The net CO₂ balance showed the predominance of the photosynthetic activity over community respiration, indicating the role of the salt marsh as a CO₂ sink. When considering the yearly-averaged net fluxes integrated to the whole area

of the Patos Lagoon Estuary marshes, the total CO₂ sink was estimated as -87.6 Mg C yr⁻¹. This paper is the first to measure and study the vegetation-atmosphere CO₂ fluxes of a salt marsh environment of Brazil. The results will contribute to the knowledge on the global carbon budget and for marsh conservation and management plans, including climate change policies.

KEYWORDS

CO₂ Fluxes, Eddy covariance, coastal carbon, salt marsh, Patos Lagoon Estuary (Brazil), temporal variability

Introduction

Salt marshes are among the most biologically productive ecosystems in the world, providing a range of valuable ecosystem services to coastal communities (Adam, 1993; Himes-Cornell et al., 2018). Being sources and sinks of nutrients and organic matter to estuaries, salt marshes regulate local biogeochemical cycles, immobilize pollutants and provide habitat for wildlife. Positioned at the intertidal zone at the interface between land and ocean, salt marshes reduce the energy of waves and currents, bind the sediments, provide flood defense and shoreline erosion control, therefore protecting the coast against sea level rise. With high rates of primary production, plant biomass growth and sediment vertical accretion, salt marshes are highly efficient in organic carbon sequestration and storage, together with mangrove forest and seagrass meadows (Duarte et al., 2005; McLeod et al., 2011; Macreadie et al., 2012). Compared to mangrove and seagrass ecosystems, salt marshes have the highest capacity for carbon sequestration, showing accumulation rates up to $244.7 \pm 26.1 \text{ g C m}^{-2} \text{ yr}^{-1}$ (Chmura et al., 2003; Ouyang and Lee, 2014) and storing an average of 130 Mg C ha⁻¹ (Howe et al., 2009), mostly in the soil and roots and detritus. Despite of their low areal cover relative to the ocean and other terrestrial ecosystems (0.1 – 2%), total carbon accumulation rates in global salt marsh soil are estimated at $\sim 10.2 \text{ Tg C yr}^{-1}$ (Ouyang and Lee, 2014). While the global storage capacity of coastal wetlands is lower compared to the size of terrestrial carbon sinks, the carbon sequestration capacity by salt marsh sediments per unit area is ranked highest amongst coastal wetland and forested terrestrial ecosystems. Furthermore, salt marshes can immobilize the organic carbon for centuries or millennia, whereas terrestrial forests usually only store organic carbon for decades (Macreadie et al., 2012). Therefore, salt marshes are well recognized as blue carbon ecosystems with potential to contribute to regulation of atmospheric CO₂ concentrations and mitigate climate change (MacLeod et al., 2011).

Despite their importance in providing ecosystem services, salt marshes have been destroyed for centuries (Duarte et al., 2013).

Between 2 and 60% of salt marshes have been lost from the temperate regions of the Earth during last 50 years, particularly due to landscape conversion for housing and farming (Lokwood and Drakeford, 2021). Once the marsh soil is disturbed, the oxidized organic matter is decomposed and large amounts of ancient buried C can be released into the atmosphere as CO₂, therefore contributing to greenhouse gases (GHG) emissions (Pendleton et al., 2012; Lovelock et al., 2017). Therefore, both conservation and restoration of salt marshes can maintain carbon sinks and avoid further emissions.

Both salt marshes and mangroves are recognized by the International Panel on Climate Change (IPCC) as potential nature-based solutions for atmospheric CO₂ reduction (IPCC, 2021) and therefore eligible to be included within national greenhouse gas accounting frameworks (IPCC, 2014). Additionally, efforts are emerging to use salt marsh conservation and restoration in carbon offset programs, like the “Reducing Emissions from Deforestation and Forest Degradation in Developing Countries (REDD)” initiative for tropical forests (Gibbs et al., 2007). However, the mitigation capacity of a blue carbon ecosystem is a balance between the CO₂ sequestered and emitted (Taillard et al., 2018) and those processes are affected by spatial and temporal variability in natural and anthropogenic disturbances.

While blue carbon science has advanced at unprecedented rates over the last decade, some aspects are still controversial (Lovelock and Duarte, 2019). Among the emerging questions are ones related to the net flux of CO₂ and other greenhouse gases between the vegetation/soil/water system and the atmosphere (Macreadie et al., 2019). Even though those ecosystems are significant carbon reservoirs, they can be temporally net emitters of CO₂ to atmosphere, depending on the natural dynamics of organic and inorganic carbon exchange. There is a lack of empirical evidence of CO₂ fluxes and the processes controlling the exchanges of carbon between the vegetation/soil/water system and overlying atmosphere at the ecosystem level (e.g. Goulden et al., 2007) and how the CO₂ fluxes can be influenced by tidal cycles, hydrology, weather, and climate

conditions (Polsenaere et al., 2012). Furthermore, anthropogenic disturbances can shift the system from carbon source to sinks (Pendleton et al., 2012; Lovelock et al., 2017). Thus, accurate global blue carbon budgets are limited by uncertainties in CO₂ net fluxes.

Micrometeorological flux methods like the eddy covariance (EC) techniques allow the study of whole ecosystem fluxes of CO₂ to estimate gross primary production, net ecosystem exchange, and ecosystem respiration (Forbrich and Giblin, 2015). The balance between CO₂ released and taken up by the ecosystem is measured, without disturbing the soil or vegetation, and modeling approaches allow the partitioning into the component fluxes of primary production and respiration. Developed initially for terrestrial ecosystems, the EC technique is not yet widely applied in coastal wetland studies, where tidal and hydrological dynamics offer challenges (e.g. Barr et al., 2010; Forbrich and Giblin, 2015; Chu et al., 2021; Hawman et al., 2021; Hill et al., 2021). The knowledge gaps of CO₂ fluxes are particularly large for South America, where the great majority of EC studies are concentrated in the terrestrial ecosystems, with few studies performed in coastal wetlands (e.g. Tonti et al., 2018; Freire et al., 2022) and the coastal and open ocean (Pezzi et al., 2016; Oliveira et al., 2019; Santini et al., 2020; Pezzi et al., 2021; Souza et al., 2021).

In the Southwestern Atlantic Ocean, southern South America, salt marshes dominate the intertidal estuarine habitats of the subtropical and temperate coastline covering approximately 5,000 km of coastline from 29° S to 54° S with an area of approximately 220,000 ha (Isacch et al., 2006; Martinetto et al., 2016). Extensive coastal wetlands are found surrounding the Patos Lagoon Estuary (Costa et al., 2003), a dominant feature of the southern Brazil coastal plain that is of high ecological and social relevance (Odebrecht et al., 2010; Odebrecht et al., 2017). Well preserved and highly productive salt marshes occupy about 70 km² of the margins of Patos Lagoon Estuary (Nogueira and Costa, 2003; Costa and Marangoni, 2010). The Patos Lagoon salt marshes are strongly affected by seasonal changes of light, temperature and hydrological cycles (Costa, 1997a; Costa, 1997b; Costa e Marangoni, 2010). Preliminary results show these salt marshes store an average of 220 Mg C ha⁻¹ (Paterson, 2016), which is in the high range of the global observations. A large area of the Patos Lagoon salt marshes has been lost and degraded since the early nineteenth century by urbanization, agriculture activities, industrial and port expansion (Costa, 1997a; Costa, 1997b; Seeliger, 2010). About 16% of the area was lost since the nineteenth century, although during past five decades those habitats has been stable (Marangoni and Costa, 2009).

The Patos Lagoon dynamics, including that of its estuarine region are dominated by low frequency perturbations (e.g. weekly, seasonal) but some of the interannual variability of the estuary and thus all ecosystem dynamics are related to climate forcing including ENSO (El Niño - Southern Oscillation). The

natural funneling of the estuary toward the Atlantic Ocean makes the intensification of the outflow currents a major regulator of the circulation of the lagoon (Möller Jr. and Fernandes, 2010). The low tidal amplitudes (~0.4 m) associated with the low tidal energies in the estuary make the balance between the continental discharge and the winds the major forcing mechanism for the local circulation when analyzing dynamics at longer temporal scales (Möller et al., 2001). Therefore, the local salt marshes are microtidal, with their primary production and biomass cycles strong related to the annual and interannual flooding and dry periods (Costa, 1997a; Costa and Marangoni, 2010).

The present study aims to report the first ever EC measurements of the CO₂ exchanges between the salt marsh vegetation and the atmosphere in Brazil. We assessed the daily and seasonal variability of the CO₂ fluxes between the vegetation and the atmosphere to describe the balance between photosynthesis and respiration. The primary scientific hypothesis is that, although the seasonal and interannual variability in the salt marsh biomass, climate and hydrology would be predominant forcing mechanisms for the fluxes' variability, the Patos Lagoon salt marshes are sinks of CO₂ with potential to contribute to mitigation of climate change. The CO₂ fluxes reported here add to the knowledge of CO₂ fluxes from the southern hemisphere, which are not yet fully explored in blue carbon studies.

Material and methods

The study was carried out in Pólvora Island (32° 01'14.24"S, 52° 06'17.35"W), an area of well preserved salt marsh located in the Patos Lagoon Estuary, southern Brazil (Figure 1). The island holds a research station and education center (Eco-Museum), managed by the Oceanographic Museum, Federal University of Rio Grande. The Patos Lagoon Estuary is part of the Brazilian Long Term Ecological Research (BR-LTER). Salt marsh in the region has been studied since 1992, with a focus on plant abundance and distribution, primary production, plant-animal interactions, biogeochemical aspects (Costa, 1997b; Costa and Marangoni, 2010) and, more recently, carbon stocks and sequestration (Patterson, 2016). Pólvora Island is located in the meso-mixohaline region of the estuary with salinity ranging between 5-25 practical salinity units (PSU). Across the topography gradient, *Spartina alterniflora* Loisel dominates in the low marsh, *Bolboschoenus maritimus* (L.) Palla in the low-mid marsh, *Spartina densiflora* Brongn in the mid-high marsh, *Schoenoplectus americanus* (Rchb.) Palla (also known as *Scirpus americanus* or *S. olneyi*) and *Juncus roemerianus* Scheele comprise the community at the highest elevations. The vegetation spatial distribution and zonation are characterized by mosaics that reflect the flooding and salinity gradients. Most of the area (93.2%) is occupied by mid-high marsh, whereas



FIGURE 1

Location of the Patos Lagoon in southern South America and Pólvora Island in Patos Lagoon Estuary. The study site is represented by the yellow star in the consecutive maps. (left) Landsat 8 (OLI) image of Patos Lagoon of 24 May 2018 provided by NASA Earth Observatory. (right) Pólvora Island image of 13 June 2021 provided by Google Earth Pro®.

marshes in creeks and muddy, flat areas occupy 5.3% and the rest (1.5%) are low marshes (Nogueira and Costa, 2003).

The regions climate is subtropical humid (Cfa) according to Koeppen-Geiger criteria (Reboita and Krushe, 2018), with four distinct seasons and average maximum temperature in January of 24.2°C and an average minimum temperature of 13.2°C in July. The annual precipitation is around 1360 mm distributed over all months, although the winter period presents a slightly higher precipitation (120–130 mm/month) compared to the summer (90–100 mm/month). The increased rainfall in winter is due to the more frequent penetration of atmospheric systems (cold fronts) to this region. These systems bring cold air masses and are associated with several meteorological phenomena such as frontal systems crossing the area from the Pacific Ocean, cold fronts and cyclones developed in southern Brazil or in the vicinity and atmospheric blocking, among others (Reboita et al., 2010).

The annual cycle of sunshine hours is from 10 h (winter) up to 14 h (summer). The ENSO events also influence the precipitation, with El Niño (La Niña) producing higher (lower) precipitation with respect to the climatological average at a determined period (Silva et al., 2021). For our data collection period (July 2016 up to April 2017), a moderate La Niña¹ event occurred from July until December, inducing lower precipitation than the normal climatological values.

Micrometeorological measurements

In order to take the vegetation/soil-atmosphere CO₂ flux data used here, a 3 m tall, micrometeorological tower was installed in January 2016 (32° 01'17.08"S, 52° 06'10.20"W) in Pólvora Island (Supplementary Figure 1). The installation and maintenance of the tower and sensors was a multi-institutional effort carried out between (1) the Center for Weather Forecast and Climate Studies (CPTEC) of the National Institute for Space Research (INPE); (2) the Institute of Oceanography (IO) and the Oceanographic Museum Prof. Eliézer de Carvalho Rios of the Federal University of Rio Grande (FURG); and (3) the State Center for Remote Sensing and Meteorology Research (CEPSRM) of the Federal University of Rio Grande do Sul (UFRGS). After installation, the tower was fully operational with all sensors operating from July 2016 to April 2017, apart from a week in October 2016 (due to battery failure) and from mid-November to the end of December 2016 when sensors were being serviced. Precipitation data were not collected due to a failure on the rain gauge electronics. Sensors were periodically serviced at about every 3-months period, mainly for cleaning, and no dataset was found to drift from the expected range of measurements during the time of our experiment.

Although the island's topography is flat and very close to the water level, subjecting the terrain to periodical flooding (Costa, 1997a; Costa and Marangoni, 2010), the tower's position in the high-mid marsh avoided water suppressing the vegetation at the site during our study period.

Supplementary Table 1 provides a list of sensors used in the tower. Most of sensors operated in the 30 s period (1/30 Hz frequency) but the IRGASON (Campbell Scientific Corporation, Logan, Utah, USA), an integrated 3D sonic anemometer with and

¹ https://origin.cpc.ncep.noaa.gov/products/analysis_monitoring/ensostuff/ONI_v5.php

open path gas analyzer operated at the 10 Hz frequency necessary for the EC estimates. The IRGASON has also a thermometer and a barometer to make auxiliary measurements at the same frequency as the wind and gas concentration.

As suggested by Verbeeck et al. (2011), the chosen position for the tower installation suitable for EC measurements, lying on very flat terrain that extends about 1,500 m in the northwestern/southeastern direction by about 200 m in the northeastern/southwestern direction (Supplementary Figure 2). The tower's location lies on an area dominated by *Spartina densiflora* (Supplementary Figure 3). The shortest distance between the tower's position in Pólvora Island and Rio Grandes's city center is 700 m. As the island is located north of the city and prevailing winds during our experiment were from the northeastern/eastern quadrants (Supplementary Figure 4) where there are no settlements, we do not expect significant urban contamination of our CO₂ measurements.

In order to estimate the source area and the contribution of a specific target to the surface/atmosphere fluxes, footprint (or fetch) models are used in association with the EC measurements. In this paper, we used the 2D footprint model described by Kljun et al. (2004) and Kljun et al. (2015) and freely available by the ToviTM s. The software uses meteorological information like windspeed and direction, surface turbulent fluxes (especially momentum and sensible heat fluxes), the atmospheric stability estimate (including the Monin-Obukhov Length), and information of the vegetation like height, displacement heights and roughness length. In our case, although these parameters vary with the seasonal cycle (Costa et al., 2003), we found that the roughness parameter variation up to a value of 1 m did not affect the calculation of the footprint area. Using the extremely high roughness parameter of 1 m, the footprint was computed as between 200–300 m (area of ~0.25 km²) for both winter-spring and summer-fall periods (Supplementary Figure 5). As we observed spatial homogeneity of the salt marsh vegetation in all directions around the instrument tower for both study periods, we assumed that all CO₂ flux measurements presented in this work were solely related to the salt marsh vegetation and represent its typical behavior.

As conventionally needed for the EC calculations, the original (3 m height) windspeed measured by the IRGASON 3D sonic anemometer was converted into its 10 m height equivalent (U_{10}) using the Coupled Ocean-Atmosphere Response Experiment (COARE) version 3.5 bulk algorithm (Edson et al., 2013). The atmospheric pressure data collected by the IRGASON barometer were extremely noisy from March 15, 2017 onward and they were not used here. The original data collected at 3 m height were also converted into sea level pressure (SLP, 0 m height) in a similar way. Both conversions make our data easily compared in the future to most atmospheric datasets in the world.

Auxiliary environmental data: water level, precipitation and wind

In order to assess the relations between water level and the micrometeorological measurements made throughout the study period, we used water pressure (proxy to water level) data gathered by the Laboratory of Coastal and Estuarine Oceanography (LOCOSTE) of IO-FURG during the period of this study. Water pressure data were taken by a thermo-conductivimeter (CT) SeaBird SBE 37-SM moored in the estuary's mouth about a kilometer away from the Pólvora Island in a depth between 4.5 and 5 m. The instrument provided a pressure mean (4.63 dbar) over the 2-years time period. This 2-years mean value was subtracted from the daily means to provide the water pressure anomaly (WPA) data used here.

As precipitation data was not directly collected by the rain gauge installed in the micrometeorological tower, we used data from the Brazilian National Institute of Meteorology (INMET)² available for the period of this study. INMET maintains the automatic weather station #A802 (a.k.a. 83995) in Rio Grande city at the position 32°04'43" S; 52°10'03" W inside the Federal University of Rio Grande (FURG) at a distance of around 9 km from the site of our micrometeorological tower. The data presented many gaps making its use as a robust time series impossible. Nonetheless, we used the data to characterize the synoptic meteorological conditions of the study area.

In order to investigate the climatology of the wind field of our study area, we used hourly values (not shown) from a meteorological reanalysis database provided by the European Centre for Medium Range Weather Forecast (ECMWF) named ERA5³. It uses a 4D variational assimilation scheme (Hersbach et al., 2020). Briefly, ERA5 consists of hourly atmospheric variables computed at a ~30 km grid size for more than 130 height levels in the atmosphere from the Earth's surface up to 60 km. The wind data used here were extracted from the grid point including Rio Grande city (32°S, 52 °W) for the period from 2010–2020 at 100 m height in the atmosphere. The analysis of these data (not shown) indicated that during our study period the winds were close to the climatological means for each of the seasons.

Eddy covariance estimates of CO₂ fluxes

The eddy covariance method correlates the turbulent fluxes of a determined scalar between two determined environments,

² <https://mapas.inmet.gov.br/>

³ <https://cds.climate.copernicus.eu/cdsapp#!/dataset/reanalysis-era5-single-levels?tab=overview>

for instance the interface of surface (vegetation/soil/water) and the atmosphere. The parameters are measured by sensors installed in micrometeorological towers and are used to estimate the net exchanges of CO₂, water and energy between the surface and the atmosphere (Stull, 1988; Jung et al., 2011; Edson et al., 2013). The EC method measures the covariance between the turbulent fluctuations of a scalar and vertical windspeed around their mean during a determined sampling interval. For instance, here we use a sampling frequency of 10 Hz for the fast response sensors and a time interval of 30 min for the computation of the fluxes. The high frequency fluctuations correspond to measurements of the transport of energy by the small atmospheric eddies. The time interval window (e.g. 30 min) data is then computed in order to resolve and include the transport by the large-scale eddies (Kaimal and Finnigan, 1994; Miller et al., 2010).

Using the IRGASON, we measured the 3D wind velocity vector components (u, v, w) and the density of H₂O(v) and CO₂ in order to calculate their mixing ratio (H₂O(v)/CO₂) in the atmosphere to further calculate the turbulent CO₂ EC fluxes (FCO₂ in μmol m⁻² s⁻¹) at the vegetation/soil-atmosphere interface as:

$$FCO_2 = \rho_a \overline{w'c'} \quad (1)$$

where, ρ_a is the dry air density, w is the vertical component of the wind velocity and c is the mixing ratio (e.g. H₂O(v)/CO₂). The means are represented by over bars and the turbulent fluctuations are represented by the primes. All data were processed using the open source software EddyPro[®] v.6.2.1⁴. At this step, we configured the proper corrections for flux computation as wind rotation, planar fit, corrections for air temperature, atmospheric pressure and humidity etc (Webb et al., 1980; Miller et al., 2010; Aubinet et al., 2012). EddyPro[®] follows the scheme proposed by Foken et al. (2004) for the data quality-control. Necessary spectral corrections were made for both low- and high-frequency bands following the methods described by Moncrieff et al. (2004). The statistical tests used to clear spikes on the micrometeorological time series were performed according to Vickers and Mahrt (1997) using 30 min long time intervals and detrended time series derived from the original data. The methodology used here is similar to that used by Oliveira et al. (2019); Santini et al. (2020) and Pezzi et al. (2021).

Once the CO₂ fluxes were computed for the two periods of this study, we used the synchronized radiation series to separate the data into daytime (from about 6 a.m. up to 18 p.m. local time) and nighttime series (from about 18 p.m. up to 6 a.m. local time), from which we calculated the basic statistics (mean and standard deviation) for both daily periods. Then we computed the net CO₂ fluxes to assess the role of the salt marsh

environment as a sink (negative net fluxes) or a source (positive net fluxes) of CO₂ to/from the atmosphere. Using only the daily values of minimum (nighttime) and maximum (daytime) values, we also computed the maximum daily amplitude of the CO₂ fluxes and statistics of the series at the monthly scale and for the two periods analyzed here (winter-spring and summer-fall).

Wavelet and cross-wavelet analysis

A wavelet transform was used to determine the temporal variability of the CO₂ fluxes and to estimate the coefficients of cross-correlations (*r*) between these fluxes and atmospheric and water level variables. From all meteorological variables collected by the instrument tower, the following were used for the analysis: air temperature, relative humidity and windspeed. Apart from correlating the fluxes with the meteorological variables and water level anomaly, we also correlated the water level with windspeed to support the assumption that these variables are highly correlated (Möller et al., 2001). All variables were averaged to a daily temporal resolution before the analysis.

The cross-wavelet analysis and wavelet coherence were performed according to the methodology proposed by Grinsted et al. (2004). We used a cone of influence (*p*>0.05) to separate valid data from the red noise. Briefly, the cross-wavelet spectrum analysis emphasizes the common power of the two-time series, while the wavelet coherence emphasizes the correlations between temporal cycles imprinted on two time series, e.g. the coherence fluctuations. We thus determine the local correlation of significant oscillations observed among the CO₂ EC fluxes and environmental variables. We used the software STATISTICA7.0[®] to perform the cross-correlations and Matlab7.0[®] to perform the wavelet and cross-wavelet computations.

Results

Salt marsh-atmosphere CO₂ fluxes and associated environmental variables

Figures 2, 3 present the time series of CO₂ fluxes at the salt marsh-atmosphere interface and the environmental variables SLP, air temperature and water level anomaly for the two sampling periods of this study (July–November 2016 and January–April 2017, respectively). Supplementary Figures 6, 7 present the time series of windspeed, relative humidity, incoming shortwave radiation and precipitation for the different study periods.

The CO₂ fluxes show a typical diurnal cycle, for both winter-spring and summer-fall periods (Figures 2A, 3A). This daily

⁴ http://www.licor.com/env/products/eddy_covariance/software.html

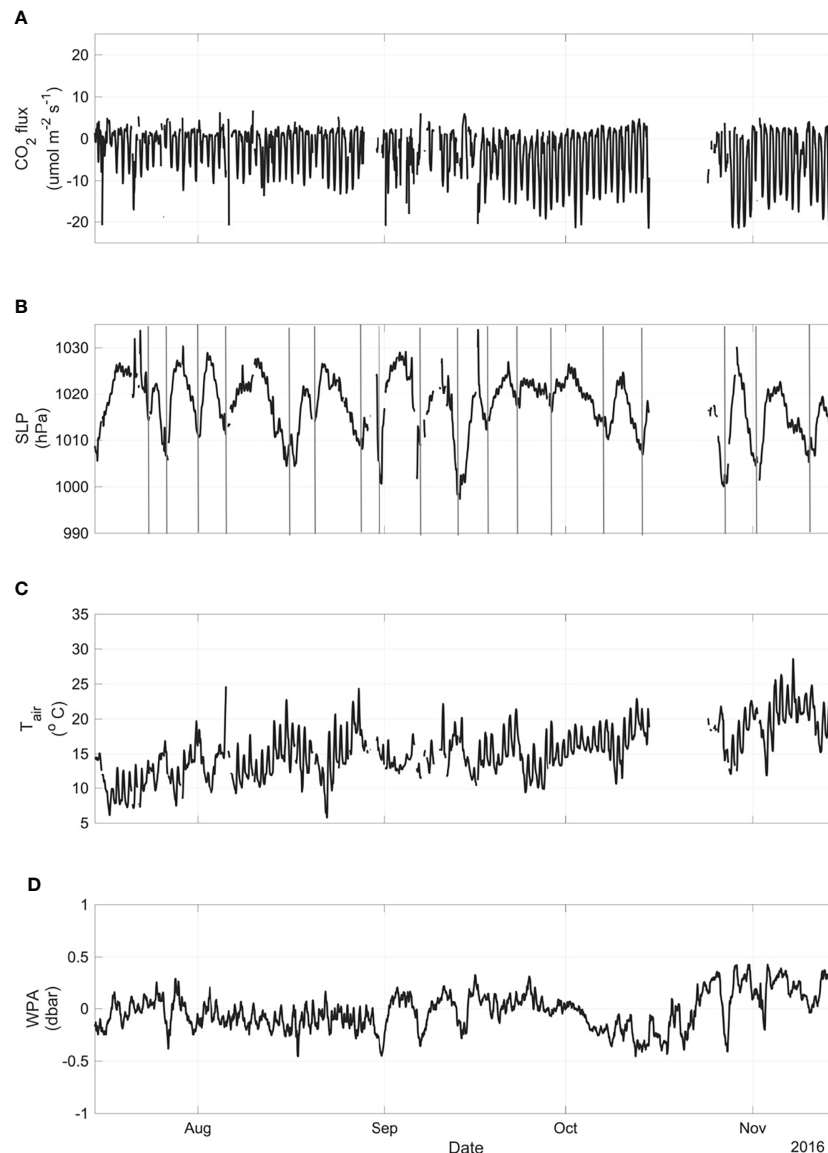


FIGURE 2

Time series of (A) CO_2 fluxes at the salt marsh-atmosphere interface; (B) sea level pressure (SLP); (C) air temperature (T_{air}); (D) water pressure anomaly (WPA) for the period spanning from July up to November 2016. The vertical gray lines in (A) indicate the pressure troughs associated with the passage of atmospheric cold fronts in the study area.

cycle, which is related to the photosynthetic activity and the community respiration, dominates the temporal modulation of the series. It is also noticeable that, for both study periods, the amplitudes of the daytime periods' CO_2 absorption (negative fluxes - influx) are larger than that released during nighttime periods (positive fluxes - eflux), suggesting a positive net balance of photosynthetic activity over the community respiration.

The average maximum negative and positive values of the CO_2 fluxes observed, respectively, during daytime and nighttime along the temporal series represent the daily amplitudes of the salt marsh-atmosphere CO_2 fluxes (Table 2). The values are a

proxy of the maximum photosynthetic rates (daytime negative values) and community respiration (nighttime positive values) for each month during the two studied periods. The peaks of negative (-16.38 to $-16.57 \mu\text{mol m}^{-2} \text{s}^{-1}$) and positive values (4.39 to $4.92 \mu\text{mol m}^{-2} \text{s}^{-1}$) of CO_2 fluxes occurred during austral summer (January-February 2017), therefore resulting in the highest amplitudes between day and night (20.77 to $21.49 \mu\text{mol m}^{-2} \text{s}^{-1}$). The amplitudes of the CO_2 fluxes signal are larger during summer (January-February) than during the winter (July-August), while the fluxes' variability is lower in summer months.

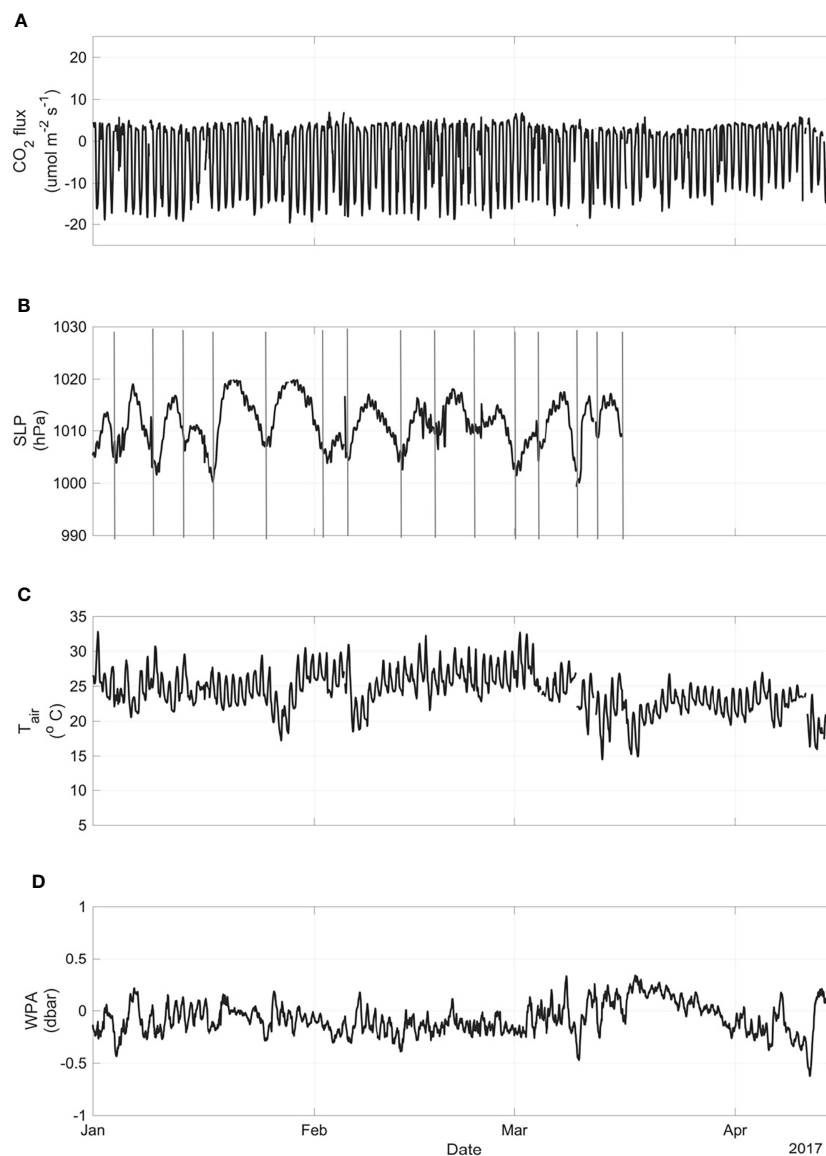


FIGURE 3

Time series of (A) CO_2 fluxes at the salt marsh-atmosphere interface; (B) sea level pressure (SLP); (C) air temperature (T_{air}); (D) water pressure anomaly (WPA) for the period spanning from July up to November 2016. The vertical gray lines in (A) indicate the pressure troughs associated with the passage of atmospheric cold fronts in the study area. The mean values of net CO_2 flux are negative and almost the same for both periods of this study (-3.23 to $-3.20 \mu\text{mol m}^{-2} \text{s}^{-1}$) (Table 1). Mean value of night fluxes (a proxy of community respiration) is about 4.6 times higher in summer-fall than in winter-spring (Table 1). Daytime mean fluxes, related to the community photosynthetic activity, varied between (-6.71 to $-7.95 \mu\text{mol m}^{-2} \text{s}^{-1}$) between the two periods analyzed. The mean value of nighttime fluxes, on the other hand varied between 0.67 (winter-spring) to $2.95 \mu\text{mol m}^{-2} \text{s}^{-1}$ (summer-fall). Variability in mean values of CO_2 fluxes is higher during daytime when compared to the nighttime measurements, for both periods (Table 1), following the high variability in the incoming shortwave radiation, a variable dependent on the cloudiness (Supplementary Figures 6C, 7C).

Using Table 1 data for the net CO_2 seasonal fluxes, the annual average of the CO_2 taken up by the salt marsh can be estimated as $-3.215 \mu\text{mol CO}_2 \text{ m}^{-2} \text{s}^{-1}$ or $-3.215 \times 10^{-6} \text{ mol CO}_2 \text{ m}^{-2} \text{s}^{-1}$. Considering that the mass of carbon in a mol of CO_2 is 12 g and applying the correct transformations of units, this results in a theoretical fixation tax of carbon close to $-1217 \text{ g C m}^{-2} \text{yr}^{-1}$.

Extrapolating this value for the total extension of the Patos Lagoon salt marshes (72 km^2 ; Nogueira and Costa, 2003) gives us an annual carbon fixation rate for the entire area covered by the Patos Lagoon marshes close to $-87.6 \times 10^9 \text{ g C yr}^{-1}$ ($-87.6 \text{ Mg C yr}^{-1}$).

Some of the CO_2 flux cycles seen in Figures 2A, 3A follow the cycles presented by the environmental variables studied here.

TABLE 1 Mean (\pm standard deviation) values of salt marsh-atmosphere CO₂ flux during daytime, nighttime and daily cycle net balance, for both studied periods.

Period	Daytime – influx ($\mu\text{mol m}^{-2} \text{s}^{-1}$)	Nighttime – efflux ($\mu\text{mol m}^{-2} \text{s}^{-1}$)	Net flux ($\mu\text{mol m}^{-2} \text{s}^{-1}$)
July–November 2016 (winter–spring)	-6.71 ± 5.55	0.67 ± 2.93	-3.23 ± 5.82
January–April 2017 (summer–fall)	-7.95 ± 6.44	2.95 ± 2.10	-3.20 ± 7.38

The sea level pressure time series, for instance, show a clear temporal variability in the scale of 3–7 days (Figures 2B, 3B), in agreement with the characteristics of the passage of atmospheric synoptic systems alternating high and low pressures over time. The frequencies of occurrence of high-pressure systems were higher in the winter–spring period (Figure 2B) than in the summer–fall period (Figure 3B) making the amplitude of the pressure differences during episodes of frontal passage in summer–fall (1000 to 1023 hPa) greater than winter–spring (1000 to 1020 hPa).

The air temperature (Figures 2C, 3C), relative humidity (Supplementary Figures 6B, 7B) and the incoming shortwave radiation (Supplementary Figures 6C, 7C) are clearly modulated by the diurnal cycle. As expected for our study area, relative humidity reaches 100% more frequently during the winter–spring period than during the summer–fall. The water pressure anomalies (Figures 2D, 3D) also show a clear diurnal cycle in both study periods and generally follow the atmospheric pressure variability at the synoptic scale. The precipitation data provided by INMET (Supplementary Figures 6D, 7D)

show that episodes of heavy rainfall with values of more than 20 mm h⁻¹ are common in Rio Grande city, especially during the summer–fall period.

Windspeed at 10 m height (U_{10}) time series present cycles that are clearly related to the variability of the atmospheric transient systems, as both variables describe the fluctuations related to the atmospheric systems' passage in our study area (Supplementary Figures 6A, 7A). The wind, though, has a prominent diurnal component, probably related to the sea breeze. Windspeed values are often smaller than 5 m s⁻¹ but sometimes reach more than 10 m s⁻¹ in bursts or gusts related to low pressures occurring in winter–spring. ERA5 climatology for Rio Grande city (not shown) revealed that the windspeed presents a clear seasonal variation and it is stronger (around 8.2 m s⁻¹) during winter than during summer (7.3 m s⁻¹). Also, the more frequent wind direction is usually from NE–E during summer, albeit some events from NW–W also occur during winter. This is also observed in the wind data provided by the micrometeorological tower (Supplementary Figures 4, 6A, 7A).

TABLE 2 Mean and standard deviation for the daytime (nighttime) monthly average of maximum (minimum) values of the CO₂ flux measured during both study periods.

Period	Daytime maximum ($\mu\text{mol m}^{-2} \text{s}^{-1}$)	Nighttime maximum ($\mu\text{mol m}^{-2} \text{s}^{-1}$)	Amplitude of the mean daily signal ($\mu\text{mol m}^{-2} \text{s}^{-1}$)	N
July	-9.94 ± 4.87	3.44 ± 1.46	13.38	17
August	-9.78 ± 3.38	3.04 ± 1.64	12.82	30
Setembro	-13.07 ± 5.09	2.69 ± 1.46	15.76	30
October	-15.19 ± 4.90	2.81 ± 1.06	18.00	21
November	-15.80 ± 2.92	2.94 ± 0.90	18.74	13
July–November 2016 (winter–spring)	-12.31 ± 5.06	2.92 ± 1.42	15.24	111
January	-16.38 ± 2.82	4.39 ± 0.92	20.77	31
February	-16.57 ± 1.96	4.92 ± 0.78	21.49	28
March	-14.36 ± 2.68	3.83 ± 1.12	18.19	31
April	-11.78 ± 2.16	4.43 ± 0.94	16.20	13
January–Abril 2017 (summer–fall)	-15.10 ± 3.28	4.33 ± 1.11	19.42	103

The amplitude of the mean daily signal and the number of observing days (N) per month are also presented.

Wavelet and cross-wavelet analysis

The results of time series analysis (wavelet and cross-wavelet) made clear the dominant period cycles of the studied variables CO₂ fluxes, windspeed and water pressure anomaly (Figures 4–7). As previously observed in the original time series (Figures 2A, 3A), CO₂ fluxes in the interface salt marsh-atmosphere show a marked diurnal cycle (~24h). Our wavelet results indicate that the diurnal cycle accounts for the highest energetic spectral content of our CO₂ fluxes time series in both periods of this study (Figures 4A and 6A). The same diurnal cycle was observed in the other variables, although not very well distributed in time and not energetic (Figures 4B, C, 6B, C). The CO₂ fluxes, windspeed and water pressure anomaly present significant energy periods centered at 64 to 512 hours (~3 to 21 days), which are associated with the synoptic atmospheric scales (gray lines) seen in Figures 2B, 3B.

Figures 5 and 7 present highly coherent, cross-energy peaks are scattered between semi-diurnal or diurnal cycles (~12 to 24 h) and low-frequency ones, mostly between 64 to 512 hours (~3 to 21 days) as already seen in the individual power spectra

(Figures 4 and 6). The semi-diurnal coherences are in phase, showing that the CO₂ fluxes directly respond to both windspeed and water pressure anomaly. Episodes of high correlations, however, were not continuous throughout the entire time series, but rather associated to episodes of high amplitude of the variables involved.

A noticeable episode of high cross-energy between CO₂ fluxes against windspeed and water pressure anomaly centered at 128 hours (~5.33 days) occurred between Julian days ~250 to ~270, corresponding to 6 to 26 September 2016⁵ (Figure 5) coincided with a period of high water pressure anomalies (~10 dbar) recorded by the CT instrument located in the Patos Lagoon Estuary (Figure 2D). At the same period, windspeed was relatively low, ranging between 3–6 m s⁻¹ (Supplementary Figure 6A). The cross-wavelet coherence of CO₂ fluxes against windspeed is very high and in phase during the period of Julian days ~250 to ~270 (Figure 5A) while the coherence between CO₂ fluxes and water pressure

⁵ <https://landweb.modaps.eosdis.nasa.gov/browse/calendar.html>

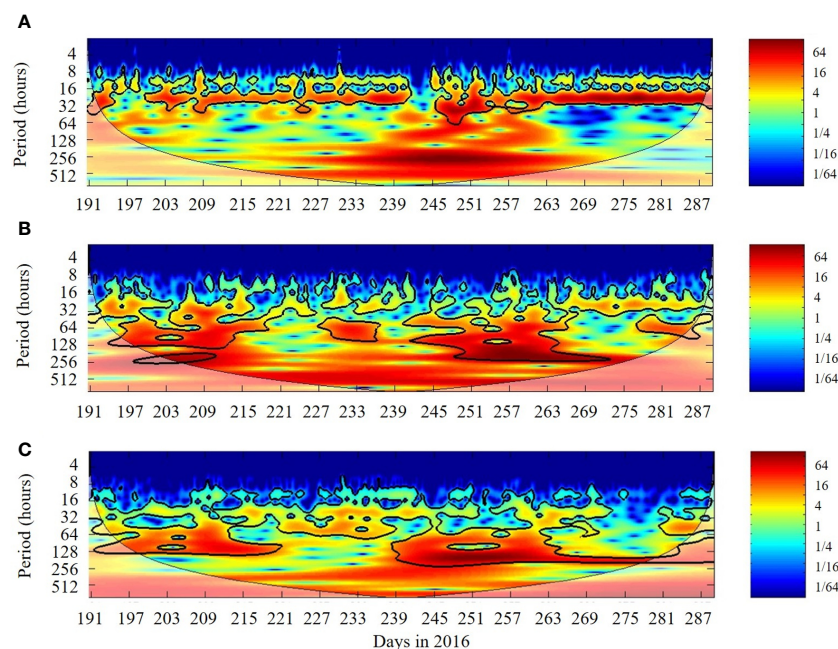


FIGURE 4

Wavelet power spectrum of CO₂ fluxes (A), windspeed (B) and water pressure anomaly (C) for the period spanning from July up to November 2016. The contours are for variance units. The 5% significance level against red noise is shown as a thick contour (cone of influence). Blurred regions indicate values outside the cone of influence. The 95% significance level is shown by heavy black contours. The horizontal scale represents the Julian days in July–November 2016 period. The results of the cross-wavelet analysis for the winter–spring (Figure 5) and summer–fall periods (Figure 7) are presented as the common power (energy) spectrum of the two-time series or the wavelet coherences that emphasize the correlations between variations of two series, i.e., coherence fluctuations. The analysis indicates the local correlation ($0 \leq r \leq 1$) of significant oscillations observed between the CO₂ fluxes and windspeed and water pressure anomaly. The relative phase between the variables is presented as vectors: they point toward the right (left) at the horizontal when the variables are totally in phase (out of phase).

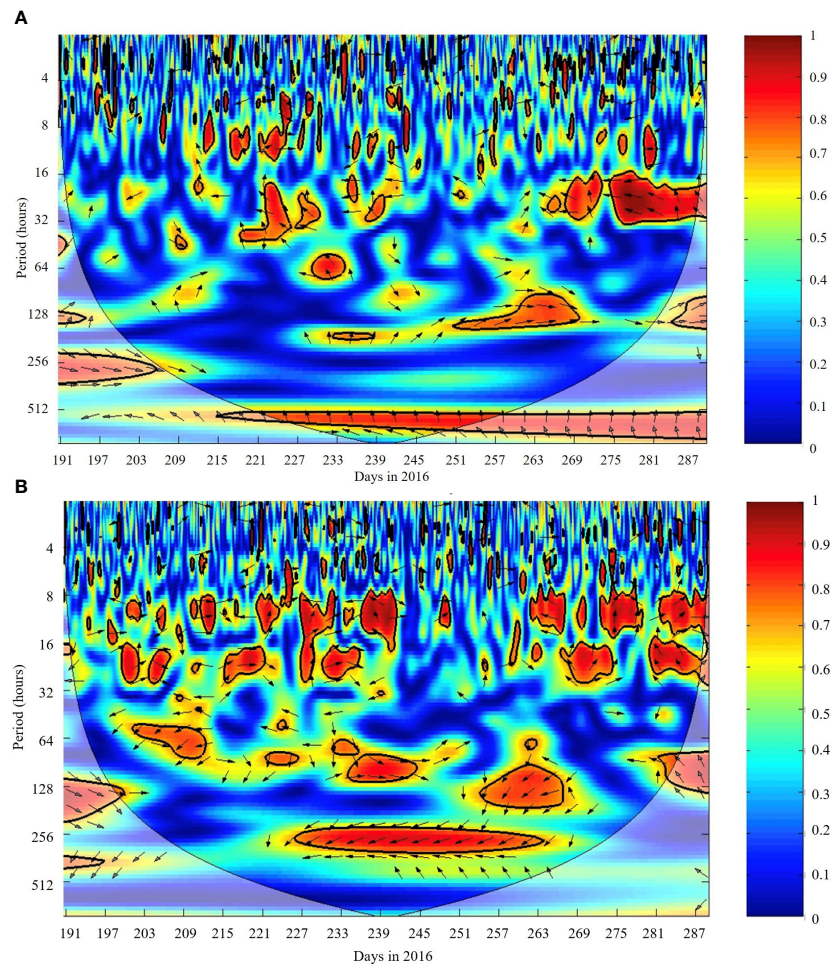


FIGURE 5
Cross-wavelet coherence of CO₂ fluxes and windspeed **(A)** and CO₂ fluxes and water pressure anomaly **(B)** for the period spanning from July up to November 2016. The contours are for variance units. The 5% significance level against red noise is shown as a thick contour (cone of influence). Blurred regions indicate values outside the cone of influence. The vectors indicate the relative phase between the variables. The horizontal scale represents the Julian days in July–November 2016 period.

anomaly for the same period, although still high, is out of phase (Figure 5B).

The cross-wavelet results between CO₂ fluxes and windspeed shows two high-coherence, in phase peaks centered at about 64h (~3 days) in periods ranging from Julian days 40–50 (9–19 February 2017) and Julian days 80–90 (21–31 March 2017 - Figure 7A). Other peak in Figure 7A occurs at the ~265 hours period (~11 days) during Julian days 20–40 (20 January to 9 February 2017). The variables were time-lagged at about 3 days (a quarter of a 11-day cycle).

The cross-wavelet coherence spectra of CO₂ fluxes and water pressure anomaly (Figure 7B) shows a prominent out of phase, high-coherence peak centered at about 192h (8 days) in periods ranging from Julian days 20–80 (20 January to 21 March 2017). During this period the water level anomaly, albeit positive, was about 5 dbar lower than the subsequent period - fall (Figure 3D).

Discussion

The present study is, to our knowledge, the first to measure gas exchange in a Brazilian saltmarsh ecosystem. Our results suggest that subtropical salt marsh habitats are net sinks of carbon. Our study also described the different temporal scales dominating of the salt marsh-atmosphere CO₂ flux cycles, emphasizing the control of the diurnal cycle by aspects linked to the plant's physiology and the control of longer periods' cycles by environmental factors.

The salt marsh-atmosphere CO₂ EC fluxes measured in Pólvora Island presented a clear cycle at the diurnal scale during all seasons of our study in 2016–2017, forced by the balance between photosynthesis (negative fluxes) and community respiration (positive fluxes). The mean daytime fluxes were $-6.71 \pm 5.55 \mu\text{mol m}^{-2} \text{s}^{-1}$ ($-7.95 \pm 6.44 \mu\text{mol m}^{-2}$

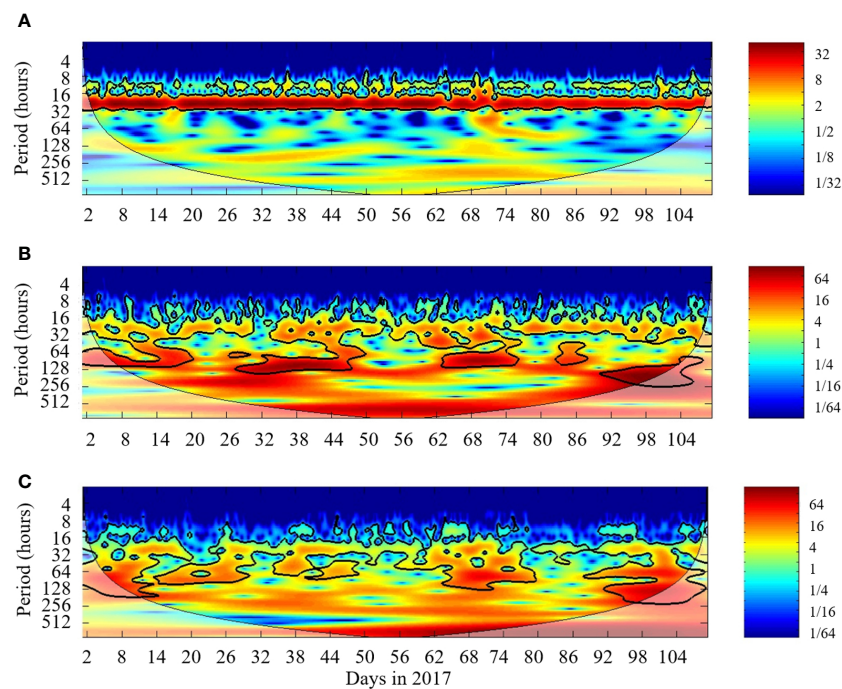


FIGURE 6

Wavelet power spectrum of CO₂ fluxes (A), windspeed (B) and water pressure anomaly (C) for the period spanning from January up to April 2017. The contours are for variance units. The 5% significance level against red noise is shown as a thick contour (cone of influence). Blurred regions indicate values outside the cone of influence. The 95% significance level is shown by heavy black contours. The horizontal scale represents the Julian days in January–April 2017 period.

s⁻¹) for the winter-spring (summer-fall) season. During nighttime, the mean CO₂ fluxes were $0.67 \pm 2.93 \mu\text{mol m}^{-2} \text{s}^{-1}$ ($2.95 \pm 2.10 \mu\text{mol m}^{-2} \text{s}^{-1}$) in winter-spring (summer-fall). Although there is high variability in the data, the effectiveness of the salt marsh as a CO₂ sink was attested by the computation of the net CO₂ balance with a predominance of the photosynthetic activity over respiration and net flux of about $3.2 \mu\text{mol m}^{-2} \text{s}^{-1}$ throughout the period of this study.

Our results showed a clear seasonal cycle, with differences of CO₂ fluxes between winter and summer (Tables 1, 2). This pattern is similar to what found by Tonti et al. (2018), for EC measurements taken in a salt marsh in Argentina (about 38° S) in 2014. These authors related the summer uptake increase of CO₂ by the salt marsh vegetation to both the increase of the air temperature and the duration of the day, consequently increasing the photosynthetic activity in that season. In agreement to the range of results presented in this work (Table 2), Tonti et al. (2018) reported a $-12.9 \mu\text{mol m}^{-2} \text{s}^{-1}$ uptake peak during daytime in March 2014. During daytime in winter, on the other hand, the CO₂ uptake by the vegetation was lower than in summer, peaking at $-4.6 \mu\text{mol m}^{-2} \text{s}^{-1}$ in August 2014. The results of both studies suggest that the seasonal cycle of air temperature, daylength (light) and plant responses are important forcing mechanisms for the vegetation-atmosphere

annual CO₂ flux amplitudes in Southwestern Atlantic salt marshes. The annual fixation rate of carbon in this ecosystem, estimated as $-1217 \text{ g C m}^{-2} \text{yr}^{-1}$, represents the amount of carbon fixed from the atmosphere in the plant and not necessarily sequestered by the plant for growth and/or deposited in the sediment. Nevertheless, this fixation rate is about 5 times the mean carbon uptake of salt marshes in other locations (i.e. mean of $-245 \text{ g C m}^{-2} \text{yr}^{-1}$, Ouyang and Lee, 2014).

The existing knowledge of CO₂ fluxes between the vegetation and the atmosphere in Brazil are restricted to terrestrial biomes. A recent study reported the seasonal behavior of the gross primary production (GPP) - a variable directly related to the fluxes - in four terrestrial biomes: Pantanal, Amazonia, Caatinga and Cerrado (Costa et al., 2022). Analyzing data from one particular location in each biome in distinct periods ranging from 2004 to 2016, the authors described how the seasonal cycle of meteorological variables such as the global incident radiation, air temperature and water vapor deficit, as well as precipitation were the key modulating factors of seasonality in GPP for all biomes.

Armani et al. (2020) presented a study of the EC CO₂ and heat fluxes measured in a reservoir located in the Paraná River, southern Brazil, during 2013. The micrometeorological

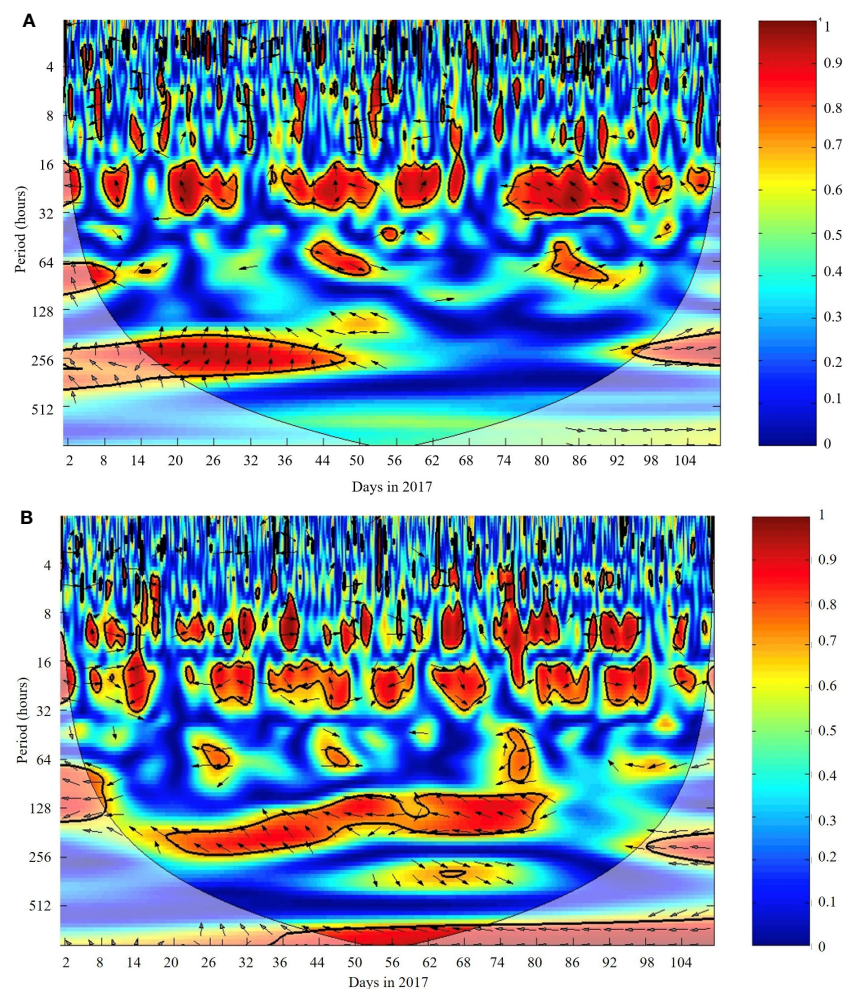


FIGURE 7
Cross-wavelet coherence of CO₂ fluxes and windspeed (A) and CO₂ fluxes and water pressure anomaly (B) for the period spanning from January up to April 2017. The contours are for variance units. The 5% significance level against red noise is shown as a thick contour (cone of influence). Blurred regions indicate values outside the cone of influence. The vectors indicate the relative phase between the variables. The horizontal scale represents the Julian days in January–April 2017 period.

instruments were deployed in a tower installed in one of the reservoir's islands which is flat and almost submerged, located at 25°03'25.72" S, 54°24'33.67" W. The authors reported remarkable seasonality of the CO₂ fluxes: in the warm season, the CO₂ fluxes were negative (CO₂ uptake by the vegetation) during daytime due to photosynthesis and positive (CO₂ emittance by the vegetation) at nighttime due to the respiration activity. This result agrees with our findings and supports the idea that the plant's physiology is the major driver of the vegetation/atmosphere CO₂ fluxes. During the cold season, however, Armani et al. (2020) found that both daytime and nighttime CO₂ fluxes were predominantly negative, suggesting an imposition of the atmosphere's CO₂ concentration and the occurrence of stronger winds on the CO₂ fluxes. The authors also reported that 90% of the CO₂

flux measurements made in their study area ranged between -102.68 to 151.72 $\mu\text{mol m}^{-2} \text{s}^{-1}$. In average, the CO₂ flux was 12.78 $\mu\text{mol m}^{-2} \text{s}^{-1}$, indicating that the reservoir was a source of CO₂ to the atmosphere.

The amplitudes of the salt marsh-atmosphere CO₂ fluxes' diurnal cycle for both study periods seen in Figures 2A, 3A demonstrate that they were modulated by the passage of transient atmospheric systems, such as cold fronts, and by the level variation of the island's surrounding waters. Beside the seasonal changes in sunlight (daylength) and air temperature, differences between the spring-summer and winter-fall periods are marked by the variation in the level of marsh inundation that is usually higher in winter-spring months than in the summer. The salt marsh inundation is locally driven by the Patos Lagoon discharge and windspeed which tend to be higher in winter.

The time series of the meteorological variables collected in our study area (Figures 2, 3 and Supplementary Figures 6, 7) attest the predominance of both the seasonal variability and the short-term, synoptic scale (3 to 7 days) events in our study area. The sea level pressure (Figures 2B, 3D) and windspeed data (Supplementary Figures 6A, 7A) clearly show the cycles related to the passage of atmospheric synoptic systems during both study periods. In addition, the diurnal cycle is also prominent in these time series and particularly visible in the air temperature series (Figures 2C, 3C). The seasonal cycle is very clear, as expected, in the air temperature series with values generally above 20°C from November 2016 onwards.

Using precipitation data of Rio Grande city in the period 1913–2016, Silva et al. (2021) describe that the monthly means of this variable are uniformly distributed along the year without distinguishable dry and wet seasons. On analyzing the period 1950–1980, however, the authors noticed that the summer–fall season was dryer, and the winter was wetter than during the whole period 1913–2016. Wetter summers, including the month of November, were predominant during the period 1980–2010. Silva et al. (2021) also report that the major modes of variability of the precipitation in Rio Grande, which can be extrapolated to the study area, are related to the seasonal cycle and to a ~5-years and a 8-years period oscillation linked to the ENSO phenomenon. The authors described that the 5-years (8-years) ENSO cycle is associated to the positive (negative) phase of the Pacific Decadal Oscillation, demonstrating that the teleconnections are important for characterizing the climate of the study area. As described before, during both periods of this study, a moderate La Niña event induced lower precipitation than the normal climatological values. This situation may have produced CO₂ fluxes lower than average.

Figures 4–7 show that patterns in winds and water level had strongly influenced our CO₂ fluxes. This result corroborates the findings of Möller et al. (2001). The authors studied the subtidal circulation of the Patos Lagoon Estuary analyzing time series of wind, outflow (discharge) and water level collected *in situ* together with numerical model outputs. They emphasize the importance of the wind forcing in the modulation of the estuary outflow, pointing out to the effects of the passage of meteorological fronts in the temporal scale of 3 to 16 days that produce an inversion of the pressure gradient between the inner and outer parts of the Patos Lagoon. Winds blowing from the southern quadrant produce a pressure gradient from the sea toward the estuary (landward) while northerly winds do the opposite (seaward). Möller et al. (2001) did not report on eventual time lag between the variables, however they pointed out to a phase lag that occurs between the inner Patos Lagoon and the adjacent coastal waters of the South Atlantic Ocean. This lag is modulated by the along-shore (along-estuary) winds and

by the morphology of the estuary that acts by filtering tidal and longer period oscillations generated outside the estuary.

Forbrich and Giblin (2015) studied CO₂ fluxes using the EC technique between a salt marsh vegetation in New England, USA, and the atmosphere in the months of May to October between 3 years of measurements (2012–2014). They noticed a considerable loss of CO₂ transfer in the marsh-atmosphere interface during both night and day under situations of tidal inundation (spring tides at ~15-day periodicity in their case). The authors, using NDVI data estimated from satellites, report areas of low elevation marshes susceptible to suffer reductions in their CO₂ fluxes during inundation events.

Although our site in the Pólvora Island is not subject to high tidal amplitudes (Möller et al., 2001) and the precipitation in the vicinity is not very distinct among all seasons when analyzed at the long-term scale (Silva et al., 2021), it is expected that wetter seasons or individual episodes would impact (diminishing) the vegetation/soil-atmosphere CO₂ fluxes. As pointed out by Möller et al. (2001), a wetter estuary (marsh) in the vicinity of our study area is related to the increase in the Patos Lagoon outflow (water level) that, on the other hand, is forced by northerly winds and the increase in precipitation, especially during wintertime.

The episode of Julian days ~250 to ~270 (ordinal calendar days 6 to 26 September 2016 - Figure 5) represents a period of very high water pressure anomalies (Figure 2D) and low windspeed (Supplementary Figure 6A) resulting in a very high, in phase (out of phase) cross-wavelet coherence of CO₂ fluxes against windspeed (water pressure anomaly), showing that high water levels reduce CO₂ uptake in the marsh and corroborating the results from Forbrich and Giblin (2015). Other similar episodes throughout the time series shown in Figure 5B, where the CO₂ fluxes are out of phase with the water pressure anomaly, confirm the findings of Forbrich and Giblin (2015) of a negative correlation between water level and salt marsh-atmosphere CO₂ fluxes.

The results presented in Table 2 for the amplitudes of the diurnal CO₂ fluxes also show that these amplitudes are higher during the dryer season of the summer (January–February) 2017 with respect to the winter (July–August) 2016. It is clear from Table 2 that, during the summer, higher CO₂ fluxes occurred during both daytime and nighttime periods. A study using the EC technique in a tropical mangrove (Freire et al., 2022) indicated that the highest values of vegetation-atmosphere CO₂ fluxes occurred during the wet season, in contradiction to our results for the Patos Lagoon salt marsh. In both ecosystems, however, the precipitation or water level seem to be major drivers for the vegetation-atmosphere CO₂ flux variability.

Krauss et al. (2016) point out that, although salt marshes absorb the atmospheric CO₂, these ecosystems also emit CO₂

and two other greenhouse gases (CH_4 and NO_2). Nevertheless, the authors report that the carbon sequester in wetlands is much greater than most ecosystems and, as a consequence, these environments draw general interest as greenhouse gas sinks. Studying the Louisiana (USA) wetlands, [Krauss et al. \(2016\)](#) reported an uptake rate of CO_2 by the marshes of $-337 \text{ g C m}^{-2} \text{ yr}^{-1}$ which is about 3.6 times less than our estimate of $-1217 \text{ g C m}^{-2} \text{ yr}^{-1}$ for the Patos Lagoon marshes. The authors also offered a comparison between EC measurements of greenhouse gas fluxes and estimates obtained from the more traditional technique of chambers, describing that the different spatial and temporal sampling footprints of the EC and the chambers techniques require further understating to make direct comparisons between these techniques possible.

As all techniques, the EC CO_2 flux estimates also present a range of limitations. [Oliveira et al. \(2019\)](#), for instance, described that EC CO_2 fluxes are computed using an estimate of the turbulent mixing ratio between the water vapor and the CO_2 in the atmosphere that is performed before any calculations of the surface-atmosphere CO_2 fluxes. These measurements, along with the original concentrations of these gases in the atmosphere need to be estimated at the same frequency as the vertical component of the wind and all instruments need to be calibrated and frequently serviced, as was the case in this work. At the same time, an accurate dry air density value is necessary in the calculations and a correct setting up of the EddyPro[®] routines should be applied. [Hollinger and Richardson \(2005\)](#), however, consider that the EC technique the best method to quantify surface to atmosphere fluxes with uncertainties in the order of only 5%.

Conclusion

This work presents the first results of vegetation/soil-atmosphere CO_2 flux measurements made using the eddy covariance technique for a salt marsh environment in Brazil. The major findings demonstrate that the local marsh biome is an effective sink for the atmospheric CO_2 during both periods of this study: July–November 2016 (characterizing the winter-spring seasons) and January–April 2017 (summer-fall seasons). The amplitude of the daytime (CO_2 fixed) and nighttime (CO_2 released) fluxes are dependent on the seasons, being higher during the summertime.

Our results also show that the CO_2 fluxes in the Patos Lagoon Estuary salt marshes are primary dependent on the diurnal cycle related to the photosynthetic and community respiration processes. For longer time scales, from the atmospheric synoptic cycles to the seasonal cycle, the results

demonstrate that the CO_2 fluxes are correlated and phase dependent on the winds and water level cycles. Considering the whole area of the Patos Lagoon Estuary salt marshes, this work also offers the first estimate of an annual, area-integrated net CO_2 flux indicating the sink of atmospheric CO_2 of $-87.6 \text{ Mg C yr}^{-1}$ averaged over all seasons. It is important to remember that, although not clearly seen in our data, the second semester of 2016 was a La Niña period, supposing a drier condition for our study area. Our results, in this case, may be overestimated compared to others “normal” years.

The importance of salt marshes is well known, especially when taking into account their role as a source of organic matter and nutrients that support fisheries. The predicted sea level rise imposed by the global warming represents a great risk for these environments ([Boorman, 1999](#)). The lower CO_2 sink of the salt marsh with higher water levels in the lagoon suggest that sea level rise could result in lower productivity. Although in Brazil the future expected sea level rise is not very well understood, its impacts add onto the negative pressures already imposed by urban expansion in the coastal regions. The past reduction of the salt marsh extent due to urban expansion in the Patos Lagoon Estuary is well documented ([Costa, 1997a](#); [Costa, 1997b](#); [Marangoni and Costa, 2009](#); [Seeliger, 2010](#)) and greatly impacts this environment in southern Brazil.

Taking into account the relevance of Patos Lagoon salt marshes for the maintenance of local estuarine fisheries and coastal protection (), the present study provided further basis for the conservation plans and climate change policies. Our work contributes to the present knowledge on the global carbon budget and for the conservation and management of Brazilian coastal wetlands.

Data availability statement

The raw data used in this study can be made available by the authors under request.

Author contributions

RS and MC conceived “the study”. RS, MC and GF wrote the manuscript. RS, MC and RA provided the infrastructure, equipments and gave the logistic support. MS, WP and FF processed the data and produced most of the figures. MS, RA, OM and LP revised the text. All authors contributed to the article and approved the final version of the manuscript.

Funding

This research was funded by the Brazilian agencies CNPq, CAPES, FINEP and FAPERGS through the following projects: (i) National Institute for Science and Technology of the Cryosphere (CNPq 704222/2009 + FAPERGS 17/2551-0000518-0); (ii) Polar Marine Meteorological Laboratory, Multiusers Equipment INPE 2016 (FINEP 01.16.0076.00); (iii) Use and Development of the BESM Model for Studying the Ocean-Atmosphere-Cryosphere in High and Medium Latitudes (CAPES 88887- 145668/2017-00) and (iv) Brazilian Research Network on Global Climate Change - Rede CLIMA (FINEP 01.13.0353-00). RS, GF, OM and LP. are partly funded by e (Rede CLIMAFINEP/Grant 01.13.0353-00) fellowships of the CNPq Scientific Productivity Program (CNPq/308642/2021-0; CNPq/307048/2018-7; CNPq/4029906/2019-5 and CNPq/304858/2019-6, respectively).

Acknowledgments

The authors acknowledge the Brazilian National Institute of Meteorology (INMET) and the European Centre for Medium Range Weather Forecast (ECMWF) for providing the supplementary meteorological data used here. We thank Prof. Lauro Barcellos, head of the FURG Museum Complex for the support to this project and by providing the access and infrastructures for the field campaigns. We acknowledge the support provided by INPE's Southern Space Coordination (INPE/COESU, Santa Maria – Brazil), by the Institute of Oceanography of Rio Grande University (IO-FURG, Rio Grande - Brazil) and by the Micrometeorology Group, Physics Department, Federal University of Santa Maria (UFSM, Santa Maria - Brazil) for setting up the micrometeorological tower, for the sensor's maintenance and for the data recovery. We are especially thankful to Catherine Lovelock and two reviewers for their extensive revisions and recommendations that improved

the quality of this paper. We thank Joel Rubert, Eliane Klering and Carlos Fujita for their technical assistance during the field works and for the data pre-processing during all phases of this work. The EddyPro[®] software is available for download at https://www.licor.com/env/products/eddy_covariance/software.html. The Tovi[™] software is available for download at <https://www.licor.com/shop/software/tovi/register/>.

Conflict of interest

The authors declare that the research was conducted in the absence of any commercial or financial relationships that could be construed as a potential conflict of interest.

Publisher's note

All claims expressed in this article are solely those of the authors and do not necessarily represent those of their affiliated organizations, or those of the publisher, the editors and the reviewers. Any product that may be evaluated in this article, or claim that may be made by its manufacturer, is not guaranteed or endorsed by the publisher.

Supplementary material

The Supplementary Material for this article can be found online at: <https://www.frontiersin.org/articles/10.3389/fmars.2022.892857/full#supplementary-material>

References

- Adam, P. (1993). *Saltmarsh ecology* (Cambridge: Cambridge University Press).
- Armani, F. A. S., Dias, N. L., and Damázio, J. M. (2020). Eddy-covariance CO₂ fluxes over itaipu lake, southern Brazil. *Rev. Bras. Recursos Hídricos* 25, e43. doi: 10.1590/2318-0331.2520202000060
- Aubinet, M., Vesala, T., and Papale, D. (2012). *Eddy covariance: a practical guide to measurement and data analysis* (London: Springer Science & Business Media).
- Barr, J. G., Engel, V., Fuentes, J. D., Zieman, J. C., O'Halloran, T. L., Smith, T. J.III, et al. (2010). Controls on mangrove forest-atmosphere carbon dioxide exchanges in western Everglades national park. *J. Geophys. Res.: Biogeosci.* 115 (G2), G02020. doi: 10.1029/2009JG001186
- Boorman, L. A. (1999). Salt marshes – present functioning and future change. *Mangroves Salt Marshes* 3, 227–241. doi: 10.1023/A:1009998812838
- Chmura, G. L., Anisfeld, S. C., Cahoon, D. R., and Lynch, J. C. (2003). Global carbon sequestration in tidal, saline wetland soils. *Global Biogeochem. Cycles* 17 (4), 1111. doi: 10.1029/2002GB001917
- Chu, X., Han, G., Wei, S., Xing, Q., He, W., Sun, B., et al. (2021). Seasonal not annual precipitation drives 8-year variability of interannual net CO₂ exchange in a salt marsh. *Agric. For. Meteorol.* 308, 108557. doi: 10.1016/j.agrformet.2021.108557
- Costa, C. S. B. (1997a). "Tidal marshes and wetlands," in *Subtropical convergence environments: the coast and sea in the southwestern Atlantic*. Eds. C. Seeliger U. Odebrecht and J. P. Castello (Berlin: Springer Science & Business Media), 24–26.
- Costa, C. S. B. (1997b). "Irregularly flooded marginal marshes," in *1997: Subtropical convergence environments: the coast and sea in the southwestern Atlantic*. Eds. U. Seeliger, C. Odebrecht and J. P. Castello (Berlin: Springer Science & Business Media), 73–77.
- Costa, C. S. B., and Marangoni, J. C. (2010). "The salt marsh communities," in *2010: The patos lagoon estuary – a century of transformations*. Eds. U. Seeliger and C. Odebrecht (Berlin: Rio Grande: FURG), 125–133.

- Costa, C. S., Marangoni, J. C., and Azevedo, A. M. (2003). Plant zonation in irregularly flooded salt marshes: relative importance of stress tolerance and biological interactions. *J. Ecol.* 91 (6), 951–965. doi: 10.1046/j.1365-2745.2003.00821.x
- Costa, G. B., Santos e Silva, C. M., Mendes, K. R., dos Santos, J. G. M., Neves, T. T. A. T., Silva, A. S., et al. (2022). WUE and CO₂ estimations by eddy covariance and remote sensing in different tropical biomes. *Remote Sens.* 14, 3241. doi: 10.3390/rs14143241
- Duarte, C. M., Losada, I. J., Hendriks, I. E., Mazarrasa, I., and Marbà, N. (2013). The role of coastal plant communities for climate change mitigation and adaptation. *Nat. Climate Change* 3 (11), 961–968. doi: 10.1038/nclimate1970
- Duarte, C. M., Middelburg, J. J., and Caraco, N. (2005). Major role of marine vegetation on the oceanic carbon cycle. *Biogeosciences* 2 (1), 1–8. doi: 10.5194/bg-2-1-2005
- Edson, J. B., Jampana, V., Weller, R. A., Bigorre, S. P., Plueddemann, A. J., Fairall, C. W., et al. (2013). On the exchange of momentum over the open ocean. *J. Physical Oceanography* 43, 1589–1610. doi: 10.1175/JPO-D-12-0173.1
- Foken, T., Göckede, M., Mauder, M., Mahrt, L., Amiro, B. D., and Munger, J. W. (2004). *Post-field data quality control Handbook of micrometeorology. a guide for surface flux measurements*. Eds. X. Lee, W. J. Massman and B. E. Law (Berlin: Springer Science & Business Media), 181–208.
- Forbrich, I., and Giblin, A. E. (2015). Marsh-atmosphere CO₂ exchange in a new England salt marsh. *J. Geophys. Research:Biogeosci.* 120, 1825–1838. doi: 10.1002/2015JG003044
- Freire, A. S. C., Vitorino, M. I., de Souza, A. M. L., and Germano, M. F. (2021). Analysis of the energy balance and CO₂ flow under the influence of the seasonality of climatic elements in a mangrove ecosystem in Eastern Amazon. *Int. J. Biometeorol.* 66, 347–359. doi: 10.1007/s00484-021-02224-8
- Gibbs, H. K., Brown, S., Niles, J. O., and Foley, J. A. (2007). Monitoring and estimating tropical forest carbon stocks: making REDD a reality. *Environ. Res. Lett.* 2 (4), 045023. doi: 10.1088/1748-9326/2/4/045023
- Goulden, M. L., Litvak, M., and Miller, S. D. (2007). Factors that control typha marsh evapotranspiration. *Aquat. Bot.* 86 (2), 97–106. doi: 10.1016/j.aquabot.2006.09.005
- Grinsted, A., Moore, J. C., and Jevrejeva, S. (2004). Application of the cross wavelet transform and wavelet coherence to geophysical time series. *Nonlinear Process. Geophys.* 11 (5/6), 561–566. doi: 10.5194/npg-11-561-2004
- Hawman, P. A., Mishra, D. R., O'Connell, J. L., Cotten, D. L., Narron, C. R., and Mao, L. (2021). Salt marsh light use efficiency is driven by environmental gradients and species-specific physiology and morphology. *J. Geophys. Research:Biogeosci.* 126 (5), e2020JG006213. doi: 10.1029/2020JG006213
- Hersbach, H., Bell, B., Berrisford, P., Hirahara, S., Horányi, A., Muñoz-Sabater, J., et al. (2020). The ERA5 global reanalysis. *Q. J. R. Meteorol. Soc.* 146 (730), 1999–2049. doi: 10.1002/qj.3803
- Hill, A. C., Vázquez-Lule, A., and Vargas, R. (2021). Linking vegetation spectral reflectance with ecosystem carbon phenology in a temperate salt marsh. *Agric. For. Meteorol.* 307, 108481. doi: 10.1016/j.agrformet.2021.108481
- Himes-Cornell, A., Pendleton, L., and Atiyah, P. (2018). Valuing ecosystem services from blue forests: A systematic review of the valuation of salt marshes, sea grass beds and mangrove forests. *Ecosyst. Serv.* 30, 36–48. doi: 10.1016/j.ecoser.2018.01.006
- Hollinger, D. Y., and Richardson, A. D. (2005). Uncertainty in eddy covariance measurements and its application to physiological models. *Tree Physiol.* 25 (7), 873–885. doi: 10.1093/treephys/25.7.873
- Howe, A. J., Rodríguez, J. F., and Saco, P. M. (2009). Surface evolution and carbon sequestration in disturbed and undisturbed wetland soils of the hunter estuary, southeast Australia. *Estuar. Coast. Shelf. Sci.* 84 (1), 75–83. doi: 10.1016/j.ecss.2009.06.006
- IPCC (2014). “Climate change 2014,” in *Synthesis report. contribution of working groups I, II and III to the fifth assessment report of the intergovernmental panel on climate change*. Eds. R. K. Pachauri and L. A. Meyer (Geneva, Switzerland: IPCC), 151 pp
- IPCC (2021). “Summary for policymakers,” in *Climate change 2021: The physical science basis. contribution of working group I to the sixth assessment report of the intergovernmental panel on climate change*. Eds. V. Masson-Delmotte, P. Zhai, A. Pirani, S. L. Connors, C. Péan, S. Berger, N. Caud, Y. Chen, L. Goldfarb, M. I. Gomis, M. Huang, K. Leitzell, E. Lonnoy, J. B. R. Matthews, T. K. Maycock, T. Waterfield, O. Yelekçi, R. Yu and B. Zhou (Cambridge, United Kingdom and New York, NY, USA: Cambridge University Press), 3–32. doi: 10.1017/9781009157896.001
- Isaac, V. J., Martins, A. S., Haimovici, M., and Andriguetto-Filho, J. M. (2006). “A pesca marinha e estuarina do Brasil no início do século XXI,” in *Recursos, tecnologias, aspectos socioeconômicos e institucionais* (Belém: UFPA), 11–40.
- Jung, M., Reichstein, M., Margolis, H. A., Cescatti, A., Richardson, A. D., Arain, M. A., et al. (2011). Global patterns of land-atmosphere fluxes of carbon dioxide, latent heat, and sensible heat derived from eddy covariance, satellite, and meteorological observations. *J. Geophys. Res.: Biogeosci.* 116 (G3), G00J07. doi: 10.1029/2010jg001566
- Kaimal, J. C., and Finnigan, J. J. (1994). *Atmospheric boundary layer flows: their structure and measurement* (Oxford: Oxford University Press). doi: 10.1093/oso/9780195062397.001.0001
- Kljun, N., Calanca, P., Rotach, M. W., and Schmid, H. P. (2004). A simple parameterisation for flux footprint predictions. *Boundary-Layer. Meteorol.* 112 (3), 503–523. doi: 10.1023/b:boun.0000030653.71031.96
- Kljun, N., Calanca, P., Rotach, M. W., and Schmid, H. P. (2015). A simple two-dimensional parameterisation for flux footprint prediction (FFP). *Geoscientific Model. Dev.* 8 (11), 3695–3713. doi: 10.5194/gmd-8-3695-2015
- Krauss, K. W., Holm, G. O., Perez, B. C., McWhorter, D. E., Cormier, N., Moss, R. F., et al. (2016). Component greenhouse gas fluxes and radiative balance from two deltaic marshes in Louisiana: Pairing chamber techniques and eddy covariance. *J. Geophys. Res.: Biogeosci.* 121 (6), 1503–1521. doi: 10.1002/2015jg003224
- Lockwood, B., and Drakeford, B. M. (2021). The value of carbon sequestration by saltmarsh in Chichester harbour, united kingdom. *J. Environ. Econ. Policy* 10 (3), 278–292. doi: 10.1080/21606544.2020.1868345
- Lovelock, C. E., Atwood, T., Baldock, J., Duarte, C. M., Hickey, S., Lavery, P. S., et al. (2017). Assessing the risk of carbon dioxide emissions from blue carbon ecosystems. *Front. Ecol. Environ.* 15 (5), 257–265. doi: 10.1002/fee.1491
- Lovelock, C. E., and Duarte, C. M. (2019). Dimensions of blue carbon and emerging perspectives. *Biol. Lett.* 15 (3), 20180781. doi: 10.1098/rsbl.2018.0781
- Macreadie, P. I., Allen, K., Kelaher, B. P., Ralph, P. J., and Skilbeck, C. G. (2012). Paleoreconstruction of estuarine sediments reveal human-induced weakening of coastal carbon sinks. *Global Change Biol.* 18 (3), 891–901. doi: 10.1111/j.1365-2486.2011.02582.x
- Macreadie, P. I., Anton, A., Raven, J. A., Beaumont, N., Connolly, R. M., Friess, D. A., et al. (2019). The future of Blue Carbon science. *Nat. Commun.* 10, 3998. doi: 10.1038/s41467-019-11693-w
- Marangoni, J. C., and Costa, C. S. B. (2009). Natural and anthropogenic effects on salt marsh over five decades in the patos lagoon (Southern Brazil). *Braz. J. Oceanogr.* 57 (4), 345–350. doi: 10.1590/S1679-87592009000400009
- Martinetto, P., Montemayor, D. I., Alberti, J., Costa, C. S., and Iribarne, O. (2016). Crab bioturbation and herbivory may account for variability in carbon sequestration and stocks in south west Atlantic salt marshes. *Front. Mar. Sci.* 3, 122. doi: 10.3389/fmars.2016.00122
- McLeod, E., Chmura, G. L., Bouillon, S., Salm, R., Björk, M., Duarte, C. M., et al. (2011). A blueprint for blue carbon: toward an improved understanding of the role of vegetated coastal habitats in sequestering CO₂. *Front. Ecol. Environ.* 9 (10), 552–560. doi: 10.1890/110004
- Miller, S. D., Marandino, C., and Saltzman, E. S. (2010). Ship-based measurement of air-sea CO₂ exchange by eddy covariance. *J. Geophys. Res.: Atmos.* 115 (D2), D02304. doi: 10.1029/2009JD012193
- Möller, O. O., Castaing, P., Salomon, J. C., and Lazure, P. (2001). The influence of local and non-local forcing effects on the subtidal circulation of patos lagoon. *Estuaries* 24 (2), 297–311. doi: 10.2307/1352953
- Möller, O., and Fernandes, E. (2010). “Hydrology and hydrodynamics,” in *The patos lagoon estuary – a century of transformations*. Eds. U. Seeliger and C. Odebrecht (Rio Grande: FURG), 17–27.
- Moncrieff, J., Clement, R., Finnigan, J., and Meyers, T. (2004). “Averaging, detrending, and filtering of eddy covariance time series,” in *Handbook of micrometeorology* (Dordrecht: Springer), 7–31.
- Nogueira, R. X. S., and Costa, C. S. B. (2003). “Patos lagoon (RS – Brazil) salt marsh mapping using infrared digital 35 mm aerial photographs,” in *Proceedings, IX congresso da associação brasileira de estudos do quaternário, II congresso do quaternário de países de língua ibérica, II congresso sobre planejamento e gestão da zona costeira dos países de expressão portuguesa*. (São Paulo: Associação Brasileira de Estudos do Quaternário). 2003, 1–5. Available in http://www.abequa.org.br/trabalhos/gerenciamento_199.pdf.
- Odebrecht, C., Bergesch, M., Rörig, L. R., and Abreu, P. C. (2010). Phytoplankton interannual variability at cassino beach, southern Brazil, (1992–2007), with emphasis on the surf zone diatom *Asterionellopsis glacialis*. *Estuar. Coasts* 33 (2), 570–583. doi: 10.1007/s12237-009-9176-6
- Odebrecht, C., Secchi, E. R., Abreu, P. C., Muelbert, J. H., and Uiblein, F. (2017). Biota of the patos lagoon estuary and adjacent marine coast: long-term changes induced by natural and human-related factors. *Mar. Biol. Res.* 13 (1), 3–8. doi: 10.1080/17451000.2017.1288037
- Oliveira, R. R., Pezzi, L. P., Souza, R. B., Santini, M. F., Cunha, L. C., and Pacheco, F. S. (2019). First measurements of the ocean-atmosphere CO₂ fluxes at the cabo frio upwelling system region, southwestern Atlantic ocean. *Continental Shelf. Res.* 181, 135–142. doi: 10.1016/j.csr.2019.05.008
- Ouyang, X., and Lee, S. Y. (2014). Updated estimates of carbon accumulation rates in coastal marsh sediments. *Biogeosciences* 11, 5057–5071. doi: 10.5194/bg-11-5057-2014

- Patterson, E., Johnson, B., Dostie, P., and Copertino, M. (2016). "Stocks and sources of carbon buried in the salt marshes and seagrass beds of patos lagoon estuary, southern Brazil," in *EGU general assembly 2016 conference abstracts*. (Vienna: European Geoscience Union - EGU), EPSC2016-10792.
- Pendleton, L., Donato, D. C., Murray, B. C., Crooks, S., Jenkins, W. A., Sifleet, S., et al. (2012). Estimating global "Blue carbon" emissions from conversion and degradation of vegetated coastal ecosystems. *PLoS One* 7 (9), e43542. doi: 10.1371/journal.pone.0043542
- Pezzi, L. P., de Souza, R. B., Santini, M. F., Miller, A. J., Carvalho, J. T., Parise, C. K., et al. (2021). Oceanic eddy-induced modifications to air-sea heat and CO₂ fluxes in the Brazil-malvinas confluence. *Sci. Rep.* 11 (1), 1–15. doi: 10.1038/s41598-021-89985-9
- Pezzi, L. P., Souza, R. B., Farias, P. C., Acevedo, O., and Miller, A. J. (2016). Air-sea interaction at the southern Brazilian continental shelf: *In situ* observations. *J. Geophys. Res.: Oceans* 121 (9), 6671–6695. doi: 10.1002/2016JC011774
- Polsenaere, P., Lamaud, E., Lafon, V., Bonnefond, J. M., Bretel, P., Delille, B., et al. (2012). Spatial and temporal CO₂ exchanges measured by eddy covariance over a temperate intertidal flat and their relationships to net ecosystem production. *Biogeosciences* 9 (1), 249–268. doi: 10.5194/bg-9-249-2012
- Reboita, M. S., Gan, M. A., Rocha, R. P. D., and Ambrizzi, T. (2010). Regimes de precipitação na América do Sul: uma revisão bibliográfica. *Rev. Bras. Meteorol.* 25, 185–204. doi: 10.1590/S0102-77862010000200004
- Reboita, M. S., and Kruche, N. (2018). Normais climatológicas provisórias de 1991 a 2010 para Rio Grande, RS. *Rev. Bras. Meteorol.* 33, 165–179. doi: 10.1590/0102-7786333101
- Santini, M. F., Souza, R. B., Pezzi, L. P., and Swart, S. (2020). Observations of air-sea heat fluxes in the southwestern Atlantic under high-frequency ocean and atmospheric perturbations. *Q. J. R. Meteorol. Soc.* 146 (733), 4226–4251. doi: 10.1002/qj.3905
- Seeliger, U. (2010). "Introduction," in *The Patos Lagoon estuary – a century of transformations*. Eds. U. Seeliger and C. Odebrecht (Rio Grande: FURG), 11–13.
- Silva, T. R., Reis, I., Klering, E., and Maier, E. L. B. (2021). Precipitação em Rio Grande – RS, (1913 – 2016): Análise descritiva e da variabilidade. *Rev. Bras. Geograf. Física* 14 (2), 537–553. doi: 10.26848/rbgf.v14.2
- Souza, R., Pezzi, L., Swart, S., Oliveira, F., and Santini, M. (2021). Air-sea interactions over eddies in the Brazil-malvinas confluence. *Remote Sens.* 13 (7), 1335. doi: 10.3390/rs13071335
- Stull, R. B. (1988). *An introduction to boundary layer meteorology*. Vol. 13 (Dordrecht: Kluwer Academic Publishers).
- Taillard, P., Friess, D. A., and Lupascu, M. (2018). Mangrove blue carbon strategies for climate change mitigation are most effective at the national scale. *Biol. Lett.* 14, e20180251.
- Tonti, N. E., Gassmann, M. I., and Pérez, C. F. (2018). First results of energy and mass exchange in a salt marsh on southeastern south America. *Agric. For. Meteorol.* 263, 59–68. doi: 10.1016/j.agrformet.2018.08.001
- Verbeeck, H., Peylin, P., Bacour, C., Bonal, D., Steppe, K., and Ciais, P. (2011). Seasonal patterns of CO₂ fluxes in Amazon forests: Fusion of eddy covariance data and the ORCHIDEE model. *J. Geophys. Res.: Biogeosci.* 116, G02018. doi: 10.1029/2010jg001544
- Vickers, D., and Mahrt, L. (1997). Quality control and flux sampling problems for tower and aircraft data. *J. Atmos. Oceanic Technol.* 14, 512–26. doi: 10.1175/1520-0426(1998)015<0416:FSEFAA>2.0.CO;2
- Webb, E. K., Pearman, G. I., and Leuning, R. (1980). Correction of flux measurements for density effects due to heat and water vapour transfer. *Q. J. R. Meteorol. Soc.* 106 (447), 85–100. doi: 10.1002/qj.49710644707

Frontiers in Marine Science

Explores ocean-based solutions for emerging global challenges

The third most-cited marine and freshwater biology journal, advancing our understanding of marine systems and addressing global challenges including overfishing, pollution, and climate change.

Discover the latest Research Topics

[See more →](#)

Frontiers

Avenue du Tribunal-Fédéral 34
1005 Lausanne, Switzerland
frontiersin.org

Contact us

+41 (0)21 510 17 00
frontiersin.org/about/contact

